

The 5th Asia Color Association Conference
ACA 2019 Nagoya



Proceedings

29 Nov. - 2 Dec. 2019
Meijo University, Nagoya, JAPAN

The 5th Asia Color Association Conference
ACA 2019 Nagoya



29 Nov. - 2 Dec. 2019

Meijo University, Nagoya, JAPAN

Proceedings

The Asia Color Association (ACA)

The Color Science Association of Japan(CSAJ)

Contents

Invitation Address	4
Greeting of Mitsuo Ikeda, the ACA coordinator.....	5
Welcome Message.....	6
Committees	7
Cosponsor/ Sponsors/ Exhibitors	8
Timetable	9
Oral Presentation Program.....	11
Poster Presentation Program	13
Floor Map.....	15
Keynote Speech, Invited Talks, Seminar, Workshop	16
Keynote Speech 1.....	17
Keynote Speech 2.....	18
Invited Talks.....	19
Seminar	24
Workshop	26
Oral Papers.....	31
Poster Papers.....	361
Design concept behind the ACA2019 Nagoya Logo.....	713
Sponsors / Exhibitors	714
Advertisement	

Proceedings

© 2019 the Asia Color Association (ACA)

<http://www.color-science.jp/ACA2019/top/index.html>

DISCLAIMER

Matters of copyright all images and text association with the papers contained within the ACA 2019 Book of Abstracts are the responsibility of the authors. The ACA and the Color Science Association of Japan (CSAJ) do not accept responsibility for any liabilities arising from the publication of any of the submission.

COPYRIGHT

Reproduction of this document or parts thereof by any means whatsoever is prohibited without the written permission of the Asia Color Association. All copies of the individual articles remain the intellectual property of the individual authors and/or their affiliated institutions.

Published November, 2019
by the Steering Committee of ACA 2019 Nagoya
Editors: Taiichiro Ishida, Takashi Tsujino
Graphical design: Manami Tada
Printed by Tsujino Planning Office, Inc.

Invitation Address

Dear Ladies and Gentlemen,

As the conference chair of the fifth Asia Color Association Conference, it is my great pleasure to welcome all of our participants to “ACA2019 Nagoya” in Aichi, Japan. This marks the fifth anniversary since the first ACA conference was held in Thailand. That first conference was at Rajamangala University of Technology Thanyaburi in 2013, and it has since been held in Taiwan, China, and Thailand again. Therefore, it is a great honor for Meijo University to provide a venue for the ACA conference for the first time in Japan. We are privileged to present to you, through the theme of “Color Communications”, the new concept of the ACA conference for up to the next five years.



The ACA conference aims to become a focal point of exchange among Asian scientists and designers specializing in color. This is the first time the ACA conference is being held in Japan, making it possible for young researchers from Asian countries to come to an event they would otherwise have difficulty attending. This is especially true with Meijo University, which is located in Nagoya, the third largest urban area in Japan. Nagoya has, of course, achieved significant development in the textile, ceramic and automobile industries. I believe that every participant of the ACA conference is going to enjoy this exciting and traditional city and create new networks with each other during this “Color Communications” conference.

I would like to thank all the contributions and cooperation given by the committee members, especially the Steering Committee and the Program Committee, and also acknowledge the contribution made by sponsoring companies and organizations. I offer my sincerest hope that this conference will prove to be most fruitful to all participants, and that the results of its success will become a valuable asset to be passed on to the future. Thank you for joining us to experience this “Color Communications” conference in Nagoya, Aichi, Japan.

Sincerely yours,

Teiji Tachibana

Conference Chair, ACA2019 Nagoya
Chairman, Meijo Educational Foundation

Greeting of Mitsuo Ikeda, the ACA coordinator

I, as the coordinator of ACA, feel particularly happy to see the 5th ACA conference is held in Japan, one of the most advanced countries in the world in the color science and design. Since ACA was established in 2013, it went to Thailand in 2013, Taiwan in 2014, China in 2016, and Thailand again in 2018, but not to Japan. I hoped for many years the ACA to go to Japan. Now it is realized and we are here. I asked Dr Kawasumi of Meijo University of Japan some years ago if she can invite the ACA to Japan recognizing that it should be a very hard work for her if she once accepts it. And she accepted. On behalf of the ACA board I would like to thank Dr Kawasumi for organizing the conference and for leading the conference to a great success.



The ACA set four mottos at the time of establishment. 1. Economical conferences so that any body, particularly young people can attend, 2. No rigid membership. Any countries, regions, and individuals are welcome to take parts in ACA. 3. The language is English, but no fluent English is required, broken English is ok. And 4, No conference in the year when AIC is held in Asia. The mottos 1 and 3 were already realized as we can see many young scientists and designers are attending in this conference. Thanks to many air companies which nowadays provide people with economical ticket and to hotels for providing with economical rooms to stay that can be searched for through internet. Some young people are afraid to attend at the conference because they have no confidence to communicate in English. But they need not to worry about this. All the attendants are similar on this point and you will get help from others.

There was a heartwarming article on a recent newspaper to report a happening in the 5000 meters track and field world championship. An athlete from a small country, Guinea Bissau in West Africa was running backmost at the last round for the goal and noticed an athlete running in front him was fluttering because of dehydration symptoms. The Guinea Bissau athlete caught up him, lent his shoulder and finished goal together. Audience applauded his action. I am sure that ACA has the same spirit. Attendants coming from advanced countries in the field of color science and design are willing to help those coming from developing countries in the field of color science and design. I am convinced that the 5th ACA conference will be successful and profitable to every body to attend at the conference.

At the last but not the least, I would like to thank Meijo university and the president Mr. Tachibana who invited the 5th ACA to Meijo university and took the responsibility as the conference chair. Also acknowledge the Color Science Association of Japan for becoming the cosponsor.

Mitsuo Ikeda
Coordinator of ACA

Welcome Message

Dear colleagues in the field of color science and design,

On behalf of the steering committee of ACA2019 Nagoya, I would like to welcome you all to the fifth Asia Color Association Conference at Meijo University, Nagoya, Japan. This conference is being cosponsored by the Color Science Association of Japan in cooperation with Aichi Prefectural Government, Nagoya Chamber of Commerce and Industry, and Meijo University. The theme of this conference is “Color Communications”, and we anticipate seeing more than two hundred delegates from all over the world enjoying it.



This conference is providing a place where scientists and designers specializing in color, especially young researchers and students in Asian countries, can communicate and interact with each other. Therefore, it is hoped that you will expand your knowledge and experience, and will create new networks in your fields.

With this in view, one hundred thirty nine abstracts have been received from eleven countries. This is the largest number ever at an ACA conference, and so the program committee has organized twelve sessions. In addition to these regular presentations, the ACA2019 Nagoya conference will be highlighted by two keynote speeches, nine invited talks, one seminar series, two workshops, and also some exciting exchange programs. I believe that these programs are going to provide a unique opportunity for you to present your research activities and discuss your mutual interests with others for the future advancement of your fields.

I am grateful for the efforts made by the members of the program and the steering committees, and I would like to express my gratitude to all of the authors for contributing their works, to all of the special session organizers for their hard work, and to all of the sponsoring companies and organizations for their cooperation. I sincerely hope that this conference will be highly successful and fruitful to you and that you will fully enjoy the conference, the academic atmosphere at Meijo University, and the exciting city of Nagoya.

Sincerely Yours,

Mikiko Kawasumi

General Chair, Steering Committee of ACA2019 Nagoya

Committees

Conference Chair:

Teiji Tachibana, President of Meijo University

International Advisory Committee:

Mitsuo Ikeda, Rajamangala University of Technology Thanyaburi, Thailand (Chair)

Tien-Rein Lee, Huafan University, Taiwan

Haisong Xu, Zhejiang University, China

Adi Djoko Guritno, Universitas Gadjah Mada, Indonesia

Chanprapha Phuangsuwan, Rajamangala University of Technology Thanyaburi, Thailand

Naoyuki Osaka, Kyoto University, Japan

Hirohisa Yaguchi, Chiba University, Japan

Miho Saito, Waseda University, Japan

Miyoshi Ayama, Utsunomiya University, Japan

Takahiko Horiuchi, Chiba University, Japan

Hiroyasu Koshimizu, Chukyo University, Japan

Toshio Fukuda, Meijo University, Japan

Movie Editor:

Tadashi Osumi, SHOCHIKU Co., Ltd

Program Committee:

Katsunori Okajima, Yokohama National University (Chair)

Tomoko Obama, Shizuoka University of Art and Culture (Co-chair)

Steering Committee:

General Chair:

Mikiko Kawasumi, Meijo University

Finance:

Yoko Mizokami, Chiba University (Chair)

Misako Yamagishi, Aichi Shukutoku University

Hisayo Ishihara, Sugiyama Jogakuen University

Shosuke Yagihashi, Color Science Association of Japan

Registration:

Shinji Nakamura, Nihon Fukushi University (Chair)

Yasuhiro Seya, Aichi Shukutoku University

Takashi Hanari, Sugiyama Jogakuen University

Publication:

Taiichiro Ishida, Kyoto University (Chair)

Takashi Tsujino, TPO

Public Relationship:

Hiroyuki Shinoda, Ritsumeikan University (Chair)

Manami Tada, Chic-design

Facility:

Eiji Kamei, Meijo University (Chair)

Atsushi Tsukada, Meijo University

Sponsorship:

Norihiro Ikeda, Kictec (Chair)

Masato Hotta, Asahi University

Kanoko Washizu, Nagoya University of Arts and Sciences

Reception Desk:

Takashi Sakamoto, National Institute of Advanced Industrial Science and Technology (Chair)

Hideki Sakai, Osaka City University

Kanoko Washizu, Nagoya University of Arts and Sciences

Hospitality:

Chiho Watanabe, Toyoda Gosei (Chair)

Yoshiko Sumiyoshi & Special Interest Group on Environmental Color Design for Daily Living

Excursion:

Tomoko Obama, Shizuoka University of Art and Culture (Chair)

Yumiko Sobue, Atelier Tricolor

Coordination with CSAJ:

Shinya Takahashi, President of Color Science Association of Japan

Michiru Shimokawa, Board member of Color Science Association of Japan

MC:

Yasuki Yamauchi, Yamagata University

Yoko Yamauchi, Studio die Sonne

Camera:

Takashi Hanari, Sugiyama Jogakuen University

Ryosuke Yamagata, Nagoya University of Arts and Sciences

Cosponsor / Sponsors / Exhibitors

Cosponsored by

The Color Science Association of Japan

In cooperation with

Aichi Prefectural Government
Nagoya Chamber of Commerce & Industry
Meijo University

With the support of

Secom Science and Technology
Foundation
Daiko Foundation

The Illuminating Engineering Institute of
Japan
Vision Society of Japan
Japan Society of Kansei Engineering
The Institute of Image Information and
Television Engineers
Japan Society of Colour Material
Information Processing Society of Japan
The Institute of Electrical Engineers of
Japan
The Institute of Electronics, Information
and Communication Engineers
The Japanese Society of Printing Science
and Technology
The Japan Society of Home Economics
The Imaging Society of Japan
The Japanese Society of Ophthalmological
Optics
The Japan Society of Mechanical
Engineers
The Japanese Psychonomic Society
Architectural Institute of Japan
The Optical Society of Japan
Japan Lighting Manufacturers Association
Japanese Society for The Science of
Design
Coating Equipment Manufacturers
Association, Japan
The Japan Ergonomics Society

Sponsors/Exhibitors

Sponsored by

KICTEC INC.
ITO OPTICAL INDUSTRIAL CO., LTD.
TOYODA GOSEI CO., LTD
TOYOTA HOUSING CORPORATION
OFFICE COLOR SCIENCE CO.,LTD.
KONICA MINOLTA JAPAN, Inc.
SHOFU INC.
Shinto Tsushin Co., Ltd.
DENTALPRO Co.,Ltd.
The grant of Secom Science and Technology
Foundation
The grant of Daiko Foundation

Exhibitors:

NAMOTO Co., Ltd.
JAPAN COLOR ENTERPRISE CO.,LTD.
EBA JAPAN CO., LTD.
NIPPON DENSHOKU INDUSTRIES CO., LTD
KONICA MINOLTA JAPAN, Inc.

Movie:

SHOCHIKU Co., Ltd

Oral Presentation ★ Sat. 30 Nov. 2019

Room A

Room A West 3F		
SAT-1A	COLOR PREFERENCE <1> Diversity Akira Asano(JP) / Tien-Rein Lee(TW)	
SAT-1A-1	Kim Min-Kyong	KR Invited Talk: Personal Color Analysis for Korean Women's (For women in their 20s and 30s)
SAT-1A-2	Masaya Nishimoto and Shigeki Nakauchi	JP Preference for Color Composition of Art Paintings and its Individual Differences
SAT-1A-3	Hathaichanok Khemthong, Prathana Thammachat, Natthamon Piengthisong and Chanida Saksirikosol	TH Use of Smoke in Advertising Hot Drink Photography Production
SAT-1A-4	Pantakan Sukontee, Chanprapha Phuangsuan, Hiroyuki Iyota, Hideki Sakai and Mitsuo Ikeda	TH Color of Cooked Rice to Improve Appetite for Elderly
SAT-1A-5	Ploy Srisuro, Warin Chuen-Aram and Thitapa Rodsong	TH Color Satisfaction on Printed Media of Foundation for Rehabilitation and Development of Children and Family (FORDEC)
SAT-2A	COLOR PREFERENCE <2> Marketing Tomoko Obama(JP) / Adi Djoko(ID)	
SAT-2A-1	Adi Djoko Guritno, Novita Erma Kristanti and Melinda Sugiana Dharmawati	ID Discoloration of Tuna Fillets (Thunnus Albacores) to Increase Added Value Using Industrial Gases
SAT-2A-2	Novita Erma Kristanti and Annisa Nurul Ghifari	ID Identifying Soybean (Glycine Max L. Merr) by Color Analysis in Supply Chains to Improve Consumer Preferences
SAT-2A-3	Nafis Khuriyati, M. Affan Fajar Falah, Mirwan Ushada and Bayu Kristiawan	ID Chili Color and Spiciness
SAT-2A-4	Wahyu Supartono and Devina Nikasari	ID Optimization of Blue Rice Production using Taguchi Method
SAT-2A-5	Cancellation	
SAT-2A-6	Eri Oomae (Zhou Xin)	CH Invited Talk: Asia Color Trend Book

Room B

Room B West 4F		
SAT-1B	LIGHTING & COLOR TEMPERATURE Taiichiro Ishida(JP) / Chanprapha Phuangsuan(TH)	
SAT-1B-1	Pei-Tzu Huang and Hung-Shing Chen	TW Spectral Design of Lighting Indicator for Detecting 5000 K White-Light LED
SAT-1B-2	Phubet Chitapanya, Chanprapha Phuangsuan and Mitsuo Ikeda	TH Color Appearance of Objects in the Environment Lit with LED Lamps
SAT-1B-3	Taiichiro Ishida and Yusuke Tateishi	JP Influence of Correlated Color Temperature and Duv of Lighting on Visual Impressions of a Space
SAT-1B-4	Nana Itoh and Ken Sagawa	JP Spans of Fundamental Colors — Comparison Among Normal Color Vision of Young and Older People, Defective Color Vision, and Low Vision
SAT-1B-5	Youngshin Kwak	KR Invited Talk: Vision Experiment on Perception of Correlated Colour Temperature
SAT-2B	COSMETICS & SKIN COLOR Takashi Sakamoto(JP) / Takanori Igarashi(JP)	
SAT-2B-1	Yoko Mizokami	JP Invited Talk: Color Perception Specific to Facial Skin
SAT-2B-2	Kumiko Kikuchi	JP Invited Talk: Image-based Measurement of Human Skin Color and its Application in Cosmetics Field
SAT-2B-3	Taiga Mikami, Yuanyuan He, Helene Midtjord, Suguru Tanaka, Kumiko Kikuchi and Yoko Mizokami	JP International Comparison of Facial Skin Brightness Perception with Differences in Skin Color
SAT-2B-4	Nutticha Pattarasoponkun, Chanprapha Phuangsuan and Mitsuo Ikeda	TH Skin Color of Thai People
SAT-2B-5	Kanokwan Sordang, Chanprapha Phuangsuan, Natsuki Tsuji, Mikiko Kawasumi and Mitsuo Ikeda	TH Color of Lipstick to Make Thai Girls Healthier

Room C

Room C West 4F		
SAT-1C	COLOR MANAGEMENT Motonori Doi(JP) / Changjun Li(CN)	
SAT-1C-1	Phil Green	UK Communicating Colour with an Advanced Colour Management Framework
SAT-1C-2	Yuki Akizuki, Futoshi Ohyama and Satoshi Iwamoto	JP The Issue of Color Appearance in Telemedicine System
SAT-1C-3	Kazuji Matsumoto and Misao Takamatsu	JP Development of Portable Spectral Gonio-Photometer
SAT-1C-4	Xiandou Zhang, Mengmeng Wang, Minchen Wei, Shangfei Li and Shuo Liu	CN Metamer Mismatching for Different Number of Camera Combinations
SAT-1C-5	Congcong Zhang, Xiaoxuan Liu, Cheng Gao, Zhifeng Wang, Yang Xu and Changjun Li	CN Local Adaptation Approach for Camera Characterization Based on Lightness
SAT-1C-6	Pei-Li Sun, Wei-Chih Su, Hung-Shing Chen and Hung-Chung Li	TW A Low-cost Method to Predict Color Appearance of Fluorescent Samples under Various Illumination Conditions
SAT-2C	COLOR PERCEPTION Naoyuki Osaka(JP) / I-Ping Chen(TW)	
SAT-2C-1	Akira Asano, Yuri Yoshii and Chie Muraki Asano	JP Relationship between Observers' Interests to Colors and the Precision of Color Categorization
SAT-2C-2	Tsuei-Ju Hsieh, Ichiro Kuriki and I-Ping Chen	TW Modern Mandarin Basic Color Terms Acquired from Color Naming Task and Statistics Corpus Linguistics
SAT-2C-3	Nischanade Panitanang, Chanprapha Phuangsuan, Ichiro Kuriki, Rumi Tokunaga and Mitsuo Ikeda	TH Thai Basic Color Terms and New Candidate Nomination
SAT-2C-4	Ichiro Kuriki	JP About Neural Representation of Colors in Visual Cortex
SAT-2C-5	Janejira Mepean, Mitsuo Ikeda and Chanprapha Phuangsuan	TH Simultaneous Color Contrast on a Display Determined by Different Viewing Distances
SAT-2C-6	Saran Chantra, Mitsuo Ikeda, Hideki Sakai, Hiroyuki Iyota and Chanprapha Phuangsuan	TH Device Independent Simultaneous Lightness Contrast
SAT-2C-7	Keizo Shinomori and John S. Werner	JP Variation of Brown Perception in Chromatic Central Fields

◆ Presentation: 15 min, including 3 min for Q&A

◆ Invited Talk: 30 min

Room A

Room A West 3F			
SUN-1A	COLOR CULTURE < 1 > Psychology & Design Vincent C. Sun(TW) / Youngshin Kwak(KR)		
SUN-1A-1	Tien-Rein Lee and Vincent Ching-Wen Sun	TW	Invited Talk: From Vernacular to Divine Classics: A New Color Survey Approach
SUN-1A-2	Tadayuki Wakata	JP	The Relationship between Psychological Brightness, Vividness and Impression
SUN-1A-3	Waiyawut Wuthiastarn	TH	The Study of How the First - Time Voters Memorize the Color of Political Parties
SUN-1A-4	Wipada Pumila, Chanprapha Phuangsuwan, Yoko Mizokami and Mitsuo Ikeda	TH	Colors for Female and Male Image by Thai and Japanese People
SUN-1A-5	Kieko Yamada, Mikiko Kawasumi and Akihiko Goto	JP	Analysis of Pale Color Preference for Jeans Products
SUN-2A	COLOR CULTURE < 2 > Region & Environment Tomoko Obama(JP) / Kitirochna Rattanakasamsuk(TH)		
SUN-2A-1	Kohji Yoshimura	JP	Invited Talk: Japanese Color Terms Denoting the Aesthetic Sense of Japanese Culture
SUN-2A-2	Akiyo Makino	JP	Practical Research for Developing Local Identity Color Method
SUN-2A-3	Kanchaporn Jankeaw, Kitirochna Rattanakasamsuk, Ryo Kihara and Mikiko Kawasumi	TH	Representative Colors of Grapes
SUN-2A-4	Lu Chen	CN	The Study on Color Design of Architecture in Korea and China Commercial Street between Korean and Chinese
SUN-2A-5	Li Li, Changyu Diao and Jinjin Mao	CN	Evaluation of Color Reproduction in Ancient Painting Based on Eigenspace Interpolation
SUN-2A-6	Ryu Furusawa	JP	Analyzing Painting by Computing Valeur of Colors

Room B

Room B West 4F			
SUN-1B	COLOR APPEARANCE < 1 > Constancy Keizo Shinomori(JP) / Xiandou Zhang(CN)		
SUN-1B-1	Shuo Liu, Xiandou Zhang, Mengmeng Wang and Shangfei Li	CN	The Post-processing of Color Constancy Methods for the Outdoor Natural Scenes
SUN-1B-2	Akira Kito and Taiichiro Ishida	JP	Color Constancy under an Illuminant Having Multiple Peaks in the Spectral Distribution
SUN-1B-3	Supattra Jinhpol, Mitsuo Ikeda, Chanprapha Phuangsuwan and Yoko Mizokami	TH	Effect of Haze Value and Materials on the Color Appearance in the Tissue Experiment of the Simultaneous Color Contrast
SUN-1B-4	Piyamon Nguensawat, Mitsuo Ikeda, Chanprapha Phuangsuwan and Yoko Mizokami	TH	Effect of Viewing Distance to the Simultaneous Color Contrast
SUN-1B-5	Chanprapha Phuangsuwan	TH	Invited Talk: Chromatic Adaptation to Illumination
SUN-2B	COLOR APPEARANCE < 2 > Diversity Ichiro Kuriki(JP) / Katsunori Okajima(JP)		
SUN-2B-1	Boonchai Waleetorncheepsawat	TH	Color Boundary by Category of Thai Elderly
SUN-2B-2	Yuki Mori and Chihiro Hiramatsu	JP	Color-Temperature Association in Children and Adults with Various Color Vision Types
SUN-2B-3	Miyoshi Ayama, Minoru Ohkoba, Kota Knari, Hiroto Mikami, Tomoharu Ishikawa, Shoko Hira and Sakuichi Ohtsuka	JP	Color Representations of Red-Green Color Deficient and Normal Observers using Color Cards and Color Names
SUN-2B-4	Kei Ito	GE	Invited Talk: Best Colors for Safety Signs

Room C

Room C West 4F			
SUN-1C	COLOR IMAGING < 1 > Vision & Technology Takahiro Horiuchi(JP) / Phil Green(UK)		
SUN-1C-1	Masayuki Osumi	JP	Sparkle and Graininess Index of Effect Coating using Spectral Imaging
SUN-1C-2	Motonori Doi, Akira Kimachi and Shogo Nishi	JP	Appearance Reproduction of Skin with Pigment Concentration Pattern Generated by Deep Convolutional Generative Adversarial Networks
SUN-1C-3	Sei-ichi Tsujimura and Katsunori Okajima	JP	A Weak Melanopsin Contribution to Color Perception
SUN-1C-4	Helene Midtjord, Phil Green and Peter Nussbaum	NO	Perception of Vividness of Emissive Colours by Norwegian Observers
SUN-1C-5	Hiroki Ishiyama, Midori Tanaka and Takahiko Horiuchi	JP	Contribution of Color Information in Instantaneous Identification of Copper Materials
SUN-1C-6	Nozomi Tobaru, Noriko Yata, Yoshitsugu Manabe and Yoko Mizokami	JP	Formulation of Metal Texture Evaluation from Image Features Considering Visual Characteristics
SUN-2C	COLOR IMAGING < 2 > Neural network & Printing Yoshitsugu Manabe(JP) / Haisong Xu(CN)		
SUN-2C-1	Hao Yan, Qingmei Huang, Defen Chen, Lialian Zhang and Pan Guo	CN	Research on Blur Discrimination Thresholds of Three-channel for Color Image
SUN-2C-2	Zhengnan Ye, Haisong Xu, Jueqin Qiu and Yang Lu	CN	Simulation of a Multispectral Imaging System based on Multichannel Filter Array
SUN-2C-3	Hung-Chung Li, Pei-Li Sun and Yennun Huang	TW	A DNN-based Model for Ciecarn02 Application
SUN-2C-4	Takuma Hirose, Noriko Yata and Yoshitsugu Manabe	JP	Analysis of the Process of Color Constancy Networks by CNN
SUN-2C-5	Tsukasa Hirabayashi, Noriko Yata and Yoshitsugu Manabe	JP	Removal of Shadow and Reflection over Printed Matter by CNN with Considering Area Information
SUN-2C-6	Pakornsit Pongto, Sureeporn Khampaeng, Ploypassorn Punkhor, Pichayada Katemake, Supaporn Noppakundilokrat, Kanitha, Tananu Wong, and Theeranun Janjarasskul	TH	Development of a Color Strip from Colorants in Grape for Alkali Indicator
SUN-2C-7	Duantemdoung Dethsuphar, Jennyssia Rattanavanh, Pichayada Katemake, Chawan Koopipat, Dhamrongruchna Hoontrakul, Prompong Pienpinijtham and Supaporn Noppakundilokrat	TH	Application of Multi-color Channels of LED for Art Examination

◆ Presentation: 15 min, including 3 min for Q&A

◆ Invited Talk: 30 min

Poster Presentation <P1>

AM Short Oral Presentation (2 min) @Room B (West 4F)
 PM Poster Presentation (60 min) @Room P1 (West 3F)

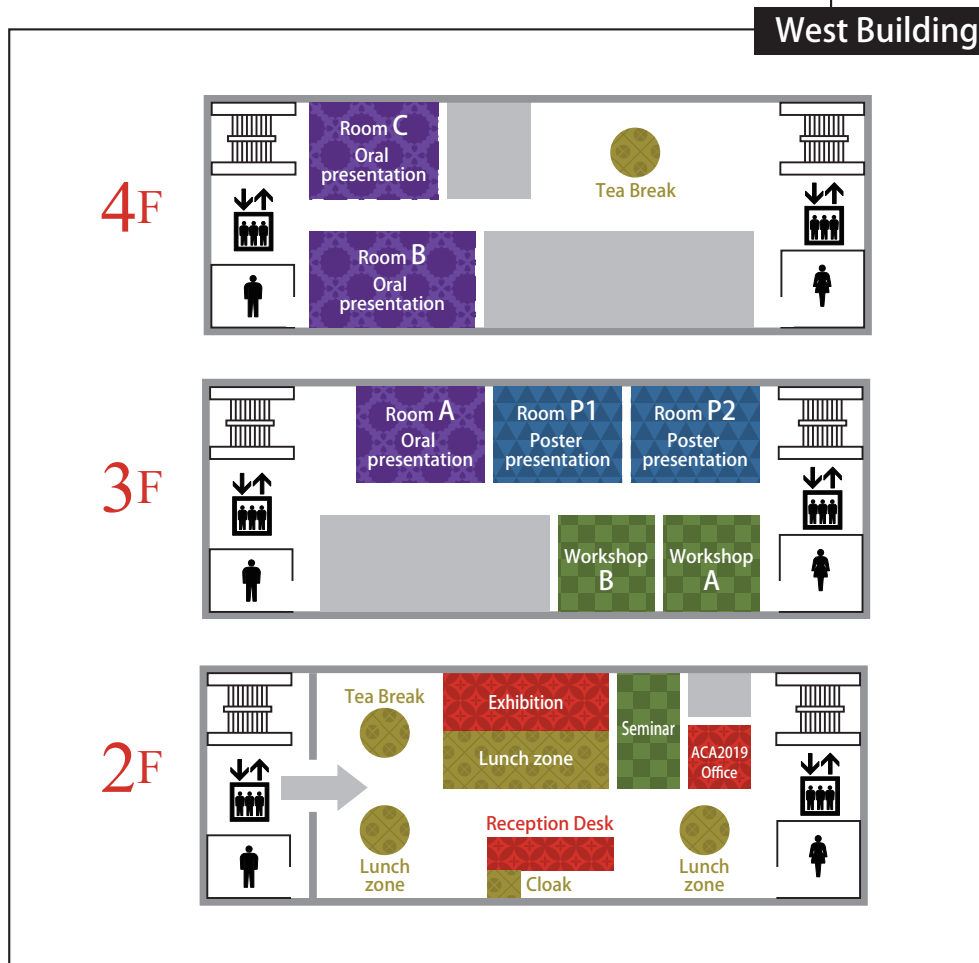
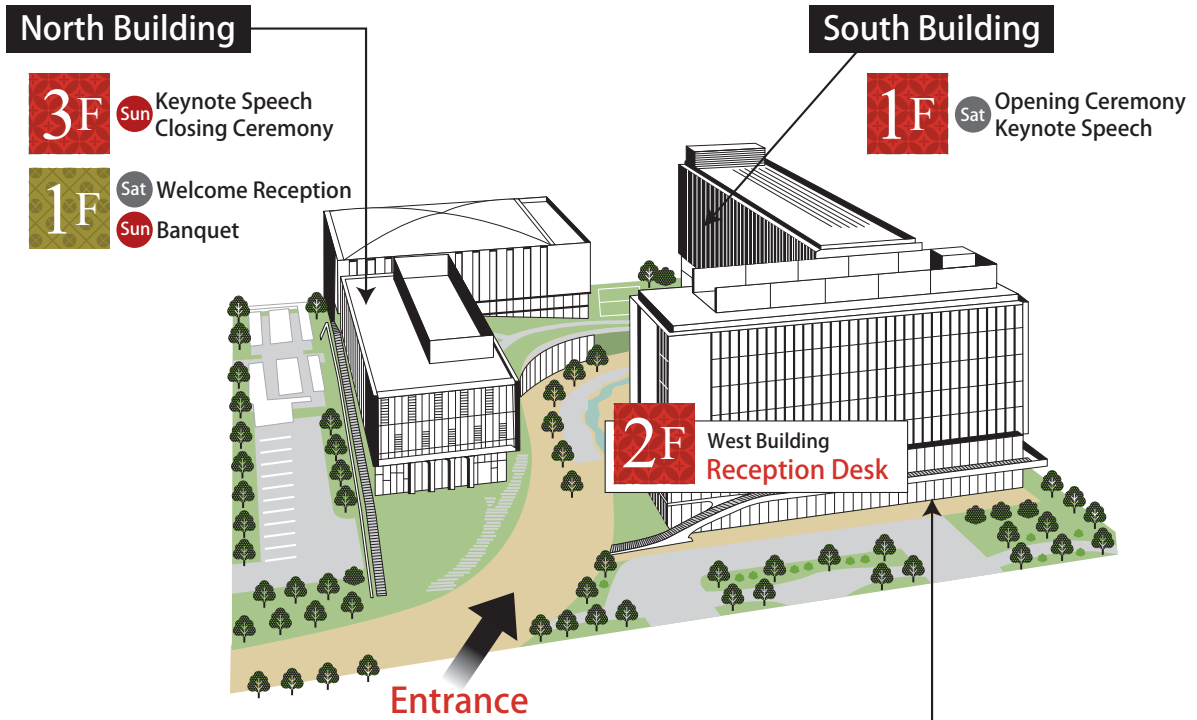
Room P1 West 3F				
Sat	1	P1-1	Hiroko Nakamura and Yasuhiro Seya	JP Effect of the Red Background on Impression Toward Dogs
Sun	2	P1-2	Yasuhiro Seya	JP Effects of Weapon Presence on Spatial Allocation of Visual Attention
Sat	3	P1-3	Cao Congjun, Fan Jingshang, Kang Yu and Sun Bangyong	CN Comparative Study of Uniformity of CAM16-UCS and CAM02-UCS
Sun	4	P1-4	Kazuho Fukuda and Kotoe Hara	JP Effect of Object Recognition on the Object-color Appearance Mode Limitation
Sat	5	P1-5	Onsucha Upakit, Chanprapha Phuangsuan and Mitsuo Ikeda	TH Size Constancy Demonstrated on Photographs
Sun	6	P1-6	Arikuni Makiguchi, Tomohiro Moriya, Kazuki Tashiro and Masashi Ohkawa	JP Color System Transform from RGB to L*a*b* using Neural Network-Consideration in Hues of PB, P and RP -
Sat	7	P1-7	Alton Mao, M. James Shyu, Simon Lin, Ya-Ning Chen and Eric Yen	TW Analysis of Faded Colors by using Spectral Approach with Non-negative Matrix Factorization
Sun	8	P1-8	Daisuke Kondo, Hayato Fujita and Isamu Motoyoshi	JP Material Rendering Property of Illumination
Sat	9	P1-9	Natthawadee Tibkawin and Pensri Charoensit	TH Development of Natural Colorant from Tectona Grandis Leaf Extract by Complex with β -Cyclodextrin
Sun	10	P1-10	Vipusit Piankarnka and Nuttakunlaya Piankarnka	TH Development of Pictorial Medication Labels for Chronic Disease Patients at Health Promotion Hospital, Chawai
Sat	11	P1-11	Sayaka Kitahara, Masato Hotta, Taiho Idono, Kazuki Oike, Shusuke Kusakabe and Toru Nikaido	JP Effects of Finishing and Polishing Procedures on Surface Roughness and Gloss of Flowable Resin Composites Containing S-PRG Filler
Sun	12	P1-12	Yasuhiro Baba	JP An Aspect of Wartime Japanese Color Science: On Shoji Sato's Corrective Practice Method for Colorblindness
Sat	13	P1-13	Mai Isomi, Hideki Sakai, Tsugumichi Watanabe and Hiroyuki Iyota	JP Measurement of Wet Colors of Bricks and Gravels by using a Non-Contact Colorimetric System with Dome Illumination
Sun	14	P1-14	Takashi Sakamoto, Saki Tomita and Toshikazu Kato	JP Age and Gender Differences Found in Verbalized Impressions for Two-Color Combinations
Sat	15	P1-15	Yukiko Shimada, Yuko Ohgami and Katsuhiro Mogi	JP Characteristics of the Sex Differences in Art Drawings by Junior High School Students using Color Stickers
Sun	16	P1-16	Kitirochna Rattanakasamsuk and Mikiko Kawasumi	TH Comparison of Color Interference in Gender Identification between Thai and Japanese
Sat	17	P1-17	Zhang Rong	CN Color in Product Design -Interpretation of Lifestyle
Sun	18	P1-18	Yen-Ching Tseng and Yuh-Chang Wei	TW A Systematic Process in Developing a Color Scheme Based on Landscape and Urban Environmental Color Analysis
Sat	19	P1-19	Ho Joo Bae	JP Study on Representation by Color of "Wakuwaku" Feeling -Make a Coloring Book to get Exciting Emotional Effects
Sun	20	P1-20	Aya Hirouchi, Hiroyuki Iyota, Mai Isomi, Hiroyuki Yamamoto and Hideki Sakai	JP Automatization of 2D-Image Recording System for Analysis of Change in Food Appearance using Dome Illumination with Digital Camera
Sat	21	P1-21	Misao Takamatsu and Kazuji Matsumoto	JP Transparency Measurement for Japanese Female's Skin and Phantom Model by SRS (Spatially Resolved Spectroscopy Instrument) and Estimation with Viewing Study
Sun	22	P1-22	Chanida Saksirikosol, Ladinpat Artsawameathawong, Songpon Raksa and Jaranee Jarenros	TH The Effect of Color Filters on Beauty Photography
Sat	23	P1-23	Tomohiko Akagi, Satoshi Ikehata and Takeharu Seno	JP The Color Black is Most Important and Special for Making Professional Wrestlers Attractive and Fearful
Sun	24	P1-24	Kohei Takaishi, Kahoko Imazu, Junko Fujimoto, Tomoharu Ishikawa, Shino Okuda and Miyoshi Ayama	JP Relation between Contrast Impact of Two-Piece Garments and KANSEI Evaluation
Sat	25	P1-25	Norifumi Kawabata and Toshiya Nakaguchi	JP Color Laparoscopic Image Diagnosis for Automatic Detection of Coded Defect Region
Sun	26	P1-26	Adedayo Jeremiah Adeyekun	ID The Art and Appreciation of Colours in Architecture
Sat	27	P1-27	Takuya Aoki, Takeharu Seno and Akiyoshi Kitaoka	JP A Picture Book of Motion Illusions in Stationary Images -- A New Method to Investigate Vection --
Sun	28	P1-28	Shinji Nakamura	JP Stability of Color Preference assessed by Various Methodologies
Sat	29	P1-29	Aya Mizukoshi	JP An Examination of the Effects of Decision Making on Color Preference Due to Layouts of a Color Chart
Sun	30	P1-30	Yoshihiko Azuma and Kou Yasuda	JP The Effects of Color Preference on Color Memory
Sat	31	P1-31	Pratthana Thammachart, Hathaichanok Khemthong, Natthamon Piengthisong, Chanida Saksirikosol and Kitirochna Rattanakasamsuk	TH Preference of Coffee Image Color Tone in Advertising
Sun	32	P1-32	Kyoko Hidaka	JP A Comparison between Itten's and Albers' Bauhaus Colour Theories
Sat	33	P1-33	Shin'Ya Takahashi and Noriko Aotani	JP Knowledge of Traditional Color Names and Aspects of Japanese Culture to Feel Proud of
Sun	34	P1-34	Riko Miyake and Shin'Ya Takahashi	JP Color Features of the Waterscape Drawing and Drawer's Personality in the Aged

Poster Presentation <P2>

AM Short Oral Presentation (2 min) @Room C (West 4F)
 PM Poster Presentation (60 min) @Room P2 (West 3F)

Room P2 West 3F				
Sat	1	P2-1	Kohei Wakai and Hideaki Hayashi	JP Example of the Color Correction and the Removal of Unpleasant Elements in a Commercial Facility
Sun	2	P2-2	Erina Kakehashi, Keiichi Muramatsu and Haruo Hibino	JP Holistic Color Combination Analysis Including Lightness, Chroma, and Hue on Papilionidae Butterflies
Sat	3	P2-3	Makoto Inagami	JP Effects of Environmental Color Properties on Perceived Spaciousness at Exterior Locations
Sun	4	P2-4	Masako Nunokawa	JP The Relationship between "Kawaii" Color and Inspiration
Sat	5	P2-5	Yoshiko Kato, Yuka Shimada and Miku Kato	JP Dress with Motif of Ostwald Color System
Sun	6	P2-6	Chenxi Li, Lisheng Wang, Kaifeng Li and Wei Ye	CN Research on Defect Detection of Textile Color Image Based on Deep Learning
Sat	7	P2-7	Kotaro Matsumura	JP Study on Impression Degree for the Color of the Concrete in Japanese
Sun	8	P2-8	Suwat Puenpa, Kitirochna Rattanakasamsuk and Ploy Srisuro	TH Relationship between Proper Contrast and Image Satisfaction
Sat	9	P2-9	Satoko Taguchi, Shino Okuda, Miho Muguruma, Miho Matoba, Atsuko Miyaji, Fumiyoshi Kirino and Katsunori Okajima	JP Color Materials used in the Reproduction of Shosoin Imperial Treasures "The Red-stained Ivory Shaku Ruler with Bachiru Decoration" Collected by Nara Women's University
Sun	10	P2-10	Shuichi Mogi, Masafumi Kamei, Masato Sakurai, Tomoharu Ishikawa and Miyoshi Ayama	JP Color Appearance Model of Small Field Stimuli in the Fovea and Periphery
Sat	11	P2-11	Takumi Nakajima, Tomoharu Isikawa, Junki Tsunetou, Yoshiko Yanagida, Mutsumi Yanaka, Minoru Mitsui, Kazuya Sasaki and Miyoshi Ayama	JP Influence of Subject Attribute Differences on Texture Evaluation of Beige Fabrics - Comparison between Subjects' Knowledge of Clothes and Differences in Their Background -
Sun	12	P2-12	Tomoya Fujiwara, Takumi Matsumoto, Hinako Kunugi, Tomoharu Ishikawa and Miyoshi Ayama	JP Effect of Metric Chroma on the Total Color Impression of Images
Sat	13	P2-13	Minoru Ohkoba, Kota Kanari, Hiroto Mikami, Tomoharu Ishikawa, Shoko Hira, Sakuichi Ohtsuka and Miyoshi Ayama	JP Hue Circle Perception of Congenital Red-Green Color Vision Deficiencies —Experimental Data and Estimation using Colorimetric Values—
Sun	14	P2-14	Masashi Tozuka, Hirotsuka Matsushima, Kakeru Yokoyama and Hiroshi Takahashi	JP Effects of Light Color Change Programs of Led Lighting on Subsequent Work Efficiency
Sat	15	P2-15	Shu Sasaki, Hiroki Asahara, Taiki Sanada and Takayuki Misu	JP Psychological and Physiological Effects of the Led Lighting Color on a Living Space
Sun	16	P2-16	Masako Omori and Reiko Hashimoto	JP The Effect of Lighting Environment Change and Cataract Cloudiness on Color Discrimination and Contrast Sensitivity
Sat	17	P2-17	Mayuko Nakamura and Taiichiro Ishida	JP How does a Two-Dimensional Array of LED Lights Affect Appearance of Texture of Object's Surface?
Sun	18	P2-18	Akiho Kito and Taiichiro Ishida	JP Comfortable Light Distribution in a Room Produced by Artificial Lighting with Daylighting from a Window
Sat	19	P2-19	Airi Hashimoto and Hiroyuki Shinoda	JP Color Identification Affected by Illuminance Level, Stimulus Size and Observation Period During the Execution of Visual Tracking Task
Sun	20	P2-20	Yasuko Kosaka and Hiroyuki Shinoda	JP Effect of Color Shift Caused by Colored Light Addition or Subtraction on Subjective Evaluation of Image Quality
Sat	21	P2-21	Shun Ito and Hiroyuki Shinoda	JP Contrast Effect of Window View and Indoor Space on the Perceived Brightness of a Room Evaluated by Rating Scale
Sun	22	P2-22	Ryuta Tetsuo and Hiroyuki Shinoda	JP Display Primaries' Spectral Power Distributions Acquired from RGB Images by Using Gradient Descent
Sat	23	P2-23	Toru Sugiura and Hiroyuki Shinoda	JP Effect of Dual Task Execution and Illuminance Level Decline on Spatial Resolution
Sun	24	P2-24	Anukul Radsamrong, Pichayada Katemake, Éric Dinet and Alain Tremeau	TH Contrast of Colored Pairs Enhanced by using 3 Selective Wavelengths for People with Low Vision
Sat	25	P2-25	Naoko Takahashi, Chen Xu, Yuki Motomura and Chihiro Hiramatsu	JP Neural Responses to Colors with Different Saliency
Sun	26	P2-26	Kajitsu Yoshitake, Kyoko Kido, Satoshi Hano, Shigehito Katsura and Shoji Sunaga	JP Development of a Color Sample Set from the Viewpoint of Dichromats for Color Universal Design
Sat	27	P2-27	Takeharu Seno, Masaki Ogawa, Shoji Sunaga and Hiroyuki Ito	JP Effects of Colors on the Illusory Self-motion Perception (Vection)
Sun	28	P2-28	Shigehito Katsura, Yoshino Tanaka, Kei Kawamoto and Shoji Sunaga	JP Emotional Responses of Dichromats to Colors and Color Names
Sat	29	P2-29	Suguru Tanaka, Kumiko Kikuchi and Yoko Mizokami	JP Influence of Hue on The Brightness Perception of Faces in the Different Type of Skin Color
Sun	30	P2-30	Taishi Masumitsu and Yoko Mizokami	JP Contribution of Saturation and Lightness Contrast on Colorfulness Adaptation of Images
Sat	31	P2-31	Tomohiro Funaki and Yoko Mizokami	JP Effect of the Acquired Memory Color of Objects on Color Constancy
Sun	32	P2-32	Takuto Ito, Tomonori Tashiro and Yasuki Yamauchi	JP Effects of Display on Depth Discrimination of Moving Stimuli
Sat	33	P2-33	Shoko Isawa, Kazutaka Takeo, Nanako Koda, Tomonori Tashiro and Yasuki Yamauchi	JP How Can the Watercolor Effect be Enhanced by Stimulus Configuration?
Sun	34	P2-34	Tomonori Tashiro, Yuto Nakamura, Yuta Terashima, Syori Yamada, Takehiro Nagai and Yasuki Yamauchi	JP Towards Consistent Color Appearance - Evaluation of Closeness of Color Images with a Trendline -

Floor Map



Keynote Speech, Invited Talks, Seminar, Workshop

Keynote Speech 1

Saturday, 30 Nov., 2019 DS Hall (South 1F)

Inside the Minds of Automotive Color Designers

Mr. Scott Kanamaru

Toyota Motor Corporation (Japan)

What is automotive color design?

How are the colors created?

What inspires the designer to create a new automotive color?

According to a study, “Color” is often ranked highly when consumers are asked the important factors when purchasing a vehicle. In recent years, variation of automotive body colors are increasing, further challenging new innovative expressions. All of these colors are specifically designed by automotive Color Designers, and there is a story to each and every color that is available in the market. Find out how automotive color designers actually create these colors, and how color / material / finishing have the power to change the image of automotive design.



Profile

Mr. Scott Kanamaru

Toyota Motor Corporation

Color Management Department

Project General Manager

Born in Japan, and moved to the United States during childhood.

Received B.A. in Economics, and pursued a certificate program in Visual Art (UCLA).

Grew up in Los Angeles, and have over 20 years of experience in automotive color design.



Keynote Speech 2

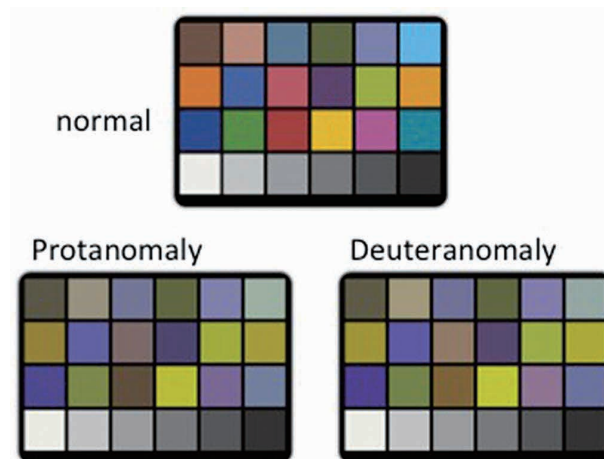
Sunday, 1 Dec., 2019 DN301 (North 3F)

Individual Colorimetry

Prof. Dr. Hirohisa Yaguchi

Chiba University (Japan)

Do people see different colors? The most widely used CIE color system is based on a single observer, called the CIE 1931 standard colorimetric observer. However, color vision is more or less different in individuals. Recently, we have developed a color appearance model for anomalous trichromats and aged people. Even if the colorimetric values of two stimuli with different spectral powers such as an object color and a display color are equal, different colors may be seen. It is considered to be a problem of observer metamerism, which is caused by the fact that the color matching function of a real observer is different from that of a standard colorimetric observer. We have analyzed the problem of observer with our color appearance model for individuals. In the near future, it would be desirable to establish a colorimetric system for individual color vision.



Profile

Hirohisa Yaguchi is Professor Emeritus at Chiba University. He got his PhD at Tokyo Institute of Technology in 1980. In 1982, he moved to National Research Council Canada. He came back to Chiba University in 1986, and retired from Professor in 2016. He was the Steering Committee Chair of the midterm meeting of AIC2015 Tokyo. Also, he served as an Executive Committee Member of AIC from 2002 to 2005.

Invited Talks

SAT-1A-1

Personal Color Analysis for Korean Women's (For women in their 20s and 30s) Min-kyoung Kim, KMK color Institute, Seoul, South Korea (Republic of Korea)

In modern society, it is becoming important to establish individual characteristics and unique personal identities. As a result, the Personal Color sector has already settled in the beauty and fashion industries. The purpose of this study is to analyze in personal color whether the color decided according to the fashion color is suitable for Asian people. Even if it is the same color, the color that matches the seasonal color tone is different. The purpose of this study is to analyze the colors that match Asian people's favorite colors. If we research and analyze color preferences, we will be able to use trend color and personal color effortlessly in the future, The goal of this research is to investigate the internationally renowned, and Korean stars' fashion and make up of K-POP.



In order to know the personal colors that Asian women's are looking for, it is necessary to analyze the color of the four seasons and diagnose the color to match. The personal color diagnosis system consists of 1:1 individual consulting and image-making through styles, images and beauty make-up through personal color analysis.

Profile

Ms.Min-kyoung Kim
Korea's 1st Colorist
Korea KMK Color Research Institute / Design Center (CEO)
Korea Society of Color & Personal Identity (president)
Ecole de Marge Verlair Korea (CEO)

SAT-2A-6

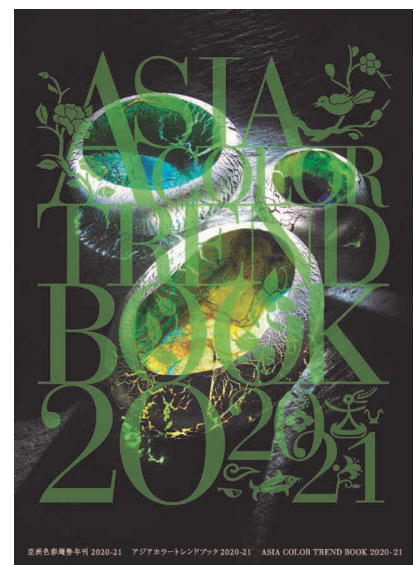
Asia Color Trend Book Eri Omae (Zhou Xin), DIC Color & Design Inc., China

With the increasing importance of Asian markets in the world economy, re-explore Asian culture and philosophy, the relationship between Asia and the world achieved structural transformation. "Asia Color Trend Book" published since 2008, as a world's only trend book focused on Asia, continue to disseminate the compactness and sense of humor, ambition and vitality of Asians, forecasting visual, color and material trend. (<http://www.asia-color-trend.com/>)



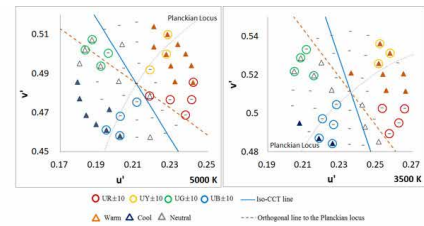
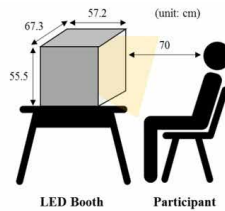
Profile

Ms.Eri Omae (Zhou Xin)
Editor-in-chief of Asia Color Trend Book /
Creative director of DIC Color & Design Inc./
Art director of Jinze Arts Centre (China)



Vision Experiment on Perception of Correlated Colour Temperature Youngshin Kwak, Ulsan National Institute of Science and Technology (UNIST), South Korea

The correlated color temperature (CCT) is widely used to describe the colors of display whites. The users can easily estimate the color of the display white based on CCT information. High CCT such as 7,000K means bluish white and low CCT such as 4,000K means yellowish white. However current CCT calculation method doesn't



match with the visual appearance. Our study shows that CCT is highly correlated with warm-cool feeling of the white color, where warm-cool feeling is determined based on hue perception mainly. A series of hue perception experiments using the color stimuli near Planckian locus indicates that the orthogonal line from the Planckian locus in CIE $u'v'$ chromaticity diagram can be used as the perception-based iso-CCT.

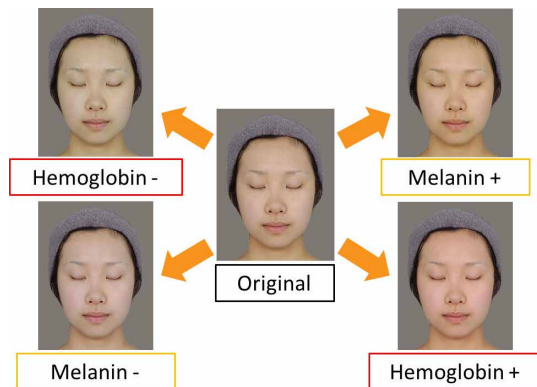


Profile

Dr. Youngshin Kwak is the associate professor at Human Factors Engineering Department, Ulsan National Institute of Science and Technology (UNIST), South Korea. She received her PhD from the Colour & Imaging Institute, University of Derby, UK, in July 2003 and then worked for Samsung Electronics. In February 2009, she joined UNIST. Prof. Kwak is currently CIE Division1 (Vision and Colour) director.

Color Perception Specific to Facial Skin Yoko Mizokami, Chiba University, Japan

Skin color is essential for obtaining various information on our mind and body, such as health, age, and face impression. Therefore, we must have developed visual sensitivity tuned to skin. It has been suggested the existence of color perception specific to facial skin. For example, we have showed that sensitivity to changes in reddish (or hemoglobin increasing) direction of the skin is better than other color directions. Reddish skin looks brighter than yellowish skin even if they have the same lightness. These perceptions may link to the property of skin color determined by pigments of skin. Our results of international comparison also suggest that other factors such as ethnicities, environments, and cultures may also influence facial color perception.

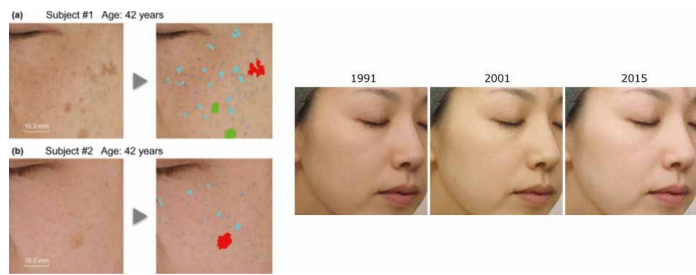


Profile

Dr. Yoko Mizokami is a Professor in the Department of Imaging Sciences, Graduate School of Engineering, Chiba University. She received a Ph.D. in Engineering in 2002 from Ritsumeikan University. After finishing a postdoctoral fellow at the University of Nevada, Reno, Department of Psychology, she moved to Chiba University in 2006.

Image-based Measurement of Human Skin Color and Its Application in Cosmetics Field Kumiko Kikuchi, SHISEIDO Global Innovation Center, Japan

Understanding the skin color and skin color heterogeneity is important for many industries, especially in the cosmetics and aesthetic fields. For objective measurement of skin color, the tristimulus colorimeter and reflectance spectrophotometer have been used for more than 50 years. In addition, various image analysis methods have been developed for quantitative evaluation of the skin color heterogeneity. Facial skin pigmentation is one of the causes of skin color heterogeneity and often affects perception of health and beauty. In



order to characterize the individual pigmented spots within a cheek image, we established a simple object-counting algorithm and provided precise information on pigmented spots such as variations in size, color shade, and distribution pattern. In this presentation, some recent results of our research which relate to skin color and skin color heterogeneity will be introduced.

Profile

Dr. Kumiko Kikuchi is a research scientist at SHISEIDO Global Innovation Center, Japan. She received a Ph.D. in Engineering in 2016 from Chiba University. Her research interests lie in skin color, including skin color perception, development of measurement methods and spectral imaging of human skin.

Chromatic Adaptation to Illumination

Chanprapha Phuangsuwan, Color Research Center, Rajamangala University of Technology Thanyaburi, Thailand

I like to demonstrate that the chromatic adaptation takes place to illumination not to color of object based on the concept of the recognized visual space of illumination RVSI developed by Ikeda. The concept emphasizes the chromatic adaptation to the illumination that fills a space where a subject stay. A flow chart of this action is (1) to recognize a space, and (2) to understand the illumination in the space. Punggrassamee et al. (2015) showed that color appearance of physically achromatic patch depends on illumination of a space where a subject stay by using two rooms technique. Phuangsuwan et al. (2013) showed that the color constancy occurs even in a 2D picture if a subject recognizes a space in the picture and understands the illumination in the space. Recently we investigated the simultaneous color contrast for various devices; a paper, a projector, a display and a real scene (two-room technique) and explained the device dependent color contrast by the strength how much a subject transfer the color on



devices to illumination. The same explanation was successfully applied to the simultaneous color contrast in after image and in a colored paper covered with a tissue.

Keywords: Chromatic adaptation, adapt to illumination, RVSI Theory, Devices, 2D picture

Profile

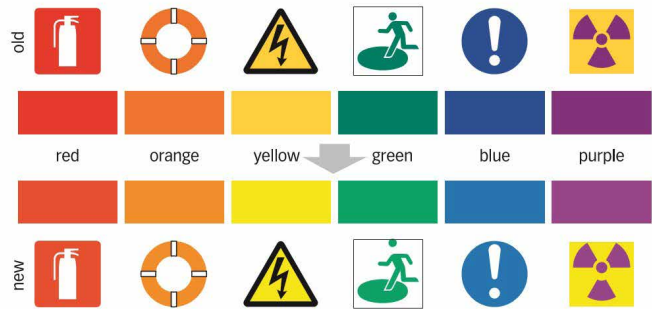
Dr. Chanprapha Phuangsuwan

Received a Ph.D. at the Faculty of Science, Chulalongkorn University, Thailand in 2012 and returned to Rajamangala University of Technology Thanyaburi (RMUTT) as a lecturer, presently an assistant professor. The research interest is to investigate the color appearance of objects in relation to the space recognition. I serve the director of Color Research Center CRC of RMUTT.

Best Colors for Safety Signs

Kei Ito, University of Cologne, Germany

Signs that convey information about danger and disaster must be painted in the colors that all kinds of people can recognize unambiguously. Special care should be taken for the people with color blindness, low-vision, cataract, and aged, because they have difficulty distinguishing certain ranges of colors. Colors convey certain meaning, for example red for danger and green for safely. We therefore cannot “change” the colors for safety signs.



However, by carefully adjusting the hue, saturation and brightness, colors can become much more distinguishable even for those people. The Japanese Industry Standard (JIS) for Safety Colors and the colors for the disaster information system of the Japan Meteorological Agency and TV broadcasters have recently been revised towards this aim. The concepts and backgrounds of these revisions will be explained.



Profile

Professor at the University of Cologne, Germany. He got his PhD for neuroscience at the University of Tokyo. After working at various institutes in Germany and Japan he became Associate Professor at the University of Tokyo before moving to Cologne. He studies sensory processing system of the brain as well as Universal Design of color and vision.

Japanese Color Terms Denoting the Aesthetic Sense of Japanese Culture

Kohji Yoshimura, Kansai Gaidai University, Japan

In different regions and countries, it is thought that there are some important colors exemplifying that area. In other words, in any region the people there can have some colors or color combinations that are commonly appreciated, valued, and employed in a certain way. However, the actual colors in this world vary significantly. There are really no colors and color combinations that are not found in other regions and countries. In Japan there are colors considered representative of the culture such as indigo (expressing ‘Japanese blue’), browns and mouse colors called the “forty-eight browns and 100 mouse colors” in literal English translation



(in reality, more than 100 browns and mouse colors are included in these Japanese color terms), and red and white indicating celebration.



Profile

Professor emeritus of Kansai Gaidai University, and part-time lecturer at Kansai University. He serves as a consultant to the Kansai Branch of the Color Science Association of Japan, and is on the board of the Japan Society of Stylistics and the Association for Japanese and English Language and Culture.

From Vernacular to Divine Classics: A New Color Survey Approach

Tien-Rein Lee, Huafan University, Taiwan

Vincent Ching-Wen Sun, Chinese Culture University, Taiwan

Surveys of color can be accomplished with a variety of ways, from questionnaire rating to self-painting target colors. Different survey methods aim to explore different aspects about “color,” which carries dissimilar meanings for variable research approaches. The present study suggests a new color survey approach which aims to find corresponding colors for a variety of items and reveal the color categories in them. We applied the basic color category investigation method of Sun and Chen (2018), which is based on the surveying procedures for basic color term by the World Color Survey (WCS) project. In our new color survey approach, we expand the survey to the color related terms found in ancient Chinese religious texts and also in western scriptures.

Profile



Prof. Lee was President of the Chinese Culture University from 2003 to 2009, and has acquired this position again from August 2013 to January 2018. He is now the President of Hua-fan University in Shihding, New Taipei City, Taiwan. As the Founding President of the Color Association of Taiwan (CAT), Prof. Lee is a color research pioneer establishing color studies and color application networks in Taiwan, with China, Asia, and worldwide. He has taken position of International Color Association (AIC) President in 2018.

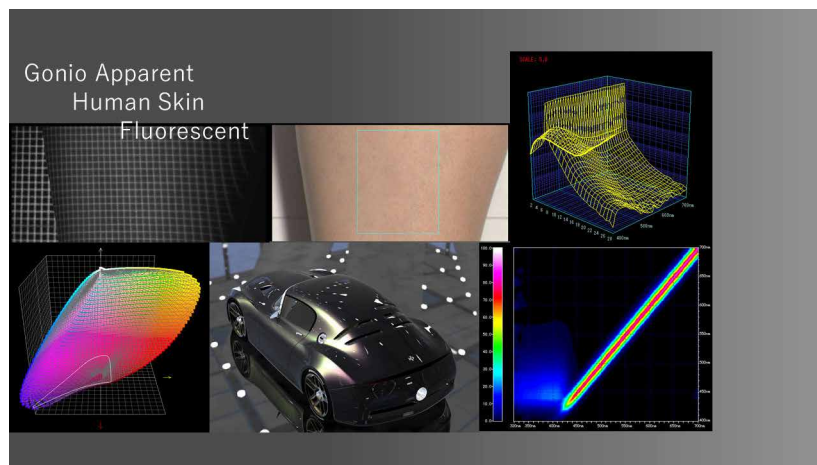


Dr. Vincent Ching-Wen Sun is assistant professor at the Department of Mass Communication, Chinese Culture University, Taipei, Taiwan. He studied color vision with professors Joel Pokorny and Vivianne Smith, at the University of Chicago, and received his Ph.D. on 1998. Dr. Sun joined the Chinese Culture University in 2000. In addition to his department, Dr. Sun is also serving at the Center for Visual Communication and Color Research of the University, and the Color Association of Taiwan.

Practical Colorimetry for Various Objects

Masayuki Osumi, President, Office Color Science Co., Ltd., Japan

In the fields of recent R&D and especially affective engineering, targets for the object color measurement are diversified. For example, in the case of product development, design has become the important determinant for buying, and the perception of various materials where special surface structures are developed. These days, the importance of colorimetry is increasing, due to such reason as globalization and manufacturing. There is a demand to conduct examinations and evaluations of products by precise methods of measurement. The purpose of this seminar is to deepen the understanding of colorimetry under the theme of diversifying object colors. The intension is to acquire the knowledge for measuring relatively difficult objects included gonio-apparent and fluorescent colors through practice by using the latest measuring instruments and also using a spectral imaging system.



Courses of the Seminar

Three types run twice, over the three days.
The capacity of each seminar is 8 people.
A reservation is required for each seminar.

Seminar A (75mins., 8 people × 2)

Basics of Colorimetry and Actual Measurement

29 Nov. 13:00-14:15 (75 mins., 8 people)

30 Nov. 12:45-14:00 (75 mins., 8 people)

Learn the basics of instrumental color measurement and experience actual measurements using commercial instruments. Deepen knowledge about the issues of disagreement with vision by using samples, such as opaque, semitransparent, high gloss and low gloss.

- What is Colorimetry?
- Actual Object Colors
- Optics Geometry Condition of Measurement
- Integrating Sphere Measurement and Edge Loss Error (Measurement training with actual instruments)
- Measurement by Surface Analyzer (Measurement training with actual instruments)

Seminar B (75mins., 8 people × 2)

Metallic Color and Fluorescent Color

29 Nov. 14:30-15:45 (75 mins., 8 people)

30 Nov. 14:15-15:30 (75 mins., 8 people)

Understand optical characteristics of effect color and fluorescent color that have relatively high degree of difficulty for measurement. Experience colorimetric measurements with the latest portable instruments.

- Structure and Optics Properties of Metallic Color
- Actual Measurement of Metallic Color (Measurement training with actual instruments)
- Characteristics of Automotive Coat Color based on Measurement Examples
- Expression Mechanism and Methods for Measurement of Fluorescent Color
- Actual Measurement of Fluorescent Color (Measurement training with actual instruments)

Seminar C (90mins., 8 people × 2)

Spectral Imaging and Measurement of Images

29 Nov. 16:00-17:30 (90 mins., 8 people)

1 Dec. 12:45-14:15 (90 mins., 8 people)

Various merits are provided by applying spectral imaging to measurement of images. Learn actual spectral imaging by using instruments with liquid crystalline tunable filter.

- Methods for measurement of Spectral Imaging
- Merits of Spectral Imaging and Issues for Practice
- Measurement of Painting Arts (Measurement training with actual instruments)
- Measurement of Skin (Measurement training with actual instruments)
- Measurement of Metallic Color (Measurement training with actual instruments)
- Future Colorimetric Technology

For detailed information on participation and reservation, see the seminar pages on AIC2019 website <<http://www.color-science.jp/ACA2019/Seminar/index.html>>



Profile

Mr. Masayuki Osumi

Specialized in color measurement, color matching, CG and color evaluation technology.

Established Office Color Science Co., Ltd. in 2004.

Developed technologies uniting measurement, color matching and CG based on effect colors (metallic and pearlescent colors), and specialized in R&D of CCM and color simulation systems for automotive coatings. Provide the systems to automotive, electronic equipment, paint and material industries, as well as acting as a technical adviser. Customers are in Europe, U.S.A., China, India, Korea and Japan.

Workshop

Workshop A1(30mins., 5 people × 8)

"Workshop for Making Your Own Lip-color Compact"

30 Nov. PM

1 Dec. PM

This workshop is for anyone who wants to make her (or his, of course) self-prepared lip-color compact. You can pick and mix up your favorite colors from 10 different natural and skin-friendly pigments made from color mica, such as Jojoba Oil, Caster Oil and Vitamin E. Our team, including fashion and color specialists, can help you choose colors for achieving the best results based on a personal-color analysis.



Workshop A2(15mins., 4 people × 16)

"Workshop for Making a Notebook Bound in Japanese Style"

30 Nov. PM

1 Dec. PM

In this workshop, you bind sheets of paper, using a needle and thread, to make a Japanese-style notebook. You can choose your favorite Japanese patterned paper and color of thread so as to create a unique notebook of your own. The binding method will be the Japanese style which has been developed over a thousand years.





Profile

The Study Group of Environmental Color Design for Daily Living is composed of a wide range of experts specializing in makeup consulting, color analysis, and aroma colorings.

Workshop B (All the time)

Workshop for Creating Your Own Music Suited to COLORSCAPE

30 Nov. 12:45-18:15

1 Dec. 9:00-11:15, 12:45-16:45

In this workshop, you can enjoy the collaboration between color and music by using the mobile application "mupic".

The examples of Asian COLORSCAPE with music will be presented, and then you can try to adjust parameters for each COLORSCAPE by yourself.



See detailed information on Workshop B both in English and Japanese on AIC2019 website

<http://www.color-science.jp/ACA2019/Workshop/mupic_Colorscape_of_Asia_191107.pdf>

Profile

The Study Group of Landscape of Japanese Color Environment is composed of a wide range of experts specializing in landscape design, color engineering, and color psychology.



Android



iOS

“mupic” is a revolutionary application that automatically generates music from color features of images. You can arrange the music to your liking. Let’s make your own original music and video!

Mechanism of creating music from an image

- (1) According to the color and expression of the image, it is categorized into five feelings: Neutral, Anger, Sadness, Happiness, Surprise.
- (2) Extracting seven colors from the image, it is converted into a score with two octaves and four bars.
- (3) Music’s key and melody are generated from the most common color on the whole image, and codes are generated from the major colors of the four bars.
- (4) The music is generated as a composition with a melody played by an instrument, cords by seven instruments corresponding to seven colors, a bass with an instrument, and beats.

Arrange Your Own Music

The music will change if you adjust the three color palettes, “Landscape”, “Rainbow Color”, and “Primary Color” that extract colors. You can also work out the music by selecting a genre and changing instruments, composition methods, and volume which are corresponding to the key, tempo, melody, chord, and bass.

Your Own Music and Your Own Video

The generated music can be integrated with the image and saved as a video, and then you can share it on SNS. If the user owns the copyright of the image, the one can have the right of the music and video.

Web/SNS

- URL: <http://mupic.jp/>
- Twitter: <https://twitter.com/MUPIC3>
- Facebook: <https://www.instagram.com/mupic.sns/>
- Instagram: <https://www.facebook.com/mupic.sns>

Contact

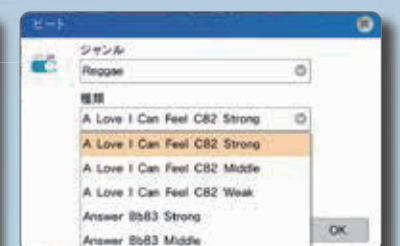
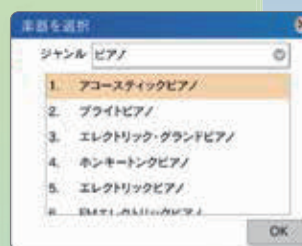
Diva corporation

- mupic Division
- URL: <https://divakk.co.jp/>
- email: support@mupic.jp

Music generated from “Happiness”



Music generated from “Landscape” and “Natural”



Arrange music with various instruments and beats

Colorscape of Asia

Create your own music from COLORSCAPE!

アジアの色景 風景の色から音楽を作ろう!

アジアに住む我々はどうな「色彩の風景」に生きているのでしょうか？風景が住んでいる人々の色彩の感性を育み、人々の感性が風景の色彩を変化させていく、という相互作用の中で、「色彩の風景」は成長していきます。しかし、住んでいる人々はどうな感性が形成されているのか客観的に判断することはできません。感性の違いに気が付くのはたいていの場合、移住してきた人々、旅人になるでしょう。風景の違い、感性の違いは、色彩のようにグラデーションです。アジアという広域において、「色彩の風景」はどうな共通点と差異があり、どのように変化していくのでしょうか？色彩から、アジアにおける人々の交流の歴史や気候の共通性など、さまざまな要素が発見できるでしょう。

今回、画像の色彩から音楽を作るアプリケーション「mupic」によって、色彩の違いを音楽で感じるという試みを行います。画像は、縦 2 オクターブ、横 4 小節の楽譜に見立てられています。画像の主要色はキー、横に 4 分割された小節の主要色はコードが当てはめられています。また、画像から 7 つの色が抽出され、7 つの色にはそれぞれ楽器が当てはめられています。ブースでは、アジアの風景を撮影している 2 人の写真家の写真から、音楽を作るデモンストレーションを行っています。写真が変わったり、設定を変えれば、音楽も変わりますので、是非実際使用していただければ幸いです。

もしあなたが持っているスマートフォンが iPhone であるならば、mupic をダウンロードして、あなたの住んでいる街の写真から音楽を作って、Twitter、Facebook、Instagram にハッシュタグをつけて投稿してみてください。「アジアの色景」を、音楽にして発信いたしましょう。

In Asia, what kind of "COLORSCAPE - color landscape" do people dwell in?

The colorscape grows through interactions where landscape nurtures color sensibilities of people living in the landscape while their sensitivity changes the color of the landscape.

However, it is hard for people to appreciate detachedly what kind of sensibility has been formed in a specific landscape. The ones who often notice the differences in sensitivity are migrants and travelers.

Variations in landscapes, as well as sensibilities, exist in gradation like colors. In a wide range of Asia, what are similarities and differences in colorscape, and how would they change?

Through colors, you can discover several things, for instance, histories of people's exchange and commonalities of climate in Asia.

In ACA2019, we would like to try to grasp differences in color through music by using the mobile application "mupic" that creates music based on colors on an image.

In the application, an image is converted to a score with two octaves and four bars. The primary color of the photograph transforms into a key, and the main colors on the four-bar give codes. Besides, seven colors are extracted from the image, and each color is assigned a musical instrument.

At our booth, we demonstrate "mupic," producing music by using photographs by two photographers who captured sceneries in Asia. If you change images or adjust the parameters of the application, the music will change. Please stop by our booth to try it out.

If you have an iPhone, you can download "mupic." Make music from photos of a city you live in and post it on Twitter, Facebook, and Instagram with the below hashtags.

Let's share Asian COLORSCAPE as music!



Android



iPhone

hashtag(ハッシュタグ)
#colorscape
#asia
#mupic
<http://mupic.jp/>

美しい日本の
色彩環境を創る研究会
*Landscape of
Japanese Color Environment*



台湾 Taiwan

港 千尋
Chihiro Minato

写真家、著述家。多摩美術大学教授。1960年、神奈川県生まれ。写真展「市民の色 Chromatic citizen」で第31回伊奈信男賞受賞。『記憶』(講談社選書メチエ、1997年)でサントリー学芸賞受賞。2007年、「ベネチア・ビエンナーレ日本館」コミッショナー、2012年、「台北ビエンナーレ」共同キュレーター、「あいちトリエンナーレ2016」芸術監督。

Born in Kanagawa, 1960, Minato is a photographer and visual anthropologist, and currently, he is a professor at Tama Art University. He received the Ina Nobuo Award for his photo exhibition Chromatic citizen in 2006, and he was appointed as the commissioner for the Japan pavilion at the 52nd Venice Biennale Art Exhibition in 2007. He served as the co-curator of the Taipei Biennale in 2012 and as the artistic director of Aichi Triennale 2016.

タイ Thailand

山内 亮二
Ryoji Yamauchi

写真家。1986年、岐阜県生まれ。2011年、名古屋学芸大学大学院メディア造形研究科終了。主な展覧会に「Musing in the Land of Smiles」新宿・大阪ニコンサロン(東京・大阪、2015年)、「Quiet River, Seoul」コニカミノルタプラザ(東京、2013年)など。2015年、ニコンサロンJuna21、2013年、コニカミノルタフォトプレミオ入賞。

Born in Gifu, 1986, Yamauchi is a photographer. He holds a master's degree from the department of visual media at Nagoya University of Arts and Sciences. His exhibitions include "Musing in the Land of Smiles (Nikon Salon, Osaka and Tokyo, 2015) and "Quiet River, Seoul" (Konica Minolta Plaza, Tokyo, 2013). In 2015, he was a prizewinner of the Konica Minolta Photo Premio.



■ mupic制作チーム

The team of mupic

DOZAN11 (ドーズンイレブン)

1996年、三木道三としてデビュー。2001年、『Lifetime Respect』(徳間ジャパン・コミュニケーションズ)が、日本のレゲエで初のオリコン週間ランキング1位を記録する。2002年、47都道府県ツアーの後、活動休止。休止中は他のミュージシャンの作詞、作曲、プロデュースを手掛ける。「DOZAN11」の名で、2014年に活動を再開し、アルバム『Japan be Irie !!』(ユニバーサル・ミュージック・ジャパン)をリリース。2018年、画像から音楽を自動作成するアプリ『mupic』のプロデューサーとなり、2019年5月1日正式版をリリースする。

DOZAN11

DOZAN11 made his debut as a singer, MIKIDOZAN, in 1996. His song "Lifetime Respect" got the first place in the Japanese music chart in 2001, which was the first time for the reggae music. After the tour across Japan in 2002, he suspended its activity while putting his hand to songwriting, music composition and production for other musicians. In 2014, he re-started his music career as DOZAN11 and released the album "Japan be Irie!!" (Universal Music Japan). In 2018, he became a producer of the mobile application "mupic," and released the official one in May 2019.

青柳 臣一 (アオヤギ・シンイチ)

C#、および、Xamarinを使ったクロスプラットフォーム開発の日本における第一人者。2017年、『Xamarinネイティブによるモバイルアプリ開発 C#によるAndroid/iOS UI制御の基礎』(翔泳社)を刊行。株式会社ディーバ代表取締役。mupicの共同プロデューサー。mupicの開発は株式会社ディーバにて担当。青柳は開発チームのリーダーとしてマネージメントをすると同時にリードプログラマーとしてプログラミングも担当する。

Shinichi Aoyagi

Aoyagi is a leading expert on developments of cross-platform using C# and Xamarin in Japan. In 2017, he published "The Developments of Mobile Application by Xamarin Native - The basics of UI Control by C# for Android/iOS" (Shoei-Sha). He is a representative director of DIVA CORPORATION and a co-producer of mupic. He has been a management leader of the development as well as a leading programmer of mupic.

三木 学 (ミキ・マナブ)

文筆家、編集者、色彩研究者、ソフト企画開発。独自のイメージ研究を基に、ジャンルやメディアを横断した著述・編集を行う。色彩分析ソフト『FeelimageAnalyzer』(ビバコンピュータ)の企画開発。都市やアート作品の色彩分析を多数行う。スライドショーや共感覚研究を発展させ、画像の色から音楽を生成するスライドショーシステムを企画開発。mupicのディレクションを担当。共編著に『大大阪モダン建築』、『新・大阪モダン建築』、『フランスの色景』(すべて青幻舎)など。

Manabu Miki

Miki is a writer, editor, color researcher, and a planner of software based on his unique research on image, crossing different genres and media. He developed the software FeelimageAnalyzer (viva computer), which analyzes colors, and he carried out the software with cities and artworks. Researching on the slide show and synesthesia, he developed a slide show system that generates music from colors on an image. He is a director of mupic and co-editor of books, including "Great Osaka Modern Architecture," "Modern Osaka Architecture in Osaka 1945-1973," and "Colorscape de France" (SEIGENSHA Art Publishing).

Proceedings

Oral Papers

Preference for color composition of art paintings and its individual differences

Masaya Nishimoto¹, Shigeki Nakauchi^{1*}

¹ Department of Computer Science and Engineering, Toyohashi University of Technology, Japan.

*Corresponding author: Shigeki Nakauchi¹, nakauchi@tut.jp

Keywords: preference, color composition, art paintings

ABSTRACT

Several studies have shown that participants preferred the original art paintings rather than the hue-rotated fake paintings even for abstract paintings although they have never seen them before. This study aims to confirm the robustness of this “original preferred judgement” for color composition of art paintings and to explore the individual differences of preference due to age, gender, household income by recruiting more than 30K participants with broad age groups. 4-AFC paradigm was used to measure the preference for art paintings. Participants were asked to select the most preferable one among four images of original (0 deg) and three hue-rotated "fake" paintings (90, 180 and 270 deg in hue angle) which have the same luminance and mean chromaticity as the original paintings. As a result, original paintings were selected as most preferable replicating our previous findings. Furthermore, individual and gender differences tend to be decreased according to age, suggesting that the preference patterns would converge to a certain universal form, presumably due to biological factors in addition to cultural, educational and/or social feedbacks.

1. INTRODUCTION

Although well-known hypothesis for explaining the aesthetics of art painting is that it depends on the degree to which it mimics natural image statistics, Nascimento et al. [1] have reported that the color preference for the art paintings does not depend on the similarity to natural images, showing that the color of the paintings tend to be biased to reddish from the natural image. Recently, Kondo et al. [2] have reported that the original-preferred judgement for art paintings (participants preferred the originals which they have never seen before rather than the hue-rotated fake paintings) is universal throughout several nationalities and languages. These results showed that color composition similar to the original art paintings was preferred regardless of culture, living environment, type of painting, and specialty. Nakauchi et al. [3] have shown that the participants' selection rate for the original paintings was correlated with certain image color statistics, suggesting that original paintings might attract participants' preference implicitly in a universal form.

The original preferred judgement mentioned above was impressive and attracting phenomenon but this was observed for a limited number of participants (less than 100) in our previous studies. Furthermore, it was not clear yet what factors effect on the individual differences in preference among participants. Therefore, this study aims to confirm the robustness of this “original preferred judgement” for the color composition of art paintings by recruiting more than 30K participants with broad age groups and to explore the relationship between individual differences in preference judgements and participants' age, gender and household income.

2. METHODS

Number of Japanese participants was 30,777 (male=16,837, female=13,940, ranging from 15 to 97 years old as shown in Fig.1). They were divided into 50 groups which were presented the same 24 sets of paintings selected from three genres (8 paintings from each genre) among abstract, poster, symbolic, still life and flower. Participants were asked to choose the most preferable painting among 4 images according to 4-AFC paradigm: original and hue-rotated images (90, 180, 270deg) with the same luminance and mean chromaticity as the original. It is worth to mention that such a large number of participants (~600 participants in each group) enabled us to analyze the individual differences in preference for color composition of art paintings.

3. RESULTS

3.1. Selection Rate for the Original Paintings

First, in order to confirm robustness of the original preference judgement, we investigated the selection rate for the original and three hue-rotated images and its gender dependency. As shown in Fig.2, the original paintings were selected more frequently than other hue-rotated images ($F = 25187.6479, p = 0.000, \eta^2 = 0.3803$) as observed in our previous studies. While, there was no difference between male and female. ($F = 0.000, p = 1.000, \eta^2 = 0.000$).

Next, we investigated the individual differences in the original selection rate. As a result, we found no effect on the original selection rate of age ($F = 4.900, p = 0.000, \eta^2 = 0.0025$) as shown in Fig.3. Also, household income ($F = 3.2654, p = 0.011, \eta^2 = 0.0011$), nor education level ($F = 11.6103, p = 0.0000, \eta^2 = 0.0056$) showed no clear effects on the original selection rate, suggesting that behind the original preference judgement there might exist biological rationale or mechanisms in addition to that acquired by experience or training. Note that to apply the statistical test, the number of participants for each factor relating to individual difference was normalized to the same to eliminate the bias due to the number of people.

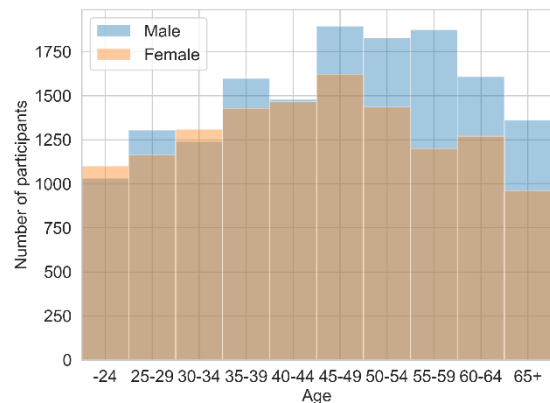


Figure 1. Age distribution of participants

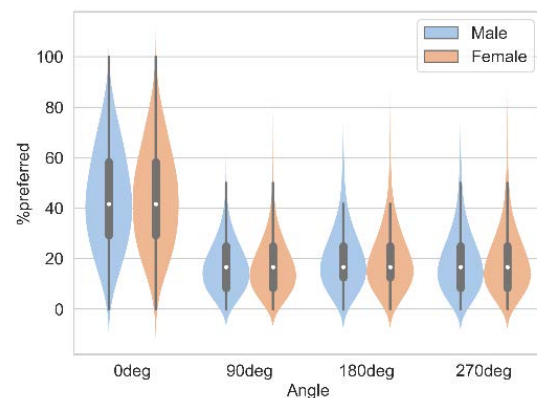


Figure 2. Selection rate for original and hue-rotated images

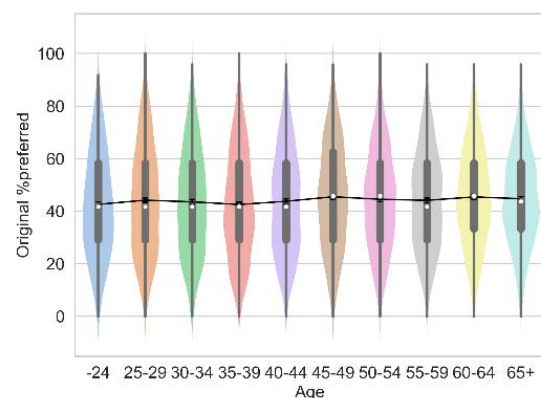


Figure 3. Age dependency in original selection rate

3.2. Variation in Painting Selection Pattern

We could find no effects on the original selection rate by any individual factors. Next, we focus on the selection pattern for a set of paintings rather than the average selection rate. Participants within the same group were presented the same 24 paintings as described in section 2. Original selection rate may differ depending on each painting presented to each participant as explained in Fig.4. To quantify this variability in selection pattern in each group (how similar the participants' preferences are in each group), we defined "variation" index as shown in the right panel of the Fig.4.

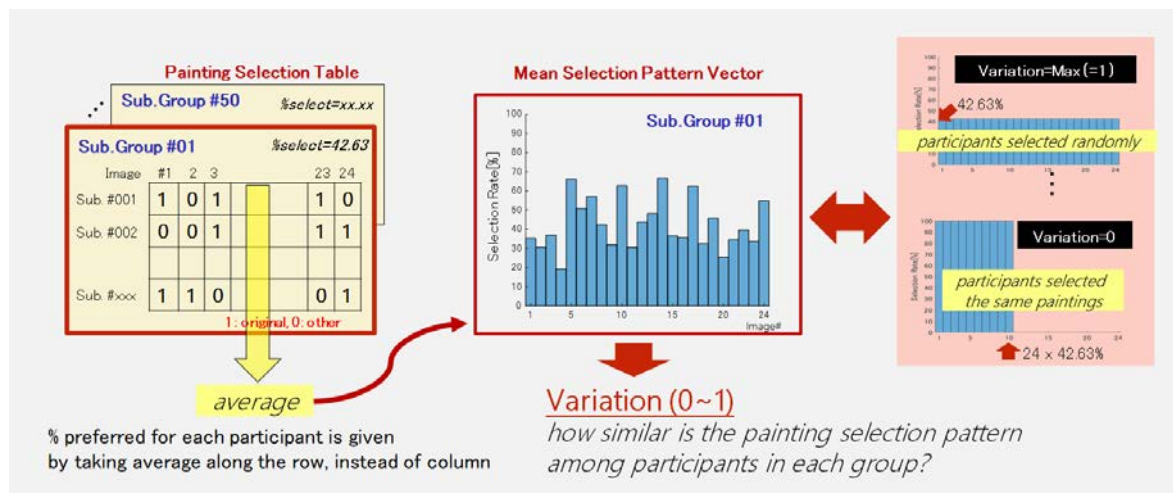


Figure 4. Painting Selection Pattern & Variation

Figure 5 shows the variation index for male and female in each age range (distribution of the variation is shown in violin plot, means for male and female are shown by blue and red lines). It was found that participants variation decreased as age ($F = 8.954, p = 0.000, \eta^2 = 0.1413$) and variation for female was lower than that of male ($F = 110.038, p = 0.0183, \eta^2 = 0.0702$). This implies that preference for color composition become similar as the age increases, and difference in preference between female and male gets closer ($F = 8.433, p = 0.000, \eta^2 = 0.0811$).

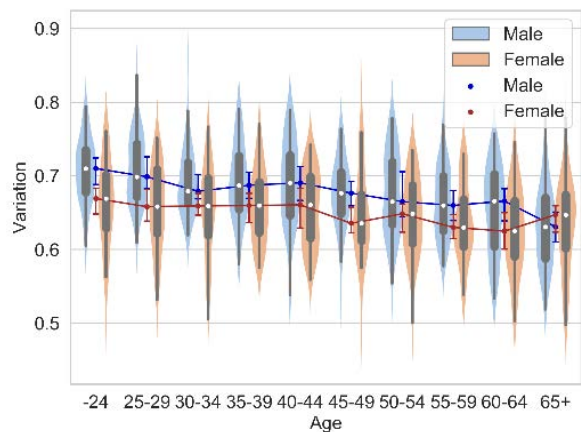


Figure 5. Variation : Age \times Gender

While, we found that no dependency of the variation on the household income ($F = 0.2075, p = 0.9341, \eta^2 = 0.0034$) and education level ($F = 1.5385, p = 0.2058, \eta^2 = 0.0230$).

3.3. Gender Similarity in Painting Selection Pattern

Finally, we investigated similarity of the original selection pattern between female and male for each age range. Figure 6 shows the correlation coefficient of the original selection pattern between gender and implying that the selection pattern become similar with the advance of age ($F = 4.9136$, $p = 0.000$, $\eta^2 = 0.0828$).

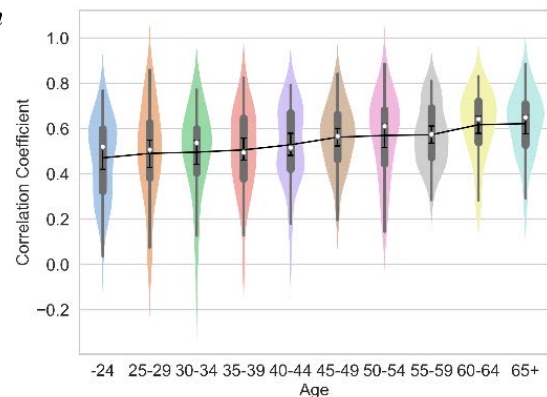


Figure 6. Gender Similarity

4. DISCUSSION & CONCLUSIONS

Original paintings were selected as most preferable (44.12 % among four choices) duplicating our previous findings. While, there was no significant difference in the original selection rate in terms of age, gender, household income, and educational level. We then analyzed the individual differences in the painting-selection patterns among participants and found that (1) the individual differences decreased according to the age, meaning that elderly participants tended to select similar paintings than younger participants, (2) the individual differences among female participants was smaller than that of male, (3) no significant trends were found in household incomes and educational background.

Furthermore, similarity analysis in the painting-selection patterns between female and male participants showed that similarity between gender decreased according to the age, female-male difference in the painting-selection patterns was bigger in young than elderly participants. These findings strongly imply that the original-preference judgement for art paintings are acquired not only during school age in the educational environment as shown in our previous report investigating children of 6-to-12 years old [4]. Also, the individual differences in the preference patterns for color composition of art paintings are affected both by age and gender, and tend to be decreased, suggesting that the preference patterns converge to a certain universal form presumably due to educational, cultural and/or environmental feedbacks.

ACKNOWLEDGEMENT

This work was supported by NTTDATA Institute of Management Consulting, Inc. for recruiting participants and data collection, and by KAKENHI (No.15H05922 and No.18KK0280).

REFERENCES

1. Nascimento, S. M., Linhares, J. M., Montagner, C., João, C. A., Amano, K., Alfaro, C., & Bailão, A. (2017). The colors of paintings and viewers' preferences. *Vision research*, 130, 76-84.
2. Kondo, T., Okada, N., Maruchi, K., Misaki, Y., Higashi, H., Monteiro AR, J., Montagner, C., Linhares MM, J., Nascimento MC, S., Nakauchi, S. (2017). Chromatic composition and preferences of paintings – Comparative study for Japanese and Portuguese observers and paintings, 24th symposium of the International Colour Vision Society, p.95.
3. Nakauchi, S., Kondo, T., Higashi, H., Linhares, M.M. J., Nascimento, M.C. S. (2018). Color statistics underlying preference judgement for art paintings, Vision Sciences Society 18th Annual Meeting, p.229.
4. Imura, T., Kondo, T., Shirai, N., Nakauchi, S. (2018). Preference for chromatic composition of art paintings by children aged 6- to 12-year old, European Conference on Visual Perception, p.27.

USE OF SMOKE IN ADVERTISING HOT DRINK PHOTOGRAPHY PRODUCTION

Hathaichanok Khemthong^{1*} Pratthana Thammachat¹, Natthamon Piengthisong¹
and Chanida Saksirikosol²

¹ *Department of Advertising and Public Relations Technology, Faculty of Mass Communication Technology,
Rajamangala University of Technology Thanyaburi, Thailand.*

² *Color Research Center, Rajamangala University of Technology Thanyaburi, Thailand.*

*Corresponding author: Hathaichanok Khemthong, e-mail: hathaichanokkt@gmail.com

Keywords: Smoke, Stick Incense, Advertising, Advertising Photography, Photography Production

ABSTRACT

The sole purpose of a business is to sell products and services to earn profits. Advertising helps a business to earn profits by enabling more people to know about the products and services and thus resulting in more sales. Key factors of advertising are a clear and eye-catching headline, a description of a good value, an attractive offer that perhaps includes a time-sensitive discount and/or “low cost to you, high value to them” premium, a logical reason for the offer, a reason for an immediate reply, and clear, understandable directions for the customer to follow. As mentioned above, an image for advertisement pays important and needs an artificial treat. In this paper types of smoke for making hot drink image attractive were investigated. Four types of smoke from stick incense, cigarette, electronic cigarette, and dry ice were used to make artificial smoke. The control factors in the process of photo production were the direction of smoke, light, hot drink, and surrounding. The images of hot drink were presented on an LCD display (27 inches; EIZO) one by one to the observers. The viewing distance was 50 centimeters. The observers were asked to assess the images with the criteria of “like” to “dislike” by 5 scales. The result showed the highest average of like at 4.03 for the hot drink image that used an electronic cigarette. The reason for selecting smoke from an electronic cigarette was that the smoke looked realistic than others.

INTRODUCTION

Currently, the photograph became an important component for advertisement. The attractive photograph is able to alter a customer’s attention to the presented product. According to the ability of photographs which communicate and describe the information itself, the customer received the information from photograph easier than text advertisement. Therefore, the photographer needs to be created an attractive photo by knowing the basic knowledge of photography and understanding product properties.

One of the factors that effected the interesting of advertising photograph of hot beverage is smoke. The smoke is able to increase the realistic photo’s feeling including people excitement for the product. The smoke also creates the perception of a fresh and hot product. Thus, the photographer needs to learn the process of creating various type of smoke and concern about the type of beverage.

Each smoke has different properties, such as the smoke from incense appeared in greyish white with higher flow. The intensity of smoke depends on the amount of incense. The smoke from dry ice showed in white color with lower flow and the intensity of smoke will crow in the early phase. The smoke from cigarette also appeared in white with higher flow. Thus, the intensity, color, and floating of the smoke are used to create an effect for the photo. The effect is able to generate a

different perception of each photo. The production of an advertising photograph for hot beverage needs to create an attraction to the customer. Therefore, the purpose of the study is to investigate the effectiveness of smoke in photograph production for a hot beverage.

METHODOLOGY

The photograph taking process has set the same direction of a camera, position of the product, additional instrument for each type of smoke. The light aperture was set as f-stop 8 with same light origin and direction. The creating smoke instrument consists of incense, dry ice, cigarette, and electric cigarette as shown in Figure 1. Each smoke instrument was applied to the product in order to create an effect of smoke in a photo as shown in Figure 2.

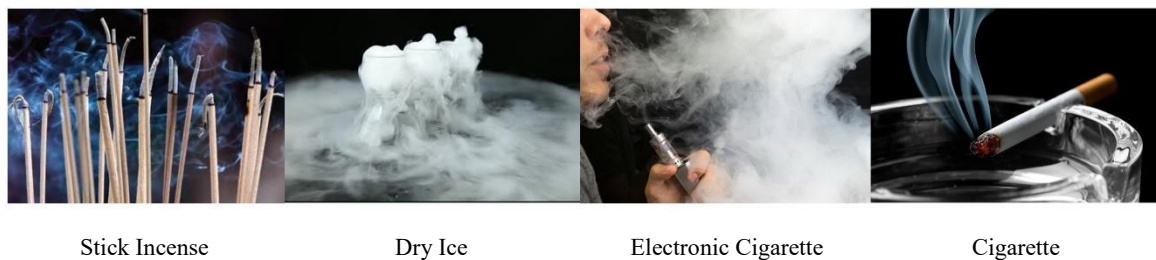


Figure 1. Type of Smoke



Figure 2. Hot Drink Photography with 4 Types of Smoke

In the evaluation process, the participants were asked to rate a suitable of each smoke with a Likert scale. Each type of smoke was randomly showed to the participants. The environment room was set in 300 Lux of light via 27 inches' monitor. Participants sit apart from monitor 50 centimeters.

RESULT

The result of an appropriate smoke for hot beverage photograph is showed in Figure3.

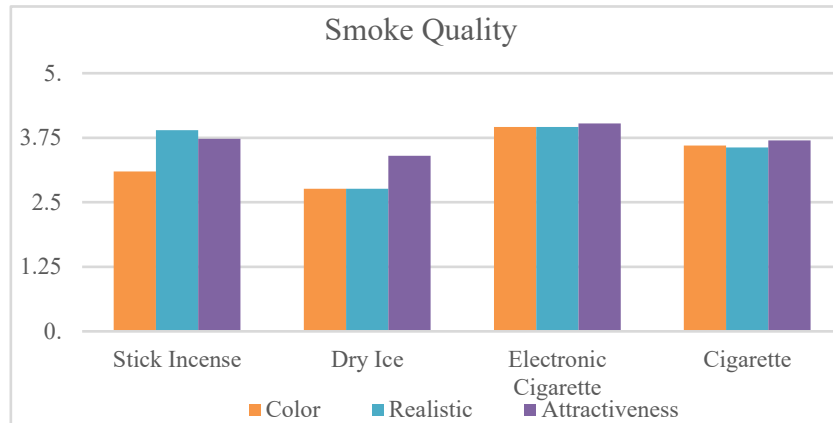


Figure 3. Comparison of Smoke Quality

The evaluation of smoke color in hot beverage advertising photograph showed that the smoke from an electric cigarette was appropriate for the product at an average of 3.96. The second appropriate instrument was cigarette with 3.6 and followed by the incense and dry ice at 3.1 and 2.76, respectively.

The result of the realistic score showed that the smoke from a cigarette had the highest score for realistic perception at 3.96, followed by the smoke from incense, electric cigarette, and dry ice at 3.9, 3.56 and 2.76, respectively.

The result of attractive perception and buying preference of the product showed that the highest score in smoke from an electric cigarette was 4.03, followed by incense, cigarette, and dry ice 3.73, 3.7 and 3.4, respectively.

CONCLUSION

In conclusion, the smoke production for hot beverage advertising photograph is able to create a realistic perception in a photo. Moreover, it increases the interesting of a photo that effected to customer buying preference. The most appropriate instruments for smoke production are from electric cigarette and cigarette.

ACKNOWLEDGEMENT

I appreciate the help of the Faculty of Mass Communication Technology and The Department of Advertising and Public Relations Technology for supporting the instruments and the location. I also would like to thank all participants for the great cooperation.

REFERENCES

1. Kasama Keawjumng. (2012). *Smoke Technique for Hot Food Photography;Steak*.
2. Steven Raichlen. (2016). *Project Smoke*. Workman Publishing Company.
3. Alison Park-Whitfield. (2012). *Food Styling and Photography for Dummies*. Wiley Publisher.

COLOR OF COOKED RICE TO IMPROVE APPETITE FOR ELDERLY

Pantakan Sukontee^{1*} Chanprapha Phuangsuan¹, Hiroyuki Iyota², Hideki Sakai³, Mitsuo Ikeda¹.

¹ *Color Research Center, Faculty of Mass Communication Technology, Rajamangala University of Technology Thanyaburi, Thailand.*

² *Graduate School of Engineering, Osaka city University, Japan*

³ *Graduate School of Human Life Science, Osaka city University, Japan*

*Corresponding author: Pantakan Sukontee, 1159108020127@mail.rmutt.ac.th, 453opolopol@gmail.com

Keywords: Color of cooked rice, Thai herb, elderly, appetite.

ABSTRACT

In the next few years, we will step into the aging society completely and many changes will take place with aging. The most common problem in the elderly is anorexia, they get bored to eat any foods. To improve this situation we hypothesized that if we change the color of rice changes from white to some other color by herbs such as butterfly pea, yellow by turmeric, red by roselle, green by pandanus leaf. Four chromatic colors and plus white rice were prepared to be presented by LCD display. In each of color rice, we changed the saturation by using Adobe Photoshop from the original color that was measured directly from real rice. Three steps of higher saturation were added to the original color and three steps of lower saturation were added to the original color. Finally, the total stimuli were 25 pictures. The preference questionnaire was "like" and "dislike" with scale 3 to -3, meaning like or dislike. We found that Thai elderlies preferred no vivid color of rice in red, yellow, green and blue. Japanese elderlies mostly preferred white color of rice and showed a small preference for red and yellow color by the reason that Japanese are familiar with the red and yellow rice for their daily life.

INTRODUCTION

Population of elderly people is increasing rapidly in Thailand. The United Nations [1] predicted that in the years 2001-2100 would be the century of the elderly, in which Europe has the highest number of elderly people in the world and Asia has the 4th highest number of elderly people in the world. Thailand is the country with the 4th highest proportion of elderly people in Asia and the 2nd in ASEAN. Department of Older Persons (DOP) of the Foundation of Thai Gerontology Research and Development Institute (TGRI) reported [2] the status of Thai elderly population in 2017 that there are 11 million elderly people aged 60 years or over in Thailand which counted as 17% of the total population of 65.5 million. Thailand is rapidly aging and it is expected that in not over than 4 years Thailand will become a completely aging society. When we step into the aging society many changes will take place with aging. One of them is a decrease of appetite for food, which decreases with age and often they get bored to eat any foods. To improve this situation rice may be colored. In Thailand, colored rice stained by herbs is common on market as it is thought some colored rice is good for health. In this report, we will investigate the effect of color of rice for appetite for elderly people.

EXPERIMENT

Subjects

There were 4 groups of subjects participated in this study, 30 Thai elderly people (age range from 61 to 80 years old), 100 Thai young people (age range from 18 to 25 years old), 15 Japanese elderly people (age range from 61 to 82 years old), and 21 Japanese young people (age range from 21 to 25 years old), totally 166 people.

Preparing stimuli

Five rice colors stained by herbs; purple by butterfly pea, green by pandanus leaf, red by roselle, yellow by turmeric, and white without stain as shown in Fig. 1 (d). The rice was cooked by a normal rice cooker (Sharp KSH-Q18) with standard water. After the cooking we measured the colors of rice by using Konica Minolta Luminometer CS-100A (Fig. 1 (b)) and we took photographs for each cooked rice on dishes under controlled illumination of experimental booth by using DSLR camera Canon EOS kiss x7i (Fig. 1 (c)). The booth was built to have the size of 150 cm in width, 60 cm in depth, and 180 cm height. It was illuminated by 8 daylight fluorescent lamps (TOSHIBA FL18W/T8/EX-D); 6 lamps were hanged on the ceiling and the others two lamps were set at the beside the dish of rice as you can see in Fig.1 (a). The illuminance of the booth was 3,194 lx, color temperature was 6,500 K.

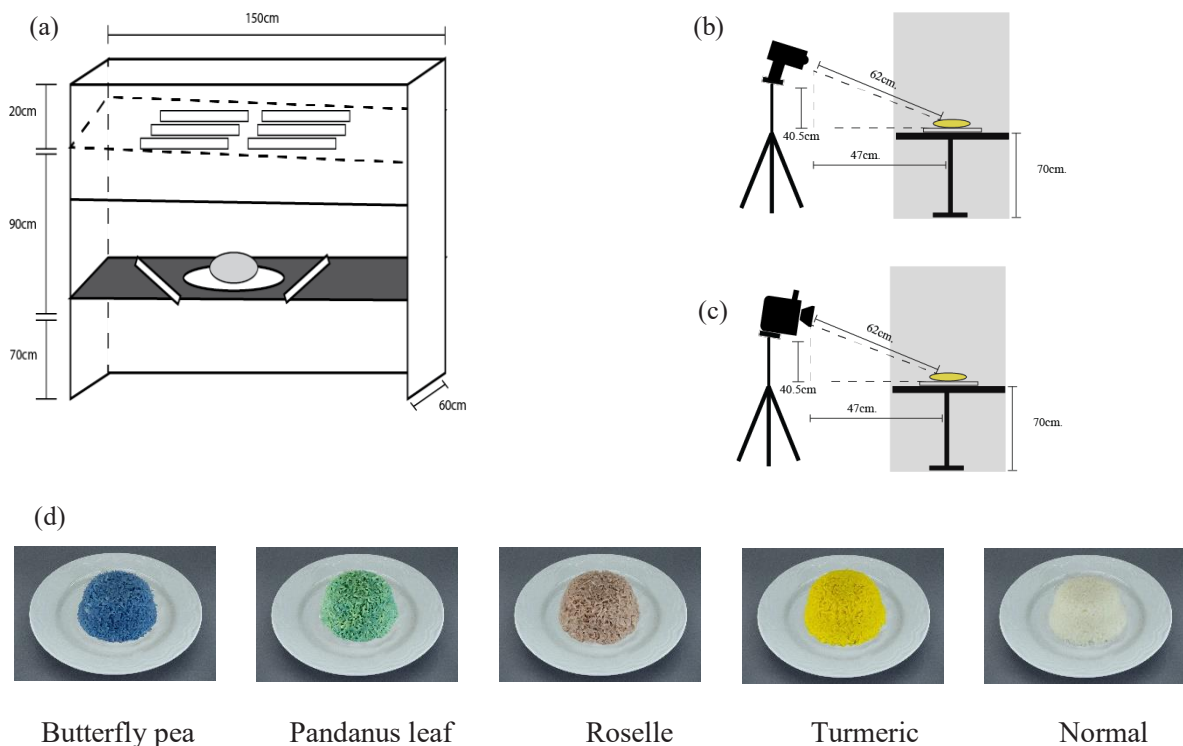


Figure 1. Preparing stimuli. (a) structure of experimental booth used for measuring rice colors and taking photos. (b) Measuring color of rice by using luminometer CS100A, (c) Taking photos of colored rice. (d) Photographs of colored rice.

Five colored rice photographs were then adjusted for temperature and tint by using the Adobe LightRoom on the LDC display (Eizo Cs2420) to make the color of photographs to match the real rice. The matched colors are shown in Fig. 2 (a) by open symbols. The colored filled symbols represent the color of real rice. After that, we adjusted the saturation of the photograph by using the Adobe Photoshop CC to decrease and increase saturation by 5 steps; two photographs of higher saturation than the original photograph (2, 1) and two photographs of lower saturation than the original photograph (-2, -1). The saturation of the original color was coded as 0. The results are shown in Fig. 2b with black filled triangles for the original. It was not possible to make saturation higher for the bellow photographs. There were 25 photographs as shown in Fig. 2 (b).

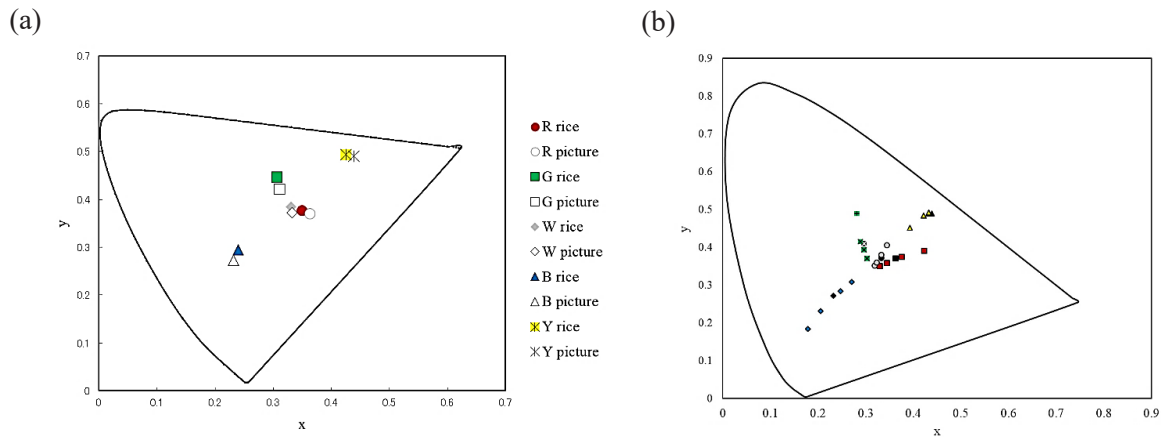


Figure 2. Rice colors. (a) Matching colors of rice photographs. (b) Adjusting saturation of rice photographs.

Procedure

For the convenience of moving experimental equipment to collect data from the elderly subject outside, we created an experimental box made of black board as shown in Fig. 3(a), of the size 45 cm in width, 91.2 cm in depth, and 30 cm height, to prevent light from outside keeping the inside the box dark. A subject looked at the 25 rice photographs which were presented one by one on the 14-inch labtop display (Asus A45V) through an aperture of the size 7.5 cm x 10 cm (Fig. 3(b)). The visual angle of a picture on the display was 12.4° high. The subject was asked to rank the picture by 7-point scale, from “like” down to “dislike”; -3 (dislike at all), -2 (dislike), -1 (rather dislike), 0 (so so), 1 (quite like), 2 (like), 3 (really like).

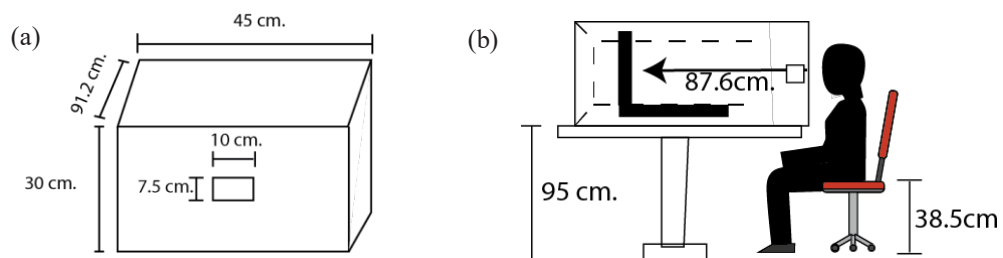


Figure 3. (a) An experimental box. (b) View of doing experiment.

RESULTS AND DISCUSSION

The scores to show saturation effect from 30 Thai elderlies are shown in Figure 4 for difference colors. The score did not change for saturation except the yellow rice. They did not like very vivid yellow rice. We averaged score of subject of each group for each color and the results are shown in Figure 5. Here, the scores of different saturation were averaged. The left above figure shows the score rated by Thai elderly subjects, we can see that red rice has the highest score of 1.67. White rice gave score 1.47, they like but not much. Other rice colors have the score less than 1 but all positive, which means they feel so so. For the Thai young subjects (right top figure), it seems that they like rice in every color, but there is no rice with a distinctive preference score than other colors, in which every rice color has less than 1.5, the highest score is 1.38. The averaged score of Japanese subjects shown at the bottom (both elderly and young groups) shows similar results for elderly and young people. The highest is white rice and the second is red and then yellow, but the green and blue rice gave minus score which means they dislike.

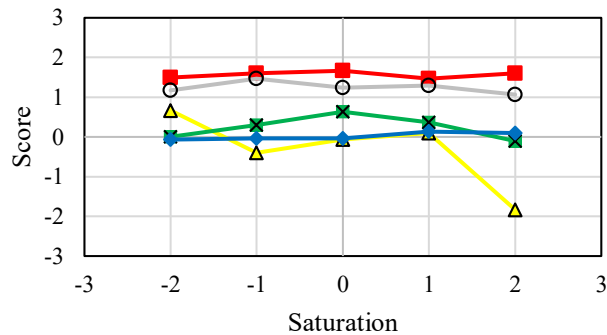


Figure 4. Score for different saturation of four colour of rice. Subjects Thai elderlies.

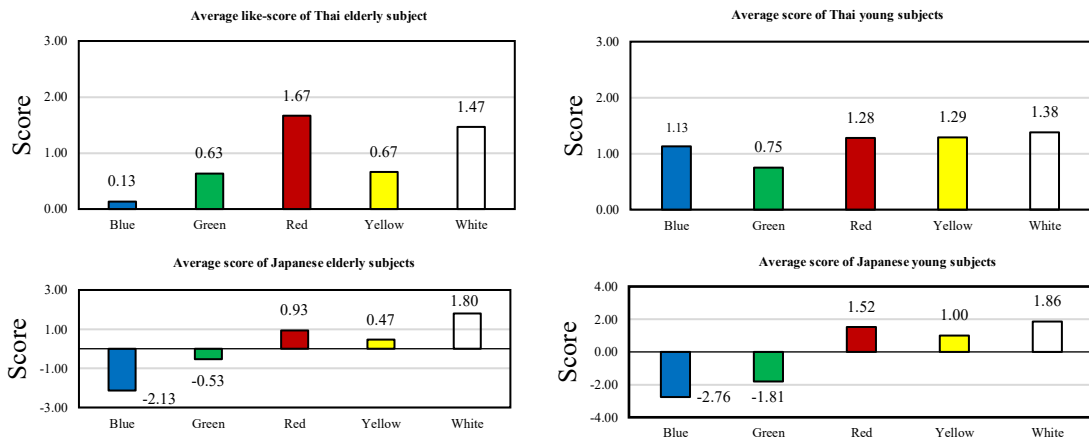


Figure 5. The averaged score of subjects. The left top shows Thai elderly subjects score, the right top shows Thai young subjects score, the left bottom shows Japanese elderly subjects score, and right bottom shows Japanese young subjects score.

If we compare Thai elderly subjects with Japanese elderly subjects in Figure 5, both Thai and Japanese elderly prefer white rice and red rice. Thai elderly subjects prefer red rice the most, secondly white rice, while the Japanese elderly subjects like white rice the most and the second red rice but they dislike blue rice and green rice. When we compare the results of Thai elderly subjects and Thai young subjects Thai young subjects like all the colors but the Thai elderly subjects like red and white, but so so for blue, green, and yellow rice. The comparison between Thai young subjects and Japanese young subjects shows clearly difference in blue rice and green rice, Thai young subjects like all the colors but Japanese young subjects dislike blue and green rice, they prefer white rice. Japanese subjects, both young and elderly subjects prefer white rice the most, like red rice, and they feel “so so” for yellow rice. But all Japanese subjects dislike blue and green.

When we look at the overall result we can conclude that the four groups of subjects prefer white rice and red rice, but do not like blue rice nore green rice. We also interviewed some subjects for voting reason and they pointed out that they preferred the white rice because it is a normal color that they always found in daily life, and the red rice looks like red bean in Japan and looks like Thai food named “Khao khluk kapi, Rice Mixed with Shrimp paste”. It influenced subjects to feel want to taste. Whereas, the blue rice and green rice remind them the fungus and chemicals that may be toxic. To ensure the results of the experiment, we should repeat the experiment by controlling the color of the blue and green rice not to have too much saturation.

ACKNOWLEDGEMENT

Pantakan Sukontee thanks RMUTT for providing him with scholarships Co - operative education Rajamangala University of Technology Thanyaburi that made Pantakan to do internship abroad. He also thanks students of Professors Iyota and Sakai laboratories to be a good friends to Pantakan and for serving as subjects for this experiment.

REFERENCES

1. Vapattanawong, P. (2019). *Station of the Thai elderly 2017: Foundation of Thai Gerontology Research and Development Institute.*, from <http://thaitgri.org/?wpdmpro=situation-of-the-thai-elderly-2017>
2. United Nations. (2015). *World Population Ageing 2015*. Retrieved September 26, 2019, from https://www.un.org/en/development/desa/population/publications/pdf/ageing/WPA2015_Report.pdf.

COLOR SATISFACTION ON PRINTED MEDIA OF FOUNDATION FOR REHABILITATION AND DEVELOPMENT OF CHILDREN AND FAMILY (FORDEC)

Ploy Srisuro^{1*} and Warin Chuen-Aram¹ and Thitapa Rodsong¹

¹*Advertising and Public Relations Department, Faculty of Mass Communication Technology, Rajamangala University of Technology Thanyaburi, Thailand.*

*Corresponding author: Ploy Srisuro, ploy@rmutt.ac.th, srisuro@yahoo.com

Keywords: Satisfaction, Brochure, Color, Design, Categorical Scale

ABSTRACT

This research aimed to investigate the level of color satisfaction for image, design, typography, and color of the printed media of the Foundation for Rehabilitation and Development of Children and Family (FORDEC). The brochures were designed in A4 size, in 3 folds, on coated paper, and 210 g/m². The brochure was printed by light blue, blue and yellow as main colors. The images and graphics were printed by purple, red, orange and pale yellow. The brochure was presented to subjects and they were asked to assess for the overall satisfaction, content, images, design, typography, and color of text and color of the background and the overall colors by 5 categorical scales between “Dislike” and “Like”. One hundred subjects living in Suanluang District, Bangkok participated in the experiment. The result showed that the satisfaction of the content, images, design, typography, and color were 4.22, 4.38, 4.35, 4.28, and 4.34, respectively. The brochures were successfully designed.

INTRODUCTION

Public Relations tools have been playing a significant role to convey the messages for the organization, such as the policy, missions, objectives, activities, and performances. They also transmit knowledge about the organization to the target group to build trust and credibility. Therefore, the marketers or PR officers of the organization should thoroughly understand the functions and principles of Public Relations tools so that they can select and use the right tools to reach the right target [1].

Printed media is one of the traditional media used to reach the target group. The production cost is lower than other advertising or public relations tools. The content is flexible so that the marketers or PR officers can choose the right content. The printed media is tangible, long-lasting and can be passed along to other audience. Therefore, many organizations, both in private and public sectors, choose printed media to be the key PR tool [2].

Nowadays, there are many Non-profit Organizations (NGO) established in Thailand. Like any other organizations in the private or public sector, NGOs need to convey and communicate their work to the public to seek cooperation. As a consequence, NGOs use various communication tools, for example, TV commercial, radio spot, printed media, and social media. However, each NGOs has a different mission and social services. They need to raise awareness as well as to educate the social problems and the solutions to the target group[3].

The Foundation for Rehabilitation and Development of Children and Family (FORDEC) is a non-profit organization, established on February 14, 1998, by Dr. Amporn Wathanavongs. The objectives of the organization are to help rehabilitate children and youth who are poor, handicapped, abused, wandering, homeless, addicted to drugs, and HIV/AIDS+ by providing them with the opportunities for physical and intellectual growth, to uplift their living conditions regardless of race and religion, and uphold the protection of children's rights. Also, the organization aims to promote cultural and moral values, good habits and spiritual values among children and youth so that they will become future productive citizens.

For poor families and the needy, the organization tries to help develop these families to have good health, decent housing and occupational assistance to increase family income for the attainment of their better living conditions. Moreover, the organization would like to work or cooperate with other similar agencies for public interest. The vision and mission statement of the organization is to be a public/charitable organization dedicated to helping underprivileged children in difficult circumstances and disadvantaged regardless of race color or religion to uplift their living condition. Also, the organization holds to one's principles of doing good with the integrity and sincere to a donor and client, with professional management by quality and service with love.

According to the interview session with the Director of FORDEC, the communication tools used for the organization are online media and printed media which are brochures and posters. Considering the printed media, the content especially the printed words are too much and look dense. The audience would take a longer time to read and understand the message. The images and pictures used for design are unattractive and cannot convey the message of the printed material as shown in Figure 1.



Figure 1. FORDEC Current Brochure

Therefore, the researchers decided to create and redesign the brochures for FORDEC by using new concept, colors, and typography. The researchers assessed the level of the satisfaction of the target group toward the design, images, content, typography, and color of the current brochures. So we hope that the new brochures would be more attractive and be used effectively. Ultimately, the brochures will be a successful tool to reach the target group.

METHODOLOGY

To study the level of color satisfaction on printed media, the researchers first needed to analyze the current printed media in terms of the content and design. After that, the researchers redesigned the brochures according to the media production principle and then had the subjects assess the level of color satisfaction toward the new brochures.

The Subjects

In 2018 living in Suanluang District, Bangkok the same location as the Foundation, the population for the assessment process was around 115,756 people. According to Taro Yamane Sample Size Determination, the subjects were selected by using the accidental sampling method. The subjects were divided into two periods of times as the following.

- 1) The first assessment: 30 subjects assessed the current brochure.
- 2) The second assessment: 100 subjects assessed the new brochure.

The Printed Media Production

According to the media production principle, the new brochures were created and produced in the following steps.

1) Pre-prepress: the design and planning process. The researchers set the objectives and the printed format, the target group as well as the printing schedule.

2) Prepress: the manuscript preparation process. The researchers prepared the content and images by considering the vision and mission statement of the organization. With the results from the subjects and the aids from the design experts, the researchers created the draft, thumbnail sketch, rough layout. Then, the researchers developed the layout and artwork and made sure that the artwork was correct.

3) Press: the printing process. After the proofreading, the researchers were sending the artwork to the printer.

4) After-press: the finishing process. The researchers checked the correctness and clarity of color and images as well as the folding.

The Satisfaction Assessment Process

The subjects, both from the first and second satisfaction assessment, were asked to answer the questionnaire. The questions were in 5 categorical scales between “Dislike” and “Like” and were divided into 5 categories which were content, images, design, typography, and color. For the content, the topics were about attraction and easy understanding. For the images, the topics were about the clarification, sharpness, and attraction. For the design, the topics were about creativity, presentation format appropriateness, and beauty and attraction. For the typography, the topics were about clear visibility, easy reading, and outstanding format. For the color, the topics were about overall appropriateness, outstanding color for the characters, and the beauty of background color.

RESULT

The Satisfaction Assessment of Current Brochure

The subjects were 30 people who were 14 males, 16 females, mostly were 15-25 years old (57%) with a bachelor degree (84%). The result of the satisfaction assessment of current brochure was shown as Figure 2.

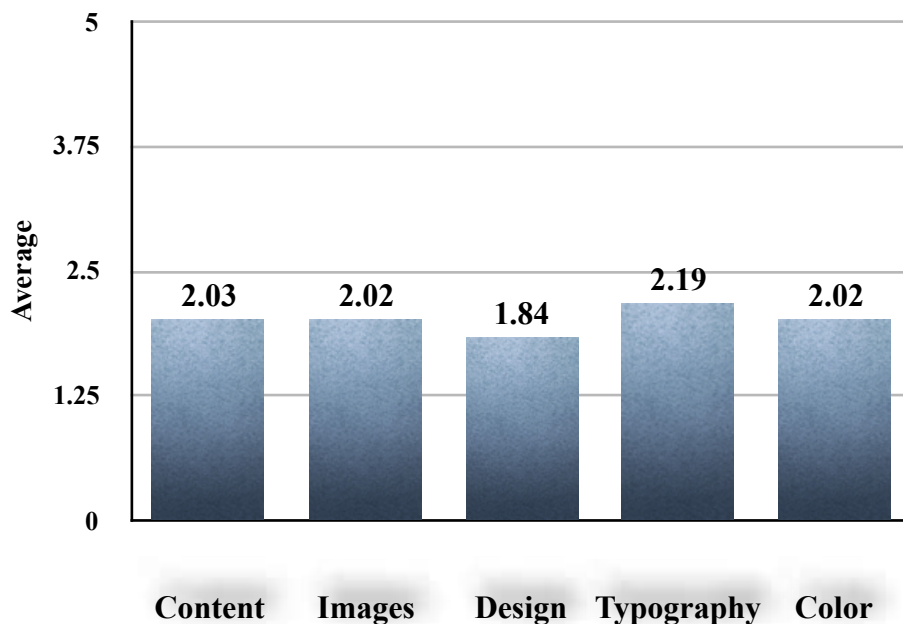


Figure 2. Satisfaction Assessment of Current Brochure

The result showed that the subjects were not satisfied with the current brochure because the average score (\bar{X}) in all categories was very low. The average score of the satisfaction of the content, images, design, typography, and color were 2.03, 2.02, 1.84, 2.19 and 2.02, respectively. Considering the color category, the average scores under the topics of the overall appropriateness, outstanding color for the characters, and the beauty of background color were 1.97, 2.43 and 1.67, respectively.

The Printed Media Production

The researchers used the result from the satisfaction assessment of current brochure to be part of the redesigning process as the following.

1) Pre-prepress: The objectives of the new brochures were to give detailed information about the organization, background, mission, and donation channel to encourage the cooperation from the target group. The format was 3-fold printed on an A4 size of 210 g/m2 coated paper. The brochures were 2 sheets of paper. The first sheet was giving out the information about the foundation joining form and the donation channel. The second sheet was the core content about the information of the foundation, the important statistics and the background of the foundation.

2) Prepress: To convey the messages, the researchers selected the content of foundation background, objectives, main projects, and donation. For the images, the researchers carefully chose the images representing the tasks of the foundation. Then the researchers created the drafts, thumbnail sketch, and rough layout of 2 sheets of paper as the following.

- The first sheet was designed to look like an envelop that can be cut and mailed back to the foundation as shown in Figure 3. The front page was showing the name and the slogan of the foundation, the address, and the donation channel. The back page included the foundation joining form, the donation form and the mission of the foundation.

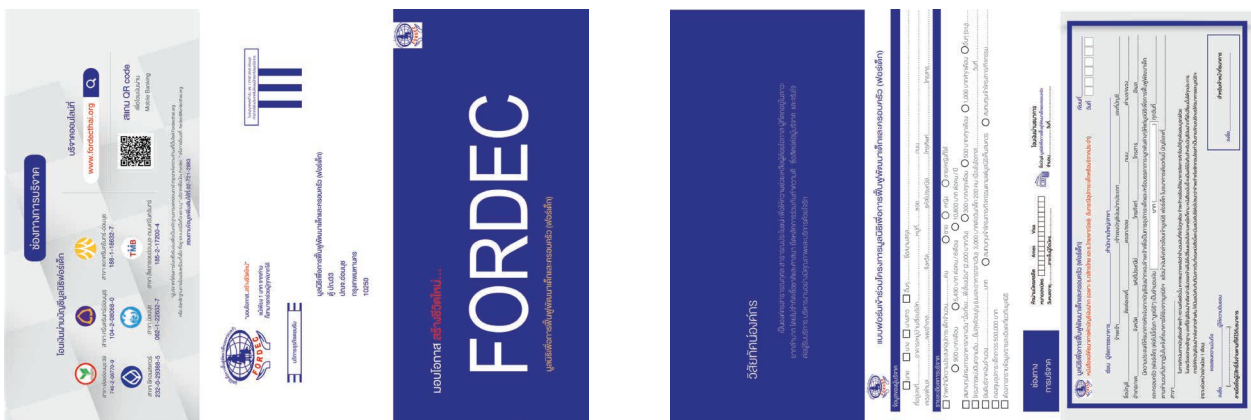


Figure 3. FORDEC New Brochure: The first sheet, front page (left) and back page (right)

- The second sheet was designed to publicize the foundation as shown in Figure 4. The front page included the cover, main activities, and projects. The bold graphics, QR codes, and statistics were used to make the brochure interesting and easier to read. The back page was displaying objectives, a timeline of the foundation, and the quotation from the founder. It was designed with the icons, pictographs, images, and QR code to attract the target group to seek more information.

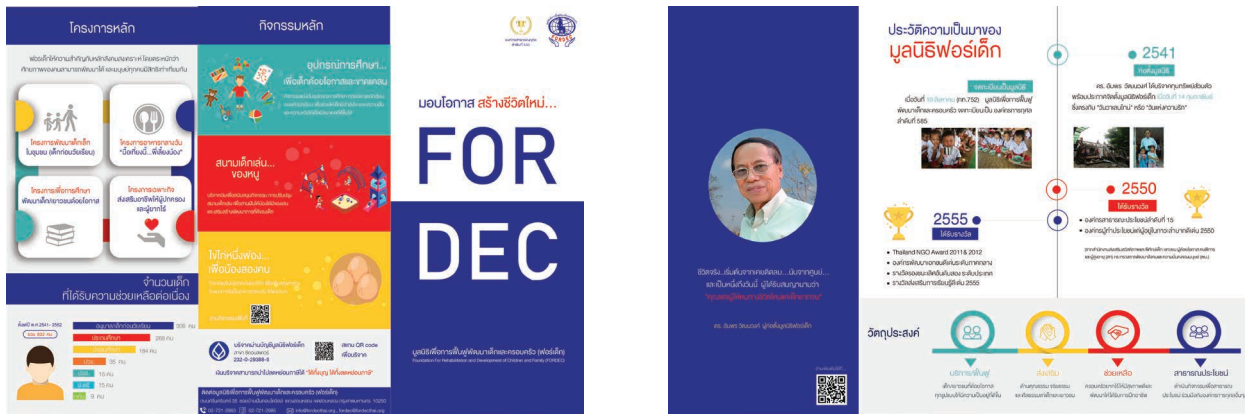


Figure 4. FORDEC New Brochure: The second sheet, front page (left) and back page (right)

The researchers used blue, light blue and pale yellow as main colors. Since blue represents the color of the foundation, the researchers used blue, light blue and yellow as the base colors and used the split complementary colors which were red, orange, purple and pale yellow for the images and graphics.

3) Press: The researchers proofread the artwork and check the spelling and grammar. Then, the brochures were printed on high-quality paper.

4) After-press: The color and images were correct and seen. The folding was neat and well-trimmed.

The Satisfaction Assessment of Current Brochure VS New Brochure

The subjects were 100 people who were 28 males, 72 females, mostly were 15-25 years old (58%) with a bachelor degree (72%). The comparison result of the satisfaction assessment of current brochure versus new brochure was shown as Figure 5.

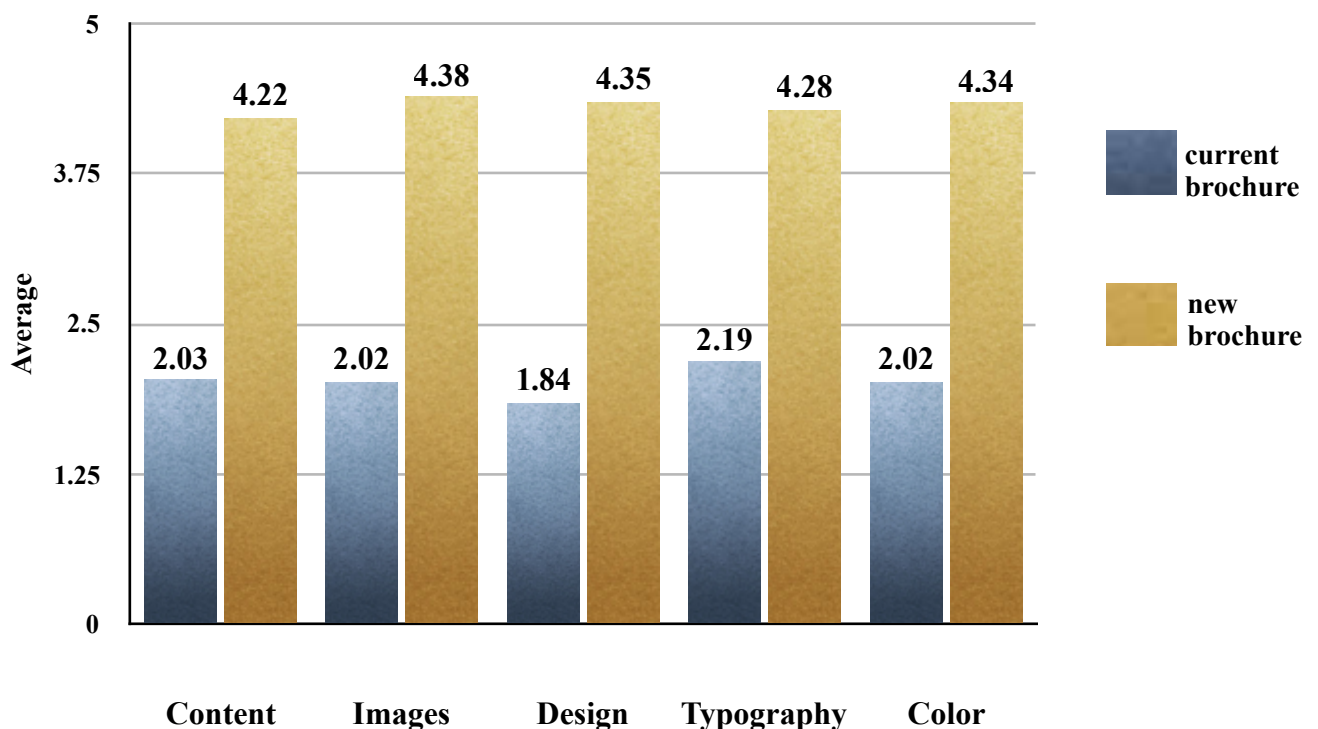


Figure 5. Comparison Satisfaction Assessment of Current Brochure VS New Brochure

The result showed that the subjects were very satisfied with the new brochure in all categories. The average score (\bar{X}) of the content, images, design, typography, and color were 4.22, 4.38, 4.35, 4.28 and 4.34, respectively. The score was higher than the result from the satisfaction assessment of the current brochure. Considering the color category, the average scores under the topics of the overall appropriateness, outstanding color for the characters, and the beauty of background color were 4.37, 4.33, and 4.31, respectively

CONCLUSION

Before, the brochures for FORDEC were simply designed in Word Program by the staff of the foundation who had limited design knowledge. Light blue and pink were chosen to represent the color of girls and boys, and easy-to-find from the program. These two colors also convey the feeling of love, affectionate and caring. The researchers, therefore, redesigned the new brochures with the concept of less text, more visual and eye-catching colors. The split complementary scheme created the same strong visual contrast as the complementary color scheme, but with less tension. The color contrast and saturation were increased. Combined with new design, composition and graphics usage, the content was easy to read and understand. The chosen colors still represent the organization identity. Therefore, the new brochures are more attractive. The average score of the color category of new brochures is 46.4 percent higher than current brochures.

ACKNOWLEDGEMENT

This work was supported by the Color Research Center and the Faculty of Mass Communication Technology, Rajamangala University of Technology Thanyaburi (RMUTT), Thailand.

REFERENCES

1. Shinaworn, A. (2010). *Public Relations Media*. Bangkok: Chulalongkorn University Printing House.
2. Seitel, F. P. (2017). *The practice of public relations*. Harlow: Pearson Education.
3. Drucker, P. F. (2016). *Managing the non-profit organization: practices and principles*. London and New York: Routledge, Taylor & Francis Group.

SPECTRAL DESIGN OF LIGHTING INDICATOR FOR DETECTING 5000 K WHITE-LIGHT LED

Pei-Tzu Huang¹ and Hung-Shing Chen^{2*}

¹ Graduate Institute of Color & Illumination Technology, National Taiwan University of Science and Technology, Taiwan

² Graduate Institute of Electro-Optical Engineering, National Taiwan University of Science and Technology, Taiwan

*Corresponding author: Hung-Shing Chen, bridge@mail.ntust.edu.tw

Keywords: Metamerism, Lighting indicator, White-light LED, Singular value decomposition

ABSTRACT

This study aims to design the reflection spectra of novel lighting indicator, which has the capability of showing similar color under 5000 K white-light LED, while showing difference colors under CIE daylight series. We applied singular value decomposition to rebuild the reflection spectra of 18 color patches chosen from ColorChecker, and successfully developed 13 pairs of metamer. The simulation results show that these metameric colors perform well.

INTRODUCTION

Metamerism is a phenomenon that two objects or colors with different spectra show similar color under a particular light source, but show different colors under the other source [1]. Currently, several lighting indicators are sold for detecting standard illuminants. For example, X-rite PANTONE product: lighting indicator stickers (D50 and D65) (Figure 1) [2]. The design principle takes use of metamerism property, more lighting environments match the light source indicated by the lighting indicator sticker, the color pair on the lighting indicator will become closer. Since the printing industry uses D50 as a standard illuminant, we found when using the D50 lighting indicator, which can observe two different colors under light sources of A, CWF, and TL84. However, these lighting indicator stickers cannot work well for general white-light LEDs. In view of the longevity and power saving of LED, other energy-consuming light sources may be replaced by LEDs in the future. CIE is also actively establishing standard spectral data for white LEDs [3]. This study aims to design the reflection spectra of metamer that can show similar color under 5000 K white-light LED, but indicate different colors in CIE daylight series.

METHOD

From the view of Colorimetry, as long as the reflectance spectrum of an object is obtained by color measuring, its tristimulus values can be calculated by the spectral power distribution of illuminant and CIE Color Matching Functions (CMFs) according to Equation (1) [4]:

$$\mathbf{T} = \mathbf{M} \cdot \mathbf{R} \quad (1)$$

where \mathbf{T} is a $3 \times n$ matrix of tristimulus values, \mathbf{M} is a 3×36 matrix of the wavelength-by-wavelength product of the illuminant with any of the CMFs, and \mathbf{R} is a $36 \times n$ matrix of the spectral reflectance values. This study defines the visible spectral range of 380 ~ 730 nm, with an interval of 10 nm. Therefore, there are 36 spectral reflectance values in total. Due to the existence of metamerism, if the reflectance spectrum (Equation (2)) is derived from the tristimulus values of an object, there may be N solutions ($N > 1$) [4].

$$\mathbf{R} = \mathbf{M}^{\dagger} \cdot \mathbf{T} \quad (2)$$

Since \mathbf{M} is not a square matrix, if we calculate the inverse matrix directly, an infinite set of pseudo-inverse matrices \mathbf{M}^{\dagger} of non-unique solutions could be obtained. Therefore, we replace \mathbf{R} in Equation (1) by \mathbf{BC} , and Equation (3) is used in this study to find the optimal solution [4]:

$$\mathbf{T} = \mathbf{M} \cdot \mathbf{B} \cdot \mathbf{C} \quad (3)$$

where \mathbf{B} is a 36×3 matrix of three basis functions that describe a particular set of reflectance spectra, which can be obtained by singular value decomposition (SVD), and \mathbf{C} is a $3 \times n$ matrix of unknown coefficients. In this study, singular value decomposition was applied to decompose a particular set of reflectance spectra to obtain a series of basis functions, and we can multiply the specific basis functions with matrix \mathbf{M} to form a square matrix, and then performed inverse matrix operation on it. Imagining that \mathbf{A} is a $m \times n$ matrix and \mathbf{A}^T is its transposed matrix, SVD can be utilized to decompose matrix \mathbf{A} according to Equation (4) [4]:

$$\mathbf{A} = \mathbf{U} \cdot \mathbf{S} \cdot \mathbf{V}^T \quad (4)$$

where the columns of the $m \times m$ matrix \mathbf{U} are the eigenvectors of \mathbf{AA}^T . The columns of the $n \times n$ matrix \mathbf{V} are the eigenvectors of $\mathbf{A}^T\mathbf{A}$, and \mathbf{V}^T is the transposed matrix of \mathbf{V} . The matrix \mathbf{S} is a $m \times n$ diagonal matrix, and the elements on the diagonal are non-negative square roots of eigenvalue of \mathbf{AA}^T and $\mathbf{A}^T\mathbf{A}$, which are the singular values of matrix \mathbf{A} . Accordingly, they are arranged in descending order from large to small and correspond to the columns vectors of \mathbf{U} and \mathbf{V} . The matrix \mathbf{V} thus obtained is used as the basis functions that can describe a particular set of reflectance spectra, then \mathbf{MB} becomes a square matrix that can be inverted. Therefore, we can solve \mathbf{C} according to Equation (5) [4].

$$\mathbf{C} = (\mathbf{M} \cdot \mathbf{B})^{-1} \cdot \mathbf{T}_{ref} \quad (5)$$

Here, \mathbf{T}_{ref} is a 3×1 matrix representing the tristimulus values of a particular reference color. Substituting Equation (5) by $\mathbf{R} = \mathbf{BC}$, we can calculate the predicted reflectance spectrum R_{pre} from Equation (6) [4].

$$R_{pre} = \mathbf{B} \cdot (\mathbf{M} \cdot \mathbf{B})^{-1} \cdot \mathbf{T}_{ref} \quad (6)$$

In this study, we selected 35 color samples from TOCOL *fan deck-A/B* and TOCOL Color Book-B (Figure 2) [5], inputted their CMY dot coverages into Adobe Photoshop software, then printed them by an inkjet printer (HP Officejet 7500A). After that, we measured their reflectance spectra of color samples with a spectrophotometer (X-rite i1 pro2).



Figure 1. PANTONE lighting indicators

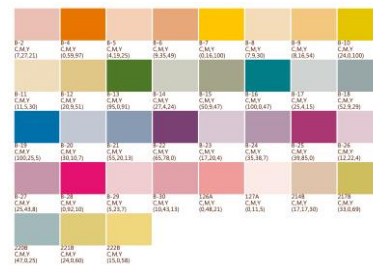


Figure 2. 35 color samples (TOCOL)

Next, we used MATLAB to perform SVD on the reflectance spectra of the 35 color samples with the operation of command “*svds*”. Table 1 shows the maximum 6 singular values and their percentages of singular value sum (referred to as contribution rate). The corresponding 6 sets of basis functions are shown in Figure 3.

Table 1: The maximum 6 singular values and their contribution rate

	Singular value	Contribution rate (%)
basis function 1	19.2	73.9
basis function 2	3.4	13.3
basis function 3	1.7	6.4
basis function 4	0.8	3.2
basis function 5	0.3	1.3
basis function 6	0.2	0.7
Total		98.8

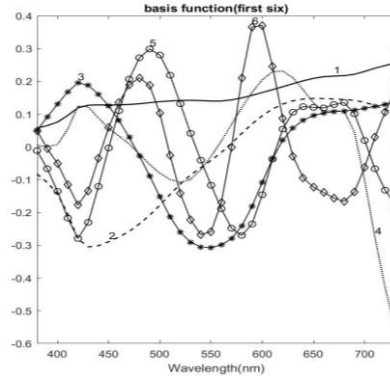


Figure 3. The resultant of 6 sets of basis functions

Since only three sets of basis functions are needed in Equation (3) to calculate the predicted reflectance spectra, the next step is to recombine the six basis functions. The combination method is to select the “basis function 1” that has the largest contribution rate, and then arbitrarily select two basis functions from basis functions 2, 3, 4, 5, 6 for combination, therefore, a total of 10 sets of basis function combinations are generated as shown in Table 2.

Table 2: The basis function combinations and their contribution rates

Combination	Spectrum No.	Contribution rate (%)
basis function 1, 2, 3	$R_{pre,1}$	93.6
basis function 1, 2, 4	$R_{pre,2}$	90.4
basis function 1, 2, 5	$R_{pre,3}$	88.5
basis function 1, 2, 6	$R_{pre,4}$	87.9
basis function 1, 3, 4	$R_{pre,5}$	83.5
basis function 1, 3, 5	$R_{pre,6}$	81.6
basis function 1, 3, 6	$R_{pre,7}$	81.0
basis function 1, 4, 5	$R_{pre,8}$	78.4
basis function 1, 4, 6	$R_{pre,9}$	77.8
basis function 1, 5, 6	$R_{pre,10}$	76.0

Because there are 10 combinations of basis functions in total, Equation (6) can be rewritten as Equation (7):

$$R_{pre,i} = \mathbf{B}_i \cdot (\mathbf{M} \cdot \mathbf{B}_i)^{-1} \cdot T_{ref} \text{ for } i=1,2, \dots, 10 \quad (7)$$

Furthermore, we used 18 color patches on the ColorChecker Color Rendition Chart (No. 1 ~ 18 in the chart name *Checker 1 ~ Checker 18*) as the reference colors for rebuilding the metameric color pair. Figure 4 shows the CIE a^*b^* color distributions of these 18 color patches.

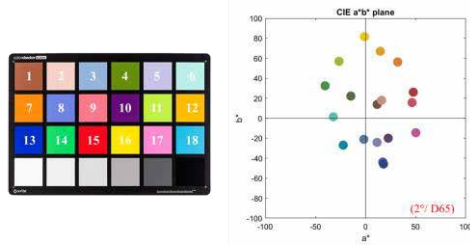


Figure 4. CIE a^*b^* color distributions of the 18 color patches of the ColorChecker

Substituting the tristimulus values of the reference colors into Equation (7), totally 180 predicted reflectance spectra (18 reference colors \times 10 predicted reflectance spectra) can be obtained. Notice that some of the predicted reflectance spectra may be partially outside of the range of 0 ~ 1, which means that they do not meet the actual definition. Therefore, the spectral reflectance values must be corrected into 0 ~ 1 according to Equation (8). Taking *Checker 4* as an example, the 10 predicted reflectance spectra of this reference color are shown in Figure 5.

$$0 \leq R_{pre,i} \leq 1 \text{ for } i=1,2, \dots,10 \quad (8)$$

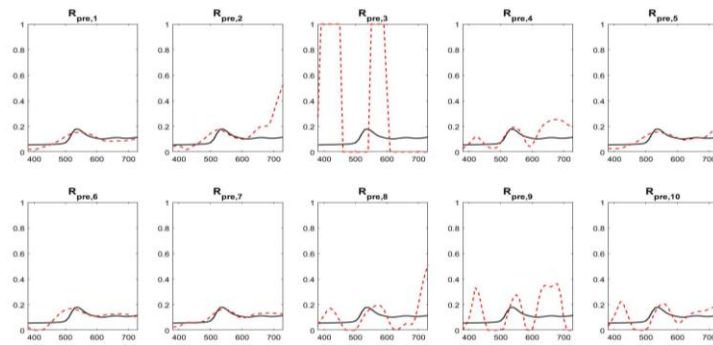


Figure 5. Predicted reflectance spectra of *Checker 4* (black curves represent reflectance spectra of reference color, and red curves represent predicted reflectance spectra)

Among the 180 predicted reflectance spectra (18 reference colors \times 10 predicted reflectance spectra), it is aimed to pick out the metamer which can show similar color under 5000 K white-light LED, while show difference colors under the CIE daylight series. Therefore, we set three conditions to screen out the metamer candidates. The screening process is shown in Figure 6.

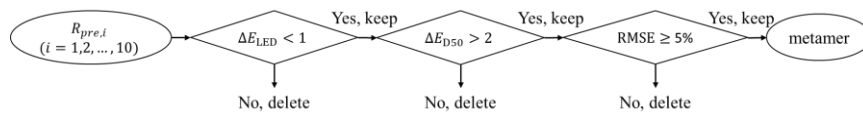


Figure 6. Screening process for the metamer

Condition 1: Calculate color differences between reference color and each predicted color with the color-difference formula CIEDE2000. Under the condition of 5000 K white LED, the reasonable color difference should be less than 1 ($\Delta E_{LED} < 1$). Taking the predicted spectra of *Checker 4* as an example, the color difference values are arranged in Table 3, where $R_{pre,1}$, $R_{pre,2}$, $R_{pre,4}$, $R_{pre,5}$, $R_{pre,6}$, $R_{pre,7}$ and $R_{pre,8}$ match Condition 1 (Figure 7(a)).

Condition 2: Calculate color differences between reference color and each predicted color with the color-difference formula CIEDE2000. Under the condition of D50 illuminant, the reasonable color difference should be greater than 2 ($\Delta E_{D50} > 2$). Taking the predicted spectra of *Checker 4* as an example, the color difference values are arranged in Table 3, where $R_{pre,4}$ and $R_{pre,6}$ match Condition 2 (Figure 7(b)).

Condition 3: Root-mean-square error (RMSE) of spectra between reference color and predicted color should be larger than 5%. Taking the predicted spectra of *Checker 4* as an example, the RMSE values are shown in Table 3, where only $R_{pre,6}$ matches Condition 3 consequently (Figure 7(c)).

Table 3: Color differences and RMSE values of the predicted spectra of *Checker 4*

Predicted spectra	ΔE_{LED}	ΔE_{D50}	RMSE
$R_{pre,1}$	0.0	1.9	
$R_{pre,2}$	0.0	0.9	
$R_{pre,3}$	44.6		
$R_{pre,4}$	0.0	3.9	7 %
$R_{pre,5}$	0.0	1.6	
$R_{pre,6}$	0.0	2.1	4 %
$R_{pre,7}$	0.0	0.5	
$R_{pre,8}$	0.5	1.8	
$R_{pre,9}$	3.1		
$R_{pre,10}$	1.3		

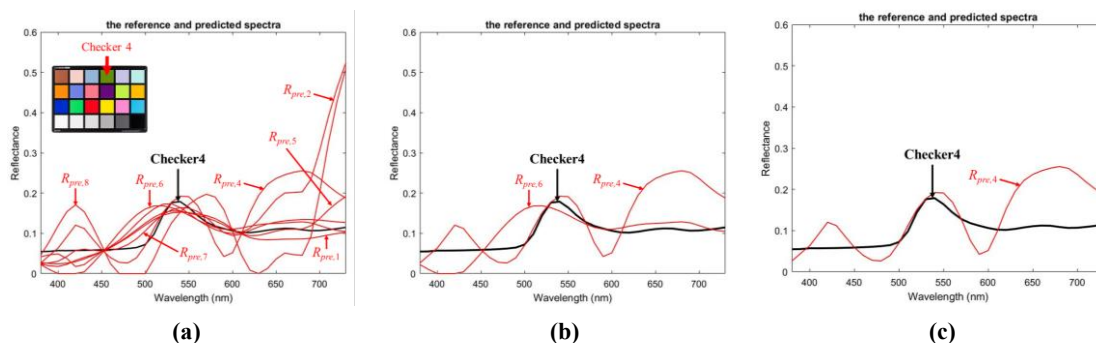


Figure 7. Screening example of *Checker 4*, (a) 6 predicted spectra which meet Condition 1, (b) 2 predicted spectra which meet Condition 2, (c) only 1 predicted spectrum which meets Condition 3

RESULTS

Totally 18 reference colors selected from the ColorChecker Color Rendition Chart were screened through these three conditions, the predicted spectra of reference colors such as *Cherckers 7, 12, 13, 15, 16* did not meet the 3 conditions, that is, the 5 reference colors do not produce the metamer. Table 4 shows the color difference values under 5000 K white LED, D40, D50, D65 respectively, and RMSE values of 13 pairs of metameric color pairs, which produced from the rest of 13 reference colors (listed by the best pair). Finally, Table 5 demonstrates partial examples of metamer and their simulated colors in this study.

Table 4: 13 pairs of metameric color pairs that match the three conditions

No.	ΔE_{LED}	ΔE_{D40}	ΔE_{D50}	ΔE_{D65}	RMSE
1	0.1	5.0	5.0	5.7	7 %
2	0.0	5.1	4.5	4.5	26 %
3	0.0	6.8	4.1	2.0	29 %
4	0.0	5.2	3.9	3.0	7 %
5	0.0	5.0	4.0	3.2	9 %
6	0.0	6.3	5.2	4.9	24 %
8	0.9	9.3	5.9	3.8	25 %
9	0.9	4.0	3.1	2.8	19 %
10	0.0	8.0	6.3	5.3	17 %
11	0.3	8.0	6.2	4.9	30 %

14	0.0	4.1	3.3	2.8	9 %
17	0.0	4.1	3.2	2.5	25 %
18	0.0	6.4	4.6	3.2	35 %

Table 5: Examples of metamer and the simulated colors (upper part is reference color, and lower part is predicted color)

No.	Reflectance spectra	Color	No.	Reflectance spectra	Color
1		 $\Delta E_{D50} = 5.0,$ <i>Checker 1</i>	2		 $\Delta E_{D50} = 4.1,$ <i>Checker 3</i>
3		 $\Delta E_{D50} = 5.2,$ <i>Checker 6</i>	4		 $\Delta E_{D50} = 6.3,$ <i>Checker 10</i>
5		 $\Delta E_{D50} = 3.2,$ <i>Checker 17</i>	6		 $\Delta E_{D50} = 4.6,$ <i>Checker 18</i>

CONCLUSION

This study successfully designed 13 pairs of metamer as the lighting indicator which have the capability of showing the similar color appearance under 5000 K white-light LED, while showing difference colors under the CIE daylight series. In this study, singular value decomposition is used to obtain the basis functions from the reflectance spectra of the 35 color samples, and the following three constraining conditions are designed to determine the metamer: (a) color difference (ΔE_{00}) under 5000 K white LED is less than 1, (b) color difference (ΔE_{00}) under D50 is greater than 2, and (c) the root-mean-square error of spectra between reference color and predicted color is larger than 5%. Consequently, the metameric color pairs meeting these conditions performed well in the simulation results, and future research will output the finished product in a multi-color (≥ 7 -color) inkjet printer to verify its performance.

REFERENCES

1. Berns, R. S. (2000). *Billmeyer and Saltzman's Principles of Color Technology, 3rd ed.* New York, NY: John Wiley & Sons, Inc.
2. PANTONE. Retrieved from <https://www.pantone.com/products/graphics/lighting-indicator-stickers-d50>.
3. Lv, X., & Luo, M.R. (2019). *LED Simulators for the Reproduction of the New CIE Standard LED Sources*. Proceedings of 29th CIE Session 2019, 93-100. doi:10.25039/x46.2019.OP16.
4. Westland, S., & Ripamonti, C. (2004). *Computational Colour Science using MATLAB, 1st ed.* West Sussex, England: John Wiley & Sons Ltd.
5. TOCOL. Retrieved from <https://www.tocol.net/test/material>

Color appearance of objects in the environment lit with LED lamps

Phubet Chitapanya^{1*}, Chanprapha Phuangsuwan ² and Mitsuo Ikeda²

¹Graduate School, Faculty of Mass Communication Technology, Rajamangala University of Technology Thanyaburi, Thailand.

²Color Research Center, Rajamangala University of Technology Thanyaburi, Thailand.

*Corresponding author: Phubet Chitapanya, phubet_c@mail.rmutt.ac.th

Keywords: Color appearance, color constancy, LED, color chip, elementary color naming, RVSI

ABSTRACT

LED (Light-Emitting Diode) is a narrow band of wavelengths lamp becoming to be all around us which is able to produce various colored illumination with less electric consumption. The one problem of LED is a poor property of CRI (Color rendering index) and it might affect the ability to see color of objects safely. To know color appearance of objects, 26 color chips which size is 6×6 inch covered 8 hues and Test color sample (R1-R15) were printed. The chips were placed one by one as a test stimulus on a table under experimental room which only illuminated by LED controlling lamp connected to a computer outside the room. The size of the room was 210 cm long, 110 cm wide, and 200 cm, and was decorated with various to simulate a normal room. There were thirteen illuminations which covered also 6 hues on $u'v'$ color space and two saturation steps. The room illumination was fixed to be about 100 lx under all illuminations. 30 subjects including experience subjects and naïve subject were participated in this experiment by judging color of the chips by the elementary color naming method. There was 2-minute adaptation before doing experiment. The result showed the relative area was decreased under green illumination more than the other when increasing saturation.

INTRODUCTION

The ability to stably see color under various colored illumination called color constancy had been investigating all the time. Many researchers used an experiment methodology working with 2-dimensional test patch on a monitor. Chanprapa and Ikeda's experiment¹⁾ showed that when a subject could perceive a test patch as a three-dimensional, he or she could get higher color constancy perception. It's not only the dimensional space affecting to color perception. The difference of spectral power distribution of LEDs can influence the effect from the other light type. There has been some research where color appearance of objects was investigated under LED light but not under vivid colored light. Ruiqing's experiment^{2,3)} showed the result of color constancy index was low on some color categories under blue and yellow illuminations. In this study, we try to determine the limit of color constancy under various illuminations by elementary naming method working on a real object represented by color stimulus in a realistic room in which subject has to judge each of color chip with their absolute judgement. By doing experiment by the method, area of color perception under each colored illumination could be compare to under white light as a ratio.

EXPERIMENT

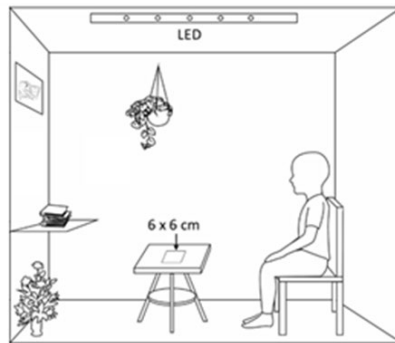


Figure 1. Experimental booth.

Apparatus

This experiment was done inside a booth which illuminated by LED light of RGB type (Philips color kinetics). The room is decorated by books, flowers, fruit model, and picture, giving a daily life situation to a subject as shown in figure 1. The size of the booth is 135 cm long, 82cm wide, and 172cm high. A stool of the height 52 cm was placed in front of a subject and a test stimulus object which size is 6 cm \times 6 cm was placed at the center of a gray paper on the stool.

Illuminations

In the figure 2. shows spectral power distributions of the red, green, and blue lights of the LEDs, as measured by Konica Minolta CL-500A Illuminance Spectrophotometer. By mixing the three of each colored light, thirteen illuminations were prepared as shown in figure 3. The square symbol indicated neutral illumination following D65 chromaticity ordinates defined by CIE. Twelve hues, (R)red, (Y)yellow, (G)green, (C)cyan, (B)blue, and (M)magenta were investigated in this experiment. Red, green, and blue hue were the maximum intensity of red LED, green LED, and blue LED respectively. The other hues were designed by half distance of $u'v'$ chromaticity diagram between each pair of colored LEDs. The twelves hues were connected by the red line indicating the gamut of our LEDs such as R2, Y2, ...G2. In each hue, different saturation was also prepared by the half distance of $u'v'$ diagram between neutral ordinates and their points on the red line. The less saturations were connected by the blue line such as R1, Y1, ...G1. All of illuminations was fixed at 100lx on the table which test stimulus placed over there.

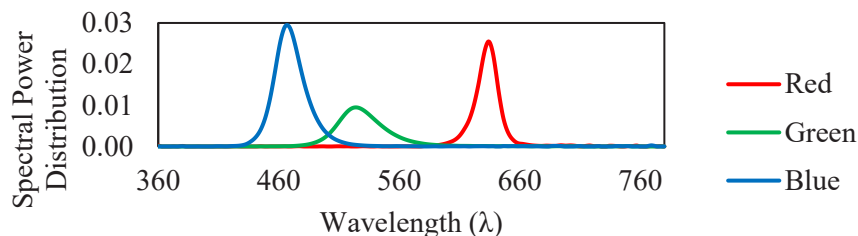


Figure 2. Spectral power distribution of red, green, and blue LED light.

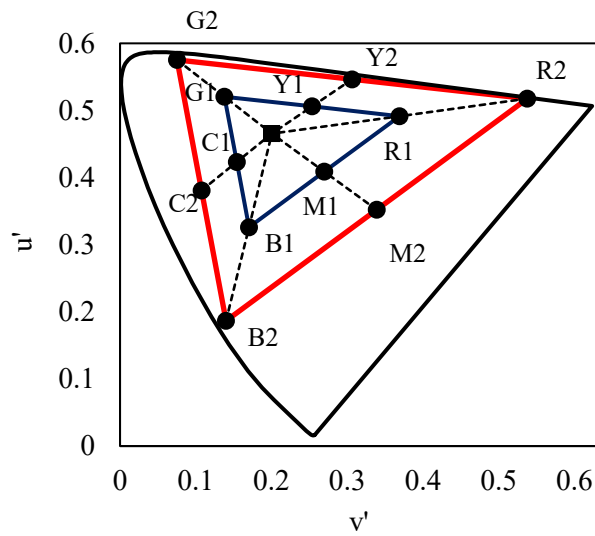


Figure 3. Illumination conditions.

Stimuli

Following CIE test color sample, fifteen color chips as TCS01-TCS15 were reproduced ($\Delta E \approx 4$) by Konica Minolta Accurio press C83HC digital printer which is designed for nearly stimulated color as a monitor as shown by open square in figure 4. The solid circle indicates eight color chips which is covered 8 hues around achromatic point representing as saturation color chips. The difference angle of each hue was 45° . Three achromatic color chip, black, gray, and white were shown in figure 4 as solid square symbols. Totally, twenty-six color stimuli were used in this experiment.

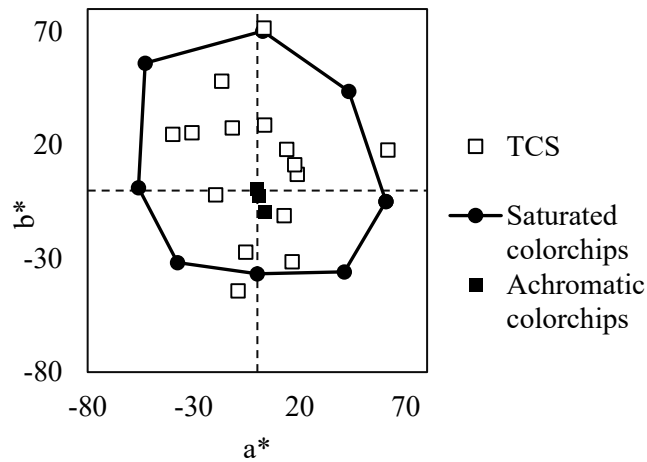


Figure 4. Color stimuli.

PROCEDURE

Thirty subjects were participated in this experiment. All of them have normal color vision tested by Farnsworth–Munsell 100 Hue Test. Twenty-five subjects were naïve. They were university students taking color vision class and they all got a score credit for doing this experiment. Five subjects were experience subjects who had a chance to do similar procedure.

In the beginning of each colored illumination, a subject had to adapt to the light for 2 minutes then each color stimuli would be placed on a table one by one. A subject had to judge color chip by using elementary color naming method. A subject had to judge an element as 100% composed of chromaticness, whiteness, and blackness. If a subject named at least percentages of chromaticness, he or she had to judge which color that he or she saw as another 100% hue element composed of red, green, blue, and yellow in which could mix to produce this color chip. As elementary color naming relating to opponent color theory, a subject couldn't judge red and green, or blue and yellow mixing together.

RESULT

The result can be transferred color naming result in each color judgement to polar diagram as shown in figure 5. In each circle plot represents the result from subject PC's perception. The colored on each plot shows the physical chromaticity of each stimulus under D65 illumination measured by Konica Minolta FD-7. The result is connected by the black line indicating the area of color perception.

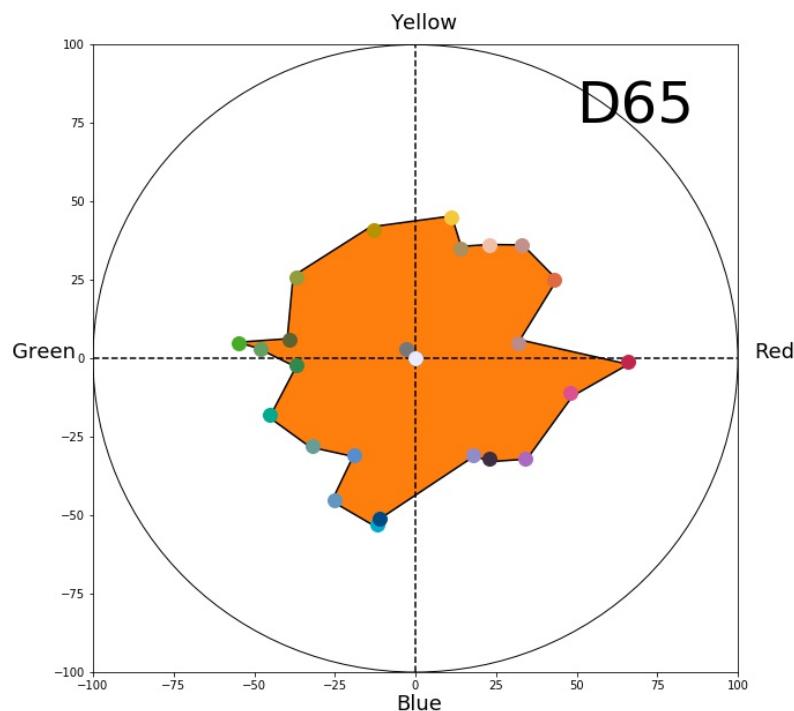


Figure 5. Example of average result of all subject under D65 illumination. The orange area shows the area perception. Each color of each plot was the chromaticity of each color under D65 light.

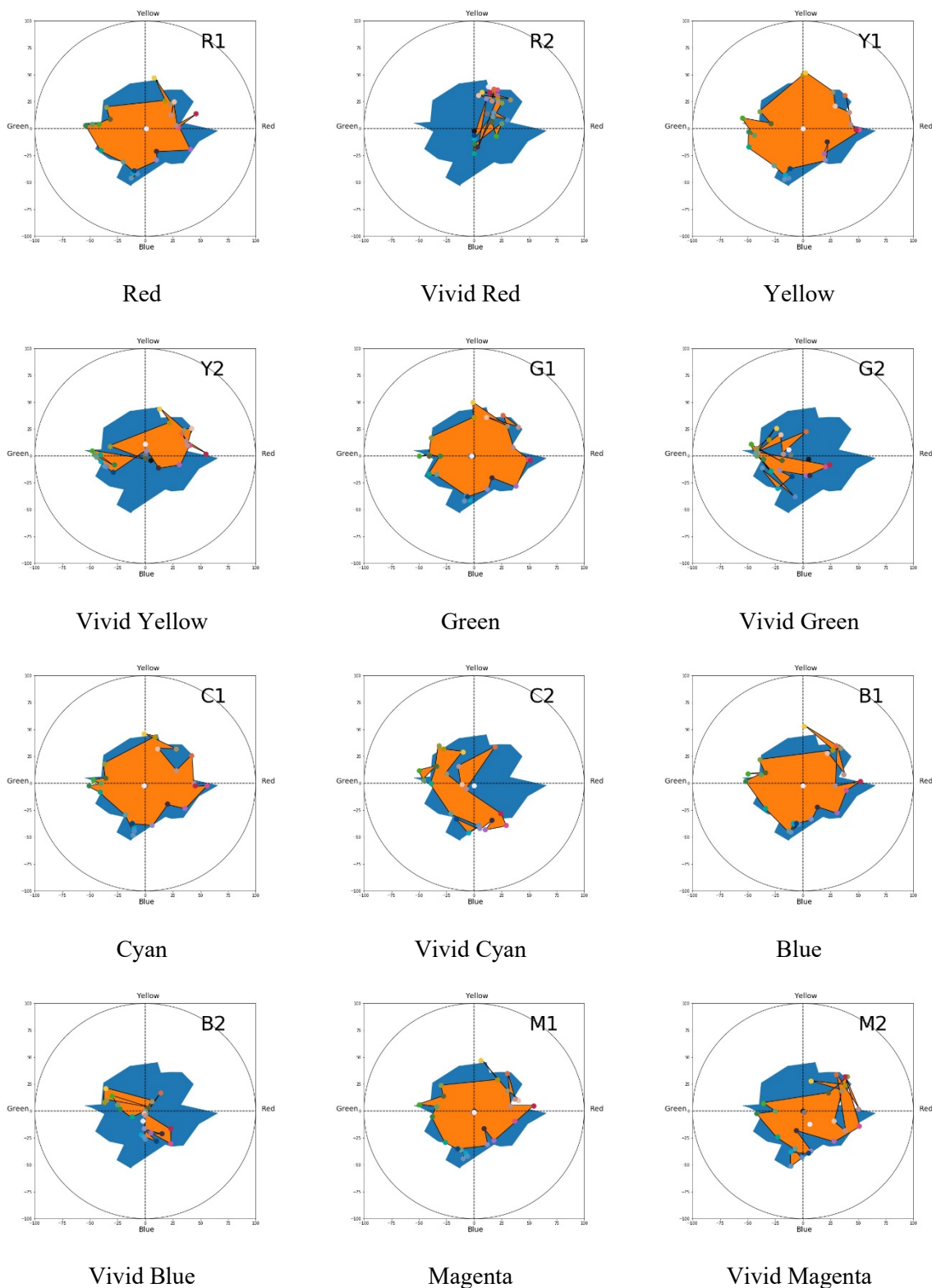


Figure 6. Average result of all subjects. The orange area indicates the result under each test illumination, while the blue area is the area under D65.

Figure 6 shows the average result of all subject in each colored illumination from R1, R2, ..., M2. The orange surfaces are the area of color perception based on how it shifts from color perception under D65. Blue surfaces are the color perception area under white illumination.

An area inside the orange shape can be calculated by Eq. (1). Then, take area ratio under test illumination by area under D65 to investigate how much area quantitative is changed compared to the normal light. The result of area comparison is showed in figure 7. Perfect color constancy is perfect when area ratio equals to 1. To compare result under various illumination, a slope (m) of any colored direction was measured by fixed curve shown that under green illumination, area ratio was decreased as $m = -5.2$, then yellow, cyan, blue, red, and magenta as $m = -5.0, -4.7, -2.9, -2.9,$ and 2.8 respectively.

$$Area = \left| \frac{(x_1y_2 - y_1x_2) + (x_2y_3 - y_2x_3) \dots + (x_ny_1 - y_nx_1)}{2} \right| \quad (1)$$

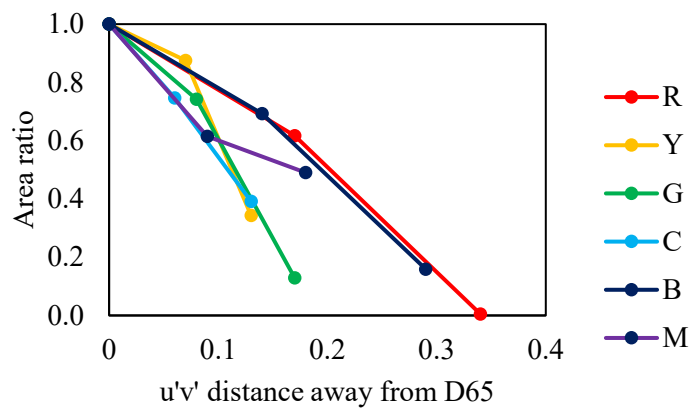


Figure 7. Area ratio comparison

ACKNOWLEDGEMENT

I'd like to thank Thai research and researchers for industries (RRI), and Konica Minolta's printing solution co., ltd. for supporting.

REFERENCES

1. Phuangsuwan, C., Ikeda, M., & Katemake, P. (2013). Color constancy demonstrated in a photographic picture by means of a D-up viewer. *Optical Review*, 20(1), 74–81. doi: 10.1007/s10043-013-0012-7
2. Ma, R., Liao, N., Yan, P., & Shinomori, K. (2018). Categorical color constancy under RGB-LED light sources. *Color Research & Application*, 43(5), 655–674. doi: 10.1002/col.22241
3. Ma, R., Liao, N., Yan, P., & Shinomori, K. (2019). Influences of lighting time course and background on categorical colour constancy with RGB-LED light sources. *Color Research & Application*, 44(5), 694–708. doi: 10.1002/col.22392

INFLUENCE OF CORRELATED COLOR TEMPERATURE AND Duv OF LIGHTING ON VISUAL IMPRESSIONS OF A SPACE

Taiichiro Ishida*, Yusuke Tateishi

Department of Architecture and Architectural Engineering, Kyoto University, JAPAN

*Corresponding author: Taiichiro Ishida, ishida@archi.kyoto-u.ac.jp

Keywords: color of lighting, correlated color temperature, Duv, LED, visual impression

ABSTRACT

LED light sources have been widely used in our living environment. One of the novel characteristics of LED lights is that color of the light can be controlled flexibly, opening new possibilities of lighting design using colored light. In this study we focused on the color of lights close to the blackbody locus. Colors of illumination close to the blackbody locus are often described by single parameter; correlated color temperatures (CCT). However, colors of the light having the same CCT should appear more or less different if their deviations from the blackbody locus are different. The value of Duv provides information on the distance and direction of a color deviation from the blackbody locus on the CIE 1960 uv color coordinate. It is important to consider both CCT and Duv to know how colors of the lighting appear and how it influences on our visual impressions of the lighting space. The aim of this study was to examine effects of CCT and Duv of illumination on our visual impressions of the lighting space.

The experiment was conducted in an experimental booth. The color of lighting in the booth could be controlled precisely by tuning the color of nine LED downlights attached on the ceiling. Subjects viewed the interior space illuminated by one of the lighting conditions and evaluated visual impression of the lighting for nine items; brightness, comfort, spaciousness, activity, warmth, naturalness, stimulating, preference and suitability.

The results of the study were plotted on the CIE 1960 uv color coordinate to see the effects of CCT and Duv. Visual impressions of comfort, naturalness, preference and suitability were found to have higher evaluation close to the blackbody locus, indicating the influence of Duv. Visual impressions of warmth and stimulating were significantly influenced by CCT.

The results of this study provided the information how the visual impression of the light changes along the wide range of the blackbody locus. This would provide a scientific basis to consider effects of the CCT and Duv of lighting.

Keywords: color of lighting, correlated color temperature, Duv, visual impression, LED

INTRODUCTION

Advances in LED technology have opened new possibilities of lighting design using colored light. We should understand how people response to various colors of lighting [1]. Ishida and Nakagawa examined visual impression of colors of illumination selected from a wide range of a chromaticity diagram [2]. This data could provide useful information for understanding how we response to color of lighting. In practical point of view, colors of illumination close to the blackbody locus have been more significant. Colors of lighting close to the blackbody locus are often described by single parameter; correlated color temperatures (CCT). Effects of illuminance and correlated color temperature of lighting on visual impression of lighting have been investigated in several studies [3][4]. However, colors of the light having the same CCT should appear different depending on their deviations from the blackbody locus. The value of Duv provides information on the distance and direction of a color deviation from the blackbody locus on the CIE 1960 uv color coordinate. It is important to consider both CCT and Duv to know how

colors of the lighting appear and how it influences on our visual impressions of the lighting space [5][6]. The purpose of this study was to examine effects of CCT and Duv of lighting on our visual impressions of a space.

METHODS

We conducted an experiment in which subjects evaluated visual impressions of a room illuminated by colored light close to the blackbody locus. The size of an experimental booth was 3.0 m x 3.0 m and 2.4 m high. The color of lighting in the booth were set precisely by adjusting the color of nine LED downlights attached on the ceiling. Figure 1 shows inside of the experimental booth. We set 52 test colors of the light covering the area along the blackbody locus. The test colors are plotted on the CIE uv color coordinates as shown in Figure 2. The correlated color temperatures used for the lighting conditions were $T_{cp} = 1000000, 20000, 10000, 6666, 5000, 4000, 3333, 2857, 2500,$ and 2222 K, having equal interval of the reciprocal correlated color temperatures. The values of D_{uv} were set from $+0.03$ to -0.04 with 0.01 interval. The illuminance at the center of a table placed on the floor was set 100 lx for all conditions.

Subjects viewed the interior space illuminated with one of the lighting conditions and evaluated visual impression of the lighting for nine items; brightness, comfort, spaciousness, activity, warmth, naturalness, awakening, preference and suitability. Along with evaluation of the visual impressions, subjects evaluated appearance of color of lighting at the start and the end of presenting a test color lighting. In evaluating color appearance, the subjects answered color appearance of lighting by selecting up to two colors out of the 6 color terms; red, orange, yellow, green, blue, purple. Also, they gave a score for saturation of the color of lighting with score 10 for saturation of color of the reference lighting shown at the beginning of each experiment session. When color of lighting appeared as white, they could answer "white".

The experiment procedure was as follows:

- (1) showing the reference lighting (the most saturated color condition) as an anchor for the color saturation judgement.
- (2) showing the standard lighting ($T_c=5000K, D_{uv}=0$) for 60 seconds.
- (3) showing one of the test color lighting.
- (4) 1st evaluation of color appearance of the lighting
- (5) after 60 seconds, evaluation of visual impressions of a booth illuminated by the test color
- (6) 2nd evaluation of color appearance of the lighting
- (7) back to step (2)

Seven subjects, 6 males and 1 female, students at the Department of Architecture, Kyoto University participated in the experiment.



Figure 1: a photo of the experimental booth

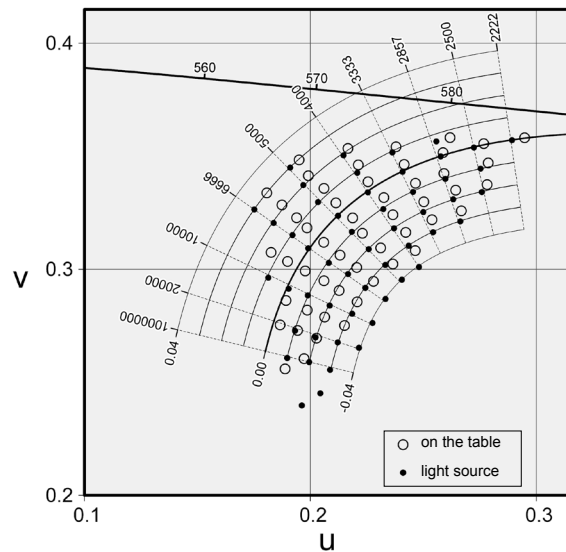


Figure 2: Chromaticity coordinates of the test colors of lighting

RESULTS

The results of the evaluation of color appearance are plotted in Figure 3(a)(b). Color of each circle indicate the color term given by the subjects and the size of the circle indicate evaluated saturation of the color of the lights. As shown in the graphs, the evaluated saturation of the color of the lighting decreased after 60 seconds, indicating effects of color adaptation.

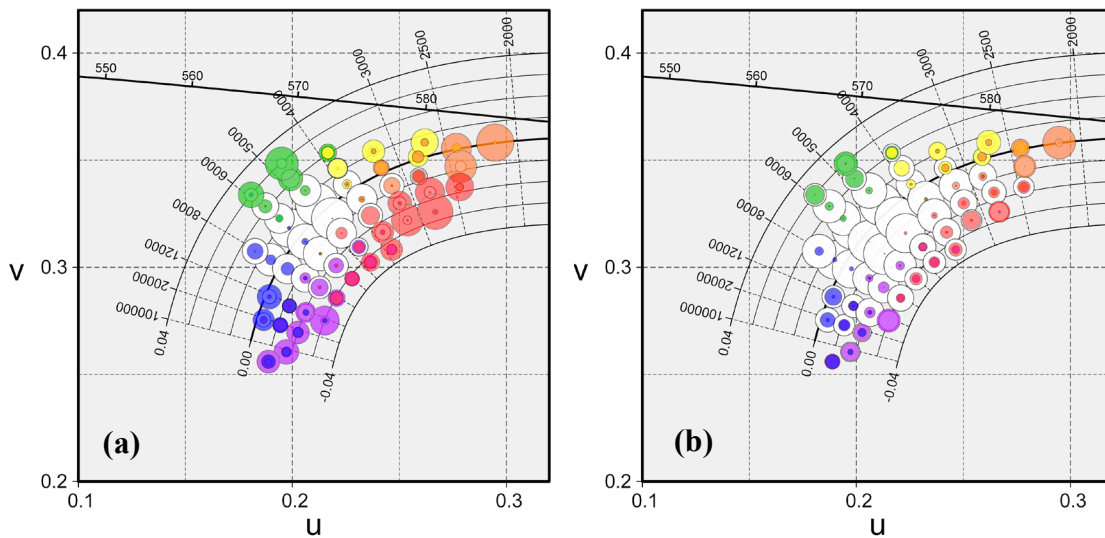


Figure 3: The results of evaluation of color appearance of lighting
(a) immediately after presenting test color of lighting
(b) 60 sec after presenting test color of lighting

Visual impression of a lighting space

The results of the evaluation of visual impressions of color of the test lighting were plotted on the CIE 1960 uv color coordinate in Figure 4. Data circles were plotted on the chromaticities measured on the table. The size of each circle indicates the absolute value of the visual impression score average over the subjects.

Visual impressions of comfort, naturalness, preference and suitability were found to have higher evaluation close to the blackbody locus, indicating influence of Duv. The colors of the lights just below the blackbody locus seems to give higher comfortable impression [5].

Visual impressions of warmth and stimulating were significantly influenced by CCT. The higher color temperatures give us awakening and cool impressions.

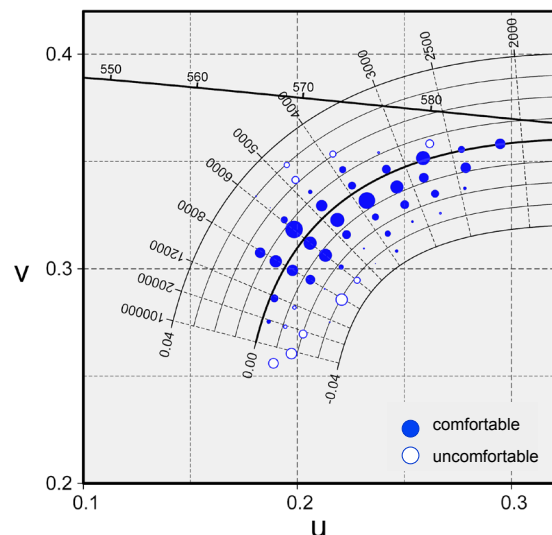


Figure 4: The result of evaluation of visual impression of a lighting space. comfortableness.

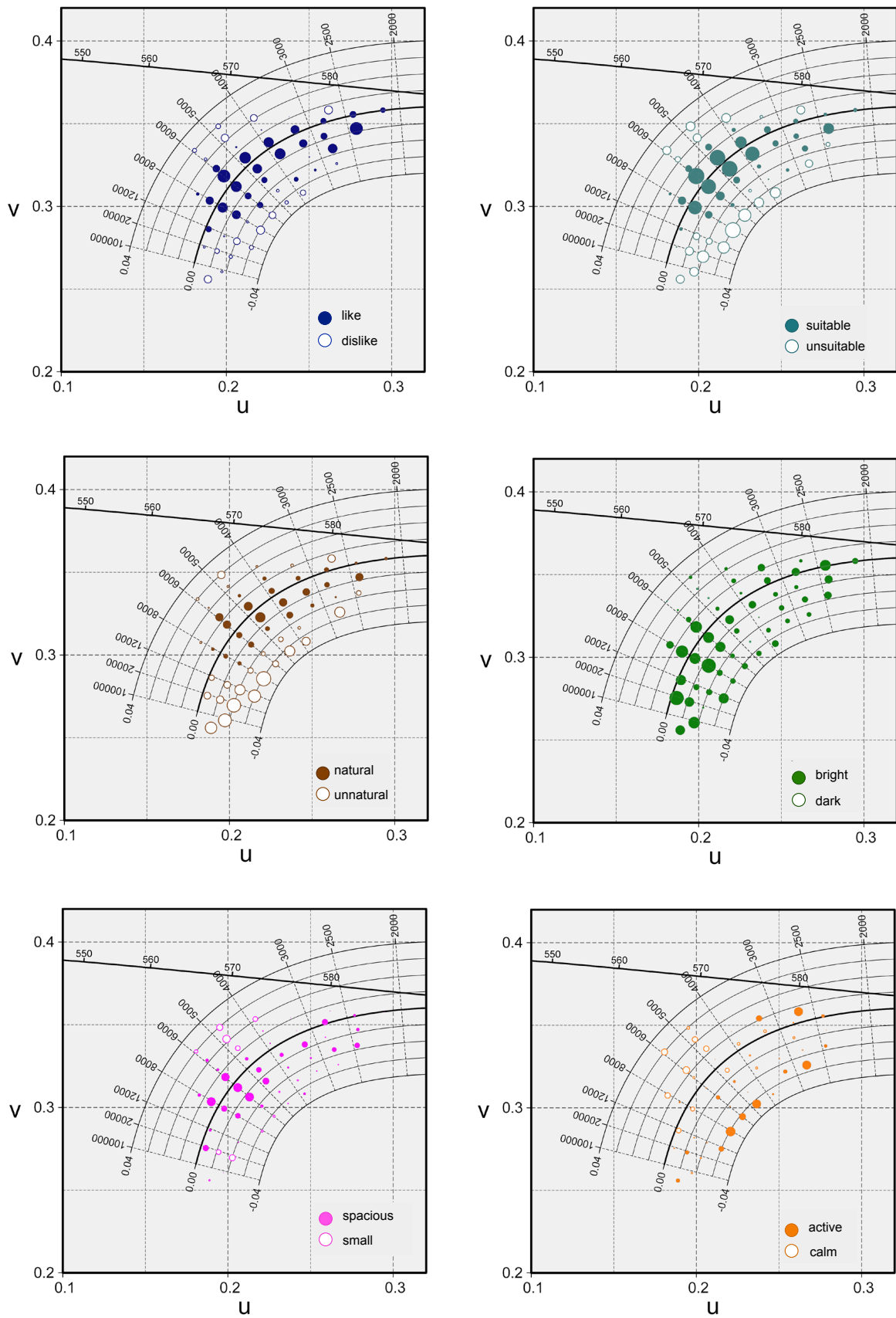


Figure 4: (continued) The results of evaluation of visual impressions of a lighting space; preference, suitability, naturalness, brightness, spaciousness, activeness.

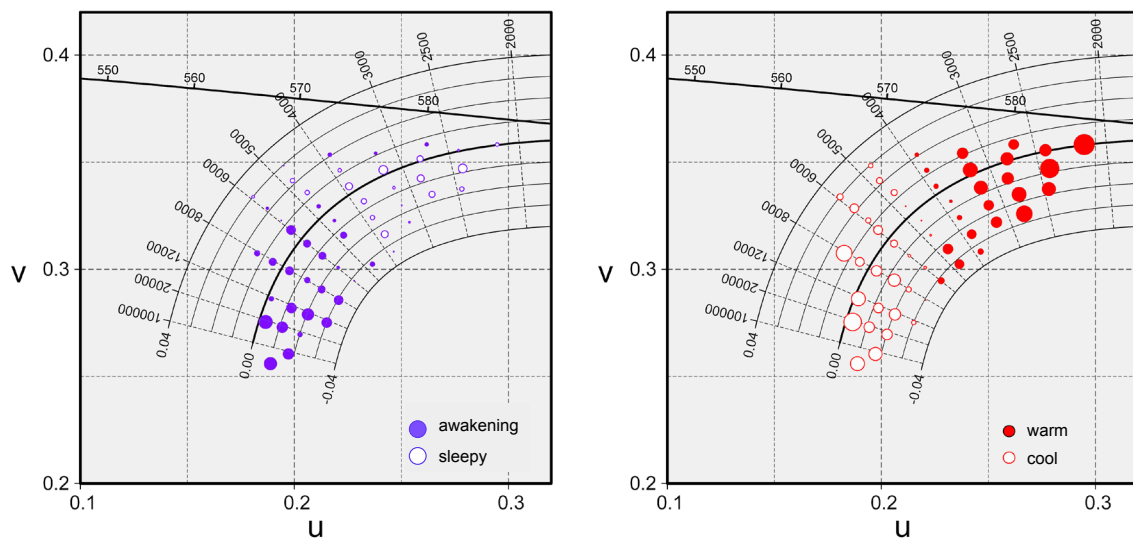


Figure 4: (continued) The result of evaluation of visual impression of a lighting space; awakening, warmth.

The results of this study would provide useful information to understand how the visual impression of the lighting changes within an area adjacent to the blackbody locus and to consider effects of the CCT and Duv of lighting. Further analysis of the results would be reported at the conference.

REFERENCES

1. ISHIDA, T. 2016, Color and Light in our living environment: Exploring psychological effects of color of lighting, *Proceedings of the 3rd conference of Asia Color Association*, pp.13-16.
2. ISHIDA, T. and NAKAGAWA, M. 2013. Evaluation of visual impressions of a space illuminated by a coloured light selected from a wide range of the chromaticity diagram, *Proceedings of the 12th Congress of International Colour Association*, 1689-1692.
3. KRUITHOF, A. 1941. Tubular luminescence lamps for general illumination, *Philips Technical Review*, vol. 6, pp. 65-96.
4. ISHIDA, T., IKEYAMA, K. and TODA, N. 2007. Psychological evaluation of lighting with a wide range of color temperatures and illuminances, *Proceedings of 26th Session of the CIE*, vol.1, pp.D1-178-181.
5. OHNO, Y and FEIN, M., 2014, "VISION EXPERIMENT ON ACCEPTABLE AND PREFERRED WHITE LIGHT CHROMATICITY FOR LIGHTING," *Proceedings of CIE 2014 Lighting Quality and Energy Efficiency*.
6. Watanabe, N. *et al.*, 2018, "Influence of chromaticity of illumination on spatial impression" *Proceedings of Annual Conference of the Illuminating Engineering Institute of Japan*, pp. 6-P-06. (in Japanese)

SPANS OF FUNDAMENTAL COLORS — COMPARISON AMONG NORMAL COLOR VISION OF YOUNG AND OLDER PEOPLE, DEFECTIVE COLOR VISION, AND LOW VISION

Nana Itoh* and Ken Sagawa

*National Institute of Advanced Industrial Science and Technology, AIST, Japan.
1-1-1 Higashi, Tsukuba, Ibaraki 305-8566, Japan*

*Corresponding author: Nana Itoh, nana-itoh@aist.go.jp

Keywords: Fundamental color, normal color vision, defective color vision, low vision, accessible design

ABSTRACT

INTRODUCTION: This study provides basic database and method to be used for accessible design with regard to color identification and conspicuous color combinations. Special care has been taken for the diversity of color vision including aging effect and visual disabilities such as defective color vision and low vision. The database were for grouping of similar colors to a total of 13 fundamental colors (red, yellow-red, yellow, green-yellow, green, blue-green, blue, purple-blue, purple red-purple, white, gray and black), all expressed as an area in Munsell Color Space which was measured by subjective evaluation of similarity in color appearance between a reference (of the 13 fundamental colors) and test colors distributed in the whole color space.

DATA: The span was defined as an area where colors are similar with some extent to each fundamental color. The similarity is high for colors close to a reference color but become lower as colors depart from the reference. By setting an appropriate criterion, a contour was drawn to form a group of colors that were similar to the fundamental color. These similarity data were collected from a total of 45 young and 45 older people, 59 color defective people (29 protanopes and 30 deuteranopes) and 69 low vision people, and the spans of fundamental colors were defined for the four groups of different types of color vision.

COMPARISON: Comparison among the measured spans for those 4 different groups revealed that aging effect exists for the size of span (larger for young people and smaller for older people) but not for the position in the color space. This aging effect might be caused by desaturating effect on colors for older people due to increased light scattering in the eye with age. Similar results were obtained for low vision with much worse colour identification but no serious hue shift. Considerable differences in size and position were observed for defective color vision for both protanope and deuteranope. The results apparently showed the different color appearance was associated for defective color vision. The spans for defective color vision were extended for the direction of red-green in color space meaning that color confusion of red and green occurs for defective colour vision.

APPLICATION: Application of those data was aimed to create conspicuous color combination for those four types of color vision. The goal is to provide color combination that are conspicuous to all those 4 group, but it was turned out difficult to find a common area of the span for those four different groups. A compromised method for color combinations was proposed, therefore, depending on the cases where care for defective color vision is critical such as for safety or emergency signs or color is the only information to discriminate, and on the other cases where care

is preferable but not mandate as non-color information can be associated. For those two cases conspicuous color combinations were considered and proposed on the bases of present data.

INTRODUCTION

AIST (National Institute of Advance Industrial Science and Technology, Japan) has been promoting accessible design to cope with the diversity of society by means of ergonomic design for products, services and environments. One of the critical problems in designing visual signs is to create discriminable or conspicuous colour combinations for all people including different types of color vision, such as defective color vision or low vision. AIST started to study this challenging project with developing database for spans of fundamental colours which are grouping of similar colors in a whole color space into a limited number of major colors, and developing a method to create color combinations picking up colors from different groups which result in conspicuous color combinations. The database were developed first for young and older people with normal color vision to take into account aging effect, and then extended to low vision and to defective color vision recently [1]-[4].

Being based on those studies and data it has been clear that a large variety exists in the spans of fundamental colors among different types of color vision mentioned above, and color combinations which are conspicuous to all those color vision types are necessary to develop for application. In this paper, overview of different types of color spans for different types of color vision and a method for color combinations conspicuous to all those different types are to be presented.

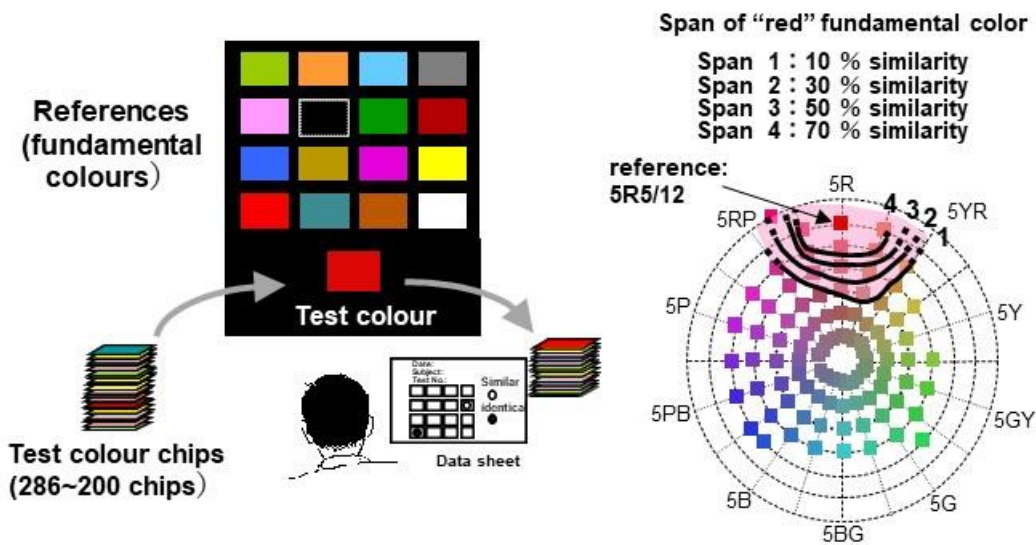
METHOD

The method to measure a span of fundamental colour is the same as we have employed first in the measurements for younger people and older people [1], but the number of reference and test colours were slightly differed for different groups in the later experiments.

As shown in Figure 1 (a), reference colors include 13 fundamental colors being based on Munsell Color System (5R5/12, 5YR7/12, 5Y8/12, 5GY5/8, 5G5/8, 5BG5/8, 5B5/8, 5PB5/10, 5P5/10, 5RP5/10, N1.0, N5.0, N9.5) plus a few more additional colors (totally 16 in case of Fig1 (a)), and test colors more than 200 test colors with variable hue, value, and chroma.

The subject was given one of the test colors and asked to select any similar colour(s) from the set of reference colours that were displayed randomly in front of the subject (see Figure 1(a)). No limitation of number of selected colors including nothing was clearly informed to the subjects. This trial was repeated until all the test colors were completed. To make sure the selection of “similar” judgement, the subject was also asked to select the colours that look “identical” to the reference. These two different criteria helped the subject to distinguish the judgement between “similar” and “identical”. This measurement was conducted for a number of subjects as shown in Table 1. Defective color vision and low vision were diagnosed by medical checks.

Data collected from a number of subjects for each group were summarized to obtain the rate of selection for “similar” colors over the whole subjects participated for a given pair of reference vs test colour, and that data were sorted out with regard to each reference (=fundamental) color. These probability-similar data were used to specify the span of similarity to a fundamental colour by four different levels from Span 1(10% similarity) to Span 4 (70% similarity). Figure 1 (b) illustrates this data analysis with the red fundamental color taken as an example at value 5 plane of Munsell Color System.



a) measurement procedure

b) an example of color span data (red)

Figure 1. Measurements of the spans of fundamental colors; a) procedure for a trial, and b) an example of the span data for red color from Span 1 to Span 4

Table 1: Subjects for the measurements of spans of fundamental colors

Subject groups	Number of total subjects participated	Age (years)	Remarks
young people	45	19–26	normal trichromat
older people	45	60–76	normal trichromat
people with defective colour vision	59	14-66	Protanope (29) Deuteranope (30)
people with low vision	69	19–79	Retinitis pigmentosa (13) Glaucoma (8) Cataract (8) Optic atrophy (6) Aphakia (3) Others (31)

DATA: SPANS OF FUNADAMENTAL COLORS

Figure 2 shows the Span 3 data as an example, as most useful data, for some of the fundamental colors, e.g. red, yellow, green, blue and purple, expressed in the Munsell Color System at Value 5 plane except for yellow for which Value 7 is used as a major lightness plane for effective expression of the data. In each diagram the 50% similarity area (Span 3) to each reference color is

shown for all the five different types of subjects, young and older normal color vision, P-type and D-type color defects, and low vision, using different lines and different colors. For red color, for example, (the upper-leftmost diagram) a smaller span is seen for low vision and for older people and a larger one for young people with a center at about 5R5/12, which is the location of the red reference color. However, this centering characteristics is not seen for P- and D-type color defects, and the spans protruding to the green area is clearly seen for both types of color defects though a slight difference in the directions is seen between P-type and D-type. This implicates the basic color perception mechanism is clearly different for color defects from young people, older people and low vision. This also implies that people with low vision have basically the same color mechanism (trichromacy) as normal color vision. Similar discussion can apply to other fundamental colors shown in Figure 2 where P- and D-type of color defects show largely different shapes of the span from young, older and low vision people. Data for green color (the upper-rightmost diagram) is a good example to see the difference between color defects and normal color vision including low vision.

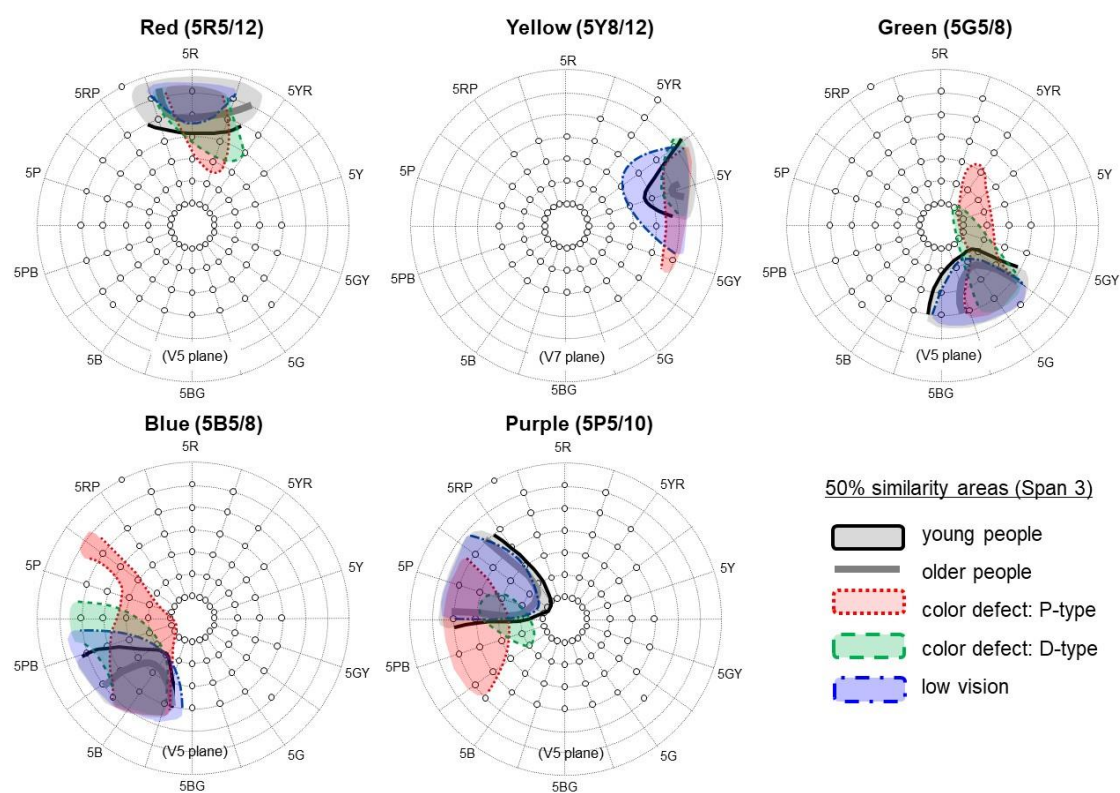


Figure 2. Span 3 data (the 50% similarity area), for some of the fundamental colors, red, yellow, green, blue and purple, expressed in Munsell Color System. Data are for Value 5 plane except for yellow for which Value 7 is used.

Data were obtained for other spans of similarity, for Span 1 (similarity 10%), Span 2 (similarity 30%), and Span 4 (similarity 70%) though not all shown here. Figure 3 shows the data for Span 1 for the same reference colors as Figure 2. With decreasing similarity, the span generally increases its area keeping the basic characteristics as mentioned above. It should be noted, however, the span for low vision becomes remarkably larger at Span 1, as shown in Figure 3, extending its area in

particular to green-to-blue direction which shows the decreased differentiation between green and blue for low vision.

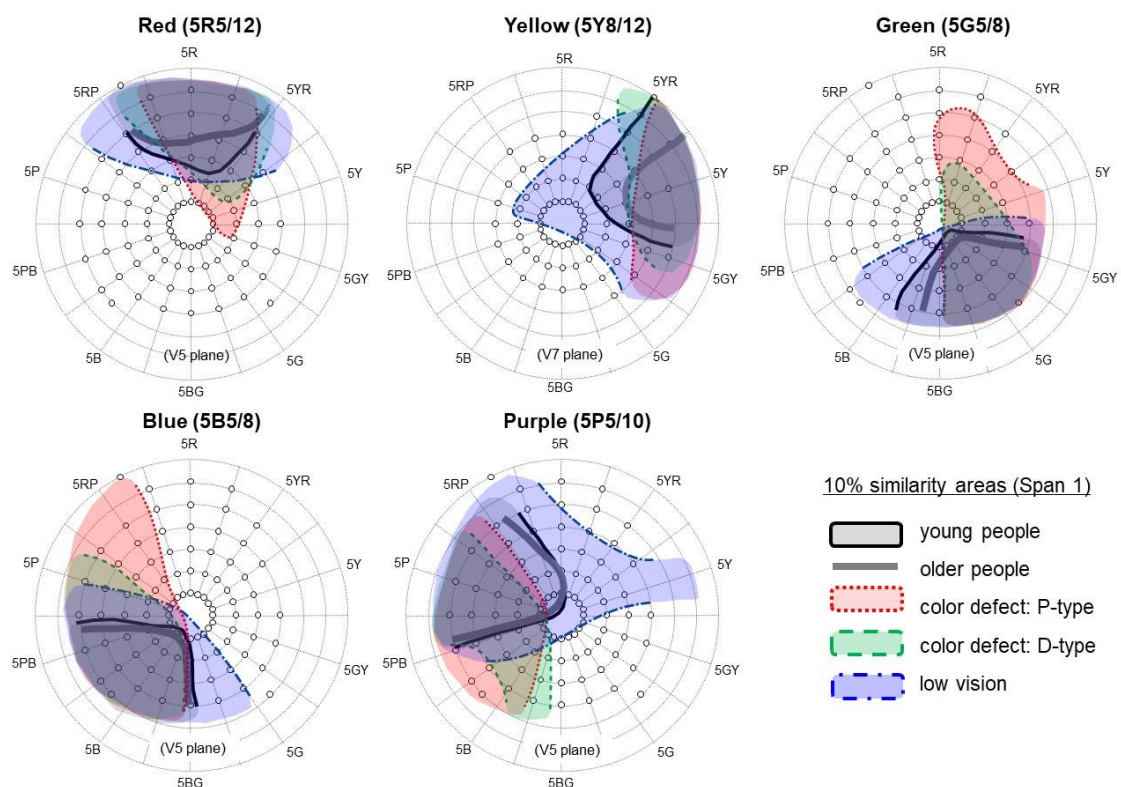


Figure 3. Same data as Figure 2 but for Span 1 data (the 10% similarity area).

DISCUSSION: A METHOD FOR COLOR COMBINATION FOR ALL TYPES OF COLOR VISION

One of the purposes of measuring spans of fundamental colors is to create a simple and consistent method for conspicuous color combination. As already shown in our previous reports the separation or overlapping of the spans of two different fundamental colors should be a reasonable criterion for evaluating conspicuity of a color combination of the two colors. Any two fundamental colors whose spans are separated differ much each other and, on the contrary, any two colors whose spans are overlapped may confuse in some case. This basic rationale can also apply to a combined group of the 5 different groups regarding them as a single mixed-up group.

To define the span of the mixed group, we drew up a new span including all the 5 spans of young /older people, P/D-types of color defect, and low vision for each of 4 different levels of spans respectively. Figure 4 shows the new span of Span 3 (50% similarity) which was drawn from the data in Figure 2 as an outer contour for all the 5 spans. It is noted again that the new spans of Span 3 are shown in Value 5 and Value 7 plane of Munsell Color System. In the new spans, red fundamental color is separated from yellow, blue, and purple, but slightly overlapped with green. This means red and green might be confused, even at the 50% similarity, for some people among the 5 different color vision groups. Yellow can be combined any other fundamental colors as long as these 5 colors are concerned. Green can be combined with yellow and purple but cannot be combined with red and blue for clear separation. Blue can be combined with red and yellow but the

COMMUNICATING COLOUR WITH AN ADVANCED COLOUR MANAGEMENT FRAMEWORK

Phil Green^{1*}

Faculty of Information Technology and Electrical Engineering, Department of Computer Science, NTNU, Norway.

*Corresponding author: Phil Green philip.green@ntnu.no

Keywords: colour management, profile connection space, ICC profile, spectral data

ABSTRACT

For the past 25 years, the most widely-used means of inter-operable communication of colour between different devices, media, platforms and applications has been the ICC profile and colour management architecture. These are based on exchange of colour information through a well-defined profile connection space (PCS), and a set of transform elements which can be used to convert between this PCS and any device or colorimetric colour encoding.

Having a well-defined PCS and small set of transform elements makes colour communication unambiguous, and relatively straightforward to implement through the wide availability of applications and APIs to generate profiles and apply them to image data. This has helped in industrial applications (such as colour management for cameras, displays and printers) and also in research where the colour management framework can be used to efficiently perform many of the routine tasks in implementing a colour reproduction workflow.

While there is scope to use colorimetry based on different illuminants with the fixed ICC PCS by applying a well-defined and invertible chromatic adaptation transform, today the restrictions of a single fixed PCS and small set of transform elements limit the ability to perform many of the tasks that are now expected. In particular, there is increasingly a demand to communicate spectral data rather than just colorimetry; and there is often a need to communicate colour appearance beyond the 0:45° geometry, diffuse reflection and standard observer which are all assumed in ICC v4. Moreover, experience has shown that the limited set of transform elements provided in ICC v4 cannot handle many of the processing tasks required to fully communicate appearance.

Recently ICC released a new specification defining a new colour management architecture and profile format, known as iccMAX. This complements and extends the current v4 architecture, while also retaining backwards compatibility with v4. It provides support for many of the features that colour scientists and engineers have asked for, including the ability to handle spectral data and alternative connection spaces, where the illuminants, observers or illumination geometries differ from the standard v4 PCS.

There have already been many interesting uses of the new specification and an associated reference implementation, a selection of which is summarised in this paper.

Habib used iccMAX to encode a spectral reconstruction transform, which computes spectral reflectance from colorimetry using classical PCA. All stages in the reconstruction workflow were encoded in a single iccMAX profile, and by connecting this profile via the PCS to a device profile it is possible to obtain spectral reflectance estimates from device data.

Conni implemented different chromatic adaptation models as functional transforms in iccMAX, enabling evaluation of state-of-the-art CATs; and Habib also encoded transforms to estimate spectral reflectances from chromatically adapted data, thus enabling spectral output when a

chromatic adaptation step is required. Derhak demonstrated transforms for HDR displays; and Green demonstrated transforms for colour vision deficient observers, enabling flexible simulation or Daltonization in cone space and on spectral data.

These and other iccMAX examples are described in the paper, together with the potential for future applications.

INTRODUCTION

The ICC colour management architecture is a standard method of communicating colour between different media. First agreed by a consortium of vendors in 1994 as means achieving interoperability between applications, devices and operating systems with a common interest in reproducing colour across different media, it was approved as an ISO specification in 2005 [1]. The first ICC specification addressed the need to take a colour signal from one device and reproduce it on another. Since every device records or outputs colour differently, the same data produces different colours on different devices. The solution was to define a transform between the data encoding of each device and an intermediate CIE-based Profile Connection Space. To ensure inter-operability, almost all aspects of the transformation were defined in the specification. PCS colorimetry was based on the CIE 1932 standard observer, the CIE D50 illuminant, and the 0:45 measurement and viewing geometry. A file format - the ICC profile - was defined as standard container for the device-to-PCS transform, and a small number of basic transform elements (matrix, curve and look-up table) were specified. These transforms are applied by a colour management module (CMM), a software routine that is often integrated into the host PC's operating systems.

Several different rendering intents (styles of colour management transform) are supported by the specification. The default mode of connecting media is to scale both source and destination white points to the PCS white, ensuring that the media white of the source is always mapped to the media white of the destination. This default behaviour is known as media-relative, but there is also provision to undo the media-relative scaling in order to achieve a match relative to a perfect white diffuser. It was also recognised that users may have different colour reproduction goals, so the Media-relative and ICC-absolute colorimetric rendering intents support accurate colour matching, while the Perceptual and Saturation intents support the goal of pleasing reproduction without the criterion of accuracy.

As well as connecting devices and media, the different ICC profile classes support connection of colour spaces and colour name systems to the PCS, direct connection of devices, and an 'abstract' PCS-to-PCS connection that allows adjustment of the PCS colorimetry (for example, to achieve a certain 'look' in a series of images).

In the most common colour reproduction workflow, an image is first acquired by a camera and then output on a display and possibly a printer. The source image will usually be rendered to a standard output-referred RGB colour space representing a display system, and a profile is assigned to the image to define the transform from this standard RGB colour space to the PCS. On the host, the CMM converts from the source colour space to the profile for the connected display for viewing, or to a printer profile for printing. The matrix, curve and LUT transform elements are computationally efficient and the time taken to perform the conversion between colour encodings is negligible for most use cases.

Although standardised in graphic arts, D50 colorimetry is not universal. The ICC specification supports other illuminants by requiring that all data is chromatically adapted to D50, using a simplified linear version of the Bradford chromatic adaptation transform. It has been shown that this transform is transitive and invertible, carries no penalty in terms of accuracy or computational cost, and performs similarly to other CATs in predicting corresponding colours under different illuminants [2]. Other colour matching functions or measurement geometries could also be

supported by a similar process of transforming to the ICC PCS, but in this case the transform required to do so is not obvious.

This first-generation colour management architecture, ICC.1, has undergone a number of minor revisions and a major revision between version 2 and version 4 of the specification. This reduced ambiguities in earlier versions and added a Perceptual PCS with a defined dynamic range and gamut.

Today ICC colour management is ubiquitous in colour reproduction workflows. For consumers, it is largely invisible as applications automatically call on the CMM to interpret the colours of an image or document according to the embedded profile, and select and apply the profiles provided by the vendors of those output devices connected to the host system. For professional users, selection of the optimal transform is of great importance and this is achieved by selecting the most suitable profile and also selecting the rendering intent that matches the user's colour reproduction goals. For automated use, the profile creator defines an intended rendering intent in the profile header which can be applied by the CMM, or over-ridden according to application or user choices.

One important element of a colour managed workflow is the PDF file format [3], which has become a dominant means of exchanging page information, whether intended for display or print. PDF format subsets have been standardised for specific purposes, most of which are associated with ICC profile classes defined in ICC.1. The ICC profile is embedded in the PDF file to tell the receiver how to interpret the colours in the document, and an OutputIntent profile can also be included to specify the intended reproduction target. The most common readers of PDF files are able to correctly interpret all supported ICC.1 profiles and apply them on viewing or printing.

ICC.1 is also widely used in colour imaging research and development, where the availability of profile creators and colour management-aware applications enable components of a colour reproduction workflow to be greatly simplified and made more efficient.

THE NEED FOR A NEW ARCHITECTURE

Since the first ICC specification in 1994, digital colour management has been incorporated into the workflow of a number of industries outside the graphic arts. These include motion picture, broadcast, the web, medical imaging and digital photography, many of which have requirements that do not fit well with the fixed colorimetric PCS model of ICC.1.

Within printing, the scope of colour management has similarly widened and new requirements have emerged. As well as traditional print on paper, many other materials are now being printed, ranging from textiles to floor and wall coverings, ceramics, glass, metals and wood. In the field of packaging, more elaborate finishes are being created by the use of additional ink colours (known as spot colours) and special effects such as metallic and pearlescent inks and varnishes. Although many of these processes are not in themselves novel, colour managed workflows demand that final reproductions can be accurately simulated on a display or on a digital proof printer, which requires a high degree of colour management and the ability to model the measurement and viewing geometries of textured and non-diffuse materials.

These new and emerging processes have thrown up a variety of situations where ICC.1 colour management is unable to completely satisfy the need. A comprehensive outline is outside the scope of this paper, but the most important issues can be summarized as:

1. A need to connect colour encodings using a connection space different from the ICC.1 PCS based on D50 colorimetry
2. A need for more flexible and programmable transform elements.

INTRODUCING iccMAX

Rather than incrementally revising the ICC.1 specification, ICC chose to develop a comprehensive next-generation colour management architecture while maintaining backwards-compatibility with ICC.1 [4]. The resulting specification, known as iccMAX, has been published as ISO 20677 [5]. ICC.1 continues to meet most colour management needs, and so iccMAX is not intended as a replacement but as an extension for requirements that cannot be met with ICC.1.

iccMAX introduces flexibility in the way the PCS is defined. An iccMAX profile can have a PCS that is colorimetric, spectral or multiplex (i.e. multiple arbitrary channels). A colorimetric PCS can be based on any illuminant (encoded as a spectral power definition in the profile's spectralViewingConditions tag), and any observer (encoded as colour matching functions in the spectralViewingConditions tag).

In iccMAX, new transform elements are encoded in a flexible multiProcessElementType. This provides the connections between encodings, and completely defines the transformation from tag input to tag output. It supports a full range of data type precisions up to 64-bit floating point, and an arbitrary sequence of processing elements. The supported processing elements include:

- Sets of 1-dimensional functions that are made up of parametric and sampled curve segments
- A 1-D to N-D transform
- An N x M linear matrix transform
- An N x M multi-dimensional lookup table
- A programmable Calculator element
- Elements that provide for late binding of observer and/or illuminant to provide efficient custom colorimetric processing

Connections

Whereas in an ICC.1 profile the PCS is unambiguously defined as D50 colorimetry (with chromatic adaptation applied if the source or destination are not also D50), iccMAX supports many very different PCSs. If both source and destination profiles have the same PCS definition, they can be connected; otherwise the workflow has to apply the default path using the CustomToStandardPCS and StandardToCustomPCS tags.

The colorimetric observer and illuminant are defined in a spectralViewingConditions tag type. If desired, the connection can be modified at run-time by over-riding the transform within the profile with the connection conditions defined in another profile.

Calc

The Calculator element (Calc) provides a mechanism for encoding more complex device models. It avoids limitations of CLUT accuracy and storage requirements when many input channels are used. It defines a script based expression calculator, employing a PostScript-like stack-based language, to determine output channels from input channels. Finite memory storage is provided for temporary results, and nearly all operations are vector based (operating on multiple channels at the same time). Calculator element operators include: stack operations, input / output channel access, temporary memory access, math operators including arithmetic, exponential, log and trigonometric operators, inequalities (<, ≤, =, ≥, >), logical and conditional operators, high-level matrix operators (transpose and linear matrix solver), polar – to - Cartesian conversion, and error handling. The Calculator element incorporates support for conversions between XYZ and CIELAB. The Calculator element also provides the ability to embed and invoke other processing sub-elements within the context of the Calculator element's script.

RefIccMax

To aid adoption, ICC has provided a Reference Implementation [6], which is freely available from ICC. This is a comprehensive library of source code with a test suite of example profiles and test images. Compiled versions of the executables are available for Windows, Linux and MacOS. A feature of the Reference Implementation is a utility to convert between the binary format of the ICC profile and a human readable XML representation, greatly simplifying the process of profile creation.

ICS

Since the iccMAX specification is considerably more complex than ICC.1, it is not envisaged that developers will implement all its features. Instead, only those elements required for a given application need to be implemented. Understanding the particular subset requirements is aided by having an Interoperability Conformance Specification (ICS) for the application, which identifies the required and optional tags needed.

Previous work using iccMAX

There have already been many interesting uses of the new specification, and a selection of them is summarised below. All have made use of the RefIccMax reference implementation.

Derhak implemented different chromatic adaptation models in iccMAX [7], enabling evaluation of state-of-the-art CATs. Test reflectance spectra were transformed to XYZ for different reference illuminants (encoded as Profile Connection Conditions in iccMAX profiles), and chromatic adaptation transforms to and from D50 were applied in the CustomToStandardPCS and StandardToCustomPCS tags.

Green [8] demonstrated transforms for colour vision deficient observers, enabling flexible simulation or Daltonization in cone space and on spectral data. For simulation profiles, the different steps were encoded as a succession of matrices in a multiProcessingElement, enabling adjustment of the cone space to accommodate different conditions of colour vision deficiency. A form of Daltonization was also demonstrated in which the illuminant in the spectralViewingConditions tag was modified to enhance red-green separation when applied to spectral reflectance data.

Habib [9] used iccMAX to encode a spectral reconstruction transform, which computes spectral reflectance from colorimetry using classical PCA. All stages in the reconstruction workflow were encoded in a single iccMAX profile, and by connecting this profile via the PCS to a device profile it is possible to obtain spectral reflectance estimates from device data. The PCA transform was encoded as a Calc element, using matrix and arithmetic operators provided in the Calc language. Habib also used a similar approach to estimate spectral reflectances from chromatically adapted data [10] [11], thus enabling spectral output when an intermediate chromatic adaptation step is required to be performed on colorimetric data.

CONCLUSIONS

The iccMAX specification is a next-generation architecture that supports a wide range of new colour management functionality. It extends the ICC.2 specification with a flexible PCS, which can be spectral or multiplex, or based on colorimetry different from the ICC.1 D50 PCS. Backwards compatibility is achieved by continued support for all transform elements defined in ICC.1, and for non-standard PCS profiles by encoding a custom-to-standard PCS transform and its inverse in the profile.

iccMAX transform flexibility is achieved by support for floating-point data and a wider range of transform elements which, unlike in ICC.1, can be applied in any number and order. In addition the Calc element allows complex functional transforms to be encoded.

iccMAX has already been used in a number of colour imaging research projects, and a complete reference implementation is available. It is envisaged that the new architecture will be of interest to both researchers and commercial developers in colour imaging.

REFERENCES

1. ISO 15076-1:2010 *Image technology colour management — Architecture, profile format, and data structure*, ISO, Geneva
2. Green, P. and Habib, T. (2019) Chromatic adaptation in colour management, *Computational Color Imaging*, doi: 10.1007/978-3-030-13940-7
3. ISO 32000-1:2008 *Document management — Portable document format — Part 1: PDF 1.7* ISO, Geneva
4. Derhak, M., Green, P. and Lianza, T. (2015) Introducing iccMAX - New Frontiers in Color Management, *Proc. SPIE 9395, Color Imaging XX: Display, Processing, Hardcopy, and Applications*, 93950L, 2015
5. ISO 20677:2019, *Image technology colour management — Extensions to architecture, profile format, and data structure*, ISO, Geneva
6. ICC, *iccMAX Reference Implementation*, <http://www.color.org/iccmax/>
7. Derhak, M., Green, P. and Conni, M. (2018) Color appearance processing with iccMAX, *Electronic Imaging, Color Imaging XXIII: Displaying, Processing, Hardcopy, and Applications*, pp. 323-1-323-6 doi:10.2352/ISSN.2470-1173.2018.16.COLOR-323
8. Green, P and Nussbaum, P. (2016) Colour vision deficiency transforms using ICC profiles, *Electronic Imaging, Color Imaging XXI: Displaying, Processing, Hardcopy, and Applications*, pp. 1-5(5) doi.org/10.2352/ISSN.2470-1173.2016.20.COLOR-328
9. Habib, T and Green, P. (2019) Spectral Estimation of Chromatically Adapted Corresponding Colors *Computational Color Imaging*, doi: 10.1007/978-3-030-13940-7
10. Habib, T. (2018) *Spectral estimation using iccMAX*, coursework project for IMT4884 at NTNU
11. Habib, T. (2019) *Getting spectral data when you don't have spectral measurements*, ICC Color Experts' Day Bressanone, <http://www.color.org/events/bressanone/18.Habib-Bressanone.pdf>

THE ISSUE OF COLOR APPEARANCE IN TELEMEDICINE SYSTEM

Yuki Akizuki^{1*}, Futoshi Ohyama² and Satoshi Iwamoto²

¹ *Environment and Humanity Department, Faculty of Human Development, University of Toyama, Japan.*

² *Faculty of Nursing, School of Medicine, Tokai University, Japan.*

*Yuki Akizuki, akizuki@edu.u-toyama.ac.jp

Keywords: Telemedicine, Smartphone, Color Reproduction, Color Difference

ABSTRACT

In Japan, the medical practice with communication equipment as computer, facsimiles and mobile telephones (Telemedicine) is on the way as part of efforts to tackle super-aging society and doctor shortage. Usually a doctor examines/sees a patient face-to-face. As treatment in the chronic phase for some significant period, the doctor can use telemedicine methods as complementary practices. The color reproduction of telemedicine communication equipment become a challenge to dermatological treatment such as decubitus care and atopic dermatitis. Smartphone has been spreading explosively since 2010 everywhere in the world, and its display has advanced by means of technological innovation. The organic light-emitting diodes (OLED) are used for smartphone displays in 2018, and they have higher definition with larger size, higher luminance and deeper black, higher contrast and higher visibility, and wider color gamut. On the other hand, problems about color appearance of OLED smartphone displays occur. The wider color gamut by OLED smartphone displays may lead to excessive color representation like cinema film and may produce different color appearance from actual color. Many medical staffs use smartphone for recording diseased parts. And they sometimes discuss the treatment policies while viewing the images. In telemedicine treatment, frequency of smartphone use will become even greater. Because of these factors, this research examined the issue of color appearance in telemedicine system with the use of smartphone.

For this experiment, 24 color charts of Macbeth Color Checker and two photoprints of decubitus were used as visual targets. In a darkroom, these visual targets were illuminated at 500 lx by six kinds of light sources (an incandescent lamp of 2468K, three fluorescent lamps of 2832K, 5064K, 6458K, and two LED lamps of 2651K and 5041K). We used REALAPS 2.0+Clum Color system made by Visual Technology Laboratory in Japan as measuring equipment for color tristimulus values CIE XYZ. We used iPhone XS Max made in 2018 too. Experimental results were summarized as follows. (1) Under lower color temperature lighting conditions than 3000K such as incandescent lamp, color reproduction of the smartphones display was not good, and the color tristimulus values were strange as compared with the values under higher color temperature lighting conditions. (2) Brightness of color on the smartphone display tended to express higher than the real color. (3) Saturation of color on the smartphone display tended to express higher than the real color, especially when the object colors were high-chroma. (4) Judgement of decubitus symptom, color difference tended to be over evaluated.

INTRODUCTION

Smartphone display has advanced by means of technological innovation. OLED are used for smartphone displays in 2018, and they have higher definition with larger size, higher luminance and deeper black, higher contrast and higher visibility, and wider color gamut. On the other hand, a problem about color appearance of OLED smartphone displays occurs. The wider color gamut by

OLED smartphone displays may lead to excessive color representation like cinema film. And it may produce different color appearance from actual color.

In Japan, Telemedicine is on the way as part of efforts to tackle super-aging society and doctor shortage. Usually a doctor examines/sees a patient face-to-face. As treatment in the chronic phase for some significant period, the doctor can use telemedicine methods as complementary practices. The color reproduction of telemedicine equipment becomes a challenge to dermatological treatment such as decubitus care and atopic dermatitis.

The medical data such as images of the affected parts are handled carefully in term of the individual information protection policy. But some medical staffs use smartphone to collect the observation data for better medicine/surgery supports, and they discuss the treatment strategy with their colleagues in person while viewing the data. In telemedicine treatment, frequency of smartphone use will become even greater.

EXPERIMENTS

The experiment was carried on a dark room at Faculty of Human development of University of Toyama, without the sunlight coming in from the windows.

iPhone XS Max made in 2018 was used in this experiment. The smartphone is the latest one. The display size of 6.5 inch was the biggest at that time in the world. The display resolution was 2688 x 1242 pixel (458 pixels per inch). The OLED were used for its displays.

“REALAPS 2.0+Clum Color system” made by Visual Technology Laboratory in Japan was used in this experiment as measuring equipment for color tristimulus values of CIE-XYZ two-dimensionally. The calculation program of “REALAPS 2.0+Clum Color system” was running under Windows 10. A digital camera “Lumix-GX7” made by Panasonic was included for the standard specification of the system. The camera’s conditions were set as the shutter speed to 1/30, the aperture of f/4, and the sensitivity ISO-200.

In a darkroom, the visual targets were illuminated at 500 lx by six kinds of light sources; an incandescent lamp of 2468K, three fluorescent lamps of 2832K, 5064K, 6458K, and two LED lamps of 2651K and 5041K. The spectral power distributions of these light sources are shown in Figure 1. These data were measured by an illuminance spectrophotometer CL-500A (Konica Minolta).

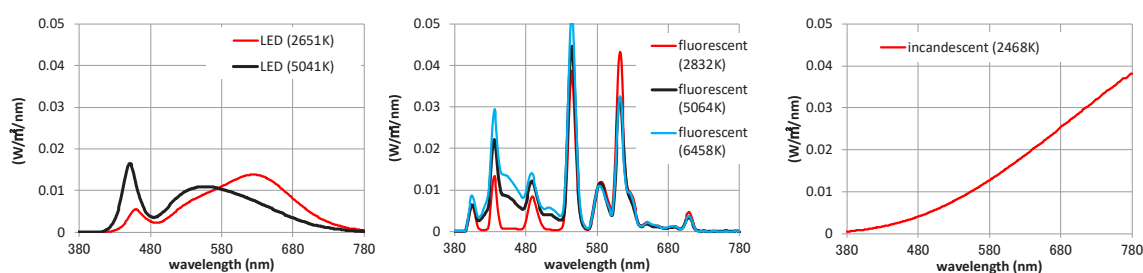


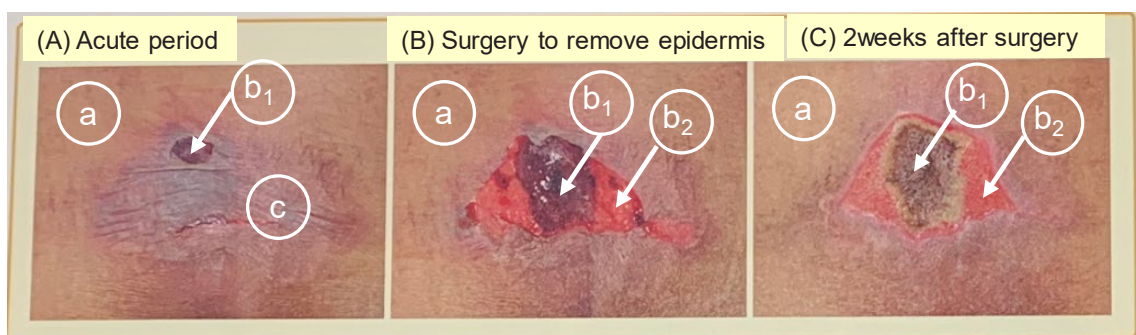
Figure 1: Spectral power distributions of light sources.

For this experiment, 24 chips of the GretagMacbeth ColorChecker (Figure 2) and photoprints of decubitus [1] were used as visual targets. The decubitus photoprints of two typical patients are shown in Figure 3. The spectral reflectance data of 24 chips of the GretagMacbeth ColorChecker and the decubitus photoprints were measured by a portable spectrophotometers CM-2600d (Konica Minolta).

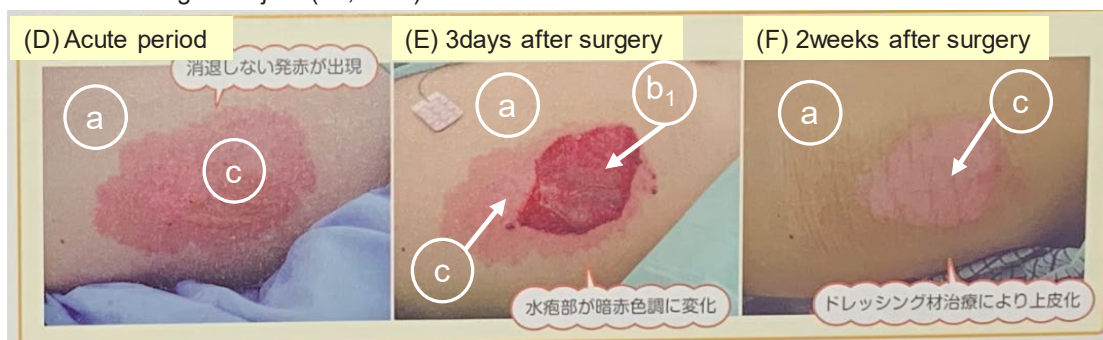


Figure 2: GretagMacbeth ColorChecker.

Elderly subject (79, female)



Midlife overweight subject (47, male)



a=skin, b1&b2=exposed affected area, c=bulged epidermis skin

Figure 3: Decubitus photoprints of two typical patients [1].

The experimental procedure is outlined below.

- 1) Take images of visual targets by “Lumix-GX7” under a certain light source.
- 2) Take images of visual targets by iPhone under the same light source.
- 3) Take images of the iPhone’s display which shows each visual target images by “Lumix-GX7” without the light.
- 4) Read color tristimulus values of CIE-XYZ in the images of procedure-1 and procedure-3 by using “REALAPS 2.0+Clum Color system”.
- 5) Calculate CIE-L*a*b* and C_{ab}* from CIE-XYZ of “REALAPS 2.0+Clum Color system”.
- 6) Experiment under other light sources following from procedure-1 to procedure-5.

RESULTS

“REALAPS 2.0+Clum Color system” is developed for inexpensive and readily available experiment to measure color tristimulus values of CIE-XYZ two-dimensionally, but the accuracy of measurement is not precise enough. Therefore, we also calculated the theoretical CIE-XYZ with the spectral power distributions data of light sources and the spectral reflectance data of visual targets by using a spreadsheet program “NIST Color Quality Scale ver.9.0.1” [2].

Figure 4 shows the comparison results of No.20 light gray chip of the GretagMacbeth ColorChecker under six light sources. Each light source result was connected in ascending order of color temperature. Under lower color temperature lighting conditions than 3000K (open circle dots), color reproduction of the smartphones display was not good, and the color tristimulus values were strange as compared with the values under higher color temperature lighting conditions. Most results of the GretagMacbeth ColorChecker indicated a similar tendency.

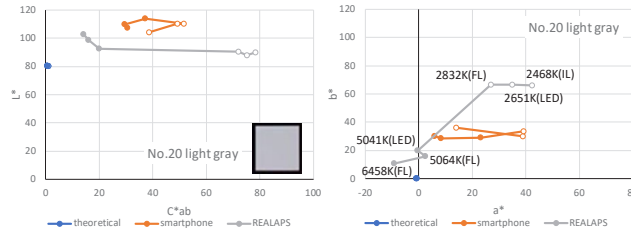


Figure 4: Result of an Achromatic Chip (No.20) under six light sources.

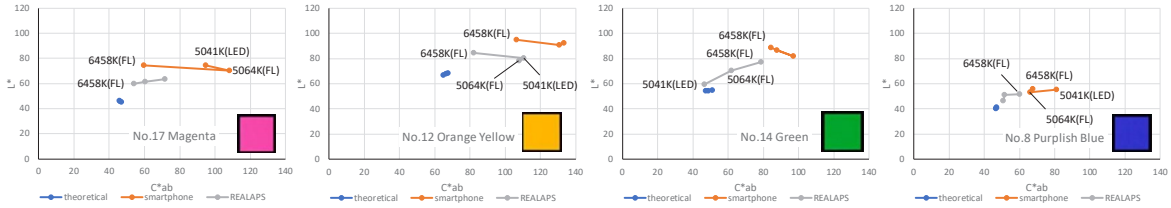


Figure 5: Results of High- Chromatic Chips (No.17, 12, 14, 8) under three light sources.

Figure 5 shows the comparison results of four high-chromatic chips of the GretagMacbeth ColorChecker under three light sources than 5000K. Brightness L^* and saturation C^*_{ab} on the smartphone display tended to express higher than the real color. Most results of the GretagMacbeth ColorChecker indicated a similar tendency, especially when the object colors were high-chroma.

Figure 6 shows the comparison results of decubitus photoprints under three light sources than 5000K. Brightness L^* and saturation C^*_{ab} on the smartphone display tended to express higher than the real color too. Therefore, the judgement of decubitus symptom by using smartphone's images might be over evaluated and misconstrued.

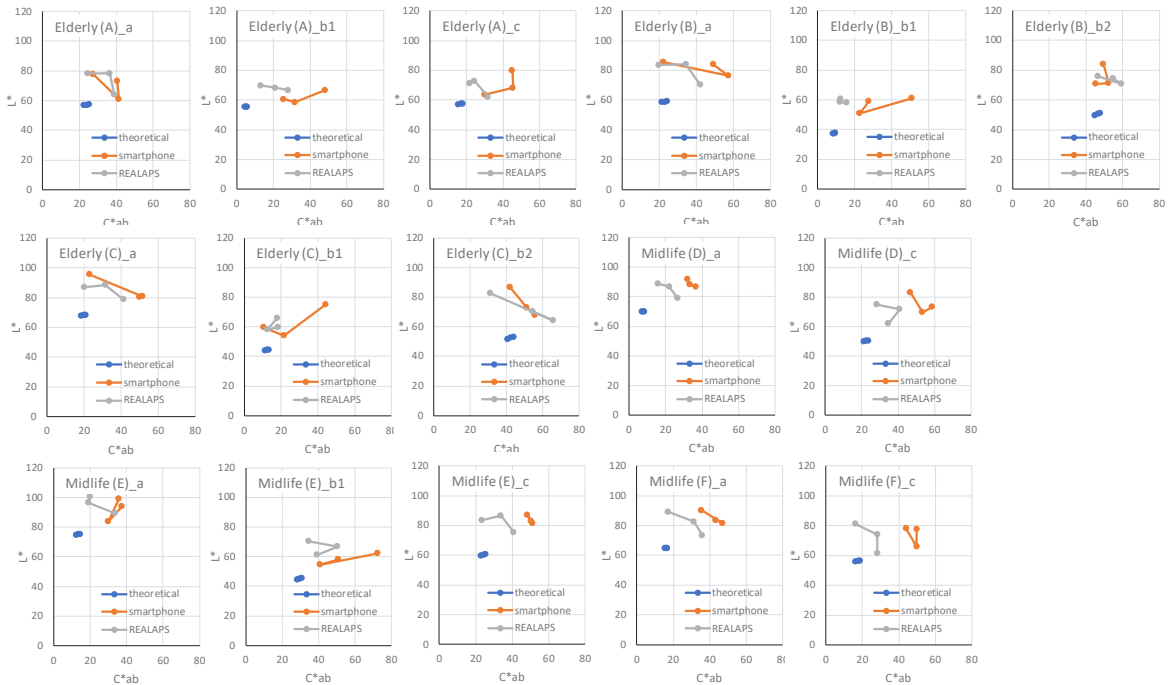


Figure 6: Comparison Results of Decubitus Photoprints under three light sources.

The color differences ΔE^*_{ab} among four combinations in Decubitus Photoprints were calculated; ΔE^*_{ab} between skin and bulged epidermis (A-a&c, D-a&c, F-a&c, E-a&c), skin and exposed affected pinkish area (B-a&b2, C-a&b2), skin and exposed affected dark-reddish area (A-a&b1, B-a&b1, C-a&b1), and both exposed affected area (B-b1&b2, C-b1&b2) in Figure 3. The results were shown in Figure 7. In the case of the combination between skin and bulged epidermis, the theoretical ΔE^*_{ab} of CQS were not large, and ΔE^*_{ab} of REALAPS and Smartphone were 10 points larger than the theoretical ΔE^*_{ab} of CQS. In the case of high-chromatic combinations including exposed affected area, the ΔE^*_{ab} of REALAPS and Smartphone were extremely larger than the theoretical ΔE^*_{ab} of CQS. It should be noted that it is necessary to be cautious when we use smartphones in Telemedicine because of their color gap against the reality.

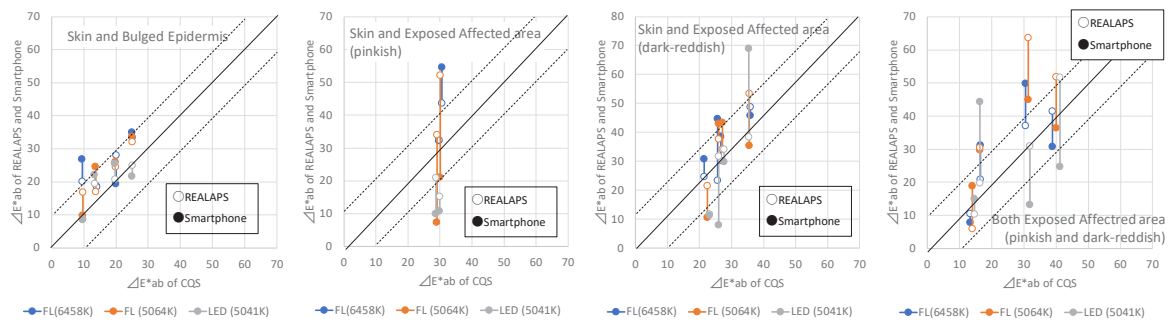


Figure 7: Results of color differences in Decubitus Photoprints.

CONCLUSIONS

The wider color gamut, higher luminance and higher contrast by OLED smartphone displays can express attractive but excessive color representation like cinema film. And it should produce different color appearance from actual color. It is necessary to be cautious when we use smartphones in Telemedicine treatment because of their color gap against the reality.

ACKNOWLEDGEMENT

This research was supported by JSPS KAKENHI Grant Number JP16K06607 and JP16H05570. The authors would like to thank Dr. Yoshi Ohno who let us to use “NIST Color Quality Scale (CQS) ver.9.0.1”, and Mr. Takahiro Goto who supported the experiment and analysis.

REFERENCES

1. Igaku Syuppan. (2016). The basis of decubitus care, WOC Nursing, Vol.4, No.9.
2. Davis, W. Ohno, Y. 2010. Color quality scale. Optical Engineering, Vol.49 (3), 033602. <https://doi.org/10.1117/1.3360335>

DEVELOPMENT OF PORTABLE SPECTRAL GONIO-PHOTOMETER.

Kazuji Matsumoto* and Misao Takamatsu

Spectral Application Research Laboratory Inc.

Nakaku Hayaumachou 2-7Hayauma Bldg.5F Hamamatsu City Shizuoka Pref. Japan

*Corresponding author: Kazuji Matsumoto, kazuji_sarli@plum.ocn.ne.jp

Keywords: portable, appearance, gonio-photometry, specular reflection, glossiness, texture

ABSTRACT

We developed portable spectral gonio-photometer for examining human's skin appearance mainly.

This instrument consists of three parts, light box, probe unit and spectral imaging unit. These parts are joined by optical fibers, probe (20mm×115mm (attachment area) ×80mm (height)) is designed for smooth contact to human's skin.

In the probe, photons are irradiated by Optical fiber in the direction of 45 degree to sample.

And, dispersive reflected photons are gathered by 33 point's optical fiber respectively.

33 receiving fibers are conducted to the slit of spectral imaging unit directly. Photon's energy in each dispersive degree trough optical components in the spectral imaging unit are transferred to 2nd dimensional sensor like CMOS or CCD.

Receiving degree of light information is described by X axis, and spectral information is described in Y axis in 2nd dimensional sensor.

In short, as spectral reflective information every 5 degree is attainable in 45 degree's irradiated illumination, information for appearance of samples could be expressed numerically.

Though this instrument was designed for an evaluation of TSUYA (glossiness) of human's skin mainly, Appearance to various natural and human made substances like TSUYA-kan (Glossiness), Shitsu-kan (Texture) and etc.) could be quantitative. We can point up a distinctive feature as follows.

As this is small and portable, it is not needed to make favorite shape's sample from a row mass's sample for fitting specimen's space in stand-alone type's it (non-destructive), and capable to carry it to field.

By using developed portable spectral gonio-photometer, we measured samples including with high specular reflection and low specular reflection and compared this data with measuring data by stand-alone gonio-photometer. And we measured human's skin. We will report these result and consideration.

INTRODUCTION

Until now, Spectral gonio-photometer was used for measurement of optical properties of materials, especially for measuring the appearance of substances precisely. Optical reflection's spectral radiation degree in each angle from substances might be captured by gonio-photometer.

For example, the difference between genuine leather and synthesized leather was researched.

Or, to find out the factors to give more genuine like appearance in synthesized materials.

And in the field of cosmetics, In order to decide the most suitable shape of micro order's small lods for raising quality of foundation's filler, the spectral gonio-photometer was used [1]. So, the spectral gonio-photometer were very effective for measuring appearance.

But, these specimen or samples measured by gonio-photometer were a piece of samples or block of samples. In short, these specimen and samples were a piece of samples. For measurement to large samples, it has been needed to make small sample or specimen for fitting specimen box of stand-alone gonio photometer. specimen needs to be extracted.

For animals or precious substances, specimens' extraction from a hole body is too difficult. Or, for human's skin, specimen's extraction is impossible. Then, Since non-destructive technique or non-invasive measurement for gonio-photometry is already needed, and would be very significant technique in the very near future, we started to develop portable type's spectral gonio-photometer.

PORTABLE GONIO INSTRUMENT

Portable Spectral Gonio-photometer was constructed by these three parts. First one is light box. Second one is Probe. Third one is small imaging Spectrometer. These three parts are combined by fiber probe.

Light box: 5mW Halogen light tube is included. Color temperature compensating filter LB 145 was added to fit 6500°K spectral curve to JISZ8720, Lights irradiates optical fiber to probe through M8 connector of this light box.

Probe: Irradiated fiber (quartz core distance 600microns graded index's type fiber) is set in 45 degree to the sample's perpendicular line. And light receiving fibers set in each 5 degree from 5 degree to 175 degree. In figure, for easy understanding the structure of gonio-photometric optics, shape for drawing is abbreviated. (Fig.1). all 33 receiving fibers are introduced to the spectral imaging unit (Spect-100vis (SARLI)).

Spectral Imaging Unit: 33 fibers are located in order at slit position of spectral imaging unit .

Light from each fiber position by respective angle position must be focused to defined position of 2nd dimensional sensor (CMOS or CCD) through plural lens1, prizm1, grating ,prizm2 and plural lens2. And, light from each fiber must be focused to defined wavelength's position by dispersive optical element (like prism, grating and prism) and plural lens1 &2. (Fig.2)

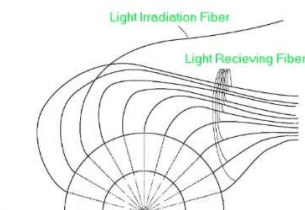


Fig.1 Potable Gonio Probe

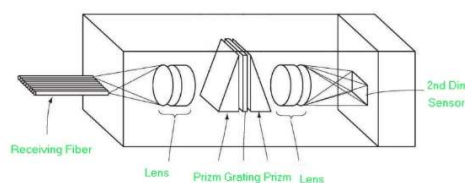


Fig.2 Imaging Spectro-photometer for fiber input

So, on 2nd dimensional optical sensor, optical wavelength's reflection distribution could be acquired in each reflection angle in 5degree respectively in one shot measurement.

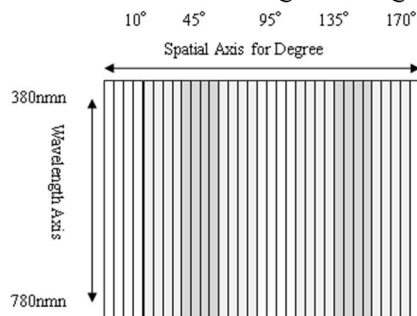


Fig.3 Image on 2nd dimensional sensor

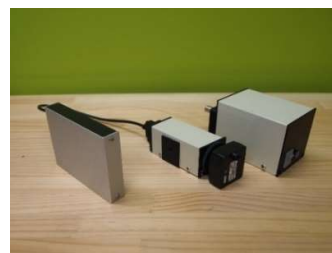


Fig.4 Developed portable spectral gonio-photometer

Photons gathered in each pixels is transformed to electric signal on sensor, and amplified by operational Amp , and transferred to A/D converter, and digital signal would be converted by A/D converter. These data would be transmitted to Personal Computer(PC) or Tablet(Tb) trough standard electrical interface (USB2.0 or USB3.0), and calculated to a well known graphic expression (reflection distribution curve at each receiving angle) and color expression calculation (like XYZ, Lab etc.) in PC or Tb.

TEST MEASUREMENT

1. Skin

To know about skin's appearance in deep, it is said that it's a lack of 45-0 degree color meas. method or measurement with integrating sphere. There is a gap over color measurement by these instrument and human's perception [2]. In order to research internal skin's phenomenon, we have already set about Specially Resolved Spectroscopy (SRS) in the field of skin study [3][4] [5].

Though gonio-photometry have a big potential for research of surface appearance more in detail compared to 45-0degree measurement and integrating sphere measurement, Orthodox type standalone's instrument has difficulty for skin's measurement .

To this skin's fields, developed instrument [portable gonio] are very effective. Because, it is very easy to access skin measurement. We can measure skin like these style in figure 5&6.



Fig. 5 forehead's measurement by Gonio-probe



Fig.6 arm's measurement by Gonio-probe

To this skin's fields, developed instrument [portable small gonio] are very effective. Because, it is very easy to access skin measurement. We can measure skin in these style in figure 5&6.

In first trial, we measured both forehead and arm for author's one.

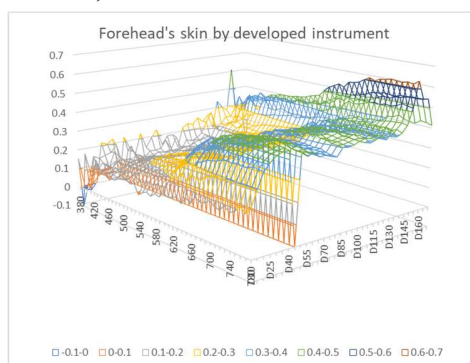


Fig.7 forehead's skin by developed instrument

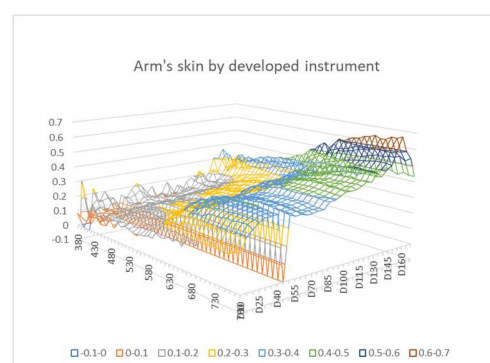


Fig.8 arm's skin by developed instrument

2. Table's woods (coated and noncoated)

Measuring furniture in non-destructive is easy. In the fields of wood or lumber, It could be measured by cutting them for adjusting sample size. But, To the field of furniture like Desk and Table, There is needs to measure substances in non-destructive or needs to measure final shape of goods or products. We examined table's woods. There is two types woods. First one is non-coated , and second one is coated woods.

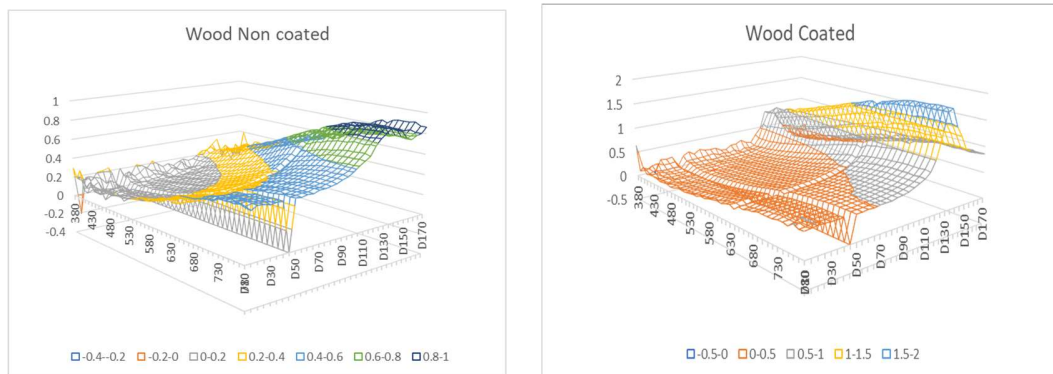


Fig.9 Wood non-coated by developed instrument Fig.10 Wood coated by developed instrument

3. Light Interference Pigment (Chroma Flair Plate)

To compare the results measured by developed small portable gonio-photometer and the results measured by standalone type gonio-photometer on the market, distinctive samples for gonio-photometry might be used. It is Chroma Flair Plate(CBC) by light interference pigment.

Chroma Flair plate by Light Interference Pigment is a sample plate has a wide range of hues depending on the angle at which it is viewed and the angle of incidence of light.

In this study, Cyan/Purple 230 and Silver/Green 060 were used. And, for standalone type's gonio-photometer, GCMS4 system (Murakami Color Res. Lab.) was selected.

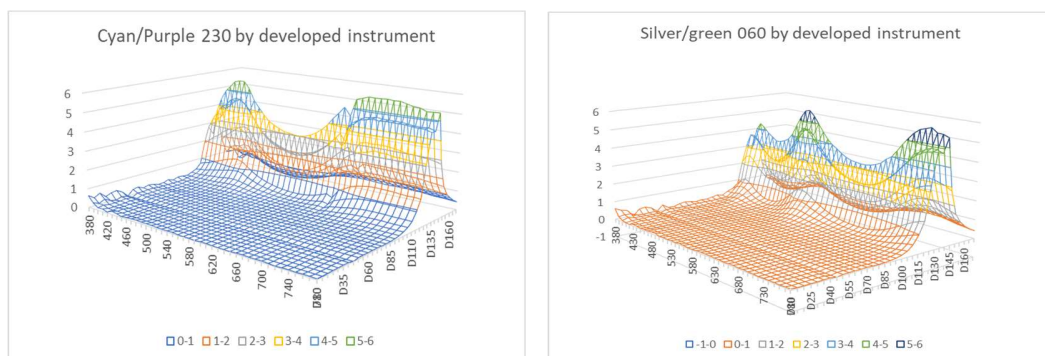


Fig.11 Cyan/Purple 230 by dev. instrument

Fig.12 Silver/Green 060 by dev. instrument

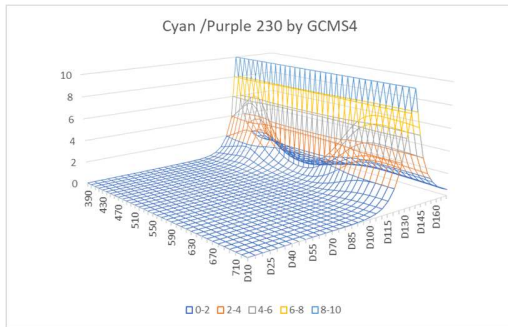


Fig.13 Cyan/Purple 230 by GCMS4

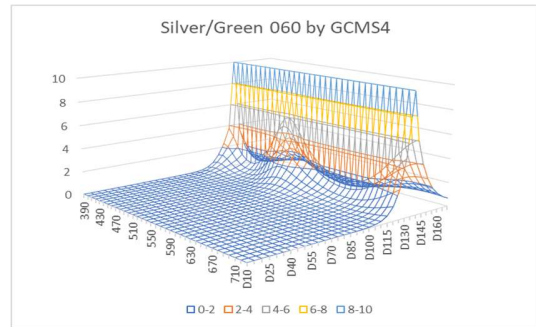


Fig.14 Silver/Green 060 by GCMS4

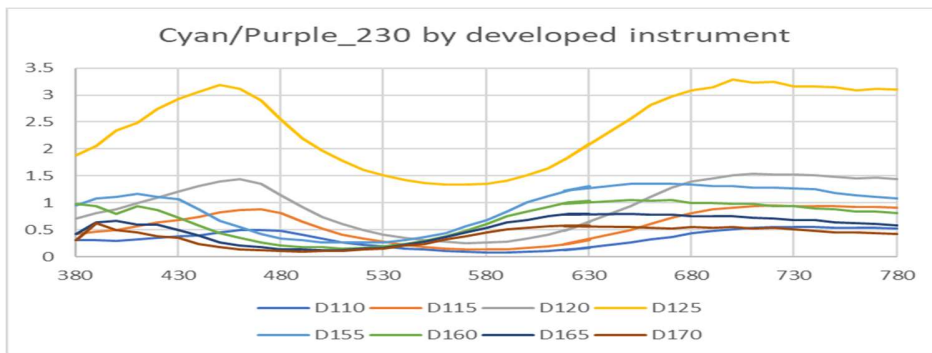


Fig.15 Spectral changes on Cyan/Purple_230 by developed instrument

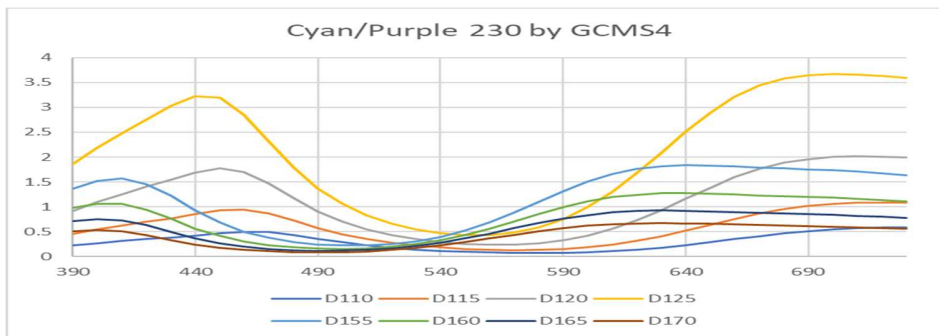


Fig.16 Spectral changes on Cyan/Purple_230 by GCMS4

RESULTS AND DISCUSSION

1. Skin

In viewing comparison, forehead's skin has more glosser than arm's skin. From this test by developed instrument, forehead's skin's specular reflection's peak is more shaper than arm's one.

From this results, In the very faint differences in reflection's appearance in skin, developed portable spectral gonio-photometer could acquire these very faint differences in skin.

In the skin's measurement specular reflection's peak were about from 135 degree to 155 degree. These result were caused by the existence of surface's curve of skin.

2. Woods

In this test, we got very clear result of the difference of coated samples and non-coated samples. Specular peak and reflection of coated samples were more higher than non-coated samples.

3. Samples on light interference pigment (Comparison with market's Gonio instrument)

In the comparison's test by samples (Cyan/Purple 230 and Silver/Green 060) to stand-alone type gonio-photometer in market, we got mainly one point's difference and find out a common result. The most difference point is the peak signal level in the specular peak's level. In our portable gonio is approx. 50~100 times compared with defusing angle area's (approximately 45-100degree) reflection. On the other hand, Standalone's type is approx. 500~2000 times compared with defusing area's reflection. And specular peak's shape is difference.

These difference must be induced by the viewing angle of each fiber. At present, there are no lens in front of light incident fiber and receiving fibers. So, lighting beam and receiving beam has 20 ~25degree angle in considering the cost effectiveness. On the other hand, Standalone's type gonio-photometer, the peak of specular reflection could be more sharp. This reason is like this, stand-alone type's beam is more close to parallel. We are thinking future's probe optics (to including lens or not.)

But, the spectral shape are mostly same in Fig.15 & Fig.16. From this data, in this regard portable can stand comparison with stand-alone gonio-photometer. To S/N, as portable measurement was in one shot in 30m second, there could be more stable data in plural acquisition.

CONCLUSIONS

Portable spectral gonio-photometer was developed. As the difference especially peak value of specular reflection's value between the result by developed portable spectral gonio-photometer and market's standalone gonio-photometer, we got the significant data, the spectral shape were mostly common.

And, we showed the merit of portable spectral gonio-photometer especially in non-destructive measurement. We can give the chance to measure the difference by faint difference appearance of substances, especially for skins of human and small sample or etc. from this instrument.

REFERENCES

1. Sakizaka, Y., Suzuki, Y., Nishikata, K., Mouri, K., (2006). Development of makeup's substances for controlling reflection from skin(1st). *J.Soc. Cosmet. Chem. Jpn.*, 40(4), 278-286.
2. Munakata, A., (2018). Color appearance in skin color and cosmetics. (Hadairo to kesyou no iromoyou) *JCSA (Tokai region lecture) 2018.12.22*
3. Takamatsu, M., Matsumoto, K., (2018). Development of skin transparency meter using SRS. *JCSAJ*, 42(3+), 83-86.
4. Takamatsu, M., Matsumoto, K., (2018). Proposal of colourimetry by spatially resolved spectroscopy. *IGC Proceedings year 2018*, 4-9.
5. Matsumoto, K., (2017). Absorbing coefficient and scattering coefficient on the basis of Diffusion theory from Kubelka-Munk Theory. *IGC Proceedings year 2017*, 10-17.

Metamer Mismatching for different number of camera combinations

XIANDOU ZHANG,^{1,*} MENG MENG WANG,¹ MINCHEN WEI,² SHANGFEI LI¹ And SHUO LIU¹

¹*Department of Digital Media Technology, Hangzhou Dianzi University, China*

²*Department of Building Services Engineering, Hong Kong Polytechnic University, Hong Kong*

* XIANDOU ZHANG, xiandouzhang@126.com

Keywords: metamer mismatching, digital imaging, multiple cameras, color difference

ABSTRACT

Metamer mismatching refers to the phenomenon that the colors are the same for different objects captured by a camera under one illuminant while different under other illuminants, which cause lots of potential problems in the fields of color reproduction and computer vision applications. Multiple cameras have been widely used in the cell phones, surveillance devices, automobiles as the increasing requirement of high-quality images in the entertainment, security and autopilot fields. Most of the past work focus on the image fusion, depth of field simulation and high dynamic range imaging in extreme lighting environment, not much work on making the best use of the multiple cameras to improve the object distinguish ability and color enhancement. This study would investigate how the metamer mismatching problems are affected by the number and shape of the sensor spectral sensitivity functions of different camera combinations.

INTRODUCTION

Metamer mismatching is a phenomenon that two different objects have the same color responses under a certain condition, but may difference after the condition changes. As the camera does not have the color constant characteristic like the human, it must be confused about which one is true when this happens. One commonly associated strategy to solve this problem is to estimate the spectral reflectance of the object with the multispectral imaging systems [1-6]. However, they are usually bulky, expensive, and low efficiency. There are many researchers have proved that adding additional sensors can reduce the degree of metamerism or improve the accuracy of color identification and reproduction. Prasad [7] investigated how frequently metameric mismatch happened when using three consumer cameras and proposed three methods [8] to add an additional sensor to an RGB digital imaging system to reduce the problem of camera metamerism. Nishino [9, 10] designed optimal spectral filters to enhance the color discrimination of skin colors. Morovic et al. [11] tried to increase the number of narrow-band sensors to reduce the frequency of metameric mismatch in a scene. Multiple cameras have been widely used in the cell phones, surveillance devices, automobiles as the increasing requirement of high-quality images in the entertainment, security and autopilot fields. Although most of the past work focus on the image fusion, depth of field simulation and high dynamic range imaging in extreme lighting environment, not much work on making the best use of the multiple cameras to improve the object distinguish ability and color enhancement. This study aims to investigate whether multiple cameras could solve this problem, and discuss the degree of the metamer mismatching would be affected by the number and shape of the sensor spectral sensitivity functions. The theoretical and practical metamer mismatching volumes, and color difference as the measurable indicators.

Metamer Mismatching Calculation Method

For a given object with spectral reflectance r , the metamer set is defined as other spectral reflectance with the similar color response with that of r under the first illuminant/observer environment, while the color responses are different under the second illuminant/observer environment. The metamer mismatching body is defined as the color response distributions under the second illuminant/observer environment for all the metamer reflectance with r . The volume of the color response distributions under the second illuminant/observer environment are adopted to evaluate how the metamer mismatching degree varied with the number and shape of the sensor spectral sensitivity functions of different camera combinations when the illuminant/observer environment changes. The volumes are determined by the boundary of the color response distributions. So, the key issue is how to define or find the metamer spectral reflectance whose color response under the second illuminant/observer environment distributed on the boundary of the metamer mismatching body.

Both the theoretical and practical metamer spectral reflectance on the boundary are defined and found respectively. Previous studies have proposed different methods to define the theoretical metameric spectral reflectance corresponding to the optimal colors distributed on the boundary of the metamer mismatching bodies [12-14]. Logvinenko et al. [13] defined the theoretical metameric spectral reflectance by the step functions with $2N-1$ transitions for the imaging systems with N sensors. Mackiewicz et al. [14], however, argued that the theoretical metameric spectral reflectance with $2N-1$ transitions would cause the metamer mismatching volume to be significantly smaller and proposed using the spherical sampling with a linear programming optimization method to derive the theoretical metameric spectral reflectance. Both the two methods were used to calculate the theoretical spectral reflectance metameric to the neutral gray (i.e., Munsell N7.5/) under the illuminant A, D200, F4 and LED respectively with CIE1964XYZ as the observer, and then the metamer mismatching volumes are calculated for each color responses set under illuminant D65. The results are shown in Table 1, which denote that the metamer mismatching volumes are much smaller for the Logvinenko's method than that for the Mackiewicz's method. Therefore, the Mackiewicz's method were used to calculate the theoretical metameric spectral reflectance in this study.

Table 1. Comparison of metamer mismatching volumes calculated using the Logvinenko and Mackiewicz's methods.

	A to D65	D200 to D65	F4 to D65	LED to D65
Logvinenko	392.59	70.32	17283.52	3320.57
Mackiewicz	547.05	115.27	24569.23	5195.45

The practical metameric spectral reflectances are also used to investigate how the metamer mismatching volumes vary with the number and shape of the sensor spectral sensitivity functions. To simulate the practical imaging process, the color responses corresponding to the metameric spectral reflectance under the second illuminant/observer environment were normalized with the maximum color responses of an ideal white to 255. As it is hard to find the spectral reflectance set with exactly the same color response under the first illuminant/observer environment, the following equation is used to determine whether the two stimuluses are metameric pairs or not,

$$\sqrt{(\psi_1^1 - \psi_2^1)^2 + (\psi_1^2 - \psi_2^2)^2 + \dots + (\psi_1^N - \psi_2^N)^2} < T, \quad (1)$$

where $(\psi_1^1, \psi_1^2, \dots, \psi_1^N)$ and $(\psi_2^1, \psi_2^2, \dots, \psi_2^N)$ are the color responses of two samples, T is a threshold that used to control the color similarity between the two samples.

For each given spectral reflectance, the metameric spectral reflectances under the first illuminant/observer environment are defined or found with the above two methods respectively. Then the color response under the second illuminant/observer environment were calculated for each metameric spectral reflectances set, based on with the metamer mismatching volumes are calculated.

EXPERIMENT

To analyze how the metamer mismatching volumes are affected by the number and shape of the sensor spectral sensitivity functions, the spectral sensitivity functions database [15] were adopted, which including the spectral sensitivity functions of professional DSLRs, point-and-shoot, industrial and mobile cameras. The criteria to select the spectral sensitivity functions is that they are as different as possible. Finally, three sets of spectral sensitivity functions CMF1, CMF2 and CMF3 were selected, as shown in figure 1. Seven different camera combinations were formed, they are CMF1, CMF2, CMF3, CMF1&CMF2, CMF1&CMF3, CMF2&CMF3, CMF1&CMF2&CMF3.

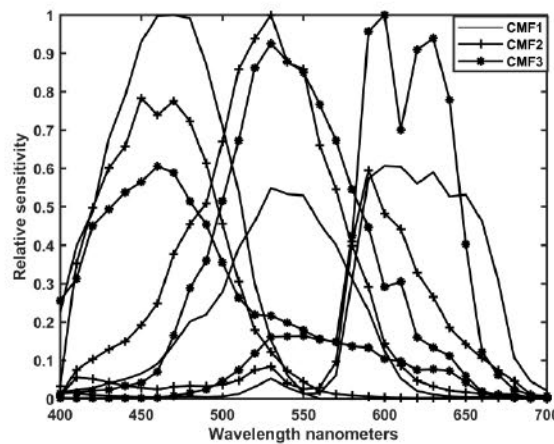


Figure 1. Spectral sensitivity functions of the three selected cameras

Four illuminants, CIE Illuminant A, D65, F4, and a mobile phone LED flashlight (3016 K), were selected to evaluate the degree of metamer mismatching. 1600 samples in the Munsell color atlas [16] were used to further investigate how metamer mismatching varies with different colors. For the color responses with the designed spectral sensitivity function combinations of Munsell samples under each of the four test illuminants, 1000 theoretical metameric spectral reflectances were generated by the Mackiewicz's method. Then the CIE1964XYZ tristimulus values of the 1000 theoretical metameric spectral reflectances were calculated under illuminant D65, based on which the volumes of the metamer mismatch bodies are calculated. The practical metamer mismatching volumes are calculated with the similar method except the metameric spectral reflectances are selected from the 47,586,022 unique practical spectral reflectances date set, which derived from the multispectral images of real scenes [17-19]. In addition, the threshold value of T is determined as 3 which ensure the color response of the selected spectral reflectance are similar to the candidate sample under the first illuminant/observer environment and most of the 1600 Munsell samples could find more than 50 metameric spectral reflectances.

EXPERIMENT RESULTS

The previous studies have investigated how the average metamer mismatching volumes vary with the value and chroma of the Munsell samples [17]. The variation relationship between the volume and the Munsell value, chroma in this study are similar as that in the previous study results, so this study only compares how the metamer mismatching volumes of the neutral Munsell color changes with different sensor combinations for simplification. The theoretical metamer

mismatching volumes for the Munsell neutral samples and the average color differences between each Munsell neutral sample and its corresponding 1000 metameric optimal surface colors were shown in Figure 2 and 3 respectively. It can be observed that the volume was reduced when the camera number increase. In addition, the volumes reduce more quickly when the sensor number changed from 3 to 6 than that from 6 to 9. The variation relationship between the color differences and the sensor sets are similar as that of the volumes and the sensor set. However, the color differences don't significantly change with the illuminants, and the largest color differences happened to be the Munsell N5.5/ sample. Moreover, the color differences of samples with lower Munsell values is higher than that of samples with higher Munsell values. This was likely due to the fact that the human visual system is more sensitive to dark colors. It is worthy to note that both the volumes and color differences are the largest for the CMF1&CMF3 combination comparing to that of the CMF1&CMF2 and CMF2&CMF3 combinations. The reason is that the shape of the spectral sensitivity functions between the CMF1 and CMF3 are much more similar than that CMF1&CMF2 and CMF2&CMF3 combinations, which indicates that the more different of the spectral sensitivity functions, the smaller of the metamer mismatching volumes and color differences.

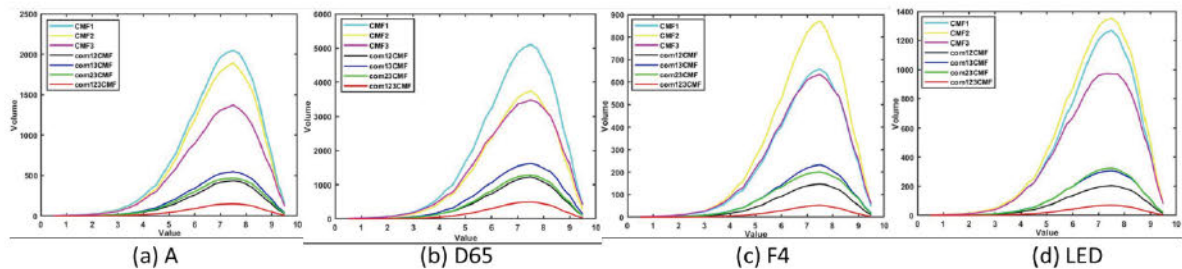


Figure 2. Theoretical metamer mismatching volumes for the Munsell neutral samples under each illuminant

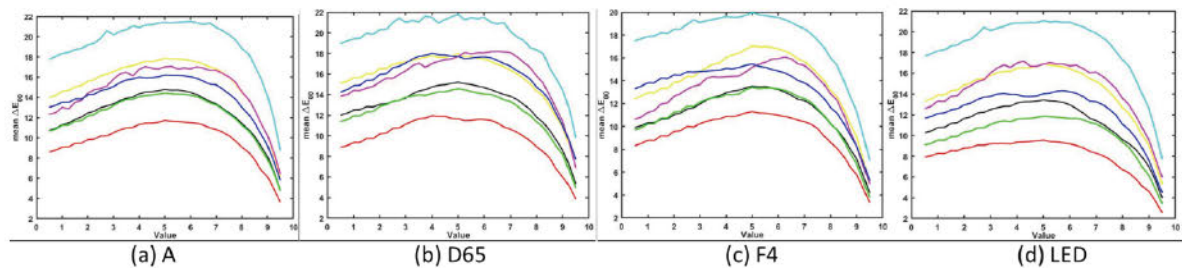


Figure 3. Average color differences between each Munsell neutral sample and its corresponding 1000 theoretical metameric spectral reflectances under each illuminant

The practical metamer mismatching volumes for the Munsell neutral samples and the average color differences between each Munsell neutral sample and its corresponding metameric real surface colors were shown in Figure 4 and 5, respectively. It can be observed that both the metamer mismatching volume and color difference are much smaller than the theoretical cases. Similarly, the more sensors used to acquire the color information, the smaller degree of the metamer mismatching volume and color differences. The degree of the metamer mismatching volume and color differences for the CMF1&CMF3 combination are larger than that of the CMF1&CMF2 and CMF2&CMF3 combinations

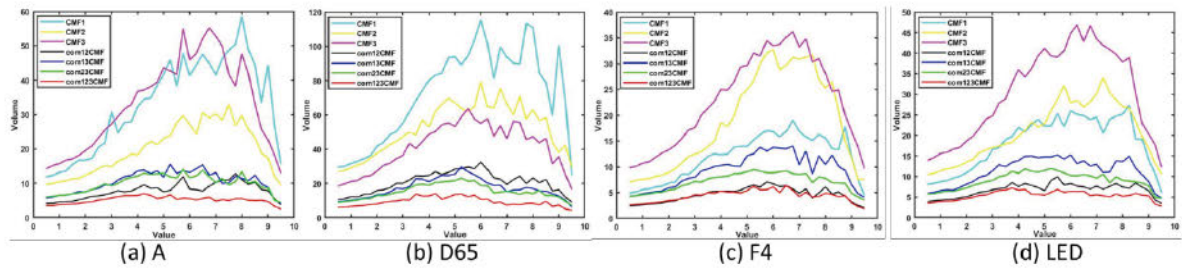


Figure 4. Practical metamer mismatching volumes for the Munsell neutral samples under each illuminant

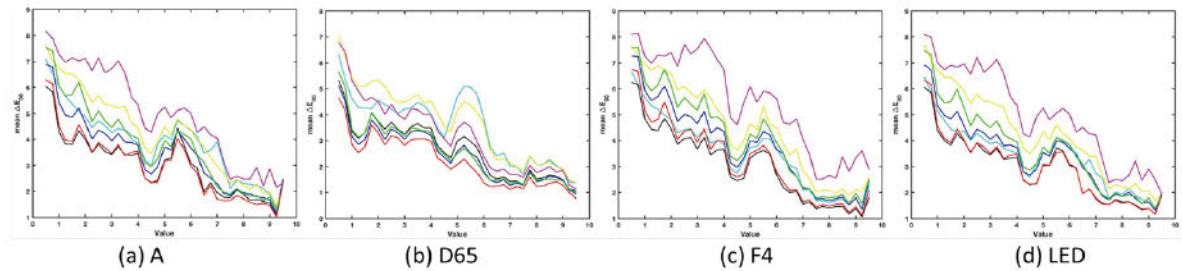


Figure 5. Average color differences between each Munsell neutral sample and its corresponding metameric real spectral reflectance under each illuminant

CONCLUSION

This study aims to investigate how the metamer mismatching affected by the number and shape of the sensor spectral sensitivity functions. The spectral sensitivity functions of different cameras were used to compose different camera combinations. The metameric spectral reflectances were either derived from the theoretical step functions or selected from a large dataset containing 47,586,022 distinct real surface samples. Both the theoretical and practical metamer mismatching were characterized using metamer mismatching volumes and color differences. It was found that both the metamer mismatching volumes and color differences were significantly reduced with the increase of sensors. In addition, the more different of the spectral sensitivity functions, the smaller of the metamer mismatching volumes and color differences.

ACKNOWLEDGEMENT

The authors thank the funding support of National Natural Science Foundation of China (NSFC) (61675060, 61205168).

REFERENCES

1. Maloney, L. T. (1986). Evaluation of linear models of surface spectral reflectance with small numbers of parameters. *J Opt Soc Am A*. 1986; 3(10): 1673-1683.
2. Burns, P. D., & Berns, R. S. (1997). Error propagation analysis in color measurement and imaging. *Color Res Appl*. 2015; 22(4): 280-289.
3. Haneishi, H. (2000). System design for accurately estimating the spectral reflectance of art paintings. *Appl Opt*. 2000; 39(35): 6621-6632.
4. Imai, F. H., & Berns, R. S. (1999). A Comparative Analysis of Spectral Reflectance Reconstruction in Various Spaces Using a Trichromatic Camera System. *Color and Imaging Conference 1999*, pp 21-25.
5. Garcíabeltran, A., Nieves, J. L., Hernandezandres, J., & Romero, J. (2015). Linear bases for spectral reflectance functions of acrylic paints. *Color Res Appl*. 2015; 23(1): 39-45.

6. Praefcke, W, Keusen, T. (1995). Multispectral color system with an encoding format compatible with the conventional tristimulus mode. *Color and Imaging Conference Final Program and Proceedings 1995*, pp 112-114.
7. Prasad, D. K., & Wenhe, L. (2015). Metrics and statistics of frequency of occurrence of metamerism in consumer cameras for natural scenes. *J Opt Soc Am A*. 2015; 32(7): 1390-1402.
8. Prasad, & Dilip, K. (2016). Strategies for Resolving Camera Metamers Using 3+1 Channel. *In Proceedings of IEEE Conference on Computer Vision and Pattern Recognition Workshops 2016*, pp 954-962.
9. Nishino, K., Kaarna, A., Miyazawa, K., Oda, H., & Nakauchi, S. (2012). Optical implementation of spectral filtering for the enhancement of skin color discrimination. *Color Res Appl*. 2012; 37(1): 53-58.
10. Nishino, K., Nakamura, M., Matsumoto, M., Tanno, O., & Nakauchi, S. (2011). Optical filter for highlighting spectral features part i: design and development of the filter for discrimination of human skin with and without an application of cosmetic foundation. *Opt Express*. 2011; 19(7): 6020-6030.
11. Morovič, Peter, & Haneishi, H. (2007). The effect of sensor shape and number on surface metamerism of colour input devices. *Color and Imaging Conference 2007*, pp 18-24.
12. Wyszecki, G. W., & Stiles, W. S. (1968). Color science: concepts and methods, quantitative data and formulas. *Phys Today*. 1968; 21(6): 83-84.
13. Logvinenko, A. D, Funt, B., & Godau, C. (2014). Metamer mismatching. *IEEE Trans Image Process*. 2014; 23(1): 34-43.
14. Mackiewicz, M., Rivertz, H. J., & Finlayson, G. D. (2019). Spherical sampling methods for the calculation of metamer mismatch volumes. *J Opt Soc Am A*. 2019; 36(1): 96-104.
15. Jiang, J, Liu, D., Gu, J., & Susstrunk, S. (2013). What is the space of spectral sensitivity functions for digital color cameras? *Workshop on Applications of Computer Vision 2013*, pp 168-179.
16. Munsell Book of Color—Glossy Edition (X-Rite Corporation, Grand Rapids, Michigan).
17. Zhang, X., Funt, B., & Mirzaei, H. (2016). Metamer mismatching in practice versus theory. *J Opt Soc Am A*. 2016; 33(3): A238.
18. Chakrabarti, A., & Zickler, T. (2011). Statistics of real-world hyperspectral images. *In Proceedings of IEEE Conference on Computer Vision and Pattern Recognition 2011*, pp 193-200.
19. Arad, B., & Benshahar, O. (2016). Sparse Recovery of Hyperspectral Signal from Natural RGB Images. *In the European Conference on Computer Vision 2016*, pp 19-34.

LOCAL ADAPTATION APPROACH FOR CAMERA CHARACTERIZATION BASED ON LIGHTNESS

Congcong Zhang¹, Xiaoxuan Liu¹, Cheng Gao¹, Zhifeng Wang¹, Yang Xu¹, and Changjun Li^{1*}

¹ *School of Computer and Software Engineering, University of Science and Technology Liaoning, Anshan, China*

*Corresponding author : cjliustl@sina.com

Keywords: Camera characterization, local adaptation, training samples, cross-media color reproduction

ABSTRACT

In this paper, we investigate a special local adaptation method. The method belongs to local adaptation in the sense the map can be selected based on the given camera response. However, each time the selected map is one of the three already available and it does not need to be computed once again. Hence, the method will be efficient in terms of computational time. The proposed method only need three maps. They are computed once for all. To be more specific, the whole training samples (G) can further be divided into two groups. In one group (G_L) each sample has the lightness L being smaller than 50 and in another group (G_H) each sample has the lightness L being not smaller than 50. Thus, three mappings: M_0 , M_L , M_H can be trained using the whole training samples (G), subgroup G_L , and subgroup G_H respectively. For any given camera response, using map M_0 to map the given camera response to get the initial estimation to corresponding colorimetric value XYZ . Hence an estimated L is obtained. According to the estimated L , then either the map M_L or M_H is used for final estimation. Our proposed method is compared with the Amiri and Fairchild method [Color Research and Application 2018, vol. 43: 675-684]. The results clearly show our proposed method outperforms Amiri and Fairchild method not only in computational cost, but also in prediction accuracy.

INTRODUCTION

Camera characterization has widely applications in cross-media colour reproduction and non-contact colour measurement. Hence it has been intensively researched for last several decades. Polynomial models[1] has been widely used for the camera characterization. Suppose n is the order of the polynomial. n is normally can be 1, 2, 3, or 4. Let C be the column vector formed by the camera response signal R, G, B and u be the column vector formed by traistimulus values (TSV) X, Y, Z , and A_n be the set formed by camera response signal C defined by:

$$A_n = A_n(c) = \left\{ R^{j_1} G^{j_2} B^{j_3} \mid j_1 + j_2 + j_3 \leq n, j_1, j_2, j_3 \text{ are nonnegative integers} \right\} \quad (1)$$

Thus, A_n has 4, 10, 20 and 35 elements when $n=1, 2, 3$ and 4 respectively. Let v_n be the column vector formed by all elements of A_n in certain order. Polynomial model is to find a map M so that for a given camera response C , we have

$$u = Mv_n \quad (2)$$

The mapping M is a matrix having 3 rows. Its number of column depends on the order n of the polynomial. It is normally obtained by the training samples. We used the X-Rite Digital ColorChecker Semi Gloss (SG) as training chart. Thus, let $u^{(k)}$ and $c^{(k)}$ be the TSV and camera response vectors for each of the colours in the chart, and $v_n^{(k)}$ is the vector formed from $c^{(k)}$ via $A_n(c^{(k)})$. Thus, we have the mapping M satisfies:

$$U = (u^{(1)}, u^{(2)}, \dots, u^{(m)}) = M(v_n^{(1)}, v_n^{(2)}, \dots, v_n^{(m)}) = MV \quad (3)$$

resulting in

$$M = UV^+ \quad (4)$$

Here, $m=140$, and V^+ is the pseudo inverse [2] of the matrix V . When the map M is obtained, for any given sample, its camera response C hence the vector v_n can be obtained. Thus, sample's TSV can be estimated using Eq. (2).

Note that in addition to the above polynomial model, Finlayson [3] proposed another kind of polynomial model, named as root polynomial model. In order to define the root polynomial model we also need a new set $B_n(c)$. In order to define $B_n(c)$, we need to define set $B_{n,n}(c)$ first (here n is again the polynomial order):

$$B_{n,n}(c) = \left\{ (R^{j_1} G^{j_2} B^{j_3})^{1/n} \mid \alpha (R^{j_1} G^{j_2} B^{j_3})^{1/n} = ((\alpha R)^{j_1} (\alpha G)^{j_2} (\alpha B)^{j_3})^{1/n} \right\} \quad (5)$$

Note the nonnegative indexes j_1, j_2, j_3 should satisfy $j_1 + j_2 + j_3 = n$. Then, the sets $B_n(c)$ can be defined using the following equation:

$$B_1 = B_{1,1}(c), B_2 = B_1 \cup B_{2,2}(c), B_3 = B_2 \cup B_{3,3}(c), B_4 = B_3 \cup B_{4,4}(c) \quad (6)$$

Note $B_n(c)$ has 3, 6, 13, 22 elements for $n=1, 2, 3$ and 4 respectively. We also can form a vector named as $v_{n,r}$ using the elements in $B_n(c)$ in certain order. Here, the subscript r is referred to the root polynomial model. It can be shown that for any positive real number α , $v_{n,r} = v_{n,r}(c)$ satisfies :

$$v_{n,r}(\alpha c) = \alpha v_{n,r}(c) \quad (7)$$

While, vector v_n does not satisfy the above property. When the root polynomial model is used, $v_n^{(k)}$ is replaced by $v_{n,r}^{(k)}$ in eq. (3) for getting the map.

Many papers [4,5] have reported that the polynomial model can be improved by local adaptive approach. In this paper, we only consider the Amiri and Fairchild method [5] which is given in detail next.

AMIRI AND FAIRCHILD (AF) METHOD

Firstly, we note that Amiri and Fairchild used the raw data rather than jpg data. The raw data is then converted to tiff using an available software (XnConvert), giving the camera response signal C . Secondly, the camera response is linearized. In the training chart, there are 6 grey scale colours from black to white via grey. The linearization is completed in each of the channel. For example, we try to find a function $f(R)$ so that $f(R)$ has linear relationship to the X values, i.e.,

$$X = a \cdot f(R) + b \quad (8)$$

In this paper, we choose $a = 1$, $b = 0$ and it was found that $f(R)$ is a polynomial of R of order 3. Similarly, functions $g(G)$ (related Y) and $h(B)$ (related to Z) were found.

For the Amiri and Fairchild (AF) method, the camera signal C is transformed to c_L using the above linearization approach.

Thirdly, a general map is obtained using camera signal c_L and a polynomial model of order 3. In fact, they made a modification to the polynomial model. As before, from c_L we can have $A_3(c_L)$. Note in the set $A_3(c_L)$ has 20 elements, however, when forming the vector v_3 they only used 17 elements of them, we denote this vector as \tilde{v}_3 . Thus, TSV vectors $u^{(k)}$, and camera signals $c_L^{(k)}$ and $\tilde{v}_3^{(k)}$ from the training chart, and Eqs. (3) and (4) can be used for finding a general map M named as M_G .

Finally, for any given sample, the camera response signal c_L , hence \tilde{v}_3 can be obtained. Then, an estimated TSV u_e can be obtained using equation: $u_e = M_G \tilde{v}_3$. For each colour in the training set, "distance" between u_e and $u^{(k)}$ can be computed. The distance is noted as $cd(u^{(k)}, u_e)$. Next, a weight w_k can be computed, which is inversely proportional to the distance. Thus, each sample in the training set, there is a weight associated to it. Hence, a new map (named as M_a) can be obtained using the following equation:

$$UW = (w_1 u^{(1)}, w_2 u^{(2)}, \dots, w_p u^{(m)}) = M_a (w_1 \tilde{v}_3^{(1)}, w_2 \tilde{v}_3^{(2)}, \dots, w_p \tilde{v}_3^{(m)}) = M_a \tilde{V}W \quad (9)$$

resulting in

$$M_a = UW(\tilde{V}W)^+ \quad (10)$$

Here, W is a diagonal matrix formed from all weights, \tilde{V} is a matrix formed by all $\tilde{v}_3^{(k)}$. In the end, the predicted TSV u_p is given by

$$u_p = M_a \tilde{v}_3 \quad (11)$$

Arimi and Fairchild [5] reported the local adaptive approach performs better. In other words, u_p is closer to the true TSV vector than u_e is. However, we note that the above local adaptive map M_a is needed for every given sample. Hence it needs more computational time compared with the traditional polynomial model.

THE PROPOSED METHOD

Firstly, similar to the AF method, we use the raw data as well. However, we used a different raw data converter provided by Professor Sun from National Taiwan University of Science and Technology. This software is different from XnConvert used by Amiri and Fairchild. We also need a general map named as M_0 obtained using the full set (G) of training samples. The only difference is that we used the root polynomial model of order 3, i.e. $u^{(k)}$ and $v_{3,r}^{(k)}$ are used in eq. (3) for getting the general map M_0 . Secondly, we further sort the whole set of training samples into two groups G_L and G_H according to the CIELAB lightness scale transformed from $u^{(k)}$. Samples in G_L have lightness less than 50, and samples in G_H have lightness not less than 50. Thus, two more maps M_L and M_H can be obtained using the groups G_L and G_H receptively. More exactly, for M_L , signals $u^{(k)}$ and $v_1^{(k)}$ from group G_L are used with eq. 3, and for M_H , signals $u^{(k)}$ and $v_{2,r}^{(k)}$ from group G_H are used with eq. (3). That is to say, M_L is obtained using the polynomial model of order 1 and M_H is obtained using the root polynomial model of order 2.

For each given sample, the camera response signal c , hence $v_{3,r}$, v_1 , $v_{2,r}$ can be obtained. Then, an estimated TSV u_e is obtained using the general mapping, i.e., $u_e = M_0 v_{3,r}$. According to the estimated TSV u_e , the estimated lightness L_e for the given sample can be obtained. Final TSV prediction is given by

$$u_p = \begin{cases} M_L v_1 & \text{if } L_e < 50 \\ M_H v_{2,r} & \text{if } L_e \geq 50 \end{cases} \quad (12)$$

Note that the above proposed method does not need to compute the local adaptive map for any given sample. Hence, it certainly takes less computational tome compared with the AF method. In the next section, the proposed method is also shown to be more accurate than the AF method does.

Table 1: Performance of the proposed and AF method in terms of average (Mean), maximum (Max) and median (Median) CIE2000 colour differences

Samples	Method	Nikon D610			Canon EOS 60D		
		Mean	Max	Median	Mean	Max	Median
MCC	Proposed	1.45	6.08	1.24	1.52	4.93	1.36
	AF	3.89	7.51	4.11	3.86	7.01	4.20
Textile	Proposed	4.10	8.61	3.68	2.83	7.65	2.49
	AF	6.13	18.75	6.04	4.28	9.08	4.33
Printed	Proposed	4.92	12.83	4.37	2.85	13.20	2.19
	AF	6.77	15.07	6.65	5.51	18.89	5.41

PERFORMANCE OF THE PROPOSED METHOD

The X-Rite Digital ColorChecker Semi Gloss (SG) was used as training chart and the Macbeth ColorChecker (MCC) was used as the testing chart. Furthermore, set of 48 textiles and set of 44 printed samples were also used for the testing as shown in Figure 1. Two cameras were used. They are the Nikon D610 and Canon EOS 60D . The setting is fixed on ISO 320, aperture 4.5, exposure time 1/30 for Nikon D610 and on ISO 400, aperture 4.5, exposure time 1/60 for Canon EOS 60D. The performance of the proposed method and the AF method is listed in Table 1 in terms of average (Mean), maximum (Max) and median (Median) CIE2000 colour differences.

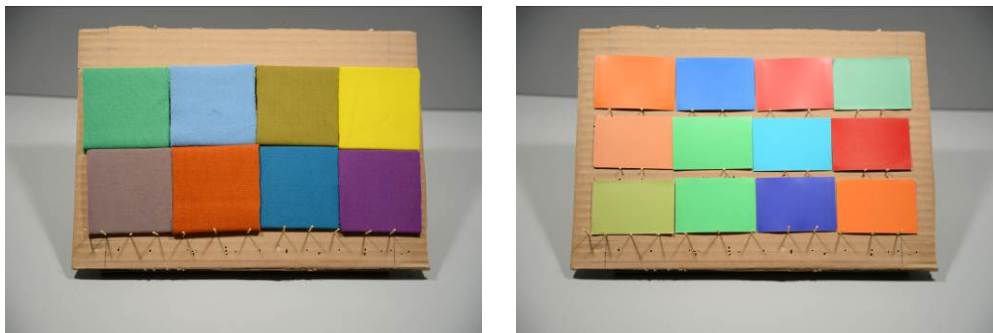


Figure 1. Textiles (left diagram) and printed (right) samples

It can be seen from Table 1 that the proposed method performs better than the AF method in all the cases, which is unexpected. For each method, it performs the best for predicting the MCC, second best for predicting the textile samples and the worst for the printed samples.

CONCLUSIONS

This paper proposes a simple local adaptation according the lightness scale. The proposed method needs three maps using the training samples. They are the general map M_0 , lower lightness map M_L , and higher lightness M_H . M_0 was trained using the full set of training samples using the root polynomial model of order 3. M_L was obtained using the low lightness group G_L and the polynomial model of order 1, and M_H was obtained using the high lightness group G_H and root polynomial of order 2. The proposed method is compared with the AF method using the MCC chart and textiles and printed samples. Testing results showed that our proposed method is better than the AF method in predicting accuracy, which is unexpected. Some of the differences may play important roles, which will be further investigated. The differences include raw data converters, different polynomials and orders.

ACKNOWLEDGEMENT

The work is supported by the Natural Science Foundation of China with grant numbers 61575090 and 61775169. The authors thank Professor Sun from National Taiwan University of Science and Technology for providing the software for converting the raw data. The authors also thank Professor Mikiko Kawasumi for providing documents related to the visa application.

REFERENCES

1. Hong, G. W., Luo, M. R., & Rhodes, P. A. (2001). A study of digital camera colorimetric characterization based on polynomial modeling. *Color Research & Application*, 26(1), 76-84. doi:10.1002/1520-6378(200102)26:13.0.CO;2-3
2. Golub, G. H. and Van Loan, C. F. (2013). *Matrix Computations*, fourth edition. The Johns Hopkins University Press, Maryland, USA.
3. Finlayson, G. D., Mackiewicz, M., & Hurlbert, A. (2015). Color Correction Using Root-Polynomial Regression. *IEEE Transactions on Image Processing*, 24(5), 1460-1470. doi:10.1109/tip.2015.2405336
4. Cao, B., Liao, N., & Cheng, H. (2017). Spectral reflectance reconstruction from RGB images based on weighting smaller color difference group. *Color Research & Application*, 42(3), 327-332. doi: 10.1002/col.22091
5. Maali Amiri, M., & Fairchild, M. D. (2018). A strategy toward spectral and colorimetric color reproduction using ordinary digital cameras. *Color Research & Application*, 43(5), 675-684. doi:10.1002/col.22231

A LOW-COST METHOD TO PREDICT COLOR APPEARANCE OF FLUORESCENT SAMPLES UNDER VARIOUS ILLUMINATION CONDITIONS

Pei-Li Sun^{1*}, Wei-Chih Su¹, Hung-Shing Chen¹ and Hung-Chung Li²

¹*Graduate Institute of Color and Illumination Technology, National Taiwan University of Science and Technology, Taiwan.*

²*Academia Sinica, Taiwan.*

*Corresponding author: Pei-Li Sun, plsun@mail.ntust.edu.tw

Keywords: Fluorescent Effect, Visual Color Difference, Textile Printing, Color Reproduction

ABSTRACT

A low-cost method to predict color appearance of fluorescent samples under various illumination conditions is proposed. It starts with XYZ measurement of test samples under reference conditions. User then compares a paired visual reference to estimate relative intensity of the UV light in a test condition. The XYZ values reflected by visible light and excited by the UV light are estimated separately and finally combine in the XYZ space to predict its color appearance roughly.

INTRODUCTION

Nowadays, inkjet printing is more and more popular in textile industry [1]. To widen color gamut of textile, fluorescent inks and substrates are sometime used [2]. Methods for predicting color appearance of fluorescent samples in various illumination conditions therefore are needed for fashion designers to optimize their products especially when a pattern contains both fluorescent and non-fluorescent areas. To accurately predict the fluorescent effect, the radiance ratio between each pair of emission wavelength and excitation wavelength need to be measured (as a bi-spectral Donaldson matrix [3]). However, it requires the use of an expensive measurement instrument and complex calculation [4]. To reduce the cost and complexity, we propose a low-cost method to obtain a rough estimation of the fluorescent effect.

METHOD

The proposed method includes 7 steps:

First, we define two reference conditions: (E1) illuminant A simulator and (E2) illuminant A simulator plus UV LED light strips (peak at 365nm) respectively.

Second, a paired visual reference samples (C1 and C2) were printed in light green. C1 has no fluorescent effect but C2 has strong fluorescent effect. The C1 and C2 samples look very similar under the E1 condition, but C2 sample is much brighter in the E2 condition as it has more fluorescent agent.

Third, a test sample C3 is measured by a non-contact colorimeter (we used Minolta CS-150) under E1 and E2 conditions respectively. Note, contact measurement is not recommended as we found the commonly used instrument such as X-rite i1 Pro 2 and X-rite Ci64uv cannot excite fluorescent sample fully as the peak of the built-in UV LEDs are around 395nm. The 395nm UV light can excite optical brightening agents for papers, but most of fluorescent inks used in textile industry need 365nm UV light to excite the colors.

Fourth, the test condition E3 contains both UV light and VIS (visible) light. The user is asked to scale the visual lightness difference between the C1 and C2 samples based on the grades of a non-fluorescent gray-difference scale (we used SDCE Grey Scale). The visual scaling value is a rough estimation of the relative intensity of UV radiation to the VIS radiation in the E3 condition.

Fifth, the XYZ measurements of the C3 separate as VIS reflection and UV excitation components respectively, where the VIS component in the reference condition is XYZ_{E1} and the UV component is XYZ_{E2} minus XYZ_{E1} . Note if the difference is negative, the XYZ_{E2} must increase proportionally to make the resulted UV component (XYZ_{UV}) all to be positive.

Sixth, VIS component under E3 condition is estimated by an artificial neural network trained by textile spectral samples of ISO SOCS database [5] with frequently used CIE standard illuminants. If the type of visible light in the E3 is known, the network can predict the VIS part of XYZ value of the C3 sample under the E3 condition more accurately. It is a rough way to predict color mismatch (or color metamerism) under different illumination conditions.

EXPERIMENT

To test the proposed method, 20 lighting conditions were estimated. It contains all combinations of 5 built-in visible light sources in a X-rite Spectralight III (including A, D65, CWF, Horizon (HZ) and TL84 where the illuminance measured by Konica Minolta CL-200 were 1554, 1613, 1660, 1172 and 2230 lx respectively) and 4 radiation levels of 365nm UV LED strips (in 0, 165, 262 and 358 mW/cm² respectively measured by an Analytik Jena UVP UVX-36 Sensor). The UV LED strips were assembled by ourselves. 16 saturate fluorescent samples (in different hue) printed by a 6 primary Mimaki TS34-1800A textile inkjet printer were used to test the accuracy of color prediction in the condition E3 based on the measurement of condition E1 and E2. The 6 primary inks consisted of non-fluorescent CMYK, Fy (fluorescent yellow) and Fp (fluorescent pink).

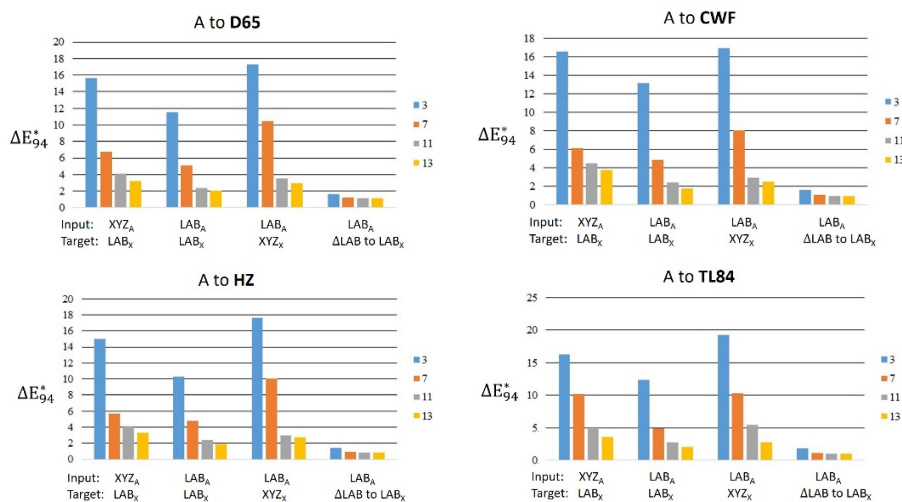


Figure 1. Prediction errors using artificial neural networks

PREDICTING XYZ VALUES OF VIS REFLECTION

The proposed method predicts the VIS reflection and the UV excitation of the C3 sample separately. In the VIS part, the source lumination (E1) is illuminant A, but the destination (VIS part of the E3) is one of illuminant X (X represents A, D65, CWF, HZ or TL84). To predict XYZ value from illuminant A to illuminant X without known spectral reflectance, three types of transformation can be considered: (1) Convert XYZ_A to XYZ_X using CIELAB with reference whites of the two

conditions. (2) Convert XYZ_A to XYZ_X using a chromatic adaptation transform (CAT) such as Bradford CAT. (3) Convert XYZ_A to XYZ_X using an artificial neural network (ANN) trained by textile spectral samples. We did an independent test for the XYZ_A to XYZ_X transformation using 2,832 textile spectral samples from ISO SOCS database [5]. 70% samples for training, 30% samples for testing. A multilayer perceptron ANN model was used. The model has two hidden layers. 4 training methods were tested: (1) input XYZ_A , predict LAB_X , (2) input LAB_A , predict LAB_X , (3) input LAB_A , predict XYZ_X , and (4) input LAB_A , predict ΔL^* , Δa^* , Δb^* to the LAB_X . Figure 1 shows the mean errors by using different numbers of neuron in the two layers. As can be seen, the mean errors are around $1\Delta E_{94}^*$ when using more than 7 neurons in each layer. The method (4) with 11 neurons in each layer were used in the final test in the Results section.

PREDICTING XYZ VALUES OF UV EXCITATION

The light green visual sample pair were predicted by ink amount CMYK_{FpFy}=(15,5,90,0,0,0) and (2,1,13,8,0,85) respectively. The ink amount is in [0 100] range. In the E1 condition (i.e., illuminant A), the LAB values of the paired samples are (84.8, -6.8, 70.0) and (86.0, -10.3, 72.4) respectively. The ΔL^* and ΔE_{94}^* are 1.2 and 2.2 respectively. However, in the E2 condition (i.e., A+UV), the ΔL^* and ΔE_{94}^* increase to 6.0 and 14.8 respectively. The ΔL^* can be used to generate a 1D look-up-table to estimate the ratio of irradiance between the UV and the visual lights. The relative irradiance ratio between the E3 and the E2 conditions can be estimated visually by scaling the lightness difference referring to a gray-difference scale (figure 2) in the two conditions.

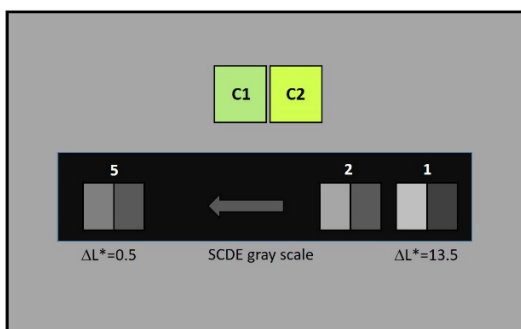


Figure 2. Visual estimation of UV intensity by a paired color samples and a gray-different scale.

However, the UV irradiance might not linearly relate to the sample C3's XYZ value of UV excitation. Therefore, three cases were tested: (1) Assume only XYZ_{UV} of the sample in E2 condition is known, use the UV irradiance ratio to scale the XYZ_{UV} . (2) Assume XYZ_{UV} under different UV irradiance ratio are known, use the UV irradiance ratio to look-up the mean XYZ_{UV} of 5 VIS lighting conditions. (3) Assume XYZ_{UV} under all conditions are known, use the UV irradiance ratio and VIS lighting to look-up the specific XYZ_{UV} . The test assume that visual estimation is accurate (as colorimeter) and the fluorescent lighting is 365nm UV LED. The results of the test are shown in the next section.

RESULTS

The test used 16 fluorescent samples, 5 VIS lighting \times 4 UV irradiance levels. In the VIS XYZ transformation, three methods including (1) CIELAB, (2) Barfdord CAT, and (3) optimal ANN were tested. In the UV XYZ estimation, three above mentioned cases were tested. The mean color differences of all 16 samples under 5 VIS lighting are listed as Table 1. The maximum color differences for each conditions are about 2 times to the mean differences. As can be seen in the 0 UV intensity column of Table 1, VIS transformation method has small impact on the prediction errors where optimal ANN is slightly better than Bardford CAT and CIELAB white point transform. The

errors increase a bit as UV intensity increases. On the other hand, the UV estimation method has more significant impact on the perdition errors. Case 3 is better than Case 2, and Case 2 is better than Case 1. It indicates that linear scaling based on an estimation of UV irradiance ratio is not good enough to predict the XYZ values excited by UV light. To achieve more accurate results, a model to correlate the UV intensity and the XYZ values is needed.

Table 1: Mean color difference of the test (unit: ΔE_{94}^*)

Method		UV intensity (mW/cm ²)			
VIS transform	UV estimation	0	165	262	358
1	1	5.90	5.36	6.07	6.12
	2	3.93	3.80	4.31	4.54
	3	1.66	1.95	2.86	2.23
2	1	4.72	4.54	5.13	4.91
	2	3.20	3.40	4.28	4.09
	3	1.63	1.86	2.96	2.62
3	1	4.22	4.16	4.44	4.54
	2	2.73	2.80	3.48	3.81
	3	1.48	1.88	1.87	1.88

CONCLUSIONS

A low-cost method to predict color appearance of fluorescent samples under various illumination conditions is proposed. It uses paired reference samples (with/without fluorescent agent) for a user to visually estimate relative intensity of the UV and visual lights in a test condition (E3). The visual-based method does not require spectral measurement of the test condition therefore is friendly to the fashion designers. The testing results were acceptable. However, it is not good enough. It still has many problems to be solved: (1) In the test, we assumed the type of visible light in E3 condition is known. It's better to find a way to predict the type automatically. (2) In the test, we assumed that the UV source in the E3 lighting is a 365nm UV LED. However, if the UV light spectrally mismatched, the prediction would be inaccurate. (3) The UV sensitivity curve of the fluorescent sample in the visual comparison (C2) might be different from the test sample (C3) which mix CMYKFyFp inks with halftone patterns. More studies are needed to make the fluorescent colors more predictable.

ACKNOWLEDGEMENT

The study was partly supported by Printing Technology Research Institute of Taiwan.

REFERENCES

1. Moser, L. S. (2003). ITMA 2003 Review: Textile printing, *Journal of Textile and Apparel Technology and Management*, 3(3), 1-15.
2. Kan, C. and Yuen, C. (2012), Digital Ink-jet printing on textiles, *Research Journal of Textile and Apparel*, 16(2), 1-24. doi:10.1108/RJTA-16-02-2012-B001
3. Donaldson, R. (1954) Spectrophotometry of fluorescent pigments, *British Journal of Applied Physics*, 5(6), 210.
4. Tominaga, S., Kato, T., Hirai, K. and Horiuchi, T. (2016). Spectral Image analysis of mutual illumination between florescent objects, *JOSA A*, 33(8), 1476-1487.
5. ISO/TR 16066:2003, *Graphic technology — Standard object colour spectra database for colour reproduction evaluation (SOCS)*
6. Dordevic, D., Javorsek, A. and Hladnik, A. (2009). Comparison of CMCCAT2000 and Bradford chromatic adaptation transforms, *Tekstilec*, 52(4), 91–101.

DISCOLORATION OF TUNA FILLETS (*Thunnus albacores*) TO INCREASE ADDED VALUE USING INDUSTRIAL GASES

Adi Djoko Guritno^{1*}, Novita Erma Kristanti¹, Melinda Sugiana Dharmawati²

¹ Department of Agroindustrial Technology, Faculty of Agricultural Technology, Universitas Gadjah Mada., Indonesia.

² Post Graduate Student, Study Program of Agroindustrial Technology, Faculty of Agricultural Technology, Universitas Gadjah Mada., Indonesia. Jl.Flora 1, Bukaksumur, Yogyakarta 55281, Indonesia

*Corresponding author: Adi Djoko Guritno, adidjoko@tip-ugm.org

Keywords: tuna fillet, industrial gases, storage, discoloration, quality

ABSTRACT

Currently in Indonesia, the marine fisheries sector recorded an increase in export value of 11.06% from 2017 to 2018, of which tuna (*Thunnus albacores*) as one of its main commodities recorded an increase of 8.9% (production) and \$ 41 million (export value) in 2018. Related to this, quality attributes are very important to control, one of which is the color of fish. This study applied several industrial gases (oxygen (O₂), nitrogen (N₂), and carbon dioxide (CO₂)) applied to tuna fillets for color changes associated to consumers preference so it will increase the added value. The objectives of this study are 1) measuring tuna fillet discoloration with industrial gas applications and 2) analysing the organoleptic characteristics of tuna fillet based on industrial gas treatment. There are two color testing methods carried out in this study, namely organoleptic testing carried out by 30 panellists, and color testing using chroma meters for 12 days of storage. Based on the results of organoleptic testing, panellists preferred tuna fillets that were given N₂ gas treatment. This can be seen from day 0 to day 12 where fish with N₂ gas treatment had the highest score (average 6) compared to others. In addition, the decrease in the quality of tuna fillets with N₂ gas during storage was not significant with a decrease in score of only 1.12 points (day 3) and 0.59 points (day 9). The results of testing with chromameter showed that the lightness values always decreased during storage, but tuna fillets with N₂ gas treatment had the highest and most stable light levels compared to other treatments. Whereas, for color assessment, tuna fish fillets show very red color (as an indicator of freshness) which is very drastic on the 6th day. But with this condition, tuna fillet with N₂ gas produces a high value of a while whereas CO₂ produces a high value of b. Based on the results of the study, N₂ and CO₂ gas made it possible to combine on tuna fillets during storage. Where N₂ and CO₂ when used in storage are suitable to be applied at temperatures higher than the boiling point, so that the two gases will in the form of gases have ability to freeze organic matter and include maintaining the quality of fish.

INTRODUCTION

According to the Ministry of Maritime Affairs and Fisheries, in 2011 to 2014 the fisheries sector experienced continuous growth, in terms of capture fisheries growth from 2011 to 2014 was 4.74%, 3.67%, 7.24%, and 7.66% [1]. fishery products have perishable characteristics and are different from other sectors, so a special approach is needed for the handling process, one of which is maintaining quality. Safeguarding fish quality or controlling fish quality is also one of the priority programs of the Ministry of Maritime Affairs and Fisheries of the Republic of Indonesia in 2018 [2]. In addition, according to the Ministry of Maritime Affairs and Fisheries from 2010 to 2014, there was an increase

in fish consumption with an average growth of 5.78% so that the need for quality control on fish supply chain actors to keep maintaining increased fish consumption in Indonesia [1].

In capturing these opportunities, of course the government needs to build adequate infrastructure to support the national fisheries business. In addition, business actors need to understand the pre-harvest process to obtain high fish production and good product handling processes in relation to maintaining the quality of fish up to the hands of consumers. According to FAO, post-harvest handling, processing, preservation, packaging, storage and transportation of fish require special care to maintain the quality and nutritional attributes of fish, avoid waste and losses experienced [3]. One important activity that businesses need to understand is the process of preserving and packaging fish to reduce the rate of spoilage that occurs so that it is possible to be distributed and marketed throughout the world.

Fish is a commodity that has a high protein and water content so that this commodity is a commodity that is easily damaged. The process of preserving and packaging becomes a critical point in the process of handling fresh fish, where producers need to understand the preservation techniques that are able to minimize their impact on the product and packaging techniques that are able to optimize the shelf life of fish, especially during the distribution process. Fresh fish that are allowed to stand at room temperature for a certain period of time can trigger odor appearance and also result in a decrease in freshness and quality of fish. The higher the temperature, the faster the fish will begin to emit unwanted odors. One method that can be used to maintain fish quality is to apply a combination of industrial gas in the preservation process and its packaging techniques. In this study, industrial gas application will be carried out on tuna to see its effect on quality. The objectives of this study are 1) measuring tuna fillet discoloration with industrial gas applications and 2) analysing the organoleptic characteristics of tuna fillet based on industrial gas treatment.

RESEARCH METHOD

The object taken in this study is tuna (*Thunnus albacores*). Determination of the area of fish sampling is on the island of Java, especially on the coast of the island of Java. Materials used in this study were tuna fillets, industrial gas N₂, CO₂, O₂, and Mixed Gas (30% N₂, 30% O₂, 40% CO₂) and vacuum packaging. While the equipment used in this study is the chromameter Konica Minolta and freezer as storage. Color testing was carried out after the application of industrial gas in tuna fillets. There are two color testing methods carried out in this study, namely organoleptic testing carried out by 30 panellists, and color testing using chroma meters for 12 days of storage. This study applies the Modified Atmosphere Packaging method. Modified Atmosphere Packaging (MAP) is the air inside the packaging is replaced by a specific gas or a mixture of gases that differ from the air composition. The proportions of each gas are established, the mixture is introduced into the packaging and no further control is carried out during storage [4].

RESULT AND ANALYSIS

Modified Atmosphere Packaging method has been applied to tuna by adding industrial gas N₂, CO₂, O₂, and Mixed Gas (30% N₂, 30% O₂, 40% CO₂) in vacuum packaging. As an evaluation step, organoleptic quality testing and color testing using chromameter is carried out. Organoleptic testing was carried out by 30 panellists who tested quality attributes, namely the attributes of color, odor, texture, and overall. Tests are carried out using scoring, with a rating score of 1 to 9. Based on the organoleptic test results of tuna, panellists prefer fish with the addition of N₂ gas treatment on each storage day it is characterized by the highest score compared to other gas treatments. Meanwhile, the treatment of O₂ gas and mixed gas for color attributes is less preferred by consumers, it can be seen that the assessment score is quite low and the value always decreases dramatically from day 0 to day 12 storage. For fish and fishery products, most gas mixtures do not include oxygen because high oxygen systems, in most cases, provide limited benefit to shelf life extension of fishery products [5,6]. This may be explained by the high rate of perishability of seafood, which results from

psychrophilic spoilage bacteria growth that is combined with muscle degradation by endogenous enzymes and oxidative deterioration of the lipids, often rich in highly unsaturated fatty acids [7]. Furthermore, on the odor attribute there is also a significant difference in the level of consumer preference on each gas treatment and storage day. In this attribute, panellists prefer fish without the addition of gas treatment. In tuna, additional mixed gas treatment is not preferred by panellists on each storage day.

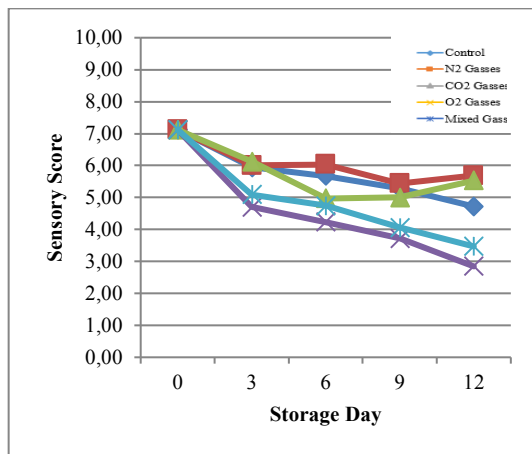


Figure 1. Sensory test score results for color attribute

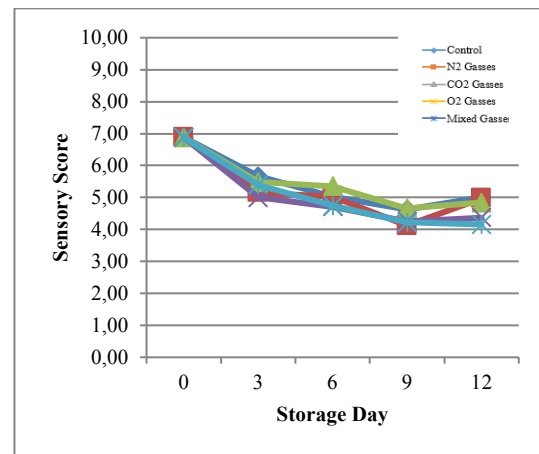


Figure 2. Sensory test score results for smell attributes

In texture attributes, the treatment of industrial gas in tuna does not provide a significant difference in the level of panellist preference, meaning that industrial gas administration does not significantly affect the quality of tuna in terms of texture. To attribute this texture to the whole fish, panellists also prefer fish texture without the addition of industrial gas treatment. Then for fish with the addition of mixed gas and O₂ treatment has the lowest scoring results compared to other gas treatments. The last sensory testing attribute is the overall attribute. In this attribute, for tuna, the additional treatment of N₂ gas can maintain the level of consumer preferences on days 6 to 12 and the tuna with additional N₂ gas treatment has the highest sensory testing score compared to other additional treatments. Based on the results of this study, the application of industrial gas only affects the preference of panelists on the color attributes and overall attributes. Therefore, the need for further measurements on the color attributes to determine changes in quality in more detail in tuna.

Overall, the test results show that fish with MAP treatment can maintain a longer shelf life when compared to fish without MAP treatment. Better results if fish with MAP treatment are stored at temperatures below 0°C. It is well established that holding seafood at the super chilled temperature range, which is defined as the range of temperature below 0°C and slightly above the temperature in which freezing is discernible [8], leads to longer shelf life extension than that achieved for product held under optimal refrigerated temperatures [9]. As stated by Davis, fish spoil more than twice as fast at 5°C than at 0°C, and four times as fast at 10°C [10].

This color test is carried out using a chromameter that produces three assessment outputs, namely the value of L, value a, and value b. The L value indicates the brightness level of the shrimp where the higher the L value, the brighter the color of the shrimp. From the results of the measurement of the value of L it is known that in all treatments in the sample always decreased brightness during the storage period. The N₂ gas treatment in tuna gives the highest L value compared to other treatments.

A positive value on the chromameter shows the intensity of the red color that is getting stronger, while a negative value shows the intensity of the green color that is getting stronger. In tuna samples, from day 0 to day 3 showed a positive trend especially in fish given additional CO₂ gas treatment.

However, a drastic decrease in the level of red color occurs on the 6th day, this indicates that the fish are not well consumed because there is an indication of a decrease in quality in terms of color appearance.

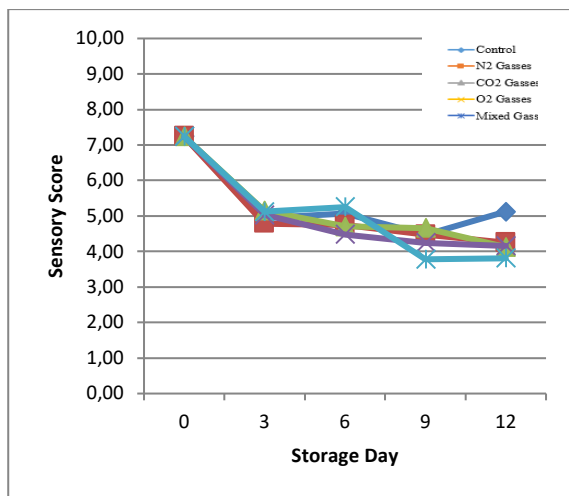


Figure 3. Sensory test score results for texture attributes

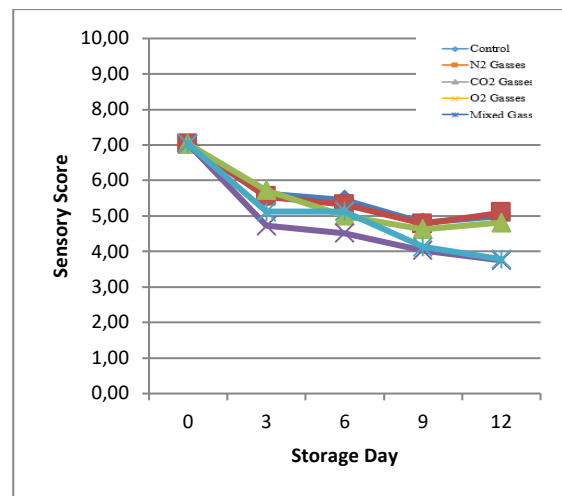


Figure 4. Sensory test score results for overall attributes

Furthermore, for the measurement of the positive b value on the chromameter shows the intensity of the yellow color that is getting stronger, while the negative value of b shows the intensity of the blue color that is getting stronger. In tuna, the N₂ gas treatment gives the highest value of b compared to other gas treatments.

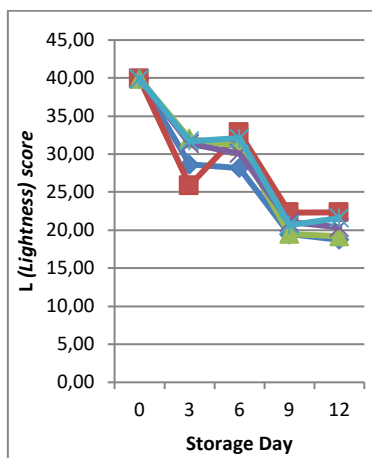


Figure 5. The value of L score in tuna fish

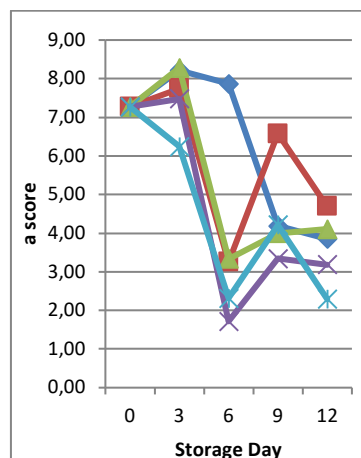


Figure 6. the value of a score in tuna fish

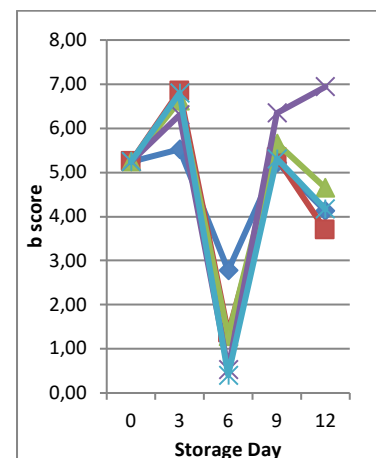


Figure 7. The value of b score in tuna fish

The conclusion is the color measurement is good fish consumed before the 6th day, because after the 6th day there has been a decline in the quality of fish, especially in terms of color. Then, for tuna fish the addition of N₂ gas can increase the brightness of the fish's color appearance.

CONCLUSION

The result of the study is, the application of industrial gas only affects the preference of panelists on the color attributes and overall attributes. Therefore, the need for further measurements on the color attributes to determine changes in quality in more detail in tuna. Overall, the test results show that fish with MAP treatment can maintain a longer shelf life when compared to fish without MAP treatment. The conclusion is the color measurement is good fish consumed before the 6th day, because after the 6th day there has been a decline in the quality of fish, especially in terms of color. Then, for tuna fish the addition of N₂ gas can increase the brightness of the fish's color appearance.

REFERENCE

1. Ministry of Maritime Affairs and Fisheries. 2015. Analysis of Marine Fisheries Data. 2015. Jakarta: Center for Statistical Data and Information
2. Ministry of Maritime Affairs and Fisheries. 2018. Indonesian Fisheries Productivity. In the 9th Merdeka Barat Forum Presentation of the Ministry of Communication and Information
3. FAO. 2016. The State of World Fisheries and Aquaculture 2016. Food and Agriculture Organization of the United Nations: Rome.
4. Silliker, J. H. and Wolfe, S. K. Microbiological safety considerations in controlled-atmosphere storage of meats. *Food Technology*, 1980, 34, 59-63.
5. Kropf, D.H.; Mancini, R.A. Packaging: Modified and controlled atmosphere. In Encyclopaedia of Meat Sciences, 2nd ed.; Dikeman, M., Devine, C., Eds.; Elsevier Academic Press: New York, NY, USA, 2014; Volume III, pp. 9–12.
6. Tsironi, T.; Tsevdou, M.; Velliou, E.; Taoukis, P. Modelling the effect of temperature and CO₂ on microbial spoilage of chilled gilthead seabream fillets. In Proceedings of the IV International Symposium on Applications of Modelling as an Innovative Technology in the Agri-Food-Chain: Model-IT 802, Madrid, Spain, 9–11 June 2008; pp. 345–350.
7. Davis, H.K. Fish and shellfish. In Principles and Applications of Modified Atmosphere Packaging of Foods, 2nd ed.; Blackstone, B.A., Ed.; Blackie Academic and Professional: London, UK, 2009; pp. 194–239.
8. Kaale, L.D.; Eikevik, T.M. The development of ice crystals in food products during the super chilling process and following storage, a review. *Trends Food Sci. Technol.* 2014, 39, 91–103.
9. Sivertsvik, M.; Rosnes, J.T.; Kleiberg, G.H. Effect of modified atmosphere packaging and super chilled storage on the microbial and sensory quality of Atlantic salmon (*Salmo salar*) fillets. *J. Food Sci.* 2003, 68, 451–458.
10. Davis, H.K. Fish and shellfish. In Principles and Applications of Modified Atmosphere Packaging of Foods, 2nd ed.; Blackstone, B.A., Ed.; Blackie Academic and Professional: London, UK, 2009; pp. 194–239.

ACKNOWLEDGMENT

Authors wish to acknowledge financial support from Ministry of Research, Technology and Higher Education of the Republic of Indonesia through Universitas Gadjah Mada Grants of “Penelitian Terapan Unggulan Perguruan Tinggi” No. 2769./UN1.DITLIT/DIT-LIT/LT/2019.

IDENTIFYING SOYBEAN (*Glycine max L. Merr*) BY COLOR ANALYSIS IN SUPPLY CHAINS TO IMPROVE CONSUMER PREFERENCES

Novita Erma Kristanti¹, Annisa Nurul Ghifari²

¹Lecturer at Department of Agroindustrial Technology, Faculty of Agricultural Technology, Universitas Gadjah Mada, Indonesia

²Student at Department of Agroindustrial Technology, Faculty of Agricultural Technology, Universitas Gadjah Mada, Indonesia

*Corresponding author: Novita Erma Kristanti, e-mail : novita_erma@ugm.ac.id

Keywords: quality, soybeans, supply chain, color, consumer preferences

ABSTRACT

Agricultural commodities affect the nutritional status and health of the population, especially through the production of food. Demand for soybean consumption in Indonesia every year to increase more than 2.2 million tons per year. The quality of food is determined by four factors, namely color, flavor, texture, and nutritional value to increase sensory acceptability factors because they are directly perceived by senses (Bourne, 2002). This study aims to identifying color measurements at each tier of the soybean supply chain and determine strategies for increasing consumer preferences.

The research method is descriptive quantitative with a convenience sampling through in-depth interviews to responden in each tier in the soybean supply chain. They are farmers, collectors, cooperatives, traders and fermented soybean processing industries consisting of fermented soybean and animal feed industries in soybean production centers in Indonesia. Measurement the soybean color test using the Minolta brand colorimeter CR-400. The colorimeter tool has a working principle such as, a spectrophotometer that has a relation with filters X, Y, and Z. This tool is equipped with direct integration for conversion of values L, a, and b. The value of consumer preference is determined by the consumer perception test using a sensory test with the value of the Likert scale score from 1 until 5. The score of 5 indicates very like.

Analysis of color test results from each tier of the soybean supply chain requires data correlation test analysis so that the resulting data is more accurate. This analysis uses L data as the dependent variable and Chromameter value, a and b as independent variables and the results show that the R value (correlation coefficient) is 0.993, which means that the dependent and independent variables can be categorized as having a very strong correlation. The results of the calculation show that the tier of fermented soybean industry has the color content (L) 56,456, (a) 5,666 and (b) 19,626 with the level of consumer a preference score of 4.5. The highest tier in supply chain is cooperative are color content (L) 57,876 (a) 5,967 and (b) 23,27 with a preference score of 4.8. It is means a manage inventory of soybeans and efficient supply chain in tiers can affect the quality of colors soybean for to improve consumer preferences.

I. INTRODUCTION

Soybean (*Glicine max L.Merr*) is a food commodity as raw materials for the food of the people because is being a healthy source of vegetable protein, is also known as cheap and affordable by most people of Indonesia. Soybean production declined sharply since 1992 until today, from 1.87 million tons to only about 700 thousand tons. Demand for soybean consumption in Indonesia every year to increase more than 2.2 million tons per year. Currently, Indonesia has one of the largest soybean importers in the world. Every year the number of imported soybean average of over 1 million tons of the total average of over 2 million tons (Anonymous, 2013). Processed soy products, among others, tempeh, tofu, soybean milk and others. Soybean self-sufficiency is a government program that will be achieved in 2017. The compliance efforts including through the development of soybean seed production in soybean production centers, improvement of postharvest management to improve the quality of soybean yield and policy support. In general, business actors in soy trade system can be classified into several, namely farmers, traders, middlemen traders / wholesalers, cooperative, distributors, importers and retailers.

Color is an important quality aspect of food, both food that is processed at the factory and those that do not undergo processing. Color is an attribute of quality that together with texture and flavor has an important role in the reception of a food. Color provides clues to chemical changes in a food such as changes that occur during heating, namely browning and caramelization (De Man, 1999).

Color is the perception felt by the human visual system that is influenced by three factors, namely the source of light, reflection of the sample, and the visual sensitivity of the observer (Gunasekaran, 2003). Color from the light spectrum, which is the distribution of light energy and wavelengths that interact with the eye. Color has a certain electromagnetic wavelength between 380 nm to 780 nm and occupies a 3 (three) dimensional space namely the type of color, color saturation, and brightness or turbidity of the color (Hoffman, 2013). The type of color (hue) is a sensation received by the human neural network in the form of shades, such as red, yellow, green, and others.

Color saturation (chroma, saturation) is a sensation of the weakness of color with white, black, and gray is a color with a color saturation close to 0 (zero). Brightness or color turbidity (value, lightness, brightness) is a clear, turbid sensation of color. The RGB color model is a color model based on the concept of adding strong primary light namely Red, Green, and Blue to form a broad array of colors such as cyan, magenta, and yellow. The concept of RGB color is often found on various equipment such as televisions, photo cameras, computer monitors, and color scanners. In the computer program calculation, the color model is presented with the component values, as in RGB (r, g, b) each value is between 0 and 255 so each component has 256 levels. When combined, there are 256x256x256 or 16,777,216 RGB color combinations that can be formed. There are some weaknesses in the RGB color system, which are calculations for RGB which are quite complex, and are not good for representing images based on human vision because humans do not see objects on a combination of red, green and blue colors (Yam, 2004).

The color diagram: $L^* a^* b^*$ can be illustrated in Figure 1 below:

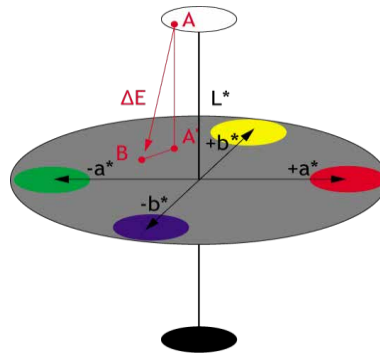


Figure 1. Color Chart $L^*a^*b^*$

II. METHOD AND MATERIAL

1. Identification of problems and setting goals
Identify the problems that exist in the supply chain in soybean commodities and their relation to the quality of soybeans during the distribution process and examine them so that they are right on target and can set the objectives of the research to be conducted.
2. Literature and literature studies
Literature study is conducted to support the steps taken in solving problems, which include literature studies on supply chain management and soybean quality. This literature study was obtained through books, journals, websites and other supporting information.
3. Determination of research objects and areas
The object and region in this study are the supply chain of yellow soybean commodity in Central Java and Yogyakarta Special Region. The determination of this region is based on the presence of a large enough soybean commodity production center in the area as illustrated in
4. Identification of tiers in the supply chain
Identification of tiers in the soybean commodity supply chain in Central Java is carried out through supply chain tracking from farmer to consumer level. This identification is done to make it easier to find information, data and determine logistical activities according to their level.
5. Data collection
Data collection begins with conducting interviews with supply chain actors regarding the flow of goods used. In addition, soybean samples were taken in each tier and research was conducted at the Laboratory. Secondary data is needed to find out the data on Indonesian national standard quality for soybeans and data from Central Java. Color measurement in tier soybean.
6. Analysis of results
From the results of quality observations in each tier will be obtained results in the form of data that can be used for further processing for data analysis and can be seen how the condition of soybean quality in each supply chain tier and soybeans as what is the best quality.

III.RESULT

Before analyzing the color test results of each grobogan variety soybean supply chain tier, data correlation test analysis is needed. This analysis uses L data as dependent variables and chroma values, a and b as independent variables and the results show that the value of R (correlation coefficient) is 0.993, which means that the dependent and independent variables can be categorized as having a very strong linear relationship

After the correlation test is done and the results have a very strong correlation, the next step is to be able to do color analysis on each soybean tier

Table 1. Test Result Soybean Color in Each Tier

No	Location	Average		
		L	a	b
1	Tier 1 (Farmer)	59.156	2.976	23.78
2	Tier 2 (Collectors)	58.84	4.567	21.073
3	Tier 3 (Traders)	57.433	3.8	20.8
4	Tier 4 (Cooperative)	57.876	5.967	23.27
5	Tier 5 (Wholesalers)	57.33	4.36	19.01
6	Tier 6 (Soybean Industry)	56.053	4.833	19.87

The soybean color test was carried out using the Minolta type CR-400 colorimeter. The colorimeter tool has a working principle such as, a spectrophotometer which has a reluctant with filters X, Y, and Z. This tool is equipped with direct integration for the conversion of values of L, a, and b.

1. Farmers

Because of the good storage process, the colors found in Farmers obtained L = 59,156, a = 2,967 and b = 23.78. From the L test results obtained 59,156 results in which the susceptibility of the luminance or lighting component values from 0 (black) to 100 (white) and indigo a * shows 2,967 two chromatic components namely a * (from green to red) and b * shows 23.78 (of blue to yellow) which varies in value from -120 to 120. So it can be concluded that the color of this soybean is yellow and bright. There is no green or red color.

2. Traders

At this collector's location soybeans were also tested using chromameter colors and the results obtained L = 58.84, a = 4,567 and b = 21,073. From these results it can be said to be almost the same as the previous tier situation.

This insignificant color change can be influenced by similar storage factors. At farmer level, soybeans are stored in the conductor and no air can enter. Then at the level of collectors, soybeans are stored in white sacks and are equally protected by sunlight or air so that the color difference is also not so significantly different.

3. Wholesalers

Wholesaler level, values of L = 57,433, a = 3.8 and b = 20.8 are obtained. At this location, large traders also store soybeans for 2-3 months for existing stock and for several months experience the difference in color from soybean seeds. But despite the differences in the way of storage there was no significant change in the value of L. Soybeans in this location are still in good condition for the brightness level.

4.Soybean Industry

Laboratory test results for soybeans in this location are L = 56,053, a = 4,833 and b = 19.87. Soybean used to make tempeh here has a bright color not much different from other soybeans. This is because soybeans brought in these industries already meet the requirements of soybean quality standards and

are good for processing into soybeans. The average color values in the last tier are almost the same because they are in the last tier ready to be consumed by consumers

Based on the results of testing the quality of soybeans, it is known that local soybean quality is better than imported soybean, especially for acceptance in the processing industry and tofu. The use of imported soybean motivated limited supply of the local soybean. In fact, in terms of quality of the final product, more local soybean providing good quality color, texture better and more advantageous in terms of cost.

CONCLUSION

A manage inventory of soybeans and efficient supply chain in tiers can affect the quality of colors soybean for to improve consumer preferences, Soybean Color measurement very important to improve consumer preferences, The highest tier in supply chain is cooperative are color content (L) 57,876 (a) 5,967 and (b) 23,27 with a preference score of 4.8.

ACKNOWLEDGEMENT

The research team thanks to everyone who contributors as research founder from Universitas Gadjah Mada and supporting from all respondents to all participation, especially to Anisa Ghifari as member of team

REFERENCES

1. Adam Tim, dan Goyal Vidhan K. 2003. *Investment opportunity set and its proxy variables: theory and evidence. Working Paper. Department of Finance.* Hong Kong University of Science & Technology, 1–35.
2. De Man, J.M. 1999. *Principles of Food Chemistry.* Westport, Connecticut: The AVI Publishing Company Inc.
3. Hoffman, G. 2013. *Gamut visualizations and Out-of-gamut Distances.* Retrieved June 26, 2014, from http://www.inf.ufes.br/thomas_graphics/Postscript/GenoHoffman/gamshow.pdf.
4. Hunter Lab. 2008. *Colorimeters versus spectrophotometers.* Retrieve Mei 13, 2014, from Hunter Lab website: http://www.hunterlab.com/appnotes/an03_95r.pdf.
5. Hutching, J.B. 1999. *Food Color and Appearance 2nd ed. A Chapman and Hall Food Science Book, an Aspen Publ.* Gaithersburg: Maryland.
6. Yam, K.L, dan Papadakis S.E. 2004. *A simple digital imaging method for measuring and analyzing color of food surface. Journal of Food Engineering* 61, 137–142.

CHILI COLOR AND SPICINESS

Nafis Khuriyati* M. Affan Fajar Falah, Mirwan Ushada, and Bayu Kristiawan

*Department of Agroindustrial Technology, Faculty of Agricultural Technology, Universitas Gadjah Mada,
Indonesia
Flora street No.1, Bulaksumur Yogyakarta, Indonesia 55281*

*Corresponding author: Nafis Khuriyati, nafis.khuriyati@ugm.ac.id

Keywords: Chili, color, capsaicin, spiciness

ABSTRACT

Chilies are a commodity that is closely related to the spicy taste. Various dishes contain chilies as the enhancer of their taste. Chilies contain nutrients that are important for health, one of which is capsaicin which gives a spicy flavor and aroma to the chilies. The spicy level is often associated with chili colors because colors are the attributes that are first used by consumers to assess the chilies' quality. This paper aims to determine the relationship between the colors of chilies and their level of spiciness represented by the capsaicin content. Chilies (*Capsicum annum* L var. Helix) from various levels of ripeness with a range of colors from green until red were used as samples. Sample measurements were conducted on two kinds of chili properties, physical and chemical. The physical property was colors measured by using chromameter while the chemical property was the capsaicin content measured by using the Thin Layer Chromatography method. Multiple Linear Regression was applied to determine the relationship between colors and capsaicin. The spiciness of the chilies represented by the capsaicin content could be determined based on the chili colors, especially the green and orange chilies.

INTRODUCTION

Chilies (*Capsicum annum* L.) are one of the horticultural plants, which belong to a vegetable type, that have small-sized fruit with a spicy flavor and the main seasoning for Indonesian cuisine. The chemical composition of a fresh chili consists of calories, protein, fat, sugar, calcium, phosphorus, iron, vitamin A, vitamin B, vitamin C, and water. In addition, chili also contains a mixture of alkaloids containing capsaicinoid, capsantin, carotenoids, alkaloids, resins, essential oils. Components in chili that cause spicy taste are capsaicinoid. Among the components in capsaicinoid in fresh chili are capsaicin and dihydrocapsaicin, which account for 90% of the total sources of spiciness [1].

During this time, the quality of a chili is determined by its color, size, shape, and defect level. A color is the first quality attribute in food that is evaluated by the consumer; therefore, it is an important component of food quality that can determine the market's acceptance. Chili colors reflect chillies' level of freshness and maturity [2]. People evaluate a food product based on visual perception to predict the taste of the product as a way of making a decision whether the product will be consumed or not. Given that chilies are as a source of nutrition, their appearance in terms of colors is expected to predict their nutritional content as well.

People often conclude that the redder the chili color, the higher the level of spiciness. The content of capsaicin, as determined by the Bajaj method [3], in ripe fruit is generally higher than that of green fruit. A chili contains 0.1% -1% spicy taste that comes from the content of capsaicin and dihydrocapsaicin substances. Compared with the large chili and paprika, the capsaicin content in cayenne peppers is quite higher than that of the two other chillies [4]. The chilli quality parameters based on SNI 4480-2016 have not considered the content of capsaicin (spiciness level) and there is no classification of quality levels based on spiciness according to the Scoville Heat Unit (SHU) because the technology is not yet available. Therefore, spiciness can be used as one of the new parameters to determine the quality classification of chillies. This study aims to develop mathematical models that are able to predict the content of a chili which includes capsaicin based on L *, a *, and b color values. The results of this study can also be used as a basis for developing nondestructive methods in determining the content of chillies.

MATERIAL AND METHODS

Material

The chili samples (*Capsicum annuum* L var. Helix) were obtained from coastal area of Bugel Village in Kulon Progo Regency, one of the highest chilli producing area in Yogyakarta Special Province, Indonesia. Sampling was done in the afternoon from 15.00 to 16.00 WIB (Western Standard Time) when the harvesting activity by farmers was taking place. The samples were chillies in their various growing stages with color variations of green, dark green, green tinge of red, orange, red, and dark red. Samples were brought into a laboratory for measurements.

Physical and chemical properties measurement

Sample measurements were conducted on two kinds of chili properties, physical and chemical. The measured physical property was colors and chemical property was capsaicin content. The color was measured using chromameter (Konica Minolta CR-400). Measurement of each sample was taken at three points namely the tip, middle, and base of a chili. The capsaicin level was measured using Thin Layer Chromatography (TLC) method.

Development of Prediction Model

The all color data generated from the measurement with the chromameter were used as the calibration dataset to construct models for capsaicin level by using the Multiple Linear Regression (MLR). The MLR was chosen because independent variables (X) were used more than two times and the dependent variable (Y) was only once. Multiple linear regression model can be expressed in the following general form:

$$Y = \beta_0 + \beta_1 X_1 + \beta_2 X_2 + \dots + \beta_k X_k + e \quad (1)$$

where k denotes the number of variables in the model.

The goal was to discover the regression coefficient β that has a minimal e. The program used to perform multiple linear regression analysis was IBM SPSS 23. The accuracy of the models were assessed using R^2 .

RESULTS AND DISCUSSION

Sample Characteristics

The measurement of physical properties included the parameter of length, diameter, and weight that were used to determine the characteristics of 117 samples (Table 1).

Table 1: Sample characteristics

	Length (cm)	Diameter (cm)				Weight (g)
		Base	Middle	Tip	Average	
Minimum	6.70	0.05	0.45	0.11	0.32	1.260
Maximum	16.10	0.95	0.93	0.75	0.71	4.78
Mean	10.62	0.47	0.67	0.34	0.49	3.00
Standard Deviation	1.61	0.26	0.09	0.22	0.0	0.77

The 117 chili samples were grouped into six categories based on the color (green, dark green, green tinge of red, orange, red, dark red). Until now there has been no classification of chili colors, so that in this study the grouping of chili color was based on the observation of color changes during the growth of chili. Each color group consists of some sample groups. The total number of sample group was 30. The grouping was performed because of the weight of one chili was not sufficient for testing the chemical content, so that each test sample (sample group) consisted of several chilies as shown in Table 2.

Table 2: Sample grouping

Color group	Number of sample	Number of sample group	Average of weight per sample group (g)
Green	21	5	2.73
Dark Green	23	5	2.89
Green tinge of red	28	7	2.82
Orange	21	5	2.76
Red	15	5	3.69
Dark Red	9	3	3.92
Total	117	30	

Chili Color

The result of color measurement by using chromameter in each color group can be seen in Table 3. The table shows different values of L* a* b in each color group. The a* values in the green group are all negative, which means the chili is green. This is also the case for dark green sample groups.

Table 3: Color of chili sample

Color Group	L*	a*	b*
Green	32.92±1.87	-9.21±2.42	17.20±3.36
Dark green	29.07±0.56	-3.24±5.15	12.10±1.72
Tinge	30.33±3.91	22.05±7.04	15.35±3.73
Orange	20.00±1.88	37.19±3.37	34.98±0.82
Red	36.80±2.15	37.57±3.14	24.54±3.36
Dark red	34.95±0.58	36.33±0.76	18.98±0.21

Capsaicin content

The test used a total of 30 samples consisting of a combination of several chilies grouped based on colors and levels of the ripeness of chilies. Descriptive statistics of capsaicin content can be seen in Table 4. The content of capsaicin tends to increase following the color change from green to orange

which then decreases to red green. This is consistent with the research conducted by Sukrasno, et al. [5] which discovered that the capsaicinoid content was affected by fruit age; the highest content was found in old but unripe fruit, which is characterized by a change in color from pale green or yellow to red.

Tabel 4: Capsaicin content (mg/100g)

	Colors of Chili Sample					
	Green	Dark Green	Tinge	Orange	Red	Dark Red
Minimum	449.790	162.030	109.010	395.900	351.770	71.570
Maximum	569.040	606.290	747.920	592.480	490.620	284.940
Range	119.250	444.260	638.910	196.580	138.850	213.370
Average	486.146	302.234	390.999	494.018	442.520	153.217
Standard Deviation	48.923	181.881	266.065	75.974	53.167	115.163

Prediction Model for Capsaicin Level

The L*a*b values obtained from the chromameter are associated with capsaicin using multiple linear regression. The regression models of capsaicin with L*, a*, and b as the independent variables are shown below.

$$\text{Capsaicin} = 432.918 - 8.077 L^* - 2.810 a^* + 15.157 b^* \quad (2)$$

Table 5: Performance of prediction model.

Statistic metrics	Capsaicin model
R	0.275
R ₂	0.076
Adjusted R ₂	-0.031
Standard error	183.579

The correlation value between variables is 0.275 and the percentage of the effect of the independent variable on the dependent variable (R₂) is 0.076 which means the influence of the independent variable on the dependent variable is 7.6% and the rest is influenced by other variables. Based on the results of the F-test, the model is not good for predicting capsaicin content. Previous research showed that the models for predicting vitamin C and total carotene content had adjusted R₂ values into 0.893 and 0.675. Both models can be used to predict the chemical content of chilies ranging from green to red [6].

Because model (2) cannot be used to predict the capsaicin content, the color change approach that occurs in chilies is from green to red. The models in each color group are obtained as in the table below.

Tabel 6: Model Regresi Chromameter Capsaicin Setiap Perubahan Warna

Color group	Prediction Model	R ₂
Green	$\hat{Y} = 3513.771 - 95.553 L^* - 190.612 a^* - 95.103 b^*$	0.964
Dark green	$\hat{Y} = 5581.608 - 172.834 L^* - 4.970 a^* - 22.347 b^*$	0.400
Tinge	$\hat{Y} = - 2119.974 + 149.938 L^* - 7.722 a^* - 131.503 b^*$	0.799
Orange	$\hat{Y} = 2991.230 - 86.589 L^* - 13.671 a^* + 46.026 b^*$	0.987
Red	$\hat{Y} = 2155.361 - 107.322 L^* + 11.436 a^* + 73.581 b^*$	0.704

The capsaicin content could not be predicted from all color groups based on L, a, and b values. Only from the green and orange color groups that it could be predicted very well because they had R₂ value above 0.900 while the R₂ value the other color groups were still below 0.800.

CONCLUSION

The capsaicin content that represents the spiciness of chili (*Capsicum annum* L) can be predicted based on the colors of L* a* b* for the green and orange color groups.

ACKNOWLEDGEMENT

This research was financially supported by Ministry of Research, Technology, and Higher Education of the Republic of Indonesia via 2018 Research Grants of Penelitian Terapan Unggulan Perguruan Tinggi-Universitas Gadjah Mada 2018 (No 1943/UN1/DITLIT/DIT-LIT/LT/2018).

REFERENCE LIST

1. Handoko, L. P., Variyana, Y., Mahfud. (2017). Studi efektifitas ekstraksi (Capsaicin) dan cabai (Capsicum) dengan metode MASE (microwave assisted soxhlet extraction) [Study on the effectiveness of extraction (Capsaicin) and chili (Capsicum) with MASE (microwave assisted soxhlet extraction method)]. *Jurnal Teknik ITS*, 6(2), 384-386 (in Bahasa)
2. Wu, D., Da-Wen, S. (2012). Colour measurements by computer vision for food quality control. *Journal of Food Science and Technology*, 29, 5-20
3. Bajaj, K. L. (1980). Colorimetric determination of capsicum fruits. *Journal of the association official Analytical Chemists* 63, 1314-1316
4. Cahyono, B. (2003). *Cabai Rawit : Teknis Budidaya dan Analisis Usaha Tani*. [Chili: Cultivation Techniques and Analysis of Farming Enterprises]. Yogyakarta: Penerbit Kanisius. (in Bahasa)
5. Sukrasno, Kusmardiyani, S., Tarini, S., Sugiarto, N. C. (1997). Kandungan kapsaisin dan dihidrokapsaisin pada berbagai buah capsicum. [The content of capsaicin and dihydrocapsaicin in various capsicum fruit]. *JMS*, 2(1), 28-34. (in Bahasa)
6. Khuriyati, N., M. Affan F.F., Mirwan, U., Bayu, K., Nugrahanto., A.W., (2018). Color as a predictor of chili content. Proceeding of the 2nd International Conference on Tropical Agriculture, 43-52.

OPTIMIZATION OF BLUE RICE PRODUCTION USING TAGUCHI METHOD

Wahyu Supartono and Devina Fitria Nikasari

Department of Agroindustrial Technology – Faculty of Agricultural Technology
Universitas Gadjah Mada – Yogyakarta 55281 – INDONESIA

*Corresponding author: Wahyu Supartono, wstono@ugm.ac.id

Keywords: Blue rice, butterfly pea, Taguchi method, Optimization

ABSTRACT

Recently trend of food diversification increases significantly, so that the new food products with their uniqueness are promoted into the market. One of them is blue rice, which is produced from rice and blue coloring agent by using butterfly pea (*Clitoria ternatae*) flower. This blue flower could be used as natural and organic food coloring agent and it is already applied in several foods within ASEAN countries such as Indonesia. The plants are grown easily founded in this region. Normally they will be dried by sun drying for several days before extracted to become coloring agent.

This research was aimed to find out “best formula” for producing blue rice that was prepared with butterfly pea flower by soaking them at certain temperature and time. The main goal was to determine the best combination of type of rice, concentration of butterfly pea, length of soaking time and temperature applied in the solution. Taguchi Method was conducted to find best combination among factors that were chosen in this experiment. Four factors (type of rice, concentration, time and temperature) were applied with 3 treatments, so that there were 9 experiments were conducted. Parameters for final products were color and texture of rice. The blue color was measured using Chromameter with L-a-b and texture was determined by Universal Testing Machine

The results of this research showed that the blue color of rice (-b value) were: -12,21 ; -11,25; -9,56; **-13,43**; -11,87; -11,31; -13,13; -10,31; -9,34. If the highest value of blue color was used as main parameter of this rice, so the best combination were achieved by type of rice (premium quality: *Pandan Wangi*), concentration 11X dilution of main solution (6 g dried butterfly pea flower powder/L), soaking time 30 minutes and temperature of solution 50°C.

INTRODUCTION

Rice is staple food for Indonesian society, so they have a proverb “they are not eating yet, if they do not consume rice”. Rice has been cooking in many variations for daily consumption, which is processed in traditional ways like yellow rice. This rice is cooked with coconut milk and colored by using curcumin. Currently colored rice becomes new trend in Indonesian culinary, such as green and blue rice that is cooked with natural coloring agent and served with some Indonesian foods.

Blue rice is becoming popular parallely with development of Indonesian culinary, so the food providers are trying to show their uniqueness and specialty in their foods and drinks. The blue rice is produced by adding blue coloring agent extracted from butterfly pea flowers. The color will enhance product performance and consumer attraction, so they are trying to use coloring agents as tool for innovation.

Butterfly pea (*Clitoria ternatea L.*) is tropical plant that is easily grown and founded in the ASEAN countries. The blue flower served as an organic coloring agent as well as antioxidant provider, that have positive medical effect on certain diseases. This flower is used in Thailand as

natural coloring agent (Kungsuwan, 2014). It contains anthocyanin as red, purple and blue pigment. It grows in Java island and uses as coloring agent for blue rice.

The research was aimed to find good combination to produce blue rice with butterfly pea flower powder. Quality parameter of blue rice such as color, texture and change of rice will be optimized. The optimization was focused on rice variant, butterfly pea concentration, time for soaking and temperature when the soaking process starts.

METHODOLOGY

This research was conducted at Laboratory of Quality Analysis and Standardization – Department of Agroindustrial Technology – Faculty of Agricultural Technology – Universitas Gadjah Mada. It was aimed to find out “best formula” for producing blue rice that was prepared with butterfly pea flower by soaking them at certain temperature and time. The main goal was to determine the best combination of type of rice, concentration of butterfly pea, length of soaking time and temperature applied in the solution. Sample of butterfly pea flowers was provided by farmers from Sleman District – Yogyakarta, who supply thee flowers to restaurant in Yogyakarta area.

The Taguchi Method was conducted to find best combination among factors that were chosen in this experiment. Four factors (type of rice, concentration, time and temperature) were applied with 3 treatments, so that there were 9 experiments were conducted. Parameters for final products were color and texture of rice. The blue color was measured using Chromameter with L-a-b and texture was determined by Universal Testing Machine. The Design for experiment by using Taguchi Method was as follow;

Table 1. Levels of Factors in the research

Factor	Code	Level 1	Level 2	Level 3
Type of rice	A	<i>C4</i>	<i>Pandan Wangi</i>	<i>Menthik Wangi</i>
Butterfly pea concentration (g/L)	B	6.1	4.2	3.2
Soaking time (min)	C	15	30	60
Soaking temperature (°C)	D	25	40	50

Based on these factors and levels in the research, the treatments or experiments that were conducted based on Taguchi Method and orthogonal matrix $L_9(3^4)$ where L = Latin Square Design; 9 = number of experiments; 3 = number of level; 4 = number of factors.

To take the temperature for soaking Yu et.al (2017) suggested that soaking initial temperature was for 25, 40 and 50°C, and furthermore time for soaking was variert such from 15, 30 and 60 minutes (Miah et.al, 2002).

Table 2. Matriks Ortogonal $L_9(3^4)$

Experiments	Factor A	Factor B	Factor C	Factor D
	1	2	3	4
1	1	1	1	1
2	1	2	2	2
3	1	3	3	3
4	2	1	2	2
5	2	2	3	1
6	2	3	1	2
7	3	1	3	2

8	3	2	1	3
9	3	3	2	1

RESULTS AND DISCUSSION

The research yielded some variation of blue rice product based on the applied parameters during the process.

1. Color

Color is the most important factor in the blue rice, because it will attract the consumer to test and to buy it. Optimization of added butterfly pea flower powder in the solvent before it is added to rice was determined in this research. Color indicator for this rice was lightness (L), redness (a) and yellowness (b). The lightness depicted the brightness of color and it has scale 0 (black) to 100 (white). The redness was not dominated but small contribution was measured. For yellowness, blue color was in this range but in negative value (-b) and it gave biggest contribution.

Nine experiments were taken place and the result was shown in the following table 3.

Table 3. Color response in average

Experiments	L	A	-b
1	54.560	1.720	12.210
2	55.890	1.760	11.250
3	55.880	1.430	9.560
4	54.270	2.610	13.430
5	57.030	2.130	11.870
6	57.580	2.120	11.310
7	53.310	1.720	13.130
8	57.920	1.590	10.310
9	57.230	1,320	9,40
Total	503.670	16.400	102.410
Average	55.963	1.822	11.379

For further decision it was needed to calculate Signal to Noise Ratio (SNR) and the result guided to convince for finding best value especially for yellowness (-b) where blue color was in this range. The SNR for yellowness was depicted in the table 4 as follow.

Table 4. SNR for color - *Yellowness* (-b)

Level	A	B	C	D
1	20.700	22.139	20.874	20.812
2	21.661	20.848	20.968	21.413
3	20.592	19.966	21.111	20.728
Delta	1.070	2.174	0.237	0.685
Rank	2	1	4	3

For yellowness (-b) the responses were shown by factors B, A, D and C respectively. The factor B (22.139) or concentration of butterfly pea contributed highest value among other factors and played important role in producing blue rice. Combining table 3 and table 4 in color response, it could be summarized that experiment 4 gave highest value of redness and yellowness, but not the lightness, which was at experiment 8 reached highest value. It was strengthened by highest value of factor B or concentration of butterfly pea flower powder 6.1 g/L

2. Texture

Texture of rice is chosen as important quality parameters of rice when it is consumed. The rice was cooked and added with coloring agent. In this research two aspects, hardness and gumminess, were measured by using Universal Testing Machine (UTM). The result on texture response by using UTM was resumed in table 5.

Table 5. Average of Texture Response

Experiment	Hardness	Gumminess
1	65.253	19.244
2	65.845	33.412
3	58.214	31.383
4	67.113	23.478
5	56.464	17.716
6	64.845	17.382
7	45.795	22.459
8	65.159	18.427
9	44.656	22.039
Average	59.260	22.838

Furthermore this average result should be analyzed by using SNR value, which results were shown in the table 6 and table 7.

Table 6. Results of Effect Factor on SNR for *Hardness*

Level	A	B	C	D
1	-36,311	-35,839	-37,075	-35,170
2	-36,564	-36,230	-35,512	-35,634
3	-34,401	-35,208	-34,689	-36,472
Delta	2,164	1,022	2,387	1,301
Rank	1	4	2	3

Table 7. Results of Effect Factor on SNR for *gumminess*

Level	A	B	C	D
1	28.050	26.052	23.214	21.999
2	22.228	21.934	28.120	27.214

3	24.726	27.018	23.671	25.791
Delta	5.823	5.084	4.906	5.215
Rank	1	3	4	2

Based on the results in table 5 the best hardness of cooked rice reached when it showed low value (soft) and for gumminess it was better when it has low value as well. The experiment 2 depicted lowest value for gumminess and experiment 9 showed the lowest value for hardness. Further analysis showed in the table 6 and 7 (rank of the gap), where the factor A (type of rice) gave highest contribution for hardness and gumminess of blue rice.

To find the best combination all the results were tested with Grey Relation Grade, in which relation among factors could be determined (Singh et.al, 2018). The result of Grey Relation Grade was shown in table 8 as follow.

Tabel 8. Response on *Grey Relational Grade*

Level	A	B	C	D
1	0.628	0.725	0.622	0.533
2	0.700	0.579	0.589	0.647
3	0.521	0.544	0.553	0.668
Delta	0.179	0.181	0.069	0.134
Rank	2	1	4	3

Based on Grey Relation Grade it could be determined, that best parameter for cooking blue rice were factor A level 2 (premium quality rice: Pandan Wangi), factor B level 1 (concentration of butterfly pea solution/6.1 g/L), factor C level 2 (soaking time for 30 minutes) and factor D level 3 (temperature of solution, when start to soak the rice/50°C).

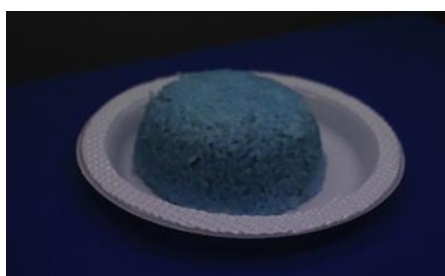


Figure 1. Blue rice – cooking with best parameter

CONCLUSION

Based on the research results it could be concluded some points as follow:

- a. The powder of butterfly pea flower can be used as blue coloring agent for cooking rice.
- b. The parameters for blue rice were color and texture, that were optimized by using Taguchi Method.
- c. The best parameter achieved were type of rice (quality premium rice/Pandan Wangi), concentration of 6.1 g/L, soaking time 30 minutes and temperature for soaking 50°C.

ACKNOWLEDGMENT

This research was financially supported by Faculty of Agricultural Technology – Universitas Gadjah Mada and part of research on natural coloring agent at Laboratory Quality Analysis and Standardization – Department of Agroindustrial Technology at same faculty and university.

REFERENCES

1. Kungsuwan, K; Singh, K; Phetkao, S; Utama-ang. 2014. Effect of pH and anthocyanin concentration on color and antioxidant activity of *Clitoria ternatea* extract. Food and Applied Bioscience Journal 2 (1): 31-46.
2. Miah, M.A.K; Haque, A; Douglas, P; Clarke, B. 2002. Parboiling rice. Part I: Effect of hot soaking time on quality of milled rice. International Journal of Food Science and Technology, 37: 527-537
3. Yu, Y; Pan, F; Ramaswamy, H.S; Zhu, S; Yu, L; Zhang, Q. 2017. Effect of Soaking and Single/Two Cycle High Pressure Treatment on Water Absorption, Color, Morphology and Cooked Texture of Brown Rice. Journal Food Science Technology 54 (6): 1655-1664.
4. Singh, R; Rashmi, Bhingole, P; Avikal, S. 2018. Grey Based Taguchi Optimization for Heat Treated Welded Joint. Materials Today: Proceedings 5: 19156-19165

COLOR PERCEPTION SPECIFIC TO FACIAL SKIN

Yoko Mizokami^{1*}

¹*Department of Imaging Sciences, Graduate School of Engineering, Chiba University, Japan*

*Corresponding author: Yoko Mizokami, mizokami@faculty.chiba-u.jp

Keywords: Color perception, Skin, Face

ABSTRACT

Skin color is essential for obtaining various information on our mind and body, such as health, age, and face impression. Therefore, we must have developed visual sensitivity tuned to skin. It has been suggested the existence of color perception specific to facial skin. For example, we have shown that sensitivity to changes in reddish (or hemoglobin increasing) direction of the skin is better than other color directions. Reddish skin looks brighter than yellowish skin even if they have the same lightness. These perceptions may link to the property of skin color determined by pigments of the skin. Our results of international comparison also suggest that other factors such as ethnicities, environments, and cultures may also influence facial color perception.

INTRODUCTION

Skin color is one of the colors that we see most often, and it becomes a cue to know important information in everyday life. For example, when we see the complexion of people, we judge that they are healthy if it is reddish. We consider that they are in bad physical condition if it is pale. Also, skin color helps to recognize expressions, such as angry and sad. Information obtained from skin color is not only a cue to understand the physical condition but also an essential factor for good communication. Thus, accurate color measurement, color reproduction, and color evaluation are required.

Several studies have suggested that there is a difference between the measured values of the skin and human perception for skin color. Yoshikawa et al. [1] show that when a face image is observed, even when lightness of the skin area is the same, reddish skin looks whiter than yellowish skin. Re et al. [2] state that people have a high sensitivity to change in skin redness. Tan et al. [3] show that discrimination ability is higher for color change in facial images than in uniform color patches. These studies suggest that skin color is unique for us, and people have a skin-specific color perception after recognizing the skin.

Skin color is mainly determined by two pigments, melanin produced by melanocytes in the skin and hemoglobin existing in a capillary vessel [4]. These pigments contribute to a difference in skin color, such as by race, region, season, age. Besides, these pigments are not uniformly distributed in the skin, which causes the color unevenness or texture of the skin. Several methods for analyzing the melanin and hemoglobin pigments have been proposed. Tsumura et al. [5] developed a method for extracting melanin and hemoglobin pigment images from a skin image obtained by an RGB camera. However, little has been investigated about the relationship between these pigments and color perception.

Here, we discuss two topics. The first topic is the sensitivity to changes in skin color. We investigated whether sensitivity to changes in skin color reddish (or hemoglobin increasing) direction of the skin is better than other color directions. The second topic is the brightness perception of facial skin. We have found that reddish skin looks brighter than yellowish skin even if they have the same

lightness. We show our results of international comparison, implying that other factors such as ethnicities, environments, and cultures may also influence facial color perception.

DISCRIMINATION THRESHOLDS FOR SKIN AND FACE IMAGE

We have been investigating the discrimination threshold for facial skin [6, 7]. Our purpose is to clarify whether we have different characteristics of sensitivity to changes in skin color concerning skin color pigment melanin and hemoglobin.

Here, we examined the color discrimination of face color in the direction of change in the amount of melanin and hemoglobin, which are the main pigment components consisting of skin color. We also tested the color discrimination on the a^*b^* axes in the CIELAB space and axes based on the independent component analysis (ICA) of skin color distribution. We used a Japanese female face with an averaged skin color obtained by measuring the skin of 694 Japanese females as a reference stimulus, as shown in Figure 1. Test stimuli were made by modulating the color of the reference stimuli. Color changes due to melanin and hemoglobin change in the CIELAB space was calculated based on skin reflectance data obtained by the Monte Carlo Simulation (MCS) and the spectra of the D65 illuminant. We used the MCS of a skin spectral reflectance using a nine-layered skin tissue model [8]. This model is a method to calculate a spectral reflectance of the skin by setting light absorption parameters by melanin or hemoglobin. Spectral reflectances were calculated by increasing and decreasing the parameters of melanin or hemoglobin from the average skin color. Then, CIELAB values were calculated from these spectral reflectances. Then, the color of a skin image was modulated in the direction of increase and decrease of each pigment, a^*b^* axes, or the first and second axis of ICA.

A reference and test stimuli were presented on a CRT monitor in a dark room. The visual angle of these stimuli was 13.5×10 degrees. First, observers adapted to the black screen of the monitor for 1 minute and the maximum white of the monitor for 2 minutes. After that, three face stimuli were presented successively. A reference stimulus was shown in the second, and a test stimulus was shown either first and third. The other stimulus was the same as the reference stimulus. Observer chose which of first and second stimulus was different from the reference stimulus. A staircase method was used to obtain a boundary that was discriminable from the reference stimulus. When one response finished, it moved to the next color modulation direction. This experiment was conducted five sessions per observer. Three observers with normal color vision participated.

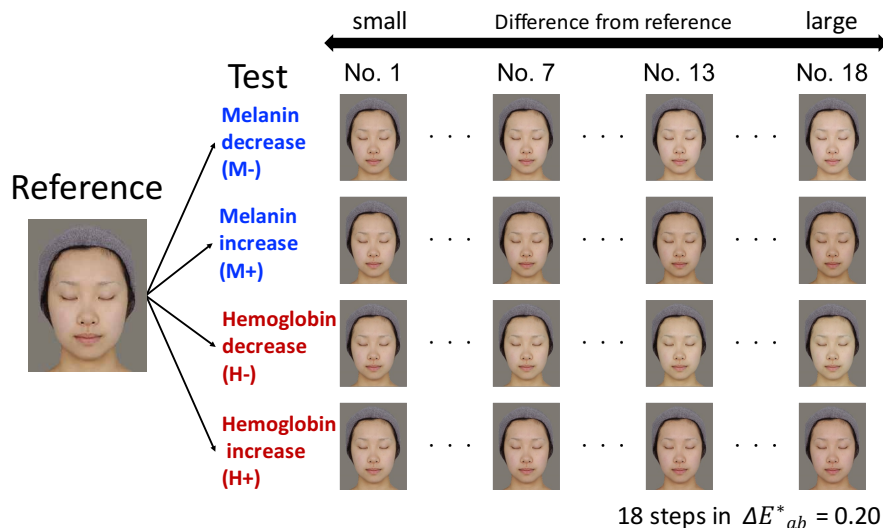


Figure 1. Color change based on pigment density based on MCS

Figure 2 shows the average of discrimination color differences ΔE_{ab}^* for all observers in each modulation direction. The discrimination color difference was defined that the average color difference for all pixels of "the reference stimulus" and "the boundary stimulus responded as discriminable." Each shows the result of the skin image in each color modification direction. The error bar represents the standard deviation. Our result showed better discrimination for changes in reddish direction in all the pigment change, a^*b^* axes, and ICA axes. It suggests that people have more sensitive to color change accompanying the increase of hemoglobin. We also tested a uniform stimulus with the same average skin color. Different tendencies were seen in the skin image and the uniform color stimulus, suggesting that skin-specific perception would exist.

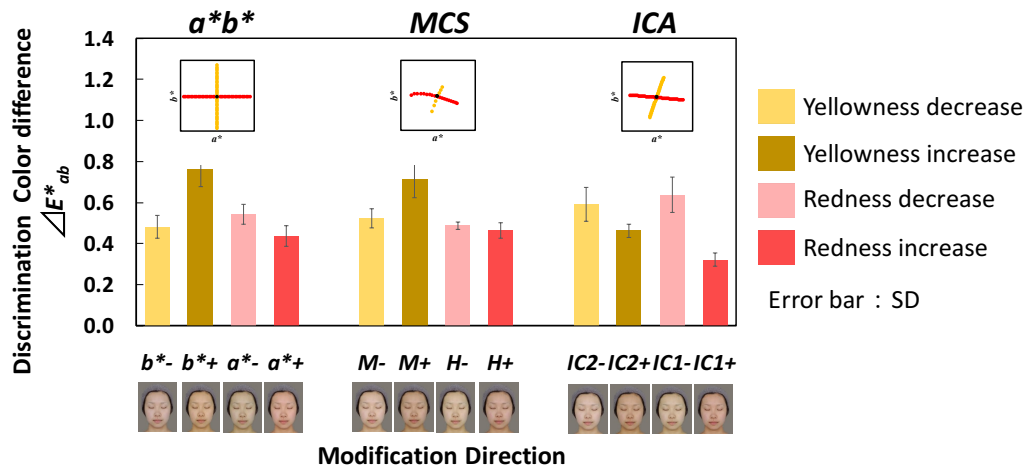


Figure 2. Results of discrimination threshold shown by the discrimination color differences ΔE_{ab}^*

BRIGHTNESS PERCEPTION OF FACIAL SKIN

The skin color distribution of young Japanese women measured with a colorimeter showed a trend that yellowish skin had higher lightness compared to reddish skin. On the other hand, it was shown that reddish skin appeared brighter than yellowish skin when both had the same lightness [1]. However, the previous result was obtained from the experiments using Japanese faces with Japanese skin color and for Japanese observers. Skin color varies among different ethnic groups, from dark to light, and from yellowish to reddish. It is not clear how the brightness perception of facial skin is influenced by the diversity of skin face colors and observers. Here, we investigate the brightness perception of facial skin for Japanese, Thai, and Chinese observers [9, 10].

We used a young Japanese female face, which was an average of forty female faces. We prepared test faces with four skin color types that were the average skin color of Japanese, Thai, Caucasian, and African. The skin color of each face was modified by changing the ratio of L^* , a^* , b^* from each test face. Test images with constant lightness and different hue angles were generated. Scale images had the same hue angle corresponding to an original face color of each skin color type and different lightness. A test image and a scale image were presented side by side on a color-calibrated tablet display. Under indoor white lighting, observers sat in front of the tablet display and adjusted the lightness of facial skin on the scale image to match the brightness of the test image and the scale image. They evaluated four groups of stimulus images (20 images in total), three times each. We conducted experiments for university students in Japan and Thailand.

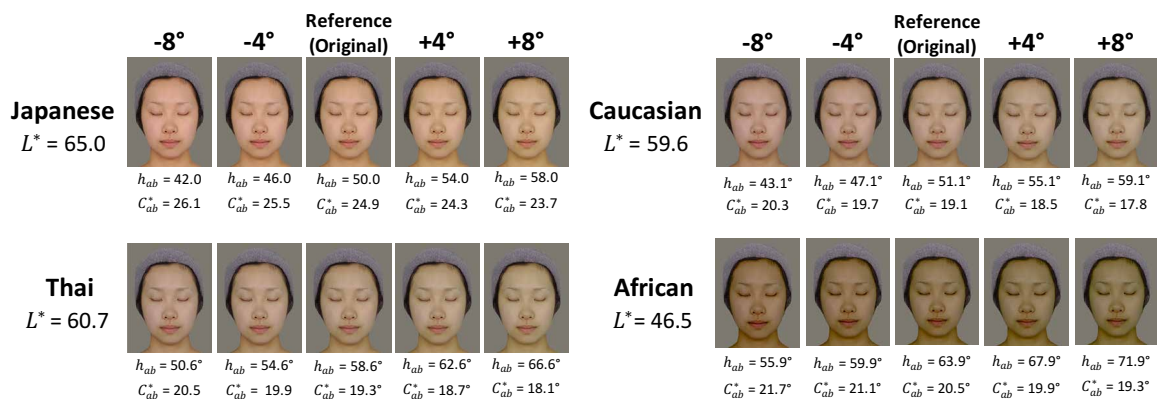


Figure 3. Modulated image of Japanese skin, Thai skin, Caucasian skin, and African skin.

As a result, Japanese observers showed a trend that reddish skin appeared brighter than yellowish skin, consistent with the previous study, whereas Thai observers showed an opposite trend, and Chinese observers did not show the systematic influence of hue. They suggest diversity in the brightness perception of facial skin.

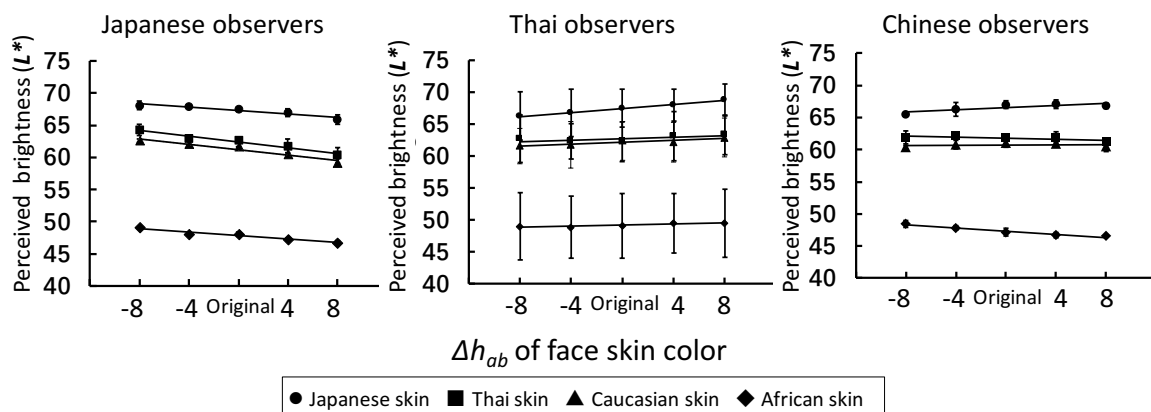


Figure 4. Results of brightness perception of Japanese, Thai, and Chinese observers (shown by matched lightness L^*).

DISCUSSION

We showed that sensitivity to changes in reddish (or hemoglobin increasing) direction of the skin is better than other color directions. Reddish skin looks brighter than yellowish skin even if they have the same lightness. The reason that discrimination color difference is smaller for hemoglobin increase direction could be because hemoglobin increase provides valuable information. For example, it is known that redness increase with blood flow provides useful information, such as judgment of breeding season [11] and emotion [12]. Changizi et al. [13] also describe that the primates' vision has evolved to discriminate skin color changes. They suggested that the M and L cone sensitivities optimize to color change with hemoglobin oxygen saturation.

Skin color is essential for obtaining various information on our mind and body, such as health, age, face impression, and attractiveness [2, 14]. Therefore, we must have developed visual sensitivity

tuned to skin. Our results of the international comparison were surprising because even observers in Asian countries showed a different trend in brightness perception of facial skin. Although the reason is not apparent yet, they imply that other factors such as ethnicities, environments, and cultures also influence facial color perception.

Facial skin perception is quite complicated and exciting. Much further investigation is needed to challenge facial skin recognition.

ACKNOWLEDGEMENT

This study was supported by JSPS KAKENHI Grant Number JP16H01663 and JP18H04183.

REFERENCES

1. Yoshikawa, H., Kikuchi, K., Yaguchi, H., Mizokami, Y., & Takata, S. (2012). Effect of Chromatic Components on Facial Skin Whiteness, *Color Research & Application*, 37(4), 281-291.
2. Re, E. D., Whitehead, D. R., Xiao, D., & Perrett, I. D. (2011). Oxygenated-blood colour change thresholds for perceived facial redness, health, and attractiveness, *PLoS One* 6(3), e17859.
3. Tan, W. K., & Stephen D. I. (2013). Colour detection thresholds in faces and colour patches, *Perception*, 42(7), 733–741.
4. Anderson, R. R., & Parrish A. J. (1981). The Optics of Human Skin, *Journal of Investigative Dermatology*, 77 (1), 13-19.
5. Tsumura, N., Haneishi, H., & Miyake, Y. (1999). Independent-component analysis of skin color image, *Journal of the Optical Society of America A*, 10(34), 1-4.
6. Hamada, K., Mizokami, Y., Kikuchi, K., & Yaguchi, H. (2017). Discrimination thresholds for skin image and uniform color stimulus, 13th Congress of the International AIC Colour Association, Proceedings, PS03-74, Jeju.
7. Mizokami, Y., Yoshida, M., Kikuchi, K., Aizu, Y., & Yaguchi, H. (2019). Characteristics of color discrimination on a face image, Vision Sciences Society, St. Pete Beach.
8. Maeda, T., Arakawa, N., Takahashi, M., & Aizu, Y. (2010). Monte Carlo simulation of spectral reflectance using a multilayered skin tissue model, *Optical Review*, 17(3), 223-229.
9. He, Y., Mikami, T., Tanaka, S., & Mizokami, Y. (2019). Comparison of brightness perception of facial skin with differences of skin color, International Colour Vision Society (ICVS) 2019.
10. He, Y., Mikami, T., Tanaka, S., & Mizokami, Y. (2019). Influence of skin color to the brightness perception of facial skin – Comparison of Japanese, Thai and Chinese, Asian Pacific Conference on Vision (APCV) 2019.
11. Rhodes, L., Argersinger, E. M., Gantert, T. L., Friscino, H. B., Hom, G., Pikounis B., Hess, L. D., & Rhodes, L. W. (1997). Effects of administration of testosterone, dihydrotestosterone, oestrogen and fadrozole, an aromatase inhibitor, on sex skin colour in intact male rhesus macaques, *Journal of Reproduction & Fertility*, 111(1), 51–57.
12. Drummond, D. P. (1997). Correlates of facial flushing and pallor in anger-provoking situations, *Personality & Individual Differences*, 23(4), 575–582.
13. Changizi, A. M., Zhang, Q., & Shimojo, S. (2016). Bare skin, blood and the evolution of primate colour vision, *Biology letters*, 2(2), 217-221.
14. Fink, B., & Grammer, K. (2001). Human (*Homo sapiens*) facial attractiveness in relation to skin texture and color, *Journal of Comparative Psychology*, 115(1), 92-99.

IMAGE-BASED MEASUREMENT OF HUMAN FACIAL SKIN COLOR AND ITS APPLICATION IN COSMETICS FIELD

Kumiko Kikuchi^{1*}

¹*Shiseido Global Innovation Center, Yokohama, Japan.*

*Corresponding author: Kumiko Kikuchi, kumiko.kikuchi1@shiseido.com

Keywords: Face, Image, Melanin, Skin color, Spectrophotometer

ABSTRACT

An important issue in cosmetics research is the determination of facial skin color and its distribution. Conventionally, spectrophotometry is used for skin color measurement and evaluation is performed by analyzing color values or the dominant chromophores in human skin (i.e., melanin and hemoglobin) from the obtained spectral data. Spectrophotometry provides one-dimensional measurements, with values measured at one point in space. To understand problems related to skin color, such as pigmented spots, acne, dark circles around eyes, and redness of the cheeks, it is necessary to perform two-dimensional measurements, which is possible with image-based methods. In this presentation, we present the advantages and disadvantages of using spectrophotometry and image-based methods in the cosmetics field. In addition, we describe our evaluation methods for determining facial skin color, and present the results of these methods.

INTRODUCTION

The ability to determine the distribution of skin color is important in many industries for product design and service optimization. In the field of cosmetics, skin color measurements are used in the development of products such as makeup and skin care products. Both general and dedicated devices have been applied to measure skin color. Analysis methods have also been developed. Spectrophotometry is commonly used for skin color measurement. A spectrophotometer probe is placed on part of the skin and data are acquired. The advantage is that skin color data for many subjects can be obtained relatively easily [1,2,3,4]. However, only the target area is measured; it is impossible to evaluate the facial skin color distribution and color heterogeneity due to spots and freckles. To solve this problem, many studies have applied image acquisition devices such as cameras for facial skin color measurement [5-7,8-11]. By using image analysis methods, it is possible to quantify conditions related to facial skin color heterogeneity. However, because many cameras use RGB sensors, their wavelength resolution is inferior to that of a spectrophotometer. Spectral cameras, which are non-contact and non-destructive measurement devices that can capture spectral data for each pixel of a two-dimensional image, have recently been applied in many fields [12,13]. In this presentation, we give examples of skin color evaluation using a spectrophotometer, a standard digital camera, and a spectral camera, and discuss the application of these devices to the development of cosmetics.

LONG-TERM CHANGES IN JAPANESE WOMEN'S FACIAL SKIN COLOR OBTAINED WITH SPECTROPHOTOMETERS

Background

It has been reported that facial skin color changes not only with age for an individual but also with the times in terms of trends of letting the skin be whiten or more suntanned [2,14].

Japanese women in the early 2000s tended to maintain a lighter facial skin color compared with that in the early 1990s, and Japanese women's facial skin lightness increased from the early 1990s to the early 2000s. Changes in Japanese women's facial skin color since 2000 have not been studied quantitatively. One reason is that the maintenance and use of a given spectrophotometer model across such a long measurement period is not feasible. Different spectrophotometer models may have different illumination diameters and measurement diameters, which affect the results of color measurements of translucent objects such as skin [15]. To compare data from the early 1990s with current data, which were obtained using a different spectrophotometer, we measured the illumination diameter and measurement diameter of the spectrophotometers and developed a method for correcting the difference in skin reflectance measured by these spectrophotometers.

Methods

The skin color for a specific part of the face was measured with different spectrophotometers, and a correction equation was established for comparing the skin color data based on the difference in the output spectral reflectance [3]. The spectral reflectance of the cheek skin of approximately 2,000 Japanese women was measured in 2005 and 2015. These spectral data were added to corrected 1991 data and 2001 data. Data for a total of 3,181 Japanese women residing in the greater Tokyo area were obtained for 1991, 2001, 2005, and 2015. The mean Munsell hue, value, and chroma were calculated for each measurement year. In addition, the concentrations of melanin and hemoglobin were calculated from the spectral data to investigate changes in skin pigmentation.

Results and Discussion

Our results showed that facial skin color significantly changed toward higher lightness, lower saturation, and higher yellowness from 1991 to 2001. From 2005 to 2015, the skin color distribution shifted toward lower saturation and increased redness (Figure 1).

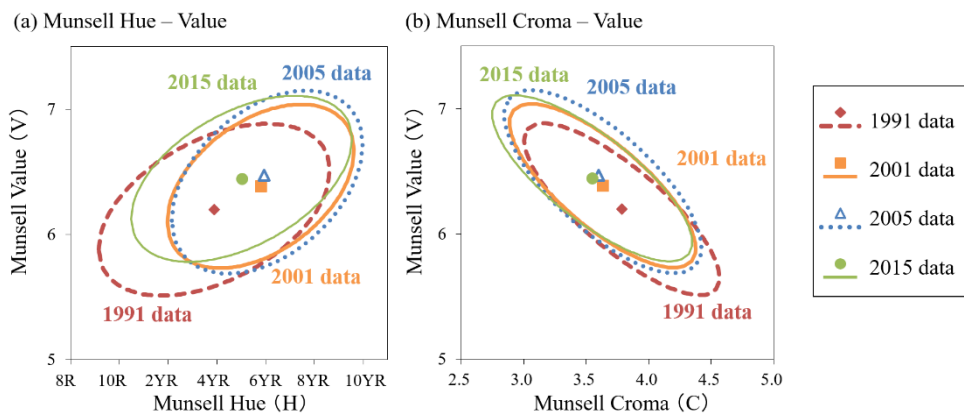


Figure 1. Mean skin color and 95% confidence ellipse for Japanese women in the Munsell color system

In addition, the concentration of hemoglobin decreased significantly from 1991 to 2001, and the melanin concentration decreased significantly from 2005 to 2015 [4]. A possible explanation for these results is that the sun-tanning behavior of Japanese women in the 2000s may have continued to decrease, as it did in the 1990s. According to trends in sunscreen product sales in Japan from 1999 to 2015, the sunscreen market approximately doubled in size from 2000 to 2015 [16]. The decrease in the frequency of sunburn may have led to a decrease in skin inflammation and a decrease in melanin pigment, leading to a change in skin color.

DEVELOPMENT OF IMAGING SYSTEM AND EVALUATION METHOD FOR FACIAL SKIN COLOR DISTRIBUTION

Background

Human facial skin color is not uniform. A person may have red cheeks, dullness around the eyes, and a suntanned forehead. Facial skin color distribution differs among individuals and influences the perception of age, health, and attractiveness of the face [17-19]. It is thus important to evaluate facial skin color distribution quantitatively. An accurate distribution is useful for the development of various products. A device that can measure a wide area of the face is required to objectively evaluate the facial skin color distribution. Some studies based on image devices have extracted color data for the target area of the facial image for quantitative analysis [8]. Because such analysis is limited to the target area, it cannot be used to obtain the skin color distribution over a wide area of the face in detail. We need to develop a measurement system and an evaluation method to measure facial skin color distribution.

Methods

A facial imaging system that consisted of an illumination unit and a high-resolution digital camera was used to measure the detailed spatial facial skin color distribution [9,10]. The illumination unit contained fluorescent lamps with a color temperature of 6700 K. These lamps were designed to provide diffuse illumination over a wide field of the subject's face to eliminate shadows and artifacts from specular reflections. The imaging system was based on a Canon CMOS digital camera (EOS Kiss X3; Canon, Tokyo, Japan).

Because the shape and size of the face varies with the individual, it is necessary to discuss not the absolute coordinates but the relative coordinates for each face to analyze parts of the face. Our evaluation method for facial skin color distribution is based on facial feature points and includes segmentation that takes into account the facial skeleton and muscle orientation. The use of facial feature points enables comparison at similar locations on the face without depending on the shape or size of the face [11]. The method mainly consists of two independent procedures: (1) the application of a specific form of the wireframe model to the frontal and left- and right-hand side facial images (i.e., normalization of coordinate information in the face area based on feature points) and (2) the averaging of the brightness of the three primary colors of pixels within each area surrounded by the wireframe (i.e., compression of image information.)

As an application of this imaging system and evaluation method, 522 healthy Japanese women aged 20-78 years were enrolled in our study. We investigated the age-related changes of facial skin color distribution. In addition, facial images were captured for the same women volunteers at different seasons of the year to investigate the seasonal changes of facial skin color distribution. 25 healthy Japanese women volunteers (age: 22-40 years; mean age: 35 years) were enrolled in this study.

Results

The results of the evaluation of the facial images of women aged 20-78 years showed that the lightness of the face decreased as age increased (Figure 2). In particular, the decrease in lightness was remarkable in the region along the cheekbone, from the temple to the center of the cheek. Furthermore, we analyzed the seasonal changes of melanin and hemoglobin distributions in the face area (Figure 3). The results showed that the melanin index increased, particularly in the cheekbone area, in the summer, when the influence of ultraviolet rays is highest. A significant increase in the hemoglobin index around the middle of the cheek was observed in winter.

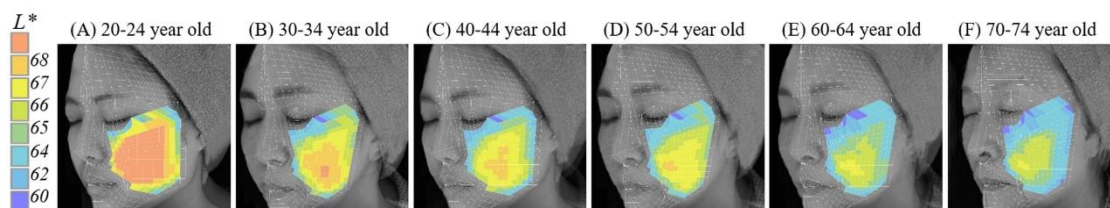


Figure 2. Average L^* distribution in the face for various age groups

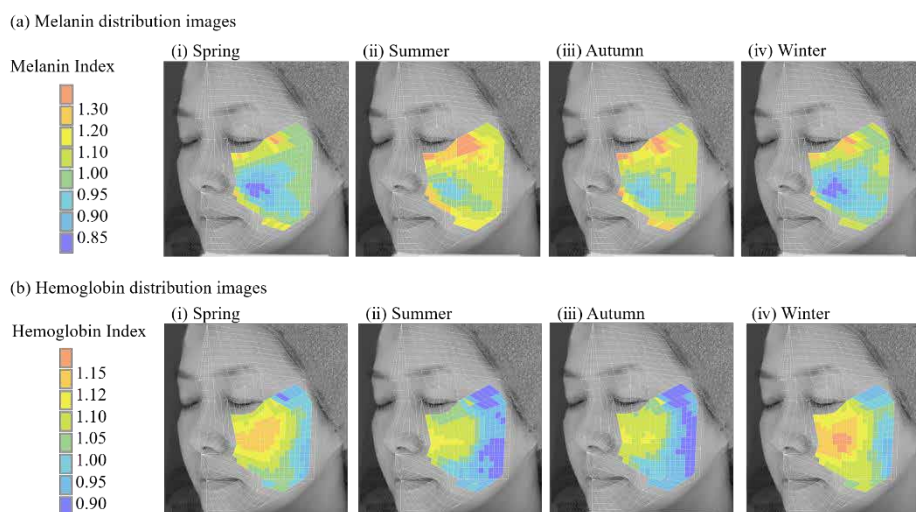


Figure 3. Seasonal changes of (a) melanin and (b) hemoglobin distribution in the face

IMAGING OF HEMOGLOBIN OXYGEN SATURATION RATIO IN THE FACE USING SPECTRAL CAMERA

Background

Contact-type spectrophotometers are widely used to measure skin color to determine color values and melanin and hemoglobin content. However, they cannot be used to obtain a two-dimensional spectral distribution. Spectral cameras, which are imaging spectrometers that provide full and contiguous spectral information for each pixel, have recently become widely used in many fields. By analyzing spectral data for each pixel of a spectral image, it is possible to construct distribution maps of the relative concentrations of melanin and oxy- and deoxyhemoglobin. In our study, we developed a spectral imaging system that is capable of capturing a wide area of the face to quantify and visualize the distribution of the relative concentrations of skin chromophores, including melanin and oxy- and deoxyhemoglobin.

Methods

The spectral imaging system developed for facial skin color measurement consisted of a spectral camera and a lighting unit for uniform irradiation of the face [13]. The distribution of skin chromophores in the face, including melanin and oxy- and deoxyhemoglobin, was calculated from the reflectance data for each pixel of the spectral images [20]. In addition, to create a mean spectral image for the study group, a face morphing method for spectral data was proposed. Using this system, we determined the characteristics of dark circles around the eyes and evaluated the effects of an anti-dark circle cosmetic.

Results

This system enables sensitive detection of skin chromophores in the face. Melanin content increased and the hemoglobin oxygen saturation ratio decreased locally in the infraorbital areas of women with dark circles compared with those of women without dark circles. In addition, we were able to detect an improvement in dark circles after 6 weeks of use of anti-dark circle cosmetic products by visualizing the distribution of the relative concentration of melanin and the hemoglobin oxygen saturation ratio (Figure 4).

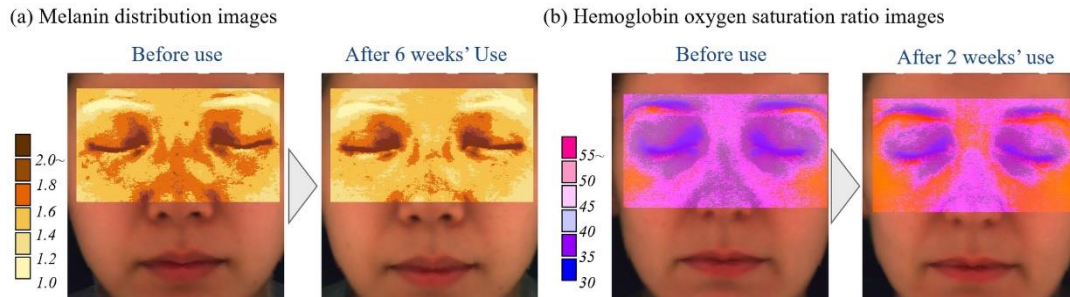


Figure 4. Mean spectral images of (a) melanin distribution and (b) hemoglobin oxygen saturation ratio in dark circles before and after cosmetic treatment

CONCLUSION

In this presentation, we described examples of skin color evaluation using a spectrophotometer, a standard digital camera, and a spectral camera. As an example application of the spectrophotometer, we presented the results of long-term changes in the skin color of Japanese women. As an example of facial skin color evaluation using the standard digital camera, we presented the analysis results of facial skin color distribution. Furthermore, we described a non-contact image processing system based on a spectral camera that is capable of capturing a wide area of the face to construct distribution maps of the relative concentrations of melanin and oxy- and deoxyhemoglobin. Our methodology and the data presented in this paper will be useful in various fields, such as dermatology, cosmetics, and computer vision.

ACKNOWLEDGEMENT

I would like to thank researchers from Shiseido Co. Ltd. for helpful discussions and suggestions. My intellectual debt is to Professor Y. Mizoami and Professor H. Yaguchi (Chiba University). I am grateful to Professor Y. Aizu (Muroran Institute of Technology) for providing spectral reflectance curves generated by a Monte Carlo simulation and helpful advice.

REFERENCES

1. Xiao, K., Yates, J. M., Zardawi, F., Sueeprasan, S., Liao, N., Gill, L., ... & Wuerger, S. (2017). Characterising the variations in ethnic skin colours: a new calibrated data base for human skin. *Skin Research and Technology*, 23(1), 21-29.
2. Yoshikawa, H., Munakata, A., Takata, S., & Yaguchi, H. (2010). Skin color change of Japanese female in the 1990s. *Journal of the Color Science Association of Japan*, 34(2), 120-130.

3. Kikuchi, K., Katagiri, C., Yoshikawa, H., Mizokami, Y., & Yaguchi, H. (2016) A correction method for skin reflectance obtained with different spectrophotometers and its application: changes in the skin color of Japanese women for 25 years. *Journal of the Color Science Association of Japan*, 40(6),195-205.
4. Kikuchi, K., Katagiri, C., Yoshikawa, H., Mizokami, Y., & Yaguchi, H. (2018). Long-term changes in Japanese women's facial skin color. *Color Research & Application*, 43(1), 119-129.
5. Miyamoto, K., Takiwaki, H., Hillebrand, G. G., & Arase, S. (2002). Development of a digital imaging system for objective measurement of hyperpigmented spots on the face. *Skin Research and Technology*, 8(4), 227-235.
6. Tsumura, N., Haneishi, H., & Miyake, Y. (1999). Independent-component analysis of skin color image. *JOSA A*, 16(9), 2169-2176.
7. Tsumura, N., Ojima, N., Sato, K., Shiraishi, M., Shimizu, H., Nabeshima, H., ... & Miyake, Y. (2003). Image-based skin color and texture analysis/synthesis by extracting hemoglobin and melanin information in the skin. *ACM Transactions on Graphics (TOG)*, 22(3), 770-779.
8. De Rigal, J., Des Mazis, I., Diridollou, S., Querleux, B., Yang, G., Leroy, F., & Barbosa, V. H. (2010). The effect of age on skin color and color heterogeneity in four ethnic groups. *Skin Research and Technology*, 16(2), 168-178.
9. Kikuchi, K., Masuda, Y., Yamashita, T., Kawai, E., & Hirao, T. (2015). Image analysis of skin color heterogeneity focusing on skin chromophores and the age-related changes in facial skin. *Skin Research and Technology*, 21(2), 175-183.
10. Kikuchi, K., Masuda, Y., Yamashita, T., Sato, K., Katagiri, C., Hirao, T., ... & Yaguchi, H. (2016). A new quantitative evaluation method for age-related changes of individual pigmented spots in facial skin. *Skin Research and Technology*, 22(3), 318-324.
11. Yoshikawa, H., Kikuchi, K., Takata, S., & Yaguchi, H. (2009). Development of a visual and quantitative evaluation method for facial skin color. In *Proceedings of 11th Congress of the International Colour Association*. Sydney, Australia.
12. Kikuchi, M., Igarashi, T., Sato, H., Fujiura, T. (2017). Development of a skin color evaluation method based on hyperspectral imaging based on erythema and melanin indexes. In *Proceedings of 13th Congress of the International Colour Association*. Jeju, South Korea.
13. Kikuchi, K., Masuda, Y., & Hirao, T. (2013). Imaging of hemoglobin oxygen saturation ratio in the face by spectral camera and its application to evaluate dark circles. *Skin Research and Technology*, 19(4), 499-507.
14. Mizukoshi, K., Futagawa, M., Yamakawa, Y. (2013). Long-term change, regional and individual difference assessment of Japanese female skin condition. *Journal of Society Cosmetic Chemists Japan*, 47(2), 119-127.
15. Osumi, M. (2015). Let's Try Measuring Colors: Introduction to the Scientific Method Used in Color Research (Part 6). *Journal of the Color Science Association of Japan*, 39(2), 85-89.
16. Fuji Keizai. Kesyohin Marketing Youran [Japanese Cosmetics and Toiletries: Marketing Research Report. 2001-2015]. Tokyo, Japan: Fuji Keizai Co., Ltd.; 2001-2015.
17. Matts, P. J., Fink, B., Grammer, K., & Burquest, M. (2007). Color homogeneity and visual perception of age, health, and attractiveness of female facial skin. *Journal of the American Academy of Dermatology*, 57(6), 977-984.
18. Fink, B., Bunse, L., Matts, P. J., & D'Emiliano, D. (2012). Visible skin colouration predicts perception of male facial age, health and attractiveness. *International Journal of Cosmetic Science*, 34(4), 307-310.
19. Arce-Lopera, C., Igarashi, T., Nakao, K., & Okajima, K. (2013). Image statistics on the age perception of human skin. *Skin Research and Technology*, 19(1), 273-278.
20. Masuda, Y., Yamashita, T., Hirao, T., & Takahashi, M. (2009). An innovative method to measure skin pigmentation. *Skin Research and Technology*, 15(2), 224-229.

INTERNATIONAL COMPARISON OF FACIAL SKIN BRIGHTNESS PERCEPTION WITH DIFFERENCES IN SKIN COLOR

Taiga Mikami^{1*}, Yuanyuan He¹, Helene Midtjord², Suguru Tanaka¹,
Kumiko Kikuchi³ and Yoko Mizokami¹

¹*Graduate School of Science and Engineering, Chiba University, Japan.*

²*Department of Science and Technology, Norwegian University, Norway.*

³*Shiseido Global Innovation Center, Japan.*

*Corresponding author: Taiga Mikami, afsa5561@chiba-u.jp

Keywords: Skin color, face, brightness

ABSTRACT

The color of human skin is one of the most common colors which we see in every life. Skin color varies among different ethnic groups, from dark to light, and from yellowish to reddish. The skin color distribution of young Japanese females measured with a colorimeter showed a trend that yellowish skin had higher lightness compared to reddish skin. On the other hand, it was shown that reddish skin appeared brighter than yellowish skin when both had the same lightness (Yoshikawa et al., 2012). This suggests that the perception of facial skin color is different from that of ordinary objects. However, the previous result was obtained from the experiments using Japanese faces with Japanese skin color for Japanese observers. Our recent study comparing the brightness perception of Japanese and Thai observers showed the opposite trend (He et al., ICVS 2019). It is not clear how the brightness perception of facial skin is influenced by the diversity of skin face colors and observers. Here, we investigate the brightness perception of facial skin for Japanese, Thai, Chinese, and European observers. We used a young Japanese female face, which was an average of 40 female faces. We prepared test faces with four skin color types that were the average skin color of Japanese, Thai, Caucasian, and African. Test images with constant lightness and five hue angles, including the average skin color, were generated for each test face. The skin color of test images was modified by changing the hue angle in CIELAB from that of each test face. Scale images had the same hue angle as an original face color of each test face and different lightness levels. A test image and a scale image were presented side by side on a color-calibrated tablet display. Under indoor white lighting, observers sat in front of the tablet display and adjusted the brightness of face on the scale image to match that on the test image. They evaluated four groups of stimulus images (20 images in total), three times each. We conducted experiments in Japan, Thailand, China, and Norway. As a result, Japanese observers showed a trend that reddish skin appeared brighter than yellowish skin, but Thai, Chinese, and European observers showed the opposite or different trends. It implies that there is the influence of ethnicities or environments on the brightness perception of facial skin. Besides, since only Japanese observers consistently showed a trend that reddish skin appeared brighter than yellowish skin, the perception of skin brightness in Japanese may be affected by Japanese cultural characteristics.

INTRODUCTION

The color of human skin is one of the most common colors which we see every day. Skin color varies in ethnicity, such as Asian and European, and it can range from dark to light, and reddish to yellowish. It is an important clue when knowing information about humans. The skin color data of Japanese women measured by a colorimeter show a trend that reddish skin is darker than yellowish

skin. However, a previous study by Yoshikawa et al. revealed that Japanese observers perceived that reddish skin was brighter than yellowish skin even with the same average lightness [1]. This suggests that the perception of facial skin color is different from that of ordinary objects. However, the previous result was obtained from the experiments using Japanese faces with Japanese skin color for Japanese observers. Our recent study comparing the brightness perception of Japanese, Thai, and Chinese observers showed a different trend from Japanese.²⁾ It is not clear how the brightness perception of facial skin is influenced by the diversity of skin face colors and observers.

In this research, we investigate the brightness perception of facial skin for Japanese, Thai, Chinese, and European observers.

EXPERIMENT

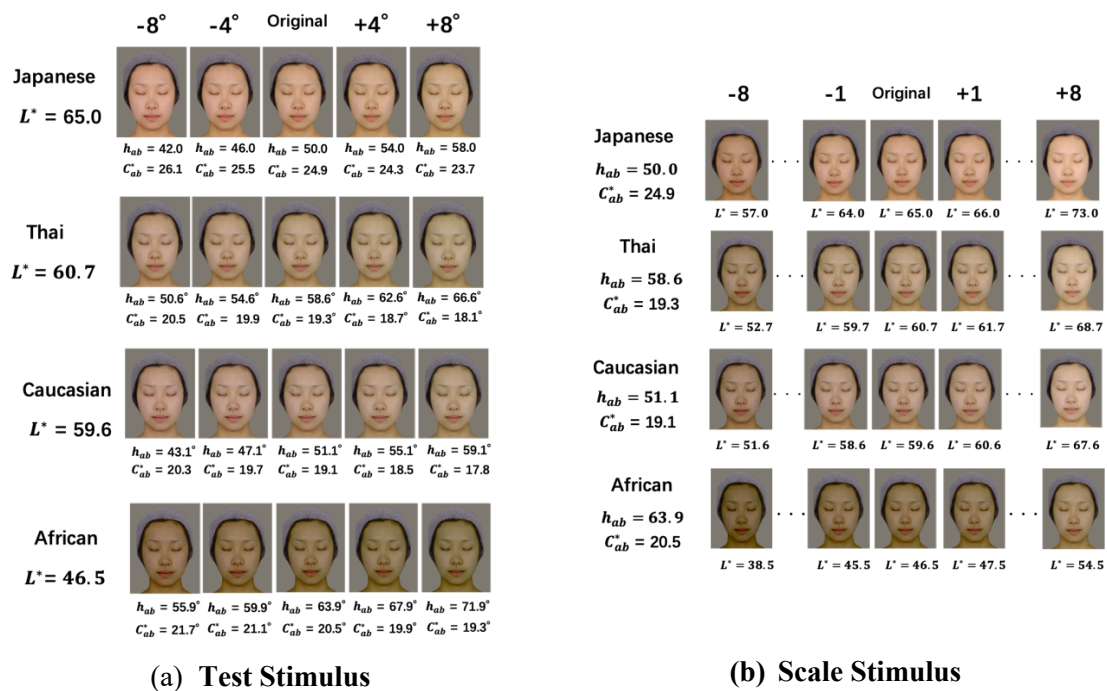
In this experiment, stimuli images are presented on a tablet display to make international comparison easier. An observer sits in front of the tablet display and adjusts the lightness of a scale image by operating the keyboard until the brightness of the scale image matches the brightness of a test image with different hues.

Methods

The experiment was carried out using a calibrated tablet display (Apple iPad Pro A1701). The viewing distance was about 40 cm, and the visual angle of stimulus images was $6.25^\circ \times 8.2^\circ$. Experiments were conducted in Japan, Thailand, and Norway.

Stimulus

In this experiment, we created a test stimulus and scale stimulus by modifying color in the CIELAB color space. The test stimulus and scale stimulus are shown in Figure 1. Each race is reproduced by changing only the hue and brightness of the face, using one facial shape of a Japanese woman. It is to consider only the influence of differences in skin color,



(a) Test Stimulus

(b) Scale Stimulus

Figure 1. Stimulus images

The hue of the test image was converted while maintaining the same lightness. The hue angle was calculated from the a^* and b^* of each race. The modulation was performed twice by 4° each in the positive or yellowish direction, and in the negative or reddish direction. A total of 5 evaluation stimuli was created for each race (Japanese, Thai, Caucasian, African). A step of 4° (-8° , -4° , 0° , 4° , 8°) hue changing was made so that the change in hue from the original of each race was distinguishable. The higher the hue angle is, the more yellowish the skin is, and the smaller the hue angle is, the more reddish the skin is. A scale stimulus is a stimulus image used as a scale for evaluating a test stimulus. In this experiment, the standard lightness L^* was modulated at the interval of one step in the positive and negative directions, and a total of 17 stimuli with different L^* were created for each race. The step of change in lightness was chosen so that observers could adjust the lightness accurately. The hue angle was fixed by each race's original.

Procedure

A method of adjustment was used in which observers adjusted the brightness of the scale stimulus to match the brightness of the test stimulus. The experiment was conducted in a room with white lighting. Although we did not fix the position of the face, the observer did not make a sizeable positional shift, and the viewing distance was kept about the same. An experimental procedure is shown below. There was no limit for presentation time.

1. Experimental descriptions and questionnaires were given.
2. An observer used a "J-key" (increasing lightness) and the "F-key" (reducing lightness) to adjust the lightness of the scale stimulus until the brightness of the test stimulus matched with the brightness of the scale stimulus.
3. After the adjustment finished, the observer pressed an "enter" button to proceed to the evaluation of the next test stimulus image.
4. The observer repeated the above evaluation steps for a total of 20 test images stimuli in one session.
5. A total of 3 sessions were conducted.

Observers

Fifty-five observers with normal color vision participated in total. Table 1 shows the information of observers, including nationality, gender, and mean age. We recruited observers from various countries in Europe, but the total number of observers in each country was small (Norwegian, 8; Italian, 1; Georgian, 1; Swiss, 1; Macedonian, 1). Therefore, in this study, we compiled them as European states.

Table 1. Information of observers in each group

Nationality (area)	Number of Male	Number of Female	Mean Age
Japanese	9	1	22.0
Thai	12	11	22.5
Chinese	6	5	25.9
European	7	4	37.7

RESULTS AND DISCUSSION

The average results of each observer group are shown in Figure 2. The horizontal axis is the hue angle of the test stimulus. In the horizontal axis, the greater the hue angle is, the greater the yellowness of the test image is, and the smaller the hue angle is, the higher the redness of the test image is. The vertical axis is perceived brightness, which corresponding to L^* value that the observer matched to the brightness of the test stimulus by adjusting the scale stimulus. Error bars are standard deviations.

For all stimuli, only Japanese observers showed the trend of the downward slope. In other words, Japanese observers judged that reddish skin was brighter than yellowish skin. Thai and European observers judged that reddish skin was darker, and these two results have similar trends. Chinese observers did not show a similar trend to the Japanese observers except for African skin color.

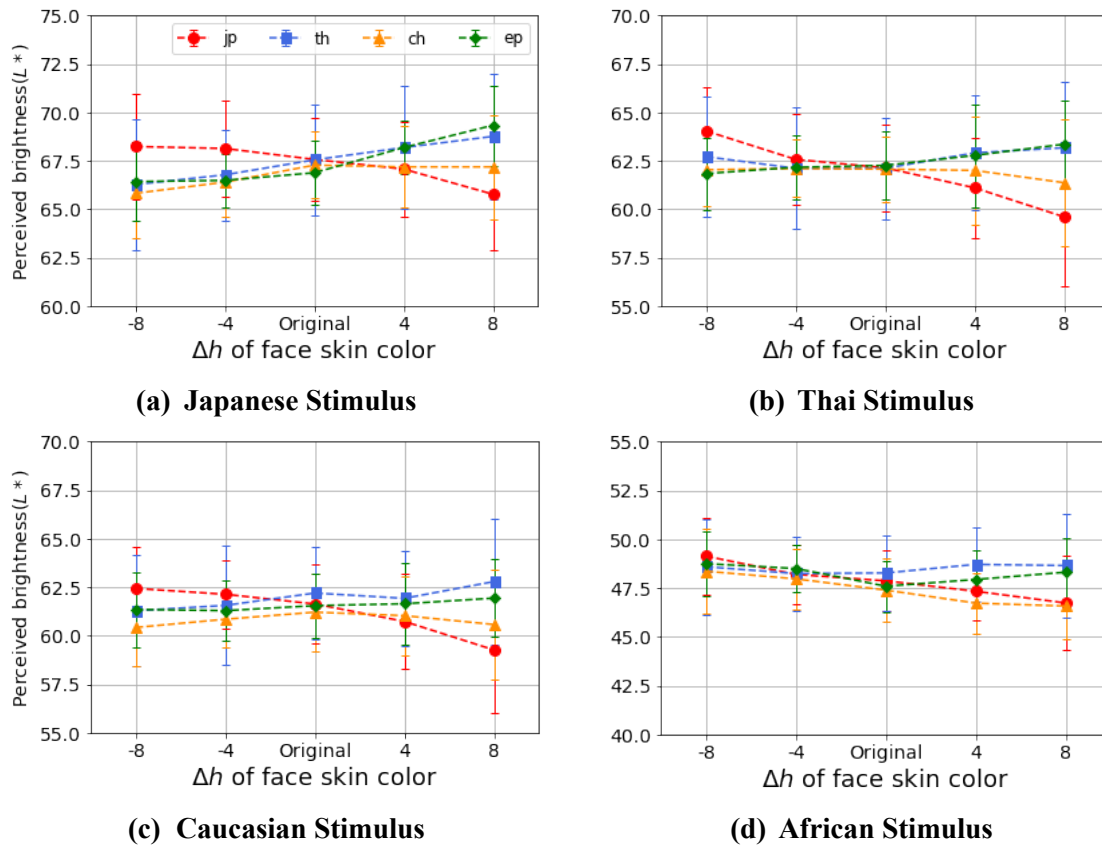


Figure 2. The average results of the observers for stimuli with different types of face color

In this study, we added European observers who were not from the Asian area. European observers showed a tendency similar to Thai, and the opposite of Japanese observers. We compared perceptions of skin brightness in four categories: Japan, Thailand, China, and Europe, but only Japanese observers perceived reddish skin brighter. This may be because the stimulus is only Japanese shape. Japanese people often look at Japanese faces, and this familiarity of the face might have influences. It would be necessary to conduct similar experiments not only with Japanese face stimuli but also with the face of other races. Some observers reported that a facial skin seemed that it was not the skin color change, but the lighting change when it was not Japanese skin color. The recognition of lighting conditions might change the recognition of skin brightness. As another possibility, different cultural settings may have caused perceptual differences. If the observer categorizes that a face is reddish or yellowish, the cultural setting may affect the decision. In other studies, Fink et al. [4] suggested that reddish skin symbolizes healthy, attractive, and good blood circulation. We need further investigation of the differences between Japan, Thailand, China, and Europe.

CONCLUSION

In this study, we added the results of European observers to our previous results (He et al. [2, 3]). European observers perceived yellowish skin brighter, and it was the opposite result from Japanese observers. It implies that there is the influence of ethnicities or environments on the brightness perception of facial skin. Besides, consistent with previous studies, Japanese people perceive reddish skin brighter. The perception of Japanese may be affected by Japanese cultural characteristics. It is necessary to conduct further experiments to clarify this issue.

ACKNOWLEDGEMENT

This work was supported by JSPS KAKENHI JP 16H01663 & 18H04183.

REFERENCES

1. Yoshikawa, H., Kikuchi, K., Yaguchi, H., Mizokami, Y., & Takata, S. (2012). Effect of chromatic components on facial skin whiteness. *Color Research & Application*, 37 (4), 281-291.
2. He, Y., Mikami, T., Tanaka, S., & Mizokami, Y. (2019). Influence of skin color to the brightness perception of facial skin – Comparison of Japanese, Thai and Chinese, Asian Pacific Conference on Vision (APCV) 2019.
3. He, Y., Mikami, T., Tanaka, S., & Mizokami, Y. (2019). Comparison of brightness perception of facial skin with differences of skin color, ICVS2019,
4. Fink, B., & Grammer, K. (2001), Human (*Homo sapiens*) facial attractiveness in relation to skin texture and color, *Journal of Comparative Psychology* 115(1), 92-99.

SKIN COLOR OF THAI PEOPLE

Nutticha Pattarasoponkun¹, Chanprapha Phuangsuan² and Mitsuo Ikeda²

¹*Graduate School, Faculty of Mass Communication Technology, Rajamangala University of Technology Thanyaburi, Thailand.*

²*Color Research Center, Rajamangala University of Technology Thanyaburi, Thailand.*

*Corresponding author: Nutticha Pattarasoponkun, nootoon2538@gmail.com

Keywords: Thai skin color, young Thai people, skin tone, skin color scale

ABSTRACT

To do a proper cosmetic treatment for faces statistics of skin color is important. Color of cheek, forehead, chin, and inner arm were measured for 107 Thai subjects and compared with Garnier skin color scale which is popular among Thai young girls. It was found that Thai skin color is mostly characterized by L* value. Thai skin color is not properly expressed by Garnier skin color scale to imply a need of development of skin color scale proper to Thai people.

INTRODUCTION

Garnier skin color scale is very popular among young girls in Thailand. It is used to judge face skin color so that cosmetics is properly chosen to make the face more charming. Atitaya Sangngiew et al.1) measured skin color of young Thai people and compared the results with the Garnier skin color scale. It was found that the Garnier skin color scale did not express the skin color of young Thai people properly and it was pointed out that it is important to collect more data of Thai skin color to see if the Garnier skin color scale cannot be applied to Thai people. If not, a new skin color scale may be developed to suit Thai girls. The measurement by Sangngiew, however, was limited only to teenagers of Thai university and it is necessary to obtain skin color of larger number of Thai people and of wide range of age. In the present paper the measurement was carried out for Thai people of the age covering 18 to 82 years old and for farmers who get strong tan.

EXPERIMENT

Color of left and right cheeks, forehead, chin and inner arm of subjects were measured with Konica Minolta CR-20, a colorimeter of contact type. At the same time the experimenter judged the subject's face to categorize them into three tones, white skin tone, tan skin tone and dark skin tone by the visual inspection following Garnier's classification. 107 subjects participated in the measurement as summarized in Table 1. Subjects of the age 19 to 30 years old were all students or staffs of Rajamangala University of Technology Thanyaburi and the students were given credit of workshop by becoming the subjects. Fifteen subjects of over 31 years old were people living in Saraburi, a northern city near Ayuttaya of Thailand.

Table 1: Subject distribution

Rank of age	Males	Females
19-30 years old	48	44
31-40 years old	2	2
41-50 years old	-	1
51-60 years old	1	2
61-70 years old	2	4
71-87 years old	-	1

Two examples of Garnier skin color are shown in Fig.1. They were purchased at different time and specified old (a) and new (b). They are different in size. The scale has 16 colors and their L^* , a^* , and b^* were measured with Konica Minolta spectrodensitometer FD-7.

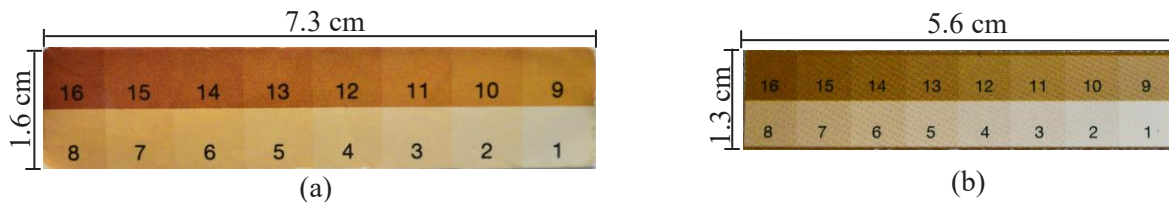


Figure 1 Pictures of Garnier skin color scales available in Thailand, a, old, b, new.

RESULTS

Color of two Garnier skin color scales were measured and their values are given in Table 2 and plotted on L^* - a^* graph in Fig. 2, by xes for the old one and crosses for the new one. Color patches for white, tan, and dark are indicated for both scales. The two scales are quite different and a proper and accurate reproduction of color is desired.

Table 2: Color specification of old and new Garnier skin color scales.

Data Name	L^*	a^*	b^*
Garnier 1	83.92	2.47	16.03
Garnier 2	82.02	3.9	20.54
Garnier 3	80.85	5.36	24.41
Garnier 4	77.33	6.57	28.2
Garnier 5	75.73	7.51	31.91
Garnier 6	72.75	9.49	34.96
Garnier 7	70.62	11.15	37.1
Garnier 8	65.92	12.37	36.34
Garnier 9	62.99	12.36	41.6
Garnier 10	59.03	13.78	41.08
Garnier 11	55.04	16.25	42.42
Garnier 12	53.55	15.35	35.04
Garnier 13	48.81	17.94	37.37
Garnier 14	45.21	19.74	36.38
Garnier 15	43.07	22.02	33.84
Garnier 16	40.33	23.46	31.17

(a) : Old scale

Data Name	L^*	a^*	b^*
Garnier 1	88.74	0.08	8.14
Garnier 2	86.69	1.6	9.91
Garnier 3	82.87	2.11	12.66
Garnier 4	77.80	2.80	14.05
Garnier 5	78.90	4.35	19.39
Garnier 6	74.59	5.15	22.14
Garnier 7	71.16	5.68	23.55
Garnier 8	64.27	5.86	24.55
Garnier 9	67.05	6.77	26.71
Garnier 10	64.00	7.89	29.04
Garnier 11	62.05	8.38	32.11
Garnier 12	59.16	8.32	32.86
Garnier 13	55	9.65	33.62
Garnier 14	52.00	8.67	34.81
Garnier 15	48.86	8.73	34.63
Garnier 16	45.95	9.72	34.88

(b) : New scale

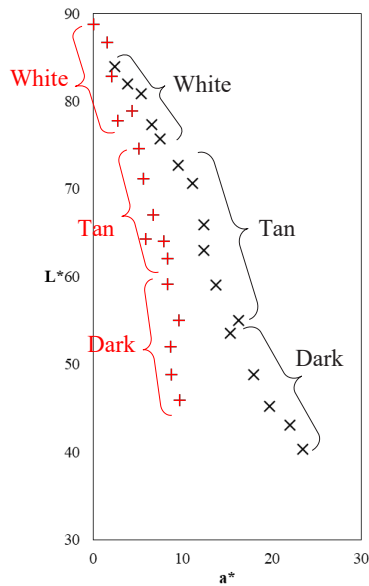


Figure 2 Plot of old and new Garnier skin color scale with regions of white, tan, and dark tone. Xes, old, +. New.

Skin colors of left and right cheeks were measured and were averaged. The results of cheek, chin, forehead, and inner arm are plotted on a^*-b^* , L^*-a^* , and L^*-b^* , graphs for all 107 subjects in Fig. 3, 4, and 5. The old Garnier skin color scale is shown by xes. Open circles are the colors of subjects judged “white” by the experimenter, gray circles are for “tan” and filled circles for “dark”. Difference of skin color appears mostly in L^* as a wide distribution in direction of L^* . The graph of cheek in Fig. 4 is reproduced as Fig. 6. Data of Saraburi people are shown by open triangles and they overlap with data taken at RMUTT, which implies that this widely spread aggregation along L^* direction fairly well represents Thai skin color. It is quite clear that old Garnier skin color scale does not represent Thai skin color as it locates far from Thai skin color aggregation. The upper people in the aggregation have white face tone, the bottom dark tone, and the middle people the tan tone. The new Garnier color scale shown by crosses passes Thai skin color but the tone ranges does not agree with tons of Thai skin.

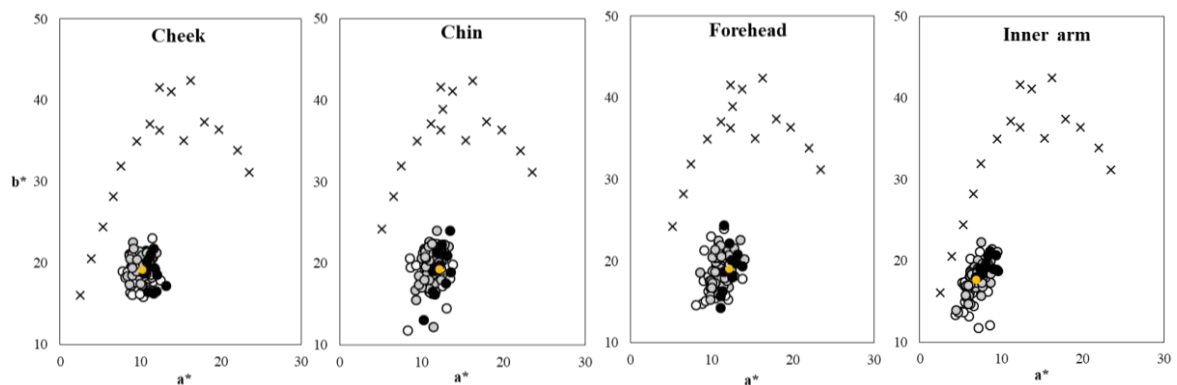


Figure 3 Skin colors of cheek, chin, forehead, and inner arm plotted on a^*-b^* graphs.

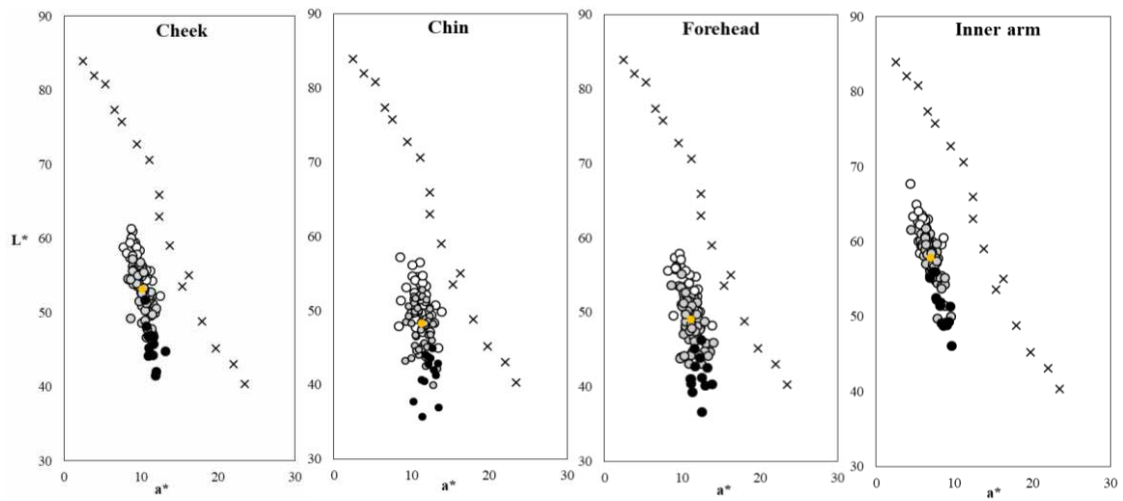


Figure 4 Skin colors of cheek, chin, forehead, and inner arm plotted on L*-a* graphs.

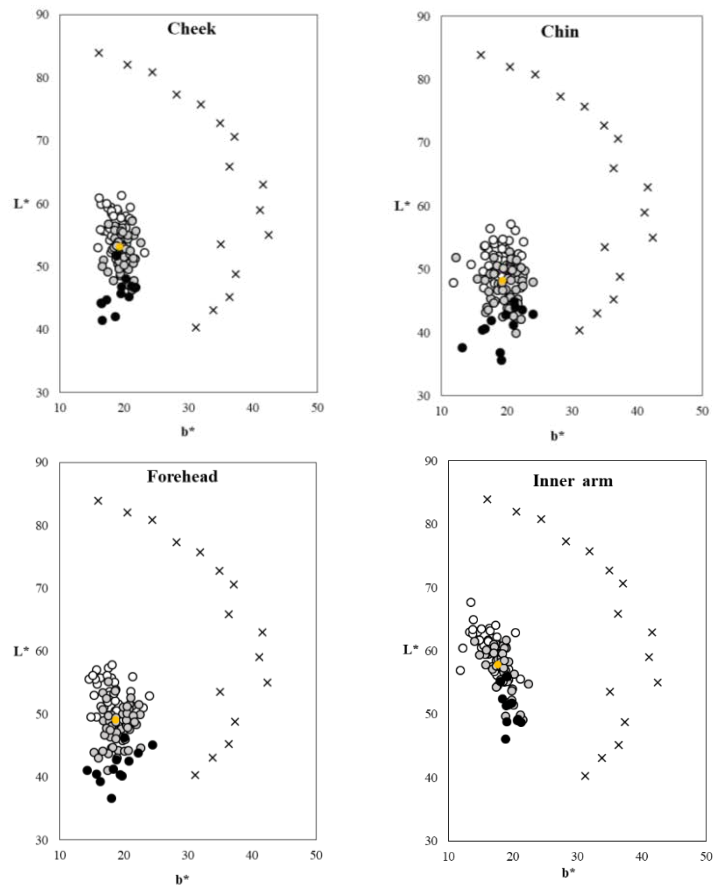


Figure 5 Skin colors of cheek, chin, forehead, and inner arm plotted on L*-b* graphs.

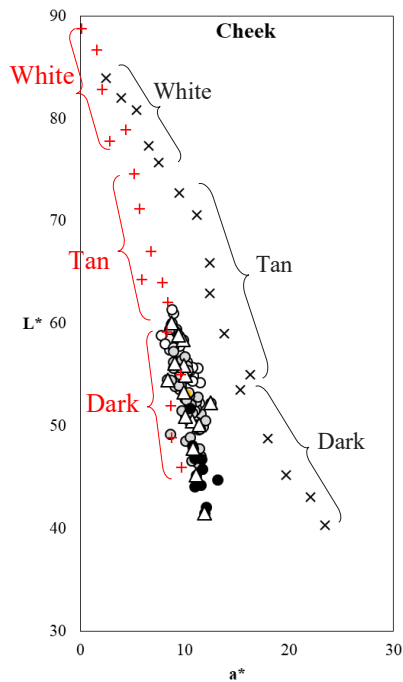


Figure 6 Skin colors of cheek plotted on L*-a* graph. Open circles, white tone skin; gray circles, tan; filled circles, dark tone skin; open triangles, Saraburi people.

In Fig. 7 colors of cheek and inner arm are plotted for Saraburi people. L* of cheek is lower than that of inner arm to imply their cheeks got tanned for many years of living. There was one female farmer of the age 66. Her cheek and inner arm colors are shown by a filled triangle and an open triangle, respectively. Her cheek is very dark, the lowest among people measured but inner arm is same as other people.

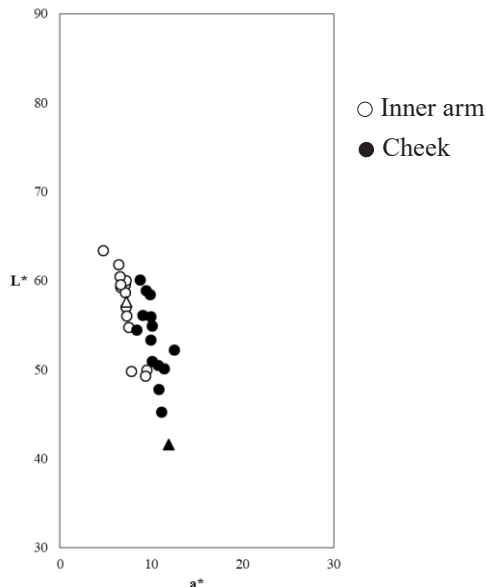


Figure 7 Comparison between cheek and inner arm for Saraburi people. A filled triangle shows cheek color of a female farmer and an open triangle inner arm of the same person.

CONCLUSION AND DISCUSSION

Thai skin colors were mostly characterized by L^* which distributed from 40 to 60. On the other hand they did not differ among people in a^* and b^* . A female farmer showed the lowest L^* value among all the 107 subjects measured. Her face was tanned because of many years of field work. This suggests importance of collecting data from different professions.

Garnier skin color scale did not represent Thai skin color. It is important to develop a scale to match with Thai skin color, which is our future work.

ACKNOWLEDGMENT

We acknowledge Centasia Co., a Bangkok distributor of Konica Minolta Sensing Co. for providing us Konica Minolta CR-20 for many months. Without the instrument the present experiment must have become difficult.

REFERENCES

1. Atitaya Sangngiew, Chanprapha Phuangwsuwan, Mitsuo Ikeda. Skin color of Thai people. Proc. *Conference of the Color Science Association of Japan*, 2019.

COLOR OF LIPSTICK TO MAKE THAI GIRLS HEALTHIER

Kanokwan Somdang^{1*}, Chanprapha Phuangsuwan¹, Natsuki Tsuji², Mikiko Kawasumi² and Mitsuo Ikeda¹

¹ *Color Research Center, Faculty of Mass Communication Technology, Rajamangala University of Technology Thanyaburi, Thailand.*

² *Faculty Science and Technology, Meijo University, Japan.*

*Corresponding author: Kanokwan Somdang, 1159108020788@mail.ac.th, Sooskaaksah@gmail.com

Keywords: Lipstick color, Healthier, Thai, Japanese

ABSTRACT

Color of lipstick changes impression of a girl to a great extent and it is useful to investigate what color gives a certain impression. In this present work we classified skin color of Thai young girls to three groups, white, tan, and dark, and their skin color were measured by Konica Minolta CM-512m3A. For Japanese girls, the color data skin was taken from Yoshikawa (2005) and they classified color skin by two groups as reddish and yellowish tones. Six colors of lipstick were selected by matching with Munsell color book which was showed by Munsell hues as 10RP, 5R and 10R and kept Value at 5 and Chroma at 8 and 14. Facial stimuli of six colors skin tone were created by a Photoshop. The colors of lipstick were stained by the same software. The six facial images were presented on a display EIZO LCD type by one type of skin color tone (with 6 colors of lipstick) and subjects assessed of impression with four categories “healthy”, “Unhealthy”, “Bright”, “Dark” and another impression, “like” and “dislike” to find out the individual favorite color of lipstick. The lipstick colors showed “healthy” impression at 10RP 5/14 for white and dark skin tones, 10R 5/8 for tan. The selected color lipsticks for “unhealthy” impression were showed 10R 5/14 for white and dark. For tan skin tone showed 5R 5/14 for unhealthy impression. The color lipsticks were selected for “bright” impression 10R 5/14 for white and tan, 10RP 5/8 for dark skin tone. The impression of “dark showed at the color lipsticks 5R 5/8 for white and 10R 5/8 for tan and dark skin tones. But for the popular like impression showed the color of lipstick at 5R 5/14, 10RP 5/14 and 10R 5/8 respectively, without considering to the skin color tone.

INTRODUCTION

Many researches have studied about the color appearance of the face skin in term of clothing colors [1], effect of facial redness [2] and so on. We can easily detect the healthiness and attractiveness by looking at the face. It has various factor to make a criterion of healthiness and attractiveness such as skin color tone, color of lip, color of hair, color of clothes and the style of making up. Lip is becoming the importance role for every gender, without adding color to lip it causes less confident to go outside or to meet other people. Our hypothesis was to use the right color of lip it can give a good looking such as healthiness and attractiveness. We employed the graphic of woman facial images and simulated 3 types of skin tone for Thai peoples and 2 types skin tone for Japanese people. We employed six colors of lipstick to simulate facial images lip. The experiment was carried out on a display. We asked the observers with the adjectives “healthy, unhealthy, bright and dark”.

EXPERIMENT

Stimuli

The color of the facial image stimuli was set to the average skin color of Thai and Japanese females (the average of Thai color skin measured from 39 females by Spectrophotometer Konica Minolta CM-512m3A and for the average Japanese color skin we took values from Yoshikawa [3]).

Categories of Thai color skin tone were white, tan and dark and Japanese skin colors tone were yellowish and reddish. The physical color measurement data are shown in Table 1. We were control the color of facial images based on the color Yxy value which was measured from the cheeks of participants. Figure 1 (a) showed the stimuli represented to 5 skin tones.

Table 1: Yxy chromaticity values of skin color and of facial images on display.

Countries	Skin color tone	Real face			Monitor		
		Y	x	y	Y	x	y
Thailand	White	25.606	0.369	0.362	25.992	0.366	0.363
	Tan	22.835	0.378	0.366	22.723	0.376	0.366
	Dark	20.803	0.385	0.371	18.700	0.385	0.371
Japan	Reddish white	32.080	0.388	0.361	31.877	0.388	0.360
	Yellowish white	39.730	0.370	0.363	39.870	0.370	0.365

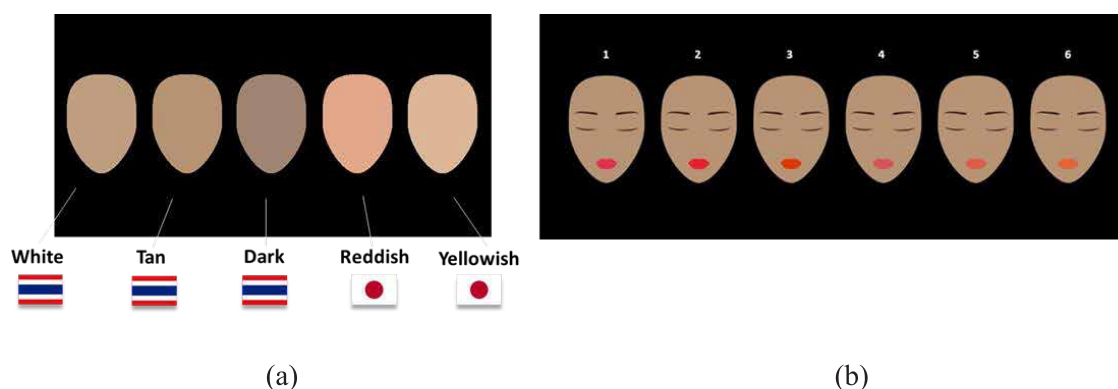
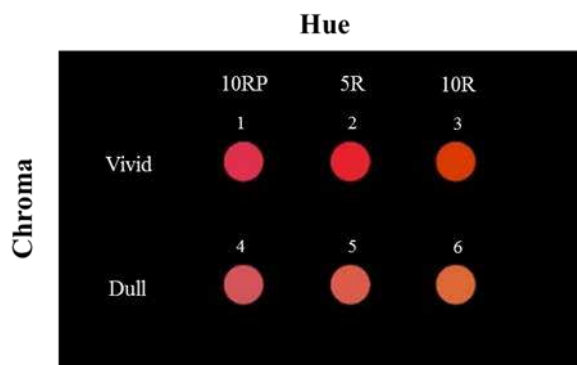


Figure 1. (a), Skin color tone on facial images. (b), Facial images with the 6 selected color lipsticks.

Six popular colors of lipstick were employed to investigate the healthy and brightness impression. Those colors of lipstick were matched with the Munsell color system shown in Fig. 2. They were three hues; 10RP, 5R and 10R of which value was fixed at 5 and Chroma at 8, th represented dull color and those with Chroma 14 and Value 5 vivid color. We adopted six colors of lipstick to lip on the facial images stimuli



(five colors tone) as shown in Fig. 1 (b). Total stimuli were 30 facial images (6 colors of sipstick x 5 skin colors tone). Fig. 1 (b) shows 6 facial images with different colors of lipstick for a color skin tone.

Figure 2. Six popular colors of lipstick expressed by Munsell color system.

Procedure

The facial images stimuli were shown on the display with the randomly skin color tone. The questionnaire was prepared by the Google form so that subjects can be select the color of lipstick which gave the impression of “healthy”, unhealthy”, “bright” and “dark”. And the last question was “What is your favorite color of lipstick among 6 colors?”. Subject selected under the experimental booth which was a dark room. No repetition in this experiment.

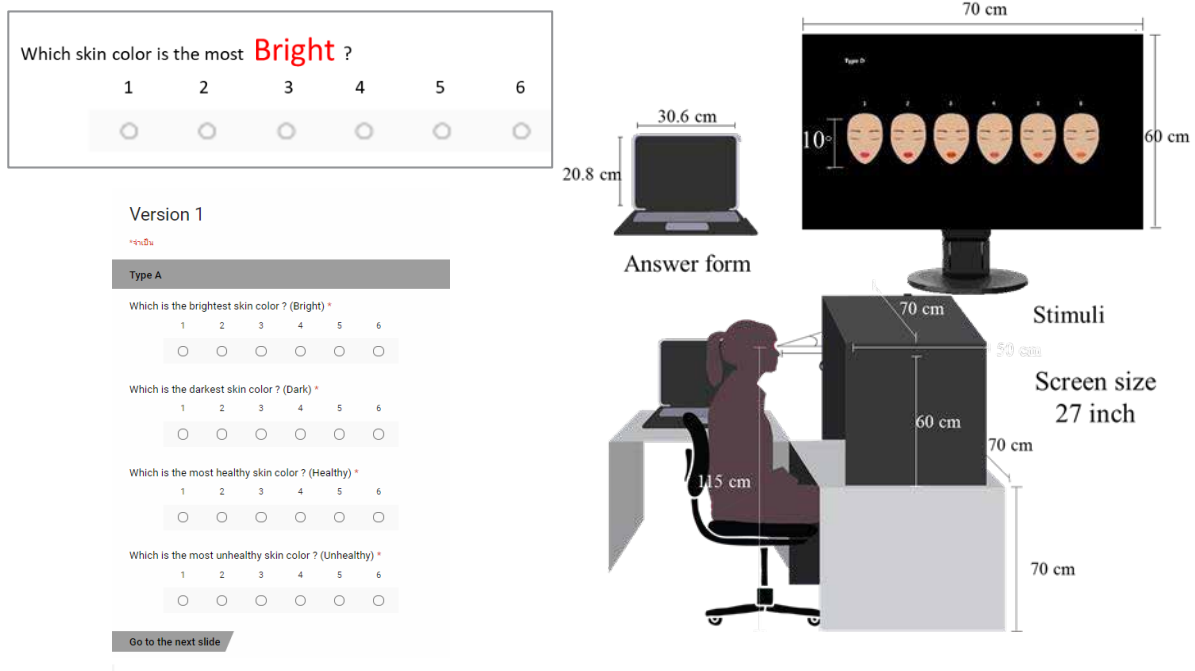


Figure 3. Data sheet, experimental booth and stimuli on the display.

Subjects

Thirty three Japanese and thirty eight Thai served as subjects. Their age ranged from 19 to 50 years old for Japanese and 18 to 44 years old for Thai. They were checked for normal color vision by Ishihara test.

RESULTS

Fig. 4 showed the results of color lipsticks that gave the impression as healthy, unhealthy, bright and dark for white, tan and dark skin tones of Thai and for reddish and yellowish for Japanese. The abscissa showed three hues of lipsticks and ordinate showed Chroma values at 8 for dull and at 14 for vivid color. The results of selected color of lipstick in four categories; healthy, unhealthy, bright and dark of Thai subjects' impression were showed in the Fig. 4. The lipstick colors showed the “healthy” impression for 10RP 5/8 for white and dark skin tone, 10R 5/14 for tan skin tone respectively. The selected color of lipsticks for “unhealthy” impression were 10R 5/8 for white and dark. For tan skin tone it was 5R 5/8 for unhealthy impression. The color lipsticks for “bright” impression was 10RP 5/8 for white and tan, 10RP 5/14 for dark skin. The impression of “dark” was color lipsticks 5R 5/14 for white, 10R 5/14 for dark skin and for tan skin, the impression of “dark” was two color of lipstick as 5R 5/14 and 10R 5/14.

The selected color of lipsticks from Japanese subjects agreed with Thai results. Reddish skin color showed 10R 5/14 but for yellowish skin showed 10RP 5/8 for the “healthy” impression. “Unhealthy” impression was given by 5R 5/8 for reddish and 10R 5/8 for yellowish skin. “Bright” showed 10RP 5/8 both reddish and yellowish skin. “Dark” impression was 5R 5/8 for reddish and 10R 5/14 for yellowish skin.

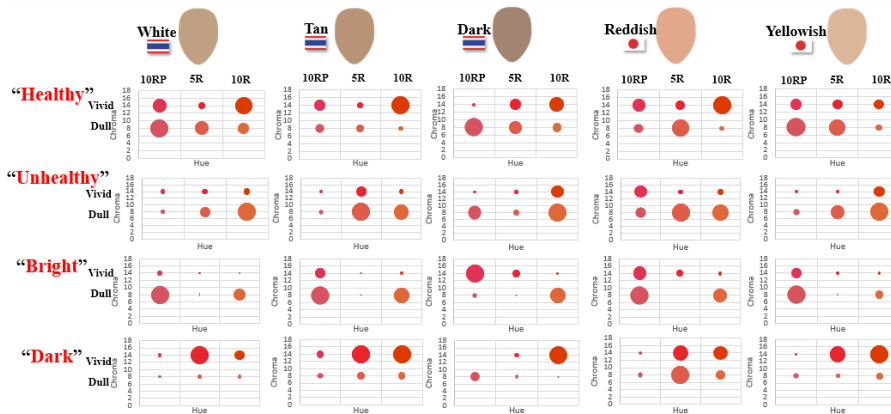
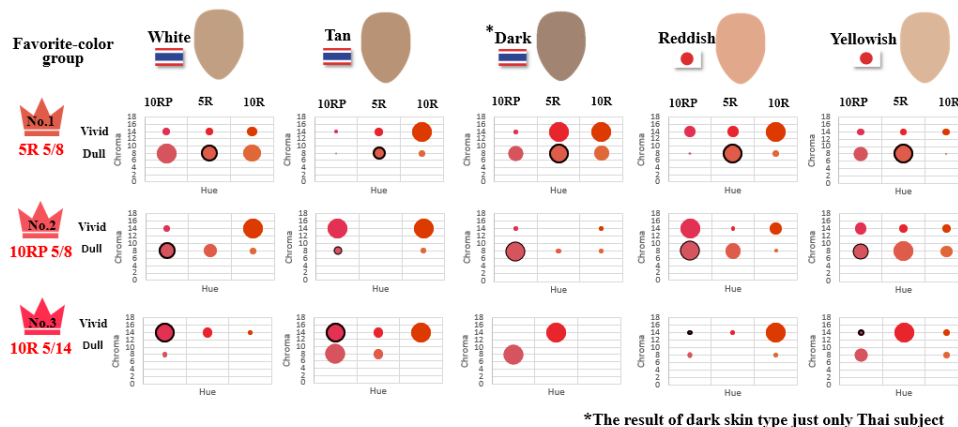


Figure 4. Results of color lipstick for healthy, unhealthy, bright and dark.

CONCLUSION

The color of lipsticks affected to the impression of the face. The individual preference of color lipsticks did not relate to the impression, which was found in the last question “what is favorite your color lipstick?” The most favorite color of lipstick was 5R 5/8, 10RP 5/8 and 10RP 5/14 respectively as shown in Fig. 5. In this experiment we could not find out the systematic preference of lipstick color with different color skin tones. We need a further experiment to investigate on this topic.



*The result of dark skin type just only Thai subject

Figure 5. Three ranking of favorite color of lipstick compared with the healthy impression results, the bubble with black line indicate favorite color of lipstick.

ACKNOWLEDGEMENT

Kanokwan somdang thanks RMUTT for providing her with the Student development foundation of RMUTT scholarship for her transportation to do an internship at Meijo University for 3 months. Also thanks students at Associate Professor Kawasumi's laboratory at Meijo University who helped her experiment and for serving subjects.

REFERENCES

1. Nakajima, Y., He, S., & Fuchida, T. (2018). Effects of adjacent chromatic clothing colours on facial skin colour appearance. *AILISBOA 2018 colour & human comfort*.
2. Re, D. E., Whitehead, R. D., Xiao, D., & Perrett, D. I. (2011). Oxygenated-Blood Colour Change Thresholds for Perceived Facial Redness, Health, and Attractiveness. *PLoS ONE*, 6(3). doi: 10.1371/journal.pone.0017859
3. Yoshikawa, H. (2005). Colorimetric Approach to the Skin Color. *Journal of the Color Science Association of Japan*, 29(2).

RELATIONSHIP BETWEEN OBSERVERS' INTERESTS TO COLORS AND THE PRECISION OF COLOR CATEGORIZATION

Akira Asano^{1*}, Yuri Yoshii¹, and Chie Muraki Asano²

¹*Faculty of Informatics, Kansai University, Japan.*

²*Sapporo Campus, Faculty of Education, Hokkaido University of Education, Japan.*

*Corresponding author: Akira Asano, a.asano@kansai-u.ac.jp

Keywords: color name, precision of color name, interests to colors

ABSTRACT

The relationship between human interests in colors and the precision of color categorization are investigated. The correlation between the precision of color categorization and the detail of the color names assigned by observers is evaluated through an experiment of the segmentation of the continuous color circle to color categories and the assignments of a color name to each segment by the observers. The experimental result shows that the details of color names and the number of the color categories are positively correlated and suggests that human interests in colors and the precision of color categorization are also positively correlated. The result also shows that a tendency of hue dependency of human color categorization due to the characteristic of the HSV color model.

INTRODUCTION

The usage of words for color expressions is different according to each observer. For example, some observers express a color by detailed words while some express by basic color names like "red" and "blue." It is expected that observers who are highly interested in colors do not use basic color names, but common and detailed color names and/or expressions originally invented by the observer.

We investigate the relationship between the observer's interests to colors and the precision of color categorization through an experiment of categorizing the colors in the color circle and naming of each categorized color. Each observer divides a color circle of continuous color transition by drawing a line at each position that the observer regards as the boundary of two different colors and assigns a name to each segment of the color circle. It is evaluated how detailed the assigned names are, and it is regarded as an index of the observer's interests in colors. We obtained the result that the details of color names and the number of the color categories were positively and moderately strongly correlated. It suggests that human interests in colors and the precision of color categorization are also positively correlated.

It is also investigated the dependence of the precision of the categorization on hues in this research. It is known that the precision of the human color categorization depends on hues. We employed the HSV color circle [1] in our experiment because a color circle of continuous color transition is easily generated based on the HSV system. It is said that the HSV color model fits the human color sense, however, the range of green is recognized wider than those of other hues, in comparison with the PCCS system [2], which is precisely adopted to human color sensitivity. We investigated the



Fig. 1. HSV color circle used in the experiment.

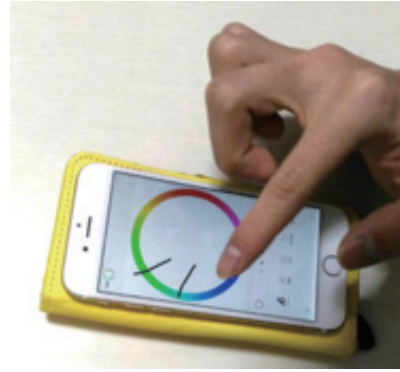


Fig. 2. Drawing color boundaries.

difference of precision of the categorization at a fixed range around each hue on the color circle. It was found that there was a tendency that the categorization was rather rough in green while rather detailed in orange.

METHODS

The HSV color circle as shown in Fig. 1 is presented to observers. The observer is requested to draw a line on the location where it is recognized as a boundary of two different colors on the color circle. The observer is also requested to name each color segment between two adjacent boundaries by a word without any limitation on the expressions. The precision and originality of the words are evaluated as a score, which is used as the index of the observer's interests in colors. The density of the boundaries on each hue is also evaluated.

The procedure of the experiment is as follows:

- 1) A color circle of continuous color transition based on the HSV color model was generated on the screen of smartphones and tablets. We employed Apple iPhone and iPad with an LCD only.
- 2) Each observer was requested to draw a line at each position that the observer regarded as the boundary of two different colors, as shown in Fig. 2. The number of the line segments were not limited.
- 3) The observer assigned a name to each segment between two adjacent boundaries on the color circle. The observer expressed the color names without any limitations.
- 4) The number of boundaries was counted, and the positions of the boundaries were recorded numerically under the definition of angles as shown in Fig. 3.
- 5) The color names assigned in 3) were evaluated according to the following scoring policy:
 - score 1: basic color names, such as “red” and “blue”
 - score 2: simple but more detailed color names, such as “orange” and “light red”
 - score 3: detailed and commonly used color names, such as “marine blue”
 - score 4: originally created color name, such as “tomato color”

The observers were 42 university students and all of them had normal color vision. All the observers used Japanese language to name colors.

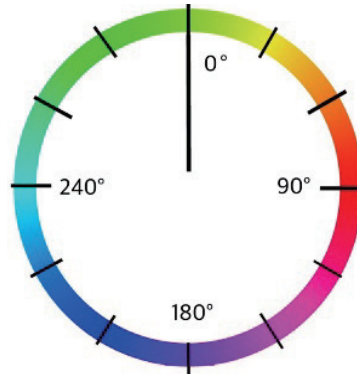


Fig. 3. Definition of angles.

EXPERIMENTAL RESULTS AND DISCUSSION

The scattergram in Fig. 4 shows the number of boundaries and the average score on the assigned color names for each observer. The correlation coefficient is 0.592. It indicates that the precision of the color categorization, measured by the number of boundaries, and the details of the assigned color names, measured by the scoring policy described in the previous section, are positively correlated. It suggests that the precision of color categorization and human interests in colors are also positively correlated.

Table 1 shows the average numbers of boundaries over all the observers in the range of ± 30 degrees at each position at the interval of 20 degrees on the color circle. It shows a tendency of hue dependency of human color categorization; The density of boundaries is smaller for green and larger for orange.

CONCLUSIONS AND FUTURE REMARKS

This research has investigated the relationship between the precision of color categorization by observers and interests in colors of the observers, through the experiment of the segmentation of the continuous color circle to color categories and the assignments of a color name to each segment by the observers. The experimental result suggests that the precision of color categorization and human interests in colors are positively correlated. The result also shows a tendency of hue dependency of human color categorization due to the characteristic of the HSV color model.

In our experiment, some observers had specific knowledge on color sciences and were probably more sensitive to colors. A further research is needed to incorporate the effect of the observers' specific knowledge. It is expected, as a future research, to measure human emotion, or *kansei*, to colors and its personal differences more precisely based on the generation of a continuous color circle in a uniform color space according to human color recognition and the investigation of the measurements of human interests in colors more objectively and precisely.

ACKNOWLEDGEMENTS

The authors thank Professor Katsunori Okajima, Yokohama National University, Japan, Dr. Mikiko Kawasumi, Meijo University, Japan, and students of their research groups for their cooperation in

the experiments. This research is partially financially supported by JSPS KAKENHI Grant Nos. 15K00706 and 19K12692, and Kansai University Researcher Grant 2016.

REFERENCES

1. Berns, R. S. (2019). *Billmeyer and Saltzman's principles of color technology*, Wiley.
2. Nayatani, Y. (2004). Proposal of an Opponent-Colors System Based on Color-Appearance and Color-Vision Studies, *COLOR research and application*, 29(2), 135-150.

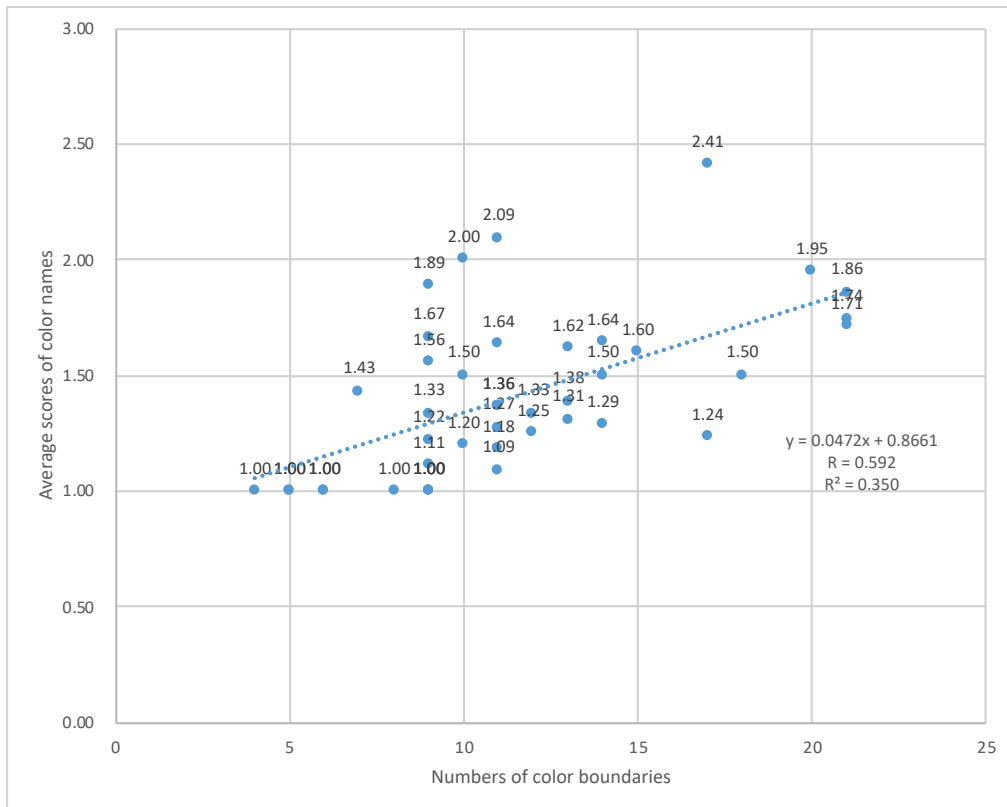


Fig. 4. Relationship between the number of color boundaries and the average score of the assigned color names.

Table 1. Number of color boundaries in the range of ± 30 degrees at each hue of 20 degree interval.

hue(deg)	180	200	220	240	260	280	300	320	340
avr. # of boundaries	3.45	3.43	3.50	3.60	3.31	3.33	2.88	2.90	3.29
	0	20	40	60	80	100	120	140	160
	3.33	3.86	3.98	4.40	4.14	3.69	3.86	3.57	3.55

MODERN MANDARIN BASIC COLOR TERMS ACQUIRED FROM COLOR NAMING TASK AND STATISTICS CORPUS LINGUISTICS

Tsuei-Ju Hsieh¹, Ichiro Kuriki², I-Ping Chen³ *

¹*Department of Information Communication, Associate Professor, Chinese Culture University, Taiwan.*

²*Research Institute of Electrical Communication, Associate Professor, Tohoku University, Japan.*

³*Institute of Applied Arts, Professor, National Chiao-Tung University, Taiwan.*

*Corresponding author: I-Ping Chen, iping@faculty.nctu.edu.tw

Keywords: Mandarin Basic Color Terms; World Color Survey (WCS); unconstrained color-naming task; statistics corpus linguistics; color categories

ABSTRACT

The uncertain developmental status of Mandarin Basic Color Terms (hereafter BCTs) in Berlin and Kay's survey (1969) has led many expanded studies with various approaches. Due to the diverse nature of color synonym terms in Mandarin, many studies had employed specific selection methods to narrow the list of candidate Mandarin BCTs down prior to the chip-term matching task. This study compares the Mandarin BCTs acquired from two different approaches, the unconstrained color-naming task and the statistics corpus linguistics. The unconstrained color-naming task duplicated the method in the World Color Survey (WCS), and the number of Mandarin BCTs was found eleven with a K-means clustering analysis, which agrees with the number asserted in most previous studies. However, there is a discrepancy between studies on what color terms comprises the eleven Mandarin BCTs. The disagreement of the wording for color categories of pink, brown, and orange is particularly evident. Our current results show these three color categories are most frequently named 粉紅 Fenhong, 咖啡 Ka-fei, and 橘 Ju, which are not consistent with previous studies. Therefore, we employed the method of statistic linguistic corpus to seek Mandarin BCTs of consensual. We compared the eleven BCTs found in the previous color-naming task with the frequency statics of color terms delivered from an authentic linguistic database. The Mandarin BCTs accessed with two methods do overlap considerably. The top eleven popular color terms from the linguistic database are white (白), red (紅), black (黑), yellow(黃), green(綠), blue(藍), brown(咖啡), grey(灰), pink(粉紅), purple(紫), and orange(橙). These terms almost match those revealed in the color-naming task. The only difference lies in the orange terms. The term “橘 Ju” is mostly used in the color-naming task, but “橙 Cheng” is ranked prior to “橘 Ju” according to the linguistic database. Despite this slight divergence, the results from the statistic corpus linguistics strongly support the validity our findings in the color-naming task.

INTRODUCTION

Basic color terms (hereafter BCTs) are the terms used to name various color shades within the color category. Due to the nature of perceptual categorization, given human color vision is capable of discriminating millions of colors, the number of color categories with corresponding color terms is quite limited across cultures. For example, various colors of bluish tone are conventionally named “blue” in English, and the boundaries of the blue category could vary in different languages. The color term used to indicate a particular range of color with high consensus (i.e., psychologically salient) is known as the BCT. The common number of BCTs within many developed languages has

been recognized eleven. However, the number of Mandarin Chinese BCTs had raised considerable debates. The earlier study asserted that the number of Mandarin BCTs was six (Berlin & Kay, 1969), but many subsequent studies clarified the number should be eleven. (Lu, 1997; Hsieh & Chen, 2011; Lin & Luo, 2012; Sun & Chen, 2018). Despite the number of BCTs in Mandarin has developed consensus, the color terms comprising the eleven Mandarin BCTs are quite inconsistent among studies. Due to the considerable amount of extant color synonyms in Mandarin, several studies had narrowed the list of candidate BCTs down with certain selection methods before the chip-term matching procedure. Relevant studies such as Lin et al. (2001), Hsieh et al. (2011), Lu (1995), and Sun et al. (2018). These studies filtered some color terms from a greater pool of color terms. The method was known as “constrained method”, which limits the participants to perform color term-color chips matching by using given color terms. Another opposite type of method is known as “unconstrained method”, such as using the free-naming task to access the spontaneous naming responses to the given color stimuli. The color terms elicited from free recall served better representation role of color basic color categories, and avoid the researchers’ judgment involving the selection of color terms.

Although most studies agree with the number of BCTs in Mandarin is eleven, there is much less consensus on what color terms comprise this BCTs set. The first debatable case is the pink category, which has been reported to be consensually named “粉紅”, literally the “pale red”, in studies adopting unconstrained method (Lin et al., 2001a; Hsieh et al., 2011). However, a free recall survey conducted at the end of last century (Lu, 1997) found the color term for pink category elicited without any stimulus was “桃”. This term also means “peach” in Mandarin. Another color category named with diverged color terms is orange, in which “橘” (literally tangerine) is mostly used (Lin, et al., 2001 b; Hsieh et al, 2011). But another term “橙” (literally orange) was also reported (Lu, 1997). The most controversial color category in terms of naming is brown, with multiple terms were identified: “棕 (tsong)” (Lin, et al., 2001a; Gao & Sutrop, 2014), “褐 (he)” (Lu, 1997; Gao & Sutrop, 2014) and “咖啡 (ka-fei)” (Hsieh et al., 2011). The inconsistent wording of naming a color category may be due merely to the time changes of common idioms or colloquial expressions. Therefore, the current study adopts two approaches with different methodological advantages to address this issue.

METHOD

The present study adopts two distinct approaches to identify the BCTs and compare their consistency. First, we repeated the experiment from previous studies by using a set of color chips from the World Color Survey (shown in Figure 1(a)) and applied k-means cluster analysis, in which the number of clusters was optimized by the gap statistic analysis (Tibshirani et al., 2001; Lindsey & Brown, 2006, 2009, 2014; Kuriki et al., 2017). Participants were 41 healthy college students of the Chinese Cultural University of Taipei, who speak Mandarin as their first language. The 330 color chips from the Munsell Book of Color, Glossy Edition (www.munsell.com) were mounted on cardboard covered with a medium gray sheet that corresponds to N5/ in Munsell notation. The color chips were presented one-by-one in a standard light cabinet, VeriVide CAC60 (VeriVide, Leicester, U.K.) and illuminated with VeriVide F20T12 / D65 Light Tube (CIE Ra = 98, approximate illuminance on the tabletop was 351 lux). The participants were shown each color chip in a pseudo-random order, pre-defined by experimenters, and participants were asked to name each color chip by a single color term (monolexic restriction).

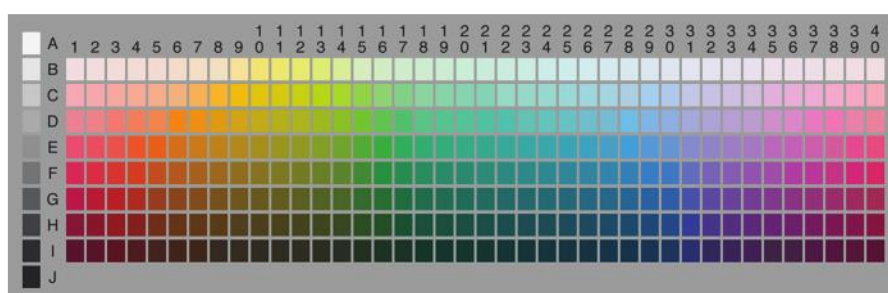
On the other hand, we adopted the method of statistics linguistic corpus to find the popularity of color terms from the corpus of contemporary Mandarin. We searched the database, Accumulated Word Frequency in Modern Chinese Corpus, by inputting the color terms acquired from the color-

naming task. The database is a part of “Academia Sinica Balanced Corpus of Modern Chinese”, which is authentically established and maintained by the Institute of Linguistics in Academia Sinica Taiwan (<https://ckip.iis.sinica.edu.tw/CKIP/engversion/20corpus.htm>). The linguistic corpus targets at 10 million words with part-of-speech tagging with finely processed Chinese word segmentation. It is considered a practical representation of Modern Chinese Mandarin as the topical distribution of the corpus covers topics include philosophy (8%), literature (13%), life (28%), society (38%), science (8%), and art (5%) (Chen, Huang, Chang & Hsu, 1996). As a result, we believe the frequency of the concerned color terms delivered by this linguistic corpus database would fairly represent the popularity status of the color terms.

RESULT

Figure 1(a) shows the color chips set we adopted, as the same set in world color survey (WCS). Figure 1(b) is the popularity rank order plot (Zipf chart) of our Mandarin Chinese data. The horizontal and vertical axes represent logarithms of rank order and populations, respectively. After verifying with a k-means clustering analysis, the result confirmed eleven color categories, including eight chromatic categories. The eleven color terms correspondingly is “紅 (hong; red),” “綠 (lü; green),” “藍 (lan; blue),” “黃 (huang; yellow),” “紫 (zi; purple),” “橘 (cheng; orange),” “灰 (hui; gray),” “咖啡 (coffee; brown),” “白 (bai; white),” “粉紅 (fenhong; pink),” and “黑 (hei; black).”

(b)



(a)

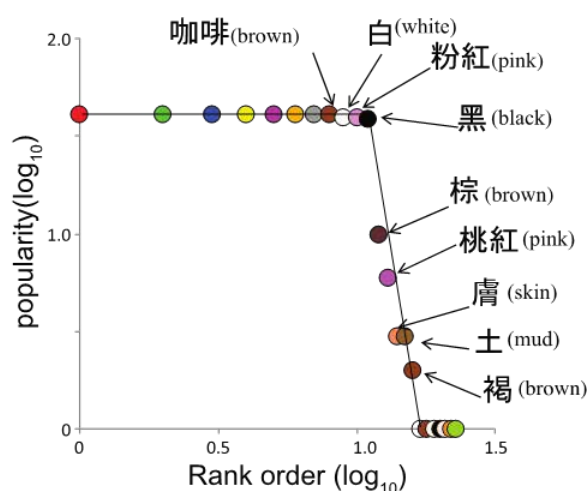


Figure 1. (a) Color chips set of WCS (b) Popularity rank order plot (Zipf chart) of our Mandarin Chinese data. The horizontal and vertical axes represent logarithms of rank order and populations, respectively.

Figure 2 shows the frequency rank order of the color terms from the Accumulated Word Frequency in Balanced Modern Chinese Corpus Sinica. Note that the scale of horizontal and vertical axes is linear. Comparing with the color terms found in previous color naming task, the terms for color categories of white, red, black, yellow, green, blue, brown, gray, pink, and purple are matched, despite several non-basic terms such as “青 (ching; grue)” and “膚 (fu; skin)” appear in the popularity rank. There are two cases of multiple terms indicating the same categories have emerged. Specifically the terms “咖啡 (coffee; brown),” “褐 (he; tan or brown),” and “棕 (tzong; palm or brown)” which all refer brown category, and “橙 (cheng; orange)” and “橘 (ju; tangerine)” both refer orange category. The rank order of “咖啡 (coffee; brown)” is prior to the other brown terms, therefore the result converges with the rank order in Figure 1(b). In the case of orange category, a rather popular term from the linguistic corpus is “橙(cheng; orange)”, which conflicts with the term we found with color naming method, “橘 (ju; tangerine).”

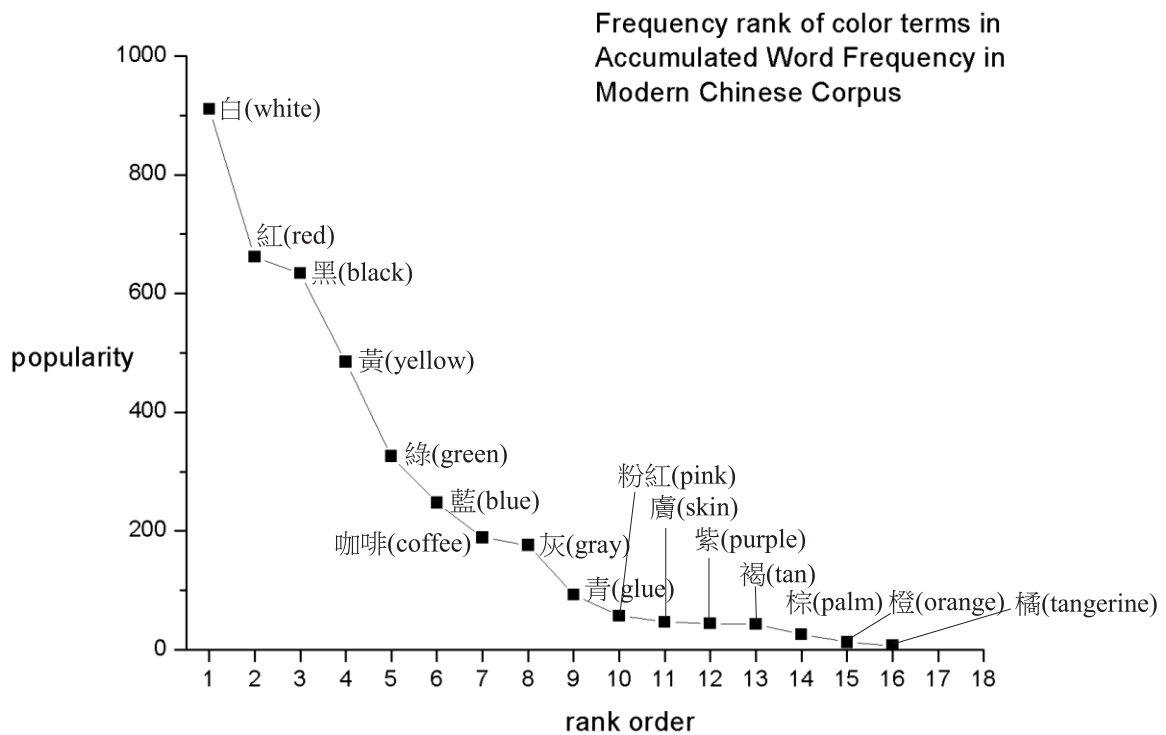


Figure 2. Frequency rank order of the color terms from the Accumulated Word Frequency in Balanced Modern Chinese Corpus Sinica.

One of the plausible explanations of this minor discrepancy is that this linguistic corpus database shows color terms collected partially from Modern Chinese literature, namely the collection of written language. However, the color-naming task in the current study required the participants to

name colors by speaking instead of writing. Perhaps “橘 (ju)” is a plain-spoken word choice to the participants. Another possibility is that “橙 (cheng)” appears more frequently than “橘 (ju)” in color-irrelevant contexts. For example, “橙 (cheng)” is used in “柳橙汁 (liǔ chéngzhī; orange juice),” which is a common term in daily life, and therefore raises the frequency count of the character “橙 (cheng).” It should be taken into consideration that using the method of “balanced” linguistic corpus could include the terms applied in various context. To illustrate the idea, Figure 3 shows the composition of four landmark basic color terms with each part of speech composition. These different type of part of speech of the color term applications constitute the frequency count in Figure 2. The accumulated count of term “紅(red)” is 662, as shown in Figure2, and this quantity includes at least three types of part of speech of the term. For example, the tag “Na” represents a part of speech which “紅色” or “紅” are used as a noun. Despite this slight divergence in the orange category, the comparative results from the statistic corpus linguistics strongly support the validity our findings in the color-naming task.

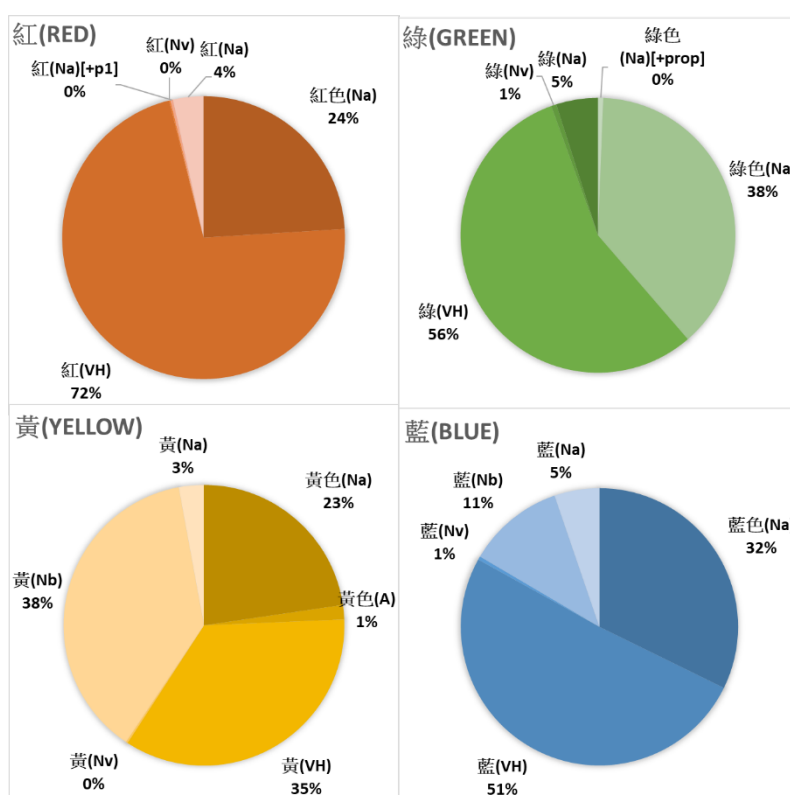


Figure 3. An example of the part of speech composition within an accumulate frequency of a color term reported by the Modern Chinese Balanced Linguistic Corpus

REFERENCES

- Berlin, B. & Kay, P. (1969). Basic Color Terms: Their Universality and Evolution. Berkeley: University of California Press.

2. Chen, K. J., Huang, C. R., Chang, L. P., & Hsu, H. L. (1996). Sinica corpus: Design methodology for balanced corpora. *Proceedings of the 11th Pacific Asia Conference on Language, Information and Computation* (pp. 167–176).
3. Gao, J., & Sutrop, U. (2014). The basic color terms of Mandarin Chinese: A theory-driven experimental study. *Studies in Language*, 38(2), 335–359. doi: 10.1075/sl.38.2.03gao
4. Hsieh, T. J., & Chen, I. P. (2011). Categorical formation of Mandarin color terms at different
5. luminance levels. *Color Research & Application*, 36(6), 449–461. doi: 10.1002/col.20638
6. Kuriki, I., Lange, R., Muto, Y., Brown, A. M., Fukuda, K., Tokunaga, R., Lindsey D.T., Uchikawa K., & Shioiri, S. (2017). The modern Japanese color lexicon. *Journal of Vision*, 17(3), 1. Doi: 10.1167/17.3.1
7. Lin, H., Luo, M.R., MacDonald, L.W. & Tarrant A.W.S. (2001b) A cross-cultural colour-naming study: Part II – Using a Constrained Method. *Color Research and Application*, 26(3), 193–208. Doi: 10.1002/col.1017
8. Lin H., Luo M.R., MacDonald L.W. & Tarrant A.W.S. (2001a) A cross-cultural colour-naming study: Part I – Using an Unconstrained Method, *Color Research and Application*, 26(2), 40–60. Doi: 10.1002/1520-6378(200102)26:13.0.CO;2-X
9. Lindsey, D. T., & Brown, A. M. (2006). Universality of color names. *Proceedings of the National Academy of Sciences*, 103(44), 16608–16613. Doi: 10.1073/pnas.0607708103
10. Lindsey, D. T., & Brown, A. M. (2009). World Color Survey color naming reveals universal motifs and their within-language diversity. *Proceedings of the National Academy of Sciences*, 106(47), 19785–19790. Doi: 10.1073/pnas.0910981106
11. Lindsey, D. T., & Brown, A. M. (2014). The color lexicon of American English. *Journal of vision*, 14(2), 17. doi:10.1167/14.2.17
12. Lu, C-F. (1997) Basic Mandarin Color Terms. *Color Research and Application*, 22(1), 4–10. doi: 10.1002/(SICI)1520-6378(199702)22:1<4::AID-COL3>3.0.CO;2-Z
13. Sun, V. C., & Chen, C. C. (2018). Basic color categories and Mandarin Chinese color terms. *Plos One*, 13(11), e0206699. doi: 10.1371/journal.pone.0206699
14. Tibshirani, R., Walther, G., & Hastie, T. (2001). Estimating the number of clusters in a data set via the gap statistic. *Journal of the Royal Statistical Society: Series B (Statistical Methodology)*, 63(2), 411–423. Doi: 10.1111/1467-9868.00293

THAI BASIC COLOR TERMS AND NEW CANDIDATE NOMINATION

Nischanade Panitanang^{1*} Chanprapha Phuangsuan², Ichiro Kuriki³, Rumi Tokunaga⁴,
and Mitsuo Ikeda².

¹*Graduated School, Faculty of Mass Communication Technology, Rajamangala University of Technology Thanyaburi, Thailand.*

²*Color Research Center, Rajamangala University of Technology Thanyaburi, Thailand.*

³*Research Institute of Electrical Communication, Tohoku University, Japan*

⁴*College of Liberal Arts and Sciences, Chiba University, Japan.*

*Corresponding author: Nischanade Panitanang, nischanade_p@mail.rmutt.ac.th

Keywords: Thai color names, Color categories, World color survey, Elementary color naming, Basic color term.

ABSTRACT

Due to a variety color names used in the world which is different depending on the speaker's habitat and it raises questions about the universality cross-linguistic of the color name. We conducted a survey of Thai color names from 161 Thai native speakers. 330 Munsell color chips taken from the Munsell Book of Color Glossy Edition, 320 chromatic chips, Munsell Value ranging from 2 to 9 with 40 equally spaced Munsell Hue (2.5 R to 10 RP, in hue steps of 2.5) at the maximum chroma of each value in each hue, and 10 achromatic chips of Value from 1.5 to 9.5. Subjects were asked to name the color chips using monolexemic color term. The results showed mean number of color terms used per subject was 18.94 ± 5.02 (Mode = 19). There were 12 color terms used by more than 80% of subjects including the eleven basic color term as found in Berlin and Kay (1969) plus "Fa" (Sky/light blue), Notice that, "Fa" was used by 100% of subjects, more than some BCTs such as white and black which were used by 98.76% and 93.17% of subjects, respectively. In order to examine the quantity of perception for "Fa" and the neighboring colors, we took the color chips that are located on their border to re-examine by elementary color naming method. The result of experiment 2 showed that Thai subjects perceive "Fa" (Sky/light blue) as distinct from other colors. This might be evident for promoting "Fa" to be a candidate of 12th Thai basic color terms.

INTRODUCTION

Color terminology varies according to the speakers in different social environments. To define the number of universal color categories, Brent Berlin and Paul Kay (B&K, 1969) [1] investigated the color terminology systems of twenty languages and they proposed eleven basic color terms (11 BCTs) for a total universal list of color categories which most languages share all or fewer color terms drawn from these 11 BCTs; red, orange, yellow, green, blue, purple, pink, brown, gray, black, and white. Shortly after their work was published, there were largely accepted by psychologists and vision researchers. However, there were also arguments, mainly by anthropologists, regarding the number of language and number of subjects in each language they explored. Therefore, World Color Survey (WCS) was established in 1976 to examine and expand the finding of Berlin and Key. There were recently works as according to the WCS project, Linsey and brown (L&B, 2014) [2] they obtained data from 51 American English subjects who are American English native speakers and found that there are 20 distinct color categories composed of 11 BCTs as found in B&K, 1969 plus 9 non-basic color terms (non-BCTa). In the modern Japanese color lexicon, Kuriki et al. (2017) found

Experimental booth and illumination

Both Experiments were conducted under controlled experiment by using then same experimental booth as shown in Fig 2. The booth has the size of 150 cm (L) x 90 cm (H) x 60 cm (W) illuminated by 6 daylight fluorescent lamps (TOSHIBA FL18W/T8/EX-D) which hung overhead from the ceiling provided illuminance of 2,509 lx measured by using Konica Minolta CL-500A Illuminance Spectrophotometer, the correlated color temperature (CCT) was 5,859 Kelvin, color rendering index (RI) was 97. The color chips were presented on the gray background, luminance was 22 cd/m², surrounded by white wall, luminance was 81 cd/m².

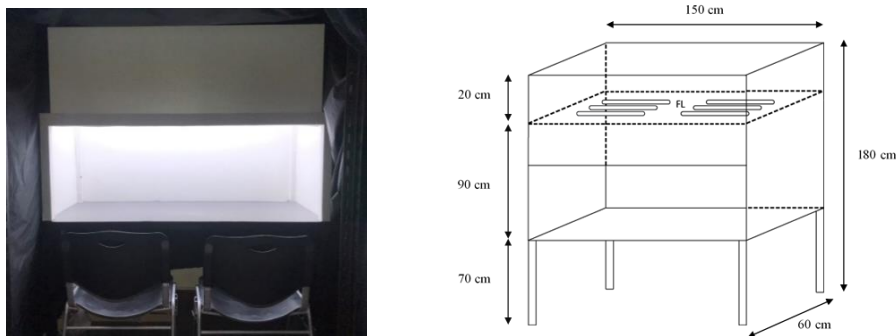


Figure 2. The experimental booth and its specification.

Procedure

Experiment 1. After tested the color vision, a subject was presented the color chip one by one and he/she was asked to provided color name for a color chip by free-naming with some conditions; 1) the color name must be single word, 2) the word must be a general color name, 3) the word must normally use to name the color of any type of object or something in everyday life. In the same time, if he/she provided any non-basic color terms (non-BCTs) then he/she was asked to provide additional information of only the color name in 11 BCTs, forced naming. Subjects conducted the experiment only one session.

Experiment 2. We re-examine the color chips located along the boundary of the Thai-BCTs candidate by using elementary color naming method to obtained quantities of subject's perception for the new candidate of Thai basic color term and its neighboring colors. Subjects assessed the amounts of chromaticness, whiteness, and blackness in percentage (a total is 100), and assessed the apparent hue by unique red, yellow, green, and blue in percentage (a total is 100). Subjects can provide only one or two hue which is not an opponent color (can't response red plus green or yellow plus blue). Each subject performed only one session for this experiment.

RESULTS AND DISCUSSION

Color terms obtained form 161 subjects show a total of 114 color terms. Figure 3 shows mean number of color terms used by 161 Thai native speakers is 18.94 ± 5.04 , maximum is 41, minimum is 12 and mode is 19 color terms. Here we can see that all Thai subjects used at least 12 color terms.

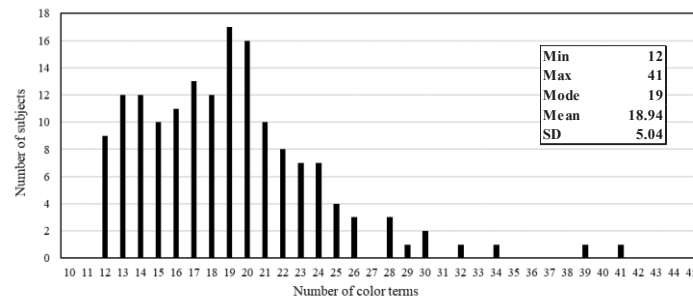


Figure 3. Number of color terms.

Figure 4 illustrated top of twenty popular list used by Thai subjects includes 11-BCTs as found in B&K 1969 and 8 non-basic color terms; Fa (Sky/light blue), Khi-ma (Horse feces/dark yellow-green), Lueat-mu (Pig blood/dark red), Ban-yen (Four o'clock flower/Magenta), Khai-kai (Chicken egg/pale brown), Nuea (Skin), Tha-le (Ocean), Old rose, and Cream. It is worth noting that, there is a non-BCTs, Fa (Sky/light blue), used by 100% of subjects (Figure 4a) and it has the 4th highest frequency of use (Figure 4b), representing 9.58%, which is higher than many basic color terms including blue, representing 6.57%. Considering other non-BCTs, it is found that there are 2 colors that are used by more than 50% of the subjects, namely (Horse feces/dark yellow-green) and Lueat-mu (Pig blood/dark red), representing 74.53% and 68.32 respectively. Both of these color names are the names of specific colors that are commonly used among Thai people but might rarely found in other countries.

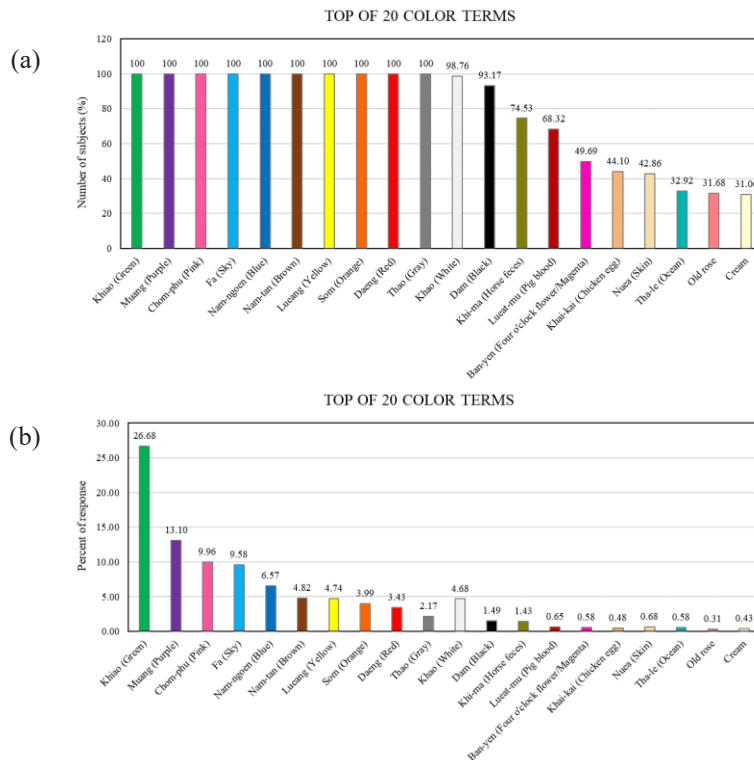


Figure 4. Twenty popular lists. (a) Number of subjects who used the color terms. (b) Percent of response for each color term.

Figure 5 shows color terms pattern plotted on the WCS color chart by using the highest proportion of color names used for each color chips, (a) the result of forced naming and (b) the result of free-naming. In the free-naming there are 14 color terms illustrated; 11BCTs plus Fa (Sky), Lueatmu (Pig blood), and Nuea (Skin). It is interesting “Fa” area is quite large, which is larger than many basic colors. This indicates the Thai subjects perceived blue and light blue as different colors and they thought it should be classified in different categories.

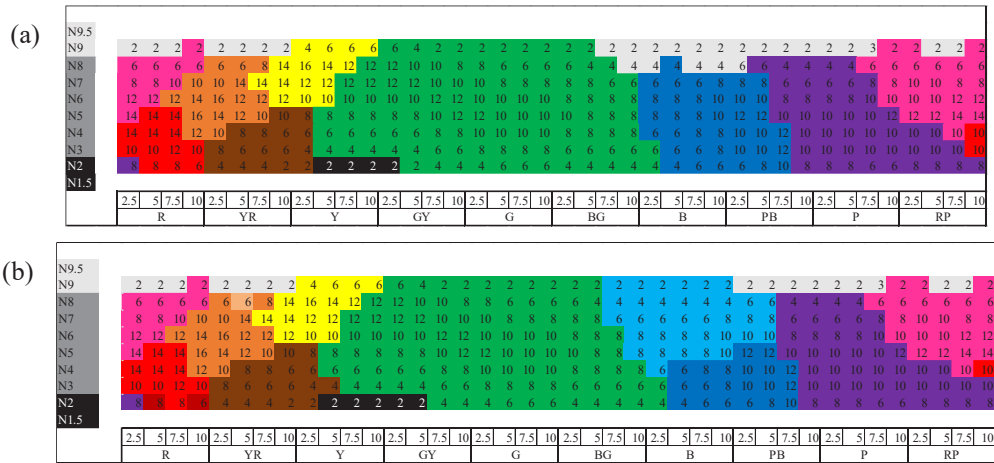


Figure 5. Color terms pattern of Free-naming (a) and Forced naming (b). The false colors represent each color name.

Due to the color term “Fa” has vary high frequency of use Due to the attractiveness of the color blue used by 100% of observers and has a very high frequency of use when compared to other color names Therefore, we have enumerated the frequency of color terms used in forced-naming instead of “Fa” as shown in Figure 6. We can see that the color terms are vary, which caused by the difficulty of the decision because the subjects thought that “Fa” is a unique color and they didn’t know should they classified into which group.

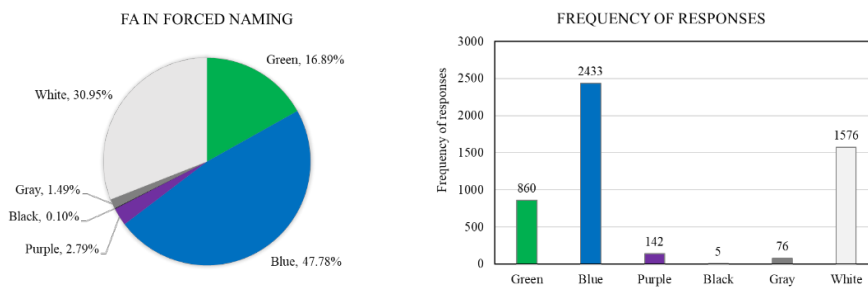


Figure 6. Forced-naming of Fa. Left figure illustrates color terms in 11BCTs and their proportion of used and the right figure illustrates their frequency of responses.

In order to examine the difference between “Fa” and its neighboring colors in term of subjects’ perception, we took the color chips along the edge of “Fa” and its neighboring to re-examine by using elementary color naming method as mentioned in the Experiment 2. Figure 7 shows the area of perception for the color chips along the boundary of “Fa” and its neighboring colors. Here, we can see some difference for “Fa” and “Purple” borders, there are no area, but the position is clearly

separated, also for “White”. In the case of “Fa” and “Green” they overlap in some parts which “Fa” is shifted to “Blue” axis side, and they almost overlap in “Fa” and “Blue”, implying that there is not much difference in hues. However, when considered in terms of chromaticness there are some difference, subjects perceived “Fa” is less chromaticness than “Blue”. Note that, most subjects who participated in the Experiment 2 are naïve and they were trained before starting the experiment, so there may be some variability in the response. However, the advantage of using this method is getting the absolute value in subjects’ perception.

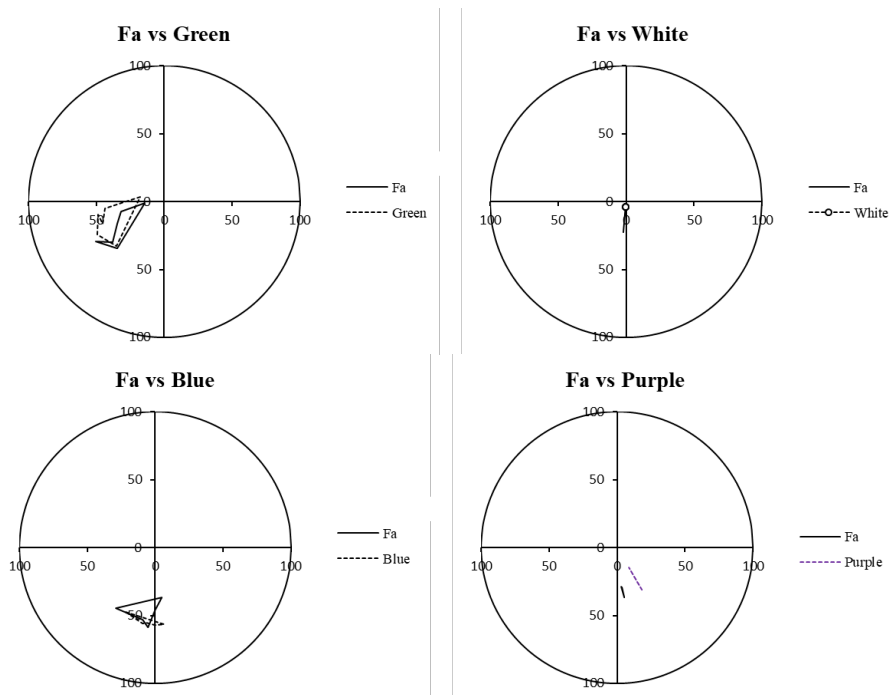


Figure 7. Area of color perception on polar diagrams for the color chips located on border. Fa is shown by solid line, the other colors show by dotted lines separate into each color.

ACKNOWLEDGEMENT

We would like to thank the Research Institute of Electrical Communication of Tohoku University and the College of Liberal Arts and Sciences of Chiba University for kindly supplying us the Munsell color chips and the experimental equipment.

REFERENCES

1. Berlin, B., & Kay, P. (1969). Basic color terms: Their universality and evolution. Berkeley, CA: University of California Press.
2. Cook, R. S., Kay, P., Regier, T. (2005). The World Color Survey database: History and use. In Cohen, Henri, & Claire Lefebvre (Eds.), Handbook of Categorization in the Cognitive Sciences (pp. 224– 241). Amsterdam: Elsevier.
3. Lindsey, D. T., Brown, A. M. (2014). The color lexicon of American English. Journal of Vision, 14(2), 1-25.
4. Kuriki, I., Fukuda, K., Tokunaga R., Lindse D. T., Uchikawa K., Shioiri S. (2017). The modern Japanese color lexicon. Journal of Vision, 17(3), 1–18.

ABOUT NEURAL REPRESENTATION OF COLORS IN VISUAL CORTEX

Ichiro Kuriki^{1*}

¹*Research Institute of Electrical Communication, Tohoku University, Japan.*

*Corresponding author: ikuriki@riec.tohoku.ac.jp

Keywords: Cortical color representation, unique hues, cardinal axes.

ABSTRACT

This presentation introduces several studies on the representation of color signal, which is strongly related to color appearance, in visual cortex. First, a summary of previous studies in psychophysics in humans and electrophysiology in macaque visual cortex will be presented to familiarize audience with the issues in the cortical representation of color. One example is the discrepancy between cone opponent responses and perceptually pure hues of red, green, blue, and yellow (so-called “unique hues”) [1]. The unique hues are different among individuals and are systematically deviated from colors that stimulates cone-opponent channels (L-M, S-(L+M)) exclusively. It implies that hue-representation mechanism in human visual cortex is not solely established by cone-opponent signals; i.e., Cartesian coordinates. To address this issue, I would like to introduce our attempts using functional brain imaging techniques. In one study, we used functional MRI (fMRI) to measure the variation of hue selectivity in human visual cortex [2]. Our result revealed the presence of cortical neurons that are selective to hues in the inter-axial directions of color space, which takes cone-opponent responses as two chromatic axes [3,4]. This is consistent with electrophysiological studies of neurons in macaque V1 [5,6]. We also demonstrated the presence of hue-selective adaptation to diagonal hues, which strongly supports that color representation is not based on cone-opponent responses. However, the population distribution of hue selectivity was strongly asymmetric, probably due to the method of measurement to increase the signal-to-noise ratio of the responses to each hue. We also tried to elucidate the tuning bandwidth of hue-selective SSVEP responses by masking technique, which exhibited a tuning bandwidth similar to previous psychophysical studies [7]. These studies proved that human visual cortex represent colors not in the cone-opponent signals (L-M and S-(L+M)) to represent red-green and yellow-blue components, respectively, but various hue-selective mechanisms may be representing color appearance as neural signal. We will extend the study to explore the relations between neural representation and color appearance.

INTRODUCTION

Classical framework by Hering’s opponent hue theory gives idea about how hue perception can be better organized when considering red/green and blue/yellow hues constitute exclusive pairs and they are orthogonally arranged on a hue circle. This idea lead to the classical study by Jameson and Hurvich on chromatic valence curve [8], in which, e.g., reddish appearance was cancelled out by adding more greenish light and perceived reddishness was quantified by the energy of green light added (hue cancellation). This study was also considered as a basis of elementary color naming technique. In this method, unique hues (red, yellow, green, and blue) are used as landmark of color space, and all colors along hue circle can be named by the weighted combination of two landmark colors. For example, purple is a mixture of red and blue in this framework. By adding achromatic colors, unique white and black, desaturation of colors can be also described.

Physiological studies have revealed that the responses of three types of cone photoreceptors are reorganized into two differential signal of cone responses, namely L-M and S-(L+M). This opponent representation is considered to constitute color signal in the early stage of visual stream [4], and often used in the fundamental axes of color space in basic color vision studies. The colors that exclusively stimulate cone-opponent channels roughly give idea of red-green and blue-yellow *flavor* of hues in

L-M and S-(L+M) channels, respectively. However, it has been also reported by several studies that these two channels do not exactly coincide with the four landmark colors [1]. Also, when the four landmark colors are marked on a hue circle in cone-opponent space, the angles between four colors would not be equally spaced. Ironically, it means the cone-opponent space is not suitable to represent color appearance based on the Hering's opponent color framework. Rather, five primary hues of the Munsell color system (R, G, Y, B, and P), which is designed to equally divide color space, would distribute more equally spaced in the hue circle.

This whole story implies that the neural system that represent color appearance has to be located somewhere after the cortical level of the visual information processing stream. Therefore, the primary research question is where and how color appearance is encoded in the human brain. In this presentation, I will introduce two studies that gives some idea about this issue.

fMRI study

If cone-opponent system represents entire colors, only neurons that represent L-M and S-(L+M) axes can be found, and representation of intermediate hues are the combination of cone-opponent neurons responses. For example, magenta can be represented by positive responses of L-M and S-(L+M). The pair 45 deg and 225 deg and another pair 135 deg and 315 deg yield identical axial components. The scale of L-M and S-(L+M) axes were equated by the multiples of detection threshold and it was roughly 1:10 in L- vs S-cone contrast with respect to the gray background (Figure 1A). If these two pairs of stimuli were alternately presented at higher temporal frequency than fMRI can resolve, brain activity recorded by fMRI for both pair of stimuli would evoke almost indistinguishable. On the other hand, if brain activity for these two pairs of stimuli are discriminable, it implies that the cortical representation of colors can be other than cone-opponent form.

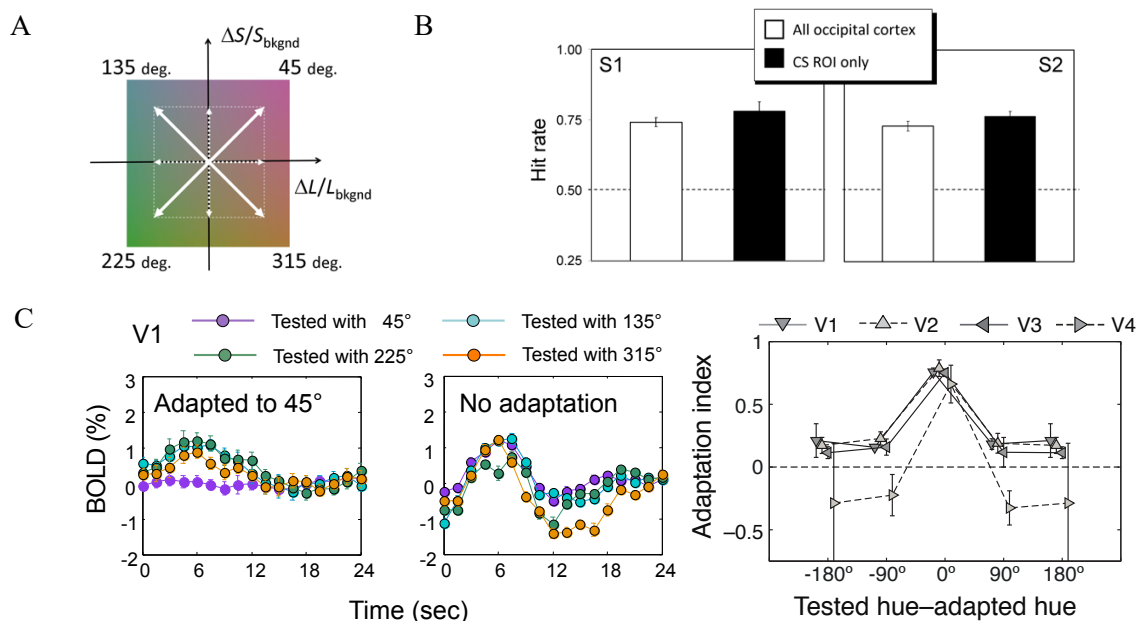


Figure 1. A. Cone-opponent color space used in this study. B. Result of fMRI decoding for color stimuli, using all visual cortex (open bar) or calcarine sulcus (V1) only (filled bar). Performance is around 75% in both subjects and sufficiently higher than chance level. C. Result of fMRI adaptation. (left) BOLD signal time course for four test hues during adaptation to 45 deg and (middle) without adaptation to hue. (right) Adaptation index was defined as follows: A.I. = 1.0 - (BOLD_{adapted} / BOLD_{no-adapt}). All visual area shows adaptation effect selective to adapted hue.

Similarly, if BOLD responses to one of the four intermediate directions (45, 135, 225, or 315 deg) is severely impaired after adaptation to the same stimulus and responses to non-adapted hues are intact, it also supports the presence of neurons that are selective to the intermediate hue. For example, 45 deg can be represented as the combination of positive L-M and positive S responses. 135 deg hue share positive S channel with 45 deg, and 315 deg hue does L-M channel with 45 deg. If 45 deg adaptation yielded adaptation of these axial mechanisms, BOLD responses to other hue probes (135 and 315 deg) would be reduced. If brain activity for adjacent hues were not reduced by 1/2, it would prove the presence of neurons selective to intermediate directions.

The result of decoding experiment [9] is shown in Figure 1B. Decoding of brain activity was conducted by SVM and the chance level for the comparison between 45-225 pair vs 135-315 pair was 50%. The results of using primary visual cortex (Calcarine Sulcus) showed performance significantly above 50%. This result is consistent with other similar studies [10-12].

The result of fMRI adaptation study [2] is shown in Figure 1C. The response to four intermediate directions of the cone-opponent space showed sharply selective adaptation (Fig.1C, left panel). The brain activity to the test 90 deg away from the adapted color showed adaptation effect far less than 1/2 for the test by adapted color (Fig.1C, right panel).

These results imply that the color representation of cortical level is no longer cone-opponent. Including studies in macaque monkeys [5, 6], the cortical neurons seem to respond to individual hue, rather than to code a color by the combination of cone-opponent responses.

SSVEP study on hue selectivity

Nevertheless, it is difficult to consider that such hue-selective neurons are prepared in each retinotopic point for dozens of hues that also differ in lightness levels. Therefore, the variation and population of such hue-selective neurons like macaque studies [5,6] is an important issue. This attempt by fMRI was conducted in our previous study [2] but it was only partially successful. We could find abundant voxels that are selective to various hue directions, but the population histogram of the hue-selective voxels was strongly asymmetric. It was neither uniformly distributed nor concentrated around cone-opponent axes; it lacks +L-M and -L+M selective responses, probably because of our analysis method to derive hue-selectivity of voxels in our fMRI data, and it also had strong individual differences in asymmetry.

Therefore, we next made an attempt by using an EEG recording method called SSVEP. We presented counterphase reversals of check pattern at 5 Hz that changes its color between gray and a particular hue. The hue of test stimulus varied along a hue circle in a cone-opponent space, same as our fMRI studies [2, 8], at the speed of 24 s per cycle. Each cycle of hue change started from one of 24 points on the hue circle, chosen randomly, and the results were averaged after 24 trials. The hue changes were presented along 3 levels of chromatic saturation (full gamut, 1/2, and 1/4) and two directions of hue changes (CW/CCW) were also recorded. Mainly, the amplitude of 5 Hz component of the EEG responses was analyzed.

Figure 2A shows the result of SSVEP amplitudes, averaged across 18 subjects for 3 levels of chromatic saturation [7]. The amplitude level for 3 saturation conditions are changing progressively (Figure 2B), and it confirms that the SSVEP profile represents the locus of hue selectivity. The locus of SSVEP amplitude appears much round shaped than the radial histogram of hue selective voxels in fMRI [2]. However, the shape of averaged locus was, again, neither circular nor symmetric around the cone-opponent axes. This confirms the presence of hue-selective neurons in intermediate direction in human visual cortex.

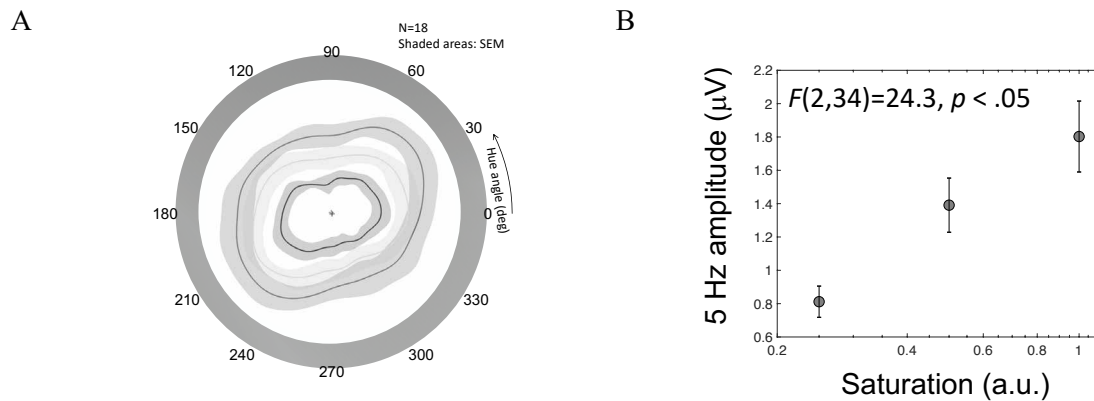


Figure 2. A. SSVEP amplitude profile. The space of hue circle for this study is the same as Fig.1A. Outer, medium, and inner loci represents conditions with full, 1/2, and 1/4 saturation, respectively. Average of 18 subjects and shaded area shows ± 1 SEM. Systematic elongation along diagonal direction. B. SSVEP amplitude for 5 Hz (color flicker component) as a function of saturation.

To estimate the underlying mechanisms, a curve fitting was attempted by predicted response of two ellipses; one was predicted from iso-Chroma contour of Munsell color system and the other was predicted from cone-opponent responses. We tested whether the Munsell-based model, cone-opponent model, or the weighted sum of these two can best explain the data by using AIC. The result turned out that the combination of the two mechanisms or Munsell-based model explains best with smallest number of model parameters. This implies that the SSVEP response is based partly on cone-opponent responses, a format fed from LGN to the visual cortex, and does on color-appearance based (Munsell) mechanism. The latter component may be reflecting the perceptual saliency difference along the hue circle.

DISCUSSIONS

From neurons' point of view, how can color appearance be represented? According to what we have found in the visual cortex of the humans by fMRI and EEG (SSVEP) responses, together with studies in non-human primates [5,6] the cortical neurons represent colors in the hue-selective manner, not as the combinations of cone-opponent responses that is the format of color signal fed from retinal ganglion cells via LGN [4].

The possible neural system behind the brain activity studies in infants may be those studied in macaque visual cortex [13-16]. These studies suggest that a set of hue-selective neurons are aligned in an order of spectrum along the cortical surface. If the cortical distance on the surface between two colors is proportional to the perceptual distance between two colors, it would also explain why small color difference is easy to evaluate and large color difference is difficult.

This color representation leads to the categorical representation of color at higher visual cortex. Although the presence of categorical color representation is reported in the past [17,18], how they are transformed from the representation at the early level of visual cortex is unclear. Before that, how the characteristic of color representation is changing across visual cortices is still unclear. In addition, the basic question about the discrepancy between opponent color theory by Hering's landmark colors (unique hues) and neural representation of color at the cone-opponent level is unsolved.

We would like to further pursue such a question by improving the combination of psychophysical and brain imaging techniques.

ACKNOWLEDGEMENT

I thank authors of studies that are introduced in this presentation. Nakamura S., Matsumiya K., Shioiri S., Sun P., Ueno K., Tanaka K. and Chen K. for fMRI studies [2,8,13]. I also thank Andersen S.K. and Kaneko S for the SSVEP study [7]. These studies were supported by JSPS Kakenhi #s JP 24330205, 15H03460, and 18H04995 to IK.

REFERENCES

1. De Valois, R. L. (2000). Cottaris NP, Elfar SD, Mahon LE, and Wilson JA. Some transformations of color information from lateral geniculate nucleus to striate cortex. *Proc Natl Acad Sci USA*, 97, 4997-5002.
2. Kuriki, I., Sun, P., Ueno, K., Tanaka, K., & Cheng, K. (2015). Hue selectivity in human visual cortex revealed by functional magnetic resonance imaging. *Cerebral Cortex*, 25(12), 4869-4884.
3. MacLeod, D. I., & Boynton, R. M. (1979). Chromaticity diagram showing cone excitation by stimuli of equal luminance. *JOSA*, 69(8), 1183-1186.
4. Derrington, A. M., Krauskopf, J., & Lennie, P. (1984). Chromatic mechanisms in lateral geniculate nucleus of macaque. *The Journal of physiology*, 357(1), 241-265.
5. Hanazawa, A., Komatsu, H., & Murakami, I. (2000). Neural selectivity for hue and saturation of colour in the primary visual cortex of the monkey. *European Journal of Neuroscience*, 12(5), 1753-1763.
6. Wachtler, T., Sejnowski, T. J., & Albright, T. D. (2003). Representation of color stimuli in awake macaque primary visual cortex. *Neuron*, 37(4), 681-691.
7. Kaneko, S., Kuriki, I., & Andersen, S. (2018). SSVEP amplitudes reflect hue selectivity in the human brain. *Journal of Vision*, 18(10), 575-575.
8. Hurvich, L. M., & Jameson, D. (1957). An opponent-process theory of color vision. *Psychological review*, 64(6p1), 384.
9. Kuriki, I., Nakamura, S., Sun, P., Ueno, K., Matsumiya, K., Tanaka, K., ... & Cheng, K. (2011). Decoding color responses in human visual cortex. *IEICE transactions on fundamentals of electronics, communications and computer sciences*, 94(2), 473-479.
10. Parkes, L. M., Marsman, J. B. C., Oxley, D. C., Goulermas, J. Y., & Wuerger, S. M. (2009). Multivoxel fMRI analysis of color tuning in human primary visual cortex. *Journal of Vision*, 9(1), 1-1.
11. Goddard, E., Mannion, D. J., McDonald, J. S., Solomon, S. G., & Clifford, C. W. (2011). Color responsiveness argues against a dorsal component of human V4. *Journal of Vision*, 11(4), 3-3.
12. Brouwer, G. J., & Heeger, D. J. (2009). Decoding and reconstructing color from responses in human visual cortex. *Journal of Neuroscience*, 29(44), 13992-14003.
13. Cheng, K. (2018). Exploration of human visual cortex using high spatial resolution functional magnetic resonance imaging. *NeuroImage*, 164, 4-9.
14. Xiao, Y., Casti, A., Xiao, J., & Kaplan, E. (2007). Hue maps in primate striate cortex. *Neuroimage*, 35(2), 771-786.
15. Lu, H. D., & Roe, A. W. (2007). Functional organization of color domains in V1 and V2 of macaque monkey revealed by optical imaging. *Cerebral Cortex*, 18(3), 516-533.
16. Tanigawa, H., Lu, H. D., & Roe, A. W. (2010). Functional organization for color and orientation in macaque V4. *Nature Neuroscience*, 13(12), 1542.
17. Komatsu, H., Ideura, Y., Kaji, S., & Yamane, S. (1992). Color selectivity of neurons in the inferior temporal cortex of the awake macaque monkey. *Journal of Neuroscience*, 12(2), 408-424.
18. Brouwer, G. J., & Heeger, D. J. (2013). Categorical clustering of the neural representation of color. *Journal of Neuroscience*, 33(39), 15454-15465.

SIMULTANEOUS COLOR CONTRAST ON A DISPLAY DETERMINED BY DIFFERENT VIEWING DISTANCES

Janejira Mepean^{1*}, Mitsuo Ikeda² and Chanprapha Phuangsuan ²

¹ Faculty of Mass Communication Technology, Rajamangala University of Technology Thanyaburi, Thailand.

² Color Research Center Rajamangala University of Technology Thanyaburi, Thailand.

*Corresponding author: Janejira Mepean, janjira672@gmail.com

Keywords: Chromatic adaptation, Color appearance, Elementary color naming, Simultaneous color contrast, Viewing distance.

ABSTRACT

The simultaneous color contrast phenomenon is considered as the effect of chromatic adaptation to the color initiated by the surrounding color of the stimulus. If the stimulus is seen at an extremely short viewing distance the subject's recognition of the stimulus as an object may be reduced because the stimulus becomes very large not to recognize the edges. The vividness of the color appearance of the central gray patch may become large at the viewing distance. The color appearance of the test patch was measured as a function of the viewing distance when the stimulus was presented on a TV display. In general the vividness increased for shorter viewing distance with some subjects but an opposite results were obtained from other subjects. An explanation was given as that the display is a self-luminous display and some subjects felt or recognized colored light of surround even at a far distance of 5 meter and eyes adapted to the color and saw a vivid color at the test stimulus.

INTRODUCTION

It is known that the simultaneous color contrast SCC is a phenomenon to show the chromatic adaptation. Stimulus pattern of SCC is a large colored field with a small achromatic patch at the center. It was pointed out that the large colored surrounding field works as an adapting color and the color appearance of the central gray patch is a result of the chromatic adaptation to the surrounding color [1, 2, 3]. If one observes the pattern from a far distance the pattern appears a mere object and no strong chromatic adaptation should take place. But if the view distance becomes short so that the surrounding field occupies a large area of the retina, it becomes hard to recognize the pattern an object and the surrounding is recognized as just a shining field, which should cause the visual system to adapt to the illumination, thus a strong chromatic adaptation takes place. The present research is to investigate if this hypothesis is correct by using a display to present the SCC stimulus.

EXPERIMENT

A Samsung 55" television display UA55H6340TK was used to present a SCC stimulus. The stimulus was a rectangle of 68 cm high and 121 cm wide as a surround having a gray test patch of 11.5 x 11.5 cm² at the center. Five colors, red, yellow, green, blue and whitewere employed for the surround. Their chromaticities are listed in Table 1 and shown in Fig 1

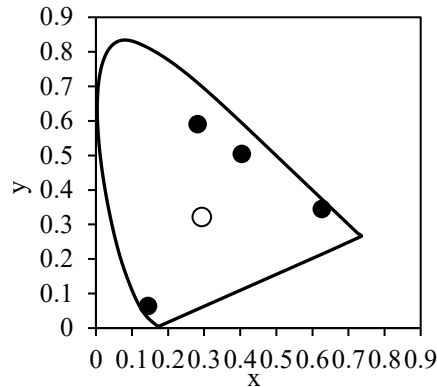


Figure. 1 Chromaticity points of surrounds, red, yellow, green, blue and white.

The bottom line in Table 1 gives specifications of the central test patch. The luminance of the surrounds and the test patch are also given in the table

Table 1: Color specifications of surrounds.

Color	Y (cd/m ²)	x	y
R	43.6	0.626	0.345
Y	185	0.404	0.504
G	140	0.282	0.591
B	16.4	0.144	0.064
W	209	0.294	0.321

To change the visual angle of the SCC pattern the viewing distance was changed to 5, 3, 1.5, 0.3 and 0.15 meters and their visual angles varied from 13.8° to 152.2° as shown in Table 2. The subjects were asked to judge the colors of the central patch by the elementary color naming method. Six subjects of normal color vision participated in the experiment and the judgement was repeated for five times for each condition. The experiment was carried out in a room illuminated at 236 lx at the subject's eye level.

Table 2: Visual angle of the test patch and the surrounds at different viewing distance.

Distance (cm)	Visual angle (width)	
	Test patch (°)	Surround (°)
15	42	152.2
30	22	127.3
150	4.4	44
300	2.2	22.8
500	1.3	13.8

RESULTS

The color appearance of the surrounds is shown in Fig. 2 on a polar diagram normally used in the opponent colors theory. The apparent hue is shown by the angle for Red axis in the anticlockwise direction. Unique hues of red, yellow, green, and blue are shown at 0°, 90°, 180°, and 270°.

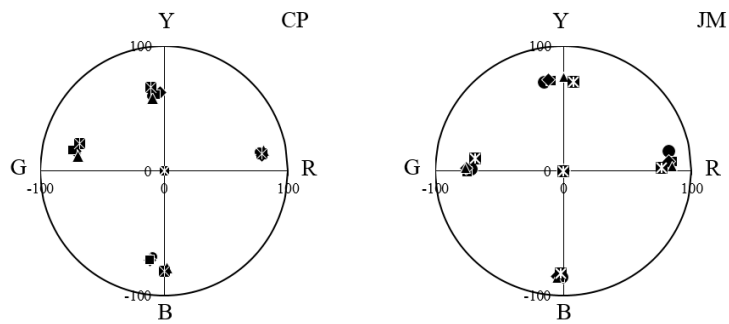


Figure. 2 Color appearance of surrounds plotted on a polar diagram for two subjects. Viewing distance, *, 15 cm, ▲, 30 cm, ◆, 150 cm, ■, 300 cm, ● 500 cm.

The amount of chromaticness is taken along the radius direction starting at the origin as 0 and ending at the circumference as 100. Figure 2 shows results of two subjects, CP and JM. At each group there are five points corresponding to five viewing distances. Each point is the average of five repetitions. Four surrounds appeared to them almost unique hues.

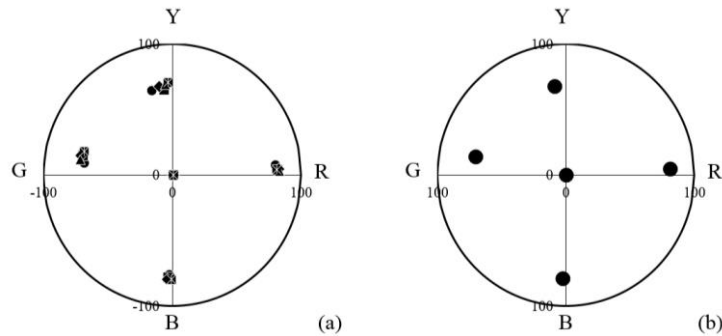


Figure. 3 Left, Color appearance of surrounds obtained by 6 subjects. Right, Averaged color appearance of 6 subjects for surrounds.

In Fig. 3 the averages of six subjects are plotted for different viewing distance in (a) and for the averages of different viewing distance in (b). As we see in (a) there seems to be no difference among different viewing distance. In Fig. 4 the amount of chromaticness is plotted for different viewing distance for different surround. Color appearance of surround did not change for viewing distance.

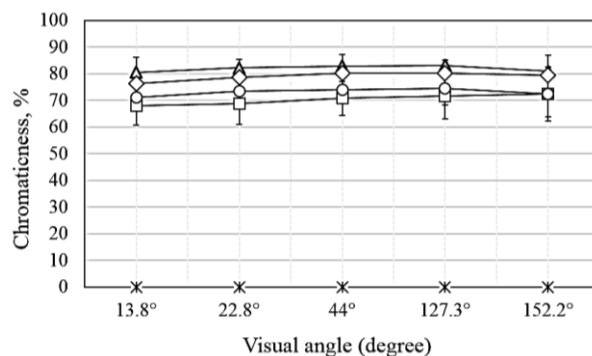


Figure. 4 Amount of chromaticness of surrounds for different viewing angle. ▲, red surround; □, yellow; ○, green; ◇, blue, *, white.

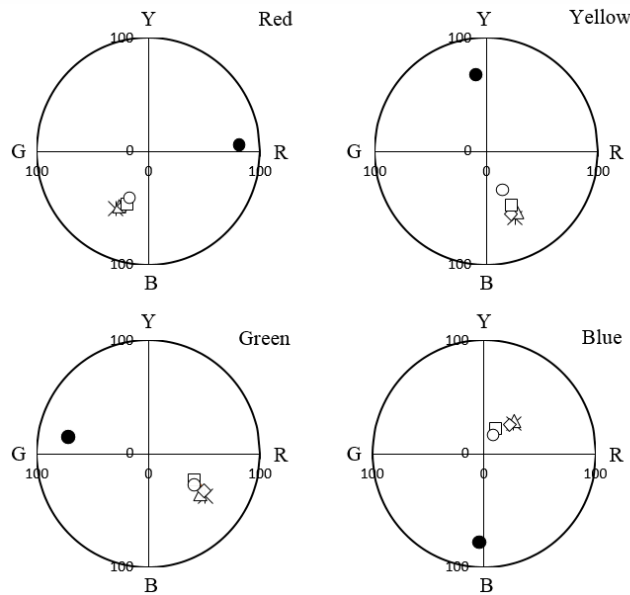


Figure. 5 Color appearance of surround and test patch shown on polar diagrams for four surrounding colors.

The average of color appearance of test patch is also shown on polar diagram in Fig. 5. Different figures give results of different surrounding colors. Filled circles show the color appearance of surround as appeared in Fig. 3. Other symbols correspond to the viewing distance; \circ , 5 m, \square , 3 m, \diamond , 1.5 m, Δ , 0.3 m, $*$, 0.15 m. There is a tendency of the amount of chromaticness increased for shorter distance, which is particularly evident with yellow surround.

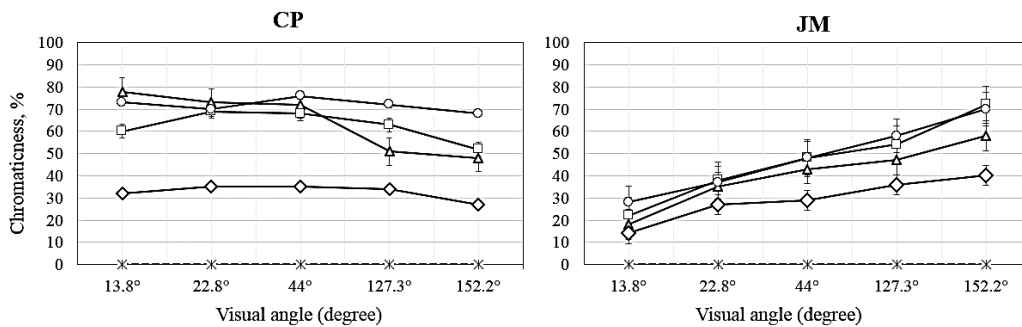


Figure. 6 Amount of chromaticness of test patch for viewing angle from two subjects. Symbols represent colors of surround. Δ , red surround; \square , yellow; \circ , green; \diamond , blue, $*$, white.

To see the change of amount of chromaticness more clearly Fig. 6 is prepared for subjects CP and JM. Along the abscissa the viewing distance is taken and along the ordinate the amount of chromaticness. There is difference in the amount among surrounding color, the largest with green, and then yellow, red, and blue, the blue the smallest in both subjects. But the trend of change differs. While JM showed increase for shorter viewing distance or larger visual angle, CP did not show such trend, rather opposite. The amount slightly decreased for larger visual angle. The subject expressed that she can see a vivid color for the test patch even at the 5 m viewing distance.

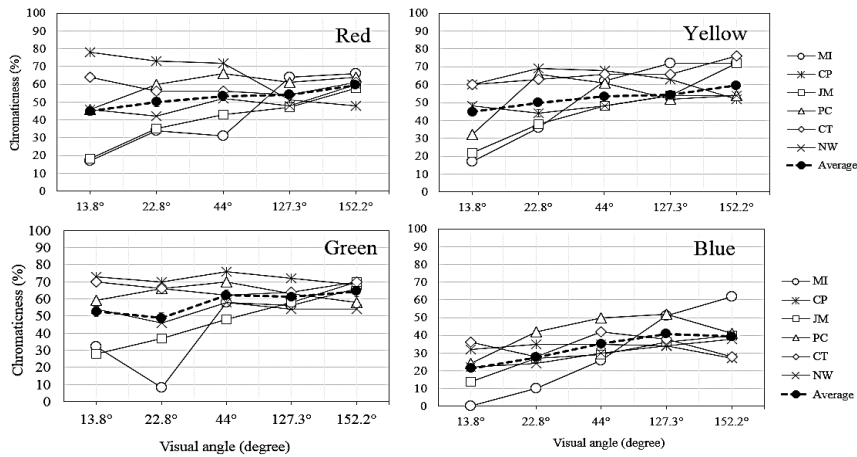


Figure. 7 Amount of chromaticness of test patch for viewing angle for six subjects. Symbols represent subjects.

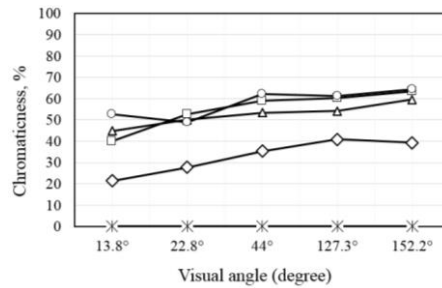


Figure. 8 Averaged amount of chromaticness of test patch for viewing angle. Symbols represent color of surround, Δ , red surround; \square , yellow; \circ green; \diamond blue, $*$, white.

Figure 7 shows the individual difference by different symbols. With red, yellow, and green surrounds the value diverges greatly at the longest viewing distance but they converge at shortest distance. Thick dashed lines show the average of six subjects. Although there is variance among subjects the dashed lines show a gradual increase for shorter viewing distance. Those dashed curves are summarized in Fig. 8. The blue curve locates separately at the low level indicating that the blue surrounding is weak to induce color at the test patch.

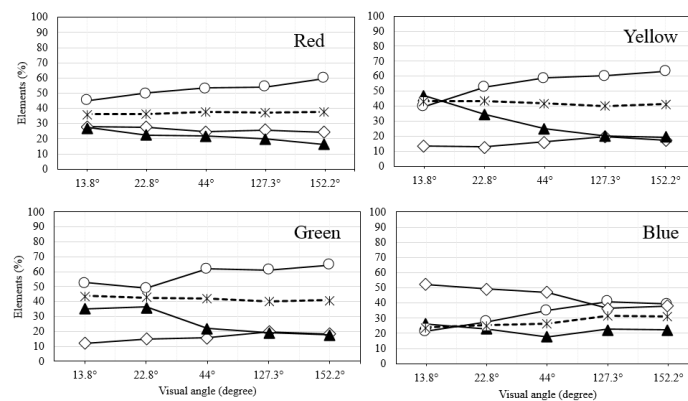


Figure. 9 Amounts of elements plotted for viewing angle. \circ chromticness; \blacktriangle , blackness; \diamond , whiteness. Dashed lines is the average of the chromaticness and blackness.

In the experiment whiteness and blackness were also measured beside chromaticness. They are shown in Fig. 9 with different symbols; ○, chromaticness, ◇, whiteness, ▲, blackness. It is interesting to note, particularly in the green surround, that the chromaticness curve and the blackness curve show symmetric relation. Dashed lines are average of chromaticness and blackness and they are almost straight lines suggesting chromaticness and blackness are symmetrical. In other words, the increase of chromaticness for shorter viewing distance was given by the reduction of blackness amount.

CONCLUSION AND DISCUSSION

The simultaneous color contrast was investigated for different viewing distance which changed the visual angle for the stimulus. It was anticipated that increase of visual angle or decrease of viewing distance increases the vividness of the color appearance of the central test patch because the recognition of the stimulus as an object reduces for short distance. The expectation was found in some subjects but opposite result was found by other subjects. We can think of some reasons for this unexpected result. A display is a self-luminous display. The surround gave light impression already at 5 m viewing distance, which gave strong chromatic adaptation and caused vivid color of the test patch. When the viewing distance was short as 15 cm, subjects could see color dots of the television display that was used in this experiment, which bothered the subjects to judge the color appearance of the test patch. An author of this paper observed the same SCC stimulus presented on an EIZO display which did not give color dots t 15 cm, She reported the color appearance of the test patch became more vivid. The SCC stimulus was composed of a central small gray patch and a large surround. Both had clear edges to give an object recognition to subjects. But if the subject saw light impression even at 5 m distance the chromatic adaptation must be strong to give vivid color for the test patch. It is needed to do a similar experiment by using EIZO in the future to clarify questions raised in this experiment.

ACKNOWLEDGEMENT

Janejira Mepean, the senior author, acknowledges Dr. Fusako Ikeda for giving Mepean the Fusako Scholarship to study at graduate school of Rajamangala University of Technology Thanyaburi.

REFERENCES

1. Ikeda, M. (2004) Color appearance explained, predicted and confirmed by the concept of recognized visual space of illumination. *Opt. Rev.*, 11, 217-225.
2. Srirat, P., Phuangsuwan, P., & Ikeda, M. (2014) Chromatic adaptation to illumination investigated with two rooms technique. *Jr. Col. Assoc. Jpn*, 38(3), 176-177.
3. Phuangsuwan, C., Ikeda, M., & Mepean, J. (2018). Learning to de-escalate: Color appearance of afterimages compared to the chromatic adaptation to illumination. *Color Research and Application*, 43(3), 349-357. doi: 10.1002/col.22207

DEVICE INDEPENDENT SIMULTANEOUS LIGHTNESS CONTRAST

Saran Chantra^{1*}, Mitsuo Ikeda¹, Hideki Sakai², Hiroyuki Iyota³ Chanprapha Phuangsuan¹

¹*Color Research Center, Faculty of Mass Communication Technology,
Rajamangala University of Technology Thanyaburi, Thailand.*

²*Graduate School of Human Life Science, Osaka City University, Japan.*

³*Graduate School of Engineering, Osaka City University, Japan.*

*Corresponding author: Saran Chantra, 1159108020192@mail.rmutt.ac.th, Saranchantra@gmail.com

Keywords: Simultaneous lightness contrast, Devices, Projector, Paper stimulus, Two - rooms arrangement

ABSTRACT

The simultaneous lightness contrast phenomenon was investigated with four different devices; a paper stimulus, a two - rooms arrangement, a display, and a projector. Luminances of the central gray patch and surround were made equal among the devices. Except the paper stimulus the strength of SLC was about same among other devices to imply device independent SLC.

INTRODUCTION

There are two kinds of simultaneous contrast phenomenon, simultaneous color contrast SCC and simultaneous lightness contrast SLC. The pattern for the phenomenon is usually a large area surrounding a small gray patch at the center. When the surround is made of a color the gray patch appears colored complementally to the surrounding color, which is SCC phenomenon, while the surround is achromatic the gray patch appears also achromatic but darker or brighter depending on the lightness of the surround, which is called SLC phenomenon. Those patterns are often shown in textbooks. But if they are demonstrated on printed paper the SLC shows a clear effect, while the SCC does not. A concept of recognized visual space of illumination RVSI proposed by Ikeda explains the SCC by the chromatic adaptation [1]. The concept asserts that the chromatic adaptation takes place to the illumination in a space where the observer stays and not to the color of objects that the observer is looking at. The simultaneous color contrast phenomenon is explained by this concept in a way that the color of the surrounding is transferred to the illumination color in the observer's recognition and he/she adapts to the illumination. Difference between the results of SCC and SLC is interpreted as that to an observer it is easier to recognize the illumination level than the illumination color on the printed simultaneous contrast pattern. The degree of the easiness greatly differs in the SCL among devices to demonstrate the phenomenon, such as printed paper, a display, a projector, or a two - rooms technique [2]. If the recognition of illumination level is easy for any devices the SLC effect should not differ among devices on the contrary to the SCC which is quite dependent on devices [3]. In this paper the SLC was measured for four different devices, a printed paper, a display, a projector, and a two - rooms technique Fig. 1. Two kinds of SLC stimuli were prepared, one with a white surround and the other with a black surround. Both surrounds had a same gray central patch. The luminance of the surround and that of the central test patch were made equal for difference devices and the visual size of the pattern was also made about same. The experiment was done in a room without the ceiling lamps. Subjects were asked to judge the

appearance of the central test patch by the elementary color naming method, namely the amounts of whiteness and blackness in percentage. Experiments were carried out at Rajamangala University of Technology Thanyaburi, Thailand and at Osaka City University, Japan, where the senior author spent for three months for internship under supervision of Professors Iyota and Sakai.

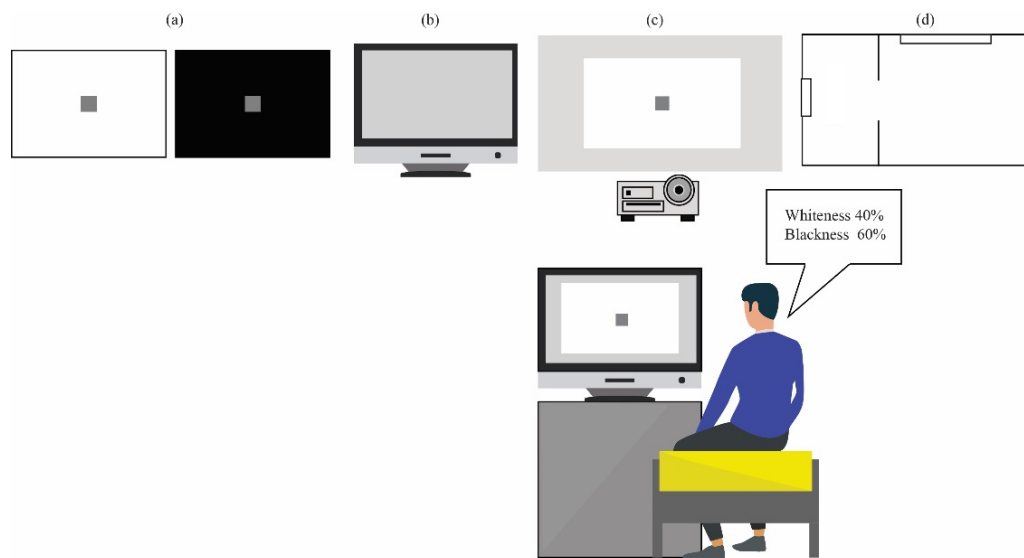


Figure 1. Four devices used for the simultaneous lightness contrast experiment.

EXPERIMENT

Stimuli we used was a small square gray patch placed at the center of a large surround of black or white. They were presented as papers, a display, a projector and in a two-rooms arrangement [2]. Their dimensions and luminance are summarized in Table 1. In spite of different devices they were made equal as much as possible. Y shows the luminance when the paper stimulus was measured in a room of the illuminance 890 lx. L* values of black surround was 26 at OCU and 22 at RMUTT and that of white surround was 95 at OCU and 93 at RMUTT. Except the paper stimuli all the devices were observed in a dark room. Fourteen subjects participated in the experiments, 7 at OCU and 7 at RMUTT. They observed devices in a pseudo - random order.

Table 1: Experimental condition

Device	S (cm)	T (cm)	Dist. (cm)	Visual angle (°)		Test patch			White surround			Black surround		
				S (°)	T (°)	Y	x	y	Y	x	y	Y	x	y
Obj.	21x30	2x2	70	17x24	1.63	89.4	0.31	0.44	231	0.31	0.45	25.4	0.31	0.44
Disp.	53x35	3x3	110	27x18	1.63	89.4	0.31	0.45	231	0.31	0.45	25.5	0.31	0.46
Proj.	60x92	4x4	135	25x38	1.63	88.4	0.29	0.46	231	0.29	0.46	24.3	0.29	0.46
Two-rms.	37x24	3x3	120	18x11	1.62	88.6	0.31	0.45	232	0.31	0.45	25.5	0.31	0.44

RESULTS

Results of two subjects, AH of OCU and SJ of RMUTT are shown in Fig. 2 and 3 for surround and gray test patch, respectively. The amount of whiteness was very high for the white surround (\circ) in the all the devices, but for the black surround (\bullet) it varied for different devices. While it was 0 and 5 with the paper stimulus from AH and SJ, respectively, it was 75 and 26 with the two rooms arrangement and 63 and 34 with display. This is understandable if we notice that the paper stimulus appeared really black but the front wall of the two - rooms arrangement was white. Even the room illuminance was set at a low level to give the same luminance as for the paper the white wall appeared dark but still white as the color constancy tells us. The left figure of Fig. 4 gives the amount of whiteness of test patch with white surround (\circ) and with black surround (\bullet). The amount of whiteness with black surround is much higher than the amount of whiteness with white surround. There is seen a large difference between the object stimulus and the two rooms stimulus, but the amount of whiteness remained about the same among other devices, two-rooms, display, and projector, implying the device independent.

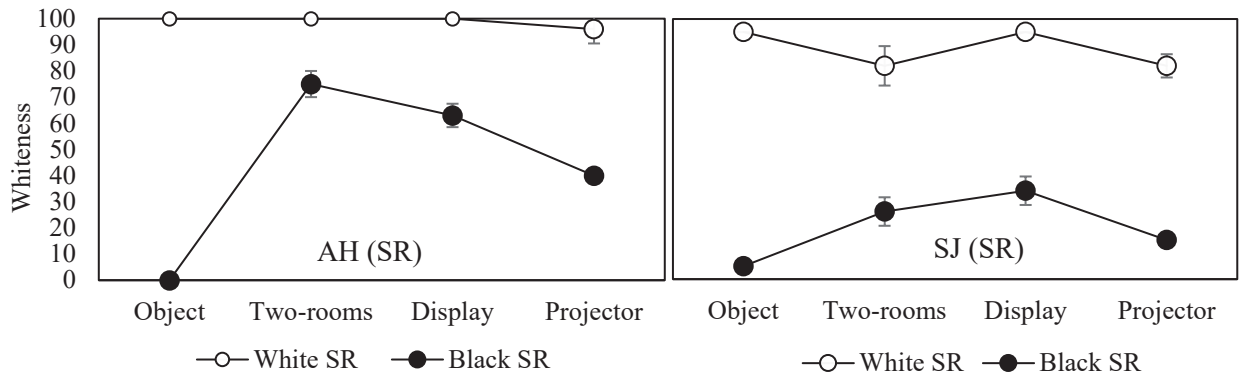


Figure 2. The amount of whiteness of white surround (\circ) and of black surround (\bullet).
Subject AH (left) and SJ (right).

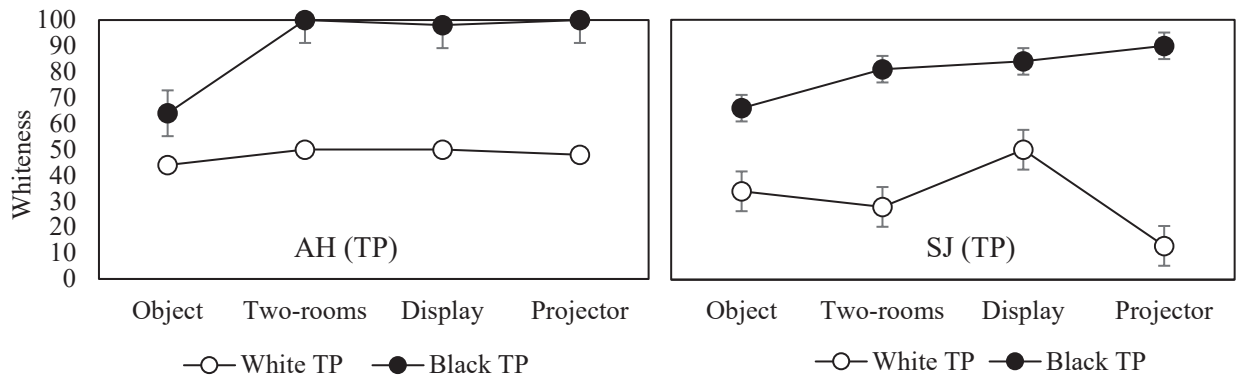


Figure 3. The amount of whiteness of test patch with white surround (\circ) and with black surround (\bullet). Subject AH (left) and SJ (right)

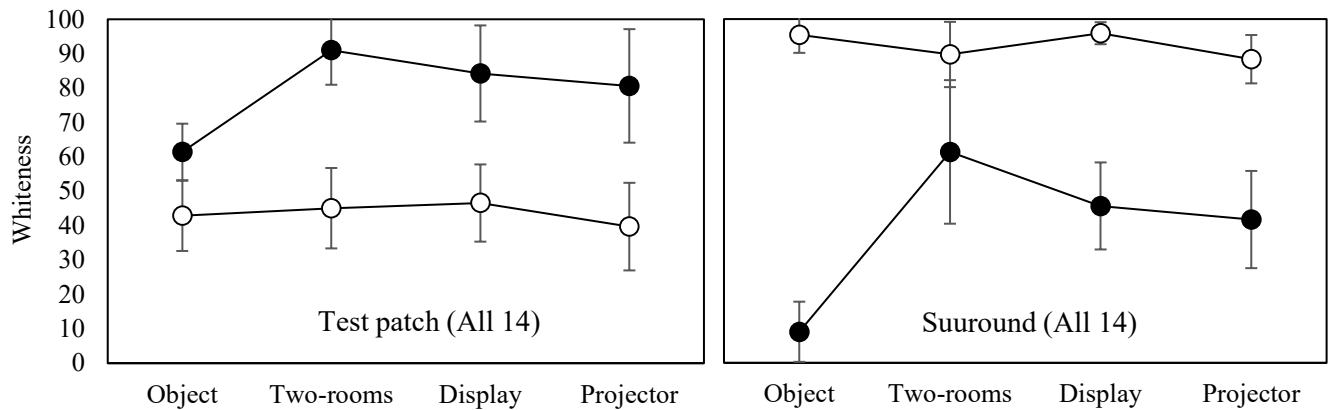


Figure 4. Averaged results of 14 subjects for the amount of whiteness of test patch (left) and of surround (right). (●), black surround, (○), white surround.

DISCUSSION AND CONCLUSION

Although we found the device independent SLC for two - rooms arrangement, a display, and a projector, the amount of whiteness with black surround in the object stimulus was smaller than other devices. With white surround the amount of whiteness was about the same for all the four devices (○) in the left figure of Fig. 4. We noticed that the white surround appeared white in all the four devices, but the black surround appeared different. That of object stimulus appeared really black as shown by only 9 of the whiteness amount as seen in the right figure of Fig. 4 but the other stimuli appeared gray although the luminance was made same as shown in Table 1. We calculated a ratio of whiteness amount of test patch to that of surround. The results are shown in Fig. 5 for the black surround (●) and for the white surround (○). The ratio of the object stimulus is much higher than other devices. The effect of surround to the test patch appearance is significantly large in the object stimulus. This might be caused by a really black surround in the object stimulus.

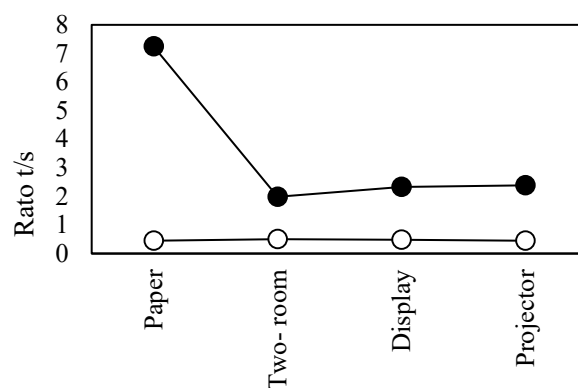


Figure 5. Ratio of whiteness amount of test patch to surround. (●), black surround, (○), white surround.

ACKNOWLEDGEMENT

Saran Chantra thanks RMUTT for providing him with scholarships Co - operative education Rajamangala University of Technology Thanyaburi that made Saran to do internship abroad. He thanks students at Iyota and Sakai laboratories to be a good friends to Saran and for serving as subjects of this experiment.

REFERENCES

1. Ikeda, M. (2004). Color Appearance Explained, Predicted and Confirmed by the Concept of Recognized Visual Space of Illumination. *Optical Review*, 11(4), 217–225. doi: 10.1007/s10043-004-0217-x
2. Phuangsuwan, C., & Ikeda, M. (2017). Chromatic adaptation to illumination investigated with adapting and adapted color. *Color Research & Application*, 42(5), 571–579. doi: 10.1002/col.22117
3. Phuangsuwan, C., & Ikeda, M. (2019). Device dependent simultaneous color contrast. *Proc of Col. Sc. Assoc. Jpn.*

VARIATION OF BROWN PERCEPTION IN CHROMATIC CENTRAL FIELDS

Keizo Shinomori^{1*} and John S. Werner²

¹*School of Information / Vision and Affective Science Integrated Research Focused Laboratory, Research Institute, Kochi University of Technology, Japan.*

²*Department of Ophthalmology and Vision Science / Department of Neurobiology, Physiology and Behavior, University of California, Davis, U.S.A.*

*Corresponding author: Keizo Shinomori, shinomori.keizo@kochi-tech.ac.jp

Keywords: Brown, Darkness, Color perception, Color appearance, Blackness induction

ABSTRACT

Brown, gray and black are considered among eleven basic colors. However, they are different in production and reproduction with other basic colors; these colors cannot be perceived in a single light in a completely dark surround. A relatively bright environment or a surround field is required to induce blackness (or darkness) in a central field. Brown perception is considered to have a more complex mechanism because some special chromatic conditions are additionally required in the center field. Brown perception has been investigated in terms of color categories, and color chips categorized as "brown" are known. However, how the chromatic conditions of the center field change the perception of brown is not yet known.

In this research, we investigated the relations between brown perception and chromatic conditions of the center field surrounded by a white annulus on a CRT monitor. In order to avoid the difficulty and unexpected bias in estimating the magnitude of the brownness perceived in the center field, we employed a paired-comparison method. Two white annuli of fixed luminance were simultaneously presented side by side, and the observer indicated which chromatic center field appeared more brown by pressing a left or right button. All win-loss scores of central field conditions were transformed to z-scores after the comparison of all combinations of the conditions. Although the results of this method are in ordinal scale, the results were reliable. We changed the chromaticity coordinates of the center field in terms of a dominant wavelength and saturation to obtain the best area of the center color in chromaticity coordinates.

Although the measurements are not complete, we have already obtained some interesting findings from five observers. The best brown perception was obtained at dominant wavelengths of 580-590 nm, which are longer than the one for a tritan yellow (on a line passing through D65). The observer variation is relatively large compared to other basic colors like yellow. It may suggest that the brown perception is not so strongly normalized by the natural environment as it is different with red-green and blue-yellow opponent responses which are strongly normalized to zero at the white daylight (D65). It may also be influenced by individual preferences for light vs. dark brown as the best exemplar of this contrast color.

INTRODUCTION

Brown, gray and black are considered among eleven basic colors [1]. However, they are different in production and reproduction with other basic colors; these colors cannot be perceived in a single light in a completely-dark surround. For gray and black perception, a relatively bright environment or a surround field is required to induce blackness (or darkness) in a central field [2, 3]. Brown perception is considered to have a more complex mechanism since some special chromatic conditions

are additionally required in the center field. Brown perception has been investigated in terms of color categories, and color chips categorized as "brown" are known [4, 5, 6, 7]. However, how the chromatic conditions of the center field change the perception of brown is not yet known. Thus, we investigated the relations between brown perception and chromatic conditions of the center field surrounded by a white annulus.

METHODS

In this research, we presented the center-surround stimuli on a CRT monitor. In order to avoid the difficulty and unexpected bias of estimating the magnitude of the brownness perceived in the center field, we employed a paired-comparison method. Two white annuli of fixed luminance were simultaneously presented side by side, and the observer indicated which chromatic center field appeared a better brown by pressing a left or right button. All win-loss scores of the central field conditions were transformed to z-scores after the comparison of all combinations of the conditions. Although the results of this method are in ordinal scale, the results were reliable.

We changed the chromaticity coordinates of the center field in terms of a dominant wavelength and saturation to obtain the best area of the center color in chromaticity coordinates. Because we expected that S-cone contribution would be an important factor for color vision processing [8, 9] including brown perception, the strength of saturation was controlled by the amount of S-cone stimulation. In Experiment 1, we changed a dominant wavelength and S-cone troland (td) of the center field, which was defined by chromaticity coordinates of the center color. We used three logarithmic S-cone td settings (-1.83, -1.41, and -1.20) for main stimuli and two log S-cone td settings for Red and Green (-1.06) and for Blue (-0.42). The S-cone td of the Red and Green of the center color was the same as the one of D65 in the equal luminance (5 cd/m²). The Blue and Yellow were on the tritan line passing through D65. These four colors were used as control conditions of the center color. The luminance of the center and the annulus were 5 cd/m² and 60 cd/m², respectively. In experiment 2, we changed the luminance of the white annulus from 13.1 to 99.6 cd/m² with two colors in the center (590 nm at -1.83 log S-cone td and 595 nm at -1.20 log S-cone td), while the luminance of the center field was fixed to 5 cd/m². In both experiments, the diameter of the center field was 1.00 deg., and outer- and inner-diameters of the annulus were 1.04 and 9.48 deg., respectively.

RESULTS AND DISCUSSION

Although the measurements are not complete, we have already obtained some interesting findings from five observers. Figure 1 shows the z-score of brownness obtained for one observer with -1.83 log S-cone td centers. The dominant wavelength of tritan yellow was 566.3 nm. The data of Blue, Green and Red center colors were plotted at the point of 545, 500 and 645 nm on the abscissa, respectively, for better presentation. On this observer, two sets of the center colors (560-590 nm and 575-610 nm) were tested in separate sessions; red crosses denote the average of these two sets of measurements. As shown in Fig. 1, the best brown perception was obtained at dominant wavelengths of 580-590 nm, which are longer than the one for a tritan yellow (on a line passing through D65). The observer variation is relatively large compared to other basic colors like yellow. It may suggest that the brown perception is not so strongly normalized by the natural environment as it is different with red-green and blue-yellow opponent responses which are strongly normalized to zero at the white daylight (D65).

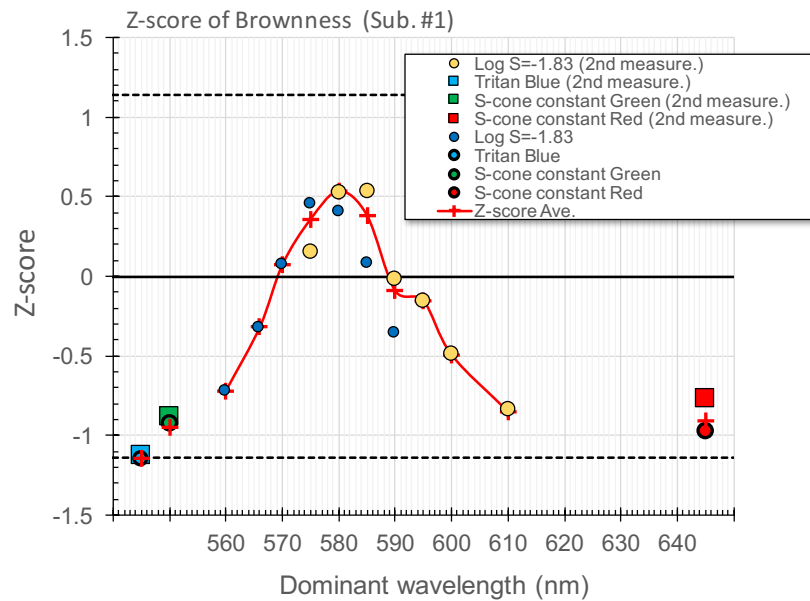


Figure 1. Z-score for Brownness from one observer tested for the condition of $\log S\text{-cone td} = -1.83$.

In Experiment 2, results show that the luminance of the annulus for the best brown perception was different between observers. For one observer, the peak luminance for best brown perception was in the range of the luminance used in the first experiment. The results from another observer showed that the best brown perception was obtained at the maximum annulus luminance. It shows that some observers prefer to have more darkness or blackness in the center field for the better brown perception. Thus, it may also be influenced by individual preferences for light vs. dark brown as the best exemplar of this contrast color.

ACKNOWLEDGEMENT

This research was supported by JSPS KAKENHI Grant Number 18H03323, and by Focused Research Laboratory Support Grant of Kochi University of Technology to KS. Also supported by the National Eye Institute grant EY 024239 to JSW.

REFERENCES

- Berlin, B., & Kay, P. (1969). *Basic color terms: Their universality and evolution*. Berkeley, CA: University of California Press. ISBN 1-57586-162-3
- Shinomori, K., Nakano, Y., & Uchikawa, K. (1994). Influence of the illuminance and spectral composition of surround fields on spatially induced blackness. *Journal of the Optical Society of America, A*, 11(9), 2383-2388. doi:10.1364/josaa.11.002383
- Shinomori, K., Scheffrin, B. E., & Werner, J. S. (1997). Spectral mechanisms of spatially-induced blackness: Data and quantitative model. *Journal of the Optical Society of America, A*, 14(2), 372-387. doi: 10.1364/josaa.14.000372

4. Bartleson, C. J. (1976). Brown. *Color Research and Application*, 1(4), 181-191. doi: 10.1111/j.1520-6378.1976.tb00041.x
5. Fuld, K., Werner, J. S., & Wooten, B. R. (1983) The possible elemental nature of brown. *Vision Research*, 23(6), 631-637. doi: 10.1016/0042-6989(83)90069-X
6. Lindsey, D. T., & Brown, A. M. (2014) The color lexicon of American English. *Journal of Vision*, 14(2):17, 1-25. doi: 10.1167/14.2.17
7. Kuriki, I., Lange, R., Muto, Y., Brown, A. M., Fukuda, K., Tokunaga, R., Lindsey, D. T., Uchikawa, K. & Shioiri, S. (2017) The modern Japanese color lexicon. *Journal of Vision*, 17(3):1, 1-18. doi: 10.1167/17.3.1
8. Shinomori, K., & Werner, J. S. (2008) The impulse response of S-cone pathways in detection of increments and decrements, *Visual Neuroscience*, 25(3), 341-347. doi: 10.1017/S0952523808080218
9. Shinomori, K. & Werner, J. S. (2012) Aging of human short-wave cone pathways, *Proceedings of the National Academy of Science of the United States of America (PNAS)*, 109(33), 13422-13427. doi:10.1073/pnas.1119770109

FROM VERNACULAR TO DIVINE CLASSICS: A NEW COLOR SURVEY APPROACH

Tien-Rein Lee^{12*} and Vincent Ching-Wen Sun²

No. 1, Huafan Rd., Shihding Dist., New Taipei City 223, Taiwan R.O.C

¹President, Huafan University, Taiwan.

²Department of Mass Communication, Chinese Culture University, Taiwan.

*Corresponding author: Tien-Rein Lee, trleex@faculty.pccu.edu.tw

Keywords: Color Survey, Color Categories, Divine Classics

ABSTRACT

The present study suggests a color survey approach which aims to find corresponding colors for varieties of items and reveal the color categories in them. Basic color categories are common among people with diverse languages and cultures, as Sun and Chen (*J*) suggested. In their Berlin & Kay style color survey with both “basic” color words and color-related words, they found that no matter the words used, the results showed concentrated and overlapping color sample distributions when the chosen samples displayed on a standard World Color Survey (WCS)(2) color palette. The distributions suggest a set of common basic color categories among the language users. We propose a color survey applying this procedure, but use those color related terms found in ancient Chinese religious texts and also western scriptures, to see how those color related terms correspond to the real perceptual colors, and whether associated basic color categories can be found.

INTRODUCTION

There are various ways to execute color surveys, and different understandings of color are revealed by different survey methods. Generally, a “color” is given by the surveyor, then surveying about the color is executed. In semantic differential scale (SD scale) studies, a color stimulus, usually a color sample, such as a Munsell chip, is presented and the observer fills the SD scale to the stimulus. Some researchers used objects with various colors, and combinations of color plus objects were surveyed. Preference rating methods are also commonly used for color survey. In this method, subjects are asked to rate colors in a multipoint preference scale. The colors could be presented as a swatch, a colored object, or just a given color name. Looking for associations of color is another color survey approach. Subjects are encouraged to freely generate associations about a given survey color.

Anyway, color surveys can also be carried out by asking subjects generate colors to a given terms. Axel Venn (2011), in his book “Colours of Health and Care,” showed a couple of color patterns that subjects drew on respond sheet with watercolor to a sort of selected words. However, it is hard to find meanings from the beautiful and creative color patterns drawn by subjects, and leaves the survey short of scientific usage.

Berlin and Kay (1969) used basic color terms, which were determined by linguistic criteria, to survey their corresponding colors on a sample board constructed by Munsell chips. Though their research originally focused on linguistic color lexicons, the study and the later World Color Survey (WCS) paid more attention on the color distributions on the sample board, which depicts a perceptual surface color representation. Those studies suggested that there are common basic color terms which correspond to similar perceptual colors among different languages.

However, Sun and Chen (1) suggested that there are basic color categories which are common among people speak same or different languages. In their study, with NCS color chips and computer-aided procedures, Mandarin speakers in Taiwan chose the color samples that they considered to correspond to a test Chinese word displayed on a computer monitor. The test words they used included both “basic” color words and color-related words. They found that no matter the words used, the results showed concentrated and overlapping color sample distributions when the chosen samples displayed on a standard color palette, as used by the classical Berlin and Kay (3) and the later World Color Survey (WCS). The distributions are consistent with the basic color terms suggested by WCS, suggesting a set of common deeper basic color categories among the language users. Based on Sun and Chen’s (2018) findings, we propose a color survey applying Sun and Chen’s survey procedures, but use those color related terms found in ancient Chinese religious texts and also western scriptures, to see how those color related terms correspond to the real perceptual colors, and whether basic color categories can be found and associated to those ancient religious color terms.

COLOR TERMS IN RELIGIOUS CLASSICS

Explore the Color terms used in Buddhist Avatamsaka Sutra (The Flower Garland Sutra) Buddha Shakyamuni preached it in heaven shortly after his attainment of Buddhahood. The sutra reveals different causes and ways of cultivation of many great Bodhisattvas, such as Ten Grades of Faith, Ten Stages of Wisdom, Ten Activities, Ten Transference of Merits, Ten Stages of Bodhisattvas, Absolute Universal Enlightenment, Wonderful Enlightenment, etc. It also reveals how to enter Avatamsaka World (Buddha's world) from the Saha World. "The Flower Adornment Sutra" -- whose full title is the "Great Means Expansive Buddha Flower Adornment Sutra" -- is the longest Sutra in Mahayana Buddhism. Referred to by Buddhist scholars as "the King of Kings of Buddhist scripture" and the "epitome of Buddhist Thought, Buddhist sentiment, and Buddhist experience," the Flower Adornment Sutra is 81 rolls (bamboo scrolls) long and contains more than 700,000 Chinese characters. There were many color terms were used to describe the In Book 44, and will be applied as the survey terms.

In addition to the color terms found in the previously mentioned classics, color terms appearing in the Christian bible scriptures will also be used in the survey. Taiwanese scholar Wen-Chang Lin (2008) codified the color terms listed in the Chinese Union version holy bible and suggested the spiritual meanings and corresponding colors of these terms. The present study will also use these terms as the surveying color terms.

THE SURVEY

A WCS style color sample board is to be built with original Munsell color chips, which is shown in the Figure 1. The same survey procedures used by Sun and Chen will be used. The sample board will be illuminated with Macbeth D65 fluorescent tubes. The color terms are displayed on a touch screen behind the board, which is also used to collect subjects’ answers about which color samples are for the survey term. The collected data of all subjects are going to be plotted as a frequency distribution on the WCS palette, and further analyses will reveal whether these religious color terms fit the basic color categories found by previous studies, or they reveal other characteristic color categories.

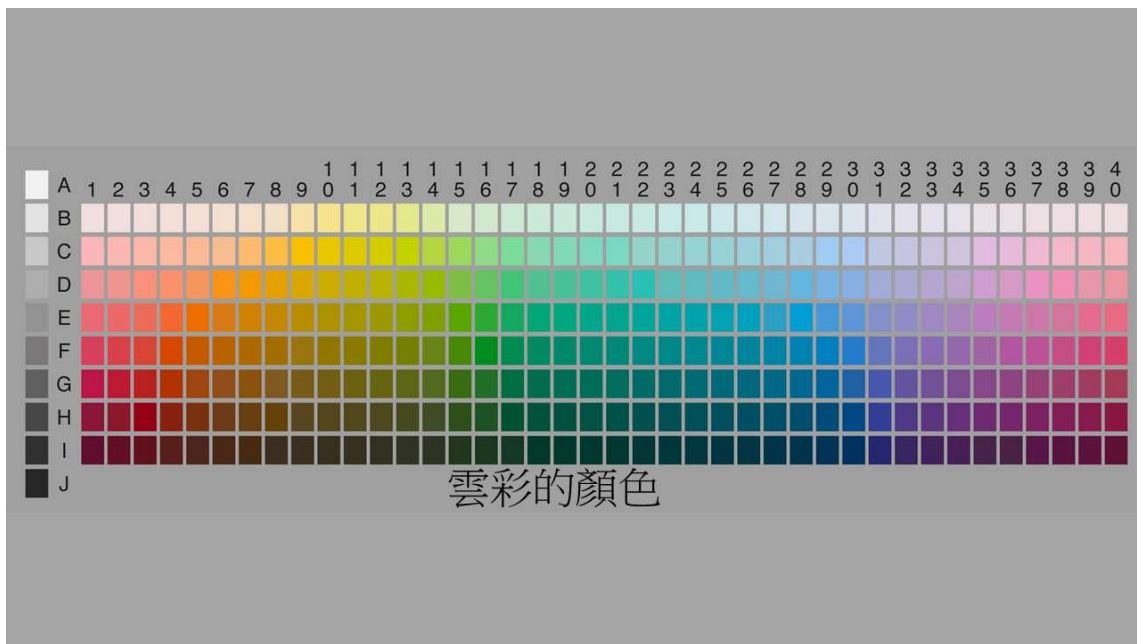


Figure 1. The color sample board proposed to build will be same as those used in the WCS. In the present study, the surveyed terms will be presented under the board, and the respondents pick all the color samples associated with the term with the aid of a touch screen.

ACKNOWLEDGEMENT

ACA2019 organizing committee thanks everyone who contributes to ACA2019.

REFERENCES

1. Sun, V. C., and Chen, C.-C. (2018) Basic color categories and Mandarin Chinese color terms, *PloS one 13*, e0206699.
2. Kay, P., Berlin, B., Maffi, L., Merrifield, W. R., and Cook, R. (2009) *The world color survey*, CSLI Publications Stanford, Calif.
3. Berlin, B., and Kay, P. (1969) *Basic color terms : their universality and evolution*, Center for the Study of Language and Information, Stanford, Calif.

THE RELATIONSHIP BETWEEN PSYCHOLOGICAL BRIGHTNESS, VIVIDNESS AND IMPRESSION

Tadayuki Wakata¹

¹ *Global Education Canter, WASEDA Univ., Japan.*

Tadayuki Wakata, wakata@aoni.waseda.jp

Keywords: Impression, Brightness, Vividness, PCCS tone

ABSTRACT

Our previous research showed the relationship between impression, psychological brightness, and color vividness. These studies suggested that psychological brightness and vividness combine to form a single dimension that corresponds to impressions of color. This study not only aims to confirm the results from the previous studies but also to quantify the relationship between these three variables. For this purpose, 65 participants evaluated 25 color stimuli (comprising 12 tones, 12 hues, and 1 achromatic color) by using the Visual Analog Scale (VAS), which considers brightness/darkness and vividness/dullness. The participants' impressions were then assessed by means of a seven-step Semantic Differential (SD) method that utilized 20 adjective pairs of color selected by referencing previous studies. The results from the SD method were then described through factor analysis and interpreted according to tone, achromatic color, and hue. According to the analysis, these components all revealed three factors, and thus, a dimension that combined brightness and vividness was obtained. Moreover, the scores from the factor and principal component analyses were calculated, and a regression analysis was used to quantify the relationship between impression and the dimension of brightness and vividness. The factor and principal component scores were applied to the dependent and independent values, respectively. Three equations were found for tone and four for hue. The results from the study confirm that the dimension of integrated brightness and vividness can explain color impression.

INTRODUCTION

A lot of research has been done on color impressions, such as Osgood's studies (Osgood .et. al;1964, Osgood .et. al;1975). Previous studies have primarily focused on the impressions of a single color (Wakata&Saito;2012, Wakata&Saito;2017). However, there is also a wider range of color expressions in everyday life, for example, "reddish color" and "pale color." In this case, "reddish color" indicates that the hue of "red" is common, but brightness and vividness may be different than a more average shade of red. "Pale color" denotes that brightness and vividness are roughly the same, but the hue could be different. The Practical Color Coordinate System (PCCS) was developed by the Japan Color Research Institute in 1964. PCCS has three attributes of color: hue, brightness, and saturation. Further, it has "tone," which is a combination of brightness and saturation. PCCS consists of 12 different tones and can indicate color by hue and tone, using the "hue-tone system." The use of tone allows for a wider range of color expression.

However, although tone is composed of brightness and saturation, there is not a 1:1 correspondence between psychological brightness and vividness. It is also important how the psychological brightness and vividness give the impression of color.

Previous researches showed the relationship between impression, psychological brightness, and color vividness (Wakata&Saito;2015, Wakata&Saito;2017). These studies suggested that psychological brightness and vividness combine to form a single dimension that corresponds to

impressions of color. This study not only aims to confirm the results from the previous studies but also to quantify the relationship between these three variables.

METHOD

Color stimuli: The color selection was done by using criteria of the Practical Color Co-ordinate System(PCCS). The tone stimuli used 12 tones [vivid: v, bright: b, strong: s, deep: dp, light: lt, soft: sf, dull: d, dark: dk, pale: p, light grayish: ltg, grayish: g, dark grayish: dkg,]. Each of these had a color wheel that consisted of 12 hues (1.5cm×1.5cm) pasted onto a piece of cardboard next to them (10cm×10cm) (Figure 1). The hue stimulus were the following 12 hues [2:R, 4:rO, 6:yO, 8:Y, 10:YG, 12:G, 14:BG, 16:gB, 18:B, 20:V, 22:P, 24:RP] that each had 12 tones (3cm×1.5cm) pasted in a belt-shape a piece of cardboard(5cm×21cm) (Figure 1). Additionally, there was a gray scale that was pasted onto the piece of cardboard in the same manner as the hue stimuli that was made up of 9 neutral color shades [1.5Bk – 9.5W]. The cardboard that was used was a neutral gray. There were a total of color stimuli 25 that consisted of the 12 tones, the 12 hues and the 1 neutral color.

Evaluation Items: The impressions were assessed using 7 step Semantic Differential (SD) method that utilized 20 adjective pair words selected by referencing prior studies (Table 1). The color stimuli were assessed using the Visual Analog Scale(VAS) that looks at brightness/darkness and vividness/dullness. Each of the assessments was done using an application that was running on the iPad.

Environment and Participants: The environment where the experiment was conducted was a university classroom with normal fluorescent lighting (800-1,000 lx). There were 65 participants in the experiment (average age of 21.48±1.21, 26 males, and 39 females).

Procedure: The brightness and vividness of the color stimuli were assessed using the VAS and the impression was assessed using the SD method by presenting one color stimulus at a time. Several groups were set up for the presentation of the stimuli and the order of the adjective pairs in SD method, and these groups were randomly matched up to each of the participants as a counterbalance consideration.

Table1. Adjective pairs words SD method

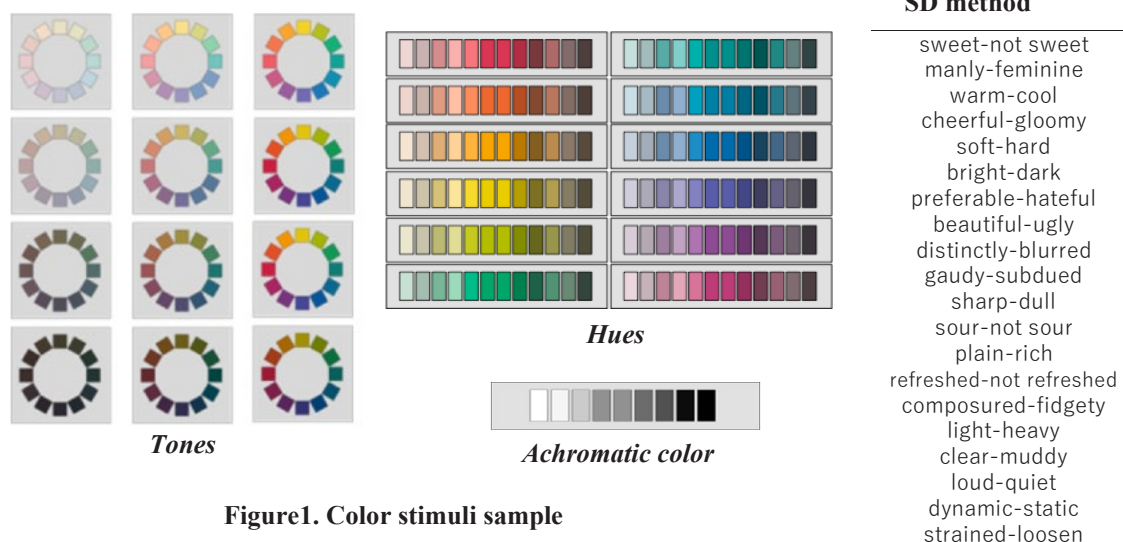


Figure1. Color stimuli sample

※This experiment was part of a multimodal study. In another part of the study, participants evaluated 30 fragrances and 40 musical pieces using the semantic differential (SD) method, and matched and mismatched colors were selected for these stimuli.

RESULT

Factor analysis: Factor analysis was conducted using scores from the SD method for tone stimuli, with achromatic color stimuli and hue stimuli. The results showed that tones had three factors and hues had four factors (Table 2,3). Tone indicated evaluation, potency, and activity, whereas hue showed activity, evaluation, potency, and tint. This suggested that tone and hue differ in impression structure. The dimension of color impression is shown as factors 3 and 4, as in previous studies (Wakata&Saito;2012, Wakata&Saito;2017).

Result of brightness and vividness by VAS: The mean was calculated for each color stimuli (Table 4,5) and plotted on figure2. This revealed that tone was plotted over a wider range than hue. The results for tone showed that vivid tone received the highest brightness score in figure 2, and bright and strong were plotted with high brightness as well. These tones were in the middle range of lightness in the PCCS. This suggested that saturation as rated by the PCCS affected psychological brightness. This finding seemed to suggest that the Helmholtz–Kohlrausch effect was observed. These results supported the findings of previous studies. The results of hue stimuli indicated that warm colors (e.g., red, orange, yellow) were higher than cool colors (e.g., blue, violet) in brightness and vividness. The hue stimuli shared a common hue, but tones were different as lightness and saturation varied. Nevertheless, psychological brightness and vividness change were observed, which suggested that hue affects brightness and vividness.

Table2. Factor loadings (Tone + Achromatic color)

	+	-	Fac1	Fac2	Fac3
beautiful - ugly			0.850	0.131	-0.110
clear - muddy			0.841	0.098	-0.071
sharp - dull			0.666	-0.408	0.189
refreshed - not refreshed			0.608	-0.149	0.064
preferable - hateful			0.584	0.146	-0.003
bright - dark			0.487	0.353	0.280
soft - hard			-0.079	0.793	-0.083
strained - loosen			0.321	-0.686	0.063
manly - feminine			-0.184	-0.679	-0.013
sweet - not sweet			0.067	0.653	0.209
distinctly - blurred			0.514	-0.520	0.370
light - heavy			0.461	0.507	-0.159
warm - cool			-0.013	0.494	0.448
loud - quiet			0.021	-0.042	0.828
dynamic - static			0.063	0.029	0.771
plain - rich			0.458	0.253	-0.595
gaudy - subdued			0.402	0.086	0.517
cheerful - gloomy			0.348	0.302	0.468
		Fac1	1.000	0.472	0.611
Factor Correlation		Fac2	0.472	1.000	0.152
		Fac3	0.611	0.152	1.000

Table3. Factor loadings (Hue)

	+	-	Fac1	Fac2	Fac3	Fac4
loud - quiet			0.861	-0.109	-0.073	-0.089
dynamic - static			0.817	-0.067	-0.019	-0.036
composured - fidgety			-0.725	0.420	0.201	-0.041
gaudy - subdued			0.481	0.456	-0.131	-0.112
cheerful - gloomy			0.466	0.353	0.251	0.043
sour - not sour			0.400	-0.182	0.096	0.220
beautiful - ugly			-0.219	0.754	0.013	-0.079
preferable - hateful			-0.330	0.721	0.119	-0.119
clear - muddy			-0.016	0.615	-0.244	0.215
distinctly - blurred			0.211	0.555	-0.445	-0.006
bright - dark			0.331	0.422	0.254	0.170
refreshed - not refreshed			-0.089	0.417	-0.142	0.269
soft - hard			-0.124	-0.056	0.711	0.054
sharp - dull			0.122	0.160	-0.639	-0.057
warm - cool			0.295	0.071	0.552	-0.138
sweet - not sweet			0.304	-0.053	0.428	-0.070
plain - rich			-0.081	-0.086	-0.109	0.672
light - heavy			0.105	0.138	0.228	0.662
		Fac1	1.000	0.336	0.305	-0.026
Factor Correlation		Fac2	0.336	1.000	0.296	0.245
		Fac3	0.305	0.296	1.000	-0.182
		Fac4	-0.026	0.245	-0.182	1.000

Table4. Mean(SD) of brightness, vividness, “brilliantness.” (VAS values and PCA scores of Tone + Achromatic color)

	brightness/darkness	vividness/dullness	PCA_ “brilliantness.”
v	81.185 (20.924)	83.646 (23.427)	1.199 (0.760)
b	78.000 (14.732)	74.200 (18.525)	0.973 (0.532)
s	76.031 (18.306)	79.554 (19.081)	1.035 (0.608)
dp	40.231 (20.931)	50.585 (23.943)	-0.116 (0.701)
lt	74.369 (17.294)	52.369 (24.053)	0.516 (0.599)
sf	62.846 (21.777)	43.400 (24.586)	0.152 (0.672)
d	35.015 (19.410)	31.092 (18.943)	-0.559 (0.601)
dk	21.723 (19.177)	26.385 (20.025)	-0.878 (0.629)
p	77.031 (24.059)	38.062 (27.440)	0.305 (0.686)
ltg	63.031 (24.610)	33.108 (26.714)	-0.030 (0.696)
g	22.569 (18.562)	18.108 (16.159)	-1.012 (0.512)
dkg	8.815 (15.705)	22.369 (26.664)	-1.177 (0.650)
Gy	32.692 (22.933)	41.723 (27.920)	-0.409 (0.793)

Table5. Mean(SD) of brightness, vividness, “brilliantness.” (VAS values and PCA scores of Hue)

	brightness/darkness	vividness/dullness	PCA_ “brilliantness.”
2R	60.508 (19.027)	59.754 (19.431)	0.442 (0.910)
4rO	63.892 (20.796)	57.246 (21.680)	0.465 (0.906)
6yO	61.446 (18.547)	49.462 (21.007)	0.194 (0.872)
8Y	61.723 (21.745)	49.108 (22.632)	0.192 (1.052)
10YG	54.277 (20.745)	49.231 (19.991)	-0.002 (0.944)
12G	54.631 (21.312)	55.738 (21.880)	0.180 (0.987)
14bG	47.123 (19.039)	51.969 (21.537)	-0.119 (0.925)
16BG	42.492 (20.561)	50.277 (21.657)	-0.286 (0.944)
18B	42.862 (19.977)	52.015 (23.817)	-0.231 (1.004)
20V	32.000 (15.522)	39.585 (20.058)	-0.847 (0.713)
22P	40.431 (20.900)	50.215 (22.116)	-0.343 (0.997)
24RP	58.600 (19.859)	58.308 (23.931)	0.353 (0.936)

Principal component analysis: Principal component analysis (PCA) was conducted using scores from the VAS for tone stimuli, with achromatic color stimuli and hue stimuli. It was aimed to get combine dimensions of psychological brightness and vividness. The mean of the PCA scores was calculated for each color stimuli, and then plotted on figure 3, 4 and table 4, 5. These results showed the same tendency as the visual analog scale (VAS) plot, and supported the findings of previous studies(Wakata&Saito;2012, Wakata&Saito;2017). This new attribute was named “brilliantness.”

Correlation coefficients between Factor score, brightness and vividness of VAS and PCA scores: Analyses for correlation coefficients between factor score, brightness and vividness of the VAS and PCA scores (“brilliantness”) were conducted (Table 6, 7). These results showed that psychological brightness and vividness corresponded to impression; furthermore, this tendency was also observed in the combine dimension of psychological brightness and vividness.

Regression Analysis: Regression analysis was conducted on PCA (“brilliantness”) and factor scores. The dependent value was factor score, and the independent value was PCA score (“brilliantness”). In total, seven formulas were obtained (Table 8). Focusing on the tone, it was suggested that Factors 1 and 3 could be explained by the correlation between brightness and vividness. Hue results showed the highest adjusted R² value in the second factor equation. The first factor of tone and the second factor of hue are common evaluation words for beautiful–ugly, clear–muddy, refreshed–not refreshed, preferable–hateful, and bright–dark. This dimension of impression is particularly sensitive to brightness and vividness.

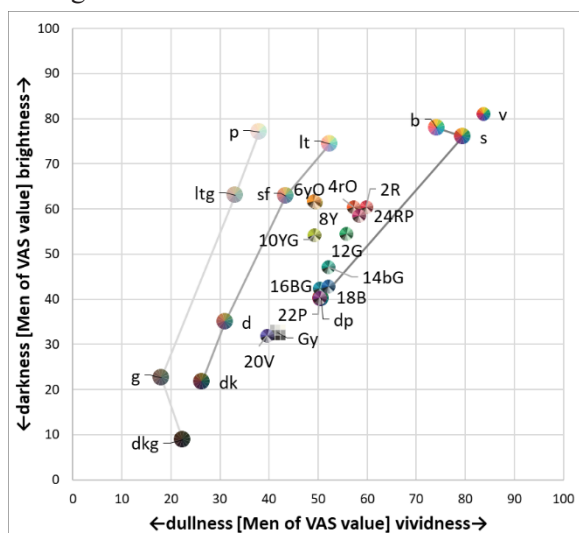


Figure2. Mean of brightness, vividness(VAS values)

Table6. Correlation coefficients
[Factor score – brightness, vividness and “brilliantness”]
of VAS and PCA scores
(Tone + Achromatic color)

	Fac1	Fac2	Fac3
VAS_brightness	0.958	0.827	0.706
VAS_vividbness	0.890	0.309	0.958
PCA “brilliantnes	0.985	0.624	0.874

Table7. Correlation coefficients
[Factor score – brightness, vividness and “brilliantness”]
of VAS and PCA scores
(hue)

	Fac1	Fac2	Fac3	Fac4
VAS_brightness	0.805	0.797	0.870	0.151
VAS_vividbness	0.500	0.872	0.566	-0.044
PCA “brilliantnes	0.762	0.895	0.833	0.092

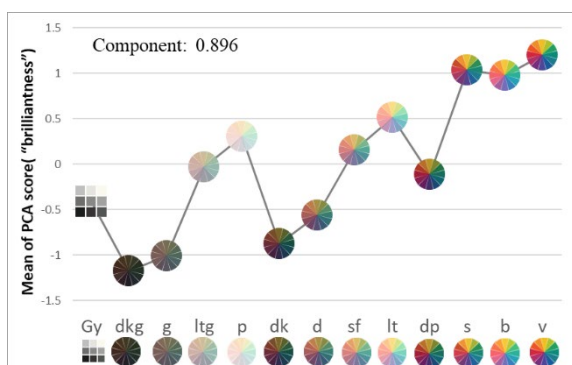


Figure3. Mean of “brilliantness.”
(PCA scores of Tone + Achromatic color)

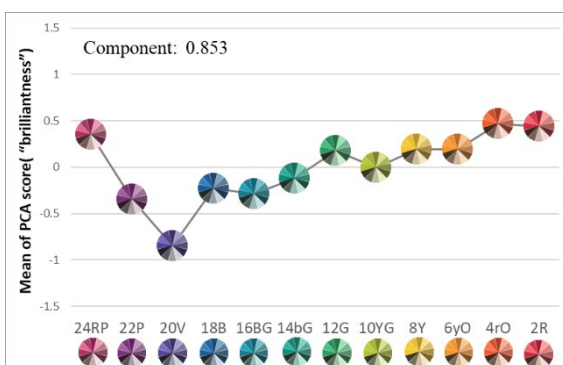


Figure4. Mean of “brilliantness.”
(PCA scores of hue)

Table8. Result of regression analysis

<i>Fac1_tone</i>	$Y = 0.944^{***} + 0.0000$	($R^2 = 0.967$)	$F_{(1,12)} = 351.743, p < .001$
<i>Fac2_tone</i>	$Y = 0.605^* - 0.0010$	($R^2 = 0.334$)	$F_{(1,12)} = 7.015, p < .050$
<i>Fac3_tone</i>	$Y = 0.855^{***} + 0.0000$	($R^2 = 0.742$)	$F_{(1,12)} = 35.54, p < .001$
<i>Fac1_hue</i>	$Y = 1.289^{**} - 0.001$	($R^2 = 0.538$)	$F_{(1,11)} = 13.826, p < .010$
<i>Fac2_hue</i>	$Y = 0.663^{***} - 0.001$	($R^2 = 0.782$)	$F_{(1,11)} = 40.361, p < .001$
<i>Fac3_hue</i>	$Y = 1.119^{**} - 0.001$	($R^2 = 0.663$)	$F_{(1,11)} = 22.625, p < .010$
<i>Fac4_hue</i>	$Y = 0.092_{n.s.} - 0.002$	($R^2 = -0.091$)	$F_{(1,11)} = 0.085, n.s.$

*: $p < .050$, **: $p < .010$, ***: $p < .001$

CONCLUSION

Color impression was revealed to have three dimensions for tone and four dimensions for hue. Psychological color brightness and vividness were shown to be related to each other, and it was able to obtain an integrated dimension. This new attribute was named “brilliantness”. The results of this study showed that “brilliantness” and the dimension of color impression were correlated.

ACKNOWLEDGEMENT

This work was supported by JSPS KAKENHI Grant Number 16K16139.

REFERENCES

- Osgood, C. E., Suci, G. J., & Tannenbaum, P. H. (1964). *The measurement of meaning*. University of Illinois Press.
- Osgood, C. E., May, W. H., & Miron, M. S. (1975). *Cross Cultural Universal of affective meaning*. University of Illinois Press.
- Wakata, T., & Saito, M. (2012). The impression of tones and hue in gradation of Practical Color Co-Ordinate System (PCCS), *AIC 2012 Taipei*, 322-325.
- Wakata, T., & Saito, M. (2015). A Study of Relationship between Physical Value and Psychological Value in PCCS. *International Color Association 2015, Tokyo*, 1087-1090.
- Wakata, T., & Saito, M. (2017). A study of common dimensions on the impression of color, fragrance and music. *日本色彩学会誌 41(3)*, 54-57.

Appendix. Mean(SD) of factor score (Left: Tone + Achromatic color, Right: Hue)

	Fac1	Fac2	Fac3		Fac1	Fac2	Fac3	Fac4
v	1.100 (0.522)	-0.040 (0.505)	1.509 (0.655)	2R	0.920 (0.710)	0.370 (0.874)	0.507 (0.705)	-0.311 (0.629)
b	0.914 (0.582)	0.538 (0.579)	0.963 (0.642)	4rO	0.744 (0.769)	0.237 (0.895)	0.603 (0.723)	-0.241 (0.662)
s	0.832 (0.646)	-0.054 (0.482)	1.270 (0.615)	6yO	0.552 (0.866)	0.150 (0.967)	0.605 (0.752)	-0.004 (0.733)
dp	-0.357 (0.639)	-0.452 (0.594)	0.105 (0.619)	8Y	0.723 (0.509)	-0.039 (0.906)	0.028 (0.927)	0.355 (0.865)
lt	0.649 (0.497)	1.039 (0.608)	0.154 (0.517)	10YG	-0.458 (0.530)	-0.113 (0.931)	0.161 (0.726)	0.420 (0.723)
sf	0.223 (0.692)	0.701 (0.684)	-0.064 (0.535)	12G	-0.419 (0.636)	0.138 (0.995)	0.139 (0.636)	0.432 (0.845)
d	-0.612 (0.590)	-0.236 (0.532)	-0.358 (0.559)	14bG	-0.542 (0.668)	-0.050 (0.868)	-0.424 (0.724)	0.295 (0.870)
dk	-0.935 (0.673)	-0.659 (0.612)	-0.557 (0.513)	16BG	-0.670 (0.774)	-0.111 (0.805)	-0.635 (0.868)	0.291 (0.861)
p	0.425 (0.535)	1.129 (0.651)	-0.368 (0.620)	18B	-0.771 (0.723)	0.123 (0.855)	-0.769 (0.689)	0.234 (0.711)
ltg	-0.039 (0.669)	0.758 (0.680)	-0.644 (0.616)	20V	-0.554 (0.777)	-0.591 (0.821)	-0.520 (0.702)	-0.429 (0.682)
g	-0.975 (0.660)	-0.619 (0.527)	-0.661 (0.595)	22P	-0.155 (0.718)	-0.420 (0.844)	-0.307 (0.703)	-0.629 (0.744)
dkg	-1.077 (0.718)	-1.177 (0.669)	-0.638 (0.569)	24RP	0.617 (0.940)	0.298 (0.921)	0.607 (0.890)	-0.431 (0.844)
Gy	-0.151 (0.755)	-0.937 (0.534)	-0.713 (0.582)					

THE STUDY OF HOW THE FIRST - TIME VOTERS MEMORIZE THE COLOR OF POLITICAL PARTIES

Waiyawut Wuthiastarn^{1*}

(39 Rangsit – Nakornnayok Rajamangala University of Technology Thanyaburi)

¹*Color Research Centre, Faculty of Mass Communication Technology, Rajamangala University of Technology Thanyaburi, Thailand*

*Corresponding author: Waiyawut Wuthiastarn, e-mail waiyawut_w@rmutt.ac.th

Keywords: colors of political parties, color code, memorize of color, first-time voters

ABSTRACT

Because of coup d'etat, the last general election voted in Thailand was 3rd of July, 2011. This has waited for 8 years for the next election voting. In 2019 the waiting had over. The election was on 24 of March 2019. The election commissions informed that the new voters were 6.4 million peoples. More than 100 political parties were registered. One of the simple strategies among the parties was to select the representative color for the political parties. They proposed the term "Color of Political Party" to be memorized for voting. In this paper, we aimed to study the factors of the memorable color of the political party for the new voter. From 132 parties, the researcher selected 2 political parties that were well-known which were Future Forward Party (orange color) and Democrat Party (blue sky color). New voters or first-time voters who participated in this survey were 419 students from the Rajamangala University of Technology Thanyaburi, Pathum Thani Province. The result showed that the new voters tended to memorize the wrong color code of the sample political parties. Most of the new voters couldn't memorize the colors of the political parties, except these two parties.

INTRODUCTION

In political campaign communication, the colors are used in elections to memorize of the voters. Each political party use representative colors that are different from the rival party. Luigi Marini (2017) found that right wing political parties tend to use color in the blue range. On the other hand, left wing political parties tend to use red color. The new political parties would not use the color that political parties have been used previously. However, the colors of political parties are vary according to the context of local areas. (Marini, L., 2017) [1]

Rifka Sibarani (2018) studied another theory of Roland Barthes in Indonesia president election campaign. She found that the parties uses color to create an ideology of political parties. The yellow symbolizes the authority of the Golongan Karya Party. The red color represents the labor history of the communist ideology of the political party PDI Perjuangan. Blue represents a new liberal concept with the patriotism of Susilo Bambang Yudhoyono. While the political parties of Joko Widodo use a combination of red-white-black to show the aggressiveness of his political party. (Sibarani, R., 2018) [3] In addition, the colors of political parties are used in the campaign in other countries as well. For example, in Taiwan, the New Party uses yellow to represent the party while the Democratic Progressive Party uses green. In Canada, the New Democrat uses orange, while the Liberal Party uses red, and the Conservative of Canada uses blue. Most U.S. political parties use red,

white and blue together. However, television broadcasting often uses red for Republican and blue for Democrat. There are still political parties that use other colors, for example, green for the Green party and yellow for the Libertarian Party.

On the other hand, according to the Ecological Valence Theory (EVT's), Palmer and Schloss (2010) studied effects of the color preferences and found that the voters closely associated red with the Republican Party and blue with the Democratic Party especially on the election date. They suggested that mass media has an effect on the color preferences of the voters. The color satisfaction of the voters depends on their experiences toward the political party. (Palmer, S. E. & Schloee, K.B., 2010)[2]

In Thailand, the coup d'etat happened on 22nd of May, 2014 by General Prayut Chan-o-cha. Thais waited for 8 years for the general election. The election was on 24 of March 2019. The Election Commissions of Thailand informed that new voters were 6.4 million peoples while there were 132 political parties. Therefore, the new voters must know and remember every political party. One of the simple strategies among the parties was to select the representative color for the political parties. According to the survey of the color usage of political parties in Thailand conducted by SALMON LAB.[4] found that blue colors were used by up to 30 political parties (36.59 percent). For example, the elder political party which is Democratic Party (no.2) as shown in Figure 1,



Figure 1 Political Parties that use blue color.

SALMON LAB,[4] survey found that followed by green 12 political parties (14.63 percent). For example, Dee Power Party (no.1), Green Party (no.3), Thai Teachers for People Party (no.11) as shown in Figure 2.



Figure 2 Political Parties that use green color.

And multi-colors. As shown in Figure 3, 12 parties (14.63 percent) used multi colors for their logos. For example, Thai Local Power Party (no.7) used green, red, and blue. The Kasikornthai Party (no.6) uses orange, purple, green, sky blue, and blue. The Prachachat Party (no. 12) uses yellow, brown, purple, green, orange, blue, violet, and red.



Figure 3. Political Parties that use more than one color.

RESEACH DESIGN

The research question was to find the memorable colors of the Political Party and other factors associated with the color from new voters. This was an online study in Google form. A logo of political parties edited by Photoshop CS6 in black and white, 2 x 2 inches was placed on the top of the questionnaire. And then, the participants were asked to select the color name of red, blue, green, yellow, pink, orange, and brown that represent the color of 27 political parties from the parties that had party-list members of the House of Representatives. The participants were 419 voters who were students of the faculty of Mass Communication Technology, Rajamangala University of Technology Thanyaburi, Pathum Thani, Thailand.

RESULT AND DISCUSSION

The 419 participants was 100 persons for 18 years old, 182 for 19 years old, 97 for 20 years old, 30 for 21 years old, 4 for 22 years old, 2 for 23 years old, and 4 for 24 years old. They selected color representative the political parties shown in the Figure 4

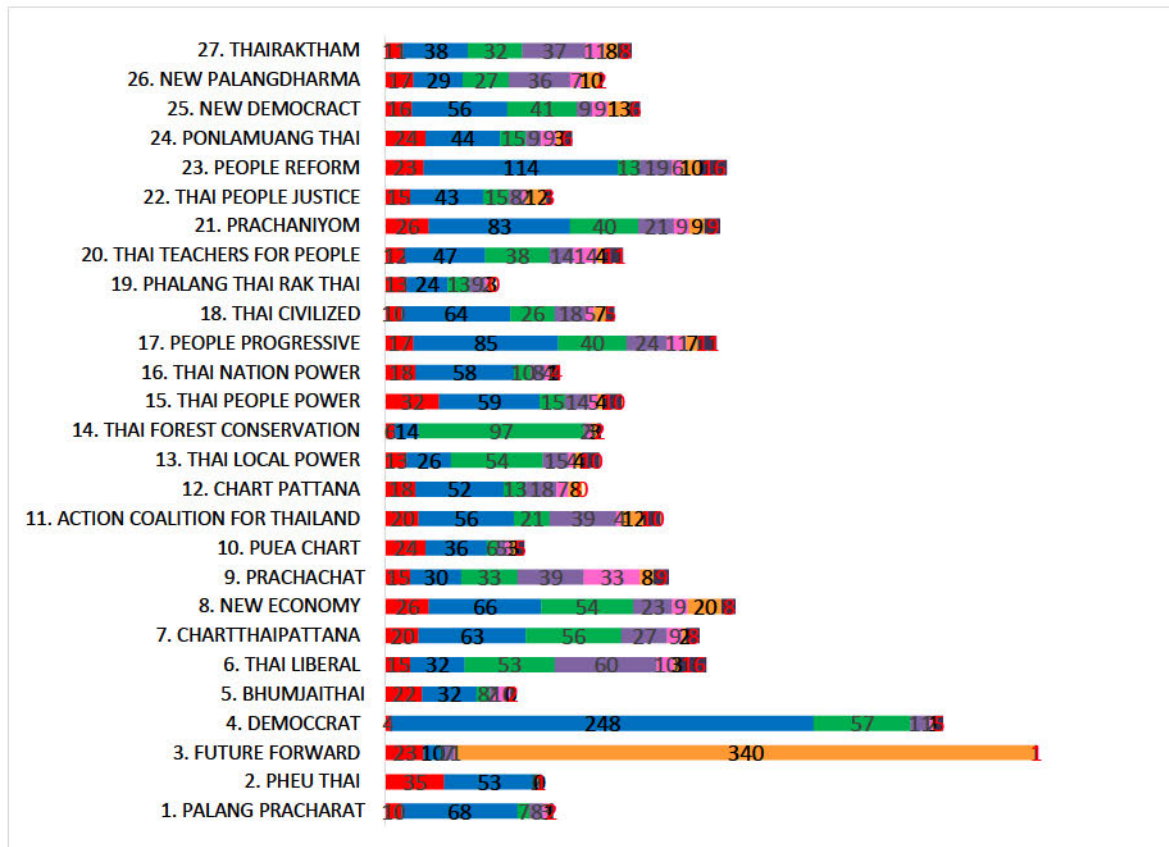


Figure 4. The memorable colors of the Political Party

The result shown that the new voters memorized orange color as the Future Forward Party (no.3) according to the Ecological Valence Theory (EVT's) that effects of the color preferences. (Palmer, S. E.& Schloee, K.B., 2010)[2] The younger voters preferred the Future Forward Party because of 6,330,617 votes from number of the new comer were 6.4 million peoples (The Election Commissions of Thailand,2019)[5]. The blue color as Democrat Party (no.4) because this party was the oldest political party established in 1946. The colors of others of political parties was distribution. They used blue color, which was a color in the blue range that represents the conservative while Future Forward Party a new liberal political party, used the opposite color (orange). It was similar to the study of previous study found that political parties with the right wing parties tend to use color in the blue range as the party's color and political parties with left wing parties tend to use red color instead. (Marini, L., 2017)[1]

ACKNOWLEDGEMENT

This acknowledgment for Miss Ploy Srisuro, and my colleagues and the freshman and sophomore students of Mass Communication Technology, Rajamangala University of Technology Thanyaburi they were a good participants in this research.

REFERENCES

1. Marini, L.(2017) *Red parties and blue parties, the political of party colours: Use and percprtion of non-verbal Cues of Ideology*. Paper presented at Political Studied Association (PSA) Conference, University of Stratchlyde, Glasgow, Scotland, 10-12 April 2017.
2. Palmer, S. E.& Schloee, K.B.(2010) *An ecological valence theory of color preferences*. Paper presented at Proceedings of the National Academy of Science, United State of America, 107(19):8877-82, May 2010
3. Sibarani, R.(2018) *Indonesia's Political Colour: From the New Oder to Joko Widodo*. ILMU KOMUNIKASI, 15(2),189-202.
4. SALMON LAB, [online], <https://lab.sal.mm/2019/03/political-parties-colors/61824/>
5. The Election Commissions of Thailand, [online], https://www.ect.go.th/ect_th/

COLORS FOR FEMALE AND MALE IMAGE BY THAI AND JAPANESE PEOPLE

Wipada Pumila^{1*}, Chanprapha Phuangsuwan¹, Yoko Mizokami², and Mitsuo Ikeda¹

¹*Color Research Center, Faculty of Mass Communication Technology, Rajamangala University of Technology Thanyaburi, Thailand.*

²*Graduate School of Engineering, Chiba University, Japan.*

*Corresponding author: Wipada Pumila, 1159108020382@mail.rmutt.ac.th, vipada.pumila@gmail.com

Keywords: Color, Female image, Male image, Thai, Japanese

ABSTRACT

We can put meaning to color, which is called color coding. In Thailand, the color codes are not so much utilized. One example is toilet sign. In many countries a male toilet is coded by blue or black while a female by red. But in Thailand such color code is not used and, in some cases, both female and male toilets are shown by red. In order to utilize the color code in public society it is necessary to investigate what color has what image to the people. The present paper investigated the colors for female image and for male image latent in Thai people. 72 color chips covering hues and saturation taken from Munsell Book of Color were arranged in two rings and female subjects were asked to choose representative hue that matches with their impression for female by ranking 1-3, the second they asked to select color chip from the hue that they chose one color. The same experiment was done for male subjects also. We obtained the color chip that female subjects chose, and that male subject chose. The result showed that the first choice for female image was 2.5R7/8 and for male image was 10B 6/10. For Japanese subjects' color choice of female was 7.5RP6/12 and male image 5PB 4/12. Results of color choice represented to female and male images from Thai and Japanese people showed slightly different. However, those colors appeared same tone as male was blue tone and female was pink tone.

INTRODUCTION

Pink and blue colors are common color when we think about the color code that represents to females and males. For example, the product of Hello-Kitty also use pink for girl and blue for boy [1]. In many countries their coded the color for female by red or pink and blue or black for male. In Thailand the color codes used for female and male are not specified. We surveyed the color of toilet sign around university, supermarket and department store and found that no systematic used of color. Sometime both female and male used the same black color and just using a difference of pictograms to discriminate or sometimes they use red color for male toilet and blue for female toilet as shown in Fig. 1 (a). In Japan, Male's toilet is shown by blue or black while female's toilet by red as shown in Fig. 1 (b). It is easy to find out where toilet is in a clouded place like in the department store. In advance, there is also a movement to introduce gender-neutral toilets that can be used by anyone. In Tokyo's Shibuya, one of the first municipalities to issue same-sex partnership certificates providing some of the same rights as a marriage certificate, the municipal office annex toilets have rainbow colored signage reminiscent of the LGBT movement's multicolored flag. New gender-free toilet signage depicting a figure wearing pants on one side and a skirt on the other can be found at places like the Mega Don Quijote discount shop in Shibuya, as well as in hotels in Kyoto catering to ever-increasing numbers of foreign tourists[2].



Figure 1. (a) Used of toilet color sign in Thailand. (b) Used of toilet color in Japan.



Figure 2. A new gender-free toilet signage.

Thailand is now aging society. More than 10 million elderly people were increasing for 10 percent of the total population since the year 2014. The prediction shows that in 2031 we will be “aged society”. To prepare the environment suitable for elderly is necessary. Color code is one idea to help the elderly this paper we aimed to utilize the color for female and male and propose to apply for the toilet sign.

EXPERIMENT

Stimuli

Seventy-two color chips from glossy Munsell color book were used to make the hue ring as shown in Fig. 3. Those color chips were pasted on the gray paper about N5 and it contained 40 hues. The color chips were kept the value 6 and chroma 8 and for achromatic chips ranged from N1 to N9 with interval 0.25 (for example N1, N 1.25, N1.50, N1.75) except N4, N5 and N6 had no value at step 0.75.

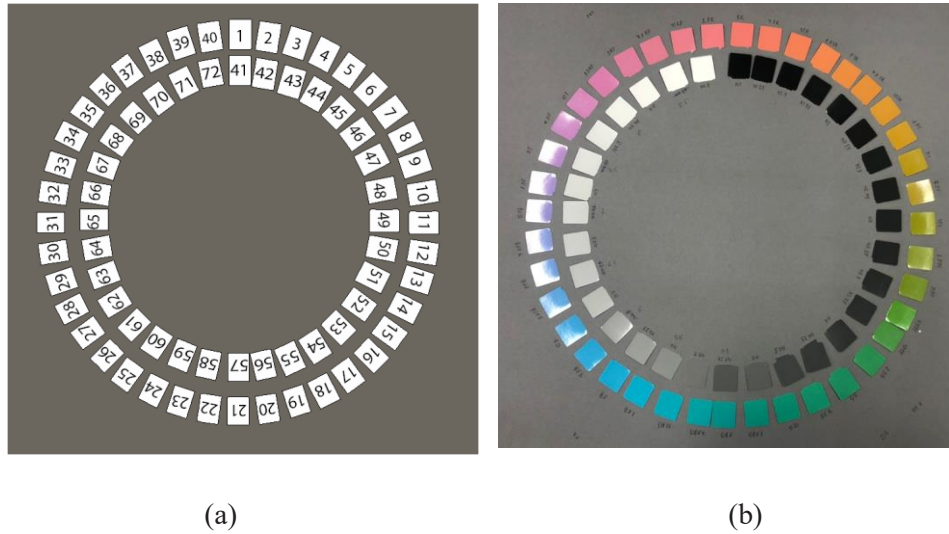


Figure 3. (a) Scheme of hue ring. (b) Hue ring.

Procedure

Subject asked to think about the color image for female and male under the normal daily life environment. Illuminance was ranged from 500 -3000 lx. The subjects were asked to select the 3 ranking of hues first. After getting three representative hues the experimenter will be opened the Munsell book into the corresponding hue that he/she chose in each ranking and then subject looked around the color chips which were showed in many values and chromas then selected one of color chip that imaged to female or male to the subject. Subjects continue selected the color chips for the second and third ranks respectively. The experiment duration was 3-5 minutes for each subject, and no repetition on this experiment.

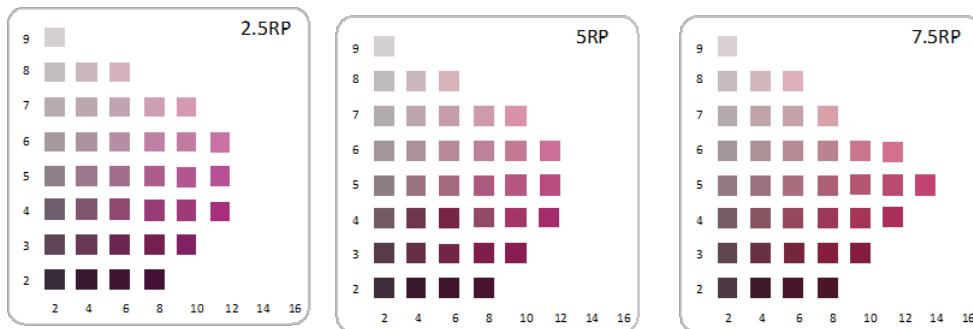


Figure 4. Example of Munsell sheet in the book.

Subjects

One hundred Japanese subjects (age ranged from 17-47-year-old) participated in this experiment and those subjects were divided into 50 females and 50 males. For Thai people was also the same number as Japanese and age ranged from 18-44-year-old.

RESULTS AND DISCUSSION

The results of selected hue for the first rank of male image from Thai and Japanese people are showed in the Fig. 5. The abscissa indicates Munsell hue and ordinate indicates number of subjects that selected in each hue. The munsell hue 10B was high frequency selected by Thai people and 5PB for Japanese choice. Figure 6 showed the result of munsell hue represented to female image. Munsell hue 2.5R was showed high frequency selected female image for Thai people and 7.5RP for Japanese people. In addition, the selected hues were varied distribution into 32 hues.

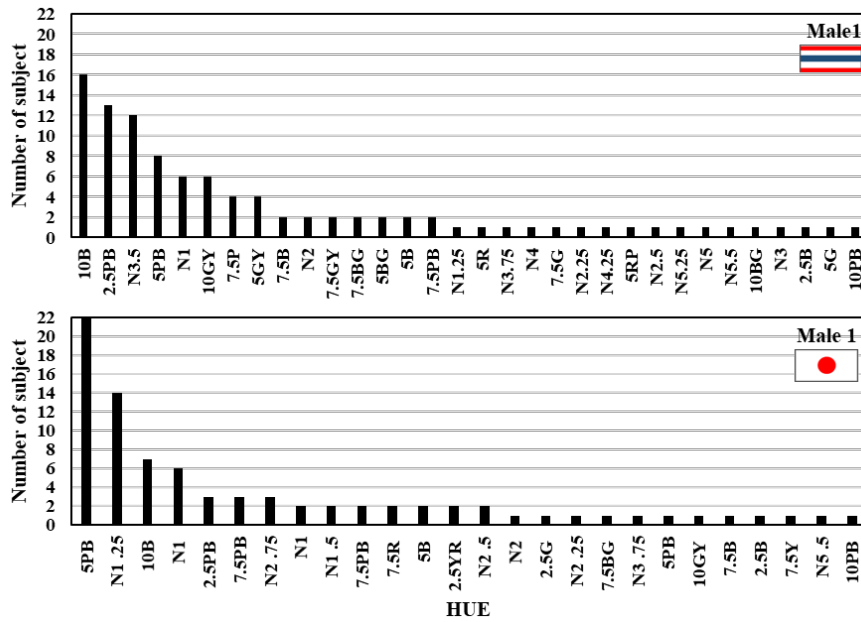


Figure 5. Result of selecting hue represented to male image of Thai and Japanese.

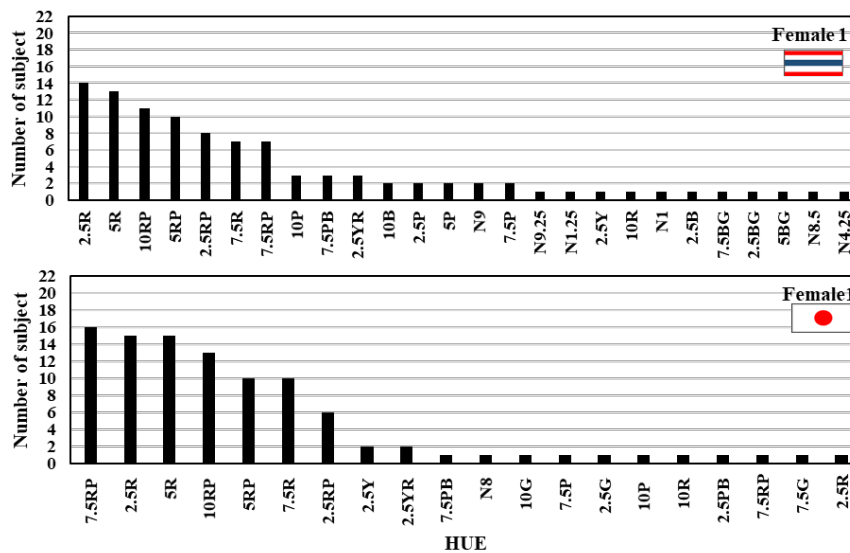


Figure 6. Result of selecting hue represented to female image of Thai and Japanese.

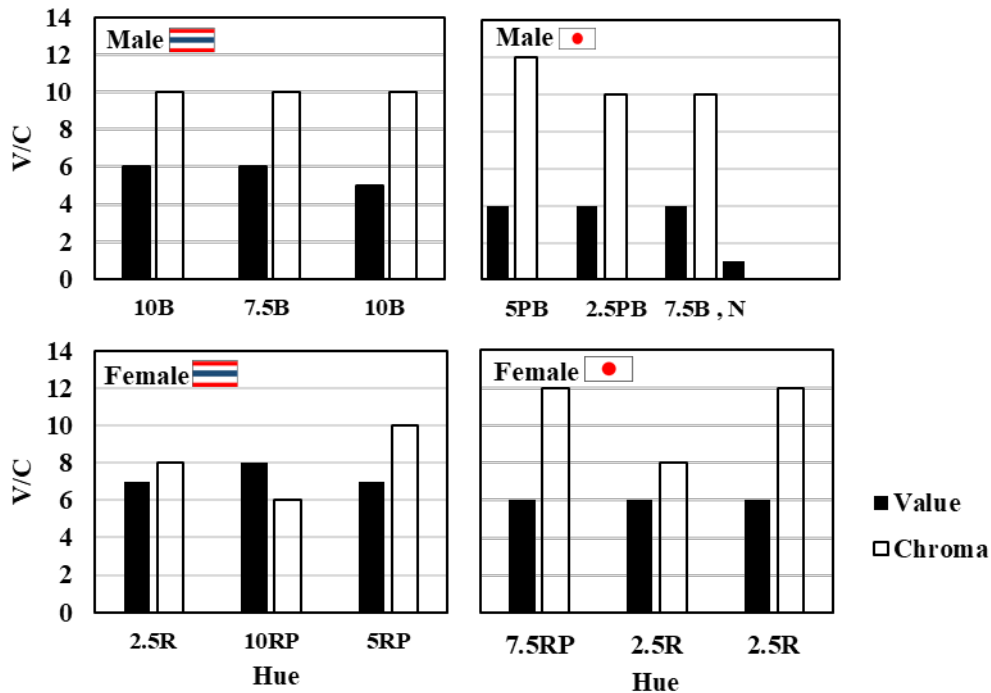


Figure 7. Results of hue/vale/chroma in three ranking from Thai and Japanese.

Three ranks of color selected by Thai and Japanese are shown in Fig. 7. The abscissa indicates Munsell hue from rank 1 to 3 and ordinate indicates value and chroma. Left column was the result of Thai and Japanese on the right column. Solid bars represent to value and chroma. The colors representative male image of Thai people was 10B 6/10, 7.5B 6/10 and 10B 5/10 respectively. Color representative male image from Japanese was showed 5PB 4/12, 2.5 4/10 and 7.5B 4/10 plus N1 respectively. In the two bottoms graph are the results of female image which 2.5R 7/8, 10RP 8/6 and 5RP 7/10 respectively. For Japanese, the female image was showed 7.5RP 6/12, 2.5R 6/8 and 2.5R 6/12 respectively. In figure 8 is comparison of only first rank of selecting color that represented male and female image of Thai and Japanese. 10B 5/10 was high frequency selected for male image for Thai people and its color was lighter than Japanese selected color 5PB 4/12 which was lower value and higher chroma. In the point of view of author in Japanese selected color for male image it might be caused by their get used to with the color code which normally seen at the toilet sign. In the case of Thai people selected color for male image it may come from their organized image or experience from other products color that normally use blue color tone for male.

The result of color representing to female image was showed high selected at 2.5R 7/8 for Thai. The color appearance for 2.5R 7/8 was pink slightly red. And for Japanese showed 7.5RP 6/12, it's colored quite pink slightly blue which is similarly to the female toilet sign in Japan. This finding is agreed with Anya C. Hurlbert et. al. that showed the color preference difference between male and female by using CRT display and using forced-choice 'color-picking' task with colorimetrically controlled stimuli separating the relative contributions of hue, saturation and lightness. Their results showed average color for female preference at reddish-purple region and male preference showed at blue-green region. In addition, color preference of male and female slightly differed by counties such as UK preferred reddish purple for female and bluish green for male. However, China preferred reddish yellow for female and reddish purple for male.

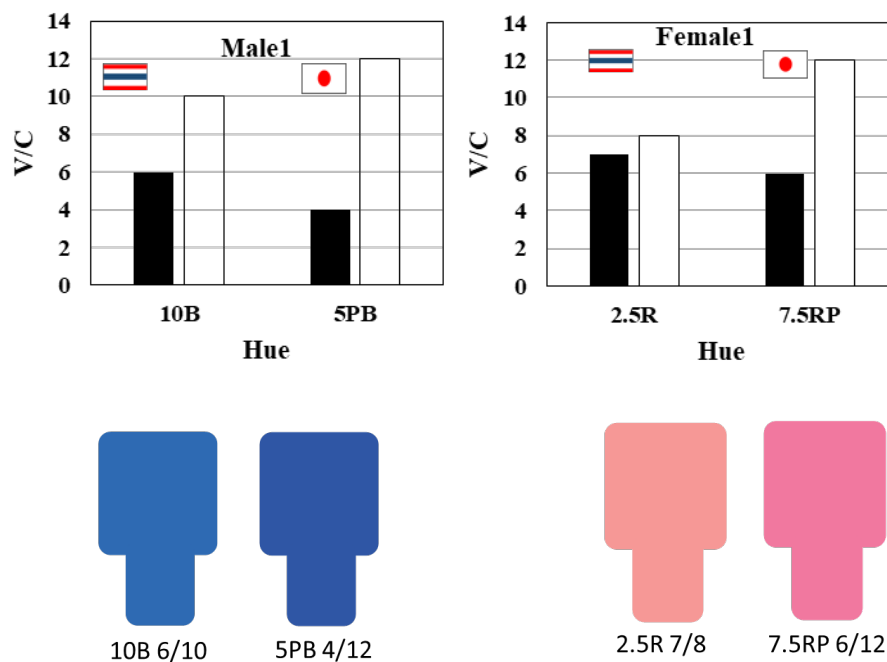


Figure 8. Comparison of color that representative to male and female image of Thai and Japanese. Solid bars indicate value and opened bars indicate chroma.

ACKNOWLEDGEMENT

Wipada Pumila thanks RMUTT for giving her the Co-operative Education, Rajamangala University of Technology Thanyaburi scholarship that made her to spend at Chiba University for 3 months to carry out internship. Also thanks students at Prof Mizokami's laboratory at Chiba University who helped her experiment and for serving subjects.

REFERENCES

1. Rost, L.C. (2018). An alternative to pink & blue: Colors for gender data. Retrieved September 22, 2019. <https://blog.datawrapp.de/gendercolor/>.
2. Maritomo. (2019). Japan's Toilet Signage Goes Global. Retrieved September 22, 2019, from <https://www.nippon.com/en/guide-to-japan/gu006004/japan's-toilet-signage-goes-global.html>.
3. Hurlbert, A. C., & Ling, Y. (2007). Biological components of sex differences in color preference. *Current Biology*, 17(16), 623–625. doi: 10.1016/j.cub.2007.06.022

ANALYSIS OF PALE COLOR PREFERENCE FOR JEANS PRODUCTS

Kieko Yamada^{1*}, Mikiko Kawasumi² and Akihiko Goto³

¹*Yamada Sarashi Some Kougyo Co., Ltd. / Japan*

²*Department of Information Engineering, Faculty of Science and Technology, Meijo University / Japan*

³*Department of Information Systems engineering, Faculty of Design Technology, Osaka Sangyo University / Japan*

*Kieko Yamada, kieko@yamadasarashi.com

Keywords: Pale Color, White Jeans, Dye, Bleach, Dye-Works, Color Psychology preference

ABSTRACT

Color stimulates human senses and has a great influence on human behavior [1][2]. This fact is becoming well known, and the psychological effect of color is now an essential element in corporate strategy and marketing. From now on, it is expected that the research demand for the color psychology field will increase more and more for the purpose of differentiation and high added values.

A lot of studies were established about primary, dark, and glossy colors, and there are many case studies are referenced by companies. However specific studies about white and pale colors are still under development and have not been adequately discussed.

White and pale colors are often used as background colors, but changing the perspective, it is more common to spend time in a light space based on white in daily life. It can be said that there are many opportunities to affect people and occupies an important position among the various shades. Based on the above background, this study conducted an evaluation experiment, using pale-colored jeans in order to investigate and clarify the psychological effects of white and pale colors on people.

Pale colors have lower color discrimination than dark color, so it may be preferable to combine it with products that are familiar to daily life when conducting evaluation experiments. Jeans are adopted on this study, because now they are widely established as a part of fashion [3], that they have acquired sufficient cognition, have strong candidates, and by having a certain surface area, makes easily recognize the differences compared to white.

Beach-dyeing technique was used to make the samples of pale-colored jeans. An appropriate amount of dye, which was prepared to dye into pale color was added to white jeans, and stirring was performed while adding sodium sulfate until the dye was fixed. In order to compare and evaluate each hue, seven pale colored jeans were successfully created by repeating the same process.

The samples prepared were subjected to hue research and quantified using the CIE L * a * b * system. The SD method was used to evaluate the sensitivity of the pale-colored jeans. Several adjectives for white and pale colors were defined in advance for evaluation. To minimize bias of evaluators, who are 95 female college students belong to various department of Osaka Seikei University, the method, conforming some pictures of worn pale-colored jeans on the website was adopted. In addition, the questionnaires were filled in after checking actual jeans samples that they touch and see closely. About the result gathered by the questionnaire, the relative evaluation was performed on the correlation between each hue, and the evaluation was performed in various ways. Expecting this research to help clarify the psychological effects of white and pale colors, adding values to cloth materials, taking as an example the color evaluation of jeans worn and widely used

on a daily life. And this experiment can be applied for product marketing, planning or academic fields of psychology.

EXPERIMENTS

Pale samples creation

Bleaching and dyeing technique was applied for making jeans samples for evaluation experiments. At First, jeans were put into an aqueous solution in which a surfactant was dissolved in order to remove chemicals and impurities added to the white jeans prepared in advance, and mechanical stirring was performed for 10 minutes while maintaining a constant temperature (80-100 ° C). Samples were put into the industrial dyeing machine shown in Figure 1 and water was permeated into the dough. They were put into the aqueous solution in which the dye is dissolved. The aqueous solution was mechanically stirred for 1-2 hours while maintaining a constant temperature (90-100 ° C). Finally, the dye was fixed by adding an appropriate amount of mirabilite (sodium sulfate decahydrate). Multiple light-colored jeans samples were created by repeating the above bleaching and dying process while adjusting the dye composition.



Figure 1. The image of the dyeing machine and the bleached jeans which are in process of dyeing.

Six types of pale colored samples were created, yellow, orange, red, purple, blue, and green. White was added as a reference for comparison, and a total of 7 types of samples shown in Figure 2 were prepared.



Figure 2. The image of pale colored samples and bleached white one.

Color measurement

Color measurement was performed to verify the correlation of the prepared samples. Quantification was performed by measuring luminance and chrominance coordinates using the popular CIE L * a * b * color system standardized by CIE and adopted by JIS Z 8781-4. Table 1 shows the average value of color measurement at 5 locations for each sample, and Fig. 3 shows the visualization of this.

Table 1: The scoring result of pale colored and bleached jeans examined by using CIE L*a*b* method.

Color name	Chromaticity	
	a*	b*
White	2.786	-9.454
Yellow	0.754	-0.336
Orange	3.538	-1.326
Red	4.62	-6.278
Purple	2.842	-8.096
Blue	-0.126	-6.822
Green	-0.646	-4.908



■ Indicator explanation

a* : (+) Red - Green (-)

b* : (+) Yellow - Blue (-)

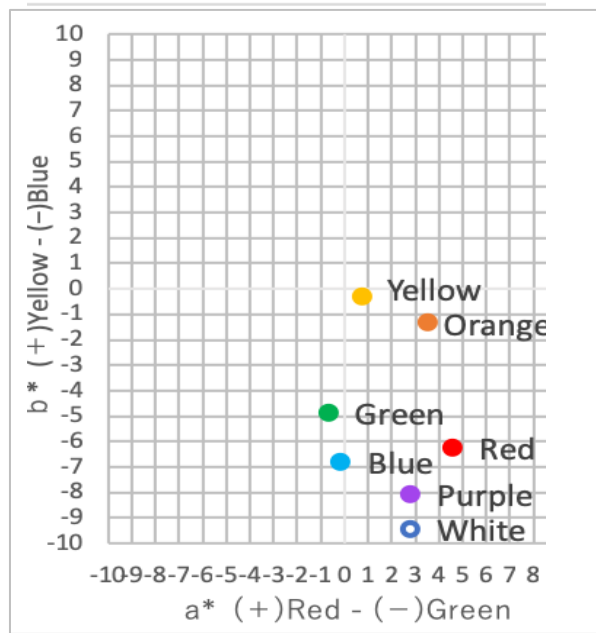


Figure 3. The figure of colorimetric result.

ASSESSMENT

Evaluation experiment method

In evaluating the light-colored jeans sample, the details were defined and studied from the viewpoint described below.

Selection of evaluation experiment participants As mentioned in the abstract, the evaluation experiment participants were young women with a strong interest in fashion. Under the cooperation of Osaka Seikei University, about 100 female university students in their late teens to early 20s were selected as participants.

Definition of evaluation experiment answer The Web answer format was adopted as a method for answering the evaluation experiment participants. First, participants in the evaluation experiment visually check the white and the samples stained in each color in a dedicated booth. After that, the actual wearing images were browsed on the website and the evaluation items were answered. There are many advantages such as being able to respond quickly compared to the paper response method [5], and it is thought that data collection with a high effective response rate will be possible by concentrating responses. And also, aim to reduce the difference in feeling depending on individual devices by checking the actual product under the same conditions.

Definition and quantification of evaluation experiment items The SD method was used to evaluate psychological effects. For each jeans samples, a five-point scoring was performed for 10 questions. In defining the answer items, more than 50 adjective expressions have been collected and organized, which were commonly used in color and fashion. The expression used for the white description is extracted and selected.

RESULTS AND CONCLUSION

Summary of aggregate results

In this evaluation experiment, Figure 4 shows the item evaluation for the hue when white is set to a median of 3, in order to evaluate with white as the reference.

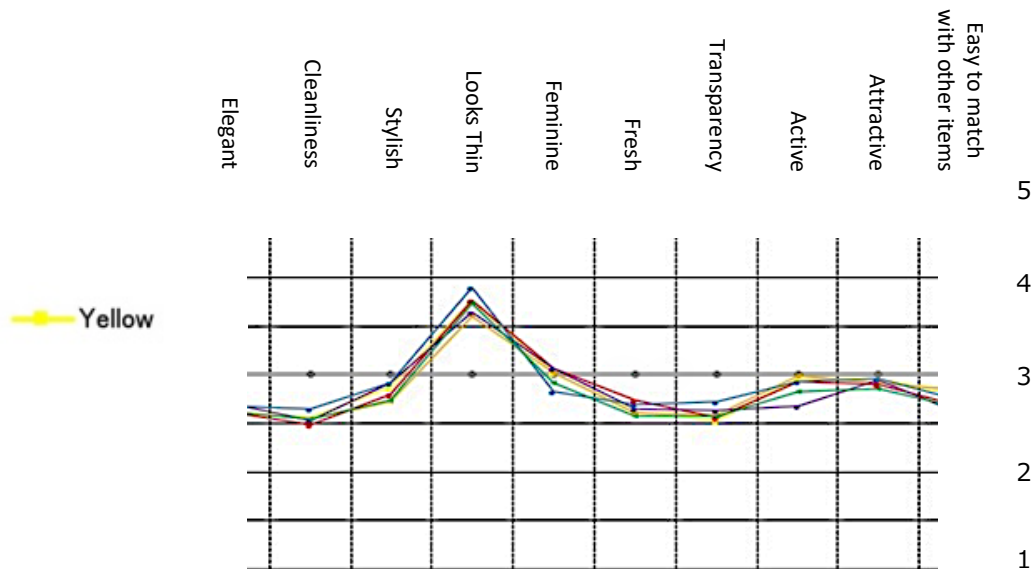


Figure 4. The result of assessments survey about pale color jeans.

It can be seemed that there is a big difference between white and other pale colors as an overall trend. Conversely, the difference in evaluation values between pale colors is extremely small. According to these results, adding a small amount of color to white can cause a significant difference. Focusing on each pale colored samples, the negative results were generally obtained about the adjective of “look thin” in comparison to white with color added since white is known as an expansive color. On the other hand, considering to the correlation of each colors, for example, it is generally known that blue has an effect of enhancing cleanliness and transparency when compared with other colors, and it is reproduced in pale colors.

Focused on respondents

It was analyzed from the perspective of whether the overall trend described above applies to all respondents. It was performed a cluster analysis using the Ward method and classified respondents. Respondents were classified into three levels, such as 1) Respondents with sharp answers. 2) Respondents with neutral answers. 3) Respondents with high score overall. The results of each response are summarized in Figure 5. Regarding the distribution of scores, there is a difference in each cluster, but there is no big difference in the overall trend, and it cannot be said that the individual sensibility of the respondents has a big influence on the whole. This study also revealed that adding other colors to white produces clusters with different response trends, although the overall trend is not significantly affected. The following was found through this study.

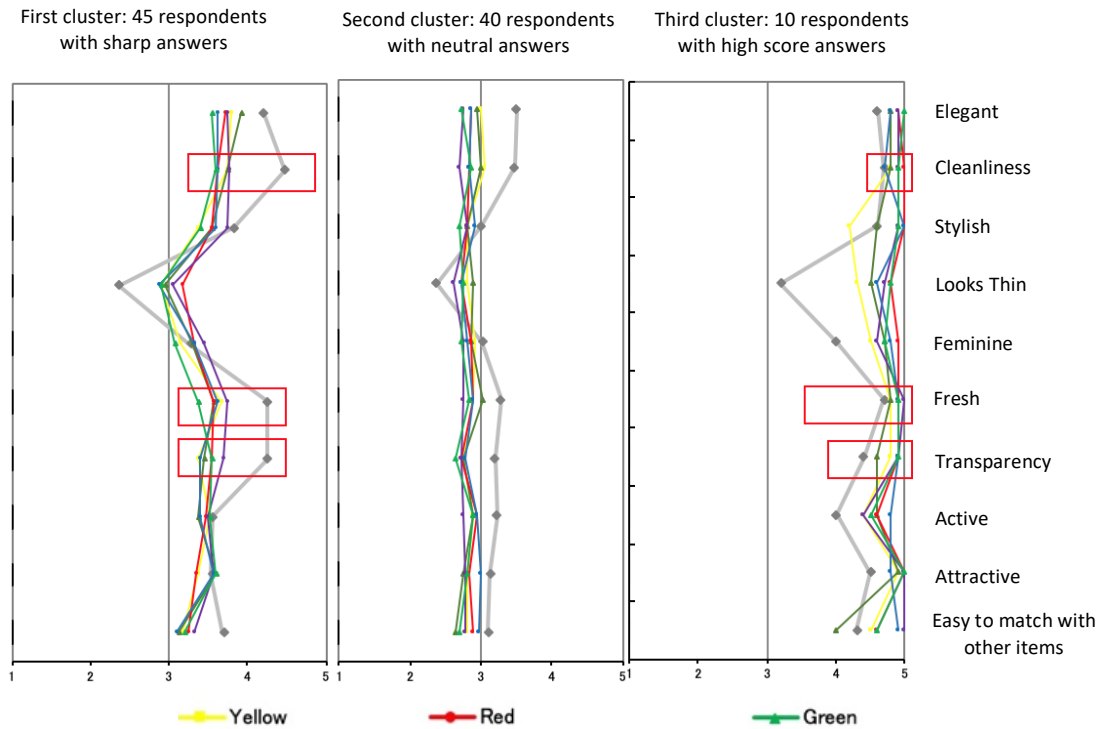


Figure 5. The comparison of response trends between three types of clusters.

- ✓ There was a huge difference in sensitivity evaluation results between white and pale colors.
- ✓ There was no significant differences in sensitivity evaluation results between each pale colors.
- ✓ As for the adjectives used in this study, the result is that only “looks thin” is superior to white in pale colors, and white is dominant in other major items.

As future prospects, it will be considered to detect response differences by changing the evaluation method, modify the adjectives adopted, evaluate using other products, or change the shade of pale colors. For example, it is assumed that it becomes possible to unravel a branch point where the difference between light colors becomes clear by strengthening the shades of light colors. Hoping that the continuation will contribute to the commercial and academic use of white and pale colors.

REFERENCES

- [1] Nomura Junichi, (2004) The secret of colors. p43.
- [2] Kawasumi Mikiko and Nishina Ken, (2017) Comparative Analysis of Silver Color Preferences for Metallic Products between Japan and Thailand. *Journal of Japan Society of Kansei Engineering*.p1.
- [3] Fuseya Setsuko, (2005) Young Women's Consciousness and Estimation of Jeans: Relating to the Physical Types and the Wearing Effects. *The journal of Wayo Women's University*.45. p84.

THE POST-PROCESSING OF COLOR CONSTANCY METHODS FOR THE OUTDOOR NATURAL SCENES

Shuo Liu, Xiandou Zhang*, Mengmeng Wang, Shangfei Li

Department of Digital Media Technology, Hangzhou Dianzi University, China

* Xiandou Zhang, xiandouzhang@126.com

Keywords: Color constancy, Gamut mapping, Digital imaging

ABSTRACT

In this study, a post-processing color constancy method for outdoor natural scenes was proposed. Comparing to the color constancy method that directly estimates the color of light sources, we focus on how to improve the accuracy and robustness of these methods. Daylights are the most frequently encountered in outdoor natural environment. The color of daylights could be significantly changing with the geographic regions, weather, season and different times of day. Fortunately, the colors of daylights are mainly distributed around the blackbody locus in the chromaticity diagram. The predicted color of the light source for the outdoor natural scenes should be distributed around the daylight color locus. Based on the observation of the color distribution of outdoor daylights, the estimation results of the color constancy methods are processed to improve the accuracy. The experimental results show that the proposed method could significantly improve the accuracy and the robustness of the mainstream color constancy method. The proposed method also has the low computational cost and higher robustness advantages comparing with other post-processing methods.

INTRODUCTION

Color constancy is a visual property that the human visual system can maintain a relatively constant color perception of an object even when the color of the light source changes. The digital imaging systems do not have the constant visual characteristics of the human visual system. When imaging, image color is easily affected by the color of light sources, resulting in the image color cast. There are mainly two steps for the digital imaging systems to simulate the color constancy ability of the human visual system, light source color estimation and color correction. The color correction step is usually implemented by a simple 3×3 diagonal matrix transformation, so the mainly work focus on the estimation of the light source color. The state-of-the-art estimation methods can be divided into two categories, statistical and learning methods. The statistical methods employ the assumptions and the statistics of the image's color distribution to predict the color of the light sources. The learning methods predict the color based on the model derived from the large set of training images. The prediction errors could be large when the captured image doesn't satisfy the assumptions for the statistical methods and there are not similar images contained in the training images for the learning methods.

A viable and effective strategy to improve the accuracy of these methods is to design a post-processing step to map the estimation result to a more realistic value. The Corrected Moment (CM) method [1] is essentially a correction method based on color moments or edge moments. The as-projective-as-possible bias correction (APAP) method [2] corrects the estimation results by establishing a mapping matrix between the estimated color and ground truth color, and uses look-up-table technology to optimize the performance.

Although there are various lighting environments which might be encountered in outdoor natural environment, daylights are the most frequently encountered in outdoor natural environment. The color of daylights significantly changes with the geographic regions, weather, season and different

times of a day, fortunately the colors of daylights are mainly distributed around the blackbody locus in the chromaticity diagram. So, if the light color estimated by the color constancy method in the daylight environment is large different from the day light colors, the large probability of the result is wrong. On this observation, this paper proposes a color constancy post-processing method for outdoor natural scenes. The main idea is to construct the color gamut of the daylights, and design strategies to map the estimated color into the corresponding color gamut.

PRELIMINARY

The image formation process of the digital imaging devices could be simply denoted as Eq. (1),

$$\rho_k = \int_{\omega} E(\lambda)S(\lambda)C_k(\lambda) \quad (1)$$

where ρ_k ($k = R, G, B$) represent the color responses, $E(\lambda)$, $S(\lambda)$ and $C_k(\lambda)$ represent the spectral power distribution of the light source, the spectral reflectance of the object and the spectral sensitivity functions of the RGB sensors respectively. λ is the wavelength and ω is the visible light spectrum. An important step in color constancy is to estimate the color of the light source, which could be represented as

$$E_k = \int_{\omega} E(\lambda)C_k(\lambda) \quad (2)$$

As the intensity of the light source is hardly to be estimated, usually only the chromaticity coordinates of the light source are estimated. The chromaticity coordinates r and g could be calculated by

$$r = \frac{\rho_R}{\rho_R + \rho_G + \rho_B}, \quad g = \frac{\rho_G}{\rho_R + \rho_G + \rho_B} \quad (3)$$

Usually the vector angles are used to evaluate the estimation accuracy. The calculation method is shown in eq. (4).

$$L = \frac{180}{\pi} \arccos \left(\frac{(\rho_k^g \cdot \rho_k^e)}{\|\rho_k^g\| \|\rho_k^e\|} \right) \quad (4)$$

where ρ_k^e and ρ_k^g represent the estimated and ground truth color respectively.

POST PROCESSING METHOD

The post processing method mainly includes two steps, gamut determination and gamut mapping. Firstly, the color distributions of the daylights should be determined. The color distributions of the daylights could be derived from simulation if the spectral sensitivity functions of the camera and the spectral power distributions of different daylights are known. If not, the color distributions of the daylights could also be collected from the known training images and the corresponding color of daylights.

Based on the collected color distributions of the daylights, the color gamut of the daylights is determined by the following methods. The chromaticity color space is firstly divided into lots of small bins, and the number of light sources located in each bin are calculated. The bins with little day lights are eliminated as they might be noises. Only the bins with certain number of day lights are kept, and based on which the gamut boundary is determined with the convex hull method. For a color constancy method, If the estimated color of the light source distributed in the built color gamut, the estimated color doesn't change. If not, the estimated color is mapped into the color gamut.

EXPERIMENT & RESULT

The images captured in the outdoor lighting environments are extracted from the widely used ColorChecker [3,4] and NUS [5] dataset. The ColorChecker dataset (Shi and Funt reprocessed versions) contains 568 indoor and outdoor scene images, taken with Canon 5D and Canon 1D SLR cameras. The images in the NUS dataset are captured with eight different brands of cameras. 306 outdoor images captured by Canon 5D in the ColorChecker dataset and 1241 outdoor images in the NUS dataset are extracted to evaluate the proposed method.

The color of the light sources is firstly estimated with different widely color constancy methods. The selected statistical based color constancy methods are Gray World (GW) [6], White Patch (WP) [7], Gray Edge (GE) [8], Shades-of-Gray (SoG) [9]. The selected learning-based methods are Gamut Mapping (GM) [10], FFCC [11], FC4 [12]. Then the estimated color of the light sources are processed with the proposed post processing method.

Table 1. Post-processing results of the ColorChecker dataset

	Original Methods				Proposed(Min-D)			
	median	mean	worst05%	worst25%	median	mean	worst05%	worst25%
GW	3.92	5.16	16.32	11.30	2.85	3.02	7.10	5.59
WP	2.52	4.29	22.14	11.38	1.85	2.36	7.59	5.29
Modified WP	4.10	5.00	16.02	10.60	3.25	3.22	7.38	5.94
GE-1	3.35	4.29	13.20	8.78	2.80	3.01	6.66	5.34
GE-2	3.32	4.29	12.92	8.72	2.77	2.99	6.71	5.33
SoG(p=6)	1.77	3.28	15.56	8.65	1.51	2.14	6.94	4.97
GM	1.97	3.38	15.70	8.54	1.51	2.14	6.67	4.81
FFCC	0.86	1.34	5.60	3.26	0.83	1.29	5.05	3.10
FC4	0.87	1.17	4.57	2.53	0.82	1.11	4.21	2.45

Table 2. Post-processing results of the NUS dataset

	Original Methods				Proposed(Min-D)			
	median	mean	worst05%	worst25%	median	mean	worst05%	worst25%
GW	2.98	3.98	13.21	8.82	2.34	2.75	8.20	5.44
WP	5.42	7.46	19.58	17.01	2.23	2.68	7.67	5.40
Modified WP	3.34	4.92	21.23	11.63	2.67	3.11	9.05	6.08
GE-1	2.51	3.54	14.03	8.05	2.09	2.51	7.26	5.08
GE-2	2.51	3.47	13.43	7.77	2.01	2.44	7.26	4.91
SoG(p=6)	3.32	4.92	16.69	11.60	2.24	2.58	7.40	5.03
GM	3.11	4.36	13.73	9.74	2.16	2.66	8.00	5.44
FFCC	1.21	1.74	7.13	3.99	1.21	1.74	6.91	3.96

The results are shown in table 1 and table 2 for the ColorChecker and NUS dataset respectively. The tables show that the proposed post processing method could improve color estimation accuracy of the light sources as a whole, especially it could significantly reduce large estimation errors. It is worthy to note that the estimation accuracy of the deep learning method (FFCC, FC4) is much higher than that of other color constancy methods, while the proposed method still could further improve the performance of the deep learning method in the large error reduction.

CONCLUSION

We developed a color constancy post-processing method for outdoor natural scenes based on the distribution characteristics of daylight in chromaticity diagrams. The analysis of the collected light source shows that the outdoor light source, especially daylight, is distributed within a certain color gamut, and the effect of optimizing the illumination estimation result can be achieved by map the estimated color into the corresponding color gamut. Experiments on the benchmark dataset show that the proposed method can improve the accuracy of the color constancy method, especially it could reduce the large estimation errors.

ACKNOWLEDGEMENT

The authors thank the funding support of National Natural Science Foundation of China (NSFC) (61675060, 61205168).

REFERENCES

1. Finlayson, G. (2013). Corrected-moment illuminant estimation. *IEEE International Conference on Computer Vision*, pp. 1904-1911.
2. M. Afifi, A. Punnappurath, G. Finlayson, and M. Brown, (2019). As-projective-as-possible bias correction for illumination estimation algorithms. *J. Opt. Soc. Am. A* 36, 71-78.
3. Shi, L., and B. Funt. "Re-processed Version of the Gehler Color Constancy Dataset of 568 Images," accessed from <http://www.cs.sfu.ca/~colour/data/>
4. P. V. Gehler, C. Rother, A. Blake, T. Minka and T. Sharp, (2008). Bayesian color constancy revisited. *IEEE Conference on Computer Vision and Pattern Recognition*, Anchorage, AK, pp. 1-8.
5. Cheng, D., Prasad, D. K., & Brown, M. S. (2014). Illuminant estimation for color constancy: why spatial-domain methods work and the role of the color distribution. *Journal of the Optical Society of America A*, 31(5), 1049.
6. Buchsbaum, G.. (1980). A spatial processor model for object colour perception. *Journal of the Franklin Institute*, 310(1), 1-26.
7. Cardei, V. C., Funt, B., & Barnard, K. (1999). White Point Estimation for Uncalibrated Images. *Color and Imaging Conference*.
8. Van, d. W. J., Gevers, T., & Gijsenij, A. (2010). Edge-based color constancy. *IEEE Trans Image Process*, 16(9), 2207-2214.
9. Finlayson, Graham & Trezzi, Elisabetta. (2004). Shades of Gray and Colour Constancy. Proceedings of the 12th Color Imaging Conference. 37-41.
10. Forsyth, D. A. (1990). A novel algorithm for color constancy. *International Journal of Computer Vision*, 5(1), 5-35.
11. J. T. Barron and Y. Tsai, (2017). Fast Fourier Color Constancy. *IEEE Conference on Computer Vision and Pattern Recognition (CVPR)*, Honolulu, HI, pp. 6950-6958.
12. Hu, Y., Wang, B., & Lin, S. (2017). FC⁴: Fully Convolutional Color Constancy with Confidence-Weighted Pooling. *IEEE Conference on Computer Vision and Pattern Recognition (CVPR)*. IEEE.

COLOR CONSTANCY UNDER AN ILLUMINANT HAVING MULTIPLE PEAKS IN THE SPECTRAL DISTRIBUTION

Akira Kito^{1*} and Taiichiro Ishida¹

¹*Department of Architecture and Architectural Engineering, Graduate School of Engineering, Kyoto University, Japan.*

*Corresponding author: Akira Kito, kito.akira.58m@st.kyoto-u.ac.jp

Keywords: Color Constancy, Color Appearance, Color Vision, LED Light Source, Spectral Distribution

ABSTRACT

We perceive surface colors as constant despite changes in color of an illuminant in a scene. This observation is referred as color constancy. Several studies on color constancy have shown that color constancy works well under an illuminant having a broadband spectral distribution [1]. In recent years white LED light sources have been widely used in our living environment. The spectral distribution of typical white LEDs includes narrow peaks, resulting in lower color rendering property. Little is known about the influences of narrow peaks in spectral distribution of illuminants on color constancy. It would be important to reveal the effect.

In this study, we investigated how color constancy works under an illuminant having multiple peaks in the spectral distribution. We prepared a lighting equipment (the MP illuminant) using three LEDs of red, green and blue colors. The intensity of each LED can be adjusted separately. We set five illumination conditions by using the MP illuminant. The spectral distribution of these illumination conditions had three peaks and the correlated color temperatures were 2800, 4000, 5000, 6500 and 13000 K. We arranged for another lighting equipment (the BB illuminant) having a broadband spectral distribution. Five illumination conditions were set by using it. The correlated color temperatures of the conditions using the BB illuminant were the same as those using the BB illuminant, respectively. We used the color category rating method to measure color appearance [2]. Observers answered color appearance of a chip by selecting up to three colors out of eleven basic color terms (red, orange, yellow, green, blue, purple, pink, brown, white, black and gray) and assigned a weighting score to each of the selected colors to make a total of 10.

The result shows that the degrees of color constancy are the same for all color chips under the BB illuminant, but they vary greatly for each color chips under the MP illuminant. For some color chips, color constancy works better under the MP illuminant than under the BB illuminant. It is worth investigating effects of the number of peaks in the spectral distribution on appearance of colors in future study.

INTRODUCTION

Today white LED light sources have been widely used in our living environment. LEDs have higher luminous efficiency and longer life than conventional light sources. Color-tunable LEDs have been put into practical use. RGB-LED light sources using red, blue and green LEDs can change the light source color.

The spectral distribution of typical white LEDs includes narrow peaks. The narrow peaks in the spectral distribution should influence perceived appearance of surface colors. In this study we were interested in effects of peaky spectral distribution of LED light sources on color constancy. When a color of an illuminant having multiple peaks in the spectral distribution is changed, the chromaticity of a surface under the illuminant would be changed in a different way from that when an illuminant having a broadband spectral distribution is changed in the same way. We considered that this should affect color constancy.

METHODS

Subjects looked at color chips in an experimental box and answered the color appearance under several lighting conditions. Nine students participated in the experiment, all of whom had normal color vision. The dimension of the experimental box was 30 cm high, 40 cm wide, and 30 cm deep. The bottom of the box was painted gray (N5) and the wall was covered with black paper. One test chip and five surround chips were placed in the box. We selected 27 Munsell chips as test chips. The surround chips provided clues to the illuminant. They were identical for all lighting conditions.

We have prepared two light sources with different characteristics of spectral distributions. One of the light sources was composed of red, green and blue LEDs and has three peaks at approximately 450, 535 and 645 nm in the spectral distribution. We could change the color by adjusting the intensity of each LED separately. The other light source simulated daylight and had a broadband spectral distribution. The color of this light source could be changed along the blackbody locus. We referred the light sources with multiple (three) peaks in the spectral distribution as the MP illuminant and those with a broadband spectral distribution as the BB illuminant. Five correlated color temperatures (T_{cp}) were set for each illuminant: 2800K, 4000K, 5000K, 6500K, and 13000K. The experiment used 10 lighting conditions. Figure 1 shows the spectral distribution of the lighting conditions. The illuminance was set to 200 lx at the position of the test chip.

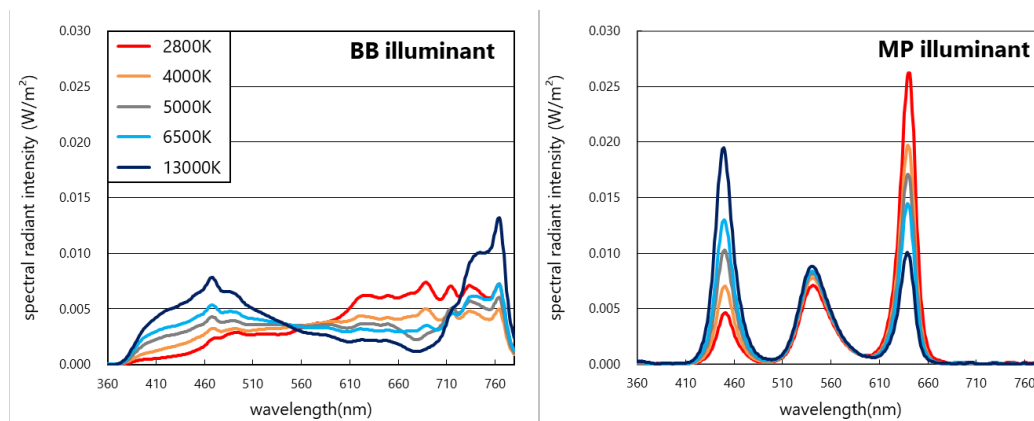


Figure 1. Spectral Distribution of the Lighting Conditions

We used the categorical rating method to measure color appearance [2]. The observers answered color appearance of a chip by selecting up to three colors out of eleven basic color terms (red, orange, yellow, green, blue, purple, pink, brown, white, black and gray) and assigned a weighting score to each of the selected colors to make a total of 10.

One session was composed of 6 blocks, and one block was composed of 9 trials. One block corresponded to one lighting condition. Before starting a block, the subjects adapted to the BB 5000K lighting condition for 60 seconds and then adapted to the test lighting condition for 60 seconds. The second adaptation was skipped when the test lighting condition was the BB 5000K condition. In each trial, they observed the test color chip for 30 seconds and evaluated the color appearance of the test chip. Each of the subjects participated in 5 sessions and performed 270 trials.

RESULTS

The results of color categorical rating for the test chips were summarized in Figure 2. We can see from this figure how the color appearance of each of the test chips changed with T_{cp} of the BB illuminant and the MP illuminant. Our main concern here is differences of the color appearance between the BB illuminant and the MP illuminant. Some color chips, for example, color chips of BG hue, the MP illuminant has a higher “green” score.

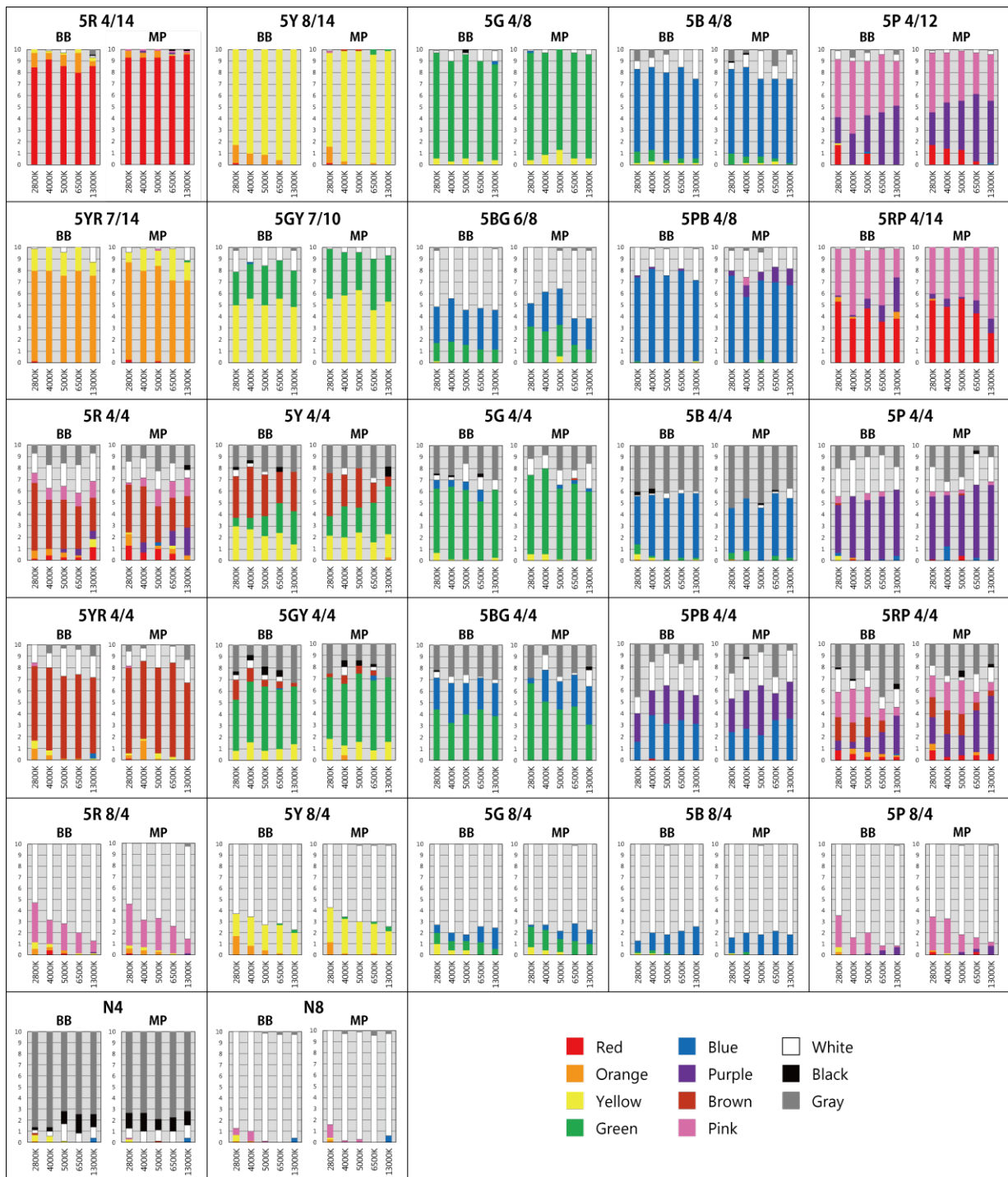


Figure 2. The Results of Color Categorical Rating for the Color Chips

DISCUSSION

To evaluate color constancy quantitatively, we first confirmed how much the chromaticity of a color chip was shifted with the change of T_{cp} under each illuminant. Figure 3 shows shifts of chromaticity of the color chips plotted on CIE u'v' diagram. A series of five points connected by a line presents

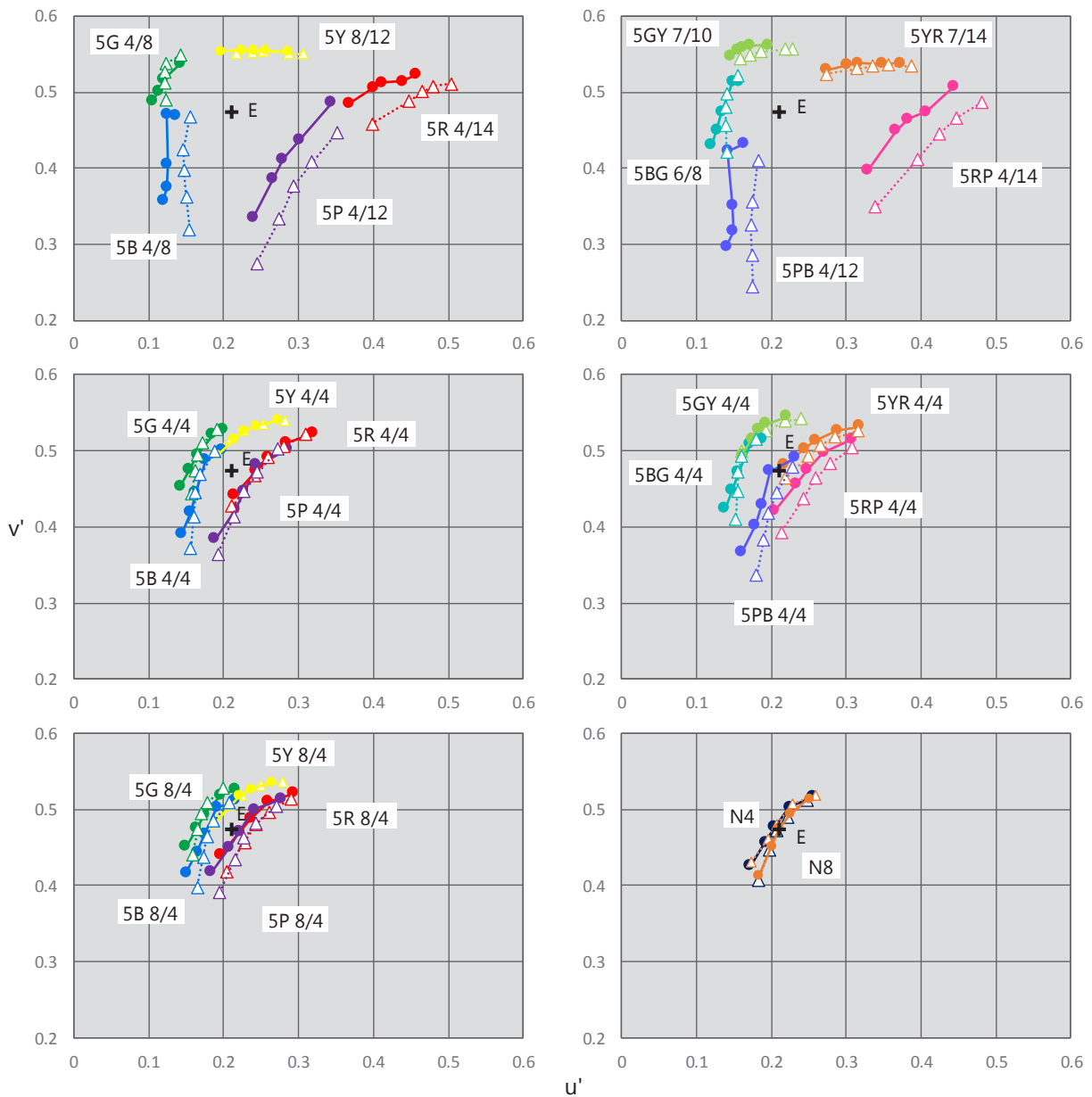


Figure 3. The Chromaticity of the Color Chips on the CIE $u'v'$ Diagram

the chromaticity points of the same color chips under five T_{cp} conditions of the illuminants. The filled circles and the solid lines represent the chromaticity under the BB illuminant, and the open triangles and the dashed lines represent the chromaticity under the MP illuminant.

Next, we transformed the color category rating data obtained in the experiment to elemental colors. Table 1 shows regression coefficients to predict elemental colors from color category rating data [2].

This conversion makes it possible to plot color appearance of the color chips on the coordinate plane with the R-G component on the horizontal axis and the Y-B component on the vertical axis. We focused on the distance between the point representing the color appearance under a given condition and the point representing the color appearance under the 5000K condition of the same illuminant. Hereafter we referred this distance as a color appearance shift. Figure 4 shows the average color appearance of all subjects. The colored circles represent the color appearance under a given

Table 1: Regression Coefficients to Predict Elemental Colors from Color Category Ratings

Elemental color	Color category										
	R	Or	Y	G	B	P	Pk	Bn	W	N	Bk
Red	0.924	0.528	-0.037	-0.006	-0.007	0.334	0.732	0.292	0.016	-0.007	-0.033
Green	0.010	-0.013	0.007	0.847	0.004	-0.007	-0.017	0.019	0.022	0.022	-0.145
Yellow	-0.022	0.407	0.872	-0.012	-0.009	-0.001	-0.003	0.188	0.007	0.016	-0.034
Blue	-0.027	-0.013	-0.030	0.030	0.920	0.468	0.009	0.012	0.022	0.006	-0.060
White	0.033	0.047	0.139	0.045	0.015	0.055	0.226	0.070	0.939	0.512	-0.134
Black	0.083	0.044	0.050	0.099	0.083	0.150	0.053	0.421	-0.008	0.449	1.395

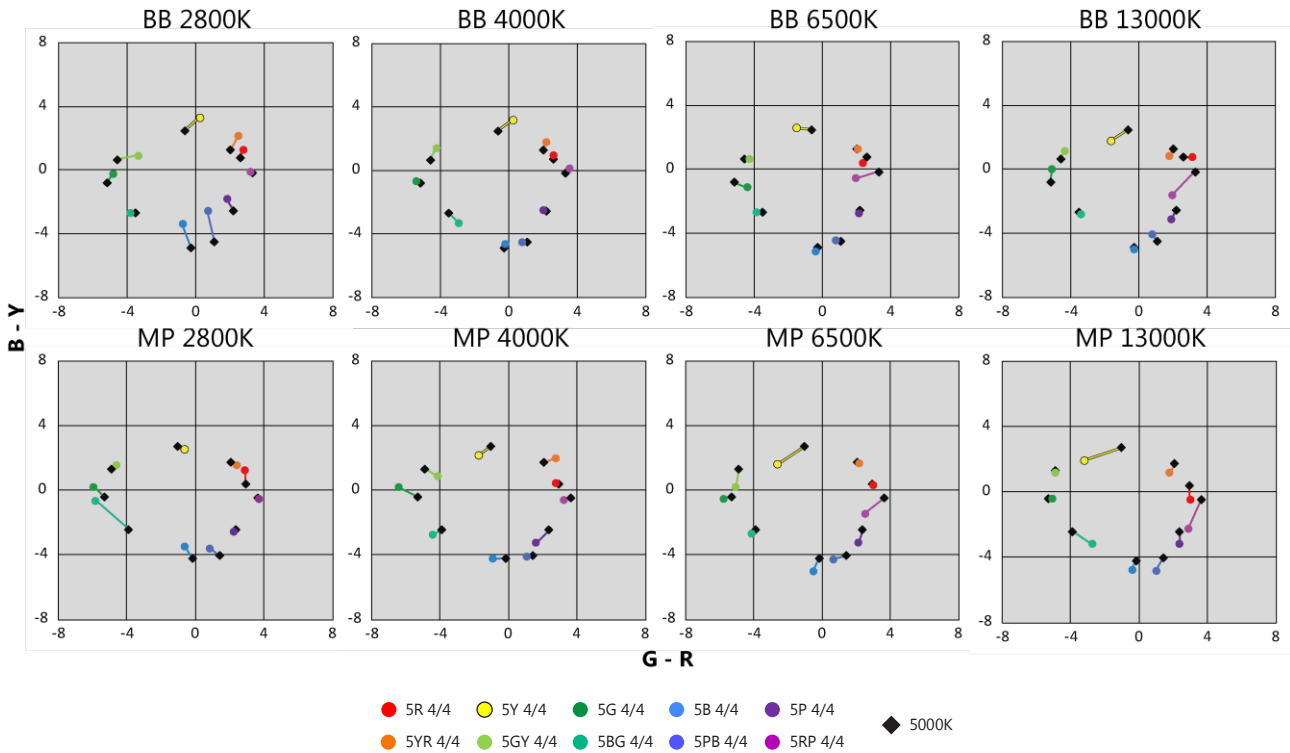


Figure 4. The Color Appearance of the Low-value and Low-Chroma Color Chips on the R-G / Y-B Diagram

condition, and the black diamonds represent the color appearance under the 5000K condition. The color appearance shift of 5BG 4/4 is comparatively large.

We introduced an index for color constancy. For each series of the chromaticity shift shown in Figure 3, we calculated the distances between the chromaticity points under the 5000K condition and the chromaticity points under the other T_{cp} condition. We defined the maximum distance within a series of chromaticity shift as the chromaticity shift index ΔE_{wv} . This index could denote physical changes of the color of the chips. We also defined an index showing perceived color changes. The color appearance shift index ΔE_{app} was defined in the same way by calculating the maximum distance on R-G, Y-B coordinate shown in Figure 4. Using these two indices, we defined the color constancy index (CCI) as follows.

$$CCI = \frac{\Delta E_{app}}{\Delta E_{wv}} \quad (1)$$

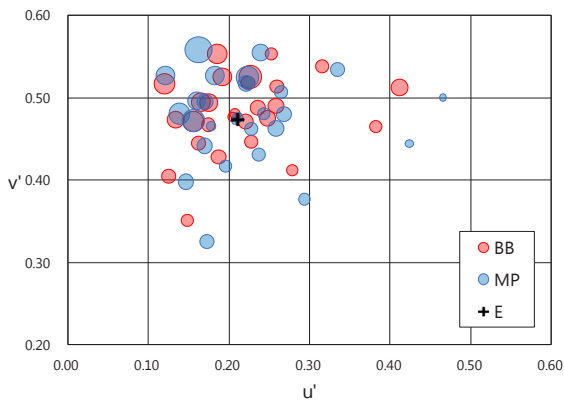


Figure 5. The CCI under the BB and the MP Illuminants

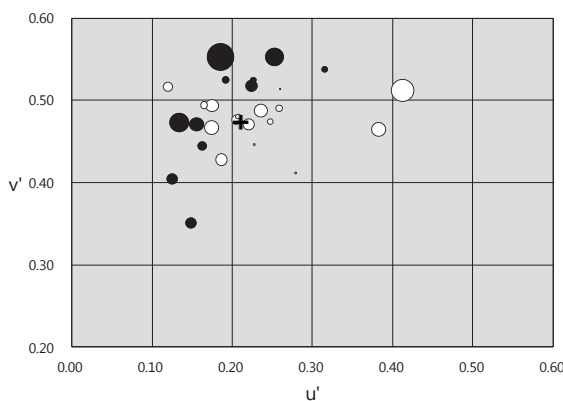


Figure 7. The Difference between the CCIs under the BB and the MP Illuminants

MP illuminant was 21.6 and that under the BB illuminant was 14.4.

Figure 7 shows the difference between the CCI under the BB illuminant and that under the MP illuminant. The circle is painted black if the CCI under the MP illuminant is larger than that under the BB illuminant, and vice versa. For high-saturation color chips of Y, GY, BG, and B hues, the CCI under the MP illuminant is larger (black circles), indicating color constancy was not functioning well under the MP illuminant. The properties of multiple peak spectral distributions such as the number of peaks, peak wavelength, must influence perceiving color appearance with changing color of lighting.

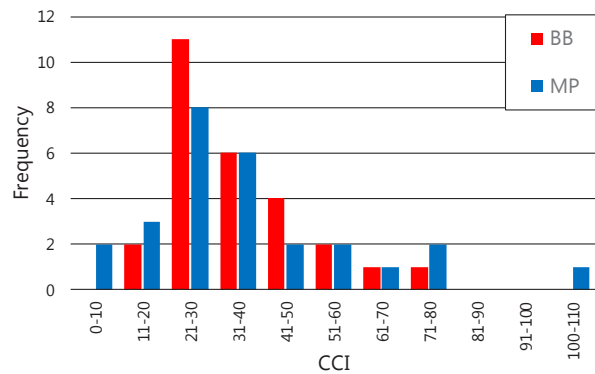


Figure 6. The Histogram of the CCIs under the BB and the MP Illuminants

Smaller CCI means that color constancy works better. Figure 5 shows the CCIs of 27 color chips. The coordinates indicate the chromaticity of the color chips under the condition of BB 5000K, and the sizes of the circles indicate the CCI value. The red circles represent the BB illuminant and the blue circles represent the MP illuminant. The CCI is relatively larger in the upper left region, especially for the MP illuminant condition. It indicates that color constancy were degraded for colors close to green. It is interesting to note that the variation of CCI values of the MP illuminant is larger than that of the BB illuminant. This may indicate that if an illuminant having peaky spectral distribution is used, appearance of colors in some regions of a color space change significantly with changes in T_{cp} of the illuminant. Figure 6 shows the CCI distribution as a histogram. The standard deviation of CCI under the

REFERENCES

1. Lucassen, M. P. and Walraven, J. (1996). Color Constancy under Natural and Artificial Illumination. *Vision Research*, 37(17), 2699-2711.
2. Ishida, T., Yamauchi, Y., Nagai, T., Kurimoto, H., Shoji, Y. and Tajima, T. (2015). Evaluation of color appearance under LED and OLED lighting based on the data obtained by a new color category rating method. *Proceedings of Midterm Meeting of the International Colour Association*, 1158-1163
3. Ma, R., Liao, N., Yan, P. and Shinomori, K. (2018). Categorical color constancy under RGB-LED light sources. *Color Research & Application*, 43, 655-674

EFFECT OF HAZE VALUE AND MATERIALS ON THE COLOR APPEARANCE IN THE TISSUE EXPERIMENT OF THE SIMULTANEOUS COLOR CONTRAST

Supattra Jinphol^{1*}, Mitsuo Ikeda¹, Chanprapha Phuangsuan¹, Yoko Mizokami²

¹*Color Research Center, Faculty of Mass Communication Technology, Rajamangala University of Technology Thanyaburi, Thailand.*

²*Graduate School of Engineering, Chiba University, Japan.*

*Corresponding author: Supattra Jinphol, 11591080200077@mail.rmutt.ac.th, supattra4762@gmail.com

Keywords: Simultaneous color contrast, paper stimuli, display stimuli, tissue, chromatic adaptation

ABSTRACT

A stimulus of the simultaneous color contrast is a small gray patch surrounded by a color. When the stimulus is made by a paper the gray patch does not give a vivid color. But when we observe the stimulus through a paper tissue the phenomenon is enhanced and the gray patch presents a vivid complementary color to the surrounding color. In this report various materials such as a tissue, ground glass and fabrics were employed and the effect to the simultaneous color contrast was investigated. There was found no effect of materials. The effect increased for higher haze value of the cover sheet to HV 80, beyond which it started to decrease. The effect was measured for display stimuli. When the stimulus on a display was observed through a tissue the color of the gray patch became more vivid than the color seen on paper stimuli through a tissue.

INTRODUCTION

When a gray patch is surrounded by a color, the patch appears roughly opposite color of the surrounding color, which is called the simultaneous color contrast SCC phenomenon. When the pattern is made of printed papers the phenomenon is not strong and the central gray remains gray if not colored. It was pointed out in text books [1][2] that if the pattern is covered by a white tissue the phenomenon becomes evident and the color of the gray patch appears vivid. No quantitative description is not given in these text books and we thought it worthwhile to investigate quantitatively the effect of tissue by using the elementary color naming method. It is considered that the effect of tissue is the effect of scattering light from the surface. The properties expressed by the haze value. If the haze value of the tissue is changed the effect of SCC is expected to change. In this report the haze value of the tissue is changed by adopting number of sheets and the SCC is measured for them. We are interested if different materials beside tissue may give different effect and some appropriate materials will be investigated for the SCC.

STIMULI

To obtain different haze value of cover sheets, commercially available sheets of various materials were collected, tissue papers of 5 different brands, 4 different fabrics including silk, and a ground glass of 5 mm thickness. Tissues of different brands did not show difference in HV and we employed only one of them in the experiment. Fig. 1 shows HV of different materials. Along the abscissa number of sheets of tissue and silk fabric is taken and along the ordinate the HV. A tissue had HV of over 80 with one sheet, much higher than HV of a silk fabric. It became equivalent to that of one tissue when 5 sheets were overlaid. Other materials, a ground glass, a Toray fabric, and a lining fabric gave a similar HV as one sheet of tissue as shown by symbols, \diamond , * and Δ , respectively.

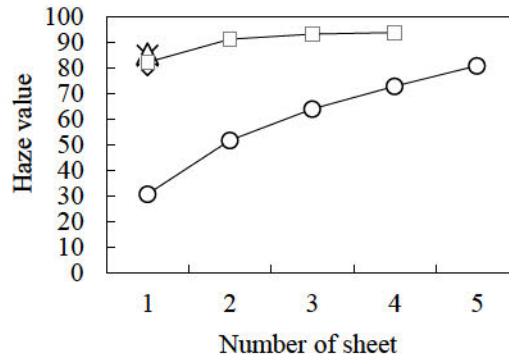


Figure 1 Haze value of cover sheet for different number of sheets. Symbols indicate materials, ○, silk fabric, □, tissue, ◇, ground glass, △, lining fabric, and *, Toray fabric.

SCC stimuli were made of printed papers of four colors and of the size 23x23 cm². At the center a gray patch of Mussel Value of about N5 of the size 3 x 3 cm² was pasted. The four colors of the surround were red, yellow, green, and blue and their chromaticities are shown by open circles in Fig. 2. A cross indicates the chromaticity of the central gray test patch. Their values are listed on Table 1 including L*, a* and b*. Small filled circles indicate surround colors with one tissue and their colors are very much desaturated coming close to a white. Open squares are chromaticities of four colors when they are presented on a display, which is employed in Experiment 2. Those paper test stimuli were placed on a table in a room lit with ceiling fluorescent lamps of the daylight type. On the table the illuminance was 1116 lx.

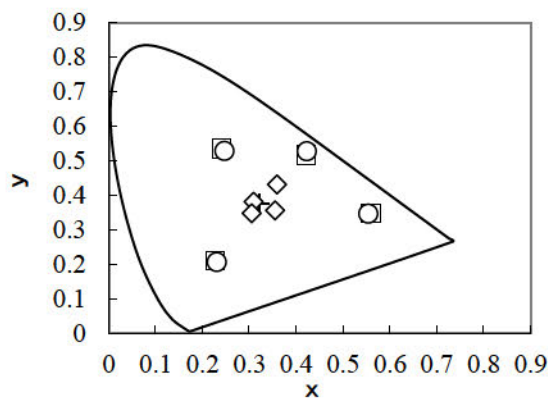


Figure 2. Chromaticities of four colors of surround in Experiment 1 (○), in Experiment 2 (□), ◇ shows paper stimuli with a tissue and cross shows a white color of tissue.

Table 1: Color specifications

Color	Y	x	y	L*	a*	b*
R	63.4	0.554	0.346	41.02	62.56	45.88
Y	166	0.423	0.527	86.27	-14.9	90.19
G	36.7	0.247	0.528	44.61	-72.22	30.07
B	13.5	0.231	0.206	19.9	24.84	-43.18
Test	53.4	0.315	0.364	59.31	-0.09	0.62

Experiment 1

In this experiment paper stimuli were investigated. Three subjects participated in the experiment. When a subject entered the experimental booth, he/she was presented a test stimulus with a cover sheet. He / She judged the color of the gray test patch by the elementary color naming method, namely amounts of chromaticness, whiteness, and blackness in percentage. If there was chromaticness he/she judged amounts of unique hues in percentage. After the judgment another cover sheet was given. This process was continued until all the cover sheets, 13 sheets altogether, were investigated. In the case of the frosted glass, only the frosted surface up was investigated.

RESULTS

Results of Experiment 1

Results are shown in Fig. 3 for the subject SJ for four surrounding colors. The abscissa gives HV and the ordinate the amount of chromaticness after the elementary color naming. Each point is the average of three repetitions. An open circle at HV=0 was given without a cover sheet, namely a direct observation of the test patch. The amount of chromaticness was 12 %. Filled circles are from silk fabric and open diamonds are from tissue. One tissue had HV of about 80 and the subject observed 23% of chromaticness for red surrounding, 33 % for yellow, 20 % for green, and 20 % for blue. They were all higher value compared to 12% of the direct observation of the test patch. Fig. 4 shows results of another subject SC. In her case the amount of chromaticness was not significantly larger than that of the direct observation for red and green surroundings, but it was larger for yellow and blue surroundings.

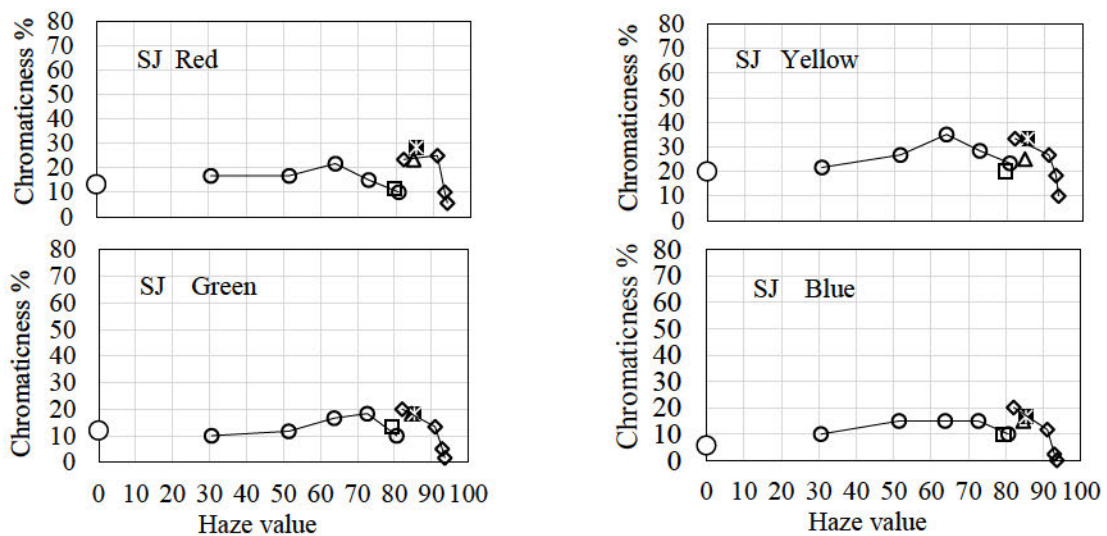
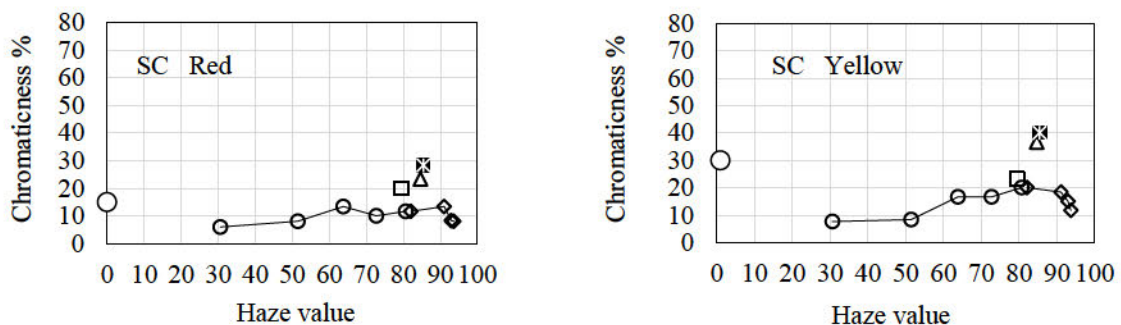


Figure 3. Amount of chromaticness plotted for HV of different materials judged by the subject SJ.



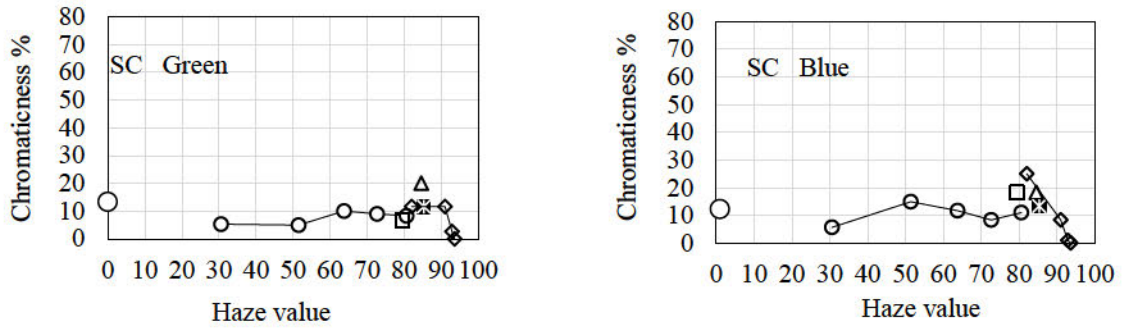


Figure 4. *ibid.* but for the subject SC.

Fig. 5 gives the average of three subjects. Open circles are from silk fabric and open triangles are from tissue. By observing both curves we may say that the increase of HV induced more chromaticness but the results from tissue indicate the amount of chromaticnes begins to reduce at HV of 80.

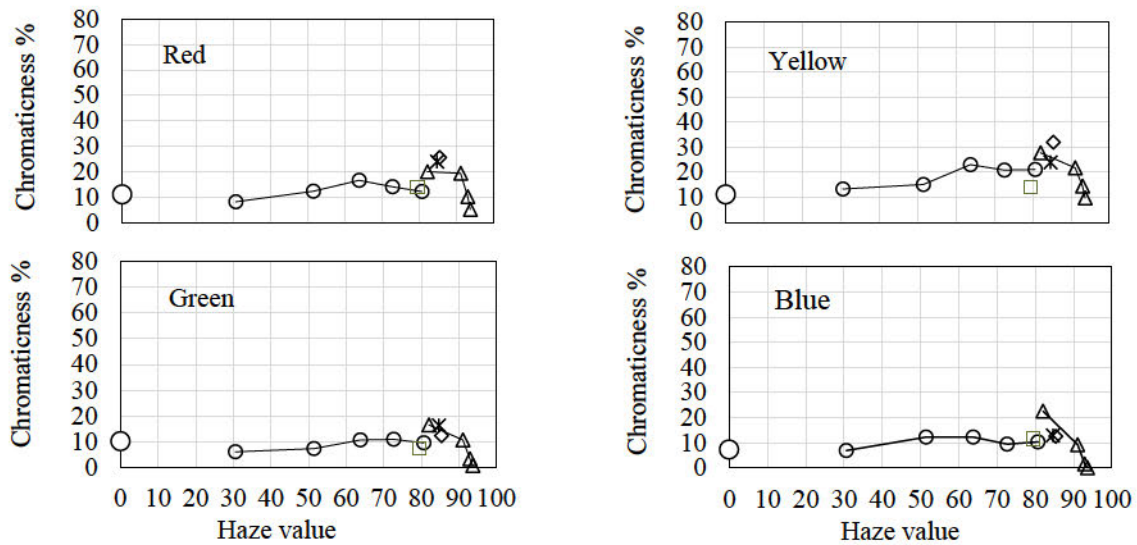
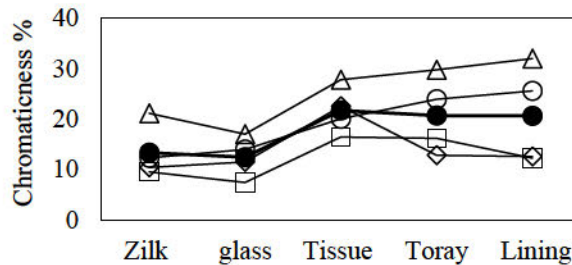


Figure 5. Averaged amount of chromaticness of three subjects plotted for HV.

Different material gave different effect on the SCC. The amounts of chromaticnes at around 80 are taken from Fig. 5 and shown in Fig. 6 for different materials. Symbols indicate the color of surrounds, \circ , red; Δ , yellow; \square , green; \diamond , blue. Solid circles with a thick lines are the verge. Tissue cover seems to give the strongest effect for the SCC phenomenon. The effect is rather small with silk and ground glass.



Figurer 6. Amount of chromaticness for different materials of HV 80.

EXPERIMENT 2

In this experiment a display is used to present the SCC stimulus and the experiment was carried out at Chiba University, Japan and Rajamangala University of Technology Thanyaburi RMUTT as one of the authors SJ of MUTT stayed at Chiba U to do internship.

Experiment 2

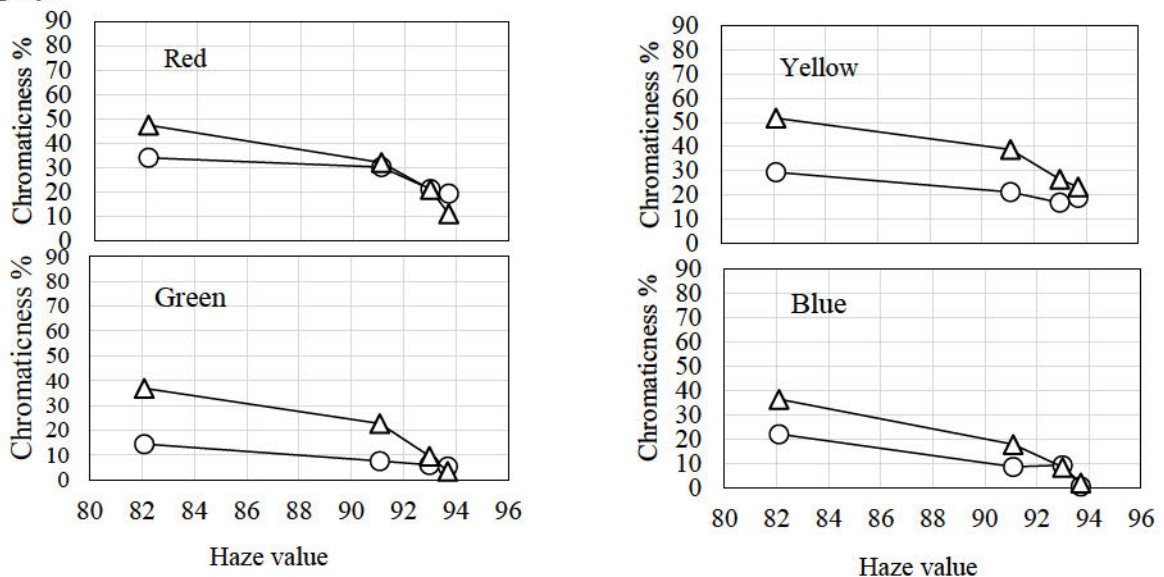
The same colors, red, yellow, green, and blue were employed which were made same as Experiment 1. Their chromaticities were shown by open squares in Fig. 1. The chromaticity points completely overlap with those at RMUTT (○). The display was EIZO.

In Chiba experiment surrounding colors of display were made same as paper stimuli with tissue of different number. To do this the colors of paper stimuli with different number of tissue were measured. At each presentation of SCC stimulus on display subjects adapted for 1 minute before judging color appearance. Five subjects, two Japanese and three Thai participated in the experiment. Each subject repeated for five times of judgment.

In RMUTT experiment colors and shape of paper stimuli were reproduced on a display and the color judgment was made for tissues overlaid on the display. The display was laid down horizontally to make the observing condition exactly same as for the paper experiment. No adaptation time was given. Three Thai students participated in the experiment and the judgment was repeated for three times in both display and in paper experiment.

RESULTS OF EXPERIMENT 2

Results of Chiba U are shown in Fig. 7. Along the abscissa HV is taken and along the ordinate the amount of chromaticness is taken. Results of display are indicated by open circles and those of paper stimulus by open triangles. For all the colors of surround the chromaticness was larger with display.



Figurer 7. Amount of chromaticness for different HV with display stimuli (○) and paper stimuli (Δ). Data obtained at Chiba U.

Results of RMUTT are shown in Fig. 8. On the contrary to Chiba results chromaticness was larger with display.

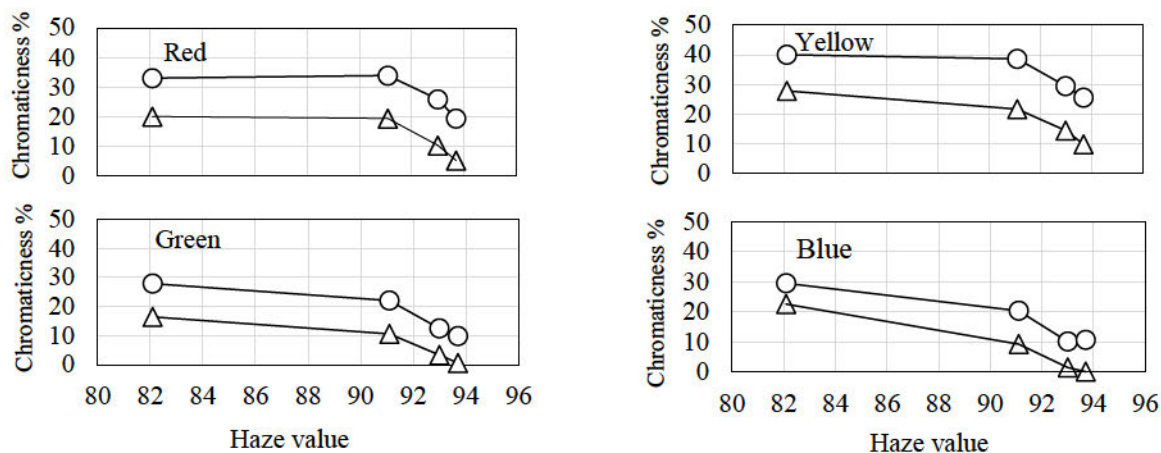


Figure 8. Amount of chromaticness for different HV with display stimuli (○) and paper stimuli (△). Data obtained at RMUTT.

CONCLUSION AND DISCUSSION

Amount of chromaticness gradually increased with increase of HV of tissue when the color appearance of the central gray patch surrounded by some color was measured by the elementary color naming method. The increase stopped at around HV=80, beyond which the amount rapidly decreased. Different materials were employed as a cover sheet, but no significant difference was found for the SCC phenomenon.

Paper stimuli and display stimuli were compared for the effect of SCC. Results of Chiba University showed larger chromaticness with paper stimuli than the display stimuli. Stimuli on the display were made same with paper stimuli with tissue in color but the appearance of the shape of the test patch was not made same. While it is blurred in the paper stimuli it remained sharp in the display stimuli. Graham and Brown²⁾ pointed out that the fact that a tissue obscures contours as well as to reduce saturation and evidence of texture may increase the vividness of the induced color. This explanation may apply to the difference of the results between two universities. In the case of RMUTT subjects noticed the stimuli appeared brighter with display. This might cause the chromatic adaptation to surrounding color worked stronger than the paper stimuli.

ACKNOWLEDGEMENT

Suppattra Jinphol thanks RMUTT for giving her the Co-operative Education, Rajamangala University of Technology Thanyaburi scholarship that made her to spend at Chiba University for 3 months to carry out internship. Also thanks students at Prof Mizokami's laboratory at Chiba University who helped her experiment and for serving subjects.

REFERENCES

1. Parsons, J H (1924). *An introduction to the study of color vision*. 2nd ed. 139. Cambridge Press
2. Graham, C H. and Brown, J L, John Wiley & Sons. (1965). *Vision and visual perception*, Chapter 16 "Color contrast and color appearance: Brightness constancy and color constancy" p.461.

EFFECT OF VIEWING DISTANCE TO THE SIMULTANEOUS COLOR CONTRAST

Piyamon Nguensawat^{1*}, Mitsuo Ikeda¹, Chanprapha Phuangsuan¹, Yoko Mizokami²

¹ *Color Research Center, Faculty of Mass Communication Technology, Rajamangala University of Technology Thanyaburi, Thailand.*

² *Graduate School of Engineering, Chiba University, Japan.*

*Corresponding author: Piyamon Nguensawat, 1159108020622@mail.rmutt.ac.th, nammon.png@gmail.com

Keywords: Simultaneous color contrast, Visual angle, Recognized visual space of illumination, Chromatic adaptation

ABSTRACT

When a small gray patch is surrounded by a colored field the patch appears a color roughly complementary to the surrounding color. This is a phenomenon called the simultaneous color contrast SCC. When the stimulus pattern is made of a paper the phenomenon is quite small. In the present research the visual field size for the SCC stimulus was extremely enlarged by making the stimulus horizontally curved and the color appearance of the gray patch was measured by the elementary color naming method for different observing distance. The vividness of the color of the gray patch increased for shorter distance to confirm the prediction based on the concept of recognized visual space of illumination RVSI [1] but partly. Even in the case of the shortest viewing distance the amount of chromaticness did not significantly increase.

INTRODUCTION

Chromatic adaptation is a popular subject in the study of color vision and the concept of recognized visual space of illumination RVSI proposed by Ikeda asserts that the human visual system adapts to the illumination color of the space where the observer stays and not to the object color that he/she is looking at [1]. Thus, the effect of the simultaneous color contrast SCC is not strong on a printed paper as the observer recognizes an object for the paper and hardly recognizes the illumination on the paper. If, however, the SCC pattern occupies a large area of the retina it becomes hard for the observer to recognize the pattern as an object. Then, the adaptation to illumination that is transferred from the object color should become apparent and the effect of SCC should become large. In the present experiment a paper pattern of SCC is presented as to make an arc with convex toward a subject to delete the recognition for an object and emphasize recognition of illumination. If the viewing distance becomes very short so that the eyes come inside the arc of the stimulus the subject cannot recognize the edges of the stimulus. An object appearance is composed of two, one is its shape or contours and the other is the color or light filling in the contours. If the subject cannot see the edges he/she only recognizes color or light and the color appearance of the central gray patch should become vivid. The color appearance was measured as a function of the viewing distance by the elementary color naming method.

EXPERIMENT

Four colored papers, red, yellow, green, and blue of which size was 66 cm wide and 52.5 cm high were held at a frame to serve a SCC stimulus as shown by a thick semicircle line in Fig. 1. The radius of the circle was 22 cm. A subject S stood in front of the stimulus at distance d from the gray test

patch T. The visual angle of the stimulus for the subject was determined by the opening size of the semicircle indicated by a dotted line (44 cm) and the viewing distance.

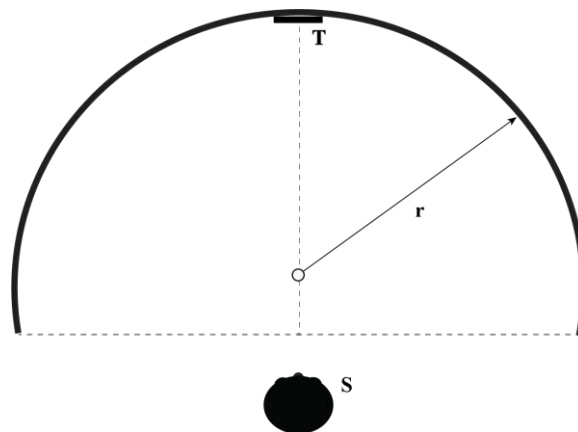


Figure 1. Experimental arrangement seen from above.

Relation of the viewing distance to the visual angle is shown in Fig. 2. It becomes more than 180° when the eyes come close to the test patch. At 27 cm both edges of the stimulus disappeared from the subject's visual field.

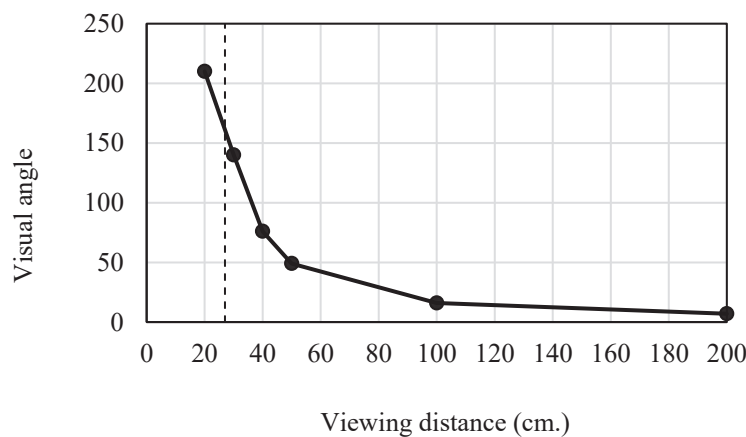


Figure 2. Visual angle-viewing distance relation.

The SCC stimulus was illuminated by two fluorescent lamps of the daylight type placed at upper position of the stimulus the ceiling lamps of the same type of fluorescent was lit during the experiment. The vertical plane illuminance at the test patch was 667 lx. Under this illumination the chromaticities of the gray test patch were $x=.323$ and $y=.352$, which is indicated by a cross in Fig. 3. Its illuminance was 57 cd/m^2 . Chromatic points of four surroundings are shown by open circles. Their luminance was 41, 138, 33, and 27 cd/m^2 , respectively for red, yellow, green and blue.

Three subjects participated in the experiment. The subjects' task was to judge the color of the test patch by the elementary color naming method by using two eyes. The viewing distance was randomly chosen from dashed line indicates the visual and the vertical 20, 30, 40, 50, 100, and 200 cm. When a subject saw the test patch its color appearance sometime changed gradually. In such case the subject was instructed to wait until the appearance became stable. This particularly happened at very short viewing distances such as 2 and 3 cm. In such case the adapting time became one or two minutes.

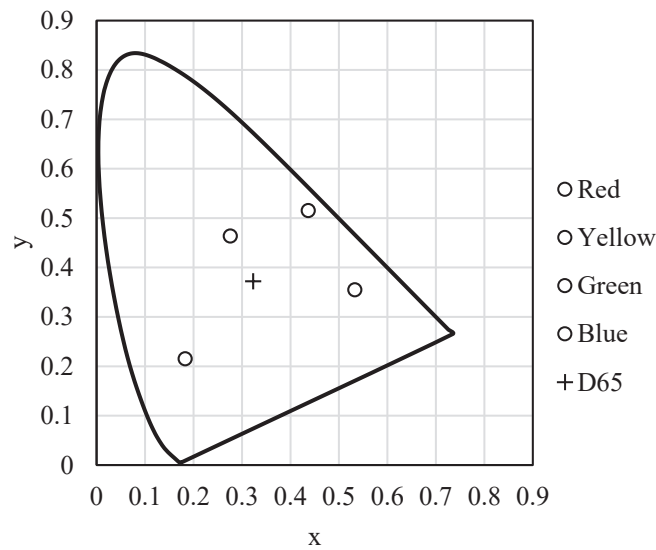


Figure 3. Chromaticities of red, yellow, green and blue surrounds, shown by open circles, and of gray test patch shown by a cross.

RESULTS

Results are shown in Fig. 4 for all three subjects, PN, SJ, and MI. They repeated the judgement for 8, 7, and 6 times. There were 4 months past from the first experiment to the last experiment. The abscissa gives the visual angle in degrees and the ordinate the amount of chromaticness in %. The vertical dashed line indicate the visual angle beyond which subjects could not see edges of the SCC stimulus. Colors of the stimulus were indicated by different symbols, circles for red, triangles for yellow, squares for green, and diamonds for blue. Each subject showed small amount of chromaticness at the viewing distance 200 cm and rapid increase for 100 cm distance. After that a gradual increase was observed. But there are difference observed among individuals. The subjects SJ and MI did not see or only small amount of color on the test patch at 200 cm, implying no simultaneous color contrast for any color of surrounding, while the subject PN could see a large amount of color at the viewing distance, especially for the yellow surrounding. She experienced a strong simultaneous contrast phenomenon for the yellow surrounding for all the viewing distances. In her case the phenomenon was weak for the blue surrounding. MI did not see any color for the blue surrounding and the amount of chromaticness was zero for all the viewing distance.

Fig. 5 gives the average of the three subjects shown in Fig. 4. All the colors showed a similar shape of curve, a rather rapid increase at small visual angle and a gradual increase up to the largest visual angle employed. The SCC phenomenon was strongest for the yellow surrounding and smallest for the blue surrounding. It is seen in Fig. 5 that any sudden change of chromaticness amount was observed at the visual angle shown by a dashed line.

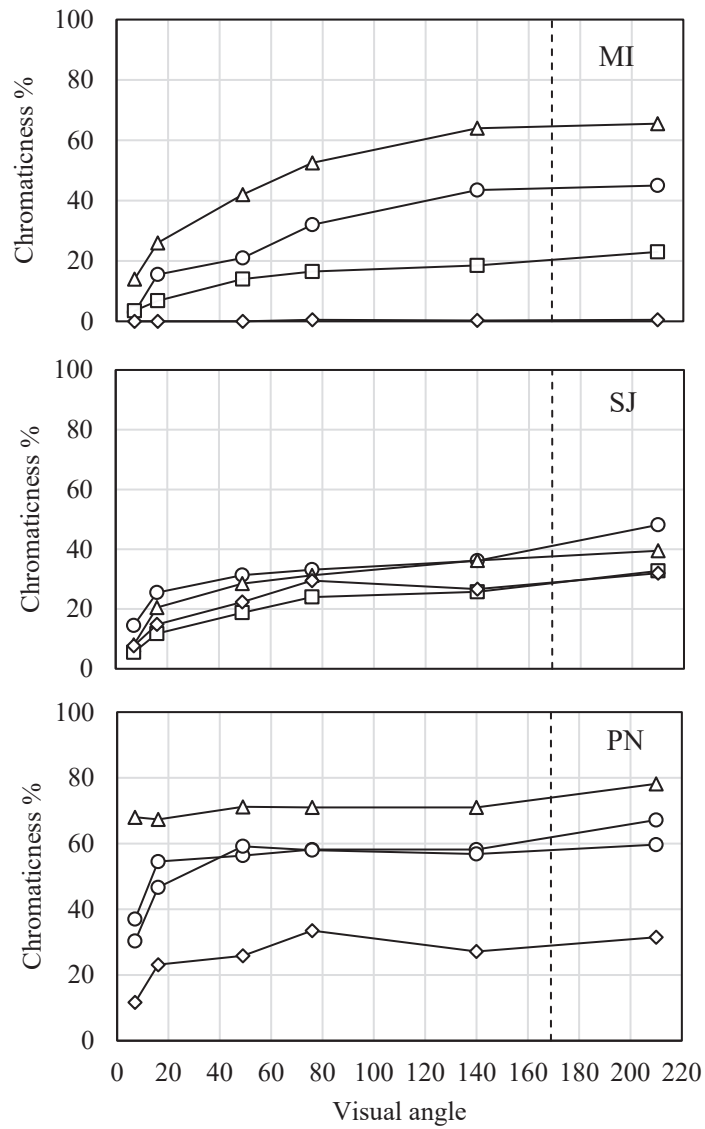


Figure 4. Amount of chromaticness plotted for viewing visual angle for three subjects○, red surround;△, yellow;□, green;◇, blue.

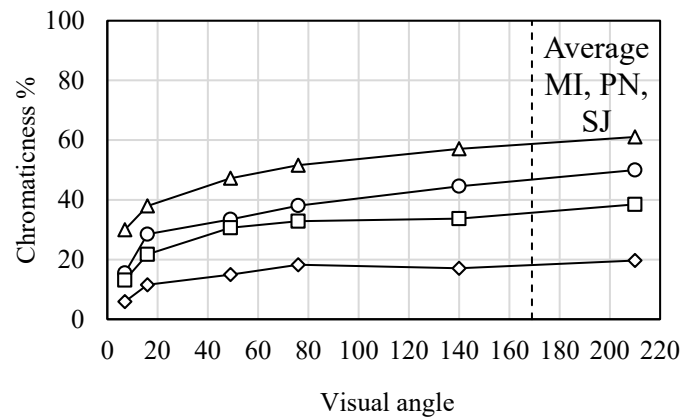


Figure 5. Average of chromaticness amount plotted for viewing visual angle.

The apparent hue of the induced test patch color was obtained by the amounts of red, yellow, green, and blue unique colors and it can be shown on a polar diagram used in the opponent colors theory. Fig. 6 shows the average of three subjects of the apparent hue of the surrounding (open symbols) and the apparent hue of the test patch (filled symbols). The angle from the red axis in the anticlockwise direction gives the apparent hue angle and the distance from the origin to a point shows the amount of chromaticness, the circumference showing 100 % of chromaticness. Surrounding colors were almost unique red, yellow, green, and blue as seen by their points almost on the horizontal and vertical axes. The induced color by the red surrounding was greenish blue or cyan, which is not green, the opponent color to the red as already confirmed [2]. This indicates that the SCC does not follow the opponent colors theory. It is true with the green surrounding, which induced blueish red color to the test patch. Yellow and blue surroundings gave the test patch almost opponent colors, blue and yellow, respectively.

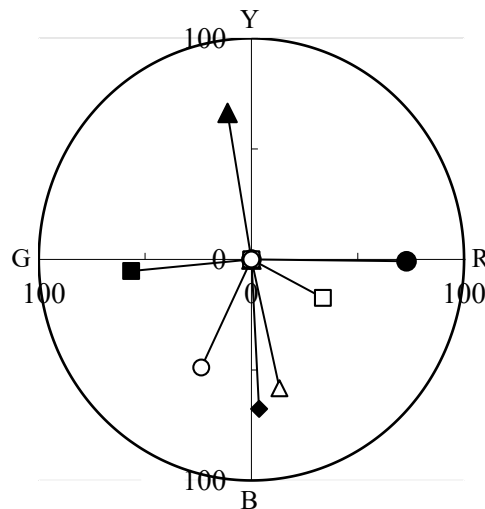


Figure 6. Apparent hue of surrounds (filled symbols) and the corresponding test patch (open symbols) plotted in a polar diagram.

DISCUSSION AND CONCLUSION

The simultaneous color contrast phenomenon became larger for shorter viewing distance, namely for larger visual angle. This is in accordance with the concept of the recognized visual space of illumination RVSI proposed by Ikeda, which insists that the chromatic adaptation takes place to the illumination not to the color of object [1]. In the SCC the illumination comes from the color of the surrounding. The surround is composed of a shape or contours or outlines and color or light. If the former recognition is reduced the remained is the color or light and a subject get larger chromatic adaptation. When the viewing distance was extremely shortened as the visual angle exceeded to extinguish the edges of the stimulus this situation should occur and the SCC phenomenon becomes very strong. Fig. 5, however, did not indicate the expectation as the chromaticness mount did not significantly increase beyond the dashed line.

ACKNOWLEDGEMENT

Piyamon Nguensawat thanks RMUTT for giving her the scholarships, the student development foundation of RMUTT that made her to spend at Chiba University for 3 months to carry out internship. Also thanks students at Prof Mizokami's laboratory at Chiba University who helped her experiment and for serving subjects.

REFERENCES

1. Ikeda M. (2004). Color appearance explained, predicted and confirmed by the concept of recognized visual space of illumination. *Opt. Rev.* 11, 217-225.
2. Phuangsuwan C. and Ikeda M. (2017). Chromatic adaptation to illumination investigated with adapting and adapted color. *Color. Col Res Appl.* 42, 571-579. doi.org/10.1002/col.22117

CHROMATIC ADAPTATION TO ILLUMINATION

Chanprapha Phuangsuan*

Color Research Center, Rajamangala University of Technology Thanyaburi, Thailand

*Corresponding author: Chanprapha Phuangsuan, Phuangsuan@rmutt.ac.th

Keywords: Chromatic adaptation, adapt to illumination, RVSI Theory, Devices, 2D picture

ABSTRACT

Here we like to demonstrate chromatic adaptation to illumination based on the concept of the recognized visual space of illumination RVSI developed by Ikeda. Pungrassamee et al. (2005) also showed that color appearance of achromatic patch depended on which illumination that subject adapted to. Phuangsuan et al. (2013) showed that to recognize the 3D space on 2D picture so that subject could adapt to the illumination in the 2D picture the color constancy occurred in this circumstance. Recently we demonstrate the chromatic adaptation to illumination under various devices; paper, projector, display and real scene (two-room technique). The result suggests that at projector and display show the strong chromatic adaptation almost same as in the real scene.

INTRODUCTION

It is a classical topic, “Chromatic adaptation”, which was taken up by many researchers proposing great theory in the past up to now. [1] For example, a white and a black paper under the strong sunlight reflecting a lot of light to our visual system, they are perceived white for the white paper as white and the black paper as black. Another example that is a white paper under an incandescent light, but we perceive it a white paper in spite of the yellowish light. Our visual system has ability of discount color from illumination that is called “color constancy”. The well-known Von Kries coefficient law describes the relationship between the illuminant and the human visual system sensitivity. [2] Illumination is a big factor which affects our color perception. Ikeda proposed the Recognized Visual Space of Illumination, RVSI theory [1-2] to explain how our color vision works. It emphasizes the adaptation to illumination. The theory says when a person enters to a room (space) he/she recognizes the space and understands the illumination, then adapts to illumination in the space. After that he/she perceives real color of an object. The color constancy takes place. This is an action of the brain. RVSI for the illumination is constructed. Pungrassamee also demonstrated the color appearance of a gray patch depending on which illumination he/she adapted. [3] It is a common understanding that the color constancy does not take place for a 2D photograph. Nevertheless, according to the RVSI concept there is a possibility of the color constancy in a 2D photograph. Namely if we can recognize a 3D space in the photograph, we can understand the illumination and consequently the color constancy holds. This was indeed proved by Phuangsuan by two approaches, color appearance and chromatic adaptation. [4] Currently, color vision researches normally conduct the psychophysical experiment by using self-luminous display. It is interested to know how our color vision work with the self-luminous circumstance. Phuangsuan demonstrated chromatic adaptation through simultaneous color contrast phenomenon on various devices such as paper, two-room technique, display and projector and found that the chromatic adaptation was device dependent.

EXPERIMENT

Chromatic adaptation to illumination will be described by color appearance through two-room technique and D-up viewer, second by simultaneous color contrast on various devices.

Refer to Pungrassamee's work, the color appearance was measured for a gray test patch which was placed in a test room illuminated by daylight lamps and was looked at from a subject room illuminated by one of four colored illuminations, red, yellow, green and blue, through windows of various sizes as shown in Fig. 1.



Figure 1. Front view in the subject room (left) and view of the test room under different size of windows (right) [3].

Based on the above experiment we simulated the same circumstance but, on photograph, and giving a perceived space to photograph by using D-up viewer and checked the color appearance of the gray test patch at the center of the front wall (see the left figure of Fig. 2). The experimental room was built as we called a two rooms technique or stimulus and environment independent technique. On the separating wall a window was opened to show the test patch from test patch room. The middle figure of Fig. 2 shows a different size of window from W1 to W5 and at W1 and W2 a subject could see only a gray test patch but from W3 to W5 subject gradually sees the objects in the test room. Four colors of light were adopted to illuminate the subject room and it was red, yellow, green and blue. Twenty photographs were prepared (4 color lights x 5 sizes of window). The task of subject was to judge the color of a gray test patch through the window on the front wall in the real room by elementary color naming method which judged the percentage of chromaticness, whiteness and blackness totaling 100%, and then judged the color by unique red, yellow, green and blue in percentage. The subject was asked to move out from the real room and was asked to judge the color of gray test patch in a photograph on a LCD display through a D-up viewer by the color naming method as before. The subject was asked to do the experiment five times. Five subjects who have a normal color vision participated in this experiment.

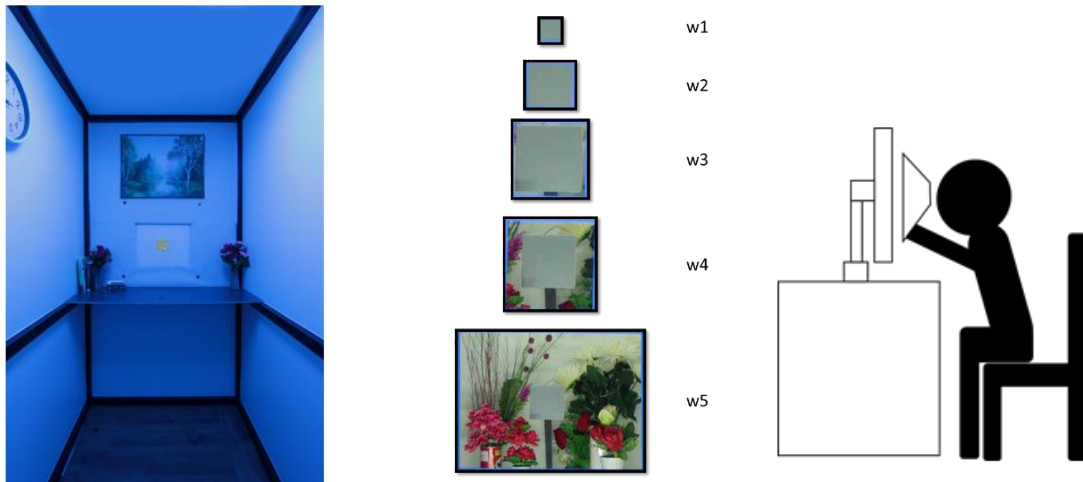


Figure 2. Front view in the subject room (left), view of the test room through different sizes of window (middle) and photograph on display observing through D-up viewer (right).

The concept of RVSI theory that says recognition of a space and adaptation to the illumination in the space is very important for the color perception. Here we demonstrate the chromatic adaptation to illumination by the phenomenon called “simultaneous color contrast” under the various devices. The most common and traditional pattern was presented on a paper as often demonstrated on textbooks, which we call object color mode experiment. The recently many researchers use display unit, with which people can manipulate stimulus pattern easily for various experimental conditions. It is possible that different devices give different data to draw different conclusions about the simultaneous color contrast. In this experiment the central gray patch was an achromatic paper of Munsell Value N6. A similar visual field was prepared with four different devices; object stimulus made of a paper covered with a tissue (Fig. 3 c) and without the tissue (Fig. 3 d), a display (Fig. 3b), a projected pattern (Fig. 3 d), and two rooms technique (Fig. 3 a). Four colors, red, yellow, green, and blue were employed for the surround and they were of a large size. We reproduced the similar colors for all the five devices. The luminance of the surround was set similar among five. In the object with tissue the color appearance of stimulus was judged with a commercially available tissue paper placed on and over the stimulus. Both object and tissue object were observed under fluorescent lamps of the daylight type as shown in Fig.3c, d. Figure 3a illustrates the two-rooms technique. The illuminance level in the test room was adjusted so that the appearance at W was the object color mode and the horizontal plane illuminance was 30 lx just in front of the gray test patch T. The subject room was illuminated by LED lamps and when it was red, for example, a stimulus pattern of the simultaneous color contrast of red surround was produced on the retina. The color appearance was judged by the elementary color naming method. When a stimulus was presented a subject adapted to the field for about one minute and judged the color appearance of the central patch, and then the surround. Four colors were pseudo-randomly presented. The judgment was done for the central test patch and for the surround. For each stimulus condition the judgment was repeated for five times on different day or time. Five subjects participated in the experiment.

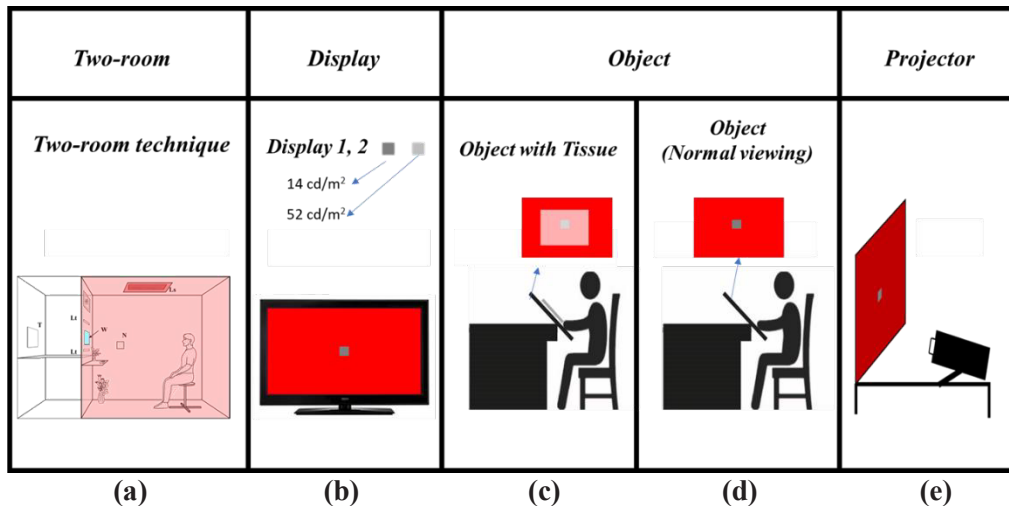


Figure 3. Different devices. a, two-rooms technique; b, display; c, object with tissue; d, object without tissue; e, projector.

RESULTS AND DISCUSSION

Pungrassamee et. al. found the color appearance of test patch was dependent on the color of illumination to which the subject adapted. The results were plotted on a polar diagram used in the opponent color theory as shown in Fig. 4. The results were under the yellow light (■) and the test patch was green color condition. The open small symbols represent the color appearance of green test patch under W1 and W2 and filled small symbols were from W3 to W5. The result showed that the color of green test patch returned to the original green when subjects could recognize the illumination in the test room. In the case of W1 and W2 subjects recognized the yellow illumination in the subject room and chromatic adaptation was working for the yellow light causing to the green test patch appeared blue color because of color constancy worked for the yellow illumination in the subject room.

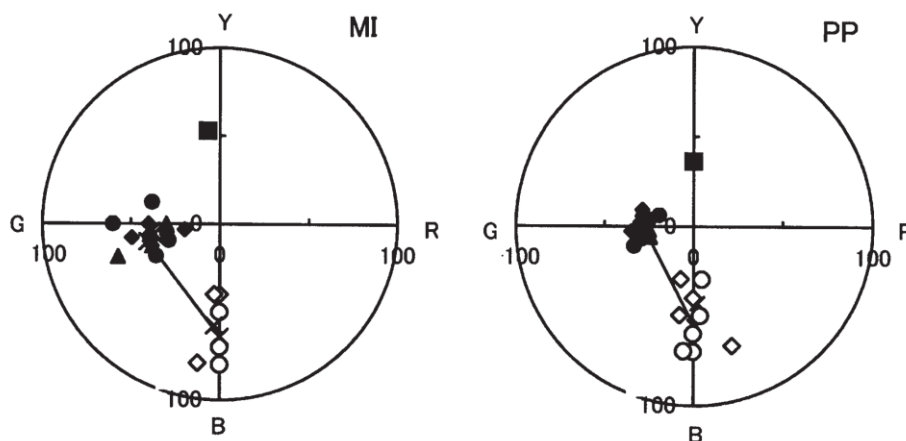


Figure 4. Example result from 2 subjects under yellow light and green color of test patch.

Figure 5 was the mean results of the gray test patch under red (■), yellow (◆), green (▲) and blue (●) lights. The polar diagram on the left most shows the results with the two-room condition, the middle shows results of D-up view condition and the right most shows results of normal view (2D) condition. Note that in the D-up view and normal view subjects observed the color of gray test patch in photographs. We found similar result as Pungrassamee in the two-room case where subjects adapted to color lights in the subject room and showed very vivid complementary color for the gray test patch for W1 and W2. The color of gray patch returned to the original at the W3 to W5. It was very interesting to confirm the prediction of RVSI theory with the D-up view experiment that the subjects could perceive a three dimensional (space) in the photographs and perceived the complementary color at gray test patch in W1 and W2 and the color almost disappeared from W3 to W5 respectively. With the normal view (2D) condition the color on the gray patch almost disappeared. The result strongly implied the chromatic adaptation to illumination was important to the color appearance of an object.

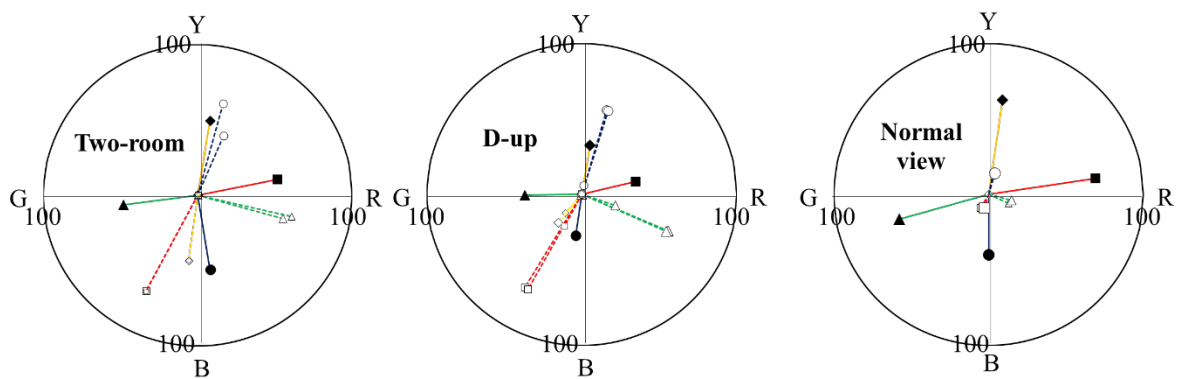


Figure 5. Mean of color appearance from W1 to W5 under red, yellow, green and blue.

The average result of chromatic adaptation to illumination through simultaneous pattern under various devices was showed in Fig. 6. Those results were the color appearance of a gray test patch which was surrounded by color red (○), yellow (△), green (□) and blue (◇). The large filled symbols were the color of surrounding. The results showed that the color of a gray test patch was complementary to the color of surrounding and it appeared the most vivid with the two-room, then display, projector, paper with tissue and paper without tissue in that order. The result suggested chromatic adaptation was working very well with devices to give light directly to the eyes like the two-rooms technique, a self-luminous display, and stimulus produced by projecting light on a white screen but not to the light reflected by an object, to which the light color belongs.

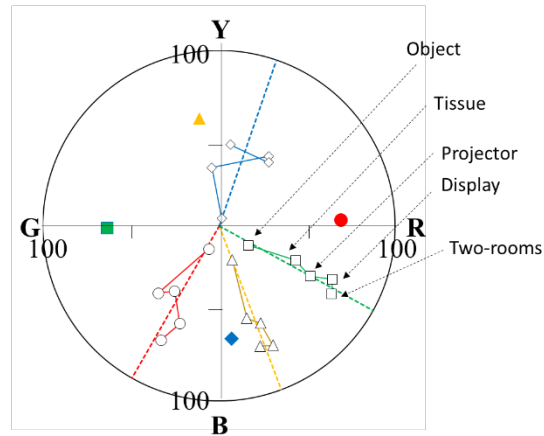


Figure 6. Averaged results of five subjects of color appearance of the central test patch for four different surrounding colors; ○, red surround; △, yellow surround, □, green surround, ◇, blue surround. Dotted lines show representative hues of respective surrounding color.

ACKNOWLEDGEMENT

I would like to thank the ACA2019 organizing committee that gave me an opportunity to give a keynote speech. Also acknowledge Prof. Ikeda for encouraging and helping me in carrying out research at Color Research Center of RMUTT.

REFERENCES

1. Fairchild, M. D. (2005). *Color Appearance Models*, 2nd Edition. England, John Wiley & Sons Ltd.
2. Foster, D. H. (2011). Color constancy. *Vision research*, 51(7), 674-700.
3. Pungrassamee, P., Ikeda, M., Katemake, P. and Hansuebsai, A. (2005). Color Appearance Determined by Recognition of Space. *Optical Review*, 12(3), 211–218.
4. Phuangsuwan, C. and Ikeda, M. (2018). Chromatic adaptation in a 2D photograph demonstrated by a D-up viewer. *Color Research and Application*, 43(4). 544-550. DOI: 10.1002/col.22214
5. Phuangsuwan, C. and Ikeda, M. (2019). Device dependent simultaneous color contrast. *Proceeding of CSAJ2019*, 43(3).

SPARKLE AND GRAININESS INDEX OF EFFECT COATING USING SPECTRAL IMAGING

Masayuki Osumi^{1*}

(Shinyokohama Bosei Bld.402, Shinyokohama 3-20-12, Kohoku-ku, Yokohama City)

¹ Office Color Science Co., Ltd., Japan.

*Corresponding author: Masayuki Osumi, masayuki-osumi@nifty.com

Keywords: Effect coating, Sparkle, Graininess, Spectral Imaging, Sphere illumination

ABSTRACT

Recent automotive exterior coatings include many types of effect pigments and apply multiplex coatings. Effect coatings have color, feel, and texture such as various sparkle and grain images related with visual perceptions depending on illumination and observation angle. In this study, a spectral imaging system was applied to measuring color and texture of effect coatings by linear lighting and diffuse lighting. It was composed of white LED illuminates, a liquid crystalline tunable filter (LCTF), and CCD imaging device with Peltier cooler and anti-blooming function. In this study, effect coating samples were used and prepared with aluminum flake and interference micas by spray application. The effect coating test panels composed of absorption pigment, aluminum flake, glass flake, and interference micas were prepared. Each panel was coated on white and black substrates. After measuring, the CIELAB color value, the spatial distribution in CIELAB color space, sparkle and graininess index were calculated. Analysis results in this study showed each value was related with characteristics of effect material. Illumination angles of linear lighting were 20, 45 and 70 degrees from normal direction, and detective direction was normal against sample, and diffuse lighting was applied integrating sphere. Sparkle index was calculated by linear lighting spectral imaging, and graininess index was calculated by diffuse lighting. The important point to note is measured panel which included interference pigment has wide distribution with all over the optimal color area. This result suggests that recent effect materials need spectral imaging measurement to get high accurate $L^*a^*b^*$ value of sparkle and grain texture. As an example, the measuring result of Xirallic Crystal Silver interference effect pigment (Merck GmbH) with FW200 carbon black pigment is shown in this study. The distribution in CIELAB color space calculated from measured spectral imaging of 20 degrees illumination was quite wide and distributed in optimal color area. Especially, Xirallic Crystal Silver has large number of color occurrence of 20 degrees illumination. Gonio-photometric spectral imaging was quite useful for evaluation of effect coatings to measure colorful sparkle index.

INTRODUCTION

Effect coating has color, feel, and texture such as various sparkle and graininess images related with visual perceptions depending on incident and observation optical geometry. On the other hand, the color matching work to reproduce effect coatings by hand is very difficult and requires high human skill in industrial processing. It is required high accurate quality control method using sparkle and graininess parameter. The main idea of evaluation is the use of combined color and imaging information by spectral imaging with various optics dimensional illumination. In this study, the sparkle index is applied to measuring texture of effect coatings by linear lighting and the graininess index is applying diffuse lighting. After measuring, the CIELAB color value, the spatial distribution in CIELAB color space, sparkle and graininess index were calculated. Analysis results in this study showed each value was related with characteristics of effect material.

METHOD

Sample Measurement

The spectral imaging system was composed of white LED illuminations, LCTF, and CCD imaging device with Peltier cooling unit. The CCD device captures the images via the LCTF from 420 to 700nm with each 10nm and 380 dpi resolution of 772 by 580 pixels. To get highly accurate spectrum reflectance and imaging information, each wavelength image was compensated by measured lattice pattern to get small shift amount of x and y direction. Before measuring, the lattice pattern composed of white and black line was applied to compensation for registration error which was caused by LCTF optical aberration of each wavelength image. For the sparkle index measurement, illuminations angles of linear lighting were 20, 45 and 70 degrees from normal direction, and detective direction was normal against sample (Shown in Figure 1). On the other hand, for the graininess index, illumination applied 20cm diameter integrating sphere with light trap to make specula component included and excluded measurements (Shown in Figure 2).

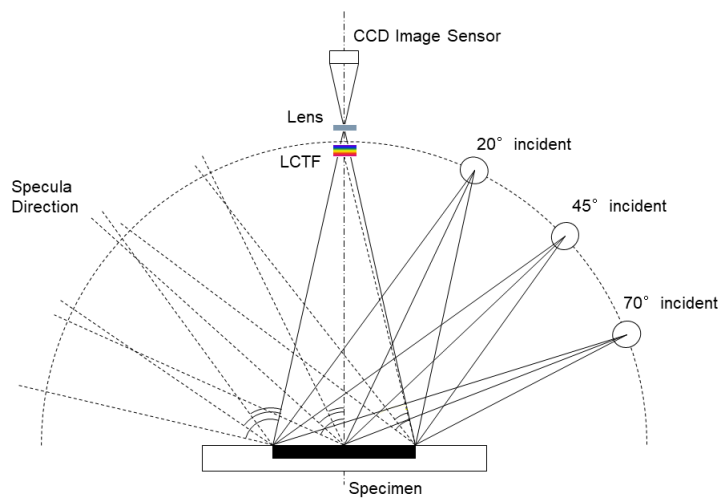


Figure 1. Optical Geometry of Spectral Imaging System for Sparkle Index

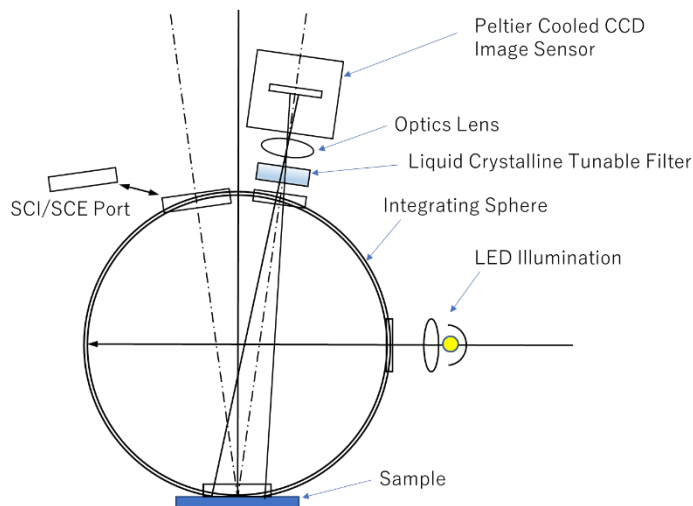


Figure 2. Optical Geometry of Spectral Imaging System for Graininess Index

Sample Preparation

The effect coating test panels were prepared composed of aluminum flake, glass flake, absorption pigment and interference micas. Each panel was coated by spray application on black and white substrates metal panel (LENETA Metopic Panel T12G). The thickness of base coat layer was 20 micrometers, and the applied transparent clear top coat layer thickness was 35 micrometers.

Index calculation

Sparkle Intensity (S_i) as follows:

$$\text{Sparkle Intensity } [S_i] = \frac{1}{T} \sum_{\substack{0 \leq i \leq m \\ 0 \leq j \leq n}} [P(i, j) - Bl] \quad P(i, j) > Bl \quad (1)$$

where $P(i, j)$: Each pixel Image Value, L^* , C^* , $L^* \times C^*$
 Bl : Baseline
 T : Number of pixel ($m \times n$)

Sparkle Area (S_a) as follows:

$$\text{Sparkle Area } [S_a] = \alpha \left\{ \frac{1}{T} \sum_{\substack{0 \leq i \leq m \\ 0 \leq j \leq n}} [1] \right\}^2 \quad P(i, j) > Bl \quad (2)$$

where α : Normalization factor
 $P(i, j)$: Each pixel Image Value, L^* , C^* , $L^* \times C^*$
 Bl : Baseline
 T : Number of pixel ($m \times n$)

Laplacian filter (L_f) as follows:

$$\text{Laplacian Filter } [L_f] = \alpha \frac{1}{T} \sum_{\substack{1 < i < m \\ 1 < j < n}} |M(i, j) \times L| \quad (3)$$

where α : Normalization factor
 $M(i, j)$: 3×3 Matrix pixel Image Value, L^* , C^* , $L^* \times C^*$
 Bl : Baseline
 T : Number of pixel ($m \times n$)
 L : Laplacian filter 3×3 Matrix

$$L = \begin{bmatrix} 0 & -1 & 0 \\ -1 & 4 & -1 \\ 0 & -1 & 0 \end{bmatrix} \quad (4)$$

RESULT

Sparkle distribution in CIELAB color space

As an example, the measuring result of Xirallic Crystal Silver with FW200 carbon black pigment is shown in Figure 3. The distribution in CIELAB color space calculated from measured spectral imaging of 20 degrees illuminant is shown in this figure. Right side shows the frequency of occurrence projected to L^*-a^* plane, and left side shows the frequency of occurrence to projected a^*-b^* plane at $L^* = 15$ with optimal color area. The important point to note is measured color occurrence area has quite wide distribution with all over the optimal color area. This result suggests that recent effect materials need spectral imaging measurement to get high accurate $L^*a^*b^*$ value of sparkle texture.

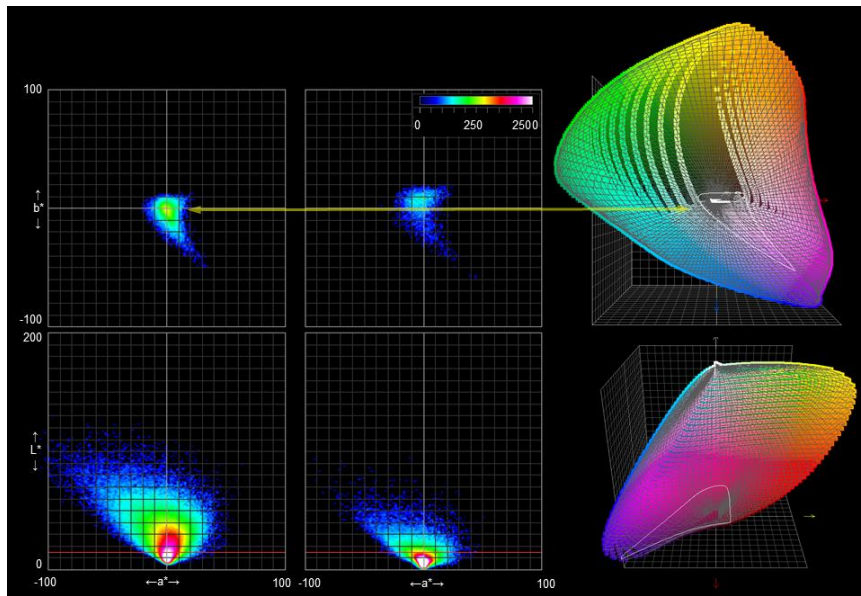


**Figure 3. Image Distribution with Optimal Colour Area in CIELAB Colour Space
Xirallic Crystal Silver/FW200 = 1.0/0.3%**

Sparkle Measurement

The measurement result of gonio-photometric spectral imaging with a-specula angle is shown in Figure 4. X axis of measurement image is related with specula direction, and system can measure from 3.5 to 80.8 deg. a-specula angle by 20, 45, and 70 deg. incident illuminations. Each pixel has spectral information, and calculated L^* , C^* , L^* multiply C^* value.

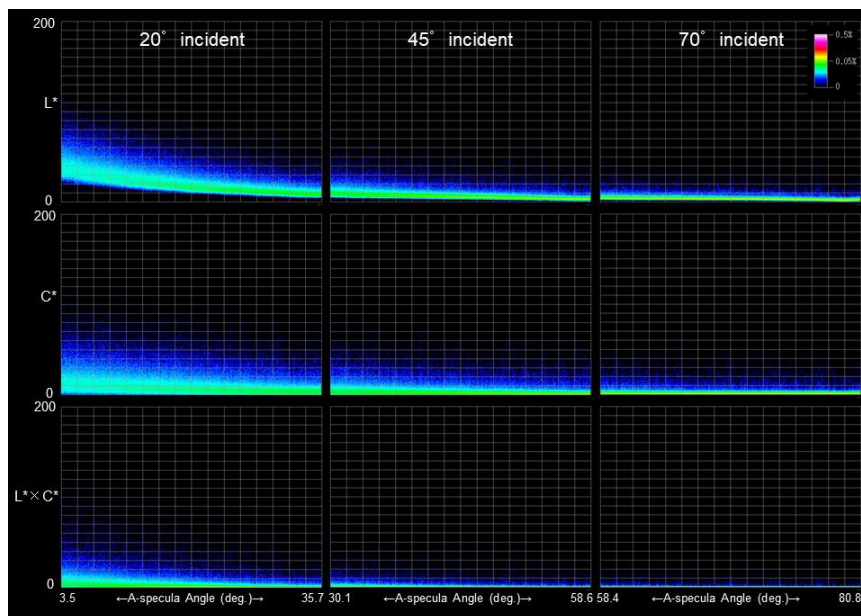


**Figure 4. Measurement Result of Gonio-photometric Spectral Imaging
 L^* , C^* , $L^* \times C^*$ Distribution with A-specula Angle, Xirallic Crystal Silver/FW200 = 1.0/0.3%**

Xirallic Crystal Silver has Al_2O_3 synthetic mica and strong sparkle appears. Nearby 3.5 deg. C^* distribution is very wide and recognized a lot of high chromatic sparkle. The calculation results

of Xirallic Crystal Silver three sparkle index, sparkle intensity, sparkle area, and Laplacian filter are shown in Figure 5 and 6. Figure 5 is nearby 3.5 deg. result, and Figure 6 is nearby 35.0 deg. by 20 deg. incident illumination.

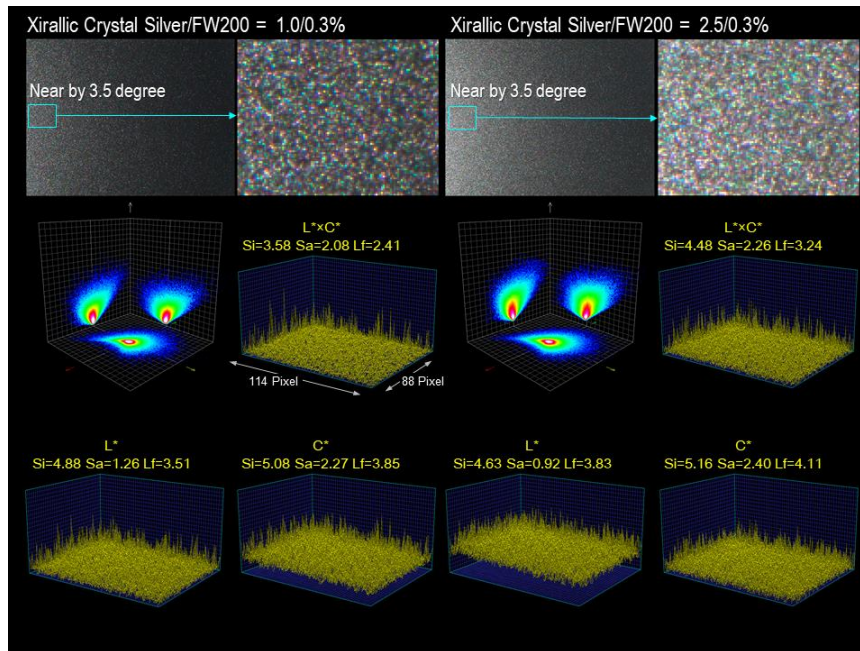


Figure 5. Measurement Result of Gonio-photometric Spectral Imaging Xirallic Crystal Silver/FW200=1.0/0.3% and Xirallic Crystal Silver/FW200 = 2.5/0.3% Incident 20 deg., A-specula nearby 3.5 deg.

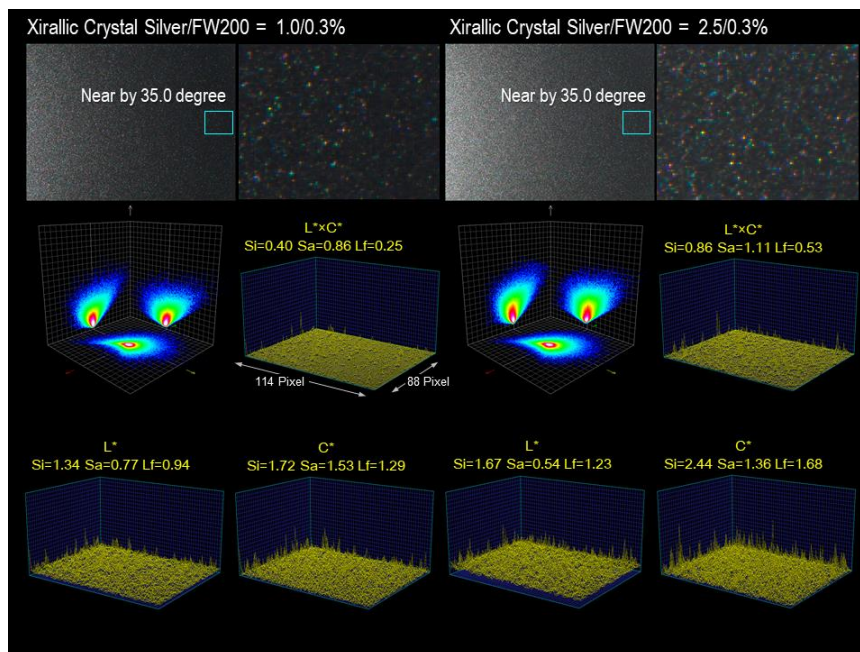


Figure 6. Measurement Result of Gonio-photometric Spectral Imaging Xirallic Crystal Silver/FW200=1.0/0.3% and Xirallic Crystal Silver/FW200 = 2.5/0.3% Incident 20 deg., A-specula nearby 35.0 deg.

Graininess Measurement

In the case of graininess measurement, integrating sphere illumination is applied. Sphere has light trap and measured specula component include (SCI) and exclude (SCE). Measurement image under D65 is shown in figure 7. SCE applied light trap and dark spot in measured image. On the other hand, SCI has not dark spot region, but surface reflection was included in measured image, and brighter than SCE image.

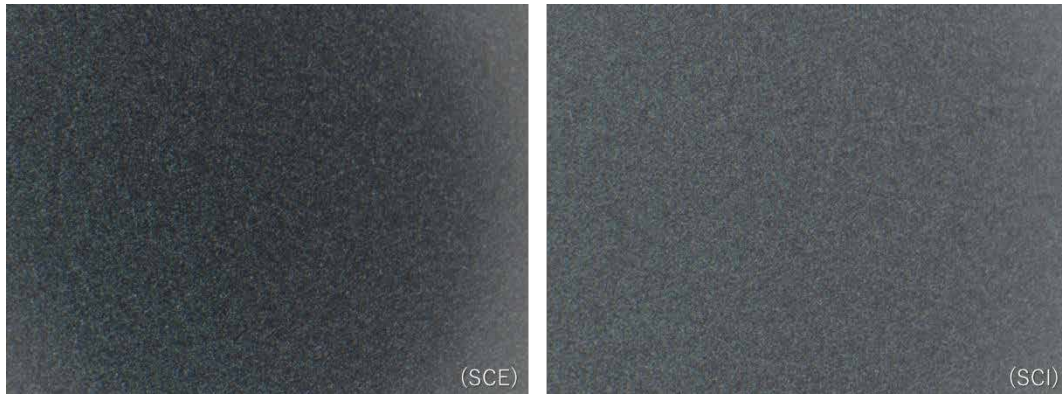


Figure 7. Measurement Result of Integrating sphere illuminate Spectral Imaging

Center of both measurement image which size is 400 by 400 pixels, L^* distribution is calculated and shown in figure 8, average L^* value is 24.93, standard deviation is 5.42 of SCE, average L^* value is 39.14, standard deviation is 4.61 of SCI. SCE measurement result is darker and high contrast. SCI measuring image has good uniformity, but SCE image has high contrast and better for graininess index measurement.

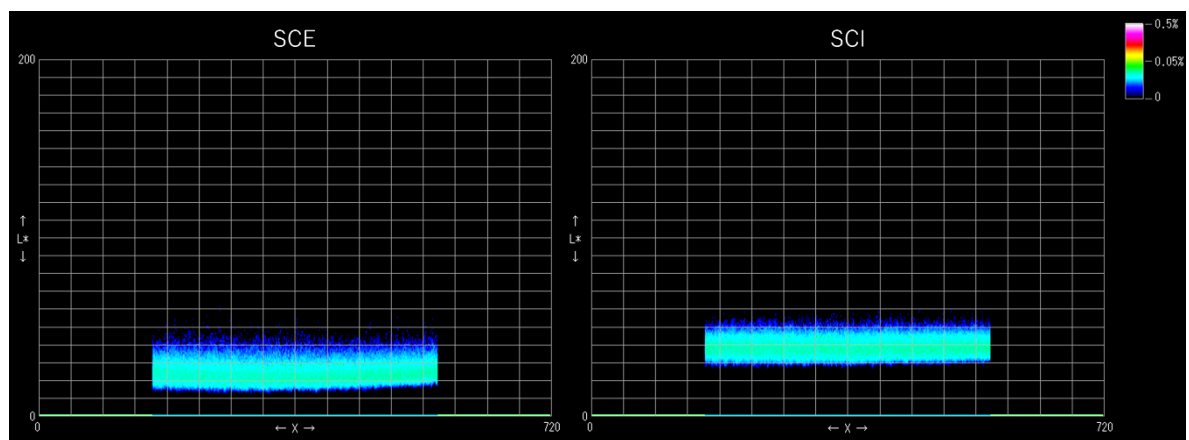


Figure 8. L^* distribution of Integrating sphere illuminate Spectral Imaging

REFERENCES

1. Hensley, D. Wyble. (2012). *Spectral Imaging Using a Liquid Crystal Tunable Filter*, Munsell Colour Science Laboratory, Technical Report November
2. Ferrero, A., Campos, J., Rabal, A. M., and Pons, A. (2013). *A single analytical model for sparkle and graininess patterns in texture of effect coatings*, Opt. Express 21, 26812– 26819
3. Ferrero, A., Velazquez, J. L., Perales, E., Campos, J., and Martinez Verdu, F. M. (2018). *Definition of a measurement scale of graininess from reflectance and visual measurements*, Opt. Express 26, 30116-30127

APPEARANCE REPRODUCTION OF SKIN WITH PIGMENT CONCENTRATION PATTERN GENERATED BY DEEP CONVOLUTIONAL GENERATIVE ADVERSARIAL NETWORKS

Motonori Doi^{1*}, Akira Kimachi² and Shogo Nishi²

¹ *Department of Telecommunications and Computer Networks, Faculty of Information and Communication Engineering, Osaka Electro-Communication University, Japan.*

² *Department of Engineering Informatics, Faculty of Information and Communication Engineering, Osaka Electro-Communication University, Japan.*

*Corresponding author: Motonori Doi, e-mail (doi@osakac.ac.jp)

Keywords: Appearance reproduction, Skin image, Pigment concentration, DCGAN

ABSTRACT

The appearance of human skin surface is important in color science. We focus on the local appearance of human skin with pigment concentrations. The color texture results from the non-uniformity of local pigment distributions in human skin layers, which include three pigments: melanin, oxy-hemoglobin, and deoxy-hemoglobin. We have studied pigment distribution estimation from multispectral images of human skin surface and its application to reproducing skin image appearance under different pigment distributions. In the procedure of reproducing the skin image appearance, different pigment distribution patterns were generated manually. For photorealistic appearance reproduction, this paper proposes appearance reproduction of skin with realistic pigment distribution patterns generated by deep convolutional generative adversarial networks (DCGANs). The DCGAN is a method to generate new images close to those in a training data set based on machine learning algorithms. By using the DCGAN, we can obtain many pigment concentration patterns from a small sample data set of real images. In the pigment distribution estimation of our method, color texture components derived from pigment distributions are separated from skin spectral images by using the multi-resolution analysis. Then, pigment distributions in the color texture component are estimated by using the Kubelka-Munk theory. In the appearance reproduction, skin images of different appearance were reproduced from pigment distributions of melanin, oxy-hemoglobin, and deoxy-hemoglobin. The pigment distribution pattern is generated by the DCGAN in this paper. In the experiments, we generated pigment concentration images by the DCGAN from nevus images in the ISIC (The International Skin Imaging Collaboration) archive. The pigment concentration images were converted to the pigment distribution pattern by the image processing procedures of thresholding, grayscaling and grayscale inversion. We demonstrated successful results of reproducing realistic skin images with a stain, an inflammation, and a bruise with the pigment distribution pattern generated by using the DCGAN.

INTRODUCTION

Appearance reproduction is one of the most important topics in color science. The appearance of skin surface with pigment colors has been analyzed in many research fields including computer graphics, medical imaging and diagnosis, and cosmetics applications. We focus on the local appearance of human skin with pigment concentrations. The color texture results from the non-uniformity of local pigment distributions in human skin layers, which include three pigments: melanin, oxy-hemoglobin, and deoxy-hemoglobin. For example, spots of melanin appear as moles or stains on skin, and bruises are observed as blue spot owing to deoxy-hemoglobin absorption.

The authors proposed a method to estimate the local skin properties from multispectral images of human skin surface and its application to reproducing the skin image appearance under different pigment distribution [1]. It is difficult to create photorealistic pigment distribution patterns manually. Therefore, a simple pigment distribution pattern was generated manually in the work.

For more photorealistic appearance reproduction, this paper proposes appearance reproduction of skin with realistic pigment distribution patterns generated by deep convolutional generative adversarial networks (DCGANs) [2]. The DCGAN is a method to generate new images close to those in training data set based on machine learning algorithms. By using the DCGAN, we can obtain many realistic pigment distribution patterns.

SKIN APPEARANCE REPRODUCTION

Figure 1 shows the scheme of the proposed method. Pigment distribution is estimated from multispectral images of human skin surface by our previous method [1]. The pigment concentration pattern is generated by the DCGAN. The appearance of skin is reproduced from the estimated pigment distribution in the skin and the generated pigment concentration.

In the pigment distribution estimation, color texture components derived from pigment distributions are separated from skin spectral images by using the multi-resolution analysis. Skin surface has various textures. We defined a simple model of the skin texture composed of sulcus cutis, shading, and color texture components derived from pigment distributions. We assumed that these textures have different fineness. Therefore, the textures are decomposed according to different fineness by a method based on multi-resolution analysis (MRA) with wavelet functions. Figure 2 shows the skin image decomposition into the three skin textures. Color texture components exist mainly in the middle frequency component. Then, the pigment distributions in the color texture components are estimated by using the Kubelka-Munk theory (KMT). The KMT is convenient for calculating the optical values of reflectance and transmittance within a layer consisting of turbid materials [4-5]. We defined an optics model of skin layers. The skin model involves the two turbid layers of the epidermis including melanin and the dermis including oxy-hemoglobin and deoxy-hemoglobin, as shown in Figure 3 [1]. Based on this model, we estimate the pigment distribution from multispectral images of skin by the method using the KMT.

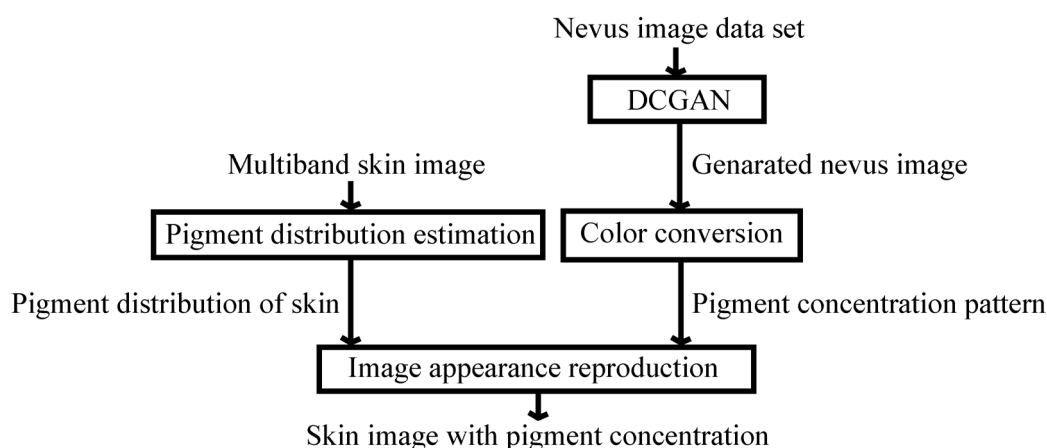


Figure 1. The flow chart of the proposed appearance reproduction of skin with pigment concentration generated by DCGAN

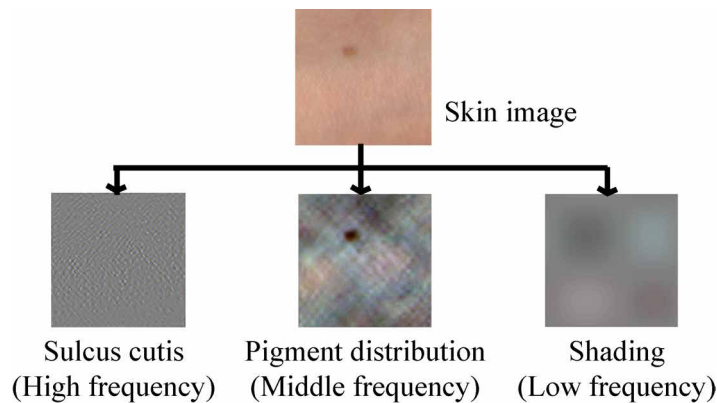


Figure 2. Skin image decomposition

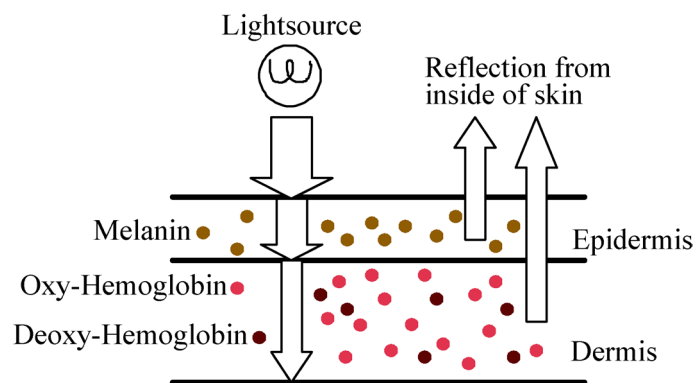


Figure 3. Skin optics model [1]

Image appearance is reproduced through the reverse process of pigment distribution estimation. In the appearance reproduction, skin images with pigment concentration were reproduced from given pigment distributions of melanin, oxy-hemoglobin, and deoxy-hemoglobin.

GENERATING PIGMENT CONCENTRATION PATTERN BY DCGAN

The DCGAN is a method to generate new images close those in training data set based on machine learning algorithms. By using the DCGAN, we can obtain many pigment concentration patterns from a small sample data set of real images including pigment concentrations. A simple structure of the DCGAN is shown in Figure 4. The DCGAN consists of networks of a generator and a discriminator. The generator generates images from random noises. The discriminator judges the output from the generator as a real image or a generated image. The generator is trained to generate images that are judged as real images by the discriminator. The discriminator is trained to make correct judgement. Through repetitive training, the DCGAN produces realistic images.

EXPERIMENTS

We conducted experiments to evaluate the proposed method. The image data set includes 156 nevus images obtained from the ISIC (The International Skin Imaging Collaboration) archive [6]. The image data set includes microscopic images taken under various illuminations. New nevus images were generated by a DCGAN with four-layer networks of a generator and a discriminator.

The networks were repetitively trained 500 times. The original nevus images are shown in Figure 5. The generated images are shown in Figure 6. The generated images exhibit noises. We use the middle frequency component of the image as a distribution pattern according to our skin texture model. The noises in this frequency component image were negligible. Figure 7 shows the pigment distribution patterns converted from the generated images. High pixel values indicate high density in the pigment distribution pattern. Figure 8 shows the original skin image, and Figure 9 shows the reproduced skin image with generated concentration patterns of melanin, oxy-hemoglobin and deoxy-hemoglobin, respectively. Pigment concentrations of these images correspond to a stain, an inflammation, and a bruise respectively. In comparison, Figure 10 shows the generated image in our previous method with a simple pigment distribution pattern [1]. We demonstrated successful results of generating realistic skin images with a stain, an inflammation, and a bruise with pigment distribution patterns generated by using the DCGAN.

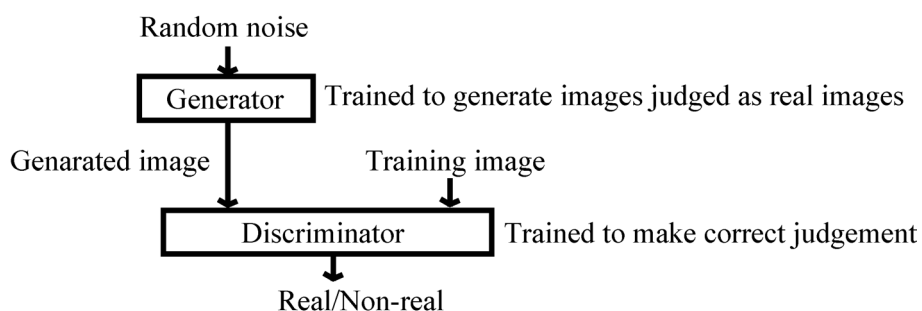


Figure 4. Structure of DCGAN



Figure 5. Nevus images in the data set taken from the ISIC archive [1]

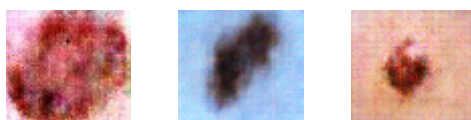


Figure 6. Generated images by the DCGAN



**Figure 7. Generated pigment concentration patterns
(High pixel values indicate high density in a pigment distribution pattern.)**



Figure 8. Original skin image

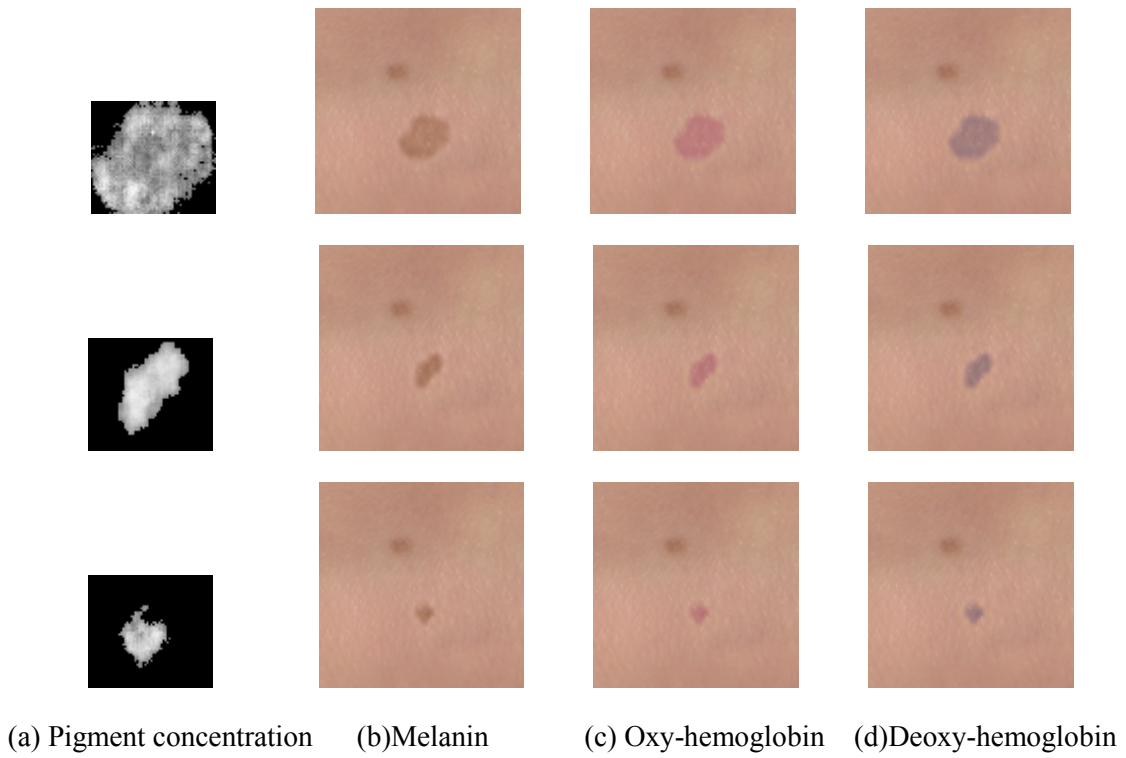


Figure 9. Reproduced skin images with pigment concentration patterns generated by the DCGAN



Figure 10. Reproduced skin images with a simple pigment concentration pattern [1]

CONCLUSIONS

This paper proposes appearance reproduction of skin with realistic pigment distribution patterns generated by the DCGAN. New nevus images are generated from real nevus images by the DCGAN. The generated images are converted to pigment distribution patterns by the image processing procedures of thresholding, grayscaling and grayscale inversion. Then, skin images with pigment concentrations are generated in multispectral images by the method based on MRA and KMT. In the experiments, we demonstrated successful results of generating realistic skin images with a stain, an inflammation, and a bruise with the pigment distribution pattern generated by using the DCGAN.

ACKNOWLEDGEMENT

This work was supported by Grants-in-Aid for Scientific Research (KAKENHI) (No. 17K00255).

We are grateful to Mr. Koki Ito for assistance in experiments.

REFERENCES

1. Doi, M., Kimachi, A., Nishi, S., & Tominaga, S. (2016). Estimation of Local Skin Properties from Spectral Images and its Application to Appearance Reproduction. *The Journal of Image Science and Technology*, 60(5), 1-11.
2. Radford, A., Metz, L. & Chintala, S. (2015). Unsupervised Representation Learning with Deep Convolutional Generative Adversarial Networks, *6th International Conference on Learning Representations*.
3. Mallat, S. G. (1989). A theory for multiresolution signal decomposition: the wavelet representation, *IEEE Transactions on Pattern Analysis and Machine Intelligence*, 11(7), 674-693.
4. Kubelka, P. (1948). New Contributions to the Optics of Intensely Light-Scattering Materials. Part I. *Journal of Optical Society of America*, 38(5), 448.
5. Kubelka, P. (1954). New Contributions to the Optics of Intensely Light-Scattering Materials. Part II: Nonhomogeneous Layers. *Journal of Optical Society of America*, 44(4), 330.
6. ISIC Archive, [Online]. Available: <https://isic-archive.com/> [Accessed: 31-Jan-2019]

A WEAK MELANOPSIN CONTRIBUTION TO COLOR PERCEPTION

Sei-ich Tsujimura^{1*}, Katsunori Okajima²

¹*Faculty of Design and Architecture, Nagoya City University, 2-1-10, Kita Chikusa, Chikusa-ku, Nagoya, 464-0083 Japan*

²*Faculty of Environment and Information Sciences, Yokohama National University, Japan*

*Corresponding author: Sei-ich Tsujimura
tsujimura@sda.nagoya-cu.ac.jp

Keywords: melanopsin, chromatic mechanisms, color perception

ABSTRACT

The discovery of melanopsin-containing retinal ganglion cells (melanopsin cells) has led to a fundamental reassessment of non-image forming processing, such as circadian photoentrainment and pupillary light reflex, suggesting that melanopsin cells play an important role in encoding ambient illuminance in the brain function. Growing evidence indicates that melanopsin cells contribute not only to non-image forming processing but also to visual perception. This study is intended to present an investigation of color perception in human vision in relation to melanopsin and cone stimulations. A four-primary stimulation system that enables independent stimulation of each photoreceptor class was used to control stimulation of the three cone types and melanopsin in the human eye. We measured temporal contrast sensitivity functions to the red-green and blue-yellow isoluminant stimuli. In each mechanism color discrimination thresholds were measured for the following isoluminant stimuli; isoluminant stimulus with melanopsin modulation and without melanopsin modulation. The results showed the contrast sensitivity functions for color discrimination formed a band-pass filter with a peak frequency of ~5 Hz for red-green color mechanism and of ~1 Hz for blue-yellow color mechanism. The shapes of contrast sensitivity functions were similar for all the red-green isoluminant stimuli, indicating that there is weak interaction between signals from melanopsin and M-L cone-opponent mechanism.

INTRODUCTION

The melanopsin-containing retinal ganglion cells (melanopsin cells) contribute to non-image forming processing, such as circadian photoentrainment and pupillary light reflex, suggesting that melanopsin cells play an important role in encoding ambient illuminance. Several studies indicate that melanopsin cells contribute not only to non-image forming processing but also to visual perception. For example, a blind human patient lacking functional classical photoreceptors can detect a monochromatic light stimulus [1], suggesting that melanopsin-mediated signals may support conscious awareness. There is a strong input of melanopsin signals to a large portion of neurons in the lateral geniculate nucleus [2]; these neurons showed sustained activation to a steady-state light step. Furthermore, the melanopsin-mediated signals influence brightness perception in both mice and humans [3, 4]. Although these results support the fact that melanopsin plays an important role in the conventional visual pathway, their functional role is not yet clear. This study is intended to present an investigation of color perception in human vision in relation to melanopsin and cone stimulations.

METHODS

A personal computer controlled the four-primary illumination system. Four different types of light-emitting diode were used. The annular ring test stimulus was superposed on the circular adaptation field using a beam splitter (Figure 1). A detailed description of the illumination system has previously been published [3, 5, 6].

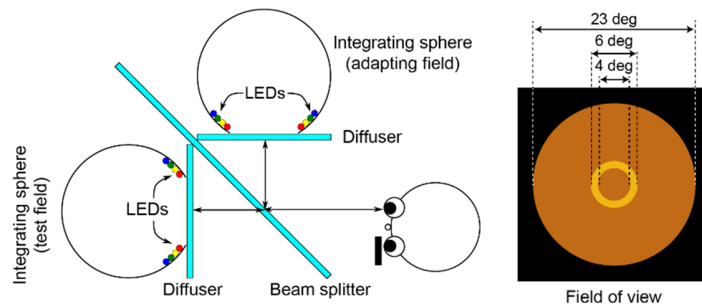


Figure 1. Eight-channel, four-primary stimulation system.

Colour discrimination thresholds were measured for the following isoluminant stimuli; isoluminant stimulus without melanopsin modulation and the isoluminant stimulus with a melanopsin modulation. The ratio of contrast of melanopsin to colour was 1.73 in cone contrast throughout. The contrast of isoluminant stimulus and that of melanopsin stimulus varied in the same way. We used two test stimuli; the M-L isoluminant stimulus corresponded to an isoluminant green-red stimulus that was modulated along M-L cone-opponent direction. Similarly, S cone stimulus corresponded to an isoluminant blue-yellow stimulus that was modulated along the S-cone direction. After the initial adaptation to the background for five minutes, a sinusoidally modulated test stimulus was shown for one second with the temporal frequencies ranging between 0.25 Hz and 40 Hz.

The luminance of the adapting field was 241.0 cd/m^2 , and the CIE color coordinates (CIE 1964) were (0.50,0.49). The receptor stimulations were 176.9 cd/m^2 , 64.1 cd/m^2 , and 5.7 cd/m^2 for the L-, M-, and S-cones and 54.6 cd/m^2 for melanopsin. The spectral sensitivity of melanopsin was estimated from a pigment template nomogram with a peak wavelength (λ_{max}) of 480 nm [7]. The lens and macular pigment density spectra in the peripheral visual field were those used by Stockman et al. [8, 9]. Although we assumed that short-wavelength sensitive cones (S-cones) and melanopsin do not affect the photopic luminance efficiency function (i.e., luminance) we used photopic luminance units (cd m^{-2}). Similar to S-cone stimulation [10], the melanopsin stimulation was defined as the amount of melanopsin stimulation that is produced by an equal energy spectrum of luminance 1.0 cd m^{-2} . The resultant spectral sensitivity function of melanopsin in the peripheral visual field displayed a peak of 872.1 (i.e., K_m) at a peak wavelength of 493 nm. The shape of spectral sensitivity curve we estimated is similar to that proposed by Lucas and his colleagues [11]. We further considered the human macular pigment density at 10-deg for the estimation.

RESULTS

Figure 2 showed the contrast sensitivity functions to the red-green isoluminant stimuli. Sensitivities to the isoluminant stimulus (open circles) and with a melanopsin modulation (open squares) were plotted.

The contrast sensitivity functions for colour discrimination formed a band-pass filter with a peak frequency of ~ 5 Hz for red-green colour mechanism. The shapes of contrast sensitivity functions were similar between with and without modulation of melanopsin stimulation and no significant difference in sensitivity for all frequencies (paired t-test with Bonferroni correction). It indicated that there is little or no contribution of melanopsin modulation in red-green colour discrimination over all temporal frequencies.

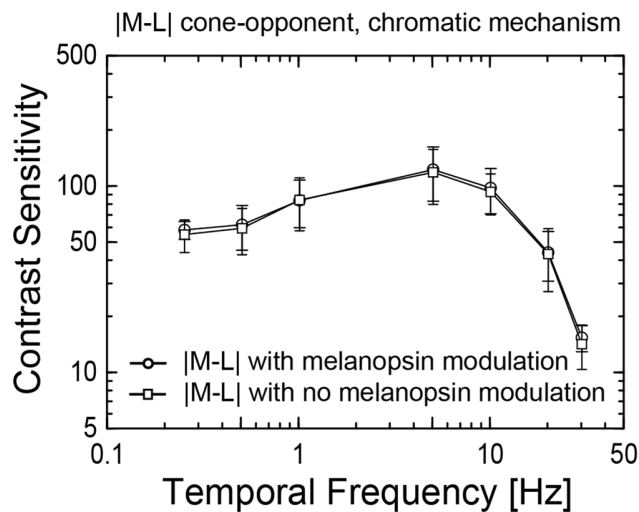


Figure 2. Contrast sensitivity functions for isoluminant colour stimulus with and without modulation of melanopsin stimulation, averaged from 5 subjects.

ACKNOWLEDGEMENT

This study was supported by the Ministry of Education, Science, Sports and Culture of Japan, Grants-in-Aid for Scientific Research (B) 26280103 and (B) 17H01808 to S.T and 18H04111 to K.O.

REFERENCES

1. Zaidi, F.H., J.T. Hull, S.N. Peirson, K. Wulff, D. Aeschbach, J.J. Gooley, G.C. Brainard, K. Gregory-Evans, J.F. Rizzo, C.A. Czeisler, R.G. Foster, M.J. Moseley, and S.W. Lockley, (2007). *Short-wavelength light sensitivity of circadian, pupillary, and visual awareness in humans lacking an outer retina*. *Current Biology*. **17**(24): 2122-2128.

2. Brown, T.M., C. Gias, M. Hatori, S.R. Keding, M. Semo, P.J. Coffey, J. Gigg, H.D. Piggins, S. Panda, and R.J. Lucas, (2010). *Melanopsin Contributions to Irradiance Coding in the Thalamo-Cortical Visual System*. Plos Biology. **8**(12).
3. Brown, T.M., S. Tsujimura, A.E. Allen, J. Wynne, R. Bedford, G. Vickery, A. Vugler, and R.J. Lucas, (2012). *Melanopsin-based brightness discrimination in mice and humans*. Curr Biol. **22**(12): 1134-41.
4. Yamakawa, M., S.I. Tsujimura, and K. Okajima, (2019). *A quantitative analysis of the contribution of melanopsin to brightness perception*. Sci Rep. **9**(1): 7568.
5. Tsujimura, S., K. Ukai, D. Ohama, A. Nuruki, and K. Yunokuchi, (2010). *Contribution of human melanopsin retinal ganglion cells to steady-state pupil responses*. Proc Biol Sci. **277**(1693): 2485-92.
6. Tsujimura, S. and Y. Tokuda, (2011). *Delayed response of human melanopsin retinal ganglion cells on the pupillary light reflex*. Ophthalmic and Physiological Optics. **31**(5): 469-479.
7. Lucas, R.J., R.H. Douglas, and R.G. Foster, (2001). *Characterization of an ocular photopigment capable of driving pupillary constriction in mice*. Nat Neurosci. **4**(6): 621-6.
8. Stockman, A., L.T. Sharpe, and C. Fach, (1999). *The spectral sensitivity of the human short-wavelength sensitive cones derived from thresholds and color matches*. Vision Res. **39**(17): 2901-27.
9. Stockman, A. and L.T. Sharpe, (2000). *The spectral sensitivities of the middle- and long-wavelength-sensitive cones derived from measurements in observers of known genotype*. Vision Res. **40**(13): 1711-37.
10. Boynton, R.M. and N. Kambe, (1980). *Chromatic difference steps of moderate size measured along theoretically critical axes*. Color Research & Application. **5**(1): 13-23.
11. Lucas, R.J., S.N. Peirson, D.M. Berson, T.M. Brown, H.M. Cooper, C.A. Czeisler, M.G. Figueiro, P.D. Gamlin, S.W. Lockley, and J.B. O'Hagan, (2014). *Measuring and using light in the melanopsin age*. Trends in neurosciences. **37**(1): 1-9.

PERCEPTION OF VIVIDNESS OF EMISSIVE COLOURS BY NORWEGIAN OBSERVERS

Helene Midtfjord*, Phil Green and Peter Nussbaum

(NTNU, Gjøvik, Norway)

Faculty of Information Technology and Electrical Engineering, Department of Computer Science, Norway.

*Corresponding author: helene.midtfjord@ntnu.no

Keywords: Colour appearance, Vividness, Display colours, Psychophysics

ABSTRACT

Vividness is a widely used term in the English language, and as a colour appearance attribute it has been investigated as a visual scale that express chroma and colourfulness. Studies have shown that perception of vividness of colour samples among English and Korean observers correlate well with chroma. In this study, we investigate if the same tendency is seen among Norwegian observers, where the language does not include a direct translation for vividness. A hundred colour samples on display were judged on a six-point categorical scale by 19 Norwegian observers. The visual data obtained in our experiment show strong correlation with chroma. We also see that lightness and the eccentricity factor are significant parameters in describing the visual data, indicating that the perception of vividness is not judged only according to chroma.

INTRODUCTION

Vividness is a term which receives increased attention in colour research. Previous work in colour science shows that the vividness term is a useful descriptor for colours as it correlates well with the intuitive perception of colourfulness of colour samples [1]. Unlike chroma, which can be operationally defined in terms of polar coordinates in CIELAB space, the term vividness does not have a universally-agreed operational definition, and its general meaning can only be the way it is used in the language [2]. This leads to the possibility that the interpretation of the term is to some degree dependent on context. We note that while vivid is a widely-used term in the English language, there is not always a precisely-equivalent term in other languages, rendering its interpretation even more subjective.

The Oxford English Dictionary defines vividness as *intensely bright, brilliant and glaring* [3]. Berns define vividness as: "*an attribute of colour used to indicate the degree of departure of the colour from a neutral back colour*" [4]. Berns' vividness model is given by the following equation:

$$V = \sqrt{(L^*)^2 + (a^*)^2 + (b^*)^2} = \sqrt{(L^*)^2 + (C_{ab}^*)^2}, \quad (1)$$

where L^* , a^* , b^* and C_{ab}^* are the CIELAB correlates for lightness, redness-greenness and yellowness-blueness, and chroma respectively. Berns points out that in real life experience, such as pigment mixing and shadow series, the colour transition include simultaneous change in lightness and chroma, which can be described by the vividness colour dimension.

Recently, a visual experiment was conducted which goal was to test attributes' relationship with the chroma dimension when judged by ordinary people without colour science training [1]. The

experiment was conducted with English and Korean observers, and it showed strong correlation between perception of vividness and chroma. Two models have been proposed based on the data from this experiment [5][6]. In our work we investigate Norwegian observers' perception of vividness through a similar experiment. Vividness models from literature are tested, and we propose a model that fits with our data.

EXPERIMENTAL METHOD

To investigate Norwegian observers' perception of vividness as a colour appearance attributes, a psychophysical experiment was conducted. 19 Norwegian observers in age group 20-30 years participated in the experiment. They were all naïve observers, so that their assessments reflect ordinary peoples view of vividness, as opposed to colour experts'. Colour samples were showed on a display in a random sequence in a dimply lit room. The observers were asked to rate the vividness of display colours based on a 6-point categorical scale categorised as "1: *very dull*", "2: *dull*", "3: *a little dull*", "4: *a little vivid*", "5: *vivid*" and "6: *very vivid*". The judgement was made by clicking on one of the six category buttons on the display. A white and a black reference was always visible on the display. The interface of the experiment is shown in Figure 1.

Vivid is not a word with a direct translation to the Norwegian language, and the observers were given two descriptors in Norwegian to help them understanding the term if they were not familiar with it. The descriptors were the words *tydelig* and *livlig*, which translates into *distinct* and *lively*.

A hundred colours were displayed as 3x3 inch patches on a light grey background. The samples were chosen to be evenly distributed in lightness and chroma for seven hue angles in CIELAB colour space. The radiance of the display colours was measured with a Minolta CS-2000 telespectroradiometer. Tristimulus XYZ values for each colour sample were calculated using the CIE 1964 (2-degree observer) and k set to 683Φ [7]. The tristimulus values of the white point was XYZ = [110, 123, 122]. CIELAB data were calculated from the computed XYZ values using the normalized XYZ values from the display white point. The measurements of the samples are shown in Figure 2.

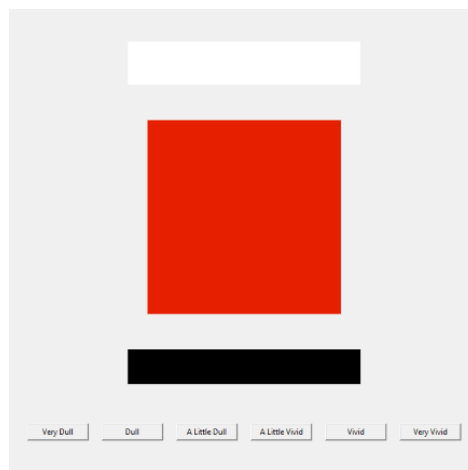


Figure 1: Figure 1: A screen shot of a red colour sample in the experiment interface. The colour samples are placed between a black and a white reference, and there are six category buttons.

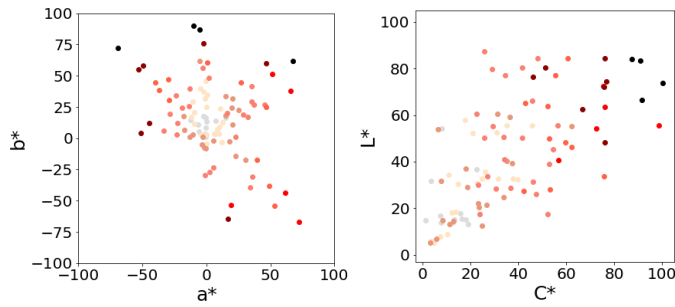


Figure 2. Distribution of colour samples according to their a*-b* coordinates (left) and L*-C*ab coordinates (right) in CIELAB colour space. The points are colour coded according to the sample's vividness score from the experiment; more chromatic and darker colour indicate higher vividness.

EXPERIMENTAL RESULTS

To investigate Norwegian observers' perception of vividness the visual data was compared with CIELAB lightness, chroma and hue, and CAM16 predictions [8]. Table 1 shows the correlation coefficient between the predicted attributes and the visual data. There is a strong correlation between chroma and our visual data, and a substantial correlation between the visual data and lightness. According to the coefficient of determination, R^2 , CIELAB chroma explains 76% of the variations in the data, while lightness explains 42%. According to ANOVA, both chroma and lightness are significant factors for predicting our visual results.

	L*	C*ab	h*	C	M	S	J	Q	h	H
r	0.65	0.87	0.16	0.91	0.91	0.67	0.61	0.62	0.15	0.15

Table 1: Correlation coefficient between the visual data and the colour appearance attributes in terms of CIELAB and CAM16.

Hue angle on the other hand explains approximately nothing of the variations in the data. However, a linear regression model which includes the colour centres as factors show that the hue centres has a significant effect on the prediction of visual vividness in our data. CAM16 chroma has an even stronger prediction of our data; CAM16 chroma explains 83% of the data. In the computations of CAM16 chroma the eccentricity factor, e_t , is included to correct for the fact that perceived achromatic colours are not at the centre of colours for low saturation [8][9]. In a previous study we showed that a linear model with CIELAB chroma and categorical coefficients for red, yellow, blue and green predicted vividness data when the coefficients take on values that are similar to the eccentricity factor for the respective hues [10]. This indicate that perceived vividness might be explained by a hue dependent factor. A simple, linear model was fitted to our data which includes CIELAB chroma, lightness and the eccentricity factor, e_t :

$$V = 0.2L^* + C_{ab}^* + 44e_t - 30, \quad (3)$$

A simple, linear model with CAM16 lightness and chroma was fitted to our data. The model is given by:

$$V = 0.2J + C - 20, \quad (4)$$

How well these models predict the visual data obtained in our experiment was tested together with models proposed in other literature. Figure 3 shows plots of the visual data against vividness models. We see that Berns' model in Equation 1 explain 68% of the variations in the visual data, while the models proposed by Li et al. [5] and Cho et al. [6] does not predict our data very well. The performance of Equation 3 and 4 are included in Figure 3, and we see that the models which is fitted to our data, predicts 84% and 89% of the variations in the data, respectively.

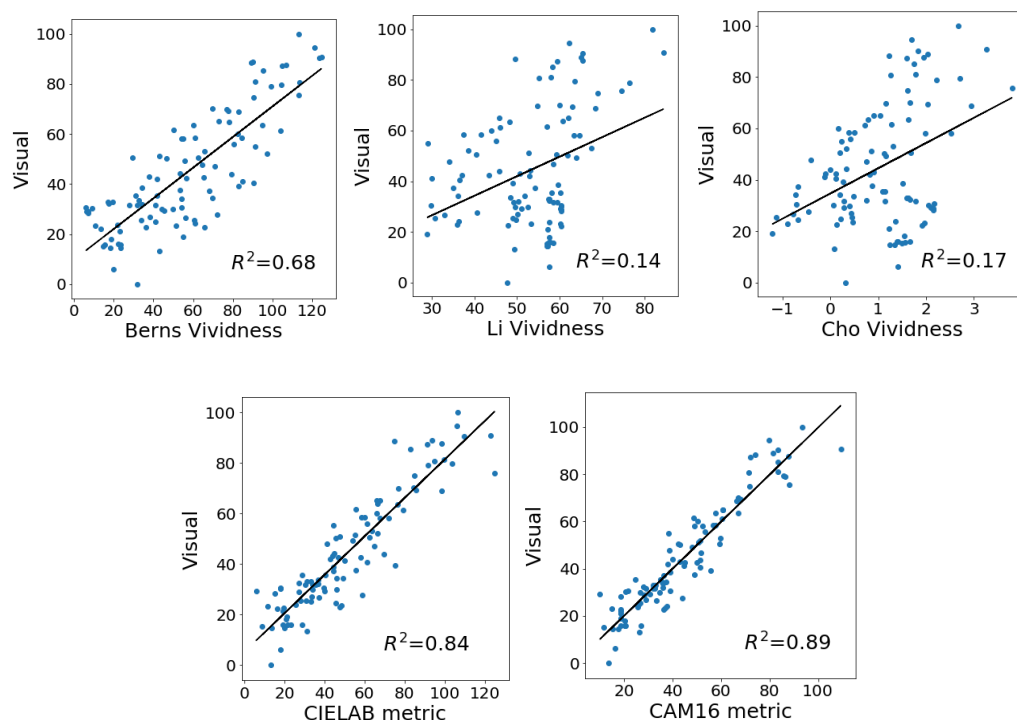


Figure 3. Plots of visual data against vividness models proposed by Berns [4], Li et al. [5], Cho et al. [6] and Equation 3 and 4.

The coefficient of determination for the visual data and different predictors are given in Table 2. We see that lightness predicts a large portion of the variance in the visual data for yellow colour samples quite well, but not for blue. We see that chroma is a good predictor for the combined dataset, and that it is an even better predictor for the colours separately. CAM16 predictions perform better than CIELAB predictions. We see that Berns' vividness model performs the best out of the models found in literature. Studies have shown that Berns' clarity predicts visual vividness quite well [1], but this is not the case for our data. Equation 3 and 4 give good predictions of our visual data; the predictions is better for the colours separately than for the combined dataset. This indicates that we have still not found the optimal relationship between hue angle and visual vividness.

DISCUSSION

Results indicate that the observers judged vividness of colours according to both chroma and lightness. In a previous study with international observers we found that lightness was not a significant predictor for visual vividness [10]. The previous experiment also included 3x3 inch colour patches on display, but the experiment differs in several aspects from the current. E.g. there was a different distribution of colour samples used; the previous experiment included samples with high

lightness and low chroma as opposed to this experiment. Also, the interface and viewing conditions were different; the previous study included both background and surround regions, where the background was darker than in this study, which will influence the perceived colour. The previous experiment also differed from the current experiment by having a brighter display, and by not including references for black and white. It is a possibility that the achromatic references gave a better foundation for predicting vividness according to the lightness scale, and this is the reason we see a significant effect from lightness in combination with chroma for the data obtained in this experiment and not in the previous.

R ²	All	Red	Brown	Yellow	Green	Turquoise	Blue	Purple
CIE L	0.42	0.46	0.64	0.72	0.37	0.49	0.17	0.25
CIE C	0.76	0.89	0.93	0.82	0.88	0.83	0.84	0.81
CAM16 J	0.37	0.29	0.51	0.81	0.43	0.52	0.11	0.12
CAM16 C	0.83	0.90	0.93	0.83	0.90	0.92	0.88	0.84
Berns V	0.68	0.73	0.85	0.80	0.68	0.64	0.47	0.75
Berns T	0.00	0.00	0.06	0.00	0.04	0.18	0.04	0.05
Li et al.	0.14	0.22	0.30	0.07	0.30	0.00	0.15	0.12
Cho et al.	0.17	0.10	0.23	0.10	0.22	0.03	0.20	0.35
Eq. 3	0.84	0.89	0.93	0.82	0.87	0.88	0.93	0.86
Eq. 4	0.89	0.91	0.95	0.86	0.88	0.94	0.93	0.89

Table 2: Coefficient of determination for the visual data and colour appearance attributes in terms of CIELAB and CAM16, together with Berns' vividness and clarity models [4], vividness models by Li et al. [5] and Cho et al. [6], and Equation 3 and 4.

CONCLUSION

Norwegian observers without colour science training were asked to evaluate vividness of colour samples on display on a six-point categorical scale from very vivid to very dull. The results show that both chroma and lightness have a significant effect on describing how the observers evaluated the percept. A model based on CIELAB lightness, chroma and the eccentricity factor, or a model based on CAM16 chroma and lightness predicted the visual data best. Berns' vividness model explains some of the variations in our visual data, while other models which are based on a dataset for English and Korean observers does not work for predicting our visual data.

REFERENCES

1. Cho, Y. J., Ou, L. C., & Luo, R. (2017). A Cross-cultural comparison of saturation, vividness, blackness and whiteness scales. *Color Research & Application*, 42(2), 203-215.
2. Malcolm, N. (1954). Wittgenstein's Philosophical investigations. *The Philosophical Review*, 63(4), 530-559.
3. Oxford (1995). The Concise Oxford Dictionary of Current English (9th edn), *Oxford University Press*.
4. Berns, R. S. (2014). Extending CIELAB: Vividness, depth, and clarity. *Color Research & Application*, 39(4), 322-330.

5. Li, C., Liu, X., Xiao, K., Ji Cho, Y., & Luo, M. R. (2018, November). An Extension of CAM16 for Predicting Size Effect and New Colour Appearance Perceptions. In *Color and Imaging Conference* (Vol. 2018, No. 1, pp. 264-267). Society for Imaging Science and Technology.
6. Cho, Y. J., Ou, L. C., Cui, G., & Luo, R. (2017). New colour appearance scales for describing saturation, vividness, blackness, and whiteness. *Color Research & Application*, 42(5), 552-563.
7. ISO 11664-3: 2013 (2013). Colorimetry--Part 3: Colorimetry - Part 3: {CIE} tristimulus values. *International Organization for Standardization*.
8. Li, C., Li, Z., Wang, Z., Xu, Y., Luo, M. R., Cui, G., ... & Pointer, M. (2017). Comprehensive color solutions: CAM16, CAT16, and CAM16-UCS. *Color Research & Application*, 42(6), 703-718.
9. Moroney, N., Fairchild, M. D., Hunt, R. W., Li, C., Luo, M. R., & Newman, T. (2002). The CIECAM02 color appearance model. *Color and Imaging Conference* (Vol. 2002, No. 1, pp. 23-27). Society for Imaging Science and Technology.
10. Midtjord, H., Green, P., Nussbaum, P. (2019). Vividness as a colour appearance attribute. *Color and Imaging Conference*. Society for Imaging Science and Technology.

CONTRIBUTION OF COLOR INFORMATION IN INSTANTANEOUS IDENTIFICATION OF COPPER MATERIALS

Hiroki Ishiyama¹ Midori Tanaka² Takahiko Horiuchi^{1*}

¹*Graduate School of Science and Engineering, Chiba University, Japan.*

²*College of Liberal Arts and Sciences, Chiba University, Japan.*

*Corresponding author: Takahiko Horiuchi, horiuchi@faculty.chiba-u.jp

Keywords: Material perception, Instantaneous identification, Metallic object, Visual experiment

ABSTRACT

Humans can easily identify metallic materials without using higher-order physical information. In this study, we conduct a psychophysical experiment based on the hypothesis that color information affects the instantaneous identification of copper. We created four types of copper metal balls as test images using computer graphics. The surrounding color scene was reflected on the balls of the test images. In each test image, we generated test stimuli in which the color gamut was expanded in ten steps, such that a part of the reflected color was deviated from the color gamut of the copper material. In our experiment, we checked the accuracy and speed of copper material identification using rapid presentations. The experimental results revealed the following: (1) Compared to the color gamut of the reflected colors of real copper objects, stimuli could not be easily identified as copper material when they were too narrow or wide; (2) A reproduced color image with a color gamut slightly wider than that of a real copper object was easily identified as copper material; (3) When the presentation time was shortened, identifying the copper material was difficult. However, the color gamut boundary identifiable as the copper material was stable; (4) The minimum presentation time required to identify the copper material varied depending on the reflected surrounding scene. The identification task was successfully performed when the presentation time was 300 ms. However, in a simple reflection scene, participants identified the copper material in less than 100 ms. Thus, color distribution in an object contributes to the instantaneous perception of metals by humans.

INTRODUCTION

Metallic materials are common in our daily life. Copper has the same chromaticity as orange and reddish brown, but it can be identified as a metallic color using higher-order physical information associated with the gloss phenomena, such as spatial light reflection. However, as we can instantly perceive that a material made of copper is metallic, it is natural to consider that complex physical information is not processed in early vision.

Conventional studies reported that humans could quickly identify materials. Motoyoshi et al. focused on the perception of surface gloss [1]. They hypothesized that simple image statistics contributed to the identification of surface gloss and showed that the skewness of the luminance histogram and sub-band filter outputs correlated to surface gloss and inversely correlated to surface albedo. They also found evidence that human observers use skewness, or a similar measure of histogram asymmetry, to judge the characteristics of surfaces. Sharan et al. investigated the speed of material categorization [2]. They displayed images classified into nine categories based on the material with short presentation times of 40, 80, and 120 ms, and found that the categories could be identified quickly, requiring only 100 ms more than simple baseline tasks. However, they did not

investigate metal objects or discuss metal perception. Based on both the results, it is expected that metallic objects can be identified using simple image features.

In this study, we conducted a psychophysical experiment based on the hypothesis that color information affects the spontaneous identification of copper materials. Reference [1] discussed only luminance information for the perception of surface gloss. This was the first study to investigate color information.

ANALYSIS OF COPPER MATERIAL

First, we measured the reflected color of a copper object to analyze the properties of the color generated by metal objects. The X-Rite ColorChecker under the illuminant at a temperature of 6000 K was reflected on a real copper board, and spectral power distributions of the original color patch and reflected components were measured using a spectroradiometer (Konica Minolta CS-2000). Subsequently, we derived a spectral reflectance of the copper board from the data. To simulate changes in the color gamut from the original object to the reflected color, we used the spectral reflectance database [3], which included 24 colors of the Macbeth color checker and 1269 colors of the Munsell color chart. A partial dataset of the database was used as the surface spectral reflectance of the original object. Using the derived spectral reflectance of the copper board, we calculated the spectral power distribution of the reflected color component.

Figure 1 shows the changes in the color gamut from the original color to the reflected color. The green points represent the chromaticity of the original object, and the orange points represent the chromaticity of the reflected component on the copper board. The colored area represents the color gamut. The arrows extending from the chromaticity points show the changes in chromaticity. The color gamut of the reflected color generally shrank compared to that of the original object, and each metal type had a unique color gamut.

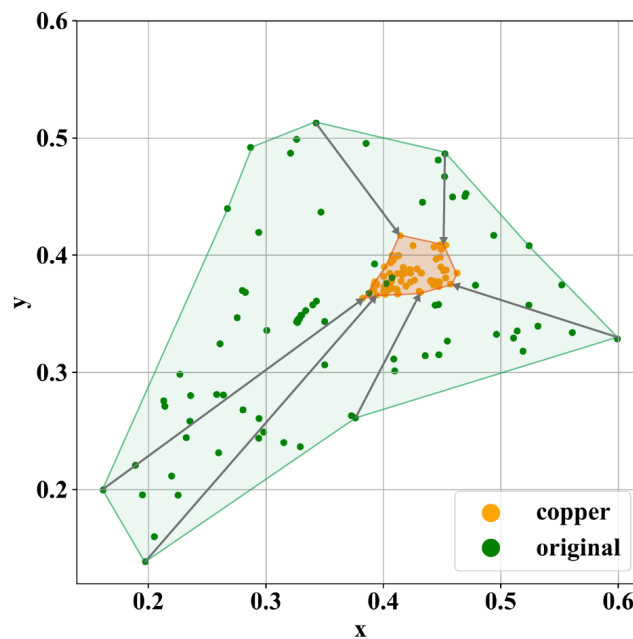


Figure 1. Changes in the color gamut

EXPERIMENT

Test Stimuli

To verify whether color information has an effect on the identification of metals, we focused on the color gamut of the reflected color component from a copper object. As the test stimulus, we considered using either a real metal or computer graphics (CGs). Subsequently, in this study, we decided to create a copper material image using CGs, which could freely set the color.

The image was created using a 3D software (MAXON Computer, Cinema4D). The reflection property of a spherical surface was provided by the Trowbridge-Reitz model (GGX). Only the specular reflection was set with parameters of a metal sphere. The copper material in the layer Fresnel preset was applied. Four types of high dynamic range images in Ref. [4] were used as images of environment scenes. Therefore, four types of original scenes were generated. As these original scenes exceeded the color gamut of the copper board from the previous section, the color gamut was normalized such that 98% of all pixels would exist within the color gamut. Figure 2 shows the normalized images. Further, in each spherical image, we generated 10 samples that extended the color gamut of a specific object reflected in the image by extending the distance from the white point to the chromaticity point of each pixel at equal intervals. The intervals were the ratio to the distance measured subjectively for each normalized image, as follows: 0.6, 4.0, 0.5, and 0.6 for scenes 1, 2, 3, and 4, respectively. In other words, when the color gamut of the normalized spherical image was 1, the ratio of the maximum color gamut for each scene was determined as follows: 6.4, 37.0, 5.5, and 6.4 for scenes 1, 2, 3, and 4, respectively. The ratio of scene 2 was high because the allowable range of the color gamut of the sky region was large in the preparation experiment. Figure 4 shows a partial sample for scene 2.

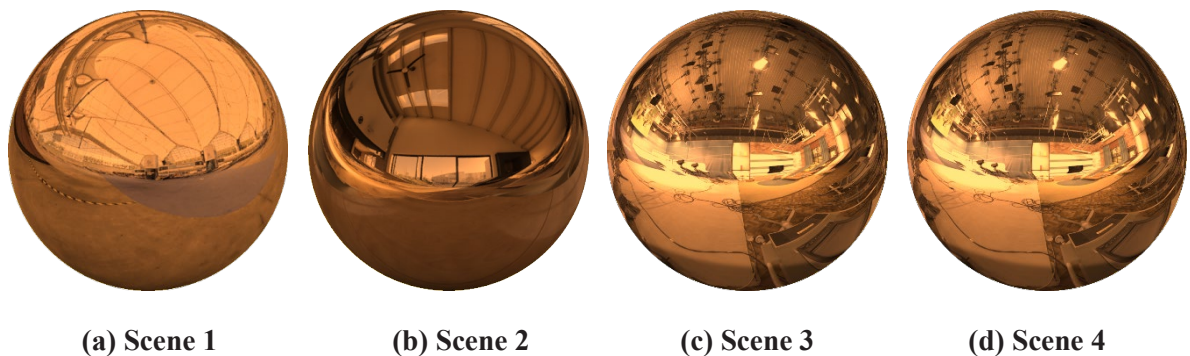


Figure 2. Four types of normalized spherical images

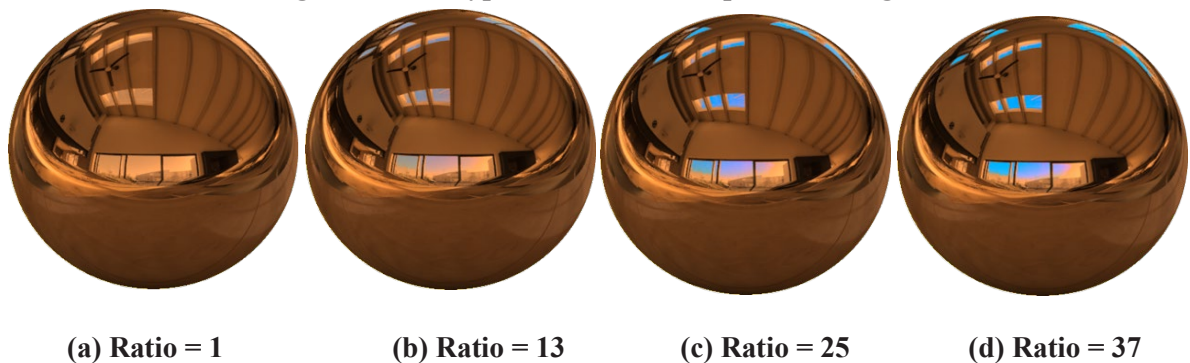


Figure 3. A partial sample for Scene 2

Procedure

The experiment followed the procedure by Sharan et al. [1], but the presentation times were 40, 80, and 120 ms. Their experiments aimed at categorizing materials into a single stimulus image. This study aimed at the perception of metals using chromaticity change, and the presentation time was too short to perceive differences among the stimuli. In our experiment, an initial stimulus was presented for 100, 200, 300, 400, or 500 ms. The initial stimulus was followed by four perceptual masks appearing for 33 ms (Fig. 4). We created the masks using the Portilla-Simoncelli texture synthesis method [5], which matches the statistics of the mask images to the statistics of the stimulus images at multiple scales and orientations, thereby allowing for more effective masking compared to the commonly used pink noise masks. Finally, a second stimulus was presented for the same duration as the initial stimulus. In each trial, the task was to report which stimuli were perceived as a copper material. All 45 combinations of 10 samples were evaluated for each scene using two Alternative Forced Choice Task.

For all experiments, stimuli were displayed centrally on a calibrated liquid crystal display monitor (ColorEdge CG-277, EIZO) against a gray background. The vertical scanning frequency of the display was 61 Hz, and it included the AdobeRGB color gamut. The viewing distance was 95 cm, and the viewing angle of the stimulus image was 12° , based on the experiment by Sharan et al. [1]. The experiment was performed under fluorescent lamps. Seven university students with normal color vision participated. Figure 5 shows the experimental setup.

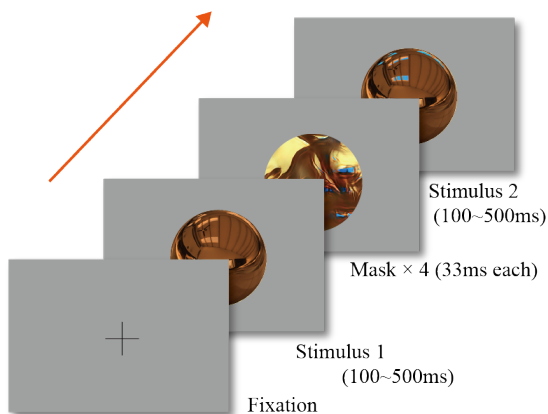


Figure 4. Procedure of the experiment

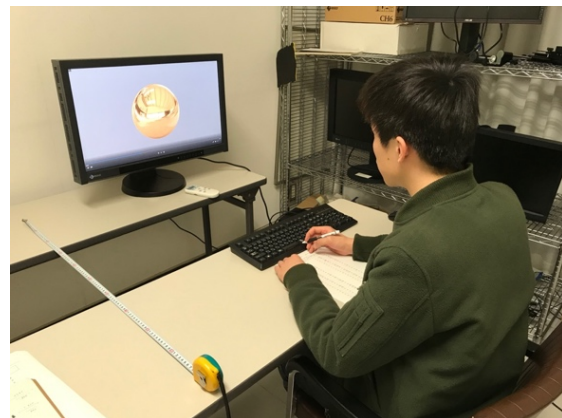


Figure 5. Experimental environment

RESULTS

Fig. 6 shows the results of an experiment by representing the Z-score for scene 2. The horizontal axis indicates the magnification rate of the color gamut of 10 samples from the normalized image, and the vertical axis indicates the Z-value. The experimental results revealed the following:

- (1) Compared to the color gamut of the reflected colors of real copper objects, stimuli could not be easily identified as copper material when they were too narrow or wide.
- (2) A reproduced color image with a color gamut slightly wider than that of the reflection of a real copper object was easily identified as a copper material.

(3) When the presentation time was shortened, identifying the copper material was difficult. However, the color gamut boundary identifiable as the copper material was stable.

(4) The minimum presentation time required to identify the copper material varied depending on the reflected surrounding scene.

The identification task was successfully performed when the presentation time was 300 ms. However, in a simple reflection scene, participants identified the copper material in less than 100 ms. Thus, color distribution in an object contributes to the spontaneous perception of metals by humans.

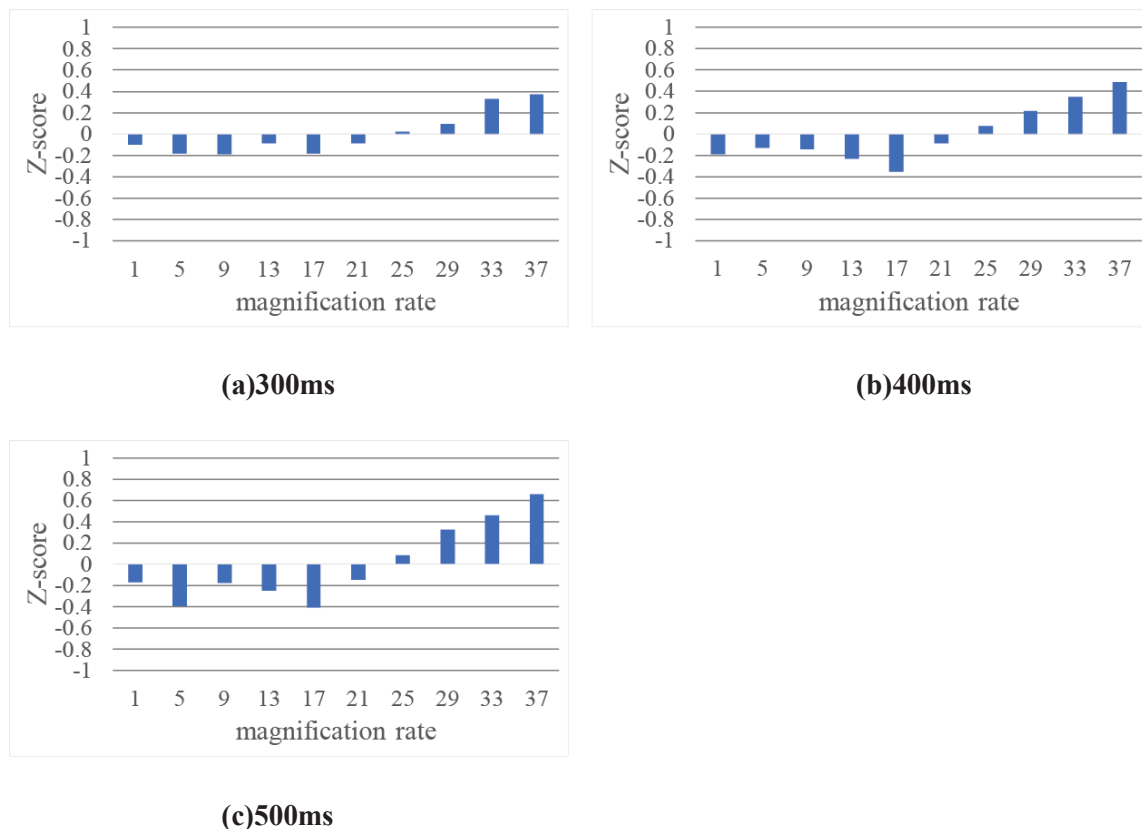


Figure 6. Z-score for Scene 2

CONCLUSIONS

This study investigated the effect of color information in the instantaneous perception of copper. In our experiment, we checked the accuracy and speed of copper material identification using rapid presentations. We confirmed that color distribution in an object contributed to spontaneous perception of metals by humans. Participants identified copper materials in only a few hundred milliseconds, and the color gamut and speed of recognition were scene-dependent. In the future, studies should be conducted on verification of different metals in various scenes.

ACKNOWLEDGEMENT

This work was supported by Grant-in-Aid for Scientific Research on Innovative Areas (No. 15H05926) from MEXT, Japan.

REFERENCES

1. Sharan, L., Rosenholtz, R., & Adelson, E. H. (2014). Accuracy and speed of material categorization in real-world images. *Journal of Vision*, 14(9), 1-24.
2. Motoyoshi, I., Nishida, S., Sharan, L., & Adelson E. H. (2007). Image statistics and the perception of surface qualities. *Nature*, 447, 206-209.
3. Barnard, K., Martin, L., Funt, B., & Coath, A. (2002). A Data Set for Colour Research, *Color Research and Application*, 27(3), 147-151.
4. sIBL Archive, <http://www.hdrlabs.com/sibl/archive.html>.
5. Portilla, J., & Simoncelli, E. P. (2000). A Parametric Texture Model based on Joint Statistics of Complex Wavelet Coefficients. *International Journal of Computer Vision*, 40, 49-70.

FORMULATION OF METAL TEXTURE EVALUATION FROM IMAGE FEATURES CONSIDERING VISUAL CHARACTERISTICS

Nozomi Tobaru^{1*}, Noriko Yata¹, Yoshitsugu Manabe¹, Yoko Mizokami¹

¹Chiba University, Japan.

*Corresponding author: Nozomi Tobaru, tobaru90226@chiba-u.jp

Keywords: Material perception, Evolutionary computation, Psychophysics computational, Modeling

ABSTRACT

In recent years, computer graphics (CG) have been developed, and it has become possible to express texture more realistically. However, since the producer needs to adjust many parameters to represent detailed CG, high ability and experience are required. Therefore, CG parameters can be set more quickly if there is an objective index for judging the texture.

The relationship between textures and physical properties has not been cleared yet although the perception of texture for objects varies greatly depending on the physical properties of the object surface. Therefore, it is not possible to easily judge what kind of textures is from which physical properties.

We focus on the texture of metal and propose a method to estimate the metallic feeling that represents how it looks like metal from the image feature obtained from a single image.

In this research, Cartesian Genetic Programming (CGP), which is a type of evolutionary calculation, optimizes the combination of operation nodes. It formulates the objective variable by constructing a network that realizes the input/output relationship that matches the learning data. CG data are used to create learning data because it is difficult to prepare real objects of various textures. For the generation of CG images, PBRT (physically based rendering from theory to implementation), which is a physics-based renderer used in academic applications, is used. First, the feature amounts of images are calculated in each of the object area and the background area of the generated CG images. Next, a subjective evaluation experiment is performed on the generated CG images by the rating scale method, and the human perception of metal texture is quantified as a metallic feeling. The input variable is an image feature quantity, and the output value is a metallic feeling. Then learning by CGP is performed, and a formula for evaluating the texture of the metal is estimated. As a result, it was confirmed that the object area information is more important than the background area information. Moreover, it turned out that the over-learning by illumination light can be reduced by including the information of the background area.

1. INTRODUCTION

The perception of the texture of human objects varies greatly depending on the physical properties of the object surface. It is not possible to determine physical properties that cause texture because the relationship between texture and physical properties has not cleared. This study proposes a method for constructing an evaluation formula with high readability in consideration of human visual characteristics for judging how looks like metal from image features calculated from a single image.

2. PROPOSED METHOD

In this chapter, we describe a proposed method that formulates the relationship between image features and metal texture using evolutionary computation.

2.1. Overview

In this study, the objective variable is defined by constructing a network that optimizes the combination of operation nodes by Cartesian Genetic Programming (CGP) [1]. Although it is formulated, a large amount of learning data is required to improve versatility. However, since it is difficult to prepare real objects with various textures, learning data is created using CG images. The degrees of look like metal in the image is used as metallic feelings. The flow of the proposed method is following.

1. Generate CG images with various textures.
2. Perform a subjective evaluation experiment and correlate each CG parameter with a metallic feeling.
3. Calculate the image feature.
4. Formulate by CGP and evaluate.

2.2. Generating CG images

We use physics-based rendering to make the CG images more realistic. It is a rendering method that measures physical phenomena and models them more precisely by mathematical formulas. This research uses PBRT (physically based rendering from theory to implementation) [2], which is a physical base renderer used for academic purposes, to reproduce various textures using metal, plastic, and glass models. The reflection on the object surface is reproduced by environment mapping, but the data is expanded by changing the environment map and camera position. Figure 1 shows examples of changing the reflection parameters for each of the three models. Figure 2 shows examples of changing the environment map [2][5].

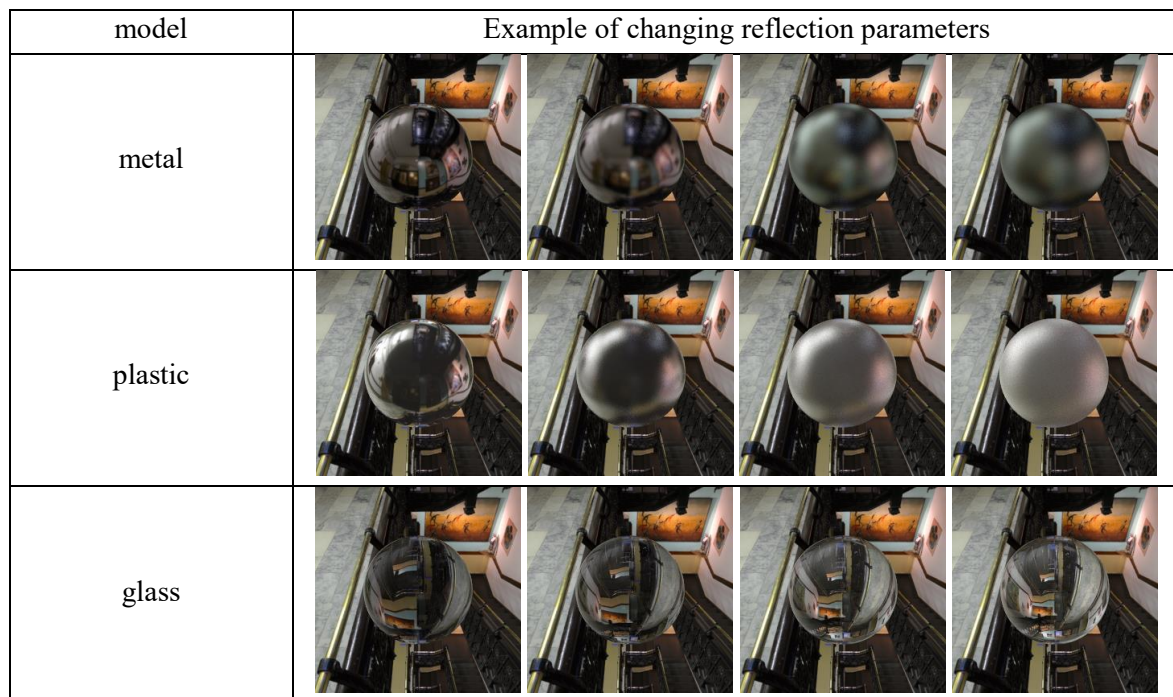


Figure 1. Example of changing the reflection parameters for each of the three models

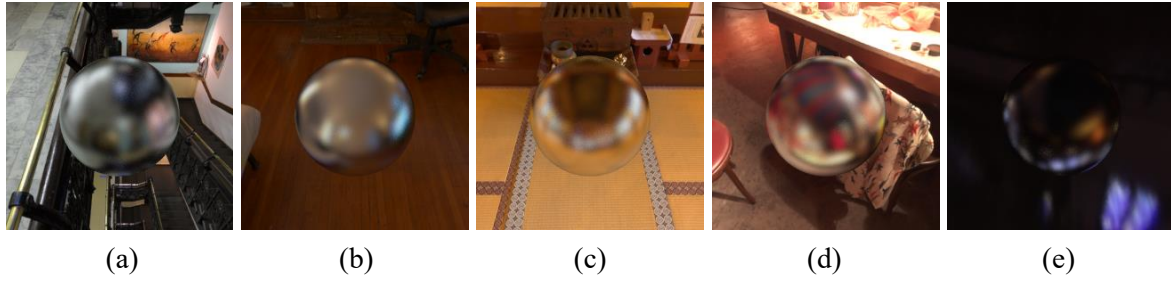


Figure 2. Example of changing the environment map

2.3. Subjective evaluation experiment

Based on the rating scale method, subjects are asked to evaluate whether the CG image of various parameters generated looks like metal in four stages (1 to 4). The average value of the judgment results of multiple people is used as the correct value for the metallic feeling and is associated with each parameter. For the expanded data, the value of the result of subjective evaluation for CG images with the same parameters is used.

2.4. Image feature calculation

The method employs the following 26 types of features with considering visual characteristics.

- Average \bar{V} and variance V_V of brightness V values in HSV color system
- Average \bar{E} and variance V_E of edge extracted images
- Median size S of SIFT[3] feature vector
- Histogram features in wavelet pyramid images

Calculate the following parameters with W_1 as the horizontal subband image and W_2 as the vertical subband image.

- Average $\overline{W_1}, \overline{W_2}$
- Variance V_{W_1}, V_{W_2}
- Kurtosis U_{W_1}, U_{W_2}
- Skewness K_{W_1}, K_{W_2}
- 10, 50, 90 percentile value $W_{1(10\%)}, W_{1(50\%)}, W_{1(90\%)}, W_{2(10\%)}, W_{2(50\%)}, W_{2(90\%)}$
- Features in luminance histogram
 - Average \bar{L}
 - Variance V_L
 - Kurtosis U_L
 - Skewness K_L
 - 10, 50, 90 percentile value $L_{10\%}, L_{50\%}, L_{90\%}$

2.5. Formulation with CGP

CGP can search a network that outputs a value closest to the correct value using the dataset of feature values for input, and metallic feelings for the correct values. And it can construct an estimation formula from the network. This research uses SPEA2[4] as a search method to construct a network having high accuracy and small size for easy to understand the relationship between

features and metallic feeling. We also experiment and compare the case of using 1 + 4ES which only consider to accuracy as a search method.

3. EXPERIMENT

In the experiment, 150 types of CG images with different parameters were prepared and correlated with metallic feelings through subjective evaluation experiments. Next, 1350 training images were generated using three types of environment maps shown in Figure 2 (a) to (c), and 26 types of feature quantities were calculated for each of the object region and background region. Then, learning data was prepared for two cases with and without features of the background region. In particular, when learning was performed with 52 variables using SPEA2, the usage rate of the feature amount of the object region was 89%, and the usage rate of the feature amount of the background region was 11%. The estimation formula with the highest fitness for the training data is shown below. The background region features are suffixed with B.

$$M_{26(SPEA2)} = \exp(W_{2(90\%)}) + \frac{\frac{V_V - V_E}{\sqrt{|V_V - V_E|}}}{\exp(\sqrt{|V_V - V_E|} - \sqrt{|W_{2(50\%)|})}} \quad (1)$$

$$M_{52(SPEA2)} = \exp(W_{2(90\%)}) + \frac{V_E - V_V}{(\bar{V}_B + L_{90\%}) \cdot (1 - 2 \cdot W_{1(90\%)})} \quad (2)$$

$$M_{26(1+4ES)} = \exp(W_{2(90\%)}) - \bar{E} - \frac{\frac{V_E}{W_{1(90\%)}} - L_{90\%} + W_{1(10\%)}}{\sqrt{\left| \frac{V_E}{W_{1(90\%)}} - L_{90\%} + W_{1(10\%)} \right|}} \quad (3)$$

$$M_{52(1+4ES)} = \exp(W_{2(90\%)}) + \frac{\exp(2 \cdot S_B) \cdot (\bar{E}_B + V_V - \frac{V_E}{W_{1(90\%)}})}{\sqrt{\left| \bar{E}_B + V_V - \frac{V_E}{W_{1(90\%)}} \right|}} \quad (4)$$

In addition, verification data was created using 450 images for verification generated by two types of environment maps shown in Figure 2 (d) to (e) different from the training images.

Table 1 shows the results of calculating the mean square error (RMSE) between the correct value of the metal feeling and the output of the estimation formula with the highest fitness for the verification data.

Table 1: Performance evaluation of estimation formula by RMSE

(a) Environment map1		
	26 variables (without background features)	52 variables (with background features)
SPEA2	0.515	0.539
1+4ES	0.427	0.488

(b) Environment map2		
	26 variables (without background features)	52 variables (with background features)
SPEA2	0.602	0.680
1+4ES	1.108	0.601

4. DISCUSSION

It can be seen that Eq. (1) to (4) contain the term $\exp(W_{2(90\%)})$ or $\exp(W_{2(90\%)} - \bar{E})$. $W_{2(90\%)}$ is the 90% tile value of the vertical subband image in the wavelet pyramid image. It is used as a substitute for the maximum value to eliminate the effects of high values due to noises. The wavelet transform can perform edge detection and corner detection considering the spatial frequency. Therefore, it is considered that the reflection of the spatial frequency with high human contrast sensitivity is successfully acquired.

Besides, V_V and V_E values are also often used. V_V is the variance of brightness and is a parameter selected in consideration of the property that the brightness contrast of metal is higher than that of other materials. V_E is the variance of the pixel values of an image whose edges are extracted by a Laplacian filter, and it is expected to measure the number of reflections. Since these values are often used, it is thought that the variance of brightness and the variance of edge-extracted images are physical properties that affect the metallic appearance.

Table 1 (a) shows that RMSE is smaller and accuracy is higher when 1 + 4ES is used. It is because 1 + 4ES is only intended to improve accuracy. On the other hand, SPEA2 aims to reduce the size of the expression, so an expression with relatively high readability is obtained. It can also be seen that the 26 variables are more accurate. The usage rate of the parameters in the background region is as low as 11%, which is less important than the information in the object region.

Looking at Table 1 (b), the accuracy of 1+4ES is worse in the case of 26 variables. It is thought to be because the over-learning could not support the verification environment map 2, which is darker than the training environment map. On the other hand, since SPEA2 maintains accuracy, it can be considered that it has the effect of preventing overlearning by limiting the size of the expression. For 52 variables, 1 + 4ES is more accurate. It was possible to cope with changes in illumination light by including background information. Therefore, it is considered that including background information has the effect of preventing overlearning for illumination light.

5. SUMMARY

In this study, we investigated a method of constructing a metal texture evaluation formula based on image features considering visual characteristics by evolutionary computation and investigated its relationship. In the future, we would like to increase the environment map of images during training so that they can be applied to real objects. We would also like to investigate changes in the importance of background features when environmental changes become large.

REFERENCES

1. Julian F. Miller, Peter Thomson: *Cartesian Genetic Programming*, Proc. Genetic Programming Lecture Notes in Computer Science, Volume 1802, pp 121-132 (2000)
2. Matt Pharr, Wenzel Jakob, Greg Humphreys: *Physically Based Rendering From Theory to Implementation*, Morgan Kaufmann Publishers, pp.533-549 (2017)
3. D. G. Lowe: Object Recognition from Local Scale-Invariant Features, Proc. of IEEE International Conference on Computer Vision (ICCV), pp.1150-1157 (1999)
4. E. Zitzler, M. Laumanns, and L. Thiele: *SPEA2: Improving the Strength Pareto Evolutionary Algorithm for Multi-objective Optimization*, Proc. of EUROGEN'02, pp.95-100 (2002)
5. sIBL Archive Free HDRI sets for smart Image-Based Lighting:
<http://www.hdrilabs.com/sibl/archive.html>

PRACTICAL RESEARCH FOR DEVELOPING LOCAL IDENTITY COLOR METHOD

Akiyo Makino¹

¹*Regional Co-creation Center for Industry and Society, Kagoshima University, Japan.*

Keywords: Local identity color, Local branding, Kagoshima pref.

ABSTRACT

Aiming at the construction of a color planning method to contribute to local branding, we studied practically in Kagoshima Prefecture, where regional revitalization is one of the most urgent issues as in the whole country. The characteristics of colors derived from local resources used for local branding are “semantic assignment type”, “local color”, “usability”, and “public collaboration”, and we named it “local identity color”. For local resources, 138 elements selected from seven areas in the prefecture and categorized to “product brands”, “environmental brands”, and “communication brands”. Then, Munsell values were calculated using either mechanical colorimetry, perceptual measurement or impression survey depending on the nature of the object. In order to cultivate local people's attachment and pride, and to aim for sustainable and independent use of colors, we conducted a local referendum and clarified the colors they would like to bring to the future. Based on it, we made the color guide samples for the top 20 colors. In the future, we will continue to develop color guides that can be used with love and pride based on the opinions of local residents as the color of “Kagonma”. To construct of a color planning method, we would like to receive evaluations from local people and improve them.

INTRODUCTION

Colors exist everywhere in the world as local resources, and it also affects human perception, cognition, emotions, impressions, value formation, etc. Such features have been used for visual identities to express the corporate philosophy and product value as branding strategy. In recent years, it has also been used as local branding.

However, take a survey of general ‘local branding’ in Japan, there are less well-designed color plan that guarantees consistency between the local brands in a broad sense and the local brands in a narrow sense. As a result, the impression for an area may be scattered even though it is in the same area, and therefore, there is a difficult to express their attractiveness enough. There is a need for the color plan that connect local brands in a broad sense and a narrow sense and contribute to regional revitalization.

The aim of this study was to establish a method for this purpose, and we decided to examine it practically in Kagoshima Prefecture, where regional revitalization is one of the most urgent issues as with it throughout Japan.

LOCAL BRANDING AND COLOR

In this study, the definition of local branding as follows; a strategic approach to create sustainable economic and cultural development of the local area by creating, establishing and strengthening

new value to resources that originally and potentially existing resources such as history, culture, tradition, climate, people, people's lives, buildings, industries, and so on.

Aoki (2004) considered that the image connection between the whole local area and individual elements is important in order to build a stronger local brand. Tanaka et al. (2012) pointed out that stronger local branding requires a new approach to bundle various resources with higher-level concepts, that is, to integrate the image of local resources. Akazawa et al. (2015) showed the importance of unified visual design. Ohori (2011) introduced the potential of the local community's vitality by introducing and clarifying a new element of the concept of "local identity" defined as "regional personality and uniqueness".

Hirata et al. (2013) clarified the characteristics of landscape color guidelines that can be used for local branding, focusing on the regional value improvement given by landscape colors. According to the survey, the feature was a "semantic assignment type" given a name that would represent a local resource with a specific color number. By searching for psychological theories that support this view, we can find an associative network model of memory by Collins & Loftus (1975). Keller (1991) relies on this associative network model of memory and cites two brand dimensions: brand recognition and brand image. This shows the possibility that strong brand recognition and image can be obtained if the image of specific color and regionality is more strongly associated.

Therefore, if local brands in a broad sense and narrow sense are integrated, and a "semantic assignment type" color planning method that expresses "individuality and uniqueness of the local area" can be developed, it may contribute to regional revitalization. In this study, the color derived from local resources was called "local identity color" and examined as follows.

CONCEPT OF LOCAL IDENTITY COLOR

In order to connect local brands in a broad sense and a narrow sense, and to give consistency to both sides, local identity color offers "semantic assignment type" (described the above), "local colors", "usability", and "public collaboration".

As for "local colors", Ozaki (1999), a practical study of "semantic assignment type" color guides on local colors, was related to the natural environment, history and culture, and Miyauchi (2008) was related to the natural environment, heritage tradition, temperament human. In local brand research, local brands are explained by the shape of an umbrella made up of multiple local brands (Aoki, 2004), and the narrow sense was categorized into "product brands", "environment brands", and "communication brands" (Aoki, 2004; Hakuodo, 2006; Hirata et al., 2013). Therefore, the same configuration was used for this study.

As for "usability", from the efforts in Sapporo City, Shinagawa-juku and Hakuba Village, is considered below.

1. Description of color samples and numerical color data
2. Clarified color concept
3. Enhancement of color schemes and usage examples
4. Building own color system

As for "public collaboration", "Traditional colors of Hyogo Gokoku" (DIC Graphics, 2018) cooperated with a local newspaper and selected five symbol colors in a referendum. This procedure contributed to the nurturing of local attachment and pride to the residents and to the sustainable and proactive use of colors.

EXPERIMENTAL

The process up to the construction of the color guide required to share and utilize the local identity color among related parties is as follows.

1.Examination of basic matters

- ①Purpose: To make a color guide prototype to contribute to local branding in the target area.
- ②Target site: The entire Kagoshima prefecture.
- ③Application: “product brands” is mainly set as clothing, “environmental brands” is a signboard, and “communication brands” is a homepage.
- ④Color system and description: Munsell value, CMYK value, RGB value, name of survey target, explanatory text on survey target, etc. Some colors also have DIC color guide numbers.
- ⑤ Number of recorded colors: According to Yamaba et al. (2015) and “70 colors of landscape colors in Sapporo”, the upper limit is “more than 500 colors and no more than 1,000 colors” and the lower limit is “70 colors”. In this study, the target number of recordings was set to about 100 colors.
- ⑥Local resources: We referred to the landscape and emotion color survey in the target area (Kagoshima Prefecture, 1975) and the creative meal event (Era, 2010) based on the image colors of the seven districts in the prefecture. Local resources were selected based on 33 kinds of tourist information pamphlets issued by local governments, prefecture homepages, and Makino (2017). Then, referring to the prefectural administrative organization rules, local resources selected from seven areas in the prefecture and categorized to “product brands”, “environmental brands”, and “communication brands”.
- ⑦Method: The Munsell value was calculated using either mechanical colorimetry or visual colorimetric impression survey depending on the nature of the object. In addition, referring to Japan Color Research Institute (2004), CMYK values and RGB values were clarified from the obtained Munsell values.
- ⑧Color guide base material: We considered developing an color guide that using architectural paint based on the Munsell value, and effective use of existing color charts with reference to the method of Nagata et al. (2015).

2.Survey

The survey was conducted between April 2016 and January 2019. Mechanical colorimetry was performed mainly for liquid and black materials using a spectrophotometer (CR-20 and CM-5 manufactured by Konica Minolta Sensing). Perceptual measurement was conducted for elements belonging to any of “product brands”, “environmental brands”, and “communication brands”, using Japan Paint Manufacturers Association 2017 J Edition color swatches and Japan Standards Association JIS Standard Color Gloss 9th Edition, with reference to Japan Color Design Laboratory (2008) and Suzuki (2014). The observation period of all survey subjects was from 3 hours after sunrise to 3 hours before sunset. The observer was a normal color vision person who confirmed that there was no abnormality in color vision using the Ishihara color vision test.

The impression survey used color charts based on PCCS's 132 chromatic colors (12 colors × 11 tones) and 5 achromatic colors, totaling 137 colors, using Kagoshima Prefecture's characteristic words and place names. The subjects were 99 university students aged 18-21, and the most frequently selected color was used as the representative color.

3. Prototyping

At the Kagoshima Prefecture's largest design event “Kagoshima Design Fair 2019”, we conducted a local referendum (Fig.1). We got 1,530 effective votes by visitors and clarified the colors that they would like to bring to the future. Based on it, we made the color guide prototype for the top 20 colors (Fig.2). After that, the results of the local referendum (Table.1) were reported on the Kagoshima University website and introduced in local newspapers and TV programs.

For sustainable use by local people in the future, it is necessary to protect the intellectual properties of the color guide. Therefore, we tried to obtain trademark rights for the results of this research. We decided to name the color guide “Kagonma Color” and we did the procedures for the trademark registration, because local people sometimes call their hometown “Kagonma” instead of “Kagoshima”.



Fig. 1. Local referendum and Flyer



Fig. 2. Color guide prototype

RESULTS AND DISCUSSION

We received various opinions about the “Kagonma Color” from local people. Based on these, we will conduct the additional research and try to fix the color guide that can be used with attachment and pride. At the same time, we will consider creating a concept sheet and color scheme proposal, according to the assumed usage site. In addition to the use of the existing color order system, creating an original color system is also effective for promoting understanding. To construct of a color planning method to contribute to local branding, we would like to receive evaluations from local people and improve them.

Table 1. The results of the local referendum

■ 1位～20位

no.	順位	投票数	カラー	意味	マンセル値に基づく系統色名(LS Z B102)	説明	マンセル	R	G	B	C	M	Y	K
1	1位	139	赤	「きばいやんせ」のイメージ	ごくあざやかな赤	鹿児島弁で「頑張ってください」の意。元気を奮ける地域のこぼ	4R4.5/14	205	45	71	25	93	66	0
2	2位	91	青	「鶴江湾」のイメージ	明るいきみの青	鹿児島県の薩摩半島と大隅半島に挟まれた湾。湾名の元は薩摩家次公の歌	5B 6/8	0	162	192	76	22	24	0
3	3位	87	青	ルリカケス	こい紫みの青	奄美大島、加計呂群島、諸島のみに生息。県の鳥。国指定天然記念物	7.5PB3/10	52	66	137	90	83	22	0
4	4位	80	赤	「桜島」のイメージ	明るいきみの赤	鶴江湾にある活火山。現在も約5,000人が桜島と共生して生活している	7RP7.5/8	247	163	185	3	49	12	0
5	5位	79	赤	キンカン	ごくあざやかな赤	生で皮ごと食べられる。爽やかな芳香。鹿児島県は全国第2位の生産量	5YR6.5/14	242	132	0	5	60	94	0
6	6位	54	緑	「大隅」のイメージ	つよい緑	鶴江湾の東岸にある半島。生命を支える食料基地として全国的に有名	4G6/8	60	166	117	73	16	66	0
7	7位	49	赤	薩摩切子の金赤	ごくあざやかな赤	幻の色。純金をガラスの材料に使用しており、華やかな高級感がある	5R4/14	187	24	51	34	100	84	1
8	8位	47	赤	桜島小みかん	ごくあざやかな赤	世界一小さいミカン。桜島、旭島地域などで生産される	2.5YR6/14	235	111	14	9	69	95	0
9	9位	44	青	薩摩切子の藍	ごく暗いきみの青	薩摩切子を代表する伝統色。清々しくも凛とした色合いが特徴	5PB2/2	42	49	63	86	80	63	39
10	10位	41	紫	薩摩切子の烏津紫	こい紫みの青	金とコバルトを使用。透明度が高く、鮮やかで高貴な紫	5P3/8	95	55	112	76	91	36	2
11	11位	36	青	坊津	やわらかい青	日本三大津の一つ。江戸時代には海外貿易の拠点として栄えた	10B6/6	98	155	185	65	31	22	0
12	12位	35	赤	薩摩切子の紅(べに)	こい赤	絹を使って染色させたシックな赤色。重厚感が漂う	5R3/10	139	23	43	48	100	87	19
13	12位	35	緑	龍川の滝	こい青緑	南大隅町にある滝。幾何学模様の節理とエメラルドブルーの水色が美しい	10BG4/8	0	112	127	87	51	48	1
14	14位	30	黄	「てけてけ」のイメージ	ごくあざやかな黄	そこそこ、適当に、適当。心のゆとりを表す地域のこぼ	5Y8/13	236	197	0	14	25	92	0
15	15位	26	紫	ミヤマキリシマ	明るいきみの紫	県の花。霧島山系一帯を中心に自生する。「深い山に咲くツツジ」の意	5RP6/8	200	125	153	27	61	24	0
16	16位	24	灰	桜島の灰	暗い灰色	桜島から日常的に地上に降り込む灰。厄介者であり自然の恵みの一部	N3	71	72	72	75	68	65	27
17	17位	23	青	土盛海岸	やわらかいきみの青	奄美大島にある海岸。輝く水面はブルーエンジェルとも言われる	5B7/4	132	182	194	53	19	24	0
18	17位	23	紫	シバザクラ	ごくあざやかな紫みの赤	春の到来を告げる花。霧島高原では日本一早く咲くシバザクラが楽しめる	2.5RP4/12	159	55	125	48	90	25	0
19	19位	22	緑	薩摩西郷梅	うすいきみ緑	さつま町名産。初夏の味覚。実が大きく、果肉は厚くて柔らかいのが特徴	7.5GY8/6	173	212	138	40	5	57	0
20	20位	21	赤	オッのコンボ	ごくあざやかな紫みの赤	江戸時代から鹿児島に伝わる。台所に置く起き上り小法師人形	7.5R4/14	185	32	33	34	99	100	2

■ 21位～50位

21	21位	20	赤	プリンセスのや	7.5R4/14	185	32	33	34	99	100	2			
22	21位	20	緑	イヌマキ	7.5GY8/6	173	212	138	40	5	57	0			
23	23位	19	青	佐多岬から見た黒船	5PB8/4	183	202	226	33	17	7	0			
24	23位	19	黒	「鹿児島県」のイメージ	N1.5	38	38	38	82	77	75	56			
25	25位	16	赤	タカエビ	10R6/12	233	110	67	9	70	78	0			
26	26位	15	赤	朝雲の赤	5R4/14	187	24	51	34	100	84	1			
27	26位	15	黄	拍車海岸のルーピン	2.5YR/14	252	190	0	5	32	90	0			
28	26位	15	黒	大島輪	N1.5	38	38	38	82	77	75	56			
29	29位	14	黄	マンゴーの実	7.5YR7/14	245	151	0	5	62	88	0			
30	29位	14	黄	丸炭炭	2.5YR/12	248	191	19	7	31	88	0			
31	29位	14	黄	可憐の新茶	2.5GY5/6	119	127	48	62	46	99	3			
32	29位	14	黒	「薩摩」のイメージ	N1.5	38	38	38	82	77	75	56			
33	33位	13	赤	ハイビスカス	7.5R4/12	176	49	43	38	93	93	4			
34	34位	12	黄	薩摩切子の黄	7.5Y8.5/12	238	216	0	14	15	90	0			
35	35位	11	赤	シラス	10YR6.5/2	175	158	138	38	38	45	0			
36	35位	11	青	鹿児島市街から見た桜島	5G4/2	80	101	90	74	56	65	11			
37	35位	11	青	鹿児島市街から見た鶴江湾	5BG7/1	162	177	174	42	25	30	0			
38	35位	11	黒	黒豚	N2.5	60	60	60	77	71	69	37			
39	39位	10	赤	霧島神宮	10R5/10	194	90	57	30	76	82	0			
40	39位	10	青	薩摩切子の緑	5BG3/6	0	83	81	92	60	67	22			
41	39位	10	青	丸池湧水	5BG7/2	150	180	175	47	22	32	0			
42	42位	9	青	薩摩黒切子	5B3/1	63	73	77	79	68	63	25			
43	42位	9	赤	かるかん	N9.3	235	235	235	9	7	7	0			
44	44位	8	赤	カイコウス	5R4/14	187	24	51	34	100	84	1			
45	44位	8	赤	薩摩焼	7.5R3/6	116	51	47	53	86	81	29			
46	46位	7	赤	タンカン	2.5YR5/12	196	90	17	30	76	100	0			
47	46位	7	赤	縄文杉	5YR4/4	127	87	63	55	68	78	15			
48	46位	7	黄	指輪の紫の花	10Y7/8	183	177	62	37	27	85	0			
49	46位	7	黄	黒島	5GY7/2	170	177	149	40	26	44	0			
50	46位	7	黄	アコウ	7.5GY5/4	105	129	88	66	44	74	2			

■ 51位～75位

51	51位	6	黒	黒薩摩	10YR4/1	103	95	85	66	62	65	12			
52	51位	6	青	黒之瀬戸	5B4/4	52	103	118	83	57	49	4			
53	53位	5	赤	安納芋	10R5/6	169	104	85	42	67	66	1			
54	53位	5	赤	薩摩黒田宮学生記念塔	10R4/6	142	78	62	49	76	77	12			
55	53位	5	赤	えががね	10R3/6	115	52	41	53	85	87	30			
56	53位	5	黄	朝雲の黄	10YR7/12	230	159	0	14	45	95	0			
57	53位	5	黄	しろくま	5Y9/1.5	234	227	203	11	11	23	0			
58	53位	5	黒	黒入のリュウキウフコフガイ	5GY5/4	114	127	80	63	46	78	3			
59	53位	5	赤	紅サツマ	10RP4/4	127	84	91	58	73	58	8			
60	53位	5	黒	黒糖	N2.5	60	60	60	77	71	69	37			
61	61位	4	赤	赤ぢよか	5YR2/1	57	47	43	74	75	76	49			
62	61位	4	赤	黒牛	5YR2/1	57	47	43	74	75	76	49			
63	61位	4	赤	薩摩硫黄島地	7.5YR5/8	169	107	39	42	65	98	3			
64	61位	4	赤	地蔵黒成産	7.5YR6/1.5	160	145	132	44	43	46	0			
65	61位	4	赤	黒野	5Y2/1	52	48	41	76	73	79	50			
66	61位	4	赤	漢生の火クス	2.5GY4/4	94	100	51	69	55	94	16			
67	61位	4	青	西郷隆盛銅像	10GY8/2	185	206	182	33	12	33	0			
68	61位	4	青	香木の庵	N9.5	241	241	241	7	5	5	0			
69	69位	3	赤	国司神社の鳥居	10YR8.5/0.5	218	213	207	17	16	18	0			
70	69位	3	赤	桜島大塚	2.5YR5/3	231	212	172	13	18	36	0			
71	69位	3	赤	黒糖	2.5Y5/3	138	119	87	54	54	70	3			
72	69位	3	赤	薩摩焼酎	5Y6/0.5	150	147	141	48	40	41	0			
73	69位	3	赤	獅子島の化石	5Y5/0.5	124	121	115	59	52	53	1			
74	69位	3	赤	ソテツ	5GY3/2	68	74	56	75	63	80	32			
75	75位	2	赤	豊稔	10R2/2	65	43	41	70	79	76	50			
76	75位	2	赤	あくまき	2.5YR3/4	102	61	46	58	77	83	33			
77	75位	2	赤	黒色徳研土器	5YR3/1	81	69	64	70	70	70	30			
78	75位	2	赤	薩摩焼石	5YR3/1	81	69	64	70	70	70	30			
79	75位	2	赤	薩摩焼が	7.5YR5/8	169	107	39	42	65	98	3			
80	75位	2	赤	赤土/レイショの土	7.5YR5/6	161	110	63	44	62	83	3			

■75位～104位

no.	順位	投票数	カラー	意味	マンセル	R	G	B	C	M	Y	K
81	75位	2		延喜神社の延喜	10YR7.5/6	224	180	117	16	34	58	0
82	75位	2		薩摩つばね	10YR7/6	209	166	104	23	39	63	0
83	75位	2		白鷺拳	10YR8.5/3	235	210	176	11	21	33	0
84	75位	2		鹿児島ラーメン	10YR8/3	220	196	164	17	25	37	0
85	75位	2		茶花節	10YR6/3	167	143	114	42	45	56	0
86	75位	2		宿結城灰岩	10YR4/1	103	95	85	66	62	65	12
87	75位	2		西田博	10YR4/1	103	95	85	66	62	65	12
88	75位	2		アマミノクロウサギ	10YR3/0.5	75	71	67	73	68	69	29
89	75位	2		竹製器	2.5Y8/4	221	197	148	18	25	46	0
90	75位	2		タケノコ	2.5Y9/3	244	225	184	7	14	32	0
91	75位	2		出水武尊聖数の石造	2.5Y4/1	102	95	85	66	61	65	13
92	75位	2		砂瀬しんぎ	2.5Y3/1	77	71	62	71	67	73	31
93	75位	2		長目の浜	5Y7/0.5	176	173	166	36	30	32	0
94	75位	2		十島の島バナナ	2.5GY4/4	94	100	51	69	55	94	16
95	75位	2		竹島	5GY8/2	197	203	172	28	16	36	0
96	75位	2		東串島のピーマン	5GY3/2	68	74	56	75	63	80	32
97	75位	2		普賢の青ゆき	5GY3/2	68	74	56	75	63	80	32
98	75位	2		飯島のキビナゴ	5GY8/0.5	199	201	192	26	18	24	0
99	75位	2		種子島	N6.5	160	160	160	43	35	33	0
100	75位	2		薩摩深木対馬	N3.5	84	84	84	72	65	62	17
101	75位	2		黒野野宿	N2.5	60	60	60	77	71	69	37
102	75位	2		はやとの風	N1.5	38	38	38	82	77	75	56
103	75位	2		甘口醤油	N1	28	28	28	84	80	78	64
104	104位	1		美人館	10R6/2	166	142	136	42	46	42	0
105	104位	1		ボセの飯室	2.5YR5/6	167	106	78	42	66	72	2
106	104位	1		げたんば	5YR3/3	94	65	49	62	73	81	33
107	104位	1		第五郎どんの輪染帯衣	5YR3/2	88	67	56	66	71	75	32
108	104位	1		奥十島のエドヒガン	5YR7.5/1	196	185	179	27	27	27	27
109	104位	1		ボンタン漬	10YR7.5/6	224	180	117	16	34	58	0
110	104位	1		ゴールドビーチ	10YR5/3	141	117	90	53	56	67	3

■104位～125位

no.	順位	投票数	カラー	意味	マンセル	R	G	B	C	M	Y	K
111	104位	1		吹上浜	10YR6/2	162	145	125	44	43	50	0
112	104位	1		薩生和紙	10YR9/0.5	231	226	220	12	11	13	0
113	104位	1		薩米の手ネイチョウ	5Y8/8	226	199	90	18	23	71	0
114	104位	1		オオゴマダラの羽織	5Y9/1.5	234	227	203	11	11	23	0
115	104位	1		ミキ	5Y9/1	232	227	210	12	11	19	0
116	104位	1		花瀬公園の石畳	5Y2/1	52	48	41	76	73	79	50
117	104位	1		さつま町の田の神さま	5Y5/0.5	124	121	115	59	52	53	1
118	104位	1		だっきしよ豆腐	10Y8.5/1	216	215	197	19	14	24	0
119	104位	1		志布志のワナギ	2.5GY3/1	71	72	63	74	66	73	31
120	104位	1		東串島のキュウリ	5GY3/2	68	74	56	75	63	80	32
121	104位	1		ハンダマ	5RP3/2	87	65	74	70	76	62	25
122	104位	1		ナベツル	N3.5	84	84	84	72	65	62	17
123	104位	1		クロダイ	N2.5	60	60	60	77	71	69	37
124	104位	1		川辺仙道の漆黒	N1	28	28	28	84	80	78	64
125	125位	0		パッションフルーツ	5R3/2	90	65	65	66	74	68	29
126	125位	0		高麗餅	5YR5/3	146	115	97	51	58	62	2
127	125位	0		長射伊勢	7.5YR6/1.5	160	145	132	44	43	46	0
128	125位	0		芭蕉布	10YR7/3	194	170	139	29	35	46	0
129	125位	0		ちゃんぽもち	2.5Y7/6	203	169	99	27	36	66	0
130	125位	0		普賢島の白こま	2.5Y8/2	211	199	172	22	22	34	0
131	125位	0		ガジュマル	2.5Y4/2	107	94	73	63	61	73	15
132	125位	0		川辺仙道の金吾	5Y7/6	195	172	94	31	33	70	0
133	125位	0		東エンドウ	5GY7/4	166	179	126	42	24	57	0
134	125位	0		長島島のブリ	5BG3/1	64	74	73	78	67	66	27
135	125位	0		エラブコリ	N9.5	241	241	241	7	5	5	0
136	125位	0		薩摩黒合鴨	N2	49	49	49	79	74	72	47
137	125位	0		人工黒糖おろすみ	N2	49	49	49	79	74	72	47
138	125位	0		黒湯泉	N1.5	38	38	38	82	77	75	56

※「カラー」は実際のマンセル値による表示とずれることがあります。

ACKNOWLEDGEMENT

The authors thank everyone who contributed to the present research, including Kagoshima Prefecture, Kagoshima City and local residents.

REFERENCES

1. Collins, A.M. and Loftus E. F.,(1975). *A spreading-activation theory of semantis processing*, Psychological Review, 82,407-428.
2. Keller, K.L.(1991). *Cue Compatibility and Framing in Advertising*, Journal of Marketing Research, 28, 42-57.
3. Makino, A.(2017). *Designing symbol color for regional revitalization- A study of black in Kagoshima -*, Journal of the Color Science Association of Japan 43(3+), 55, 2019.

REPRESENTATIVE COLORS OF GRAPES

Kanchaporn Jankeaw^{1*}, Kitirochana Rattanakasamsuk¹, Ryo Kihara² and Mikiko Kawasumi²

¹ *Color Research Center, Faculty of Mass Communication Technology, Rajamangala University of Technology Thanyaburi, Thailand.*

² *Faculty of Science and Technology, Meijo University, Japan.*

*Corresponding author: Kanchaporn Jankeaw, 1159108020135@mail.rmutt.ac.th, bbkan.day@gmail.com

Keywords: Grape Color, Color Memory, Representative Color

ABSTRACT

In the market, grapes are categorized into three kinds as red grapes, green grapes, and black grapes. For red grapes, the range of color sometimes can be from red, reddish brown to reddish purple. For green grapes, the range of color can be from greenish yellow, light green to dark green. For black grapes, the range of color includes black, dark blue, dark purple. We can see that the color of each kind of grape is a wide variety. However, the perception of grape color for the customer may not match with the real grape color. In this research, we want to investigate the representative color of each kind of grapes. The subject is 20 females and 20 males aged between 19-23 years old who have normal color vision. The experiment is divided into two parts. In the first part, the representative hue of grapes is identified. The stimulus is a gray background and 40 Munsell color chips. These 40 color chips are varied in hue cover every hue in Munsell color. Each color chip has chroma 8 and value 5. These 40 color chips are attached on the gray background to form the Munsell ring. Size of each color chips is two degrees of visual angle. Subject's task is to indicate the color chip which represented the color of red grape, green grape and black grape in their memory. In each trial, the subject must select at least a color chip. If the subject thinks the range of color of grape is wide, they can select more than a color chip to cover that range. This process repeats until 3 kinds of color of grapes are selected. Each subject must repeat totally 3 judgments (3 colors of grapes x 1 judgments). The result shows that the range of representative hue of red grape covers from 2.5RP, 5RP, 7.5RP, 10 RP, 2.5R, 5R and 7.5R. For green grape, the range of representative hue of green grape covers from 2.5GY, 5GY, and 7.5GY, 10GY. For the black grape, the range of representative hue of black grape covers from 5PB, 7.5PB, 10 PB, 2.5P, and 5P. These selective hues of each grape color will be used in the next part. In the second part, Munsell value and chroma of the representative color of grape will be identified. Munsell color chart of the selective hues from the first part will be presented to the subject. The subject will be asked to select every color chip which represented the color of red grape, green grape, and black grapes. The result will be used as a database for creating a color scheme for grape packaging design.

INTRODUCTION

Grapes are the 6th most popular fruit in the world [1]. Grapes can be divided into 3 main colors, which are green grapes, red grapes, and black grapes [2] [3]. Although grapes are popularly consumed as fresh fruits but grapes can be processed into other products. Product presentation is important to attract and create memories for consumers, and color is an important element on the product packaging. Previous research revealed that people make a subconscious judgment about a person, environment, or product within 90 seconds of initial viewing and that between 62% and 90% of that assessment is based on color alone [4]. Therefore, the researcher has the idea that studying color to find colors that represent grape will help increase interest in grape products and can increase value to the product. The research was divided into two parts. The first part, each subject identified the representative hue of green grapes, red grapes, and black grapes by selecting hue from Munsell

ring. For the second part, each subject identified Munsell value and chroma in the Munsell color chart.

EXPERIMENT

PART I: HUE IDENTIFICATION

The first part of experiment is to select hue that represents three types of grape color, green, red, and black grapes. The criterion of the hue identification is that the selected hue must represent the subject's image color of green grapes, red grapes and black grapes. The subject can be select an unlimited number of hue per type of green grapes, red grapes and black grapes.

Apparatus

The apparatus was a test room size of 93 cm × 62 cm × 78.5 cm. The test room was made of the whiteboard and top on the room was covered with white wax paper to filter and diffuse light. The illuminance of the subject room was measured by an Illuminance meter (Konica Minolta T - 10) and was kept constant between 1000-1200 lux. The stimulus was 40 Munsell color chips which represent the entire hue in Munsell color (Munsell Book Glossy Collection X-rite). Each color chip has chroma 8 and value 5. These color chips were pasted on a gray background paper (N6) to form the Munsell ring. The Munsell ring was placed on the wall in front of the subject. A chin rest (Takei Scientific Instruments T.K.K 930a) is used to fix the subject head's position. Each color chip contains 2 degrees of the visual angle.

Subject

The subjects were 30 undergraduates from the Department of Information Engineering at Meijo University. There were 15 females and 15 males. All of them had normal color vision.

Experimental Procedure

Before starting the experiment, the subject sees a set of photographs of 3 grape colors on a laptop. After 2 hours or more, the experiment starts. In each trial, the Munsell ring was randomly rotated. The experimenter selected a type of grapes and told to the subjects. The subject then imagined the color of that type of grape. After that, the subject select the color chips which represented the Hue of the subject's image color. There was no limitation of the number of the selected color chips. The experimenter recorded the selected Hue. These selected hues of each grape color will be used in the next part.

Result

The result of experiment 1 was shown in Figure 1. The radius of the radar graph was the frequency of the selected hue. Red line, green line and purple represented the result of the hue identification of red grape, green grape and black grape, respectively. If a Munsell hue was chosen by higher than 20% of the subject, that Munsell hue will be used in the next part of the experiment. This criterion was represented by the dashed circle line.

For the red grape, there most selected hue was 5RP and 7.5R. The other selected hue were 2.5RP, 7.5RP, 10RP, 2.5R, and 5R. For the green grape, 4 Munsell hue; 2.5GY, 5GY, 7.5 GY, and 10GY; were selected. For the black grape, 7.5PB, 10PB, 2.5P, and 5P were selected. These selected Hue were used in the next part of the experiment.

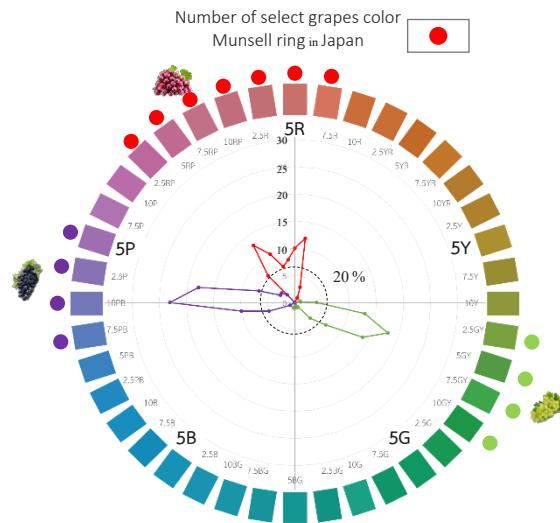


Figure 1. The selected Hue of red, green and black grapes

PART II: MUNSELL VALUE AND CHROMA IDENTIFICATION

The second part of the experiment is to identify Munsell value and chroma that represents three types of grape color, green, red, and black grapes. There are two types of value and chroma Identification. The first type is based on the subject's image color of those three grapes. The second type is based on the color which is suitable for the packaging of grape products. The subject can select unlimited number of color chips for each type of identification.

Apparatus

The test room was the same room which were used in the first part of the experiment. The illuminance of the test room was measured by an Illuminance meter (KONICA MINOLTA T - 10) and was kept constant between 1000-1200 lux. Table 1 shows the selected hue used in this part of experiment. For each hue, there was a Munsell color chart which contained several color chips. The color chips were varied in value and chroma as shown in Figure 2. A viewing mask was used when the subject selects the color chips. This viewing mask was made from 15 cm × 21 cm gray sheet (N6). There was a 1.5 cm × 2 cm square aperture at the center of the viewing mask. A laptop was used for presenting the grape's photo before the experiment started.

Table 1: The selected hue of each type of grapes

Grapes Color	Selected Hue
Green	2.5GY, 5GY, 7.5GY, 10GY
Red	2.5RP, 5RP, 7.5RP, 10RP, 2.5R, 5R, 7.5R
Black	7.5PB, 10PB, 2.5P, 5P



Figure 2: Figure 2: Munsell color chart and viewing mask

Subject

The subjects were 40 undergraduates from the Department of Information Engineering at Meijo University. All of them had a normal color vision they are female 20 people and male 20 people.

Experimental Procedure

Before starting the experiment, a set of photographs of red grape, green grape and black grape were presented to the subject. After 2 hours or more, the experiment starts. There are two tasks for each subject. The first task is to identify the image color of grapes. In each trial, the experimenter selected a type of grapes and told to the subjects. The Munsell color charts of the selected hue which corresponded to the type of grape were placed on the table. The subject then imagined the color of that type of grape. After that, the subject using the viewing mask to see the color chip through the hole, one by one color. When the subject selected the desired color, the mask will be placed on that color. The subject can choose an unlimited number of colors for each type of grapes color. This procedure was repeated until all type of grape were selected. For the second task, the procedure was same as the procedure of the first task except from the criterion of selecting color. The criterion of this task is to identify the color which were suitable for the packaging of the grape product. These two tasks were done in the separated session.

Result

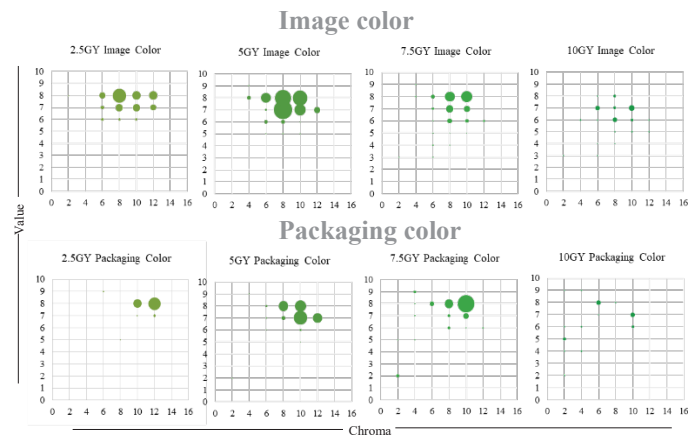


Figure 3. Comparative result between image color and packaging color of green grapes

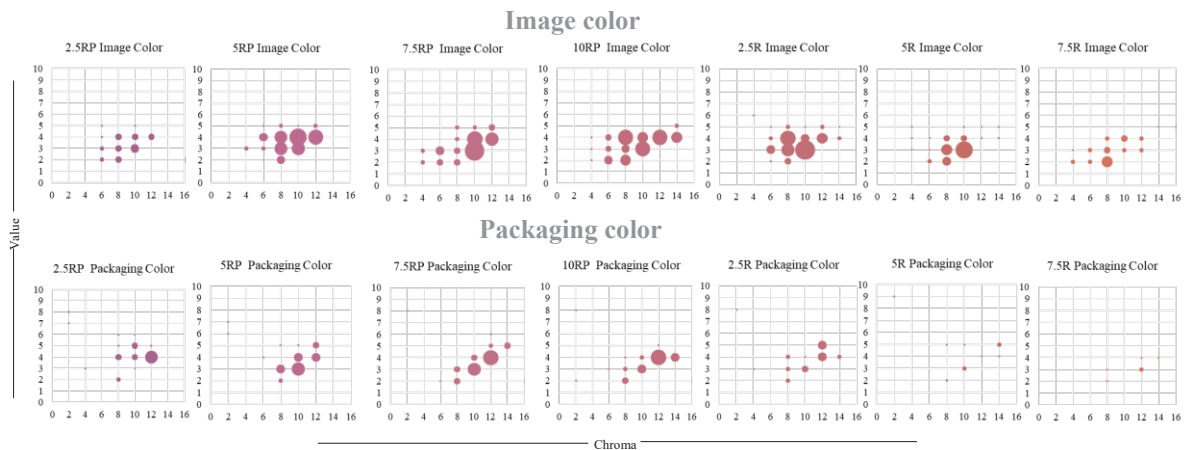


Figure 4. Comparative result between image color and packaging color of red grapes

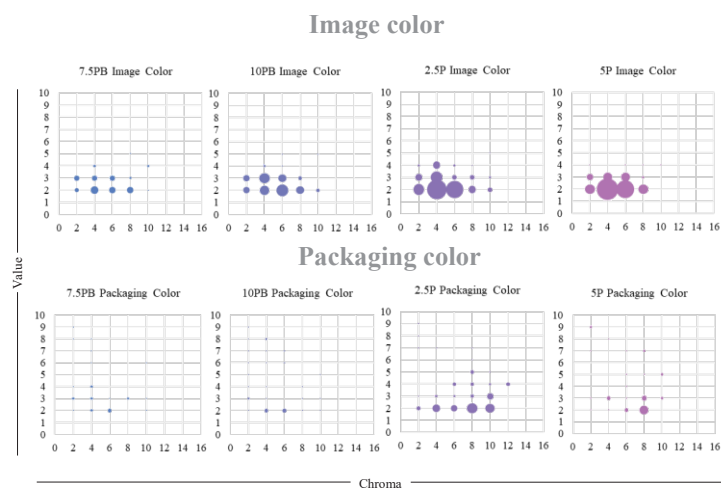


Figure 5. Comparative result between image color and packaging color of black grapes

Figure 3 shows the image color and the packaging color of the green grape. The bubble size represented the frequency of the selected color. There was some difference between these two kinds of color. Most of the image color of the green grape was greenish yellow with chroma range of 8-10 and value range of 7-8. For the packaging color, the suitable colors were more vivid and slightly darker than the image color.

Figure 4 shows the image color and the packaging color of the red grape. The image color of red grapes covered wide range of color. The Munsell hue range was from 2.5RP to 7.5R. However, the popular color of red grape was divided in to two groups; reddish purple and slightly purplish red. For the packaging color, the reddish purple was more popular.

Figure 5 shows the image color and the packaging color of the black grape. Even though this kind of grape was called as the black grapes, but the image color was darkish purple with low chroma (range of 2-4) and low value (range of 2-3). The packaging color was considerably different from image color. The subject preferred more vivid purple for the grape product packaging.

Based on our result we created the color palette for the grape packaging design. Table 2 shows Munsell color notation of the colors which were obtained from two methods. The first method was the top five rank of the selected Munsell color chips. The second method was five color calculated from K-mean cluster analysis. For the packaging design, the top 5 rank should be used as the primary color of the packaging. And the color from K-mean cluster analysis should be the secondary color to make the packaging more colorful. For the future work, the quality of these color palette must be examined. It is necessary to use these color palettes for designing the packaging of grape products.

CONCLUSION

The color palettes obtained from the image color have more variety of colors than those obtained from the packaging color. But color in the color palettes of packaging color will have more vibrant colors. To design grapes packaging, colors in the popular colors' palette can be use as primary colors. If the packaging with a variety of colors is required, color in the palettes from K-Means Cluster Analysis can be used as the secondary color.

Table 2: The color palettes from top 5 and K-Means Cluster Analysis

Grapes Color	Top 5				K-Means Cluster Analysis			
	Image Color		Packaging Color		Image Color		Packaging Color	
Green	5GY 7/8		7.5GY 8/10		5GY 7/10		5GY 8/11	
	5GY 8/8		5GY 7/10		5GY 8/9		7.5GY 6/9	
	5GY 8/10		2.5GY 8/12		7.5GY 6/9		5GY 8/9	
	2.5GY 8/8		5GY 8/10		7.5GY 7/5		7.5GY 8/5	
	5GY 7/10		5GY 8/8		7.5GY 4/5		7.5GY 4/2	
	7.5GY 8/10		5GY 7/12					
Red	7.5RP 3/10		7.5RP 4/12		10RP 4/10		5RP 4/11	
	5RP 4/10		10RP 4/12		5R 3/8		10RP 3/9	
	5R 3/10		2.5RP 4/12		5RP 4/8		2.5R 5/13	
	5RP 4/12		5RP 3/10		2.5R 3/5		7.5RP 8/2	
	7.5RP 4/10		7.5RP 3/10		2.5R 5/13		7.5RP 3/5	
	10RP 4/8							
	10RP 3/10							
	10RP 4/12							
2.5R 4/8								
Black	5P 2/4		2.5P 2/8		2.5P 3/3		10PB 3/4	
	2.5P 2/4		2.5P 2/10		5P 2/5		2.5P 2/8	
	2.5P 2/6		2.5P 2/4		10PB 2/7		10PB 4/9	
	5P 2/6		2.5P 2/6		10PB 4/8		10PB 7/3	
	2.5P 3/4		2.5P 3/10		10PB 3/3		2.5P 6/7	

ACKNOWLEDGEMENT

I would like to express my sincere gratitude to Scholarships of Co-operative Education from Rajamangala University of Technology Thanyaburi (RMUTT) for supporting my internship at Meijo University. Special thanks to Professor Mikiko Kawasumi who accepted me for internship for 3 months. Thanks to the staffs and students of Meijo University and everyone who participated as subjects in the experiment.

REFERENCES

1. Misachi, J. (2017). The Most Popular Fruit in the World. Retrieved September 10, 2019, from <https://www.worldatlas.com/articles/the-most-popular-fruit-in-the-world.html>.
2. Lancaster, J. E., Lister, C. E., Reay, P. F., & Triggs, C. M. (1997). Influence of Pigment Composition on Skin Color in a Wide Range of Fruit and Vegetables. *Journal of the American Society for Horticultural Science*, 122(4), 594–598. doi: 10.21273/jashs.122.4.594
3. Carreño, J., Martínez, A., Almela, L., & Fernández-López, J. A. (1996). Measuring the color of table grapes. *Color Research & Application*, 21(1), 50–54. doi: 10.1002/(sici)1520-6378(199602)21:1<50::aid-col5>3.0.co;2-4
4. Morton, J. (2010). Why Color Matters. Retrieved September 20, 2019, from <https://colormatters.com/color-and-design/why-color-matters>

The study on Color Design of Architecture in Korea and China Commercial Street between Korean and Chinese

Lu, Chen^{1*}

¹*School of Art and Design Faculty, Shanghai University Of Engineering Science, CHINA.*

*Corresponding author: Chen Lu, 215826091@qq.com

Keywords: Color design, Architecture, Korean and Chinese

ABSTRACT

The purpose of this study is to grasp the simplification of Architecture color in Korea and China commercial street. The basic of research is divided into four parts. The paper is the result of the basic research. In this study the current state of architectural color for traditional commercial streets and modern commercial streets in Korea and China was analyzed and a color palette was derived. In addition, a color coordination palette was created by using the color palette to evaluate the images of commercial streets in Korea and China, and to compare and analyze them. Finally, the form factors and color scheme of Korean and Chinese traditional and modern commercial street architecture were evaluated, and based on the results design direction for commercial streets in China was suggested.

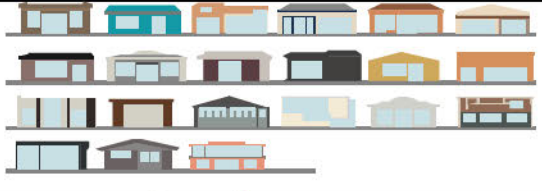
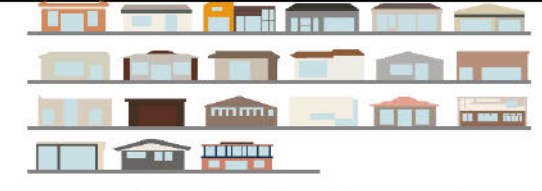
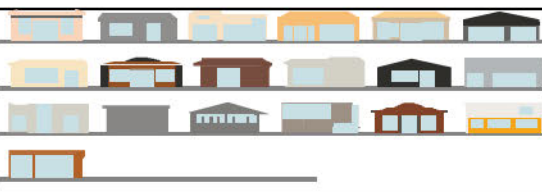
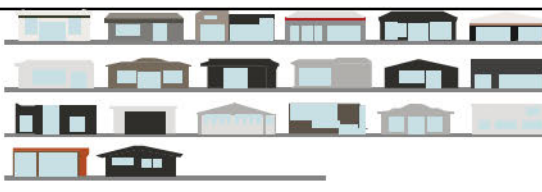
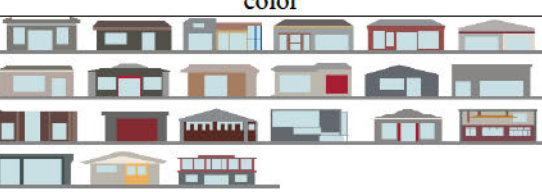
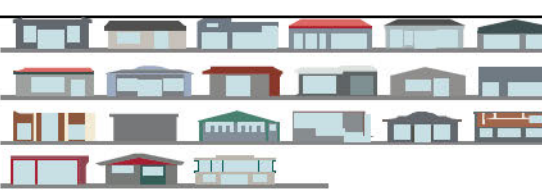
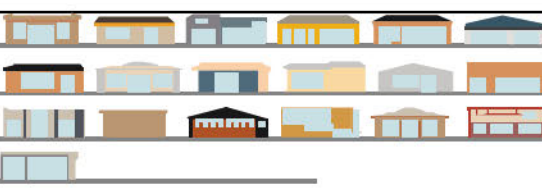
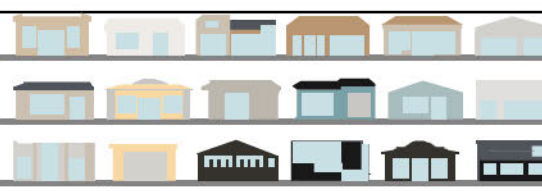
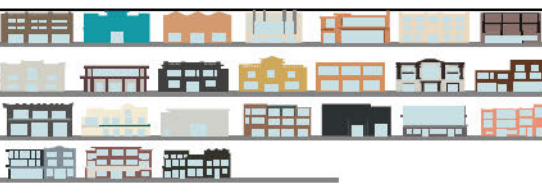
INTRODUCTION

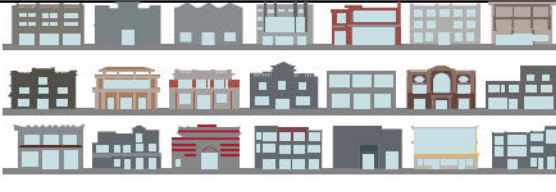
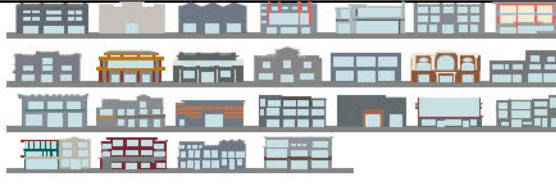
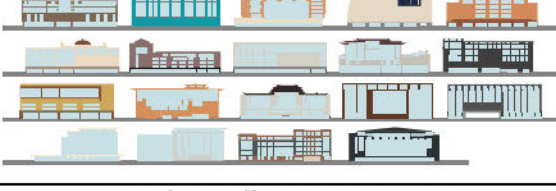
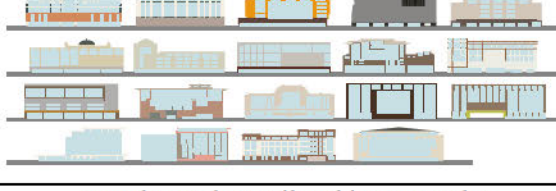
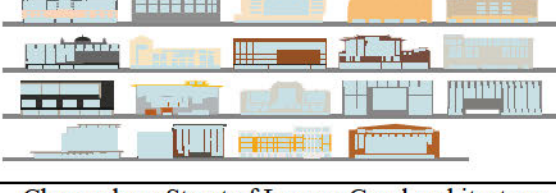
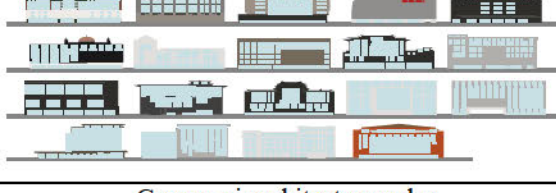
In this paper, the basic of model Architecture color is from the eight commercial streets between Korea and China. The eight commercial streets are selected and founded in Seoul and Beijing which are Insadong-gil, Samcheongdong-gil, Cheongdong Street of Luxury Good and Garosu-gi and Nanluoguxiang, Qianmendajie, Wangfujing, Xidan. This study is aimed at design of architecture color in commercial street between Korea and China.

GENERAL GUIDELINE

In this study, I measure architecture façade color. The current study uses NCS color Scan 2.0 and NCS Index original-1950 color atlas to measure physiological signals. This study is a study on the images elevation of commercial streets in Korea and China. This study is performed an operational definition to remove all variables except color. Firstly, digital camera is used to photograph building elevation and removed all parameters excluding architecture such as roads, cars and public facilities, signboards. The architecture façade was made with using AUTO CAD. Secondly, representative color of architecture of Korea and China commercial street were applied to Adobe Illustrator CS 6. I used the architecture façade color from eight commercial streets and the CAD model of China commercial streets. I made the new model of simplification of architecture color in China commercial street. I divided the model of China commercial streets into two parts. The first part is China tradition commercial street with two model style. The second part is China modern commercial street with two model style. The model of simplification of architecture color in China commercial street are as follows(Table1).The vocabulary and opinion scale of image evaluation about simplification of architecture color in Korea and China commercial street are as follows (Table 2).

Table 1: The model of simplification of architecture color in China commercial street

China tradition commercial street model 1	
	
Insadong-gil architecture color	Samcheongdong-gil architecture color
	
Cheongdong Street of Luxury Good architecture color	Garosu-gi architecture color
	
Nanluoguxiang architecture color	Qianmendajie architecture color
	
Wangfujing architecture color	Xidan architecture color
China tradition commercial street model 2	
	
Insadong-gil architecture color	Samcheongdong-gil architecture color
	

Cheongdong Street of Luxury Good architecture color	Garosu-gi architecture color
	
Nanluoguxiang architecture color	Qianmendajie architecture color
	
Wangfujing architecture color	Xidan architecture color
China modern commercial street model 1	
	
Insadong-gil architecture color	Samcheongdong-gil architecture color
	
Cheongdong Street of Luxury Good architecture color	Garosu-gi architecture color
	
Nanluoguxiang architecture color	Qianmendajie architecture color
	
Wangfujing architecture color	Xidan architecture color
China modern commercial street model 2	

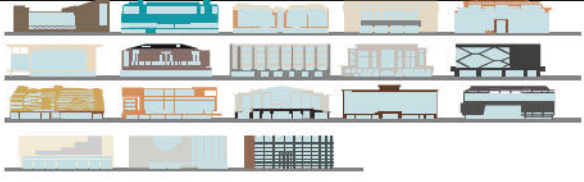
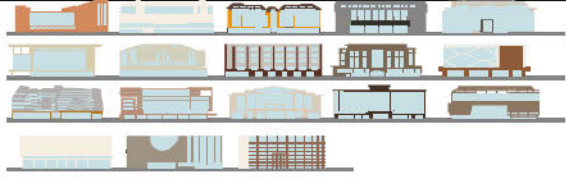
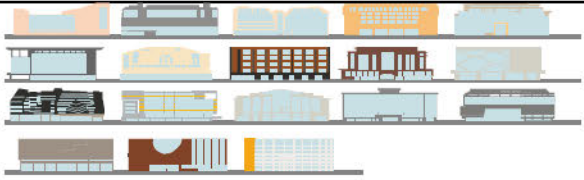
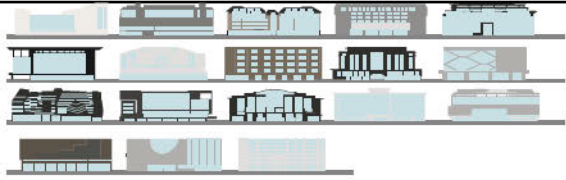
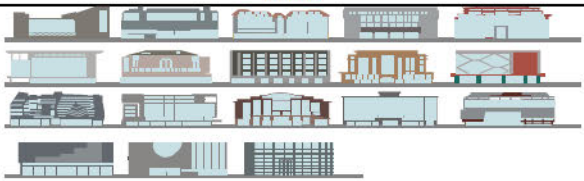
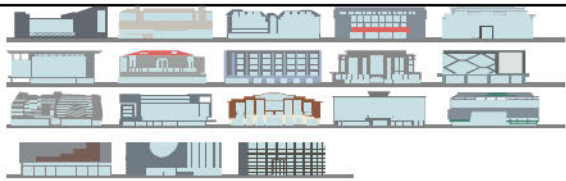
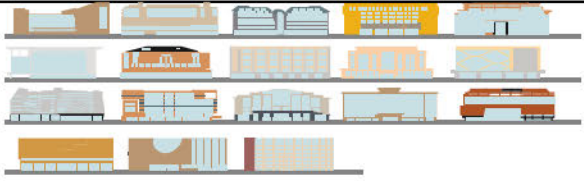
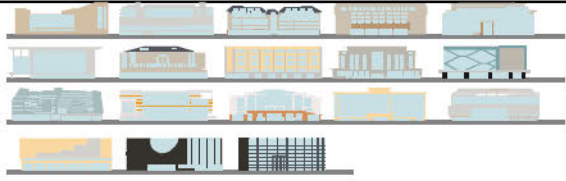
	
Insadong-gil architecture color	Samcheongdong-gil architecture color
	
Cheongdong Street of Luxury Good architecture color	Garosu-gi architecture color
	
Nanluoguxiang architecture color	Qianmendajie architecture color
	
Wangfujing architecture color	Xidan architecture color

Table2: Vocabulary and opinion scale

Vocabulary	Alteration	Refined	Happy	Warm	
	Bright	Energetic	Distinctive	Modern	
	Soft	Successive	Harmonious	Classy	
	Unity	Order	Comfortable	Natural	
	Impressive	Calm	Traditional		
Opinion scale	very	quite	average	few	absolutely
	5	4	3	2	1

RESULTS AND DISCUSSION

In this study the current state of architectural color for traditional commercial streets and modern commercial streets in Korea and China was analyzed and a color palette was derived. In addition, a color coordination palette was created by using the color palette to evaluate the images of commercial streets in Korea and China, and to compare and analyze them. Finally, the form factors and color scheme of Korean and Chinese traditional and modern commercial street architecture were evaluated, and based on the results; design direction for commercial streets in China and Koera was suggested.

Following are the main results:

1) Analysis on image evaluation of shape and color coordination palette of buildings in commercial streets

According to the analysis, the 'traditional' image from the Korean perspective on the shape of the building and the color coordination palette was the most influenced by the shape of the Wangfujing Street (modern) architecture and the color coordination palette of Nanluoguxiang (traditional). Also, the 'modern' image was the most influenced by Xidan Street (modern) architecture form and Garosu-gi Road (modern) color coordination palette.

According to the analysis, the 'traditional' image from the Chinese perspective was the most influenced by Qianmendajie (traditional) architecture and the color coordination palette of Nanluoguxiang (traditional), and the 'modern' image was the most influenced by the shape of Xidan Street (modern) architecture and the color coordination palette of the Wangfujing Street (modern) as follows (Table 3).

Table 3: Image from the Korean and Chinese perspective

R ² =0.9316										
Project Variable	Sort	Sample Size	Standardize Sort Quantitative Analysis	Correlation Coefficient	Variable Scope	Variable Amount	Standardize Sort	Quantitative Scattergram	Standardize Sort	Quantitative Scattergram
Form	Nanluoxuqilano	4	0.022					10.022		
	Qianmendajie	4	0.022	0.402	0.169	27.86%		10.022		
	Wangfujing	4	0.059					10.059		
	Xidan	4	-0.108							
Color Palette	Insadong-ol	8	0.084							
	Samcheongdong-ol	8	0.184					0.184		
	Cheongseong Street of Luxury Goods	8	0.184	0.824	0.500	78.64%				
	Garosu-gil	8	0.184							
	Nanluoxuqilano	8	0.234					0.234		
	Qianmendajie	8	-0.116							
	Wangfujing	8	-0.366							
	Xidan	8	-0.241							

R ² =0.8854										
Project Variable	Sort	Sample Size	Standardize Sort Quantitative Analysis	Correlation Coefficient	Variable Scope	Variable Amount	Standardize Sort	Quantitative Scattergram	Standardize Sort	Quantitative Scattergram
Form	Nanluoxuqilano	4	-0.216							
	Qianmendajie	4	-0.166	0.706	0.500	87.08%				
	Wangfujing	4	0.007					0.007		
	Xidan	4	0.284					0.284		
Color Palette	Insadong-ol	8	0.084							
	Samcheongdong-ol	8	-0.041							
	Cheongseong Street of Luxury Goods	8	-0.256	0.764	0.550	62.97%				
	Garosu-gil	8	0.484					0.484		
	Nanluoxuqilano	8	-0.016							
	Qianmendajie	8	0.084					0.084		
	Wangfujing	8	-0.366							
	Xidan	8	0.084							

R ² =0.9564										
Project Variable	Sort	Sample Size	Standardize Sort Quantitative Analysis	Correlation Coefficient	Variable Scope	Variable Amount	Standardize Sort	Quantitative Scattergram	Standardize Sort	Quantitative Scattergram
Form	Nanluoxuqilano	4	-0.059							
	Qianmendajie	4	0.106	0.678	0.175	43.75%		0.106		
	Wangfujing	4	0.019					0.019		
	Xidan	4	-0.056							
Color Palette	Insadong-ol	8	0.091							
	Samcheongdong-ol	8	0.006							
	Cheongseong Street of Luxury Goods	8	-0.004	0.669	0.225	56.25%				
	Garosu-gil	8	-0.044							
	Nanluoxuqilano	8	0.181					0.181		
	Qianmendajie	8	0.056					0.056		
	Wangfujing	8	-0.059							
	Xidan	8	-0.019							

R ² =0.9557										
Project Variable	Sort	Sample Size	Standardize Sort Quantitative Analysis	Correlation Coefficient	Variable Scope	Variable Amount	Standardize Sort	Quantitative Scattergram	Standardize Sort	Quantitative Scattergram
Form	Nanluoxuqilano (traditional)	4	-0.056							
	Qianmendajie (traditional)	4	-0.005	0.841	0.112	85.63%				
	Wangfujing (modern)	4	0.006					0.006		
	Xidan (modern)	4	0.056					0.056		
Color Palette	Insadong-ol	8	-0.069							
	Samcheongdong-ol	8	-0.019							
	Cheongseong Street of Luxury Goods	8	-0.069	0.646	0.325	74.97%				
	Garosu-gil	8	-0.144							
	Nanluoxuqilano	8	0.056					0.056		
	Qianmendajie	8	0.056					0.056		
	Wangfujing	8	0.181					0.181		
	Xidan	8	0.006							

RESULTS AND DISCUSSION

The purpose of this study is to grasp the simplification of Architecture color in Korea and China commercial street. The results of this study have evaluated and analyzed the color, color tone, and color images of buildings according to commercial streets in Korea and China, which have following limitations for further studies. Because this study only discusses the color, it is necessary to carry out research on various types of perception factors such as shape and material of commercial street architecture.

The relationship between architecture façade of the two areas, which environment are different from each other, as a primary reasearch purpose, and it is thought that such a research as this purpose should be regarded as important data for the research related to the traditional commercial streets of Korea and China in the future.

REFERENCES

1. Moon Bae Eun. Color design handbook, Korea. 2011.
2. Kuni Hiroshi Narumi. A technique of urban design, Japan. 1989.
3. Lu Chen, Jiseon Ryu, Jinsook Lee. A Study on Comparative Analysis of Architecture Color in Traditional Commercial Street between Korea and China, Korea. 2015.
4. Lu Chen, Jiseon Ryu, Jinsook Lee. A Study on Comparative Analysis of Color Application Characteristics of Building Elevation and Outdoor Advertisement on Traditional Commercial Streets in Korea and China, Korea. 2015.
5. Ji-Hyeun, Lee. A Study of Color Planning in the Interior Space of a High Speed Train Station-Focusing on Analysis of Natural Color System(NCS), Korea. 2015.

EVALUATION OF COLOR REPRODUCTION IN ANCIENT PAINTING BASED ON EIGENSPACE INTERPOLATION

Li Li, Changyu Diao* and Jinjin Mao

Cultural Heritage Institute, Zhejiang University, China.

*Corresponding author: Changyu Diao, dcy@zju.edu.cn

Keywords: Eigenspace Interpolation, Color Reproduction, Typical Color

ABSTRACT

Ancient paintings and other material cultural heritage require high fidelity and integrity in the process of inheritance and dissemination. It can make users do research and education more accurately by precise expression. However, there have many difficulties in printing and publishing for ancient paintings in practice, such as color distortion, aliasing, and so on. And the evaluation of color reproduction mainly depends on visual inspection at present, which has disadvantages in accuracy and efficiency, and also brings great difficulties for later adjustment and restoration. In order to solve the problem, we designed a method of color eigenspace interpolation for evaluation of color reproduction in ancient paintings. The algorithm framework mainly includes three aspects. Firstly, the color differences of typical colors between printed samples and reference are calculated using color science. Typical colors are extracted by clustering method based on each image. Secondly, the corresponding relationships of typical color blocks are mapped to the pixels by the eigenspace interpolation method. Then, the color differences of pixels are obtained by inverse Distance Weight interpolation. It is believed that color differences refined to pixels can improve the accuracy of color reproduction evaluation in ancient paintings. The experimental results show that the evaluation algorithm based on eigenspace interpolation can quickly and accurately give the quantitative results of color reproduction for ancient paintings.

INTRODUCTION

Cultural heritage contains rich historical, artistic and scientific value. The more precise expression users have, the more accurately they carry out scientific research, education, exhibition and other purposes. But in practice, there have many problems in printing and publishing for ancient paintings, such as color distortion and aliasing. At present, the evaluation of color reproduction on ancient paintings mainly relies on visual measurement. It has problems in accuracy and efficiency, and also brings great difficulties for later adjustment and repairment. Therefore, an accurate, quantitative and efficient evaluation of color reproduction is an important guarantee to ensure the precise transmission in the process of printing and dissemination.

Color reproduction aims to reconstruct the real color by establishing the mapping relationship between different devices color space, according to the observation environment and other parameters. The evaluation of color reproduction purposes to analyze its reproduction effect. It is very popular in the field of color science and has rich research results, which are widely used in optical engineering, pharmaceutical industry and biology etc. At present, studies on evaluation of color reproduction can be described in the following categories. One is to study the external factors affecting color reproduction, such as device color space, ambient light, paper quality and so on. For example, Norberg [1] analyzed the effect of paper whiteness on color reproduction. Another is to analyse the methods of color reproduction and evaluation, such as Zhang studied the reproduction

theory of digital image from acquisition to reproduction in[2], Tong[3] tested and compared various color difference evaluation methods. The third one is to research specific application scenarios, for example, Yamaguchi[4] studied color reproduction of multispectral images.

However, there are few studies on the evaluation of color reproduction for ancient paintings. Diao [5] introduced the algorithm of estimating the color reproducibility of ancient paintings by using typical color blocks. And the analysis of color difference was consistent with the visual perception and printing knowledge. But there may be some errors when the color differences of typical color blocks were directly used as the color difference value of pixels, which would affect the analysis of color information and the calculation of model in the virtual restoration of ancient paintings. To solve this problem, this paper attempts to map the color differences of typical color blocks to the pixels and achieve a relatively accurate evaluation of the color reproduction by using the color eigenspace interpolation algorithm and the inverse distance weight space interpolation algorithm.

METHODS

Because of its rarity, ancient paintings will be subject to some constraints in data collection and evaluation of color reproduction. Therefore, this paper is mainly attention on the color differences between reference samples and printing samples. Spatial interpolation algorithms based on color eigenspace are used for experiment.

The color eigenspace interpolation algorithm selects representative colors, which are clustered of ancient paintings, as feature vectors and transforms the measured discrete data into continuous data surfaces. We mainly use two kinds of color eigenspace interpolation algorithms. One is tetrahedral interpolation algorithm, which is mainly used for color mapping from scanned samples to printed samples to unify typical color blocks and pixels in the same environmental parameters as possible. The other one is IDW algorithm, which is used to interpolate the color differences of discrete typical colors to the pixels. Tetrahedron interpolation algorithm [5] takes tetrahedron as the basic unit of spatial interpolation, and chooses typical colors' values as the vertex coordinates of tetrahedron. Firstly, the corresponding tetrahedron of the interpolation point is found, then the weights of four vertices are calculated by weighting function, and finally the interpolation value is obtained. This algorithm is excellent on color correction and has been applied in many engineering projects.

The IDW interpolation uses a set of linear weights of discrete points to determine the values of interpolation points. And weight is calculated by an inverse distance function. In this paper ,it uses color values as point coordinates. This study assumes that the mapped variables are affected by the distance between the sampling points and the mapped variables. The algorithm is described as follows.

Given N discrete points with color differences of typical color blocks $Z(L_1, a_1, b_1, E_1)$ $Z(L_2, a_2, b_2, E_2)$ $Z(L_3, a_3, b_3, E_3)$ $Z(L_n, a_n, b_n, E_n)$, find $Z(L, a, b, E)$ of interpolation points (L, a, b) .

Step1. Calculate the distances from the interpolation point to discrete points using Euclidean distance function.

$$d_i = \sqrt{(L - L_i)^2 + (a - a_i)^2 + (b - b_i)^2} \quad (1)$$

where (L, a, b) is color coordinates of interpolation points, (L_i, a_i, b_i) is color coordinates of discrete points.

Step2. Get the weights of discrete points.

$$w_i = \frac{d_i^{-P}}{\sum_1^n d_i^{-P}} \quad (2)$$

where P is power parameter, and is a positive real number, default $P = 2$, n is number of discrete points.

Step3. Obtain the value of interpolation point.

$$Z(L, a, b, E) = \sum_1^n w_i * Z(L_i, a_i, b_i, E_i) \quad (3)$$

Based on the above methods, firstly, the CIELAB values of the typical colors in the reference samples and printed samples are collected by spectrophotometer, secondly, the colors of scanned samples are corrected by tetrahedral interpolation algorithm, thirdly, the colors differences of the typical colors between printings and reference are calculated, and finally, the color differences of pixels are mapped by IDW based on color eigenspace. The workflow is shown in Figure 1.

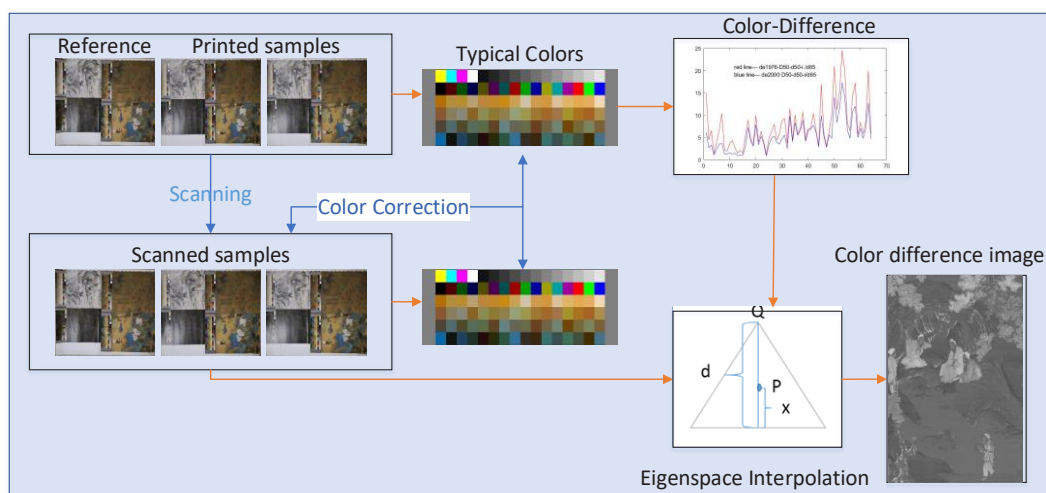


Figure1. The scheme of evaluation based on Eigenspace interpolation

RESULTS and DISCUSSIONS

We obtained typical color blocks of ancient paintings by clustering algorithm in the previous work. In this paper, the test samples were printed with the typical color blocks without adjusting the printing parameters. And the samples were scanned using the same scanning parameters. According to the research needs, the publishing house provided reference samples and two printed samples of four ancient paintings, each of which contained 64 typical color blocks. We choose one of the ancient paintings as an example to show the results.

Firstly, the color values of typical color blocks in the samples from the perspective of 2 degrees of D50 light source were collected by spectrophotometer (Konica cm-700d, 8mm). Then, the

quantitative analysis of color differences was carried out by using CIEDE2000 formula [6]. The statistical results of color differences are shown in Fig. 2. It implies that the trends of color difference of 64 typical colors in two test samples are consistent. After sorting the values, it indicates that the differences are relatively small in sensitive zones of human eyes, while the differences of less attention of human eyes are relatively large. The results of quantitative analysis conform to the rule of visual perception.

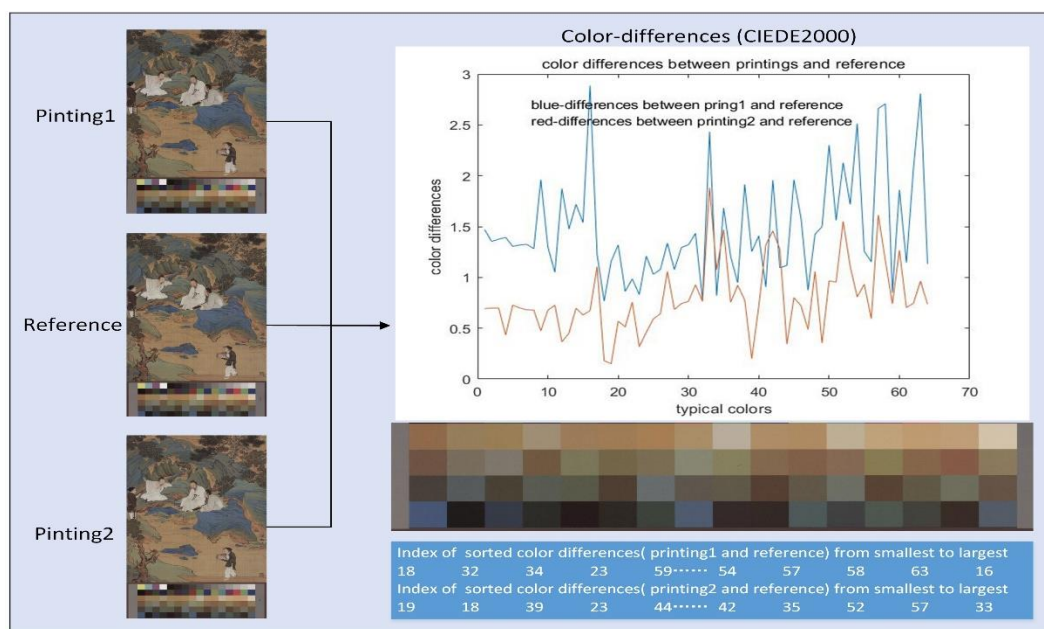


Figure2. The color-differences of typical colors between printings and reference

However, it is not accurate enough in describing the color difference of the whole image by using typical color blocks rather than pixels. Therefore, we attempt to obtain the color differences of the pixels by interpolating algorithm to get the estimation of the whole image's color difference, according to the distance between the pixel and 64 typical colors. Before color difference interpolation, first we use the tetrahedral space interpolation algorithm to re-fit the scanned data and get the similar color values as the printed sample. Then, the inverse distance weights of points in scanned sample are calculated. Fig. 3 shows distance values and weight values of a certain point in the image. It shows that the weights vary with distances.

Given the weight results and the color difference values of typical color blocks, the color difference values of the pixels were obtained. Next, we compared the results of using typical blocks color differences as pixels color differences with those obtained by our algorithm, as shown in the Figure 4. The histogram of the fist algorithm is discrete and ours is continuous and more uniform. In the surface graph, it shows that the first is step-like surface and ours results fluctuate in a small range. By comparison, the results of our algorithm are more uniform and continuous and also can map the color differences of typical color blocks to pixels, which are in line with visual perception.

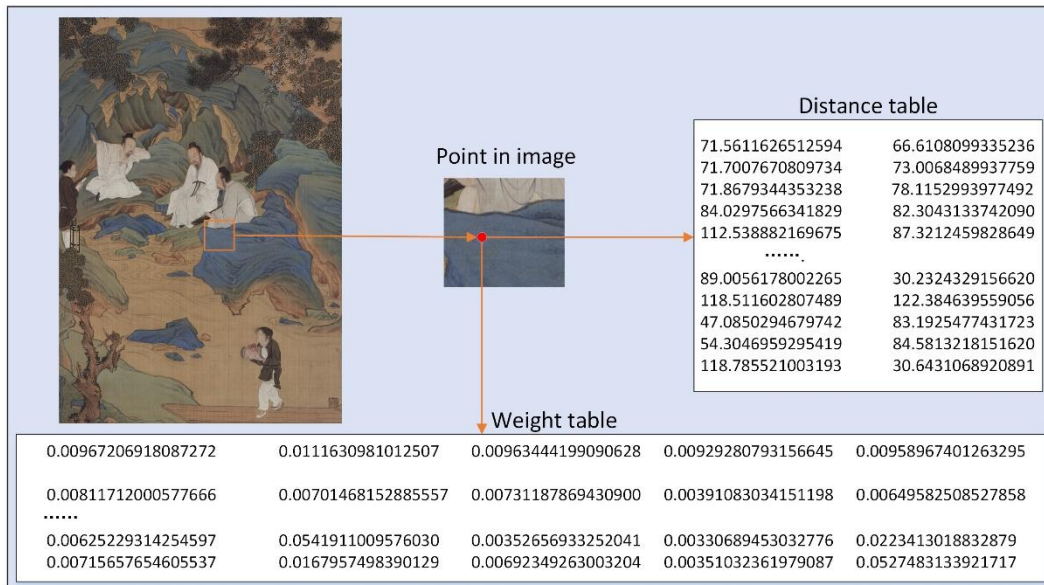


Figure3. The weight table of one points

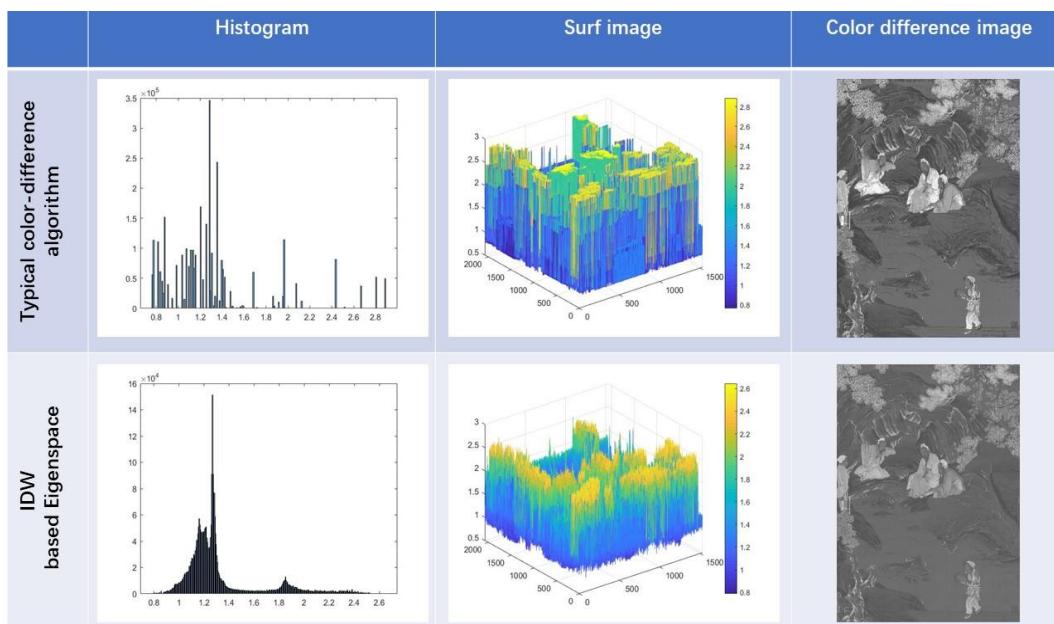


Figure4. The comparison diagram of color differences

CONCLUSIONS

The experimental results support that quantitative analysis of color reproduction can be more accurate by using interpolated color differences of pixels than using the color differences of typical color blocks, and more convenient to adjust the color of ancient paintings. It is believed that the quantitative algorithm of color reproduction based on eigenspace interpolation can quickly and accurately give the analysis results of color reproduction for ancient paintings. However, there are some unavoidable errors in the current processing, such as data transmission between devices and

color space conversion and color correction, which may cause data loss, so the evaluation of reproducibility in this study is only a relatively accurate value. In view of the problem of the restoration and evaluation for ancient paintings, we will try to further study from the perspective of hyperspectral data analysis in the future.

ACKNOWLEDGEMENT

The author would like to thank Professor Haisong Xu for his guidance and suggestions, and thank colleagues of the cultural relics digitization team for their support, so that the research can proceed smoothly. And this work is supported by the Fundamental Research Funds for the Central Universities(2018FZA128), Zhejiang Province Foundation for Cultural Heritage Preservation Technology (2017010) and Key Scientific Research Base for Digital Conservation of Cave Temples (Zhejiang University), State Administration for Cultural Heritage.

REFERENCES

1. Norberg, O. (2007). Paper whiteness and its effect on the reproduction of colors. *Electronic Imaging*.
2. X. Zhang. (2010). Study of color reproduction theory and method for digital image. *Doctoral dissertation, Zhejiang University, 2010*.
3. Q. Tong, H. Xu, et al. Testing color difference evaluation methods for color digital images. *Chinese Optics Letters*, 11 (7): 073301 (2013).
4. Yamaguchi, M., Ohsawa, K., & Murakami, Y. (2001). Color image reproduction based on multispectral and multiprimary imaging: experimental evaluation. *Proceedings of SPIE - The International Society for Optical Engineering*, 4663, 15-26.
5. C. Diao, et al. (2018). Color Correction and Reproduction Assessment of Cultural Heritage Images. *ACA2018*.
6. ISO/CIE, (2014) . ISO/CIE 11664-6:2014 Colorimetry — Part 6: CIEDE2000 Colour-Difference Formula. Vienna: CIE.

Analyzing Painting by Computing Valeur of Colors

Ryu Furusawa

(ryu.furusawa@gmail.com)

*Department of New Media Studies, Graduate School of Film and New Media,
Tokyo University of the Arts / Japan*

Keywords: valeur, simultaneous contrast, impression evaluation, psychophysics

ABSTRACT

In many cases, there is a difference between the perceived colors and actual colors in paintings because of conditions such as the surrounding colors. Analyzing that difference leads to grasping the impression created by the image. This paper proposes a mathematical method to verify the impression created by complex images such as paintings using the concept of “valeur,” which has long been used in handling the colors of paintings within the history of Western art. This paper defines the valeur of a pixel using mathematics in a digital image. It is the sum of the color differences between a single pixel and all other pixels divided by the square of their distance. Specifically, we explain how to find the valeur of any given pixel. We use the CIE Lab color space for this calculation. First, we find the color differences for all pixels constituting the image. Then, we divide the those by the square of the inter-pixel distance. Finally, we calculate the sum. By repeating this operation for the image resolution, we can obtain an array of valeur for the target image, which can be used to easily generate a visual image. This approach makes it possible to grasp the parts of an image that create the strongest impressions, as well as quantify perceived color and show this as a visible image. In this paper, we take pictures by La Tour and Monet as examples, and present the process of examining color contrast and valeur. Furthermore, this paper identifies the potential of color analysis of images through the valeur concept.

1 Introduction

There have been many attempts to analyze colors in paintings by mathematical methods which use digital images.^{1 2} This research is different from prior research in that it applies a mathematical interpretation of “valeur” to color analysis. First, this paper starts with an explanation of the meaning of “valeur” which is concept of color for painting.

2 Meaning and Usage of Valeur

“Valeur” is a French word which is translated as “Lichten Werte” in German, “value” in English, “valore” in Italian, “shikika” or “kouka” in Japanese, and it is technical term for the color property of paints on the picture plane. There are several definitions given in art dictionaries, which are briefly summarized as follows. “Valeur” is the degree of impression that is given by some elements of the color on the picture plane (hue, saturation, lightness, matiere, amount, etc.) in relationship with the entire picture plane. The “degree of impression,” is also considered to be the degree of depth within the pictorial space. For example, in the case of a portrait, the pictorial space is often seen in subtle degrees in depth such as the roundness of the human body, the space beneath the nose, or the space between fingers. In the case of landscapes, the degree of depth can extend over several kilometers including oceans and mountains. For abstract paintings, the pictorial space is related to the figure and ground. Shikanosuke Oka described the proper handling of valeur simply as “representing the intended position using color.”³ In terms of the use of valeur, the painter refers to the color of a portion of the picture plane, such as “valeur is strong” versus “weak,” or “fitting” versus “poorly fitting.” Even if the painter feels that valeur for part of the picture plane is strange, technical experience is needed in order to elucidate those factors. Although the general audience can identify discomfort regarding colors, even great painters struggle to understand the source of that discomfort. The term valeur also treats those factors as a black box, which makes a useful word in such cases. The valeur concept can be traced back to chiaroscuro, which is a technique from the Renaissance era that used contrasts between light and dark, and the color perspective which Leonardo da Vinci developed.⁴ The first use of the term valeur can be traced to the end of the 19th century in France for Impressionism and Post-Impressionism.⁵ During the Post-Impressionism era,

artists and critics circulated various color theories interpreting contemporary psychology and optics, which painters put into practice in manifold ways. In comparison with the colors that painters can sense from the model, the range of color that can be represented within a painting is narrow. In order to extend that range, painters developed techniques including brush stroke division, complementary color contrast and pointillism. There were many different senses of color conveyed from the pictures that used those techniques. And, a wide variety of terms were used to represent those different senses of color. It seems that *valeur* came into use as a term to handle those new senses of color.



Figure 1. Still Life with Vessels | Francisco de Zurbarán | 1650

3 Contrast and Valeur

The range of light perceived from the model is broad however, the range of the color that can be represented within the picture is narrow. Simultaneous contrast effect was developed as a way to overcome this gap. Colorist painters such as Da Vinci had an experience-based grasp of simultaneous contrast effect even before it was identified by Michel Eugène Chevreul in the 19th century.

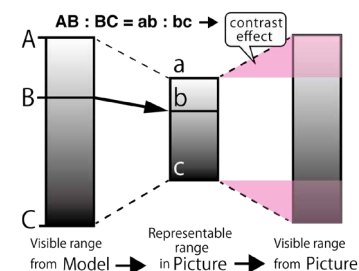


Figure 2. Schematic representation of the relation between valeur and effect of contrast. (expanded from referring Ichiro Sato.⁷)

For example, a still life by Spanish painter Francisco de Zurbarán during the Baroque period was drawn realistically with highlights of the row of vessels (Figure 1). To draw such realistic highlights, it is necessary to apply the highlights with the strongest white and reduce the overall tone in accordance with lightness of the white. Adjusting this degree of tone (*valeur*) brings together the conditions for lightness contrast on the surface of the painting (the strength of the effect depends on the relationship between color and the size of the surrounding surface), and as a result the reflected light from the vessel drawn in the painting really looks like it is reflecting light. Matisse is reported to have said the following : "You are representing the model, or any other subject, not copying it; and there can be no color relations between it and your picture; it is the relation between the colors in your picture which are the equivalent of the relation between the colors in your model that must be considered."⁶ In other words, the important thing for painting while maintaining reality is that relationship of color for model should be scaled for the picture. Thus, a close relationship can be seen between the contrast effect and *chiaroscuro*. Applying the appropriate *valeur* leads to bringing out the potential of the contrast effect. And, it gives viewers a rich color experience beyond the light and dark range that looks like the painting surface is emitting light (Figure 2).⁷ Of course, this involves not only simultaneous contrast, but also other color appearance phenomena.

While this model apply Figure 1, A is highlights of vessel, B is point of unhighlights of white vessel, C is background dark. This relationship same to condition of fitting *valeur*. If you mistake a few lightness of point "b", the *valeur* is broken, effect of contrast disappear.

During the Impressionism movement, more works consciously used lightness contrast as well as other color phenomena such as hue contrast and complementary contrast. Examples include pointillism by Seurat and modulation by Cézanne and cloisonnism by Gauguin. These contrasts are not simply generated by the juxtaposition of two color fields. Rather, the magnitude of the effect depends on conditions such as the balance of the surface area. After this research was first consolidated by Chevreul, it was also practiced by Impressionist painters as well as Joseph Albers. Research has been undertaken by psychologists. In 1891 A. Kirschmann clarified various conditions such as the induction area of simultaneous contrast and the size and distance of the area. Those ideas were verified in 1965 by C.H. Graham and J.L. Brown and summarized as

During the Impressionism movement, more works consciously used lightness contrast as well as other color phenomena such as hue contrast and complementary contrast. Examples include pointillism by Seurat and modulation by Cézanne and cloisonnism by Gauguin. These contrasts are not simply generated by the juxtaposition of two color fields. Rather, the magnitude of the effect depends on conditions such as the balance of the surface area. After this research was first consolidated by Chevreul, it was also practiced by Impressionist painters as well as Joseph Albers. Research has been undertaken by psychologists. In 1891 A. Kirschmann clarified various conditions such as the induction area of simultaneous contrast and the size and distance of the area. Those ideas were verified in 1965 by C.H. Graham and J.L. Brown and summarized as

Kirschmann's Law⁸. For example, Kirschmann's Law can be seen in "Impression, Sunrise" by Monet (Figure 9). The color of the sun reduces as much as possible the lightness contrast with the surrounding area, and the area of the surrounding grey is larger than the sun. As a result, the chroma contrast impact is magnified as much as possible. Thus, the color of the sun echoes throughout the entire picture and is directly linked to the overall impression of this picture.

4 Computing Valeur

In this research, quantified analysis of valeur using digital images is studied separately from the influence of the viewing environment which includes illuminance. The goal is to calculate the simultaneous contrast and visual impression by digital image analysis. The influence of the viewing environment is not dealt with. Prior research on models for computing the effect of simultaneous contrast was investigated using only schematic figure which have a simple composition. Thus previously there is not many attempt to simulate the effect on the complex surface such as a painting. In this research, the method of elucidating the mathematical valeur calculates units of a single pixel constituting the digital image quantized. The single pixel of valeur is regarded as the accumulation of influence received from all other pixels.

4-1 Base Model

In this paper proposes a "computing valeur quantification algorithm." It aims to comprehensively calculate stimulations received from a variety of images using the concept valeur discussed above. Specifically it combine the equation of color difference in CIE-Lab color space and Coulomb's law (inversely proportional to the square of the distance) which has been introduced by research of the induction field model in vision⁹ to calculate the decrease contrast effect in accordance with inter-pixel distance. First, a bitmap image can be represented in units of pixels. All pixels that are on the screen hold specific values of "position" and "color" and have the potential for exerting reciprocal force within the overall relationship. The effect resulting from change in a single pixel will be insignificant, but their aggregate effect accumulates gradually to form the overall impression. The effect of a single pixel on the whole is determined as the sum of color differences between all pixels. This method captures the way in which contrast effect's strength depends on the size of the entire area. The specific method is as follows.

- ① All pixels holds some values of "position"(X, Y) and "color" (L *, a *, b *).
- ② Valeur of reference pixel $p1$ is calculated by the equation "color difference / distance ^ 2" with respect to the pixels $p2$.
- ③ The calculation is implemented for all of the pixels. The sum of the calculated values is used to find the valuer of a single pixel with in a complex image.
- ④ Implement algorithm ② ③ for all pixels.



Figure 3 (Left). Original (800-627px) | Magdalene with the Smoking Flame | Georges de La Tour|1640.
Figure 4 (Right). Intensity mapping valeur (heat map) calculated using (Eq.1).

n is the number of the all pixel in the image. d is the pixel distance between $P1$ and $P2$. Vs is valeur the of pixel can be represented by the following equation.

$$V_s = \sum_{i=1}^n \frac{\sqrt{\Delta_L^2 + \Delta_a^2 + \Delta_b^2}}{\Delta_d^2} \quad (1)$$

The value for each pixel calculated in this way makes sense in comparison with other pixels. As a simple method is generating an intensity mapping image (heat map) from the value data sequence obtained by normalization in image processing. This method makes it possible to simply represent the impression created by with the image through the composite information of color and position. Furthermore, this method makes it easy to identify the locations that create a strong impression. In the painting in Figure 3, at first glance, the candle area would appear to be the brightest region, but the heat map shows that the peak of value is in the skull highlight (Figure 4), and this point contrast effect is more strongly perceived. (There aren't measurable lightness differences in the original image.)

4-2 Valeur Vector

The optical illusion of lightness contrast shown in Figure 5, the rectangular in the center appears to have gradation, even though it has the same identical in lightness throughout. The heat map created using Eq. 1 shows that highest value occurs at the rectangular corners (Figure 6). In addition, the heat map shows that both the inner and outer sides of the rectangular edge are affected. The visual impression is understandable this way, but the grey is not possible to predict the direction of the gradation within the rectangle by the lightness contrast effect.

In the basic model (Eq.1), the accumulation of the color difference formula can only be handled as a positive value, The value vector handled here not only measures the color difference due to the Euclidean distance in the Lab color space, but it also combined with calculation vector of the color difference by measuring each L * a * b * difference.

$$V_s(L) = \sum_{i=1}^n \frac{P_s L - P_i L}{d^2}$$

$$V_s(a) = \sum_{i=1}^n \frac{P_s a - P_i a}{d^2} \quad (2)$$

$$V_s(b) = \sum_{i=1}^n \frac{P_s b - P_i b}{d^2}$$

As described above, each pixel takes three values (L *, a *, b *) and it is easy to determine whether the vector direction is positive or negative. L * represents a lightness and it goes in the direction of dark it has a negative value and brighter if it is positive. A positive value for a* indicates the red direction, the opposite is green. The b* range is blue for positive values and to yellow for negative values. Figure 7 is a heat map that maps only the value data for L*. Blue shows negative values data, red is positive values. Eq. 2 is applied to "Impression, Sunrise" by Monet and displayed Intensity maps showing the value vector (Figure 8). This is mapping for range of CIELAB with reference axis point of neutral grey to be mapped to 0 intensity. The region of the sun in the L * mapping image (center-right) is not displayed at all. In other words, the lightness contrast not occur at all in this special painting which is composed of only the difference of a* b*. Conversely, in the

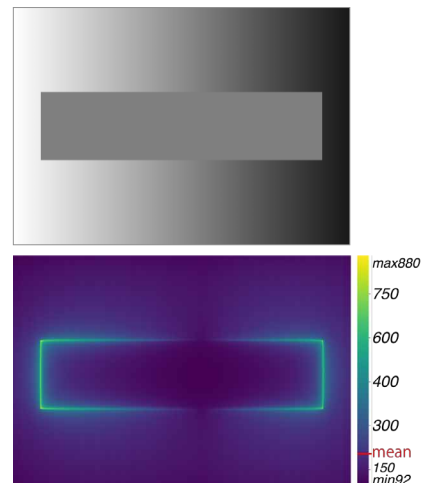


Figure 5(Top). Original (842×595px)
Figure 6(Bottom). Heat map using (Eq.1).

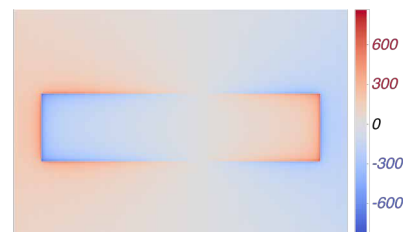


Figure 7. Heat map using (Eq.2).

case of the Rembrandt self-portraits (Figure 9), it can be seen that lightness contrast is larger than the hue contrast and chroma contrast.

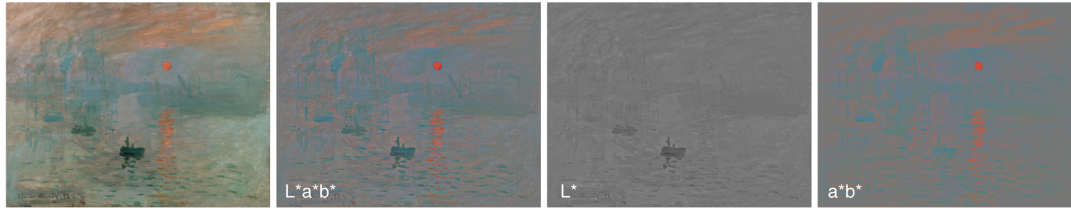


Figure 8. Mapping of the valeur vector for Impression, Sunrise | Claude Monet | 1874. Left: Original (620×800px). Center-Left: Mapping of the valeur vector. Center-Right: Mapping of only L* valeur vector. Right: Mapping of only a*b* valeur vector.



Figure 9. Mapping of the valeur vector for Self-Portrait with Two Circles | Rembrandt van Rijn | 1665-1669. Left: Original (842×595px), Center-Left: Mapping of the valeur vector, Center-Right: Mapping of only L* valeur vector. Right: Mapping of only a*b* valeur vector.

4-3 Cancellation and Simulation

Furthermore, a version of the image with the contrast effect cancelled out can be created by subtracting the calculated valeur from the original image. When doing this operation, the valeur value should be compressed to 2% to 5% because the raw data of the valeur range is larger than the CIELAB data range. This version with the contrast effect cancelled out is illustrated in Figure 10. However, the compression rate is at present determined by subjective judgment. In the case of this optical illusion figure, we have adopted numerical values so that the appearance is similar to the original uniform grey. Figure 10 appears blurred because there is a difference between the size of the contrast effect for the central grey rectangle in comparison with the contrast effect created by the rectangle's edges. It can be surmised that the contrast effect at the edges resulted in excessive cancellation/subtraction from the original image. This cancellation operation is summarized as follows. The original image data is I . $V(I)$ is (Eq.2). A is the raw data array of valeur calculated from $V(I)$. k is the compression ratio. I' is the cancellation image (Figure 10). I'' is the simulation of the contrast effect (Figure 11).

$$A = V(I)$$

$$I' = I - V(I) * k \quad (3)$$

$$I'' = I + V(I) * k \quad (4)$$

I'' is perceived in excess because the contrast effect is doubled through looking at it. The magnitude of the effect can be easily verified using image editing software or by hiding the extraneous area in the image by hand.

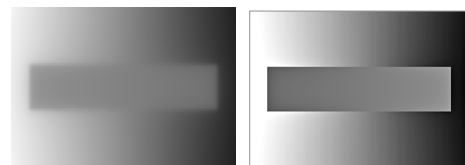


Figure 10 (Left). Cancellation image
Figure 11 (Right). Simulation image

5 Toward Color Analysis of Paintings

There are a variety of ways to undertake painting analysis through computing valeur. Viewing the mapped image in contrast to the original can lead to various discoveries. When performing further analysis of the detailed composition, it is necessary to determine the sum of the valeur of pixels for each component in the picture. The sum of the valeur of this particular surface is the “overall valeur”. Calculating the ratio of the “overall valeur” to the total valeur of the entire image makes it possible to calculate the contribution of that area to the impression of the entire image. Figure 12 shows an example of the calculation. In this figure the ratio of the overall valeur to the total valeur is shown in the bottom. Region A, D which have higher overall valeur ratio than area ratio (A:B:C:D:E:F = 17.2% : 22.3% : 16.4% : 12.4% : 11.4% : 20.4%) tends to appear as the figure. Lower region B, C, E, F is the ground. Furthermore, overall valeur can be applied as it is to color proportion theory. Figure 13 shows the recombination of Johannes Itten's 12-color wheel based on overall valeur equivalence. Each color area ratio reconstituted to equalize overall valeur. The result changes significantly by background color and color order of color wheel. It has great potential for offering a new viewpoint on past harmony theory.

6 Conclusions

This paper demonstrates the possibility of composition analysis and development that could lead to color harmony theory. Although this computational model is incomplete yet, it already demonstrated the ability of color analysis of pictures by using valeur visualized images which can be used to capture the degree of impression of the painting and the effect of simultaneous contrast. Future work includes refinement of the computational model and its implementation for real time color analysis and development of new color expression of art.

REFERENCES

1. Kobayashi, M. (2011). Color Aspects of Painting Arts Deduced from a Mathematical Model: *Color Association of Japan*, 35(4), p.310-315
2. Fujihata, M. (1997). Color as a concept. Tokyo: Bijutsu Shuppan-Sha
3. Oka, S. (1954). *Matiere of oil painting* [Translated from Japanese]. Tokyo: Bijutsu Shuppan-Sha. p.212
4. Archive Larousse: Dictionnaire de la Peinture - valeur: Larousse. (Accessed 2019 Sep 20). <https://www.larousse.fr/archives/peinture/page/1289#t154717>
5. Fabbri. (1984). GRANDE ENCILOPEDIA de'Il ARTE. Milan:Fabbri
6. Flam, J. D. (1978). MATISSE ON ART. New York, NY: E.P.Dutton. p.45
7. Sato, I., & Oil painting Technique and Material, Tokyo University of the Arts. (2014). An Introduction to Paint Making -Theory and practice for painter-. Tokyo: Tokyo Geidai Press. p.28
8. Graham, C. H., & Brown, J. L. (1965). Color contrast and color appearance. In C. H. Graham (Ed.), *Vision and visual perception*. New York, NY: John Wiley & Sons. p.452-478.
9. Nagaishi, M. (2003). Evaluation of Sensibility Using Induction Field in Vision: *Cognitive Studies*, 10(2), p.326-333.
10. Furusawa, R., & Yanagawa, T., & Ohara, T. (2017). Evaluation of Valeur: *AMC Journal*, 2. Tokyo: Art Media Center, Tokyo University of the Arts. p.22-33

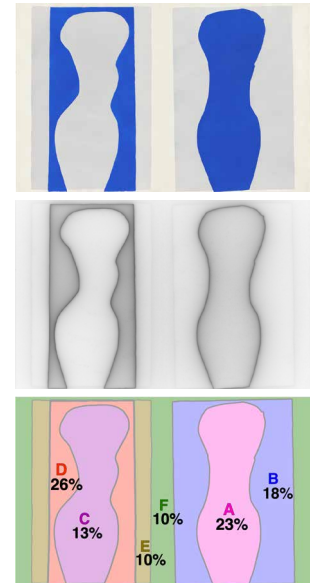


Figure 12. Forms | Henri Matisse | P.62 - 63 from Jazz (1947)
Top: Original
Center: Grayscale mapping using (Eq.1).
Bottom: The ratio of the overall valeur.



Figure 13. The recombination of Johannes Itten's 12-color wheel. (colors is not critical.)

COLOR BOUNDARY BY CATEGORY OF THAI ELDERLY

Boonchai Waleetorncheepsawat^{1*}

¹*School of Science and Technology, Sukhothai Thammathirat Open University, Thailand.*

*Corresponding author: Boonchai Waleetorncheepsawat, e-mail: boonchai.wal@stou.ac.th

Keywords: Color Boundary, Color Category, Elderly

ABSTRACT

The population of elderly in Thailand is increasing. Elderly color vision deteriorated when they are getting aged, mostly due to the increasing degree of cataract. To name colors identification correctly in daily communication task, the database of color boundary by category of Thai elderlies for each basic color terms should be observed. Since elderly deal with both monitor colors and printed colors, and many experiment has been done on monitor colors, this experiment will focus on printed colors. The 1.5 x 1.5 inch color chips generated and printed by inkjet printing to match the predefined 12 colors across color wheel of a*b* graph. There are 3 sets of color chips with the similar hue angle but differ in Lightness, The plane of Lightness for each color set are L*3, L*5, and L*7. Three sets of color chips with different Lightness were prepared and experimented together. The 11 Berlin and Kay Basic Color Terms were used as target for color category. They are: Blue, Green, Red, Yellow, Pink, Purple, Orange, Black, Gray, White, and Brown. Since the Thai are so familiar with the pale shade of Blue as called Light Blue, which we call the Light Blue naturally as “Fah” or Sky color. In this experiment we collect data of Blue color name but divided into normal Blue (some what called Dark Blue, and the Light Blue. The experiment conducted under daylight viewing condition, in the real living environment of the elderly, with 6500 K and 200-400 lx lighting. There are 13 elderies aged between 60-77 years old with normal color vision participated in this experiment. The color naming of each Berlin and Kay colors terms will be shown on the desk and subject pick up color chip one by one to call the color of that chip the color boundary tendency of elderly. This research focus on experimenting with printed color, instead of monitor color which are more widely experimented. For the result of this experiment, color boundary for each color category of each Lightness will be shown and guide to the understanding of color boundary tendency of Thai elderlies.

INTRODUCTION

Elderly infrastructure and design is becoming the hot issue for social awareness in Thailand. The proportion of elderly population in this country is rising quickly, and Thailand will become the elderly society in the near future. Elderly color vision deteriorated when they are getting aged, mostly due to the increasing degree of cataract. To name color identification correctly in daily communication task, the knowledge and database of color naming and color boundary should be observed and inform for the better color awareness for elderly. The basic color terms has been researched and standardized in many countries. However, the color naming communication are subject to local language identity and color understanding of the local population. We observe the color naming to match Berlin and Kay 11 basic color terms, but we intentionally divided the Blue color into Normal Blue (dark blue) and Light Blue (sky blue) since we found that Thai people are generally familiar with these 2 colors and easily differentiate them. Another issue for our color chip experiment is that it is quite common for elderly to see color of print and package, which are surface color. Previous research have been done with monitor color and we want to stay with printed color which is predominantly used in elderly daily life.

METHODOLOGY

The 1.5 x 1.5 inch color chips generated and printed by inkjet printing to match the predefined 12 colors across color wheel of a*b* graph. The major hue angle between each color chip was set to 30 degree. The computer generated color print was measured with Techkon SpectroDen spectrophotometer for the color value and hue angle. The printed chart was finetuned to guarantee the even distribution of color hue angle. Each step of measured hue angle was with 30 degree increment from 30 degree to 360 degree. The color chart was made into 3 Lightness of L* 30, 50 and 70. Chart background was printed to make it N5 gray color. Each color chips were coded with number for recoding. The color value recorded were plotted into graph to show the color distribution of overall color chips, as shown below.

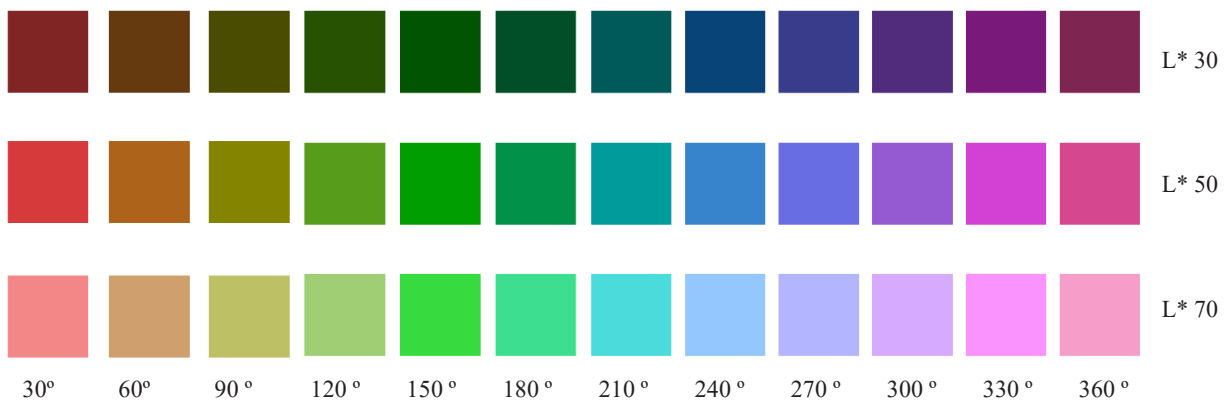


Figure 1. The chips created at 30 degree increment at L* 30, 50 and 70

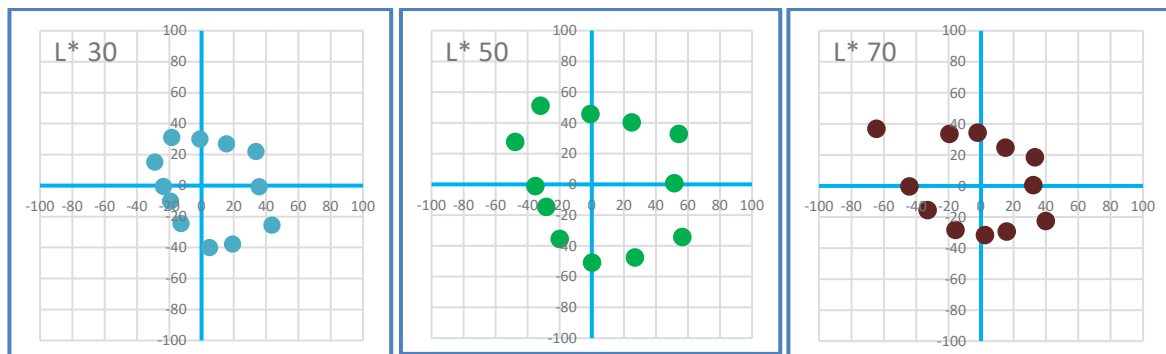


Figure 2. The a*b* plot of color chips stimuli at L* 30, 50 and 70

The 11 Berlin and Kay Basic Color Terms were used as target for color category. They are: Blue (dark and light Blue), Green, Red, Yellow, Pink, Purple, Orange, Black, Gray, White, and Brown. The experiment conducted under daylight viewing condition, in the real living environment of the elderly home or office, with 6500 K or near daylight color temperature. Konica Minolta CL500A illuminometer was used to measure the illuminant and color temperature of the experiment area. The illuminant were controlled between 200 – 400 lx. To experiment, the total 36 chips in different colors of 3 Lightness were shown to the subject randomly.

Subject picked up a color chip, looked and assigned the color name to match a basic color term. Experiment recorded the code of each color chips to the certain color name of 11 basic Berlin & Kay color terms. After finish each round subject continue to experiment in the same environment to finish 3 rounds. There were 13 elderly (8 female and 5 male) aged between 60-77 years old (mean 64) with normal color vision participated in this experiment. For the result of this experiment, color boundary for each color category from the group of subjects was shown in separate Lightness. The result will guide to the understanding of color boundary tendency of Thai elderly.



Figure 3. Printed color chart with code, and experimental environment

The stimuli color chips was coded as A for Lightness of L^* 30, B for Lightness of L^* 50, and C for Lightness of L^* 70 respectively. The hue angle of 30 degree was coded as 3, hue angle of 60 degree as 6, respectively. Then each color chips are coded as A3, A6, A9, A12, A15, A18, A21, A24, A27, A30, A33, A36 respectively for the set of L^* 30 lightness. The code changed to B3 to B 36 for the chip set of L^* 50 lightness, and C3 to C36 for L^* 70 respectively. For the Berlin and Kay color names. The abbreviation of color names are given as follow: R for red, G for green, Y for yellow, B for blue, BL for light blue, BR for brown, PI for pink, PU for purple, OR for orange, WH for white, GR for gray, and BK for black. In the table below, the codes and abbreviated names are used.

RESULT AND DISCUSSION

The color name data collected from the experiment was input into computer for analysis. The “countif” function was used to see the frequency of calling each color by each subjects. The frequency of giving color names to the color chips was analyzed into table for each Lightness, shown below in table 1 to table 3 below. The total count for each color by all subjects was analyzed in the subsequence table below for each lightness. From the frequency table, the more frequent color names of each color chip will be assigned for that color value in the a^*b^* graph of its lightness. Color chips that has been given scattered color names or has no predominant color name given to it will be assigned to the average color instead. For example the color chip A36 in table 1 was named 13 Red and 13 Purple, then the color given to the position in a^*b^* graph is Purple-Red.

From our observation in the experiment, we found that the more tendency of Green and Blue color names were given to the near threshold of color change. However, the elderly who was operated and has new lens of clear vision, compared to the one that has not been operated, with the same age (77). The elderly with more degree of cataract tend to give the color names as green, brown or gray, rather than the clear color names.

Table 1: Frequency of color chips assigned to each basic colors at L* 30

L* 30												
Each chip	A3	A6	A9	A12	A15	A18	A21	A24	A27	A30	A33	A36
Red	14	0	0	0	0	0	0	0	0	0	0	13
Green	0	0	20	37	36	35	23	0	0	0	0	0
Yellow	0	0	0	0	0	0	0	0	0	0	0	0
Blue	0	0	0	2	3	3	10	27	38	0	0	0
Light Blue	0	0	0	0	0	1	5	7	0	0	0	0
Brown	23	38	8	0	0	0	0	0	0	0	3	8
Pink	0	0	0	0	0	0	0	0	0	0	1	3
Purple	0	0	0	0	0	0	0	0	1	39	35	13
Orange	2	1	0	0	0	0	0	0	0	0	0	2
White	0	0	0	0	0	0	0	0	0	0	0	0
Gray	0	0	10	0	0	0	1	5	0	0	0	0
Black	0	0	1	0	0	0	0	0	0	0	0	0

All subjects; for color chips with L* 30

R	G	Y	B	BL	BR	PI	PU	OR	WH	GR	BK
27	151	0	83	13	80	4	88	5	0	16	1

Table 2: Frequency of color chips assigned to each basic colors at L* 50

L* 50												
Each chip	B3	B6	B9	B12	B15	B18	B21	B24	B27	B30	B33	B36
Red	21	0	0	0	0	0	0	0	0	0	2	2
Green	0	0	17	39	39	36	15	1	0	0	0	0
Yellow	0	0	17	0	0	0	0	0	0	0	0	0
Blue	0	0	0	0	0	1	1	1	10	0	0	0
Light Blue	0	0	0	0	0	2	21	37	28	1	0	0
Brown	0	24	0	0	0	0	0	0	0	0	0	1
Pink	3	0	0	0	0	0	0	0	0	0	23	34
Purple	0	0	1	0	0	0	0	0	1	38	14	1
Orange	15	15	0	0	0	0	0	0	0	0	0	1
White	0	0	0	0	0	0	0	0	0	0	0	0
Gray	0	0	4	0	0	0	2	0	0	0	0	0
Black	0	0	0	0	0	0	0	0	0	0	0	0

All subjects; for color chips with L* 50

R	G	Y	B	BL	BR	PI	PU	OR	WH	GR	BK
25	147	17	13	89	25	60	55	31	0	6	0

Table 3: Frequency of color chips assigned to each basic colors at L* 70

L* 70												
Each chip	C3	C6	C9	C12	C15	C18	C21	C24	C27	C30	C33	C36
Red	1	0	0	0	0	0	0	0	0	0	0	0
Green	0	0	10	37	39	32	6	1	0	0	0	0
Yellow	0	8	24	2	0	0	0	0	0	0	0	0
Blue	0	0	0	0	0	0	0	0	0	0	0	0
Light Blue	0	0	0	0	0	7	32	34	13	0	0	0
Brown	3	6	0	0	0	0	0	0	0	0	0	0
Pink	16	4	0	0	0	0	0	0	0	1	37	38
Purple	0	0	0	0	0	0	0	0	13	35	2	0
Orange	19	17	0	0	0	0	0	0	0	0	0	0
White	0	0	0	0	0	0	0	0	0	0	0	0
Gray	0	4	5	0	0	0	1	3	12	3	0	1
Black	0	0	0	0	0	0	0	0	0	0	0	0

All subjects; for color chips with L* 70

R	G	Y	B	BL	BR	PI	PU	OR	WH	GR	BK
1	125	34	0	86	9	96	50	36	0	29	0

The frequency of color names was allocated to the a*b* location of each color chips in the correlated Lightness. Then the color diagram of popular color names was plotted in the graph below. In this graph we can see the different location of blue color that put into dark blue and light blue.

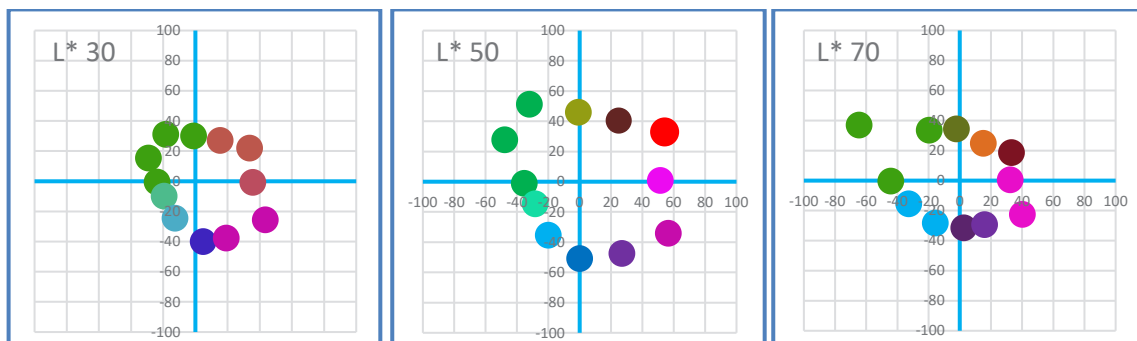


Figure 4. The color names of each stimuli at L* 30, 50 and 70

From our experiment, we found that elderly has more tendency of giving Green and Blue color names for those stimuli that may not very clear in color or near threshold of color change. This is interesting to aware of Green tone color is specific color name is require from the given of elderly. The safe color for communicate color with elderly is the clean and clear color name.

For Thai people, compare to universal, we support the idea to use the Blue color name that familiar to Thai people. Blue color for Thai is obviously and easily separated into dark blue and light blue. Thai are familiar with the light blue color naturally.

We also found that light color such as yellow is not very clear when control under the same lightness. The lightness of color take important role on seeing color clearly.

ACKNOWLEDGEMENT

The author thank Sukhothai Thammathirat Open University for supporting the fund to attend the ACA2019 conference in Nagoya, Japan.

REFERENCES

1. Berlin, B. & KAY, P. (1958) *Basic Color Terms: Their Universality and Evolution*, University of California Press, Berkeley
2. Ikeda, M & Obama, T. (2008). Desaturation of Color by Environment Light in Cataract Eyes. *Color Research and Application*, vol. 33, pp. 142-147
3. Sagawa, K. & Yasuro, T. (2003) Spans of Categorical Colours Measured by Similarity of Colours. *Proceedings of the 25th Session of the CIE*, San Diego, USA, Vol.1, D1-64 - D1-67

COLOR-TEMPERATURE ASSOCIATION IN CHILDREN AND ADULTS WITH VARIOUS COLOR VISION TYPES

Yuki Mori^{1*} and Chihiro Hiramatsu²

¹*Human Science Course, Graduate School of Design, Kyushu University, Japan.*

²*Department of Human Science, Faculty of design, Kyushu University, Japan.*

*Corresponding author: Yuki Mori, aiyou403@gmail.com

Keywords: Apparent Warmth, Color Vision Diversity, Multimodal Perception, Development

ABSTRACT

Many people tend to associate particular colors with physical temperatures. For example, red is usually associated with hot while blue is associated with cold. However, the process through which these associations are formed remains unclear. These associations may be acquired through learning during development and association patterns may differ among individuals with different color vision types. In order to reveal how these associations are acquired through developmental stages, we investigated the color-temperature association patterns in children and adults with various color vision types. As stimuli, we used 20 Munsell colors consisting of five hues (red, yellow, green, blue, and purple) and four tones (vivid, light, soft, and dark). Each tone consisted of a combination of lightness and saturation. This enabled us to examine the effect of lightness and saturation on the color-temperature association, which has not been clarified by previous studies. Sets of two pieces of colored paper were presented to participants and they were asked to choose one colored paper that felt warmer than the other. We found that dichromatic adults and trichromatic children 10 years and older showed similar association patterns as trichromatic adults. Conversely, trichromatic children under 10 years and dichromatic children tended to present different association patterns compared to other participants. Regression analysis revealed that hue, lightness, and saturation of colors had strong effects on the association between color and temperature in both dichromatic and trichromatic individuals of all ages, although the association patterns with regard to the lightness of color, were not equal among participants. These results indicate that children may acquire the same association patterns observed in trichromatic adults (the majority in the population) through social interaction and/or automatically learn these association patterns through interaction with objects in the environment, although the acquisition speed may differ between color vision types. Further research with various color vision types along different developmental stages could clarify these processes more precisely.

INTRODUCTION

It is well known that color and apparent warmth have psychological associations. For example, red, orange, and yellow are usually associated with warmth while blue is associated with coolness [1, 2]. These trends have been reported in many previous studies, regardless of age or region. Previous studies found that patterns similar to those established among adults were observed in elder children [3]. It was also reported that dichromatic adults exhibited similar association patterns as trichromatic adults, though there were differences in perception for specific colors, especially red and green, among differing color vision types [4]. This evidence indicates that dichromats may acquire associations similar those of trichromatic adults through development. However, little is known about the process by which people obtain the association between color and temperature or how the association patterns change during the course of development for different color vision types.

EXPERIMENTAL METHODS

The color vision types of participants were determined via an anomaloscope, the Ishihara pseudo-isochromatic plates, and Farnsworth Munsell 100 Hue Test. Participants in the experiment included 7 trichromatic adults (3 men and 4 women, 20-23 years old), 38 trichromatic children (15 men and 23 women, 6-17 years old), 3 adult males with deuteranopia (20-58 years old), two male children with protanopia (10-14 years old), and 6 male children with deuteranopia (6-11 years old). Twenty Munsell colors were used as stimuli (Figure 1). Stimuli consisted of five hues (red, yellow, green, blue, and purple) and four tones (vivid, light, soft, and dark). Each tone consisted of a combination of lightness and saturation. Participants were presented two pieces of colored paper (BASIC COLOR 140, Nihonshikiken, 12.8×18.2 cm) and asked to identify the color with higher apparent warmth by pointing out one piece of colored paper. There were 70 sets of two color combinations and each combination was presented once. To evaluate the apparent warmth for each participant, one point was added to the color selected to be “warmer” in appearance. Warmth index was calculated by dividing the points of each color by 7 (maximum point). Pearson correlation coefficients between groups of participants were calculated using the average warmth index of every color in each group.

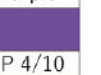
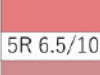
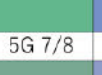
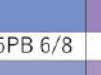
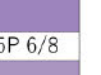
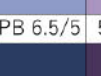
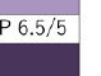
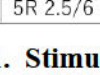
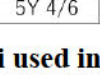
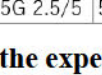
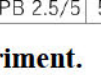
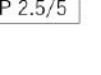
Tone	Red	Yellow	Green	Blue	Purple
vivid	 5R 4/14	 5Y 8/14	 5G 5.5/10	 5PB 4/10	 5P 4/10
light	 5R 6.5/10	 5Y 8.5/10	 5G 7/8	 5PB 6/8	 5P 6/8
soft	 5R 6.5/6	 5Y 7.5/6	 5G 6.5/5	 5PB 6.5/5	 5P 6.5/5
dark	 5R 2.5/6	 5Y 4/6	 5G 2.5/5	 5PB 2.5/5	 5P 2.5/5

Figure 1. Stimuli used in the experiment.

H V/C (e.g., 5R 4/14) indicates Hue Lightness/Saturation of each color. “5” means the representative color of each hue.

RESULTS

Association patterns differed depending on the age and color vision of participants (Figure 2, 3). Trichromatic children tended to show association patterns similar to trichromatic adults beginning at around 10 years old. The same tendency was observed in children with deuteranopia. Dichromatic adults also tended to exhibit association patterns similar to trichromatic adults. In contrast, children with protanopia followed different association patterns. Correlation coefficients between groups of participants (Table 1) showed that the association patterns of trichromatic adults were similar to those of trichromatic children aged 10 years and over, dichromatic adults, and children with deuteranopia aged 10 years and over, while these patterns were differed from those of children with protanopia and children with deuteranopia under 10 years.

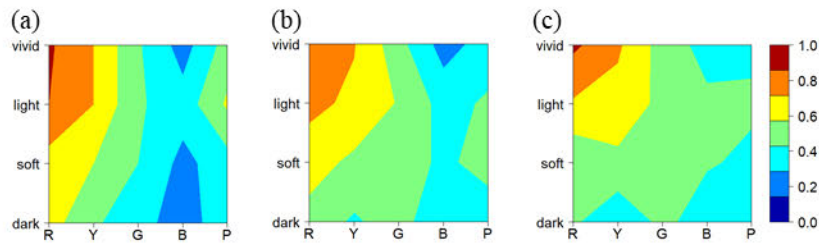


Figure 2. Average warmth index of trichromatic participants

(a): adults, (b): children 10 years and over, (c): children under 10 year

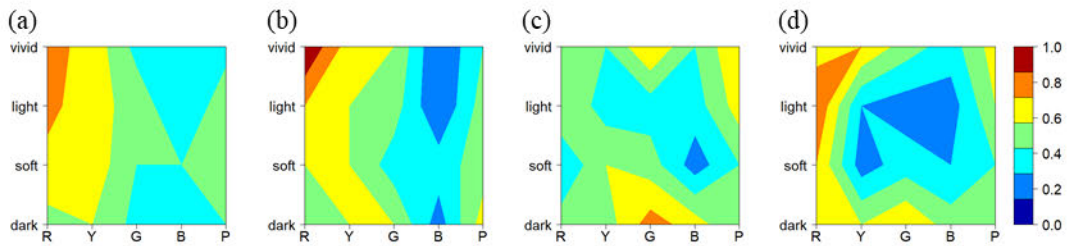


Figure 3. Average warmth index of dichromatic participants.

(a): adults (all deuteranopes), (b): children (10 years and over, deuteranopes), (c): children (under 10 years, deuteranopes), (d) children (protanopes)

Table 1: Correlation between groups of participants.

Group	Correlation between groups						
	Trichromatic adults	Trichromatic children (under 10 years)	Trichromatic children (10 years and over)	Adults with deuteranopia	Children with protanopia (10 years and 14 years)	Children with deuteranopia (under 10 years)	Children with deuteranopia (10 years and over)
Trichromatic adults	1						
Trichromatic children (under 10 years)	.794**	1					
Trichromatic children (10 years and over)	.955**	.863**	1				
Adults with deuteranopia	.900**	.715**	.909**	1			
Children with protanopia (10 years and 14 years)	.473*	0	.400	.367	1		
Children with deuteranopia (under 10 years)	.056	.211	-.027	-.124	.425	1	
Children with deuteranopia (10 years and over)	.881**	.740**	.900**	.956**	.453*	.022	1

*p<.05, **p<.01.

DISCUSSION

Elder trichromatic children and children with deuteranopia tended to exhibit similar association patterns as trichromatic adults. This result suggests that the association between color and apparent temperature might be influenced by trichromatic adults (the majority of modern society) through the process of socialization. In contrast, different association patterns were observed in older children with protanopia. Although the data obtained were limited, this may indicate that intrinsic association in protanopes is stronger than associations acquired via social learning through the process of socialization.

ACKNOWLEDGEMENT

We appreciate advice on the experimental design for Dr. Ichiro Kuriki. This work was supported by JSPS KAKENHI Grant Numbers JP17H05952, JP18K18694, and the NTT-Kyushu University Collaborative Research Program for Fundamental Sciences to CH.

REFERENCES

1. Newhall, S. M. (1941). Warmth and coolness of colors. *Psychological Record*, 4, 198-212.
2. Wright, B. (1962). The influence of hue, brightness, and color on apparent warmth. *American Journal of Psychology*, 75, 232-241.
3. Morgan, A. G., Goodson, E. F., & Jones, T. (1975). Age Differences in the Associations between Felt Temperatures and Color Choices. *American Journal of Psychology*, 88(1), 125-130.
4. Sato, K., & Inoue, T. (2016). Perception of color emotions for single colors in red-green defective observers. *PeerJ*, 4(e2751). doi:10.7717/peerj.2751.

COLOR REPRESENTATIONS OF RED-GREEN COLOR DEFICIENT AND NORMAL OBSERVERS USING COLOR CARDS AND COLOR NAMES

Miyoshi Ayama^{1*}, Minoru Ohkoba¹, Kota Kanari¹, Hiroto Mikami¹, Tomoharu Ishikawa¹, Shoko Hira², Sakuichi Ohtsuka²

¹Graduate School of Engineering, Utsunomiya University, Japan.

² Graduate School of Science and Engineering, Kagoshima University, Japan.

*Corresponding author: Miyoshi Ayama, miyoshi@is.utsunomiya-u.ac.jp

Keywords: Congenital color deficiency, hue circle, color name, difference scaling, MDS

ABSTRACT

Studies on the wavelength-hue relations of spectral lights reported that results of congenital red-green color vision deficient observers (CVDs) show a certain degree of overlap depending on the degree of deficiency in the responses of “red”, “orange”, “yellow”, and “green” [1,2]. On the other hand, their color naming performance is comparable with normal color vision observers (NCVs) in the surface colors [3,4]. In these studies, MDS analysis is utilized to represent the color stimulus space, but configuration of many color stimuli is complicated to grasp the difference among color vision property. In that sense, results of Shepard and Cooper [5] is simple and interesting. MDS results based on similarity ranking using color cards for CVDs showed distorted configuration bending at turquoise and yellow, while those based on color names became circular configuration similar to those of NCVs. However, they did not assess the degree of distortion in individual results. The aim of the study is to quantitatively compare the results of difference scaling test using color cards and color names. For some of the observers, relation to the saturation evaluation results of our previous study [6] was also investigated.

In the experiment, 20 colors, high and medium chroma for each of 10 basic hues of Munsell color system, were chosen, and all combinations of 10 hues, i.e., 45 paired cards were prepared for each of high and medium chroma groups. Observers were asked to scale the psychological difference between 2 colors in the pair or the pair of 2 color names, using 5 levels of 1:very close to 5:very far. Nine protan, 8 deutan, and 8 NCV observers participated the experiments using high chroma colors and color names only, while 7 protan, 5 deutan, and 6 NCVs participated the experiment using medium chroma colors, too. Color vision of observers were examined using anomaloscope, panel D-15, and Ishihara charts.

MDS results of the NCVs became circular configuration similar to Munsell hue circle for high and medium chroma cards as well as the color names only. U-shaped curves bending at 5Y and 5PB were found in the MDS results of the CVDs in the experiments using color cards. Degree of distortion decreased in the results of color names only. Most of the observers in this study participated our previous experiment to evaluate perceptual saturation difference of the series of red, yellow, green, and blue stimuli of different metric chroma. Medium level of correlation was observed between saturation evaluations of red and green, and the degree of distortion. In observing reflective surface under general white lighting and/or using color names, CVDs seem to utilize several strategies to cover their deficiency, probably based on their knowledge and experience. Our results suggest that sensitivity to saturation-difference of individual observers contribute to such strategy.

INTRODUCTION

It is well known that discriminability of green, yellow, orange, and red is low in congenital red-green color deficient observers (CVDs). However, CVDs use color names in everyday conversation without any serious problems apparently. Previous studies on color recognition of CVDs have reported that their color naming ability, especially for surface colors observed in rich environmental information, is comparable to those of NCVs [1-4,7]. In this study, color representations of congenital red-green CVDs obtained using color cards and color names are compared with those of NCVs to investigate how and to what degree the color representation in brain differs between CVD and NCV observers.

EXPERIMENT

The first and second columns in Table 1 indicate the Munsell notations of the colors with high and medium chroma, respectively, used in the color card experiment, and the third column shows the color names used in the color name experiment. All combinations of 10 hues, i.e., 45 paired cards were prepared for each of high and medium chroma groups. Figure 1(a) shows the experimental set-up and the example of color card used in the experiment. In the color name experiment, the answer sheet on which all pairs of color name were listed as shown in Figure 1(b) was used.

First, observers were asked to scale the psychological difference between 2 colors in the pair or the pair of 2 color names, using 5 levels of 1:very close, 2:rather close, 3:neither close nor far, 4:rather far, and 5:very far. In this study, we call the judgement “difference scaling”, because judgement when an observer perceives large difference in the pair, larger score should be assigned. Forty-five cards were presented in a random order, and this sequence was repeated again in a different random order with flipping the left and right. After the color card experiment, similar difference scaling was carried out using the answer sheet on which all pairs of 10 color names were written. Nine protan (6 protanopes and 3 protanomalous labeled P3 to P11), 8 deutan (6 deuteranope and 2 deuteranomalous labeled D7 to D14) and, 8 NCV (labeled N11 to N18) observers participated the experiments in the difference scaling test using high chroma colors and color names only, while 8 protan, 5 deutan, and 7 NCVs participated the experiment using medium chroma colors. Color vision of observers was examined using anomaloscope, panel D-15, and Ishihara charts. Classification of the type indicated above is mainly based on the results of anomaloscope.

Table 1 Munsell notation of the color chips, color names, and the labels

High	Medium	Color Name	Label
5R4/14	5R4/4	Red	R
5YR6.5/14	5YR6.5/4	Orange	YR
5Y8/14	5Y8/4	Yellow	Y
5GY6.5/10	5GY6.5/4	Yellow-Green	GY
5G4.5/10	5G4.5/4	Green	G
5BG/4/9	5BG/4/3	Blue-Green	BG
5B4/8	5B4/3	Blue	B
5PB/4/12	5PB/4/4	Blue-Purple	PB
5P4/11	5P4/3	Purple	P
5PR/4/12	5PR/4/4	Red-Purple	PR

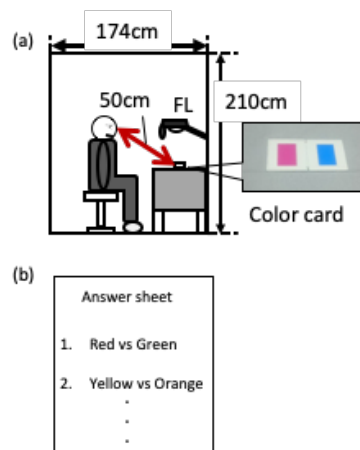


Figure 1. Experimental setup, color cards (a), and the answer sheet (b) FL:Fluorescent lamp.

RESULTS

Figure 2 shows the results of difference scaling in the pairs including “R”. Figure 2(a), (b), and (c) indicate the results of high chroma color cards, medium chroma color cards, and color names, respectively. Solid, broken, and dotted lines represent the average results of normal, protan, and deutan observers, and the bars are the standard errors. Results of NCVs are single peaked curve with a plateau in the range from Y to PB in Figure 2(a), and from Y to BG in Figure 2(b). Perceptual difference against “R” is the largest at “G” or “BG” in both color cards and color name experiments. On the other hand, results of CVD observers show double peaked curves in all results. Dip appears at “BG” and “G” for protan and deutan, respectively in color cards. Dips are deeper in medium chroma card condition than those in high chroma condition as shown in Figure 2(b). This indicates that for protan observers, for example, the perceptual difference between “R” and “BG” is smaller than that between “R” and “Y”, reflecting their low discriminability between reddish and greenish colors, especially in the case of desaturated colors. Dips of CVDs’ results are shallow in the color name condition and the curves become closer to the curve of NCVs as shown in Figure 2 (c).

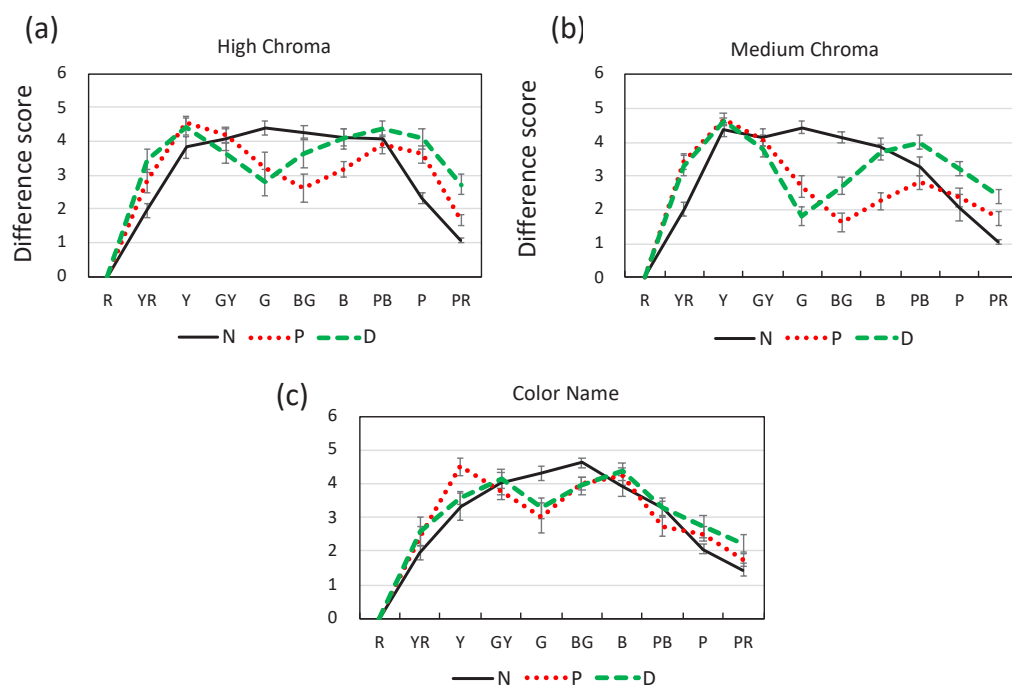


Figure 2. Results of difference scaling. (a): High chroma color cards, (b): medium chroma color cards, and (c): color names

Using the results of difference scaling for all pairs, color representations for NCVs and CVDs are derived using 2 dimensional MDS analysis (non-metric MDS) for all observers for all conditions. Figure 3 shows the results of 3 observers, N11 of NCV, P4 of protanope, and D8 of deutanope. Results based on the experiment using medium chroma cards are essentially similar to those of high chroma cards, and thus not shown here to save space. As shown in the figure, color space of the N11 is circular for both high chroma color cards and color name conditions. Color chips or names are arranged in the same order as that of Munsell hue circle, though a small irregularity is seen in the B and PB in Figure 3(a). Primary axis (horizontal) is roughly R vs BG for both of Figure 3(a) and (d) for N11, whereas the secondary axis (vertical) is roughly P vs GY in Figure 3 (a) and PB vs GY in Figure 3 (d), respectively. They do not exactly correspond to the red-green and yellow-blue axes, but

close to them. On the other hand, color space of CVD observers, especially based on the color card experiment largely deviate from circular shape as shown in Figure 3 (b) and (c). They show U-shaped configuration bending at Y and PB that is consisted with those reported in previous studies [5, 6, 8]. Distance between Y and PB is comparable to that of NCVs', while those between YR and GY or R and G are very short in Figure 3 (b) and (c), reflecting their low discriminability between these pairs in the color card experiment. In a complementary paper [9], results of other observers showing U-shaped configuration are indicated, and the estimation of MDS configuration using colorimetric values is challenged. It is worth mentioning that similar U-shaped configuration is obtained for NCVs when the a^* values of the stimuli are changed to zero while keeping the b^* values, called 'R-G neutral- and Y-B only changed-' stimuli, in display experiment recently reported by Hira et al [10].

On the other hand, distortion from circular shape decreases in the results based on color name experiment as shown in Figure 3 (e) and (f). Results of D8 in Figure 3 (f) is as circular as that of N11 in Figure 3(b). This tendency is consistent with those in previous studies on MDS [5, 6, 8], as well as with the results of other studies on color naming property of CVDs reporting that CVDs' color naming ability, especially for surface colors observed in rich environmental information, is comparable to those of NCV [1-4, 7]. At some point in the growth process, CVDs recognize some kind of difference in their color vision from other people, and they might become keen to learn difference between basic color names being used by NCVs or being appeared in various sentences such as "strong contrast between red roses and green leaves". Our results suggest that color representation in CVDs' brain based on color name is different from that based on visual perception.

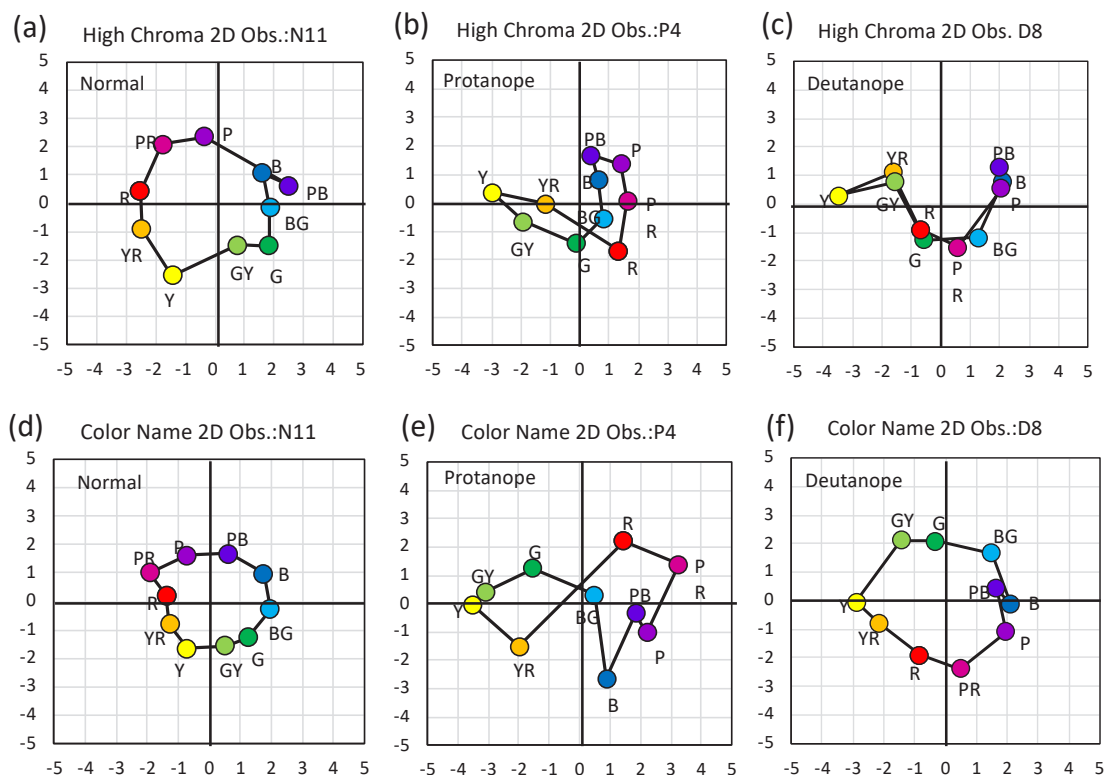


Figure 3. Color representations for NCV and CVD observers based on difference scaling using high chroma color cards ((a), (b), and (c)), and color names ((d), (e), and (f)).

To evaluate the degree of shape distortion of the MDS results, we define the distortion index described in Figure 4. In addition to the shape distortion, MDS results of CVD are vertically flatter than those of NCV. Thus the sum of the distance from horizontal axis in CVDs' is generally smaller than that of NCVs' as shown in the right-hand plot in Figure 4. Also, nearly 80% of CVDs in this study show U-shaped results bending at Y and PB. The distance between Y and PB denoted as (Y – PB) is roughly an indicator of horizontal width of the MDS results. Therefore, the sum divided by (Y – PB) were calculated for each observer. When the shape is circular as shown in Figure 3(a), the index value is about 2. In the cases of distorted shapes shown in Figure 3 (b), (c), and (e), the values are 0.93, 0.18, and 1.39, respectively.

Most of the observers in this study participated our previous experiment to evaluate perceptual saturation difference of the series of red (R1 to R3), yellow (Y1 to Y3), green (G1 to G3), and blue (B1 to B2) stimuli of different metric chroma [6]. Before the saturation evaluation, scaling of perceptual lightness difference was examined using a series of achromatic pairs of various ΔL^* s, and no significant difference was found between CVDs and NCVs indicating that ΔL^* can be utilized as a common measure for perceptual difference. Then the pair of R_i and R_{i+1} ($i=0, 1, 2$), for example, were compared with the series of achromatic pair, and the certain achromatic pair with the lightness difference of ΔL^* was determined that gave an observer the same perceptual difference as the saturation difference in a given chromatic pair. R2-R3 (G2-G3) was the pair of the most saturated and secondary saturated reds (greens). Because all of R (G) stimuli were nearly the same hue and set in equal brightness for each observer, difference between R2 and R3 should be the saturation difference. In the experiment, ΔL^* of R2-R3 and G2-G3 pairs for CVDs were significantly smaller than that for NCVs [6], indicating that the CVDs perceived some kind of saturation difference in reddish and greenish pairs, but the amount of difference is smaller than that of NCVs.

We compared the results of difference scaling in this study with the results of saturation difference in our previous study. Figure 5 shows the relation between them. Horizontal and vertical axes are the distortion index (sum/(Y-PB)) and the average ΔL^* obtained in R2-R3 and G2-G3 pairs in previous study, respectively. Medium level of correlation was observed between saturation evaluations of red and green, and the degree of distortion in the MDS configuration.

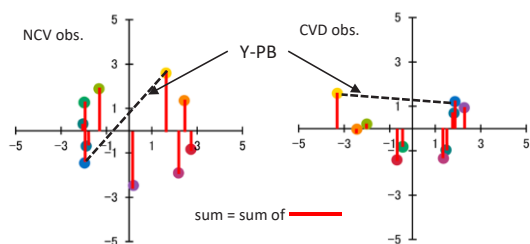


Figure 4. Index to express the distortion from circular shape

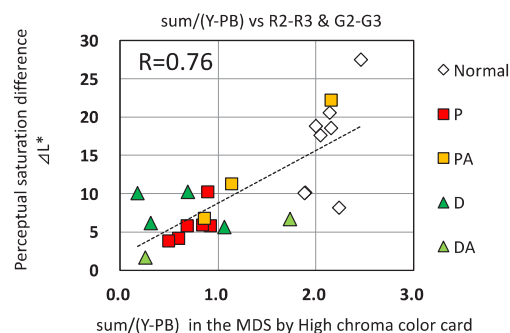


Figure 5. Relation between distortion index and perceptual saturation difference

CONCLUSION

MDS results of the NCVs became circular configuration similar to Munsell hue circle for high and medium chroma cards as well as the color names only. U-shaped curves bending at 5Y and 5PB were found in the MDS results of the CVDs in the experiments using color cards. Degree of distortion from circular shape decreased in the results of color names only, sometimes as circular as that of

NCVs, indicating that CVDs' color representation based on color names is close to that of NCVs'. This indicates that CVDs have color representation in their brain very similar to that of NCVs' based on the knowledge and experience of color names, whereas that based on color perception difference differs.

Medium level of correlation was observed between the degree of distortion from circular shape in the MDS results in this study and the saturation evaluation of red and green stimuli in previous study. In observing reflective surface under general white lighting, CVDs seem to utilize several strategies to cover their deficiency. Our results suggest that the residual sensitivity to saturation-difference in individual observers contribute to such strategy.

REFERENCES

1. Paramei, G. V. (1996). Color Space of Normally sighted and color-deficient observers reconstructed from color name. *American Psychological Society*, 7(5), 311-317.
2. Nagy, B. V., Nemeth, Z., Samu, K., & Abraham, G. (2014). Variability and systematic difference in normal, protan, and deutan color naming, *Frontiers in Psychology*, 5, Article 1416, 1-7. doi:10.3389/fpsyg.2014.01416
3. Bonnardel, V. (2006). Color naming and categorization in inherited color vision deficiencies, *Visual Neuroscience*, 23, 637-643.
4. Lillo, J., Moreira, H., Alvaro, L., Davies, I. (2014). Use of basic color terms by red-green dichromats: I. General Description. *Color Research & Application*, 39(4), 360-371.
5. Shepard, R.N., Cooper, L. A. (1992). Representation of colors in the blind, color-blind, and normally sighted, *Psychological Science*, 3(2), 97-104.
6. Kanari, K., Ishikawa, T., Ayama, M. (2017). Perceived saturation difference of congenital red-green color vision deficiencies. *Proceedings of the 13th AIC Congress 2017*, USB.
7. Jameson, D., Hurvich L. M. (1978). Dichromatic color language: "Reds" and "Greens" don't look alike but their colors do. *Sensory Processes*, 2, 146-155.
8. Hira, S., Nakamichi, M., Kanari, K., Karakama, Y., Fukuda, H., Ayama, M., Ohtsuka, S. (2017). Individual differences in chromatic perception: Continuous variation from dichromacy to trichromacy. *Proceedings of the 24th International Display Workshops*, 992-995.
9. Ohkoba M., Kanari, K., Mikami, H., Ishikawa, T., Hira, Ohtsuka, S., S.Ayama, M. (2019) . Hue circle perception of congenital red-green color deficiencies -Experimental data and estimation using colorimetric values-, *Proceedings of the 5th Asia Color Association Conference*. Electric file.
10. Hira, S., Sako, A., Uto, R., Kanari, K., Ohkoba, M., Ishikawa, T., Ayama, M., Ohtsuka, S. (2019). Immanent dichromatic in trichromatic observer: based on MDS analyses of R-G neutral- and Y-B only changed-stimuli observation results. *Proceedings of the 26th International Display Workshops*.

RESEARCH ON BLUR DISCRIMINATION THRESHOLDS OF THREE-CHANNEL FOR COLOR IMAGE

Hao Yan ¹ Qingmei Huang ^{1*} Defen Chen ¹ Lialian Zhang ¹ Pan Guo ¹

(¹National Laboratory of Color Science and Engineering, School of Optics and Photonics, Beijing Institute of Technology, Beijing, China, 100081)

*Corresponding author: Qingmei Huang, huangqm@bit.edu.cn

Keywords: Blur discrimination threshold; Quest psychological experiment method; Opponent color space

ABSTRACT

On the basis of modern theory of color vision, the blur discrimination thresholds of color image with three channels(luminance, red-green and the yellow-blue channel) in the opponent color space(DKL space) is studied through visual experiments in this paper. The visual evaluation experiment is designed by the psychophysical method based on Quest algorithm. Finding the blur discrimination thresholds of color image according to the DKL space is of great significance for helping us understand color perception of image. It also has a wide range of applications in areas such as color image compression during color image transmission.

Two (flowers and artificial object) typical images in the McGill standard color image database were chosen as the experimental images. After converting the color space of the image from RGB to DKL space, Gaussian low-pass filtering is used to establish the fuzzy image database. Quest algorithm which is a psychological physical method is used to design the visual evaluation experiment. Ten volunteers were invited to participate in the visual evaluation experiment for each of the three channels of the two images. The experimenter data is statistically analyzed, and then the three-channels blur discrimination thresholds of two typical images were obtained. The influence of image information on the blur discrimination thresholds of color image is analyzed from the two features of image texture and color.

1.INTRODUCTION

In humans, around 80%-90% of all information is obtained visually. Visual information is an indispensable part of the information composition. the study of color image blur discrimination thresholds in DKL color space provides important application value for digital image compression, transmission and display, and provides a research basis for human eye vision resolution threshold.

Huw C. Owens^[1] discussed the blur discrimination thresholds of red-green, blue-yellow and luminance channels according to the modulated square wave. For all observers (three), the blur discrimination thresholds for red-green, and luminance channels are similar, and the threshold for yellow-blue channels is higher. Ferzli et al. proposed a “just noticeable difference” model^[2] to establish the relations between image data and human perception, and they also presented a perceptual no-

reference image sharpness metric by measuring the spread of edges^[3,4]

This paper studies the blur discrimination thresholds of color image based on DKL color space. The main work of this paper is focuses on the actual image and divided the image into three channels. Ten observers were invited to conduct a visual evaluation experiment to determine the three-channel blur discrimination thresholds of the color image. Through experimental data analysis, the relationship between blur discrimination thresholds of image and texture of image is discussed.

2.METHOD

After completing the space conversion from RGB to the opponent color space, the typical image in McGill image database is selected for Gaussian filtering processing, and the experimental fuzzy image database is established. On this basis, the visual evaluation experiment was designed by using the principle of Quest algorithm. Finally, the observers were invited to complete the experiment and a series of experimental data was obtained.

2.1 Blurred images for experiment

2.1.1 conversion of color space for the image

A lookup table was created to firstly convert RGB space to CIEXYZ space , then to LMS space and to DKL space subsequently. The image is divided into luminance, red-green, and yellow-blue channels in the DKL space.

The formula for converting LMS space to DKL space^[5] is shown below ,(Eq 1)

$$\begin{bmatrix} D \\ K \\ L \end{bmatrix} = \begin{bmatrix} 22.0454 & 22.0454 & 0.0 \\ 13.8336 & -32.4902 & 0.0 \\ -12.7279 & -12.7279 & 9.6048 \end{bmatrix} \begin{bmatrix} L \\ M \\ S \end{bmatrix} \quad (1)$$

2.1.2 Typical image selection

The image used in the experiment is a standard color image database provided by Olmos & Kingdom of McGill University. The McGill images database are mainly used in computer vision and biological research, including 9 types of natural images: animals, flowers, leaves, fruits, land surface, artificial objects, Shadows, snow and textures. In this paper, the images of flowers and artificial objects are selected as research objects.

The more obvious the texture feature, the more information that can be observed. Based on the gray level co-occurrence matrix, the two types of image texture features are analyzed, then the image with the largest contrast was selected for experiment. Finally, two images(numbered 43 in flowers and numbered 135 in artificial object)were selected as experimental images, as shown in Figures 2.1 and 2.2 below:



Figure 2.1. Experiment image of flower



Figure 2.2. Experiment image of artificial object

2.1.3 Image blurring processing

The Gaussian low-pass filter(Eq.2) is used to filter the image to obtain the required experimental image database.

$$H(u, v) = e^{-\frac{D^2(u,v)}{2 \cdot D^2}} \quad (2)$$

In visual experiments, 0~500 is a proper range of D required by a Quest algorithm. We use parameter B(B=500-D₀) to describe the degree of blur, and B₀ was used to represent blur discrimination thresholds of color image.

2.2 Design of visual evaluation experiment

Quest algorithm is a Bayesian adaptive psychometric method^[6] and it is widely used for its effectiveness in threshold estimation. Therefore, in this study, Quest was used for visual experiment programming.

The basic idea of Quest is to place each trial at the current most probable Bayesian estimate of threshold. The procedure is implemented in three steps:

- (1) Specification of initial probability density function(Eq.3).

$$q_0(T) = A/[Be^{-C(T-\tau)} + Ce^{B(T-\tau)}] \quad (3)$$

Where T is the threshold in log units, A determines the amplitude of the fitted curve, B and C determine the slopes of the fall-off at high and low thresholds respectively, τ corresponds to the most probable log threshold value. A, B, C in this paper are 6.29, 1.22, 5.07 respectively.

- (2) A method for choosing the stimulus intensity of any trial.

A psychometric function describes the relation between some physical measure of a stimulus and the probability of a particular psychophysical response. Ours is a “2 alternative force choice” (2AFC) experiment, the psychometric function is expressed as $p(r, x, T)$ ^[6], which represents the probability of a response, r (1 or 0), for a subject with log threshold, T, to a stimulus of log intensity, x. The psychometric function(Eq.4) is given by

$$p(r, x, T) = \Psi(x - T) = 1 - \delta - (1 - \gamma - \delta)exp[-10^{\beta(x-T+\epsilon)}] \quad (4)$$

Where γ is the false positive rate, δ is the false negative rate, β determines the slope of the psychometric function and ϵ determines the threshold criterion, in this paper they are 0.5, 0.01, 3.5 and 1.5 respectively. Then the probability density function(Eq.5) after nth response is given by

$$q_n(T) = p(x_n, x_n, T) \cdot q_{n-1}(T) \quad (5)$$

The next log stimulus intensity x_{n+1} is chosen as the one corresponding to the maximum probability.

(3) A method for choosing a final threshold estimate.

The minimum variance method is been used. The standard deviation of nth response(Eq.6) is

$$V_n = \sqrt{\int (T - m_n)^2 q_n(T) dT / \int q_n(T) dT} \quad (6)$$

where m is the mean of the probability density function $q_n(T)$. When V_n reaches the termination condition, in this paper is 0.055 times sample size 131, i.e. 7.205, current T is the final threshold result.

2.3 Experimental procedure

2.3.1 Experimental procedure

The experimental sequence in the indoor lighting environment are as follows:

(1) Place the eye tracker 10 cm in front of the monitor screen to switch on the eye tracker and initiate the program software in the computer;

(2) The observer sits 45 cm in front of the eye tracker, and sets the parameters of the eye tracker according to the height and position of the observer, the position of the eye tracker, and the size of the display screen;

(3) Calibration of the human eye;

(4) The eye tracker works and the visual experiment begins;

(5) After the experiment, save the video data of the eye tracker and the original data; invite the observer to fill out the experimental information record form.

2.3.2 Experimental data

After the experiment, the experimental data of each observer is compiled, which mainly includes the following contents: (1) Eye tracker data: The line of sight of the observer in the experiment recorded by the eye tracker. (2) Experimenter judges time.(3) The number of each experiment and the corresponding blur Y. (4) The position of the clear image and the blurred image at each judgment.

3.RESULT

Figure 3.1 shows the experimental data of the luminance channel of the flower image of the observer No. 3. the x axis is the click times, and the y axis is the corresponding B value.

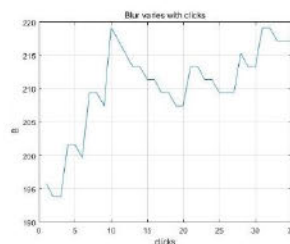


Figure 3.1 B changes with click times

The experiment was terminated at the 35th judgment, according to Quest algorithm the threshold result of this experiment is corresponding image blur degree $B = 217$.

According to the above process, the experimental results of each observer is obtained. As shown in Figure.3.2, the average blur discrimination thresholds of flower luminance, red-green, yellow-blue channel are 255.1, 378, 368.6, respectively. The average blur discrimination thresholds of artificial object luminance, red-green, yellow-blue channel are 332.8, 393.1, 416.4, respectively.

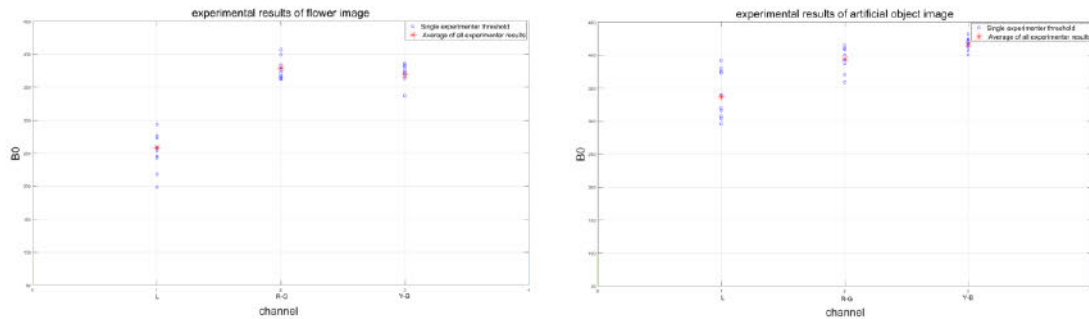


Figure 3.2 The results of blur discrimination thresholds

It can be seen from the final results of the average blur discrimination thresholds : (1) The blur discrimination thresholds of three-channel of the flower image is smaller than that of the artificial object image. (2) The blur discrimination of luminance channel of the flower image is smaller than the thresholds of red-green channel and yellow-blue channel; the blur discrimination threshold of luminance channel of the artifact object image is smaller than that of the red-green channel, and the blur discrimination threshold of red-green channel is smaller than that of the yellow-blue channel.

4. DISCUSSION

Our study analyzes the influence of image contrast and uniformity on the blur discrimination thresholds of color image. The contrast of the three channels of the flower image is larger than the contrast of the three channels of the artificial object image, and the contrast between the luminance of the flower image and the luminance channel of the artificial object image is much larger than that of the red-green channel and the yellow-blue channel, which is opposite to the relationship between the blur discrimination thresholds of the same channel in the two images; The three-channel uniformity of the artificial image is greater than the uniformity of the three channels of the flower image, and the difference between the uniformity of the luminance channel of the artificial object and the flower image is much larger than that of the red-green channel and the yellow-blue channel. The relationship between the result and the blur discrimination threshold of the same channel of the two images is obtained. In conclusion the larger the contrast of the image, the smaller the uniformity of the image, and the smaller the corresponding blur threshold of the color image.

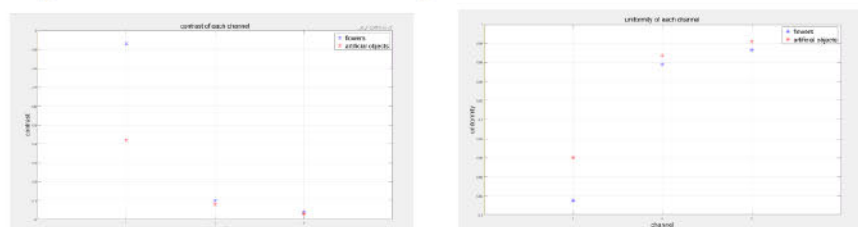


Figure4.1 Image of contrast and uniformity of three-channel

REFERENCE

- [1] Huw C. Owens, Stephen Westland, Sophie Wuerger. Blur tolerance and perceived sharpness in the chromatic and luminance domain[C]. IS&T 5th Color Imag. Conf., 1997, 235-239.
- [2] Ferzli R, Karam L J.2006. Human visual system based no-reference objective image sharpness metric, IEEE International Conference on Image Processing 2006:2949-2952.
- [3] Ferzli R, Karam L J.2007.A no-reference objective image sharpness metric based on just-noticeable blur and probability summation, IEEE International Conference on Image Processing 445-448
- [4] Ferzli R, Karam L J.2009.A No-Reference Objective Image Sharpness Metric Based on the Notion of Just Noticeable Blur (JNB), IEEE Transactions on Image Processing 18(4) 717-728
- [5] Brainard D.H..Cone contrast and opponent modulation color spaces[J]. Human Color Vision, 2nd edition. Washington DC:Optical Society of America,1996: 563–579.
- [6] Watson A B, Pelli D G.1983. *QUEST: A Bayesian adaptive psychometric method*, Perception & psychophysics 33(2): 113-120.

SIMULATION OF A MULTISPECTRAL IMAGING SYSTEM BASED ON MULTICHANNEL FILTER ARRAY

Zhengnan Ye, Haisong Xu*, Jueqin Qiu, Yang Lu

*State Key Laboratory of Modern Optical Instrumentation, College of Optical Science and Engineering,
Zhejiang University, Hangzhou 31007, China*

*Corresponding author: Haisong Xu, chsxu@zju.edu.cn

Keywords: simulation, multispectral imaging system, multichannel filter array, demosaicing, spectral reconstruction

ABSTRACT

The multispectral imaging systems implemented with color filter wheel or multiple illuminants are competent to capture multispectral images, but correspondingly extend the measurement duration for multiple exposures. The employment of multichannel filter array (MCFA) enables capturing a multispectral image at a single exposure, but at the cost of the spatial resolution. Simulation of a MCFA based 9-channel multispectral imaging system was carried out to estimate its colorimetric and spectral reproduction performance, the channels of which were selected and optimized from a set of technologically available narrow band color filters. A demosaicing method was proposed, and its performance was investigated with the comparison to the performance of the classic Bayer color filter array (CFA). The simulated imaging system was tested with a bunch of hyperspectral images of real scenes, and a spectral reconstruction method was applied to the captured images to obtain the relative spectral response. The simulation results indicate that the MCFA based multispectral imaging system losses minor spatial resolution and would be favorable for colorimetric as well as spectral reproductions.

INTRODUCTION

The multispectral imaging systems are competent to capture and reconstruct the spectral reflectance of real scenes. Since they usually possess a panchromatic image sensor capturing light signals with the modulation of multiple narrowband color filters or light grating[1], the majority of multispectral imaging systems needs an external multiple sampling mechanism like color filter wheel or linear scanning device to obtain both spatial and spectral information, which extends the measurement duration and system complexity. Hereby the multispectral camera system with multichannel filter array (MCFA) was developed to capture the spectral as well as spatial information in a single exposure, providing the capability of multispectral imaging within a convenient mosaicing camera system.

Through the simulation of a MCFA based 9-channel multispectral camera, the spectral sensitivity functions (SSFs) of the channels were selected and optimized from a set of real narrow band color filters[2]. Assuming that the neighbor ones of the green channel contribute to its response, a novel demosaicing method was proposed to improve the spatial resolution of the demosaic image. The relative spectral response of the multichannel image can be obtained via a spectral reconstruction method. The whole simulation framework was applied to a bunch of

hyperspectral images of real scenes to test its performance. Two basic methods, namely linear interpolation demosaicing and classic RGB CFA, were employed as references to our method.

MULTISPECTRAL CAMERA SYSTEM AND DEMOSAICING METHOD

The multichannel filter blocks of the simulated camera are of the size 3×3 pixels, the SSFs of which were selected and optimized from a set of real narrowband color filters in our previous work[2], as shown in Figure 1(a). A total of 8 narrow band filter SSFs are involved in the MCFA, in which the channel with 540nm central wavelength (hereafter referred to 540nm channel) possesses an extra pixel in the 9-pixel multichannel filter block for better spatial sampling rate. The FWHM of the SSFs are all around 20nm. The proposed MCFA pattern of the image sensor in our simulation is demonstrated in Figure 1(b), in which the two pixels of 540nm channel in a multichannel filter block locate at the upper left corner and bottom right corner, while the pixels of 500nm channel and 581nm channel locate at the bottom left corner and upper right corner, respectively. This specific pattern of pixel locations in a block is beneficial to the demosaicing method proposed in this study. The detailed distribution of the other channels can be found in Figure 1(b).

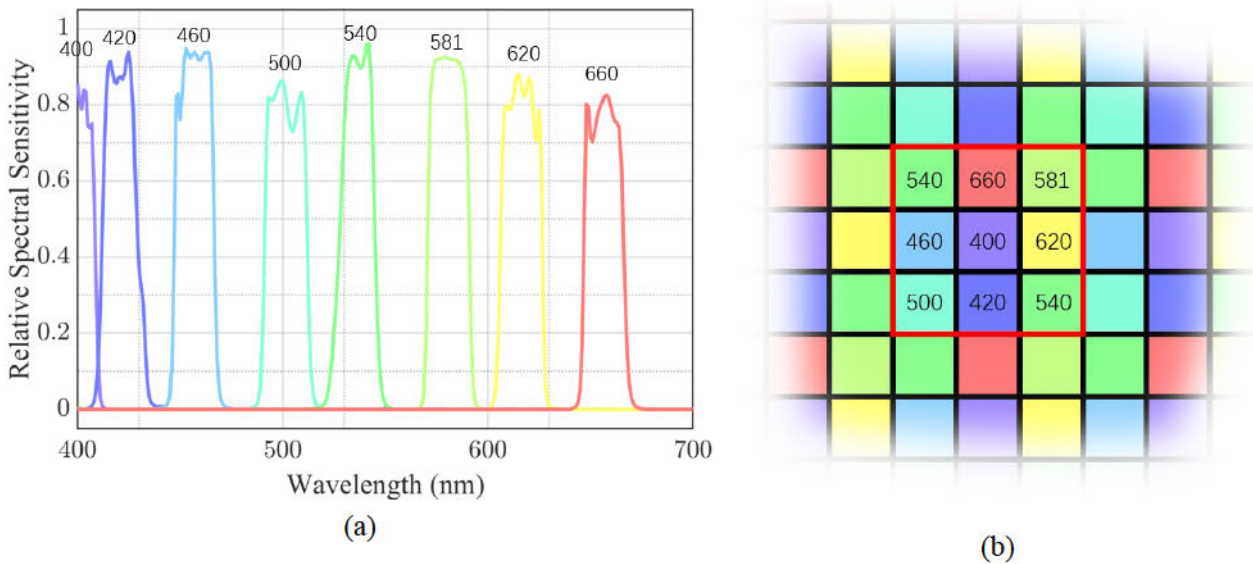


Figure 1. The MCFA of the proposed camera system: (a) the spectral sensitivity of each channel, and (b) the MCFA patterns with the numbers representing the central wavelength of the channel.

Two spectral reflectance image datasets were used in the experiment, i.e., the CAVE dataset and the spectral reflectance images captured in this study (hereafter referred to our dataset). The CAVE dataset is regarded as a standard multispectral image dataset, which consists of 31-band images at every 10nm from 400nm to 700nm, with the image size of 512×512 . The images of our dataset were all captured using a Dualix GaiaField-V10 hyperspectral camera, with the spatial and spectral resolution being 1392×2132 and 3.2nm, respectively. The captured images were corrected with the image of a white reference plate under the same illuminant, generating the corresponding 94-band spectral image from 400nm to 700nm. The CIE standard illuminant D65 and D50 were adopted to the two datasets to generate input spectral radiance image for the simulated camera. Figure 2 illustrates the appearance of the images of our dataset, together with the images of CAVE dataset, under the

standard illuminant D65.

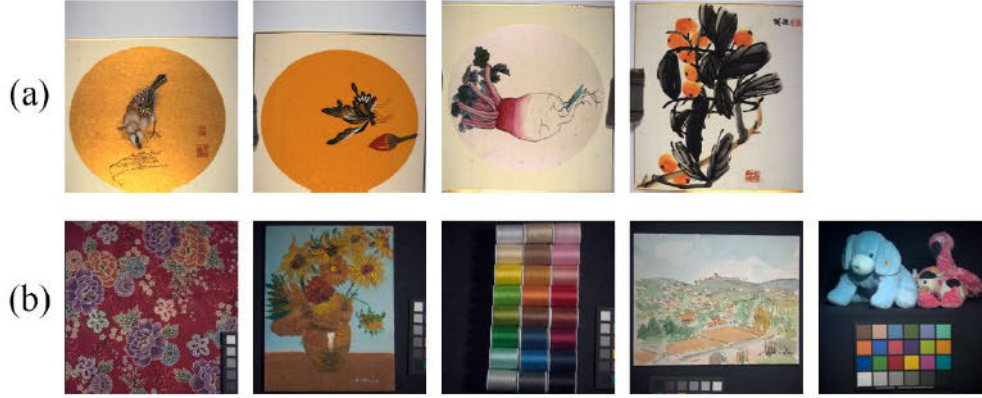


Figure 2. The color appearance of the involved spectral images: (a) our dataset and (b) CAVE dataset.

The pixel responses of a raw image are calculated by multiplying pixel radiance vector and the relevant SSF of the MCFA pattern location. The proposed demosaicing method assumes that the pixel response of 500nm or 581nm channel is potentially related to that of the 540nm channel. Thus, the responses of 540nm channel for these pixels can be deduced from the those of the 500nm and 540nm channels.

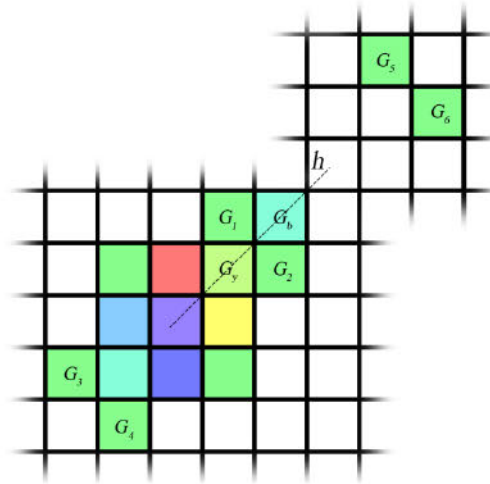


Figure 3. The reconstruction of 540nm channel response.

Following this assumption, the response of 540nm channel at the 581nm pixel can be calculated using the response of 581nm channel G_y and the response of 500nm channel G_b as

$$G_{581} = \frac{k}{2}(G_b + G_y) + \frac{1-k}{2}(G_1 + G_2) + \frac{1}{12}\left(\frac{G_3+G_4}{2}\right) - \frac{1}{12}\left(\frac{G_5+G_6}{2}\right) \quad (1)$$

Similarly, the response of 540nm channel at the 500nm pixel can be calculated as

$$G_{500} = \frac{k}{2}(G_b + G_y) + \frac{1-k}{2}(G_1 + G_2) + \frac{1}{12}\left(\frac{G_5+G_6}{2}\right) - \frac{1}{12}\left(\frac{G_3+G_4}{2}\right) \quad (2)$$

The locations of the variables with subscripts can be found in Figure 3. k is a weighting factor, being set as 0.5 in this study. The responses of G_3 , G_4 , G_5 and G_6 pixels are employed to protect the texture of h axis as shown in Figure 3. The responses of 540nm channel at the remaining pixels are rebuilt with linear interpolation to achieve the full resolution image of the 540nm channel. The other 7 channels are then demosaiced using a guide filter method[3],

which assumes that the spectral neighbor band are highly correlated, thus the ratio of the sparse channel to its full resolution neighbor channel can be regarded as a guide image of the guide filter method for sparse channel rebuilding.

The ground truth spectral image was set as the 31-band spectral image from 400nm to 700nm. A kernel spectral reconstruction method[4] was utilized in the experiment to reconstruct the 31-band spectral image from the 8-channel demosaic image and to evaluate the accuracy of the demosaicing methods. A total of 100 multispectral pixels and their corresponding ground truth spectral pixels were randomly selected from the image as the reconstruction training samples. Besides, the RGB version of the ground truth spectral image was calculated using the CIE 1931 standard observer, and the pseudo-inverse method was applied to the training samples for generating a transfer matrix to acquire RGB version of the 8-channel demosaic image.

To evaluate the performance of the proposed method, another demosaic image with all interpolated channels and a 3-channel classic CFA based RGB image using the SSF of a certain camera (Nikon D3x) were generated for comparison. A total of 100 pixels were randomly chosen as testing samples. The angular error and RMSE between demosaic image and ground truth 8-channel image were calculated to evaluate the performance of the demosaicing method. In addition, the CIEDE2000 color deference ΔE_{00} under standard illuminant D65 as well as RMSE between the reconstructed spectral image and the ground truth spectral image were also taken into consideration to evaluate the demosaicing performance.

RESULTS AND DISCUSSION

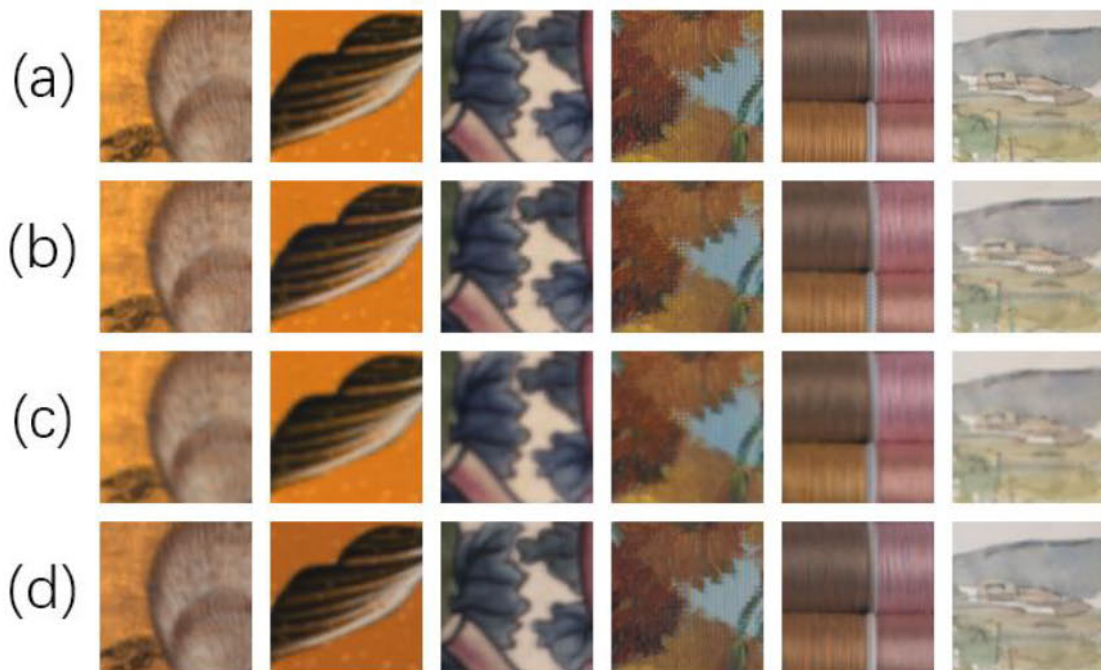


Figure 4. The partial images of the reconstructed RGB version of demosaic results: (a) the ground truth, (b) the proposed method, (c) the linear interpolating method, and (d) the classic CFA RGB image.

Some 100×100 pixel partial images of the mapped RGB version of the 8-channel images as well as the classic RGB CFA images are demonstrated in Figure 4, being compared with the

ground truth image to inspect the spatial recovering performance of the proposed demosaicing method. It can be seen that the proposed method presents better performance on spatial recovering than the linear interpolating method, being close to the performance of the classic CFA method. This method also avoids the false color artifacts in the classic CFA images to a certain extent. The result suggests that the simulated camera system with the proposed MCFA achieves balance between the spatial and multispectral performance.

The performance evaluation results are listed in Table 1. The proposed method has advantages in comparison to the linear method and the classic CFA method, showing superiority in terms of ΔE_{00} and spectral RMSE, suggesting that the proposed method performs better on spectral reconstruction. Furthermore, the proposed method also shows improvement to the linear method on angular error and 8-channel RMSE, which implies that the proposed method performs better in demosaicing accuracy.

Table 1: The evaluation results of the demosaicing methods.

		Spectral image		8-channel image	
		ΔE_{00}	RMSE	Angular error	RMSE
Our dataset	proposed	0.89	0.02579	7.56×10^{-4}	0.04101
	linear	0.98	0.02662	7.62×10^{-4}	0.04141
	RGB	1.44	0.03930	-	-
CAVE dataset	proposed	2.15	0.02181	8.60×10^{-4}	0.03773
	linear	2.50	0.02390	8.78×10^{-4}	0.04017
	RGB	3.23	0.03338	-	-

CONCLUSION

An MCFA based multispectral camera system and a corresponding demosaicing method were proposed and simulated in this study. The camera system employs an 8-channel MCFA to capture the raw image. The demosaicing method is based on an assumption that the response of 540nm channel can be estimated by its neighbor bands. The linear interpolation demosaicing method and the classic CFA method were employed to evaluate the performance of the proposed method. The results indicate that the camera system with the proposed demosaicing method achieves a balance between the spatial and the spectral performance.

REFERENCES

1. Khan, M. J., Khan, H. S., Yousaf, A., Khurshid, K., & Abbas, A. (2018). Modern trends in hyperspectral image analysis: a review. *IEEE Access*, 6, 14118-14129.
2. Xu, P., & Xu, H. (2016). Filter selection based on light source for multispectral imaging. *Optical Engineering*, 55(7), 074102.
3. Monno, Y., Kikuchi, S., Tanaka, M., & Okutomi, M. (2015). A practical one-shot multispectral imaging system using a single image sensor. *IEEE Transactions on Image Processing*, 24(10), 3048-3059.
4. Valero, E. M., Hu, Y., Hernández-Andrés, J., Eckhard, T., Nieves, J. L., Romero, J., ... & Nowack, D. (2014). Comparative performance analysis of spectral estimation algorithms and computational optimization of a multispectral imaging system for print inspection. *Color Research & Application*, 39(1), 16-27.

A DNN-BASED MODEL FOR CIECAM02 APPLICATION

Hung-Chung Li^{1*}, Pei-Li Sun², Yennun Huang¹

¹ *Research Center for Information Technology Innovation, Academia Sinica, 128 Academia Rd., Sec. 2, Nankang Dist., Taipei 11529, Taiwan, R.O.C.*

² *Graduate Institute of Color & Illumination Technology, National Taiwan Univ. of Science and Technology, No. 43, Sec. 4, Keelung Rd., Da'an Dist., Taipei 10607, Taiwan, R.O.C.*

*Corresponding author: Hung-Chung Li, pony780210@iis.sinica.edu.tw

Keywords: CIECAM02, color appearance model, artificial intelligence, deep learning, neural network

ABSTRACT

In the study, a DNN-based model for CIECAM02 application with the novel optimizer and activation functions are proposed. The predicted color appearance J_{ab} from the DNN-based model well represents those attributes of CIECAM02 with high R-squared and acceptable RMSE values. The result also verifies that the color appearance model can be adequately described by typical neural networks architecture.

INTRODUCTION

The CIECAM02 color appearance model proposed by CIE Technical Committee 8-01 has been successfully used in cross-media color reproduction [1] [2]. It can predict both relative and absolute color appearance attributes such as Lightness and Brightness considering luminance adaptation, chromatic adaptation, cone response functions, simultaneous contrast, surround effect, discounting-the-illuminant, Stevens and Hunt effects.

With the rapid development of artificial intelligence (AI) in recent years, deep neural network (DNN) has become one of the most representative models for application in various filed such as convolutional neural networks (CNNs) and long short-term memory (LSTM) respectively used in image classification and prediction of time series data. In supervised learning, the DNN utilized the back-propagation algorithm, which is based on gradient descent optimization to calculate the gradient of the loss function and update the weights of the neurons for gradually reducing the loss.

From the previous studies, some researchers have described the color appearance for human vision by modeling a neural network [3] [4] [5]. Compared with the conventional neural network, some novel optimizers like Adam [6] and activation functions were later proposed and mainly adopted for training speed up and avoiding vanishing gradient problems. Therefore, the study aims to introduce a DNN-based model with those approaches for better-predicting color appearance attributes inclusive of Lightness (J), green–red component (a) and blue–yellow component (b) derived from the CIECAM02 model.

DATA PREPARATION

To train a deep neural network, the initial step is to determine the inputs. Similar with the CIECAM02 model, the tristimulus values (XYZ) of an object, reference white (XYZ_w), absolute luminance of the adapting field (L_A), relative luminance of background (Y_b) and surround conditions (S_R) are regarded as inputs for a DNN model to conduct the learning procedure. Totally 481,401 sets of input data are obtained with spectral power distribution (SPD) of CIE Standard illuminant A, D50, and D65, spectral reflectance of Standard object color spectra database (SOCS)

and CIE 1931 color-matching functions. The tristimulus values (XYZ) are calculated with the integral of light source, spectral reflectance and CIE 1931 color-matching functions ranging from 400 nm to 700 nm as Eq. 1 where $S(\lambda)$ is the spectral power distribution of the test light sources, $\rho(\lambda)$ is the spectral reflectance of SOCS data, \bar{x} , \bar{y} , \bar{z} are the CIE 1931 color-matching functions for X, Y, Z components respectively and k is the scaling factors limiting the range of tristimulus values (XYZ) between 0 and 100. The absolute luminance of the adapting field (L_A) and the relative luminance of background (Y_b) are assigned as one-fifth of L_w and 20 respectively. All the surroundings (S_R) are tested, which are average, dim and dark conditions.

$$\begin{aligned}
 X &= k \int_{400}^{700} S(\lambda) \rho(\lambda) \bar{x}(\lambda) d\lambda \\
 Y &= k \int_{400}^{700} S(\lambda) \rho(\lambda) \bar{y}(\lambda) d\lambda, \quad k = \frac{100}{\int_{400}^{700} S(\lambda) \bar{y}(\lambda) d\lambda} \\
 Z &= k \int_{400}^{700} S(\lambda) \rho(\lambda) \bar{z}(\lambda) d\lambda
 \end{aligned} \tag{1}$$

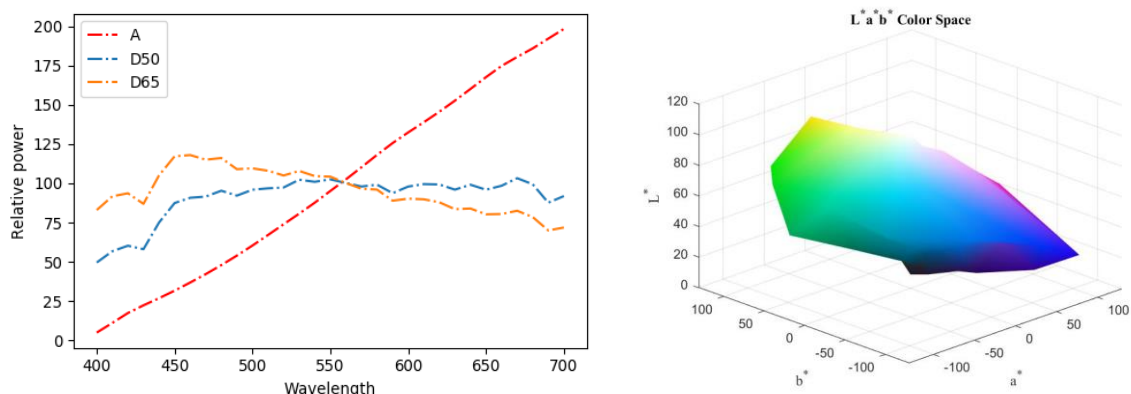


Figure 1. SPDs of light source and color gamut of SOCS

In data pre-processing, the data of reference white and surround conditions are classified into three categories respectively, and thus one-hot encoding is used. The demonstration of one-hot encoding can refer to Figure 2. Besides, the feature scaling method shown as Eq. 2 called Min-Max Normalization is applied to the input data for improving accuracy and faster convergence.

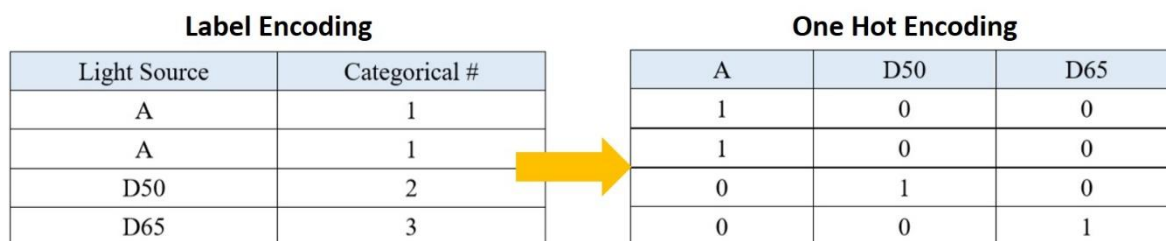


Figure 2. One-hot encoding

$$X_{scaled} = \frac{X - X_{min}}{X_{max} - X_{min}} \in [0, 1] \quad (2)$$

ARCHITECTURE OF THE DEEP NEURAL NETWORK

After the data pre-processing, a deep neural network (DNN) with 2,313 trainable parameters is built and later compiled. The architecture of the deep neural network is a multilayer perceptron (MLP) containing an input layer with 11 input variables, three hidden layers with 30 neurons and a nonlinear activation function ReLU for each layer and an output layer with three output values and a linear activation function to solve the regression problem. Figure 3 illustrates the architecture of DNN-based model. The model is implemented in Python with Keras, Pandas and Numpy modules. An optimization algorithm called adaptive moment estimation (Adam) is adopted, which is a method for stochastic optimization with an initial learning rate of 0.001. The Adam combines the advantages of Momentum and AdaGrad algorithm, which can adaptively accelerate gradients vectors and adjust learning rate.

Furthermore, the number of epochs and batch size are set as 1,500 and 128 when training. All the samples are randomly assigned as 70% for training (10% for validation) and 30% for testing. The training data and testing data are 336,980 and 144,421 sets respectively. The testing procedure is conducted five times for reliability and average the rest of the test results. Figure 4 shows the training history of DNN-based model for each epoch. Referring to Figure 4, there are fluctuations of MAE between 0.3090 and 0.2413 starting from the training procedure at epoch 798/1500.

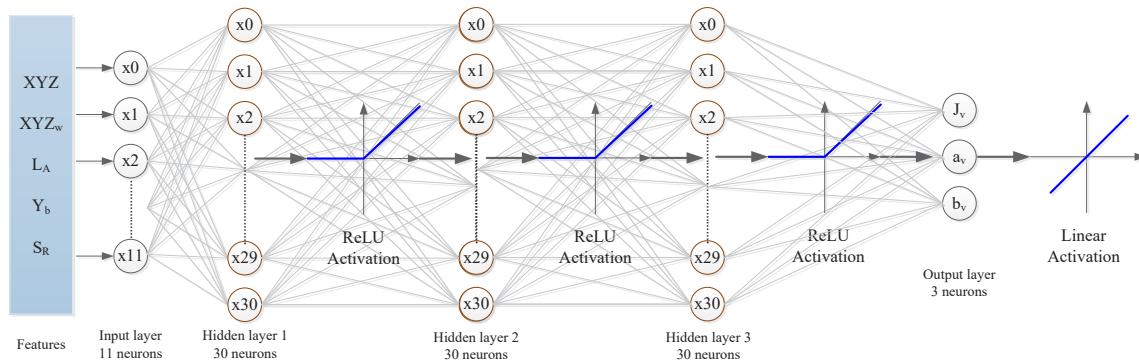


Figure 3. Architecture of the deep neural network

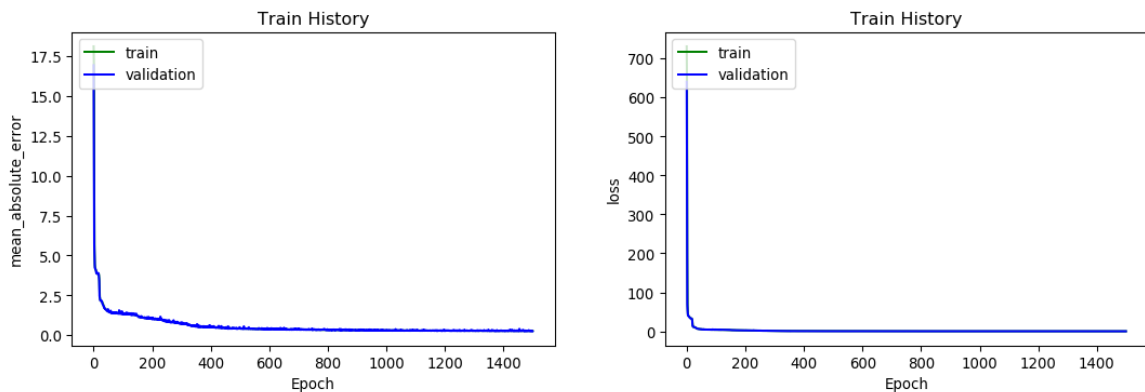


Figure 4. The history of training (Left: MAE, Right: loss)

MODEL EVALUATION

For regression analysis, coefficient of determination (R-squared) and root-mean-square error (RMSE) are mainly used to evaluate the machine learning models. The average of the test results in RMSE, mean absolute error (MAE), maximum of absolute error (Max_AE), R-squared and Pearson correlation coefficient are listed in Table 1. As a result, the mean absolute error (MAE) between CIECAM02 Jab and predicted Jab is 0.280. The R-squared for Lightness (J), green-red component (a) and blue-yellow component (b) are about 0.9998. Their RMSE are 0.207, 0.491 and 0.470 respectively. According to the test results, the Lightness (J) can be much more accurately predicted but not for green-red component (a) and blue-yellow component (b) which needs further studies. To better predict the color appearance attributes, a method called grid search can be used for finding the best hyper-parameters including parameters of the learning rate, Adam, layers, hidden units and mini-batch size for our model. Figure 5 shows the scatter plot of predicted values and the ground truth where the distribution of the data points is close to the 45-degree line that is considered as a perfect prediction. The results indicate that the DNN-based model can well predict the color appearance attributes with high R-squared and acceptable RMSE value.

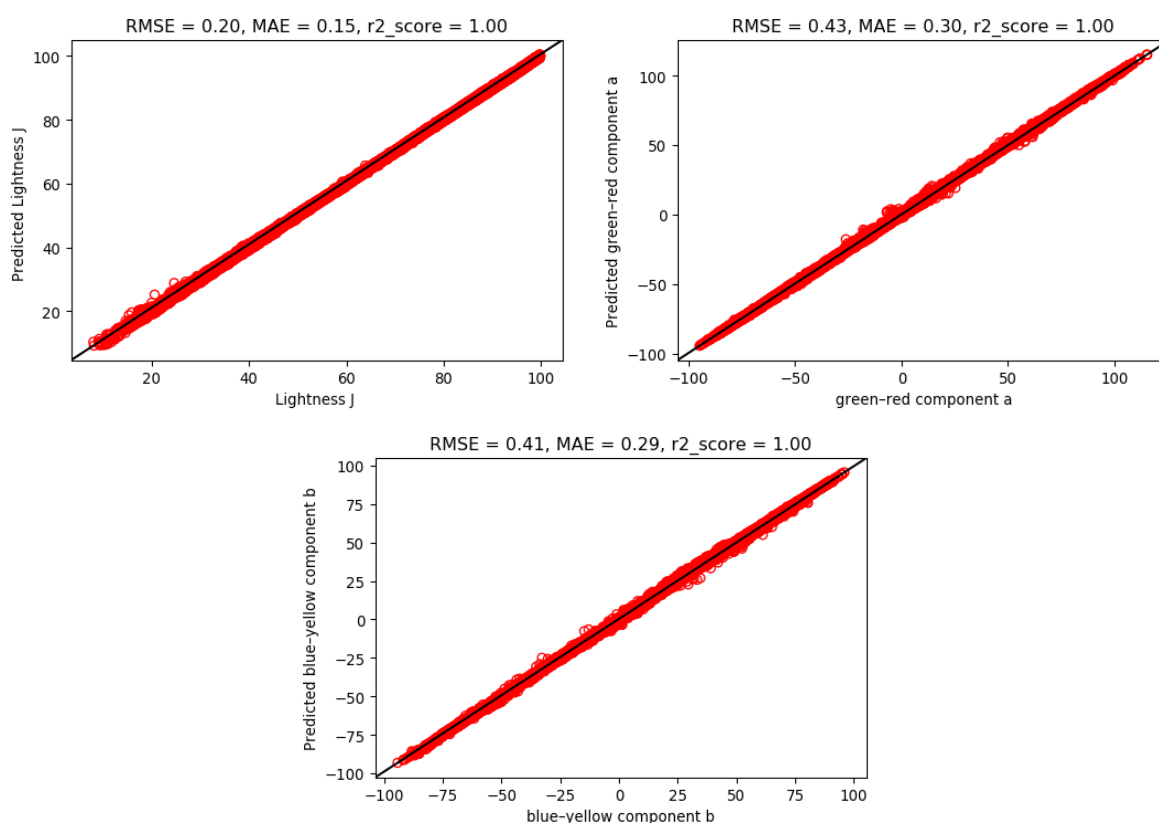


Figure 5. Scatter plot of prediction

Table 1: Test results of DNN-based model

	RMSE	MAE	Max AE	r2score	Pearson r
J	0.207	0.150	4.719	0.9998	0.9999
a	0.491	0.345	10.495	0.9998	0.9999
b	0.470	0.345	9.140	0.9997	0.9999

Three formulae are used to evaluate the color difference between CIECAM02 Jab and predicted Jab, CIE76, CIE94 and CIEDE2000 included. The test results with different formulae are shown in Table 2. With the method of CIE94 and CIEDE2000, the model performances the smaller color difference. The mean value of the color difference in CIE76 is falling into the range where expresses that the difference is unnoticeable [7]. However, there are still relatively more significant color differences for some color samples.

Table 2: Test results in color difference

	CIE76	CIE94	CIEDE2000
mean	0.581	0.345	0.343
max	10.942	8.301	11.482

CONCLUSIONS

The study aims to build a machine learning model based on a deep neural network to verify the accuracy of the prediction for color appearance attributes compared to those derived from CIECAM02. The model applies Adam as an optimizer and uses a nonlinear activation function ReLU which are widely accepted in most field of deep learning to fit the ground truth dataset. The result suggests that the prediction of green–red component (a) and blue–yellow component (b) still have room for improve by tuning hyper-parameters in the model. In addition, k-fold cross validation will be studied next to verify the reliability of the model. In conclusion, the results show that the DNN-based model can ideally predict the color appearance attributes with high R-squared and acceptable RMSE value. Moreover, training a deep neural network to express color appearance is feasible.

ACKNOWLEDGEMENT

This research project is partly supported by Ministry of Economic Affairs (RD-1070202-2)

REFERENCES

1. Fairchild, M. D. (2013). Color appearance models. John Wiley & Sons. p 289–310
2. CIE 159-2004. (2004). A color appearance model for color management systems: CIECAM02. Vienna, Austria: CIE Central Bureau.
3. Schettini, R. (2001). Approximating the CIECAM97s color appearance model by means of neural networks. *Image and Vision Computing*, 19(9-10), 691-697.
4. Chai, B., Liao, N., & Zhao, D. (2004). Approximating the CIECAM02 color appearance model by means of neural networks. *Chinese Optics Letters*, 2(11), 637-639.
5. Wu, C. Q. (2009, May). A multi-stage neural network model for human color vision. In *International Symposium on Neural Networks* (pp. 502-511). Springer, Berlin, Heidelberg.
6. Kingma, D. P., & Ba, J. (2014). Adam: A method for stochastic optimization. arXiv preprint arXiv:1412.6980.
7. Mokrzycki, W. S., & Tatol, M. (2011). Colour difference ΔE -A survey. *Machine Graphics and Vision*, 20(4), 383-411.

ANALYSIS OF THE PROCESS OF COLOR CONSTANCY NETWORKS BY CNN

Takuma Hirose^{1*}, Noriko Yata¹ and Yoshitsugu Manabe¹

¹*Chiba University, Japan.*

*Corresponding author: Takuma Hirose, hirose_t7@chiba-u.jp

Keywords: Color imaging, Color constancy, Convolutional neural network, Deep neural network

ABSTRACT

Convolutional Neural Network (CNN) attracts attention in a field of image recognition and image generation. CNN is modeled on the structure of the characteristic extraction of the human visual cortex. This research works from the thought that reproduces and analysis color constancy on CNN clues to the elucidation of the mechanism of human color constancy. Therefore, a network learns to reproduce color constancy. A visualization is utilized as an analysis of the processing of the network. First, it is necessary that a large number of images which changed the color of the illumination variously as a training data set. In this research, the data set is composed of Computer Graphics (CG) images because it is difficult to collect a large number of images, including the same scene of under various illumination color in the real world. The CG images are produced by physically based rendering from theory to implementation (PBRT), which is often used by a scientific use. Input data of CNN are the images under colored illuminant light, and grand truths are the images under the white light source of the same scene as input. Second, a network based on CNN learns the data set and reproduce color constancy on a computer. It is the color constancy network what we proposed. Finally, visualizing the feature map for the network which learned color constancy extracts what kind of character in images and how processes color constancy. The color constancy network based on pix2pix, which is a coloration network learn a converting color of an input image to achieve the color constancy. Pix2pix which are incorporated U-net and patchGAN is the image generation network which has general versatility. The color constancy network revised the most images successfully but revised some images inaccurately under red illumination. We assume the deflection of the input image cause it. As a result of visualizing the feature map of the layer, we defined the role of each filter in each layer of the network. Also, we discovered the possibility for the color information for the highlight of the object contributed to revision. It is thought that this discovery becomes a significant clue in the mechanism of the human color constancy.

INTRODUCTION

Color constancy is a phenomenon in which we humans can correctly perceive the color of objects even when the color of illumination changes. This mechanism is thought to exist in the visual system but has not been clarified yet. On the other hand, it could come to explain the mechanism of color constancy by reproducing and analyzing using Convolutional Neural Network (CNN), which imitates the structure of the human visual cortex. In this study, we attempt to reproduce and analyze the human color constancy on a computer using Generative adversarial networks: GAN[1].

RELATED WORKS

In this chapter, the following are described: Relation research of convolution neural network, realization of color homeostasis and related research of visualization of the network.

Features of GAN

GAN is a method proposed by Goodfellow et al. [1]. The network consists of a generator and a discriminator. The generator generates an output from the input noise. The discriminator is populated with either real data or generator output to identify whether the data is real or fake. The generator learns to deceive the discriminator, and the discriminator learns to detect the fakes from the generator. The whole of the system is aiming at a correct response rate of 50%. In other words, the goal is that the discriminator cannot distinguish the data generated by the generator from the real one. Also, a network called Deep Convolutional Generative Adversarial Networks (DCGAN) using CNN and GAN has been proposed. The generated images are clear, and the results cannot be distinguished from the real ones. This paper also deals with a network [2] called Conditional GAN which can control images generated by specifying labels.

previous work on color constancy

A method to realize color constancy on a computer using a physical base renderer and DCGAN has been proposed [3]. In the method, a set of two in learning data for DCGAN consists of two images of multiple objects arranged randomly. One of them is under a colored light source, and the other is under a white light source. A network learns the former as an input image and the latter as a correct image. The colors of colored lights were changed variously in each scene. Since a large number of images are necessary for learning, and color constancy is a phenomenon which occurs in the real world, it is desirable to learn using a real image. However, it is difficult to collect a large number of various scene images in which the illumination light can be changed in the real world. On the other hand, the ordinary CG image sometimes becomes a far image from the real image, because the rendering is carried out by modeling the property of simple light and the object surface. Then, this paper carries out rendering by a model capable of reproducing complicated physical phenomena such as spectral reflectance in an object surface called physical-based rendering, the spectral distribution of light, and a path propagating to a camera in detail. In Hirabayashi et al., CG images for learning were acquired using Physically Based Rendering from Theory to Implementation (PBRT) [4], which is a physical-based renderer used in academic applications.

Hirabayashi et al. used an image generation network called pix2pix[5]. pix2pix is an image generation network with high versatility such as coloring task, generation of road, and building images from label images, generation of map images from aerial photographs. For an auto-encoder which performs dimensional compression, a network called U-net which transmits a common feature quantity of input and output is used. And, cGAN is also used jointly, and among them, a technique called PatchGAN [5], in which L1 normalization is incorporated in the calculation of loss function, features of the rough image are caught by L1 normalization, and the detail is supplemented by GAN, is also incorporated. The pix2pix is improved and used in this paper.

Network visualization and understanding

CNN learns the process from the input of the image to the output of the recognition result by end-to-end, so it was not clear what kind of feature extraction and processing CNN performs for the image. Then, the research which understands the action of CNN is advanced, and there are many related kinds of research. Girshick et al. proposed a method to obtain the region of the input image from which strongly activated neurons are derived [6]. Zeiler et al. proposed DeconvNet [7] to visualize the pattern captured by the filter of convolution layer. Springenberg et al. have developed the visualization technique of convolution filter of Zeiler et al., and carried out the clear visualization of convolution filter of the higher layer of CNN by the introduction of guided backpropagation [8]. In this paper, we apply these techniques to DCGAN and analyze them.

PROPOSED METHOD

For the image generation model, a CG image in which the color of the illumination light is changed variously is input, and the CG image under the white light source of the same scene is learned as a correct image. The feature maps of model are visualized after the learning, and the information extractions in each layer are analyzed.

generation of learning CG images

PBRT (Physically Based Rendering from Theory to Implementation) [4] was used as a renderer. The object is made of 5 kinds of materials such as metal, plastic, mud, woofer, and mirror provided by PBRT as a standard, and the surface roughness and spectral reflectance are also randomly set. The illumination light is set by changing the temperature of the blackbody radiation, and the colored light source image is set randomly between 2000 K and 30,000 K and the white light source image is set at 6500 K in the same scene.

Building a network of color constancy

For automatically generated CG image for the learning, the network which reproduces the constancy of the human color is constructed using CNN which is made on the basis of the knowledge of visual cortex and is used for image recognition, etc. The color constancy neural network in this study is an image generation model. Also, since color constancy is a task to convert color to the input image, it is constructed based on the coloring model. A colored model is a model which outputs a color image when a monochrome image expressed only by luminance value without color information is given as an input. As in the previous study [3], the network was constructed referring to pix2pix [5].

Network Analysis

The feature map of each layer of the network after learning is initialized and restored. Then, the pattern which each filter catches is visualized to observe extracted information by each convolution layer from the image. Based on the technique by Zeiler et al.'s research [7], all the positions except for the maximum value of the feature map are initialized to 0 in each layer, the feature map is restored to the input layer by deconvolution and visualized, and the pattern which strongly stimulates the filter is compared and examined.

EXPERIMENTS AND RESULTS

Evaluation experiments and analysis experiments of the network are described. We used the network which had been learned with 4500 sheets of learning, one batch size, and 200 epochs.

evaluation experiment

An example of the result of inputting 496 unknown CG images not used for learning is shown in Fig. 1. The color of the object in the left figure is corrected from purple to pink, and the color of the object in the right figure is corrected from green to blue. These colors got to close to the color of the correct image. From this fact, it was confirmed that the color constancy was realized using CNN.

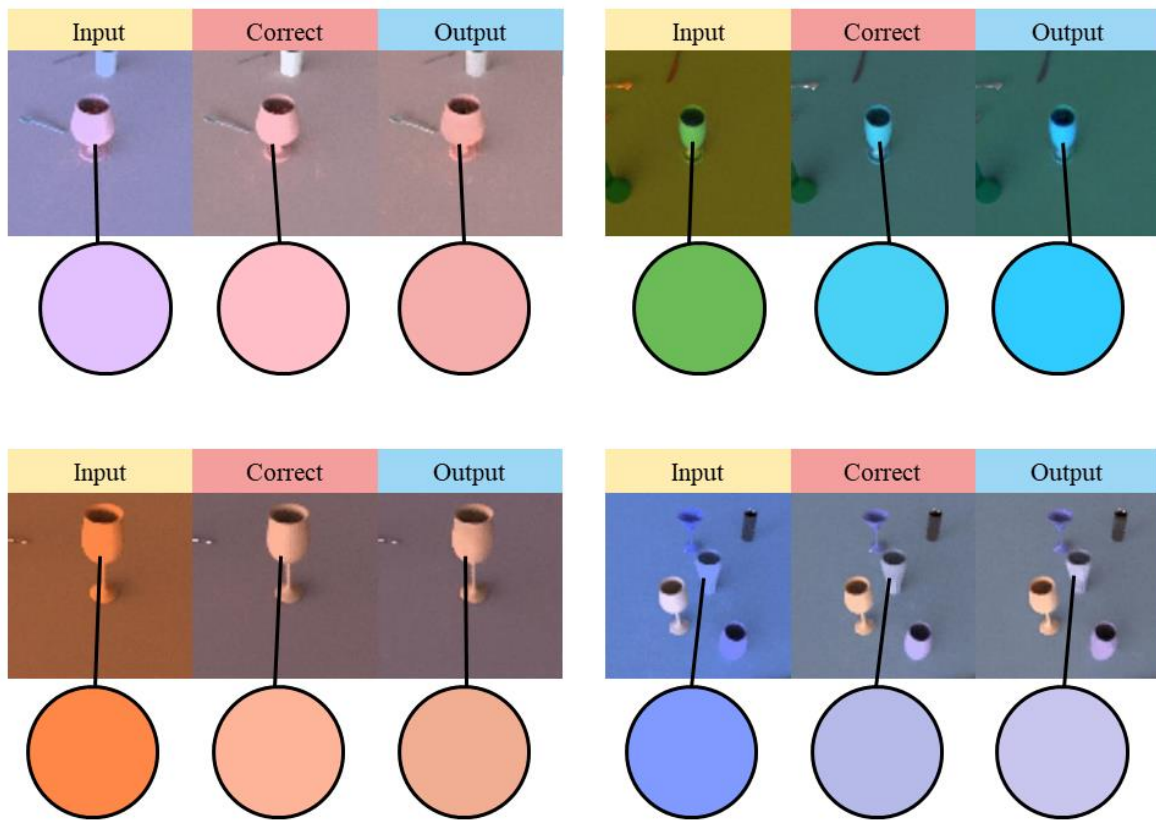


Figure 1. Comparison of object colors in the output image

analytical experiment

An example of the result of visualizing the feature map for each layer by the proposed method is shown in Fig. 2. The object is identified in the shallow layer, and the background part is identified in the deep layer, and the information which seems to be necessary for the correction of the illumination light after the color tone of the whole scene is identified in Conv7 seems to be summarized in Conv8.

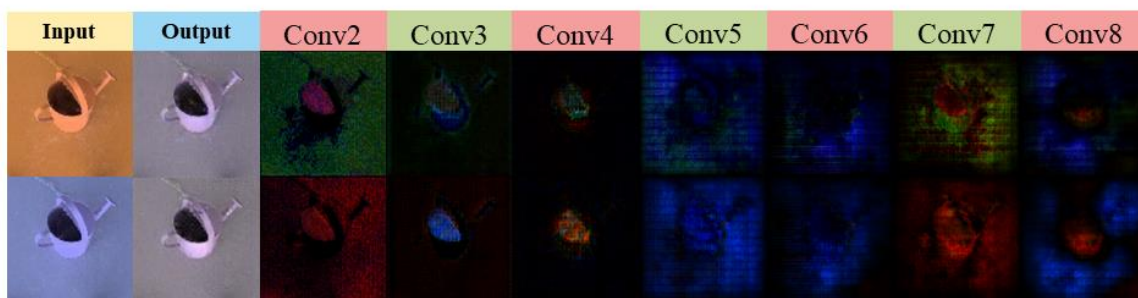


Figure 2. visualized feature map

CONCLUSION

The color constancy was reproduced by the learning using the CG image by the physical-based rendering, and the recognition pattern of each convolution layer was visualized by restoring the feature map. As future works, we will improve the reproducibility of the color constancy network, and tackle the visualization of the reverse convolution layers.

REFERENCES

1. Ian J. Goodfellow, Jean Pouget-Abadie, Mehdi Mirza, Bing Xu, David Warde-Farley, Sherjil Ozair, Aaron Courville, Yoshua Bengio. (2014). Generative adversarial nets, In *Advances in neural information processing systems*, pp. 2672-2680.
2. Mirza Mehdi, Simon Osindero. (2014). Conditional generative adversarial nets, *arXiv preprint arXiv:1411.1784*.
3. Tsukasa Hirabayashi, Yoshitsugu Manabe, Noriko Yata. (2018). Colour Constancy by Machine Learning using Physics Based Rendering Images, *Proc. of AIC2018*.
4. Matt Pharr, Wenzel Jakob, Greg Humphreys. (2016). *Physically Based Rendering, Third Edition: From Theory to Implementation 3rd Edition*, Morgan Kaufmann, Burlington, Massachusetts.
5. Phillip Isola, Jun-Yan Zhu, Tinghui Zhou, Alexei A. Efros. (2016). Image-to-Image Translation with Conditional Adversarial Networks, *arXiv:1611.07004*.
6. Ross Girshick, Jeff Donahue, Trevor Darrell, and Jitendra Malik. (2014). Rich feature hierarchies for accurate object detection and semantic segmentation, *Proceedings of the IEEE conference on computer vision and pattern recognition*, pp.580-587.
7. Matthew D Zeiler and Rob Fergus. (2014). Visualizing and understanding convolutional networks, *European Conference on Computer Vision*, pp.818-833.
8. Jost Tobias Springenberg, Alexey Dosovitskiy, Thomas Brox, Martin Riedmiller. (2014). Striving for simplicity: The all convolutional net. *arXiv preprint arXiv:1412.6806*.

Removal of shadow and reflection over printed matter by CNN with considering area information

Tsukasa Hirabayashi^{1*}, Noriko Yata² and Yoshitsugu Manabe²

¹*Graduate School of Science and Engineering, Chiba University, Japan.*

²*Graduate School of Engineering, Chiba University, Japan.*

*Corresponding author: Tsukasa Hirabayashi, afa5555@chiba-u.jp

Keywords: shadow removal, reflection removal, deep neural network, convolutional neural network, digital archive

ABSTRACT

Taking printed matter with a camera causes shadows of the camera and reflection of lighting. These shadows and reflections impair the original color of the printed matter, therefore need to be removed. However, it is a difficult problem to separate the content of the printed matter and the shadow and/or reflection. This research creates a data set for shadow and reflection removal and proposes the method to remove shadows and reflections by learning using a convolutional neural network (CNN). We collected various contents and paper materials as objects of photographs which are data set. We took shadow images and reflection images with shadows and reflections on the printed matter and shadow-reflection-free images under environmental conditions without shadows and reflections. We construct a CNN for shadow and reflection removal. The network learns to output a shadow-reflection-free image when the input is a shadow-reflection image. The shadow-reflection removal network is based on DeShadowNet, which is proposed in the research on shadow removal. This research replaces a part of DeShadowNet with U-Net and adopt the nearest neighbor upsampling. Also, printed matter area and surrounding area information would be useful for separating shadows and reflections. Therefore, a binary mask image is additionally input image to the shadow-reflection removal network. We verified whether the additional input of the mask image is effective in improving the accuracy of shadow and reflection removal. As results of the experiment, in all of RMSE, SSIM, and visual comparison, the results with inputting mask image were better. From this fact, it was confirmed that the accuracy of shadow and reflection removal was improved by inputting region information into the network.

INTRODUCTION

People sometimes take a printed matter with a camera instead of a scanner and save it. Also, if the printed matter is on a wall or is too large to fit in the scanner, you will use a camera. However, taking a printed matter with a camera causes shadows of the camera and reflection of lighting. So, these shadows and reflections need to be removed. Nevertheless, it is a difficult problem to separate the content of the printed matter and the shadow and reflection. On the other hand, in recent years, research on shadow removal and reflection removal from landscape images by CNN has been conducted [1, 2, 3, 4, 5]. From these studies, the semantic information learned and acquired by CNN is considered to be effective in removing shadows and reflections. So, this research creates a data set for shadow and reflection removal, and proposes the method to remove shadows and reflections by learning using a CNN.

PROPOSED METHOD

First, we create a data set by shooting shadow images and reflection images with shadows and reflections added to the printed matter and shadow-reflection-free images without them. Data sets are also generated from CG images based on physical-based rendering. Next, we construct a CNN for shadow and reflection removal. The network learns to output a shadow-reflection-free image when the input is a shadow-reflection image. Also, shadow and reflection removal are performed by separate networks of the same structure. Each is described below.

The data set consists of two types: real images and CG images. For creating real images, we collected various contents and paper materials as printed matter, such as photos, flyers, documents, and so on. Figure 1 shows an overview of creating real images using these printed matters. Shadow-reflection-free images are obtained by fixing the main light source and camera so that shadows and reflections did not occur on the printed matter. Next, shadow images and reflection images are obtained by shooting shadows and reflections on the printed matter with a shade or sub-light source. In addition, we change the shape and hardness of the shadows and reflections and the background of the printed matter in various ways.

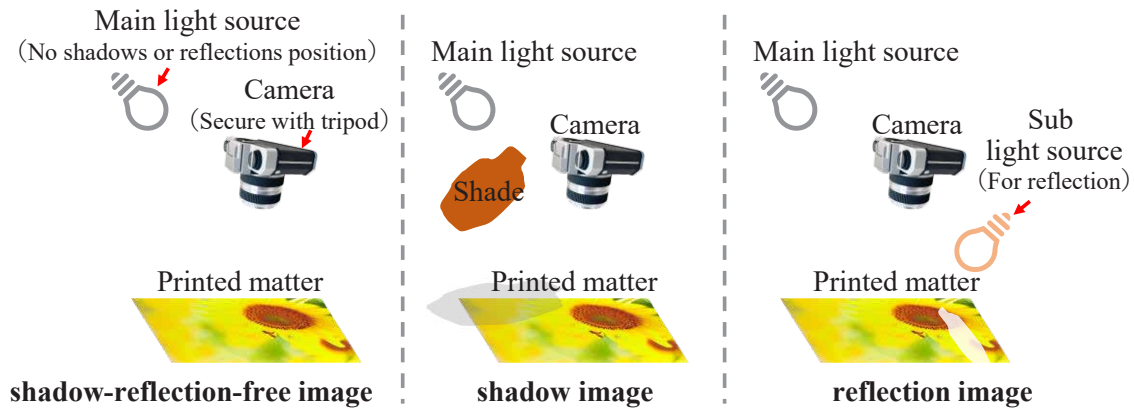


Figure 1. Overview of creating real images

CG images are used to make the dataset larger. We use PBRT of physics-based rendering to generate these CG images [6]. Images used for printed matter and background texture are collected from the Internet. And, like the real printed matter, the printed matter object in CG has wrinkles, creases, and distortion. CG scenes are arranged in the same way as when shooting real images, and shadow images, reflection images, and shadow-reflection-free images are rendered. Figure 2 shows an example of a data set of a real image and a CG image. Furthermore, the data is expanded by adapting rotation and contrast changes.

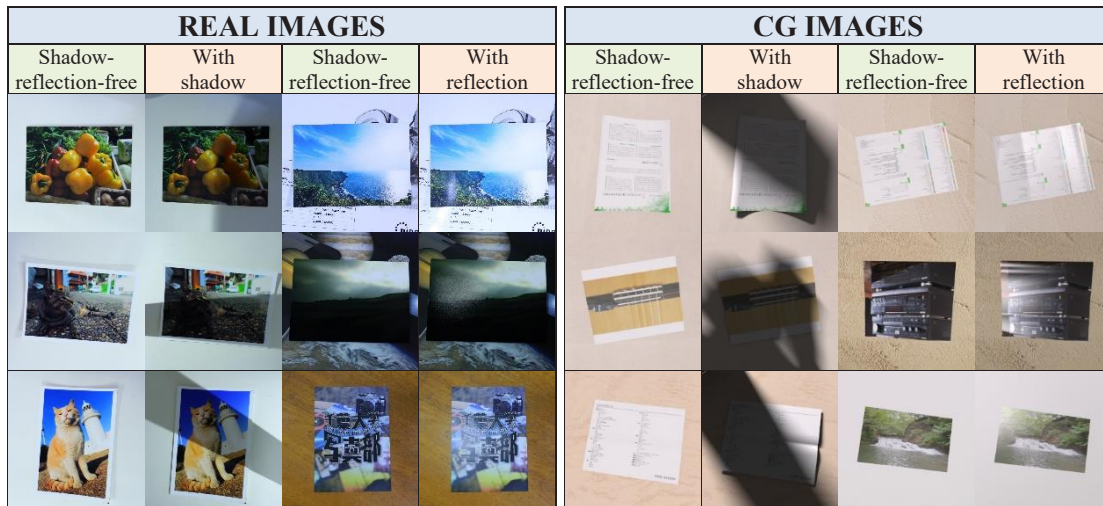


Figure 2. Example of created shadow-reflection removal data set

This paragraph describes the network configuration. We believe that the surrounding information of the printed matter provides a clue to separate the content of the printed matter from shadows and reflections. Therefore, it is necessary to distinguish between the printed matter area and the surrounding area. So, in order to distinguish them, we additionally input a mask image of the printed matter as area information into the network. The proposed network consists of a segmentation network that generates a mask image of the printed matter and a shadow-reflection removal network, as shown in Figure 3. Shadow and reflection removal are performed by separate networks of the same structure. The shadow-reflection-free image is obtained through the shadow removal network and the reflection removal network. The shadow or reflection removal network is improved and built with reference to DeShadowNet used in the study on shadow removal [1]. DeShadowNet is adapted to the multi-context network and mainly consists of three networks. The three networks are the global localization net (G-Net) with fine-tuning of VGG16 [7], the appliance modeling net (A-Net) that receives the output of the shallow layer of G-Net and the segmentation modeling net (S-Net) that receives the output of the deep layer of G-Net. The outputs of A-Net and S-Net are integrated and output. In this research, in order to increase the resolution of the output image, A-Net and S-Net are composed of U-Net [8], which is a kind of semantic segmentation network, and nearest-neighbor upsampling is applied. Figure 4 shows the structure of the shadow or reflection removal network.

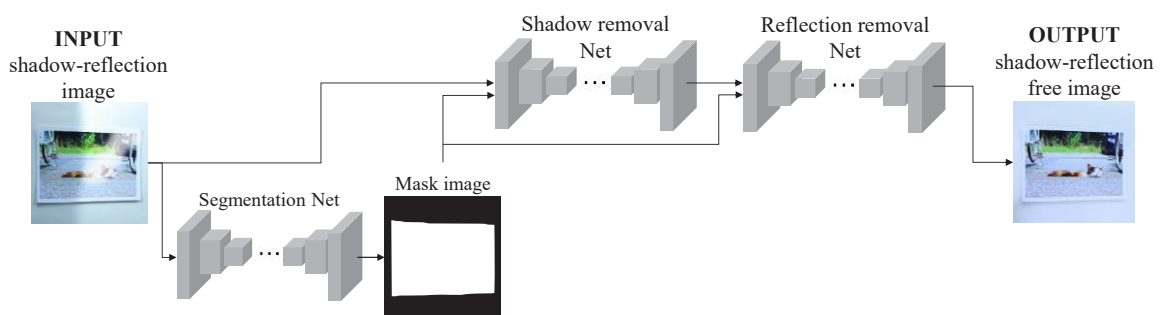


Figure 3. Network configuration with considering area information

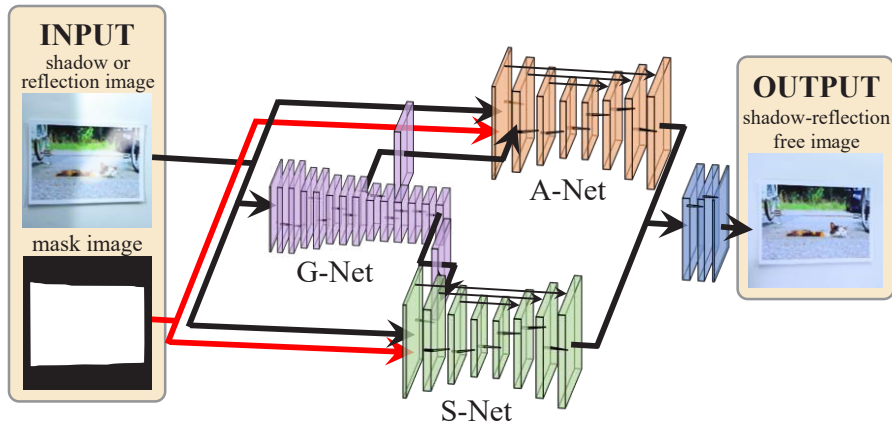


Figure 4. Structure of shadow or reflection removal network

EXPERIMENT

It is verified whether the additional input of the mask image is effective in improving the accuracy of shadow or reflection removal. First, the mask image of shadow-reflection images was created manually instead of the segmentation network. Next, the mask image was input to A-Net and S-Net, and we trained the network. For comparison, we also trained a network that did not contain the mask images. The network was pre-trained with the CG images before training with the real images. The training image size is 224×224 pixels. The training set of the CG images for the shadow and reflection removal were each 32,000 triplets (pairs). The training set of the real images were 3,072 triplets (pairs) for shadow removal and 2,496 triplets (pairs) for reflection removal. The Loss value was Mean Square Error (MSE) between the Shadow-reflection-free images as the ground truth and the output images. The optimization method was Adam, with parameter $\alpha = 0.0001$. Training time was approximately one week. The evaluation after training was performed with unknown real images. The unknown real images are 47 triplets (pairs) for shadow removal and 39 triplets (pairs) for reflection removal.

RESULTS AND DISCUSSION

As showed in Qu et al. [1], the color space is converted to CIE $L^*a^*b^*$, and RMSE and SSIM were calculated using the L^* , a^* , and b^* values between the ground truth and the output image. Table 1 shows the average evaluation values calculated for all unknown real images. The lower values of RMSE and the higher values of SSIM show that the outputs are closer to the ground truth. Both of shadow removal and reflection removal were better evaluated with mask image input. In addition, when the mask image was used to evaluate only the print area, these values got better. Figure 5 shows the output images of each network.

Table 1: The average evaluation values of each network

Removal type	Mask input	RMSE	RMSE only print area	SSIM	SSIM only print area
Shadow removal	no	11.73	7.717	0.9453	0.9754
Shadow removal	yes	10.53	5.915	0.9477	0.9772
Reflection removal	no	13.40	10.59	0.9320	0.9562
Reflection removal	yes	10.90	8.574	0.9423	0.9639

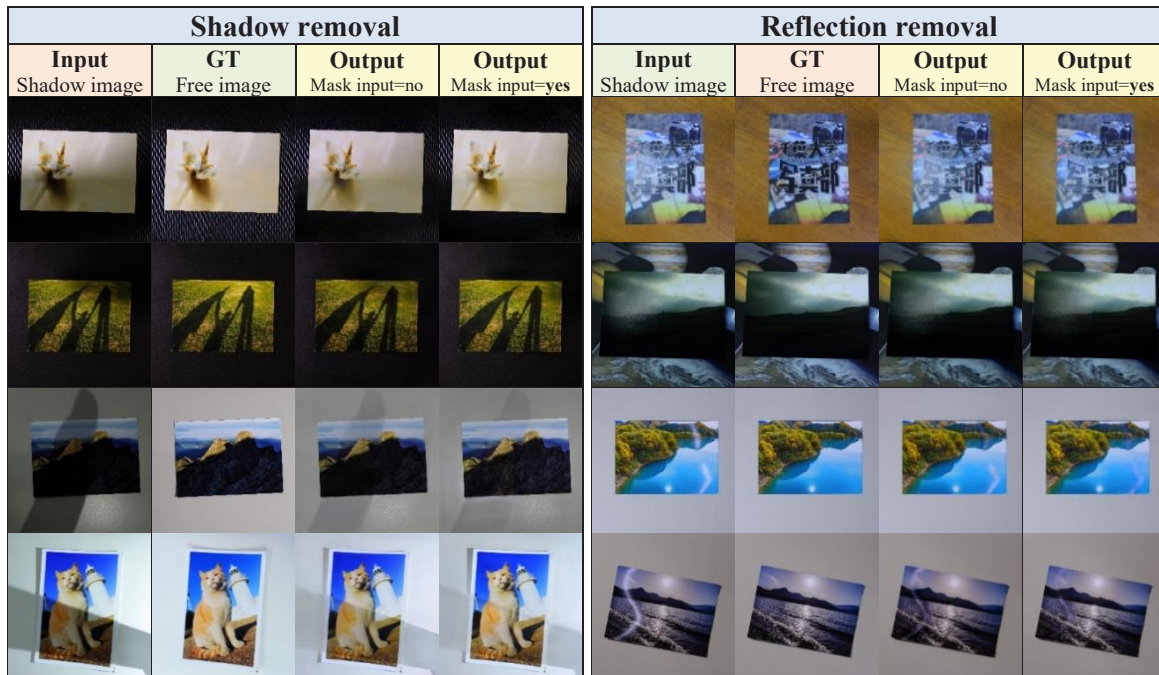


Figure 5. The output images of each network.

The images in the first and second rows of shadow removal in Figure 5 are examples of removing soft shadows. It can be confirmed that the output with mask input can be removed more clearly. The images in the third and fourth rows are examples of removal for hard shadows. It can be confirmed that the output with the mask image removes the inside of the hard shadow more and has a brightness close to the ground truth. The images in the first and second rows of reflection removal in Figure 5 are examples of removing soft reflections. It can be confirmed that the output with mask image can be removed more clearly. The images in the third and fourth rows are examples of removal for hard reflection. It can be confirmed that the output with the mask image does not leave a relatively trace of reflection. From the result, it is confirmed that the presentation of the region information by the mask image is effective in the shadow and reflection removal. The continuous shadows in and out of the printed matter are often the shadows that occur during shooting. The area information contributes to the detection of this shadow, which may have improved the accuracy. On the other hand, in the case of reflection removal, the accuracy may have been improved due to the effect of narrowing the area of interest by the area information.

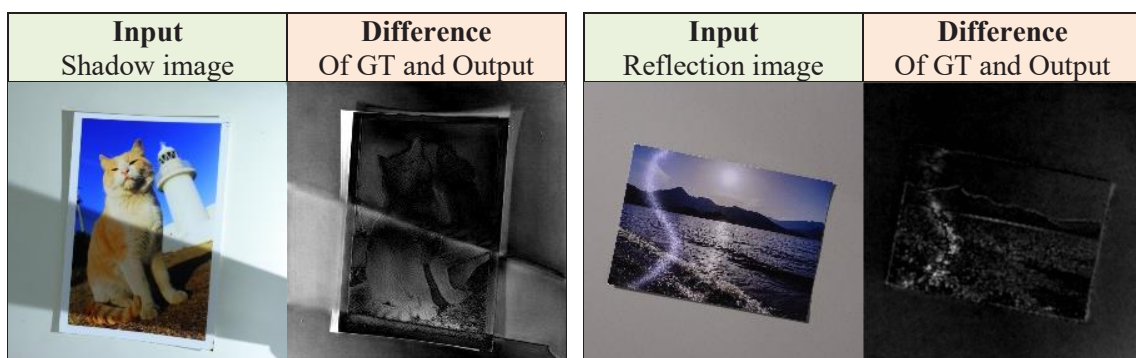


Figure 6. Luminance difference image between output image and ground truth.

There are still remain traces of hard shadows and reflections in some of the results. Figure 6 shows the luminance differences image between the output image and the ground truth shown in the fourth column of Figure 5. The pixel values of the luminance differences image are normalized to “255” for the maximum value and “0” for the minimum value. Thus, a white pixel indicates the largest error. It can be confirmed that the edges of shadows and reflections tend to remain in particular. In order to solve this problem, it is necessary to propose a new method such as that incorporates flexible structure learning.

CONCLUSIONS

Using a multi-context network, we removed the shadows and reflections that occur when shooting printed matters. From the results, it was confirmed that the accuracy of shadow and reflection removal was improved by inputting the mask image to the network as region information. In the future, we plan to conduct experiments on removal when shadows and reflections occur at the same time, and experiments using the generated mask. We aim to improve the accuracy of shadow and reflection removal examining the problems found in the results.

REFERENCES

1. Qu, L., Tian, J., He, S., Tang, Y., & Lau, R. W. (2017). *Deshadownet: A multi-context embedding deep network for shadow removal*. In Proceedings of the IEEE Conference on Computer Vision and Pattern Recognition (1), 4067-4075.
2. Hu, X., Zhu, L., Fu, C. W., Qin, J., & Heng, P. A. (2018). *Direction-aware spatial context features for shadow detection*. In Proceedings of the IEEE Conference on Computer Vision and Pattern Recognition (6), 7454-7462.
3. Wang, J., Li, X., & Yang, J. (2018). *Stacked conditional generative adversarial networks for jointly learning shadow detection and shadow removal*. In Proceedings of the IEEE Conference on Computer Vision and Pattern Recognition (6), 1788-1797.
4. Chi, Z., Wu, X., Shu, X., & Gu, J. (2018). *Single image reflection removal using deep encoder-decoder network*. arXiv preprint arXiv:1802.00094.
5. Fan, Q., Yang, J., Hua, G., Chen, B., & wipf, D. (2017). *A Generic Deep Architecture for Single Image Reflection Removal and Image Smoothing*. arXiv preprint arXiv:1708.03474.
6. Pha, M., Ja, W. and Hu, G. (2016). *Physically Based Rendering, Third Edition: From Theory to Implementation 3rd Edition*. Burlington, Morgan Kaufmann.
7. Simonyan, K., & Zisserman, A. (2014). *Very deep convolutional networks for large-scale image recognition*. arXiv preprint arXiv:1409.1556.
8. Ronneberger, O., Fischer, P., & Brox, T. (2015). *U-net: Convolutional networks for biomedical image segmentation*. In *International Conference on Medical image computing and computer-assisted intervention*. Springer, Cham. 234-241.

DEVELOPMENT OF A COLOR STRIP FROM COLORANTS IN GRAPE FOR ALKALI INDICATOR.

Pakornsit Pongto, Sureeporn Khampaeng, Ploypassorn Punkhor, Pichayada Katemake^{1*},
Supaporn Noppakundiligrat, Kanitha, Tananuwong, Theeranun Janjarasskul

¹*Department of Imaging and Printing Technology, Faculty of Science, Chulalongkorn University, Thailand.*

²*Department of Food Technology, Faculty of Science, Chulalongkorn University, Thailand.*

*Corresponding author: Pichayada Katemake, pichayada.k@chula.ac.th

Keywords: Freshness color label, Food dye, Alkali indicator

ABSTRACT

Manufactured and/or expired date on packaging is used for estimating the expired date of product under controlled condition. If the packaged product is stored in different condition as specified on the package, the expired date is invalid and the freshness of the product will not relate to the expired date. Our project is aimed to study and develop color label that directly indicate freshness of product. Natural dye from grape peel (Brenntag AC 12r WSP) called Anthocyanin was used to produce coating for paper. Seven coating formulations were mixed according to simplex lattice design using 3 components: natural dye, polyvinyl alcohol (PVA) and water and were coated on filter paper. The criteria of choosing amount of dye were color strength. The coatings on paper were tested their color changes when they were exposed to ammonia vapor. In fish, ammonia gas is released from gills as a metabolic waste from protein breakdown. The prepared paper color labels obtained from coating were attached on the PP-multilayer film and glued the film on plastic tray containing ammonia solution. Later, they were kept in the refrigerator (2-7 degrees C) The concentrations of ammonia were 0.5, 1.0, 5.0 and 10 mM. The color measurement of color label was carried out, every 30 min until 240 min, before and after keeping in the refrigerator. It was found that the change of color, indicating by CIE 1976 color difference, increased with time and concentration.

INTRODUCTION

Household packaging for food is one of many types of packaging that are of our interest. Some information on package and/or label is required by government legislation. The expiry/best before date is one of them with the aim to indicate that the package should no longer be on the supermarket shelf. The best before date relates to the freshness of the perishable food. The storage directions printed on the package of the perishable food should be strictly complied to avoid spoilage earlier than the best before date. If the packages on the supermarket shelf are stored improperly, the expiry/best before date will be unreliable. Some spoilage food causes rancid odor and slime on the surface. The packaging locks the smell inside and touching food texture is impossible. From the previous research, the development of color that responds to the acid-base time related by using natural colorant Anthocyanin is used in order to solve the problem as mentioned above, which is extracted from plants such as purple sweet potato [1], tomato [2] and grape peel. Anthocyanin extraction from grape peel has a property in response to the change of acid-base. When pH value is in between 1 – 4.5 [3], Anthocyanin appears as red while appears as blue in alkaline condition. [4] Therefore, Anthocyanin is used as food coloring to be an acid-base indicator.

The aim of this experiment is to study the effect of pH and time which relates to the color change of anthocyanin dye obtained from grape peel mixed with PVA solution. Then, predict the effect of color changes on the anthocyanin indicator paper caused by vapor of ammonia in food packaging. This research is the preliminary work before changing the coating technique (on paper substrate) to flexographic printing technique (directly on multi-layer film).

MATERIALS AND METHODS

Coating formulations with anthocyanin dye

Coating formulations were created by mixture design, defining 7 formulas and indicated the range of water, dye and PVA to 11- 2.50 ml, 0.05-0.50 g and 1.09-1.50 g respectively as shown in Table 1. PVA was boiled in water at temperature just above 80 degrees Celsius. Later, anthocyanin dye solution was added according to the formulations given in table 1.

Table 1: Coating formulations with anthocyanin dye

Formulas	Proportion		
	water	dye	PVA
1	1.00	0.00	0.00
2	0.33	0.33	0.33
3	0.67	0.17	0.17
4	0.00	1.00	0.00
5	0.17	0.17	0.67
6	0.00	0.00	1.00
7	0.17	0.67	0.17

Determination of coating formulation based on color change with alkali and time

The coating formulations (Table 1) were coated on filter paper no.1 and no.4 using K-bar number 0 which the amount of coating on paper was controlled. The anthocyanin indicator paper then was cut into small pieces before attaching on the multi-layer film, PP-nylon-PET. The ammonia, concentration of 0.5 mmol, was poured in the plastic packaging before sealing it with the multi-layer film that was already attached with the anthocyanin indicator paper. We repeated the process to have enough samples for testing the color change for 4 hours, 2 types of paper and 7 formulations. The samples were kept in the refrigerator immediately after sealing. The CIE L*a*b* values of the anthocyanin indicator paper were measured every 30 minutes for 240 minutes. The color difference (CIE ΔE^* 1976) between 0h of the anthocyanin indicator paper and every 30 minutes later were calculated and analyzed.

RESULTS AND DISCUSSION

Two types of substrate: filter no.1 and no.4 gave the same tendency of color change. The anthocyanin indicator paper with formulation 4 at 210 and 240 minutes shows highest color difference. It might be caused by the highest proportion of anthocyanin dye in the formulation 4 as shown in figure 2 and 3. This anthocyanin dye reacted with the ammonia vapor led the color change

in the indicator paper. The substrate no.4 gave higher ΔE^* than no.1 in all formulations. Again with the higher thickness of the substrate no.4, it could possibly absorb more anthocyanin dye than the substrate no.1. The color differences, ΔE^* , increased with the increase of amount of anthocyanin dye (see the proportion in table 1) and increased with the time (from 30 to 240 minutes) increased.

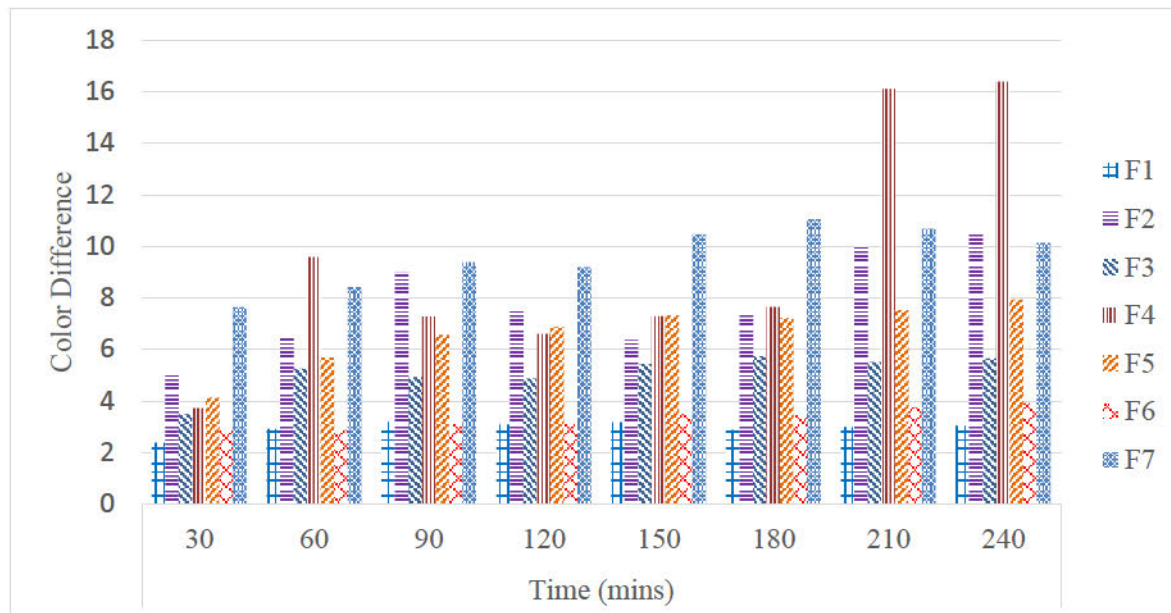


Figure 1. Color difference (CIE ΔE^* 1976) between 0h of the anthocyanin indicator paper and every 30 minutes later, filter no.1 as substrate.

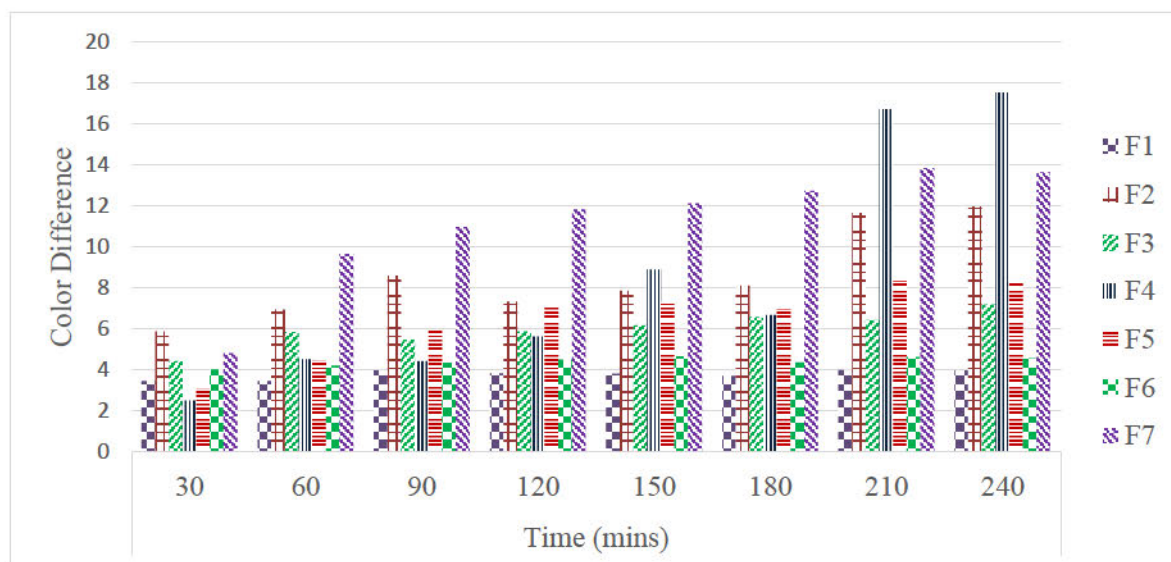


Figure 2. Color difference (CIE ΔE^* 1976) between 0h of the anthocyanin indicator paper and every 30 minutes later, filter no.4 as substrate.

To optimized the formulations then we used the mixture design based on color differences, ΔE^* for 7 formulations. The optimized formulation should give high color difference with less amount of anthocyanin dye which is the most expensive component in the formulation and at the same time the coating film should not be detached from the substrate. The optimized formulations should be in the darkest green area at the left corner in figure 3. We picked up the far right formulation that contained the highest amount of PVA and the least amount of dye in that area as shown in the small white box on the left of figure 3. The ΔE^* shown here is at 240 mins.

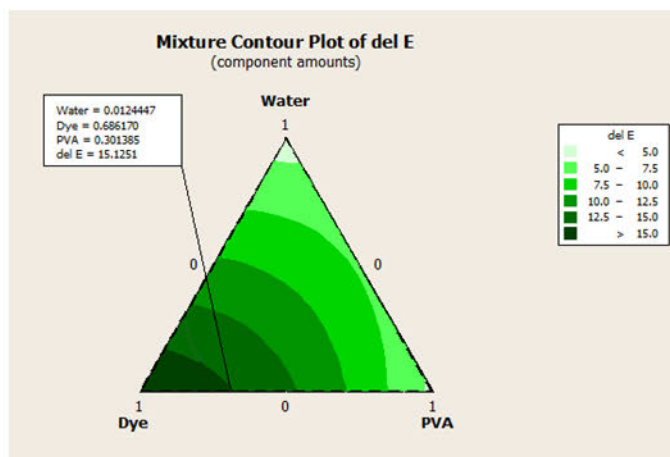


Figure 3. Mixtures of coatings contained anthocyanin dye as a function of ΔE^* .

The optimized formulation was formulated, coated on the substrate no.4 and repeat the same test. The color differences changed with time were shown in table 2. The predicted result was very close to the formulated one done according to predicted formulation.

Table 2: Color differences of the optimized formulation from 30 mins to 240 mins.

	Time (min)							
	30	60	90	120	150	180	210	240
ΔE^*	3.66	11.72	12.24	12.50	13.36	13.76	14.53	14.58

CONCLUSION

The color change in terms of CIE ΔE^* 1976 of the anthocyanin indicator paper increased with the increase of the amount of anthocyanin dye in the coating formulation and with time that related to the amount of vapor of ammonia released in the closed container. The mixture design could be used to optimize and predict the formulation efficiently.

REFERENCES

- [1] He, X. L., Li, X.L., Lu, Y.P., He, Q. Composition and color stability of anthocyanin-based extract from purple sweet potato, Food Sci. Technol, Campinas, 2015, 35(3): 468-473, Jul.-Set. 2015.
- [2] Jones, C. M., Mes, P., Myers J. R. Characterization and Inheritance of the Anthocyanin fruit (Aft) Tomato Journal of Heredity 2003; 94(6): 449–456.

[3] [Margarita Corrales) .2004 .(Extraction of anthocyanins from grape skins assisted by high hydrostatic pressure .*Journal of Food Engineering* .90; 415-421.

[4] Khoo, H. E., Azlan, A., Tan, S. T., Lim, S. M. Anthocyanidins and anthocyanins: colored pigments as food, pharmaceutical ingredients, and the potential health benefits, *Food & Nutrition research*, 2017; 61:1361779. <https://doi.org/10.1080/16546628.2017.1361779>

APPLICATION OF MULTI-COLOR CHANNELS OF LED FOR ART EXAMINATION.

Duantemdoung Dethsuphar¹, Jennyssia Rattanavanh², Pichayada Katemake^{1,*}, Chawan Koopipat¹, Dhamrongruchna Hoontrakul¹, Prompong Pienpinijtham³, Supaporn Noppakundilograt¹

¹*Department of Imaging and Printing Technology, Faculty of Science, Chulalongkorn University, Thailand.*

²*Univ Lyon, UJM Saint-Étienne, CNRS, Laboratoire Hubert Curien UMR 5516, France*

³*Department of Chemistry, Faculty of Science, Chulalongkorn University, Thailand.*

*Corresponding author: Pichayada Katemake, pichayada.k@chula.ac.th

Keywords: multi-color channels LED, tunable lamp, pigment identification, technical photography, art examination

ABSTRACT

This research was aimed to investigate if picture of pigments taken under 14 LED channels and stored as database could be used for mapping and identifying some pigments. The application could be used for identifying pigment in cultural heritage such as paintings. The experiments were separated into 2 parts: First was preparation of the database and second was mapping and identifying pigments. In preparation of the database, 50 of earth pigments, provided by Tokyo Pigment, were mixed with acacia gum and applied on acid-free water color paper using K-bar no.8. Four hundred ninety-three pigments, 10 categories, on cards from Kremer Pigments GmbH & Co.KG were collected. Pigments from both sources were photographed under visible light (halogen) and under 14 LED channels of Thouslite tunable lamp, from Thousand Lights. All digital pictures were adjusted their white balance according to the grey scale on Color Checker taken under the corresponding LED channel. Their reflectance spectra were also collected using spectrophotometer and spectroradiometer (under 14 LED channels). RAMAN spectra were also recorded. In identifying and mapping pigments, a painting painted with known pigments, used in our database, were photographed under the same LED channels and mapped the colors with database. Another painting, painted by using our database pigments but we did not know which pigments were selected, was used for mapping color and identifying pigments. The type of pigments associated with the LED channels was analyzed by using mapping of color and of reflectance methods. This method then was compared with Ultraviolet Fluorescent photography, Reflected Ultraviolet photography, Infrared photography and Infrared False Color photography.

INTRODUCTION

Technical photography (TP) techniques such as Ultraviolet Fluorescent photography, Reflected Ultraviolet photography and Infrared photography have been using for pigments identification in work of arts for several years by giving color match between images of pigments (database) and image of art, taken with the same TP technique. The post image processing is routinely applied for confirmation of information. The camera used in TP techniques does not block UV and IR that are useful for examination of varnish coatings and under-drawing of paintings. The information of the TP techniques can be found in previous research [ref].

Apart from TP techniques that we used in our research, we would like to investigate if the narrow wavelength of the visible region, 400-700 nm, could be used to identify some pigments before using other advanced technique such as Raman spectrum.

MATERIALS AND METHODS

Light sources: LEDCube-Any SPD Simulator with 14 channels was used for taking photograph of pigments and paintings. Fourteen channels included 2 achromatic channels: cool white and warm white, and 12 chromatic channels: 405nm, 425nm, 450nm, 475nm, 505nm, 525nm, 540nm, 595nm, 635nm, 660nm, 670nm, and 700nm. Halogen lamp, Infrared fluorescence lamp and UV lamp were used for taking photos with TP techniques. In this study we used Infrared (IR), Infrared Fluorescence (IRF), UV Fluorescence (UVF), UV reflectance (UVR) and visible light photography plus 2 of post processing of false colors obtained by IR and UVF images.

Cameras: Canon EOS 7D and 5D (without UV/IR filters) cameras were used for taking photographs under 14 LED channels and for taking TP respectively.

Pigments: Fifty earth pigments from Pigment Tokyo and Kremer pigments from Germany were used as our database.

Procedures: 1) Fifty earth pigments were individually mixed with acacia gum with ratio of 20:80 and applied on acid free watercolor paper with K-bar No.8 having wet film thickness of 100 μm . The acacia gum solution contained 13.6 grams of gum in 100 ml of water. 2) After the paints dried completely, we captured the earth pigment films and all Kremer pigments under 14 LED channels. Also we used 5 TP techniques for these pigments. 3) We painted 11 earth colors on acid free watercolor paper with knowing the position of individual color and they were painted without mixing or blending on the paper as shown in figure 1 (left). We naturally painted another one “the scream” using 7 earth colors with mixing and blending colors to match the original of “the scream” as much as possible as shown in figure 1 (right). 4) These 2 paintings were captured under 14 LED channels and with 5 TP techniques. 5) The pigments in the paintings were identified by matching the colors with the database carried in 2).

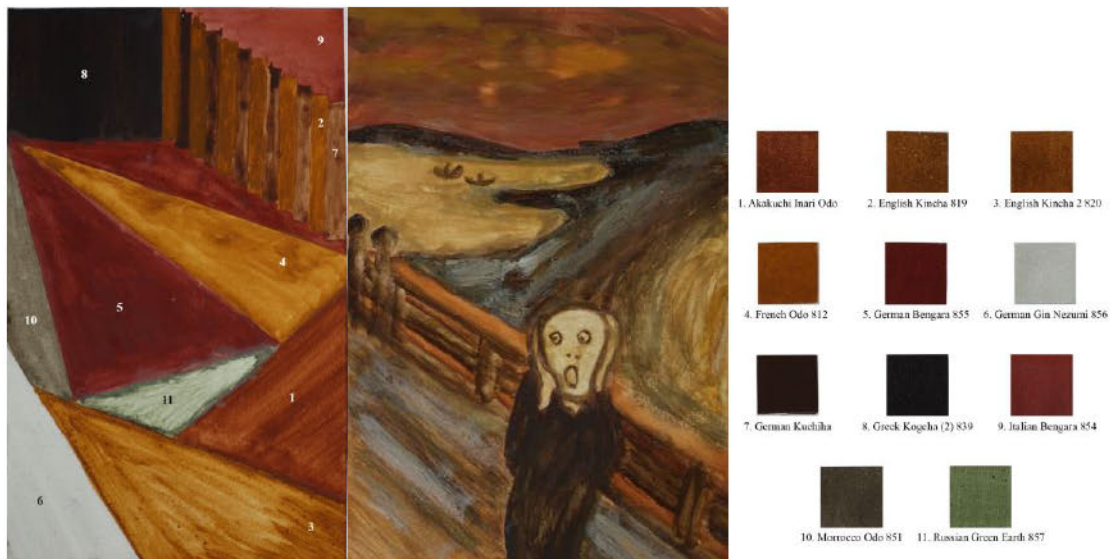


Figure 1. Paintings of 11 single earth pigments for individual area (left) and 7 earth pigments blending and mixing on paper (middle) and 11 pigments database (right). They were captured under visible light.

RESULTS AND DISCUSSION

Identify pigment under 12 LED channels

We selectively showed 4 earth colors in this section. There are 12 small pictures shown in figure 2. Each of them, captured under chromatic 12 LED channels, was divided into 2 parts: left part is the hand painting of “Italian Shudo” earth color and right part was database of the same pigment applied using K-bar No.8. For this pigment the color differences ΔE_{ab}^* (1976) between the sample from the database and the painting test were small in 660nm, 635nm and 670nm respectively.

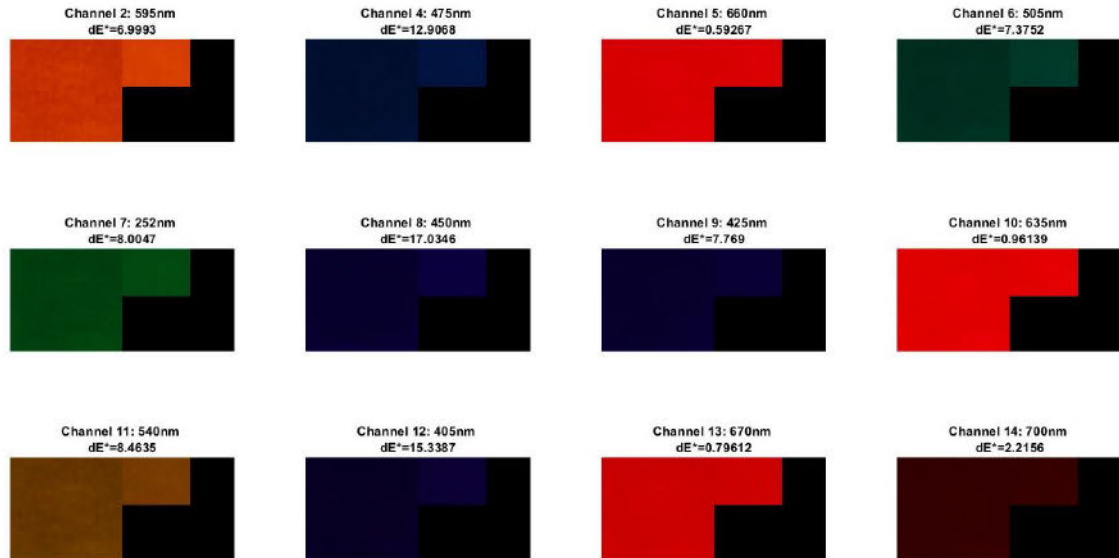


Figure 2. Italian Shudo

For the “Bohemian Green Earth 850”, shown in figure 3 the color differences are large for all channels.

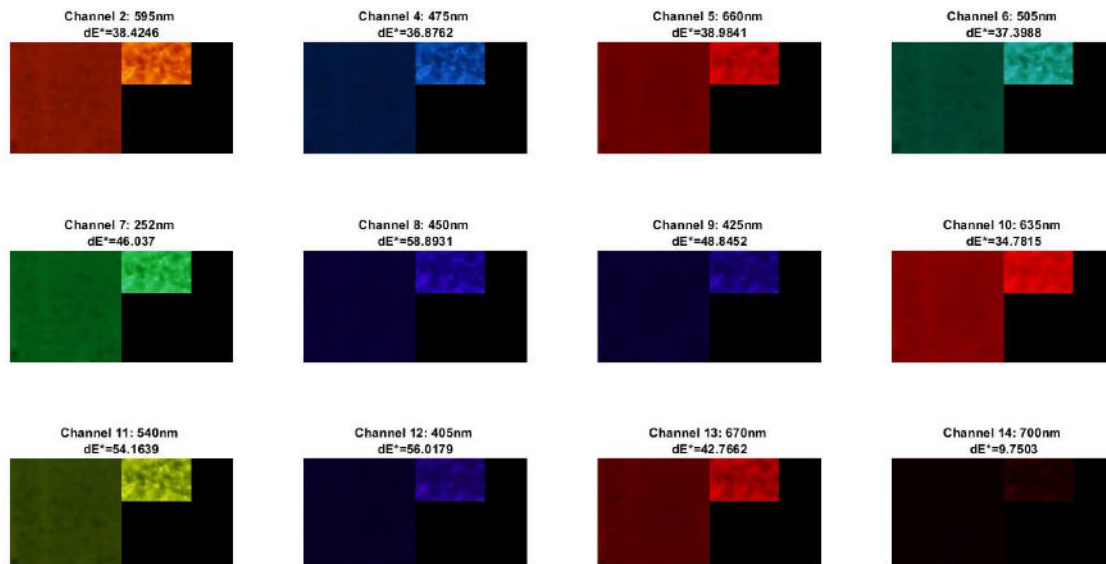


Figure 3. Bohemian Green Earth 850

For German Kogecha pigment, shown in figure 4 the color differences are too large for all channels.

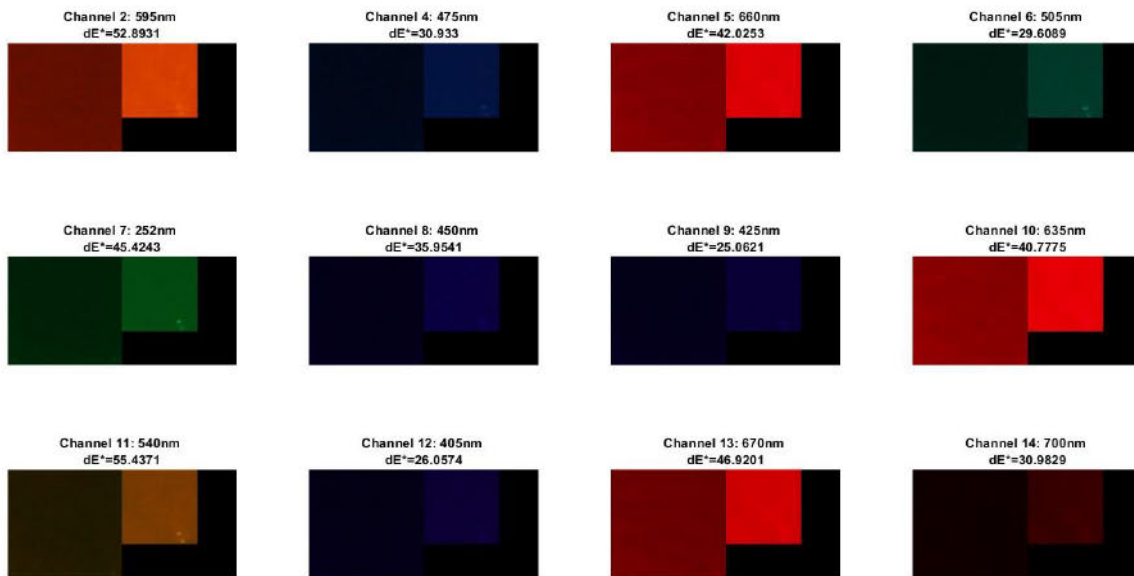


Figure 4. German Kogecha

The “German Bengara 855” (figure 5) gave small color difference, under 2, for the channels 660nm, 425nm, 635nm, 670nm and 700nm.

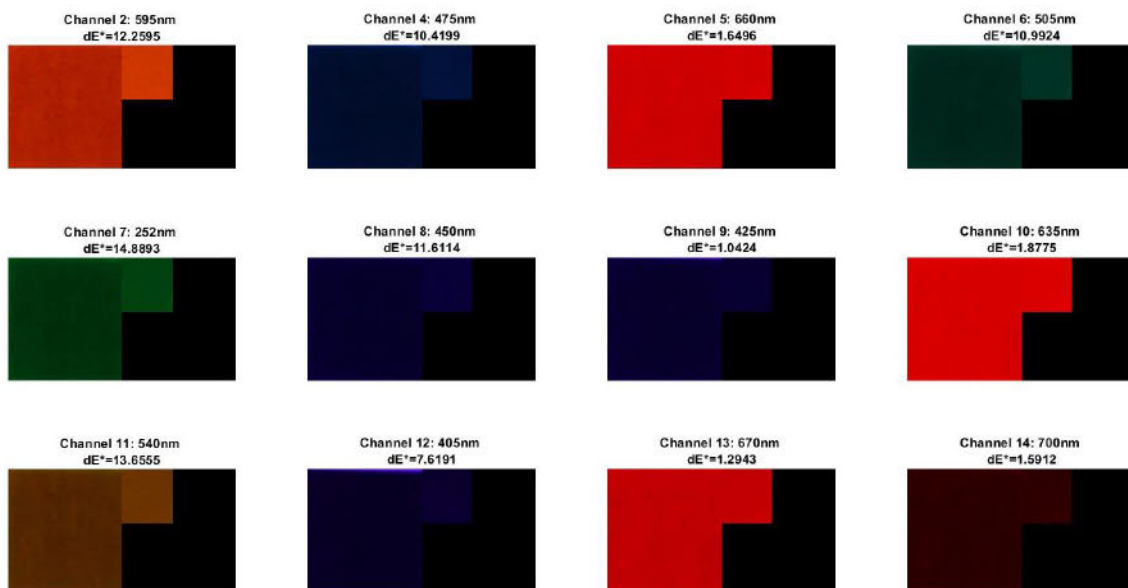


Figure 5. German Bengara 855

This technique need another post-process or another technique to further identify pigment

Identify pigment by using TP techniques

In this section we showed only the images captured with IR and UVF techniques and changed the colored channels to obtain IRFC and UVFC as shown in figure 6 and figure 7. The colors that greatly change when compared the visible image to the IRFC and to the UVFC images are the ones that easy to identify. Some colors that are similar under visible light and change to similar colors under IRFC

and UVFC, are difficult to identify by these 2 techniques. Other techniques should be applied. As an example we showed the color changed by these 2 techniques compared to the visible light (table 1).

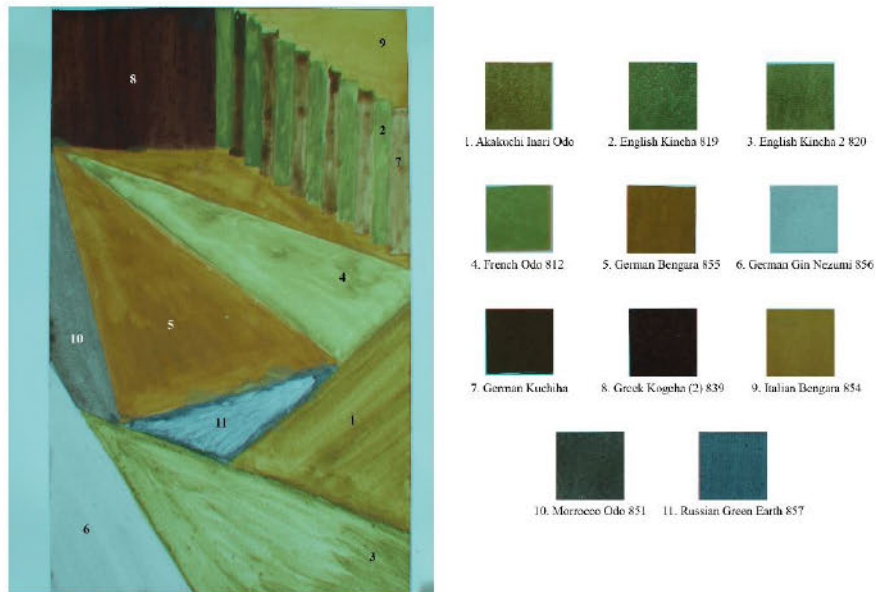


Figure 6. Infrared false color image: painting with single pigment color in each area (left), database of pigment color used in the painting (right).

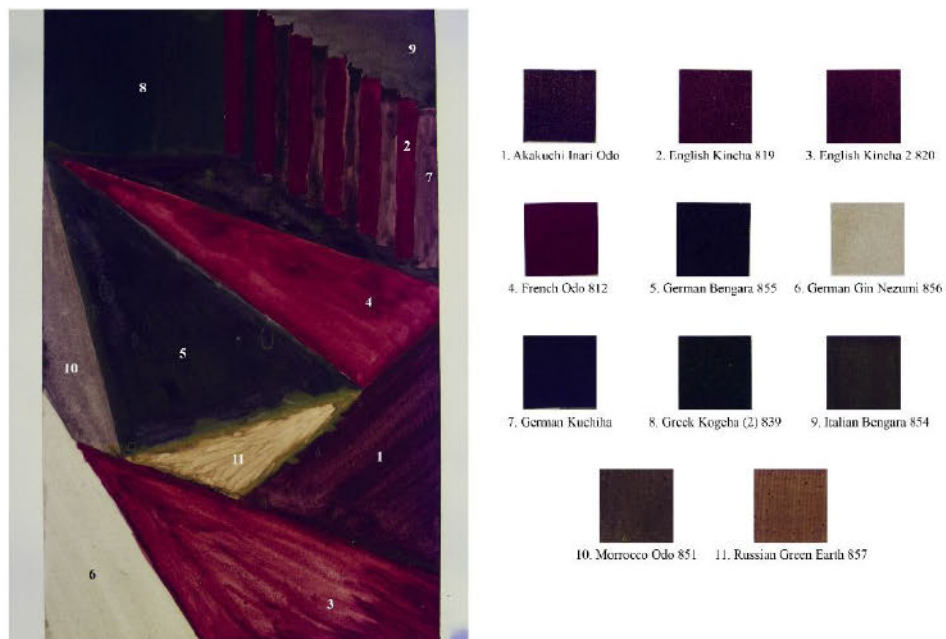
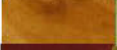
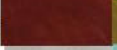
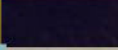
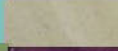


Figure 7. UV false color image: painting with single pigment color in each area (left), database of pigment color used in the painting (right).

Table 1: Examples of 7 earth colors captured under visible light, under IR plus FC post process and under UV plus FC post process

No.	Commercial name	VIS	IRFC	UVFC
1	Akakuchi Inari Odo			
2	English Kincha 819			
3	English Kincha 820			
4	French Odo 812			
5	German Bengara 855			
6	German Gin Nezumi			
7	German Kuchiha			

We could see from table 1 that the first four earth colors changed from brown to light green and dark red under visible light, IR+FC post process and UVF +FC post process. They could be grouped into these four pigments and other techniques could be used further to identified them.

CONCLUSION

Identifying pigment by capturing image under 14 channels of LED light source needs to do post process to the image and may need other technique to further identify. The TP technique, the same as the previous study, it could group and identify some pigments. Other technique could be used to confirm or to further identify.

ACKNOWLEDGEMENT

The Imaging and Nuclear Techniques for Restoration of Cultural Heritages group, the Special Task Force for Activating Research (STAR) Chulalongkorn University Centenary Academic Development Project is acknowledged.

REFERENCES

1. Cosentino, A. (n.d.). 1 Technical Photography (TP). Retrieved from <https://chsopensource.org>
2. Cosentino, A. (2014). Identification of pigments by multispectral imaging; flowchart method. *Heritage Science*. Article number: 8. <http://www.heritagesciencejournal.com>
3. Cosentino A: A practical guide to panoramic multispectral imaging. *e-Conservation Magazine*. 2013, 25: 64-73.

Proceedings

Poster Papers

EFFECT OF THE RED BACKGROUND ON IMPRESSION TOWARD DOGS

Hiroko Nakamura^{1*} and Yasuhiro Seya¹

¹*Faculty of Human informatics, Aichi Shukutoku University, Japan.*

*Corresponding author: Hiroko Nakamura, nkmr@asu.aasa.ac.jp

Keywords: Red, Color, Attraction, Animal

ABSTRACT

In this study, we investigated how color can affect impression judgment toward animals. Previous studies found that wrestlers in red uniforms were more likely to win when compared to those in blue ones, and that women in red clothes appeared more attractive. These results have been explained by assuming that reddened skin is associated with anger and reproductivity. For example, one's face turns red when aroused in anger. In a herd of primates, reddened skin functions as a sign of superiority or reproductivity. Additionally, research has shown that red increases avoidance motivation, because it is often used to signal anger, prohibition, and avoidance in daily scenarios. Although numerous studies have shown the effect of red on impression formation toward humans, it is not clear whether it can be extended toward another species' judgment. Considering that most animals have fur covering their entire skin, red may not be associated with dominance and reproductivity when impression formation is being made toward animals. Rather, red may be associated with avoidance motivation, resulting in the reduction of attractiveness.

In an online experiment, 33 university students viewed 16 dog photos presented on a red or blue background. They rated six types of impressions made toward the dogs (i.e., attractiveness, strength, healthiness, cuteness, cleverness, and warmth), as well as the willingness of having the dog, on a 6-point scale. The results showed that attractiveness, healthiness, cuteness, and warmth were higher when a dog was presented on the red background rather than on the blue one, suggesting that the red has an effect on impression formation which can be extended to other species. The enhancement of attractiveness and healthiness by red imply that the color is a sign of reproductivity when applied to other species. As a result, with the red background, dogs may have been judged as fertile.

INTRODUCTION

The present study investigates whether red affects our impression judgment toward animals. Research on color associations have indicated that people link red to activeness and warmth [1], and it is often considered a symbol to denote anger and love [2]. Recent studies revealed that red affects how one perceived the emotional state of others (e.g., anger), formulated impressions (e.g., attractiveness), and one's behavior toward others.

It has been argued that red is a sign that denotes anger and dominance which activates avoidance motivation and reduces the performance of people who see red. Hills and Barton (2005) indicated that in Olympic combat sports, wrestlers who wore a red uniform were more likely to win than wrestlers who wore a blue uniform [3]. Stephen, Oldham and Barton (2010) manipulated the redness and greenness of skin color in men's photos, and they revealed that redness was associated with aggression and dominance [4]. Men who wore red clothes were evaluated as more aggressive and dominant, and often categorized as 'angrier' than men who wore blue or grey clothes [5]. In addition,

the association between red and dominance was observed in primates. The male mandrills' reddened skin is related to levels of testosterone and dominant rank in a herd. Thus, they avoided conflict with other males with a red face [6]. It has argued that red activates an avoidance motivation because red denotes anger, dominance, and prohibition in daily life. Mehta and Zhu (2009) asked participants to solve anagrams that included approach and avoidance motivation words. The response time of avoidance related words was faster on a red background than on a blue or neutral background [7]. Together with these researches, red is linked to anger and dominance, and thus, it denotes danger and prohibition which activates avoidance motivation.

Several studies indicated that red enhances attractiveness in the context of heterosexual interaction. People perceived a person was more attractive and sexually desirable when he/she wore a red shirt or appeared on a red background [8, 9]. The link between red and sexual appearance was observed only in opposite-sex pairs (e.g., women evaluated men), and the red effect on attractiveness was observed across cultures [10]. It was also argued that red facial coloration is a sign of reproductive quality in primates. The facial coloration of the female mandrill and macaques was brighter during the follicular phase [11, 12]. In macaques, dark red-faced males received more sexual solicitation than pale pink ones [13]. These studies imply that humans and primates may use information about skin coloration to make inferences about the health and reproductive quality. Hence, it affects their evaluation of the opposite sex's attractiveness.

Although it was revealed that red is a sign to denote anger, dominance, attractiveness, and reproductive qualities, most of the study focused its effects of red on intra-species interaction, not on inter-species interaction. It is unclear whether red affects our impression judgment toward other animals such as dogs. One possible hypothesis is that red may not affect our perception toward other animals, because most mammals, except primates, have fur covering their entire skin and skin color itself is difficult to distinguish. The second hypothesis is that the effects of red can be extended to perception of other species, and that red may work as a sign to denote anger and dominance. Moreover, because the link between red and attractiveness was observed in heterosexual interaction between same species [8, 9], red may not affect perceived attractiveness in other species.

The present study tested whether red affects our impression judgment toward dogs. For this purpose, participants viewed dog photos on a red or blue background and then evaluated seven questions about the dog: "likeability: how strongly they want to have that dog", "attractiveness", "strength", "healthiness", "warmth", "cuteness", and "intelligence". If the effects of red were extended to dogs, then participants may evaluate dogs on a red background as stronger but less cute and "want to have", because red is a sign for anger and dominance. In addition, the effect of red on perceived strength and dominance may be salient in large-sized dogs that are considered more powerful and fearful than small-sized dogs. It is also possible that the color-word association affected participants' perception toward dogs, and red related words (e.g., warmth) may attribute to the overall impression of dogs on a red background. To test this possibility, we asked participants to evaluate their impressions of red and blue.

Method

Participants: Thirty-three undergraduate students ($M_{age} = 21.6$, $SD_{age} = 1.27$, 13 Male, 19 Female) participated in this experiment in exchange for a 500 yen book coupon.

Design, procedure, and materials: The stimuli used for this experiment were black and white photos of a dog on a red or blue background (Figure 1). A preliminary survey was conducted to select the dog photos. Ten undergraduate participants viewed 30 dog photos and evaluated if the dog was

large-sized or small-sized on the 5-point scale. We selected eight photos of large-sized dogs and eight photos of small-sized dogs that showed the dog's full body. The size of the dogs' photos was 450 x 450px, and the photos were surrounded in a red or blue background of 150px width. The RGB values for red were R = 255, G = 0, B = 0, and for blue, they were R = 0, G = 0, B = 255. We created a red and blue background version for each dog photo.

We used Qualtrics software (<https://www.qualtrics.com/>) and Windows PC for stimulus presentation and data collection. The experiment was conducted online and participants used a web-browser to answer the questions. Participants viewed a dog's photo on a red or blue background. There were 16 trials conducted. The background color and the dog's size in the photos were counterbalanced between participants. We used the semantic differential approach to measure "likeability (how strongly one wanted to have that dog): want to have - not want to have," "attractiveness: attractive - unattractive", "strength: strong - weak," "healthiness: healthy - unhealthy," "warmth: warm - cold," "cuteness: cute - not cute," and "intelligence: clever - unclever," on a 6-point scale. The order of presenting the photos and questions were randomized across participants. We also asked participants to evaluate their impression toward the red and blue background. Participants were presented with a 600 x 600px red or blue square, where they evaluated "likeability," "attractiveness," "strongness," "healthiness," "warmth," "cuteness," and "cleverness" of the color on a 6-point scale.

Results

Figure 1 shows the mean values and standard errors of the seven measures used (likeability, attractiveness, strength, healthiness, warmth, cuteness, intelligence). We included 2 colors (red and blue) and 2 dog sizes (large and small) to evaluate the participants' varying analysis of each measure. We concluded that there was no significant interaction between the colors and dog sizes for all the measures [$F_s(1, 31) < 1.97, p_s > .17$]. The main effects of color were seen to be significant in healthiness and warmth [$F_s(1, 31) > 4.30, p_s < .05$], they were marginally significant in attractiveness and cuteness [$F_s(1, 31) > 3.79, p_s < .10$]. Participants evaluated dogs on a red background as more healthy, warm, attractive, and cute than dogs on a blue background. The main effects of dog sizes were significant in want to have, attractiveness, strength, cuteness, and intelligence [$F_s(1, 31) > 10.81, p_s < .05$], but marginally significant in healthiness [$F(1, 31) = 3.05, p < .10$]. We found that more participants wanted to have smaller dogs when compared with larger dogs. Smaller dogs were evaluated as more attractive and cuter than larger dogs, while larger dogs were evaluated as stronger, healthier, and cleverer than smaller dogs.

Table 1 shows the evaluation results of red and blues' mean values and standard errors. In addition, we conducted a paired *t*-test for each measure. Evaluations of likeability, attractiveness, strength, healthiness, warmth and cuteness of red were higher than those of blue [$t_s(31) > 2.88, p_s < .01$], while the evaluation of intelligence of blue were higher than that of red [$t(31) = 4.68, p < .001$].

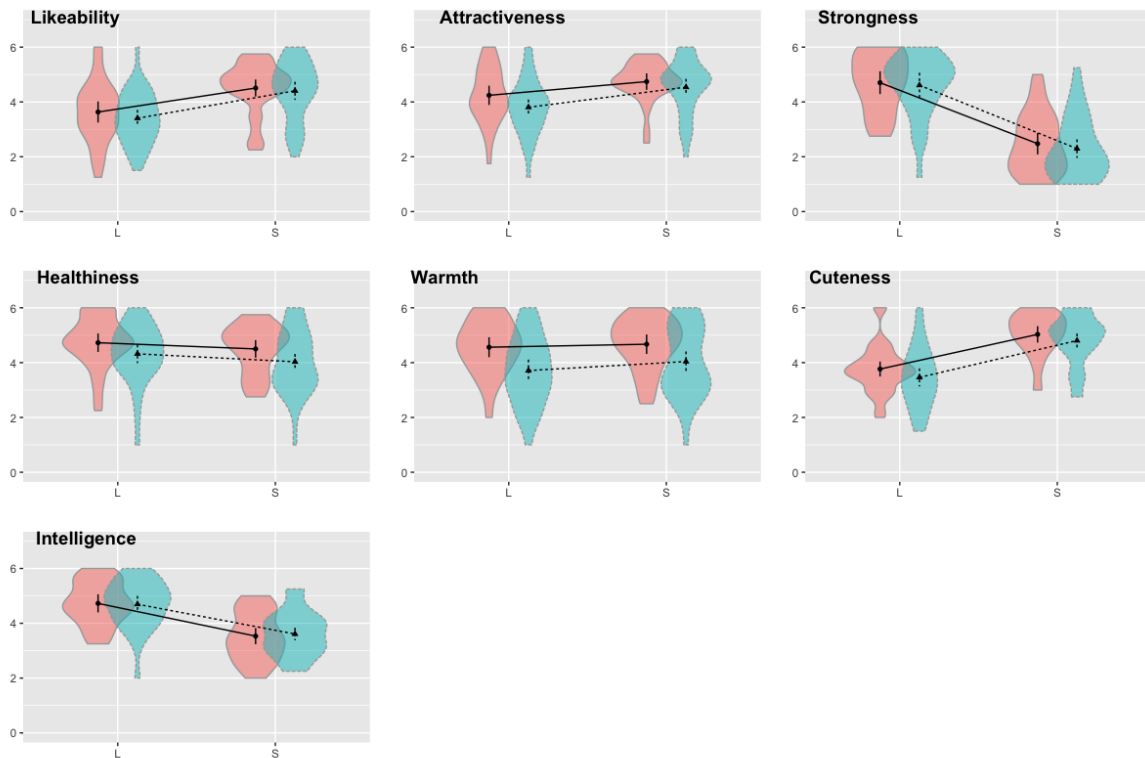


Figure 1. Seven measures' mean and standard errors (vertical lines)

Table 1: Evaluation of red and blues' mean values, standard errors, and *t*-test results

Measures	Red		Blue	
	Mean	SE	Mean	SE
Likeability	4.91	0.15	4.09	0.27
Attractiveness	5.16	0.17	3.88	0.31
Strongness	5.56	0.11	2.78	0.28
Healthiness	4.84	0.22	2.59	0.25
Warmth	5.72	0.09	1.56	0.17
Cuteness	4.09	0.24	2.72	0.23
Intelligence	3.66	0.22	5.06	0.17

DISCUSSION

The present study examined the effect of red on ones' impression judgment toward dogs. Our results revealed that participants had evaluated dogs on a red background as more attractive, warm, healthy, and cute than dogs on a blue background. Contrary to our predictions, there was no effect of red on the dogs' strength, nor was there any relationship between background color and the dogs' size. In addition, the effect of red on the impression toward dogs was not parallel with the impression

toward red and blue. Therefore, the effects of red on the impressions toward dogs were not just mirrored impressions toward red, but were a specific signal about dogs.

Our results implied that the effect of red on enhancing attractiveness [8, 9] could be extended to other species. Red skin coloration is a sign of the reproductive quality and healthiness in primates [11, 12]. Although dogs' skin is covered with fur, people tend to use red as a sign of healthiness in dogs where healthy dogs might be evaluated as young, cute, and attractive. On the other hand, there was no effect of red on the dogs' strength. It is possible that participants did not consider dogs as threatening or competitors, but considered them as companion animals. Consequently, red might not be a sign of dominance and danger but might be a sign of the dogs' attractiveness.

The present study implied that the effects of red on attractiveness can be extended to inter-species interactions. However, it is still unclear whether this effect can be extended to other animals, and whether was altered by experimental contexts (e.g., competitive settings). Further study is recommended to reveal the effects of red on impression formation.

REFERENCES

1. Oyama, T., Tanaka, Y., & Haga, J. (1963). Color-affection and color-symbolism in Japanese and American students. *Japanese Psychological Research*, 34(3), 109-121. <https://doi.org/10.4992/jjpsy.34.109>
2. Ito, K. (2008). A chronological study of color preference and color symbolism. *Bulletin of Japanese Society for the Science of Design*, 55 (4), 31-38. https://doi.org/10.11247/jssdj.55.31_2
3. Hill, R. A., & Barton, R. A. (2005). Red enhances human performance in contests. *Nature*, 435(7040), 293. <https://doi.org/10.1038/435293a>
4. Stephen, I. D., Oldham, F. H., Perrett, D. I., & Barton, R. A. (2012). Redness enhances perceived aggression, dominance and attractiveness in men's faces. *Evolutionary Psychology*, 10(3), 147470491201000312. <https://doi.org/10.1177/147470491201000312>
5. Wiedemann, D., Burt, D. M., Hill, R. A., & Barton, R. A. (2015). Red clothing increases perceived dominance, aggression and anger. *Biology Letters*, 11(5), 20150166. <https://doi.org/10.1098/rsbl.2015.0166>
6. Setchell, J. M., Smith, T., Wickings, E. J., & Knapp, L. A. (2008). Social correlates of testosterone and ornamentation in male mandrills. *Hormones and Behavior*, 54(3), 365-372. <http://dx.doi.org/10.1016/j.yhbeh.2008.05.004>
7. Mehta, R., & Zhu, R. J. (2009). Blue or red? Exploring the effect of color on cognitive task performances. *Science*, 323(5918), 1226-1229. DOI: 10.1126/science.1169144
8. Elliot, A. J., & Niesta, D. (2008). Romantic red: red enhances men's attraction to women. *Journal of Personality and Social Psychology*, 95(5), 1150-1164. DOI: 10.1037/0022-3514.95.5.1150
9. Elliot, A. J., Niesta Kayser, D., Greitemeyer, T., Lichtenfeld, S., Gramzow, R. H., Maier, M. A., & Liu, H. (2010). Red, rank, and romance in women viewing men. *Journal of Experimental Psychology: General*, 139(3), 399-417. DOI: 10.1037/a0019689
10. Elliot, A. J., Tracy, J. L., Pazda, A. D., & Beall, A. T. (2013). Red enhances women's attractiveness to men: First evidence suggesting universality. *Journal of Experimental Social Psychology*, 49(1), 165-168. <https://doi.org/10.1016/j.jesp.2012.07.017>
11. Setchell, J. M., Jean Wickings, E., & Knapp, L. A. (2006). Signal content of red facial coloration in female mandrills (*Mandrillus sphinx*). *Proceedings of the Royal Society B: Biological Sciences*, 273(1599), 2395-2400. DOI: 10.1098/rspb.2006.3573
12. Higham, J. P., Pfefferle, D., Heistermann, M., Maestripieri, D., & Stevens, M. (2013). Signaling in multiple modalities in male rhesus macaques: sex skin coloration and barks in relation to

- androgen levels, social status, and mating behavior. *Behavioral Ecology and Sociobiology*, 67(9), 1457-1469. <https://doi.org/10.1007/s00265-013-1521-x>
13. Dubuc, C., Allen, W. L., Maestriperi, D., & Higham, J. P. (2014). Is male rhesus macaque red color ornamentation attractive to females? *Behavioral Ecology and Sociobiology*, 68(7), 1215-1224. <https://doi.org/10.1007/s00265-014-1732-9>

EFFECTS OF WEAPON PRESENCE ON SPATIAL ALLOCATION OF VISUAL ATTENTION

Yasuhiro Seya^{1*}

¹*Faculty of Human Informatics, Aichi Shukutoku University, Japan.*

*Corresponding author: Yasuhiro Seya, yseya@asu.aasa.ac.jp

Keywords: Weapon focus effect, Color image, Negative emotion, Reaction time

ABSTRACT

It is well known that the presence of a weapon causes observers to narrowly focus and strongly engage their attention on the weapon. Consequently, peripheral objects around the weapon are poorly encoded. Previous studies have examined this topic by asking participants to identify a peripheral object presented immediately after an image of weapon or neutral object in the central vision. Considering that the onset of peripheral objects strongly captures observers' attention, it is not clear whether the previous findings reflect the effects of weapon presence on the spatial allocation or spatial shift of attention.

The main aim of the present study was to examine the effects of the presence of a weapon on the spatial allocation of attention by using a flanker task in which observers are not required to shift their attention at the periphery. In two experiments, the participants identified, as soon and accurately as possible, a target presented at the center of the display while ignoring flankers presented on the left and right sides of the target. The target was an arrow pointing right or left. The flankers were arrows pointing either in the same direction as the target (congruent condition) or in the opposite direction (incongruent condition). The distance of the flankers from the target was manipulated (i.e., 1, 3, and 5°). Prior to the presentation of the target and flankers, a color image of a weapon (a bloody splash was added in Experiment 2) or neutral object was presented at the center of the display, and reaction times (RTs) were measured. The results showed no RT difference between the weapon and neutral image conditions. RTs were longer in the incongruent than in the congruent conditions, with the RT difference decreasing as the distance of the flankers increased. These results suggest that the presence of a weapon, irrespective of whether it includes emotionally arousing information (e.g., bloody splash), does not affect the allocation of attentional focus.

INTRODUCTION

Eyewitnesses observing a crime are generally less likely to remember details about criminal perpetrators if they hold weapons such as guns and knives. This phenomenon is called the weapon focus effect [1]. One of the mechanisms generating this effect is the concentration of eyewitnesses' visual attention on weapons. When criminal perpetrators hold weapons, eyewitnesses shift and narrowly focus their visual attention on the weapons, leaving less attention available for viewing other items. Research has investigated the role of attentional processes in the weapon focus effect. For example, Harada, Hakoda, Kuroki, & Mitsudo [2] investigated the effects of weapon presence on attentional focus size. In their experiment, participants were asked to identify a digit presented in the peripheral vision immediately after a neutral object (e.g., cell phone) or weapon (e.g., knife). Results showed the attentional boundary derived from 50% performance was narrower when a weapon image, compared to a neutral image, preceded digit identification. Flowe, Hope, & Hillstrom [3] examined the effects of weapon presence on the spatial shift of attention by asking

their participants to look toward or away from a peripheral target that was either a weapon or a neutral image. Results showed no difference in saccadic latencies between the conditions. On the other hand, Ami & Kitagami [4] reported shorter reaction times toward a weapon image presented in peripheral vision than toward a neutral image.

The main aim of the present study was to examine the effects of the presence of a weapon on the spatial allocation of attention by using a flanker task in which observers are not required to shift their attention at the periphery. In most previous studies, the target was featured by the onset. The onset of an object is known to facilitate a spatial shift of attention (e.g., [5]). Therefore, the effects of weapon presence on spatial allocation (size of attentional focus) or spatial shift of attention were confounded in previous studies (a similar argument was made for findings regarding spatial attention during smooth pursuit eye movements [6, 7]). In a standard flanker task, one of two possible targets, e.g., an arrow pointing right or left, is presented. A target is flanked by objects that are identical (congruent condition) or opposite (incongruent condition) to the target. The observer's task is to identify the central target (e.g., right or left), and a reaction time is measured. Since attention is distributed across a certain range of space, the identification of flankers within attentional focus is also facilitated. As a result, reaction times to a central target become longer when incongruent items are presented as flankers (i.e., flanker effect).

In the present study, there were two experiments in which participants identified, as soon and accurately as possible, a target presented in the center of the display while ignoring flankers presented on the left and right sides of the target. Prior to the target and flanker presentation, either a weapon or neutral image was presented. In the task, flanker compatibility (congruent and incongruent conditions) and eccentricity (i.e., a distance between flankers and target: 1, 3, 5 degrees) were manipulated. If the presence of weapon causes observers to narrowly focus their attention, the flanker effect should rapidly decrease with increasing eccentricity of flankers.

EXPERIMENT 1

METHOD

Nine participants took part in this experiment. Mean age was 21.0 (SD±0.5) years. Prior to participation, all the participants gave written informed consent.

A personal computer was used to control the experiment, generate experimental stimuli, and record participants' response made on a keyboard. All stimuli were presented on a 24-inch monitor located in front of participants with a visual distance of 57 cm.

For the display, a fixation stimulus, a color image, a target, and flankers were presented on a grey background. The fixation stimulus was a cross, subtending 0.8 deg × 0.8 deg, and presented in black. The color image was either a weapon (four images of a knife or axe) or a neutral object (four images of a ladle or broom) subtending 2.0 deg × 2.0 deg. The target was a black arrow (head part only) pointing either right or left. The target subtended 0.8 deg × 0.8 deg. The flanker was identical to the target stimuli.

The experiment was conducted in a dark booth. Participants were given an instruction about the task and conducted practice trials until they were familiar with the task, after which the main experimental session started. At the beginning of each trial, the cross was presented at the center of the display. After participants pressed the space bar, the color image was presented for 1 sec. A blank frame was then presented for 0.5 sec, after which the target and flankers were presented at the central and peripheral locations of the display, respectively. There were three eccentricities (center-to-center distance): 1, 3, 5 deg. The participants' task was to indicate, as accurately and quickly as possible, the direction of the central target by pressing either the right or left arrow key.

The target and flankers were presented until participants pressed a key or 2,000 ms had elapsed. There were 192 trials: 16 images (8 weapons and 8 neutral objects) \times 2 congruency conditions (congruent and incongruent) \times 3 eccentricities (1, 3, and 5 deg) \times 2 targets (right and left). Image type, congruency between central target and flankers, eccentricity of flankers, and target were randomly selected for each trial. Reaction time was measured in all the trials.

RESULTS AND DISCUSSION

Figure 1 shows the results for reaction times in Experiment 1. As can be seen in the figure, regardless of the image condition, the pattern of reaction times was similar. When flankers were close to the target, reaction times were markedly longer in the incongruent condition than in the congruent condition. With increasing eccentricity, reaction times were shorter in the incongruent condition while there was no difference in the congruent condition. The data for reaction time were entered into a three-way ANOVA, which revealed significant main effects of congruency, $F(1, 8) = 48.74, p < .01$, and eccentricity, $F(2, 16) = 25.99, p < .01$. There was a significant interaction between congruency and eccentricity, $F(2, 16) = 31.55, p < .01$. Subsequent analyses showed a significant simple main effect of eccentricity in the incongruent condition, $F(2, 32) = 55.91, p < .01$, but not in the congruent condition. Multiple comparisons by using a Ryan method showed significant differences between any pair of eccentricities ($ps < .05$). Subsequent analyses also showed significant simple main effect of congruency at the 1-, $F(1, 24) = 96.46, p < .01$, and 3-deg eccentricities, $F(1, 24) = 27.40, p < .01$, but not at the 5-deg eccentricity.

The results showed no significant difference in the pattern of reaction times, suggesting that the spatial allocation of attention does not differ by images presented before a target presentation. Therefore, the weapon focus effect would not be due to the shrinkage of attentional focus by the presence of weapon. Rather, it would be due to the delay of spatial shift of attention. Another interpretation of the present results is that the lack of emotionally arousing information in the weapon images did not cause participants to narrowly focus their attention, as in the present study, simple images of weapons and neutral objects were used. This point will be further discussed in Experiment 2.

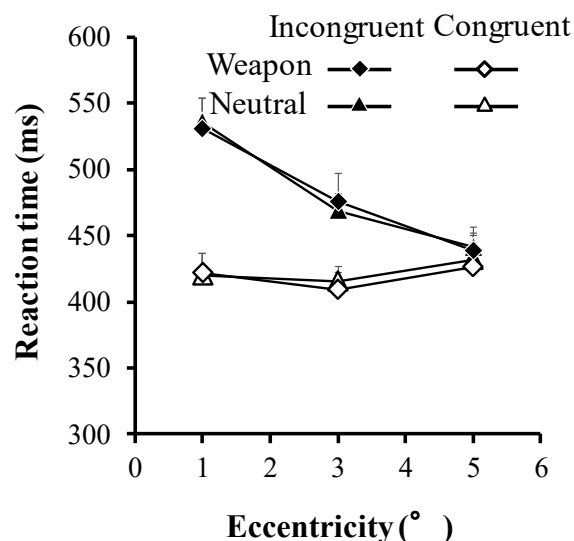


Figure 1. Mean RTs as a function of eccentricity, separated by congruency of flankers in Experiment 1.

EXPERIMENT 2

METHOD

The method used in this experiment was identical to that used in Experiment 1 with one exception: a blood splash was added to each of the weapon images. Nine participants took part in Experiment 2. The mean age was 20.7 (SD±1.5) years. Prior to participation, all the participants gave written informed consent. One of them had participated in Experiment 1.

RESULTS AND DISCUSSION

Figure 2 shows the results for reaction times in Experiment 2. As can be seen in the figure, regardless of the image condition, the pattern of reaction times was similar, which is consistent with the results of Experiment 1. A three-way ANOVA showed significant main effects of congruency, $F(1, 8) = 136.66, p < .01$, and eccentricity, $F(2, 16) = 17.25, p < .01$. There was a significant interaction between congruency and eccentricity, $F(2, 16) = 19.22, p < .01$. Subsequent analyses showed a significant simple main effect of eccentricity in the incongruent condition, $F(2, 32) = 36.28, p < .01$, but not in the congruent condition. Multiple comparisons revealed significant differences between any pair of eccentricities ($ps < .05$). Subsequent analyses also showed significant simple main effects of congruency at all the eccentricities [1 deg, $F(1, 24) = 141.78, p < .01$; 3-deg, $F(1, 24) = 44.82, p < .01$; 5-deg, $F(1, 24) = 13.90, p < .01$].

The results of Experiment 2 were clearly similar to those in Experiment 1, indicating that the presence of a weapon does not affect the allocation of attentional focus, irrespective of whether it includes emotionally arousing information (e.g., a bloody splash).

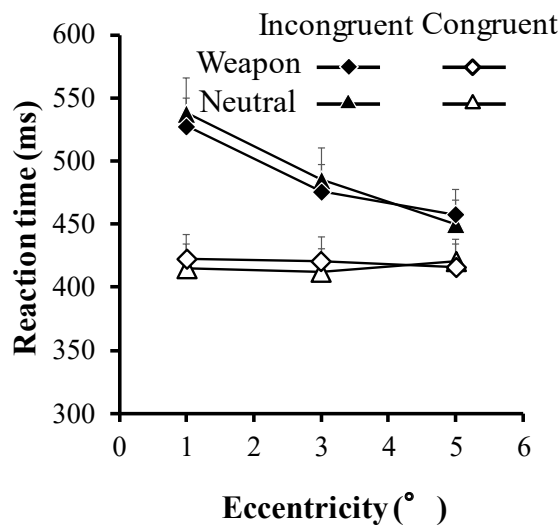


Figure 2. Mean RTs as a function of eccentricity, separated by congruency of flankers in Experiment 2.

GENERAL DISCUSSION

To examine the effects of weapon presence on spatial allocation of attention, we conducted two experiments using a flanker task. The results showed that irrespective of whether either a weapon or a neutral image was presented before the flanker task, the pattern of reaction times did not

change (Experiment 1): RTs were longer in the incongruent than in the congruent conditions, with the RT difference decreasing as the distance of the flankers increased. Even when emotionally arousing information (i.e., a splash of blood) was added to the weapon images, the results were quite similar (Experiment 2). These results suggest that the presence of a weapon per se does not affect the spatial allocation of attention. Rather, the results imply the presence of a weapon may affect the spatial shift of attention. It is also conceivable that, because no contextual information was added to the weapon images (cf. [2]), this may have resulted in no changes in attentional focus size. Indeed, Flowe et al. [3] showed no difference in spatial shift of attention between the image conditions and argued that a lack of contextual information might have resulted in the null effect (cf. [4]). Further studies are needed in the future.

ACKNOWLEDGEMENT

This study was supported by a grant from Aichi Shukutoku University 17TT06 and JSPS KAKENHI Grant Number JP17K00286.

REFERENCES

1. Loftus, E. F., Loftus, G. R., & Messo, J. (1987). Some facts about “weapon focus”. *Law and Human Behavior, 11*, 55-62.
2. Harada, Y., Hakoda, Y., Kuroki, D., & Mitsudo, H. (2015). The presence of a weapon shrinks the functional field of view. *Applied Cognitive Psychology, 29*, 592-599.
3. Flowe, H. D., Hope, L., & Hillstrom, A. P. (2013) Oculomotor examination of the weapon focus effect: Does a gun automatically engage visual attention? *PLoS ONE, 8(12): e81011*.
4. Ami, S., & Kitagami, S. (2013). Does a weapon attract eyewitness attention? *Journal of Human Environmental Studies, 12*, 7-10.
5. Seya, Y., Tsutsui, K.I., Watanabe, K., & Kimura, K. (2012). Attentional capture without awareness in complex visual tasks. *Perception, 41*, 517-531.
6. Lovejoy, L. P., Fowler, G. A., & Krauzlis, R. J. (2009). Spatial allocation of attention during smooth pursuit eye movements. *Vision Research, 49*, 1275–1285.
7. Seya, Y., & Mori, S. (2012). Spatial attention and reaction times during smooth pursuit eye movement. *Attention, Perception, & Psychophysics, 74*, 493-509.

Comparative Study of uniformity of CAM16-UCS and CAM02-UCS

Cao Congjun^{*1,2}, Fan Jingshang¹, Kang Yu¹, Sun Bangyong^{1,2}

¹*Faculty of Printing, Packaging Engineering and Digital Media Technology, Xi'an University of Technology,*

²*Printing & Packaging Engineering Technology Research Centre of Shaan Xi Province, Xi'an, Shaanxi 710048, China*

*Corresponding author: Cao Congjun, 864593346@qq.com

Key words: color appearance model; WCS; color management; image quality evaluation

ABSTRACT

Compared with the CIELAB, the CIECAM02 color appearance model has a great improvement in uniformity, but it still has poor effect in the dark blue area. The CAM16-UCS model was derived from CAM02-UCS in 2017. This paper had done two aspects works. Firstly, it compared the differences between the CAM16-UCS and CAM02-UCS in the standard deviation of the color space dimensions, the standard deviation of the flatness and the average flatness. The results showed that the uniformity of CAM16-UCS is almost the same as the CAM02-UCS. The uniformity of CAM16-UCS is slightly better than that of CAM02-UCS. Secondly, it used the two color appearance model as the WCS profile connection space (PCS), and selected the seven images dedicated to the test and evaluation in GATF4.1 to study the difference of the color conversion effects of the two color appearance spaces through subjective and objective evaluation; The subjective evaluation results show that the CAM16-UCS color appearance model is slightly better than the CAM02-UCS as the PCS; The objective evaluation results show that the peak signal-to-noise ratio (PSNR) and the structural similarity (SSIM) of the images obtained by the CAM16-UCS as PCS are higher than those by CAM02-UCS, and the mean value of the root mean square error (RMSE) is slightly lower than that by CAM02-UCS. In general, the CAM16-UCS is similar to the CAM02-UCS. The CAM16-UCS is better in the dark blue region than the CAM02-UCS, and the uniformity of the CAM16-UCS is better.

INTRODUCTION

Color images will produce cross-media color distortion problems in the process of transmission. Using the color appearance model as the profile connection spaces (PCS), color management can improve the distortion of color reproduction in different environments [1-2]. The establishment of color appearance model provided a theoretical basis for cross-media color reproduction [3]. In 1997, CIE established the CIECAM97 color appearance model [4] by combining the characteristics of the Nayatani color appearance model [5], Hunt color appearance model [6], RLAB color appearance model [7], and LLAB model [8]. In 2002, the CIE synthesized the CIECAM02 color appearance model after the related problems and improvement methods of the CIECAM97 color appearance model [9-11]. With the related research of color appearance model deepening, the study on the uniformity of color appearance model has become a hot spot. In 2003, Li et al. proposed a uniform color space and color difference evaluation formula based on CIECAM02, and then evaluated it by data set. It was

found that the color difference evaluation was better than the color difference evaluation based on CIECAM97 color model [12-13].

In 2006, Luo et al. derived the CAM02-UCS space [14]. Until 2017, Professor Li Changjun used LUTCHI and Juan data sets to conduct test research to obtain the CAM16 color appearance model, which not only solved the error in the calculation of the brightness part of the color appearance model, but also compared the CIECAM02 color appearance model to the CAM16 color appearance model. The computational complexity is lower [15].

Based on the CAM02-UCS color appearance model and the CAM16-UCS color appearance model, the differences between the color space uniformity of the two was compared by theoretical analysis and experimental verification.

THE UNIFORMITY OF CAM16-UCS AND CIECAM02-UCS

Color space visual uniformity is an important part of color management and color science. The uniformity research method mainly used the color data of scientific and industrial color difference data sets and Munsell and other related color-sequence systems to process and predict.

According to McAdam's basic theory [16], the data of the RIT data set was converted into CAM02-UCS and CAM16-UCS color space by color conversion program. The least square method was used to perform ellipse fitting on the coordinates of the data set, and the corresponding fitting ellipse was obtained [17]. The result is shown in Figure 1 and Figure 2.

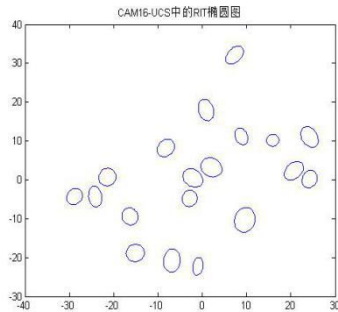


Figure 1. Ellipse in CAECAM02-UCS

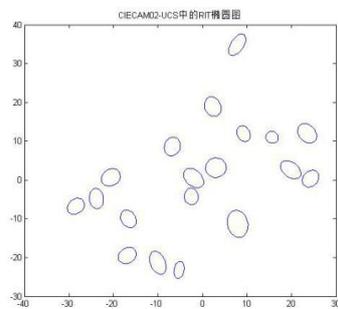


Figure 2. Ellipse in CAM16-UCS

It can be seen from the above figure that the ellipse distribution and the ellipse size of the two color appearance spaces were not much different, which indicates that the uniformity of the two color appearance spaces is not much different under the overall observation.

The correlation index of the flatness and size of the color-resolving ellipse reflects the degree of uniformity of the chromaticity plane. The flatness reflects the closeness of the ellipse to the circle; the standard deviation of the flatness and the standard deviation of the dimensions reflect the proximity of the ellipse of the entire chromaticity space. The larger the flatness, the closer the ellipse is to the circle. The flat standard deviation and the smaller the standard deviation of the dimensions indicate that the uniformity of the color space is better.

The ellipse-related parameters of the ellipse centers of the CAM02-UCS color space and the CAM16-UCS color space were processed to obtain three indexes of dimensional standard deviation, flatness standard deviation and average flatness, as shown in Table 1.

Table 1: Ellipses rasion indices of CAM02-UCS and CAM16-UCS

Statistical indicators	Average flatness	dimensional standard deviation	Flatness standard deviation
CAM02-UCS	1.4612445	0.27566321	1.23550436
CAM16-UCS	1.4445451	0.25606744	1.32738406

It can be seen from the above table that the average flatness and flatness standard deviation of the CAM16-UCS color space is slightly better than that of CAM02-UCS, and the CAM02-UCS size standard deviation is slightly better than the CAM16-UCS color space. This shows that the uniformity of CAM16-UCS is not much different from that of CAM02-UCS, and the uniformity of CAM16-UCS is slightly better than that of CAM02-UCS.

EXPERIMENTAL ANALYSIS

1. experiment procedure

In this paper, CIECAM02-UCS and CAM16-UCS were used for subjective evaluation and objective evaluation of color management of connected color space. They both used Segment Maxima GBD[8] and the SGCK. The three cases of color appearance model were compared and analyzed to evaluate the color management of CAM02-UCS and CAM16-UCS as the PCS, hereinafter referred to as CAM02-UCS method and CAM16-UCS method.

This paper selected seven images of GATF4.1 dedicated to testing and evaluation as standard images, as shown in Figure 3.



Figure 3. Experimental test chart

After the standard image was selected, the image was processed. The experimental process was as follows:

- (1) reading a standard test image as an input image, and performing a decoding operation on the input image;
- (2) Reading profile files in three environments;
- (3) Selecting CAM02-UCS or CAM16-UCS color appearance model as the PCS for color management;
- (4) Reading the device files of the LCD display and the printer, inputting the number of feature points about the source device and the target device, and extracting the color gamut boundary about all the device by using a partition maximization algorithm;
- (5) Adopting the SGCK mapping algorithm as the gamut mapping algorithm for gamut mapping;
- (6) Displaying the image the image after color management;

21 sets of images with color management of CIECAM02-UCS and CAM16-UCS color appearance models as PCS based on three environments were obtained. The evaluation of the color management consequent was also converted into an evaluation of these group images.

2. Subjective evaluation credibility analysis

In this experiment, based the three color appearance models, the 5-level scale standard was selected, and 20 observers were absolutely evaluated on the images processed by the CAM02-UCS method and CAM16-UCS method. Absolute evaluation was the classification of the evaluation image and the standard image by the observer according to his subjective visual perception. As shown in Table 2, the internationally specified 5-level absolute scale was listed.

Table 2: Absolute evaluation scale

Quality scale		Obstruction scale	
5	very good	5	Not see the image quality getting worse
4	good	4	Can see the change in image quality but does not hinder viewing
3	general	3	It is clear that the image quality is degraded, which hinders viewing
2	not good	2	Obstructing viewing
1	very bad	1	Very serious hindering viewing

Since the observers' subjective evaluation has great uncertainty, in order to test whether the subjective evaluation data was reliable, this paper used the alpha reliability coefficient method to analyze the reliability of the subjective experiment results.

The Cronbach's α in the α -coefficient coefficient method is the most commonly used reliability coefficient, and its calculation method is as follows.

$$\alpha = \left(\frac{k}{k-1} \right) * \left(1 - \frac{\sum Si^2}{ST^2} \right) \quad (1)$$

Where K is the total number of items in the scale, S_i^2 is the variance within the item of the i -th item, and ST^2 is the variance of the total score of all items. If the alpha coefficient is within the interval of 0.7-0.8, the data is available. The α reliability coefficient is shown in Table 3.

Table 3:Result of alpha reliability analysis

reliability coefficient	average	dim	dark	average value
Cronbach's α	0.889	0.923	0.943	0.921

As can be seen from the above table, the results of subjective evaluation experiment are very reliable and highly reliable, which can be used for the analysis of CAM02-UCS method and CAM16-UCS method.

3. Subjective evaluation results

After confirming that the subjective evaluation results were credible, the evaluation results were processed, and the scores of the images processed by the CAM02-UCS and CAM16-UCS methods in the three environments were respectively obtained. And the evaluation results were obtained. As shown in the table below.

Table 4:Result of subjective evaluation

image	average		dim		dark	
	CAM02-UCS	CAM16-UCS	CAM02-UCS	CAM16-UCS	CAM02-UCS	CAM16-UCS
1#Red couch	3.17	3.665	3.33	3.725	4.17	4.205
2#Memory color	3.16	3.13	3.155	3.295	3.06	3.325
3#Wedding reception	3.105	3.125	2.13	2.465	2.06	2.355
4#Lady portrait	4.41	4.29	3.98	4.2	2.975	3.045
5#Fruit	2.885	3.155	3.6	3.89	3.035	3.53
6#Group portrait	3.5	3.71	3.055	3.445	3.78	3.92
7# Neutral gray	3.96	4	4.295	4.26	3.865	4.05
average value	3.456	3.582	3.363	3.611	3.278	3.491

The results show that the color management effect of the CAM16-UCS color appearance model as the PCS was slightly better than the color management of the CAM02-UCS color appearance model .

4. Objective evaluation analysis

Objective evaluation was the use of calculation formulas to characterize image quality. In the field of digital image processing, root mean square error, peak signal-to-noise ratio and structural similarity are common and effective indicators for image quality evaluation. Therefore, these three indicators are used as the criteria for objective evaluation.

In the normal environment, the image was compared with the standard image by color management of the CAM02-UCS and CAM16-UCS color space for the connected color space, and the RMSE, PSNR and SSIM were obtained. The results of the three indicators are shown in the table below.

Table 5:Image quality evaluation results of PSNR,RMSE and SSIM

image	CAM02-UCS	CAM16-UCS
-------	-----------	-----------

	PSNR	RMSE	SSIM	PSNR	RMSE	SSIM
1#Red couch	29.849	0.001533	0.937543	30.48667	0.001511	0.945816
2#Memory color	31.8613	0.002191	0.957369	31.73853	0.002353	0.954344
3#Wedding reception	30.6527	0.002418	0.963395	31.32287	0.002616	0.969386
4#Lady portrait	33.02947	0.001097	0.944412	33.57177	0.001121	0.94719
5#Fruit	30.63237	0.001765	0.939144	32.64603	0.001621	0.952819
6#Group portrait	30.2163	0.002	0.957957	30.45577	0.002111	0.956608
7# Neutral gray	33.21507	0.001187	0.936998	33.41757	0.001242	0.939708
average value	31.35089	0.001742	0.948117	31.94846	0.001796	0.952267

As can be seen from the above table, the average value of PSNR and SSIM of the image obtained by the CAM16-UCS method was higher than that of CAM02-UCS, and the average value of RMSE was slightly lower. In CAM02-UCS, this shows that the results of the CAM16-UCS method were similar to those of the CAM02-UCS method, and the former was slightly better than the latter.

CONCLUSION

This paper theoretically analyzed the differences in uniformity between CAM16-UCS and CAM02-UCS color space, and concluded that the spatial uniformity of CAM16-UCS color appearance was slightly better than that of CAM02-UCS color space. The color management effects of CAM02-UCS and CAM16-UCS color space as PCS were compared and evaluated. The results of subjective evaluation and objective evaluation indicated that the CAM16-UCS method was slightly better than the CAM02-UCS method.

1.Ku, G. (2008). Learning to de-escalate: The effects of regret in escalation of commitment. *Organizational Behavior and Human Decision Processes*, 105(2), 221-232. doi:10.1016/j.obhdp.2007.08.002

REFERENCES

1. Kohler, T. . (2000). The Next Generation of Color Management System. *Color & Imaging Conference*.
2. Phil Green MSc PhD Reader member. 7. ICC Profiles, Color Appearance Modeling, and the Microsoft Windows Color System[M]// *Color Management: Understanding and using ICC Profiles*. John Wiley & Sons, Ltd, 2010:53-55.
3. Fairchild M D. Color Appearance Models[M]. City: JOHN WILEY & SONS, INC, 2013.
4. Luo M R, Hunt R W G. The structure of the CIE 1997 Colour Appearance Model (CIECAM97s)[J]. *Color Research & Application*, 2015, 23(3): 138-146.
5. Nayatani Y, Takahama K, Sobagaki H. Formulation of a Nonlinear Model of Chromatic Adaptation[J]. *Color Research & Application*, 2010, 6(3): 161-171.
6. Hunt R W G. A model of colour vision for predicting colour appearance[J]. *Color Research & Application*, 1982, 7(2): 297-314.
7. Fairchild M D, Berns R S. Image color - appearance specification through extension of CIELAB[J]. *Color Research & Application*, 1993, 18(3): 178-190.

8. Luo M R, Lo M C, Kuo W G. The LLAB (l:c) colour model[J]. *Color Research & Application*, 2015, 21(6): 412-429.
9. Li C J, Luo M R, Hunt R W G. A revision of the CIECAM97s model[J]. *Color Research & Application*, 2015, 25(4): 260-266.
10. Fairchild M D. 17. Testing Color Appearance Models[M]. City: John Wiley & Sons, Ltd, 2013.
11. Moroney N. The CIECAM02 Color Appearance Model[C]// The CIECAM02 Color Appearance Model. *Is&t/sid 10 Th Color Imaging Conference*. 23-27.
12. Li C, Luo M R, Cui G. Colour-Differences Evaluation Using Colour Appearance Models[C]// *Colour-Differences Evaluation Using Colour Appearance Models. Color and Imaging Conference*. 127-131.
13. Moroney N, Hewlett-Packard H. Field trials of the CIECAM02 color appearance model[C]// *Field trials of the CIECAM02 color appearance model*. 23--27.
14. Luo M R, Cui G, Li C. Uniform colour spaces based on CIECAM02 colour appearance model[J]. *Color Research & Application*, 2006, 31(4): 320-330.
15. Li C, Li Z, Wang Z, et al. Comprehensive color solutions: CAM16, CAT16, and CAM16 - UCS[J]. *Color Research & Application*, 2017, 42(1).
16. Macadam D L. Visual Sensitivities to Color Differences in Daylight*[J]. *Joptsocam*, 1942, 32: 247-274.
17. Li W, Xiao K, Cui G H. Optimized uniform colour appearance space[J]. *Journal of Beijing Institute of Technology*, 2003.

EFFECT OF OBJECT RECOGNITION ON THE OBJECT-COLOR APPEARANCE MODE LIMITATION

Kazuho Fukuda^{1*} and Kotoe Hara¹

¹*Department of Information Design, Faculty of Informatics, Kogakuin University, Tokyo, Japan*

*Corresponding author: Kazuho Fukuda, fukuda@cc.kogakuin.ac.jp

Keywords: Color Appearance Mode, Illuminant-Color, Object-Color, Object Recognition

ABSTRACT

There are two states of appearance when we see colors, illuminant-color appearance and object-color appearance. In general, the former is observed when we see a light source directly, and the latter is observed when we see a light diffusely reflected from a surface. However, artificially increasing the luminance reflected from a surface stimulus or decreasing that of surrounding causes a change in the mode of color appearance from the object-color appearance into the illuminant-color appearance. It might be expected that object recognition, for example, familiar objects or semantic contents affect the mode of color appearance because the range of lightness which we experience depends on the materials of surface. We also have shown a large gap between the gamut of measured natural objects and the gamut of the physical limitation defined by the optimal surfaces, which has rectangular spectral reflectance with one or two abrupt transitions between 0% and 100% within the visible wavelength. The hypothesis in this study was that the color, especially lightness, perception of a region is influenced by the observers' object recognition of the region. For example, the color of leaves might appear brighter than the identical color of a meaningless colored patch. In our psychophysical experiment, we compared subjective limitation of object-color perception for a target in an image with familiar objects and that in a meaningless geometrical image. To make the object image stimuli, we used five pictures of colorful familiar objects, a bird, leaves, sun flowers, balloons, and buttons, and the number of surround colors in each image was restricted to 20 colors with the MATLAB `rgb2ind` function. It was confirmed that this manipulation did not affect object recognition. To make a meaningless image stimulus, we modified the spatial element of each object image stimulus by replacing each colored region on the object image stimulus with a circle with the same color. So, the same 20 colors appeared on each pair of object image and meaningless image stimuli. It was confirmed that observers were unable to recognize the original object on the stimuli. Observer's task was to adjust the brightness of a target color in the stimuli to the subjective upper limit of object-color perception. We tested 5 colors as the target color for each pair of 5 stimuli. The results showed the significant difference in the limitations of object-color appearance mode between the object stimuli and meaningless stimuli in some conditions of target color and object. The result indicates that the limitation of object-color appearance mode is influenced by the observers' object recognition of the region in a certain degree.

INTRODUCTION

We see colors when retinal photoreceptors are stimulated by visible lights, which come from a light source directly or from a direct/diffuse reflection of illuminant at a surface. These two situations usually cause different "mode of color appearance"; the former causes illuminant-color appearance mode and the latter causes object-color (or surface-color) appearance mode. However,

artificially increasing the luminance of a target stimulus or decreasing that of surrounding stimuli in a scene causes a change in appearance of the target color from the object-color into the illuminant-color mode [1-5]. This is because the chromaticity and luminance of reflected light from an object are restricted in a certain range under a uniform illuminant because objects usually do not reflect stronger light than the illuminated light. This limitation is called as MacAdam's limit [6, 7] and the gamut of optimal colors defined by the optimal surfaces, which has rectangular spectral reflectance with abrupt transitions between 0% and 100% within the visible wavelength [8].

If a color in a scene is outside the gamut of optimal colors, it theoretically means that the color is not the reflected light from an object but that it may be a kind of light source. We have been proposing a color constancy model, optimal color hypothesis [9, 10], which estimates an illuminant with the comparison between the gamut of colors in the scene and that of optimal colors, and also have shown that the distribution of subjective object-color limitations is similar to the optimal colors [11]. We have also shown that the color appearance mode of a color influenced the contribution of the color element to the illuminant estimation for color constancy [12].

It might be expected that object recognition, for example, familiar objects or semantic contents affect color appearance mode of the surface or surroundings because the range of lightness which we experience depends on the materials of surface. It is known that, for example, the perceived chromaticity of familiar objects, fruits or vegetables, is influenced by their typical colors [13, 14]. We also showed that a large gap between the gamut of measured natural objects and the optimal colors [9, 10] by measuring a variety of natural object, flowers, leaves, stones, barks, fruits [15], and using other data set of natural objects [16]. The hypothesis in this study was that the color, especially lightness, perception of a region is influenced by the observers' object recognition of the region. For example, the color of leaves might appear brighter than the identical color of a meaningless colored patch.

METHODS

We compared subjective limitation of object-color appearance for a target in an image with familiar objects and that in a meaningless geometrical image. To make an object image stimulus (Figure 1b), we used a picture of colorful familiar objects, a bird, leaves (Figure 1a), sun flowers, balloons, or buttons, which are chosen from a copyright free images in Pixtabay [17], then the number of surround colors in each image was reduced to distinct 20 colors with the MATLAB `rgb2ind` function. It was confirmed that this manipulation did not affect object recognition. To make a meaningless image stimulus (Figure 1c), we modified the spatial element of each object image stimulus by replacing each colored region on the object image stimulus with a circle with the same color. So, the same 20 colors appeared on each pair of object image and meaningless image stimulus. It was confirmed that observers were unable to recognize the original object on the meaningless image stimuli. The stimuli were appeared at the center of a calibrated LCD color monitor, EIZO ColorEdge CG246 in a dark room. The viewing distance was 60 cm.

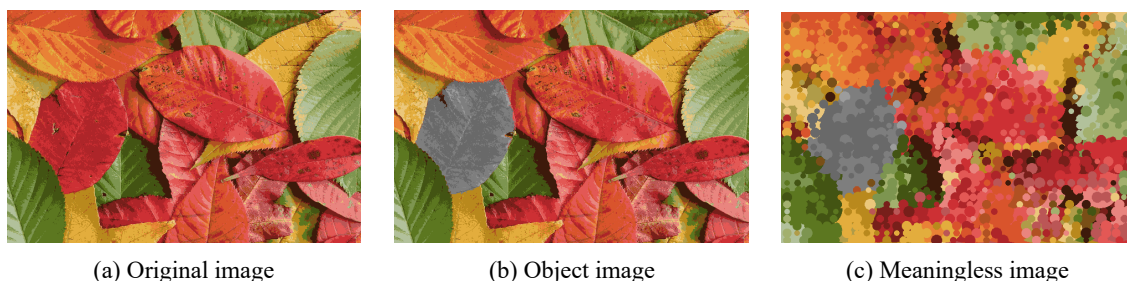


Figure 1. Example of stimuli

Observer's task was to adjust the brightness of a target color region in the stimuli to the subjective upper limit of object-color perception with no time limitation. The areas painted with light, middle, and dark gray colors in Figure 1 (b) and (c) were the target color regions. We tested 5 colors, achromatic, yellow, pale pink, red and blue as the target color for 10 stimuli, the combination of two image types (object image and meaningless image) and 5 scenes (a bird, leaves, sun flowers, balloons, or buttons). On the CIE 1931 xy chromaticity diagram, achromatic was $(x, y) = (0.34, 0.33)$, yellow was $(0.45, 0.45)$, pale pink was $(0.42, 0.36)$, red was $(0.59, 0.33)$ and blue was $(0.16, 0.08)$. Nine observers with trichromat color vision, which was determined with the Ishihara's test for color deficiency II [18], participated in the experiment and each observer performed total 50 trials (one trial for each condition)

RESULTS AND DISCUSSION

Figure 2 shows the results of luminance adjustment of the target color to the upper limit of object-color appearance mode. Each panel shows the results for one of five scenes. The abscissa indicates the target color and the ordinate indicates the mean luminance of the nine observer's settings. The bluish diamond symbols indicate the results for the object image stimuli and the dark reddish square symbols indicate those for the meaningless image stimuli. The error bars show the standard error of the mean.

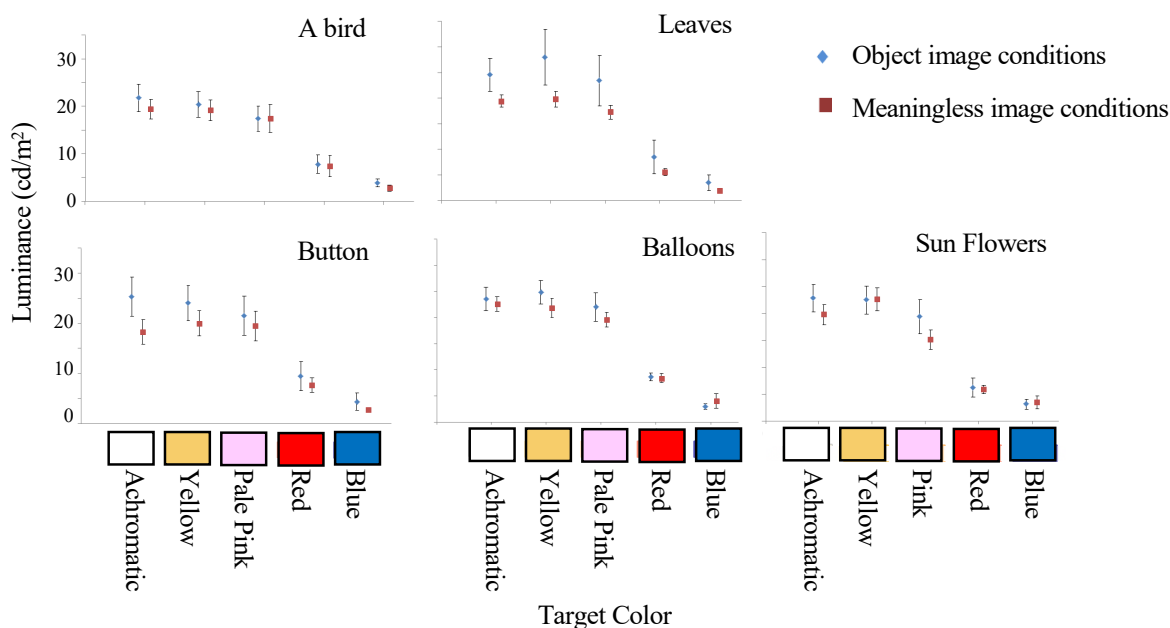


Figure 2. Result of luminance adjustment of the target color

We conducted three-way repeated measures analysis of variance (ANOVA), with target colors (achromatic, yellow, pink, red, blue), image modifications (object image, meaningless image), and scenes (a bird, leaves, buttons, balloons, sun flowers). As we found a second-order interaction ($F(16, 128) = 1.85, p < 0.03$), we also conducted two-way ANOVA with target colors and image modification, and found a significant main effect of target colors ($p < 0.01$) for all scenes, and a significant simple interaction effect of target colors and image modification for buttons ($p < 0.01$),

sun flowers ($p < 0.01$), and leaves ($p < 0.05$). Analysis of interaction showed a significant effect of image modification at achromatic target ($F(1, 8) = 13.45, p = 0.007$) and at yellow target ($F(1, 8) = 5.68, p = 0.04$) for buttons, and a trend of image modification at achromatic target for leaves ($F(1, 8) = 4.49, p = 0.07$), and for sunflowers ($F(1, 8) = 4.21, p = 0.07$). These results indicate that the limitation of object-color appearance mode especially for less saturated colors was influenced by the type of image modification of the stimuli (object image or meaningless image), the former allowed the observers clear object recognition of the scene, and the latter did not.

As the statistics shows, the significant effect of image modification appeared for the scenes of buttons, sun flowers, and leaves, not for those of a bird and balloons. It means that the effect was independent of the object types in scene whether those were artificial (buttons and balloons) or natural (sun flowers, leaves, and a bird).

Figure 3 shows the 20 colors for each scene on the CIE 1931 xy chromaticity diagram. The 20 colors widely distribute around white point toward various hue in the scene of button, where the statistics showed significant effect of image modification at achromatic and yellow target colors. On the other hand, the colors distribute very locally but more saturated toward specific hues in the scene of a bird or balloons, where the statistics showed no significant effect of image modification. It might be possible that the effect of object recognition on the object-color appearance mode limitation is influenced by the distribution of the colors contained in the scene.

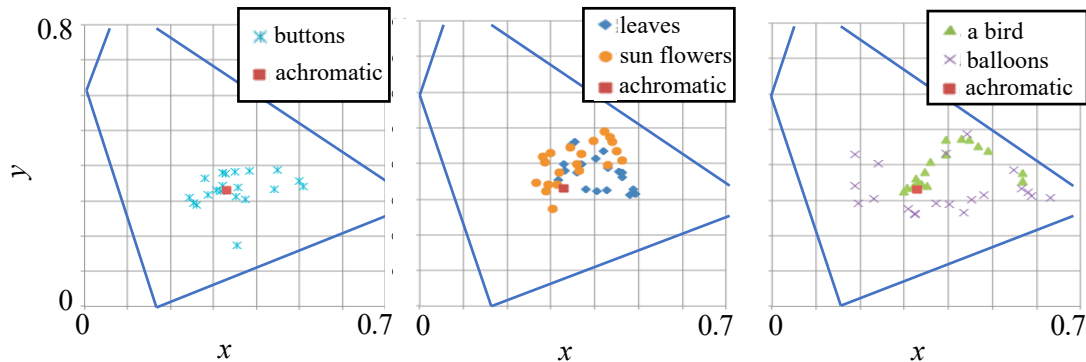


Figure 3. Distributions of the 20 colors in each stimulus plotted on the CIE 1931 xy chromaticity diagram

In this study, we investigated the effect of object recognition on the transition of color appearance mode from object-color to illuminant-color appearance. We performed a set of psychophysical experiment where the observers adjusted the color of test region to the upper limit of object-color appearance. The stimuli were 10 images, the combinations of two types of modification (familiar object image and meaningless image) and five scenes (a bird, leaves, sun flowers, balloons, or buttons). We tested 5 target colors (achromatic, yellow, pink, red, or blue) for each image. The results showed some effect of image modification on the limitations of object-color appearance mode in some conditions of target colors and scenes. The result indicates that the limitation of object-color appearance mode is influenced by the observers' object recognition to the scene in a certain degree.

ACKNOWLEDGEMENT

This research was supported by JSPS KAKENHI Grant Numbers JP17K04503 and JP 26780413.

REFERENCES

1. D. Katz. (1935). World of colour. London: *Kegan Paul*.
2. H. Uchikawa, K. Uchikawa and R. M. Boynton. (1989). Influence of achromatic surrounds on categorical color perception of surface colors, *Vision Research*, 29 (7), 881-890
3. F. Bonato and A. L. Gilchrist. (1994). The perception of luminosity on different backgrounds and in different illuminations, *Perception*. 23 (9), 991-1006
4. J. M. Speigle and D. H. Brainard. (1996). Luminosity thresholds: effects of test chromaticity and ambient illumination, *Journal of the Optical Society of America A*, 13 (3), 436-451
5. Y. Yamauchi and K. Uchikawa. (2000). Upper-limit luminance for the surface-color mode appearance, *Journal of the Optical Society of America A*, 17 (11), 1933-1941, <https://doi.org/10.1364/JOSAA.17.001933>
6. D. L. MacAdam. (1935). The Theory of the Maximum Visual Efficiency of Colored Materials, *Journal of the Optical Society of America*, 25 (8), 249-252, <https://doi.org/10.1364/JOSA.25.000249>
7. D. L. MacAdam. (1935). Maximum Visual Efficiency of Colored Materials, *Journal of the Optical Society of America*, 25 (11), 361-367, <https://doi.org/10.1364/JOSA.25.000361>
8. K. Masaoka. (2010). Fast and accurate model for optimal color computation, *Optics Letters*. 35 (12), 2031-2033
9. K. Uchikawa, K. Fukuda, Y. Kitazawa, and D. I. A. MacLeod. (2012). Estimating illuminant color based on luminance balance of surfaces, *Journal of the Optical Society of America A*, 29 (2), 133-143, <https://doi.org/10.1364/JOSAA.29.00A133>
10. T. Morimoto, K. Fukuda, and K. Uchikawa. (2016). Effects of surrounding stimulus properties on color constancy based on luminance balance. *Journal of the Optical Society of America A*, 33 (3), A214-A227, <https://doi.org/10.1364/JOSAA.33.00A214>
11. K. Fukuda, A. Numata, and K. Uchikawa. (2014). Physical Limitation of Object Color's Luminance and Critical Luminance for the Transition of Color Appearance Mode, *ITE Technical Report*, 38 (10), 49-51, https://doi.org/10.11485/itetr.38.10.0_49
12. K. Fukuda, and K. Uchikawa. (2014). Color constancy in a scene with bright colors that do not have a fully natural surface appearance. *Journal of the Optical Society of America A*, 31 (4), A239-A246 <https://doi.org/10.1364/JOSAA.31.00A239>
13. P. Siple and R. M. Springer. (1983). Memory and preference for the colors of objects. *Perception & Psychophysics*, 34 (4), 363-370.
14. M. Olkkonen, T. Hansen, and K. R. Gegenfurtner. (2008). Color appearance of familiar objects: effects of object shape, texture, and illumination changes. *Journal of Vision*, 8(5), 13.1–16. <http://doi.org/10.1167/8.5.13>
15. K. Fukuda, and K. Uchikawa, Validation of the optimal color model for illuminant estimation using spectral data in natural environment, *ITE Technical Report*, 41 (16), 151-154, <http://id.nii.ac.jp/1001/00181977/>
16. R. Brown. (2003). Background and illuminants: the yin and yang of colour constancy, *Colour Perception: Mind and the Physical World*, R. Mausfeld and D. Heyer, eds., Oxford University, 247–272.
17. Pixabay. (2019). Stunning free images & royalty free stock, <https://pixabay.com>,
18. S. Ishihara. (1996). Tests for colour blindness 38 plates-edition (in Japanese), Handaya CO. LTD

SIZE CONSTANCY DEMONSTRATED ON PHOTOGRAPHS

Onsucha Upakit¹, Chanprapha Phuangsuan² and Mitsuo Ikeda²

¹ *Faculty of Mass Communication Technology, Rajamangala University of Technology Thanyaburi, Thailand*

² *Color Research Center, Rajamangala University of Technology Thanyaburi, Thailand*
*Corresponding author: Onsucha Upakit, Onsucha_u@rmutt.ac.th, Onsucha.u@gmail.com

Keywords: Size constancy, Mountain, Photographs, D-up viewer

ABSTRACT

Size constancy is referred to the fact that our perception of the size of objects are relatively constant although the size of the retina image varies greatly with viewing distance. You can experience of the size constancy by putting your hand in front of your eyes and moving back and forth. The retinal image size changes greatly but the perception of the hand size remains almost same. When we travel to the forest, we always perceive a big mountain even though we are far away from the mountain. And we are often disappointed later to see a small mountain on the photograph. In this paper we investigate the perceived size constancy of mountain on photographs that give the same size of the real impression while we are looking at the mountain. The experiment started by taking a photograph of mountain by setting the focal length at 50 mm giving the field of view at 46°. And then the size of a mountain on a photograph was changed by software Adobe Photoshop to several sizes. The subject's task was to ask to remember the size of the mountain in the real scene. Then subject was asked to select the picture of the mountain that appeared the same perceived size of the mountain. They selected photographs of larger mountain image than the original picture so shows no size constancy. As the second step we asked the subjects to observe the photographs in a D-up viewer, which gave a 3D perception of photographs. The original photograph taken by the camera was selected to show the size constancy for a 3D photograph.

INTRODUCTION

Size constancy is a perception phenomenon in the cognitive level. [1]. We perceive the real size of object even the viewing distance changes. It is interpreted as result of the brain function called a size correction. [2]. In our retina the image size varies depending on the viewing distance. A building appears very tall and high even we are standing far from the building. This paper aims to demonstrate the size constancy of a mountain on a photograph by using a D-up viewer.

EXPERIMENT

Stimuli

We selected a well know mountain in Lopburi province, named "Khao Jeen Lae" for the experiment. The mountain height is 650 meters above the sea level. A photograph was taken by Canon EOS 5D Mark III with the focal length 70 mm, ISO200. Figure 1a shows the photograph and Fig. 1b its sketch. The mountain was kept white in the sketch and other parts were filled gray. In front of the mountain there was a forest to hide the mountain foot. The field from the forest to the subject position was a wide flat field filled with flowers. The distance to the mountain from the subject and camera was 5,600 meters which gives the visual angle of 6.6°. The original photograph was edited by Adobe Photoshop CS6 to manipulate the size of only the mountain to have 10 pictures including the original with different size of the mountain, which was presented on a display one by

one. Figure 2 show the pictures, where the original picture is number 4. The picture number 1 to 3 were smaller than the original (number 4). From picture number 5 to 10 the mountain size is bigger than the original and those of 1 to 3 smaller than the original. Other parts than the mountain remained same in those ten pictures. The size of a picture was 17.5 x 26 cm on the display. Table 1 gives the size of the mountain in each picture in centimeter (on the left two columns) and visual angle (on the right two columns). The thick outline in the table 1 shows the size of original picture.

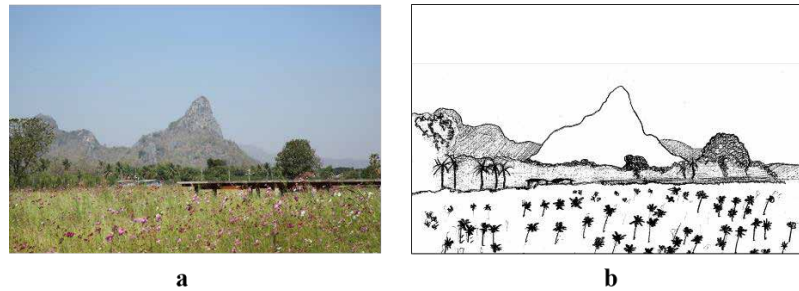


Figure 1. a, the original photograph and b, its sketch.

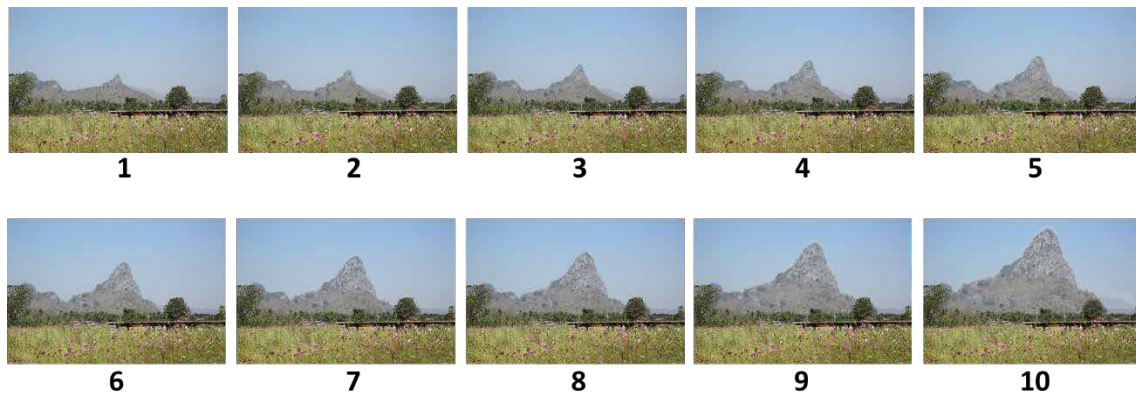


Figure 2. Pictures stimuli.

Table 1: Size of mountain in centimeter and visual angle.

Pic. No.	Size of Mountains			
	Size (cm)		Visual angle (°)	
	height	width	height	width
1	2.6	4.7	4	7.3
2	4	6.7	6.2	10.4
3	5.4	8.7	8.3	13.4
4	6.8	10.7	10.5	16.5
5	8.2	12.7	12.6	19.5
6	9.6	14.7	14.8	22.5
7	11	16.7	16.9	25.5
8	12.4	18.7	19	28.4
9	13.8	20.7	21.1	31.3
10	15.2	22.7	23.2	34.1

Apparatus

The D-up viewer was built to change the mountain scene from 2D picture to 3D perception to the subjects. The principle of the D-up viewer is to eliminate any information beside the picture and help the subject to receive only the information in the picture. A 2D picture is perceived a 3D scene. [3]. A scheme of the D-up viewer is shown in Figure 3. By a hood a subject can see only the picture displayed on a display.

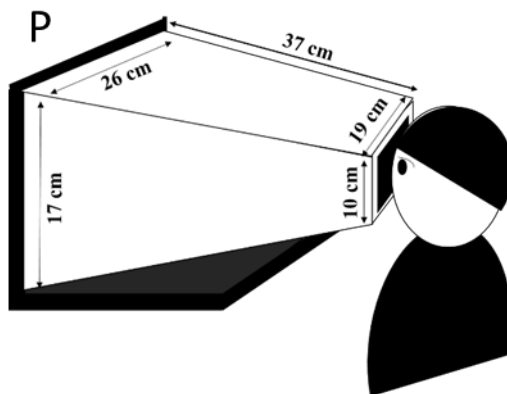


Figure 3. Observing picture through D-up viewer.

Procedure

Nine people participated in the experiment. A subject was asked to look at the mountain scenery and remember the impression of the size and then to select a picture on the LCD display that he/she felt the same size of the mountain as the impression for the real scene. Binocular view was adopted. Then, the subject did the same as before to observe the real mountain and remember size. After that he/she moved to look at the pictures through D-up viewer on the display monocularly and selected one out of 10 pictures that gave the same impression about the size of mountain as they looked at the real mountain. Notice that subjects took some time to perceive the mountain of picture as a 3D scene. The experimenter recorded the answer from the subjects by number of pictures. The observing was done for 3 times.

RESULTS AND DISCUSSION

The results are shown in the left of Fig. 4. The abscissa indicates subjects and the ordinate picture number that the subjects chose. The solid triangles with dotted line are the results of the first step of experiment, where the subjects chose a picture without D-up viewer. A red line is drawn at the picture number 4, that is the original picture. Subjects chose pictures of larger number, which means that the subjects needed much larger size (no. 7-9) of the mountain to match with the impression of the real scene. But when they observed pictures with the D-up viewer they had the same impression as the real scene for a small number of pictures, from 4 to 6.5. Only one subject (WP) chose the original picture. The results are replotted on the right of Fig. 3 with the visual angle for the ordinate. A dotted line indicates the visual angle of actual visual angle for the mountain, 6.6° . Almost all the subjects selected the size of mountain of much larger visual angle without D-up viewer in agreement with our daily experience, for example, subject PS needs the visual angle 31° to be matched with the real scene impression of 6.6° showing the size constancy. In the case of D-up viewer the visual angle showed smaller than the results from normal observation without D-up viewer. The difference of

filled circles from filled triangles at each subject indicates that the difference was supplemented by the amount gained by the size constancy function in the pictures by seeing the pictures as 3D scenes.

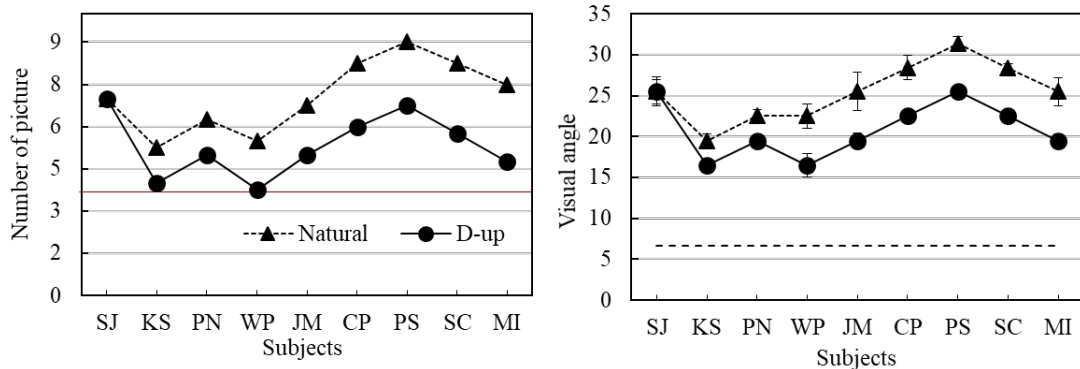


Figure 4. Observing picture through D-up viewer.

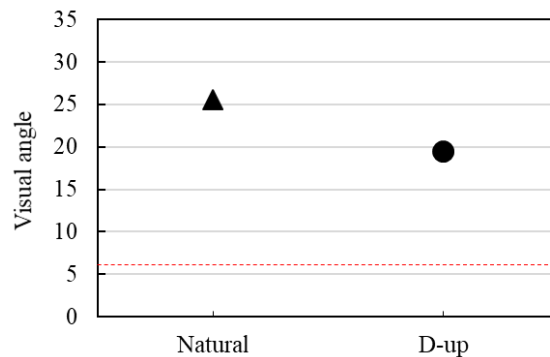


Figure 5. Averaged results of without (natural) and with D-up viewer.

The averaged results of all the subjects are shown in the Fig. 5. The ratio of the visual angle for the natural view and for the real view was 3.78 (Visual angle of natural view/Visual angle of actual retina image). For the D-up viewer observation the ratio was 3.03 (Visual angle of D-up view/Visual angle of actual retina image). Based on this experimental result we can conclude that to get the size constancy we need to perceive object as three dimensional.

ACKNOWLEDGEMENT

We thank Faculty of Mass Communication Technology for giving us the research fund 2019. We also thank students of Ikeda and Chompoo laboratory, who contributed to this research as subjects. We acknowledge Janejira Mepean, a student of the laboratory, as a research assistant.

REFERENCES

1. Sperandio, I. and Chouinard PA. (2015). The Mechanisms of Size Constancy. *Multisensory Research*, 28(3-4), 253-283.
2. Maturana, H. R., Varela, F.G., Frenk, S.G. (1972). *Size constancy and the problem of perceptual spaces*, *Cognition*, 1(1), 97-104.
3. Phuangsuwan, C, Ikeda, M, and Katemake, P. (2013). Color constancy demonstrated in a photographic picture by means of a D-up viewer. *Optical review*, 20(1), 74-81.

COLOR SYSTEM TRANSFORM FROM RGB TO $L^*a^*b^*$ USING NEURAL NETWORK – CONSIDERATION IN HUES OF PB, P AND RP –

Arikuni Makiguchi^{1*}, Tomohiro Moriya¹, Kazuki Tashiro¹, Masashi Ohkawa²

¹ Graduate School of Science and Technology, Niigata University
8050 Ikarashi 2-no-cho, Nishi-ku, Niigata 950-2181, Japan.

² Faculty of Engineering, Niigata University
8050 Ikarashi 2-no-cho, Nishi-ku, Niigata 950-2181, Japan.

*Corresponding author: Arikuni Makiguchi, f19c106c@mail.cc.niigata-u.ac.jp

Keywords: color system transform, color system conversion, neural network, RGB, $L^*a^*b^*$

ABSTRACT

Color management are getting significant in various businesses, such as fashion, printing, and advertisement. In colorimetry, colorimeters with a built-in illuminant are usually utilized, and diameter of measurement area ranges from several mm ϕ to several cm ϕ . Incidentally, color information can also be obtained by conventional imaging devices. In particular, a wide-angle imaging device, namely a digital camera, would be useful to evaluate color distribution. Color information obtained by the digital camera is, however, RGB values that is not a uniform color space, which is unsuitable for color management. It is desirable to transform RGB color system into $L^*a^*b^*$, which is well known as a uniform color system. Moreover, RGB values obtained using an imaging device strongly depend on photo-shooting conditions, such as illuminant, imaging device, lighting condition, and shutter speed, so that it is not realistic to prepare a transform formula for an arbitrary condition. Therefore, our group has proposed color system transform from RGB to $L^*a^*b^*$ using an artificial neural network (ANN), which has excellent generalization ability.

Data sets of RGB and $L^*a^*b^*$ for twelve hues, such as hues of PB, P and RP, based on JIS standard color charts were prepared in order to train and test the neural network. In this research, the ANN was composed of 3 layers: an input layer, a hidden layer and an output layer. The input layer was 3 units corresponding to the R, G and B values. The output layer was also 3 units corresponding to the L^* , a^* and b^* values. Moreover, the hidden layer is comprised of 20 units. The RGB data was obtained from RAW data of pictures taken by a digital camera, and the $L^*a^*b^*$ data was calculated using spectral reflectance of color samples in the charts.

In this study, performances of color system transform for the twelve hues of PB, P, and RP were considered with the ANN's which had been trained using only twelve training data sets selected from two designated hues out of the twelve hues. The number of training data was 12, namely 6 for each hue. In order to evaluate performance of color system transform for the trained neural network, we introduced an original index, which is defined as percentage of color difference of less than 2.5 between the network output and the expected $L^*a^*b^*$. According to the results, color-system-transform performance was found to be more than 50 % for each hue between the two hues with the training data when the other training hue except for 5P was set at 2.5PB, 5PB, 10PB or 2.5RP. According to the results, we could find usefulness of color system transformation using ANN.

INTRODUCTION

In color management, spectrophotometers and colorimeters with a built-in illuminant are usually utilized [1], and the diameter of the measurement area ranges from several mm ϕ to several cm ϕ . Color attributes can also be obtained by conventional imaging devices. In particular, a wide-angle imaging device, such as a digital camera, is useful when evaluating color distribution. Color data obtained by a digital camera is, however, in RGB values which are not a uniform color space and are unsuitable for color management. Converting a RGB color system into $L^*a^*b^*$, which is well known as a uniform color system [1], is desired. Moreover, RGB values obtained from an imaging device are strongly dependent on the photo-shooting conditions, such as illuminants, the imaging device, lighting conditions, and shutter speed. Consequently, developing a conversion formula for arbitrary conditions is not realistic. Therefore, our group would like to propose a RGB to $L^*a^*b^*$, color system conversion using an artificial neural network (ANN), which has excellent generalization ability [2]. In this study, training of ANN was carried out using only six or twelve data sets, and then performance of a color system conversion from RGB to $L^*a^*b^*$ was examined using RGB- $L^*a^*b^*$ data sets based on color samples of hues of PB, B and RP.

NEURAL NETWORK CONFIGURATION FOR COLOR SYSTEM TRANSFORM FROM RGB TO $L^*a^*b^*$

A three-layer neural network, consisting of input, hidden and output layers, is shown in Figure 1. The input and output layers have 3 units each, corresponding to RGB and $L^*a^*b^*$ values, respectively, and the hidden layer has 20 units. Each unit acts as a non-linear, multi-input/one-output system, which mimics the brain's neurons and synapses. Units of neighbor layers are connected to each other, and connection weights and biases [2] of all units must be adjusted so ANN will have the desired input-output correspondence by training. To train the network, a back propagation algorithm with momentum was used [2], and sigmoid function was used as the activation function [1]. In order to train and evaluate ANN, training and test data sets were prepared using color samples of JIS standard color charts as shown in Figure 2. In this study, photos of twelve color charts, specifically hues of 2.5PB, 5PB, 7.5PB, 10PB, 2.5P, 5P, 7.5P, 10P, 2.5RP, 5RP, 7.5RP, and 10RP, were taken with a digital camera to obtain RGB values. The setup to obtain photo data is shown in Figure 3. Distance between the camera and the opposing color chart was set 30 cm. A halogen lamp (Toshiba Neo Halo Beam JDR 110 V 75 W / K 5 S) was employed as an illuminant and was placed at a 45° angle from the face of the color chart. JPEG photo data were saved in the camera, and RGB values of each color sample were determined from bitmap image data using openCV. On the other hand, $L^*a^*b^*$ values were calculated using the spectral reflectance of each color sample and the spectral distribution of the light source [1]. The obtained RGB- $L^*a^*b^*$ data sets were divided into training and test data sets. In this study, six or twelve training data sets were selected from a single hue or two assigned hues, respectively. In training ANN, initial values of the connection weights and biases of all units were arbitrarily set between -0.3 and 0.3. The learning rate and momentum coefficient [2] of the back propagation algorithm were set at 1.0 and 0.9, respectively, as determined by the optimization results. After training, performance of the color system conversion was evaluated based on the color difference between the output values (L^*_{NW} , a^*_{NW} , b^*_{NW}) and the target values (L^*_{target} , a^*_{target} , b^*_{target}) using the test data sets, that is, all data excluding the training data. Color difference ΔE was calculated by the following equation [1].

$$\Delta E = \sqrt{(L^*_{NW} - L^*_{target})^2 + (a^*_{NW} - a^*_{target})^2 + (b^*_{NW} - b^*_{target})^2} \quad (1)$$

Here, an original performance index PI , as defined in Eq. (2) for each hue, was introduced in order to evaluate the generalization of the trained ANN with regard to performance of color system conversion.

$$PI = \frac{N_2}{N_1} \times 100 (\%), \quad (2)$$

where N_1 and N_2 are the number of test data in a hue and the number of test data with color difference less than 2.5 in a hue, respectively.

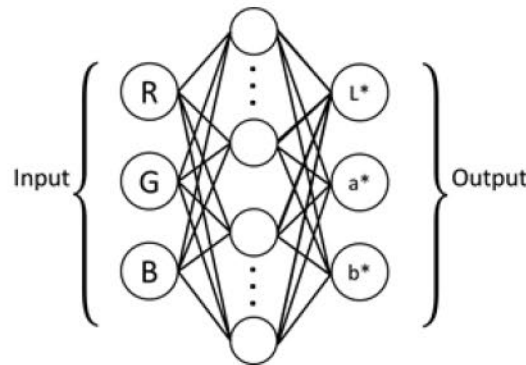


Figure 1 Configuration of a three-layer neural network

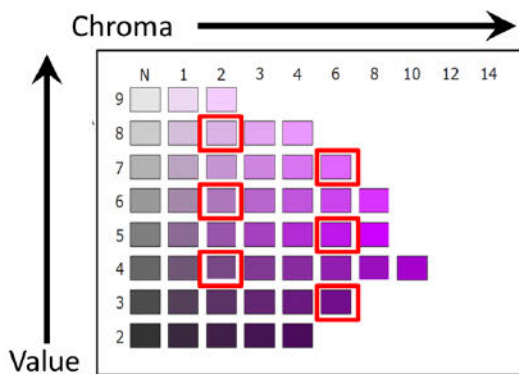


Figure 2. Example of the color chart of a hue of 5P. Color samples outlined in red represent the training data

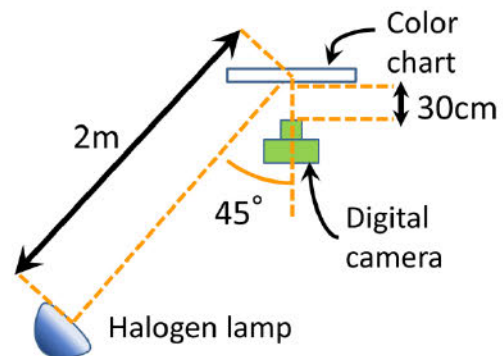


Figure 3. Layout of the camera, color chart, and halogen lamp to obtain photo data.

TRAINING OF ANN USING THE SIX-DATA SETS OF A SINGLE HUE

In the training of ANN, data sets of a single hue of 5P were used to examine the performance of color space conversion. The RGB- $L^* a^* b^*$ data sets of 8/2, 7/6, 6/2, 5/6, 4/2, and 3/6 (value/chroma) were assigned as training data (outlined in red in Figure 2). The remaining data sets were used as test data sets. Color differences calculated by Eq. (1) of a trained ANN are shown in Figure 4. In

the figure, columns and rows indicate Munsell values and Munsell chroma, respectively. Blue highlighted cells indicate color difference less than 1.2, and yellow highlighted cells indicate color difference ranging from 1.2 to less than 2.5. From the figure, the resultant color differences tend to be relatively small near the training data, and conversion performance PI is calculated to be 58.5%. Moreover, the average conversion performance for hue 5P was 59.0% for five trials with different initial values of connection weight and bias. After examining a hue of 5P, the same examination was conducted for 11 other hues. Average performances of color system conversion are shown for all 12 hues in Figure 5. Average performances of 7 hues (2.5PB to 7.5P) were higher than 50%, while the other 5 hues (10P to 10RP) were lower than 50%. The cause for such difference depending on the hue is difficult to explain, but may be attributed to the non-uniform quality of the RGB-L*a*b* data set, which is sensitive to photo-shooting conditions.

		Chroma								
		N	1	2	3	4	6	8	10	
Value	9	2.44	1.70	3.83						
	8	2.50	1.31	0.16	1.73	3.38				
	7	3.27	1.92	1.36	1.75	1.94	0.20			
	6	1.75	1.61	0.18	0.66	1.26	1.61	1.19		
	5	0.77	0.25	2.23	1.52	1.04	0.22	2.22		
	4	2.96	2.23	0.18	0.67	0.36	0.71	3.90	3.34	
	3	8.04	6.91	6.44	4.44	3.27	0.12			
	2	15.23	13.47	13.00	12.91	11.17				

Figure 4. Example of color differences of a trained ANN for hue of 5P

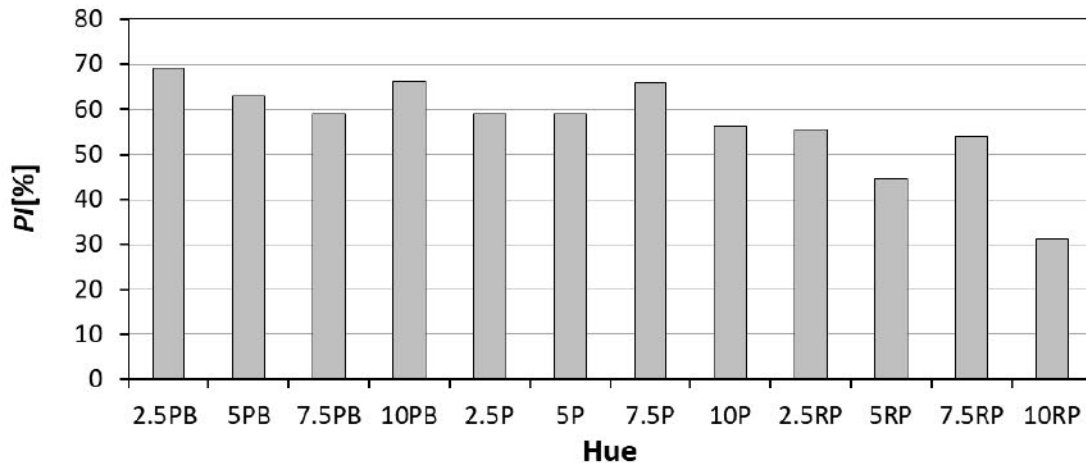


Figure 5. Average performance indices PI over five trials for each hue

TRAINING OF ANN USING THE SIX-DATA SETS OF TWO ASSIGNED HUES

Performance of color space conversion was examined in the training of ANN using the data sets of twelve hues of PB, P and RP. The training data sets were selected from only two designated hues, including the hue of 5P, out of the twelve hues, in order to reduce training cost of ANN. For each of the two hues, RGB-L*a*b* data sets of 8/2, 7/6, 6/2, 5/6, 4/2, and 3/6 (value/chroma) were

assigned as training data, as shown in Figure 2, outlined in red. Consequently, the total number of training data sets was only 12. ANN training was conducted five times under the same conditions except for the initial values of connection weight and bias. Figure 6 shows average performance of color system conversion for the trained ANN when the training data sets were selected from a hue on the PB side as well as 5P. Moreover, Figure 7 shows the average conversion performance for the training data sets from the RP side as well as 5P. The bold red circles in the figure indicate the two hues for which the training data sets were assigned. The vertical and horizontal axes represent color-system conversion performance PI and hue designation, respectively. From Figure 6, the performance of color-system conversion is found to be relatively high on the PB side, for hues with training data sets. On the other hand, on the RP side, where training data sets were not allocated, performance of color conversion gradually decreased as hue was apart from 5P. From Figure 7, the conversion performance is found to be high for the hues on the RP side, and gradually decreased as the hues became farther from 5P on the PB side. According to the results, color system conversion performance was found to be more than 50% for each hue between the two designated hues with training data in cases where the training hue other than 5P was set at 2.5PB, 5PB, 10PB or 2.5RP.

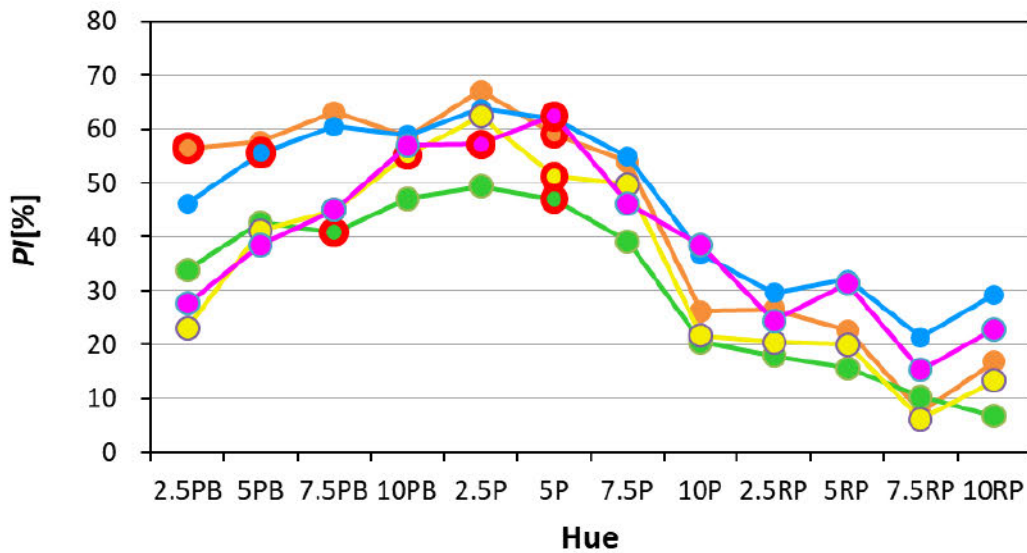


Figure 6. Performance of color conversion for a trained hue on the PB side.

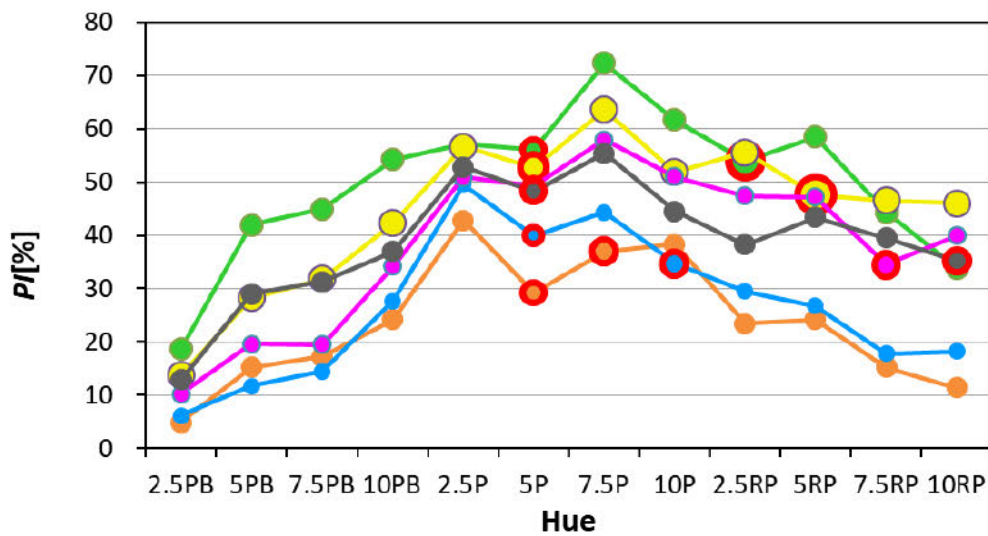


Figure 7. Performance of color conversion for a trained hue on the RP side.

CONCLUSIONS

Performance of color system conversion from RGB to $L^*a^*b^*$ using a three-layer ANN was examined for twelve hues of PB, P and RP. Regarding training of the ANN, six data sets of a single hue were used, and average conversion performance was evaluated for each hue. Performance exceeded 50% for seven hues, namely 2.5PB to 7.5P. Moreover, conversion performance in training ANN using training data sets selected from two designated hues, one of which was a hue of 5P, out of the twelve hues was examined. A number of training data sets was only 12, namely 6 for each hue. According to the results, color system conversion performance was found to be more than 50% for each hue between two designated hues with training data, in cases when the training hue other than 5P was set at 2.5PB, 5PB, 10PB or 2.5RP. While the obtained conversion performance is insufficient for color management, the feasibility of realizing a digital camera with a colorimetry function using the trained ANN was demonstrated.

REFERENCES

1. R. W. G. Hunt, and M. R. Pointer, (2011) *Measuring Colour Fourth Edition*, John Wiley & Sons, Ltd., Chapters 2, 3 and 9.
2. S. Haykin, (2008) *Neural Networks and Learning Machines Third Edition*, Pearson Education, Introduction and Chapter 4.

Analysis of Faded Colors by Using Spectral Approach with Non-negative Matrix Factorization

Alton Mao^{1*}, M. James Shyu¹, Simon Lin², Ya-Ning Chen³, Eric Yen²

1. Department of Information Communications, Chinese Culture University, Taiwan,

2. Institute of Physics, Academia Sinica, Taiwan,

3. Department of Information and Library Science, Tamkang University, Taiwan

*Corresponding author: Alton Mao, alton0803@gmail.com

Keywords: Spectral, Non-negative Matrix Factorization, Faded colors, Color restoration

ABSTRACT

The surface paints of many historical sites are faded gradually due to sun exposure day by day. However, the paint is always faded unevenly which makes the depiction of the surface colors ambiguous. In the mean time, recent progress on spectral approach makes it possible to measure an object's surface spectral reflectance values accurately and to record its physical properties. In this study the non-negative matrix factorization (NMF) method is used to extract the spectral color components. An approach to characterize a group of faded colors into specific numerical representation is proposed in this study.

INTRODUCTION

The beauty of historical sites is appreciated by their form and color in various cultures. However with time goes by, the surface paint and then the colors of many historical sites are faded commonly due to long-term sun exposure and other weathering process. When studying the color characteristics on these types of historical buildings, it is necessary to describe the color precisely in order to estimate its original color for maintenance or restoration purpose. Nevertheless, the paint is always faded unevenly which makes it necessary to develop a method to measure and to define the primary color on the historical site.

The measurement of color is usually represented by colorimetric values. Nevertheless, spectral reflectance values are involved in the computation for colorimetric values. Furthermore by using analysis in spectral manner, it is possible to measure an object's surface reflectance values accurately and factor out light source influence and to record its physical property[1].

This study deploys the NMF method to extract color features. Compared with many feature extraction methods, NMF has a non-negative nature and conforming to the physical

properties of the paint. It can effectively find the primary components from the data which include different levels of fading, and it is able to identify the association between individual components and paint[2]. Moreover, after obtaining the characteristic spectrum, linear regression is used to reconstruct each spectral reflectance data. The regression coefficient represents the ratio relationship between the paint and the substrate at the sampling position. Quantifying the degree of fading on the paint can be more effective by the coefficients. It is useful also in assisting the color restoration of the historical site.

ANALYSIS METHOD

The formation of color requires three elements: light source, object and observer as described in CIE colorimetric computation in Eq. (1). The energy distribution of the light can be represented by spectral manner, usually a continuous band in nanometers. When the light source illuminates on the object, depending on the physical properties on the surface of the object, part of the energy is absorbed and part of the energy is reflected spectrally. The spectral reflectance values are measured and used in Eq. (1) to come up with the actual colorimetric description of the object in this study. Different from other color spaces (e.g. RGB signals from digital camera), spectral reflectance values are not influenced by the light source as well as the observer, and it can describe the color information of the substance more accurately. The actual color appearance can be estimated by CIE colorimetric computation, like CIELAB color space[3].

$$\begin{aligned}
 X &= k \sum_{\lambda} S(\lambda)R(\lambda)\bar{x}(\lambda)\Delta \lambda \\
 Y &= k \sum_{\lambda} S(\lambda)R(\lambda)\bar{y}(\lambda)\Delta \lambda \\
 Z &= k \sum_{\lambda} S(\lambda)R(\lambda)\bar{z}(\lambda)\Delta \lambda \\
 k &= \frac{100}{\sum_{\lambda} S(\lambda)\bar{y}(\lambda)\Delta \lambda}
 \end{aligned} \tag{1}$$

where X, Y, Z denote the CIE tristimulus values calculated from spectral data $R(\lambda)$. $S(\lambda)$ is an illuminant, $\bar{x}(\lambda)$, $\bar{y}(\lambda)$ and $\bar{z}(\lambda)$ are the CIE standard observer color-matching functions, k is a normalizing constant.

Non-negative Matrix Factorization (NMF) is used to decompose a non-negative matrix V_{ij} into two non-negative matrices W_{ik} and H_{kj} as Eq. (2). The decomposed matrix product approximates the original matrix, and the non-negative matrix refers to the real number (R) of elements in the matrix that are all more than or equal to zero[4].

$$V \cong WH \quad (2)$$

In this study, the original spectral data matrix V_{ij} (35-j-dimensional, 380-730nm, 10nm) is decomposition into W_{ik} base matrix (35-k-dimensional characteristic spectrum) and H_{kj} weight matrix (the coefficients of characteristic spectrum). However by nature, NMF lacks the information for effectively determining the number of principal features, it can be determined by using Principal Component Analysis (PCA)[5].

EXPERIMENTAL

Two painted pillars of a historical architecture at Bogd Khan Palace Museum in Ulaanbaatar, Mongolia are the primary objects in this study. One pillar, as shown in Fig. (1a), is having the original surface painting on which the color is faded unevenly due to the sun exposure over the time. Another pillar is a newly painted surface from recent restoration as shown in Fig. (1b). The pillars are under the roof, therefore half side of each pillar is always in the shadow and the other half would expose directly to the sun.



Figure 1. Pillars of historical architecture in Ulaanbaatar, Mongolia.

An X-rite i1 Pro 2 spectrophotometer with M0 light source was used to measure the reflectance spectrum of the original and newly painted pillars. The interval between sampling points was set as 1 cm. The sampling point started from the inner shadow-side and turned a circle around the column with equal spacing as illustrated in Fig. (2). There are 28 sampling points for the pillar having the original paint. There are 30 sampling points for the newly painted pillar. The measured spectral reflectance curves are shown in Fig. (3).

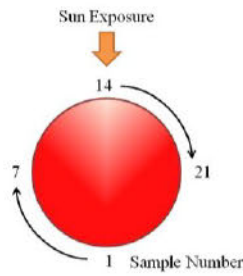


Figure 2. Illustration for the position and the sequence of the sampling on the pillar.

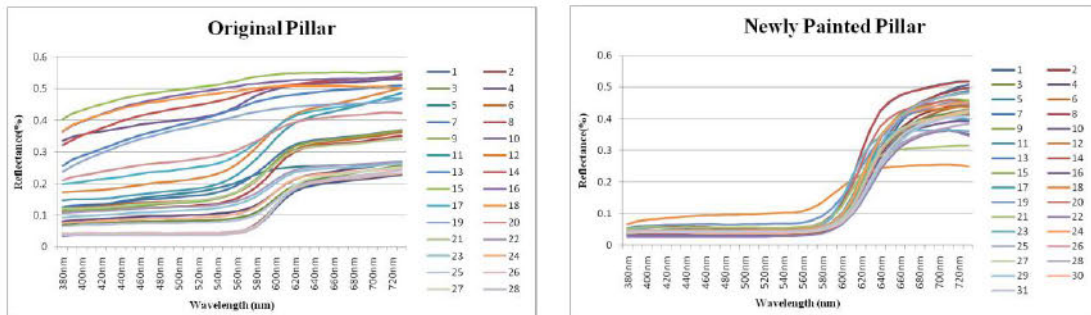


Figure 3. Spectral reflectance curves of the sampling points on the pillars.

RESULTS

The extraction of the color features was performed by using the NMF library in Python 3.7. PCA analysis was performed first to determine the number of the primary components. Two components can be found for the pillar having the original paint. The spectral reflectance curves and their corresponding color in sRGB encoding are shown in Fig. (4-a). They are dark red and light gray colors. The red one is the summarized original paint. The light gray seems to be the base paint underneath the red paint which surfaces up when the red paint faded away. The mixing ratios in between can be indicated by the coefficients as shown in Fig. (5-a).

Only one component can be found from the spectral data of the newly painted pillar. The spectral reflectance curve and its corresponding color in sRGB encoding are shown in Fig. (4-b). The regression coefficients are shown in Fig. (5-b), which may indicate the intensity of the paint on the newly painted pillar.

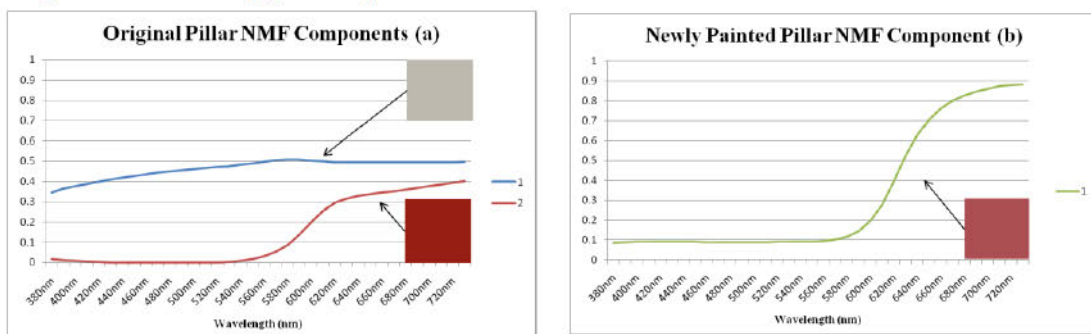


Figure 4. The NMF components of the 2 pillars and its corresponding sRGB encoding.

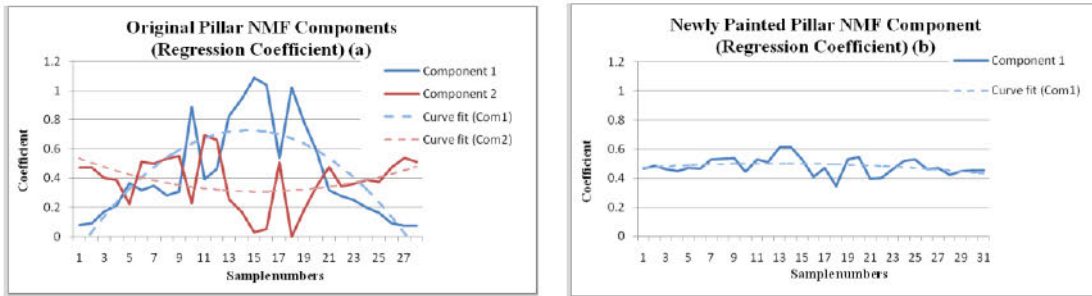


Figure 5. The regression coefficients of the NMF components.

The coefficients obtained by the linear regression with the spectral components can serve as the scalar for the amount of the paints. Due to the influence of the surface texture of the pillar and the uneven coloration, the coefficient distribution fluctuates. However, there is a trend that the variation of the coefficients matches with the level of sun exposure on the position. The first coefficient to the basic color of the original pillar is positively correlated with the degree of exposure. The maximum value is at the outermost side of the pillar facing the sunlight (No. 14), and then gradually decreases to the shadow area. The second coefficient of the original pillar, although distributed not smoothly, can still be observed that the coefficient is negatively correlated with the degree of sun exposure. The newly painted pillar is less affected by the sun exposure, consequently showing less significant variation.

The normalized spectral components are drawn together in Fig. 6. It can be seen that there are some difference between the original paint and the new paint in the spectral distribution around 620 nm region. Further study might be able to find a different paint that shows closer color characteristics to the original paint.

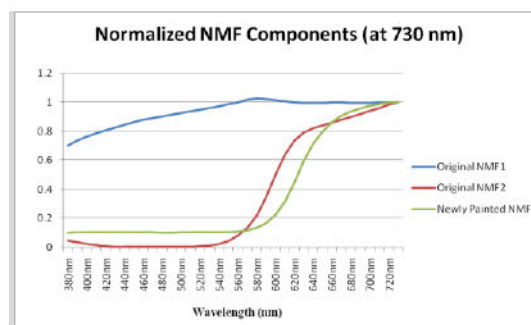


Figure 6. Normalized NMF components of original and newly painted pillars.

SUMMARY

The non-negative matrix factorization (NMF) method is used to extract the spectral color components from two sets of spectral reflectance data of a historical building. The results indicate that this method is capable to obtain the primary components in an all-positive vector form which can be co-related well with the spectral characteristics of the physical paint in this study. This method can be useful in determining the color characteristics among color samples of a faded object.

ACKNOWLEDGEMENT

This study was partially supported by the Ministry of Science and Technology of Taiwan, project number 104-2923-H-001-002-MY3 and 107-2410-H-034-039. The authors would like to express their appreciation for the supports from the Mongolian Academy of Science and Bogd Khan Palace Museum.

REFERENCES

1. Chamhee Jung, Hanhyoung Lee, Youna Song, Kyungjin Min and Yongjae Chung (2018). Analysis of painting materials of Dancheong on Korean traditional wooden building using hyper-spectral imaging technique. *Journal of Conservation Science*, 35(4), 345-361.
2. Gershon Buchsbaum, Orin Bloch (2002). Color categories revealed by non-negative matrix factorization of Munsell color spectra. *Vision Research*, 42, 559-563.
3. Roy S. Berns (3rd Eds.). (2000). *Billmeyer and Saltzman's Principles of Color Technology*. CA: Wiley-Interscience.
4. Daniel D. Lee, H. Sebastian Seung (2000). Algorithms for non-negative matrix factorization. *Neural Information Processing Systems*, 13, 535-541.
5. Xiu-rui Geng, Lu-yan Ji, Kang Sun (2016). Non-negative matrix factorization based unmixing for principal component transformed hyper-spectral data. *Frontiers of Information Technology & Electronic Engineering*, 17(5), 403-412.

MATERIAL RENDERING PROPERTY OF ILLUMINATION

Daisuke Kondo¹, Hayato Fujita¹, Isamu Motoyoshi^{1*}

¹*Department of Life Sciences, The University of Tokyo, Japan.*

*Corresponding author: Isamu Motoyoshi, imotoyosi.ac@gmail.com

Keywords: ACA, illumination, color rendering property, material perception

ABSTRACT

Particular types of illuminations can enhance the color appearance of objects. This 'color rendering property' of illumination has been extensively investigated in color science and widely introduced in various industrial fields. But, past studies on the effect of illumination on rendering have restricted themselves to the influence of the illuminant's spectrum on color perception. On the other hand, recent psychophysical studies have shown that the perception of various surface properties – glossiness, lightness, and color – strongly depend on the spatial structure of illumination, or so-called "lightfield". Here, we propose a novel concept called the 'material rendering property' of illumination which refers to the spatial and chromatic characteristics of the lightfield that enhance the material appearance of surfaces. Here, we identified lightfields with good material rendering properties by studying the relationship between the statistical structure of lightfields and the perception of surface qualities. In a series of psychophysical matching experiments, we showed computer-generated bumpy objects under 21 different natural lightfields (both outdoor and indoor scenes) to 9 observers and measured perceived surface properties including glossiness, mesoscopic roughness, and sharpness of bumps (7 levels for each dimension). Our analysis revealed that, for all three dimensions, variations in perceived surface properties were highly correlated with key statistical features of the lightfield, namely contrast, skewness, and energy correlation across orientation subbands. These results suggest that light environments with high spatial contrast and skewness, especially those produced by blobby light sources (e.g., small circular lamps), tend to enhance material rendering properties.

INTRODUCTION

Particular types of illuminations can enhance the color appearance of objects. This 'color rendering property' of illumination has been extensively investigated in color science and widely introduced in various industrial fields. But, past studies on the effect of illumination on rendering have restricted themselves to the influence of the illuminant's spectrum on color perception. On the other hand, recent psychophysical studies have shown that the perception of various surface properties – glossiness, lightness, and color – strongly depend on the spatial structure of illumination, or so-called "lightfield" [1-5].

In the present study, we propose a novel concept called the '*material rendering property*' of illumination which refers to the spatial and chromatic characteristics of the lightfield that enhance the material appearance of surfaces. Here, we identified lightfields with good material rendering properties by studying the relationship between the statistical structure of lightfields and the perception of surface qualities.

METHOD

In a series of psychophysical matching experiments, we showed computer-generated bumpy spherical objects under 21 different natural lightfields (both outdoor and indoor scenes) to 9 observers and measured perceived surface properties including glossiness, mesoscopic roughness,

and sharpness of bumps (7 levels for each dimension). The glossiness was defined as the specular reflectance. The mesoscopic roughness was defined by the amplitude of bump map. The sharpness was defined as the amount of blur of the shape distortion map which was given as a spherical image of binarized band-pass noise. On each trial in the experiment, observers freely viewed the test object having a particular surface property (e.g., specular reflectance of 0.5%) under a particular lightfield, and adjusted that property (e.g., specular reflectance) of the reference object under a fixed lightfield (Eucalyptus).

RESULTS

For the both of objects and lightfields, we computed the luminance subband image statistics that are known to be encoded in the primate visual cortex: moment statistics (contrast, skew, and kurtosis) at each spatial frequency and orientation subband, and cross correlations across different subbands. We then looked at correlations between the matched surface property and these image statistics. The analysis revealed that, for all three dimensions, variations in perceived surface properties were highly correlated with key statistical features of the lightfield, namely contrast, skewness, and energy correlation across orientation subbands.

DISCUSSION

In agreement with the results from previous studies, these results suggest that light environments with high spatial contrast and skewness, tend to enhance the material appearance of surfaces. Moreover, these results indicate that material rendering properties are enhanced in the environments with high cross-orientation correlation (e.g., blobby light sources such as small circular lamps).

ACKNOWLEDGEMENT

This study was supported by the Commissioned Research of NICT (1940101), and by JSPS KAKENHI grant-in-aid 18K19801 and JP15H05916.

REFERENCES

1. DROR, R. O., WILLSKY, A. S., & ADELSON, E. H. (2004). Statistical characterization of real-world illumination. *Journal of Vision*, 4, 821-837.
2. FLEMING, R. W., DROR, R. O., & ADELSON, E. H. (2003). Real-world illumination and the perception of surface reflectance properties. *Journal of Vision*, 3, 347-368.
3. MOTOYOSHI, I., & MATOBA, H. (2012). Variability in constancy of the perceived surface reflectance across different illumination statistics. *Vision Research*, 53(1), 30–39.
4. OLKKONEN, M., & BRAINARD, D. H. (2010). Perceived glossiness and lightness under real-world illumination. *Journal of Vision*, 10(9):5, 1-19.
5. PONT, S. C., & TE PAS, S. F. (2006). Material - Illumination ambiguities and the perception of solid objects. *Perception*, 35(10), 1331–1350.

DEVELOPMENT OF NATURAL COLORANT FROM *TECTONA GRANDIS* LEAF EXTRACT BY COMPLEX WITH β -CYCLODEXTRIN

Natthawadee Tibkawin¹ and Pensri Charoensit^{1*}

¹Department of Pharmaceutical Technology, Faculty of Pharmaceutical Sciences, Naresuan University, Phitsanulok 65000, Thailand

*Corresponding author: Pensri Charoensit, pensric@nu.ac.th

Keywords: *Tectona grandis*, teak, natural colorant, β -Cyclodextrin, solubility

ABSTRACT

Tectona grandis Linn. is commonly known as teak, which is a commercial tree of Thailand have color pigments in various parts of the tree; bark, wood, and leaf. Teak leaves have been used for textile dyeing in Thailand local wisdom. We previously studied the color extracts of teak leaf extracted from various solvents which exhibited a variety color shade of the extracts. However, these extracts had low solubility in water that caused difficulty in application. The aim of this study was to increase water solubility of teak leaf extract by complex with β -Cyclodextrin (BCD) for development a natural colorant from teak leaf. In this study, teak leaves were extracted by the maceration method with ethyl acetate. The extract was then complexed with BCD by three methods; Co-precipitation, Freeze-drying and Solvent evaporation which the colorant products were termed BCD-E1, BCD-E2 and BCD-E3. The percentage yield, solubility and color appearance of the colorants were determined. The characteristics of colorants were also evaluated by UV-Vis spectrophotometer, Colorimeter and Fourier-transform infrared spectroscopy (FTIR). Three preparing methods provided the colorants in a powder form, which had the same pink color. The results showed the colorants prepared from three methods had solubility values approximately 100 times higher than the crude extract (0.025g/100ml), which the water solubility of BCD-E2 was highest (2.49g/100ml). The percentage yields of colorants were not much difference between the preparing methods, which Freeze-drying method gave the highest yield (49.01%). After dissolving the colorants in water, the slightly differ in color appearance between the colorants was observed. This result agrees with the UV-Vis absorption spectra of the colorants that was little different in terms of intensity and wavelength. The color values of the three colorants were also different. These results suggest that the preparing method affects the color appearance of the colorants. The FT-IR spectra of colorants were identical with the BCD spectrum, but the peak of the colorants at absorption band at 1700 cm^{-1} disappeared that might refer to the chemical reaction between BCD and the teak leaf extract. In addition, the colorants prepared from three methods showed the light stability was higher than the extract after UVB light exposure. In conclusion, β -Cyclodextrin can improve water solubility and stability of *Tectona grandis* leaf extract for application as a natural colorant.

INTRODUCTION

Colorants are used in many industries such as paints, plastics, food, drugs and cosmetics. In the cosmetic industry, some metals in the environment and their natural occurrence can be present in the manufacture of synthetic colorants. Therefore, consumers can be exposed to metals as trace contaminants in cosmetic products they daily use [1]. Such research outcomes have created greater consumer awareness of the potential harmful effects of synthetic colorants and an increased interest

in natural colorants, which has prompted greater efforts for the discovery of alternative natural colorants.

Tectona grandis Linn. is commonly known as teak, which is an economic plant of Thailand. The woods are manufactured for making furniture, but the leave become an agricultural waste material. Teak leaves have traditionally been used as colorants for enhancing an appearance of food and for the dyeing of textiles and have been reported to contain coloring substances such as anthraquinones and flavonoids [2,3]. In addition, we previously studied the teak leaf extracts from various extraction solvents which provided a variety color shade. However, these extracts had low solubility in water that limit the application of the extracts in the cosmetic formulations. Therefore, the improvement in solubility of teak leaf extracts is necessary.

Cyclodextrins (CDs) have been used for the enhancing properties of host molecules such as solubility and stability. CDs are cyclic oligosaccharides with six, seven or eight glucose units named α -Cyclodextrin, β -Cyclodextrin (BCD) and γ -Cyclodextrin linked by α -(1,4)-glycosidic bonds. CDs exhibit a truncated-cone shape with a hydrophobic cavity in which a wide variety of lipophilic guest molecules can be hosted to form inclusion complexes. All CDs are non-toxic ingredients and BCD is the most widely used because its cavity fits common guests with molecular weights of 200-800 g/mol [4,5]. Ariana Zoppi et al., suggested that the formation of the inclusion complexes between BCD and three drugs, sulfadiazine, sulfamerazine or sulfamethazine, in a ratio of 1:1 molar to enhance their solubility [5]. Marcolino VA et al., demonstrated that the complexation of bixin with BCD promoted an intensification of color, increased water solubility and improved light stability of bixin complexes [6].

The aims of this work were to develop the colorant from teak leaf extract and study the effects of preparation method of teak leaf extract complexation with BCD on the solubility in water, the percentage yield and the color appearance of the colorant complexes. The characteristics of the colorant complexes were evaluated using the UV-Vis spectroscopy, Colorimetric and FT-IR techniques. Additionally, the stability against UVB light of the colorant complexes were investigated for application as a natural colorant in cosmetic industries.

EXPERIMENTAL

Plant material

Teak leaves were collected from the tree at Nan province, Thailand. The herbarium specimen (No.004299) of teak leaf has been verified by Asst. Prof. Dr. Pranee Nang-ngam, Faculty of Sciences, Naresuan University and deposited in Department of Biology, Faculty of Science, Naresuan University, Thailand.

Preparation of teak leaf extract

Teak leaves were oven-dried at 60°C for 24 h and ground to provide teak leaf powders. The powdered leaves were macerated with ethyl acetate for 48 h and the extract solutions were then filtrated. The filtrates were evaporated using a rotary evaporator and dried on water bath to obtain a crude extract. The percentage yield of the crude extract was 5.05.

Preparation of colorants from teak leaf extract complex with BCD

The colorant complexes of BCD and teak leaf extract were prepared in the weight ratio of 1:0.2 using Co-precipitation, Freeze-drying and Solvent evaporation methods.

1) Co-precipitation methods. One gram of BCD was dissolved in 40 ml of water. Two hundred milligrams of the extract was dissolved in 30 ml of ethanol and then added into the BCD solution. The mixture was refluxed at 70°C for 4 h and the ethanol was then evaporated. The mixture was

cooled down, stirred for 8 h and stored overnight at 4°C. The mixture was filtrated to be a clear solution, which then freeze dried to afford a colorant complex named as BCD-E1.

2) Freeze-drying methods. The mixture of BCD and the extract was prepared as same as co-precipitation techniques. The mixture was stirred in an incubator shaker at 180 rpm, 37°C for 7 days. Then, the ethanol was removed and the solution was filtrated to be a clear solution. The clear solution was freeze dried to obtain a colorant complex named as BCD-E2.

3) Solvent evaporation methods. The mixture of BCD and the extract was prepared as same as co-precipitation techniques. The mixture was stirred without a cap to evaporate the ethanol. The solution was stirred overnight, filtrated using filter paper and the supernatant was recovered by freeze drying to obtain a colorant complex named as BCD-E3.

The obtained colorant complexes were stored at 4°C until further use. The percentage yield of the colorant complexes were calculated by the following equation:

$$\% \text{ yield} = [\text{weight of the colorant complex} / (\text{weight of extract} + \text{weight of BCD})] \times 100 \quad (1)$$

Solubility assay

Ten milligrams of the colorant complexes were placed in test tubes. In the tubes, 10 µl of water was continuous added and mixed using a vortex mixer until a clear solution was obtained. The solution was set aside for 5 min to ensure the solubility. The solubility of the extract was determined as the same manner. The solubility of samples were calculated by the following equation:

$$\text{Solubility} = [\text{weight of the colorant complex} / \text{volume of water}] \quad (2)$$

Color determination

The sample was prepared by dissolving the extract or the colorant complexes in water at concentration of the maximum solubility. The photograph of the sample was taken by a digital camera. The color values of the sample were measured by Colorimeter (ColorQuest XE, Hunterlab, Virginia USA) in reflectance specular excluded mode with CIELAB system.

Characterization of the colorant complex

Sample was prepared by dissolving the extract or the colorant complexes in water at concentration of 0.025g/100ml. The light absorbance of the sample was determined in wavelength range of 400-800 nm by UV-Vis spectrophotometer (UV-1800 240V, Shimadzu, Kyoto Japan).

The FT-IR spectra of the colorant complex, the extract, BCD and the simple mixtures of BCD and the extract at the weight ratio of 1:0.2 were obtained at spectral range was 400-4000 cm⁻¹ using an infrared Fourier transform spectrometer (Spectrum GX, PerkinElmer Frontier, Waltham USA). The samples were diluted in KBr powder and the pellets were made to perform the measurements.

Stability study

The light stability of the extract and the colorant complexes were tested using a UV test chamber (BS-04, Opsytec Dr.Grobel, Ettlingen Germany). The samples were prepared by dissolving the extract in water at concentration of 0.025g/100ml and the colorant complexes in water at concentration of 0.2g/100ml to obtain the same amount of the extract in the sample. The samples were kept in glass vials with caps and exposed to UVB. After exposure for 30, 60, 120, 240 and 480 min, the absorbance of the sample was determined by a UV-Vis spectrophotometer. The percent retention of samples was calculated by the following equation:

$$\% \text{ Retention} = [\text{absorbance of sample at } T_1 / \text{absorbance of sample at } T_0] \times 100 \quad (3)$$

By T_0 = absorbance value of sample at initial time.

T_1 = absorbance value of sample at each time.

RESULTS AND DISCUSSION

The percentage yield, solubility and color appearance of the colorant complexes

Table 1: The percentage yield, the solubility, the color appearance and the color values of the extract and colorant complexes.

Samples	% yield	Texture appearance	Solubility in water (g/100ml)	Color appearance	Color values		
					L*	a*	b*
Extract	-		0.025		12.99	0.15	-1.91
BCD-E1	43.18		2.12		1.42	6.47	2.76
BCD-E2	49.01		2.49		0.98	0.67	0.17
BCD-E3	45.25		2.06		1.97	4.03	1.67

The percentage yield, the solubility and the color appearance of the extract and colorant complexes are shown in Table 1. The complexation the extract with BCD by the three methods changed the texture appearance from a sticky flake form of the extract to a powder form of the colorant complexes, which had the same shade as pink color. The percentage yields of the colorants prepared from the three methods were more than 40%, which Freeze-drying method (BCD-E2) gave the highest yield. For the water solubility of the colorant complexes, the obtained three colorants had the solubility values approximately 100 times higher than the extract (0.025g/100ml), which the solubility of BCD-E2 was the highest. After dissolving the three colorants in water at the maximum solubility, the same reddish-orange shade of the three colorant solutions was observed, but the color intensity was slightly different that BCD-E2 had the highest intensity. This observation agrees with the lowest L* value of BCD-E2 that imply the darkest color compared with the other colorants. These results suggest that the preparing method affects the color appearance of the colorant complexes.

The Colorant complexes characterization by UV-Vis spectrophotometer and FTIR

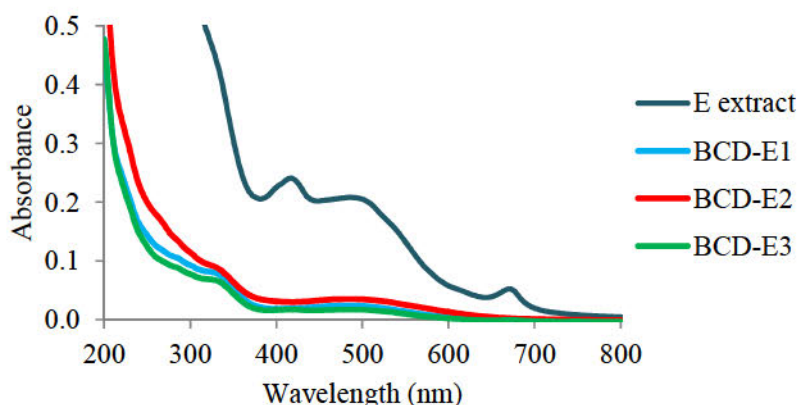


Figure 1. The absorption spectra of the extract and the colorants complexes

The absorption spectra of the extract and the three colorants after dissolving in water at concentration of 0.025g/100ml are shown in Figure 1. The lambda max of the extract appeared

three positions at 417, 485 and 672 nm. Meanwhile, the three colorants showed one lambda max, which was slightly blue-shifted to 481 nm (BCD-E1), 478 nm (BCD-E2) and 481 nm (BCD-E3). This observation maybe explained by partial shielding of the excitable electrons and chromophores in the BCD cavity and therefore is rationalized as being indicative of complex formation [7]. The absorbance value of the three colorants was about 7 times lower than the extract because the limited amount of the extract was entered into the BCD cavity of the three colorants.

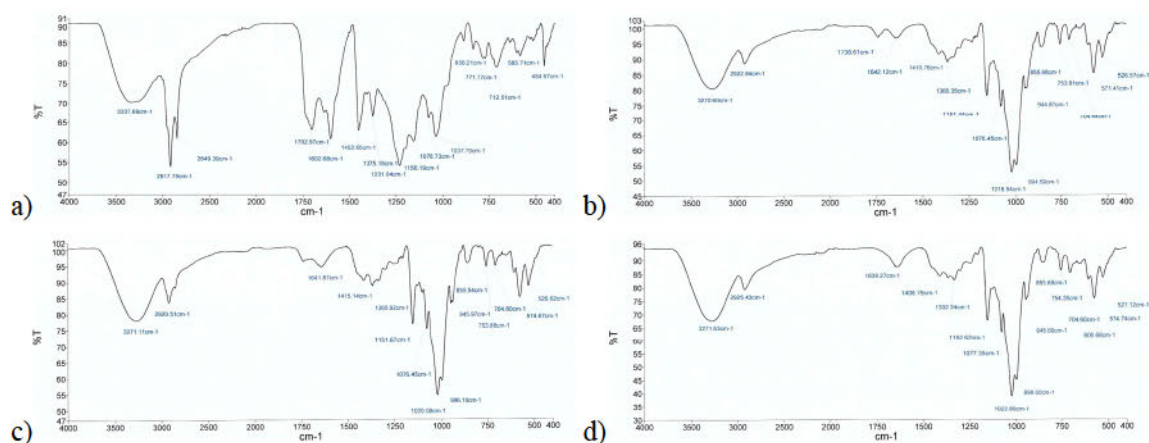


Figure 2. FT-IR spectra of (a) extract, (b) BCD, (c) simple mixture of BCD and (d) BCD-E2

FT-IR spectra of the extract and the three colorants are presented in Figure 2. There were peaks in the most significant carbonyl region ($1800\text{--}1650\text{ cm}^{-1}$) in the extract spectrum (Figure 2a) and weak peak in the carbonyl region in the BCD spectrum (Figure 2b). The spectrum of the simple mixture of BCD and extract (Figure 2c) exhibited peaks that corresponded to the components that were present in both of the spectrum of the BCD and the extract. Meanwhile, the spectrum of the BCD-E2 (Figure 2d) exhibited the most peaks conform to the BCD spectrum and a few peaks of the extract were visible. Moreover, the peak at 1700 cm^{-1} , which refers to the C=O stretching of the carbonyl group, was absent in the BCD-E2 spectrum, but showed in the simple mixture spectrum. This observation may be the compound interactions that partly due to the entry of a carbonyl group of compounds of the extract into the BCD cavity. The FT-IR spectra of BCD-E1 and BCD-E3 also shown the spectra as same as the spectra of BCD-E2 (data not shown).

Light stability of the colorant complexes

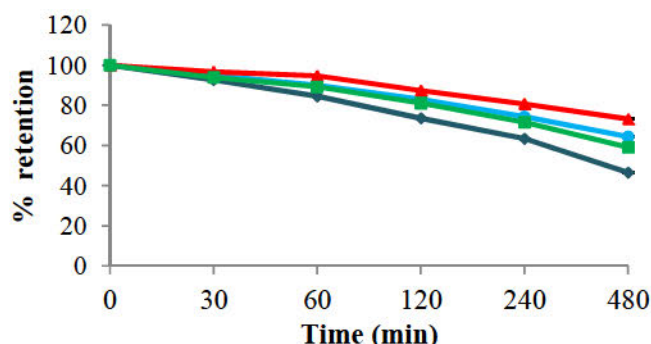


Figure 3. The colorant retention of the extract (◆), BCD-EB1 (●), BCD-EB2 (▲) and BCD-EB3 (■) after UVB exposure for various exposure times

The absorbance values at wavelength of 485 nm of the samples were calculated for the percent retention after UVB light exposure (Figure 3). The percent retentions of the extract and the three colorants were decreased as increasing UVB exposure time, but the percent retentions of three colorants were higher than the extract which obviously detected after 120 min exposure. Moreover, BCD-E2 exhibited the highest light stable compared with the other colorants. These results corroborate with the improvement of sunlight stability of curcumin by complex with BCD [8]. Therefore, the results indicated that BCD complexes protect the teak leaf extract from photodegradation and enhance its stability.

CONCLUSION

This study demonstrated that BCD can improve the water solubility and the light stability of teak leaf extract for application as a natural colorant. Some color compounds of the extract was kept into BCD cavity and may interact with BCD. In addition, BCD-E2 prepared by Freeze-drying method exhibited the best method for complexation in this work.

ACKNOWLEDGEMENT

This research was financially supported by Faculty of Pharmaceutical sciences, Naresuan University and The Center of Excellence for Innovation in Chemistry (PERCH-CIC), Thailand.

REFERENCES

1. Bocca B, Pino A, Alimonti A, Forte G. (2014). Toxic metals contained in cosmetics: A status report. *Regulatory Toxicology And Pharmacology*, 68(3), 447-467. doi:10.1016/j.yrtph.2014.02.003
2. Prusty AK, Das T, Nayak A and Das NB. (2010). Colourimetric analysis and antimicrobial study of natural dyes and dyed silk. *Journal of Cleaner Production*, 18, 1750-1756. doi:10.1016/j.jclepro.2010.06.020
3. Naira N, Karvekar MD. (2010). Isolation of phenolic compounds from the methanolic extract of *Tectona grandis*. *Research Journal of Pharmaceutical, Biological and Chemical Sciences*, 1(2), 221-225.
4. Szente L, Szejtli J. (2004). Cyclodextrins as food ingredients. *Trends in Food Science and Technology*, 15(3-4), 137-142. doi:10.1016/j.tifs.2003.09.019
5. Zoppi A, Quevedo MA, Delrivo A, Longhi MR. (2010). Complexation of sulfonamides with β -cyclodextrin studied by experimental and theoretical methods. *Journal of Pharmaceutical Sciences*, 99(7), 3166-3176. doi:10.1002/jps.22062
6. Marcolino VA, Zanin GM, Durrant LR, Benassi MDT, Matioli G. (2011). Interaction of curcumin and bixin with β -cyclodextrin: Complexation methods, stability, and applications in food. *Journal of Agricultural and Food Chemistry*, 59(7), 3348-3357. doi:10.1021/jf104223k
7. Tang B, Ma L, Wang H, Zhang G. (2002). Study on the supramolecular interaction of curcumin and β -cyclodextrin by spectrophotometry and its analytical application. *Journal of Agricultural and Food Chemistry*, 50, 1355-1361. doi:10.1021/jf0111965
8. Mangolim CS, Moriwaki C, Nogueira AC, Sato F, Baesso ML, Neto A n., et al. (2014). Curcumin- β -cyclodextrin inclusion complex: Stability, solubility, characterisation by FT-IR, FT-Raman, X-ray diffraction and photoacoustic spectroscopy, and food application. *Food Chemistry*, 153, 361-370. doi:10.1016/j.foodchem.2013.12.067

DEVELOPMENT OF PICTORIAL MEDICATION LABELS FOR CHRONIC DISEASE PATIENTS AT HEALTH PROMOTION HOSPITAL, CHAWAI

Vipusit Piankarnka^{1*}, Nuttakunlaya Piankarnka²

¹ Multimedia Technology, Faculty of Mass Communication Technology, Rajamangala University of Technology Thanyaburi, Thailand

² Clinical pharmacy, Faculty of Pharmacy, Eastern Asia University, Thailand

*Corresponding author: Natchaphak Meeusa, natchaphak.th@gmail.com

Keywords : pictorial medication label, chronic disease

ABSTRACT

This research has developed a pictorial medication labels for patients with chronic diseases at Chawai Sub-district Health Promotion Hospital. The objective to developing pictorial medication labels for providing advice on how to administer medicines in patients and evaluating understanding of drug administration orders from pictorial medication labels. Method by group discussion with community health volunteers and professional nurses in total of 8 people at Chawai Sub-district Health Promotion Hospital to design the appropriate pictorial medication labels for chronic disease patients. Assessing understanding of drug administration orders from pictorial medication labels in chronic patients at Chawai Sub-District Health Promotion Hospital in total of 30 people by using 5 pictorial medication labels. The results of the evaluation of the understanding of pictorial medication labels developed for patients with chronic diseases receiving services at Chawai Sub-District Health Promotion Hospital. It was found that 91.83% of the patients understood the pictorial medication labels. When considering the understanding of the number of tablets, number of times to take medicine, taking medication before or after meals and when taking the medicine, it was found that 100.00% of the patients had the most understanding of the amount of drug intake. The lowest perception of oral medication before or after meals was 86.67%.

INTRODUCTION

According to the 2007 survey of the elderly population in Thailand of the National Statistical Office, most of the elderly have health problems due to chronic illness, with chronic health problems such as high blood pressure 31.7 percent, Diabetes 13.3 percent and Heart disease 7.0 percent etc. [1] Which the characteristics of the elderly are often visually limited, resulting in unclear readings or inability to read books.. Pictorial labeling is one way to increase patient understanding of drug use [2]. The currently used picture drug label was developed by United State Pharmacopoeia- Dispensing Information (USP-DI) [3] may have restrictions on use in Thai people because it is inconsistent and does not reflect the Thai society and culture.

OBJECTIVES

- 1) To develop pictorial medication labels for use in information media, to advise drug administration methods for patients with chronic disease.
- 2) To assess understanding of drug administration orders from pictorial medication labels.

METHODS

This study is a research and development to develop pictorial medication labels for chronic disease patients at Chawai Sub-district Health Promotion Hospital and assess understanding of drug administration orders from pictorial medication labels. The method of research is divided into 2 steps.

1) The process of designing pictorial medication labels by creating focus group 2 times, consisting of community health volunteers and professional nurses in total of 8 people at Chawai Sub-district Health Promotion Hospital

2) The process of assessing understanding of drug administration orders from pictorial medication labels in chronic patients at Chawai Sub-District Health Promotion Hospital in total of 30 people by using 5 pictorial medication labels. Data were collected by interviewing patients directly from the interview form. The interview form is divided into 2 parts which are general information and the part of evaluating the understanding of pictorial medication labels. In which the quality of the instruments has been examined, questionnaires for understanding of drug usage orders on pictorial medication labels by testing the content validity by 3 experts.

Data collection procedures are The researcher selected a sample of patients who would join the study. By random sampling by accidental sampling, using 30 subjects. Selection of those who meet the criteria set is Chronic disease patients treated at Chawai Sub-district Health Promotion Hospital. Analyze and process data by Microsoft office excel (Mean, Percentage).

RESULTS

The results of the group discussion for the 1st development of pictorial medication labels.

Researcher began a conversation with all 8 participants about the pictorial medication labels with the original drug label to allow the group to discuss all appropriate forms, amount 6 images. Group suggestions as follows.

Picture for take medicine in the morning : Them would like to change the house to a mosque instead because the Cha Wai community most of them are Muslim, with 95% of the prayers being performed 5 times a day and would like to add more color to the part of the grass, the image of the crow is good, can be said to be breakfast.

Picture for take medicine in the lunch : Please add an accurate time clock image to the image. and most people like to watch time and the sun image in the middle shows the time accurately.

Picture for take medicine in the dinner : The picture of a bird flying back to the nest can convey the good evening.

Picture for take medicine before bed time : Them would like to change the image of a person wearing a hair cape (Headscarf) because Cha Wai community most Muslims are 95%, add color to represent darkness and the crescent image shows the night well.

Picture for take medicine before meal : Beautiful images can convey good medication before meals and In the picture, food is chicken, not pork, considered suitable for the Islamic community.

Picture for take medicine after meal : Beautiful images can reflect the medication taken after meals.

Tablet image : Request images of tablets in oval form instead of round tablets.

The results of group discussion for the 2nd development of pictorial medication labels.

Picture for take medicine in the dinner : Time is adjusted to 6:00 pm instead of 5:00 pm because the dinner time is probably more than 6:00 pm

Other : Please adjust the tablets to only 2 tablets per meal due to the number of tablets too much and prescribing medication of patients at the hospital, most not more than 2 tablets per time. Add the name-surname, drug name, strength, and telephone number of Cha-wai Sub-District Health Promotion Hospital on the drug label. By name-surname, drug name, potency placed on the top of the drug label picture and phone number placed.

Table 1 : The development of pictorial medication labels from group discussion

	Original pictorial medication labels	1st pictorial medication labels design	2nd pictorial medication labels design
Picture for take medicine in the morning			
Picture for take medicine in the lunch			
Picture for take medicine in the evening			
Picture for take medicine before bedtime			
Picture for take medicine before meal			
Picture for take medicine after meal			
Other			

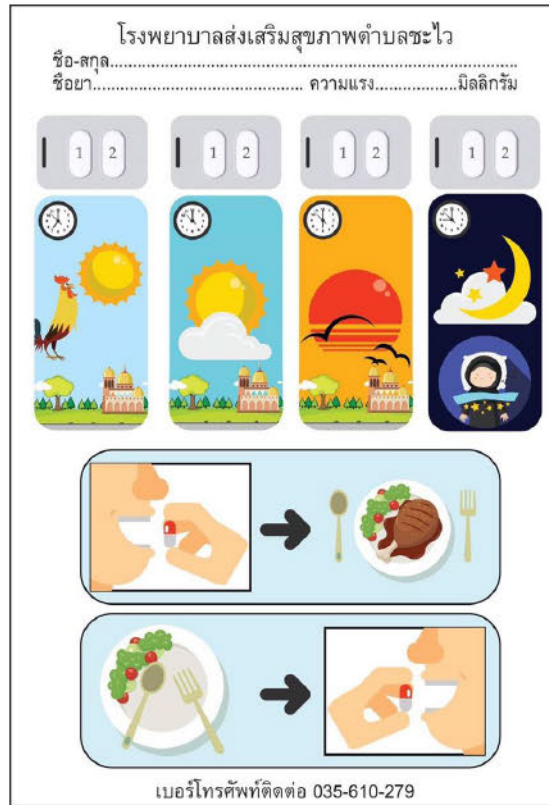


Figure 1 : Pictorial medication labels for patients with chronic disease at Cha Wai Health Promotion Hospital.

Demographic data of patients with chronic diseases that have been evaluated for understanding the pictorial medication labels.

The results showed that the patients who have been evaluated for understanding the pictorial medication labels were 15 males and 15 females and most of them aged 60 yearold up, as in Table 2.

Table 2 : Demographic data of patients (N=30)

Demographic data	Number (Percent)
Gender	
male	15 (50.00)
female	15 (50.00)
Age	
20-30 years	1 (3.33)
30-40 years	3 (10.00)
40-50 years	7 (23.33)
50-60 years	9 (30.00)
60 yearold up	10 (33.33)

Understanding of the pictorial medication labels for patients with chronic diseases receiving services at the health promotion hospital of Cha Wai Subdistrict.

From the evaluation of understanding image drug labels developed for chronic disease patients who receive services at the Health Promoting Hospital, Cha Wai Subdistrict, found that 30 patients understand the picture drug labels, accounting for 91.83 percent. When considering the understanding of the number of tablets, number of medication doses, taking medication before or after a meal, and when taking medication found that the understanding of the most number of medication doses accounted for 100.00 percent. Regarding medication intake before or after food, the lowest percentage was 86.67%, as in Table 3.

Table 3 : Percentage of correctly understanding of pictorial medication labels

Understanding of	The percentage of understanding correctly per pictorial medication labels (1-5)					Mean
	1	2	3	4	5	
1. Number of tablets	50.00	93.33	93.33	100.00	100.00	87.33
2. Number of medication doses	100.00	100.00	100.00	100.00	100.00	100.0
3. Taking medication before or after a meal	90.00	100.00	76.67	80.00	86.67	86.67
4. When taking medicine	96.67	86.67	93.33	93.33	96.67	93.33
Total mean						91.83

CONCLUSIONS

From the evaluation of understanding pictorial medication labels developed for chronic disease patients who receive services at the Health Promoting Hospital, Cha Wai Subdistrict, found that 30 patients understand the pictorial medication labels, accounting for 91.83 percent. When considering the understanding of the number of tablets, number of medication doses, taking medication before or after a meal and when taking medication found that the understanding of the most number of medication doses accounted for 100.00. Regarding medication intake before or after meals, the lowest percentage was 86.67%.

DISCUSSIONS

The results of this study confirm the findings from both domestic and international research that pictorial medication labels created from the perspective of illiterate target groups are consistent with the culture, thinking methods and way of life of the target audience. Resulting in an pictorial medication labels that has the power to communicate well the study by Wiraphon Phimaman and others (2014) found that the pictorial medication labels may be another option to increase the effectiveness of medication use of the elderly with chronic diseases. [4] As well as the research by Withni Ketpook and others (2015) Found that the pictorial medication labels may be useful in helping to communicate well for patients with language problems when used in conjunction with verbal descriptions, gestures, or real drug samples and useful in helping to remind the patient to remember when seeing the picture again. [5]

SUGGESTION

- 1) The development of pictorial medication labels in other forms, such as the development of auxiliary labels in the list of health promotion hospitals in Cha Wai Sub-district so that patients can receive more information about drugs or the development of drug labels, pictures of special effects drugs available at Cha Wai Health Promoting Hospital.
- 2) May use the pictorial medication labels with other media such as tablets that the patient actually received that day with explanations to help enhance understanding.

ACKNOWLEDGEMENT

This research was successful due to the cooperation from many parties. This is supported by Personnel at Cha Wai Health Promoting Hospital , Department of information technology, Rajamangala University of Technology Thanyaburi and Faculty of pharmacy, Eastern Asia University.

REFERENCES

1. Ministry of Social Development and Human Security. (2010). Situation of Thai elderly 2004. Retrieved April 20, 2018. from http://www.m-society.go.th/document/edoc/edoc_893.pdf.
2. Dowse, R. and Ehlers, M.S. (2001). The evaluation of pharmaceutical pictograms in a lowliterate South African population. *Patient Educ Couns*, 45, 87-99.
3. United States Pharmacopoeia Convention. (2011). USP Pictograms. Retrieved Jan 6, 2014, from <http://www.usp.org/usp-healthcare-professionals/related-topics/resources/usp-pictograms/download-pictograms>.
4. Wiraphon Phimalan, Phattharaphon Phianana, Rawi Rangsungnoen, Likit Ritthiya, and Wipada Phattharaditpitak. (2014). Development and evaluation of drug label systems for chronic disease patients. *The Isan Pharmacy Journal*, 9, 109-115. (IN THAI)
5. Withthi Ketpook, Panyaporn Songsoontornwongsasithamamai, Supanan Pungcharoenkit Kunkanok Kotchabatnamphet and Attaya Phongsanguansa. (2015). Development of pictorial medication labels for foreign patients in nopparat rajathanee hospital. *Nida Journal of Language and Communication*. 20, 1-23. (IN THAI)

EFFECTS OF FINISHING AND POLISHING PROCEDURES ON SURFACE ROUGHNESS AND GLOSS OF FLOWABLE RESIN COMPOSITES CONTAINING S-PRG FILLER

Sayaka Kitahara¹, Masato Hotta^{2*}, Taiho Idono¹, Kazuki Oike¹, Shusuke Kusakabe¹, and Toru Nikaido¹

¹ Department of Operative Dentistry, Division of Oral Functional Science and Rehabilitation, Asahi University, School of Dentistry, Japan

² Asahi University, Japan

*Corresponding author: Masato Hotta, w7mhotta@dent.asahi-u.ac.jp

Keywords: Dental esthetics, Polishing, Surface gloss, Flowable resin composite, S-PRG filler

ABSTRACT

Objective: Flowable resin composites are widely used on both anterior and posterior teeth in dental clinical work. The longevity and esthetics of tooth-colored dental restorative material greatly depend on the quality of the finishing and polishing techniques employed. High-quality finishing and polishing improve both the esthetics and longevity of flowable resin composite restorations. In addition, flowable resin composites containing S-PRG filler have superior operability, and an anti-plaque action mediated by the multi-ion release from S-PRG fillers has been reported. The purpose of the present study was to evaluate the effect of finishing and polishing procedures on the surface roughness and gloss of S-PRG filler contained flowable resin composites. **Materials and Methods:** F00 and F03 types of previous BEAUTIFIL Flow Plus (BFP, A3, SHOFU) and BEAUTIFIL Flow Plus X containing nano and submicron S-PRG fillers (BFPX, A3, SHOFU) were used. These resin composites were placed in a Teflon mold with a 10-mm inner diameter and 3-mm height, compressed by using a glass plate and plastic strips, and light cured with a curing light (Pencure, MORITA) for 1 minute. The samples were then immersed in distilled water at 37°C for 24 hours and polished (SP) with SiC papers (#600, #800, #1,000, #1,200), followed by additional polishing (CG) using CompoMaster (SHOFU) and a PRG CompoGloss Kit (SHOFU) in this order. Resin composite samples covered with only plastic strips were designated as the control (MS), and those polished with SiC papers (#600, #800, #1,000, #1,200, #2,000, #4,000, #8,000, and #10,000) were designated as the mirror polishing ones (SSP). Four samples were prepared for each group, and surface gloss and roughness were measured. Surface gloss was measured by using a glossmeter (VG-7000, Nippon Denshoku Industries); and surface roughness, with a nano-scale hybrid microscope (VN-8010, KEYENCE) 3 times for each sample. Significances of difference in the values were analyzed by using two-way analysis of variance (ANOVA, $p < 0.05$) and Fisher's PLSD test. **Results:** The lowest surface roughness (Ra values) was found in the Group MS. Significant differences were observed between the Group MS and the other Groups. Group SP provided significantly the highest Ra values and a less glossy surface than the other polished surface Groups. However, no significant differences were found between Group MS and Group CG for surface gloss. The order of finishing and polishing procedures, ranked from the lowest to the highest surface roughness was as follows: MS < SSP < CG < SP (BFP-F00, BFP-F03, BFPX-F00, BFPX-F03). The order of finishing and polishing procedures, ranked from the highest to the lowest surface gloss was the following: MS, CG, SSP > SP (BFP-F00), MS, CG > SSP > SP (BFP-F03, BFPX-F00, BFPX-F03) **Conclusions:** The results of the present study showed that the surface characteristics (roughness and gloss) following finishing and polishing with different procedures

were S-PRG filler particle size dependent. In addition, the final buffing with PRG CompoGloss produced a superior gloss of the surface of flowable resin composites containing a S-PRG filler.

INTRODUCTION

Flowable resin composites are widely used on both anterior and posterior teeth in dental clinical work. The longevity and esthetics of tooth-colored dental restorative material greatly depend on the quality of the finishing and polishing techniques employed[1-5]. High-quality finishing and polishing improve both the esthetics and longevity of flowable resin composite restorations. The purpose of this study was to evaluate the effect of finishing and polishing procedures on the surface roughness and gloss of S-PRG filler-contained flowable resin composites. The null hypothesis tested was that different finishing and polishing procedures would not affect the surface roughness and gloss of these composites.

MATERIALS AND METHODS

Four S-PRG filler-contained flowable resin composites were used in this study (Table 1) ; Beautifil Flow Plus and Beautifil Flow Plus X (F00 and F03, Shade-A3, Shofu, Kyoto). A Teflon mold with internal dimensions of 10-mm diameter and 3-mm height was used to prepare 64 specimen disks. Each mold with a flowable resin composite was covered with a Mylar strip, pressed flat with a glass slide, and light-cured with a curing light (Pencure, Morita, Kyoto) for 60 s at room temperature (23 ± 2 °C). All test materials were handled according to their manufacturer's instructions. The cured samples were then stored in distilled water at 37°C for 24 h. Four specimens of each flowable resin composite were randomly assigned to 1 of the 4 finishing and polishing procedure groups as follows:

Group MS (control group): The specimen surface was covered with a Mylar strip (no finishing and polishing procedures were applied.), Group SP: The specimens were finished and polished with a final polishing with #1,200 SiC-paper, Group SSP: The specimens were finished and polished with a final polishing with #10,000 SiC-paper. Group CG: The specimens were finished and polished with a final polishing using #1,200 SiC-paper, and then they were given a final buffing with PRG CompoGloss (Shofu).

Table 1. Materials and their compositions

Material	Code	Main composition	Manufacturer
Beautifil Flow Plus F00	BFP(F00)	Bis-GMA, TEGDMA, S-PRG filler	SHOFU
Beautifil Flow Plus F03	BFP(F03)	Bis-GMA, TEGDMA, S-PRG filler	SHOFU
Beautifil Flow Plus X F00	BFPX(F00)	Bis-GMA, Bis-MPEPP, TEGDMA, Nano S- PRG filler	SHOFU
Beautifil Flow Plus X F03	BFPX(F03)	Bis-GMA, Bis-MPEPP, TEGDMA, Nano S- PRG filler	SHOFU

The finishing and polishing procedures were carried out by the same operator. After all the specimens had been polished, they were rinsed thoroughly with distilled water and allowed to dry for 24 h before measuring the average surface roughness (Ra) and gloss (%). A nanoscal hybrid microscope (VN-8010, Keyence, Osaka) was used for assessing surface roughness (Ra); and another nanoscal hybrid microscope (atomic force microscope), for image observations. The surface roughness measurements were reported as the arithmetic mean of 5 readings. The surface gloss of the specimens was measured with a gloss meter (VG-7000, Nippon Denshoku Industries, Tokyo).

STATISTICAL ANALYSIS

Two-way analysis of variance (ANOVA) was used to evaluate the data from surface roughness and gloss measurements. Then the means of the different groups were compared by using Fisher's PLSD multiple comparison test ($\alpha=0.05$).

RESULTS

The average surface roughness and gloss of the specimens subjected to the finishing and polishing procedures are shown in Table 2. Nanoscale hybrid microscope images of the S-PRG filler-contained flowable resin composites after surface finishing and polishing procedures had been performed are shown in Figure 1.

Table 2. Surface roughness and gloss (mean (SD)) of S-PRG filler-contained flowable resin composites affected by each polishing procedure

Material (Code)	Finishing and polishing (Group)	Surface roughness (Ra: nm)	Surface gloss (%)
BFP(F00)	MS	5.0(1.2)h	80.4(5.9)b,c,d
	SP	93.0(1.4)a	15.9(1.4)g
	SSP	22.8(6.6)f	73.9(6.5)d
	CG	78.6(6.0)b	78.0(4.2)d
BFP(F03)	MS	5.3(0.8)h	80.4(4.7)b,c,d
	SP	93.8(2.6)a	13.9(4.3)g
	SSP	24.4(4.6)f	63.3(3.3)e
	CG	77.1(3.2)b	78.3(4.5)c,d
BFPX(F00)	MS	4.0(1.0)h	91.0(3.6)a
	SP	57.5(6.2)d	21.2(4.3)f,g
	SSP	23.1(4.4)g	77.5(3.3)d
	CG	40.7(11.8)e	85.2(4.5)a,b,c
BFPX(F03)	MS	3.9(0.4)h	87.8(4.7)a
	SP	66.9(5.9)c	23.5(0.7)f
	SSP	20.1(4.6)f,g	79.7(1.0)c,d
	CG	47.3(1.1)e	87.5(3.7)a,b

For each flowable resin composite in the finishing and polishing groups, different letters represent statistically significant differences among different flowable resin composites in the different finishing and polishing groups ($P<0.05$).

According to the two-way ANOVA results, there were significant differences in surface roughness and gloss. The lowest Ra values were found in Group MS (the control specimens). Significant differences were observed between the Group MS and the other Groups. Group SP showed significantly the highest Ra values and less glossy surface than the other polished surfaces. However, no significant differences were found between Group MS and Group CG for surface gloss. The order of finishing and polishing procedures, ranked from lowest to highest for surface roughness was the following:

MS<SSP<CG<SP (BFP-F00, BFP-F03, BFPX-F00, BFPX-F03)

The order of finishing and polishing procedures, ranked from highest to lowest for surface gloss was as follows:

MS, CG, SSP>SP (BFP-F00), MS, CG>SSP>SP (BFP-F03, BFPX-F00, BFPX-F03)

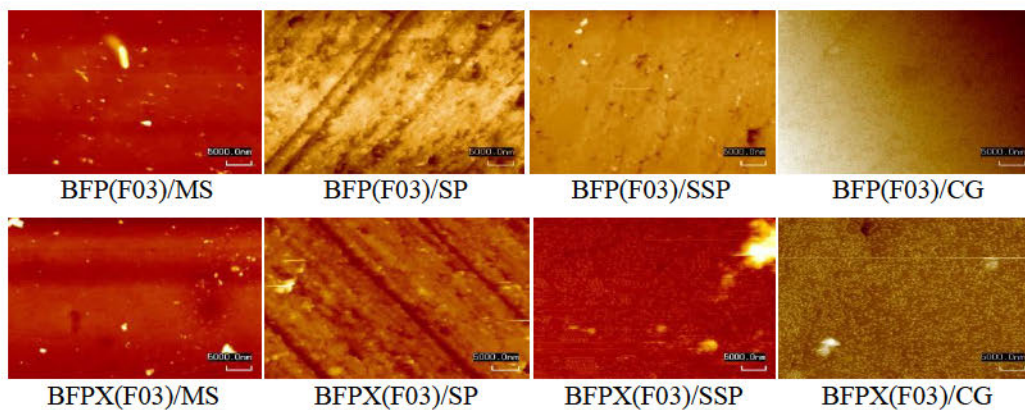


Figure 1. Nanoscale hybrid microscope images of the S-PRG filler-contained flowable resin composites (typical examples) after surface finishing and polishing procedures.

DISCUSSION

Previous studies have shown that resin composites with smaller particle sizes have lower surface roughness and higher surface gloss after polishing with several polishing systems[6,7]. However, nano-hybrid resin composites show higher roughness levels than the nanofill resin composites, due to the disruption of the filler matrix interface as a result of the loss of prepolymerized fillers[8]. Moreover, glass particles in resin composites cause high porosity and more discoloration[9].

In this study, the larger the filler particle size, the greater was the resulting Ra value and the lower was the resulting surface gloss. The finishing and polishing procedures resulted in the exposure of the filler particles. These results clearly demonstrated that a distinctive relation existed between the filler particle size of S-PRG filler-contained flowable resin composites and their surface roughness. The resulting surface gloss was influenced by filler particle size, which is critical to light dispersion. The S-PRG filler has larger particles to scatter light.

The smoothest surfaces were obtained for specimens under the Mylar strip; however, in most clinical cases, the finishing step of a restoration is necessary to remove excess resin composites and for contouring. In addition, the polymerized surface against the Mylar strip is rich in resin matrix and less resistant to abrasion[10]. After the finishing and polishing procedures applied to the group CG, the surface roughness values were not similar to those of the Group MS, but the surface gloss values were similar to them. In most studies, the lowest surface roughness values after the finishing procedures were obtained with flexible aluminum oxide discs[11-13]. Moreover, the time

used for polishing procedures might have influenced the surface roughness as well as the grain size and type of abrasives in the polishing systems[3]. The main composition of PRG CompoGloss paste is aluminum oxide, diamond, glycerin, and S-PRG filler.

CONCLUSIONS

The results of the present study showed that the surface characteristics (roughness and gloss) following finishing and polishing with different procedures were dependent on the S-PRG filler particle size. In addition, the final buffing with PRG CompoGloss produced a superior gloss of the surface of flowable resin composites containing S-PRG filler.

REFERENCES

1. Reis AF, Giannini M, Lovadino JR, Ambrosano GM. (2003). Effects of various finishing systems on the surface roughness and staining susceptibility of packable composite resins. *Dental Materials*, 19,12-18.
2. Türkün LS, Türkün M. (2004). The effect of one-step polishing system on the surface roughness of three esthetic resin composite materials. *Operative Dentistry*, 29, 203-211.
3. Gönülol N, Yilmaz. (2012). The effects of finishing and polishing techniques on surface roughness and color stability of nanocomposite. *Journal of Dentistry*, 40s, e64-e70.
4. Yoshida N, Gen T, Hotta M. (2017). Influence of final polishing of composite resin on surface property and color. *Journal of Japan Academy of Color for Dentistry*, 23, 4-17.
5. Hotta M, Kasahara Y, Aono M, Nakashima Y. (1997). Colorimetrics evaluation of light-cured composite resin – influence of finishing and polishing on various light-cured composite resins -. *Journal of Japan Academy of Color for Dentistry*, 4, 20-23.
6. Da Costa J, Adams-Belusko A, Riley K, Ferracane JL. (2010). The effect of various dentifrices on surface roughness and gloss of resin composites. *Journal of Dentistry*, 38s, 123-128.
7. Turssi CP, Saad JR, Duarte Jr SL, Rodrigues Jr AL. (2000). Composite surfaces after finishing and polishing techniques. *American Journal of Dentistry*, 13, 136-138.
8. Antonson SA, Yazici AR, Kilinc E, Antonson DE, Hardigan PC. (2011). Comparison of different finishing/polishing systems on surface roughness and gloss of resin composites. *Journal of Dentistry*, 39s, 9-17.
9. Iazzetti G, Burgess JO, Gardiner D, Ripps A. (2000). Color stability of fluoride-containing restorative materials. *Operative Dentistry*, 25, 520-525.
10. Asaka Y, Miyazaki M, Kurokawa H, Takamizawa T, Moore BK. (2006). Effect of low O₂-gas transmission rate barrier films on knoop hardness and toothbrush abrasion of resin cements. *American Journal of Dentistry*, 19, 222-226.
11. Paravina RD, Roeder L, Lu H, Vogel K, Powers JM. (2004). Effect of finishing and polishing procedures on surface roughness, gloss and color of resin-based composites. *American Journal of Dentistry*, 17, 262-266.
12. Gedik R, Hüzmüzlü F, Coskun A, Bektas D, Özdemir AK. (2005). Surface roughness of new microhybrid resin-based composites. *The Journal of the American Dental Association*, 136, 1106-1112.
13. Venturini D, Cenci MS, Demarco FF, Camacho GB, Powers JM. (2006). Effect of polishing technique and time on surface roughness, hardness and microleakage of resin composite restorations. *Operative Dentistry*, 31, 11-17.

AN ASPECT OF WARTIME JAPANESE COLOR SCIENCE: ON SHOJI SATO'S CORRECTIVE PRACTICE METHOD FOR COLORBLINDNESS

Yasuhito Baba ^{1*}

¹*Research Institute for Letters, Arts and Sciences, Waseda University, Japan.*

*Corresponding author: Yasuhito Baba, y-baba@ruri.waseda.jp

Keywords: colorblindness, discipline, Panopticon, Foucault

ABSTRACT

The purpose of this paper is to clarify the framework of the “corrective practice method,” devised by Shoji Sato for colorblindness in late Imperial Japan, through the examination of texts by his supports: Keiji Suzuki, Tadao Kondo, Zentaro Shibata, and so forth. (Contemporary medical science has since discredited this ‘method’).

Sato’s ‘method’ followed in the tradition of many other methods for correcting colorblindness using glasses and filters, as well as treatments involving chemicals. The main feature of Sato’s method was the synthesis of these preexisting methods in a unique way: it is characterized by having subjects wear colored glasses and training them to look at the pseudoisochromatic plates through the glasses. He combined the colored glasses, which had been used exclusively for “correction” before, and the pseudoisochromatic plates, which had been used for “screening.”

Although this method at first glance to be novel, Sato’s conception of this method itself was in line with an old form of power that had been handed down since the 18th century. In other words, it is a form of power called “discipline” that has become well-known through Michel Foucault’s *Discipline and Punish*. In this paper, I examine the structure of Sato’s corrective practice method in five points using Foucauldian analysis: 1. Individualization of subjects, 2. Deprivation of words from subjects, 3. Elimination of symbols and names indicating colors, 4. Confinement of subjects within the space created by the pseudoisochromatic plates, 5. Periodical tests and evaluations. Through the above analysis, I will try to show that the “corrective practice method” has continuity with the technique for creating subjects as docile bodies in modern Europe.

INTRODUCTION

While it was John Dalton who conducted the first academic study on colorblindness, his contemporary, Scottish philosopher Dugald Stewart considered color misrecognition as a defect in the “power of conception” [1]. He postulated that color misrecognition could be corrected by teaching children about color terminology and names at home and in school. In reality, however, colorblindness is related to physiological functions of the human body, so even if a child did learn the names of colors, color misrecognition would not disappear [2].

With the publication of Goethe’s *Theory of Colours* in 1810, the paradigm of optical science shifted from physical optics to physiological optics, and the focus of research on colorblindness and color vision also shifted from “concept” and “spirit” to “body” and “physiology” [3]. Along with these changes, as technologies such as steam engines and railways developed rapidly, the importance of color recognition of traffic signals increased, and colorblindness came to be regarded as a “danger” that could cause major accidents [2].

When the Lagerlunda rail accident occurred in Sweden in 1875, Swedish physiologist Frithiof Holmgren argued that the accident was caused by the misidentification of a signal by a color-blind

railroad worker [4]. This assertion led to the institutionalization of color vision testing for public transport workers in various countries. In 1877, German ophthalmologist Jakob Stilling devised the pseudoisochromatic plate (PIP) (Figure 1. Stilling's pseudoisochromatic plate) for screening color-blind people, and in 1916, Japanese military doctor Shinobu Ishihara further improved to develop the Ishihara pseudoisochromatic plate (Figure 2. Ishihara's pseudoisochromatic plate) that still remains in general use for screening in Japan.

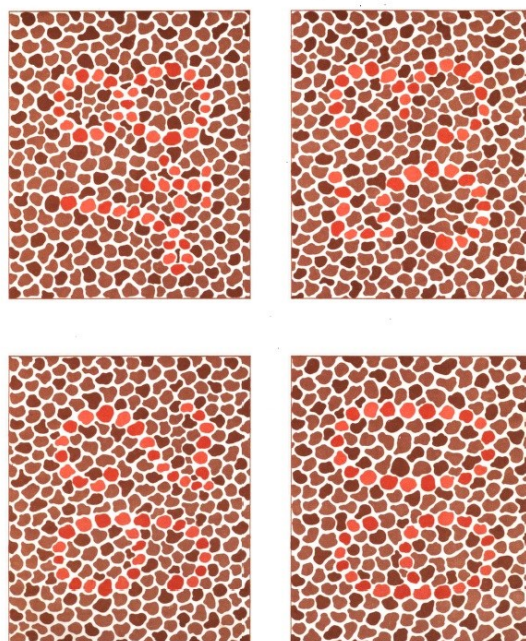


Figure 1. Stilling's pseudoisochromatic plate

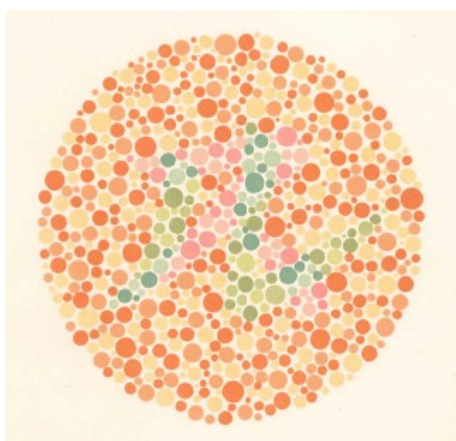


Figure 2. Ishihara's pseudoisochromatic plate

At the beginning of the 20th century, as color vision testing systems became widespread and regulations were tightened in several countries including Japan, there was an increasing demand for the development of ways to “cure” color-blind people who had been excluded from some aspects of social and economic life [5].

Indeed, since the earliest days of research on colorblindness, many methods have been devised to “cure” the condition, for example, injecting extracts of cobra venom or marigold, warming the

eyeballs, and administering electric shocks, most of which were, at best, questionable. One of these methods focused on the correction by language or names of colors. Among such early attempts, August Seebeck first used the “color filter” in 1837. He succeeded in getting color-blind people to discriminate red from green through a red and green filter. James Clerk Maxwell followed this method and made them wear glasses with red and green lenses to distinguish colors in 1855. These methods were passed on to later researchers [7]. Altogether, “corrections” using glass and filters have existed since the first half of the 19th century.

According to Ryo Seki, Shoji Sato announced the “corrective practice method” in 1935 [8]. The most notable feature of this being a combination of colored glass illustrating the influence of Seebeck and the PIP used primarily for screening color-blind people.

Furthermore, I would like to examine this “method,” describing its framework and analyzing it from the perspective of Michel Foucault’s concept of “discipline.”

THE FRAMEWORK OF SATO’S CORRECTIVE PRACTICE METHOD

Before analyzing Sato’s methods, it is important to present a simple description of his overall process of performing the corrective practice. First, before the practice, the color-blind subjects are examined using a PIP or anomaloscope to diagnose the degree and type of colorblindness [6]. Second, the “identification practice” is performed for the first month of the “first term,” which is used to understand whether two colors that appear to be equal to color-blind people are actually equal. When viewed through the colorless part of the glasses used for the practice, the labyrinth and its surrounding colors look the same, but when viewed through the red part, they look different and can be traced with a “tracing brush.” The “labyrinth” to be traced is indicated by a solid line, whereas a broken line is used to indicate the one often misrecognized by color-blind people (Figure 3. “Labyrinth”). Thus, the practice of tracing the labyrinth is repeated while alternating between the red and colorless parts of the glasses (“switching practice”). This is repeated until the subjects can easily and quickly trace through the colorless part.

During the first month of the “second term,” the discriminating practice is conducted using different plates from the ones used in the first term. Finally, in the “third term” of the practice, in addition to continuing the identification practice, “color recognition practice” is performed. This practice is an exercise to identify the presented color. Since the subjects are expected to understand the difference in hue via the identification practice and trace the labyrinth by the switching practice, they now try to understand how many colors there are in the plate by finding the same hue in the list placed at the top (see the upper part of Figure 4. Corrective practice plate). If, as a result of this process, they can discriminate between colors previously misidentified by the above-mentioned process, they move on to an element called the “sketch.”

Here, the symbols and names of the colors attached to the color pencils and paints used are erased or hidden in advance. First, the corrective practice plate is drawn, and in the case of drawing practice with a drawing book, if it contains color symbols or names then those are also hidden [9]. Moreover, after starting the practice, some subjects might not realize that they have misrecognized a color, even if they were wearing the glasses [6]. In that case, it is necessary for the instructor to step in. Attendance at practice, its progress, and grades are recorded in the “Color-blind Children’s List,” “Practice Attendance Book,” “Correction Diary,” “Correction Grade List,” “Personal Correction Grade Chart,” and “Colorblindness Test Chart.” In addition, close contact with parents is maintained throughout [6]. The effectiveness of the practice is evaluated by measuring the “reading speed” of the PIP and drawing a picture by the “color task” [6].

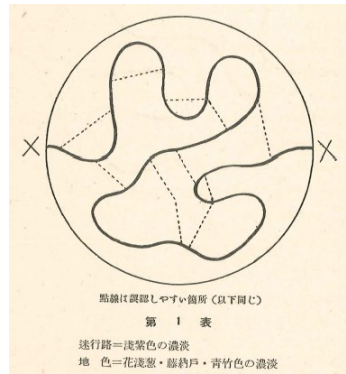


Figure 3. “Labyrinth”

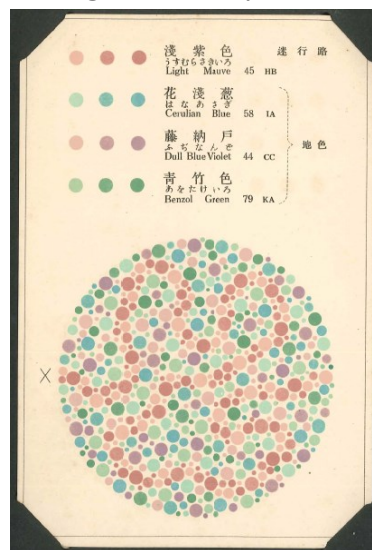


Figure 4. Corrective practice plate

DISCIPLINARY TECHNIQUE OF SATO’S CORRECTIVE PRACTICE METHOD

Strictly speaking, the above process is a “correction”, not a “treatment,” as Keiji Suzuki, who was one of the proponents of this method, admitted. In other words, this practice is repeatedly imposed on the bodies of color-blind people to discipline them in accordance with the “normal” people’s color world. This can, therefore, be compared to the disciplinary technique that Foucault described which produces “docile bodies” through “Panopticon.”

Panopticon, which is derived from the Greek word “panoptes” for “all-seeing,” is a prison designed by the British utilitarian Jeremy Bentham that Foucault deployed as a metaphor for modern society. There is a watchtower in the center of the Panopticon, and the cells are arranged in an annular form around it. Each cell has one window inside and one outside so that light can enter into the cell. Thanks to the light, the watchers in the central tower can keep track of what each prisoner is doing. On the contrary, the prisoners cannot see the inside of the watchtower, so they can be watched unilaterally without them knowing that they are being watched. Under such an imbalance of gazes, if daily training is imposed on them with sanctions as per the timetables and behavioral programs, the prisoners become conscious of being constantly watched and internalize the norm of the watcher and spontaneously subject themselves to it. Foucault calls this technique “discipline.” According to him, the system operates not only in prisons but also in major institutions that form modern society such as the military, schools, hospitals, and factories [10].

I would like to consider Sato's corrective practice method as a realization of Panopticon and analyze the process, outlined above, in a Foucauldian manner.

First, *individualization and individualizing gaze*: The subjects are separated from others as individuals, and their distance from the norm is measured and classified by identifying their unique characteristics. In addition, as the practice progresses, the results are recorded in books, and the degree of "development" and "advancement" of all the subjects can be efficiently grasped through the numerical value.

Second, *deprivation of words from subjects*: Instead of letting the subjects express their subjective processes in words when viewing the PIP, the process is translated into brush strokes by a "tracing brush." As a result, the subjects' internal thought processes are visualized and if the "brush movement" deviates from the "right" path associated with normal color vision, it can immediately be corrected by the instructor (Figure 5. A color-blind child instructed by an instructor).



Figure 5. A color-blind child instructed by an instructor

Third, *the elimination of color symbols and names*: Recognizing the color of the PIP based on color symbols and names is prohibited. The subjects are forced to practice filling the infinite gap between "color-normals" and "color-blinds" all the while being aware of the instructor's gaze who is the only person to know the true color.

Fourth, *confinement to the space created by the PIP*: The goal of the practice is to be able to read the PIP correctly. The PIP is presented as the model of the color world as it should be perceived, and at the same time, the color-blind subjects are detected and held by the same plate. In other words, after using the plate to measure the distance from the norm, the corrective practice method imposes the practice on the subjects to fill the distance through the same plates.

Subjects who have passed through these trials would become docile bodies and practice on their own without any instruction from the instructor (Figure 6. A color-blind child practicing on his own). That was considered to be the final ideal state by the advocates of the method. Thus, "after having been corrected once, all the colors they see in everyday life become objects by which their color discriminating abilities are trained constantly, and that effect will last forever" [11].

The corrective practice was also closely related to the perception of how the ideal national order should be. The proponents of the method repeatedly stressed in their writings: "It is the correction of colorblindness that is absolutely decisive for the enhancement of the national army, the development of the industry, and the individual happiness" [11]. They proposed to found a national institution to systematically implement the corrective practice method, which was only stymied by the defeat of Japan.



Figure 6. A color-blind child practicing on his own

CONCLUSIONS

The “corrective practice method” proposed by Shoji Sato in Japan in the 1930s can be regarded as one of the practices to “cure” or “correct” colorblindness that has been developed since the early days of research. This method imposes training on color-blind subjects using colored glasses and PIP. As one of the advocates of the method said, colorblindness was not “cured” by this method because this process was an example of Foucauldian “discipline.” The corrective practice method was one of the realizations of the Panopticon. Although the national institution that systematically implements the method was not realized due to the defeat of Japan, if the Panopticon structure survives, the similar practices are sure to reappear.

REFERENCES

1. Stewart, D. (1808). *Elements of the philosophy of the human mind*, The Third Edition, Corrected., Strand, London: T.Cadell & W. Davies.
2. Lanthony, P. (2013). *The history of color blindness* (C. Mailer, Trans.), Wayenborgh Publishing.
3. Crary, J. (1990). *Techniques of the observer: On vision and modernity in the nineteenth century.*, Cambridge, MA: MIT Press.
4. Holmgren, F. (1877). *De la cécité des couleurs dans ses rapport avec les chemins de fer et la marine.* Stockholm: Imprimerie Centrale.
5. Kondo, T. (1937)., Shikimou ni tsuite. *Ika Kikai Zatsugaku Zasshi*, 15(2), Nihon Iryoukiki Gakkai.
6. Shibata, Z. (1940). *Shikimou Hosei no Riron to Jissai*, Ubunkan.
7. Sharpe, L. T., & Jägle, H. (2001). I used to be color blind. *Color Research and Application*, 26(S1), S269-S272.
8. Seki, R. (1966). Shikikakuijou no Chiryou to Taisaku. *Nihon Ganka Gakkai Zasshi*, 70(11), Nihon Ganka Gakkai.
9. Sato, S. (1934). *Shikimou Hosei Rensyuhyo*, Yamakoshi Seisakujo.
10. Foucault, M. (1975). *Surveiller et punir: Naissance de la prison*. Paris: Gallimard.
11. Suzuki, K. (1937). *Shikimou Hosei Mondou*, Shikishin Hosei Rensyukai.

MEASUREMENT OF WET COLORS OF BRICKS AND GRAVELS BY USING A NON-CONTACT COLORIMETRIC SYSTEM WITH DOME ILLUMINATION

Mai Isomi^{1*}, Hideki Sakai¹, Tsugumichi Watanabe¹ and Hiroyuki Iyota²

¹ Graduate School of Human Life Science, Osaka City University, Japan.

² Graduate School of Engineering, Osaka City University, Japan.

*Corresponding author: M. Isomi, mai03isomi@gmail.com

Keywords: specular component-exclude, garden components, non-contact colorimetry

ABSTRACT

We measured the color changes of some garden components such as bricks and gravels from completely wet to completely dry. Various colored bricks and gravels are sometimes used to decorate gardens. They easily change color when they become wet. Therefore, it is helpful to know their wet colors for designing garden scenery on a rainy day. In this experiment, beige, red and brown bricks were prepared, and white, red and green gravels were prepared. We immersed them under water for 30 minutes (completely wet condition). Then, we took them from water, and measured their color changes when drying at various intervals. To measure the colors, a non-contact colorimetric system with dome illumination was used. It consists of a hemispherical dome illumination and movable light traps. The dome illumination makes it possible to obtain the unshaded images of rough surfaces of bricks and gravels. Without a light trap, however, the unshaded images are specular component-included (SCI). With a light trap in one position, a part of the image becomes specular component-excluded (SCE). When the light trap is moved to another position, another part of the image becomes SCE. Then, after moving the light traps all over the inner surface of the dome, all parts of the SCE image are obtained and can be merged into a complete SCE image.

INTRODUCTION

Various colored bricks and gravels are sometimes used to decorate gardens [1]. They easily change color when they become wet. However, it is not clear how much the color changes. It is helpful to know their wet colors for designing garden scenery in a rainy day. Therefore, we measured the change of bricks and gravels in color between a dry state that simulates sunny days and a wet state that simulates rainy days.

To measure the colors, a non-contact colorimetric system with dome illumination, which was developed by the authors for this purpose, was used [2-4]. It consists of a hemispherical diffused light irradiation and movable light traps, as shown in Figure 1.

The dome illumination makes it possible to obtain the unshaded images of rough surfaces of bricks and gravels. Without a light trap, however, the unshaded images are specular component-included (SCI). With a light trap in one position, a part of the image becomes specular component-excluded (SCE). When the light trap is moved to another position, another part of the image becomes SCE. Then, after moving the light traps all over the inner surface of the dome, all parts of the SCE image are obtained and can be merged into a complete SCE image. Since it is a non-contact method, it can measure the color of wet surfaces as they are. By using this system, we measured the color changes of bricks and gravels from completely wet to completely dry.

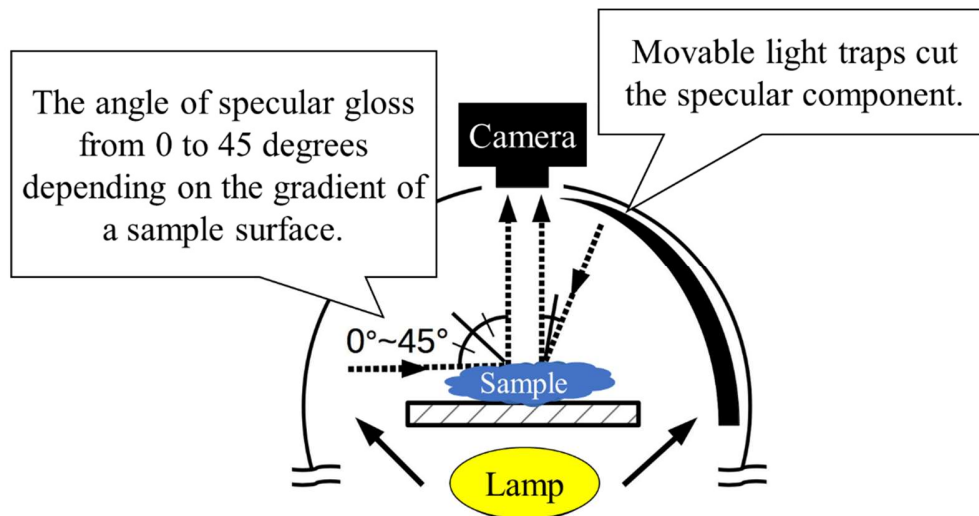


Figure 1. A non-contact colorimetric system with dome illumination

METHODS

The samples measured are beige, red, and brown block bricks and white, red, and green gravels (Figure 2). All samples are commercially available. The gravels were fixed to each other using glue when putting it in the sieve.

To measure the colors of samples, a non-contact color measurement system is used with a 300-mm-diameter dome, high-color-rendering white LED lamps ($T_{cp} = 6,200$ K, $Ra = 90$), and a digital camera Nikon D5100 (55 mm lens). The illuminance of the sample stage was set to 2,000 lx. To correct colors, the ColorGauge 24 colors (Image Science Associates, LLC) was used as the standard color chart. Samples were recorded side by side with the ColorGauge, and their recorded colors were corrected according to the designated sRGB values of the ColorGauge. Then, each pixel of color-corrected images was transformed to the $L^*a^*b^*$ value (D65/2-degree). For an accuracy verification, dry bricks were measured using a commercially available contact colorimeter (Konica Minolta spectrophotometric colorimeter CM-2600d).

In the experiment, first, after thoroughly washing with distilled water, samples were dried at 110 degrees Celsius for 60 minutes in a chamber (completely dry state). We measured their color as a completely dry state. Next, samples were immersed in distilled water for 30 minutes (completely wet state). Then, we measured the color just after pulling out of the water and at every 5 minutes up to 60 minutes, at every 10 minutes up to 90 minutes and at 120 minutes. These wetting experiments were performed in an artificial climate chamber room controlled at 23 degrees Celsius and 50 percent humidity.

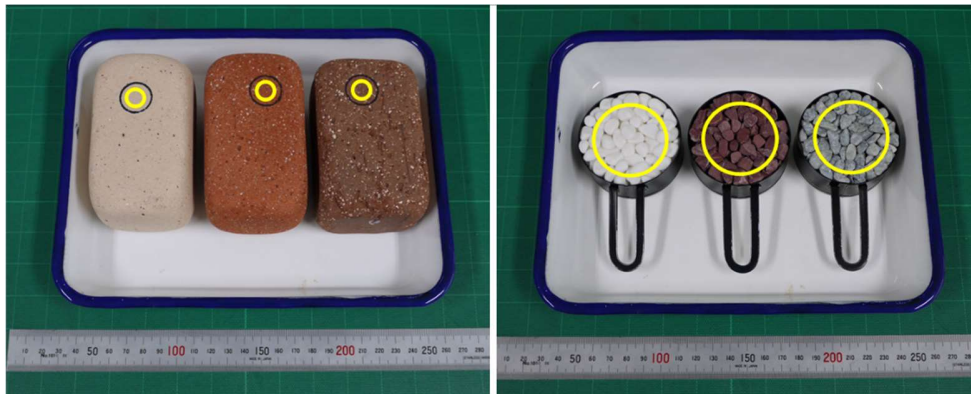


Figure 2. Sample pictures of block bricks and gravels (dried)

The yellow circles indicate the measurement areas for bricks in diameter 8 mm, and for bricks in diameter 40 mm.

RESULTS AND DISCUSSION

Figures 3 and 4 show the change in lightness and chroma with time elapsed after pulling up from water for three bricks. For the three colors of bricks, the average $L^*a^*b^*$ values of 31,188 pixels inside the yellow circles (8 mm in diameter) in Figure 2 were calculated. The diameter of 8 mm was adopted to match the measurement diameter of the contact-type colorimeter (Konica Minolta CM-2600d) used for the accuracy verification.

The color difference (ΔE^*_{ab}) between values by the system and values of the contact-type colorimeter were found to be about 5 in both the completely dry state and 120 minutes after pulling up from the water. We think that the measurement accuracy of the system is good enough to be an alternative method for visual evaluations.

In Figure 3 and 4, it can be seen that bricks with high lightness have a small change and those with low lightness have a large change. There is a rapid lightness change in the first 5 minutes for the red brick. For the beige brick, it is 20 minutes, and for brown, 40 minutes. The timing of the rapid change varies depending on the color.

Figures 5 and 6 show the change in lightness and chroma with time elapsed after pulling up from water for three gravels. For the three types of gravel, the average $L^*a^*b^*$ values of 779,776 pixels inside the yellow circles (40 mm in diameter) in Figure 2 were calculated.

In Figures 5 and 6, it can be seen that gravels with high lightness have a small change and those with low lightness have a large change. In Figure 5, the lightness gradually increases with time for all three gravels. In Figure 6, the chroma decreases with time for all three gravels. Red gravels showed especially large amount of change in chroma.

CONCLUSIONS

The findings obtained in this research are as follows:

- (1) It is possible to measure wet color by using a non-contact colorimetric system.
- (2) For bricks and gravels, those with high lightness has a small change, and those with low lightness has a large change in lightness and chroma.

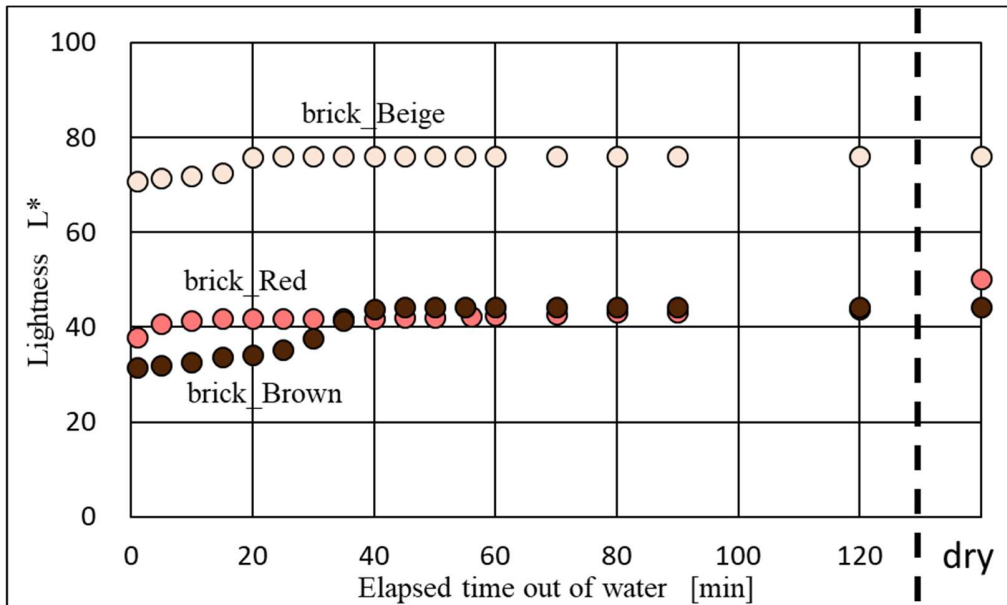


Figure 3. Lightness with time elapsed after pulling up from water (bricks)

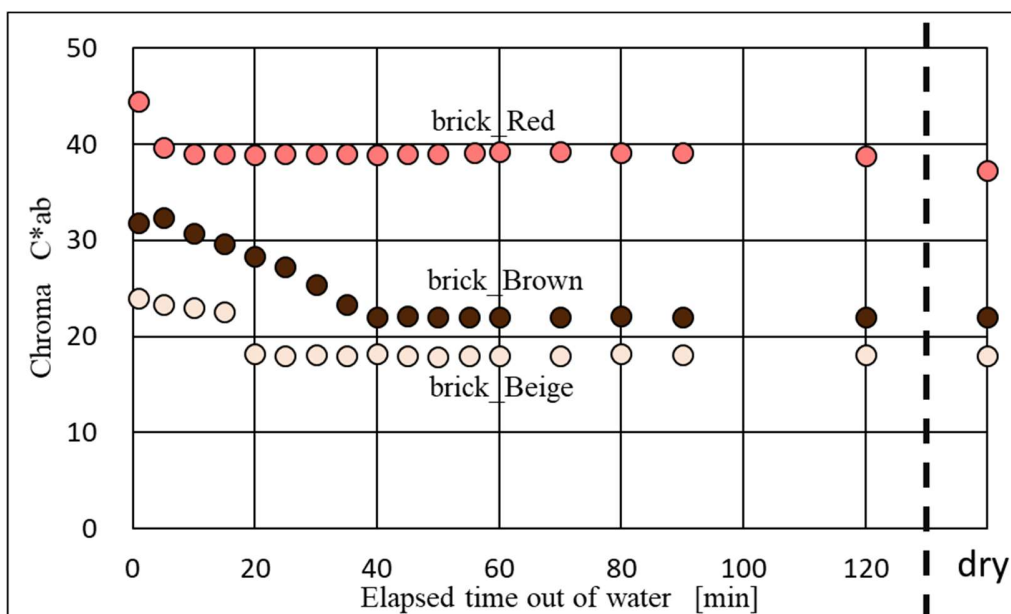


Figure 4. Chroma with time elapsed after pulling up from water (bricks)

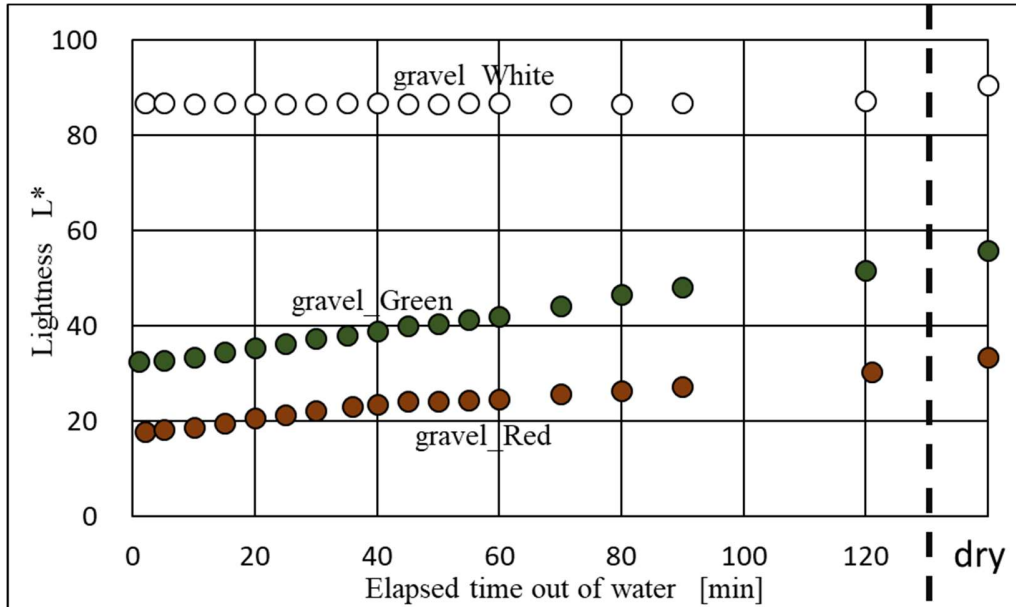


Figure 5. Lightness with time elapsed after pulling up from water (gravels)

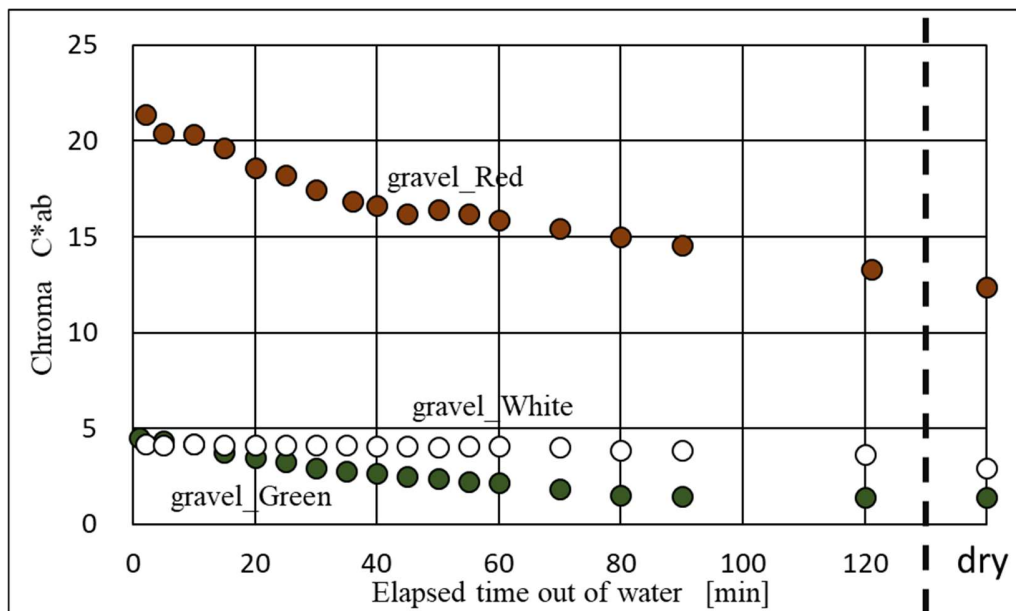


Figure 6. Chroma with time elapsed after pulling up from water (gravels)

REFERENCES

1. Sawano, T. (1999). *Creating Your Own Japanese Garden*, Japan Publications Trading, Tokyo.
2. Sakai, H., Isomi, M., and Iyota, H. (2017). Non-contact colorimetric measurement using dome illumination for free-form surfaces Part 1, *J. Color Science Assoc. Japan Vol.41(3) Supplement*, 10-11 (in Japanese)
3. Isomi, M., Sakai, H., and Iyota, H. (2017). Non-contact colorimetric measurement using dome illumination for free-form surfaces Part 2, *J. Color Science Assoc. Japan Vol.41(3) Supplement*, 12-15 (in Japanese)
4. Sakai, H., Isomi, M. and Iyota, H. (2018). Non-contact colorimetric measurement using dome illumination for complex shape objects, *Proc. the 4th Asian Color Association Conference*, 183-186
5. Sakai, H., Yoshikawa, S., and Iyota, H. (2013). Accuracy of color measurement by using digital cameras and the standard color chart, *Proc. of the 1st Asia Color Association Conference*, 248-251

AGE AND GENDER DIFFERENCES FOUND IN VERBALIZED IMPRESSIONS FOR TWO-COLOR COMBINATIONS

Takashi Sakamoto^{1*}, Saki Tomita², Toshikazu Kato³

¹*National Institute of Advanced Industrial Science and Technology (AIST), Japan.*

²*Graduate School of Science and Engineering, Chuo University, Japan.*

³*Faculty of Science and Engineering/Research Promotion Office, Chuo University, Japan.*

*Corresponding author: Takashi Sakamoto, takashi-sakamoto@aist.go.jp

Keywords: Nouns, Adjectives, Memory-recall

ABSTRACT

This paper investigated which parts of speech, namely, nouns and adjectives, were more frequently used while expressing impressions of two-color combinations. It specifically focuses on age and gender differences in the usage of nouns and adjectives. Although it is commonly believed that one's impressions of colors are represented by adjectives, results obtained in our first experiment with 20 Japanese college students (16 males and 4 females, aged 21–23 years) indicated that nouns were used more frequently than adjectives. To examine whether those findings were only peculiar to young participants, 22 elderly Japanese people (11 males and 11 females, aged 65–69 years) were observed in the second experiment with the same experimental design. In all, eight colors (red, orange, yellow, green, blue, purple, white, and black) were used to prepare 64 patterns as visual stimuli. The elderly participants were then asked to respond their recalled words verbally within 16 seconds in an open-response format. Thus, the second experiment revealed that the female elderly participants recalled more adjectives than nouns, while the male elderly participants recalled more nouns than adjectives, which was in line with our first experiment's findings. We also found that the number of recalled nouns and adjectives changed on the basis of particular color components within the two-color combinations. For example, purple components made participants recall more adjectives than nouns; a similar tendency was also observed in the case of red components. On the basis of these results, a memory recall model can be proposed that indicates red and purple directly induce specific emotions, and the adjectives used to express these emotions are easy to recall.

INTRODUCTION

While expressing one's impressions of colors, which parts of speech—nouns, adjectives, verbs, and interjections—are frequently employed? Often, one's impressions of colors are considered to be expressed in the form of adjectives, such as “beautiful,” “vivid,” “soft,” or “warm.” For example, Osgood's semantic differential method is an adjective-based research method used for impression analysis. However, words recalled in an observer's mind may not be limited to adjectives because nouns, verbs, and interjections can also be recalled.

Investigating the type, frequency, and tendency of words used for expressing impressions of colors is vital for understanding memory recall and psychological effects of colors. On the basis of this consideration, we conducted a memory recall experiment in which participants recalled and verbalized words while looking at colors with a simple arrangement. Findings from our previous research revealed that nouns were recalled more frequently than adjectives [1]. These findings were obtained when 20 young participants between the ages of 21 and 23 (16 and 4 native Japanese speakers, males and females, respectively) were studied. A possibility thus prevailed that these

findings were peculiar only to young individuals. In the present study, we aimed to verify our previous findings by studying elderly participants to increase our understanding of memory recall in people.

This paper reports and discusses our findings from an experiment performed with 22 elderly participants (11 and 11 native Japanese speakers, males and females, respectively, aged 65–69 years), employing the experimental design of the previous experiment conducted with 20 young participants. The only alteration made was regarding the duration that the participants were given to verbally respond their recalled words in an open-response format (from 8 seconds to 16 seconds), in consideration of slower reaction durations among the elderly. On the basis of these results, age and gender differences will be identified and discussed in this paper.

EXPERIMENT WITH YOUNG PARTICIPANTS

Our previous experiment involved the recall and association of nouns and adjectives for two-color combinations. It comprised of 20 Japanese individuals (16 males and 4 females, aged 20–24 years) with normal visual acuity and color vision. Two-color combinations were employed as visual stimuli to examine whether adjectives or nouns were more frequently recalled. The visual stimuli, presented using a liquid crystal display (LCD) monitor, composed of two colors from a total of eight colors—six vivid colors, black, and white (Table 1).

Table 1. Colors used in our experiments

No.	Color name	PCCS tone	Equivalent Munsell color notation		
			Hue	Value	Chroma
1	Red	v2	4R	4.5	14
2	Orange	v5	4YR	6	13.5
3	Yellow	v8	5Y	8	13
4	Green	v12	3G	5.5	11
5	Blue	v17	10B	3.5	10.5
6	Purple	v20	9PB	3.5	11.5
7	White	—	N10	—	—
8	Black	—	N0	—	—

In all, six vivid colors specified in the tone notation of the Practical Color Coordinate System (PCCS) are red (v2), orange (v5), yellow (v8), green (v12), blue (v17), and purple (v20). Two-color combinations were employed to create 64 patterns, including eight same-color combinations. When each two-color combination was presented, participants were indicated to respond verbally within eight seconds, using an open-response format; they were also provided rest of eight seconds between each set (Figure 1). Further, the participants' recalled words were classified as adjectives, nouns, verbs, interjections, or others.

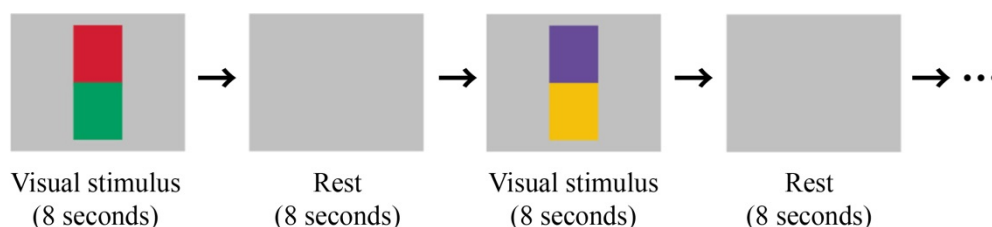


Figure 1. Example of the experimental procedure

The following results were obtained from the abovementioned experiment:

1. The number of nouns used per visual stimulus was significantly larger than the number of adjectives used per visual stimulus ($p < 0.05$) (Figure 2).
2. Significantly more nouns than adjectives were initially recalled ($p < 0.05$) (Figure 3).
3. The results of the statistical analysis revealed that nouns were more likely to be recalled than adjectives.
4. In the case of red and purple colors, no statistical significance was observed between the number of nouns and adjectives recalled.
5. In the combinations where either red or purple was included in a two-color combination, the participants recalled adjectives faster and more frequently than in combinations where these colors were not included.
6. Many negative adjectives were associated with purple, such as “dark,” “poisonous,” “cold,” “creepy,” and “sober.”

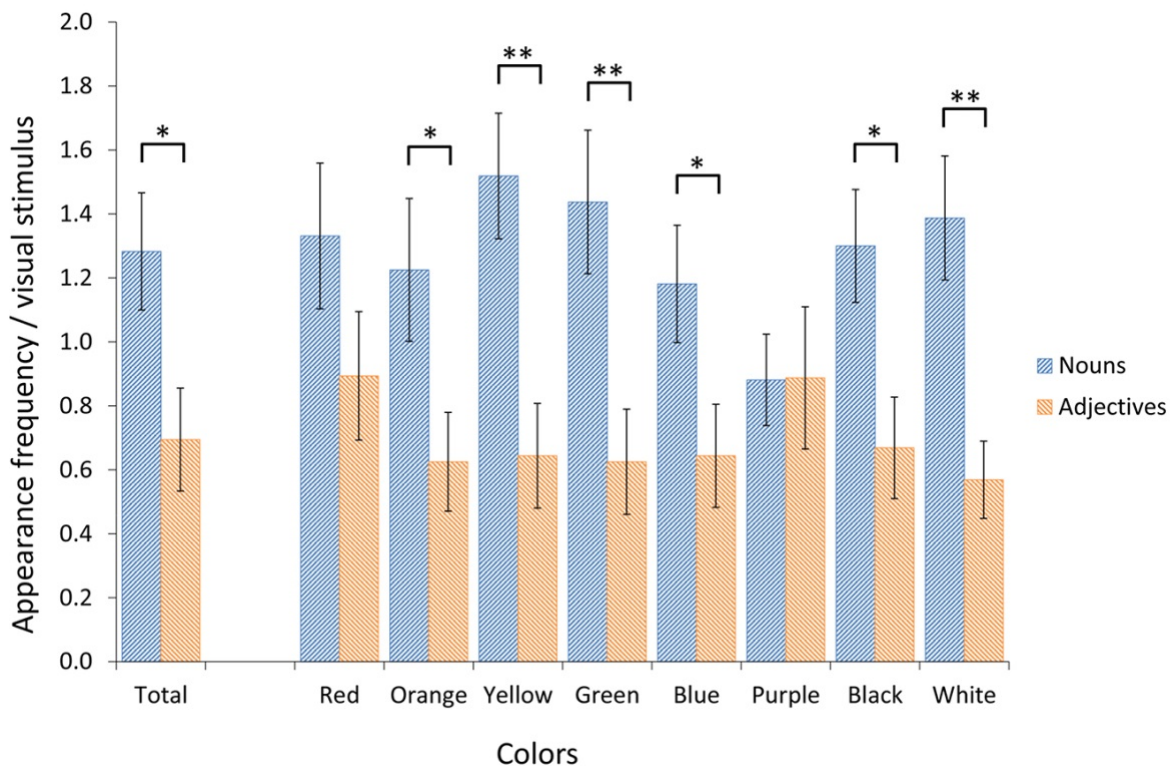


Figure 2. (Figure reprinted from [1]) Number of nouns used per visual stimulus was significantly larger than the number of adjectives ($p < 0.05$). Visual stimuli that included red or purple colors led participants to recall adjectives more frequently in comparison to other colors.

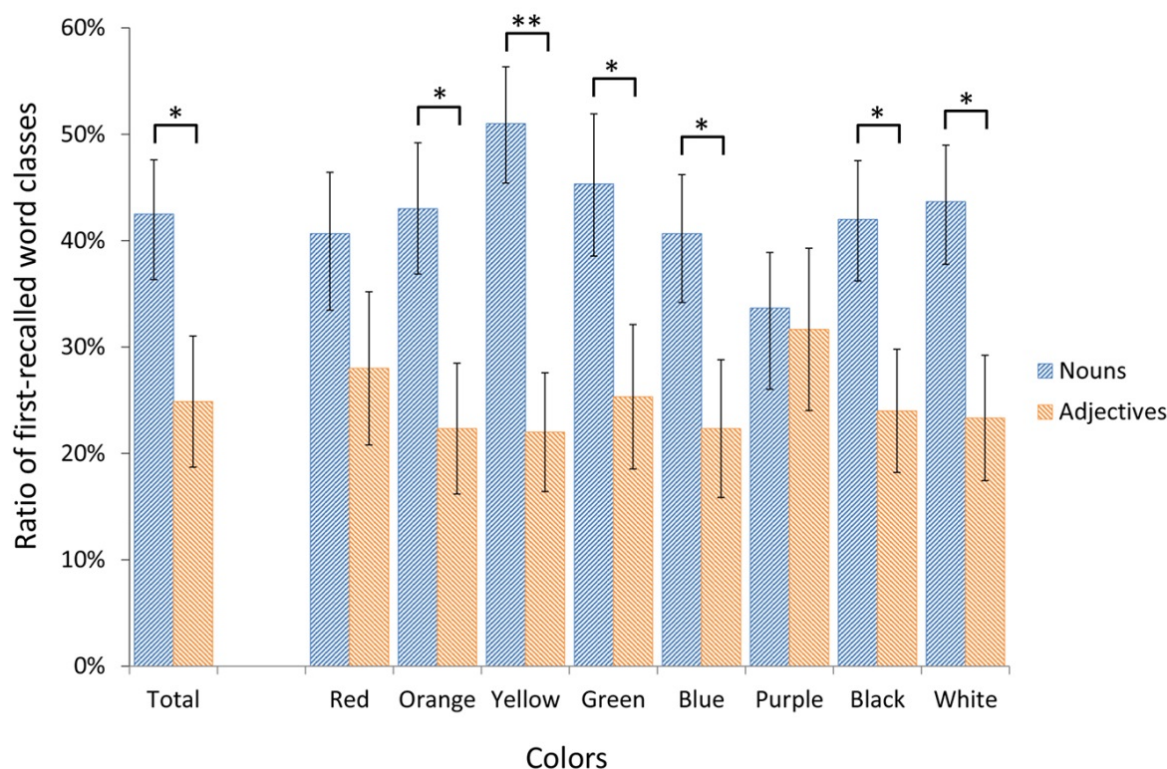


Figure 3. (Figure reprinted from [1]) Significantly larger numbers of nouns than adjectives were initially recalled ($p < 0.05$). Visual stimuli that included red or purple led observers to recall adjectives more quickly compared to other colors.

EXPERIMENT WITH THE ELDERLY PARTICIPANTS

To verify the results of the abovementioned experiment to determine age and gender differences, 22 elderly participants were studied in the second experiment with the same design. The experimenters recorded the number of nouns and adjectives the elderly participants recalled and verbalized while viewing two-color combinations. It comprised of 11 and 11 native Japanese speakers, males and females, respectively, aged 65–69 years, with normal visual acuity and color vision. This experiment also employed two-color combinations as visual stimuli, and these stimuli were presented using an LCD monitor. Additionally, eight colors and 64 patterns employed in the previous experiment were further employed. When each two-color combination was presented, the participants were instructed to respond verbally in an open-response format within 16 seconds; they were also provided a 16-second rest between each set. After the experiment, the participants' recalled words were classified as adjectives, nouns, or other parts of speech.

The results obtained were as follows:

1. Elderly female participants significantly recalled more adjectives than nouns ($p < 0.05$) (Figure 4), which was in contrast to the findings of the previous experiment.
2. Elderly male participants significantly recalled more nouns than adjectives ($p < 0.05$) (Figure 4), which was in line with the findings of the previous experiment.
3. The number of recalled nouns and adjectives changed depending on the color components of the two-color combinations. In particular, participants recalled more adjectives than nouns for red and purple colors (Figure 5).

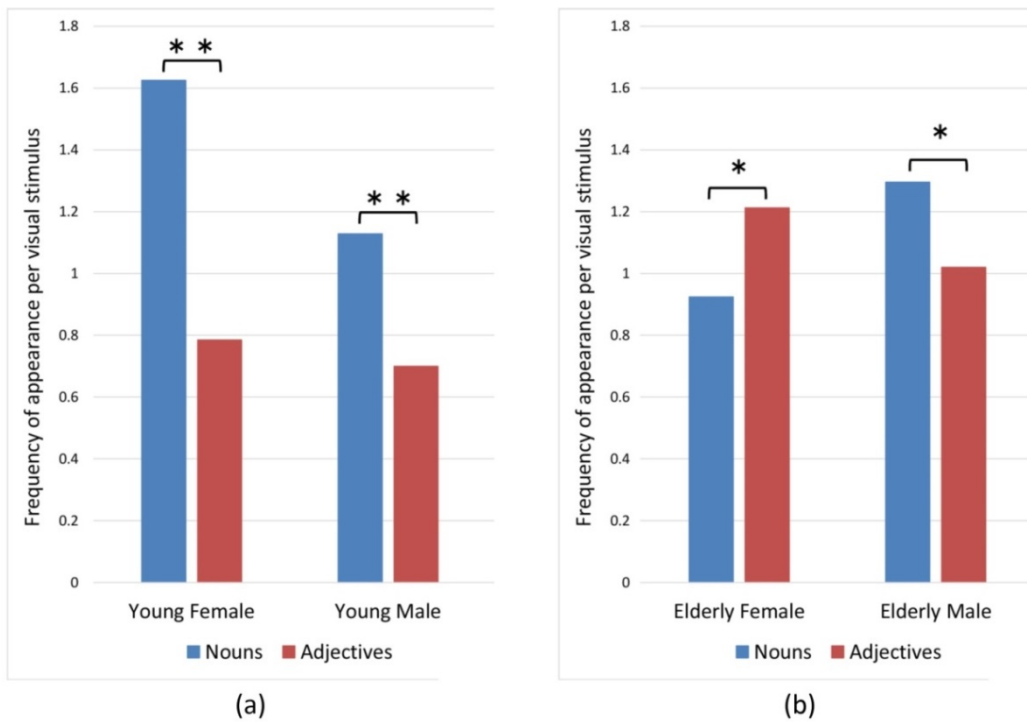


Figure 4. (a) Young male and female participants significantly recalled more nouns than adjectives ($p < 0.01$). (b) Elderly female participants significantly recalled more adjectives than nouns ($p < 0.05$); however, elderly male participants significantly recalled more nouns than adjectives ($p < 0.05$). Results (a) were obtained within 8 seconds, while Results (b) were obtained within 16 seconds, considering slow reaction durations among the elderly.

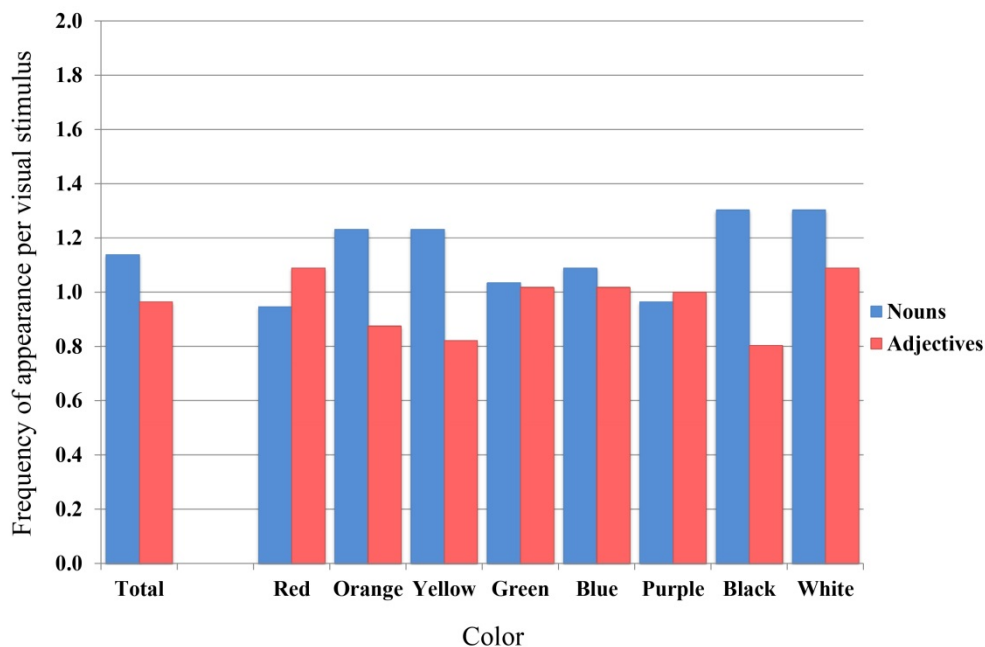


Figure 5. Number of nouns and adjectives varied according to component colors; among them, participants verbalized more adjectives than nouns when red or purple colors were included.

DISCUSSION AND CONCLUSIONS

Our experimental results revealed that nouns associated with two-color combinations were more likely to be recalled than adjectives while expressing color impressions. Specifically, young participants and male elderly participants more frequently recalled nouns than adjectives. Conversely, female elderly participants recalled more adjectives than nouns. These results suggest that female elderly participants could verbalize more adjectives than young and male elderly participants, and those adjectives may have been accumulated on the basis of their linguistic experiences, including speaking with others and reading various novels. Male elderly individuals, however, especially in Japan, spent their youth during the time when a “man should be silent” was a common notion. Due to this historical trend, elderly Japanese men may have lost a few opportunities for the advancement of their linguistic experiences. The results of the experiment with young participants were similar to those of the elderly male participants, which may be further illustrated on the basis of their few language experiences.

In both the experiments, as durations allocated to verbalize recalled words were different, it was difficult to perform a statistical comparison between them. Additionally, the ratio of male and female participants should be equal for more reliable and stable experimental control and statistical analysis. These short-comings should therefore be addressed in future studies.

ACKNOWLEDGEMENT

This work was partially supported by JSPS KAKENHI Grant Numbers 25240043 and 18H03565.

REFERENCES

1. Sakamoto, T., Tomita, S. & Kato, T. (2018). Impressions of a combination of two colors are more frequently represented by nouns than adjectives: In the Japanese case, *Proceedings of the International Colour Association Conference 2018*, Portugal, 715-719.
2. Kunugida, Y., Nagai, Y. & Taura, T. (2008). Methods of creative design focused on the process of associative concepts chains, [in Japanese], *Proceedings of the 55th Annual Meeting of Japanese Society for the Science of Design*, B14, 1-2.
3. Ito, K., & Oyama T. (2005). Affective effects of two-color combinations between different hues, [in Japanese], *Journal of the color science association of Japan*, 29(4), 291-302.
4. Makino, A. & Takahashi, S. (2012). Color impression of Onomatopoeia: a study of association colors on three-color combinations, [in Japanese], *Journal of the color science association of Japan*, 36, Supplement, 50-51.
5. Ban, H. & Tsuya, A. (2017). Generational comparison of images for color terms in Japanese and English, [in Japanese], *Proceedings of the 19th Japan Society of Kansei Engineering Conference and General Meeting*, E23.
6. Ban, H. (2005). Comparison of Images for Color Terms in Japanese and English, [in Japanese], *Journal of the Faculty of International Studies*, Toyama University of International Studies, 1, 117-128.

CHARACTERISTICS OF THE SEX DIFFERENCES IN ART DRAWINGS BY JUNIOR HIGH SCHOOL STUDENTS USING COLOR STICKERS

Yukiko Shimada^{1*}, Yuko Ohgami², and Katsuhiko Mogi³

¹ *Department of Child Studies, Faculty of Human Development, Kokugakuin University, Japan.*

² *Department of Child Development and Education, Faculty of Humanities, Wayo Women's University, Japan.*

³ *Midori Municipal Kasakake South Junior High School, Japan.*

*Corresponding author: Yukiko Shimada, y-shimada@kokugakuin.ac.jp

Keywords: Sex differences, drawing, color stickers

ABSTRACT

Junior high school students (aged 13 to 15) typically begin to have awareness of their own sex after they have developed secondary sexual characteristics. In Japanese junior high schools, male and female students attend the same classes as a rule, although some classes such as physical education and music are held separately. The aim of this study was to identify the characteristics of the sex differences in drawings made during puberty. Previous studies have pointed out the following sex differences in drawings made by preschool children: color preferences, motifs in free drawings, color biases used in free drawings, etc. However, it has been rarely examined whether these differences continue to be observed in puberty. **Method:** A total of 264 public junior high school students (130 male and 134 female) participated in the study. We assigned two kinds of sticker tasks: a black stickers task and a ten color stickers task. In the black stickers version of the task, we asked them to paste 18 black round stickers freely on a sheet which is divided into 25 squares (5×5) and to give them titles. In the ten color stickers version, we gave them 24 round stickers each for ten colors (red, pink, orange, yellow, green, blue, light blue, purple, white, and black) for a sheet divided into 49 squares (7×7). Furthermore, we let them choose the colors they liked from these ten colors. **Results and Discussion:** We examined what kind of sex differences there were regarding color preferences, the characteristics of the art work in the sticker tasks, and the titles given by the students. In terms of color preferences, male students tended to prefer red, green, and black, whereas female students tended to prefer pink and yellow, which was consistent with the previous studies. However, the difference between these color preferences was not reflected in the number of stickers used of each color. In the characteristics of the artwork made, sex differences were noticeable in the following two points,

mainly in the colored stickers version: First, female students used more colors than male students. Second, male students used more black and white than female students, whereas female students used more pink and orange than male students did. Finally, we divided the titles of each artwork into five categories (natural objects, artificial objects, animals, decorations, and other) and examined the sex differences. The result shows that male students made sticker collages of artificial objects more than female students did in both the black stickers and the colored stickers versions while female students made collages of decorations more than male students did except in the black stickers version. These results were consistent with the characteristics of sex differences in the motifs of the free drawings made in early childhood. It suggests that the characteristics of sex differences in the free drawings made in early childhood were partially carried forward into puberty.

INTRODUCTION

Preschool children's free drawings reflect sex differences in motifs, colors, shapes, and construction [1]. However, it has been rarely examined whether these sex differences continue into puberty. Junior high school students (aged 13 to 15) become aware of their own sex after they have developed secondary sexual characteristics. The aim of this study was to identify the characteristics of the sex differences in sticker collages made during puberty.

METHOD

1. *Participants*

A total of 264 public junior high school students (130 male and 134 female) participated in the survey.

2. *Materials and Tasks*

The participants were presented with a two-dimensional picture task with two components: a black stickers version and a ten color stickers version.

In the black stickers version, each participant received an A4 sheet featuring 25 square cells arranged in a 5×5 grid, together with 18 round black stickers. They affixed these stickers as they desired. In the ten color stickers version, each participant received an A4 sheet of 49 square cells arranged in a 7×7 grid, together with 24 colored stickers. There were ten colors: red, pink, orange, yellow, green, blue, light blue, purple, white, and black. Again, they affixed these stickers as they desired. In both tasks, they gave titles to their completed artwork.

The participants were given a questionnaire in which they stated their favorite color amongst the colors used in the colored stickers version. They also used the questionnaire to report whether their favorite color influenced their artwork.

3. *Procedure*

The experiment was conducted during mandatory art classes for first and second-year junior

high school students. Of the two task components, the black stickers version was conducted first. Thereafter, the ten color stickers version was conducted. Finally, the students reported their favorite sticker color and whether this color influenced their resulting artwork.

Each student worked on their artworks at their own pace, and the process as a whole lasted around 50 minutes.

This study was approved by the Ethical Committee of the Kokugakuin University.

RESULTS

1. *Black stickers version*

1.2. *Number of stickers used*

We compared the number of stickers used out of the 18 stickers by the male students, with that used by the female students to check for any sex difference. Male students used an average of 12.4 stickers, while female students used an average of 12.0, a non-significant difference.

1.3. *Artwork title*

The artwork titles were organized into five categories (Natural objects, Artificial objects, Decoration, Animals, Others). We compared the sex of each student with the picture category, revealing significant sex difference ($p < .01$). Male students were more likely to choose a title categorized as “artificial objects” while female students were more likely to choose one categorized as “decoration”.

2. *Ten color stickers version*

2.1. *Number of stickers used*

We found no significant sex difference in the number of stickers used. However, male students used black and white stickers to a greater extent than their female counterparts. Female students used pink and orange stickers to a greater extent than their male counterparts.

Next, we compared the number of different colors used (i.e. the degree of color variation). Female students used a significantly wider range of colors than the male students.

2.2. *Color preference and impact of preference*

We compared sex with favorite color, revealing significant sex differences. A residual analysis indicated that male students tended to select red, green, or black as their favorite color, while female students tended to choose pink or yellow. However, we found no significant sex difference in whether color preference influenced the resulting artwork.

2.3. *Picture title*

We compared sex with picture category, revealing significant sex differences. According to a residual analysis, male students were more likely to choose a title categorized as “artificial objects” ($p < 0.1$), which is consistent with the results for the black stickers version. However, unlike with the black stickers version, we found no sex difference in the results for the decoration category.

DISCUSSION

In this study, we sought to clarify sex differences in adolescent artwork.

We found no significant sex difference in the number of stickers the students used in either the black stickers version or the colored stickers version of the task. The implication is that male and female adolescents share a similar sensibility about white space in a two-dimensional picture.

As for the colored stickers version, we found that male students used black and white stickers to a greater extent than the female students did, whereas female students used pink and orange more frequently than their male counterparts did. These findings are in accordance with a study on preschool children by Minamoto [1]. Our study also revealed that female students used a greater range of colors than the male students. This finding is also consistent with the previous study [1]. Therefore, the sex differences in the colors junior high school students use—both in the number of different colors they use and in the specific colors they use—represent a continuation of prepubescent sex differences.

Our study also revealed a sex difference in color preference. Previous studies reported that preschool boys favor black and cool colors, while girls favor warm colors such as pink [1]. Our study also reported this finding, at least in part. Thus, the color preferences of prepubescent children—boys' preference for black and girls' preference for pink—persist in adolescence.

In titling an artwork, the male students typically opted for a title categorized as “artificial objects.” In the black stickers version, female students opted for a title categorized as “decoration.” This finding is consistent with Iijima et al.'s study [2] on children's free drawings.

These findings imply that art teachers can understand their students' art better if they understand the manifestation of sex differences in art.

ACKNOWLEDGEMENT

This research was partially supported by the Mitsubishi foundation.

REFERENCES

1. Minamoto, F. (2017). *Imagination of "the drawing": The mind of the child and the rich world*. Syunjyusya Publishing Company, Tokyo.
2. Iijima, M., Arisaka, O., et al., (2001). Sex Differences in Children's Free Drawings: A Study on Girls with Congenital Adrenal Hyperplasia, *Hormones and Behavior*, 40(2), 99-104.

COMPARISON OF COLOR INTERFERENCE IN GENDER IDENTIFICATION BETWEEN THAI AND JAPANESE

Kitirochna Rattanakasamsuk^{1*} and Mikiko Kawasumi²

¹*Color Research Center, Faculty of Mass Communication Technology, Rajamangala University of Technology Thanyaburi, Thailand.*

²*Faculty of Science and Technology, Meijo University, Japan.*

*Corresponding author: Kitirochna Rattanakasamsuk, kitirochna@rmutt.ac.th; kitirochna@gmail.com

Keywords: Color Code, Color and Gender, Gender Identification

ABSTRACT

Color was used as a code to identify gender. For example, female baby clothes are generally pink while male baby clothes are generally blue. In some culture, the color code is almost standardized for gender identification. We can see in Japan that most of the female toilet sign is red or pink, whereas the male toilet sign is blue, so it is not necessary to recognize the detail of the sign. You can identify the toilet type by just seeing the toilet sign's color. In this research, we investigated the color code usage for gender identification of Japanese and compare the results with Thai. The experiment was conducted in Thailand and Japan. In each country, the subjects are 25 female 25 male university students. The stimuli were three patterns of female and male toilet sign. Each pattern was applied by five colors included blue, navy blue, red, pink and black. Therefore, the stimuli were composed of a combination of two genders, three patterns, and five colors, totally 30 signs. The stimuli were presented on an LED monitor. The size of stimuli was between 12-15 degree of visual angle. There were two tasks for each subject. For the first task, the subjects assessed the color of the sign whether that color was identified as male or female. For the second task, the subjects assessed the details of the signs whether they were male or female. In each judgment, a sign was presented for two seconds and separated by at least five seconds blank screen. If the subject did not judge within 5 seconds of a blank screen, the blank screen will appear until each judgment was finished. The results suggested that there was a firm linkage between color and gender in Japanese culture. More than 90% of Japanese pointed out that red and pink were identified as the color of female whereas light blue, navy blue and black were identified as the color of the male. This linkage was truly strong enough so that some color could interfere their gender identification by the sign. When the female sign was applied with red or pink and the male sign was applied with blue, navy blue and black, the percentage of correct judgment is higher than 90%. However, when the female sign was applied with navy blue and the male sign was applied with pink, the correct judgment decreased significantly to be about 60%. Unlike the result of Japanese, the linkage between color and gender did not firmly hold in Thai culture. Most of all Thai subject could correctly identify gender regardless of color in sign.

INTRODUCTION

Previous research has shown that color preference was affected by many factors such as age, culture etc. Gender was one of the important factors to determine color preference [1], [2], [3]. "Men like blue and women like pink" was the belief that intentionally implanted by the marketeer in order to increase the product sale. For example, female baby clothes are generally pink while male baby clothes are generally blue. This belief was somehow transformed to be a color code and was used to identify gender. In some culture, the color code is almost standardized for gender identification. We can see in Japan that most of the female toilet sign is red or pink, whereas the male toilet sign is blue. Therefore, it is not necessary to recognize the detail of the sign. You can identify the toilet type by just seeing the toilet sign's color. We hypothesized that in the culture which color were obviously referred to gender, the color can interfere the interpretation of sign

meaning. In this research, we investigated the interference of color on gender identification of Japanese people and compare the results with Thai people.

METHODOLOGY

Subject

The subject were 50 Japanese and 50 Thai students. Each group of subjects were composed of 25 male and 25 female subject aged between 18-24 years old. All subjects had normal color vision.

Stimuli

The stimuli were three patterns of female and male toilet sign as shown in Figure 1. Each pattern was applied by five colors included blue, navy blue, red, pink and black. The color values of each color were shown in Table 1. The stimuli were composed of a combination of two genders, three patterns, and five colors, totally 30 signs. Each sign was placed on the white background. The size of the stimuli was between 12-15 degree of visual angle.

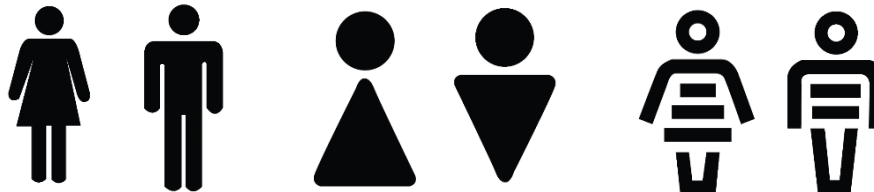


Figure 1. Three patterns of female and male sign

Table 1: Luminance and xy chromaticity of color stimuli

Color	Luminance (cd/m ²)	x	y
Black	0.4	0.320	0.369
Pink	63.2	0.462	0.305
Red	35.6	0.588	0.341
Blue	95.5	0.218	0.298
Navy Blue	37.6	0.201	0.233
White Background	250.0	0.310	0.330

Experimental Procedure

The stimuli were presented on an LED monitor which was placed inside a subject room. The background behind the monitor is a white wall. The illuminance measured at the monitor position was 400 lux.

There were two tasks for each subject. For the first task, the subject was asked to judge whether each stimulus was male or female sign. For the second task, the subject was judge whether the color of each stimulus was referred to male or female. These two tasks were done in separated session.

In each session, the subject must sit inside the room for at least two minutes before starting the experimental session. After the two minutes adaptation, the experimental start by pressing the space bar. The blank screen appeared for three seconds. Then a color stimulus was presented for two seconds. After that, the screen turned to be blank screen. The subject gave the judgement by pressing “1” on the keypad for male and “3” on the keypad for female. The blank screen continuously appeared for at least five seconds before the next stimulus was presented. If the

subject did not judge within five seconds of a blank screen, the blank screen will appear until each judgment was finished. The order of color stimulus was random. The procedure repeated until all 30 color stimuli were presented.

EXPERIMENTAL RESULTS

The relation between color and gender of Thai and Japanese was investigated. After presenting the color female or male sign, the subject would indicate whether the presented color was the color of the male or the female. The results were shown in Figure 2.

In case of Japanese subjects, more than 90% of Japanese pointed out that red and pink were identified as the color of the female whereas blue, navy blue and black were identified as the color of the male, regardless of the gender of sign.

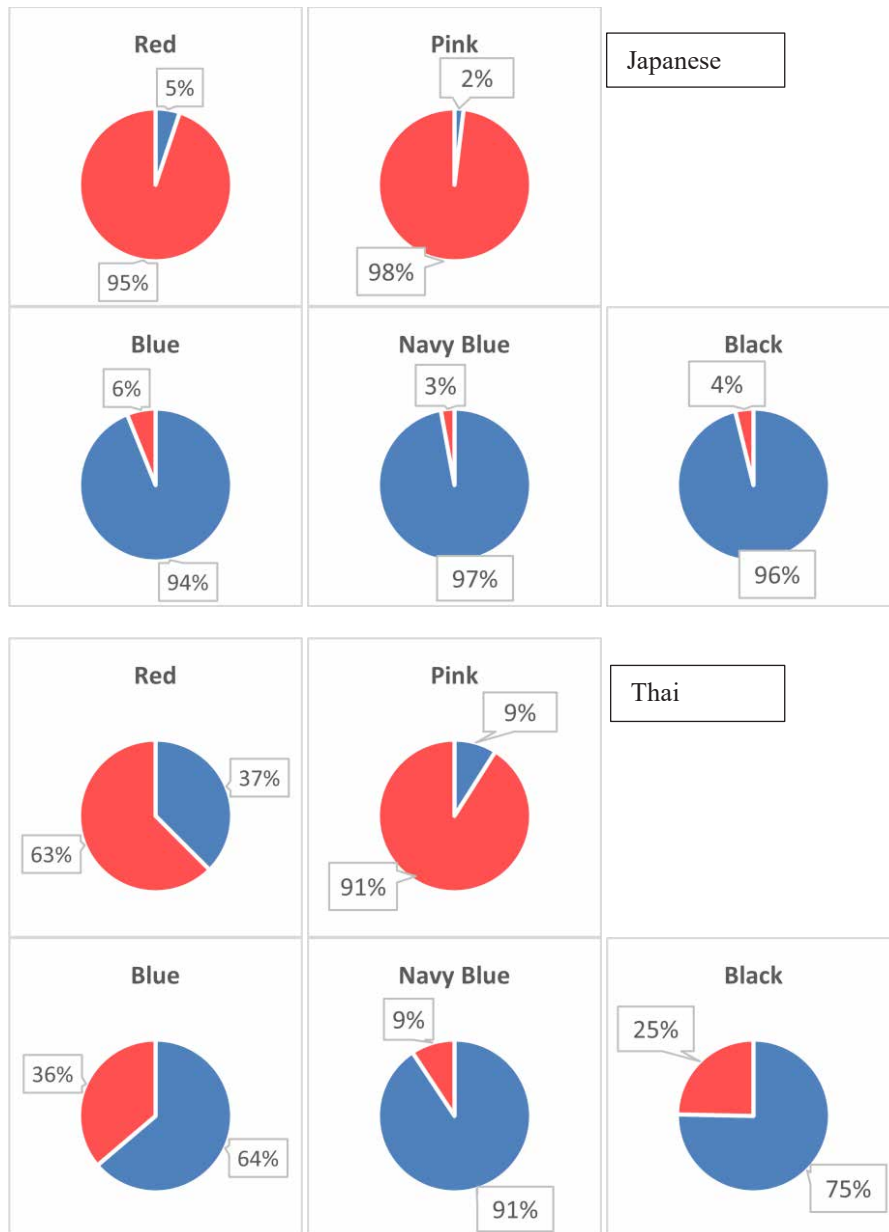


Figure 2 Color and gender relation by Japanese (above) and Thai (below). Red and blue represent female and male response, respectively.

In case of Thai subjects, only pink and navy blue were obviously identified as the color of the female and the male respectively. Black was majorly identified as the color of the male but 25% of response also identified it as the color of female. Most of Thai's responses identified that blue was the color of the male and red was the color of the female. However, about 36% of response from Thai also indicated that red was the color of the male and blue was the color of the female. Therefore, red and blue seems to be unobvious to identify their gender for Thai.

The above result showed that there was a firm linkage between these colors (red, pink, blue, navy blue and black) and their gender in Japanese culture. On the other hand, the relation between these colors and their gender were not obvious in Thai culture. The possible reason was that Japanese people familiar with the color code usage for gender identification. Red and pink always used for female objects whereas and blue, navy blue and sometime black were used for male objects. This color code was the de facto standard especially for the color of toilet sign. In contrast to Japanese, the implementation of color code in Thailand was not successful. For example, there is no standard for the color of toilet sign.

Figure 3 shows the result of gender identification of color stimuli judged by Japanese and Thai. The abscissa represents five colors of the sign. The ordinate represents percentage of response which subject identified the sign as female (red bar) and male (blue bar). For the female sign, the correct gender identification should be female which is the red bar graph. But for the male sign, the correct gender identification should be male which is the blue bar graph.

In case of Japanese, when the female sign was red and pink, the correct gender identification was higher than 90%. But when the female sign was black, blue and navy blue, the correct identification considerably decreased. Especially in case of blue and navy blue, the percentage of correct gender identification was only 64% and 50%, respectively. When the male sign was investigated, the correct gender identification of black, blue and navy blue sign was nearly 100%.

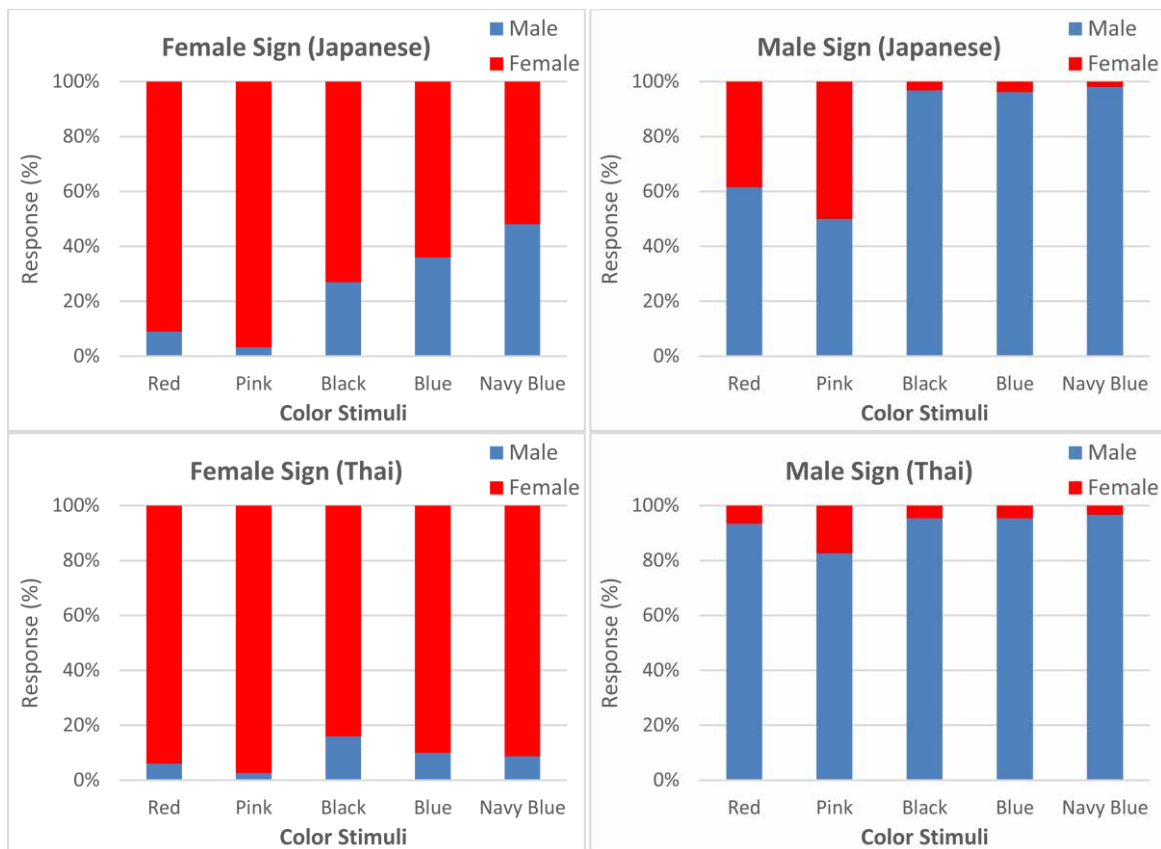


Figure 3 Gender identification of female and male color sign by Japanese and Thai.

However, the pink and red male sign made the gender identification significantly incorrect. There were only 62% and 52% correct responses for red and pink male sign.

In contrast to Japanese, color seems to be slightly affected the gender identification of male and female sign. The correct gender identification by Thai subjects was higher than 80% regardless of color. Pink and black possibly interfered the gender identification but the effect of these two colors was not clear. The wrong gender identification was still lower than 20% which considerably differed from Japanese's result.

Based on the above results, there was the evidence that the color could interfere the gender identification. The interference of color on gender identification was possibly due to the linkage between color and gender. For Japanese which the color and gender linkage was firmly hold, the interference of color on gender identification was clearly distinct. But the influence of color on gender identification would be small, if there was no linkage between color and gender in their culture. However, to the further investigation is also required to confirm this hypothesis.

CONCLUSION

Our result supported the hypothesis that the color could interfere the interpretation of the sign meaning. In the culture which color were obviously linked to gender, color would show strong influence on the gender identification like in Japanese culture.

ACKNOWLEDGEMENT

This research was partially supported by Research Fellowship Program of Meijo University, Nagoya, Japan. We would like to thank Prof. Mikiko Kawasumi for the collaboration of this research. Thanks also to Mr. Narupon Keawpilab and Ms. Kanchaporn Jankeaw for their contribution to this research.

REFERENCES

1. Bonnardel, V., Beniwal, S., Dubey, N., Pande, M., & Bimler, D. (2017). Gender difference in color preference across cultures: An archetypal pattern modulated by a female cultural stereotype. *Color Research & Application*, 43(2), 209–223. doi: 10.1002/col.22188
2. Hurlbert, A. C., & Ling, Y. (2007). Biological components of sex differences in color preference. *Current Biology*, 17(16), R623–R625. doi: 10.1016/j.cub.2007.06.022
3. Lobue, V., & Deloache, J. S. (2011). Pretty in pink: The early development of gender-stereotyped colour preferences. *British Journal of Developmental Psychology*, 29(3), 656–667. doi: 10.1111/j.2044-835x.2011.02027.x

COLOR IN PRODUCT DESIGN -INTERPRETATION OF LIFESTYLE

Zhang Rong

(Jicaixun Consultancy (Guangzhou)Co; LTD, Rm105, JiDian Building,35 Shuiyin Road Yuexiu District,510075 Guangzhou)

¹Dept. of Industrial, Academy of Arts & Design, Tsinghua University, China.

Corresponding author: Zhang Rong, e-mail: suzi222@163.com

Keywords: Lifestyle, Product and Color

ABSTRACT

We live in a world of colors all around us, and color affects all areas of our lives in different ways.

Color, as part of the emotional bond, also affects people's lifestyle in its own way.

Lifestyle implies human nature, self-expression and self-consciousness of style.

Color is one of the easiest ways to personalize your lifestyle.

The meaning of lifestyle/color design .

The lifestyle system is a set of tools to sell better products.

Through color, we hope to optimize the production system.

Color affects not only the feeling of the person most easily, but also the person's mood.

Color is the lowest input cost, the best effect in the production system.

The composition of household lifestyle,

Material Factors: Products + Decorates

Immaterial Factors: Feelings + emotions

And color is especially important! The color of lifestyle and color trend

The choice of different color combinations will affect our feelings of space design, which also represent different lifestyles.

People's different needs for lifestyle make the personalized color especially important.

We take 36 square metre small family model for example, satisfy basic function, little space, strong receive. Keep the structure of the furniture as same.

Through changing the color of furniture products, we create a different way of life.

Optimize production systems by enriching product lines at the lowest cost in the production chain.

Take the following plan as an example.

Different lifestyles: 3 color series of collocation scheme design

From color inspiration perception to systematic color analysis, and then product color collocation.

From the material combination of space, deserve to act the role of combination, search the connection between color.

Result: if we live in a color environment we like, we will feel better! Because we choose our way of life!

COLOR IN PRODUCT DESIGN -INTERPRETATION OF LIFESTYLE

We live in a world of colors all around us, and color affects all areas of our lives in different ways.

As part of our emotional bond, colors also influence human lifestyle in their own ways.

From the sociological perspective, one's lifestyle is one's mode of life.

-- Austrian psychologist Alfred Adler

One's lifestyle contains one's human nature, self-expression and self-awareness of style.

And it manifests itself through one's body, clothes, speech, pastimes, food preference, houses, cars, vacation choice, and so on, all considered to be indicators of customers' personality and awareness of style.

Home space is also a type of life mode, and its colors can particularly indicate human lifestyle.

Lifestyle can be viewed at two levels, the material and the non-material.

Materially, lifestyle mainly refers to furniture products, accessories and other concrete objects in people's household furnishing. While non-materially, it is more abstract, and involves such matter as sensations and emotions. In many cases, the color of household products will cross the material and non-material boundary and takes on both sentimental and rational features.

At the material level: furniture products /accessories

The design of furniture and accessories is the most important part of interior design.

In recent years, independent movable furniture has been gradually replaced by full house customization in China's furnishing market, which has ushered in a rapidly growing customized furniture industry.

Full house customization has been the product of a confluence of factors, including the customers, decoration companies, the industry, and so on.

To customers, customized furniture can save them a lot of labor and trouble while satisfying their basic needs for furniture functions.

To manufacturers, full house customization can be realized through standardized production and with lower cost and higher efficiency, and it can also remarkably increase per customer transaction and the sales.

But on the other hand, full house customization is unable to fully respond to the personalized needs of each customer.

And this will lead to the contradiction between manufacturers' standardized production and operation and consumers' need for customization.

So, how to resolve this contradiction between industrialized production and the need for personalized lifestyle?

Can colors help to solve this problem?

At the non-material level: sensations + emotions

Here, the non-material influence of color corresponds to people's lifestyle,

These non-material factors can awaken emotions and vibrate all our sensory organs.

Color can dominate our overall impression of certain space within a very short time, for humans can see before they feel, smell, hear, touch and taste. The taste sense is the slowest to react.

Hence, different color combinations will greatly affect our perception of the space, and that's how color psychology works. In the meantime, the choice of colors also suggests the lifestyle of different groups.

As people's need for lifestyle varies from person to person, personalized color becomes particularly important.

This shows how color works in human lifestyle.

So, can color solves this problem?

This is related to the connection between lifestyle and color design.

We hope to optimize the product line through color...

1. Color can affect human feelings;
2. Make color the link that costs the least but produces the best effect in the production system.

Mainstream modern consumption has become increasingly personalized and diversified.

With the development of urbanization, soaring housing prices, and the prevailing attitude of remaining single and unmarried, personalized small dwelling-size apartments have become more and more popular.

Skinny houses are super cozy. The residents grow closer to one another, relaxing spots to withdraw from the group are created on various levels, and an atmosphere in which everyone feels at ease is the result. On top of that, a small living space saves time and money. But the feeling of having one's own home in the city remains the same! With the growth of metropolitan areas, the demand for these popular skinny houses is also growing.

Here, let's take the small apartment of 36 m² for example. Such an apartment can satisfy people's basic needs. Despite its limited space, it can contain a lot of things within itself.

If we don't change the furniture structure, we can still create different atmospheres and demonstrate different lifestyles by changing the color of furniture.

Meanwhile, in doing so, we can enrich the product line and optimize the overall production system.

Next, we will explain in detail the color schemes that we've designed for three types of people.

First is the perception of color inspiration, then a systematical color analysis, and finally the design of color schemes.

The combination of furniture materials and of accessories at the spatial level will be examined to explore the connection between different colors.

The following examples are based on the plans of the apartments. Color combination in 3 directions.



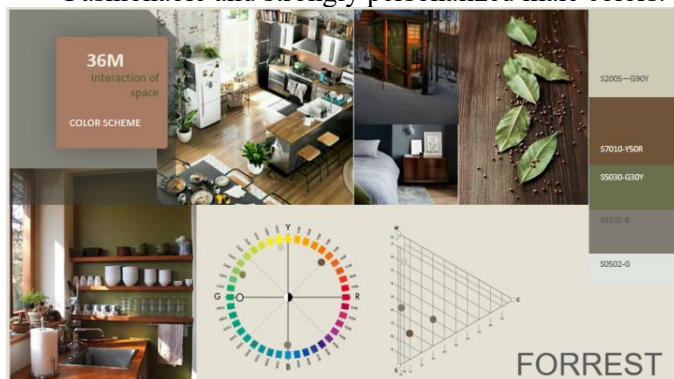
Scheme 1: A young “rebellious” and self-motivated boy, about 18-25 years old. He has a strong character, and used to study engineering in Europe. He doesn't like the boring furnishing style of his parents' house, but prefers more fashionable and personalized colors.

Forest Man Series

As to its hue selection, this series of furniture products mainly uses warm wood grain and cold medium grey, and the color of medium green which gives forth a sense of the forest is also used but only as an interspersing color. The colors S7010-Y50R and S5030-G30Y have the same whiteness, so they can produce some gradations of color, but the effect is harmonious. The overall

furniture color belongs to the blackness zone and the male color gamut. Modern wood texture and glossy dark grey, together with some interspersing medium green, light up the entire space.

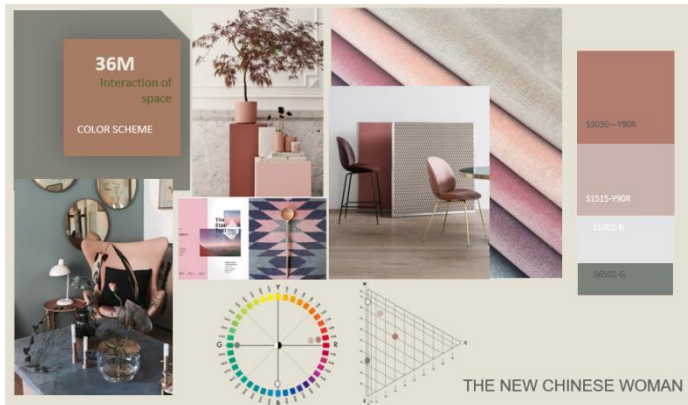
Fashionable and strongly personalized male colors.



Scheme 2 An independent and self-confident woman, about 22-28 years old. She is very busy with work, and often travels on business. As a “new woman”, she is both gentle and strong. Being a fashion chaser, she hopes that her furniture color can be exciting and heartening.

New Chinese Women Series

This series chooses pink, a soft female color, as its major hue. Specifically, it mainly uses two pink colors of the same hue, dark pink and light pink, and greyish-green is used as a contrast color. The soft pink color in the whiteness zone is the base color, together with the contrast color of greyish-green, the whole space highlights the softness and strength of women. As feminism prevails today’s world, new Chinese women are both tough and gentle.



Scheme 3 A world for two, a small but sweet home for the cohabiting couple. Due to their stressful jobs, they both prefer the Nordic style. They want their home to feel as spaciousness as possible, and wish that the home space can be both fresh and soft.

Home Series

This series of colors does a great job in simplifying what is complicated. Both the Nordic style and the Japanese style advocate the idea that colorlessness is also a kind of color, and their main aim is to make the entire space more relaxed and natural.

In this small world of 36 m² where a couple lives, the use of bright colors helps to maximize the space. This space only uses such colors as the natural and warm oak, purplish grey, and all-

matching warm white, which set off the fresh and soft life, and make the dwellers inside it feel more relaxed.



These three homes all have the same space and the same household products with the same functions, while when we design different colors for the household products according to their different users, the space is endowed with different lifestyles and also represents the lifestyle of its users.

Give free rein to your creativity and imagination! Bring your knowledge and experience into play, and use new colors boldly to create different living space.

The result: There is an important element in our lifestyle: color!

It just feels better if we can live in an environment full of colors that we like!

A SYSTEMATIC PROCESS IN DEVELOPING A COLOR SCHEME BASED ON LANDSCAPE AND URBAN ENVIRONMENTAL COLOR ANALYSIS

Yen-Ching Tseng^{1*}, Yuh-Chang Wei^{2*}

Chinese Culture University, 55 Hwa-Kang Rd., Yang-Ming-Shan, Taipei, Taiwan, R.O.C.

¹ *Department of Architecture and Urban Design, Faculty, Chinese Culture University, Taiwan*

² *Department of Information Communications, Faculty, Chinese Culture University, Taiwan*

*Corresponding authors: Yenching Tseng, yenching.tseng@gmail.com; Yuh-Chang Wei, ycwei@faculty.pccu.edu.tw

Keywords: Environmental color planning and design, Systematic process, Environmental color analysis, Color scheme

ABSTRACT

In recent years, environmental color planning and design tended to apply a scientific method in developing a color scheme. The aim of the current study is to analyze and to better understand the significance of an urban environmental color scheme from a systematic color analysis process. The color scheme project of Zhengbin Fishing Port, located in Keelung city, northern Taiwan, was chose for the study. Based on Jean-Philippe Lenclos's methodology of color geography, the environmental colors can be classified into chromatograms. The well-known NCS environment color survey tools adopted to collect the Zhengbin Fishing Port regional colors through photography, color patch mapping, color measurement, sampling, coding, and classification. An environment color database was established, which consisted of 269 NCS color patches. In accordance with the environmental color analysis, the color planner developed and carried out the color scheme. The results showed that the renovated multi-color combinations façade of seafront architecture complex at Zhangbin Fishing Port has successfully received widespread public attention. It has become a tourist attraction after its implementation through a systematic environment color analysis process.

INTRODUCTION

The theory of color geography put forward by the famous French colorist Jean-Philippe Lenclos [2] in the 1960s. The main focus of his work is on the collection, induction and extraction of local chromatograms to represent the color composition of a region, city or country, to illustrate the architectural color and local natural geographical environment (such as local materials, and to construct the relationship between the environment conditions and the human geography (local cultural traditions, customs, etc.). The work of JP Lenclos has the great influence on the research method in collecting and classifying environmental color data. Up to date, it is widely used in urban, architecture and environmental landscapes color planning.

Zhengbin Fishing Port, located in Keelung city harbor, northern Taiwan, was built in 1929. With the changes over the decades, the current urban environment was affected by the wet and rainy weather result in the rusted, mottled and faded color imagery. In order to highlight the local characteristics of Zhengbin Fishing Port, a scientific method adopted to develop a color scheme. The color scheme, based on Jean-Philippe Lenclos's methodology of color geography, used NCS environmental color survey tool [3] to conduct the regional local colors investigation and to develop a color plan. The objective of color planning is to maintain the balance between the color imagery of harbor city and Zhengbin Fishing Port area, to achieve "colorful diversity", and in support of a color scheme to enhance regional characteristics and cultural style of the

Zhengbin Fishing Port. A multi-color combinations façade of the seafront architecture complex is the target color scheme. See Figure 1.



Figure 1. Zhengbin Fishing Port located in Keelung city, northern Taiwan. A multi-color combinations façade of the seafront architecture complex is the target color scheme.

METHOD

A scientific environmental color survey conducted to collect regional colors information and to establish an environmental color database for further analysis. The investigation is through a systematic process using photography, color patch mapping, color measurement, sampling, coding, and classification. A subjective environmental color analysis will be evaluated by the color planner in order to develop a color planning strategy.

NCS Environmental Color Survey and Tools

NCS color system [1] was used for the survey. The use of NCS environmental color survey tools included digital camera, NCS color ticket, NCS colorimeter, NCS color software and NCS Chromatography Set. NCS colorimeter and color ticket comparison used for the measurements of color sampling. PhotoShop software is used for auxiliary analysis to establish the Zhengbin Fishing Port Environmental Color Database. See Figure 2.

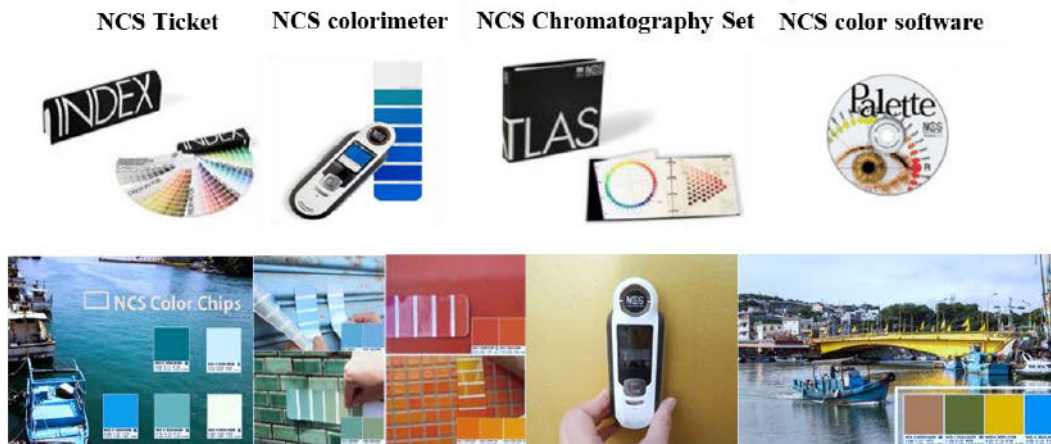


Figure 2. NCS environmental color survey tools (upper). Color survey conducted by adopting Lenclos's methodology (below).

The Procedure of Zhangbin Fishing Port Environmental Color Survey

All the factors affecting the color imagery of the landscape and urban environmental are included in the scope of investigation. Each of color samples recorded through material extraction, color matching, material lightness level measurement, on-site coloring sketches and photographs. The collected color data is analyzed, classified, and presented by means of chart chromatography. The procedure of environmental color survey has shown on Figure 3.

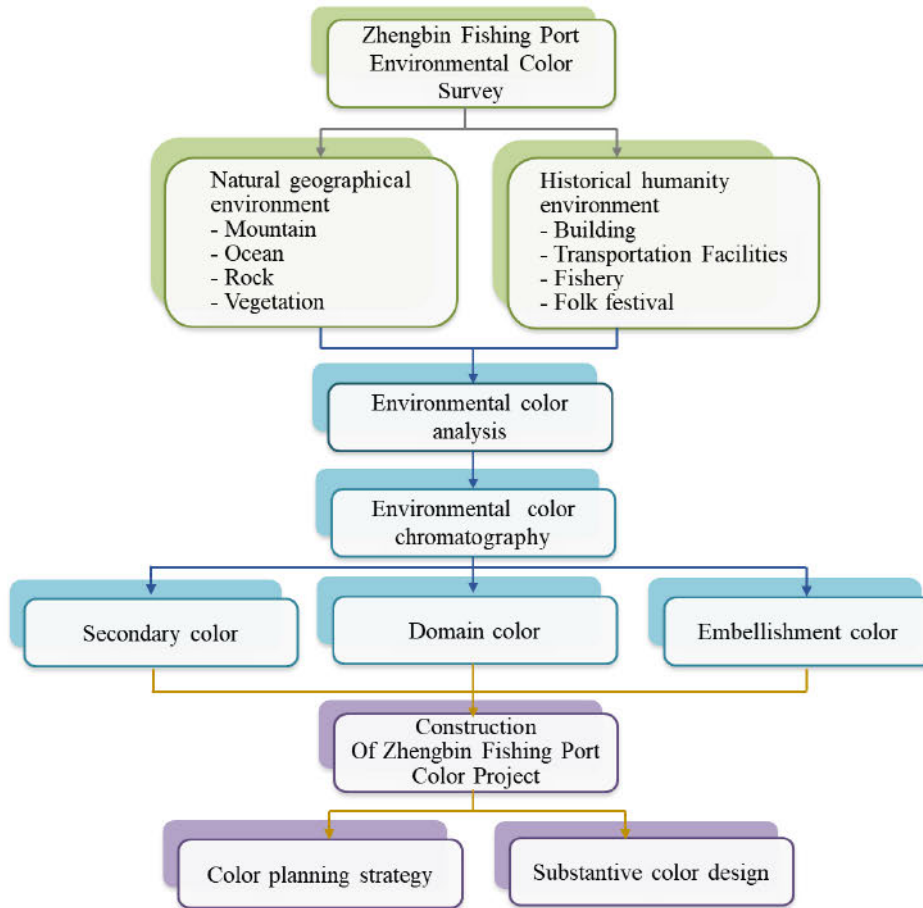


Figure 3. The flowchart of Zhangbin Fishing Port environmental color survey for the color planning and design

RESULTS

Environmental Colors Data Analysis

An environmental color database consisted of 269 color chromatograms, which extracted from the Zhengbin Fishing Port landscape and urban environmental, established and classified into hue categories (see Table 1). The color tones analyzed in each of domain color, secondary color and embellishment colors sections are described as in Table 1.

Table 1: 269 environmental color data classified and analyzed by hue range, chromatogram and color tone.

Hue Range		Chromatogram	Color Tone	
Natural	N	14	B/W gray scale	Embellishment color
Color	Y-Y90R	91	Medium-Low Lightness Medium-High Chroma	
	R-R90B	58	Medium-High Lightness Medium-Low Chroma	Secondary color
	B-B90G	51	Medium-High Lightness Medium-Low Chroma	Domain color
	G-G90Y	55	Medium-Low Lightness Medium-Low Chroma	

Further in-depth classification analysis of landscape and urban environmental colors [4] (see Table 2) in Zhangbin Fishing Port area found that regional colors were mainly based on large-area natural color - blue-green tone, supplemented by secondary area artificial color - warm embellishment color. The overall color image in this region appeared in a turbid tone with the high-lightness and low-low chroma.

Table 2: Classification analysis of landscape and urban environmental colors in Zhangbin Fishing Port area

		Landscape elements site	Chromatogram	Photos of color sample
Natural environment color	Sky			
	Sea			
	Harbor			
	Mountain			
Urban landscape color	Coastline			
	Architecture			
	Street			
	Facade			
Local humanistic color	Historical			<p>* Agenna Shipyard Relics * Tian Ho temple</p>
	Traditional			

The Color Scheme Planning & Implementation

The cause of the mediocre color resulted in the color scheme of the subsequent environmental color scheme that should be simplified to an orderly main color, and visually contrasted to enhance the regional characteristics and public interest. The collaborative discussions held by stakeholders, experts, scholars and the color planner to determine medium-high lightness and chroma of colors (warm colors) with higher contrast (see Figure 4), as the key tone for the façade of seafront architecture complex at Zhengbin Fishing Port.

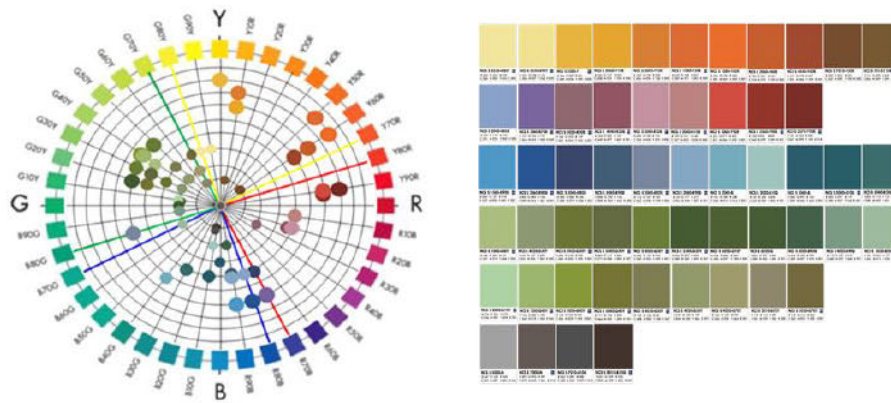


Figure 4. The color dataset, which analyzed by NCS Colour Circle and Chromatography, established based on the collaborative decision for the color scheme planning.

In accordance with the color selection from the color dataset, a proposed color scheme was designed by the color planner, based on color harmony scheme principle. The final approval of color selection of each building was decided by the residents. A renovated multi-color combinations façade of the seafront architecture complex is shown on Figure 5. It was found that color differences existed between NCS color patches and actual color paints.



Figure 5. The color painting for the façade of seafront architecture complex at Zhengbin Fishing Port complied with the results of systematic environmental color analysis.

DISCUSSIONS

Issues regarding the environmental color analysis of the natural geography and historical humanities around Zhengbin Fishing Port area are discussed as follow:

1. Urban color scheme is a complex and comprehensive work. The analysis of landscape and urban environmental colors needs a multi-dimensional viewpoint. It is necessary through a scientifically systematic process to investigate the overall appearance and characteristics of the geographical region objectively. The results of study indicated that a good color planning

strategies must look into both the macro and micro levels.

2. The results of the study indicated that the environmental color planning and design needs to concern some important factors as followings: (1) maintain continuity and order with adjacent colors, (2) keep color harmony with the surround spatial environment, (3) utilize the regional landscape characteristics in accordance with background architectural colors.

3. Urban color planning and design contain the strong publicity. The current project set up a good example that the domain colors selection for color scheme was decided according to the collaborative discussions from stakeholders, experts, scholars and the color planner. However, the residents' color preferences turned out to be a significant factor influencing the outcome of color scheme. It is a crucial to establish a smooth communication channel regarding the color consensus between stakeholders and the color planner that requires a great deal of efforts.

CONCLUSION

Zhengbin Fishing Port color scheme has captured public attention and compliments after the implementation of project. The new multi-color combinations façade of the architecture complex perceived quite harmonious with the harbor environmental landscape colors, which indeed enhanced the Zhengbin Fishing Port's regional characteristics and cultural style successfully. It has become a new landmark and tourist attraction (see Figure 6), which known as “Zhengbin Color Houses” that inspired from the Italy Venetian Island of Burano (colorful island).

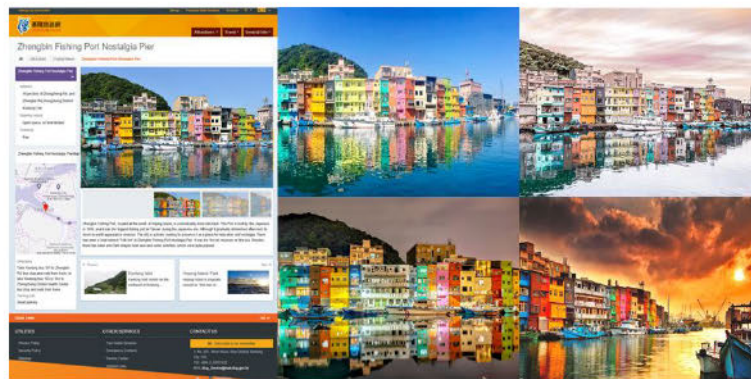


Figure 6. Keelung city government tourist website and popular photos posted by courtesy of the photographers.

ACKNOWLEDGEMENT

It is highly appreciated that all the information and materials of color project, funded by the Keelung city government, provided for this research is overwhelmingly. The photos used in this article by courtesy of the photographers are very grateful as well.

REFERENCE

1. Hård, A.; Sivik, L. & Tonnquist, G. (1996) “NCS Natural Color System - from Concepts to Research and Applications. Part I and II”. *Color Research and Application*. Vol. 21, p.180–220.
2. Lenclos, J. (1999) *Couleurs du monde*. Moniteur, Paris.
3. *Natural Color System*, https://en.wikipedia.org/wiki/Natural_Color_System1/
4. Qi, M.; Lu X. & Qian, Q. (2018) “Study on the Color Characteristics of Dalian City”. *Proceedings of 9th International Conference on Urban Planning, Architecture, Civil and Environment Engineering*. P.18~22. Kyoto: Japan.

STUDY ON REPRESENTATION BY COLOR OF "WAKUWAKU" FEELING

-Make a coloring book to get exciting emotional effects -

Hojoo Bae

*Kansei Engineering, Interdisciplinary Graduate School of Science and Technology, Shinshu University,
17st114c@shinshu-u.ac.jp, Shinshu University,3-15-1,Tokida,Ueda, Nagano ,386-8567, Japan*

Keywords: Waku Waku, Culture comparison, Feelings of excitement, Coloring book

ABSTRACT

Humans receive various information with our five senses. The sense that obtains the most information among them is visual. Particularly in the expression of emotion, "color" is also a medium for transmitting linguistic expressions of feelings as visual information. After rapid economic development in Japan, the challenge and motivation for new things from the existing generation to young people is diminished in recent society due to the declining population. The expression word, "Waku Waku" selected in the previous studies expresses excitement possessed in color - whether a certain kind of color is expressed and if differences appear by country, region, etc. This present presentation is for a coloring book created based on the results of "Waku Waku" a research in Japan, Republic of Korea and China from 2017 to until now.

1. Introduction

Human sensibility has become more noticeable with the major change in the global industry, attracting worldwide attention. In the study of the medium to which color is applied, it is the point where various fields such as design, psychology, physiology, electronics, physics etc. Research on psychological effects of color has been emphasized and developed more than ever. From my personal experience staying in Japan, many people have sought counseling and healing in order to alleviate the psychological anxiety of bullying at school and depression in their social lives. The more the mechanical industry develops, the more research to understand human sensitivity is needed for human beings. In human culture, words are used as means of expression. These words express the image in color and use language as a means of expressing human emotions. For the purpose of this study, only differences and similarities depending on gender and region were examined, which lead to opportunities to regain an "excitement feeling" which disappeared, and to be able to be link emotions that we are pleased by to the "excitement feeling".

2. Experimental

To collect data from within Japan, Republic of Korea and China using 12 colored pencils, size A4 paper, and having the subjects answer a few questions.

2.1 Subjects Used: 321men, 329 women. (Japan), 200(Republic of Korea), 165(China)

2.2 Age of subjects: 15 to 77

2.3 Colored Pencils Used: Yellow, peach, orange, red, pink, brown, light green, green, light blue, blue, and violet, black.

2.4 Duration: September 2017-Janunary 2019

2.5 Question Asked: 1, Gender 2, Age 3, Nationality 4, Occupation 5, Residency 6, longest place of residence 7, Draw something that excites those 8, Place in order the colors which were used from first to last.

3. Results and Discussion

3-1 Relation between Color and Shape

Kandinsky's theory shows that not only is there harmony shape and color, but there exists a relatively clear proportional emotional relationship in the effects of lightness and activity. The result of this survey also suggests the relationship between the lightness and activity to the word expressing the "exciting feeling". The younger the age, the more strongly the relationship of color and shape are seen in men. In Figs. 1 and 2, we wrote the words "bicycles" and "sweet foods", and they expressed the colors that correlate with that object.

Others express money and vehicles in the colors we recognize. In the line representation method, it was found that curves are much more expressed than straight lines as shown in Fig 3 and 4.



Figure 1.



Figure 2.

Male in their 20s (Japan) Female in their 10s (Japan)

3-2 Differences in Gender

Men tended to express drawings as a specific image (like a bicycle) as opposed to women, (heart ♥ or smile ☺), who would for example draw simple objects such as hearts or smiley faces. On the other hand, it was found that both men and women chose warm colors based on many rather than cold colors.



Figure 3



Figure 4

Male in their 10s (Chinese) Female in their 20s (Japan)

3-3 Age

As the age of these people get older, the time taken to answer the questionnaire becomes longer, many due to saying they have never felt the feeling of "Waku Waku" recently. Many also drew landscapes based on their experiences when they were young (Fig 5&6). There were no inherent difference in gender.



Figure 5



Figure 6

Female in their 20s (Korean) Female in their 50s (Japanese)

3-4 colors

For both men and women, the most chosen color was "red". The top three colors were warm colors: pink and orange respectively. Following that, fourth was yellow, expresses abstractly as seen in Figures 3 and 4. The tone is not strong & vivid, but instead pale and light. It seems that it was chosen because it has a tendency to show up brighter. (Fig 7)

From this survey, it is possible to explain that emotions have a close relationship with colors and shapes. It is clear that these results may vary when done on a larger scale due to the biology of humans, however this data proves that quantifiable data is possible to obtain.

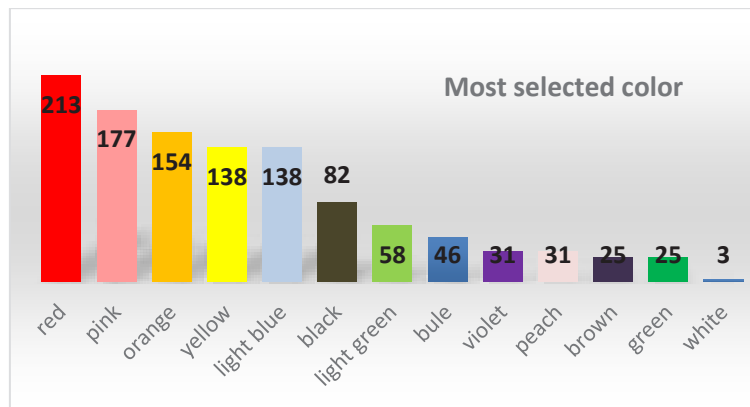


Figure 7.
Most selected color

3-5 conclusion

According to the research conclusion, we can learn a lot more things from the expression of curving line than of straight line. In the expression of curving line where the abstract expression are often used than the conceptual expression, there are countless ascending order spreading from the core to the outside, as well as the expressions soaring from the bottom to the above. We can see that in the linear expressions, there are enormous expressions spreading from the core to the outside, especially, as well as the expressions soaring from lower-left to upper-right. I would like to move on to make coloring books following this consequence, and would like to verify it. The example of coloring book will be displayed at ACA 2019Nagoya as a sample model. (Fig 8~10).

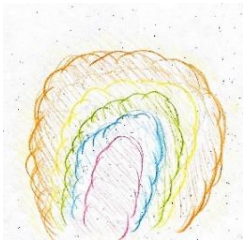


Figure 8

Female in their 20s (Japanese)



Figure 9

Female in their 20s (Japanese)



Figure10

Female in their 20s (Korean)

REFERENCES

1. Atsushi Kimura, Yoshifumi Wada, and Kaoru Nogu : The Influence of the Similarity of Emotional Effects on the Harmonious Relation between Shape and Color The Society of Society and Society, *Japanese Society for the Science of Design* 52 , No.P.1-8.2005
2. Atsushi Kimura: Consideration of Psychological Attributes and Emotional Effects of Morphological Colors, *Japanese Psychological Association*. Vol 20, 2002
3. Nodoka Ohmori, and Yumiko Wada: Gender differences in color preference and the psychological effect of color, *Health Science University*. Vol. 5, 67-76, 2009
4. Hojoo Bae and chika Sasaki.: Study on representation by color of "WAKUWAKU" Feeling -A Comparative research between Japanese and Korean University students- *Color The Society of Society and Society* 43 No.P.178,2019
5. Hojoo Bae: Comparison of idioms about color between Korea and Japan, *Color The Society of Society and Society* 36, No.P.176-177,2012
6. Hideaki Chijiwa: Why do human beings a Color's strange relationship with human psychology that at the mercy of color, Kawade Shobo Shinsha, japan.,1997
7. Fumie Minamoto : Gender differences between pictures, Tokyo shoseki, japan,1986

AUTOMATIZATION OF 2D-IMAGE RECORDING SYSTEM FOR ANALYSIS OF CHANGE IN FOOD APPEARANCE USING DOME ILLUMINATION WITH DIGITAL CAMERA

Aya Hirouchi¹, Hiroyuki Iyota^{2*}, Mai Isomi³, Hiroyuki Yamamoto², Hideki Sakai³

¹*Faculty of Mechanical Engineering, Osaka City University, Japan.*

²*Graduate School of Engineering, Osaka City University, Japan.*

³*Graduate School of Human Life Science, Osaka City University, Japan.*

*Corresponding author: H. Iyota, iyota@eng.osaka-cu.ac.jp

Keywords: process monitoring; drying; glossiness; automatic control; image analysis

ABSTRACT

The appearance of food, including its surface color and glossiness, is an important factor in the evaluation of quality. In general, the parameters associated with appearance change with time due to water evaporation and the chemical reactions that occur during thermal processing, drying, storing, and mundane exposure. To evaluate these parameters, quality control of food and process optimization is necessary. There are several available instruments for the measurement of the color and glossiness of flat and dry material surfaces. However, these tools are not suitable for the characterization of the appearance of food due to the combined effects of the roughness and moisture of food surfaces. Therefore, we have developed a device for the contactless measurement of color and glossiness using a digital camera and a dome-shaped illumination device. This instrument facilitates the acquisition of color images via specular component included (SCI) and excluded (SCE) modes for subsequent analysis with/without the shading of a region of the dome-shaped illumination.

In this investigation, we installed an automatic control system for the illumination device to capture the SCE and SCI images for long-duration monitoring. Electrical components were also installed to measure the temperature, humidity, and weight of food. The developed instrument facilitates the acquisition of images without the requirement of a human operator, while analyses of the color and glossiness change with time. Important experimental data can be obtained using this system, such as the effect of food appearance change on the process conditions.

INTRODUCTION

Color and gloss greatly affect the quality of objects/materials. For this reason, a quantitative evaluation of these indexes is required when considering the quality control of an object, such as the surfaces of processed food or building/gardening materials. However, natural objects such as food and building materials have complicated shapes and moisture is often present on the surfaces. Therefore, it is difficult to use a general contact-type colorimeter that requires close contact with the sample surface. To solve these problems, we have developed a non-contact two-dimensional (2D) color-measuring device using dome-shaped illumination and a digital camera to measure the entire complex sample [1]. In addition, we installed a light absorber, called a 'light trap', in the dome-shaped illuminator between the white dome surface and the object. By moving this light trap, we could obtain 2D images, of specular component excluded (SCE) and specular component included (SCI), recorded by a digital camera for analysis. The color of an object can be obtained from these images at the same time [2, 3].

In this research, to quantitatively evaluate the changes in color and gloss due to the drying of food and moisture in building materials, it is necessary to measure the color and gloss of materials for a long time in an arbitrary environment. Therefore, because long-term measurements are required, equipment was developed to automatically measure the temperature and humidity in the dome, as well as measure the sample mass change.

EQUIPMENT

Figure 1 shows an overview of the equipment that was remodeled. An LED was used as the light source (high color rendering LED, Ra 90, 29 W, 6200 K, illuminance 279.4 lx), as shown in Figure 1(a). The dome is made of white (opaque) acrylic; the light from the LED is reflected multiple times on the dome inner walls and irradiated from all directions on the upper surface of the sample. Thus, it is possible to suppress the occurrence of shadows due to unevenness of the sample surface. As shown in Figure 1(b) and Figure 2, a part of the upper wall surface of the dome is shielded by light traps (made of black polyester felt, at approximately 30° per light trap), such that light from the direction of the shaded body cannot be seen. By installing a single-board microcomputer (Arduino), it was possible to automate the movement of the light traps and photography, which has previously been done manually, using the optical sensor and DC motor.

A sample and a color chart (24 colors made by X-rite) with no specular reflection component from the light traps is recorded by a digital camera (Canon EOS Kiss 7) above the sample. The digital camera takes three shots while moving every 30°-position of the light traps. Then, the image analyzing software we developed in Python is used to extract and synthesize the lightest and lowest pixels from the three images. Finally, the SCI and SCE images [2] can be obtained.

Additionally, a new electronic balance was installed in the dome to measure changes to the moisture content. A temperature and humidity sensor (SENSILION, SHT75) was installed in the dome to measure drying conditions as well. The signal from the electronic balance can be stored in a personal computer at a predetermined time interval via RS-232C, and the temperature and humidity can be stored in an SD card.

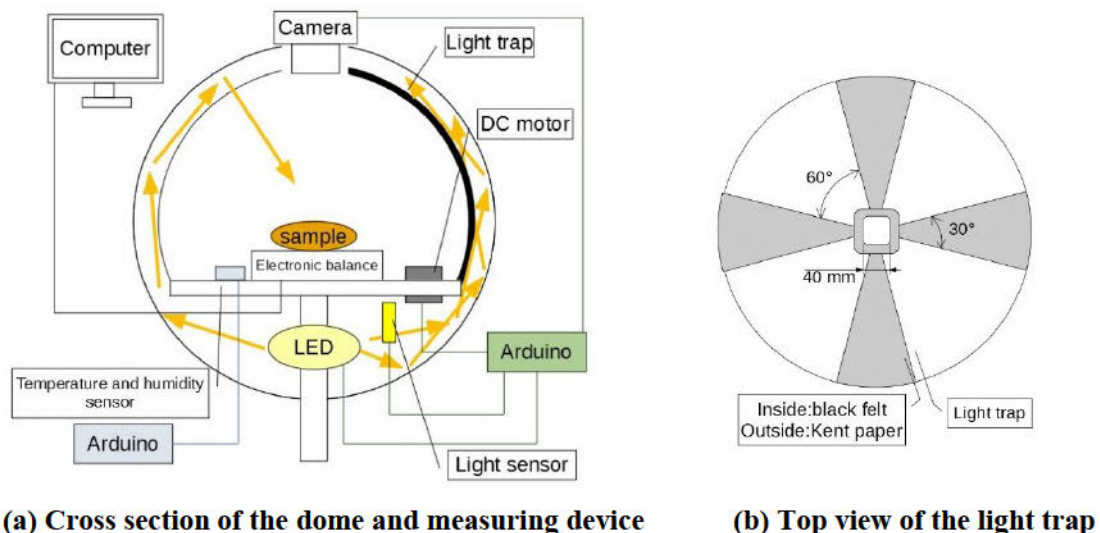


Figure 1. Overview of the developed equipment

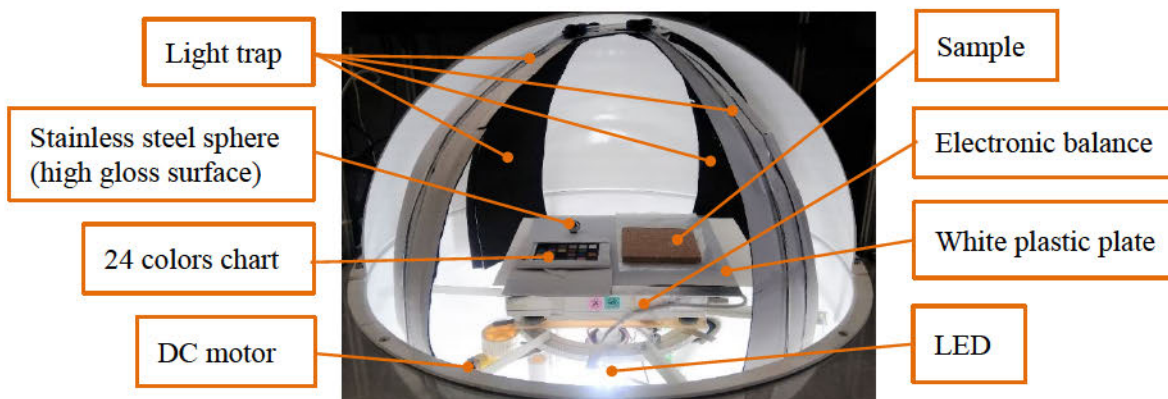


Figure 2. Photograph of the inside of the upper side

OPERATION TEST AND RESULTS

A wetted brick (JIS-B1, 120 mm × 120 mm, thickness 12 mm, dry weight 72.67 g) was used as a sample object, as shown in Figure 2. A white plastic plate was placed in the dome to record the 2D illumination distribution before the sample was placed on the stage in the dome. Then, the process was initiated in ambient conditions.

Figures 3 (a) and (b) show the SCE and SCI images before the process and those after 22 h elapsed as sample images, respectively. Here, it is demonstrated that this equipment can monitor the brick-drying process at room temperature for 22 h. In addition, the sample mass, and the temperature and humidity inside the dome were recorded. From these data, the temperature and humidity in the dome can be seen to have changed in the range of approximately 25–30 °C and approximately 35% to 50%, respectively. Furthermore, the mass of the sample continuously changed from 145.33 g to 102.77 g in this condition. Meanwhile, the moisture content of the brick decreased from 50.0% to 29.2% (wet-basis) over the 22 h.

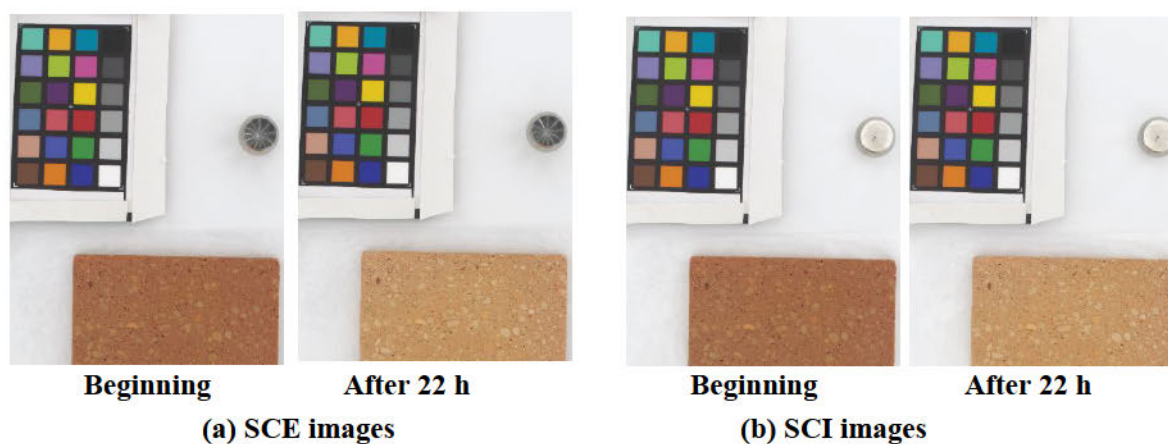


Figure 3. SCE and SCI images of the sample before and after drying

CONCLUSION

We developed an automatic experimental/recording system and demonstrated that not only can this equipment record the SCI and SCE images of an object, but can also measure the mass change

of the object during drying. Measurements of the drying conditions, such as the temperature and humidity, were also demonstrated.

REFERENCES

1. Sakai, H., Yoshikawa, S., & Iyota, H. (2013). Accuracy of color measurement by using digital cameras and the standard color chart, *Proc. of the 1st Asia Color Association Conference*, 248-251.
2. Yamamoto, H., Sakai, H., Kitamura, S., Takayama, M., & Iyota, H. (2018). Evaluation of Surface Color of Steam-Cooked Manju through Non-Contact Colorimetric, Measurement Using Dome Illumination: Effect of Processing Conditions, *Proc. of the 4th Asia Color Association Conference*, 172-177.
3. Sakai, H., Isomi, M., & Iyota, H. (2018). Non-contact colorimetric measurement using dome illumination for complex shape objects, *Proc. of the 4th Asia Color Association Conference*, 183-186.

TRANSPARENCY MEASUREMENT FOR JAPANESE FEMALE'S SKIN AND PHANTOM MODEL BY SRS (SPATIALLY RESOLVED SPECTROSCOPY INSTRUMENT) AND ESTIMATION WITH VIEWING STUDY.

Misao Takamatsu*and Kazuji Matsumoto

Spectral Application Research Laboratory Inc.

Nakaku Hayaumachou 2-7 Hayauma Bldg. 5F Hamamatsu City Shizuoka Pref. Japan

*Corresponding author: Misao Takamatsu, misao.ud@gmail.com

Keywords: skin colour, skin transparency, transparency measurement, scattering coefficient, spatially resolved spectroscopy

ABSTRACT

We developed SRS instrument, and we reported this instrument and its application in the 49th annual meeting held at Osaka (2018) and Colour measuring meeting held at Tokyo (2019) in Colour Science Association of Japan. By this instrument, absorbing coefficient of colourant substances like dyes or pigments and scattering coefficient of others for translucent substances respectively in visible range could be measured in physical theory. As a result, inverse function of scattering coefficient could be a transparent index of filler's substances on translucent materials. This index and SRS systems are effective for getting information of many translucent materials in non-invasive and non-destructive.

Meanwhile, the term of "Toumei-kan" is popularly used for the expression of beautiful skin in Japan. "Toumei-kan" means perceptual transparency in Japanese. Skin having "Toumei-kan" is strongly supported by Japanese women. As a word of "Toumei-kan" is including subjective and sensuous factor, an objective evaluation by connecting measurement result from an instrument with "Toumei-kan", is needed in beauty and cosmetics industry. But there is a controversial space in the relation between visual evaluation to "Toumei-kan" and actual scientific measured data of skin. Especially, the reports for the relation between physical transparency of skin itself and "Toumei-kan" induced from visual evaluation study are very few. One of reason is difficulty for measurement of skin transparency. We think we can contribute to such skin's colour research by using our SRS system.

We made transparent phantom models, measured it by SRS instrument and evaluated. And, we measured scattering coefficients of various aged Japanese female models by SRS instrument, and we gathered significant 6 index—"Toumei-kan", whiteness, clearness, thinness, redness, and complexion—through hearing sheet and viewing test. We will report the result of measurement by SRS and evaluation results to skin phantom and female's skin.

INTRODUCTION

"Toumei" means that an object is transparent in Japanese. "Toumei-kan" is the perceptual transparency sensing visually. This word is popularly used for the expression of beautiful skin in Japan. Skin having "Toumei-kan" is strongly supported by Japanese women. Naturally, the research on "Toumei-kan" is expected, and many studies have been reported in Japan.

Since "Toumei-kan" of skin is visual transparency, people might imagine that "Toumei-kan" is higher when physical transparency is higher. However, several papers that discuss factors related to skin whiteness instead of measurement of transparency have been reported. Seiya et al reported that

evaluation of “Toumei-kan” is correlated with L^* value of skin [1]. There are two reports that “Toumei-kan” increases as luminance of skin image increase [2][3]. Kuwabara introduced some physical factors of skin that contribute to “Toumei-kan” [4]. He explained that low melanin concentration and low hemoglobin concentration contribute to “Toumei-kan”. From these results, it is considered that “Toumei-kan” of skin is high, when the skin colour appears whitish.

On the other hand, there are few reports of physical measurements of skin transparency because it is difficult to measure the transparency of translucent objects nondestructively. Masuda’s report is known as a famous method of measuring skin transparency [5]. They throw light on the skin, blocked the surface reflected light with a slit, and detected the spread of light in the skin with a CCD camera. Visual evaluation score of Toumei-kan correlated with an index calculated from the internally reflected light. However, the cause of the high internally reflected light is not only the skin transparency but also other factors such as lower amount of pigments.

We developed SRS instrument for the main purpose of measuring skin transparency [6] [7]. This machine can measure the scattering coefficient (μ_s') and absorption coefficient (μ_a) separately. Inverse of the scattering coefficient ($1/\mu_s'$) can be assumed as skin transparency unaffected by pigments absorption. The purpose of this study is to research the relationship between physical transparency measured by SRS and perceptual “Toumei-kan”. We report the measurement results of created some skin phantoms, and the results of the measurement of 20 female models and visual evaluation of “Toumei-kan”.

SRS INSTRUMENT

The process of SRS measurement and calculation of scattering coefficient and absorption coefficient is schematically shown in the Figure 1. Figure 2 is image of SRS instrument. SRS is a method that measures spectral information at different distances from the incident light at the same time. And this is enough information to separately calculate the scattering coefficient and absorption coefficient from the light diffusion equation [8]. As our SRS instrument has 6 light receiving points, 6 relative reflections are measured. The scattering coefficient and absorption coefficient are calculated by solving 6 simultaneous equations.

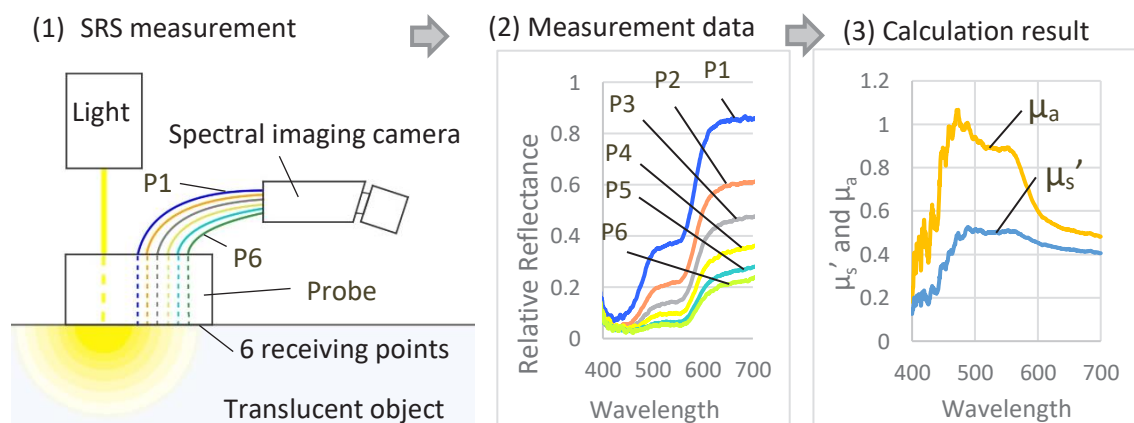


Figure 1. Pattern diagram of SRS measurement and calculation of scattering coefficient (μ_s') and absorption coefficient (μ_a).

(1) P1 is the light receiving point closest to the incident light on the probe. And there are 6 points in order. (2) When measured, 6 reflectance values are obtained. By substituting these values into the diffusion equation, 6 simultaneous equations are solved. (3) μ_s' and μ_a can be obtained.



Figure 2. Image of SRS instrument

EXPERIMENT

1. Skin phantoms

Table 1 shows a component list of the 4 skin phantoms. These phantoms were adjusted to a colour like Japanese female's skin using yellow, magenta and black ink. The ink concentration of 4 phantom was fixed. Milk was added to a phantom as scattering medium, and the concentration was changed. These phantoms were gelled with agar.

Plastic petri dish ($\Phi 85.7$ mm, D13.2mm) was used to create these phantoms. The thickness of these phantoms was 1 cm or more. These phantoms were taken into another glass petri dish lid and measured with SRS.

Table 1: Phantom composition (ml/100 ml)

	Phantom-1	Phantom-2	Phantom-3	Phantom-4
Yellow ink*	0.1			
Magenta ink*	0.038			
Black ink*	0.025			
Milk**	30	45	60	75
H ₂ O	70	55	40	25
Agar	2.5			

* "ink tank BCI-7e", canon (for inkjet printer), ** "Oishiigyunyu", Meiji

2. Measurement of skin transparency by SRS

Model's makeup was removed with baby oil (Johnson & Johnson) and skin lotion. Their skins were measured with a probe on their cheeks. Measurements were taken in a room with no lights, to avoid influence of lighting. The transparency index was calculated from the formula below (Eq. 1). \bar{y} is 10-deg colour matching functions.

$$\text{Transparency Index} = \frac{1}{\sum_{400}^{700} us'(\lambda) \cdot \bar{y}(\lambda)} \quad (1)$$

3. Visual evaluation

Visual evaluation was performed by looking directly at the models because skin transparency cannot be visually recognized in images. The evaluation was divided into 3 days. Total number of female models is 20. Their age is from 20's to 60's. Evaluators were ordinary women including models. There were 8-10 evaluators for each evaluation. During the evaluation, the model's face was illuminated by LED mini-light 600 (Ra: 92, 5000 K, Toshiba Lighting & Technology) at 920 lx. Evaluators approached about 2 m from a model so that model's skin could be observed closely. Model's makeup was removed except for eyes and eyebrows. Visual evaluation items are Toumei-kan, whiteness, and 4 skin terms that seem to be related to skin transparency: clearness, thinness, redness, and complexion. However, this report introduces results specialized on "Toumei-kan" and whiteness evaluations. The Evaluations is five phases (2, 1, 0 -1, -2). Evaluators were told to evaluate subjectively and intuitively. Evaluation of one model was executed in 1 minute.

RESULTS AND DISCUSSION

1. Skin phantom

Figure 3 are images of skin phantoms. The amount of scattering material can be recognized as the whiteness of the phantom. Phantom-4—with the most scattering material—appeared most whitish. You will be able to recognize the difference in transparency when you look at these phantoms directly. But you may not be able to recognize by the image. In order to visualize the transparency, phantoms were sliced into about 1 mm thick and sliced phantoms placed on a whiteboard and blackboard (Figure 4). Phantom-1 appears the most transparent but appears the darkest. Phantom-4 appears most opaque and whitish. Figure 5 shows the result of measuring Phantom-1 and Phantom-4 with SRS. Figure 6 show the scattering coefficient data for 4 phantoms. The scattering coefficient increases linearly as the concentration of scattering material increases.

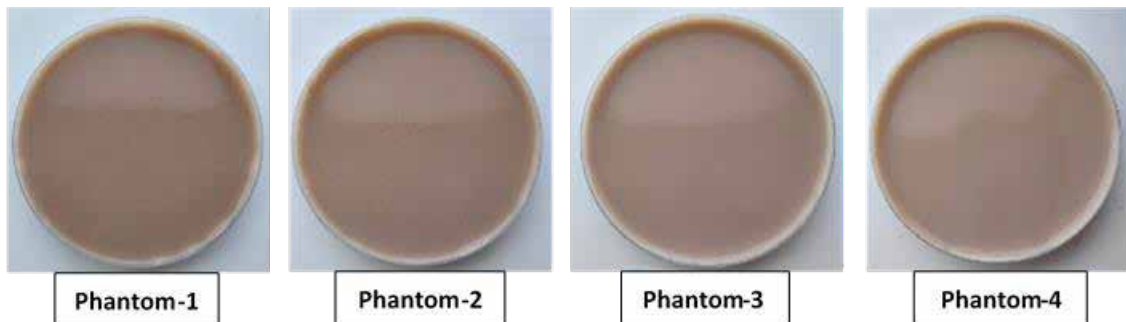


Figure 3. Images of skin phantoms

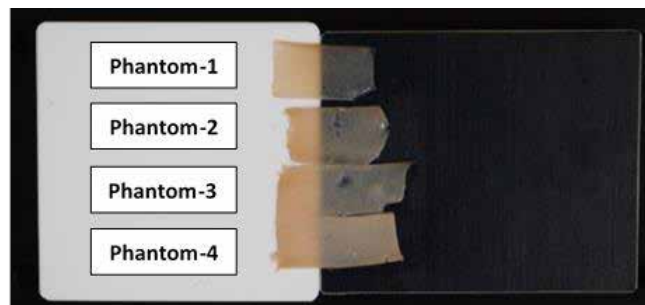


Figure 4. Images of sliced phantoms on a whiteboard and blackboard.

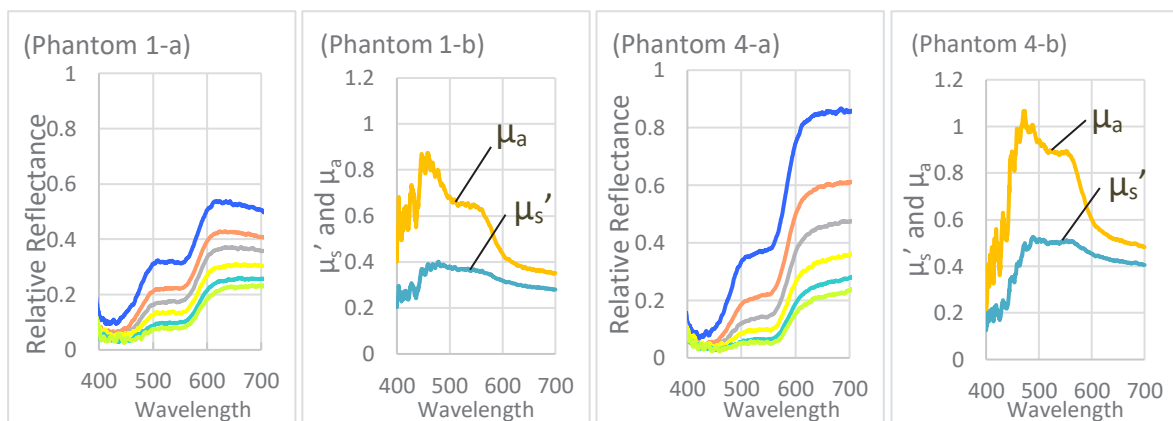


Figure 5. SRS measurement data of phantom-1 and phantom-4
Graphs of relative reflectance measured by SRS are (-a). Graphs of scattering coefficient (μ_s') and absorption coefficient (μ_a) calculated from transmittance are (-b).

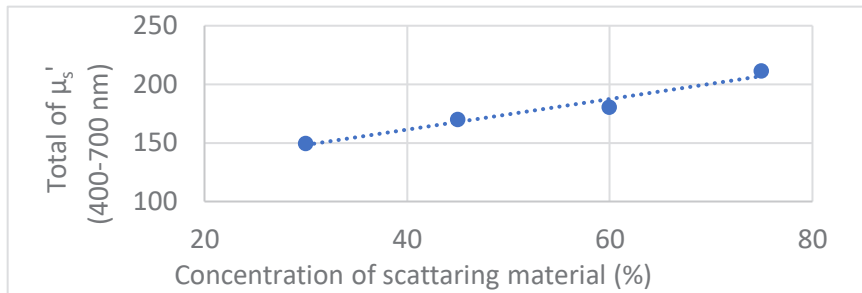


Figure 6. Total of Scattering coefficient (μ_s') between wavelengths 400 – 700 nm and scattering material concentration of phantoms

From this result, translucent objects become less transparent and appear more whitish when their scattering material concentration increases. Therefore, it is expected that skin with more scattering material appears whiter, if there is no individual difference in the amount of pigments in the skin tissue. In other words, skin with low physical transparency tend to appear whitish. Here is a notable phenomenon. From previous studies, it seems that “Toumei-kan” of skin is high, when the skin colour appears whitish. Assuming that whitish skin with a lot of scattering material tend to be perceived as highly “Toumei-kan”, perceptual transparency of skin is higher when physical transparency is lower. That means “Toumei-kan” of skin contradict its own meaning of term.

2. Visual evaluation

The correlation coefficient between visual evaluation of “Toumei-kan” and whiteness was 0.813, that is, perceptual “Toumei-kan” has a positive correlated with perceptual whiteness. This supports previous studies that skin with highly “Toumei-kan” has higher luminance, higher L^* or low pigment concentration.

The row of “all models” in Table 2 is correlation coefficient between transparency index and visual evaluation score. Both correlation values are very low. However, since the amount of pigments varies from person to person, the effect of physical transparency may not be uniform. Therefore, the three pigments—Melanin, Deoxyhemoglobin (deoxyHb) and Oxyhemoglobin (oxyHb)—was quantified from the adsorption coefficient measured by SRS. According to each index of these pigments, models were divided in half as mentioned below. A high melanin group/a low melanin group, a high oxyHb group/a low oxyHb group, and deoxyHb group/a low deoxyHb group. This quantitative calculation cannot be shown in this report. It is because there is not enough verification of the quantitative calculation of the pigments. Table 2 shows the correlation coefficient between transparency index and visual evaluation score in each group. In the low index groups, there is little correlation. But, most of the high index groups, correlation values are higher than values of all models. Therefore, it is thought that physical transparency affects perceptual “Toumei-kan” and whiteness for skin with a lot of pigments.

Table 2: correlation value between transparency index and evaluation score

Groups	Evaluation items	
	Toumei-kan	Whiteness
All models	-0.064	-0.139
Low Melanin	0.016	0.000
High Melanin	-0.457	-0.413
Low deoxyHb	0.062	-0.001
High deoxyHb	-0.569	-0.722
Low oxyHb	-0.169	-0.105
High oxyHb	0.423	0.101

In the high melanin or deoxyHb groups, the transparency index negatively correlates with whiteness score and “Toumei-kan” score. Skin phantoms appeared whiter when scattering material concentration was higher and transparency was lower. Also, in human skin, the skin colour might appear whiter when the physical transparency is lower. Even when there are many dark pigments in skin, strong scattering might hide these pigments and make the skin appear whiter. People might tend to perceive visual transparency in whitish skin. However, as mentioned above, there is a contradiction that perceptual transparency is high even though physical transparency is low.

On the other hand, high oxyhemoglobin group has a positive correlation value in “Toumei-kan” evaluation. This means that “Toumei-kan” of skin is high score when the physical transparency is high. In skin with relatively high amount of oxyhemoglobin, “Toumei-kan” might be increased when these pigment’s colour can be seen through for the high physical transparency. This case seems more faithful to the meaning of “Toumei-kan”.

In any case, it was suggested that “Toumei-kan” are affected by interaction of physical transparency and the amount of each pigment of the skin. Therefore, in order to quantify “Toumei-kan”, in addition to physical transparency, an accurate pigments index calculated from the absorption coefficient is required. As the measurement data of human skin transparency and pigment content increase, it will deepen understanding not only of “Toumei-kan” but also other skin appearance impressions.

CONCLUSIONS

SRS instrument was able to measure the difference in phantom transparency. And, it was found that the translucent object appears more whitish when the scattering is higher: the transparency is lower. Visual evaluation and measurement of female models suggested that perceptual “Toumei-kan” and whiteness of skin were affected by the interaction between physical transparency and pigments amount. Therefore, for the study of skin colour and appearance, it might be necessary to measure both physical transparency and pigment content.

REFERENCES

1. Saiya, T., Nomura, M., Takashi, H., (2002). Analysis of linguistic structure of "skin transparency" and physiological parameters of the skin. -Comparison between young and elder-. *The Japanese journal of ergonomics*, 38, 486-487.
2. Nakanishi, Y., Igarashi, T., Okajima, K., (2017). Quantitative relationships between image statistics or colourmetric values and skin transparency. *JCSAJ*, 41(6), 29-30.
3. Nishimuta, D., Igarashi, T., Okajima, K., (2014). Effects of colour and luminance on perceptual translucency of human skin. *The journal of the institute of image information and television engineers*, 68(12), J543-J545.
4. Kuwabara, T., (2010). Measurement of skin translucency. *Japanese journal of optics*, 39(11), 524-528
5. Masuda, Y., (2010). Methodology for evaluation of skin transparency and skin darkness. *FRAGRANCE JOURNAL*, 6, 37-43.
6. Takamatsu, M., Matsumoto, K., (2018). Development of skin transparency meter using SRS. *JCSAJ*, 42(3+), 83-86.
7. Takamatsu, M., Matsumoto, K., (2018). Proposal of colourimetry by spatially resolved spectroscopy. *IGC Proceedings year 2018*, 4-9.
8. Bruulsema, J. T., Hayward, J. E., Farrell, T. J., Essenpreis, M., & Patterson, M. S., (1997), Optical Properties of Phantoms and Tissue Measured in vivo from 0.9-1.3 μm using Spatially Resolved Diffuse Reflectance. *SPIE*. 2979, 325-334.

THE EFFECT OF COLOR FILTERS ON BEAUTY PHOTOGRAPHY

Chanida Saksirikosol^{1*} Ladinpat Artsawameathawong², Songpon Raksa² and Jarunee Jarernros²

¹*Color Research Center, Rajamangala University of Technology Thanyaburi, Thailand.*

²*Department of Advertising and Public Relations Technology, Faculty of Mass Communication Technology, Rajamangala University of Technology Thanyaburi, Thailand.*

*Corresponding author: Chanida Saksirikosol, e-mail: chanida_s@rmutt.ac.th

Keywords: Color Filters, Skin tone, Advertising, Advertising Photography, Beauty Photography

ABSTRACT

Nowadays the competition of the beauty business is increasing. The advertisement in the beauty business is commonly using the model who has the body talent but difficult to find out.

In advertising, the technique of making artificial beauty photograph beauty is needed. Particularly, the skincare products need to show the beauty of the model. This research aimed to investigate the suitable color filters for white, yellowish white and tan skin tones in term of beauty photograph. Lighting and model posture were kept the same in every photograph. Two-color filters, pink and brown, were used to take a photo of white, yellowish and tan skin models. These photographs were presented on the LCD display (27 inches, EIZO) one by one to the observers and then they were asked to assess the beauty of the photograph. The viewing distance was 40 centimeters. The observers were students from the department of Advertisement and Public Relations Technology, the faculty of Mass Communication Technology, RMUTT. The five scales were used to assess the beauty impression; 1=lowest beauty, 2=low beauty, 3=fairly beauty, 4=beauty, and 5=most beauty. The limit time of the assessment for each photograph was 10 seconds. The result suggested that the pink color filter gave a good beauty impression on the photograph of white and yellowish white skin model and brown color filter good on tan skin tone.

INTRODUCTION

Beauty photography was used for the advertising of a variety of skincare products to show the features of the product and to persuade the consumer to make a purchase. An important thing that makes beauty photography look attractive is the models. Generally, the model must have healthy skin in order to show the effectiveness of the product. Therefore, the special model, called body talent, is hired to represent the healthy skin. The body talent has a relatively high cost, resulting in the high cost of photo processing.

In the photography production process, there are many methods to improve photography quality, such as retouching and make-up which take longer time and require skills in the process. The control quality of the photo in the shooting process can save a lot of production time.

The important steps in the photography process that can make the image more beautiful are the lighting procedures which affect the color of the image and the quality of light. The use of a filter with the lighting procedure is one method to differentiate photography.

This research aimed to study the effect of color filters on beauty photography for white, yellowish white and tan skin tones by using 20 color filters in the photography production process.

METHODOLOGY

For the shooting process, the direction of the main light was set at the slightly front of the model and the fill light was at the opposite of the main light as shown in Figure 1. Then, 20 colored filters in pink and brown tone were alternately used when shooting the photos as shown in Figure 2.

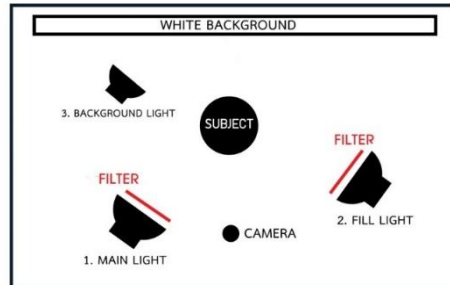


Figure 1. Plan of Lighting



Figure 2. The 20 Color Filters

The models used in the photography production process were in 3 skin types which are white, yellowish white and tan skin tone as shown in Figure 3.

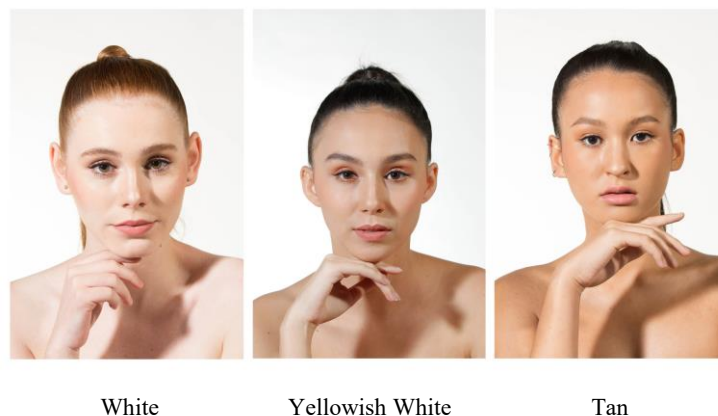


Figure 3. Skin Type

In the experimental room where the room illuminance kept constant at 300 lux, the photographs, one by one, were shown to 30 subjects through 27-inch EIZO monitor at the distance of 40 centimeters as shown in Figure 4. Then, the subjects evaluated the photographs that display healthy skin.

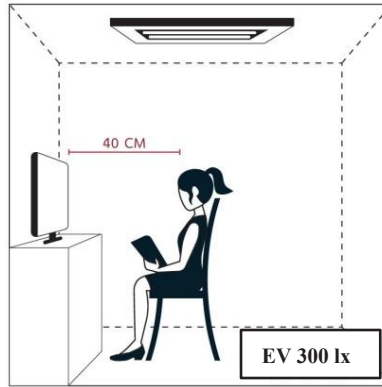


Figure 4. Experimental Room

RESULT

For the evaluation result, the effect of color filters on beauty photography for white, yellowish white and tan skin tones was shown as the following Figure5.

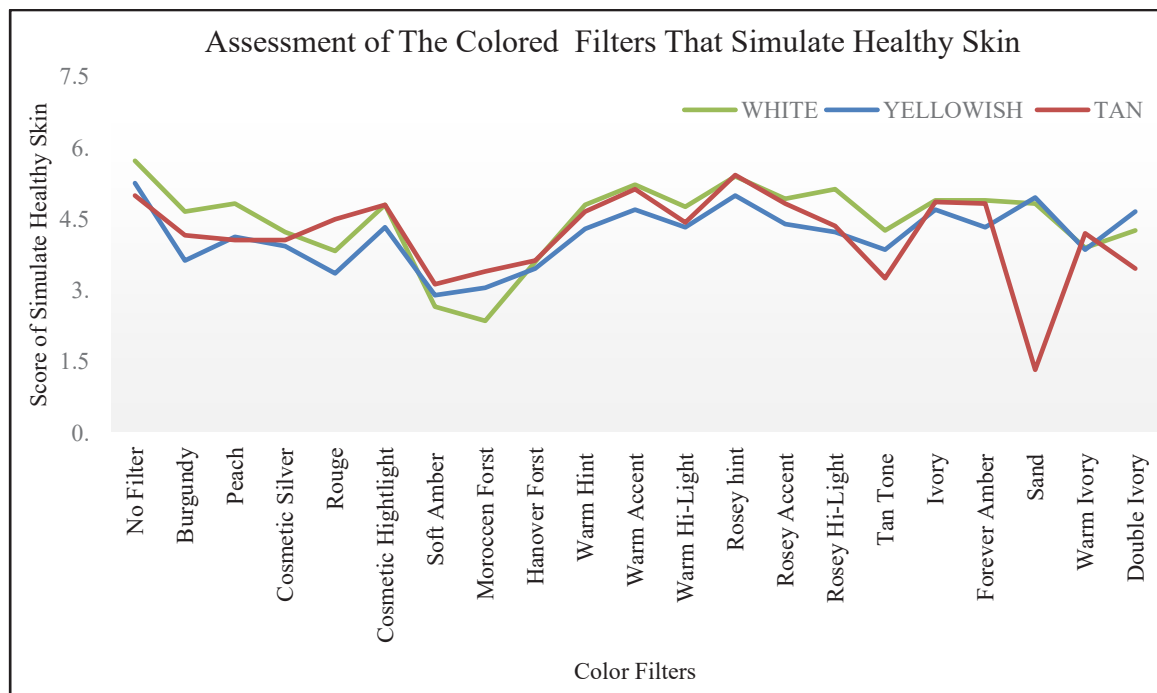


Figure 4. Assessment of The Color Filters

The result of colored filters that made the model's white skin healthy was Rosey Hint color filter, followed by Sand color filter and Warm Accent color filter, respectively.



The result of colored filters that made the model's yellowish white skin healthy was Rosey Hint color filter, followed by Warm Accent color filter and Ivory color filter, respectively.



The result of colored filters that made the model's tan skin healthy was Rosey Hint color filter, followed by Sand color filter and Rosey Accent filter, respectively.



The result showed that Rosey Hint color filter is a filter suitable with every type of skin tone and can show the healthy because it has the highest average value from 20 color filters. The color for the second and third color filter is different according to the skin color of each model.

CONCLUSION

The result showed that Rosey Hint color filter is a filter suitable with every type of skin tone and can show the healthy because it has the highest average value from 20 color filters. The color for the second and third color filter is different according to the skin color of each model.

ACKNOWLEDGEMENT

This Research was financially supported the by Faculty of Mass Communication Technology, Rajamangala University of Technology Thanyaburi, Thailand.

REFERENCES

1. François Giard & Matthieu J. Guitton. (2010). Beauty or realism: The dimensions of skin from cognitive sciences to computer graphics.
2. Elizabeth Hungerford and others. (2013). Coverage error of commercial skin pigments as compared to human facial skin tones.
3. Heliane Sanae Suzuki and others.)2011(. Phototype comparison between caucasian and asian skin types.

The color black is most important and special for making professional wrestlers attractive and fearful.

Tomohiko Akagi¹, Satoshi Ikehata², and Takeharu Seno^{1*}

¹*Faculty of Design, Kyushu University, 4-9-1 Shiobaru, Minami-ku Fukuoka, Japan.*

²*National Institute of Informatics, 2-1-2 Hitotsubashi, Chiyoda-ku, Tokyo, Japan.*

*Corresponding author: Takeharu Seno, seno@design.kyushu-u.ac.jp

Keywords: CG, Professional Wrestling, Heel, Psychological experiment, black

ABSTRACT

We examined what visual characteristics are important for the impressions of professional wrestlers. We conducted subjective estimations of the impressions of 30 Japanese pro-wrestlers. Also, we made virtual CG pro-wrestlers and conducted a psychological experiment comparing and estimating their impressions. The results showed us that some visual features create them more attractive or more evil. In conclusion, we found the fact that the color black is very special for creating attractive and evil professional wrestlers.

INTRODUCTION

Recently, in Japan, professional wrestling is becoming much more popular among all generations (Tokyo Shoukou Research, 2018; Nakamura, 2018). We examined what visual characteristics especially what colors are important for facilitating the attractiveness of the heel professional wrestlers. Recently, professional wrestling is becoming much more popular in Japan. In professional wrestling, there are two types of wrestlers, i.e. baby face and heel wrestlers. We wanted to know what visual characteristics including colors, are important for facilitating the attractiveness of the professional wrestlers.

Experiment 1

In Experiment 1, we conducted subjective estimations of the impressions of 30 Japanese pro-wrestlers. We obtained 9-item-subjective estimations, i.e. (total) Attractiveness, Nice (facial) looking, Justice, Nasty, Hateful, Youthfulness, Reliability, Strength, and Manly. We used a 10-point scale rating, for these estimations. This experiment was conducted on the internet by using Google Form. 28 volunteers (16 males, 12 females) participated in this experiment. They were ranged from 21 to 56 years old. The obtained subjective total attractiveness of the wrestlers, was significantly correlated with the nice (facial) looking of them. The subjective fearfulness was not correlated with the total attractiveness.

The image statistics showed us that the less colored and lower luminance can facilitate the impression of fearfulness. The luminance and colorfulness were significantly and negatively correlated with the attractiveness and positively correlated with fearfulness and hatefulness. In short, the color black can be a symbol feature for the heel.

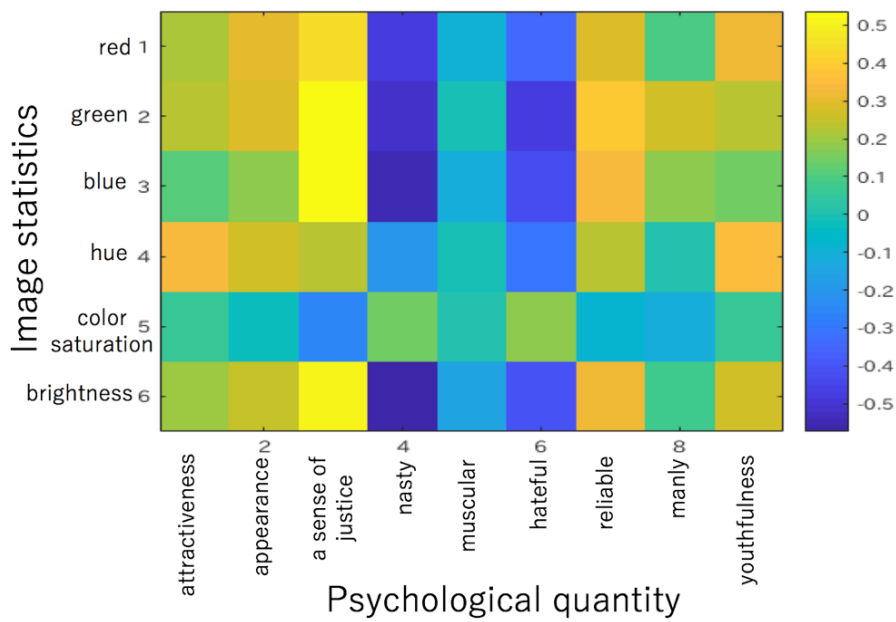


Figure 1. The correlation analyses between the image statics and impressions of professional wrestlers.

Experiment 2

In Experiment 2, we conducted a phenomenological experiment. 58 participants reported freely their subjective impressions about a famous Japanese heel character, “Baikin-Man”. Also, we obtained some free descriptions about visual features, and characteristics, of some real-existing heel wrestlers. Both two phenomenological reports, showed us that the color “black” is most effective to make the impression of “heel” and “villain”. These results suggested that the color black is special for the heel.

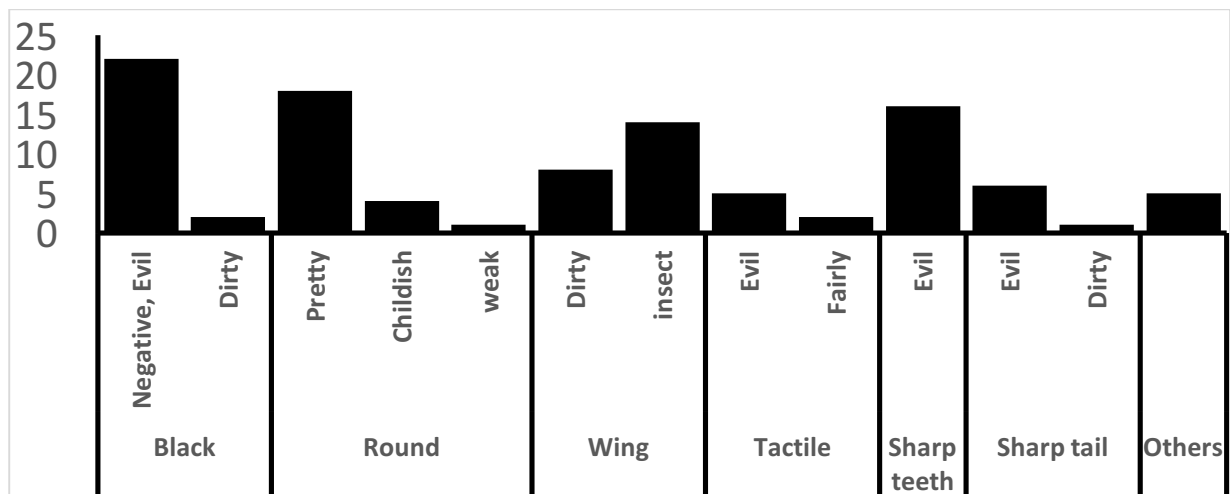


Figure 2. The results of phenomenological experiment, i.e. the impressions and those inducers of BAIKINMAN.

Experiment 3

In Experiment 3, we made 48 virtual CG pro-wrestlers and conducted a psychological experiment estimating their impressions. We set three wear-colors (red, black and white), two hair-colors (gold and black), two face types (baby face like, and heel like faces), two lengths of hair (long and short), two lengths of the wear (short and long). There were 48 types in the virtual pro-wrestlers in total. We obtained subjective impressions of the attractiveness and fearfulness of these 48 virtual wrestlers. We used a 10-point scale rating, for these estimations. 35 volunteers participated in this experiment. This experiment was conducted on the internet by using Google Form, again.

The results showed us that some visual features created them more attractive or more evil. For example, the black wear was perceived most attractive and most fearful rather than the red and white wears. Golden hair was perceived more fearful and less attractive than the black hair. The perceived attractiveness and fearfulness were negatively and significantly correlated, again.



Figure 3. Different conditions in the color of tights and hairs.

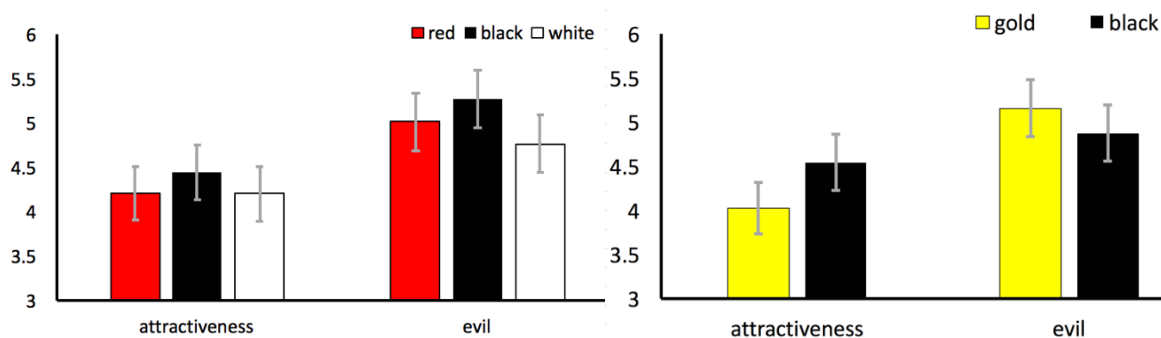


Figure 4. The results of the effects of colors on impressions of professional wrestlers.

General Discussion

All through three experiments, it was repeatedly reported that the color black is very important and special for making a heel pro-wrestler more attractive and fearful. We can conclude that the color “black” is special for the heel pro-wrestlers.

ACKNOWLEDGEMENT

This work was supported by MEXT KAKENHI (Grant number JP26700016, JP17K12869, and JP18H01100) to TS. Part of this work was carried out under the Cooperative Research Project Program of the Research Institute of Electrical Communication, Tohoku University.

REFERENCES

1. Tokyo Shoukou Research (2018). 新日本プロレスが復活、過去最高の業績を更新へ. 2018. 06. 01. http://www.tsr-net.co.jp/news/analysis/20180601_01.html (in Japanese language)
2. Nakamura, R. (2018年9月2日). 【ブシロード】木谷取締役に聞いた『イケる!』と思うビジネスのタイミング 【新日本プロレス・バンドリ!】 参照先: ウレぴあ総研: <http://ure.pia.co.jp/articles/-/303150?page=3> (in Japanese language)
3. Sports Graphic Number PLUS AUGUST 2018 ProWrestler プロレス総選挙 2018. (2018年7月10日). (in Japanese language)
4. Culin Stewart. (1907). Games of the North American Indians. 1-846. Government Printing Office, Washington D.C.
5. Ball, Michael R.,1990,Professional Wrestling As Ritual Drama In American Popluar Culture,The Edwin Mellen Press. (江夏健一監訳・山田奈緒子訳,1993,『プロレス社会学』,同文館.)

RELATION BETWEEN CONTRAST IMPACT OF TWO-PIECE GARMENTS AND KANSEI EVALUATION

Kohei Takaishi^{1*}, Kahoko Imazu³, Junko Fujimoto³,
Tomoharu Ishikawa², Shino Okuda³, Miyoshi Ayama²

¹*Graduate School of Regional Development and Creativity, Utsunomiya University, Japan.*

²*Graduate School of Engineering, Utsunomiya University, Japan.*

³*Faculty of Life and Science, Doshisha Women's College of Liberal Arts, Japan.*

*Corresponding author: Kohei Takaishi, mc196842@cc.utsunomiya-u.ac.jp

Keywords: Contrast Impact, Floral Pattern, Real Clothes, KANSEI evaluation, Fashion

ABSTRACT

Percentage of people who show unobtrusive interest in fashion seems to decrease because of diversity of values and spread of fast fashion. However, many young people still pay attention to fashion whether they are fashionista or not. Based on the observation in public spaces, we noticed that most people wear two-piece garments (blouse & skirt, or shirt & pants, etc.) with some degree of some kind of contrast such as the shirt and skirt of the same hue but different lightness, or a reddish check shirt with a simple blue-jeans etc. Thus, we assumed that people try to make some degree of contrast impression between the upper and lower garments. We call it “contrast impact” in this study. The aims of this study are to measure the strength of contrast impression of two-piece garments as the scale of “contrast impact” using real-clothes, and to investigate its relation to various KANSEI evaluation words.

In the experiment, we used mini-torsos put on simple blouse and skirt. Twenty-eight combinations of two-piece garments composed of the blouse made of cotton cloth (the same floral pattern of 5 colors of black, red, yellow, green and blue) and skirt of uniform achromatic cotton cloth (white, gray 1, gray 2, and black of which lightness is about 9.5, 7, 4, and 1.5, respectively) were prepared as test stimuli. Twelve combination of the same style but the blouse is also made of uniform achromatic cotton cloth were prepared as reference stimuli. Average luminance of the blouse and skirt of all stimuli was measured using 2D color analyzer (Konica-Minolta, CA-2500). Two experiments, Experiment 1: pair comparison for contrast impact, and Experiment 2: KANSEI evaluation, were carried out.

In the Experiment 1, each of the test stimuli was compared with each of the reference stimuli, and the observer was asked to answer which stimulus gives stronger contrast impression. For each of test stimuli, a modified contrast between the blouse and skirt of reference stimulus is employed as horizontal axis and percentage of the answer that the impression of the test stimulus is stronger than that of the reference is plotted in the vertical axis. Horizontal value that provides equivalent strength of contrast impression, 50% in the vertical axis, was employed as the contrast impact value of the test stimulus.

In the Experiment 2, only the test stimulus was presented to the observer, and she was instructed to evaluate the test stimulus by indicating a score of each of six KANSEI evaluation words on a seven-point scale (not at all:0, slightly:2, rather:4, and very much:6).

Relations between the contrast impact and each of the KANSEI evaluation words were analyzed. In the test stimuli of black floral blouses, positive correlation was found for “Bright” and “Showy”, negative correlation was found for “Subdued” and “Plain” evaluations. In the test stimuli of chromatic floral blouses, negative correlation was observed for “Pretty”, “Neat”, and “Bright”. Results suggest a possibility of KANSEI evaluation estimation using the contrast impact value.

INTRODUCTION

Percentage of people who show deep interest in fashion seems to decrease because of diversity of values and spread of fast fashion. However, many young people still pay attention to fashion whether they are fashionista or not. Based on the observation in public spaces, we noticed that most people wear two-piece garments (blouse & skirt, or shirt and pants, etc.) with some degree of some kind of contrast such as the shirt and skirt of the same hue but different lightness, or a reddish check shirt with a simple blue-jeans etc. Thus, we assumed that people try to make some degree of contrast impression between the upper and lower garments. We call it “contrast impact”, and preliminary experiment using real clothes achieved certain results [1, 2]. However, the test stimuli, combinations of blouse and skirt, were limited to those with black skirt only, and patterns of blouses in different colors were not the same. Therefore we increase the variation of combination of blouse and skirt using the same pattern of blouse for different colors. The aims of this study are to measure the strength of contrast impression of two-piece garments as the scale of “contrast impact” using variety of combinations of real-clothes, and to investigate its relation to various KANSEI evaluation words.

EXPERIMENT

In the experiment, we used mini-torso putted on simple blouse and skirt. Twenty-eight combinations of two-piece garments composed of the blouse made of cotton cloth (the same floral pattern of 5 colors of black, red, yellow, green and blue) and skirt of uniform achromatic cotton cloth (white, gray 1, gray 2, and black of which lightness is about 9.5, 7, 4, and 1.5, respectively) were prepared as test stimuli. Twelve combination of the same style but the blouse is also made of uniform achromatic cotton cloth were prepared as reference stimuli. Table 1 shows the stimuli combinations.

Two experiments, Experiment 1: pair comparison for contrast impact, and Experiment 2: KANSEI evaluation, were carried out. Figure 1 (a) shows the experimental set-up, and Figure 1 (b) and (c) show the stimuli presentation in Experiments 1 and 2, respectively. Vertical and horizontal illuminances at the mini-torso were about 650 lx and 350 lx, respectively. Average luminance of the blouse and skirt of all stimuli was measured using 2D color analyzer (Konica-Minolta, CA-2500).

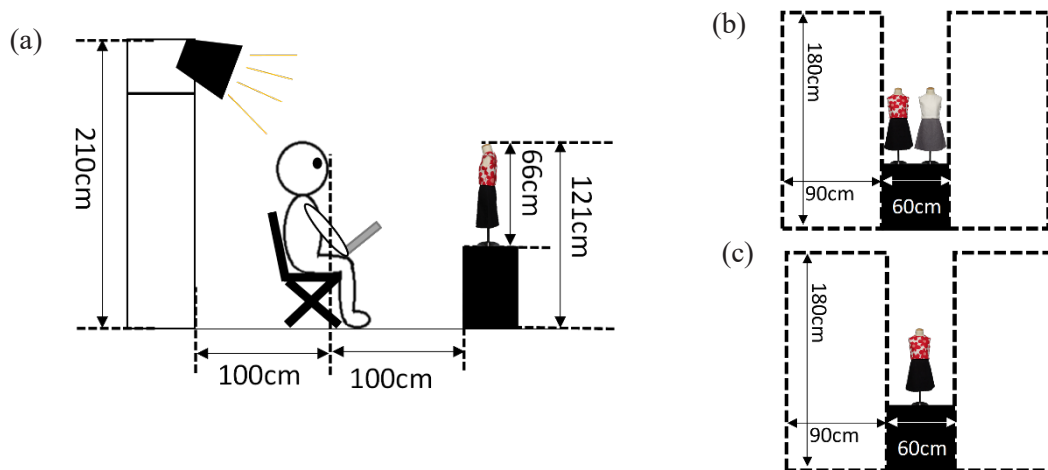


Figure 1. (a): Experimental set-up. (b) and (c): Stimuli presentations during pair comparison for the contrast impact and KANSEI evaluation, respectively.

In the Experiment 1, each of the test stimuli was compared with each of the reference stimuli, and the observer was asked to answer which stimulus gives stronger contrast impression. All combinations of the test and reference stimuli were presented 4 times throughout the experiment that means 1344 comparison were done for each observer. Figure 2 shows the stimuli presentation of pair

comparison for the contrast impact. In the Experiment 2, only the test stimulus was presented to the observer, and she was instructed to evaluate the test stimulus by indicating a score of each of six KANSEI evaluation words on a seven-point scale (not at all:0, slightly:2, rather:4, and very much:6). Six adjectives, “subdued”, “pretty”, “neat”, “bright”, “plain”, and “showy” were employed.

Five female students in each of the School of Engineering and Faculty of Life and Science participated the experiment.

Table 1. Stimuli Combinations

	Test stimuli	Reference stimuli
Blouse	   Black Small Black Middle Black Large	  White Gray1
	    Red Large Yellow Large Green Large Blue Large	  Gray2 Black
Skirt	    White Gray1 Gray2 Black	
Total	28 combinations	12 combinations

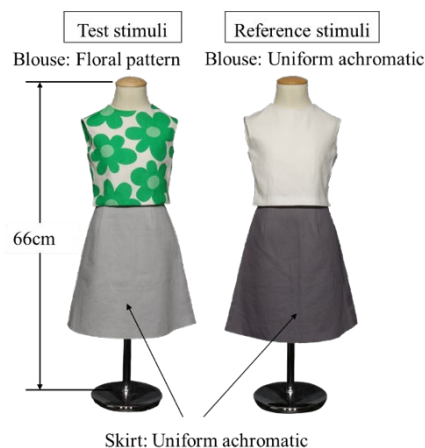


Figure 2. Stimuli presentation of pair comparison for the contrast impact experiment

RESULTS

Contrast Impact

Figure 3 indicates the way to derive the contrast impact value. The frequency that the test stimulus was chosen in 40 pair comparisons (4 repetitions for 10 observers) is plotted on the vertical axis. Horizontal axis indicates the measure of contrast impact derived from the luminance values of reference stimulus as follows. Based on the luminance measurement using the 2D color analyzer, the higher luminance of the blouse and skirt is denoted L_{high} , and the lower luminance is L_{low} . Modified Mickelson contrast with weighing coefficients k_i and k_j , indicated in the Eq. (1), was calculated and employed as the horizontal axis.

$$\chi = \frac{k_i \cdot L_{high} - k_j \cdot L_{low}}{k_i \cdot L_{high} + k_j \cdot L_{low}} \quad (1)$$

As shown in the figure, the frequency of the response that the impression of the test stimulus is stronger than that of the reference decreases as the contrast in the horizontal axis increases. Horizontal value that provides equivalent strength of contrast impression, corresponding to 20 times in the vertical axis, was employed as the contrast impact value of the test stimulus. Thus results were fitted using sigmoid function, and the point on the horizontal axis corresponds to 20 times (=50%) is determined as the contrast impact of the test stimulus. After several trial and error, we found that assigning different k_i for the cases of white, gray 1, gray 2, and black skirt gives good fittings for all combinations. Values of k_i for white, gray 1, gray 2, and black skirt are 2.0, 1.1, 0.6, and 0.5, respectively. In the cases of gray 1, gray 2, and black, these values correspond to k_j in Eq. (1) in the

combinations with lighter colors. For example, in the combination of white blouse and skirt of gray2, L_{high} and L_{low} correspond to the luminances of white and gray2, respectively. Therefore, 2.0 and 0.6 are assigned to k_i and k_j , respectively.

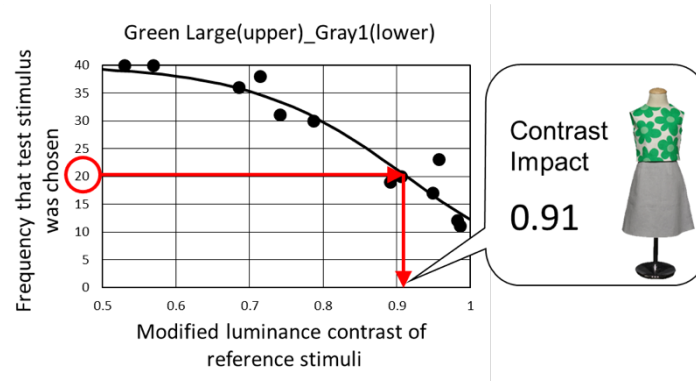


Figure 3. Way to derive the contrast impact of the test stimuli

Figure 4 shows the contrast impact values for all combinations. The combination with white skirts has higher contrast impact values in the achromatic blouses, while the combination of black skirts has higher contrast impact values in the chromatic blouses. In particular, the combination of the black-small-size blouse with black skirt is significantly lower than others. This is because the pattern of the black-small-size blouse is fine and looks nearly uniform blackish color as a whole in the viewing distance of 100cm in this study, although the pattern is still visible. Contrast impression of the combination was very weak resulting very low contrast impact value [3, 4]. On the other hand, the contrast impact value of the yellow-large-size blouse with the white skirt is lower than the others. This is because the luminance of the petal part of the floral pattern is high and the ground color is white which shows continuity to white skirt, and the contrast impression to the observers became weak.

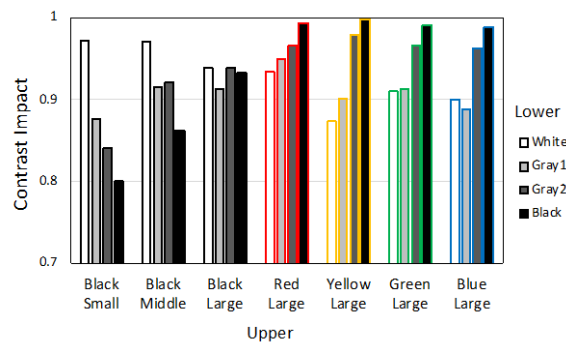


Figure 4. Contrast impact values for all combinations

Figure 5 shows the average evaluation score of “showy” in all combinations. Obviously, chromatic blouses show higher scores than achromatic blouses. Among the combinations with chromatic blouses, yellow and red are relatively high and blue are low. Among the achromatic colors, the evaluation scores increase as the floral pattern size of blouse increases from small, medium to large in all skirts. Figure 6 shows the average score of “pretty” in all combinations. Here also, higher rating scores are found for the combinations with white skirt for all blouses.

Common tendency shown in Figure 5 and 6 is that the rating score is the highest in the combinations with white skirt, the second highest are either with gray 1 or with black skirt, and those with gray 2 are the lowest.

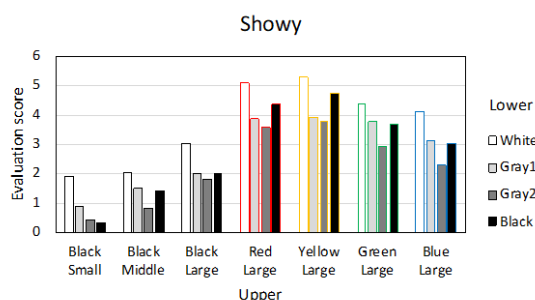


Figure 5. Evaluation score of "Showy"

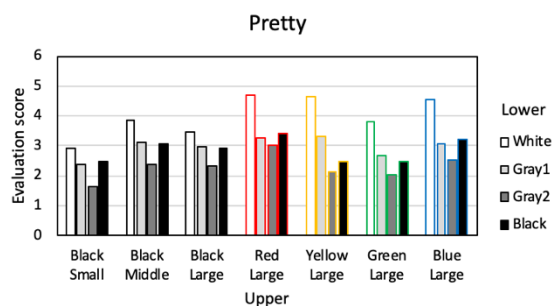


Figure 6. Evaluation score of "Pretty"

Comparing Figure 4 with Figure 5 and Figure 6, it is difficult to explain KANSEI evaluations such as "showy" and "pretty" using only the contrast impact values, although it contributes to some degree. In the "showy" results, scores of the combinations with white skirt are always high, so the average value of the luminance of the blouse and skirt was taken as one of the explanatory variables. In addition, since chromatic blouses have higher scores overall, average metric chroma of blouse is also taken into consideration. A multiple regression analysis with three variables was performed by adding the contrast impact.

Figure 7 and Figure 8 show the relationship between the standardized measured values and estimated values for the "showy" and "pretty" evaluations. The multiple regression equations for the two adjectives are shown in Eq. (2) and (3).

$$Y = 0.36 \cdot X_1 + 0.63 \cdot X_2 + 0.22 \cdot X_3 \quad (2)$$

$$Y = 0.73 \cdot X_1 - 0.10 \cdot X_2 + 0.001 \cdot X_3 \quad (3)$$

Where Y is the KANSEI evaluation score, X_1 is the average value of the average luminance of the blouse and skirt, X_2 is the average metric chroma of the blouse, and X_3 is the contrast impact value. The above three types of explanatory variables were selected mainly considering the "showy" explanation, but results for other adjectives, such as "bright" and "neat", were explained well ($R > 0.90$). However, as shown in Figure 8, the estimation of "pretty" is relatively worse. Results for "subdued" and "plain" did not show high correlation either. Factors other than these explanatory variables are needed to be investigated.

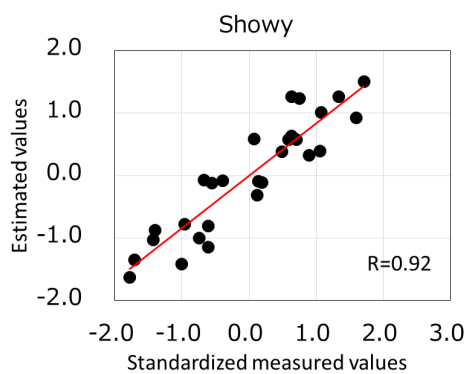


Figure 7. relationship between the standardized measured values and estimated values “Showy”

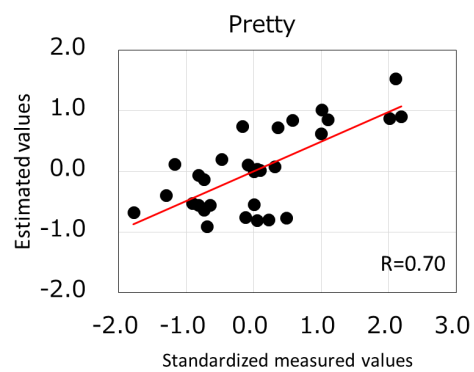


Figure 8. relationship between the standardized measured values and estimated values “Pretty”

CONCLUSION

Using the modified Mickelson contrast of the luminance of upper and lower garment of the reference stimuli (combinations of various achromatic blouse and skirt), the result of contrast impression evaluation for two-piece garments (combinations of various chromatic patterned blouse and achromatic skirt) were approximated fairly well. The contrast impact value for each combination of the test stimuli was defined using the value that gives equivalent contrast impression.

KANSEI evaluation experiment was conducted in parallel for six kinds of adjective pairs, “subdued”, “pretty”, “neat”, “bright”, “plain”, and “showy”. Multiple regression analysis using average luminance of the upper and lower garments, the average metric chroma of the blouse, and the contrast impact value was successful to explain the results of KANSEI evaluation experiment except for “pretty”.

ACKNOWLEDGEMENT

This research is supported by the Grant-in Aid from the Japan Society the Promotion of Science (No. 16K1250719 and K12179)

REFERENCES

1. Ayama, M., Tomoharu, I., & Tagaya, M. (2017). Contrast Impact of Two-Piece Garments. *Proceedings of the 13th AIC Congress 2017*.
2. Takaishi, K., Tomoharu, I., Okuda, S., & Ayama, M. (2018). Evaluation of Contrast Impression of Two-Piece Garments – Proposal of a New Index, Contrast Impact –. *Japan Society of Kansei Engineering 2018*. In Japanese.
3. Takaishi, K., Imazu, K., Fujimoto, J., Tomoharu, I., Okuda, S., & Ayama, M. (2019). The Influence of Size and Color of Pattern on Contrast Impact of Two-Piece Garments and KANSEI Evaluation. *Color Science Association of Japan 2019*. In Japanese.
4. Ayama, M., Takaishi, K., Tomoharu, I., & Okuda, S. (2019). Effect of Colorimetric Values and Contrast Impact Value on KANSEI Evaluations of Two-Piece Garments. *Japan Society of Kansei Engineering 2019*. In Japanese.

Color Laparoscopic Image Diagnosis for Automatic Detection of Coded Defect Region

Norifumi Kawabata^{1*} and Toshiya Nakaguchi²

¹ *Department of Information Sciences, Tokyo University of Science, Noda, Chiba, Japan*

² *Center for Frontier Medical Engineering, Chiba University, Chiba, Japan*

*Corresponding author: Norifumi Kawabata, norifumi@rs.tus.ac.jp

Keywords: Laparoscopic Image, Peak Signal to Noise Ratio (PSNR), S-CIELAB Color Space, CIEDE2000, Support Vector Machine (SVM)

ABSTRACT

At present, it is advanced the medical application for multi-view 3D, 4K (Quad Full HDTV, 4K UHD TV), 8K (8K UHD TV) image and video from starting engineering, broadcasting fields. And then, it is advanced every day that R&D for a new diagnosis method based on the image processing technology to support the surgical operation. On the other hand, in previous, the professional medical doctors and health care workers carried out the most of medical image diagnosis manually. As a result, it is possible to judge images accuracy in detail by human eyes, however, there is disadvantage at least that it takes a lot of time, and often occurs oversight of diagnosis because of fatigue. However, by appearing of large-scale and high-performance computer system in the past decade, it is enabled to construct the diagnostic imaging system using artificial intelligence actively. It is enabled to approach from not only medicine field but also information engineering, medical engineering. Therefore, the fusion of different research field is needed. Actually, there are many methods for surgical operation support. In this study, we consider support based on image processing technology seeing from information engineering field. In the case of carrying out surgery, medical doctors and health care workers always gaze to display, and then, they check which body region is treated one by one. Therefore, medical images are needed to present the display screen correctly. It is not clarified how degradation is perceived. Of course, we hope there is no degradation for display to carry out health care work. In this paper, first, we generated medical images cut as frame still image from laparoscopic video acquired by endoscopy. Using these images, we processed to encode and decode by H.265/HEVC in certain image regions, and we generated evaluation images. Next, we evaluated objectively seeing from the coded image quality by using PSNR (Peak Signal to Noise Ratio), considering the automatic detection of coded defect region information. Furthermore, we analyzed for color information by measuring both the luminance using S-CIELAB color space and the color difference using CIEDE2000. Finally, we try to classify effectively using Support Vector Machine (SVM), and we discussed including the automatic detection of coded defect region information whether it is possible for application of medical image diagnosis or not.

INTRODUCTION

The medical application of multi-view 3D images and 4K (Quad Full HDTV, 4K UHD TV), 8K (8K UHD TV) images as starting point of engineering and broadcasting is advanced, and then, it is ongoing for R & D of a new diagnosis method based on image processing technology to support surgery. On the other hand, in the medical image diagnosis field, medical doctors and medical workers carry out the most of diagnosis manually. This is advantage that it is possible to judge correctly and in detail for one by one. This is also disadvantage that it takes time, it often occurs oversight by fatigue at least. By large-scaling and speeding up of computer system, it is enable to

construct diagnostic imaging system using artificial intelligence actively, and then not only the approach from the medical field but also the approach from information and computer technology, medical engineering are enabled, and the fusion of different fields is needed. Actually, there are various methods for surgery support [2]. In this study, we consider support based on image processing technology seen from information and computer technology. In the case of operating surgery, medical workers always gaze display and check one by one what body region they carry out. Therefore, it is needed for images to present on display correctly. It is not clarified to perceive how degree of degradation is occurred on display. To carry out medical work, we hope this degradation should be lower.

Thus far, we studied on multi-view 3D image quality assessment [3], [4], [5]. In this case, we used 3D CG and uncompressed images in the engineering field. However, laparoscopic images (including medical image) used in this study are not always uncompressed, and image quality is not always good condition. Therefore, we need to consider image quality in the medical image diagnosis. It is hard for the only image quality to assess index of the medical image diagnosis since there are various medical images, and then laparoscopic video used in this study is different for property and status of use in particular. Also, there is a difference between color and grayscale. In color images, since it is not enough for affection by color information to reflect objective image quality such as PSNR (Peak Signal to Noise Ratio), it is hard for the only objective image quality to judge the coded image quality generally. Therefore, it is enabled to judge generally by applying color information (including brightness, color difference) and classifier.

As previous study, in the case of occurring coded defect by H.265/HEVC with all or certain viewpoints of multi-view 3D CG image, we diagnosed this image automatically by computer, and then we assessed and estimated quantitatively from point of view of the coded image quality how coded defect is enable to detect [6]. As a result, in the case of occurring the coded defect with all or certain viewpoints, we found knowledge that it is possible to detect from the point of view of coded image quality. However, this is a result based on images in the engineering field, and it is not clarified for result of medical images. Other previous study is considered degradation by coding in the engineering. However, it is not clarified for degradation of medical image [7]. Therefore, first we considered whether it is possible or not to diagnose medical image automatically using laparoscopic image enabled to support surgery in single viewpoint image.

In this paper, first we generated evaluation images after encoded and decoded by H.265/HEVC for certain image regions by using medical frame images cut from laparoscopic video acquired in endoscopy. And then, we assessed objectively from the point of view of the coded image quality by using PSNR, supposing automatic detection of coded defect region information. On the other hand, we analyzed color information measuring each luminosity by using S-CIELAB color space including visual spatial frequency characteristics, and each color differences by using CIEDE2000. Finally, we discussed including the automatic detection of the coded defect region information whether these results are applied for medical image diagnosis or not by setting classifier parameter by Support Vector Machine (SVM) effectively. This study is expanded and improved from [8].

RELATED WORK

In [9], they propose medical image diagnosis support using three-dimensional image information, and then, they are enabled to simulate laparoscopic virtual surgery. In [10], they propose algorithm to carry out 3D reconstruction suiting real time process using stereoscopic laparoscopy arranged two cameras. In [11], they propose the ultrasonic image superposition system to the endoscopy image, and then they assess accuracy of image superposition, and finally they show usefulness by animal experimentation as surgery support based on augmented reality (AR). In this study, we consider application for medical image diagnosis from a point of view of the image processing, coded image quality as medical engineering from the image informatics field.

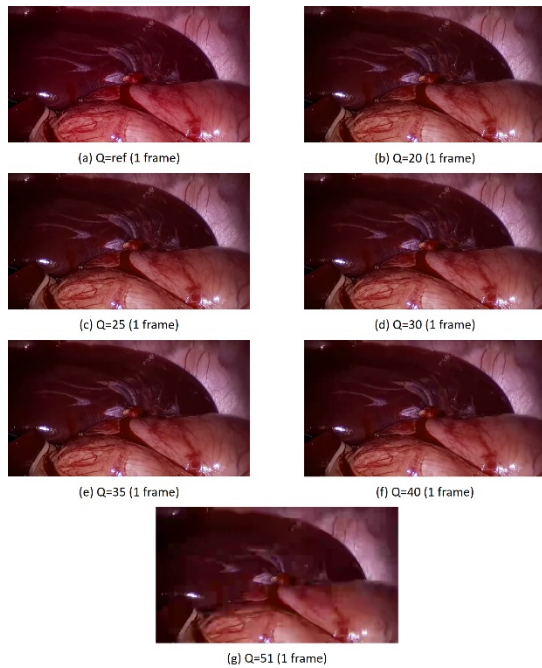


Fig. 1: Medical images used in this study

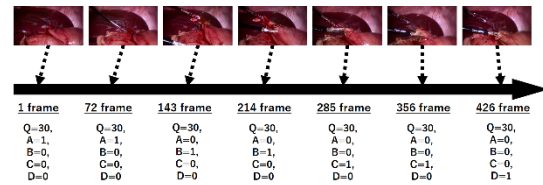
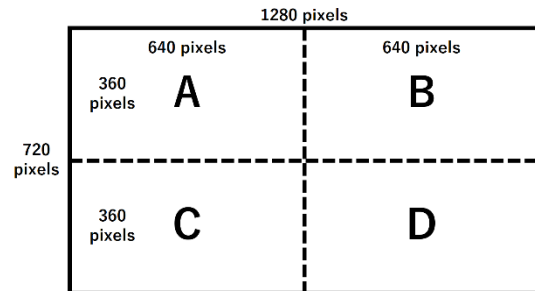


Fig. 2: Introduction of frame images



(Attention!) For each image region, in the case of processing of coding, it is defined as 1, in the case of no processing of coding, it is defined as 0.

Fig. 3: Image region used in this study

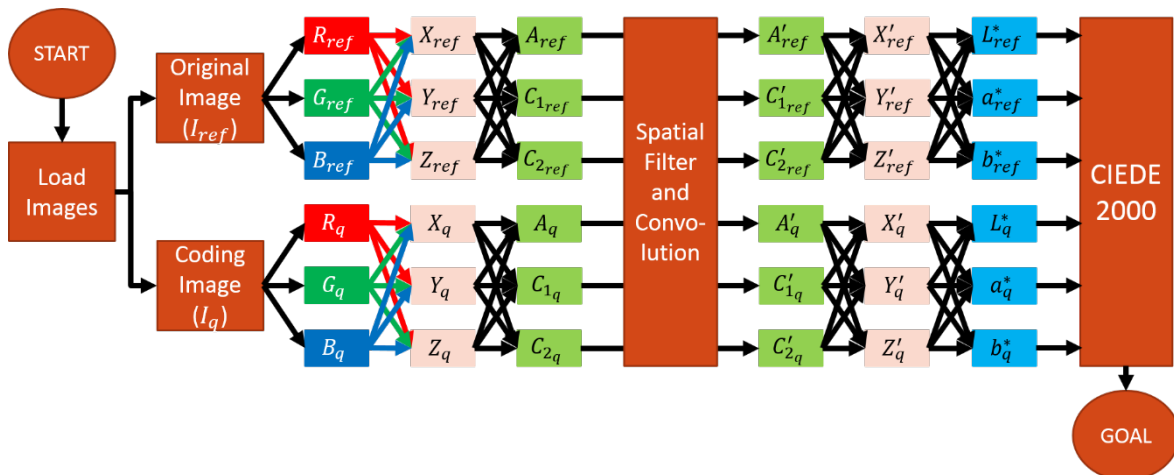


Fig. 4: Flowchart from loading images, transforming to S-CIELAB color space, CIEDE2000

EXPERIMENT

Medical image used in this study is frame image cut from surgery video (about 15 secs) under laparoscopy filmed around liver and stomach acquired in endoscopy such as Fig. 1. In this study, we do not carry out specific treatment.

Both evaluation image generation and image processing procedure are (1)-(6) as shown below. In this study, we try to process automatically for image processing by assessment.

- (1). First, we process cutting as frame still images from surgery video under laparoscopy (hereinafter, this is called laparoscopic image or video.). In this study, we cut 426 frame images from surgery video.
- (2). Next, for these frame images, we select seven frame images per interval of 71 images as shown in Fig. 2.

- (3). For seven frame images, we carry out the coded defect processing for certain image regions by H.265/HEVC [12]. In this study, we divide one image into four regions as shown in Fig. 3. Here, $A = 1$ in Fig. 2 is to process coding in image region shown in Fig. 3.
- (4). After the coded defect processing, for the laparoscopic frame original image and evaluation image, we assess the coded image quality objectively by using PSNR.
- (5). We load both original image and evaluation image (such as coded image) of laparoscopic frame image, and then we calculate luminosity L^* after transforming to S-CIELAB color space. After that, we calculate color difference ΔE_{00} by using CIEDE2000.
- (6). We process all patterns and compare each pattern. And then, we classify by using Support Vector Machine (SVM), finally, we judge whether the coded defect is detected or not.

Fig. 4 is shown from loading original image and evaluation image, transforming to S-CIELAB color space and calculating to CIEDE2000. In detail, you would like to refer to [13], [14], and [15].

In this study, we carried out three experiments. (1). Objective assessment by PSNR. (a). in the case of the coded defect for all region of laparoscopic image, (b). in the case of the coded defect for 3/4 region of laparoscopic image, (c). in the case of the coded defect for 1/2 region of laparoscopic image, (d). in the case of the coded defect for 1/4 region of laparoscopic image. (2). Measurement of luminosity L^* transforming S-CIELAB color space. (3). Measurement of color difference ΔE_{00} using CIEDE2000. We define (1) to (3) as Exp. 1 (Exp. 1-1, 1-2, 1-3, and 1-4), Exp. 2, and Exp. 3.

For experimental method, we do not experiment the multi-view 3D image quality assessment subjectively with 8 viewpoints parallax barrier method in this study to purpose objective assessment automatically by computer. As experimental main specification, computer operating environment (Windows 10 Pro, MATLAB R2016a), image resolution (1280×720 (for image region of all, 640×360 (for image region))).

For assessment method, we used PSNR. PSNR is one of index to measure image quality objectively how one image data is degraded compared to original image data. The more score is higher, the less degradation becomes. The more score is lower, the more degradation becomes.

In this study, if PSNR is more than 50 dB, assessment result is “Excellent (Poor Detection)”, if PSNR is more than 50 dB, assessment index is “Excellent (Poor Detection)”, if PSNR is between 45 and 50 dB, assessment index is “Good (Bad Detection)”, if PSNR is between 40 and 45 dB, assessment index is “Fair (Fair Detection)”, if PSNR is between 35 and 40 dB, assessment index is “Bad (Good Detection)”, and if PSNR is less than 35 dB, assessment index is “Bad (Excellent Detection)”.

RESULT AND DISCUSSION OF EXP. 1

Result of Exp. 1 is shown for laparoscopic frame image obtained from objective assessment. The vertical line is PSNR, the horizontal line is Quantization Parameter (Q).

Exp. 1-1 is the case of the coded defect processing for all region of laparoscopic frame image. From result of Exp. 1-1, in the case of $Q = 20$, PSNR is 45 dB (“Fair” (Fair Detection)), in the case of $Q = 35$, “Bad (Good Detection)”, in the case of $Q = 40, 51$, “Poor (Excellent Detection)”. On the other hand, focused on “Fair (Fair Detection)”, PSNR in $Q = 20, 25$ is satisfied. From knowledge of [6], for 3D CG images, focused on better than “Fair Detection”, in the case of $Q = ref, 20$, 1/2 of all patterns, in the case of $Q = 25, 30$, 2/3 of all patterns, in the case of $Q = 35, 40, 51$, all, are satisfied. From this, it is easy for the coded degradation to perceive objectively since for laparoscopic image used in this study, there are many patterns in the case of less than 40 dB. This is cause that original video is not uncompressed. On the other hand, laparoscopic video in this study is not treated medical work, however, since this video is filmed in the body, and then each body regions are moved irregularly, this is affected for evaluation score. Particularly, the more approach to final frame, the lower PSNR is tend.

Exp. 1-2 is the case of the coded defect processing for 3/4 region of laparoscopic frame image. From result of Exp. 1-2, for all patterns, in the case of $Q = 51$, PSNR can be judged as “Poor (Excellent Detection)”. For “1101” pattern, the difference among frame images is large. Particularly, this is seen in the middle number of frame images when Q is higher. Laparoscopic images used in this study consist of red component, and it is seen clearly and visually for the change of color and contrast in the case of coding. This tendency is represented from Exp. 2 and 3, however, in Exp. 1, we estimate the relation to color information. In 3D CG images used in Author’s references [5], [14], [15], there are change for luminance and color difference by contrast enhancement and image resolution. Therefore, we estimate applying this knowledge in laparoscopic image in this study. On the other hand, since we found new knowledge that forceps movement is affected to PSNR among frame images in this case, the image quality improvement should be considered in the case of treating medical work.

Exp. 1-3 is the case of the coded defect processing for 1/2 region of laparoscopic frame image. From result of Exp. 1-3, not in case the coded region is large such as Exp. 1-1 and 1-2 but in Exp. 1-3, the difference among patterns is larger than that of Exp. 1-1 and 1-2. Seen laparoscopic frame images in Fig. 1 and 2, body part region is divided into some regions, and around border line divided to image region, it is larger for change of color information. It is easy to affect for degradation. Particularly, we can judge that it is easy to perceive affect for coded image quality in laparoscopic image including forceps region.

Exp. 1-4 is the case of the coded defect processing for 1/4 region of laparoscopic frame image. From result of Exp. 1-4, since the coded region used in Exp. 1-4 is the least of all patterns from the point of view of image region, we estimate this result is better than other experiments. The difference among regions is largest of four experiments.

Next, we classified using SVM (Support Vector Machine) by SMO (Sequential Minimal Optimization) from result data of Exp. 1-1 to 1-4. From SVM result, in the case of Class (*Code*), Recall of “0010”, in the case of Class (Q), all patterns except for one pattern, are satisfied more than 70%. Therefore, we can judge as “Classified”. SVM classified correctly percentage is, in Class (Q), more than 80%, in Class (*Code*), more than 30%, in Class (*Frame*), more than 10%.

RESULT AND DISCUSSION OF EXP. 2

Exp. 2 is shown for luminosity L^* after transforming to S-CIELAB color space. From result, in $30 \leq Q \leq 35$, L is increasing rapidly, in $20 \leq Q \leq 25$, $40 \leq Q \leq 51$, there is no change.

RESULT AND DISCUSSION OF EXP. 3

Exp. 3 is shown for color difference ΔE_{00} . This result is different from Exp. 2. Q and ΔE_{00} are the proportional relation in $Q < 40$, however, in $40 < Q < 51$, ΔE_{00} is increasing rapidly. ΔE_{00} difference between in $Q = 20$ and in $Q = 51$ is seen by 2.3 times. This is different from L^* .

CONCLUSION

In this study, we examined medical image diagnosis method including the automatic detection of coded defect region, and then, we experimented and discussed from the point of view of coded image quality, color information, and classifier parameter.

From experimental result and discussion, it is easy to perceive degradation in the case of laparoscopic images than in that of 3D CG images, and then in case the coded defect region is small, the difference among patterns is large. From this, we find out new novelty and knowledge that it is easy to perceive degradation objectively in the border line of body parts region. On the other hand, these results are considered to relate to forceps, and are enabled to apply for medical image diagnosis. As the future work, we will apply deep learning for medical image diagnosis, region segmentation by body parts region, and we would like to advance 3D stereoscopic images [16] and high-definition images for medical application.

ACKNOWLEDGEMENT

We would like to thank them because this study is cooperated with the Center for Frontier Medical Engineering, Chiba University. There is no conflict of interest in this study.

REFERENCES

- [1]. M. Ravi and S. S. S. Sanagapati: "A Practical Design and Implementation of a Low-cost Platform for Real-Time Diagnostic Imaging," *IEEE Access*, pp.24952--24958, October 2017.
- [2]. Y. Hayashi, K. Misawa, M. Oda, D. J Hawkes, and K. Mori: "Clinical application of a surgical navigation system based on virtual laparoscopy in laparoscopic gastrectomy for gastric cancer," *Int'l J Computer Assisted Radiology and Surgery*, Vol. 11, Issue 5, pp.827--836, May 2016.
- [3]. N. Kawabata and M. Miyao: "3D CG Image Quality Metrics by Regions with 8 Viewpoints Parallax Barrier Method," *IEICE Trans. on Fundamentals*, Vol.E98-A, No.08, pp.1696--1708, August 2015.
- [4]. N. Kawabata and Y. Horita: "Statistical Analysis of Subjective Assessment for 3D CG Images with 8 Viewpoints Lenticular Lens Method," *IEEEJ Trans. on IEVC*, Vol.4, No.2, pp.101--113, December 2016.
- [5]. N. Kawabata and M. Miyao: "Multi-view 3D CG Image Quality Assessment for Contrast Enhancement Based on S-CIELAB Color Space," *IEICE Trans. on Information and Systems*, Vol.E100-D, No.07, pp.1448--1462, July 2017.
- [6]. N. Kawabata: "Image Diagnosis for Coded Defect Detection on Multi-view 3D Images," *Proc. of IMQA2018*, PS-10, pp.110--119, September 2018.
- [7]. J. Pambrun and R. Noumeir: "Limitations of the SSIM quality metric in the context of diagnostic imaging," *Proc. of IEEE ICIP*, September 2015.
- [8]. N. Kawabata and T. Nakaguchi: "Improvement of Laparoscopic Color Image Diagnosis for Automatic Detection of Coded Defect Region and Application of Effective Classifier Parameter," *IEICE Tech. Rep.*, MI2018-42, MICT2018-42, pp.21--26, November 2018 (in Japanese).
- [9]. K. Mori: "Medical Image Diagnosis Assistance by using 3-D Image Information," *Journal of ITE*, Vol.65, No.4, pp.448--452, 2011 (in Japanese).
- [10]. Y. Okada, T. Koishi, S. Ushiki, T. Nakaguchi, N. Tsumura, and Y. Miyake: "Fast Stereo Matching Method for 3D Reconstruction of Internal Organ in Laparoscopic Surgery," *Med Imag Tech* Vol.25, No.5, pp.389--398, November 2007 (in Japanese).
- [11]. R. Oguma, T. Nakaguchi, R. Nakamura, T. Yamaguchi, H. Kawahira, and H. Haneishi: "Ultrasound and Endoscopic Image Overlay System by Detecting Laparoscopic Ultrasound Probe Flexion," *Med Imag Tech* Vol.32, No.3, pp.203--211, May 2014 (in Japanese).
- [12]. F. Bossen, D. Flynn, and K. Sühring: "HM Software Manual," https://hevc.hhi.fraunhofer.de/svn/svn_HEVCSoftware/, accessed September 30, 2019.
- [13]. G. M. Johnson, M. D. Fairchild: "A Top Down Description of S-CIELAB and CIEDE2000," *Color Research & Application*, vol.28, no.6, pp.425--435, 2003.
- [14]. N. Kawabata and M. Miyao: "Multi-view 3D CG Image Quality Assessment for Contrast Enhancement Including S-CIELAB Color Space in case the Background Region is Gray Scale," *Proc. of ITC-CSCC2016*, T2-6-3, pp.579--582, July 2016.
- [15]. N. Kawabata: "Image Quality Assessment for Multi-view 3D CG Images and 5K High Definition Images Based on S-CIELAB Color Space," *Proc. of IDW'17*, Vol.24, 3D5-1, pp.849--852, December 2017.
- [16]. L. T. Cook, S. J. Dwyer, S. Batnitzky, and K. R. Lee: "A Three-Dimensional Display System for Diagnostic Imaging Applications," *IEEE Computer Graphics and Applications*, Volume 3, Issue 5, August 1983.

THE ART AND APPRECIATION OF COLOURS IN ARCHITECTURE

Adedayo Jeremiah Adeyekun

B. Tech Arch (Hons.), M.Plan (URP) MDU, India

Ph.D. Candidate in Dept. of Civil Engineering,

Jagannath University, Delhi – NCR (India)

Email: theonlyicd4life@yahoo.com

ABSTRACT

According to the father of Organic Architecture, Frank Lloyd Wright as rightly said, that the mother art is Architecture, without Architecture of our own we have no soul of our own civilization. Art and Architecture should live as a family or live as husband and wife. No Architecture is good without the application of art. A building without art is like bread without butter or tea without sugar. The use of colour in Architecture has been effectively applied since the early ages in both India as well as Europe, Middle Eastern and Chinese cultures. In Italy, during the Baroque era, architecture was assigned the role of conveying emotions and captivating the imagination of the masses visiting churches. Colour played a vital role in fulfilling this architectural ambition. Following that trajectory of radical use of colour and blending it with his curvilinear fluid forms that were done by the master architect Antonio Gaudi during his time. He was perhaps the most radical in his experimentation of colour and architectural form and showcasing to the world the magic that could happen when the two combined.

Colour plays a significant role in the perception of a space in the human mind. When lighter shades are used, it makes the space appear bigger. On the other hand, using darker shades make the same space look smaller. Hence colours can be used to adjust the proportion of a building space. In the Expression of material, we saw in the example of falling water that light painted materials seem lighter than dark coloured materials. Other visual effects of colour can make things look further away or more distant; larger or smaller; cooler or warmer. For example, a cool blue bathroom and warm red living room. This paper is a review of literature that were collected from documents, journals, books, periodical and other materials that will explore the key importance of art and appreciation of colours in Architecture.

Keywords: Art, Architecture, Colours, Building, Culture, Effect of Colours.

1.0 INTRODUCTION

Colours are a vital element of our universe, not only in the natural environment but also in the environment which is created by the humans. Colours play a noteworthy role in the human evolutionary process, in the society and spaces we live and interact. When it comes to building architecture, we often consider colours to be a principal in decoration. But, colours in architecture play a paramount role. Keeping this in mind, the role of colours in architecture is a factor in the perception of a space and its function. Colour is a visual language used to demonstrate the work of an architect. So when we try to communicate or transmit something through building design, there is no better way than doing it with colours. But to communicate with colours, one needs to first understand how colour behaves, how they influence humans and how they change their character. The impression of a colour and the message it conveys is of extreme importance in creating the psychological ambiance that supports the function of a building space.

2.0 APPLICATION OF COLOURS IN URBANISM

The use of colour on an urban scale has two very different evolutions. One comes as a natural and informal development of towns into cities and cities into neighbourhoods. This type of informal settlements often displayed a rubric of eclectic colours which were primarily a result of random application. The effect was a vibrant and lively urban scape. Taking a cue from this evolution emerged a rather carefully crafted approach of formal urbanism that intended to ultimately create a similar effect of random eclectic and vibrant urban typology via imitation. The latter is prevalent predominantly in the post-war regions of Europe and late 20th century North America. India, however, is the Mecca of colourful informal urbanism with the proliferation of colour and its celebration as a fabric of the masses.

In a recent urban project in Denmark, the use of bright colours as an activator of public life was explored by its literal application along the streets, side-walks and buildings façades.



Fig 1: Work of Bjarke Ingells Group



Fig 2: Work of Bjarke Ingells Group

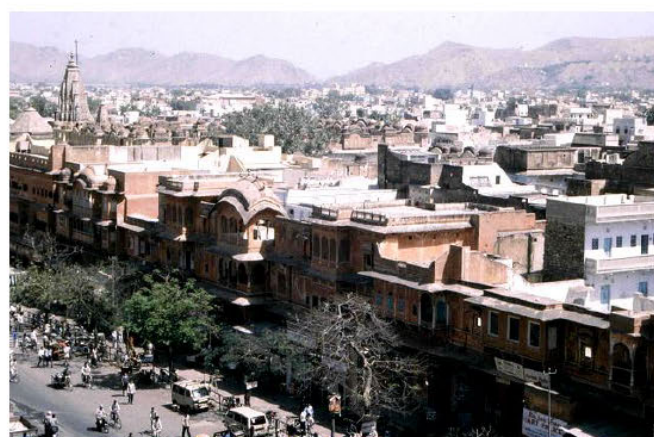


Fig. 3: Jaisalmer, the Old City of Jaipur, India.

The old city of Jaipur is known for the use of red sandstone and Jaisalmer is known for its yellow sandstones. In an era when most of the cities are turning to look same and more like concrete jungles, these Indian cities still portray a sense of uniqueness.

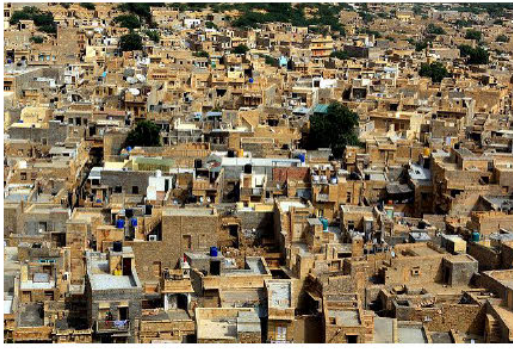


Fig. 4: Jaisalmer, the Old City of Jaipur – Yellow sandstone gives the city a sense of collective belongings



Fig. 5: Moroccan City Chefchaouen

The city is painted blue for the apparent theories of either keeping mosquitoes away or as a symbol of freedom from Hitler.

3.0 COLOURS IN BUILT ENVIRONMENT

From its traditional application as a tool for interior décor, the use of colours has once again moved outwards to the exterior of the building as continuation of the internal experience. This phenomenon is not new to the Indian context, however, the role of technology and lighting has added a new dimension to it. The building's "skin" has become a key element of evoking a response in the user and drawing them inside. The move has been further propagated by the potential impact that commercial enterprises can generate from customers as a result, this phenomena is most common in commercial office buildings and shopping malls.



Fig 6: Work of Herzog de Meuron



Fig 7: Installation of Olafur Eliasson



Fig 8: Installation of James Turrell



Fig. 9: The Nasir al-Mulk Mosque in Shiraz, Iran

The mosque is called by many different names. Mostly known as the “Pink Mosque”, it is also called the “Mosque of colours,” the “Rainbow Mosque” or the “Kaleidoscope Mosque”. This is a space where light and worship intertwine. The mosque comes to life with the sunrise and colours dance throughout the day like whirling dervishes. It reflects on the ground, walls, the arches and the towering spires. It even reflects on the visitors as if a colourful ball is hit by the first sun ray and explodes to thousands of butterflies all around. Built by the order from one of the lords of the Qajar Dynasty, Mirza Hasan ‘Ali Nasir al-Mulk, it took 12 years to complete in 1888. Its interior reveals a magnificent masterpiece of design with stunning colours.

The designers Muhammad Hasan-e-Memar and Muhammad Reza Kashi Paz-e-Shirazi used extensively stained glass on the façade and other traditional elements such as *panj kaseh-i* (five concaves), which create a breath taking effect of the interior like standing in a kaleidoscope. Once the sunlight hits the stained glass, the entire building is flooded by a vibrant rainbow of colours. In popular culture, the mosque is also called Pink Mosque, because its tiles are beautifully decorated with a pre-eminently pinkish rose colour.

Today this gorgeous mosque is still in use under protection by Nasir al Mulk's Endowment Foundation. Built in late 19th century, not very new and not very old, it is a celebration of both classic and modern times embedded in Islamic heritage. Speaking of this heritage, it has roots in Islamic art, architecture, tile making, geometry, patterns and other arts that flourished in the Golden Age of Islam. For example the “New Discoveries in the Islamic Complex of Mathematics, Architecture and Art” article, written by the president of FSTC, Professor Salim Al-Hassani, shows a very interesting link with patterns on the mosques and a sophisticated geometry, where art enter wined with science. There are many more articles you can find in Muslim Heritage website that can be linked to this mosque: muslimheritage.com/architecture, muslimheritage.com/arts, muslimheritage.com/geometry, etc.



Fig. 10: The Nasir al-Mulk Mosque in Shiraz

Japanese photographer Koach was blown away by the mosque's beauty which is best appreciated in the morning light, explaining: “You can only see the light through the stained glass in the early morning. It was built to catch the morning sun, so that if you visit at noon it will be too late to catch the light. The sight of the morning sunlight shining through the colourful stained glass, then falling over the tightly woven Persian carpet, is so bewitching that it seems to be from another world. Even if you are the world’s least religious person, you might feel your hands coming together in prayer naturally when you see the brilliance of this light. Perhaps the builders of this mosque wanted to show their “faith” through the morning light shining through this staine.

4.0 THE EFFECT OF COLOURS IN ARCHITECTURE.



Fig. 12: Coloured Architectural Glass

Colour plays a huge role in architectural design and is not just for decoration, the impression of a colour and the message the colour conveys is important in creating a physiological mood or ambiance to support the function of a space or building.



Fig. 13: Central Saint Giles by Renzo Piano in London

Central Saint Giles by Renzo Piano in London strikes out with bold use of colourful facade in grey London.



Fig. 14: Installations on the pathways and stairs in a European City providing a vibrant atmosphere for the public)

The places and spaces above, are a clear indication of the evolution of our interaction with the spaces through the times and eras. It is an important and needed approach to accept architecture, just for the fact that our daily lives are affected by all the places and their way of existence. It becomes necessary that the use of colours in appropriate and subtle ways is understood and implemented. It enhances the ability to intercept better with the surrounding and triggers our mood.

Every space can be distinguished with its approach towards the human and non-human interaction. Architecture plays an important role in promoting it, and colour in architecture helps understand that interaction better.



Fig. 15: Falcon Headquarters, Rojkind Arquitectos, San Angel, Mexico

A yellow warm and exciting colour combination translated into loud sharp trumpets and high fanfares.



Fig 16: Didden Village, MVRDV, Rotterdam, Netherlands

Blue: Deep, inner, supernatural, peaceful. Sinking towards black, it has the overtone of a mourning that is not human typical heavenly colour which is translated into sound of flute, cello, and organ.



Fig.17: Refurbishment and Extension of Arcelor Mittal R&D Headquarters Avilés, Spain

Orange Colour: A mixture of red and yellow, radiant, healthy. Translated into the sound of middle range church bell, an alto voice.

5.0 CONCLUSION

Colour has a great effect on human emotions, ergonomics and most apparent in the human aura or energy that it could be used in healing. Colour has been said to be important to the level of being a need for humans, not only to achieve some decorative or aesthetical values, but also to fulfill some needs of the human being that they cannot live without in architectural and urban contexts. According to the examples of application of colours to buildings showed above, colour plays a role in safeguarding visual efficiency and comfort of our environment. It is the soul of Architecture and without colour is like having a tree in the wilderness. Therefore, colour becomes the ingredient of beauty in the environment.

6.0 ACKNOWLEDGEMENTS

The author specially wishes to express a deep appreciation to the distinguished Prof. Prabhubhai K. Patel, a Professor Emeritus of Architecture from Indian Institute of Technology, Roorkee (Oldest Technical Institution of Asia), Prof. Olubode O. Ajayi of Chemistry Department, Federal University of Technology Akure and Mr. Raj Kumar Oberoi (Registrar of COA, New Delhi). The authors also gratefully acknowledge the financial support from Mr. Vedprakash Sharma, the Proprietor of Shri Krishna Filling Station in Farukh Nagar, Gurugram.

7.0 REFERENCE

- **Frank Lloyd Wright (1953)** The Future of Architecture. New American Library, Horizon Press, pp. 21.
- **Matheus Pereira (2008)** The Role of Colour in Architecture: Visual Effects and Psychological Stimuli.
- **Rasmussen, S.E. (1964)** Experiencing Architecture, pp. 218.
- **Piyush Bajpai (2015)** Colours and Architecture, pp 1-5.

About the Author



Adedayo Jeremiah Adeyekun (born on 22nd February 1985) is a Nigerian Professional Artist, Architect, Urban Planner, Educator and a Preacher of the Word of God. He studied Architecture at the Federal University of Technology, Akure (NIGERIA) and graduated with the degree of B.Tech in Architecture with Honours (5years) in October, 2008. He proceeded in his career in India with the degree of Master of Planning (Hons.) with specialisation in Urban and Regional Planning from Maharshi Dayanand University, Rohtak with Distinction securing a Silver Medal. A Ph.D. Candidate in Civil Engineering with specialisation in Building Technology and Construction Management at JNUB, Delhi – NCR, India. He was an associate professor in the faculty of Architecture, Savera College of Architecture, Gurugram affiliated to MDU, Rohtak. He received a medal in April 2018 for the presentation of a paper titled: Technology and Management Options towards the use of Fly Ash in Civil Engineering. His research interest is spread across the discipline of Architecture, Planning and Civil Engineering and as a researcher; he has more than 15 research papers and 4 written international books to his credit.

A picture book of motion illusions in stationary images -- a new method to investigate vection --

Takuya Aoki¹, Takeharu Seno^{1*}, and Akiyoshi Kitaoka²

¹*Faculty of Design, Kyushu University, 4-9-1 Shiobaru, Minami-ku Fukuoka, Japan.*

²*College of Comprehensive Psychology, Ritsumeikan University, 2-150 Iwakura-cho, Ibaraki, Osaka, Japan.*

*Corresponding author: Takeharu Seno, seno@design.kyushu-u.ac.jp

Keywords: vection, picture book, visual illusion, motion illusion, Active Volcano, analog contents

ABSTRACT

In this study, we challenged to make a picture book of vection. Vection is normally induced by some digital devices recently. However, it can be induced by some analogue devices too. There was no challenge at all to utilize and induce vection in a picture book. Therefore, we made a vection picture book. Also, we conducted a psychological experiment to investigate the vection strength induced by those picture books. In the near future, we will present the final product of vection picture book to children and obtain subjective oral reports by them.

INTRODUCTION

Visually induced illusory self-motion perception is named vection (Fischer & Kornmuller, 1930). Generally, vection is induced by visual stimuli projected on a large screen, or some visual, e.g. plasma, display by using some digital devices (Figure1)(e.g. Riecke et al., 2006, 2009 and 2015; Palmisano et al., 2011, 2015 and 2017; Seno et al., 2017 and 2018). Vection stimuli have been made and controlled by computers in the history of vection research. However, it is possible to induce vection by some analog methods. In fact, in the older days, there had been some inventions of the analog contents of vection, e.g. a rotating drum and a tumbling house (Figure 2).



Figure 1. Vection by some digital devices (from Riecke et al., 2015).

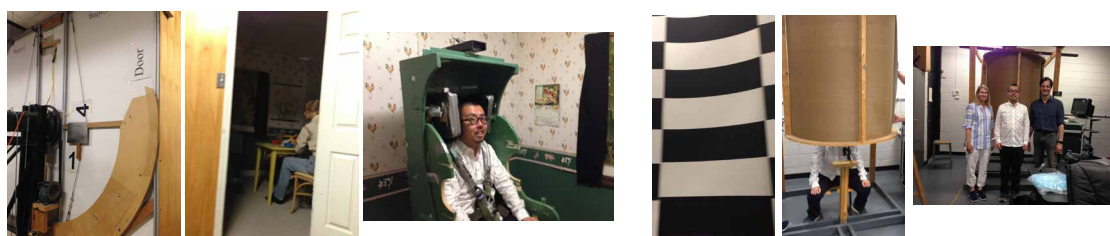


Figure 2. Vection by analogue devices (Tumbling room and Rotating drum).

MAKING AN ANALOGUE VECTION CONTENT

In this current study, we challenged to make a picture book of vection. There are various types in the picture books. In some picture books, visual illusions have been utilized for entertaining the readers, especially children. However, there was no challenge at all to utilize and induce vection in a picture book.

In our previous article (Seno, Kitaoka & Palmisano, 2013, Perception), we reported that a static image could induce enough strong vection. Kitaoka developed a visual illusion named “Active Volcano” that is entirely static but appears to keep expanding illusorily. On the basis of the ‘color-dependent Fraser–Wilcox’ illusion (Kitaoka, 2014, Perception), the direction of illusory motion is determined by the color arrangement. If color strips are repeatedly arranged in the following order—red, purple, red– purple, light red–purple, and back to red—perceived motion occurs in this direction. Owing to their radial arrangement in the Active Volcano, the image appears to expand. Yanaka and Hilano (2011) suggest the illusion is triggered by saccades, eye-blinks, or shaking the image.

We thought that this Active Volcano could be used as an analogue vection stimulus in a picture book. We printed this visual illusion into two-page high luminance A2 photo-papers. By adding the cardboard background to these papers, we created a prototype of a vection picture book. This book should be seen with sustained eye blinks at a constant frequency or seen with fluttering the book. We also employed other visual illusions invented by Kitaoka to make picture books. We employed four different visual illusions in the vection picture books.

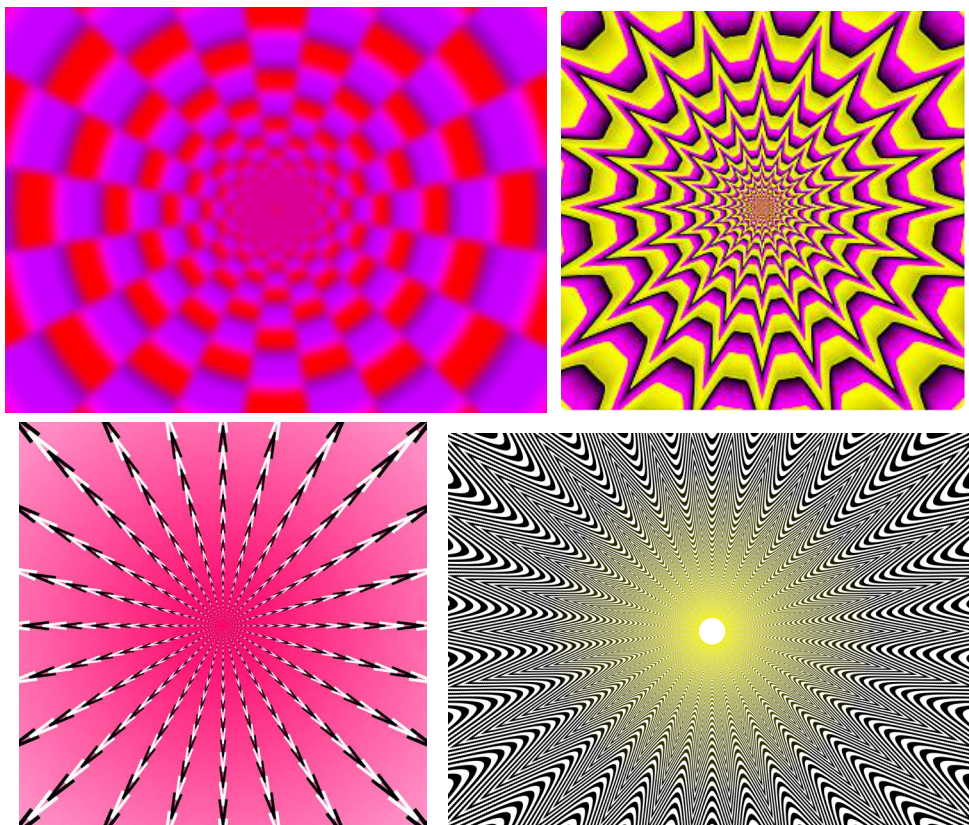


Figure 2. The four stimuli used in the picture books.

PSYCHOLOGICAL EXPERIMENT

We presented these prototypes of the picture books to thirteen naïve volunteers and obtained eight subjective statements describing their inner states, by oral reports. Before the stimulus presentation, the experimenter carefully avoided to give them any information about vection and the purpose of this study. We counted the frequency of the appearances of the words and statements related to vection. The results showed that the average number of the reported words related to vection, was 12.5. The total reported words were 104 (13 participants reported 8 words). About 12 % inner statements were related to vection. This value might indicate that our picture books could induce substantial vection.

Also by using visual analog scale (VAS), they reported subjective vection strength. We converted its strength to 0 (no vection) to 100 (very strong vection) values. The results showed that the average subjective vection strength became 46.21. This value also might indicate that our picture books could induce substantial vection. However, it should be noted here that two participants evaluated the subjective vection strength as 0 in all picture books. This indicated that some people could not perceive any vection in our picture books and it suggested that we should improve our vection picture book in the near future.

In the next step, we will conduct a more sophisticated and controlled psychological experiment to measure vection strength induced by these picture books. First, we will present an expanding-grating optic flow as a standard stimulus for 30 seconds and make the participants set its subjective vection strength, 100. Then by comparing to this 100, participants will estimate the subjective vection strength induced by the picture book. We will also present them the same but large Active Volcano projected on a plasma display by using a computer and measure its subjective vection strength for the comparison of digital and analog vections.

GENERAL DISCUSSION

In the near future, we will present the final product of vection picture book to children and obtain subjective oral reports by them. We try to analyze these oral reports by a phenomenological method. Our challenge can lead a totally new understanding of vection. Also, it has a big value as the applied research of vection. Vection still has many hidden values and we should keep trying to reveal them.



Figure 3. Our challenge and the near future of the picture book of vection.

ACKNOWLEDGEMENT

This work was supported by MEXT KAKENHI (Grant number JP26700016, JP17K12869, and JP18H01100) to TS. Part of this work was carried out under the Cooperative Research Project Program of the Research Institute of Electrical Communication, Tohoku University.

REFERENCES

1. Fischer, M. H. & Kornmuller, A. E. 1930 "Optokinetic ausgeloste Bewegungswahrnehmungen und optokinetischer Nystagmus." *Journal of Psychological Neurology*, 41, 273-308.
2. Riecke, B. E., Schulte-Pelkum, J., Avraamides, M.N., & Von Der Heyde, M. (2006). Cognitive factors can influence self-motion perception (vection) in virtual reality. *ACM Transactions on Applied Perception*, 3, 194 – 216.
3. Riecke, B. E., Valjamae, A., & Schulte-Pelkum, J. (2009). Moving sounds enhance the visually-induced self-motion illusion (circular vection) in virtual reality. *ACM Transactions on Applied Perception (TAP)*, 6(2): 7, 1-27. doi: 10.1145/1498700.1498701
4. Riecke, B. E., & Jordan, J. D. (2015). Comparing the effectiveness of different displays in enhancing illusions of self-movement (vection). *Frontiers in psychology*, 6: 713, 1-16.
5. Palmisano, S., Allison, R. S., Kim, J., & Bonato, F. (2011). Simulated viewpoint jitter shakes sensory conflict accounts of vection. *Seeing & Perceiving*, 24(2), 173-200. doi: 10.1163/187847511X570817
6. Palmisano, S., Allison, R.S, Schira, M.M. & Barry, R.J. 2015 "Future Challenges for Vection Research: Definitions, Functional Significance, Measures and Neural Bases." *Frontiers in Psychology*, 6(193), 1-15.
7. Palmisano, S., Mursic, R., & Kim, J. (2017). Vection and cybersickness generated by head-and-display motion in the Oculus Rift. *Displays*, 46, 1-8.
8. Seno, T., Sawai, K. I., Kanaya, H., Wakebe, T., Ogawa, M., Fujii, Y., & Palmisano, S. 2017 "The Oscillating Potential Model of Visually Induced Vection." *i-Perception*, 8(6), 2041669517742176.
9. Seno, T., Murata, K., Fuji, Y., Kanaya, H., Ogawa, M., Tokunaga, K. & Palmisano, S. 2018 "Vection is enhanced by increased exposure to optic flow." *i-Perception*, 9(3), 2041669518774069.
10. Seno, T., Kitaoka, A., & Palmisano, S. (2013). Vection induced by illusory motion in a stationary image. *Perception*, 42(9), 1001-1005.
11. Kitaoka, A. (2014). Color-dependent motion illusions in stationary images and their phenomenal dimorphism. *Perception*, 43(9), 914-925.
12. Yanaka K, Hilano T, 2011, "Mechanical shaking system to enhance "Optimized Fraser–Wilcox Illusion Type V"" *Perception* 40 ECVF Abstract Supplement, page 171

STABILITY OF COLOR PREFERENCE ASSESSED BY VARIOUS METHODOLOGIES

Shinji Nakamura^{1*}

¹*School of Psychology, Nihon Fukushi University, Japan*

*Corresponding author: Shinji Nakamura, shinji@n-fukushi.ac.jp

Keywords: Color Preference, Psychological Measurement, Paired Comparison, Visual Analogue Scale

ABSTRACT

In this investigation, psychological surveys were carried out in order to examine intra-individual stability/consistency concerning participant's expressed color preference against the passage of time, with employing various psychological measurement. Participant's color preference was evaluated twice with a time interval of eight months, and with methods of ranking, paired comparison and visual analogue scale. The results indicated that rank correlations between each color preference measurements were quite high, indicating that three different methodologies employed in this investigation can be considered as equivalent to assess the participant's color preference. Furthermore, color preference was quite robust against the time passage, even though there was an eight months interval between the tests. The participant's expression of their color preference was not susceptible to a detailed method to acquire it and also by a passage of time including change of seasons. The results suggested that color preference stemmed from a participant's stable personalities, just like as psychological characteristics.

INTRODUCTION

We usually have an individual color preference which can be internally represented and externally expressed without a specific effort. Color preference has been one of the biggest concerns in color sciences for long years, and many researchers have tried to accumulate wider knowledge about color preference in a various way. Color preference researches have revealed distributions of preferred/hated colors as a function of genders, ages, countries and so on, by collecting data from massive group of survey participants. In these researches, it has been indicated that color preference has a certain range of robustness against a passage of time, and colors selected as preferred or hated color did not show a huge variation within a specific participant's group. Similarly, color preference also shows a certain range of stability within an individual person on average. This suggests that individual color preference would stem from a stable characteristic of the participant's personality, not affected by transient feelings varied from day to day.

Nonetheless, it has been also indicated that the intrapersonal stability/consistency of color preference would be subject to relatively large individual differences, and widely known that there would be some persons with very high stability in their color preferences, while other persons did not show a stable preference. In our previous studies, intra-individual stability of color preference was investigated by measuring the participant's color preference twice (letting them to rank 12 fundamental colors in order of preference) with four or 14 weeks intervals, in order to examine the relationships between the consistency of the color preference and the participant's personality traits [1][2]. In this investigation, the intra-individual stability of the color preference was further examined by employing 1) much longer time interval between the color preference measurements

(eight months) and 2) various psychological methodologies in accessing the participant's color preference (methods of ranking, paired comparison and visual analogue scale).

METHODS

In the psychological surveys reported here, the participant's color preference was measured by the following three psychological methodologies, namely 1) ranking, 2) paired comparison, and 3) visual analogue scale (VAS). All participants underwent all of the three tests. Targets for preference measurements were nine different color names; red, green, blue, yellow, white, black, grey, pink and brown. They were presented as the color name in Japanese in all of the three tests (Thus, in the current investigation, we measured an abstract preference against a color name, not a specific color preference against color patches or colored object). In the ranking test, they simply made a ranking of the nine colors based on their preference. In the paired comparison test, the participants selected more preferred color from each combination of the two colors selected from the nine target color names (there were 36 different combinations of the two target colors). In the VAS test, the participants were asked to express their degree of preference against each of the target color name on the line, both of the ends represented "completely dislike (0)" and "completely like (100)". All tests were printed on A4 formatted papers, and the participants were needed approximately 20 minutes to complete them. The same tests were repeated twice with a time interval of eight months. The first test (TEST1) was on middle of April (the mid spring season in Japan) and the second test (TEST2) was on middle of December (beginning of the winter); we can consider that the tests were carried out across the seasonality in Japan. After the TEST2, each participant was requested to complete psychological questionnaires which measured their general personality traits (TIPI [3]) and public and private self-consciousness [4].

The participants were Japanese undergraduate students, ages ranged from 18 to 21 years old. In TEST1, 184 students were participated and 114 participants were took part in TEST2. The subjects of the data analyses were 89 participants who took part in both tests and who didn't have any missing values (32 males and 57 females).

RESULTS AND DISCUSSION

Data Analysis

In order to compare the result obtained three different methods employed in this investigation, all data concerning the participant's color preference judgements were converted into rank order among nine target colors. In the ranking test, the rank scores indicated by the participant were directly used for the analysis. In the paired comparison test, frequencies that the specific color was selected as more preferred (within the two target colors) were counted for each target color first, then the rank orders of the frequencies among nine colors were calculated. In the VAS test, VAS values which represent degree of preference against each target color were converted into the rank orders.

Rank order of the color preference

Figures 1 and 2 indicate distributions of participants color preference measured by the methods of ranking (left), paired comparison (middle) and VAS (right) in TEST 1 and 2, respectively. The

pattern of distributions was relatively similar across the three different methods and between TESTs 1 and 2. Achromatic colors of black and white, and chromatic color of blue were typically selected as highly favorable colors by the participants. On the other hand, achromatic grey and brown had tendencies to be less preferred alternatives. These results were consistent with the previous researches about color preference measured as a group characteristic, including ours. Concerning the result of the color pink was a little bit ambivalent. In the TEST1, about 25-30% participants selected a color pink as the most favorable color in the target colors, and approximately 30% other participants exhibited that a pink was the least preferred color. The two thirds of the participants who took part in the survey were female, and for typical Japanese a color pink is considered as “girl’s color.” Thus, the ambivalent result concerning the pink preference/avoidance might be due to different responses against a pink between the male and female participants. In TEST2, the pink preference seemed to be diminished and the avoidance might be increased. The difference between the TESTs may reflect the seasonality of the surveys; TESTs 1 and 2 were carried out in the spring and the winter in Japan respectively. Generally, Japanese people have a tendency to associate a color pink with cherry blossoms, which might be a kind of symbols of Japanese spring. This might boost pink preference in TEST1.

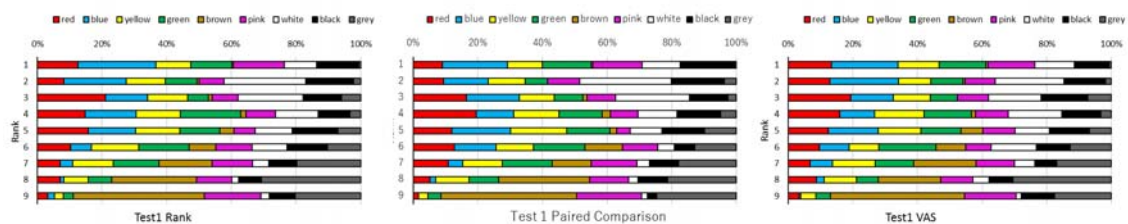


Figure 1 Distributions of the rank order of the participant’s color preference (TEST1)

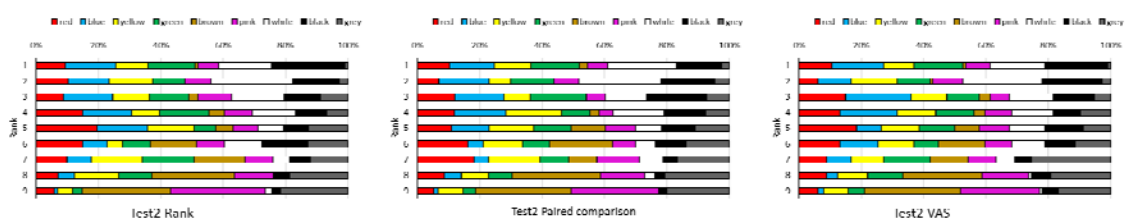


Figure 2 Distributions of the rank order of the participant’s color preference (TEST2)

Consistency between the TESTs

Table 1 indicates medians of coefficients of rank correlation of color preference between the TESTs for three different preference measurements. Coefficients of correlation were very high (around .80 in median), indicating that, the participant’s expression of their color preference was quite robust against a time passage, even when there was a long interval and seasonal change between the TESTs (8 months). This suggests that the color preference was hardly affected by the participant’s daily

feeling (which might be changed day by day), nor their living environment (which would be strongly affected by the seasonal change), at least if it was evaluated by the preferential rank order.

Table 1 Medians of coefficients of rank correlation between TESTs 1 and 2

<i>Ranking</i>	<i>Paired comparison</i>	<i>VAS</i>
0.80	0.83	0.76

Consistency between the measurements

Table 2 indicates medians of coefficients of rank correlation of color preference among the three different measurements of the color preference, namely the ranking, paired comparison and VAS. The coefficients of correlation were quite high again across the measurements. This results strongly indicate that the color preference was highly consistent within the participants, irrelevant to the methods measuring it. The participant’s color preference was less susceptible for the manner in which they expressed it, suggesting that the color preference holds a solid psychological foundation inside the participant. The color preference measured in this survey was against an abstract concept of color (not a specific colored image or colored item) and would be somewhat vague. Together with the results that the color preference was very robust against a time passage, it is astonishing that the color preference exhibited very strong intra-individual consistency/stability.

Table 2 Medians of coefficients of rank correlation among the measurements

	<i>VAS-Paired comparison</i>	<i>Paired comparison-Ranking</i>	<i>Ranking-VAS</i>
TEST1	0.86	0.88	0.98
TEST2	0.90	0.95	0.90

Conclusive remarks

In this psychological survey, the intra-individual consistency/stability of the participant’s expression of their color preference was investigated with three different psychological methodologies, namely methods of ranking, paired comparison and visual analogue scale. The measurements of the color preference with each method were repeated twice with quite long time interval (8 months). The surveys revealed that the color preference was very stable irrelevant to the different method by which and the different seasonality in which it was measured. These result suggested that the color preference would stem from the static psychological traits of the participants, not affected by their temporal feelings which can be easily changed transiently. The following research should be done in order clarify the relationship between the participant’s psychological characteristics and their color preference with considering its stability.

REFERENCES

1. Nakamura, S. and Takahashi, S (2017). Personality Characteristics Relating to Individual Consistency of Color Preference. *AIC2019 Jeju*, PS03-07.
2. Nakamura S. (2018). Personality Characteristics and Stability of Color Preference. *ACA2017 Proceeding book*, 130.
3. Gosling, S.D., P.J. Rentfrow, & W.B. Swann, Jr. (2003). A Very Brief Measure of the Big Five Personality Domains. *Journal of Research in Personality*, 37(6), 504-528.
4. Fenigstein, A., M.F.Scheier, & A.H. Buss (1975). Public and private self-consciousness: Assessment and theory. *Journal of consulting and clinical psychology*, 43(4), 522-527.

AN EXAMINATION OF THE EFFECTS OF DECISION MAKING ON COLOR PREFERENCE DUE TO LAYOUTS OF A COLOR CHART.

Aya Mizukoshi

Graduate School of Informatics, The Open University of Japan, Japan

Corresponding author: Aya Mizukoshi, 1918006600@campus.ouj.ac.jp

Keywords: Color Preference, Fixed Method, Color Chart

ABSTRACT

Two kinds of methods are typically used when studying color preference using color chips. One is called “Free Sequence Method” wherein participants select the color chips by themselves. The other is called “Fixed Method” wherein participants choose from a series of fixed color chips pasted on a board. The Free Sequence Method is more resilient to selection bias than the Fixed Method.

Totsuka claimed that the Fixed Method is not an appropriate method for preference color survey because participants’ choices are affected by the other colors present on the color chart [1]. However, previous research on color preference have mostly used the Fixed Method, probably owing to its simplicity and portability.

In the Fixed color chart, the horizontal axis has chromatic colors comprising red, orange, yellow, yellowish green, greenish blue, blue, bluish purple, purple, and reddish purple from left to right. The vertical axis is arranged in groups of different color tones.

If the Fixed Method affects decision making of participants at an unconscious level, the chromatic color sequence may have the largest effect. Thus, there may be a possibility that the layout of a color chart affects decision making related to personal color preference. This study examined whether color preferences of select Japanese college students were changed due to the layout of a color chart that includes hues and tones.

INTRODUCTION

There have been many studies conducted on color preference, and several factors are said to be responsible for color preference, such as age, sex, culture, and geographical area of residence.

Color charts are often used to study color preference, and there are two kinds of typical color survey methods. One is called “Free Sequence Method”, in which participants select the color chips by themselves. The other is called “Fixed Method”, in which an administrator shows participants fixed color chips pasted on a board.

The Free Sequence Method is more resilient to selection bias than the Fixed Method. Totsuka claimed that the Fixed Method is not an appropriate method because participants’ color preference can be easily affected by the other colors present in the color chart [1]. However, the Fixed Method is frequently used in previous research on color preference, probably because of its simplicity and portability [2].

Generally, in the Fixed Method, chromatic colors are arranged on the horizontal axis and color tones are arranged on the vertical axis. Each color is presented on a color chip, and the chips are arranged on a neutral gray cardboard panel. The horizontal axis contains the following ten chromatic colors : R, YR, Y, GY, G, BG, B, PB, P, RP), and the vertical axis is arranged by the following eight tones: vivid, light, pale, light grayish, soft, deep, dark). While the aforementioned a

rrangement of chromatic colors is common in most color charts, the arrangement of tones is not uniform.

While the Fixing Method is mostly used because of its simplicity and portability, it has been shown that it is not the only means for conducting color preference surveys. Therefore, this survey was conducted to investigate how the color arrangement on a color table affects color preference of subjects.

METHODS

Subjects

The study included 266 participants (29 male and 197 female subjects) who were first-year students at a fashion college. They were divided into two groups so that the gender ratio in each group was almost the same. Subjects in Group 1 (those who were administered color chart 1) comprised 103 students with an average age of 18.48 years. Subjects in Group 2 (those who were administered color chart 2) comprised 123 students (14 males and 109 females) with an average age of 18.93 years. There was no statistically significant difference in gender composition between the two groups. ($\chi^2=0.263$, n.s)

Prior to the survey, there was no screening test to check for factors such as color blindness in subjects, and participation was voluntary.

Environments

The survey was conducted between July 17 and August 1, 2019 in a classroom with windows on the southwest wall. Since it was conducted during class hours, the date and time varied. Therefore, in order to maintain uniform brightness in the environment, the survey was conducted using only the lights installed in the classroom.

Stimulus

The stimuli used in the study were two color charts (Color Chart 1 and Color Chart 2) with 74 colored chips (comprising 70 chromatic colors and 4 achromatic colors.) The colors were arranged on a neutral gray cardboard panel measuring 21.0 cm by 29.7 cm. Each colored chip was 1.5 cm by 2.0 cm. These colors were chosen from the 'Basic Color' product of Japan Color Enterprise Co., Ltd. This colored paper is a modified Munsell color system compatible with Japanese Industrial Standards.

As for the arrangement of chromatic colors in Color Chart 1 (Figure 1), the horizontal axis contains chromatic colors of purple, bluish purple, blue, greenish blue, green, yellowish green, yellow, orange, red, and reddish purple, from left to right. The arrangement of chromatic colors in the horizontal axis of Color Chart 2 (Figure 2) had hues of reddish purple, red, orange, yellow, yellowish green, green, greenish blue, blue, bluish purple, and purple, from left to right.

The vertical axis contains different tone groups arranged in the same order in both charts, from Vivid tone, Light tone, Pale tone, Light Grayish tone, Soft tone, Deep tone, and Dark tone, to achromatic (white, light gray, dark gray, black) colors, from top to bottom.

The subjects reported the number corresponding to their favorite color from the color table. Answers were sent to the online learning portfolio system used by our college. While there was no limit on the response time, interviews were conducted approximately 5 minutes after completion of the class.



Figure 1: Color Chart 1



Figure 2: Color Chart 2

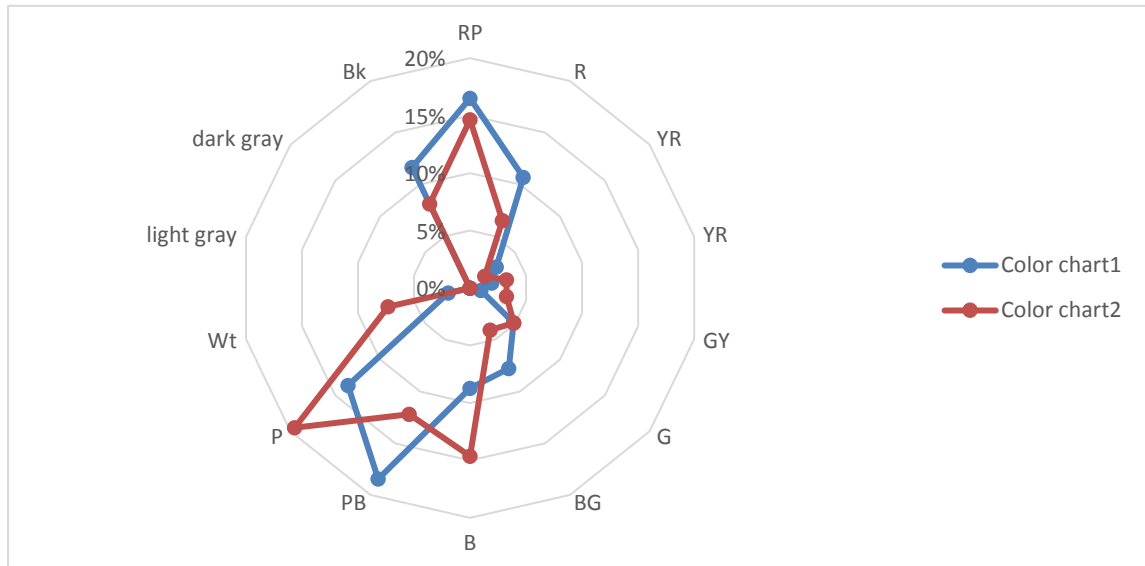
RESULT AND DISCUSSION

Figure 3 & 4 and Table 1 & 2 display the results of preference colors. The tendency of preference colors were almost the same results for both color chart. Figure 3 and Table 1 show that subjects in both groups prefer reddish-purple, red, purplish-blue, purple, and black colors. Figure 4 and Table 2 show that subjects in both groups prefer vivid tone, light tone, pale tone, soft tone, and deep tone. Additionally, both groups showed fewer responses to gray, orange, yellow, light, light gray, and dark tones.

The results of this study indicate that it is difficult to conclude whether the layout of the color chart affects color preferences. However, the majority of responses to this survey were from colors located at the top, left, and right sides of each color table.

In other words, many respondents said that they prefer blue, bluish purple, purple, reddish purple, and red colors, and prefer highly saturated and clear colors. The effect of tone placement on color preference needs to be considered.

In addition, the trends may have been influenced by the fact that number of male students was small and the students were from fashion colleges (special schools where students who are more conscious of color). Considering this point, further enquiry is necessary.



**Figure 3: Preference color tendency by chromatic colors and achromatic colors.
N= 226 (103 in Group 1, 123 in Group 2)**

**Table 1: Preference color tendency by chromatic colors and achromatic colors.
N= 226 (103 in Group 1, 123 in Group 2)**

	Color chart 1	Color Chart 2
RP	17%	15%
R	11%	7%
YR	3%	2%
Y	2%	3%
GY	1%	3%
G	5%	5%
BG	8%	4%
B	9%	15%
PB	18%	12%
P	14%	20%
Wt	2%	7%
N2.5	0%	0%
N7.5	0%	0%
Bk	12%	8%

Figure 4: Preference color tendency by tone.
N= 226 (103 in Group 1, 123 in Group 2)

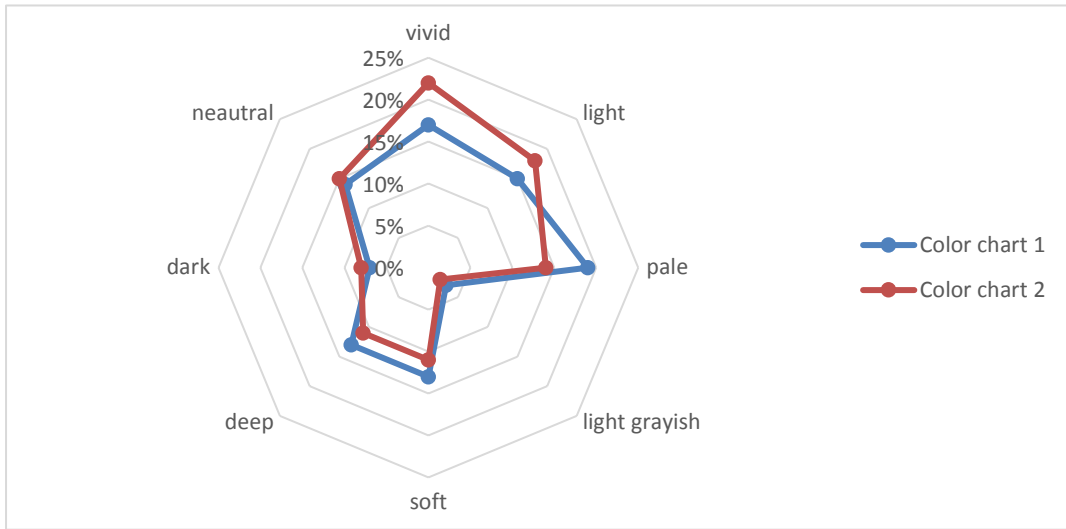


Table 2: Preference color tendency by tone
N=226 (103 in Group 1, 123 in Group 2)

tone	Color chart 1	Color chart 2
vivid tone	17%	22%
light tone	15%	18%
pale tone	19%	14%
light grayish tone	3%	2%
soft tone	13%	11%
deep tone	13%	11%
dark tone	7%	8%
neutral	14%	15%

**Table 3: Preference color tendency by hue
N=226 (103 in Group 1, 123 in Group 2)**

χ^2 test (Upper: Actual measurement, Bottom: Expected value)

	P	PB	B	BG	G	GY	Y	YR	R	RP	N
Color chart 1	14	19	9	8	5	1	2	3	11	17	14
	17.31	15.49	12.30	5.925	5.013	2.279	2.735	2.279	8.659	15.95	15.04
	9	6	5							1	
Color chart 2	24	15	18	5	6	4	4	2	8	18	19
	20.68	18.50	14.69	7.075	5.987	2.721	3.265	2.721	10.34	19.04	17.96
	1	4	5						1	9	

$\chi^2(10) = 9.113$, ns

Cramer's V = 0.201

**Table 4: Preference color tendency by tone
N=226 (103 in Group 1, 123 in Group 2)**

χ^2 test (Upper: Actual measurement, Bottom: Expected value)

	vivid	light	pale	light grayish	soft	deep	dark	neutral
Color chart 1	18	15	20	3	13	13	7	14
	20.509	16.863	16.863	2.279	11.85	11.85	7.748	15.04
Color Chart 2	27	22	17	2	13	13	10	19
	24.491	20.137	20.137	2.721	14.15	14.15	9.252	17.96

$\chi^2(7) = 3.109$, ns

Cramer's V = 0.117

ACKNOWLEDGEMENTS

We would like to thank Editage (www.editage.com) for English language editing.

REFERENCES

1. Totsuka, U. (1964). An Examination on the Investigation Method of Favorite Colors. *Journal of Home Economics of Japan*, 15(2), 92-98. doi: <https://doi.org/10.11428/jhej1951.15.92>
2. Saito, M. 1994. A cross-cultural study on color preference in three Asian cities: Comparison between Tokyo, Taipei and Tianjin. *Japan Psychological Research*, 36(4), 219-232. doi: <https://doi.org/10.4992/psycholres1954.36.219>

THE EFFECTS OF COLOR PREFERENCE ON COLOR MEMORY

Yoshihiko Azuma* and Kou Yasuda

Department of Media and Image Technology, Faculty of Engineering, Tokyo Polytechnic University, Japan.

*Corresponding author: Yoshihiko Azuma, azuma@mega.t-kougei.ac.jp

Keywords: color preference, memory retention, colored words, word recall

ABSTRACT

A digital textbook that uses a digital device such as a tablet PC can be used as a textbook for learning. The digital textbook can easily change the colors of texts contained. It is thought that keywords should be colored to be easily memorized. This research examined the effects of color preference on recall of colored words. In experiments we used an iPad to present texts to subjects. The iPad was used in a viewing booth at an illuminance of 600 lx. Four groups of sentences about American food culture were chosen and appropriate ten words were assigned as keywords in each group. Two favorite colors and two least favorite colors were obtained from a questionnaire investigation to students in a color science class and these four colors were called “test colors”. The keywords in each group of sentences were colored in the same color as one of the test colors. Thus, the keywords in the four groups of sentences differed in color. In an experiment, a subject was asked to read a group of sentences in silence and after three minutes rest, to answer the keywords as many as possible. Twelve subjects performed this task for all groups of sentences. From the experiments the rate of correct answer was calculated for each subject for each test color. Results were analyzed in two categories, favorite color and least favorite color. Average value of correct answer rate was 42.5% for the favorite color and 35% for the least favorite color. Thus, the correct answer rate for favorite color is higher than that for least favorite color. Although, a statistical analysis showed no significant difference between favorite color and least favorite color, words in favorite color might be memorized easier than those in least favorite color.

INTRODUCTION

Digital devices such as smartphones and tablet PCs have become widespread, and books can be read on electronic devices. In Japan, the Ministry of Education, Culture, Sports, Science and Technology is aiming for the full-scale spread of digital textbooks after fiscal year 2020, when the new course of study is fully implemented at elementary schools. In addition, a bill was established in May, 2018. In the bill, digital textbooks that are available in PCs and tablet devices are approved as official textbooks.

With digital textbooks, you can change the color of text as if you were marking texts with a highlighter, so you can highlight important words or words you want to memorize. In this case, does word memory performance depend on the color of the word? Several previous studies have reported that the color of letters affects the memory retention of words, suggesting that red and yellow are more accurately remembered than green and blue [1]. Meanwhile, people have a preference for colors, such as their favorite and disliked colors. Does color preference affect memory retention? Very few studies on the effects of color preference on memory retention have been reported so far. When a person colorizes important words with a marker pen, the possibility of choosing his or her favorite color is great. When the words are in a favorite color, they might be memorized more accurately than when they are in other colors.

The purpose of this study is to clarify whether there is a correlation between memory retention of words in a color and preference of the color.

EXPERIMENT

In this experiment, subjects silently read four types of stimulus sentences with several words colored, and took a memory recall test for the words, thereby examining the effect of differences in word colors on memory accuracy.

Apparatus and Experimental environment

We used an Apple iPad Air 2 with 9.7 inch display of 2048 x 1536 pixel resolution (264 ppi) to present stimuli. The iPad Air 2 was placed at about 60 degrees in the viewing booth (Figure.1). The floor illuminance of the booth was set to about 600 lx so that it is 500 lx or more according to the school environmental health standard established by the Ministry of Education, Culture, Sports, Science and Technology [2]. The illuminance on the display screen was 150 lx.



Figure 1. Viewing booth

Stimuli

As stimuli, we used four sentences extracted from books dealing with the history of American food culture [3]. Each sentence consisted of 23 characters per line, 23 lines, and approximately 500 characters including Hiragana and Kanji (Figure.2). The font type was HGS Kyokasho-tai. The character size was 18 points and the height of the characters when viewed from a viewing distance of 60 cm was a viewing angle of 0.38 degrees. Ten selected words in each stimulus sentences is colored with a specific color.

The colors used for the words were chosen from ten web-safe colors close to five primary colors:5R, 5Y, 5G, 5B, 5P and five intermediate colors:5YR, 5GY, 5BG, 5PB, 5RP of the Munsell color system by 65 students who attended the class of "color science". The students observed the ten colors displayed on the screen of the iPad and chose the two most favorite colors and the two least favorite colors. As a result, "blue" close to 5B and "purple" close to 5P were chosen to be the most favorite colors, and "olive" close to 5GY and "maroon" close to 5RP were chosen to be the least favorite colors because they were the top two answers.

Subjects

Twelve university students aged 20 to 24 with binocular vision of 0.7 or more participated in the experiment. Visual acuity of each subject was measured with Atec Autovision tester AT-1000.

Procedure

In the viewing booth set up in the darkroom, the subjects tried to silently read the stimulus sentence presented on the iPad for 90 seconds and memorize the contents. After a 3-minute break, the subjects were asked to answer the five words specified from the eight colored words within the 5-minute answer time. Then the subjects took a 3 minute break. The above task was taken as one trial. This task was done in a random order for four different types of stimulus sentences.

刺激文章 2

アメリカは地域によって入植した人種の割合が異なるため、どの人種の食文化から**文化的影響**を受けているかはおおむね地域によって分けることができる。

例えば、南部でも特に**メキシコ系アメリカ人**の割合が多いテキサス州やニューメキシコ州などでは、**テキスメクス料理**という料理が根付いている。テキサス州に接したルイジアナ州は独立戦争以前では**フランス**領であり、**ケイジャン・フレンチ**と呼ばれるフランス人入植者が多く居住していた。ケイジャン料理は、彼らのフランス料理文化に、チリペッパーなどを用いたヒスパニック系の食文化が融合したルイジアナ独特の食文化である。

西海岸最大の都市であるカリフォルニアは太平洋に面しているという地理的条件から、アメリカ最大の**アジア系人口**を誇っており、同州最大の都市であるサンフランシスコをはじめとして、アジア料理が文化として強く根付いている。

ニューイングランド地域に代表される東海岸はそれとは代わり、イギリスやイタリアなどの**ヨーロッパ**をルーツとした食文化が存在している。ボストンなど裕福なイギリス系移民の多かった地域では、ロンドンのように牡蠣やロブスター・ニシンなどの**海産物**がよく食される。

Figure 2. Stimulus sentences

RESULTS

We decided two most favorite colors and two least favorite colors, but in the experiment, there were quite a few subjects who felt dislike the favorite colors and felt like the least favorite colors. Therefore, we analyzed according to whether the subjects felt like or not. Figure.3 shows the result of averaging the correct answer rate of all subjects for each color of word. Those who liked Olive, Purple, and Maroon had a higher correct answer rate than those who disliked them, but the standard deviation was large and no significant difference was observed. In Blue, the rate of correct answers was slightly higher for those who disliked, but the reliability was low because there was only one subject who disliked Blue. Next, Table 1 shows the results of sorting by favorite color and least favorite color for each subject. Figure. 4 shows the averaged values for all subjects. The favorite color shows a slightly higher value, but as a result of t-test with a risk rate of 5%, no significant difference was found depending on color preference.

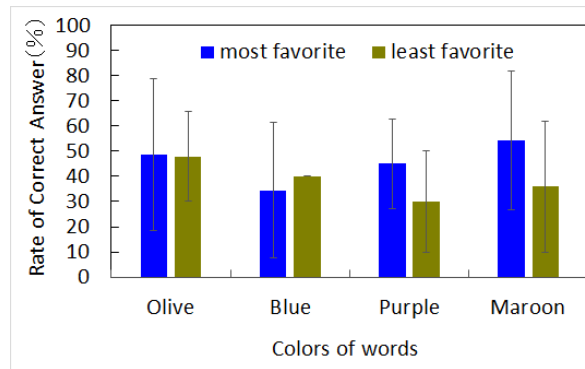


Figure 3. Rate of correct answer for each color

Table 1: Rate of correct answer for most favorite and least favorite color (%)

Subjects	Most favorite	Least favorite
A	60	20
B	10	20
C	50	50
D	26.7	0
E	33.3	40
F	53.3	40
G	70	50
H	10	40
I	70	0
J	46.7	40
K	33.3	60
L	46.7	60
Average	42.5	35.0

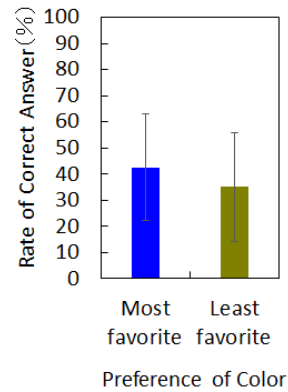


Figure 4. Average rate of correct answer

DISCUSSIONS

In the current study, the most favorite color and the least favorite color were decided by a preliminary survey, but the colors other than Blue did not necessarily match the preference of the subjects who participated in the experiment. It was better to select the color according to the subject's color preference. Otherwise, it seems that it is necessary to select colors that are liked and disliked

by the same number of subjects. Even in that case, the number of subjects this time is insufficient, and it seems necessary to increase the number of subjects further.

REFERENCES

1. Richards, C., Alonzo, M. & Barsness, M. (2016). The Effects of Warm and Cool Colors on Word Memory. *Sentience : Undergraduate Journal of Psychology*, 14 (FALL), 9-12. Retrieved from www.psych.umn.edu/sentience.
2. Ministry of Education, Culture, Sports, Science and Technology. (2009). School environmental health standards. Retrieved from www.mext.go.jp/component/a_menu/.../1292838_01.pdf (in Japanese).
3. Honma, T., Ariga, N. & Ishige, N. (2004). *Food Culture of the World (12):America*, Tokyo: Nobunkyo (in Japanese).

PREFERENCE OF COFFEE IMAGE COLOR TONE IN ADVERTISING

Pratthana Thammachat^{1*} Hathaichanok khemthong¹, Natthamon Piengthisong¹,
Chanida Saksirikosol² and Kitirochna Rattanakasamsuk²

¹ *Department of Advertising and Public Relations Technology, Faculty of Mass Communication Technology,
Rajamangala University of Technology Thanyaburi, Thailand.*

² *Color Research Center, Rajamangala University of Technology Thanyaburi, Thailand.*

*Corresponding author: Pratthana Thammachat, e-mail: pratthana.due@gmail.com

Keywords: Preference, Color Tone, Coffee Image, Advertising

ABSTRACT

The idea of an image in advertising normally creates with a favorable mental picture of the product in the mind of the customer. An attempt is made to associate the product or service with certain values. Advertiser tends to design the advertisement media by using “attractive” as the point of view. This paper aimed to investigate the preference of coffee image color tone in the advertisement. We prepared the picture of coffee which included color checker. We presented a picture on EIZO LCD display (27 inches) and asked the professional advertiser to adjust the color tone in red-green and yellow-blue by using software Adobe Lightroom. Ten professionals in the advertising industry participated in the experiment. The viewing distance of subject was 40 centimeters. The result showed clearly that the professional adjusted the coffee image to the yellow tone.

INTRODUCTION

Nowadays, people prefer to sit down in the coffee shop for chatting, talking or doing their job and business, so launching the coffee shop is the famous business and also growing sharply. It demonstrates that there is too many brand shop that enhances their branches in many areas, includes suburbs and towns. It could be called “Chain Store”. Moreover, launching the new coffee shop as SME, it has affected to have a comparative market for this business type, therefore, some owners use the advertisement for promoting their shop in the wider market as larger customers. They prefer to choose a photo of a cup of coffee to be a symbol or present their shop.

The advertisement is one channel to present the product to consumers. It is able to attract or convince them to interest in and buy that product. Hence, the advertisement has a response to make it happen by using some communication tools such as chose the famous person to be a brand ambassador or building a good image of goods and services.

Photograph is one tool of advertising to present goods or services to the consumer. Photo/picture that will be used for presenting has to be able to attract and convince the consumer to interest and buy that product, so the presenting photo has to consist of good components.

Producing photograph for advertising has to pay more attention and photographer skills in order to create a beautiful photo which matching with the brand concept. Also, when this photo presented to the consumer, it should attract the consumers to have a first impression on it, then consume or buy that product.

Furthermore, photograph color is an important component to illustrate photograph emotion. Choosing the photograph color is able to set up in the pre-production planning by identifying the color of photograph’s component or scene or products and others related in order to available with

advertisement concept. In the post-production, we should adjust the color by using many photograph editing programs.

Choosing the color tone in the coffee advertisement is able to make it charm and attract consumer, so the research objective is to study the right color tone for the coffee advertisement.

METHODOLOGY

In the production of coffee photograph, it has identified the direction of light by dividing the highlight and shadow. Also, we can take some components to include in the photograph scene in order to make a beautiful photo and able to make some smoke during taking the photo in order to make a realistic photograph. Besides, during taking a coffee photograph, the color checker will be put in the scene as shown in Figure 1.

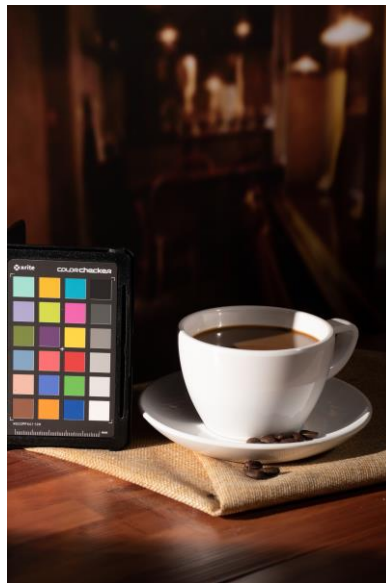


Figure 1. Coffee Photography with Color Checker

Then, the photographs were distributed to 10 professional photographers for editing color, light, and contrast. They stayed together in the experiment room with light control 300 lux and used the program of Adobe Lightroom with size 27 inch of a monitor screen.

After that, the edited photographs were collected from 10 professional photographers to measure the color through the color checker by using Luminance Meter of Konica Minolta, series CS-100A. This machine will compare the color with the color of the original photograph.

RESULT AND DISCUSSION

The result has demonstrated that both photographs are different in the color and it depends on each photographer's style.



Figure 2. The images Adjusted from 10 Professional Photographers

We compared the color average in the color checker from both edited and original photograph as shown in Figure 3 and Figure 4.

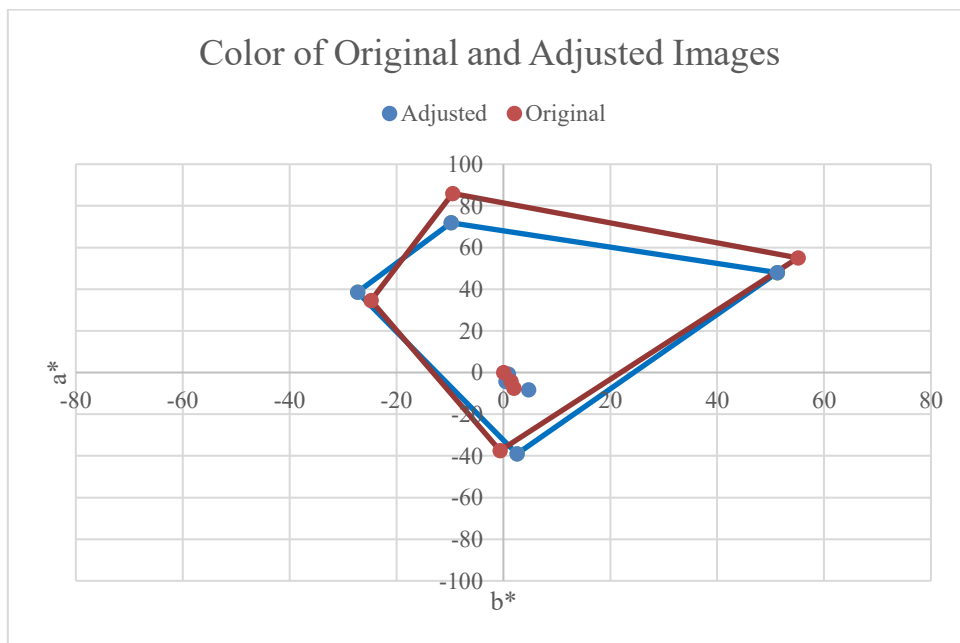


Figure 3. Comparison of Color between Original and Adjusted Images

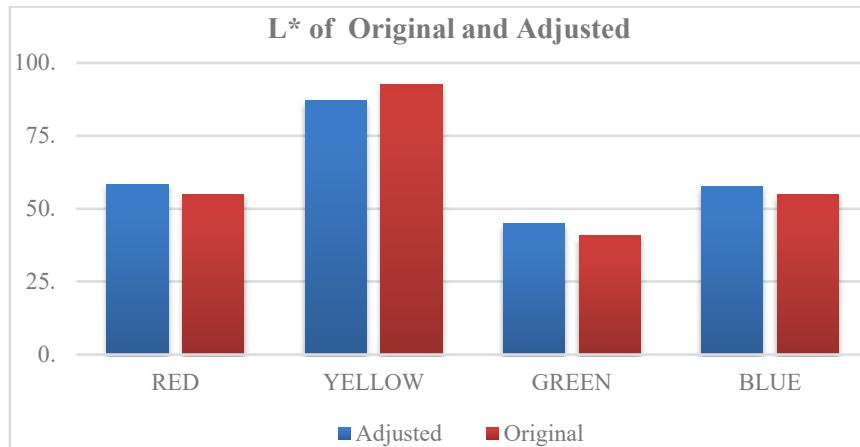


Figure 4. Comparison of L* between Original and Adjusted Images

According to the result of L* between original and edited images, it showed that the saturation of red and yellow has decreased and the lightness of yellow has decreased which means that the darkness of brown increase, but the other component has adjusted lighter in other to make the good atmosphere in overall.

The experiment photographers have recommended that they would like to adjust photo in more light with less contrast.

Form the experiment result, we have seen that the adjust photograph is more light and less saturation of orange in order to make them more similar to brown. However, we cannot set it to be a systematic rule due to the small example group. Therefore, we should enhance this study in a wider range and use a more different photographs.

CONCLUSION

According to the experiment result, it demonstrated that the color tone of the edited photo has more light in order to show the photo detail clearly, and the photo contrast has decreased and the saturation of yellow also decrease in order to make photo color to more similar with brown.

ACKNOWLEDGEMENT

We would like to thank the Communication Technology Faculty and the Department of Advertisement and Public Relations Technology for supporting place and equipment for this research. Also, we are very thankful for 10 photographers for joining this experiment.

REFERENCES

1. Wuttipong Nim-orn.) 2014(. Choosing Color for Photography. Retrieved September 16, 2019, from <https://www.dozzdiy.com>.
2. Yochuwa Samarom. (2018). Using Color in Photography. Retrieved September 16, 2019, from <https://www.photoschoolthailand.com/how-to-smartly-use-color-in-your-compositions>.
3. Alison Park-Whitfield. (2012). *Food Styling and Photography for Dummies*. Wiley Publisher.

A COMPARISON BETWEEN ITTEN'S AND ALBERS' BAUHAUS COLOUR THEORIES

Kyoko Hidaka^{1*}

¹*College of Engineering and Design, Shibaura Institute of Technology, Japan.*

*Corresponding author: Kyoko Hidaka, khidaka@shibaura-it.ac.jp

Keywords: Colour Theory, Bauhaus, Johannes Itten, Joseph Albers, Design Education

ABSTRACT

Johannes Itten (1888–1967) and Joseph Albers (1888–1976) were masters who taught colour theory at Bauhaus. From a colour theory perspective, this paper compares the characteristics of the two artists' approaches. Hideaki Chijiwa, the author of *An Outline of Color Science*, described Itten as a traditional colour theorist and Albers as a colour theorist of the new generation. Albers was indeed charismatic, for he influenced the Op Art movement in the 1960s. This paper, however, argues that Itten was not traditional because his colour scheme promoted the democratisation of modern industrial colour design.

Itten was Bauhaus' first colour theory teacher, and Albers was his successor. Itten brought in geometrical figures to colour theory, for example, colour stars or polygons based on Goethe's colour wheels, colorimetric systems and figurative notations. These geometric and algorithmic elements of the colour order system can be applied, especially to today's automatic digital colour schemes, to assist in mass production. Colour scheme algorithms can be seen at work in software such as Adobe Illustrator.

Meanwhile, Albers developed a colour theory to understand the arbitrary nature of human perception (e.g. optical illusions), which was crystallised in his seminal book *Interaction of Color*.

This contrast between the two colour theories is similar to a previous controversy about design standardisation involving Hermann Muthesius and Henry van de Velde in *Deutscher Werkbund*, which was an argument regarding mass production and artistic decorativeness. There was public demand for a colour theory that is suitable for mass production at factories as well as designs that incorporate human perception. Both colour theory approaches are indispensable when devising colour schemes. These Bauhaus masters' influence on 20th-century design education is deemed providential, and both approaches have become key to elevating Bauhaus' impact on modern design education worldwide.

INTRODUCTION

This paper compares the emphases of Itten's and Albers' approaches of colour theory from a colour theory view. Hideaki Chijiwa, the author of *An Outline of Color Science*, described Itten as a traditional colour theorist and Albers as a colour theorist of the new generation.[1] Albers set the trend of the Op Art movement in the 1960s.[2] This paper, however, argues that Itten was not traditional because his colour scheme promoted the democratisation of modern industrial colour design.

TWO DIFFERENT APPROACHES OF COLOUR THEORY

Itten was Bauhaus' first colour theory teacher at Bauhaus, and Albers was his successor. Itten brought in geometrical figures to colour theory, such as, colour stars or polygons based on Goethe's colour wheels, colorimetric systems and figurative notations.[3] These geometric and algorithmic elements of the colour order system can be applied, especially to today's automatic digital colour schemes, to assist in industrial production. Colour scheme algorithms can be seen at work in software such as Adobe Illustrator.

In stages, Albers developed a colour theory to understand the arbitrary nature of human perception (e.g. optical illusions), which was crystallised in his seminal book *Interaction of Color*.

ANALYSIS AND CONCLUSION

This contrast between the two colour theories is similar to a previous controversy about design standardisation involving Hermann Muthesius and Henry van de Velde in *Deutscher Werkbund*, which was an argument regarding mass production and artistic decorativeness. There was public demand for a colour theory that is suitable for mass production at factories as well as designs that incorporate human perception. Both colour theory approaches are significant when devising colour schemes.[4] These Bauhaus masters' influence on 20th-century design education is deemed providential, and both approaches have become key to elevating Bauhaus' impact on modern design education worldwide.

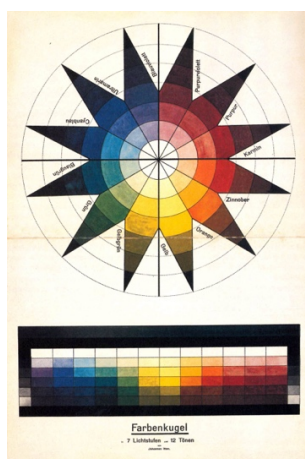


Figure 1. Itten, Colour Star (Colour Sphere) 1921, Goethe House (Weimar)

ACKNOWLEDGEMENT

This study was made possible by JSPS Grant-in-Aid for Scientific Research (C).

REFERENCES

1. Chijiwa, H. (2001). *An outline of Color Science*. Tokyo: University of Tokyo Press. p.213.
2. Albers, J. (1963). *Interaction of Color*. New Haven, CT: Yale University Press.
3. Itten, J., and Birren, F. (1970). *The Elements of Color: A Treatise on the Color System of Johannes Itten Based on His Book The Art of Color*. New York: Van Nostrand Reinhold.
4. Lara-Alvarez, C. and Reyes T. (2017). A Geometric Approach to Harmonic Color Palette Design. *Color Research & Application*. Wiley. DOI: 10.1002/col.22292

KNOWLEDGE OF TRADITIONAL COLOR NAMES AND ASPECTS OF JAPANESE CULTURE TO FEEL PROUD OF

Shin'ya Takahashi^{1*} and Noriko Aotani²

¹*School of Psychology, Tokai Gakuen University, Japan.*

²*School of Education, Tokai Gakuen University, Japan.*

*Corresponding author: Shin'ya Takahashi, takahashi-s@tokaigakuen-u.ac.jp

Keywords: traditional color names, pride in Japanese culture, 'love for one's home country' education

ABSTRACT

The present situation of Japanese young people's knowledge of, and attitude toward, traditional color names, and its relationship with individual traits including the aspects of Japanese culture which induced pride was investigated. A hundred and twenty-five university students answered the questionnaire on his/her knowledge of traditional color names, past experience of having learned these color names, motivation for learning them, their opinion about the cultural value of them, domestic and international interests in a general sense, and opinions about the validity of 24 selected items as representatives of Japanese culture. The data obtained was analyzed by the correlation analysis among processed scores, comparison of the group difference in terms of the learning experience, and the Self Organizing Map (SOM) procedure developed by Kohonen (1995). The results demonstrated that one's recognition of cultural value of the traditional color names has a stronger relationship with appreciation of Japanese culture, particularly for the traditional items, than one's knowledge about these color names. It was also indicated that the learning experience according to one's voluntary interest is more influential in raising the knowledge of the traditional color names and developing a positive attitude toward them than the learning experience at schools. These findings were discussed in light of the educational effectiveness of 'love for one's home country' education through learning traditional color names, our underlying research project.

INTRODUCTION

In our previous study, as a preliminary step of the research project on 'love for one's home country' education through learning traditional color names, we examined the relationship between Japanese young people's knowledge of traditional color names and aspects of Japanese culture of which they feel proud (Takahashi & Aotani, 2018) [1]. The reason why we directed our attention to the traditional color names is that these color names have been taught less and less in schools, although they are a rich source worthy of learning with their historical and cultural background and idiomatic uses. We thought these color names would be excellent learning materials for young people to take a new approach to appreciate the attractiveness of their home country, Japan.

Takahashi and Aotani (2018) analyzed their data by means of the Self Organizing Map developed by Kohonen (1995) [2], and found characteristic group of participants that could be labeled as a 'tradition-conscious' group, those who tended to appreciate traditional things such as 'kimono' (traditional clothes), 'shodo' (calligraphy), and 'kado' (flower arrangement), while being negative to contemporary culture. They also showed a greater knowledge of the traditional color names and a higher motivation for learning them. Another characteristic group of participants we found was labeled as a 'low motivation' group, those who had a relatively poor knowledge of the color names and a low motivation for learning them and showed an opposite tendency to the first group with regard to the aspects of Japanese culture in which they took pride.

In the present study, we reexamined the above findings in more detail. To achieve this, we collected data about pride in Japanese culture on a quantitative scale, as compared to the qualitative scale utilized by Takahashi and Aotani (2018). Participants rated, on a 5-point scale, each of the 24 cultural items as valid representatives of Japanese culture. In addition, participant's motivation for learning traditional color names, the opinion about the cultural value of these color names, and his/her domestic and international interests were measured to explore the individual traits relating to a knowledge about the traditional color names and the appreciation of Japanese culture.

METHODS

Participants

A hundred and twenty-five university students, 72 males and 53 females, answered the questionnaire. Their mean age was 18.3 years old ($SD=.60$).

Questionnaire

The questionnaire was comprised of six parts. Part 1 asked participant's knowledge of 10 Japanese traditional color names (see Table 1) using a 4-point scale from '1: do not know the name' to '4: know the detailed characteristics of the color.'

Part 2 asked participant's experience of having learned the traditional color names on three occasions; 1) at primary school, 2) at junior high or high schools, and 3) voluntarily due to his/her own interest. Participants answered each occasion in a yes/no manner.

Part 3 asked participant's motivation for learning these color names by three items, 'be intrigued,' 'want to know them more,' and 'hope to use them usually.' These items were answered on a 5-point scale from '1: do not agree at all' to '5: completely agree.'

Part 4 asked participant's opinion about the cultural value of these color names by five items, 'have high cultural value,' 'should be handed down to the future,' 'should be learned by the nation,' 'should be used in daily life,' and 'be proud of them internationally.' These items were answered on the same 5-point scale as in Part 3.

Part 5 asked participant's domestic and international interests by five items each, 'love Japanese traditional culture,' 'love my hometown,' 'Japan is the best country,' 'be proud of being Japanese,' and 'hope to get a job in my hometown' as the domestic interest items, and 'be attracted to various foreign cultures,' 'hope to speak good English,' 'want to visit many countries,' 'want to make many foreign friends,' and 'hope to work abroad' as the international interest items. These items were answered on the same 5-point scale as in Parts 3 and 4.

Finally, Part 6 instructed participants to rate, on the same 5-point scale as before, each of the 24 cultural items (see Table 3) as valid representatives of Japanese culture.

Data Analysis

In each participant, ratings of 10 items in Part 1 were averaged to yield *Knowledge* score ($\alpha=.762$). Similarly, *Motivation* ($\alpha=.848$), *Value* ($\alpha=.846$), *Domestic* ($\alpha=.695$) and *International* ($\alpha=.839$) scores were calculated from ratings in Parts 3, 4, and 5.

Ratings in Part 6 underwent the factor analysis (maximum likelihood method, Promax rotation), and five factors were obtained. The first factor loaded highly to 'kado,' 'sado (tea ceremony),' 'shodo,' 'noh and kyogen (traditional theatrical art),' 'haiku and tanka (traditional short poetry),' 'kimono,' and 'local idol,' and was labeled as *Traditional Culture*. The second factor loaded highly to 'yakitori (skewered chicken),' 'ramen (noodle),' 'sukiyaki,' 'karaoke,' 'tempura,' 'onigiri (rice ball),' and 'sushi,' and was labeled as *Food*. The third factor loaded highly to 'manga,' 'anime,' 'game,' and 'cosplay (costume play),' and was labeled as *Pop Culture*. The fourth factor loaded highly to 'jinja (shrine),' 'jiin (temple),' and 'jokaku (castle),' and was labeled as *Structure*. The fifth

factor loaded highly to ‘samurai’ and ‘ninja,’ and was labeled as *Samurai*. Then, in each participant, ratings of items listed above were averaged to produce *Traditional Culture*, *Food*, *Pop Culture*, *Structure*, and *Samurai* scores ($\alpha=.900$, $.850$, $.851$, $.883$, and $.949$, respectively). Exceptionally, rating of ‘Fujisan (Mt. Fuji)’ was used in the succeeding analysis as *Fujisan* score, because it was not exclusively loaded by any single factor.

RESULTS

Basic Statistics

Table 1 shows mean rating of knowledge of each color name examined (on its approximate background color) with its Munsell notation, as well as the total *Knowledge* score in the right column. Table 2 shows mean and SD (in parenthesis) of each score among all, male, and female participants. It was revealed that females rated significantly higher than males in *Motivation* ($t=3.10$, $df=123$, $p=.002$, $d=.56$), *Value* ($t=2.31$, $df=123$, $p=.022$, $d=.42$), *Traditional Culture* ($t=3.79$, $df=123$, $p<.001$, $d=.69$), and *Structure* ($t=2.38$, $df=123$, $p=.019$, $d=.43$). Table 3 shows mean rating of each item presented in Part 6 of the questionnaire.

Correlation Analysis

Table 4 shows correlation coefficients among scores in all participants. *Knowledge*, *Motivation*, and *Value* correlated positively with each other. Six scores of Japanese culture, *Traditional Culture*, *Food*, *Pop Culture*, *Structure*, *Samurai*, and *Fujisan* correlated positively with each other as well. *Domestic* and *International* had no correlation, while these scores correlated positively with most cultural scores. As regards relationship between color-related scores and the cultural scores, in which we have a chief interest, *Value* had stronger positive correlations with cultural scores than *Knowledge* and *Motivation*. *Value* also had a positive correlation with *Domestic*, but not with *International*.

Table 1. Color names used in the questionnaire, their Munsell notations, and mean rating of knowledge of each color, the score ranging from 1 (low) to 4 (high).

Color name	Oudo	Gunjo	Yama-buki	Enji	Uguisu	Toki	Komugi	Hada	Kohaku	Akane	Total
Munsell notation	10YR 6/7.5	7.5PB 3.5/11	10YR 7.5/13	4R 4/11	1GY 4.5/3.5	7RP 7.5/8	8YR 7/6	5YR 8/5	8YR 5.5/6.5	4R 3.5/11	(Know- ledge)
Mean (SD)	3.63 (0.50)	3.24 (0.80)	3.27 (0.72)	2.98 (1.01)	2.68 (1.01)	1.58 (0.86)	3.06 (0.91)	3.82 (0.40)	2.76 (1.10)	3.16 (0.77)	3.02 (0.47)

Table 2. Mean and SD (in parenthesis) of each score among all, male, and female participants, the score ranging from 1 (low) to 5 (high) except for *Knowledge*.

	<i>Knowledge</i>	<i>Motivation</i>	<i>Value</i>	<i>Domestic</i>	<i>International</i>
All	3.02 (.47)	3.03 (1.12)	3.00 (.82)	3.66 (.74)	3.25 (.95)
Male	2.98 (.47)	2.77 (1.10)	2.86 (.84)	3.63 (.84)	3.19 (1.01)
Female	3.07 (.47)	3.38 (1.07)	3.19 (.75)	3.69 (.59)	3.34 (.87)

[Table 2. Continued]

	<i>Trad. Cul.</i>	<i>Food</i>	<i>Pop Cul.</i>	<i>Structure</i>	<i>Samurai</i>	<i>Fujisan</i>
All	3.95 (.78)	4.00 (.77)	4.09 (.87)	4.05 (.88)	4.02 (1.02)	4.30 (1.03)
Male	3.74 (.85)	3.98 (.86)	4.02 (.93)	3.89 (1.01)	3.91 (1.08)	4.17 (1.16)
Female	4.25 (.56)	4.04 (.64)	4.18 (.78)	4.26 (.60)	4.18 (.92)	4.47 (.80)

Table 3. Mean rating and SD (in parenthesis) of each item presented in the questionnaire as the representative of Japanese culture, the score ranging from 1 (low) to 5 (high).

sushi	4.52 (.82)	manga	4.40 (.92)	haiku / tanka	3.85 (1.13)
tempura	4.10 (1.00)	cosplay	3.61 (1.18)	noh / kyogen	3.87 (1.12)
sukiyaki	3.99 (1.02)	game	3.95 (1.13)	ninja	4.02 (1.02)
ramen	3.90 (1.18)	local idol	2.75 (1.08)	samurai	4.03 (1.06)
yakitori	3.69 (1.23)	sado	4.31 (.88)	jinja	4.14 (.97)
onigiri	4.22 (1.05)	kado	4.23 (.90)	jiin	4.06 (.96)
karaoke	3.61 (1.21)	shodo	4.26 (.92)	jokaku	3.95 (.99)
anime	4.40 (.93)	kimono	4.40 (.88)	Fujisan	4.30 (1.03)

Table 4. Correlation coefficients among scores. ** $p < .01$ * $p < .05$

	K	M	V	D	I	TC	F	PC	St	Sa
<i>Knowledge</i>	----									
<i>Motivation</i>	.291**	----								
<i>Value</i>	.211*	.654**	----							
<i>Domestic</i>	.027	.102	.349**	----						
<i>International</i>	.027	.003	.065	-.046	----					
<i>Trad. Cul.</i>	.074	.205*	.383**	.272**	.259**	----				
<i>Food</i>	.093	.117	.139	.368**	.270**	.403**	----			
<i>Pop Cul.</i>	.175	.153	.215*	.197*	.123	.471**	.460**	----		
<i>Structure</i>	.158	.166	.333**	.298**	.258**	.648**	.429**	.379**	----	
<i>Samurai</i>	-.093	.168	.297**	.262**	.226*	.560**	.463**	.459**	.570**	----
<i>Fujisan</i>	-.111	.050	.140	.248**	.225*	.461**	.406**	.216*	.584**	.581**

Influence of Learning Experience

The results of Part 2 of the questionnaire, in which participants were asked their past experience of having learned the traditional color names, was Yes=45, No=80 for 'at primary school,' Yes=42, No=83 for 'at junior high or high schools,' and Yes=42, No=83 for 'voluntarily due to participant's own interest.' (These three occasions are not mutually exclusive to be answered, so some participants answered 'Yes' to more than one occasion.)

Then, we divided participants into Yes-group and No-group in each learning occasion and analyzed the group difference of scores. In the occasion of primary school, Yes-group rated higher than No-group in *Fujisan* (Yes-group 4.56, No-group 4.15; $t=2.14$, $df=123$, $p=.034$, $d=.40$). In the occasion of junior high or high schools, Yes-group rated higher than No-group in *Domestic* (Yes-group 3.92, No-group 3.53; $t=2.89$, $df=122$, $p=.005$, $d=.55$). In the occasion of voluntary interest, Yes-group rated higher than No-group in *Knowledge* (Yes-group 3.18, No-group 2.94; $t=2.81$, $df=123$, $p=.006$, $d=.53$), *Motivation* (Yes-group 3.48, No-group 2.81; $t=3.26$, $df=123$, $p=.001$, $d=.62$), and with a marginal significance in *Value* (Yes-group 3.20, No-group 2.90; $t=1.93$, $df=123$, $p=.056$, $d=.37$).

Self Organizing Map (SOM)

The data obtained was processed with a data-mining procedure to investigate the relationship among all scores and participant's attributes. The data mining procedure was based on the data-ordering and visualization capabilities of the Self Organizing Map (SOM) [2]. Based on the

principles of ‘ordered vector quantization,’ the SOM approach has the advantage that all input data are represented as vectors in a data space defined by the number of variables for each sample.

The analysis revealed that 4-cluster solution is the optimal balance between cluster size and distinguishing features (Figure 1). On maps with four attributes shown in the first row, males and participants who answered ‘No’ to the learning experience questions are shown in blue, and females and participants who answered ‘Yes’ are shown in red. On other score maps, participants are represented in colors changing from blue, green, yellow, orange to red according to each one’s score.

The maps visualize that the participants in Yes-group on *Voluntary Interest* tend to have higher scores on *Knowledge*, *Motivation*, and *Value* maps, whereas those on *Primary School* and *Junior High & High Schools* maps do not. Moreover, it is more clearly shown that the participants without learning experience on any occasions, forming the upper half of the central cluster, have low color-related scores, *Knowledge*, *Motivation*, and *Value*. We can also see that some participants in Yes-group on *Voluntary Interest*, comprising a small cluster in the lower right of maps, tend to rate low for most cultural items. They are all males and their color-related scores are also low.

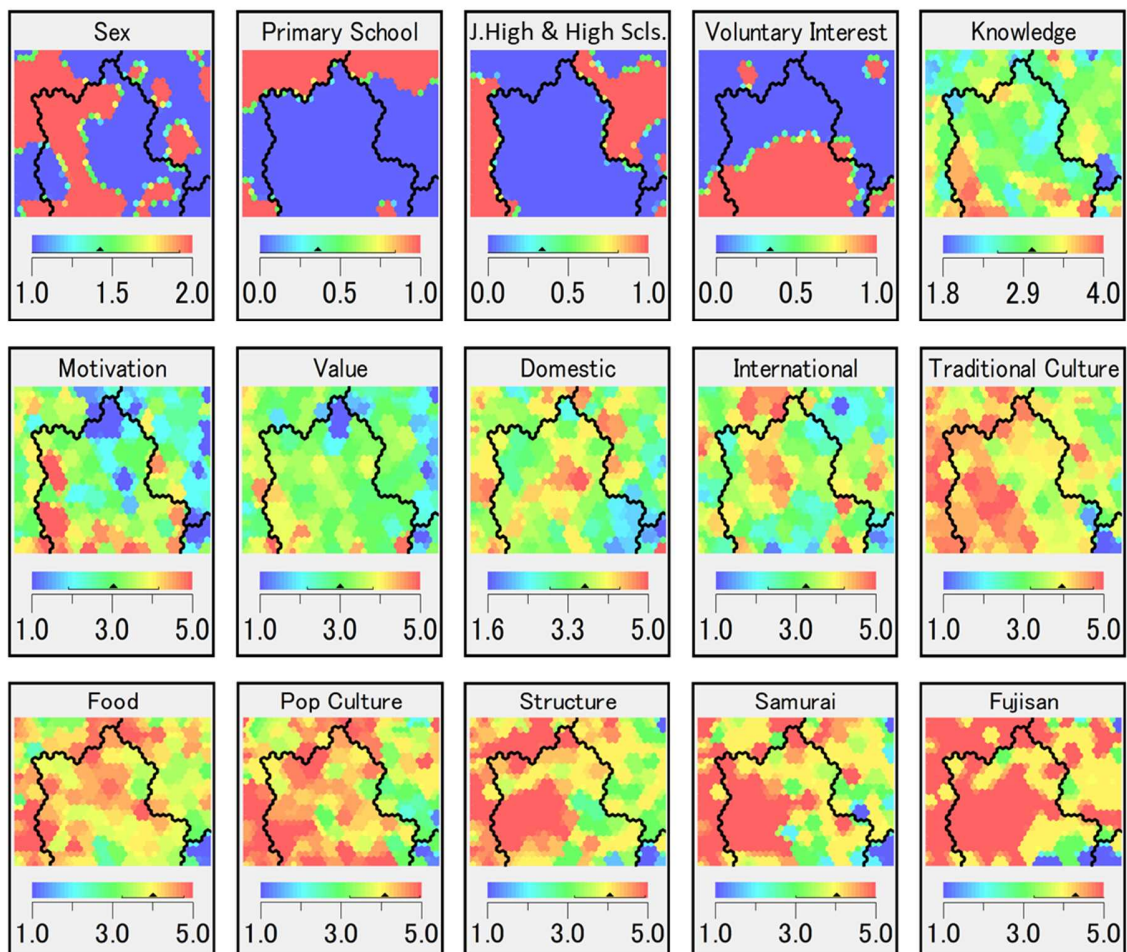


Figure 1. Results of the Self Organizing Map (SOM) analysis. The colors on maps indicate the score of each participant represented as a dot (or more precisely, a hexagon). The score range of each map is shown below the map with the mean (\blacktriangle) and SD (segment). Each participant is represented in the same position on all maps.

DISCUSSION

Participants in the present study had a rather good knowledge about the traditional color names examined. The average *Knowledge* score, 3.02, means that participants were 'able to roughly imagine the color, though not confident about its detailed characteristics.' Among these colors, the score of *Toki* (1.58) is remarkably low, that indicates the place between 'do not know the name' and 'have heard the name but cannot imagine its color at all.' The color name *Toki* derived from the bird of the same name that was very popular in Japan a hundred years ago. However, the bird's population decreased rapidly due to overhunting and development, and are rarely seen in Japan now. It would be one of the typical cases of a color name being forgotten because its source (original possessor of the color) is no longer a feature of modern life.

As shown in Table 4, three color-related scores, *Knowledge*, *Motivation*, and *Value*, correlated positively with each other. However, correlation coefficients between *Knowledge* and other two scores are lower than our previous data ($r=.430$ with *Motivation*, $r=.331$ with *Value*) [1]. In contrast, coefficient between *Motivation* and *Value* this time ($r=.654$) is higher than before ($r=.452$). These points seem to imply a clue to read the present results comprehensively, suggesting one's 'having knowledge of the color names' should be considered separately from one's 'being motivated to learn them more' or 'recognizing their cultural value.' This is seen in the relationship between color-related scores and other scores as well. Whereas *Knowledge* had no relationship with any cultural scores, *Value* correlated positively with them, particularly with *Traditional Culture*, *Structure*, and *Samurai*. *Value* also had a positive correlation with *Domestic*. Taking these results together, it could be summarized those who recognize the cultural value of the traditional color names are inclined to be domestic-oriented and tend to have a positive attitude toward traditional Japanese culture, while for those who know them well it is not necessarily so. Therefore, in order to achieve 'love for one's home country' education through learning traditional color names, it may be more important to understand the attractiveness and value of these colors and color names than to memorize just a linkage between the color and its name.

In addition, we obtained another result that is suggestive from the educational point of view. When the group difference in terms of participant's learning experience was analyzed, the learning experience according to a voluntary interest had an influence upon color-related scores; those who have learned the color names voluntarily showed higher *Knowledge*, *Motivation*, and *Value* scores than those who have not. In contrast, learning experience in schools did not have such an influence. These results show the importance of an active learning on 'love for one's home country' education by using the traditional color names. Our research project originated from the idea that the recent situation in Japanese schools where the students have rarely been taught traditional colors and their names is regrettable. Therefore, we considered the first item is to change this situation. In this respect, the present findings suggest that it is important not only to teach the traditional colors to young people, but also to make them have an interest in these colors and begin a voluntary and active learning.

REFERENCES

1. Takahashi, S. & Aotani, N. (2018). Preparatory study of indigenous education through traditional color names. *Proceedings of Education and New Development 2018*, [Ed.] M. Carmo, 443-445.
2. Kohonen, T. (1995). *Self-Organizing Maps*. New York: Springer.

COLOR FEATURES OF THE WATERSCAPE DRAWING AND DRAWER'S PERSONALITY IN THE AGED

Riko Miyake^{1*} and Shin'ya Takahashi¹

¹*School of Psychology, Tokai Gakuen University, Japan.*

*Corresponding author: Riko Miyake, miyake-r@tokaigakuen-u.ac.jp

Keywords: waterscape drawing, color features, drawer's personality, aged people

ABSTRACT

The relationship between color features of a waterscape picture drawn by the aged people and drawer's personality was investigated. Eighty-five people (44 males and 41 females), aged from 63 to 88 years, drew a picture using 24-color crayons per an instruction 'please draw freely a scene with water.' They also answered general and specific personality inventories and the semantic differential scales asking the mental image of the water. Pictures were scanned into digital image, and the color feature indices (Ave-L*, Ave-C*, Ave-h, and Hue-ENT) were calculated for the full image (whole picture) and for the water image (water-depicted area). The correlation analysis between the color feature indices and the psychological indices revealed that the old people who have a pure, violent, and joyful image of the water tended to draw bluish picture. Moreover, the old people who have a feminine image of the water tended to draw light picture, while those who have a maternal image of the water tended to draw dark picture. Participant's personality traits had weaker relationship with the color feature indices of the picture than his/her mental image of the water. In addition, some gender-specific relationships were found, positive and optimistic old males tended to draw the water in deep blue, and the old females having a pure image of the water tended to draw deep-bluish picture with complex coloring. These results were discussed by comparing with the data obtained from young participants in our previous studies.

INTRODUCTION

In the clinical psychology, client's production of water as a subject matter (e.g., drawing and sandplay) is often used as a clue to psychological assessment, because water representation is thought to have much information about producer(client)'s mental state. For example, Miyake (2009) investigated the relationship between characteristics of the waterscape drawing (free drawing of 'any scene with water') and drawer's personality, and found that those who drew a scene of water with motion (e.g., river) tended to have stronger positivity and extraversion than those who drew a scene of water without motion (e.g., pond) [1].

In the past research of the waterscape drawings, as in the case cited above, assessment was almost limited to a qualitative and subjective analysis such as an interpretation of the meaning of depicted water that is told by a client him/herself. Researchers have not paid much attention to, for example, 'how deep' or 'how dense' the water was drawn, since these aspects were thought to be ambiguous when subjectively evaluated. However, by employing the image-analyzing technique [2], we can utilize such an information as objective image feature indices.

We have investigated the relationship between color features of the waterscape drawing and drawer's personality [3,4]. In these studies, we used young people (university students) as participants and revealed some interesting findings, for example, positive and highly-motivated people tended to draw water in dark blue and females who think water joyful and alive tended to

draw light picture. In the present study, to test a generalizability of these findings, we examined aged people as participants.

METHODS

Participants

Eighty-five people, aged from 63 to 88 years (mean 74.3 years old; 44 males and 41 females), participated in the present research as paid volunteers.

Questionnaire

We employed following six inventories and scales; YG (Yatabe-Guilford) Personality Inventory (YGPI; 120 items) [5], a Japanese version of the State-Trait Anxiety Inventory-Form JYZ (STAI; 40 items) [6], a short form of the Japanese Big-Five Scale (Big-Five; 29 items) [7], the Resilience Scale for Students (RS-S; 25 items) [8], the Sense of Basic Trust Scale (Trust Scale; 11 items) [9], and the semantic differential (SD) scale asking participant's mental image of the water (30 items) [10].

Procedure

The test was conducted in a group of about 20 participants. First, participants answered YGPI, STAI, Big-Five, RS-S, and Trust Scale. Next, they drew a picture according to an instruction 'please draw freely a scene with water.' A picture was drawn by using a black pencil, a black felt-tip pen, and 24-color crayons, on an A4-size sheet of Kent paper. Most participants mainly used crayons. It took about 30 minutes for drawing. Then, after answering the Post-Drawing Inquiry (PDI) sheet in which participants were asked to give a supplementary explanation of the picture they drew, finally they answered the SD scale asking the image of the water. It took about an hour and a half to complete the whole test.

Color Feature Indices of Pictures

Pictures were scanned into digital images (Epson GT-X830, 24bit color, 72dpi, no color correction). The scan was conducted in two ways for each picture; a full image was obtained by scanning a whole picture and a water image was obtained by scanning water-depicted area (e.g., river, sea and pond) in the largest rectangle. Then, using originally-developed image-analyzing software [2], images were converted into L*-image, C*-image, and h-image, and therefrom the averaged luminance (Ave-L*), the averaged chroma (Ave-C*), the averaged hue angle (Ave-h)¹, and the hue entropy (h-ENT) were calculated as color feature indices.

Psychological Indices of Participants

Results of YGPI, STAI, and Big-Five were processed according to the test manual, and scores of twelve personality traits of YGPI, two subscales of STAI, and five subscales of Big-Five were calculated in each participant. Results of RS-S, Trust Scale, and the SD scale were subjected to the factor analysis (maximum likelihood method, Promax rotation), and four factors of RS-S (Social Support; $\alpha=.867$, Competence; $\alpha=.826$, Positive Evaluation; $\alpha=.789$, and Significant Others; $\alpha=.843$), three factors of Trust Scale (Active Interpersonal Trust; $\alpha=.736$, Passive Interpersonal Trust; $\alpha=.712$, and Basic Trust; $\alpha=.658$), and eight factors of the image of the water (Purity; $\alpha=.903$, Harmony; $\alpha=.790$, Violence; $\alpha=.711$, Speediness; $\alpha=.638$, Joy; $\alpha=.702$, Feminineness; $\alpha=.501$, Maternalism; $\alpha=.582$, and Warmth; $\alpha=.703$) were obtained.

¹ In this software, a*-plus axis is set as the origin of the hue angle, and the counter-clockwise direction takes plus value from 0 to 180, and the clockwise direction takes minus value from 0 to -180.

RESULTS

Excluding data of three participants (all males) who drew an achromatic picture by using only a pencil, data of 82 participants were analyzed.

Basic Statistics

Table 1 shows mean of psychological indices in all, male, and female participants. It was revealed that males rated significantly higher than females in Trait Anxiety ($t=2.33$, $df=80$, $p=.022$, $d=.51$), and females rated significantly higher than males in Social Support ($t=3.61$, $df=80$, $p=.001$, $d=.80$) and Positive Evaluation ($t=2.33$, $df=80$, $p<.022$, $d=.51$).

Table 2 shows mean and SD (in parenthesis) of the color feature indices in all participants. The color feature indices were calculated for the full image and the water image of each picture. The prefix 'w-' indicates the indices of the water image. There was no significant sex difference in any color feature indices.

Table 1. Mean of psychological indices, the score ranging from 0 to 20 for YGPI, from 20 to 80 for STAI, from 1 to 7 for Big-Five, Trust Scale, and SD scale, and from 1 to 4 for RS-S.

Note. D: Depression, C: Cyclic Tendency, I: Inferiority Feelings, N: Nervousness, O: Lack of Objectivity, Co: Lack of Cooperativeness, Ag: Lack of Agreeableness, G: General Activity, R: Rhythymia, T: Thinking Extraversion, A: Ascendance, S: Social Extraversion, State: State Anxiety, Trait: Trait Anxiety, Ext: Extraversion, Con: Conscientiousness, Neu: Neuroticism, Ope: Openness, Agr: Agreeableness, SS: Social Support, Com: Competence, PE: Positive Evaluation, SO: Significant Others, A-IT: Active Interpersonal Trust, P-IT: Passive Interpersonal Trust, BT: Basic Trust, Pur: Purity, Har: Harmony, Vio: Violence, Spe: Speediness, Joy: Joy, Fem: Feminineness, Mat: Maternalism, and War: Warmth.

	YGPI											
	D	C	I	N	O	Co	Ag	G	R	T	A	S
All	6.46	7.68	6.14	7.65	7.20	6.23	10.35	13.43	10.41	9.84	11.06	13.55
Male	7.02	7.83	6.88	8.60	6.72	6.70	10.64	13.20	10.48	10.02	10.78	13.20
Female	5.89	7.52	5.40	6.71	7.68	5.76	10.05	13.67	10.35	9.66	11.34	13.90

[Table 1. Continued.]

	STAI		Big-Five					RS-S			
	State	Trait	Ext	Con	Neu	Ope	Agr	SS	Com	PE	SO
All	40.40	40.48	4.73	4.62	3.82	4.49	4.75	2.83	2.87	2.93	3.30
Male	41.22	42.67	4.66	4.79	3.87	4.59	4.63	2.59	2.82	2.81	3.20
Female	39.59	38.29	4.81	4.45	3.76	4.38	4.87	3.06	2.91	3.06	3.41

[Table 1. Continued.]

	Trust Scale			SD scale (image of the water)							
	A-IT	P-IT	BT	Pur	Har	Vio	Spe	Joy	Fem	Mat	War
All	4.83	5.39	4.45	5.07	4.61	3.82	4.04	4.59	3.85	4.92	4.57
Male	4.65	5.21	4.30	4.97	4.81	3.56	4.05	4.54	3.83	4.91	4.67
Female	5.01	5.58	4.59	5.18	4.41	4.08	4.03	4.63	3.86	4.93	4.48

Table 2. Mean and SD (in parenthesis) of the color feature indices.

Ave-L*	Ave-C*	Ave-h	h-ENT	w-Ave-L*	w-Ave-C*	w-Ave-h	w-h-ENT
93.07 (5.00)	8.21 (6.55)	48.45 (26.41)	5.29 (1.54)	92.54 (6.17)	8.54 (7.59)	-44.21 (57.86)	5.73 (1.02)

Table 3. Correlation coefficients between the psychological indices and the color feature indices. Black, blue and red figures indicate the result of all, male, and female participants, respectively. Only the significant results are shown. Boldface figures: $p < .01$, otherwise: $p < .05$.

	YGPI		Big-F	RS-S	Trust	SD scale (image of the water)				
	D	T	Con	PE	A-IT	Pur	Vio	Joy	Fem	Mat
Ave-L*	-.263								.290	-.219
Ave-C*						.346			-.254	
Ave-h		.222	.374		-.325	-.263	-.288	-.422		
h-ENT	.234				.324	.395				
w-Ave-L*										
w-Ave-C*				.326						
w-Ave-h										
w-h-ENT					.263					

Correlation Analysis

Table 3 shows correlation coefficients between the color feature indices and the psychological indices. Black figures indicate the results of all participants. Blue and red figures indicate the results of male and female participants respectively, only in the case where the coefficient of all participants did not reach significance. In this table, only the significant results are shown. Two subscales of STAI showed no significant correlations with any color feature indices.

DISCUSSION

As regards the relationship between the color feature indices of pictures and the psychological indices of drawers, personality traits measured by general scales (YGPI and Big-Five) and by specific scales (STAI, RS-S, and Trust Scale) showed only a limited tendency. Significant cases of the general personality traits are a negative correlation between Depression of YGPI and Ave-L*, a positive correlation of Depression and h-ENT, and a positive correlation between Thinking Extraversion and Ave-h. These results mean that depressive old people tended to draw darker picture with complex coloring, and those who do not do deliberate thinking tended to draw yellowish picture represented by larger value of a hue angle. These relationships were not found in young people in our previous study [3]. As to the specific personality traits, Active Interpersonal Trust of Trust Scale correlated positively with w-h-ENT, indicating that the water-depicted area of a picture drawn by the old people who think others trustworthy tended to have complex coloring.

In contrast, participant's mental image of the water demonstrated stronger relationship with the color feature indices. Ave-L* correlated positively with Feminineness and negatively with Maternalism, Ave-C* correlated negatively with Feminineness, and Ave-h correlated negatively with Purity, Violence, and Joy. The results of Ave-h would be particularly interesting. Since, as noted above, smaller (negative) value of a hue angle indicates a direction toward blue, the above correlations mean that the old people who have a pure, violent, and joyful image of the water tended to draw bluish picture. In some cases, it is due to larger part of the picture being occupied by the water. At the same time, however, it should be noted that among these factors related to Ave-h, Violence did not have significant correlation with neither Purity ($r = .138$, ns) nor Joy ($r = .192$, ns), while Purity and Joy correlated positively with each other ($r = .569$, $p < .01$). Therefore, it would be better to suppose that the different psychological processes underlie between bluish pictures drawn by the old people having pure and joyful image of the water and by those having violent image of the water. This is our next problem that should be investigated in the future studies.

Next, Ave-L* correlated positively with Feminineness and negatively with Maternalism. That means the old people who have a feminine image of the water tended to draw light picture, while those who have a maternal image of the water tended to draw dark picture. Though these two images seem to overlap with each other, they mutually had no significant correlation ($r=.213$, ns). Feminineness also correlated negatively with Ave-C*, meaning that the picture drawn by a participant having such an image tended to be less vivid or pale. Considering together with the fact that Feminineness loaded highly to the items such as ‘organized’ and ‘weak’ as well as ‘feminine,’ it may represent rather calm and passive image of the water, as compared to Maternalism that loaded highly to ‘pure’ and ‘alive,’ suggesting vigorous and active image of the water.

To see the results by participant’s gender, Active Interpersonal Trust correlated negatively with Ave-h and positively with h-ENT in females, meaning that a picture drawn by an old woman who thinks others trustworthy tended to be bluish and complex in coloring. Moreover, also in females, Purity correlated positively with Ave-C* and h-ENT, indicating that an old woman having a pure image of the water tended to draw deep-bluish picture with complex coloring.² Figures 1a and 1b show, for references, the drawings by female participant with high Purity score (7.0) and high Ave-



Figure 1a. A picture drawn by a female participant with high Purity score.



Figure 1b. A picture drawn by a female participant with low Purity score.

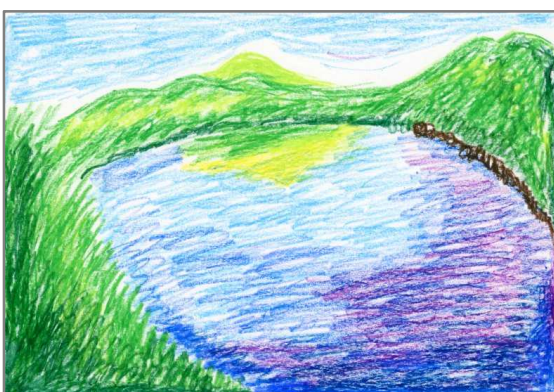


Figure 2a. A picture drawn by a male participant with high PE score.

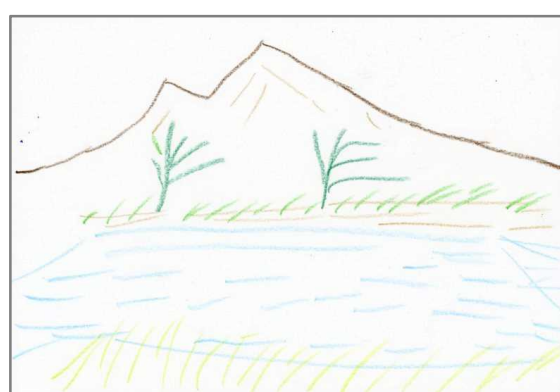


Figure 2b. A picture drawn by a male participant with low PE score.

² Purity correlated negatively with Ave-h in females ($r=-.380$, $p<.05$), whereas it did not in males ($r=-.138$, ns).

C* (16.5) and with low Purity score (3.7) and low Ave-C* (2.3), respectively.³ This tendency was not found in young female participants in our previous results [4]. It was also shown that the conscientious old females tended to draw yellowish picture, indicated by a positive correlation between Conscientiousness of Big-Five and Ave-h.

In males, on the other hand, a positive correlation between Positive Evaluation (PE) of RS-S and w-Ave-C* showed that positive and optimistic old males tended to draw the water in deep color (blue in most cases). Figures 2a and 2b show the drawings by male participant with high PE score (3.4) and high w-Ave-C* (27.4) and with low PE score (2.2) and low w-Ave-C* (1.3). This result may be fundamentally linked to our previous findings obtained from young participants, the positive correlations between Lack of Agreeableness and Rhythymia of YGPI and w-Ave-C* that was considered to suggest a relationship between deep coloring of the water and the drawer's positive and decisive personality [3].

The results of the present study given by the aged participants showed different tendency from those given by young participants in some ways. However, since obtained correlation coefficients are generally low, even if statistically significant, it would be far from conclusive. Therefore, we need larger number of participants to be examined in the future. In addition, in order to clarify the developmental changes on this subject, we need to examine participants with wider range of age as well.

REFERENCES

1. Miyake, R. (2009). The waterscape drawing method and Y-G Personality Test. *Memoirs of the Faculty of Education, Shimane University*, 43, 79-85. [In Japanese]
2. Mori, T., Uchida, Y., & Komiyama, J. (2010). Relationship between visual impressions and image information parameters of color textures. *Journal of the Japan Research Association for Textile End-Uses*, 51(5), 433-440. [In Japanese]
3. Miyake, R., Takahashi, S., & Mori, T. (2016). Relationship between color and form features of waterscape drawing and drawer's personality. *AIC2016 SANTIAGO DE CHILE Proceedings, [Ed.] I.C. Ivanovic*, 181-184.
4. Miyake, R., Takahashi, S., & Mori, T. (2017). Color features of the waterscape drawing and drawer's mental image of the water. *AIC2017 JEJU Proceedings, [Ed.] Y.J. Lee, J. Hwang, H.J. Suk, & Y.K. Park*, PS03-16.
5. Tsujioka, B., Yatabe, T., & Sonohara, T. (1982). *Yatabe-Guilford Personality Inventory*. Osaka: Institute for Psychological Testing. [In Japanese]
6. Hidano, T., Fukuhara, M., Iwawaki, S., Soga, S., & Spielberger, C.D. (2000). *State-Trait Anxiety Inventory-Form JYZ*. Tokyo: Jitsumukyoiku Shuppan. [In Japanese]
7. Namikawa, T., Tani, I., Wakita, T., Kumagai, R., Nakane, A., & Noguchi, H. (2012). Development of a short form of the Japanese Big-Five Scale, and a test of its reliability and validity. *The Japanese Journal of Psychology*, 83(2), 91-99. [In Japanese]
8. Saito, K., & Okayasu, T. (2010). Development of the Resilience Scale for Students. *Meiji University Journal of Psycho-Sociology*, 5, 22-32. [In Japanese]
9. Tani, F. (1996). Development of the Sense of Basic Trust Scale. *Proceedings of the 60th Annual Convention of the Japanese Psychological Association*, 310. [In Japanese]
10. Tada, K. (2007). A study of images of water: Using the Nine-in-One Drawing method and SD-method. *Archives of Sandplay Therapy*, 20(1), 3-18. [In Japanese]

³ All pictures in this paper are shown not as the original ones, but as the reproductions by the authors, in order to protect participants' privacies.

Example of the color correction and the removal of unpleasant elements in a commercial facility

Kohei Wakai^{1*} and Hideaki Hayashi²

¹ *Cre-Inno.inc, Japan.*

² *Landart & Design Studies, Japan*

*Corresponding author: Kohei Wakai, k-wakai@shikisa.com

Keywords: City Landscape, Color Harmony, Pictures Modification

Abstract

The purpose of this study is to confirm the influence of elements of the cityscape that are favored as beautiful or desirable.

And we propose an analysis of the color of the target landscape and improvement sofas of "dominance" rooted in the region.

In this study, the preferred color rooted in the region was extracted as "dominance", and the color of the building which seemed to be bad was changed, and it changed it to the preferred color. The building is a commercial facility located on the shore of Lake Suwa in Nagano Prefecture, Japan.

There are many buildings in Japan that ignore color harmony, but it is one of the things that we think is particularly bad.

The walls of the original building were painted in pink and yellow, and there were many more high-chroma signs and banners. These colors have an invitation, but they are disproportionate to the surrounding lakes and buildings, giving us a cluttered and unpleasant impression. In addition, the presence of electric wires and telephone poles amplifies ugliness.

We explored the change in impressions by cutting out walls, signs, banners, wires and telephone poles from the pictures of this building and its surroundings and arranging them in different colors. There were a lot of calm structures and greens which harmonized with the surface of the water on the shore of Lake Suwa, and it decided to extract these colors as "dominance" and to use it for the correction.

The results indicated that changing the color of walls and signs would not be enough, but it would be desirable to erase both signs, banners, wires and telephone poles.

We tried to change the impression by changing the color of the wall of this building to light blue (generally imagine disused lakes) but we did not get a very good evaluation.

It was found that the elements that felt uncomfortable included signs and sky splitting, so we erased both signs, banners, wires and telephone poles.

In addition, the impression was improved by reflecting regional dominance, matching the color of the wall extracted from the surroundings, and placing the trees.

The author concludes that the element that feels uncomfortable cannot remove only chroma downing.

In addition to the removal of signs, banners, wires and telephone poles, it is also necessary to derive and improve the "dominance" of the entire landscape of the region to harmonize with it. This method is an effective method to advance the improvement to the disharmony confusion of the scenery which is everywhere in the whole country.

1. Introduction

On the shore of "Lake Suwa" in Suwa City, Nagano Prefecture, Japan, there are hot springs, ryokan and museums in the city, and we can enjoy a calm atmosphere from the elegant buildings, water and trees. (Fig.1,2) But, there are some scenes that you want to express as miserable scenery.



Figure 1. Lake Suwa (Photo by Wakai)



Figure 2. Shop & Restaurants "CLASUWA" (Photo by Hayashi)

2. Objectives and assumptions

Scenic landscapes and traditions should be carefully inherited and promoted in the future, focusing on the importance of landscape formation as a whole in line with local dominance and the basic urban environment that must be protected by any industry. Therefore, the features of the whole country and the local landscape are harmonized and exist as a calm landscape, and festivals and events become more vibrant with seasonal changes. The uniqueness of the whole area will be felt naturally, and it will contribute to tourism.

3. Problem Scene

However, the scene of the karaoke place on the pink and yellow walls near the lakeside park gives a terrible impression. In addition, all signboards and banners and Electric wires and telephone poles, add to us bad impression. (Fig.3, 4)



Figure3. Karaoke place (Photo by Hayashi)



Figure4. Karaoke place (Photo by Wakai)

4. Attempts by color conversion

Assuming repainting, we tried to correct the color of the outer wall of the building. The pink and yellow parts of the outer wall were changed to light blue to match the image of the lake surface in Fig. 1. (Fig.5)。 However, it was not judged that this change of color alone would make the whole area unique and feel natural, contribute to tourism, and above all, be a landscape where residents can be proud.



Figure5. Karaoke place Color Change (Photo by Hayashi, Retouch by Wakai)

5. Correction considering “Dominance”

Removed electric wires, utility poles, signboards and banners. Then, the wall color was changed to calm black, white, and gray, and the blue of the lake surface was expressed mainly by reflection using glass, and a sketch with trees arranged was created. (Fig.6) And the photo retouching (Fig.7) was made based on this sketch.



Figure6. Karaoke place Preferable (designed by Hayashi)



Figure7. Karaoke place Preferable (designed by Hayashi, Retouch by Wakai)

6. Partial addition of bad impression

Even if the building becomes beautiful, how will the overall impression change if bad impression elements remain? we created scenes when the wires and utility poles remained (Fig. 8). We think you can understand the necessity of the removing Electric pole which is not advanced in Japan.



Figure8. Add Wire & Poles (Photo by Hayashi, Retouch by Wakai)

And when the signboard and banners remained (Fig. 9). On the other hand, we created a scene with the building as it was, with the wires, utility poles and signboards removed. (Fig. 10) How will your impression change? We will evaluate and verify these factors in next step.



Figure9. Add Signboard &Banner (Photo by Hayashi, Retouch by Wakai)



**Figure10. Erase Wire &Poles & Signboard &Banner
(Photo by Hayashi, Retouch by Wakai)**

REFERENCES

1. Hideaki Hayashi, Kohei Wakai, Mikiko Kawasumi 2018. Future of Color Environment in Beautiful Japan, Journal of the Color Science Association of Japan, Vol42, No.6 279-280.
2. Hideaki Hayashi 2018. Future of Color Environment in Beautiful Japan –For the Best Color Environment which Looks Good on Japanese People–, Journal of the Color Science Association of Japan, Vol42, No.6 Supplement 157-158.
3. Kohei Wakai 2018. Analysis of color environment~ Color distribution and language representation of images ~ Asking Why? ~. Journal of the Color Science Association of Japan, Vol42, No.6 Supplement 163-164.

HOLISTIC COLOR COMBINATION ANALYSIS INCLUDING LIGHTNESS, CHROMA, AND HUE ON PAPILIONIDAE BUTTERFLIES

Erina Kakehashi^{1*}, Keiichi Muramatsu², and Haruo Hibino¹

¹*Graduate School of Engineering, Chiba University, Japan.*

²*Graduate School of Science and Engineering, Saitama University, Japan.*

*Corresponding author: Erina Kakehashi, kakehashi@chiba-u.jp

Keywords: Quantification of color combination, holistic color harmony, Papilionidae butterfly

ABSTRACT

Clarifying the color combination rules of “beautiful things” contributes to the development of color harmony theory (e.g. paintings (Kobayashi, 1999)). Until now, by focusing on the papilionidae butterflies, we have clarified these color combination rules of hue, lightness, and chroma respectively (Kakehashi et al., 2019). In this study, we aimed to statistically clarify the holistic color combination rules of papilionidae butterflies through hue, lightness and chroma. To achieve this aim, we clarified the holistic color combination rules of 118 papilionidae butterfly images through the following steps: 1) the color similarities between two images were calculated using histogram intersection; 2) the images were classified by utilizing hierarchical cluster analysis based on the similarities obtained in step 1 (Kakehashi et al., 2018); 3) the representative colors of each resulting image cluster were analyzed by employing the Gaussian mixture model (GMM); 4) The color combination types (i.e. similar or contrast) of each cluster were determined based on the distributions of representative colors in the categorized regions of the color space (Kakehashi et al., 2019). Consequently, the following holistic color combination rules were obtained: 1) similar lightness, similar chroma, and similar hue; 2) contrasting lightness, similar chroma, and similar hue; 3) contrasting lightness, contrasting chroma, and similar hue. In particular, similar hue appeared in all clusters. These rules partly agree with the results of the previous studies (Szabó et al., 2010; Ou et al., 2018), which investigated the color combination rules of individual attributes. In present study, we used simple and orthodox methods for classifying the images which was automatic calculations. However, it is very important to classify the images based on human visual perception. In future works, we will implement further investigation considering the subjective image classification.

INTRODUCTION

Clarifying the color combination rules of “beautiful things” contributes to the development of color harmony theory. Kobayashi attempted to clarify the color combination structures of paintings to resolve color harmony issues [1]. However, the common color combination principles in paintings have not yet been clarified. We focused on the beautiful colors of papilionidae butterflies, which have been evolving regardless of the human aesthetic response [2-4]. Until now, we have clarified the common color combination rules of papilionidae butterflies particularly for each attribute (hue, lightness, and chroma) of the CIE LCh color space using conventional methods of image retrieval and image segmentation [2]. The holistic color combination of hue, lightness, and chroma is extremely important in studies on color harmony [5]. However, these holistic rules were not statistically clarified in our previous work [2]. Thus, in this study, we aimed to statistically

clarify the holistic color combination rules of papilionidae butterflies through hue, lightness, and chroma attributes.

METHOD

In the present study, we clarified the holistic color combination rules of papilionidae butterflies through the following steps: 1) the color similarities between two images were calculated using histogram intersection [6]; 2) the images were classified by utilizing hierarchical cluster analysis based on the similarities obtained in step 1) [7]; 3) the distribution characteristics of each resulting cluster were analyzed by employing the Gaussian mixture model (GMM).

Image Classification

As in our previous works [2], we used 118 butterfly images, the color space of which was unified to sRGB and converted into the CIELCh scale.

First, to calculate color similarities, we used 200-interval histograms from the combination of the CIELCh attributes (i.e., $8 h_{ab} \times 5 L^* \times 5 C_{ab}^*$ intervals) and normalized the frequencies by the ratio of each bin in the histograms. Then, the calculated similarities were subtracted from 1 and used for hierarchical cluster analysis using Ward's method. The number of clusters were determined based on the sharp increase in height among clusters (Figure 1).

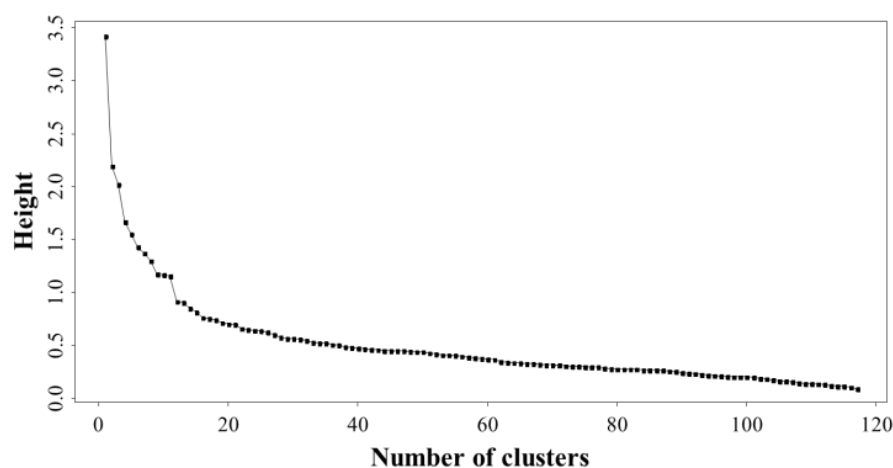


Figure 1. Height and number of clusters

Statistical analysis

The GMM was used for analysis with the `mclust` package of R as an easier method for representing color distributions compared to the previous study [1]. The GMM determines the number of Gaussian mixture components based on the likelihood of an information criterion, and it indicates the density of color distributions as a probability density function. We determined the number of components by focusing on the point whose Bayesian information criterion (BIC) values were beginning to converge (Figure 2). This was because the mixture-based density estimate curves that were simulated based on the above-mentioned number of components were frequently the visually fittest for the histograms of each attribute in our preliminary investigation. For each component of the GMM, we defined mean values as representative colors, mixing proportions as size, and covariance matrices as ranges. The mean value of each component was categorized according to the definition in Table 1. We determined the color combination types in each cluster by comparing the combinations of these categories with the color combination types defined in

Table 1. The color combination types show the color combinations which have similar or contrast. Furthermore, the components whose proportions were under 3% or variances were large were excluded from the analysis.

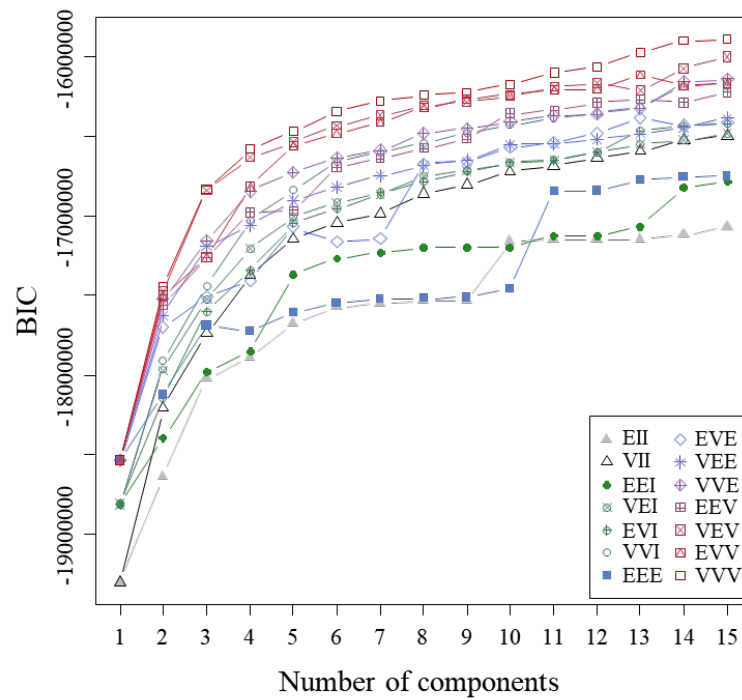


Figure 2. Examples of BIC values according to the number of components in a cluster

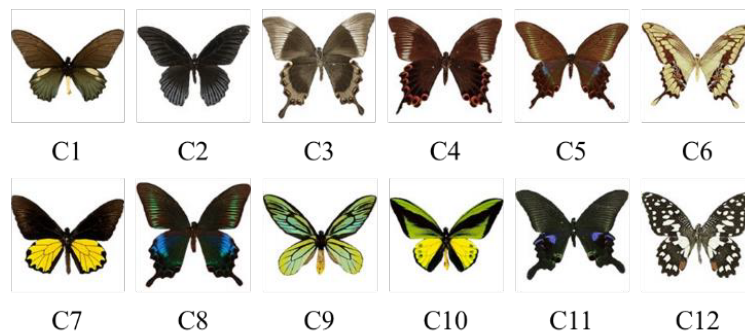


Figure 3. Examples of papilionidae butterfly in each cluster. “C1” to “C12” indicate clusters 1 to 12

RESULTS AND DISCUSSION

As a result of clustering, 118 images were classified into twelve clusters. The examples of papilionidae butterfly images included in each cluster are shown in Figure 3. Additionally, in these clusters, the mean values, proportions, and covariance matrices of each component obtained using the above-mentioned method are shown in Table 2. According to the mean values of each component in the table, clusters 2, 4, 5, 8, and 11 mainly consist of low lightness, low chroma, and the 2nd–4th hue. Clusters 1 and 12 mainly consist of low lightness, high lightness, low chroma, and

the 3rd–4th hue. Clusters 7 and 10 mainly consist of low lightness, high lightness, low chroma, high chroma, and the 2nd–4th hue. Additionally, the distribution characteristics of clusters 3, 6 and 9 are not common with the other clusters, even though these clusters mainly consist of the 3rd–4th hue.

In summary, the color combination types are similar lightness, similar chroma, and similar hue in clusters 2, 4, 5, 8, and 11, contrasting lightness, similar chroma, and similar hue in clusters 1 and 12, and contrasting lightness, contrasting chroma, and similar hue in clusters 7 and 10. In particular, similar hue is observed in all clusters. Among these color combination rules, contrasting lightness, similar chroma, and similar hue agree with the experimental color harmony theory [8-11].

Table 1: Defined Color categories and color combination types. The values of L^* and C^*_{ab} were divided into three categories, and the values of h_{ab} were divided into twelve categories. “Similar” shows the similar color categories, and “Contrast” shows the contrasting color categories. In the L^* and C^*_{ab} , we regarded the same category combinations as similar and different combinations as contrasting. In the h_{ab} , we regarded the hue category number differences less than two as similar and just six as contrasting

Range	Category	Similar	Contrast
$L^*, C^*_{ab} \leq 33$	Low	Low	High
$33 < (L^*, C^*_{ab}) \leq 66$	Middle	Middle	-
$66 < L^*, C^*_{ab}$	High	High	Low
$0 \leq h_{ab} < 30$	1	2, 3, 11, 12	7
$30 \leq h_{ab} < 60$	2	1, 3, 4, 12	8
$60 \leq h_{ab} < 90$	3	1, 2, 4, 5	9
$90 \leq h_{ab} < 120$	4	2, 3, 5, 6	10
$120 \leq h_{ab} < 150$	5	3, 4, 7, 8	11
$150 \leq h_{ab} < 180$	6	4, 5, 7, 8	12
$180 \leq h_{ab} < 210$	7	5, 6, 8, 9	1
$210 \leq h_{ab} < 240$	8	6, 7, 9, 10	2
$240 \leq h_{ab} < 270$	9	7, 8, 10, 11	3
$270 \leq h_{ab} < 300$	10	8, 9, 11, 12	4
$300 \leq h_{ab} < 330$	11	1, 9, 10, 12	5
$330 \leq h_{ab} < 360$	12	1, 2, 10, 11	6

CONCLUSION AND LIMITAION

In the present study, we aimed to statistically clarify the holistic color combination rules of papilionidae butterflies. The results were summarized following three rules:

- 1) similar lightness, similar chroma, and similar hue
- 2) contrasting lightness, similar chroma, and similar hue
- 3) contrasting lightness, contrasting chroma, and similar hue

We used simple and orthodox methods for classifying the images which was automatic calculations. However, it is very important to classify the images based on human visual perception. In future works, we will implement further investigation considering the perceptual perspective.

Table 2: Number of components (G) extracted in each cluster. Proportions (π_k), mean values (μ), and covariance matrices (Σ) for each component. “C” denotes the cluster number. For each component, μ and Σ are composed of three rows that indicate L^* , C^*_{ab} , and h_{ab} from the top respectively. The gray-colored cells show the components that have proportions under 3% or large variances

C	G	π_k	μ	Σ			C	G	π_k	μ	Σ			
				L^*	C^*_{ab}	h_{ab}					L^*	C^*_{ab}	h_{ab}	
1	1	0.625	28.27	184	72.8	74.2	7	4	0.0584	89.38	12.2	10.6	14	
			21.62	72.8	53.9	21.9				89.12	10.6	9.47	12.1	
			68.87	74.2	21.9	98.3				94.39	14	12.1	16.1	
	2	0.251	78.73	173	-73.9	94.4		8	1	0.413	45.59	752	470	-993
			16.3	-73.9	55.2	-27.1					34.57	470	500	-932
			88.16	94.4	-27.1	137					177.2	-993	-932	5790
	3	0.124	54.03	854	280	575		2	0.587	8.841	38.5	38.2	108	
			24.47	280	642	-416				9.363	38.2	49.8	77.2	
			106.3	575	-416	2770				63.86	108	77.2	1530	
2	1	0.76	13.34	61.6	25.4	32.5	9	1	0.253	83.66	45	-34.4	22.3	
			9.042	25.4	26.8	-0.021				40.5	-34.4	108	-24.5	
			67	32.5	-0.021	283				97.81	22.3	-24.5	15.2	
	2	0.24	59.13	665	117	-494		2	0.413	58.13	378	195	173	
			18.35	117	440	-397				35.05	195	220	52	
			108.8	-494	-397	3550				104.8	173	52	359	
3	1	0.248	25.59	23.7	4.05	-7.35	3	0.307	12.14	82.2	35.3	132		
			3.377	4.05	2.6	-1.85			8.414	35.3	24.3	60.6		
			73.73	-7.35	-1.85	775			64.17	132	60.6	741		
	2	0.149	49.32	748	484	-1150		4	0.0272	21.94	688	54.2	-1230	
			24.33	484	482	-1380				5.287	54.2	16	-32.9	
			209.8	-1150	-1380	6430				276.2	-1230	-32.9	5740	
3	0.603	43.18	566	8.3	321	1	0.193	28.8	432	225	-398			
		12.57	8.3	28.8	4.4			19.84	225	191	-230			
		74.05	321	4.4	337			108	-398	-230	4640			
4	1	0.285	61.28	587	93.5		253	10	2	0.405	70.61	114	111	-47.6
			26.63	93.5	330		-74.4				70.25	111	129	-39.3
			103.5	253	-74.4		4320				102.8	-47.6	-39.3	76.3
	2	0.715	13.96	60.2	49	52.9	3		0.319	3.697	11	10.4	10.1	
			18.91	49	71.3	37.1				3.971	10.4	12.1	-5.22	
			39.35	52.9	37.1	91.7				62.91	10.1	-5.22	1130	
5	1	0.687	26.39	135	56.2	95.5	4	0.0829	91.26	3.25	3.04	3.62		
			27.46	56.2	61.9	34.3			90.82	3.04	2.87	3.39		
			48.11	95.5	34.3	92.9			96.7	3.62	3.39	4.08		
	2	0.313	64.05	406	-53	314		1	0.34	45.15	985	44.7	-984	
			20.87	-53	203	-284				12.33	44.7	239	-618	
			101.1	314	-284	2180				208.1	-984	-618	6990	
6	1	0.0962	38.15	1090	234	184	11		2	0.443	13.29	87.9	25.6	112
			14.01	234	179	25.5					5.07	25.6	19.3	65.9
	2	0.747	98.13	184	25.5	6560			3	0.217	8.517	32.5	0.00291	-
			44.88	518	132	442							0.00101	

			33.53	132	192	34.9				0.0009194	0.00291	2.81E-07	-9.49E-08	
			63.92	442	34.9	458				117.8	-	-9.49E-08	4.57E-08	
	3	0.157	78.8	18	-	0.0644		1	0.601	18.03	100	24.1	59.6	
			13.68	-	0.0312	-45				7.476	24.1	13.3	28.2	
			107.7	0.0644	-45	103				83.3	59.6	28.2	274	
	1	0.259	3.645	6.51	5.21	-3.28		12	2	0.313	71.43	462	-27.9	150
			3.52	5.21	6.29	-14.3				15.07	-27.9	122	-8.88	
			54.43	-3.28	-14.3	866				105.1	150	-8.88	93.9	
	2	0.467	18.55	97.5	39.5	68.4		3	0.0866	43.49	965	741	-1010	
			16.47	39.5	37	28.8				30.8	741	787	-1180	
			57.67	68.4	28.8	146				141.3	-1010	-1180	9700	
7	3	0.216	64.2	710	181	-1210								
			29.19	181	561	-571								
			112.6	-1210	-571	4990								

REFERENCES

1. M. Kobayasi, "Analysis of color combination in fine art paintings," Proc. Int. Symp. Multispectral Imaging Color Reproduction, pp. 139-142, 1999.
2. E. Kakehashi, K. Muramatsu, J. Choi, and H. Hibino, "Lightness, chroma and hue distribution on Papilionidae butterflies," Interim Meeting of the International Color Association (AIC), 2018.
3. E. Kakehashi and K. Kasamatsu, "Investigation of color structure in the swallowtail butterfly wings," Journal of the Color Science Association of Japan, vol. 39, pp. 25-26, 2015.
4. E. Kakehashi, K. Muramatsu, J. Choi, and H. Hibino, "Hierarchical cluster analysis in color applied to the papilionidae butterflies," Journal of the Color Science Association of Japan, vol. 42, pp. 75-78, 2018.
5. M.C. Chuang and L. Ou, "Influence of a holistic color interval on color harmony," Color Res. Appl., vol. 26, pp. 29-39, 2001.
6. M.J. Swain and D.H. Ballard, "Color indexing," Int. J. Comput. Vis., vol. 7, pp. 11-32, 1991.
7. S. Krishnamachari and M.M. Abdel, "Image browsing using hierarchical clustering," Proc. IEEE Int. Symp. Computers and Communications, pp. 301-307, 1999.
8. L. Ou, P. Chong, MR. Luo, C. Minchew, "Additivity of colour harmony," Color Res. Appl., vol. 36, pp. 355-372, 2011.
9. L. Ou, MR. Luo, "A colour harmony model for two-colour combinations," Color Res. Appl., vol. 31, pp. 191-204, 2006.
10. L. Ou, Y. Yuan, T. Sato, et al., "Universal models of colour emotion and colour harmony," Color Res. Appl., vol. 43, pp. 736-748, 2018.
11. F. Szabó, P. Bodrogi, J. Schanda, "Experimental modeling of colour harmony," Color Res. Appl., vol. 35, pp. 34-49, 2010.

EFFECTS OF ENVIRONMENTAL COLOR PROPERTIES ON PERCEIVED SPACIOUSNESS AT EXTERIOR LOCATIONS

Makoto Inagami

Institutes of Innovation for Future Society, Nagoya University, Japan

Corresponding author: Makoto Inagami, inagami@coi.nagoya-u.ac.jp

Keywords: everyday environments, space perception, L^*C^*h color space, advancing and receding effects

ABSTRACT

This study investigated the relationships between environmental color properties and perceived spaciousness at exterior locations. For an experiment, I selected 42 locations with different spatial layouts and color properties. At each location, I measured the spatial layout with a 3D laser scanner and took several photographs to capture the surrounding environment. The measured data were used to calculate the spatial volume, and the photographs were converted to a panoramic image. In the experiment, the images were presented on a 27-inch monitor using a technique called VR panorama. Participants ($N=25$) explored the surrounding environment of each location and then rated its perceived spaciousness. In the present analysis, I created a multiple regression model to predict the rated spaciousness based on the spatial volume and three color variables: proportion of warm colors, proportion of cool colors, and mean lightness. The obtained model showed that the perceived spaciousness decreased with the proportion of warm colors and increased with that of cool colors. This result suggests that environmental colors have advancing and receding effects on space perception even at everyday exterior locations.

BACKGROUND & PURPOSE

Environmental designers need to select colors appropriately, because they affect not only the attractiveness of environments but also the perception of spatial properties such as distance and size. For example, surfaces in warm and cool colors are perceived to be close to and far from the viewpoint, respectively. These advancing and receding effects have been shown to increase with chroma [1]. In addition, some colors have expanding and contracting effects, which are known to be dependent on lightness [2]. That is, surfaces high in lightness are perceived to be larger than ones low in lightness.

The effects of colors on space perception have been studied not only in perceptual psychology but also in architecture. For example, Sato [3] investigated advancing and receding effects of a wall's color in a room and found that perceived spaciousness decreases with the advancing effect. In addition, Yoshida and Sato [4] found that the higher the lightness of wall and floor surfaces, the more spacious the room is perceived. Other studies [5, 6, 7] also reported the relation between wall colors and perceived spatial properties in interior spaces. On the other hand, a limited number of studies have examined such effects for exterior spaces. Takei and Ohara [8] investigated the spatial feeling caused by a building and did not obtain results consistent with advancing, receding, expanding, and contracting effects. Thus, it remains unclear how environmental colors affect space perception at exterior locations.

In this study, I conducted an experiment to examine the relationships between environmental color properties and perceived spaciousness at everyday exterior locations. Environmental psychology and ecological psychology have emphasized the fact that the environment surrounds a perceiver. Ittelson [9] wrote that “the environment surrounds, enfolds, engulfs . . .” (p. 149), and



Figure 1. Panoramic images of the environments selected for this experiment. These environments are shown in the equirectangular projection and arranged in order of spaciousness as rated in the experiment.

Gibson [10] wrote that “no animal could exist without an environment surrounding it” (p. 8). In line with this emphasis, I presented different surrounding environments using a virtual-reality technique and attempted to capture the perception of their spaces in the form of rated feelings of spaciousness.

METHODS

For the experiment, I selected 42 locations on a university campus so that they varied in spatial layout and color properties (see Figure 1). At each location, a camera (Sony $\alpha 7R$) was positioned at a height of 1.5 m above the ground. The camera was equipped with a fish-eye lens (Sigma 15mm F2.8 EX DG Diagonal Fisheye) and a panoramic tripod head (Nodal Ninja 4). From the position, several photographs were taken so that they covered the environment in all directions. The photographs were later converted to a panoramic image using stitching software (PTGui Pro ver. 9.1.6), as shown in Figure 1. The resolution of the images was 18,424 pixels wide and 9,212 pixels high. All environments were photographed on cloudy days, and the camera’s white balance was set to the cloudy mode.

In addition, I set up a 3D laser scanner (Leica Geosystems ScanStation C10) at the same position as the camera. The scanner recorded the layout of surrounding surfaces as point cloud data.

The measurement covered all directions except the bottom: 360° in azimuth and 135° in elevation. The area was scanned at an interval of approximately 0.1°. The missing data from the bottom were interpolated by assuming that the ground surface was horizontal. For this study, I sampled point cloud data at an interval of 2°, that is, from 180 directions in azimuth and 90 directions in elevation. I then calculated the mean radial distance to the surrounding environment and defined the value as “spatial volume.” Each radial distance was weighted by the cosine of the elevation angle, because the density of data (per solid angle) becomes higher as the elevation approaches ± 90°. The upper limit of radial distance was set to 200 m.

In the experiment, the selected environments were presented using a technique called VR panorama. The panoramic images were converted into the Flash file format with software (Pano2VR ver. 3.1.4) and displayed on a 27-inch monitor (EIZO FlexScan EV2736W-ZBK). This technique made it possible to explore the environments virtually while changing the viewing direction by pushing keys on a keyboard. Participants ($N = 25$) observed the environments in a random order and rated them with respect to perceived spaciousness. The ratings were normally provided on a 21-point scale ranging from 0 to 100 (i.e., 0, 5, 10, . . .), but finer scores were also available when necessary. Concerning the standard for rating, I instructed the participants to imagine being in a small room and on a large athletic field and assign the scores of 0 and 100 to the two degrees of spaciousness. The ratings were standardized to z -scores for each participant and then averaged for all participants.

For the present analysis, the color properties of the environments were quantified based on the panoramic images. The resolution of the images was reduced to 360 pixels wide and 180 pixels high, which correspond to intervals of 1° in azimuth and elevation, respectively. The RGB values of each pixel were converted to L^*C^*h values with the brightest white ($R = G = B = 255$) as a reference white point. For each image, I calculated three color variables: proportion of warm colors, proportion of cool colors, and mean lightness. I defined the warm and cool colors as $0^\circ < h < 110^\circ$ and $180^\circ < h < 270^\circ$, respectively, and calculated the proportions of the pixels meeting these conditions. In the calculation of the three variables, each pixel was weighted by the cosine of the elevation angle, in the same way as the mean radial distance.

RESULTS & DISCUSSION

I conducted a multiple regression analysis to predict the rated spaciousness based on the three color variables as well as the spatial volume. Considering that the advancing and receding effects of colors increase with chroma, I set a lower limit of C^* for the calculation of the proportion of warm and cool colors, and counted only the pixels for which C^* was equal to or higher than the limit. As shown in Table 1, I repeated the regression analysis while changing the lower limit at an interval of 5 and then selected the model that provided the highest R^2 value. Figure 2A shows a path diagram of the obtained model. The prediction accuracy of the model was statistically significant, $R^2 = 0.75$, $F(4, 37) = 28.16$, $p < 0.001$ (see also Figure 2B). The spatial volume and the proportions of warm and cool colors showed significant effects ($t(37) = 6.27$, $p < 0.001$; $t(37) = -2.51$, $p = 0.02$; $t(37) = 2.21$, $p = 0.04$, respectively), although the mean lightness did not ($t(37) = -0.99$, $p = 0.33$).

The path coefficients in Figure 2A are standardized partial regression coefficients, which indicate that perceived spaciousness decreases with the proportion of warm colors and increases with that of cool colors. These relationships are consistent with advancing and receding effects, considering that when an environmental surface is perceived closer to the viewpoint, the space between the surface and viewpoint is perceived smaller. Therefore, I conclude that environmental colors have advancing and receding effects on space perception even at everyday exterior locations.

Table 1. Comparison of the R^2 values obtained from multiple regression analyses to predict the rated spaciousness. For these analyses, the proportions of warm and cool colors were calculated with different lower limits of C^* .

Lower limit of C^* for cool colors	Lower limit of C^* for warm colors																
	0	5	10	15	20	25	30	35	40	45	50	55	60	65	70	75	80
0	0.68	0.71	0.69	0.68	0.68	0.68	0.68	0.69	0.68	0.70	0.72	0.72	0.72	0.71	0.69	0.69	0.68
5	0.68	0.71	0.69	0.68	0.68	0.68	0.69	0.69	0.69	0.70	0.73	0.72	0.72	0.71	0.70	0.69	0.68
10	0.69	0.71	0.70	0.69	0.69	0.69	0.69	0.69	0.69	0.71	0.73	0.73	0.73	0.72	0.71	0.70	0.69
15	0.71	0.73	0.72	0.71	0.71	0.71	0.71	0.72	0.71	0.73	0.75	0.75	0.74	0.74	0.73	0.72	0.72
20	0.69	0.71	0.70	0.69	0.69	0.69	0.69	0.69	0.69	0.71	0.73	0.73	0.72	0.72	0.71	0.70	0.70
25	0.68	0.70	0.69	0.68	0.68	0.68	0.68	0.69	0.68	0.70	0.72	0.72	0.72	0.71	0.70	0.69	0.68
30	0.68	0.70	0.68	0.68	0.68	0.68	0.68	0.69	0.68	0.70	0.72	0.72	0.72	0.70	0.69	0.68	0.68
35	0.68	0.70	0.68	0.68	0.68	0.68	0.68	0.69	0.68	0.70	0.72	0.72	0.72	0.71	0.69	0.69	0.68
40	0.68	0.70	0.68	0.68	0.68	0.68	0.68	0.69	0.68	0.70	0.72	0.72	0.72	0.71	0.70	0.69	0.68
45	0.68	0.70	0.69	0.68	0.68	0.68	0.68	0.69	0.69	0.71	0.73	0.72	0.72	0.71	0.69	0.69	0.68

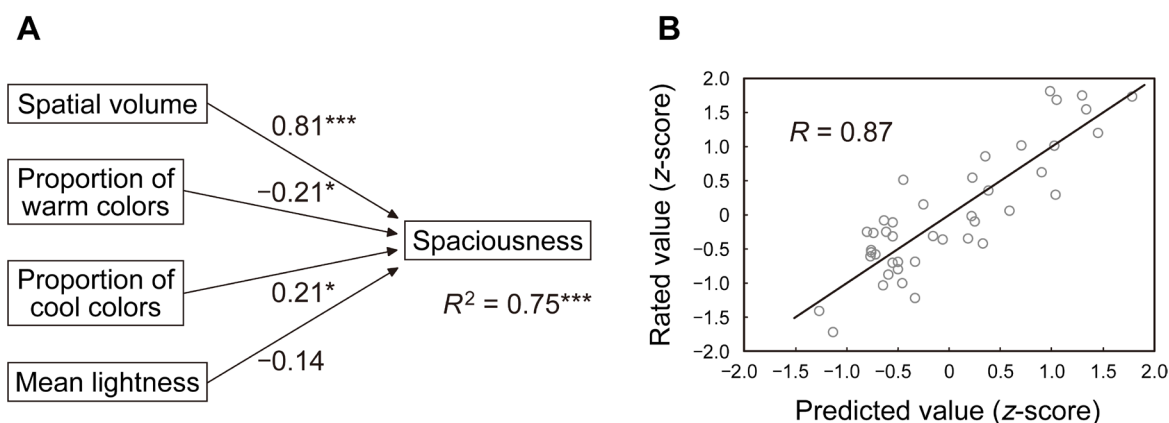


Figure 2. Multiple regression model that provided the highest R^2 value. (A) Path diagram describing the model. Significance levels are indicated as follows: $*p < 0.05$ and $*p < 0.001$. (B) Relationship between the rated and predicted values of spaciousness.**

On the other hand, the present result did not show a clear effect of the mean lightness, although expanding and contracting effects are dependent on lightness. This may be because the mean lightness had a strong correlation ($R = 0.77$) with the spatial volume. The effect of lightness needs to be re-examined in a future study where environments are sampled so that their mean lightness and spatial volume are independent.

ACKNOWLEDGMENT

This work was supported by a Grant-in-Aid for Young Scientists (B) and a Grant-in-Aid for Scientific Research (C) from the Japan Society for the Promotion of Science (No. 26820259 and No. 17K06701, respectively).

REFERENCES

1. Oyama, T. (1958), A measurement of advancement and recession of colored surfaces. *Journal of the Illuminating Engineering Institute of Japan*, 42, 526–532.
2. Oyama, T. (1962), Psychological effects of color. *Journal of the Illuminating Engineering Institute of Japan*, 46, 452–458.
3. Sato, M. (2012), Advancing and receding effects of colors on apparent distance to a wall of an interior space. *Journal of Environmental Engineering (Transactions of AIJ)*, 677, 559–565.
4. Yoshida, K. & Sato, M. (2017). Effects of wall and floor lightness on the perception of interior space: Experiments of lighting from the ceiling surface. *Journal of Architecture and Planning (Transactions of AIJ)*, 742, 3073–3079.
5. Suda, M. & Hatsumi, M. (1994). Study on effects of colors in space recognition: Study on structure of space recognition. *Journal of Architecture and Planning (Transactions of AIJ)*, 59, 99–106.
6. Ishida, T. & Shinomiya, M. (2000). Effect of the interior color on depth perception of room. *Summaries of Technical Papers of Annual Meeting Architectural Institute of Japan, D-1*, 387–388.
7. Kondo, T. & Yanase, R. (2018). Effects of wall color and wooden floor on the impression and apparent size in living space. *AIJ Journal of Technology and Design*, 57, 747–750.
8. Takei, M. & Ohara, M. (1978). Experimental study on measurement of the sense of oppression by a building (part 3): Consideration of the distance to a building, and relation between colour effect of exterior wall and the sense of oppression. *Transactions of the Architectural Institute of Japan*, 263, 71–80.
9. Ittelson, W. H. (1976). Environment perception and contemporary perceptual theory, In H. M. Proshansky, W. H. Ittelson, & L. G. Rivlin (Eds.), *Environmental psychology: People and their physical settings* (2nd ed.) (pp. 141–154). New York: Holt, Rinehart and Winston.
10. Gibson, J. J. (1979). *The ecological approach to visual perception*. Boston: Houghton Mifflin.

THE RELATIONSHIP BETWEEN “KAWAII” COLOR AND INSPIRATION

Masako Nunokawa

*Graduate School of Comprehensive Human Science Master's Program,
Kansei Behavioral and Brain Science,
1-1-1 Tennoudai, Tsukuba-shi, Ibaraki
University of Tsukuba*

*Corresponding author: Masako Nunokawa, nunoma@ka2.so-net.ne.jp

Keywords: Kawaii, color, inspiration, greeting card, impression

ABSTRACT

In recent years, content using “Kawaii”, originating in Japan, has become globalized. Such images are used especially in digital communications. In this analysis of “Kawaii” images, I verified hue, brightness, and saturation on various greeting cards found online. This highly rated image of “Kawaii” had a significantly higher average brightness value of colors used in the HSV evaluation and a higher average saturation value in the main color hue of the greeting card. In addition, there was a correlation between the impression evaluation about “Kawaii” from these images and the inspiration scale. These findings suggest that “Kawaii” images with bright colors inspire people.

INTRODUCTION

The “Kawaii” culture in Japan is now spreading all over the world. “Kawaii” is defined variously as “beautifulness”, “cool”, “lovely”, and “cute”. The original etymology of “Kawaii” is “compassion” and “sorrowful”, and even today it is expressed as “lovable”, but the “Kawaii” word may include elements of sympathy as well. In the 21st century, “Kawaii” was spread around the world by Japanese content including animation and manga. Against the backdrop of a unique view of the world, the element of “Kawaii” has come to refer to objects that appeal to sensibility as the things to empathize or sympathize. In recent years, with the advent of Instagram and other social networking services, the posting of images related to “Kawaii” has proliferated. From these trends, visualized communications with color, shape and more factors of objects are more important than in the 20th century.

There are many studies on “Kawaii”, and they generally concern “Baby Schema”. In those researches, the elements of the “Kawaii” objects are studies on objects such as babies and animals and human psychology, which are mainly evoked from memory. In addition, research on color-related impression evaluations such as Pinky is ongoing. In particular, research on “Kawaii” in Japan analyzes not only the emotions of animals and babies but also various objects and stimuli.

“Kawaii” has a positive effect during light exercise. The images chosen to evoke the feeling of “Kawaii” were largely based on shapes and attributes of human babies and animals, and those that give a gorgeous impression including colors such as those of desserts, dresses and accessories. And as a result of comparing these, both types of “Kawaii” images were evaluated as giving a pleasant feeling after browsing. In another study, Nitto (2012) found that light exercise performance improved after viewing “Kawaii” images. In the case of browsing images of food, which can stimulate the same pleasant feelings, we found that food images were not effective in improving performance. From

these studies, we found that images of “Kawaii” objects promote brain activation, including cognitive functions. But what is the influence of color?

In this study, I analyze the hue, saturation and brightness of “Kawaii” images and clarify whether the colors of the images affect human inspiration. If there is a change in the evaluation of “cute” depending on the impression of the color, and it correlates with the score on the inspiration scale, it is considered that the “Kawaii” images have elements that stimulate human creativity and inspiration.

RESEARCH PROCEDURES AND RESULTS

1. Image selection

In conducting this study, I firstly selected images for evaluation of "Kawaii" impression. I originally planned that the images for this research would be selected by Google search and Instagram hashtags, or photographic images taken by the author. However, because there was a concern that the author may be biased when selecting the images, another idea was adopted: 37 greeting cards presented on a website were selected. These greeting cards are templates that are currently offered free of charge on the “Yuubin.jp” website, which is operated by the Japan Post Group, the largest postal and delivery system in Japan. These 37 templates include “Kawaii cards” (K-cards) offered in the “Marriage” and “Birth” categories as “Kawaii” images, and “Non-Kawaii cards” (NK-cards) offered in the “Business” category (Figure 1). The two types of cards were compared and analyzed for hue, saturation, and brightness in the color analysis. Furthermore, a subjective evaluation of each card was conducted using a questionnaire, and the correlation between the evaluation of “Kawaii” and the sensitivity of inspiration was examined.



Figure 1. Selected four K-cards (Left) and four NK-cards (Right)

2. Color analysis by the software

At first, in order to examine the average values of hue, lightness, and saturation of each card, the online color analysis software “Iro-Toridori” was used for the analysis. In the first analysis, K-cards and NK-cards were compared for the average values of hue, saturation, and lightness obtained by HSV of five main hues. As a result of averaging the HSV values, the brightness of the K-cards was 18.86 and the brightness of the NK-cards was 11.35; the brightness of K-cards was significantly higher. Image based on the average values of hue, lightness, and saturation are as shown in Figure 2 below using these numerical values.

Table 1: Comparison of Hue, Brightness and Saturation of K-cards and NK-cards

(M=Mean)	Hue	brightness	saturation
K-card	64.77	18.86	90.52
NK-card	73.39	11.35	90.47

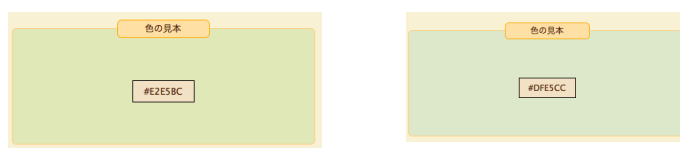


Figure 2. Color of mixed data of K-cards (Left) and NK-cards (Right)

As a second analysis, the percentage of white space that could be used to write a text message was measured for each individual card. The ratio of K-cards was 54.6% and the ratio of NK cards was 59.0%, constituting a negligible difference. In addition, I measured the occupancy of the main colors used in the image. The ratio of K-cards was 18.3% and the ratio of NK cards was 22.2%. This result shows that the ratio of main color on the NK cards was high because the NK card image is often monochromatic.

The software “Iro-toridori” is equipped with a system that evaluates the saturation and lightness at 10 levels. In the third analysis, the hue, saturation and brightness were evaluated by using these values. From the comparison of average values of saturation and brightness, the saturation average of K-cards was 2.2, and the saturation average of NK-cards was 1.2, and clearly the saturation average of K-cards was higher than that of NK-cards. Furthermore, the brightness average of K-cards was 9.0, and the brightness average of NK-cards was 8.3. There was more difference in the average saturation than in the average brightness.

The final analysis using the software was a comparison between the K-cards and NK-cards of the hue used: K-cards often use warm colors such as yellow and red, but NK-cards often use green, especially blue-green, and then yellow.

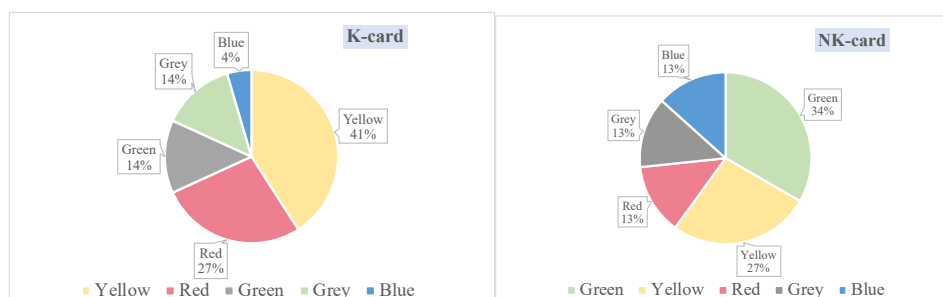


Figure 3: Comparison of main color of K-cards and NK-cards

3. Subjective evaluation of impression for images

I conducted a questionnaire with personal information concealed for subjects aged 15 to 50 who were randomly selected by "Ann and Kate", an online survey company (n = 118). 37 types of images were shown to the experimental collaborators, and a five-step Likert scale was used to ask the experimental collaborators to make a subjective evaluation of the presence or absence of a “Kawaii” impression. For the assessment, I used the inspiration scale developed by Thrash, T. M., & Elliot, A. J. (2003) and the reaction scale for “Kawaii” developed by Nittano (2016).

By the analysis of the all responses of "Kawaii", the impression rating of K-cards was M = 3.20, SD = 0.16. The impression rating of NK-cards was M = 2.62, SD = 0.22, and the evaluation of image impression about “Kawaii” was low in this case. Comparing the two, it was found that the K-cards such as “marriage” and “childbirth” greeting cards, had a strong “Kawaii” impression.

Table 2: Correlation of “Kawaii” impression score and Inspiration Score

	Score of Impression for "Kawaii"		Inspiration Score	
	M	SD	M	SD
Kawaii Card	3.20	0.16	2.94	0.12
Non-Kawaii Card	2.62	0.22	2.59	0.14

As a final analysis, in order to analyze the correlation between “Kawaii” impressions and scale of inspiration, I asked if there was any inspiration when browsing these greeting cards. The result derived from the evaluation score was $0.7 < |r| = .751 < 1.0$ and a significant correlation was recognized between the two. This result suggests that greeting cards with high “Kawaii” impression ratings stimulate more inspiration than greeting cards without a "Kawaii" impression.

DISCUSSION

In previous research, evaluations of “Kawaii” impression of objects were often analyzed by the shape or attributes of the objects and studied animals and babies. At the same time as the color comparison between “cute” objects and those that are not, there are not many attempts to simultaneously investigate issues such as the evaluation of color impression and the relevance of the inspiration. In this respect, this study is novel.

In addition, the decision to use 37 greeting cards for the images in this research made the procedure simpler and clearer because it followed the categorization already made by the image provider depending on the use of the cards.

However, greeting cards that symbolize life events such as “marriage” and “childbirth”, not just impressions from colors, have strong message characteristics and may have other stimuli other than the colors themselves. Therefore, there is a concern that the impression evaluation obtained from this questionnaire may have been influenced by other factors other than color.

Looking at the relationship between color and inspiration there is a future research direction concerning not only browsing images but also the creation of images. For example, It would be interesting to investigate each scene in terms of how the selection of colors by the creator when drawing a picture affects the impression of the color of the viewer.

REFERENCES

1. Nittono, Hiroshi. Fukushima, Michiko. Yano, Akihiro. Moriya, Hiroki. (2012) The Power of Kawaii: Viewing Cute Images Promotes a Careful Behavior and Narrows Attentional Focus. *PLOS ONE. Cognitive Neuroscience Channel*
2. Ihara, Namiha. Nittono, Hiroshi. (2012). Cute things are not always infantile: A psychophysiological study on the feeling of cuteness - *International Journal of Psychophysiology*. journal ISSN :0167-8760. DOI:10.1016/j.ijpsycho.2012.07.109
3. Nittono, Hiroshi. (2016). The two-layer model of ‘kawaii’: A behavioural science framework for understanding kawaii and cuteness. *East Asian Journal of Popular Culture. Volume 2 Number 1*. pp. 79–95
4. Nittono, Hiroshi. Ihara, Namiha. (2017). Psychophysiological Responses to *Kawaii* Pictures with or without Baby Schema. SAGE Open, 2017 - journals.sagepub.com. <https://doi.org/10.1177/2158244017709321>
5. Thrash, T. M., & Elliot, A. J. (2003). Inspiration as a psychological construct. *Journal of Personality and Social Psychology*, 84, 871-889.

Dress with Motif of Ostwald Color System

Yoshiko.Kato^{1*}, Yuka.Shimada², Miku.Kato³

1. Department of Fashion Design, Keishin High School Student, Japan
2. Department of Fashion Design, Keishin High School Teacher, Japan
3. Department of Information and Communication Meiji University, Japan.

*Corresponding author: Yoshiko Kato, pama112mi@yahoo.co.jp

Keywords: Fashion, Dress, Ostwald, Hering, Color system

ABSTRACT

In this study, a high school student studying color science embodied the color system devised by the German chemist Ostwald in 1920 as a cocktail dress^{1,2)}. In order to reproduce the theory of the Ostwald color system faithfully, she selected the hue of each part of the dress, materials used, and practiced purchase of fabric, a draft, drawing, sewing, dressing, make up and runway. As a result, The Ostwald Color System was expressed from various view points. The result which deepened understanding was obtained. In future research, I would like to embody other color systems and deepen my understanding.

INTRODUCTION

There are various types, to learn the theory of color scheme harmony and color system as one of theories of color science. It is necessary to understand each feature accurately to deepen the research. However, it is difficult for high school students who have just learned color education to understand terminology and to sort out various theories and deepen their understanding.

In previous studies, there are a study Kuge et al (1999) analyzed the relationship between PCCS and the same tone series colors of various color systems³⁾ and the other one Ishihara et al (2018) organized the color harmonization area in the theory of color harmony in apparel education⁴⁾.

However, none of these studies have yet been found to embody the theory of color harmony from diverse.

The purpose of this study is to obtain basic knowledge on how to practice color education by designing cocktail dresses and expressing theories so that high school students studying colorology can understand the Ostwald color system.

METHODO LOGY

The research method is as follows.

This is a study practiced by third-year high school students in the fashion design department in order to deepen their understanding of color science.



Figure 1. Ostwald Color System Design



Figure 2. Dress with Motif of Ostwald Color System

1. Read the text carefully to understand the Ostwald color system theory (3, 4).
2. While designing the cocktail dress, the details of the Ostwald color system are expressed in detail (Figure1).
3. Drafting. (draw a curve to keep the body line and each detail line clear.)
4. Purchase of fabric. (At this time, chose clothes approximated to the Ostwald hue ring, and the material is cotton and polyester.)
5. Cutting and sewing (Figure2). (Colors are responsive to this theory.)
6. Fitting. (Check the length of the hem, waistline, bodyline, and how each part comes out and correct them.)
7. Makeup. Put on a makeup that fits a cocktail dress.
8. Runway. In official contests, wear a coordinated cocktail dress, put on their own makeup, and runway in line with the costume concept.
9. Review of this research.

FINDING AND CASE DESCRIPTION

The contents of Ostwald's theory practiced in this study are as follows.

- (1) Before and after the tops, cut the each cloth with 24 color rings and wrapped foamed polystyrene foam.
- (2) The bulge of the sleeve is a double conical color solid, the middle part is the achromatic axis.
- (3) The red color of the waist belt express my hot feeling, because at the time of the design, the examination was approaching and I absolutely hoped to pass.
- (4) The triangle on the left hand shows an equal hue triangle, the color at the middle of the blue is the face color, infinite possibilities.

- (5) The circumference of skirt hem, the right hand wristband and the right foot hem express Color hue ring with 24 colors.
- (6) The band connecting the color ring of the right foot and the skirt is the psychological four primary colors of Herring's opposite color theory.
- (7) On the rib of the chest and the ribbon of the back, in order to think of the light source which beautifully colors this dress, represent spectral distribution of standard-illuminant A and standard illuminant D₆₅.
- (8) Contest makeup (eyehole, rouge, teak), Ostwald color cycle using approximated colors, total coordination and runway.

METHODOLOGY

High school students studying fashion learn the Ostwald color system. At this time, they make a cocktail dress made from a design drawing that incorporates theory. Then, put on makeup to match with the dress and runway. By practicing these, they can understand the Ostwald color system from a multifaceted perspective. These are the results obtained in this study. As a future subject, it is a subject for us to continue this research to represent various color systems in three dimensions.

ACKNOWLEDGEMENT

This work is awarded to the final selection of the 10th National High School Student Fashion Design Contest (sponsored by Kobe Fashion College) held in February 2019. For the understanding of this research presentation, I would like to express my heartfelt thanks to Prof. Miyoko Fukutomi, the principal of the Kobe Fashion College.

REFERENCES

1. Publication, pp.51, 82-833. A. Kitabatake. (2006). "*Science of color Rare Book Illustration*" Tokyo Yushodo Publication, pp.74-75.
2. H. Shinoda & I. Fujieda, (2007). "*A Guide to Color Engineering*". Published Tokyo, Morikita
3. Y. Kuge, N. Takei, K. Kawamoto, K. Matumoto & T. Yonaga (1999) "*Common Characteristics of Colors in the same PCCS Tone Series*" Color Science Association of Japan 23(1), pp.23-29
4. H. Ishihara, K. Washizu, K. Oosawa, H. Komachiya & K. Hata (2018) "Consideration of color harmony in the field of apparel" The Japan Society of Home Economics Abstract 70(0) pp.58-58

RESEARCH ON DEFECT DETECTION OF TEXTILE COLOR IMAGE BASED ON DEEP LEARNING

Chenxi Li¹, Lisheng Wang², Kaifeng Li², Wei Ye^{1*}

¹College of Control Science and Engineering, Zhejiang University, China.

²ZHEJIANG GRACE CO. LTD., China.

*Corresponding author: Wei Ye, wye@zju.edu.cn

Keywords: Deep Learning, Defect detect, Color Space Fusion, Color image processing

ABSTRACT

A novel deep learning model is proposed in this paper for defect detection on color images of textile. In the textile industry, product quality inspection is an important procedure. Nowadays, quality inspection is widely relying on manpower while this burdensome work consumes much human resources. With the development of image acquisition, storage technology and the computing power, collecting and processing high quality pictures from product lines becomes available. Meanwhile, deep learning methods have achieved great achievements in image processing. Together with deep neural network and high quality image, a robust textile defect detection model can be built for textile quality inspection. This paper aims at studying the effect of color image on textile defect detection and build an efficient defect detection model. A fabric defect data set is established with real data from industry site for model training and testing. Traditional image processing methods usually extract features from gray-level images while the deep learning models can take lossless color images as input. To demonstrate the difference between deep learning models and traditional methods, a GBDT model using gray level co-occurrence matrix features is built as reference. Meanwhile, several deep convolution neural network models are built using color images in different color space to demonstrate the effect of different color space. The experimental results show that the performance of the deep learning model varies with the color space and fabric design. To gather the advantages of different color space, a multi-color space model is built. By Taking images in different color space as input and apply a learnable weight on them, the multi-color space model gets more outstanding AUC and mAP on our test data.

INTRODUCTION

As a traditional industry, textile industry is going through an intelligent reform. As the reform going further, most processes have been automated, while the quality inspection process still relies on manpower. To cut cost, lift efficiency, and ensure high quality of product, automatic inspection system has been in the research industry for longtime.

As the key element of a computer vision based automatic inspection system, defect detection algorithms have been extensively studied. Many methods such as wavelet transform, Gabor transform, co-occurrence matrix, Markov random fields and shallow neural networks had been implemented in defect detection. The hardware development and the computing power of GPU allow us to use deeper neural networks to extract more efficient feature from loss-less color images. Deep CNN models which taking color images as input have shown their outstanding capability in instance detection, image classification, semantic segmentation and many other complicated tasks. So we have reasons to believe that, deep neural network can also help us to solve the problems in defect detection that can't be solved by traditional ways. Meanwhile, we also think that much more information provided by the less-destruction color images will benefit the deep model on the defect detection task.

In this paper, we compared the traditional machine learning model and the deep learning model's performance on the same defect detection task using gray level images to verify the efficiency of deep learning model. Then several deep models are trained using images from different color spaces to find out if color images benefit the model and how color space affect the performance of deep model. Based on the analysis of the previous experiment, a novel color weight block is proposed to fuse the multiple color space input images and promote the performance of the deep learning model on texture defect detection task.

RELATED WORK

Many approaches using manual features have been proposed to inspect textile defects. Zuo et al. [1] proposed to combine texture enhancement method and gray level co-occurrence matrices algorithm to extract the texture features for fabric defect inspection. Many machine learning methods are also used as classifier to extract abstract information from manual features. Shumin et al. [2] proposed to encode the fabric image with histograms of orientated gradient(HOG), and use AdaBoost to automatically select a small set of efficient HOG features as the representation of the image. Support vector machine is used to classify the fabric defects. Zhou et al. [3] presented to use dictionary learning framework to implement fabric defect detection. Combining manual features and machine learning methods, fabric defect detection algorithms achieve promising result for specific products. Most of the methods mentioned above take grey level image as input. While CNN based deep learning architecture has shown its superiority as it able to extract features of high abstraction from less-contrasted colorful images and update its parameters during training. The generalization capacity and robustness enable deep learning methods to perform better on complicated fabric defect detection problems. Wang et al. [4] proposed a light and robust convolutional neural network architecture to detect defect on product surface with high accuracy. Li et al. [5] proposed a compact convolutional neural network architecture for detection of several kinds of fabric defects. Obviously, although consume a lot of computing resources, the deep learning models are more robust and effective.

Color space is a mathematical model to represent color information as three or four different color components. A mess of researches have done to demonstrate how color space effects image related task. Shaik et al. [6] compared the difference of skin color detection and segmentation result in different color space, and draw a conclusion that YCbCr color space is more effective and efficient for the separation of image pixels in terms of color in color images. Goderio et al. [7] point out that the RGB space is not perceptually uniform, so that they use CIELab space instead in their Chronic Wounds classification task. Color space also has an impact on the performance of deep learning models. By converting the RGB dataset to 3 different color space and combine the pretrained deep CNN net and the Random Forest model, Sachin et al. [8] proposed a CNN based scene classification system, they also show that the color space do effects the accuracy of classification.

Based on these previous works, we have reason to believe that using color images, we can build a more efficient deep learning model to detect defects on the textile. We can also learn from [6-8] that different color space may lead to different result. What we want to find out in this paper are if the color space also makes difference in our defect detection task, and if so, can we take advantage of it to improve our accuracy of defect detection.

Methodology

Data Set

To build a data set for training defect detection models, a considerable volume of images of towels with varying degrees of defect are collected. The products from weaving machine were ranked as three degrees by the inspection process according to their quality. To get the distribution of defect in the real production environment, we randomly sampled products from the second and the third class products, and labeled the defect areas on pixel level. According to the color and pattern of the textile, they can be divided to 10 classes, as shown in Figure 1.

There are various degrees of defects in the images we collected from product lines. To generate defect-free images from existing samples and expand data scale, the slide windows are used to crop origin images, and a continuous label given by equation (1) according to pixel leveled label of the original image can be calculated for each sub-image. Where N denote the number of different type of defect in the sub-image. R_{sub} is the region of sub-image, R_d^i is the i -th defect region in the sub-image. $S(x)$ means the area of region x . This label means the ratio of defect area to the sub-image area. It is worth noting that when a sub-image contains more than one defect which can be overlapping with each other, its label can be larger than 1.

$$\text{label} = \sum_{i=1}^N \frac{S(R_{sub} \cap R_d^i)}{S(R_{sub})} \quad (1)$$



Figure 1. Textile Product Samples

Experiments

Table 1: Comparison of result for different model and color space

Model & color space	AUC	mAP
GBDT & Gray	0.8506	63.73%
DenseNet & Gray	0.889	95.3%
DenseNet & RGB	0.9214	98.61%
DenseNet & HSV	0.9241	98.32%
DenseNet & XYZ	0.9287	98.35%
DenseNet & LAB	0.8690	97.49%
DenseNet & YUV	0.9281	98.02%
DenseNet & YCrCb	0.9325	98.33%

At the very beginning, a GBDT [9] model using gray level co-occurrence matrix features is trained as reference. The gray level co-occurrence matrix (GLCM) [10] is a statistical method of examining texture that considers the spatial relationship of pixels in gray level image. Energy, ASM-energy, contrast, dissimilarity and correlation are calculated from 42 different matrixes with different offset and angle for each image as the texture features in our work. Gradient boosting decision tree (GBDT) is a widely-used machine learning algorithm, due to its efficiency, accuracy, and interpretability. A classify GBDT model has been trained using the features mentioned above. As shown in Table 1, the classify model get 63.73% mAP and 0.8506 AUC [11] on the test data.

As a comparison, a deep learning model is also trained on gray level images. The backbone model is DenseNet [12]. By using Dense Block shown in Figure 2 in a CNN structure, the error signal can be easily propagated to earlier layers more directly in the Dense Net. Since each layer in DenseNet receive all previous layers as input, more diversified features and tends to have richer patterns, which leads to outstanding performance. In our work, a DenseNet trained with gray level images gets 95.3% mAP and 0.889 AUC on the test data. Which proves that deep learning model does have stronger capability dealing with complicated image related task than traditional machine learning model with manual features.

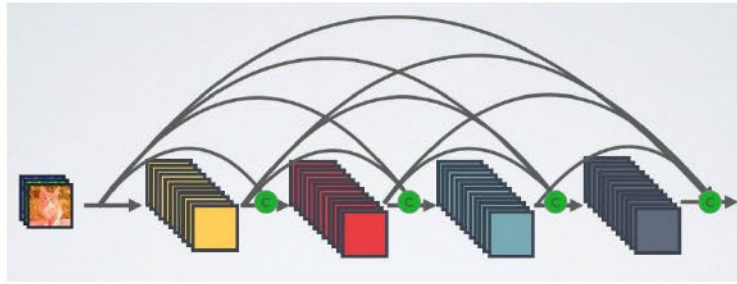


Figure 2. Dense Block

Further on, gray level images are replaced by less-destruction color images to provide richer visual information while training deep models. Meanwhile, to find out how color space effect deep model, the original RGB dataset is converted to five other common color spaces such as HSV, XYZ, LAB, YUV and YCrCb. Six different DenseNet models with the same structure were trained and test on each of these color spaces separately. The test metrics are demonstrated in Table 1. Compared to the gray level images, color images bring considerable performance boost to the deep models, the best AUC and mAP are 0.9325 and 98.33% for the color-input models. However, simply converting color space doesn't bring distinct benefit. Besides LAB color space, models from all other spaces seem to be at the same level.

Proposed Approach

Although changing color space doesn't promote model performance, we can still find something interesting after more delicate analysis. As mentioned above, the textile can be divided into 10 classes according to the pattern and color. The AUC of the models trained under different color spaces for each of these 10 classes are demonstrated in Table 2. On closer inspection, we see that each color space performs differently for different classes. Even the model using LAB color which has the worst performance on whole, has a certain class of expertise. In this context, we believe that different color spaces can be combined in a proper way to obtain better result.

Table 2: The AUC of the models trained in different color spaces for each class

Pattern	RGB	HSV	YUV	XYZ	YCrCb	LAB
Class1	0.897	0.754	0.956	0.975	0.920	0.660
Class2	0.962	0.999	0.986	0.981	0.964	0.871
Class3	0.962	0.996	0.992	0.989	0.994	0.659
Class4	0.944	0.958	0.965	1.000	0.937	0.833
Class5	0.878	0.829	0.888	0.950	0.867	0.568
Class6	0.939	0.950	0.981	0.984	0.994	0.870
Class7	0.652	0.997	0.651	0.932	0.614	0.998
Class8	0.946	0.969	0.956	0.948	0.951	0.922
Class9	0.970	0.983	0.991	0.813	0.991	0.313
Class10	0.878	0.794	0.914	0.887	0.783	0.837

The method of fusing multiple color space inputs in our work is color weight block (CWB) shown in Figure 3. In this layer, the multi-color space input with shape $h \times w \times c$, where h and w denotes the height and the width of the input image, c denotes the number of channels in all input color spaces, is converted to a color

weight vector with shape $1 \times 1 \times c$ by a FCN block. The FCN block contains a FCN [13] structure and several fully connection layers, which aims at learning the importance of the input channels. Then the weight vector will be broadcast to the input along the spatial dimension [14], so that we can get the weighted multi-color input. As different color space has the pattern class that excels at severally, the color weight layer is designed to learn which color space is more important, to emphasis the meaningful channel and depress the noneffective channels.

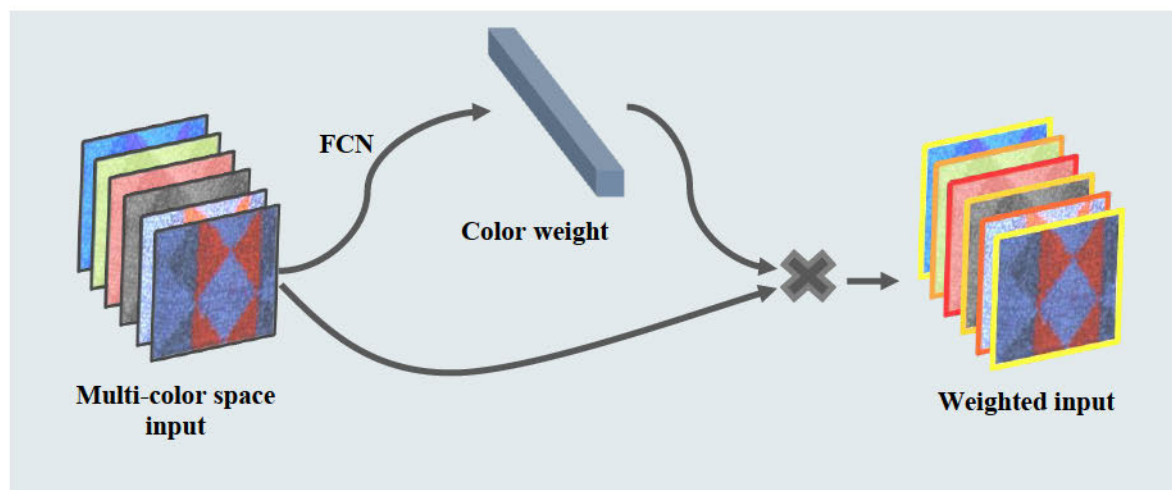


Figure 3. Color Weight Block

As shown in Table 3, considering the balance of performance and calculate quantity, we choose XYZ and YCrCb as the input. Using multi-color space images, the origin DenseNet get a slight improvement both on AUC and mAP. When we add our color weight block (CWB) to the top of the origin DenseNet, at a small computational cost, we get a significant performance boost. Which confirmed that combining different color space do benefit the defect detection task and the effectiveness of our color weight block.

Table 3: Comparison of result for input color space and model structure

Model Structure	Input Color Space	AUC	mAP
Origin DenseNet	XYZ	0.9287	98.35%
Origin DenseNet	YCrCb	0.9325	98.33%
Origin DenseNet	XYZ & YCrCb	0.9426	98.52%
DenseNet & CWB	XYZ & YCrCb	0.9673	99.40%

CONCLUSION

In this paper, we proved the positive effect of using color images and deep learning model in textile defect detection task. Meanwhile, as analyzed above, we find out that the performance of deep model varies with the color space of the input images and pattern design of the textile. In this context, the color weight block (CWB) is proposed to assists deep models to fuse the multiple color space. Using CWB and fusion color space, we get 0.9673 AUC and 99.4% mAP on our test data.

REFERENCES

1. Zuo, H., Wang, Y., Yang, X., & Wang, X. (2012, October). Fabric defect detection based on texture enhancement. In 2012 5th International Congress on Image and Signal Processing (pp. 876-880). IEEE.
2. Shumin, D., Zhoufeng, L., & Chunlei, L. (2011, July). Adaboost learning for fabric defect detection based on hog and SVM. In 2011 International conference on multimedia technology (pp. 2903-2906). IEEE.
3. Zhou, J., Semenovich, D., Sowmya, A., & Wang, J. (2014). Dictionary learning framework for fabric defect detection. *The Journal of The Textile Institute*, 105(3), 223-234.
4. Wang, T., Chen, Y., Qiao, M., & Snoussi, H. (2018). A fast and robust convolutional neural network-based defect detection model in product quality control. *The International Journal of Advanced Manufacturing Technology*, 94(9-12), 3465-3471.
5. Li, Y., Zhang, D., & Lee, D. J. (2019). Automatic fabric defect detection with a wide-and-compact network. *Neurocomputing*, 329, 329-338.
6. Shaik, K. B., Ganesan, P., Kalist, V., Sathish, B. S., & Jenitha, J. M. M. (2015). Comparative study of skin color detection and segmentation in HSV and YCbCr color space. *Procedia Computer Science*, 57, 41-48.
7. Godeiro, V., Neto, J. S., Carvalho, B., Santana, B., Ferraz, J., & Gama, R. (2018, September). CHRONIC WOUND TISSUE CLASSIFICATION USING CONVOLUTIONAL NETWORKS AND COLOR SPACE REDUCTION. In 2018 IEEE 28th International Workshop on Machine Learning for Signal Processing (MLSP) (pp. 1-6). IEEE.
8. Sachin, R., Sowmya, V., Govind, D., & Soman, K. P. (2017, September). Dependency of various color and intensity planes on CNN based image classification. In International symposium on signal processing and intelligent recognition systems (pp. 167-177). Springer, Cham.
9. Ke, G., Meng, Q., Finley, T., Wang, T., Chen, W., Ma, W., ... & Liu, T. Y. (2017). Lightgbm: A highly efficient gradient boosting decision tree. In *Advances in Neural Information Processing Systems* (pp. 3146-3154).
10. Haralick, R. M., Shanmugam, K., & Dinstein, I. H. (1973). Textural features for image classification. *IEEE Transactions on systems, man, and cybernetics*, (6), 610-621.
11. Huang, J., & Ling, C. X. (2005). Using AUC and accuracy in evaluating learning algorithms. *IEEE Transactions on knowledge and Data Engineering*, 17(3), 299-310.
12. Iandola, F., Moskewicz, M., Karayev, S., Girshick, R., Darrell, T., & Keutzer, K. (2014). Densenet: Implementing efficient convnet descriptor pyramids. arXiv preprint arXiv:1404.1869.
13. Long, J., Shelhamer, E., & Darrell, T. (2015). Fully convolutional networks for semantic segmentation. In *Proceedings of the IEEE conference on computer vision and pattern recognition* (pp. 3431-3440).
14. Hu, J., Shen, L., & Sun, G. (2018). Squeeze-and-excitation networks. In *Proceedings of the IEEE conference on computer vision and pattern recognition* (pp. 7132-7141).

Study on impression degree for the color of the concrete in Japanese.

Kotaro Matsumura*

*(152-52 Sugo, Takizawa-shi, Iwate-ken 020-0611 Japan)
Morioka Junior College, Life Style Science, Iwate Prefectural University/
Japan Society of Kansei Engineering, Japan.*

*Corresponding author: Kotaro Matsumura, mission_penguin_concrete@yahoo.co.jp

Keywords: Color of the concrete, Impression degree, gray, Greening concrete, Natural destruction

ABSTRACT

The concrete in Japan is caught by a masterpiece of the natural destruction. On the other hand, it is the construction materials which the concrete is cheap, and are strong. The concrete is about 10,000 yen at 1 cubic meter and is cheaper than mineral water. And the concrete is stronger than the wood which is used a lot by a Japanese architecture. The color of the concrete is gray. The color of the concrete is the same as the color of the stone gathered in Portland Island of England. Therefore the European peoples compare a color of the concrete to it of nature. However, Japanese are thinking about a color of nature in the green color of trees. Therefore, this study on impression of the color of the concrete is investigated by performed questioner's survey. The questionnaires' survey assumed the construction engineers who used the concrete and general people that concrete did not have relations in Japan the target persons. In addition, the number of the questionnaire collections of construction engineers were 682 cases (recovery: 39.1%), the questionnaire collections of general parsons were 147 (recovery: 100%).

From a result of this questioner's survey, the impression degree of engineers of the concrete and the impression degree of general parsons irrelevant to concrete were completely opposite. The construction engineers have a color of the concrete in goodwill. However, the students irrelevant to concrete did not like a color of the concrete. In this study, the reason was made clear by questionnaires' survey. Therefore greeting concrete which can harmonize with natural environments was examined in this study as a policy to improve value of the concrete. In Japan, a natural disaster is prevented by greeting concrete, and it is expected that the concrete corresponding to natural environments increases in future.

INTRODUCTION

Because it is thought that the concrete is a material of the natural destruction in Japan, it is avoided. On the other hand, because it is thought that the concrete is considered as an artificial stone as a substitute for the natural stone in Europe, it is liked. Therefore, this study grasps the sense of values for the color of the concrete in Japan by a questionnaire and arranges a difference with Europe. And this performs suggestion to improve the sense of values for the color of the concrete in future Japan. In addition, the person targeted for the questionnaire investigated in this study does both with the construction engineers and general persons in Japan. And this study is arranged whether there is difference in what kind of sense of values in each.

QUESTIONARIES' SURVEY METHOD

The questionnaires' survey was intended to grasp the impression degree for the color of the concrete in Japan.

The target person who performed questionnaires' survey

⇒ Construction engineers in Japan

Random sampling workers of 1,748 civil engineering works and architecture's works

The number of the collections: 682 cases (39.0 %)

⇒ General persons in Japan

The number of the collections: 147 cases (100 %)

QUESTIONARIES' SURVEY CONTENTS

The questionnaires' survey contents were considered to be contents to show to 5 from 1.

1. person's life area (selective type)
2. What are your favorite materials? (selective type)
3. Do you like the color of the concrete? (selective type)
4. What thinks you to be a cause deteriorating an image of the concrete? (description type)
5. What is the factor to improve value of the concrete? (description type)

In addition, the paper size of the questionnaire was considered to be A4, and the pages were considered to be page 2.

QUESTIONARIES' SURVEY RESULTS

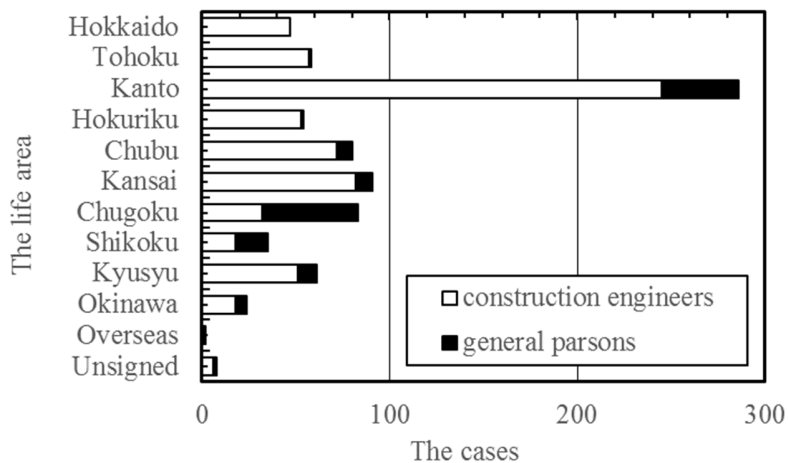


Figure 1. The life area of respondents

But construction engineers were shown in "C" and general persons were shown "G".

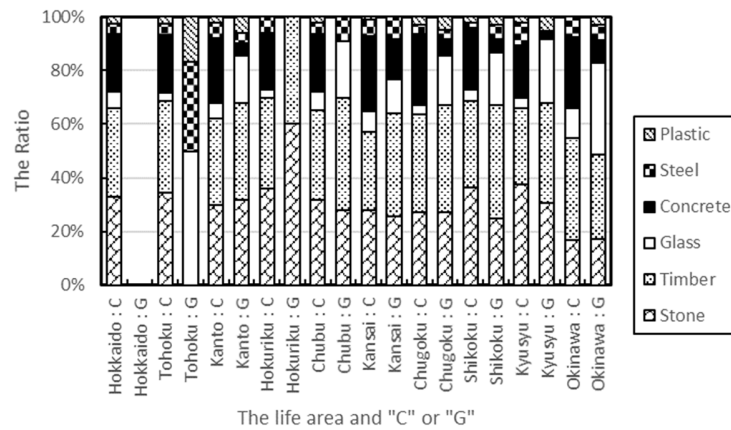


Figure 2. The favorite materials for life area

The difference by each life area was not confirmed so much. In Japan, Timber and a stone were liked regardless of a life area. Particularly, the general persons did not like concrete.

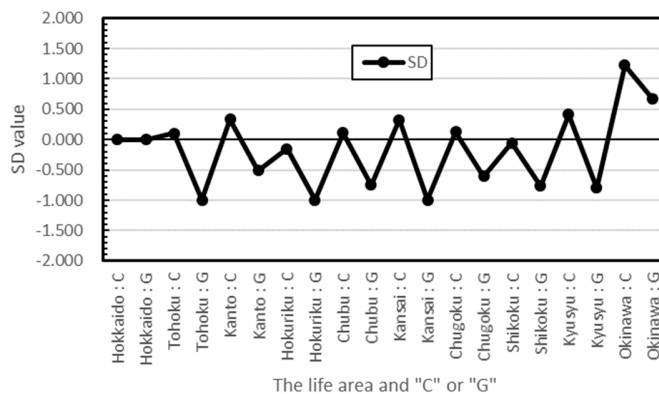


Figure 3. The preference of the color of the concrete for life area

In addition, the SD value was calculated with a value to show next. -- The like is 2 point, the like a little is 1 point, the neither is 0 point, the little dislike is -1 point, the dislike is -2 point. The general persons in Japan tended dislike the color of the concrete in other than the Okinawa. The construction engineers in Japan tended to like a little the color of the concrete.

But, about Okinawa, as for the both the construction engineers and general persons, the color of the concrete was liked. This is caused by a house of Okinawa being often made with concrete. There were many wooden buildings in Okinawa before World War II. However, after World War II, concrete houses increased by assistance to construction in the concrete house by the Operation Army of USA. Therefore, the persons which grew up after World War II in Okinawa tend to like it as the house which is not broken in a typhoon and a concrete house does not have a sense of incongruity. Because the construction engineers often use concrete in work about the area except Okinawa of Japan, a color of the concrete does not have a sense of incongruity. However, because concrete is often regarded as materials used for natural destruction, the general persons except Okinawa in Japan may tend to avoid it. Because the culture of the tree is mainstream in Japan, the Japanese thinks that concrete destroys it naturally when there is the concrete of the artifact on the land where there is a tree. Therefore, other than the construction engineers using the concrete by work avoid the concrete. In addition, by the relations, the color of the concrete is disliked, too.

The cause worsening an image of the concrete described the answer to questionnaire is shown next.

- The color of the concrete does not have an expression.
- The color of the concrete is unitary.
- The concrete changes in uneven coloring for change of properties with time.
- The surface of the concrete changes color and is dirty.
- The concrete is mineral matter and it is felt to be cold.
- The color and form that the concrete cannot harmonize with for green surrounding environment, and the concrete is hard to melt into it naturally.
- The old concrete becomes strong in the image of the dark color.
- The concrete is hard to feel warmth in achromatic color.
- The color of the concrete is felt to be it is monotonous, and cold.
- The concrete structure is easy to change color in the color of the bad image.
- The color of the concrete has bad appearance.
- The concrete is not a beautiful color.
- There is the different concrete structure of the color in green natural environments.
- The concrete is easy to become dirty by algae and mold black.

In this way, the concrete was strong in the image that a color had bad. About an image of this concrete, the differences between building engineers and general parsons in Japan were not recognized. Therefore, the Japanese is judged not to like the color of the concrete.

Table 1: The method of the value improvement to concrete

Order	The construction engineers	The general parsons
1	Production of the ship	Production of the art object
2	Harmony to natural environments	Production of artworks
3	Production of the monument	Harmony to natural environments
4	Improvement of the function	Life article
5	Artistic molding thing	Do not hit

The answer about the method of the value improvement to concrete by the questionnaires' survey is shown in table 1. In addition, the answers of the respondents in the questionnaire were considered to be a result settled by KJ method. The construction engineers in Japan had many answers such as ships being produced with concrete. In contrast, it is thought that general parsons in Japan are that an art object, artworks and life article are made. And they does not hit. It is thought that the harmony to natural environments improves value of the concrete as for both construction engineers and general parsons in Japan.

DISCUSSION

The color of the concrete is caught as a color of the environmental disruption for a Japanese. The construction engineers in Japan was thought that concrete is essential in Japan with many natural disasters. Therefore, the construction engineers made retaining walls and breakwaters of the concrete in Japanese nature. They were effective for a natural disaster. From them, In Japan, concrete has been outstanding in natural environments. When Japanese parsons demand an ease from natural environments, they see gray for the color of the concrete. Therefore, Japanese parsons dislike the concrete than the tree and the stone of nature. In addition, Japanese parsons call a city with concrete jungle because the building of the city is made with concrete. However, from the questionnaire result of this study, construction engineers and general people think that value of the concrete improves because it harmonizes natural environments. However, the impression degree of the concrete may rise when the color of the concrete changed like Greening concrete. The Greening concrete is the concrete which is available for direct planting on the concrete. Therefore, concrete may not be a masterpiece of the environmental disruption when the color of the concrete changes into the color such as the Greening concrete. Green Concrete is a concrete on which plants directly grow. It consists of a continuous void concrete a water retentive material in the void and thin soil layer sprayed on the surface. Because the surface of green concrete can raise a plant, it can let a plant grow up in the state that the ground was protected. This green concrete is coming to be used now on not only the protection of the ground but also the wall of the building. In the building of the city, it is thought that wall surface tree planting is more effective for global warming than the roof tree planting. Green concrete using on the ground is shown in figure 4. Green concrete using on the wall of the building is shown in figure 5. When this green concrete is spread widely in Japan, good concrete will be handed down to Japanese people. And concrete will be not disliked Japanese people. When green concrete spreads widely, the global warming can prevent it, too. But colors of the concrete may not become rarely disliked by vegetation to lose the eyesight of the gray at the color of the concrete.



Figure 4. The green concrete using on the ground



Figure 5. The green concrete using on the wall of the building

CONCLUSIONS

This study was impression degree for the color of the concrete in Japanese. As a result of questionnaire, Japanese parsons disliked the concrete. The also reason of the concrete was colored it. However, Japanese parsons thought that value of the concrete improved when concrete could harmonize with nature. The method that it is harmonized with if concrete is natural includes green concrete. When this green concrete is spread widely in Japan, good concrete will be handed down to Japanese people. And concrete will be not disliked Japanese people. When green concrete spreads widely, the global warming can prevent it, too. But colors of the concrete may not become rarely disliked by vegetation to lose the eyesight of the gray at the color of the concrete.

REFERENCES

1. Yoshiyuki Chinen, Masami Shiba (2015). Consideration of Underlying Historical Change in House Building Materials in Okinawa Prefecture. *Journal of the Japanese Forest Society* 97, pp.143-152, 2015
2. Kunio Yanagibashi, Toshio Yonezawa, Mamoru Sakuma and Yosaku Ikeo (1995). A Study on Green Concrete. *AIJ (Architectural Institute of Japan) journal of technology and design. Des. No.1*, pp.61-66, December 1995

RELATIONSHIP BETWEEN PROPER CONTRAST AND IMAGE SATISFACTION

Suwat Puenpa^{1*} Kitirochna Rattanakasamsuk² and Ploy Srisuro³

¹ *Photography and Cinematography Technology, Faculty of Mass Communication Technology, Rajamangala University of Technology Thanyaburi, Thailand.*

² *Color Research Center, Rajamangala University of Technology Thanyaburi, Thailand.*

³ *Advertising and Public Relations Technology, Faculty of Mass Communication Technology, Rajamangala University of Technology Thanyaburi, Thailand.*

*Corresponding author: Suwat Puenpa, suwat_p@rmutt.ac.th

Keywords: image contrast, zone system, grayscale image, photographer and image satisfaction

ABSTRACT

For an image retouching process, image contrast adjusting is a way to obtain the quality of the image. However, we observed that in the case of a grayscale image, most of the non-professional photographers think that good grayscale image must be low contrast image. Unlike most professional photographers, they prefer to retouch the image by keeping original image contrast or slightly increasing the image contrast. Therefore, we investigated whether this observation is true or not. The objective of this research was to investigate the relationship between proper contrast and image satisfaction of these two groups. The subjects were fifteen professional photographers and fifteen non-professional photographers. The stimuli were five landscape images. All image is 8-bit grayscale at zone system 5. Weber Contrast of each image was varied to seven levels which include original contrast level, one increment contrast levels, and one decrement contrast levels. The stimuli were presented on a 24-inches LED monitor situated in the experimental room. The distance between the subject's eye and the monitor was 95 centimeters. The size of the stimuli was 29 X 43 degrees. The task of the assessors was to evaluate the image satisfaction with rating scales from 1-5 which 1 is the highest dissatisfaction and 5 is the highest satisfaction. Each subject must complete 35 evaluations. The expected result was that the non-professional photographers might prefer a lower contrast image than original contrast. On the other hand, professional photographers might prefer a high contrast image.

INTRODUCTION

Landscape Photography is one of the most popular niches of photography, for both professional and non-professional photographers. It is to capture the beauty of the scenery in the natural park. The atmosphere of the fields in rural areas is extraordinarily beautiful. This invites a photographer or general person to hold the camera up to take this impressive beauty.

The Photography enthusiasts see the beautiful atmosphere through the viewfinder of a digital single lens Reflex camera (DSLR) or smart phones, that are visible and displayed in color images as if they were seen with eyes. The perfect composition, good lighting conditions and the right shooting time are the best moments in photography. On the other hand, the image becomes normal, lack of depth and interest when converted to black and white. Because the colors that appear on those photos will help to distinguish and interest themselves. And colorful photography will create great excitement in the viewing experience as opposed to black and white photos. For adjusting a color image into a black and white photo, various colors may turn out to be the same or have very similar tones or become a low contrast black and white image. Black and white photos with low contrast will cause the image to lack depth or lack of detail and make the image uninteresting.

The best black and white photos usually have some portion of the photo that is near to pure white, and some portion of the photo that is near black. This increased contrast adds interest to the scene. Therefore, a suitable black and white photo should have a different gray tone according to the Zone System. In this

regard, it is appropriate to consider the contrast level of the grayscale of black and white photos. Between professional photographers and amateur photographers, which may affect the satisfaction of high and low contrast to different black and white photos.

METHODOLOGY

Apparatus and Procedure

The relationship between appropriate contrast and satisfaction with Landscape Photography in a black and white image was studied with the following steps.

Step 1: The Preparation Process

The experimenters began researching the related information from books, articles and expert interviews to adjust the contrast of the middle tone grayscale of landscape photos. Then they set the images with a grayscale chart. The experimenters were adjusting the color image to black and white of the landscape photos with software for image enhancement. Later, 5 landscape photographs were selected by the experimenters. The objective criteria that determine whether an image that has the characteristics of pixel distribution from the darkest black, the middle gray and the whitest as shown in the histogram of Figure 1.

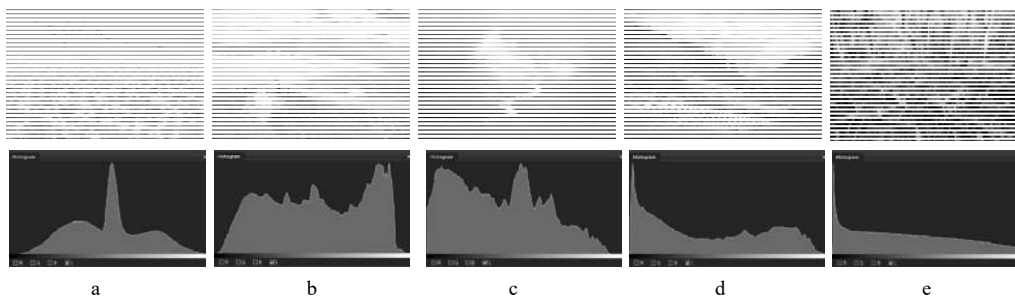


Figure 1. Histogram of Landscape Photographs

Step 2: The Adjustment Contrast Process

The Landscape photographs were adjust the contrast level, referring to the grayscale of the Ansel Adams Zone System, consisting of 7 levels, covering gray levels from deep tonalities, representing the darkest part of the image in which some detail is required (ZoneII) to white with textures and delicate values (ZoneVIII) or -3 -2 -1 0 +1 +2 +3 as an example shown in Figure 2.

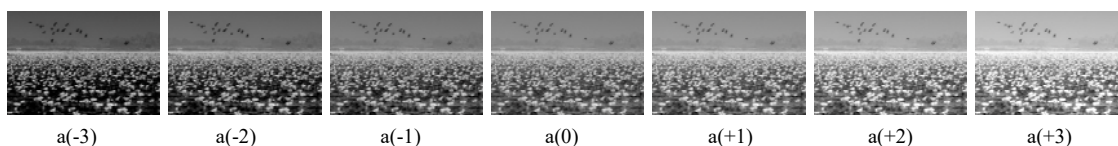


Figure 2. Seven Gray Levels of Landscape Photographs

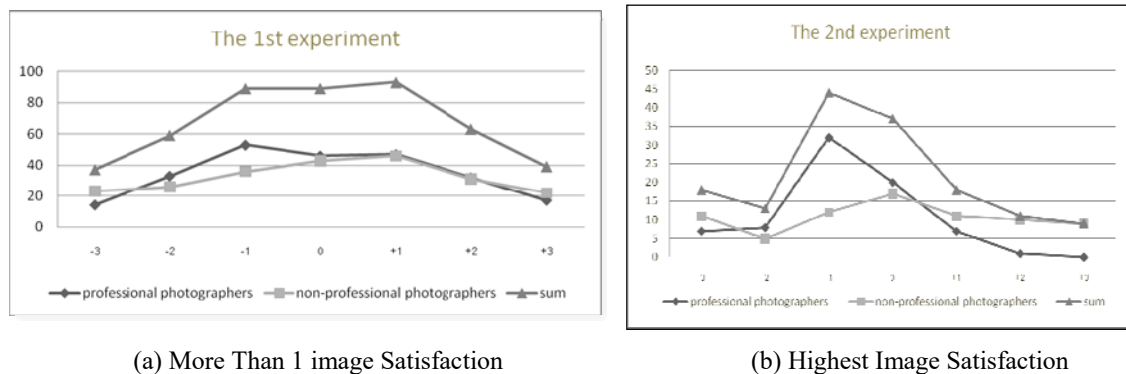
Step 3: The Evaluation Process

The Landscape images were used in all five images experiments in seven sets of contrast levels. Each image was arranged in a different presentation. The experiment was conducted in a dark room. The Landscape Photographs were presented on a 24-inch LED screen in the laboratory. The distance between the eyes of the person and the screen is controlled to be 95 centimeters. The size of the stimuli was 29x43 degrees. The assessors will have to consider a total of 35 images, evaluate 2 experiments. The first experiment, the assessors selected more than 1 image in each set. And the second experiment, the assessors were asked to select only one of the most satisfying images in each set.

RESULT AND DISCUSSION

The results from the first experiment, the assessors were able to choose the satisfaction of more than 1 photograph from Figure 3. (a). It was found that a group of professional photographers were satisfied with the image contrast between -1 0 +1 but there were trends of satisfaction with black and white photos which has a high contrast or gray tone, zone VI (Dark light). The non-professional photographers were satisfied with the contrast between 1 0 +1 but tend to be satisfied with black and white images with low contrast or gray tone, zone IV (Light dark).

In the second experiment, the assessors consider black and white photos. From figure 3. (b), it was found that a group of professional photographers were satisfied with the contrast of positions at position-1, which had quite high contrast characteristics or gray tones, Zone VI (Dark light). In contrast, the non-professional photographers were satisfied with the contrast between 1 0 +1 and tend to be satisfied with the black-and-white image which has a normal contrast to the low, gray tones, Zone IV (Light dark) or a picture that looks quite bright.



(a) More Than 1 image Satisfaction

(b) Highest Image Satisfaction

Figure 3. The Assessment Result

The study found that the grey tone images at different grayscale levels according to the Ansel Adams Zone System affects the satisfaction of the professional photographers and non-professional photographers. A group of professional photographers was satisfied with the high contrast. On the other hand, a group of non-professional photographers was satisfied with low contrast.

Additional findings during the observation of the photograph evaluation, the experimenter found the different methods for determining the photo contrast of these two assessor groups. The professional photographer group took the time to consider the details of each tone of the photos presented on the screen. While the non-professional photographer considered the contrast of the picture together with the elements of the beauty of the image. The second group was elderly and tends to be satisfied with the brighter images than the professional photographer group.

ACKNOWLEDGEMENTS

This Research was supported the by Faculty of Mass Communication Technology, Rajamangala University of Technology Thanyaburi, Thailand.

REFERENCES

1. Panyawat Leawpaibool and Suwat Puenpa (2018) Studying Landscape photography by Using the tone control with Zone System.
2. Panyawat Leawpaibool and U-krit Na Songkhla (2018). Studying black and white cityscape photography by Using the tone control with Zone System.
3. Sheppard, R. (2012). Black-and-White images: Examining The Rich Tradition and Today's Potential of Black-and-White Landscapes. *Landscape Photography: From Snapshots to Great Shots*, 159. Berkeley, CA. Peachpit Press.

COLOR MATERIALS USED IN THE REPRODUCTION OF SHOSOIN IMPERIAL TREASURES “THE RED-STAINED IVORY SHAKU RULER WITH BACHIRU DECORATION” COLLECTED BY NARA WOMEN'S UNIVERSITY

Satoko Taguchi,^{1*} Shino Okuda,² Miho Muguruma,³ Miho Matoba,⁴
Atsuko Miyaji,⁴ Fumiyoshi Kirino¹, Katsunori Okajima⁵

¹*Center for Conservation and Restoration of Cultural Properties, Faculty of Fine Arts,
Tokyo University of the Arts, Japan.*

²*Faculty of Human and Life Science, Doshisha Women's College of Liberal Arts, Japan.*

³*The Kyoto University Museum, Kyoto University, Japan.*

⁴*Division of Humanities and Social Sciences, Nara Women's University, Japan.*

⁵*Faculty of Environment and Information Sciences, Yokohama National University, Japan.*

*Corresponding author: Satoko Taguchi, taguchi.satoko@fa.geidai.ac.jp

Keywords: color materials, two-dimensional spectroradiometer, Shosoin imperial treasures

ABSTRACT

Shosoin imperial treasures is a collection of cultural properties of the Nara period that include the remains of Emperor Shomu (701-756, reigning: 724-749), which is stored at Shosoin, Todaiji Temple. In the Meiji era, the project to create reproductions of Shosoin imperial treasures started in preparation for disasters. The reproduction of Shosoin imperial treasures “the Red-stained ivory shaku ruler with bachiru decoration” (hereinafter referred to as “R-bachiru ruler” compared with the original one referred to as “O-bachiru ruler”) owned by Nara Women's University was produced by Yoshida Houshun. He was a craftsman who played an active part during the Showa era. Although Bachiru was a traditional craft technique to dye and engrave ivory, the technique was lost in the Heian period. When Houshun made the reproduction of Shosoin treasures, it was considered that the detail of the Bachiru technique was unknown. Moreover, because the analysis techniques were not enough at that time and the information of color materials was insufficient. This study aims to clarify what kinds of color material were selected by Houshun in the reproduction of Shosoin imperial treasures, and we focused on a material survey on the R-bachiru ruler. In a previous study, the coloring material used for the O-bachiru ruler was clarified according to the investigation results by the Shosoin Office, Imperial Household Agency. In this study, we measured the color materials used in R-bachiru ruler and analyzed the measured data using an optical microscope, an X-ray fluorescence (XRF), and a two-dimensional spectroradiometer. In addition, the acquired results were compared with the O-bachiru ruler. According to the investigation results, red, blue and green color materials were used in the R-bachiru ruler. The spectral reflectance of each color was measured by a two-dimensional spectroradiometer. When the blue and green spots were observed with the microscope, some particles were confirmed. Since Cu was detected by XRF analysis of blue and green spots, it is suggested that copper-based pigments were used. The red coloring material used for the O-bachiru ruler owned by Shosoin has been identified as a cochineal from the measuring results of its spectral reflectance. On the other hand, particles were not observed in the red spot of the R-bachiru ruler when using the microscope, and also elements derived from the colorant were not detected when using the XRF. Therefore, it is inferred that the dyes were used in the red spot of the R-bachiru. Overall, it was considered that Houshun had used properly dyes and pigments in making the R-bachiru ruler as well as the original one.

INTRODUCTION

The Shosoin imperial treasures is a collection of cultural properties offered by the Empress Komyo to pray for the repose of Emperor Shomu's soul, and is stored at Shosoin, Todaiji Temple, Japan. Most of the properties were imported from China (Tang) and Persia, and produced in Japan during the Nara period (8th century). The collection has more than 9000 items, and there are also many types of materials and techniques used in the treasures. Since the Meiji era, research and reproduction projects have begun to preserve the Shosoin imperial treasures in preparation for disasters. Nara Women's University has collected more than 10,000 educational materials since 1908, including the reproduction of Shosoin imperial treasures and related materials. The reproduction of Shosoin imperial treasures “the Red-stained ivory shaku ruler with bachiru decoration” (R-bachiru ruler) was created by Yoshida Houshun (1878-1951), a craftsman in early Showa era. The coloring material used for the original “the Red-stained ivory shaku ruler with bachiru decoration” (O-bachiru) ruler was clarified according to the investigation results by the Shosoin Office, Imperial Household Agency [1]. Bachiru was a traditional craft technique of dyeing and engraving ivory. This Bachiru technique was introduced from Tang to Japan during the Nara period, and was used in other treasures, such as a sash band (obidome) and stones used in the game of Go. However, the details of the technique are unknown, since it was not inherited. The bachiru technique was lost and any information of materials could not be obtained through analysis. Hence it is thought that Houshun made the reproduction of Shosoin imperial treasures through trial and error. To clarify what materials Houshun chose to restore the treasures made in the Nara period, we analyzed the color and material of the R-bachiru using XRF and a two-dimensional spectroradiometer. The obtained results are compared with the O-bachiru survey results reported by the Shosoin Office, Imperial Household Agency.

MATERIALS AND METHODS

Figure 1 shows the photograph of the R-bachiru (length 30.1cm, width 2.3 cm, thickness 0.8 cm). The R-bachiru is the reproduction of one of the Shosoin imperial treasures, Red stained ivory shaku ruler with bachiru decoration, No. 3 (Treasure Number: Middle Section 51, length 29.7 cm, width 2.3 cm, thickness 0.8 cm). R-bachiru was purchased in 1932 as an educational material by Nara Women's Higher Normal School. The name of the creator, Yoshida Houshun, has been written on the storage box.

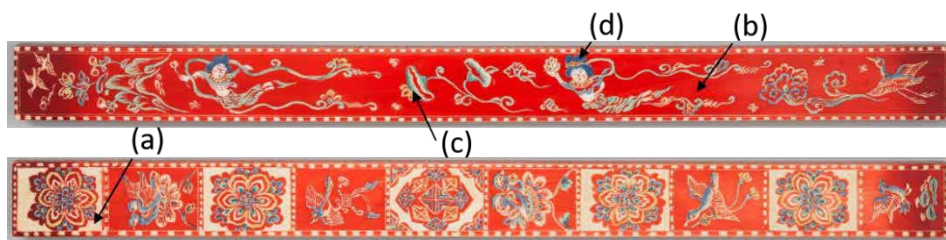


Fig. 1 The photograph of R-bachiru [2].

The composition of the materials used in the R-bachiru was determined by the measurement results using an XRF (XL3t-900S-M, Thermo-niton, voltage 50 kV, filament current 200 mA, X-ray tube: Ag, mineral mode, spot diameter 3 mm ϕ). In addition, the spectral reflectances of the R-bachiru were measured using a two-dimensional spectroradiometer (TOPCON, SR5000-HWS).

RESULTS AND DISCUSSION

The R-bachiru was colored with red, blue, green, and yellow colorants. The colors of the R-bachiru are very similar to those of the O-bachiru in appearance. However, the O-bachiru is mostly colored in red evenly whereas the redness of the R-bachiru is deeper toward the edge. It is unclear whether it depends on the dyeing process in reproduction or the aging of the R-bachiru. According to the observation of the R-bachiru using an optical microscope, it was considered that pigments were used for coloring materials because particles were observed in the blue and green regions. Since red particles were not confirmed, it is likely that a dye was used. According to the O-bachiru's material survey results by the Shosoin Office, Imperial Household Agency [2], the red is identified as cochineal and the green as atacamite ($\text{Cu}_2(\text{OH})_3\text{Cl}$).

Figure 2 shows the XRF spectra of the measurement points of Fig. 1(a)-(d). Ca, P, and Ag were detected from all measurement points, but Ag was derived from the X-ray tube of the XRF instrument. In the analysis of the measurement point (a), it could not be observed any color material, and only Ca, P, and Ag were detected. Therefore, Ca and P are considered to be due to hydroxyapatite ($\text{Ca}_{10}(\text{PO}_4)_6(\text{OH})_2$), which is the main component of ivory. In the XRF spectrum of the measurement point (b) in red, no element was detected except for an ivory-derived component. Therefore, there is a high possibility that the artist used a dye for coloring the material. There was no difference in the detected element between the dark red and the light red. In the XRF spectrum of the measurement point (c) showing blue and the (d) showing green, Cu was detected in addition to the ivory component, suggesting that the pigment mainly composed of copper by using azurite ($2\text{CuCO}_3 \cdot \text{Cu}(\text{OH})_2$) or malachite ($\text{CuCO}_3 \cdot \text{Cu}(\text{OH})_2$).

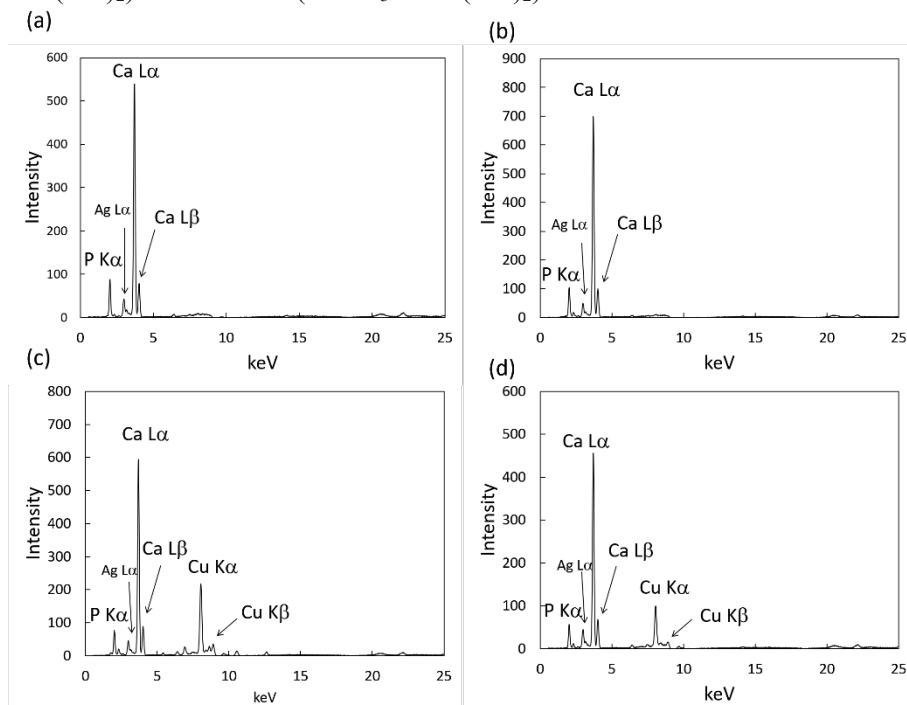


Fig. 2 XRF spectra of the R-bachiru ruler: (a) ivory, (b) red, (c) green and (d) blue.

Figure 3 shows the spectral reflectance of the measurement points (a) to (d). The result of point (a) shows that the spectral reflectance increases with increasing wavelength. The measurement result of point (b) shows that the spectral reflectance remains low when the wavelength is less than 550nm, and rapidly rises over 570nm. The spectrum of point (c) has a peak around 520 nm, and point (d) has

a peak around 470 nm. The spectral reflectance values of an ivory sample with and without various red coloring materials were reported by the Shosoin Office, Imperial Household Agency [3]. The spectral shape of the ivory sample is similar to (a), and the spectral shape of (b) is similar to that of the ivory sample colored lac lake, cochineal lake, suo lake, and akane lake. Therefore, these results suggested that the R-bachiru may have used the red dyes.

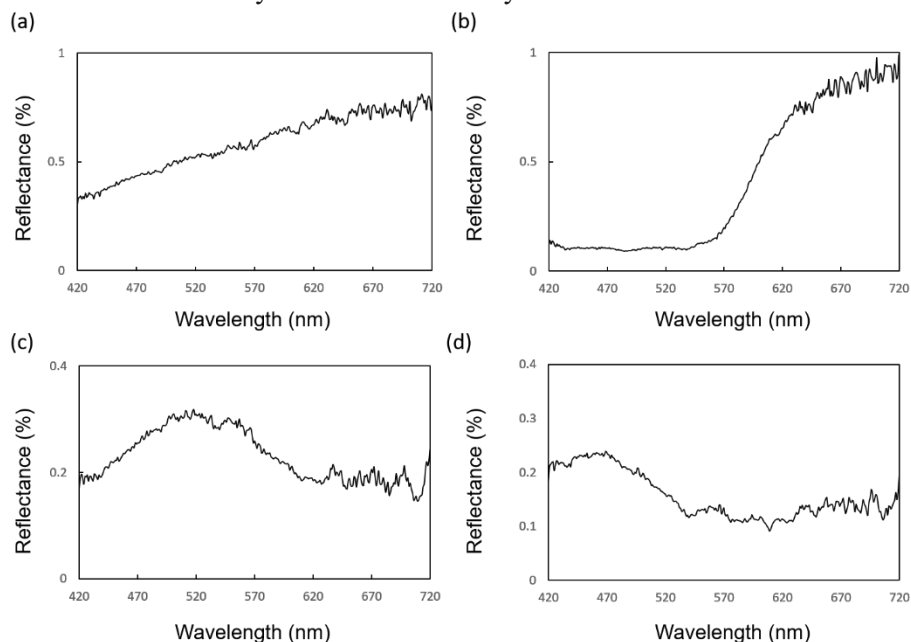


Fig. 3 Spectral reflectance of the R-bachiru ruler: (a) ivory, (b) red, (c) green and (d) blue.

CONCLUSIONS

According to the results of XRF analysis, 2D-spectral reflectance measurement and microscopic observation of the R-bachiru, we found that the red colorant used a dye, and the green and blue colorants used a pigment containing Cu. Since selected pigments and dyes for each color were used in the R-bachiru, it is suggested that Houshun might have tried to reproduce the color materials used in the O-bachiru by carefully observing the original Shosoin imperial treasures.

ACKNOWLEDGEMENTS

This work was supported by JSPS KAKENHI Grant Number 18KK0282. We would like to thank Masato Nagata for the measurement using the two-dimensional spectroradiometer.

REFERENCES

1. Nakamura, R., Tanaka, Y., Ogata, M. & Naruse, M. (2013). Annual report. *Bulletin of Office of the Shōsōin Treasure House –Shōsōin kiyō–*, 35, 66-69.
2. Educational specimens of Nara Women's University and Nara Women's Higher Normal School School (2019), Retrieved September 1, 2019, from <https://trc-adeac.trc.co.jp/WJ11F0/WJJS07U/2920155100/2920155100200020/mp000020>
3. Nakamura, R., & Naruse, M. (2015). Lac Colorant Found in the Shosoin Treasures by Visible Reflectance Spectrometry. *Archaeology and natural science*. 68, 33-46.

COLOR APPEARANCE MODEL OF SMALL FIELD STIMULI IN THE FOVEA AND PERIPHERY

Shuichi Mogi¹, Masafumi Kamei¹, Masato Sakurai², Tomoharu Ishikawa¹, Miyoshi Ayama¹

¹*Graduate School of Engineering, Utsunomiya University, Japan.*

²*Dept. of Computer Science, Faculty of Informatics, Shizuoka Institute of Science and Technology, Japan.*

*Corresponding author: Shuichi Mogi, e-mail: m.shuichiito080801@gmail.com

Keywords: Color appearance, Small field stimulus, Peripheral field, Color naming

ABSTRACT

Most of previous studies on color appearance change with eccentricity aim to investigate the change of color mechanism over the retinal eccentricity. Thus each study employed one method such as color matching, elementary color naming, or scaling chromatic component to intensively explore the focal issue. However, color appearance change in periphery is also important to design various signage, information display, or signals for transportation. Taking these applications into consideration, Sakurai et al. (2003) measured color appearance of 1.85 deg stimulus presented on various points in the entire visual field using both the opponent-colors-type color evaluation and categorical color naming. The principle of the former is the same as elementary color naming. Data obtained by the latter method reflect color categorization processed in the higher level of human brain. Unfortunately, few studies have done using both methods.

Considering the cases of presenting information on the edge of display using characters or pictograms, color appearance change of small field stimulus in near periphery along various directions is quite important. Therefore, we aim to investigate the color appearance change of small field stimulus using both methods mentioned above to reveal the change of relation between opponent-color processes and color categorization, and to provide practically useful data for color design of information display.

We employed the circular test stimulus with a diameter of 0.5 deg, and it was presented at 5, 10, and 20 deg for each of upper, lower, left and right directions as well as at 0 deg, total of 13 locations. Fifty-four color stimuli of the LCD were prepared. They were grouped into reddish, dark yellow, greenish, bluish at about 20 cd/m², and bright yellow at about 60 cd/m². Color appearance was evaluated using the hue judgment using the hue circle and saturation judgment using the saturation evaluation bar, blackness and whiteness evaluation, and a categorical color naming.

Results of the stimuli close to unique hues, of the opponent-colors-type color evaluation were compared with those of the comparable stimuli in Sakurai et al. Saturation decreases sharper, and hue changes of red and green toward yellow are larger than the corresponding cases of 1.85 deg stimuli in Sakurai et al. In the results of categorical color naming, “red” and “green” responses disappear quicker than “yellow” and “blue” responses in the periphery. Points of “undefined” responses increase with eccentricity. Vertical asymmetry of the increase of “undefined” response was more prominent than the horizontal asymmetry.

Categorical color naming results were estimated using modified Okajima et al.’s model that can derive “undefined” response in addition to basic categorical color names from the outputs of chromatic and achromatic processes. Good approximation was obtained in all positions by using the amplifying coefficients of chromatic response that decrease with eccentricity.

INTRODUCTION

The same color stimuli appear differently when presented in peripheral visual field. For example, a slightly yellowish vivid seen in the foveal vision looks pale orange when seen in peripheral vision. Such a change of color appearance in periphery has been investigated in various studies to reveal the change of color vision mechanism with retinal eccentricity from basic psychophysical point of view [1-5] as well as with eccentricity in the visual field from application point of view [6-9]. Results shown in these previous studies indicate that color vision deteriorates in periphery than in the central vision. Another factor to degrade color vision is the decrease of stimulus size. Even for the stimulus presented in the center of the visual field, i.e., seen in foveal vision, it appears desaturated in a small size [1, 10]. Some studies have shown that the decrease of saturation and the amount of hue shift with eccentricity are more eminent in a small size stimulus [1, 11, 12]. Therefore, this study aims to measure color appearance for small stimuli presented in various locations in the visual field using the two representative methods to measure color appearance, elementary color naming and categorical color naming. The former is called 'the opponent-colors type color evaluation' in this study, because the hue circle based on the opponent-colors theory is used. In addition to provide data, another aim of the study is to analyze the relation between two color naming results by examining whether the Okajima et al.'s model [13] can be applied to those data of small stimuli in periphery.

METHODS

In this study, eccentricity is defined in the stimulus location presented in the visual field. We employed the circular test stimulus with a diameter of 0.5 deg, and it was presented at 5, 10, and 20 deg for each of upper, lower, left and right directions as well as at 0 deg, total of 13 locations. Fifty-five color stimuli were prepared. They are grouped into reddish, dark yellow, greenish, bluish at about 20 cd/m², and bright yellow at about 60 cd/m². Surround was a gray of which luminance varied from 25 to 50 cd/m². Color appearance was evaluated using the opponent-colors type color evaluation (hue judgment using the hue circle and saturation judgment using the saturation evaluation bar shown in Figure 1), blackness and whiteness evaluation, and a categorical color naming. Three observers participated in the experiment.

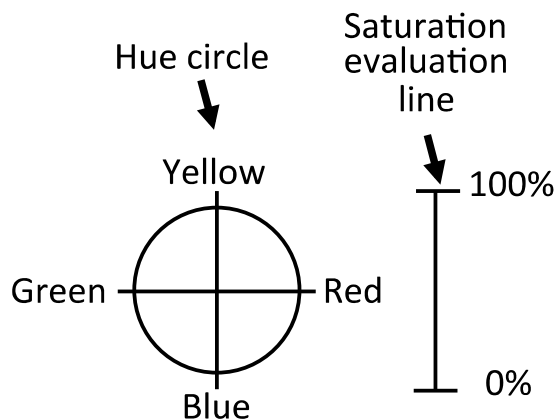


Figure 1. Figure employed in the opponent-colors-type color evaluation

RESULTS

Figure 2 indicates the results of saturation and hue judgments for the stimulus R1 in the opponent-colors type color evaluation for the observer KH. It is the most saturated red among reddish stimuli used in this study. Figure 2 (a) and (b) are the results of saturation judgement, and Figure 2 (c) and (d) are the results of hue judgement. Results along the horizontal and vertical directions are shown in Figure 2 (a) (c), and Figure 2 (c) (d), respectively. In the experiment, each observer evaluated 5 times for each stimulus at each location throughout the experiment. Broken symbols and lines denote the results of each measurement, and the solid symbols and lines indicate the average of them. As shown in Figure 2 (a) and (b), saturation curves show their peak at 0 deg and decrease with the eccentricity. Repeatability of evaluation is fairly well at 0 deg, while variability increases with eccentricity. Figure 2 (a) and (b) shows that asymmetry is larger in the vertical direction than in the horizontal direction. Figure 2 (c) and (d) show the results of hue judgement. R1 appears close to unique red at 0 deg and changes slightly yellowish as eccentricity increases.

In the categorical color naming, if the same color name was responded 3 times or more, the color name was employed as the categorical color response. If no color name qualified the criterion, it was assigned “undefined”. Response of “not seen” means no color response was obtained in 5 repetitions. Figure 3 shows the results of categorical color naming for observer KH at 0 deg and 20 deg in the upper direction. As shown in the figure, only the ‘yellow’ and ‘blue’ responses remained as chromatic color name, and many of the test stimuli result “undefined” or “not seen” at 20 deg upper.

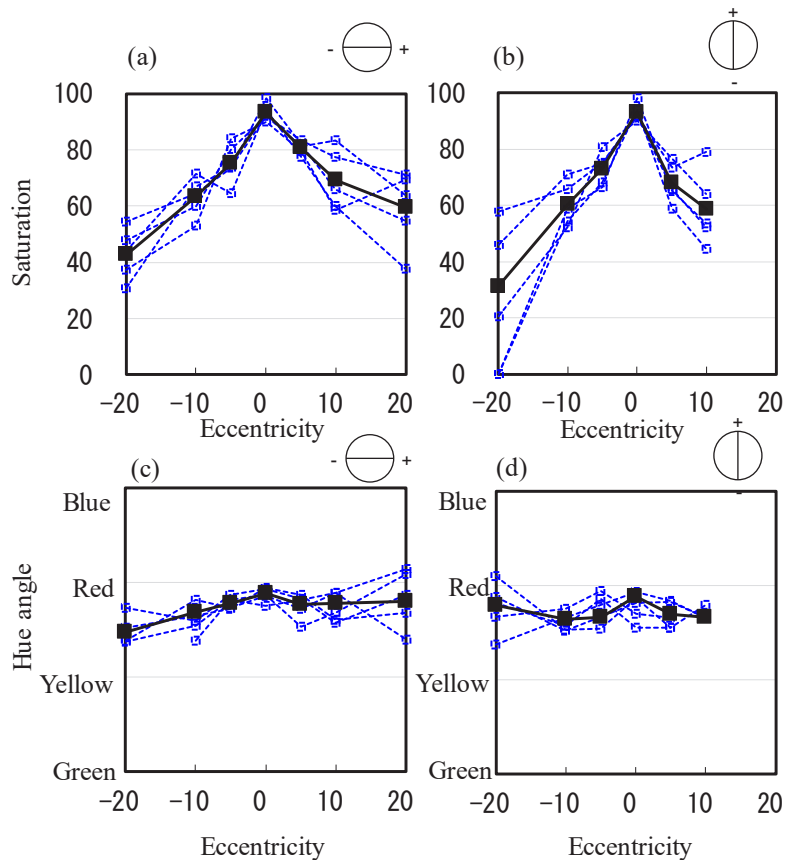


Figure 2 Results of saturation and hue judgments for R1 stimulus. Observer:KH.

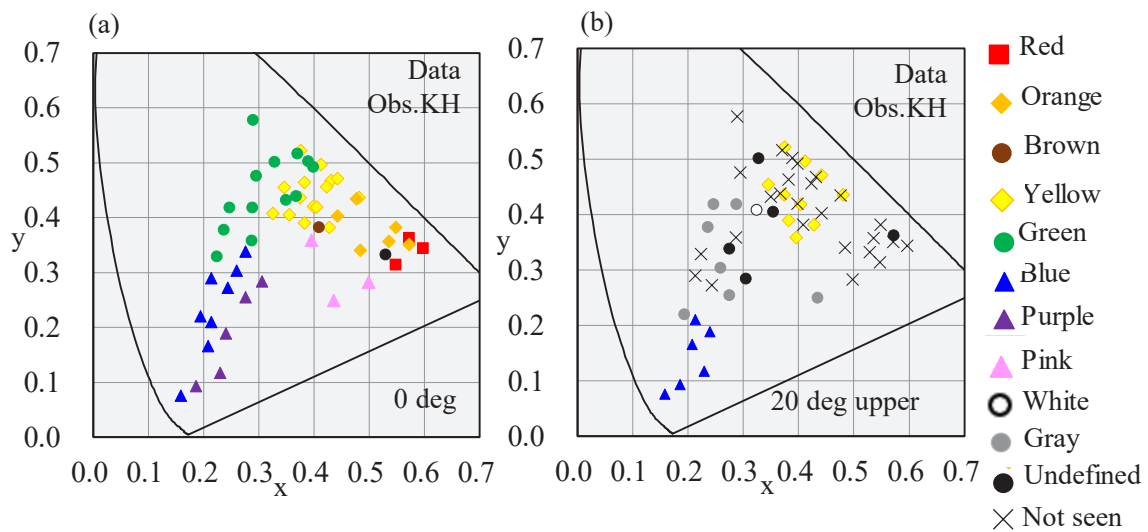


Figure 3 Results of categorical color responses observer KH. (a) and (b) are the results of 0 deg and 20 deg in the upper direction, respectively.

DISCUSSION

Okajima et al. [13] proposed a model for the relation between the results of elementary color naming and categorical color naming. It is redrawn in Figure 4. In their model, categorical responses of primary colors, such as red, yellow, green, blue, white, and black are converted to make the responses of secondary colors such as orange, pink, brown, purple, and gray, and the maximum response among all color responses determines the categorical color. The opponent-colors type color evaluation in this study is essentially the same as the elementary color naming, and the categorical color naming is the same as that employed in their study. Thus we tried to estimate the results of categorical color naming using the model modified to fit the data for small stimuli presented in various locations in the visual field.

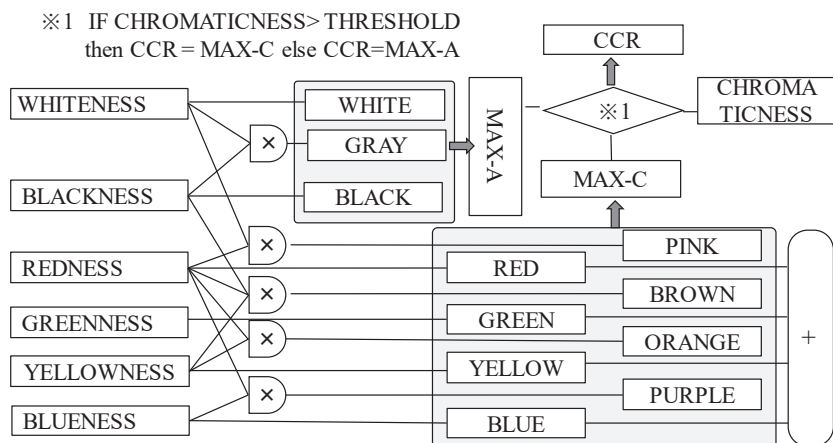


Figure 4 Okajima et al.'s model for color categorization redrawn from the Okajima et al. (2002).

The model was originally constructed for the fovea, and thus any stimulus is given some categorical color. However, as shown in Figure 3(b), categorical color name is not determined for many stimuli due to instability or inability in the naming task. Among five repetitions, same color

name appeared only twice, or sometimes response of “not seen” was obtained. In such cases, the final categorical color response is assigned “undefined” in this study, which is not derived by the original model. To derive the response of “undefined”, we made the model fitting 5 times for each location by searching the optimal combinations of amplitude coefficients for the secondary colors to determine categorical color response. When the same categorical color was derived 3 times or more, then that color name is employed as the observer’s color response, otherwise “undefined” was assigned as the final response. When the observer’s response was “not seen”, the estimation resulted “not seen” without any inputs to the primary color responses. Results for HK at 0 deg and 20 deg in the upper location are shown in Figure 5 (a) and (b), respectively. Estimation employed in this study considering the fluctuation of responses is so good at 0 deg that the percentage of correct estimation is 91%. In the case of 20 deg upper direction, it is 87.3%.

If the original version of the model was applied to the average results only, not taken the response fluctuation into consideration, the correct percent was 56.4%, much lower than that in this study.

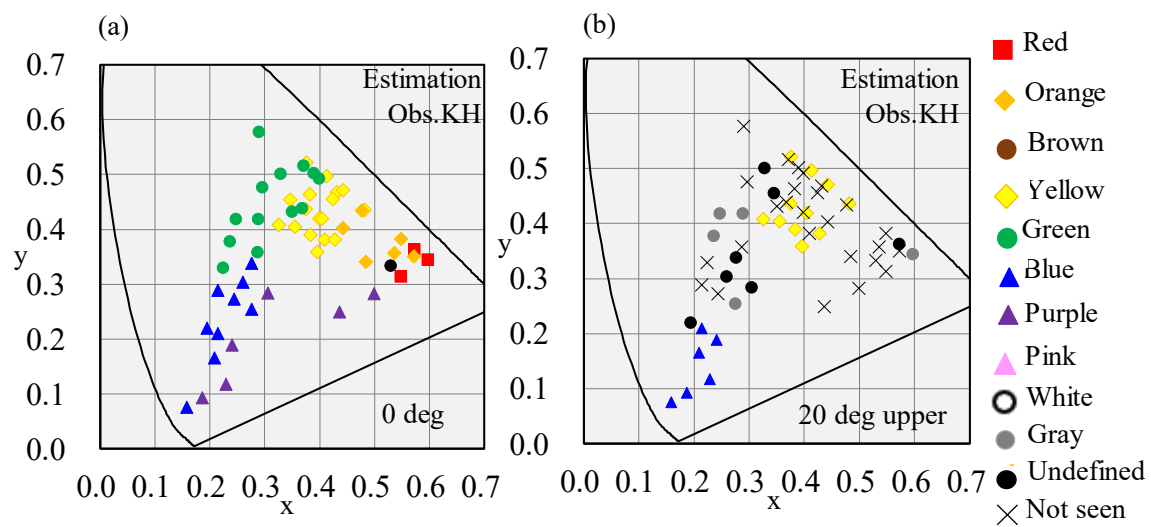


Figure 5 Estimation of categorical color response observer KH. (a) and (b) are the estimations of 0 deg and 20 deg in the upper direction, respectively.

CONCLUSION

Color appearance of small field stimulus (diameter of 0.5 deg) was investigated at the center of the visual field (0 deg) and 12 locations in near periphery using the opponent-colors type color evaluation and categorical color naming. Results at 0 deg are similar to those obtained in previous study while saturation decrease and hue shift with eccentricity are more drastic than the previous results of using the stimuli of about 2 deg diameter [7]. In the results of categorical color naming, “red” and “green” responses disappear quicker than “yellow” and “blue” responses in the periphery. Points of “undefined” and “not seen” responses increase with eccentricity. Vertical asymmetry of the increase of “undefined” response was more prominent than the horizontal asymmetry.

Categorical color response is derived from the results of opponent-colors type color evaluation using the modified version of Okajima et al.’s model. Taking into inability of color evaluation, i.e., “not seen”, as well as observer’s response fluctuation into consideration, responses of “not seen” and “undefined” can be derived by the model.

REFERENCES

1. Weitzman, D. O., & Kinney, J. A. S. (1969). Effect of stimulus size, duration and retinal location upon the appearance of color. *J. Opt. Soc. Am.* 59, 640-643.
2. Abramov, I., & Gordon, J. (1977). Color vision in the peripheral retina. I. Spectral sensitivity. *J. Opt. Soc. Am.* 67(2), 195-202.
3. Abramov, I., & Gordon, J. H Chan. (1992). Color appearance across the retina: effects of a white surround. *J. Opt. Soc. Am. A.* 9(2), 195-202.
4. Stabell, B., & Stabell, U. (1996). Peripheral colour vision: effects of rod intrusion at different eccentricities. *Vision Res.* 36(21),3407-3414.
5. Volbrecht, V., & Clark, C. L., & Nerger, J. L. & Randel, C. E. (2009). Chromatic perceptive field sizes measured at 10° eccentricity along the horizontal and vertical meridians. *J. Opt. Soc. Am. A.* 26(5), 1167-1177.
doi: 10.1364/josaa.26.001167
6. Ayama, M., & Sakurai, M. (2003). Changes in hue and saturation of chromatic lights presented in the peripheral visual field. *Color Res & Appl.* 28(6), 413-424.
doi: 10.1002/col.10194
7. Sakurai, M., & Ayama, M., & Kumagai, T. (2003). Color appearance in the entire visual field: color zone map based on unique hue component. *J. Opt. Soc. Am. A.* 20(11), 1997-2009.
doi: 10.1364/josaa.20.001997
8. McKeefry, D. J., & murray, I. J., & Parry, N. R. (2007). Perceived shifts in saturation and hue of chromatic stimuli in the near peripheral retina. *J. Opt. Soc. Am. A.* 24(10), 3168-3179.
doi:10.1364/josaa.24.003168
9. CIE TECHNICAL REPORT. (2014). *Colour appearance in peripheral vision*, CIE211.
10. Yano, T., & Yamaguchi, T., & Kubo, M. (1989). Color perception for small fields. *Kogaku.* 18(8), 425-433.
11. Nagy, A. L., & Doyal, J. A. (1993). Red-green color discrimination as a function of stimulus field size in peripheral vision. *J. Opt. Soc. Am. A.* 10(6), 1147-1156.
12. Takamatsu, M., & Nakashima, Y., & Kamiya, K. (2001). Color appearance in the small visual angles using color-naming method. *I. T. E.* 55(10), 1298-1300.
13. Okajima, K., & Robertson, A. R., & Fielder, G. H. (2002). A quantitative network model for color categorization. *Color Res. & Appl.* 27(4), 225-232.
doi:10.1002/col.10060
14. Fujisawa, K., & Ayama, M., & Komaba, A., & Hagiwara, K. (2004). Color appearance of the small field stimuli presented in periphery. *Technical Digest of 2004 ICO International Conference Optics and Photonics in Technology Frontier*, 259-260.

Influence of subject attribute differences on texture evaluation of beige fabrics - Comparison between subjects' knowledge of clothes and differences in their background -

Takumi Nakajima¹, Tomoharu Ishikawa^{1*}, Junki Tsunetou¹, Yoshiko Yanagida²,
Mutsumi Yanaka², Minoru Mitsui³, Kazuya Sasaki⁴, and Miyoshi Ayama¹

¹*Graduate School of Engineering, Utsunomiya University, 7-1-2 Yoto, Utsunomiya, Japan*

²*Faculty of Fashion Science, Bunka Gakuen University, 3-22-1 Yoyogi Shibuya, Japan*

³*Institute of Technologists, 333 Maeya, Gyoda, Japan*

⁴*Faculty of Education, Utsunomiya University, 350 Mine, Utsunomiya, Japan*

*Corresponding author: Tomoharu Ishikawa, ishikawa@is.utsunomiya-u.ac.jp

Keywords: Beige fabrics, Texture evaluation, Subject attributes, Clothes' knowledge, Observer's background

ABSTRACT

This study aimed to examine whether observers' evaluation of the texture of beige textiles is influenced by their existing knowledge of clothes and their background. The texture of 39 beige fabrics was evaluated using only tactile sensation (TE), while another experiment used both visual sensation and tactile sensation (VTE). Based on the differences in the results of the evaluation of fabric texture by the Chinese clothing student (CC) and Japanese clothing student (CJ) groups, the influence of each observer's background is discussed. Similarly, the influence of fiber knowledge is discussed for the CJ and Japanese engineering student (EJ) groups. Each fabric was mapped to a factor space composed of these three axes based on factor scores, and is discussed from the perspective of observers' knowledge of clothes and their different backgrounds. It was found that the difference in material and structure of textiles can be recognized more clearly in the order of the CJ, EJ, and CC groups. Therefore, the presence or absence of knowledge on clothes and background differences influenced observers and led to differences in their evaluation of texture.

INTRODUCTION

In recent years, with the spread of the Internet, clothes and fabrics are more frequently purchased through online shopping than by going to stores. However, the impression of the image seen on the Internet and what actually arrives may differ. Therefore, it is assumed that recognition differs between images and the real thing, because people do not fully understand the texture of clothes and fabrics from the presented images. Thus far, many reports focus on fabric texture recognition. In a past study, Nakajima et al prepared three kinds of silk fabrics with different thicknesses, and clarified the change of the texture due to the difference in the thickness of the yarn by evaluating sensitivity and measuring the texture value. ^[1] Yashima et al conducted a visual and tactile evaluation test on the glossiness of fabrics, and examined whether observers with no practical experience or designers could judge fabrics with higher accuracy. ^[2] Furthermore, paying attention to the differences in the evaluations of texture between observers with varying clothing knowledge, Tsuneto et al conducted a fabric texture evaluation experiment to examine the differences between observers and sensory modalities in the fabric texture space. ^[3] In addition, Tsuneto et al conducted a fabric texture evaluation experiment of Japanese and Chinese clothing students, and clarified the

differences in the evaluations of fabric texture by observers with different backgrounds. [4] As mentioned, the effects of the presence of knowledge and differences in the background environment on the recognition of fabric texture have been studied in comparative analyses of observer groups. However, the relationship between the presence and absence of knowledge and influence of background differences on the recognition of fabric texture by comparing three observer groups remains unclear. Therefore, the purposes of this research are to compare the experimental results of tactile sensation and visual tactile sensation of Japanese and Chinese clothing design students and Japanese engineering students, and clarify the influence on the evaluation of the fabric texture based on their clothing knowledge and background environment.

EXPERIMENT

For fabric samples, we used 39 squares of fabric measuring 20 cm by 20 cm stored for at least 24 hours at a temperature of 20°C with 65% humidity. These were chosen from combinations of fibers (seven types: cotton, hemp, fur, silk, nylon, polyester, cupra), knit/weave (five types: plain weave, oblique weave, satin weave, single, double) and thread thickness (3 types: fine, medium, thick) based on the conditions of completeness, purchase availability, and uniformity of color (beige). We carried out two types of texture evaluation experiments, namely a tactile evaluation (TE) involving only the touching of fabrics and a visual tactile evaluation (VTE) involving the touching and viewing of fabrics (Figure 1). The observers were divided into 3 groups, each with 20 students: Chinese (CC group) and Japanese (CJ group) students majoring in clothing design and Japanese students majoring in engineering (EJ group). The relationship between each observer can clarify the influence on the evaluation of texture based on differences in knowledge and the background environment by using Japanese clothing as a standard (Figure 2). The evaluation was measured on a five-point scale. The words used in the evaluation were those used in previous research by Ishikawa (Table 1).

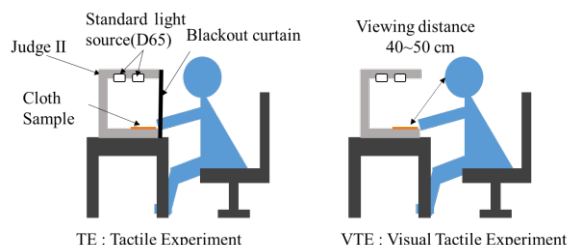


Figure 1. Outline of experiment

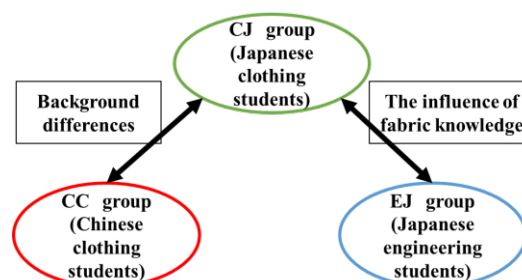


Figure 2. Observer relationship

Table 1: List of evaluation words

Experiment	Evaluation Words
TE (13 words)	Thin, Thick, Flat, Rustic, Crisp, Soft, Dry, Wet, Stretchy, Warm, Cool, Like, Comfortable
VTE (14 words)	Thin, Thick, Flat, Rustic, Crisp, Soft, Dry, Wet, Stretchy, Warm, Cool, Like, Comfortable, Glossy

ANALYSIS AND RESULTS

A factor analysis was performed of the evaluation results for the TE and VTE for each of the 20 students in the CJ, CC, and EJ groups. The factor analysis was performed using the main factor method, and varimax rotation was conducted after factor extraction. The number of factors was conditioned to have an eigenvalue of 1 or more. The TE became a three-factor structure comprising the factors wet preference, cold temperature, and flexibility. VTE became a three-factor structure comprising the factors cold temperature, flexibility, and surface. Here, in a space composed of two factors, the factor score of each cloth was assigned a symbol, and the range where the symbol is

connected for each fiber is shown in the figure. In addition, the center of gravity of the factor score in the range is indicated with a circle. This is called the cloth texture evaluation space. Figure 3 shows the fabric texture evaluation space of CC, which is composed of the wet preference and cold temperature factors of the TE (Figure 3). Figure 4 shows the fabric texture evaluation space of CJ, which is composed of the wet preference and cold temperature factors of the TE. The same graph was created in the same way for the VTE (Figure 4).

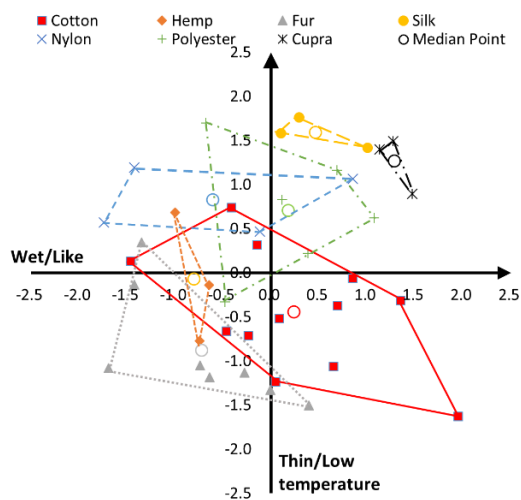


Figure 3. Wet/Like, Thin/Low temperature (CC)

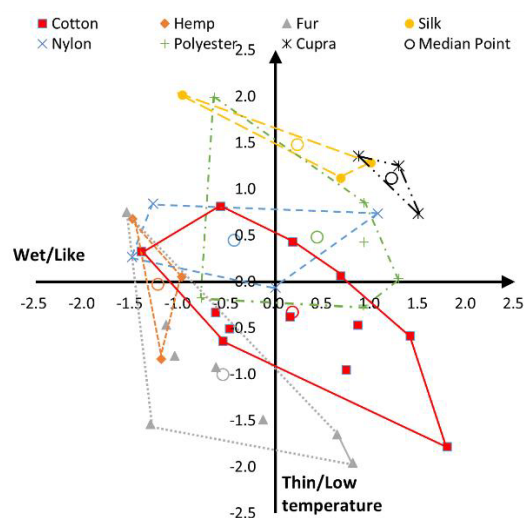


Figure 4. Wet/Like, Thin/Low temperature (CJ)

In the fabric texture space shown in Figures 3 and 4, the differences between the center of gravity position and spread range (area) in each fiber can be seen. In other words, comparing the center of gravity position and area (area) in each fiber for the three observer groups enabled examining the differences in their evaluations. Here, comparing the evaluation results of CJ and EJ entailed studying the differences in the evaluation based on knowledge of the cloth. Comparing the evaluation results of CC and CJ enabled studying the evaluations based on their background environment. In addition, for differences in the center of gravity position, that of CJ was expressed as a reference (origin (0,0)) to the center of gravity position of EJ and CC in a vector. As a result, the difference of the vector for EJ and CC, i.e., the differences in cloth knowledge and influence of background environment were compared. Here, to compare the three observer groups for the entire fabric, we calculated the sum of vectors in each fiber. Figure 5 shows the vector total of CC and EJ against CJ in the wet preference-cold temperature factor space (Figure 5). The evaluation words shown on each axis indicate the words associated with the factors. Figure 5 shows the effect of the knowledge of cloth (EJ against CJ) and evaluation of the background environment (CC against CJ) as a vector. Specifically, compared to CJ, CC in the TE demonstrated a tendency to prefer the fabric that feels thin and cold. Compared to CJ, EJ preferred the cloth that feels slightly thick and warm. Similarly, in the wet preference-flexible factor space, in the TE, CC highly evaluated soft and stretchy fabric compared to CJ. Compared to CJ, EJ evaluated their preference for crisp cloth as slightly high. In addition, in the cold temperature-flexible factor space, compared to CJ, CC evaluated the fabric with tension as a thin, cool cloth. Compared to CJ, EJ evaluated the fabric with the slight tension as a thick, warm cloth. These results are attributed to the fact that differences in cloth knowledge and background environments influenced the evaluation.

On the other hand, we compared the spread range (area) of each fiber of the fabric for the three observer groups, examining their ability to determine the fabric fibers. The size of this area was evaluated by distinguishing the thickness of the yarn in the fabric and difference in the weave. In other words, a large value indicated high judgment ability regarding the cloth. Therefore, from the total value of the spread range (area) of each fiber of the fabric in each space, the ability of the three observer groups to judge the entire fabric was compared (Figure 5). Figure 6 shows that the total area in each fabric texture space is in the order CJ>EJ>CC. Here, the ability to judge the cloth is considered high in the order CJ>EJ>CC. In addition, the area of each fabric fiber was t-tested. As a result, significant differences ($p=0.011$ and $p=0.044$) were observed for CJ and CC in the wet preference-flexible factor and cold temperature-flexible factor spaces.

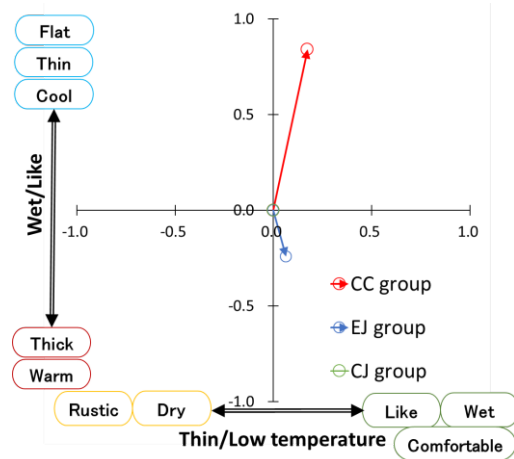


Figure 5. Wet/Like, Thin/Low temperature

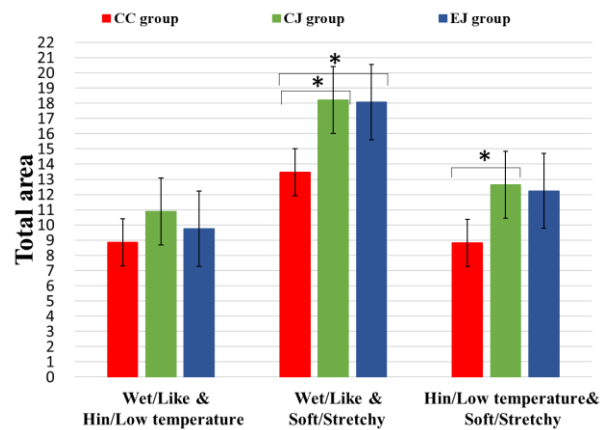


Figure 6. Total area of evaluation space

Figures 7 and 8 compare the vector sum of the entire fabric of the cold-temperature-soft preference factor space in the VTE, and spread range (area) of each fabric fiber in each space. Figure 7 shows that in the VTE, CC highly evaluated the thick, warm fabric as soft, stretchable, and preferable compared to the CJ group. The results were similar for EJ, although this group evaluated the fabric as thicker and warmer than did CC. Similarly, for the cold temperature-surface factor space, in the VTE, CC evaluated the fabric as feeling thicker and warmer, while CJ judged it as flat, glossy, and wet. EJ demonstrated the same tendency. In particular, CC more highly evaluated the fabric as flat and glossy than did EJ. In the flexible preference-surface factor space, in the VTE, CC evaluated the flat, glossy, and wet fabric as being soft, stretchable, and preferable more than did CJ. EJ demonstrated the same tendency. In addition, Figure 8 shows that the total area in each fabric texture space is in the order CJ>EJ>CC in any space. This means that the ability to judge the fabric is higher in the order CJ>EJ>CC. In addition, the area of each fabric fiber was t-tested. As a result, significant differences ($p = 0.026$ and $p = 0.021$) emerged at a significance level of 5% in the areas of CJ and CC and CC and EJ in the cold temperature-soft preference factor space. In addition, there was a significant difference at a significance level of 1% in the area of CJ and CC in the flexible preference-surface factor space ($p = 0.008$). In the area of CC and EJ, there was a significant difference at a significance level of 5% ($p = 0.019$).

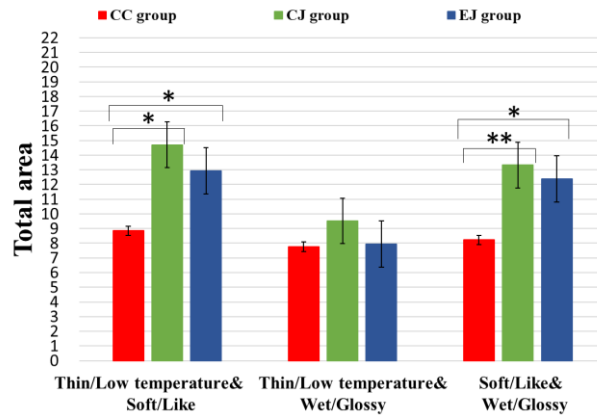
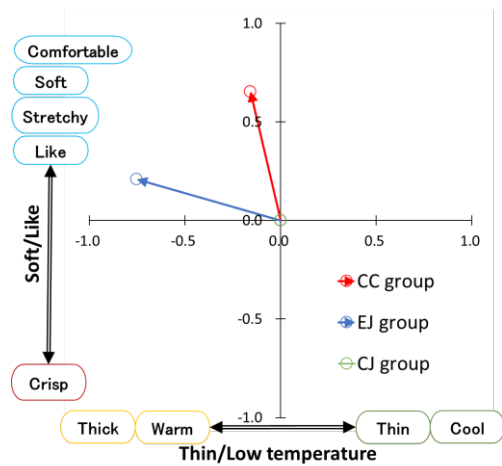


Figure 7. Soft/Like, Thin/Low temperature Figure 8. Total area of evaluation space

CONCLUSION

In this study, two types of experiments using tactile sensation and visual tactile sensation were conducted to clarify the effects of different clothing knowledge and background environments on the evaluation of fabric texture. We conducted experiments with Japanese clothing students, Chinese clothing students, and Japanese engineering students, and compared the evaluation trends among the three observer groups. A factor analysis of the results was performed, and the influence of different clothing knowledge and background environments on the evaluation of the fabric texture was examined based on the center of gravity and spread range (area) of each fabric fiber in the factor space. The results clarified that the evaluation of fabric texture in the tactile sensation experiment differed because of different knowledge and background environments. On the other hand, the evaluation of fabric texture in the visual tactile experiments revealed similar effects, although there were differences in the growth environment and knowledge. Moreover, in any evaluation space, it was clear that the total value of the evaluation spread range (area) for each fabric fiber is in the order of CJ, EJ, and CC. Furthermore, in some fabric texture evaluation spaces, it was shown that the total spread range (area) of Japanese clothing students was significantly larger than for Chinese clothing students. In other words, Japanese clothing students are more capable of accurately discriminating fabric fibers, weaving/knitting, and yarn thickness than Japanese engineering students. Furthermore, this capability was significantly lower for Chinese clothing students.

ACKNOWLEDGEMENTS

This research was supported by the Strategic Information and Communications R&D Promotion Programme (SCOPE) [152303002], Scientific Research Grants and Fundamental Research (B) [Project Number 18H03317] [Project Number 18H03458], and Centre of Excellence at Utsunomiya University (UU-COE) Research Funding went. Described here, expresses my deep gratitude.

REFERENCES

1. Kenichi, N., Haruo, K., & Mikihiro, M. (2011). Analysis of a sensory test with thin and thick fabric and a comparison of the KES hand value. *Silkworm Insect Biotech*, 80(1), 53-58 (in Japanese).
2. Kenya, Y., Moe, Y., Masayuki, T., Kyoungok, K., & Keiko, M. (2017). Development of textile proposal system (TPS) -Verification of validity for luster evaluation in textile retrieval system -. *The 12th Japan Society of Kansei Engineering Spring Competition*, 1D-1 (in Japanese).
3. Junki, T., Tomoharu, I., Mutsumi, Y., Yoshiko, Y., Kazuya, S., & Miyoshi, A. (2018). Texture Evaluation of Various Cloth Attributes - Influence of the Differences between the Subjective Knowledge and Sensory Modality -. *Journal of Textile Engineering*, 64(5), 117-126 (in Japanese).
4. Junki, T., Tomoharu, I., Mutsumi, Y., Yoshiko, Y., Kazuya, S., & Miyoshi, A. (2018). Difference of fabric texture evaluation by Japanese and Chinese. *KANSEI robotics workshop*, 13(2), 3-7 (in Japanese).
5. Tomoharu, I., Shunsuke, N., Kazuya, S., Keiko, M., & Miyoshi, A. (2015). Identification of Common Words for the Evaluation of Clothes' Appearance and Tactile Sensation in Online Shopping -An Indicator for Producing Images that Express Clothes' Textures-. *International Journal of Affective Engineering Special Issue on KEER*, 14(3), 143-149.
6. Tomoharu, I., Junki, T., Mutsumi, Y., Yoshiko, Y., Kazuya, S., & Miyoshi, A. (2017). Influence of Knowledge about Clothes and Sensation Modalities on Texture Evaluation of Beige Textile. *Association Internationale de la Couleur*, OS09-6.

EFFECT OF METRIC CHROMA ON THE TOTAL COLOR IMPRESSION OF IMAGES

T. Fujiwara^{1*}, T. Matsumoto², H. Kunugi², T. Ishikawa¹, M. Ayama^{1,3}

¹ Graduate School of Engineering, Utsunomiya University, Utsunomiya, Japan.

² Faculty of Engineering, Utsunomiya University, Utsunomiya, Japan.

³ Center for Optical Research & Education, Utsunomiya University, Utsunomiya, Japan.

* Tomoya Fujiwara, +81 28 689 6264, mt186727@cc.ustunomiya-ac.jp

Keywords: colored image; KANSEI evaluation; chroma; categorical color; CIELAB

ABSTRACT

Color was introduced in the movie in early in the 20th century, spread to color TV broadcast and color photography by 1970s, and then expanded to computer display with a rapid spread of PC. In the time of development, people in related fields eagerly elaborated to devise new technique that made beautiful color image possible. Nowadays, HDR wide color gamut display is available and even a small display of mobile phone has satisfiable color quality. Generally speaking, most people prefer color image to monochromatic image. However, why people seek or prefer color image has not been investigated systematically. Nowadays, real time color processing to enhance or reduce colors becomes possible, and any imaging device such as camera, display, and TV has its own color processing engine to render colors. In this time and age, psychological effect of color should be reconsidered, and systematic approach to reveal the effect of color is needed. Psychological effect here means how and to what degree color of image contributes to various subjective impressions, such as preference, powerfulness, comfortableness or beautifulness. These are called KANSEI evaluation recently. Before we start KANSEI evaluation experiment using images of different chromatic strength, it is appropriate to obtain a threshold of chromatic strength as the basis. We take average of metric chroma, C_{ab}^* , as an index of chromatic strength of images. Therefore, objective of the study is to reveal the threshold metric chroma for various color images that gives observers "chromatic impression" as a whole. Having a final goal to reveal psychological effect of saturation increase in digital images, BCACI, Border Chroma between Achromatic and Chromatic Impression, was investigated for normal and shuffled-mosaic natural images as the first approach. In the color naming experiment, observers were asked to respond total color impression by choosing one color name among 14 color names including basic categorical colors. BCACI was obtained by the effective metric chroma C_{ab}^* where 50% of responses were achromatic color names. Results of normal images indicate that when the metric chroma C_{ab}^* exceeds 7, observer's perception of the whole image turns from achromatic to chromatic, except "pink" and "purple" images. BCACI of shuffled-mosaic images is significantly lower than that of normal images, suggesting the effect of the meaning of contents on color impression. In mosaicked images, objects are dispersed and meaningless, although parts of contents are still visible. This lack of meaning and closeness to uniform color image might be the cause of lower BCACIs in mosaicked images. In the next step, relation between various KANSEI evaluation words and metric chroma is to be investigated. The effects of change of metric chroma on KANSEI evaluation of color images using SD (semantic differential) method for nine different image contents, used for color naming experiment.

INTRODUCTION

Border Chroma between Achromatic and Chromatic Impression

Generally, most people prefer color image to monochromatic image. However, why people seek or prefer color image has not been investigated systematically. We have investigated threshold chroma at which observers begin to perceive the image chromatic in our previous studies as the first step to reveal psychological effect of color image [1, 2]. Nine different images representing the following color names, “red”, “green”, “orange”, “yellow”, “pink”, “blue”, “purple”, “red and green”, and, “yellow and blue”, were used as the original images, and a series of images from zero to low C_{ab}^* (approximate 20% of the original one) were made for each of them. Observer was asked to choose one color name among 14 color names such as “red”, “red and green”, or “gray” etc. Frequency of achromatic color response, e.g. “gray” or “black”, decreased as the average C_{ab}^* of image increased, and the C_{ab}^* that corresponds to 50 % appearance of achromatic color response was taken as the threshold chroma. We called it BCACI, Border Chroma between Achromatic and Chromatic Impression. Our results showed that BCACI is around 7 for most of the images except “pink” and “purple”. That is when the metric chroma C_{ab}^* of the image exceeds around 7, observer’s perception of the whole image turns from achromatic to chromatic. In the case of mosaic images shuffled by every 10 x 10 pixel squares, observer was sufficed lower chroma than normal image to perceive color image [2].

KANSEI Evaluation

KANSEI is described as ‘mental sense of subjectivity’ and measured by having observers answer the quantitative degree of impressions such as sharpness, naturalness, or preference usually using bipolar adjective pairs. Only a few studies have been done on the effect of color image property on the KANSEI evaluation of image. Fedorovskaya et al. reported that preference rating increases with gamut volume and luminance for natural and/or human images, indicating that ordinary observers prefer brighter and more saturated images generally [3]. On the other hand, Sagawa showed that visual comfort tends to decrease with saturation for interior scene images [4]. These discrepancies have not been yet investigated. Furthermore, dependency on the kind of KANSEI property, as well as dependency on the contents of images are important issues to be solved, but not clarified yet.

Aim of the study

The aim of this study is to investigate the effect of metric chroma on various KANSEI evaluations of images. Our results will provide the least metric chroma required to give observers satisfiable impression for various KANSEI properties.

EXPERIMENT

Test Stimuli

Nine different color images representing the following color names, “red”, “green”, “orange”, “yellow”, “pink”, “blue”, “purple”, “red and green”, and, “yellow and blue”, based on categorical color data analysis [5] were used as the original images. Those of “blue”, “yellow”, “orange”, and “purple”, are shown in Figure 1. For each of the original test images, various chroma images were made as test stimuli. Each pixel of original image was multiplied by scaling factor k based on metric chroma C_{ab}^* in the CIELAB space, while lightness L^* is kept constant. We prepared 7 levels of scaling factor k (0, 0.08, 0.16, 0.32, 0.63, 1.0, and 1.26). Scaling factor $k=1.0$ means original image. Test stimuli of “red” image are shown in Figure 2.



Figure 1. Original image. For example blue, yellow, orange and purple image.

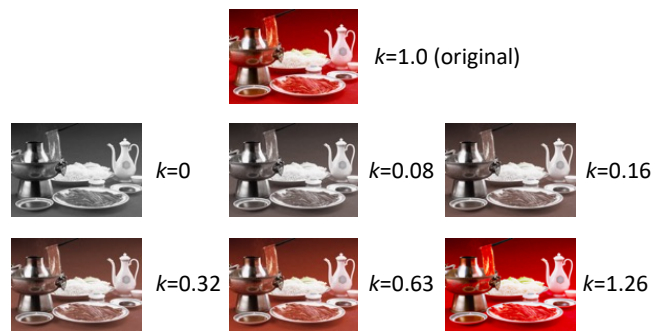


Figure 2. Test stimuli of red image

Viewing Condition

Test stimulus was presented on the display (EIZO ColorEdge CG277) with the visual distance of 120cm. Display and observer's seat were set up in a booth covered by black curtain.

Procedure

Semantic differential method (SD method) was used in the KANSEI evaluation. Table1 indicates nine adjective pairs, and we employed the seven-point scale (-3 to 3) used in the experiment. These adjective words were selected from previous studies [6-8]. An adjective pair is presented at the bottom of the display.

Figure 3 shows the flow of experiment. An observer took dark adaptation for five minutes at the beginning of each session. He/she was asked to evaluate each test stimuli for each adjective pair by marking position corresponding to observer's impression or feeling of the test stimulus on a seven-point scale between the bipolar adjective. Test stimulus was presented continuously until the observer made the response. Between the test stimulus presentation, uniform gray image (R, G, B = 38) was presented about 3 sec. Total of 63 images (7 levels of k for 9 test images) were used as test stimuli. Test stimulus was presented continuously until the observer made the response. Uniform gray image (R, G, B = 38) was presented about 3 sec between trials to avoid the effect of chromatic after image of the preceding test stimulus. One test stimulus was presented 2 times throughout the experiment. Test stimuli and adjective pairs were presented in a random order.

Observers

Four subjects, 2 males and 2 females in their twenties with normal color vision examined by Ishihara Chart, participated the experiment.

Table 1. Adjective pairs used in KANSEI evaluation

Negative	Positive	Negative	Positive
Dark	Bright	Dislike	Like
Dull	Vivid	Mundane	Impressive
Weak Contrast	Strong Contrast	Unnatural	Natural
Ugly	Beautiful	Flat	Stereoscopic
Vague	Sharp		

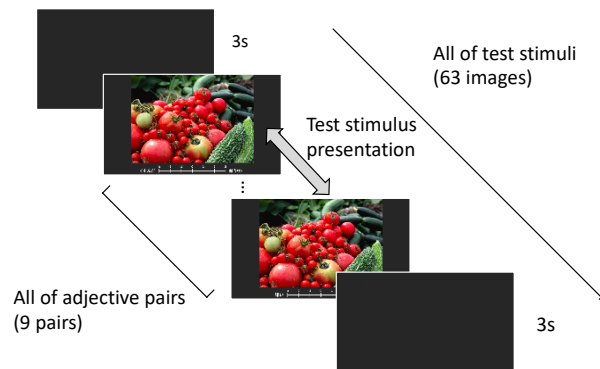


Figure 3. Experimental procedure

RESULTS

Figure 4 shows the results of “Vivid-Dull” and “Natural-Unnatural” for all images. Horizontal axis is the scaling factor k . Colored symbols and lines denote the average scores of 4 observers for each image, whereas the black circle and solid lines denote the grand average of all images. Both vividness and naturalness increase with the increase of metric chroma, consistent with the previous study [3]. Not only for them, but also for all other adjective pairs and color images, rating score increases with the scaling factor k , i.e., with metric chroma. However, in some cases, slight decrease when the k is over 1.0 was observed such as seen for “blue”, “yellow-blue”, “red-green”, and “orange” in “Natural-Unnatural” evaluation.

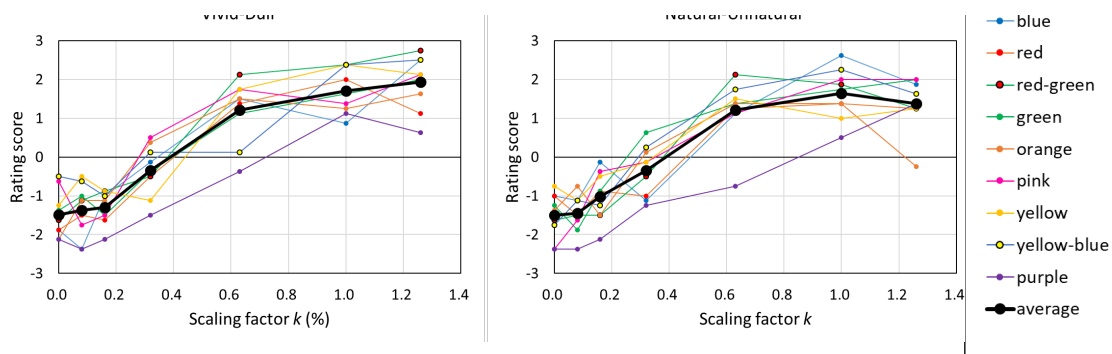


Figure 4. The results of “Vivid-Dull” and “Natural-Unnatural”.

All results in this study show negative value when the scaling factor k is zero, i.e., images are achromatic. Rating score increases with k , and changes from negative to positive. Zero crossing value is derived for all test images. When we used original image, we calculated L^* , a^* , b^* , and C_{ab}^* using a white point ($R, G, B = 255$) as a reference white. However, colorimetric values depend on individual display. So, we measured chromaticity and luminance of whole image using 2D colorimeter (CA-2500, Konica Minolta) for all original image and a uniform white image. Then average value of L^* , a^* , b^* , and C_{ab}^* was recalculated for each of the test stimuli Figure 5 shows average metric chroma C_{ab}^* of original image.

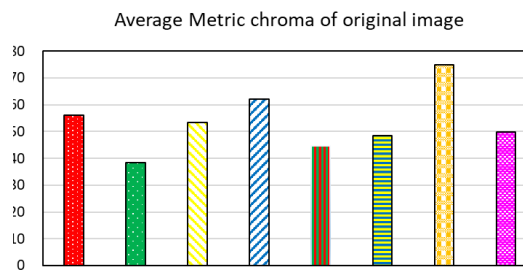


Figure 5. Average metric chroma of original image.

Scaling factor k that corresponds to zero crossing was derived by a linear interpolation between the adjacent scaling factors that gave negative and positive scores for each of the test images. Then the metric chroma corresponding to zero crossing was calculated by multiplying the k to the average C_{ab}^* of original image. Results in the adjective pairs of “Vivid-Dull” and “Natural-Unnatural” are indicated in Figure 6(a) and (b), respectively. As shown in Figure 6(a), the metric chroma C_{ab}^* for zero crossing are in the range between 14 to 25 in the result of “Vivid-Dull”. Variability is not so large compared with the results of other adjective pairs. This indicates that the vividness of images changes from negative to positive when the average metric chroma is around 20 regardless of the metric chroma of original image. On the other hand, results for “Natural-Unnatural”, variability expands from 10 to 30 as shown in Figure 6(b). Metric chroma of zero crossing is high for “red”, “blue”, “orange”, and “purple”, while it is very low in “green”. This tendency is similar to that in Figure 5, although the order is not exactly the same.

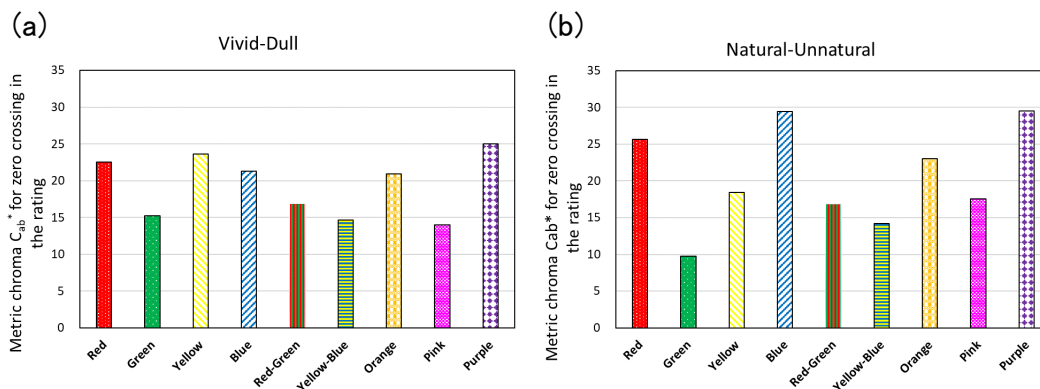


Figure 6. Zero crossing value in 2 adjective pairs, (a) “Vivid-Dull” and (b) “Natural-Unnatural”.

We calculated correlation between average metric chroma of original image (Figure 5) and the zero crossing values (Figure 6). Correlations for “Vivid-Dull” and “Natural-Unnatural” are indicated in Figure 7(a) and (b), respectively. As shown in the figures, no correlation is observed in “Vivid-Dull”, while strong positive correlation ($r=0.94$) is found in “Natural-Unnatural” if the “purple” (the most left-hand point) and “orange” (the most right-hand point) are excluded. Results of “Stereoscopic-Flat” shows similar tendency to that of “Natural-Unnatural” ($r=0.86$ without orange and purple), but no systematic tendency was observed in the results of other adjective pairs.

In our previous study, the “purple” image showed significantly smaller BCACI than other images for normal image condition, whereas its BCACI in shuffled mosaic condition was in the

variability range of all images [2]. In this study, “purple” showed the largest value for zero crossing metric chroma for most of the adjective pairs. Particular tendency of “purple” image might be due to the lack of sharp edge and certain size of uniform color area. The image of lavender field without any clear objects appears roughly a uniform color image, and impression of image does not change so much with the increase of average metric chroma. Existence of objects with sharp edge might

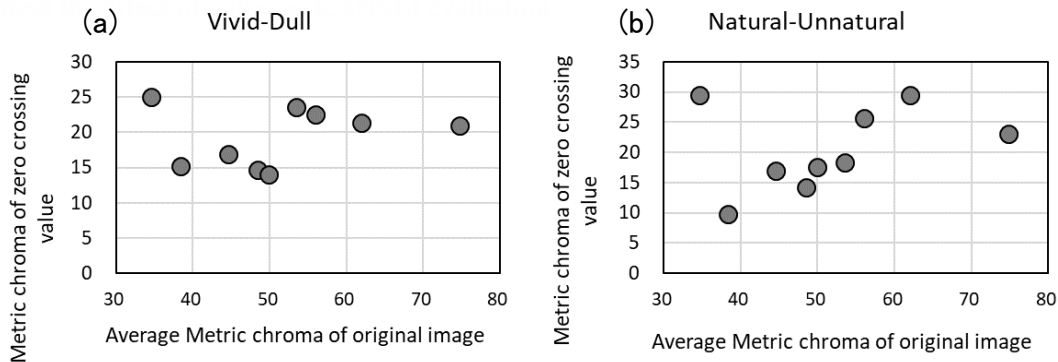


Figure 7. Correlation between zero crossing value and average metric chroma of original image.

CONCLUSION

In this research, we performed KANSEI evaluation experiment using various chroma images. Results showed that the average metric chroma where the rating score of impression changes from negative to positive are in the same range for “Vivid-Dull” evaluation. Results of the adjective pairs of “Natural-Unnatural” and “Stereoscopic-Flat” showed a correlation between zero crossing value and average metric chroma of original image if the “purple” and “orange” images were excluded. Color effect on KANSEI evaluation might relate to characteristic of image pattern that requires further investigation.

REFERENCES

1. Fujiwara, T., Nakada, S., Ishikawa, T., Ayama, M. (2018). Chromatic threshold for total color-image impression. *Proceedings of the 4th Asia Color Association Conference*, 355-360.
2. Fujiwara, T., Nakada, S., Ishikawa, T., Ayama, M. (2019). Threshold metric chroma of images for chromatic perception. *Proceedings of the 29th CIE SESSION*, 896-899.
3. Fedorovskaya, A.E. et al. (1997). Chroma variations and perceived quality of color images of natural scenes. *Col. Res. Appl.*, 22, 96-110.
4. Sagawa, K. (1999). Visual comfort to colored images evaluated by saturation distribution. *Col. Res. Appl.*, 24, 313-321.
5. Kumakura, A., Hamano, T., Ishikawa, T., Ayama, M. (2016). Color classification of images using categorical color database. *SID Symposium Digest of Technical Papers*, 47, 1246-1249.
6. Ayama, M., Fuseda, T., Hamano, T., Ishikawa, T. (2016). KANSEI evaluation of color images presented in color gamuts with different blue primaries. *JSID*. Vol.24 No.2, 74-84.
7. Kageyama, S., Inuzuka, Y., Ishikawa, T., Ayama, M. (2019). Kansei evaluation of the red object images using different red primaries. *Proceedings of the 29th CIE SESSION*, 941-946.
8. Ishikawa, T., Guan, Y., Chen, C. Y., Oguro, H., Kasuga, M., Ayama, M. (2012). Effect of tone curve and size on kansei evaluation of high dynamic range images – Comparison of Japanese and Chinese observers. *Kansei Engineering International Journal*. Vol.11 No.2, 67-79.

HUE CIRCLE PERCEPTION OF CONGENITAL RED-GREEN COLOR VISION DEFICIENCIES —EXPERIMENTAL DATA AND ESTIMATION USING COLORIMETRIC VALUES—

Minoru Ohkoba¹, Kota Kanari¹, Hiroto Mikami¹, Tomoharu Ishikawa¹, Shoko Hira²,
Sakuichi Ohtsuka², Miyoshi Ayama¹

¹*Graduate School of Engineering, Utsunomiya University, Japan.*

²*Graduate School of Science and Engineering, Kagoshima University, Japan.*

*Corresponding author: Minoru Ohkoba, e-mail: dt187102@cc.utsunomiya-u.ac.jp

Keywords: Congenital color deficiency, Hue circle, Difference ranking, MDS

ABSTRACT

Color vision of congenital color-vision deficiency (CVD) is often simply explained by the loss or spectral sensitivity shift of L or M cones that results the lack or degrade of red-green opponent process. However, a number of studies have shown that their color naming results are not so simple that they can name reddish colors as “red” and greenish colors as “green”. To investigate internal color representation of CVD observers (CVDs), Shepard and Cooper (1992) indicated the MDS representations of nine colors from red to purple using the similarity judgement by color cards and color names. Results based on color names became circular configuration similar to hue circle of the CIELAB, whereas results based on color cards showed distorted configuration bending at turquoise and yellow. We consider whether the latter test, similarity test using color cards, is employed to indicate the degree of color deficiency of individual CVD observers. In the experiment, 20 colors, high and medium chroma for each of 10 basic hues of Munsell color system, were chosen, and all combinations of 10 hues, i.e., 45 paired cards were prepared for each of high and medium chroma groups. Observers were asked to scale the psychological difference between 2 colors in the pair. Nine protan, 8 deutan, and 8 normal color vision observers (NCVs) participated the experiment using high chroma colors, while 8 protan, 5 deutan, and 7 NCV observers participated the experiment using medium chroma colors. Difference scaling using only the color names was conducted, although only the results of color cards are shown in this study. Part of the results of color names is reported in the other paper. Color vision of observers were examined using anomaloscope, panel D-15, and Ishihara charts.

Results of MDS for the NCVs became circular configuration similar to Munsell hue circle. Results of some CVDs, who were judged as protanopia or deuteranopia, showed U-shaped curves bending at 5Y and 5PB, while those of other CVDs, who were judged as protanomaly or deuteranomaly, indicated irregular shape between circle and U-shape. The simulation of the hue circle was performed by using the CIE2000 color difference value of each pair and executing MDS. The U-type configuration was simulated using the same procedure after converting negative a^* value in greenish color charts to positive values, assuming unidirectionality of a^* axis. Further investigation is needed to explore whether the assumption can describe individual differences, that would lead practical applicability of the difference scaling test employed in this study in judging characteristics of individual observer, not only CVDs but also NCVs.

INTRODUCTION

In Japan, about 5% of male is X chromosome-linked congenital color vision deficient (CVD) that means the number of people is larger than 3 million which is definitely non-negligible for designing display colors or signs. Many attempts have been made to compensate their color deficiency [1, 2].

The mechanism of their color vision is often simply explained by the loss or spectral sensitivity shift of L or M cones that results the lack or degrade of red-green opponent process. Based on this simple assumption, many CVD simulators conveniently used in a demonstration of how color objects appear for CVDs consisting of yellows, blues, and grays. However, a number of studies have shown that CVDs' color naming results are not so simple that they can name reddish colors as "red" and greenish colors as "green" [3-6]. To estimate CVDs' internal color representation, various studies that focused on hue circle have been conducted [7-11]. Especially, Shepard and Cooper carried out the similarity judgement using nine colors from red to purple and color names, and estimated internal hue circle derived by the multidimensional scaling (MDS). Results of normal color vision observers (NCVs) became circular configuration similar to the Munsell hue circle for both color cards and color names. Those of CVDs based on color names became circular configuration, whereas results based on color cards showed U-shaped configuration bending at turquoise and yellow. They used only high chroma cards such as 5R4/14. According to the panel D15 performance using high and medium chroma color chips reported by Atchison et al. [12], hue circle representation of CVDs would further degrade in the color stimuli of medium chroma. Therefore, in this study, to investigate CVDs' internal color representation more precisely, a psychological distance of color pairs using high and medium chroma color charts is measured. Also, to express internal color representation for individual observers, estimation of the MDS from colorimetric values is challenged.

EXPERIMENT

Test Stimuli

In the experiment, 20 colors, high and medium chroma chips for each of 10 basic hues of Munsell color system, were chosen (Table 1). All combinations of 10 hues, i.e., 45 paired cards were prepared for each of high and medium chroma groups. The size of one color area was 2.5cm x 3.5cm, and the two colors in a pair were placed 2.5cm apart in each card.

Table 1. Munsell color notation of the test stimuli

High Chroma Group				Medium Chroma Group							
R	5R	4/14	BG	5BG	4/9	R	5R	4/4	BG	5BG	4/3
YR	5YR	6.5/14	B	5B	4/8	YR	5YR	6.5/4	B	5B	4/3
Y	5Y	8/14	PB	5PB	4/12	Y	5Y	8/4	PB	5PB	4/4
GY	5GY	6.5/10	P	5P	4/11	GY	5GY	6.5/4	P	5P	4/3
G	5G	4.5/10	RP	5RP	4/12	G	5G	4.5/4	RP	5RP	4/4

Experimental Environment

A color card was placed on the desk covered with a grey cloth. The desk top was illuminated with white fluorescent light. Horizontal illuminance at the color card was 560lx. Observer sat in front of the desk and observed the color card in the visual distance of 50cm. Schematic of the experimental set-up is indicated in the other paper [13].

Procedure

Experiments using the test cards of high and medium chroma were conducted separately. Randomly selected color card was presented to the observer, and he was instructed to evaluate the difference of the pair with five grade difference scale (1. Very close, 2. Rather close, 3. Neither close nor far, 4. Rather far, 5. Very far). After the color card experiment, difference scaling for color names were conducted. Answer sheet on which 45 pairs of color names were written was given to the observer, and he was asked to make difference scaling described above.

Observers

Nine protan, 8 deutan, and 8 normal color vision observers participated the experiment using high chroma colors and color names, while 8 protan, 5 deutan, and 7 NCV observers participated the experiment using medium chroma colors. Prior to the experiment, all observers were examined for their color vision using Ishihara charts, panel D-15, and anomaloscope.

RESULTS

Non-metric MDS with Euclidean distance was employed for the analysis. In this study, only the results based on the color card experiment are concerned. Results based on the color name experiment are reported in the other study [13]. Figure 1 shows the MDS configuration of the representative observers for three different types of color vision based on the results of high chroma cards. Figure 2 shows the color space based on the results of medium chroma cards of the same observers shown in Figure 1.

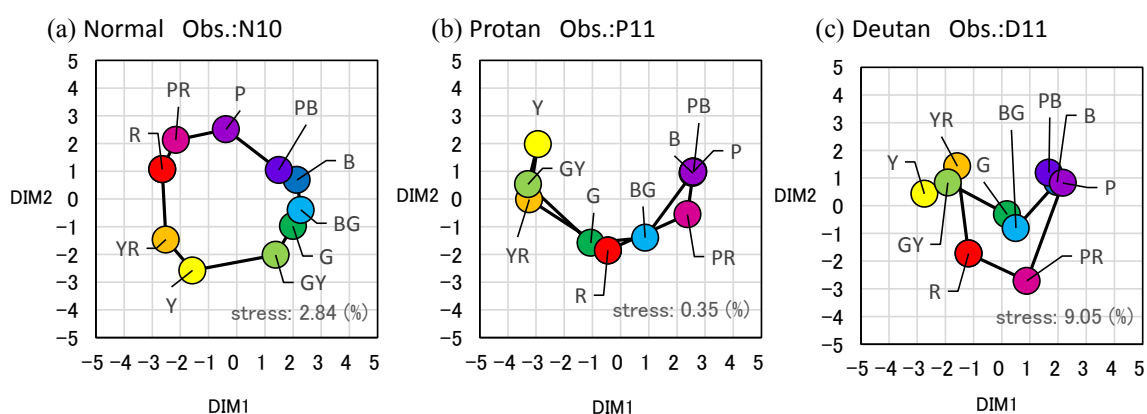


Figure 1. Results of hue circle estimation tested with high chroma cards

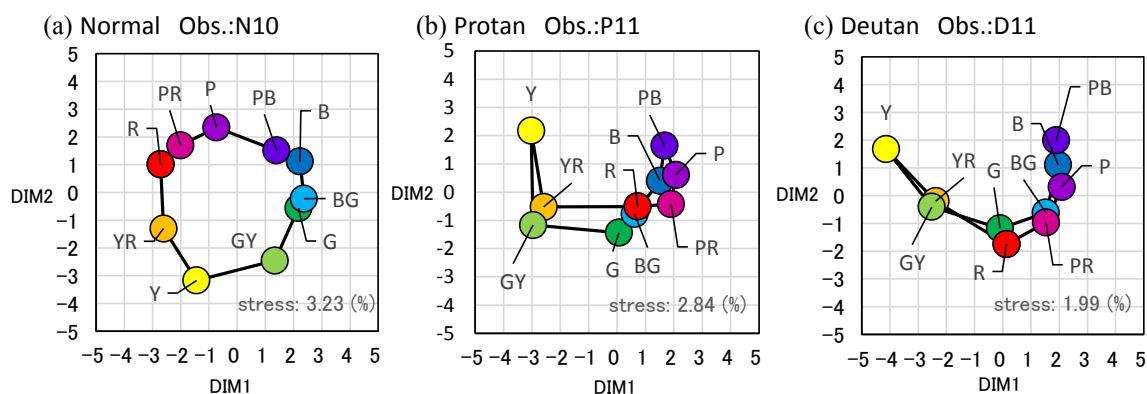


Figure 2. Results of hue circle estimation tested with medium chroma chips

As shown in figures, results of high and medium chroma are similar, while the results of medium chroma of deutan observer D11 (Figure 2(c)) show U-shape property more eminent than that of high chroma shown in Figure 1(c). Concerning to the results of this study, effect of chroma on the MDS configuration that reflects internal color representation of CVDs is not significant so far.

DISCUSSION

We tried to estimate MDS configurations of NCVs and CVDs from colorimetric values as follows. First, colorimetric values of 10 color chips were measured using spectroradiometer (Konica-Minolta, CS-2000) from the observer's position. Result of the colorimetry plotted on a^* - b^* chromaticity diagram is shown in Figure 3(a). Color differences of 45 pairs were calculated using the CIE2000 color differences formula. Then the MDS configuration shown in Figure 4(a) was obtained based on these color differences. This corresponds to the internal color representation for the standard observer, i.e. NCV.

After several trial and errors, we found the following conversion gives the U-shaped MDS configuration similar to the results shown in Figure 1(b) and (c) or Figure 2(b) and (c). When the a^* value is negative, then the point is reflected in the a^* axis as shown in Figure 3(b), while keeping the b^* constant, assuming unidirectionality of a^* axis. MDS configuration is indicated in Figure 4(b). Points in Figure 3(b) are considered as the color stimuli for CVD's visual system plotted in the NCV's color space. We understand a curiosity of this, i.e., plotting the color stimuli for CVD's visual system in the color space constructed for NCV, but the MDS configuration derived from the points in Figure 3(b) is the most successful result to simulate U-shape configuration at the present. In the related study by Hira et al. [14], U-shaped configuration is obtained for NCVs when the a^* values of the stimuli are changed to zero while keeping the b^* values as unchanged, and difference scaling is performed. They call them 'R-G neutral- and Y-B only changed-' stimuli. However, the MDS configuration would be linear if all color chips are on the y-axis, theoretically. This means that each NCV observer's residual sensation of the red-green opponent process elicited by 'R-G neutral- and Y-B only changed-' stimuli, may contribute to form U-shape MDS configuration. Considering the implication of their results, assuming non-zero a^* values in one direction indicated in Figure 3(b) is not inappropriate to express 'color chips' for CVDs.

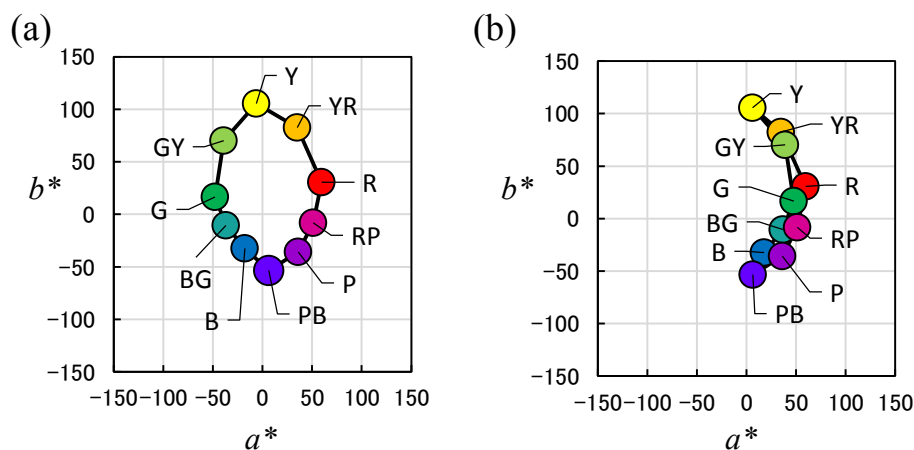


**Figure 3. a^* vs b^* of High chroma chips,
(a): Before conversion, (b): After conversion for CVD simulation**

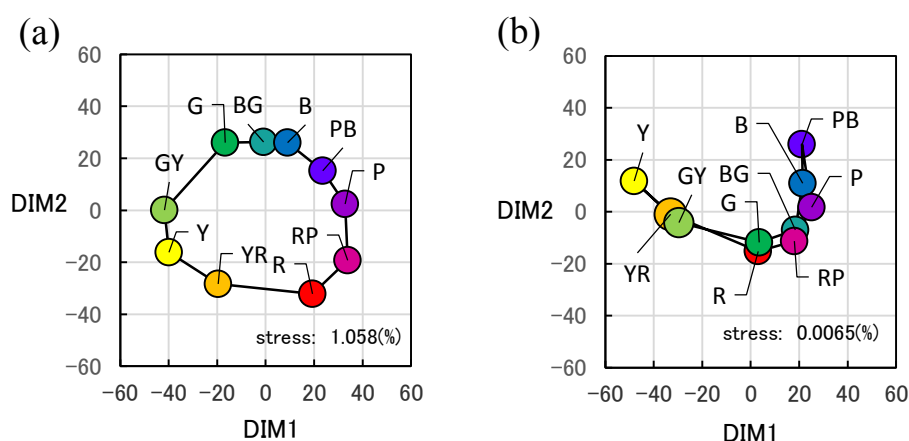


Figure 4. Results of Simulation, (a): NCVs , (b): CVDs

CONCLUDING REMARKS

Internal color representation of CVDs is investigated precisely using high and medium chroma color cards, and compared with that of NCVs. No significant difference was observed between high and medium chroma. Estimation of the MDS configuration from colorimetric values was challenged. By employing absolute values for a^* for all color chips, while taking the same b^* values as original, fairly good estimation of the U-shaped MDS configuration was obtained. Our simulation suggests that internal color representation of CVD is composed of yellow-blue component which are as strong as that of NCV, some kind of unidirectional (non-opponent) component, say weak red (or green) component, and brightness-darkness component which is not discussed here. Further investigation is needed to explore whether the assumption can describe individual differences.

REFERENCES

1. Hira, S., Matsumoto, A., Kihara, K., Ohtsuka, S. (2019). Hue rotation (HR) and hue blending (HB): Real-time image enhancement methods for digital component video signals to support red-green color-defective observers. *Journal of the Society for Information Display*, 27(7), 409-426.
2. Chen, Y.C., Guan, Y., Ishikawa, T., Eto, T., Nakatsue T., Chao, J., & Ayama, M. (2014). Preference for Color-Enhanced Images Assessed by Color Deficiencies. *Color Research & Application*, 39(3), 234-251.
3. Jameson, D., Hurvich L. M. (1978). Dichromatic color language: "Reds" and "Greens" don't look alike but their colors do. *Sensory Processes* 2, 146-155.
4. Paramei, G. V. (1996). Color space of normally sighted and color-deficient observers reconstructed from color name. *American Psychological Society*, 7(5), 311-317.
5. Bonnardel, V. (2006). Colornaming and categorization in inherited color vision deficiencies. *Visual Neuroscience*, 23, 637-643.
6. Nagy, B. V., Nemeth, Z., Samu, K., & Abraham, G. (2014). Variability and systematic difference in normal, protan, and deutan color naming, *Frontiers in Psychology*, 5, Article 1416, 1-7. doi:10.3389/fpsyg.2014.01416
7. Shepard, R.N., Cooper, L. A. (1992). Representation of colors in the blind, color-blind, and normally sighted. *Psychological Science*, 3 (2), 97-104.
8. Lillo, J., Moreira, H., Alvaro, L., Davies, I. (2014). Use of basic color terms by red-green dichromats: 1. general description. *Color research and application*, 39(4), 360-371.

9. Moreira, H., Lillo, J., Alvaro, L., Davis, I. (2014). Use of basic color terms by red-green dichromats. II. models. *Color Research & Application*, 39(4), 372-386.
10. Hira, S., Nakamichi, M., Kanari, K., Karakama, Y., Fukuda, H., Ayama, M., Ohtsuka, S. (2017). Individual differences in chromatic perception: continuous variation from dichromacy to trichromacy. *Proceedings of the International Display Workshops24*, 992-995.
11. Kanari, K., Ishikawa, T., Ayama, M. (2017). Perceived saturation difference of congenital red-green color vision deficiencies. *Proceedings of 13th AIC Congress 2017*, USB.
12. Atchison, D.A., Bowman, K. J., Vingrys, A. J. (1991). Quantitative scoring methods for D15 panel tests in the diagnosis of congenital color vision deficiencies. *Optometry and Vision Science*, 68(1), 41-48.
13. Ayama, M., Ohkoba, M., Kanari, K., Mikami, H., Ishikawa, T., Hira, S., Ohtsuka, S. (2019). Color representations of red-green color deficient and normal observers using color cards and color names. *Proceedings of the 5th Asia Color Association Conference*.
14. Hira, S., Sako, A., Uto, R., Kanari, K., Ohkoba, M., Ishikawa, T., Ayama, M., Ohtsuka, S. (2019). Immanent dichromatic in trichromatic observer: based on MDS analyses of R-G neutral- and Y-B only changed-stimuli observation results. *Proceedings of the 26th International Display Workshops*.

EFFECTS OF LIGHT COLOR CHANGE PROGRAMS OF LED LIGHTING ON SUBSEQUENT WORK EFFICIENCY

M. Tozuka, H. Matsushima, K. Yokoyama, H. Takahashi*

Department of Electrical & Electronic Engineering, Kanagawa Institute of Technology, Japan.

* Corresponding author: Hiroshi Takahashi, e-mail: htakahashi@ele.kanagawa-it.ac.jp

Keywords: Light color change program, Work efficiency, Alertness, EEG, LED

ABSTRACT

The use of light-emitting diode (LED) lighting has now become widespread. LEDs are capable of emitting light in the primary colors of red, green, and blue, and are thus able to reproduce most chromatic colors. Certain wavelengths of visible light have been found to have both physical and psychological effects on human beings. For example, some studies have reported that long-wavelength (red) light increases alertness in the daytime, while other studies have reported that colored lighting influences cognitive performance. However, the effects of light color changes before work on work efficiency levels have not yet been clarified. Therefore, in this study, we investigate the effects of light color changes before work on subsequent work efficiency.

In this experiment, the work surface illuminance was set to 200 lx. White, red, green, and blue LEDs were used in this experiment. Electroencephalogram (EEG) data from seven test subjects were recorded throughout the experiments, and the data were grouped into the following two frequency ranges: 8-12.5 Hz (alpha) and 13-30 Hz (beta). The ratio beta/alpha was used as an index of alertness level. The change program from colored light back to white light was of two types: (A) instantaneous change after 5-minute exposure and (B) a gradual change over one minute after 4-minute exposure.

Comparing the two types of light color change programs, alertness during work was found to be higher in the case of program (B) for all light colors investigated. Moreover, the results suggest that alertness decreases following exposure to green light.

As for work efficiency, the number of correct answers to the calculation task was higher in the case of program (B) for all light colors investigated.

1. INTRODUCTION

The use of light-emitting diode (LED) lighting has now become widespread. LEDs are capable of emitting light in the primary colors of red, green, and blue, and are thus able to reproduce most chromatic colors. Certain wavelengths of visible light have been found to have both physical and psychological effects on human beings. For example, some studies[1],[2],[3] have reported that long-wavelength (red) light increases alertness in the daytime, while other studies[4],[5] have reported that colored lighting influences cognitive performance. However, the effects of light color changes before work on work efficiency levels have not yet been clarified. Therefore, in this study, we investigate the effects of light color changes before work on subsequent work efficiency.

2. EXPERIMENT

Table 1 shows the experimental conditions. In this experiment, the work surface illuminance was set to 200 lx. White, red, green, and blue LEDs were used in this experiment. From the subjects electroencephalogram (EEG) data recorded throughout the experiments. Electrodes were placed on subject's scalps according to the International 10-20 system at C3 and C4. An additional electrode was attached at A1 to serve as reference electrode for those attached to the scalp. Data

were grouped into the following two frequency ranges: 8-12.5 Hz (alpha) and 13-30 Hz (beta). The ratio beta/alpha was used as an index of alertness level.

Subjects were given 3 minutes to adapt to white lighting at 200 lx as the initial condition. They were then exposed to colored light for 5 minutes, after which they performed a calculation task for 5 minutes under white light again. The change program from colored light back to white light was of two types: (A) instantaneous change after 5-minute exposure and (B) a gradual change over one minute after 4-minute exposure.

Table 1: Experimental condition

Light source	LED
Work surface illuminance	200 lx
Light source height	0.8 m
Chromaticity	White: (0.31, 0.33) Red: (0.70, 0.30) Green: (0.20, 0.72) Blue: (0.13, 0.07)
Subjects	7 males in their 20s

3. RESULTS AND DISCUSSION

Figure 1 shows the average of normalized alertness. In each frequency range, the EEG power at each interval was normalized to the power obtained during the initial white light adaptation. Comparing the two types of light color change programs, alertness during work was found to be higher in the case of program (B) for all light colors investigated. Moreover, the results suggest that alertness decreases following exposure to green light.

Figure 2 shows the number of correct answers to the calculation task. The number of correct answers was higher in the case of program (B) for all light colors investigated. The number of correct answers was the highest in the case of program (B) with blue light exposure, and then the number of correct answers was high for white light.

Figure 3 shows the relationship between the alertness and the number of correct answers. The correlation coefficient of 0.6 shows that there was a positive correlation between alertness and the number of correct answers. Working efficiency was high when work was conducted after gradually changing to white light after exposure to blue light.

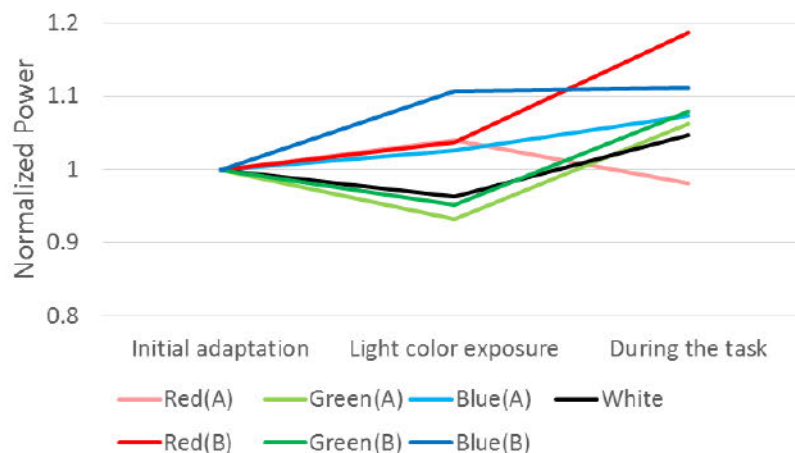


Figure 1. Average of normalized alertness

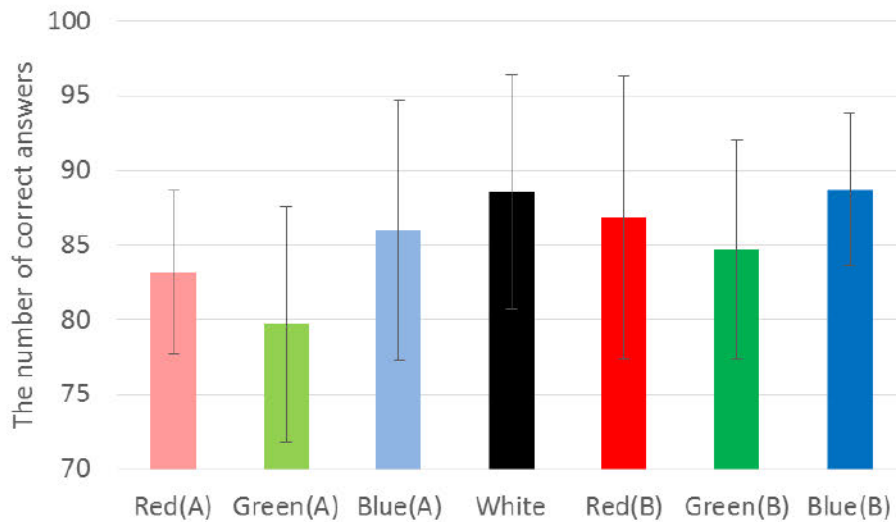


Figure 2. The number of correct answers to the calculation task

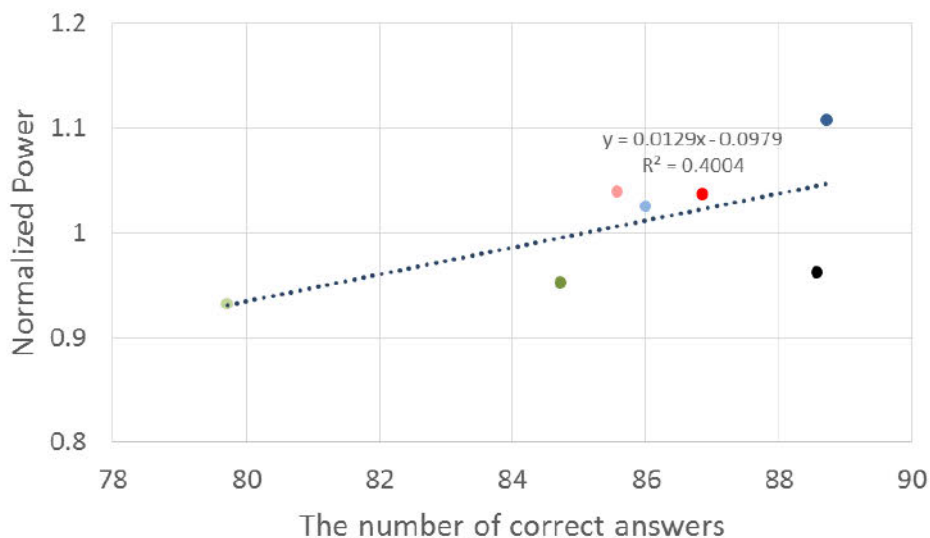


Figure 3. Relationship between the alertness and the number of correct answers

4. CONCLUSION

In this study, we conducted an experiment to clarify the effect of light color changes before work on subsequent work efficiency. The results can be summarized as follows:

- (1) For all light colors investigated, alertness during work was higher in the case of program (B).
- (2) For all light colors investigated, the number of correct answers to calculation tasks was higher in the case of program (B).
- (3) There is a positive correlation between alertness and the number of correct answers to calculation tasks.

ACKNOWLEDGEMENT

This study was approved by the Ethical Review Board for the use of human subjects of Kanagawa Institute of Technology (No. 20180322-20)

REFERENCES

1. PLITNICK, B., FIGUEIRO, MG., WOOD, B. & REA, MS. (2010). The effects of red and blue light on alertness and mood at night. *Lighting Research and Technology*, 42(4), 449-458.
2. SAHIN, L. & FIGUEIRO, MG. (2013). Alerting effects of short-wavelength (blue) and long-wavelength (red) lights in the afternoon. *Physiology & Behavior*, 116-117, 1-7.
3. SAHIN, L., WOOD, BM., PLITNICK, B., FIGUEIRO, MG. (2014). Daytime light exposure: Effects on biomarkers, measures of alertness, and performance. *Behavioural Brain Research*, 274, 176-185.
4. KOJIMA, H. and MIURA, H. (2012). Examining the Effect of Illumination Color on Cognitive Performance, *J. Illum. Engng.Inst. Jpn.*, 96(2), 95-99.
5. TAKAHASHI, H., UETSUHARA, T., KOHAMA, S. (2016). Effects of chromatic colour lighting on work efficiency. *PROCEEDINGS of the 4th CIE Expert Symposium on Colour and Visual Appearance*, 476-479.

PSYCHOLOGICAL AND PHYSIOLOGICAL EFFECTS OF THE LED LIGHTING COLOR ON A LIVING SPACE

Shu Sasaki^{1*} and Hiroki Asahara² and Taiki Sanada² and Takayuki Misu²

¹*Department of Electrical and Electronic Engineering, Graduate School of Engineering, Kanagawa Institute of Technology, Japan*

²*Department of Home Appliance Engineering, Kanagawa Institute of Technology, Japan*

*Corresponding author: Shu Sasaki, shu.sasaki1216@gmail.com

Keywords: Full Color LED, Psychological, Physiological, Lighting Color Control

ABSTRACT

The LED lighting has appeared in which the light emission color can be changed, and appropriate usage of the light color is considered. The advantage of the LED implementation of the illumination is that the chromatic light and the lighting color control is possible. However, the lighting color control is only used for entertainment light effects and no other use has been found. Therefore, new systems of using LED lighting will be added if the LED chromatic light has a psychologically and physiologically beneficial influence. The purpose of this study is to investigate the psychological and physiological effects on living organisms caused by the use of chromatic lighting in living space, and to examine new ways of using LED lighting. In the experimental environment, a laboratory simulating a single room of a general type equipped with full-color ceiling lights was prepared, and kept at a constant temperature and humidity using an air conditioner and an air purifier. The experiment used three primary colors of light, (red, blue, and green) and white. The subject was exposed to the illumination light for 10 minutes of white light, 15 minutes of one of the three primary colors (either red, blue, or green), or 10 minutes of white light for a total of 35 minutes. The lighting color of the ceiling lights was controlled from another room according to the communication standard "ECHONET lite". The experimental results show that the three primary colors affect human thermal sensation. In addition, it was found that the three primary color lights affect the face temperature in physiological evaluation.

INTRODUCTION

Nowadays, it is known that stimuli from light colors have a psychological and physiological effect on the human body [1-4]. Many studies have been carried out because it has been proved that light is perceived not only from the eyes but also from the skin in the study that conducted the demonstration experiment. The Japan Institute of Energy has announced that it will reduce electricity consumption by about 10 percent by raising the set temperature of the air conditioner during cooling by one degrees Celsius in "Home Energy Saving Measures and Summer Power Consumption Reduction (IEEJ: issued in April)". In recent years, full-color LED lighting that can produce chromatic color light has been sold, and chromatic color light can be used in a residential environment. Therefore, we thought that changing the color of the illumination light could raise the temperature of the sensation and move the set temperature of the air conditioner toward energy-saving levels. In this study, we examine the psychological effects of changing the illumination light color to the three primary colors of light, i.e. red, green and blue, and the effect of measuring the facial surface temperature and stress.

OUTLINE OF EXPERIMENT

Figure 1 shows the lighting test room. The laboratory is a room that resembles a 10.5 tatami room, and two LED lights (LEDH81718LC-LT3 manufactured by Toshiba Lighting & Technology Corp.) are installed on the ceiling. Evaluation items in the experiment were VAS (Visual Analogue Scale) as psychological evaluation, vital data (LF/HF, heart rate) by wearable electrocardiograph (hitoe) as physiological evaluation, face temperature by thermography camera (NECAvio InfRec-R300S). The illumination color was controlled by ECHONET Lite. For all light colors, the emission intensity was integrated and the integrated value was unified to 0.126. Figure 2 shows the xy chromaticity coordinates of the light colors used in the experiment.

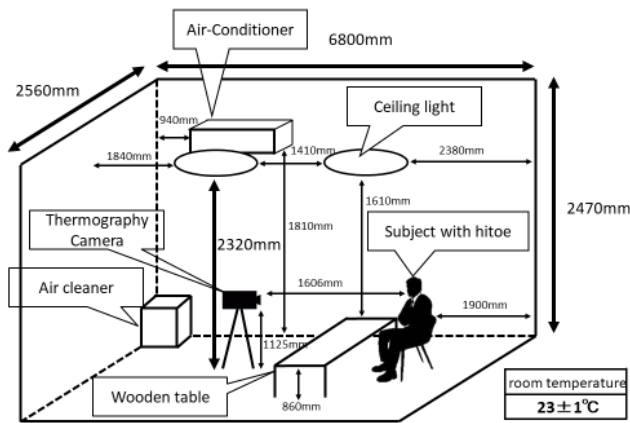


Figure 1. Illumination light color laboratory

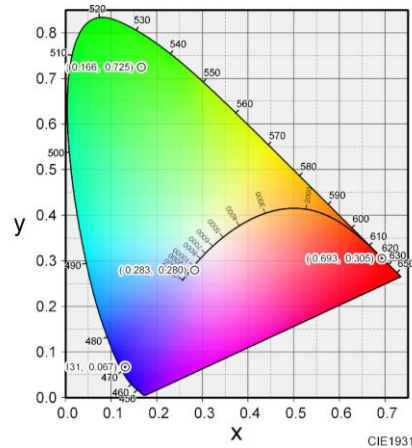


Figure 2. x-y Chromaticity diagram of the light color using the ceiling lights

EXPERIMENTAL METHOD

The subjects were five male students in their twenties with normal color vision who attended Kanagawa Institute of Technology. The subject was seated in front of a wooden table that was not directly exposed to the wind of the air conditioner. The subject was wearing a “hitoe” to measure vital data (LF/HF, heart rate, heart rate interval) [5], and a thermographic camera was installed at about 2 m from the subject's face to measure the facial surface temperature. The experiment was divided into three days, and the one-day experiment was performed for 35 minutes in total, changing the light color in the order of white 10 minutes, chromatic 15 minutes, and white 10 minutes. VAS evaluation was performed every 5 minutes from the start of the experiment. The lighting order of chromatic colors was changed for each subject. During the experiment, a simple associative question that could be answered verbally was used to unify the state.

RESULT AND DISCUSSION

In the graph of the result, how much chromatic light (R, G, B) is better than white light is obtained by subtracting the value obtained with white light color from the value obtained with chromatic light (R, G, B).

Psychological effects VAS

Figure 3 shows the measurement results of VAS. The average value of “Warmth” in Figure 3 (a) was 29 for red, 9 for green, and -24 for blue compared to white. When observed in each subject, all the

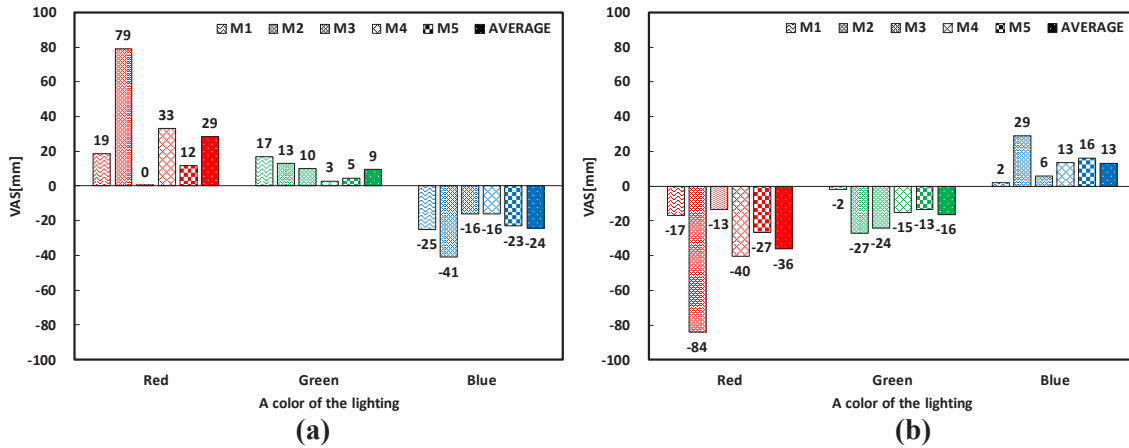


Figure 3. VAS measurement results (a) Warmth, (b) Coolness

subjects felt warm in red, while none of them felt warm in blue. All subjects felt warm with a neutral green color. This is probably because the green color used this time was close to red in the xy coordinates. The average value of “Coolness” in Figure 3 (b) is -36 for red, -16 for green, and 13 for blue compared to white. When observed in each subject, none of the subjects felt cool in red, while all of them felt cool in blue. In green, none of the subjects felt cold.

Physiological effects LF/HF, Facial surface temperature

Figure 4 shows the measurement results of the face temperature. The average changes in the face temperature of each light color when compared with white were -0.168°C for red, -0.169°C for green, and 0.045 for blue. Compared with the VAS results in the previous section, the face temperature decreased even when the subjects were feeling psychologically warm, and the face temperature increased even when they were feeling cool. Figure 5 shows the LF/HF measurement results. The LF/HF value of each light color when compared with white was 0.018 for red, 0.021 for green, and -0.058 for blue. When observed in each subject, none of the subjects felt stress in blue. Based on the results in the previous section, it can be said that blue gives a cool effect to people and has a relaxing effect.

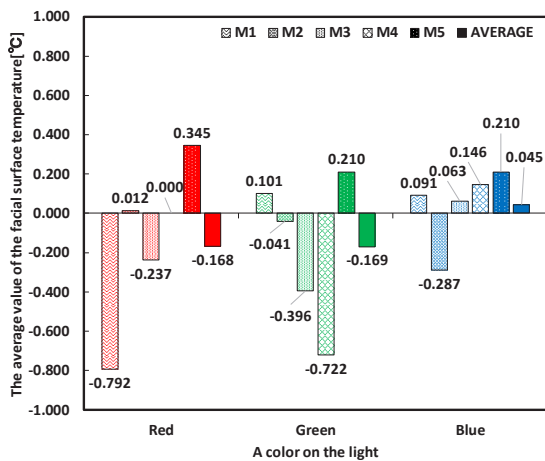


Figure 4. Measurement result of face surface temperature

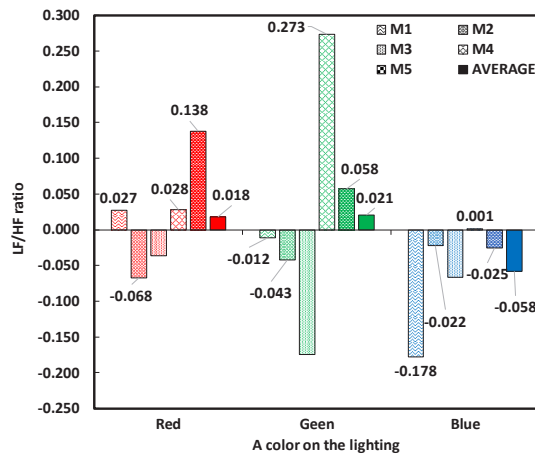


Figure 5. Measurement result of LF/HF

The measured results of the face temperature and LF/HF showed that the physiological effect of the lighting color on the subject differs from person to person.

CONCLUSION

The PSYCHOLOGICAL AND PHYSIOLOGICAL EFFECTS OF THE LED LIGHTING COLOR ON A LIVING SPACE results are summarized below.

- The average value of VAS “Warmth” was 29 for red, 9 for green, and -24 for blue compared to white. The average value of VAS “Coolness” is -36 for red, -16 for green, and 13 for blue compared to white. The lighting color has a psychological effect on people, and it has been found that red light feels warm and blue light feels cool.
- The average changes in the face temperature of each light color when compared with white were -0.168 ° C for red, -0.169 ° C for green, and 0.045 for blue. Compared with the VAS results in the previous section, the face temperature decreased even when the subjects were feeling psychologically warm, and the face temperature increased even when they were feeling cool.
- The LF/HF value of each light color when compared with white was 0.018 for red, 0.021 for green, and -0.058 for blue. This is probably because the blue light has a relaxing effect on people.
- The result of physiological effects given by the color of the illumination light differ from person to person.

REFERENCES

1. Ishikawa, Y. (1993). Light Color and Comfortable Dwelling Environment-Energy Conservation Effect of Light and Cooling by Light Color (in Japanese). *Journal of the Illuminating Engineering Institute of Japan*, Vol. 77, No. 11, pp18-20.
2. Li, D., & Jiang, X., & Koga, T., & Hirate, K. (2011). BASIC STUDY ON DISCOMFORT CAUSED BY LED LIGHTING COLORS IN WORKING SPACE. *Architectural Institute of Japan Technical Report*, Vol. 17, No. 35, pp.201-204.
3. Inoue, Y. (2008). Effects of Chromatic Light Lighting on Visibility and Atmosphere (in Japanese). *Journal of the Illuminating Engineering Institute of Japan*, Vol. 92, No. 9, pp. 637-644.
4. Kubo, H., & Inoue, Y. (2008). Physiological and Psychological Effects of Chromatic Light Lighting: Exposure to Youth Girls for 60 Minutes (in Japanese). *Journal of the Illuminating Engineering Institute of Japan*, Vol.92, No.9, pp.645-649.
5. TORAY INDUSTRIES, INC., “About hitoe”, <https://www.hitoe-toray.com/en/>

THE EFFECT OF LIGHTING ENVIRONMENT CHANGE AND CATARACT CLOUDINESS ON COLOR DISCRIMINATION AND CONTRAST SENSITIVITY

Masako Omori^{1*} and Reiko Hashimoto²

¹*Faculty of Home Economics, Kobe Women's University.*

²*Department of Human Environment Design, Sugiyama Jogakuen University.*

*Corresponding author: Masako Omori, masako@suma.kobe-wu.ac.jp

Keywords: LED, color temperature, cataract cloudiness, chromatic discrimination ability, contrast sensitivity

ABSTRACT

Recently, light-emitting diode (LED) illumination in Japan has become popular in the past several years. With the spread of LED illumination, it has become possible for people of all ages to design a comfortable living environmental. One survey found that 66-83 % of people in their 60s, 84-97 % in their 70s and 1 % older had cataracts. In this study, we focused on the effects of cataract cloudiness on the chromatic discrimination ability and contrast sensitivity with LED illumination. The subjects were thirty people aged 20's young females and more than 60's elderly people, with normal or corrected-to-normal vision. The subjects' visual functions of cataract cloudiness (CC) and near visual acuity for a 50 cm distant target (NVA) were measured. Subjects' CC was indicated on a 256 gradation and classified into four groups, (-), (+), (2+), and (3+), where (-) means 0-99, (+) 100-149, (2+) 150-199, and (3+) 200-256. NVA was classified as good (1.0-1.2), fair (0.5-0.7), or weak (0.1-0.3). In this experiment, used dimmable LED illumination (ODELIC CO., LTD) was used and, we had tested under staged illuminance conditions. Two different types of color temperature (daylight: 5700K and mesopic vision: 2600K) and two different luminance (1000Lx and 5Lx) were examined. Color temperature and luminance were measured (Minolta CL-70F). The results of the experiments showed that the chromatic discrimination ability and contrast sensitivity affected both of cataract cloudiness and illuminance conditions.

INTRODUCTION

Light Emitting Diodes (LEDs) are highly efficient and have a long lifetime, and contain almost no ultraviolet rays or infrared rays. In addition, visible light can be efficiently obtained, and fading of products due to ultraviolet rays and thermal damage due to infrared rays can be reduced. In addition, it lights instantly even at low temperatures. It does not contain environmentally hazardous substances (such as mercury and lead).

In recent years, the demand for LED lighting is expanding in a wide range of applications, including light bulb-type LED lamps used in general households, facility lighting, and outdoor lighting. There are many studies on the types of light sources and the appearance of colors. In addition, it is important to consider the visibility of the elderly in a super-aged society. Among visual function changes with aging, visual acuity, accommodation function, spatial frequency characteristics, and cataract cloudiness strongly affect the decrease in visibility. There are many studies on the effects of cataract cloudiness due to aging on visibility, especially color discrimination ability and spatial frequency characteristics. As for the spatial frequency characteristics, there are reports that high frequency components [1], high frequency components, and intermediate frequency components decrease with age [2]

[3]. There is a report that the color discrimination ability for blue light of 460 nm decreases to less than half that of young people around 60 years old [4], is best from 20 to 50 years old, and decreases after 50 years old [5]. In addition, there is a report that the color discrimination ability decreases as the illuminance decreases, and that the confusion of the blue-yellow axis increases in older people [6] [7].

In this study, in order to clarify the effects of illuminance and color temperature of LED lighting on the appearance of color, we examined the effects of aging on the lens opacity on color discrimination ability and spatial frequency characteristics.

METHODS

The subjects were 20 years of age younger subject (21.1 years \pm 0.3) and 10 elderly subject aged over 60 years of age (75.2 years \pm 5.5). The subjects were measured the cataract cloudiness (CC) before the experiment. The CC was measured with anterior ocular segment measuring instrument EAS-1000™ (NIDEK Inc.). The indication of cataract cloudiness had 256 levels (Sasaki, K. and Yamamura, T., 1991) in which 0 indicated no cloudiness and 255 maximum cloudiness.

In this study, two experiments were conducted. The first experiment, 100HueTEST (ND-100: Japan Color Research Institute) was conducted to clarify the age-related changes in color discrimination ability. In the second experiment, a contrast sensitivity test (CVS-1000E: Nikon Healthcare Japan Co., Ltd.) was performed to clarify the spatial frequency characteristics. In the two experiments, the color temperature and illuminance were changed. The experiment was conducted in a dark room using an LED illumination experiment box. The illuminance conditions were 2 conditions (daytime: 1000 lx, mesopic vision: 5 lx), and the color temperature was 2 conditions of warm color (2600K) and cool color (5700K). The subjects performed light and dark adaptation for each illumination condition. A total of 4 experiments were conducted with breaks.

RESULTS AND DISCUSSION

In this study, experiments were conducted under LED lighting with two different spectra (with color correlate temperature of 2600K and 5700K), and two different illuminance level (5Lx, 1000Lx). The mean binocular cloudiness value were 47.2 (\pm 6.2) for younger subject group and 151.5 (\pm 25.6) for elderly group. The cataract cloudiness was sever in elderly subject groups than in the younger group.

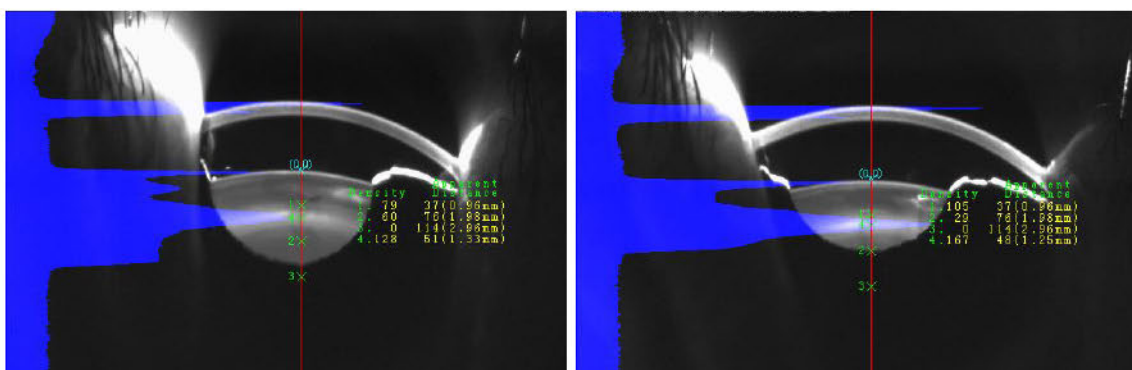


Figure 1. Cataract cloudiness of Subject A : 75 years old
(Left eye: 128, Right eye: 167)

In the two-way ANOVA, Error score was tested statistically as the dependent variable with the two independent variables of the color temperature and color group (100 hue). A significant difference in Error score was seen between color temperature ($P < 0.05$) and color group ($P < 0.001$). Multiple comparisons in the two-way ANOVA revealed significant differences in the Error score between the color No.1 and the other two groups (No.2 and No.4), and between No.3 to No.4. And also significant differences between the warm color (2600K) and cool color (5700K) ($P < 0.05$). Older subjects with high cloudiness had an increase Error score to color No.2 and No.4.

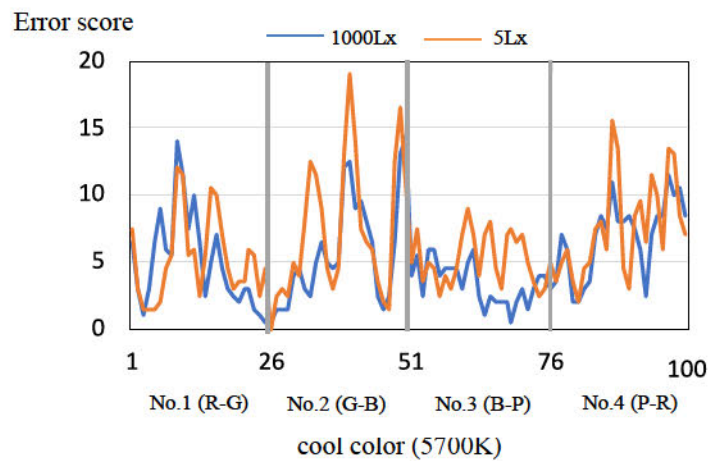
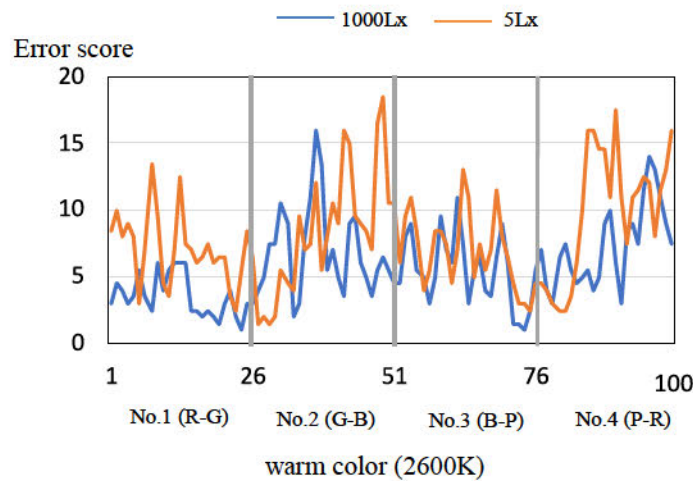


Figure 2. Result of 100Hue test
Subject A : 75 years old, cataracts cloudiness (Right: 167 •Left:128)

REFERENCES

1. Nameda N, Kawara T, Ohzu H. (1989). Human visual spatio-temporal frequency performance as a function of age. *Optom Vis Sci*, 66(11), 760-765. doi10.1097/00006324-198911000-00007
2. Derefealdt G, Lennerstrand G, Lundh B. (1979). Age variations in normal human contrast sensitivity. *Acta Ophthalmol* 57, 679-690.
3. Ginberg AP, Evans DW, Cannon MW. (1984). Large-sample norms for contrast sensitivity. *Am J Opt Physiol Opt* 61, 80-84.
4. HK Lewis, (1982). *A Biography of the Eye. Weale RA. Development, Growth, Age.* London
5. Roy MS, Podgor MJ, Collier B, et al., (1991). Color vision and age in a normal North American population. *Graefes Arch Clin Exp Ophthalmol* 229, 139-144.
6. Boyce PR, Simons RH. (1977). Hue discrimination and light sources. *Light Res Technol* 9, 125-140.
7. Bowman KJ, Cole BL. (1980). A recommendation for illumination of the Farnsworth-Munsell 100Hue Test. *Am J Optom Physiol. Opt, Nov; 57(11)*, 839-43.

HOW DOES A TWO-DIMENSIONAL ARRAY OF LED LIGHTS AFFECT APPEARANCE OF TEXTURE OF OBJECT'S SURFACE?

Mayuko Nakamura^{1*} and Taiichiro Ishida¹

¹*Department of Architecture and Architectural Engineering, Graduate School of Engineering, Kyoto University, Japan.*

*Corresponding author: Mayuko Nakamura, nakamura.mayuko.63n@st.kyoto-u.ac.jp

Keywords: Texture, Appearance, LED, Lighting

ABSTRACT

The surface of an object has both color and texture. The appearance of the texture changes not only by the physical characteristics of object surfaces but also by spatial distribution of lights. In this study, we focused on how the surface of an object does appear under an illuminant composed of a two-dimensional array of LED lights. A surface light source and a point light source have contrasting properties. The difference of the two light sources may strongly influence appearance of the surface of an object. A two-dimensional array of LED lights has unique characteristics. It consists of several LED lights, each of them can be regarded as a point light source. In another aspect, it emits light from an area like a surface light source.

In this study, the two-dimensional array of LED lights (test light condition) and the surface light source (reference light condition) illuminated the samples of materials. Subjects observed them and evaluated their appearance of texture. Two types of LED array (2x2 and 5x5) were prepared to see the effects of the spatial density of LED lights. We used 18 pairs of samples of variety of materials such as paper, textile, leather and sandpaper. Two samples of the same material were prepared and placed in a test box and a reference box separately. The subjects assigned a number to appearance of the sample under the test condition comparing with those under the reference condition being assigned 100. The evaluation items were ten. For example, “not glossy/ glossy”, “warm/ cool”, “dry/ wet”, “vague/ distinct”, “dislike/ like” and “dull/ sparkling”.

The result showed that the samples illuminated by the two-dimensional array of LED lights appeared to be more shiny, distinct and sparkling than the samples illuminated by the surface light source. The spatial density of LEDs also slightly changed the subjects' evaluation.

INTRODUCTION

When we see a surface of a real object, color cannot exist alone on the surface. The surface of an object has both color and texture. We may recognize the visual property of the object based on information of texture as well as color on the surface [1]. The appearance of the texture changes not only by the physical characteristics of object surfaces but also by lighting conditions or viewing direction [2][3].

This study focused on effects of spatial distribution of lights. Our question is how the surface of an object does appear under an illuminant composed of a two-dimensional array of LED lights. A surface light source and a point light source have contrasting properties. A surface light source emits diffused light from an area. A point light source emits directional light from a small area that can be regarded as a point. The difference of the two light sources may strongly influence appearance of the surface of an object [4]. A two-dimensional array of LED lights has unique characteristics. It consists of several LED lights, each of them can be regarded as a point light source. In another aspect, it emits light from an area like a surface light source. Our preliminary study indicated that some types of material surfaces appeared to be glossy under a two-dimensional array of LED lights¹.

¹ Unpublished study; M.Hata, (2016) Graduation thesis, Kyoto University

METHODS

The two-dimensional array of LED lights (test light condition) and the surface light source (reference light condition) were prepared to illuminate test samples. We made two types of LED array (2x2 and 5x5) to see the effects of the spatial density of LED lights. Fig. 1 shows the actual two-dimensional array of LED lights used in this experiment. The size of the light sources was approximately 70mm x 70mm. The surface light source was made by a LED bulb and a light diffusion board.

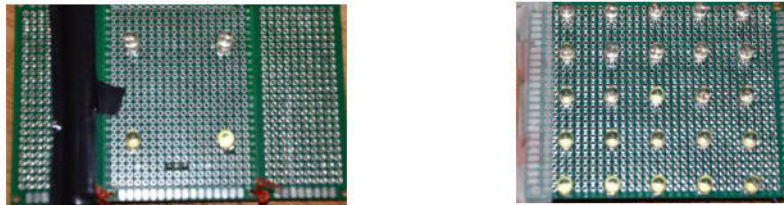


Figure 1. The two-dimensional array of LED lights (2×2) and (5×5)

Fig. 2 shows 18 samples of variety of materials such as paper, textile, leather and sandpaper. Two samples of the same material were prepared and placed in a test box and a reference box separately. A sample of materials placed in the test box were illuminated by the two-dimensional array of LED lights. The same sample of materials placed in the reference box were illuminated by the surface light source.



Figure 2. Samples of materials

Subjects observed pairs of the samples of materials and evaluated their appearance of texture. They assigned a number to appearance of the sample under the test condition comparing with that under the reference condition being assigned 100. The evaluation items include “not glossy/ glossy”, “flat/ uneven”, “smooth/ rough”, “soft/ hard”, “warm/ cool”, “dry/ wet”, “vague/ distinct”, “heavy/ light”, “dislike/ like”, and “dull/ sparkling” [2]. For example, if the sample of

materials placed in a test box appears to be glossier, the subject will assign a number greater than 100. There were seven subjects, and all were majoring in architecture.

Fig. 3 shows a simple diagram of the experimental apparatus. The left box is the test box and the right box is the reference box. Considering the small difference in texture, the two boxes can be observed simultaneously. The size of the samples was 80 mm x 80 mm. The table on which one of the samples was placed was tilted by about 40 degrees to make it easier for the subjects to see the texture of the materials. In fact, the inside of the box was covered with black paper to avoid the effects of light reflection.

Fig. 4 shows the actual viewpoint of the subjects. The illuminance at the center of the sample surface was set to about 450 lx.

Fig. 5 shows the luminance distribution on the surface of the table on which the sample was placed. The luminance distribution differed between the two conditions depending on the difference of light distribution of the light sources.

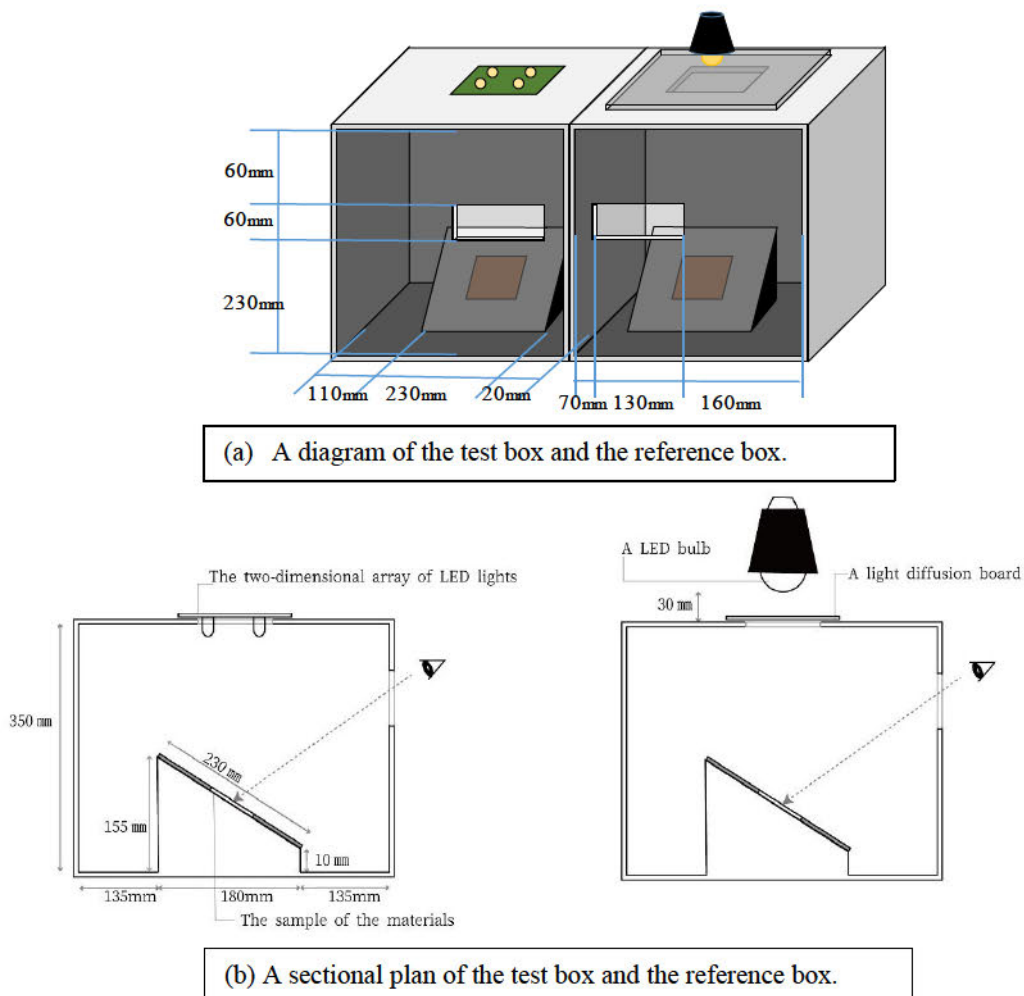


Figure 3. A diagram of the experimental apparatus. (The reference box and the test box)



Figure 4. The viewpoint of the subjects.

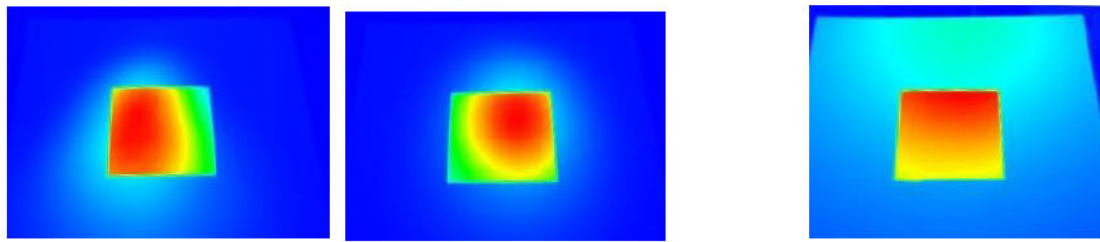
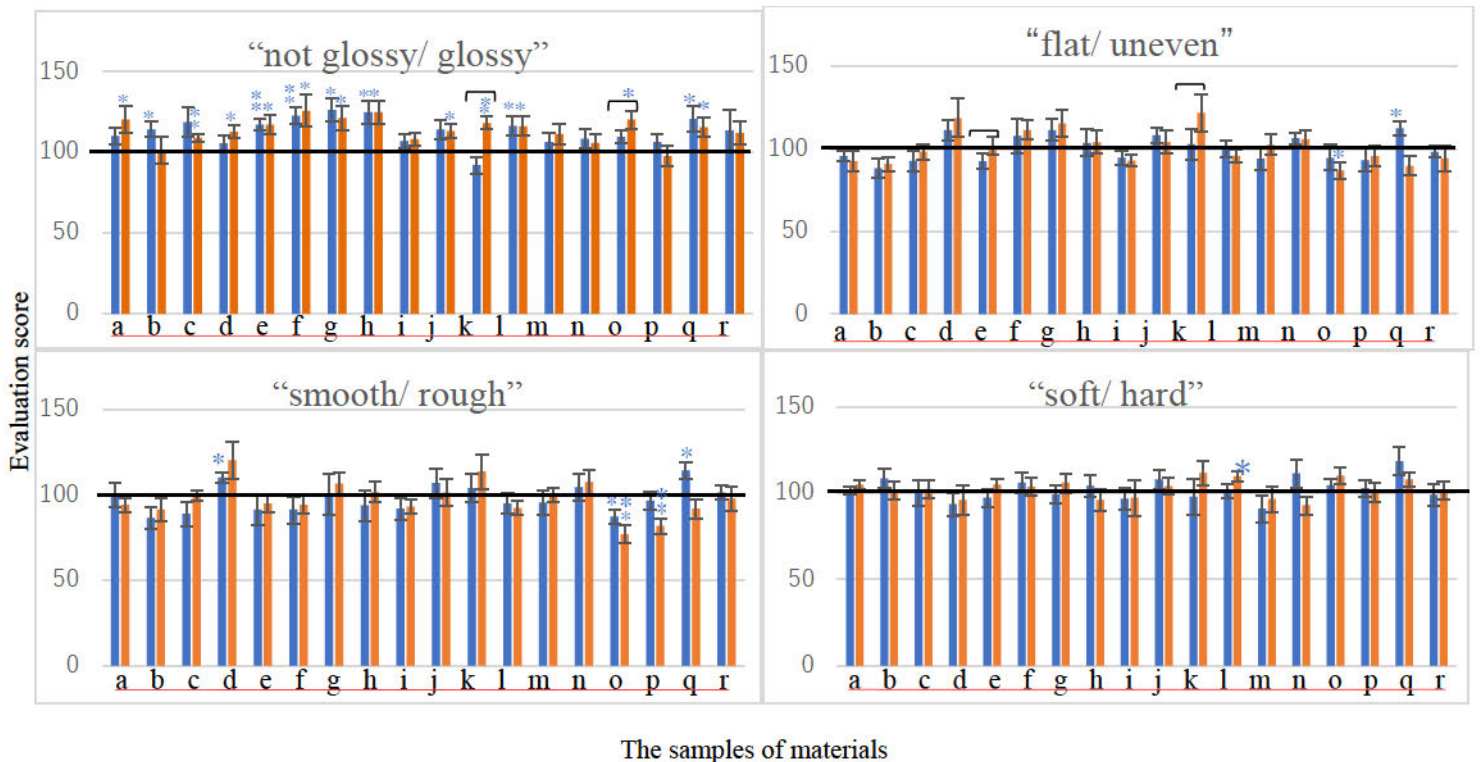
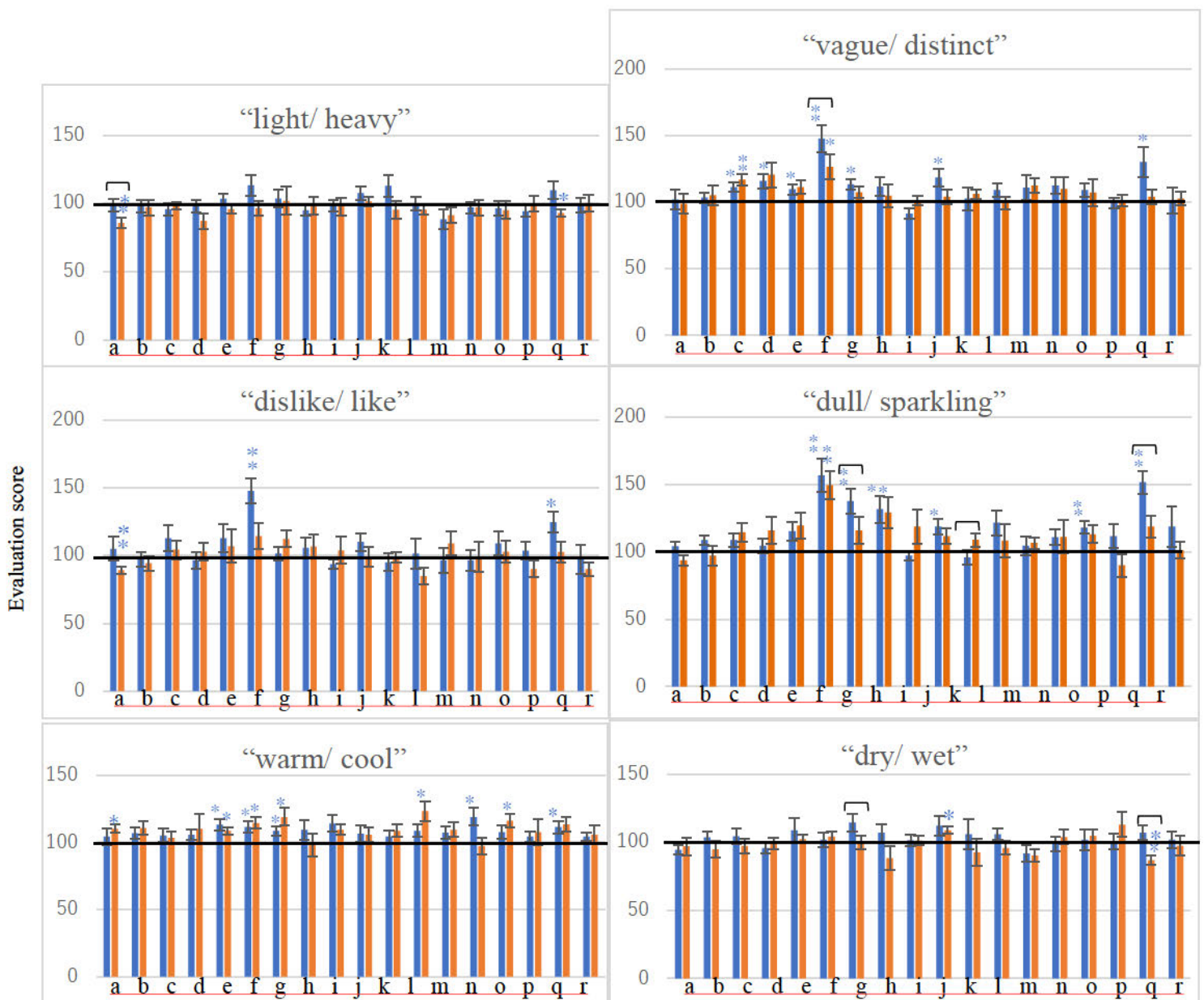


Figure5. The luminance distribution (The two-dimensional array of LED lights (2×2), (5×5) and the surface light source)

RESULTS

Fig. 6 shows relationship between the average number assigned by the subjects and the samples of materials. Among the 10 evaluation items, three items (“not glossy/ glossy”, “vague/ distinct” and “dull/ sparkling”) were given clearly different evaluation scores between the two-dimensional array of LED lights and the surface light source. The blue bar represents the results of the two-dimensional array of LED lights(2x2) and the orange bar represents (5x5). The differences between the average evaluation scores assigned by the subjects and the score of 100 mean that there are differences between appearances under the surface light source and the two-dimensional array of LED lights. The marks of '*' and '**' are given to the samples assigned significantly different scores from 100 (*: $p < 0.05$ **: $p < 0.01$). The marks of '—' are given to the samples that have a significantly different appearance when illuminated by the two-dimensional array of LED lights (2×2) and (5×5) (—: $p < 0.05$).





The samples of materials

Figure 6. Relationship between the average number assigned by the subjects and the samples of the materials. (Blue: The two-dimensional array of LED lights (2×2) Orange: (5×5))

Difference between the test condition and the reference condition (*: p<0.05 **: p<0.01)

Difference between the two-dimensional array of LED lights (2×2) and (5×5) (—:)

DISCUSSION

The result showed that texture appearance of some samples under the test condition was significantly different from the reference condition. The overall trend was that the samples illuminated by the two-dimensional array of LED lights appeared to be more shiny, distinct and sparkling than the samples illuminated by the surface light source. In this study, the spatial density of LEDs slightly changed the subjects' evaluation. Further study is needed to examine

the relation between material surfaces and a lighting method to produce more preferable appearance of the objects.

REFERENCES

1. Marcel P. Lucassen, Theo Gevers, Arjan Gijsenij. (2011) Texture affects color emotion. *COLOR research and application*, Vol.36, No.6, 426-436. Dec.2011
2. Shigeko Kitamura et al. (1998). Interpretation of the evaluation scales for appearance, and a quantitative analysis of appearance using simple texture. *J. Archit. Plann. Environ. Eng., AIJ*, No. 511, 69-74. Sep. 1998
3. T. Ishida and A. Nakashima. (2007) "Quantitative assessment of perceived gloss and roughness of material surfaces based on two-dimensional luminance distribution data," *Proceedings of the Midterm Meeting of the International Colour Association*, vol. D1, pp. 207-212.
4. Hajimu Nakamura. (1999). Lighting of clothing shop. *J. Illum. Engng. Inst. Jpn. Vol.83 No.6*, 387-392. 1999

COMFORTABLE LIGHT DISTRIBUTION IN A ROOM PRODUCED BY ARTIFICIAL LIGHTING WITH DAYLIGHTING FROM A WINDOW

Akiho Kito* and Taiichiro Ishida

*Department of Architecture and Architectural Engineering, Graduated School of Engineering,
Kyoto University, Japan.*

*Corresponding author: Akiho Kito, kito.akiho.56u@st.kyoto-u.ac.jp

Keywords: Daylighting, Comfortable Environment, Brightness

ABSTRACT

Artificial lighting is mostly used not only in nighttime but also in daytime to compensate insufficient light in a room. The Artificial lighting during daytime does not always produce comfortable lighting environment. The aim of this study was to examine comfortable light distribution in a room produced by artificial lighting with interior daylighting from a window. It would be useful to know a method to harmonize artificial lighting and daylighting in a room in terms of designing comfortable light environment and saving energy consumption.

Firstly, it is necessary to consider what kind of light distribution people feel comfortable in a room with daylighting.

Subjects observed an indoor model space with a window on one side. The ceiling of the room was divided in three parts (window side, center, backside of the window) and a fluorescent lamp attached on each part could be adjusted independently. The subject adjusted luminance of each of three fluorescent lamps to make comfortable light distribution in a room with considering daylight from a window. We set nine window conditions; the combinations of three types of window shape (square, vertically long, and horizontally long) and three luminance levels (example for square: 6000, 4000, 1000 cd/m²). The nine conditions were presented in random order for each subject. The subject's adjustment of each of three fluorescent lamps was recorded by using illuminance meter to obtain distribution of illuminance on a floor.

It was found that the preferred illuminance level of the room significantly varied depending on the subjects. In addition, it was also revealed that the comfortable light distribution was strongly influenced by the window conditions.

The results showed that comfortable light distribution in a room with daylighting can be classified into three patterns. In first pattern, the shape of the overall light distribution in the room is similar to that made by the daylighting from the window. In second pattern, the room was illuminated almost uniformly. In third pattern, brightness in the back of the room is higher than that near the window.

This study suggested that comfortable light distribution in a room with daylighting from a window could be achieved by using artificial lightings that produce the three light distribution patterns.

INTRODUCTION

It is usual to use artificial lighting not only in nighttime but also in daytime. There is daylight in daytime. Daylight provides brightness in buildings and contributes to energy saving and human health [1][2]. However, daylight is not stable, and sufficient daylight is not always available.

In most cases, artificial lighting is planned to provide a satisfactory light environment even when daylight is not available, typically at night. It is not necessarily considered to integrate artificial lighting with daylighting to create a comfortable light environment.

The aim of this study was to examine comfortable light distribution in a room produced by artificial lighting with interior daylighting from a window. It would be useful to know a method to harmonize artificial lighting and daylighting in a room in terms of designing comfortable light environment and saving energy consumption. Han et al. proposed a method of creating a comfortable lighting environment in an office space by combining daylighting from a window and artificial lighting on the ceiling. We are considering to study a general method of integrating daylighting and artificial lighting to make comfortable light environment that can apply to the variety of space types [3][4][5].

Firstly, it is necessary to consider what kind of light distribution people feel comfortable in a room with daylighting.

METHODS

1. Impression evaluation experiment

The experiment was conducted using a 1/10-scaled-model box which was lit by light from a side window. Figure 1 illustrates an experimental apparatus. The ceiling of the room was divided in three parts (window side, center, backside of the window) and a fluorescent lamp attached on each part could be adjusted independently. Subjects observed the room and tried to adjust luminance of each of three fluorescent lamps to make comfortable light distribution in a room with considering daylight from a window.

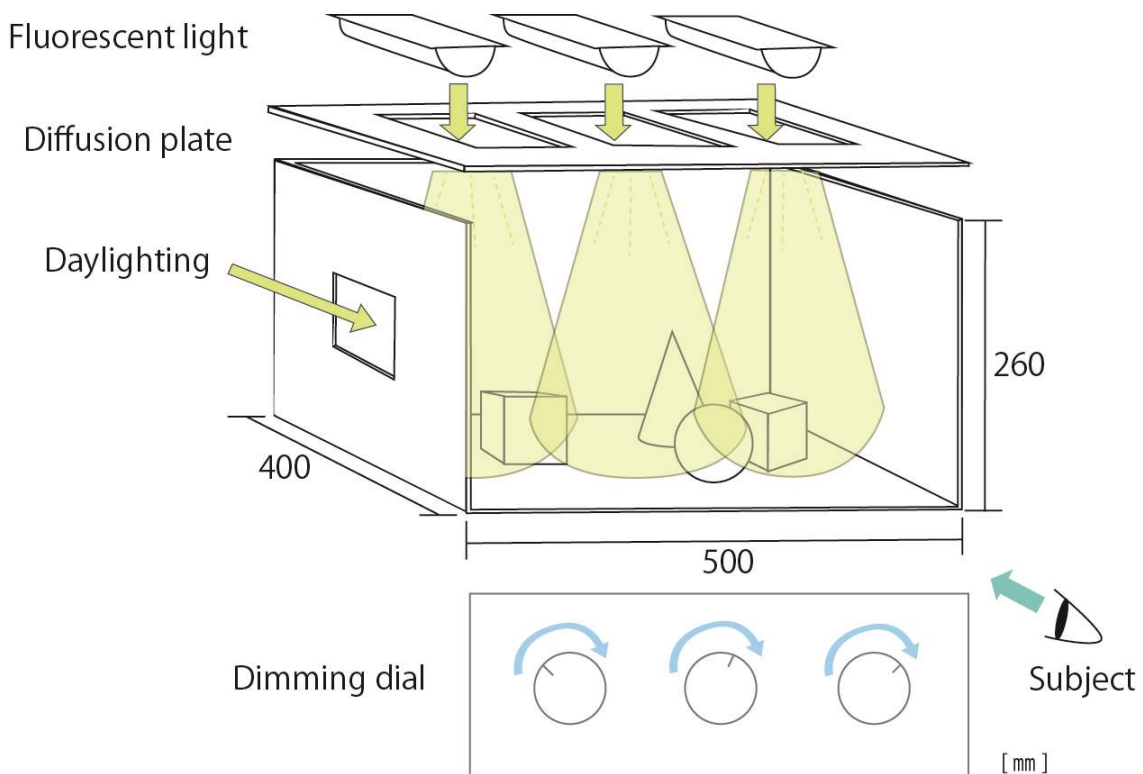


Figure 1. Experimental model box

2. Experimental condition

The experimental condition consisted of 9 window conditions; the combinations of three types of window shape (square, vertically long, and horizontally long) and three luminance levels (example of square: 6000, 4000, 1000 cd/m^2). The nine conditions were presented in random order for each subject.

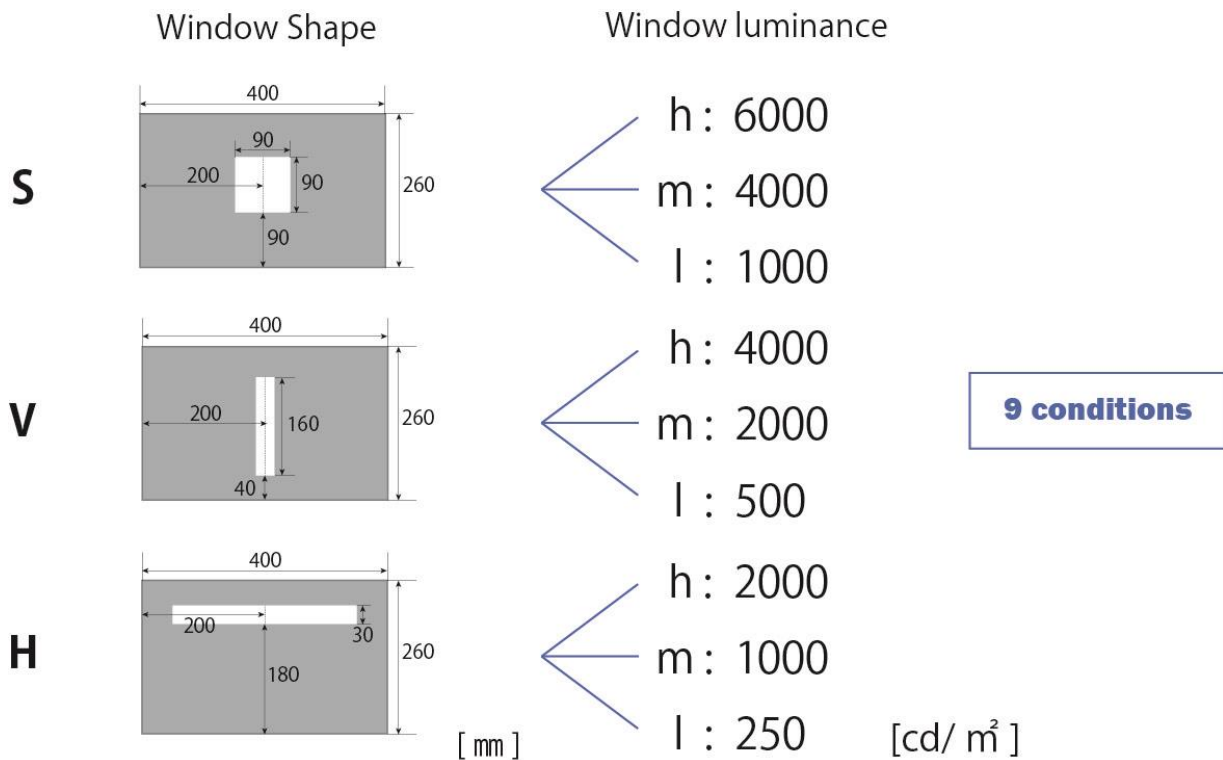


Figure 2. Experimental conditions

3. Subjects

Eight graduate and undergraduate students participated in the experiment. Of the eight subjects, 5 were male and 3 were female. Their average age was 23 years.

RESULTS

The subject's adjustment of each of three fluorescent lamps was recorded by using illuminance meter to obtain distribution of illuminance on the floor. Figure 3 shows the results of the experiment. The results of 8 subjects are plotted on a graph for each of 9 conditions. The horizontal axis is the distance from the window and the vertical axis is illuminance on the floor. The symbols of red circles indicate illuminance produced only by the light from the window. The results showed that there were large individual differences in comfortable illuminance distribution in terms of average values and also shapes of the illuminance distributions.

To grasp characteristics of the illuminance distribution adjusted by the subject, the illuminance data are replotted in Figure 4. The vertical axis is logarithmic value of the illuminance. It is clearly shown that the illuminance levels adjusted by the subjects cover a wide range of the illuminance.

To see the shape of the illuminance distribution, the illuminance value at the central position were normalized to 100 (Figure 5). We can see from this figure that there seems to be three patterns of the illuminance distribution on the floor. First, the illuminance close to the window is higher than that near the back wall. Second, the illuminance is almost uniform. Third, the illuminance in the back of the room is higher than that near the window.

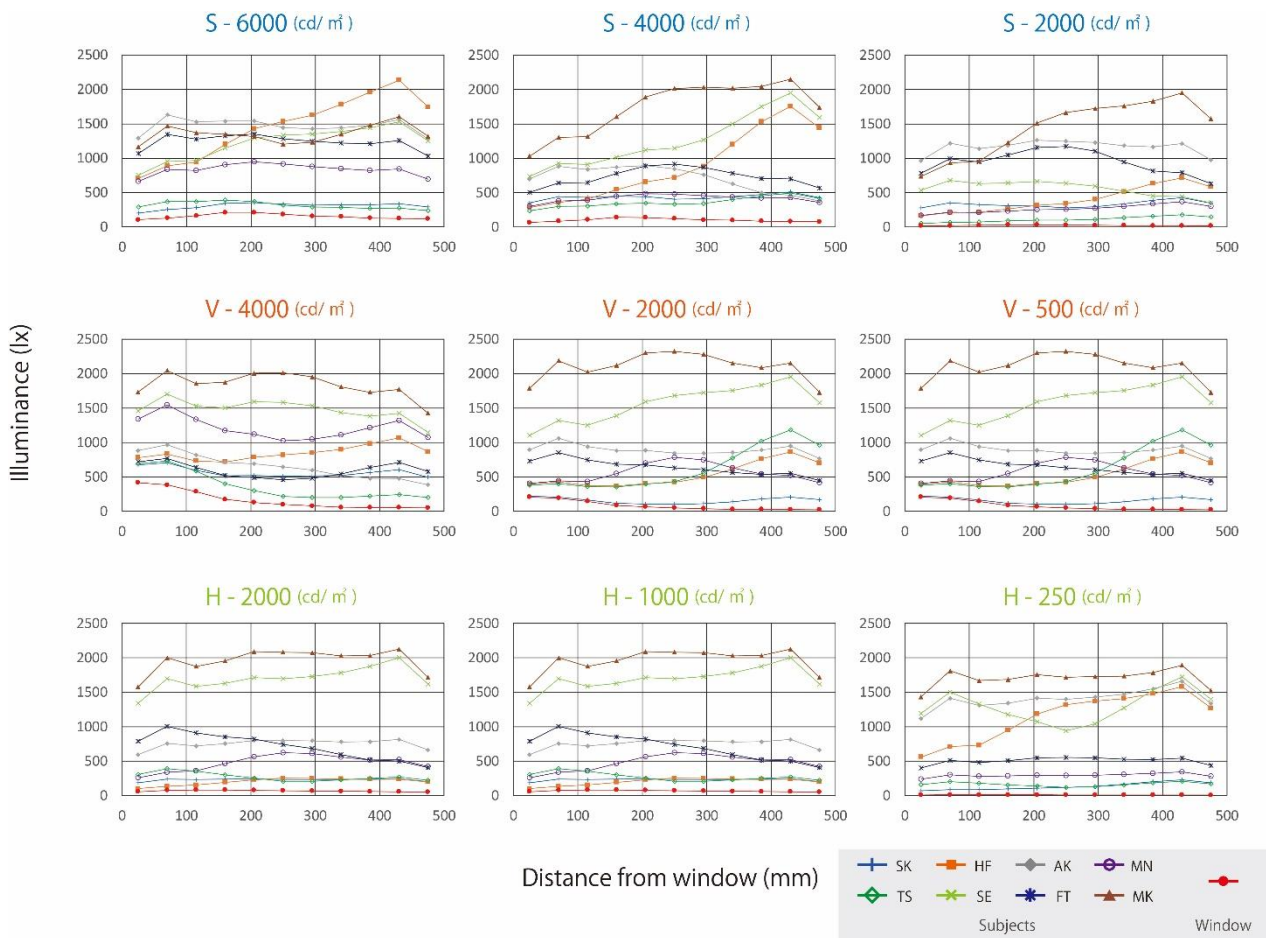


Figure 3. The results of the experiment.

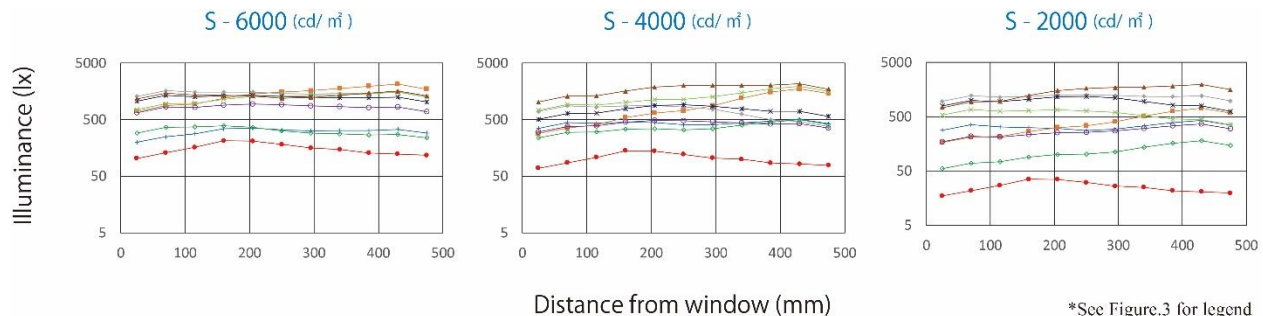


Figure 4. The results of the experiment: Logarithmic value of illuminance. (square window)

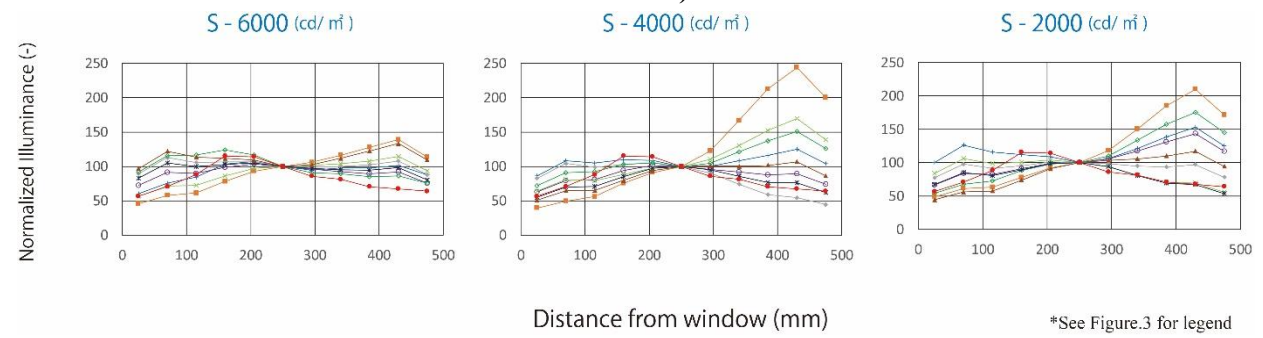


Figure 5. The results of the experiment: Normalized illuminance. (square window)

We tried to classify the comfortable illuminance distribution. By considering the characteristics shown in Figure 4 and 5, we introduced two indices shown in Figure 6. First one is the average of the illuminance values, E_M . Second one is the ratio of the average illuminance in the back of the room area and the average illuminance in the area near the window, E_B/E_W . Each of the illuminance distribution adjusted by the subjects are plotted as a point on Figure 7 showing a pattern classification by two indices E_M and E_B/E_W .

From this figure we can confirm the characteristics of the results shown in Figure 3-5. There are large individual differences in the adjustment of illuminance level, the average illuminance extends over a wide range, and there are three patterns in the illuminance distribution. The Data points in Figure 7 is scattered and does not form a clear cluster. However, it is interesting that there are many data points in the positive region of the horizontal axis, that is, the subject set the back of the room brighter.

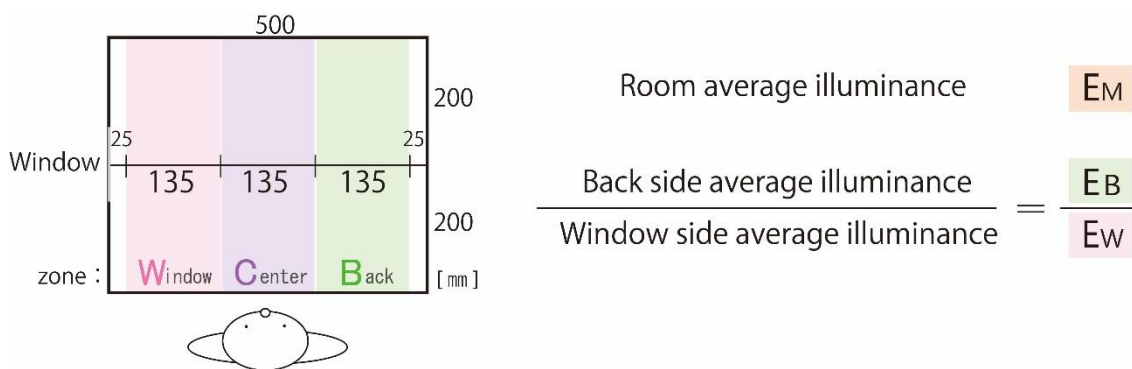


Figure 6. Indices for classification of the illuminance distribution

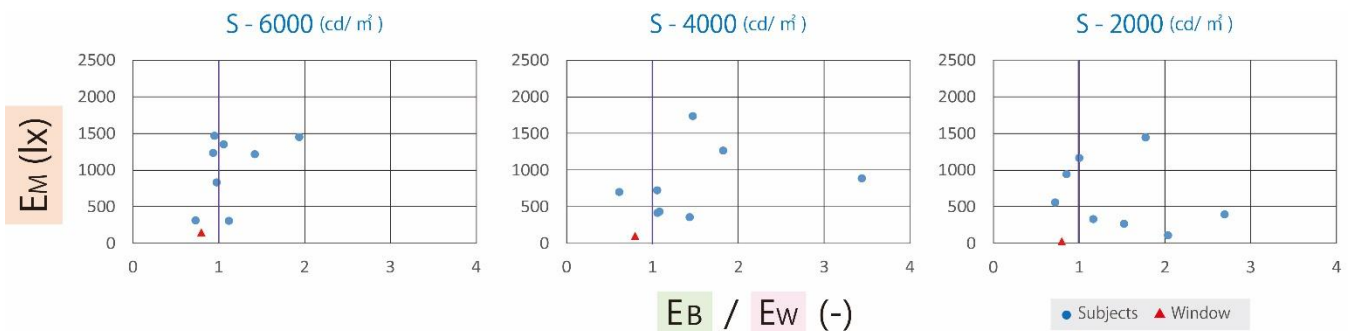


Figure 7. Data plot on E_B/E_W vs E_M graph

DISCUSSION

The results of this study suggest that that comfortable light distribution in a room with daylighting can be classified into three patterns:

- 1) the shape of the overall light distribution in the room is like that made by the daylighting from the window.
- 2) the room was illuminated almost uniformly.
- 3) brightness in the back of the room is higher than that near the window.

First pattern was seen when the subjects chose low illuminance. Second pattern was chosen by some subjects through all conditions. Third pattern was selected for both high and low illuminance, and it tended to be selected when the window luminance was not high. Finally, we mention the introspective reports of the subjects. The following are examples of the subject's views when setting comfortable lighting. "I didn't want to darken the corners.", "I adjusted the whole room to have a smooth distribution.", "I adjusted the light so that there was no shadow."

The subjects might have several different views on comfortable light distribution. There were also large individual differences in the experimental results. On the other hand, a certain pattern was found in the illuminance distribution adjusted by them. We would like to investigate a model of comfortable lighting that can apply to various spaces with daylighting.

CONCLUSION

This study suggested that comfortable light distribution in a room with daylighting from a window could be achieved by using artificial lightings that can produce the three light distribution patterns: light distribution similar to daylighting, overall uniform light distribution and light distribution brighter in the back of the room. Further research is needed to investigate how the comfortable light distributions are related to daylighting and composition of a space.

ACKNOWLEDGEMENT

This work was supported by JSPS KAKENHI Grant Number JP19K12679.

REFERENCES

1. Toshie Iwata. (2004): Comfort from Daylighting. Journal of the illuminating engineering institute of Japan, 88(10), 780-783.
2. Toshimoto Miyata. (1998): Psychological Aspect of Utilization of Daylight. Journal of the illuminating engineering institute of Japan, 82(9), 743-746.
3. S. Han and T. Ishida, "A Practical Method of Harmonizing Daylight and Artificial Light in Interior Space," Journal of light and visual environment, vol. 28, no. 3, pp. 132-138, 2004.
4. S. Han, T. Ishida, and W. Iwai, "Visual impression of lighting from a window and a ceiling: the effect of their compound ratio," Journal of light and visual environment, vol. 29, no. 1, pp. 25-33, 2005.
5. S. Han, T. Ishida, M. Iguchi, and W. Iwai, "Visual impression of lighting from a window and a ceiling: a comparison between the compound Lighting and the uniform Lighting" Journal of light and visual environment, vol. 30, no. 2, pp. 87-94, 2006.

COLOR IDENTIFICATION AFFECTED BY ILLUMINANCE LEVEL, STIMULUS SIZE AND OBSERVATION PERIOD DURING THE EXECUTION OF VISUAL TRACKING TASK

Airi Hashimoto^{1*} and Hiroyuki Shinoda²

¹ Graduate School of Information Science and Engineering, Ritsumeikan University, Japan.

² College of Information Science and Engineering, Ritsumeikan University, Japan.

*Corresponding author: Airi Hashimoto, is0274hi@ed.ritsumei.ac.jp

Keywords: eyewitness testimony, tracking task, color identification, stimulus size, observation period

ABSTRACT

Eyewitness testimony has been acknowledged as one of the most powerful forms of testimony in criminal justice. In a previous study, we reported that response to color is inconsistent as color identification is greatly affected by illuminance, stimulus size and observation period. In the experiment conducted for that study, the participant was asked to concentrate on a single task, such as color identification. However, in reality, an eyewitness is likely to observe an incident during the execution of other unrelated tasks. In the present study, the effect of a tracking task on color identification is examined, in addition to the effects of illuminance level, stimulus size and observation period.

The participant used a computer mouse to track a target that moved in a figure eight pattern on a display screen. During the tracking task, each participant was asked to find a color patch on the screen and to identify the patch's color by choosing one of 19 possibilities. After naming the color, the participant indicated their level of confidence in their color identification on a scale of 1 (not at all confident) to 5 (completely confident).

Comparisons between previous and present experimental results reveal the effect of the dual task. Some of the color stimuli in the single task experiment were identified by lighter color terms in the tracking task experiment. Moreover, confidence ratings decreased due to the smaller stimulus size. Results suggest that eyewitness statements that include descriptions of color observed in a dual task situation should be treated carefully.

INTRODUCTION

Eyewitness testimony has been acknowledged as one of the most powerful forms of testimony in criminal justice and among the most effective and important contributors to an investigation [1]. Recently, the reliability of eyewitness statements has been questioned and extensively studied in psychology [2][3]. Nevertheless, relatively little attention has been paid to the fact that visual perception can be greatly affected by conditions and that this can affect the accuracy of eyewitness descriptions. Many who are unfamiliar with this characteristic of visual perception tend to unconsciously assume that the visual perception of an eyewitness is the same as their own everyday visual experience.

Previous studies [4][5] have reported that the accuracy of eyewitnesses is affected by illuminance and viewing distance. It has also been shown that the absence or presence of colors in

a suspect's attire affects the accuracy of witness identification [6]. Other studies [7]-[10] have reported that color identification is greatly affected by illuminance and stimulus size.

Our previous study reported that color response became inconsistent because color identification is greatly affected by illuminance, stimulus size and observation period [11]. In that experiment, the participant concentrated on a single task, such as color identification. On the other hand, an eyewitness often happens to see an incident during the execution of other unrelated tasks (for example, witnessing an accident while driving). In the present study, the effect of a tracking task on color identification was examined, in addition to the effects of illuminance level, stimulus size and observation period.

EXPERIMENT

In the experiment, the participant tracked a target that moved in a figure eight pattern on a display screen (EIZO, CG2420) using a computer mouse. During the tracking task, the participant was asked to find a color patch presented in one of the two centers of the target's path over a certain period and to identify the color of the patch using one of 19 preselected color terms [12]. These terms included white, black, red, green, yellow, blue, brown, purple, pink, orange, gray, water, skin, indigo, green tea, maroon, sand, globeflower and cream. If the stimulus was undetected, the participant selected undetectable. After naming the patch color, the participant indicated their level of confidence in their color identification on a scale of 1 (not at all confident) to 5 (completely confident). The booth used in the experiment is shown in Figure 1. A numeric keypad was placed on the table in front of the participant; each participant held a computer mouse while seated on a chair at a distance of 100 cm from the display. The inside of the experimental booth was illuminated by fluorescent lamps (Panasonic, FLR40S D-SDL/M daylight color).

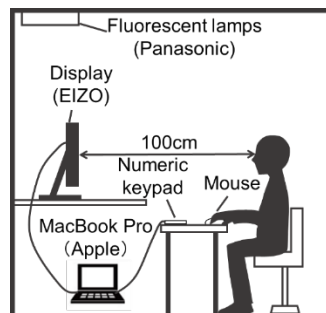


Figure 1. Experimental booth

The tracking target, cursor, and color patch were presented on an achromatic background corresponding to N5 in Munsell color. The horizontal illuminance was set to 0.2 lx at the location of the display screen. Munsell color N8 was used for the target and the cursor. Sixty-five colors were selected as stimuli from the Munsell colors and precisely simulated on the display through the calculation of CIEXYZ under the illuminance level. Sixty chromatic color samples were selected from 20 hues, with a value of 6, chroma of 2, 6, and a maximum value of 8 or 10. Five achromatic color samples (N1, N4, N6, N8, and N9) were also included. The diameter of the stimulus circle was either 5, 1 or 0.5 degrees. The duration of the stimulus presentation was either 1 or 0.5 seconds. Stimulus presentation and the recording of participant responses was done by MATLAB and the Psychophysics Toolbox Version 3 [13]-[15] on an Apple MacBook Pro 13-inch computer.

A single session consisted of the repetition of dual tasks for a stimulus of randomly selected size and duration. The stimulus presentation order in a single trial was as follows: tracking task (11-20 sec.), stimulus presentation, color term choices and confidence rate choices (see Figure 2). The

participant adapted to the illuminance for 10 minutes before the experimental session began. To examine consistency in color identification during the tracking task, the participant performed color naming twice for each of the colors and conditions in separate sessions.

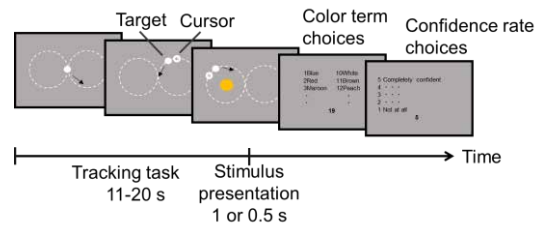


Figure 2. Experimental procedure
RESULT AND DISCUSSION

Figure 3 shows a part of the experimental result of the color identification in our previous study by one participant: (a) 0.2 lx, 5°, 0.5 s, (b) 0.2 lx, 0.5°, 0.5 s. Figure 4 shows a part of the experimental result of one participant in the present study: (a) 0.2 lx, 5°, 1 s, (b) 0.2 lx, 0.5°, 1 s, (c) 0.2 lx, 5°, 0.5 s, (d) 0.2 lx, 0.5°, 0.5 s. Symbols in the charts show responses by the participant to color stimuli of plotted chromaticities. Crosses represent color stimuli undetected in both of the two presentations.

Asterisks, open circles, and dots indicate unstable responses in the sense that the color stimulus drew two different responses by the participant. Asterisks represent color stimuli undetected in one of the presentations. Dots represent color stimuli to which both achromatic and chromatic color terms were assigned. Open circles represent color stimuli to which two different chromatic color terms were assigned.

All other symbols show stable responses in the sense that the color stimulus was identified with the same color term in both of the presentations. A broken line is the color gamut of the display; a solid line shows spectrum loci. Responses to five achromatic color stimuli are plotted on the right of the figure.

Comparisons between Figure 3(a) and 4(a), 3(b) and 4(b) reveal the effect of the dual task. Some of the color stimuli identified as “brown” and “blue” in the single task experiment, for instance, are described with light color terms such as “orange” and “water” in the tracking task experiment. The effect of stimulus size is indicated by comparing Figures 4(a) to (b) and (c) to (d). Unstable responses (dots or asterisks) increased and the number of color stimuli identified as “water”, “purple” or “unstable” increased with a stimulus size of 0.5°. Comparisons between Figures 4(a) and (c), (b) and (d) reveal the effect of presentation duration. Unstable responses (dots) and the number of color stimuli named as “water” increased.

Figure 5 shows a part of the experimental results for confidence rate: (a) 0.2 lx, 5°, 1 s, (b) 0.2 lx, 0.5°, 1 s, (c) 0.2 lx, 5°, 0.5 s, (d) 0.2 lx, 0.5°, 0.5 s. The symbols in the charts show confidence level responses by the participant to the color stimuli of the plotted chromaticities. As the symbols become a darker color, confidence level decreases. Crosses represent color stimuli undetected in both presentations. Squares represent unstable responses in the sense that the color stimulus drew two different responses by the participant.

The effect of stimulus size is can be seen by comparing Figures 5(a) to (b) and (c) to (d). Confidence decreased due to smaller stimulus size. The confidence level of 5 (completely confident) was assigned by the participant to undetectable responses.

All of the results suggest that eyewitness statements including descriptions of color observed under poor conditions should be carefully treated or interpreted. The result of the present study will help judicial officials to properly evaluate eyewitness statements that include color information.

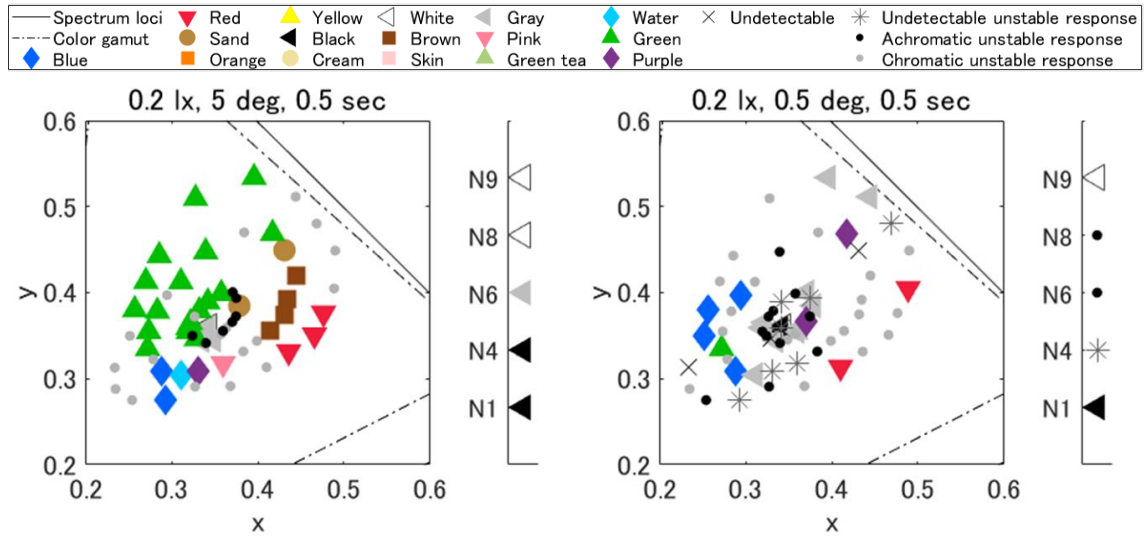


Figure 3. Result of the previous study (single task)

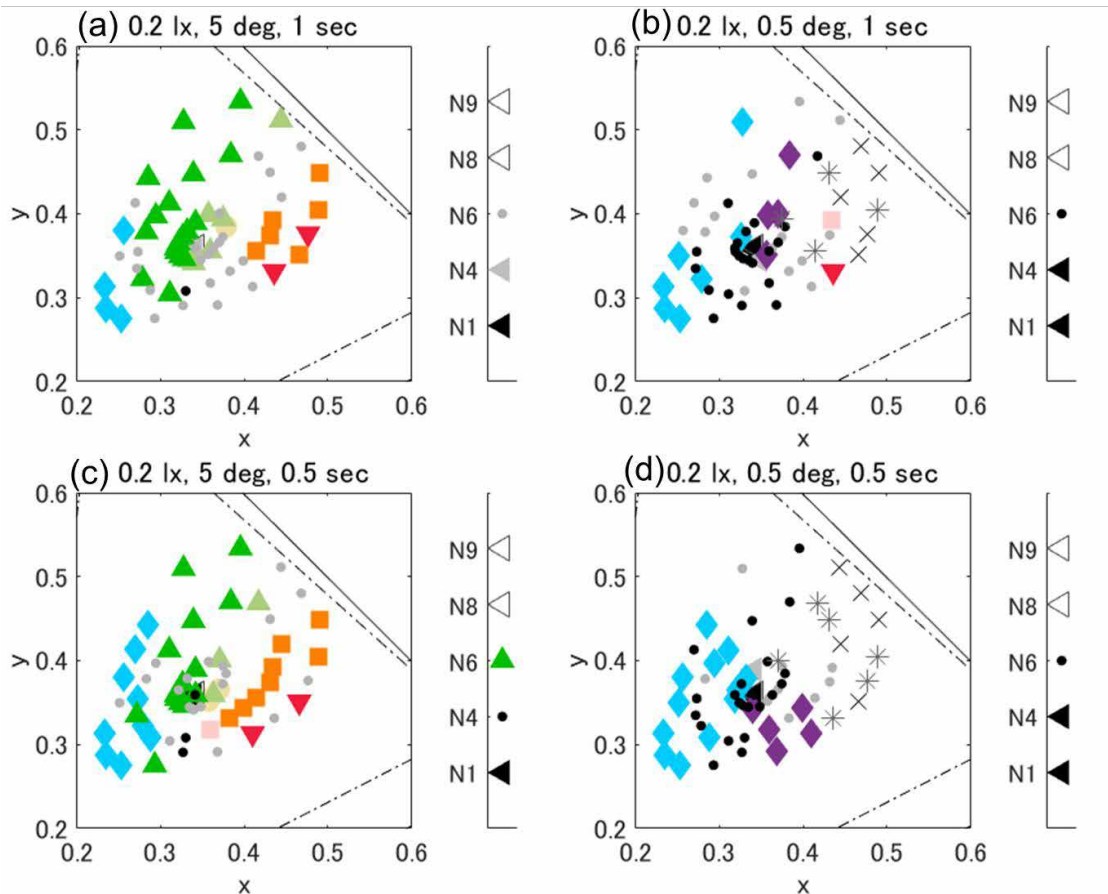


Figure 4. Result of the present study (tracking task)

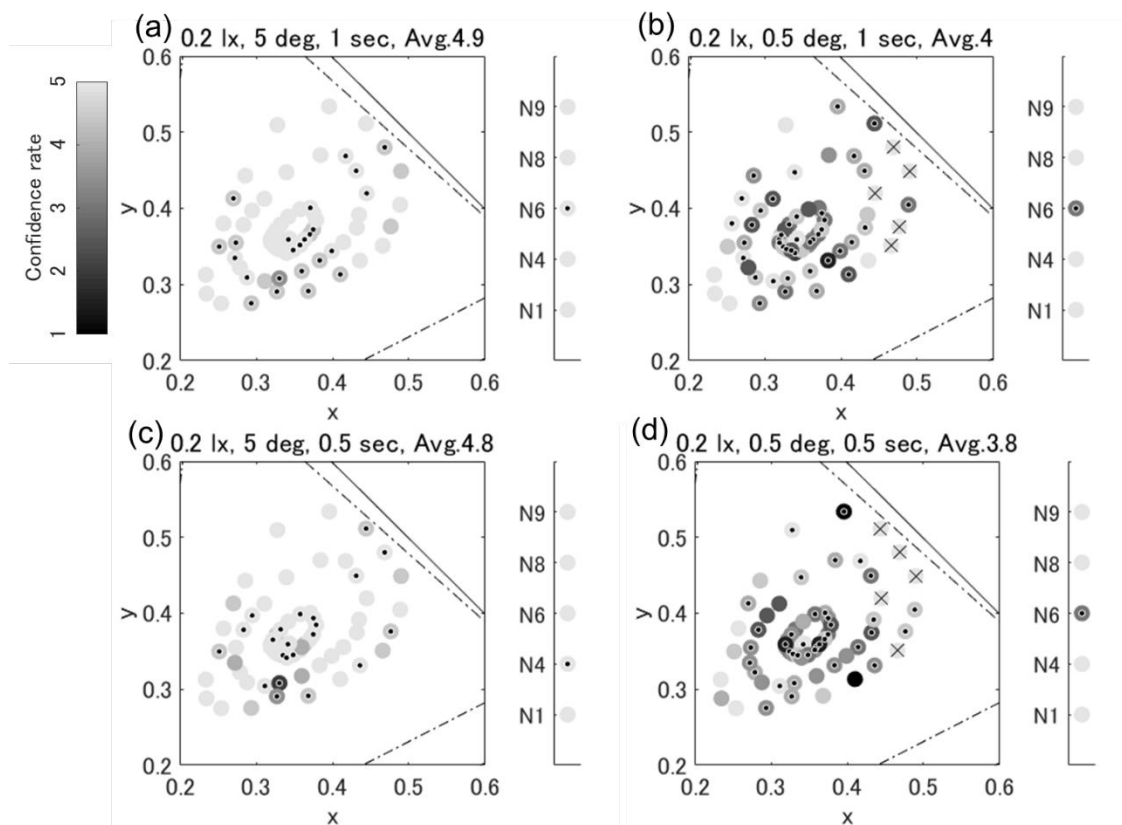


Figure 5. Result of the present study (tracking task)

REFERENCES

1. Cindy Laub, Brian H. Bornstein (2008). Juries and eyewitnesses. in Encyclopedia of Psychology and law, doi: 10.4135/9781412959537
2. Amina Memon (1980). Munsterberg's Legacy: What Does Eyewitness Research Tell Us About the Reliability of Eyewitness Testimony?. Applied Cognitive Psychology, 22, 841-851.
3. Robert Buckhout (1980). Nearly 2,000 witnesses can be wrong. Bulletin of Psychonomic Society, 16 (4), 307-310.
4. Daniel A. Yarmey (1986). Verbal, visual, and voice identification of a rape suspect under different levels of illumination. Journal of Applied Psychology, 71 (3), 363-370.
5. Willem A. Wagenaar, Juliette H. Van Der Schrier (1996). Face recognition as a function of distance and illumination: a practical tool for use in the courtroom. Psychology, Crime & Law, 2 (4) 321-332.
6. Angela D. West, Billy J. Long (1993). The Effects of Color on Eyewitness Identification Accuracy: Implications for Criminal Justice. Journal of Contemporary Criminal Justice, 9 (4) 343-360.
7. W. E. Knowles Middleton, Eleanor G. Mayo (1952). The Appearance of Colors in Twilight. Journal of the Optical Society of America, 42 (2), 116-121.
8. Taiichiro Ishida (2002). Color Identification Data Obtained from Photopic to Mesopic Illuminance Levels. Color Research and Application, 27 (4), 252-259.

9. Akira Yujiri (1990). Color Appearance of Surface Colors for Various Illuminance Levels: Effect of Stimulus Size. *Journal of Optics of Japan*, 19 (2), 97-104 (in Japanese).
10. Masaru Ryuchi, Taiichiro Ishida (2000). Color identification under mesopic lighting environment: effect of stimulus size. *Proc. AIC2000*, 39-42.
11. Airi Hashimoto, Hiroyuki Shinoda (2018). Color Identification Affected by Illuminance Levels, Stimulus Size and Observation Period. *11th ALC Proceedings*, 211-213.
12. Ichiro Kutiki, et al. (2017). The modern Japanese color lexicon. *Journal of Vision*, 17 (3), 1-18.
13. David H. Brainard (1997). The Psychophysics Toolbox. *Spatial Vision* 10, pp. 443-446.
14. Denis G. Pelli (1997). The VideoToolbox software for visual psychophysics: Transforming numbers into movies. *Spatial Vision*, 10, 437-442.
15. Mario Kleiner, David Brainard, and Denis Pelli (2007). What's new in Psychtoolbox-3?: Perception. *36 ECVF Abstract Supplement*.

EFFECT OF COLOR SHIFT CAUSED BY COLORED LIGHT ADDITION OR SUBTRACTION ON SUBJECTIVE EVALUATION OF IMAGE QUALITY

Yasuko Kosaka^{1*} and Hiroyuki Shinoda²

¹ Graduate School of Information Science and Engineering, Ritsumeikan University, Japan.

² College of Information Science and Engineering, Ritsumeikan University, Japan

*Corresponding author: Yasuko Kosaka, is0257hk@ed.ritsumei.ac.jp

Keywords: image quality, subjective evaluation, color shift, superimposition

ABSTRACT

We studied subjective image quality evaluation of images whose color is shifted uniformly. In the experiment, a reference image and a test image with a color shift were successively presented on a display screen. An observer evaluated the quality of the test image compared with the reference using a nine-grade rating scale. The result showed that color shifts caused by colored light addition degraded image quality; in contrast, some shifts caused by colored light subtraction improved the quality.

INTRODUCTION

As mobile devices, such as smartphones and tablets, are now widespread, their display screens are viewed in various lighting environments. In some situations, the colors of images may change depending on the influence of colored light. This can change the image quality. In our previous study [1] [2], image quality was subjectively evaluated when the colors of images were uniformly shifted in various hue directions with colored light superimposition, and consequently image quality was degraded. It is desirable to prevent image quality from degrading due to colored light superimposition and to perform color corrections that improve image quality. To research color shift conditions that improve image quality, this study evaluated the quality of images with uniform color shift caused not only by addition of colored light but also by subtraction.

When an additive color shift occurs, the intensity increases in inverse proportion to the contrast decrease. Conversely, when a subtractive color shift occurs, the intensity decreases in inverse proportion to the contrast increase. Therefore, it is possible to optically simulate any type of color shift caused by addition or subtraction of colored light by manipulating the intensity and the contrast of each RGB channel in a display. In the present experiment, observers with normal color vision observed two images displayed successively; a reference image with no color shift and a test image with color shift. They repeatedly performed subjective evaluation of the image quality relative to the reference image.

EXPERIMENT

Stimulus Images

In the experiment, 24 images downloaded from the Kodak lossless true color image suite [3] were processed to create reference and evaluation images. The stimulus image was created by independently manipulating the three luminance values, Y_{Ri} , Y_{Gi} and Y_{Bi} , of each pixel of the Kodak image using equation (1).

$$\begin{aligned}
Y'_{Ri} &= I_R \bar{Y}_R + I_R C_R (Y_{Ri} - \bar{Y}_R) \\
Y'_{Gi} &= I_G \bar{Y}_G + I_G C_G (Y_{Gi} - \bar{Y}_G) \\
Y'_{Bi} &= I_B \bar{Y}_B + I_B C_B (Y_{Bi} - \bar{Y}_B)
\end{aligned}
\tag{1}$$

where Y_{Ri} , Y_{Gi} , and Y_{Bi} represent the R, G, and B luminance values, respectively, of the i th pixel in the original image; Y'_{Ri} , Y'_{Gi} , and Y'_{Bi} represent the R, G, and B luminance values, respectively, of the i th pixel in the stimulus image; and \bar{Y}_R , \bar{Y}_G , and \bar{Y}_B represent the mean R, G, and B luminance values, respectively, of the original image. Images of varying intensity and contrast were reproduced by changing the intensity adjustment coefficients (I_R , I_G , I_B) and the contrast adjustment coefficients (C_R , C_G , C_B) in equation (1).

In this experiment, we set $I_R = I_G = I_B = 0.5$ and $C_R = C_G = C_B = 0.5$ to create reference images without superimposition or subtraction of colored light. I_R, I_G were selected from 0.01, 0.1, 0.2, 0.3, 0.4, 0.5, 0.6, 0.7 or 0.8, and I_B was selected from 0.01, 0.1, 0.2, 0.3, 0.4, 0.5, 0.7, 1.1 or 1.5. Various color shifts were generated by combining the three coefficients. The contrast adjustment coefficients (C_R, C_G, C_B) were set inversely proportional to the luminance adjustment coefficients, that is, $C_R = 0.25/I_R$, $C_G = 0.25/I_G$, $C_B = 0.25/I_B$.

Figure 1 shows a subset of the stimulus images. The upper left image is a reference image, and the others are test images with various color shifts. The intensity adjustment coefficients and addition or subtraction of RGB intensity relative to the reference image are shown below each image.

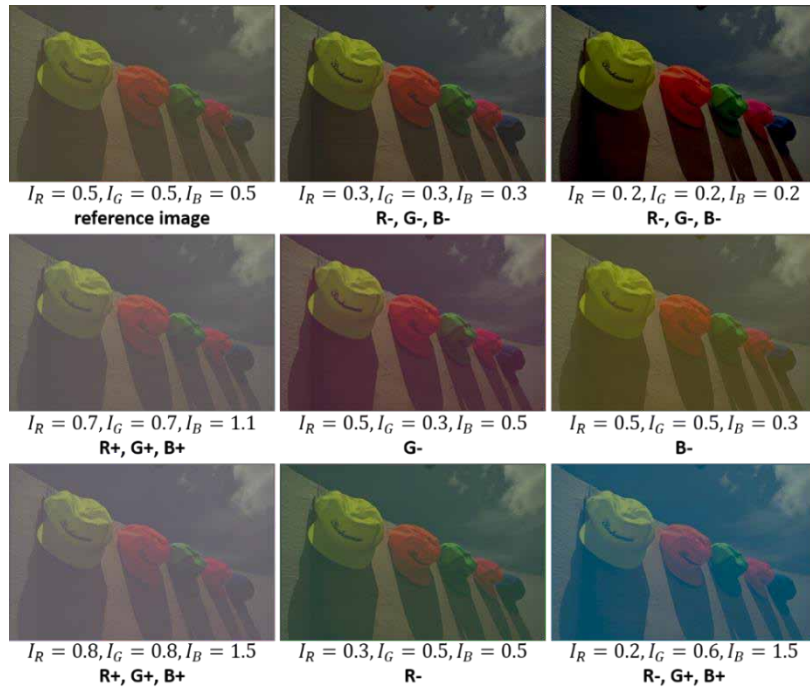


Figure 1. Subset of stimulus images

Method

The experiments were conducted in a darkroom. Figure 2 illustrates the flow of the experiment. In one sequence, an observer was presented with a reference image, a blank, and a test image in order, after which the evaluation was conducted. An observer evaluated the image quality of the test image

compared to the reference using extended degradation category rating (DCR) method presented in Table 1. DCR is one of the experimental methods prescribed in the ITU-T Recommendations published by the International Telecommunications Union [4], where an observer evaluates image degradation using a score of 1–5. As conventional DCR does not consider image improvements, we adopted extended DCR where an observer evaluates both the degradation and improvement using a scale of 1–9.

There were 189 combinations of intensity adjustment coefficients, which produced a total of 4,536 test images (24 reference by 189 color shifts). Stimulus images were generated and presented using Matlab and PsychToolbox [5] [6] [7]. There was one observer.

Table 1. Extended DCR

DCR	Evaluation criteria
1	Very annoying
2	Annoying
3	Slightly annoying
4	Deterioration perceptible, but not so annoying
5	Imperceptible
6	Improvement perceptible, but not so favorable
7	Slightly favorable
8	Favorable
9	Very favorable

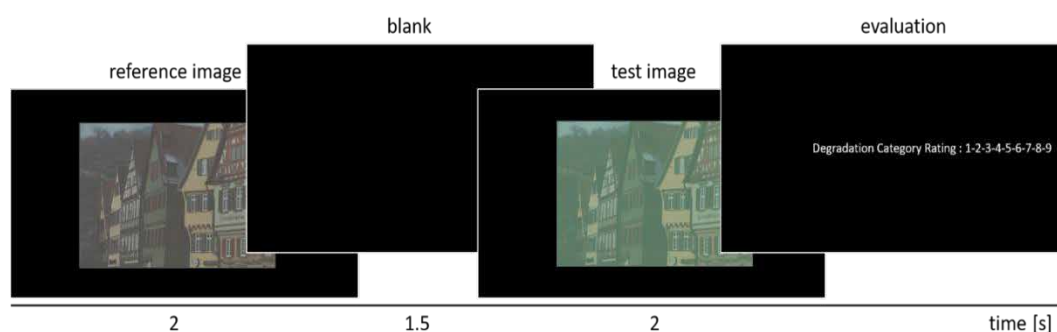


Figure 2. Experimental flow

EXPERIMENTAL RESULT

Figure 3 shows the average responses for all 24 images from one observer. The graph on the left represents the mean DCR, and the two graphs on the right represent the DCR from different viewpoints. There were three tendencies common to the results of all 24 images: 1. The DCR was 5 (imperceptible) without any color shift at $I_R = I_G = I_B = 0.5$, 2. As the color shift due to the colored light addition became larger, the DCR gradually decreased and finally reached 1 (very annoying), 3. As the color shift due to colored light subtraction became larger, the DCR gradually increased to a maximum value was 8 (favorable) or 9 (very favorable). For some images, however, the DCR decreased rapidly when the colored light subtraction exceeded a certain level.

Comparison of the DCR change due to the color shift of each RGB shows that the DCR was higher in G and B than in the R channel when colored light was subtracted. We compared the results of three images containing more R than G or B (Figure 4), containing R, G, and B almost equally (Figure 5), and containing less R than G or B (Figure 6). The color shift of G and B resulted in higher DCR scores than those for an R shift in all cases. However, the effect decreased as the R proportion increased.

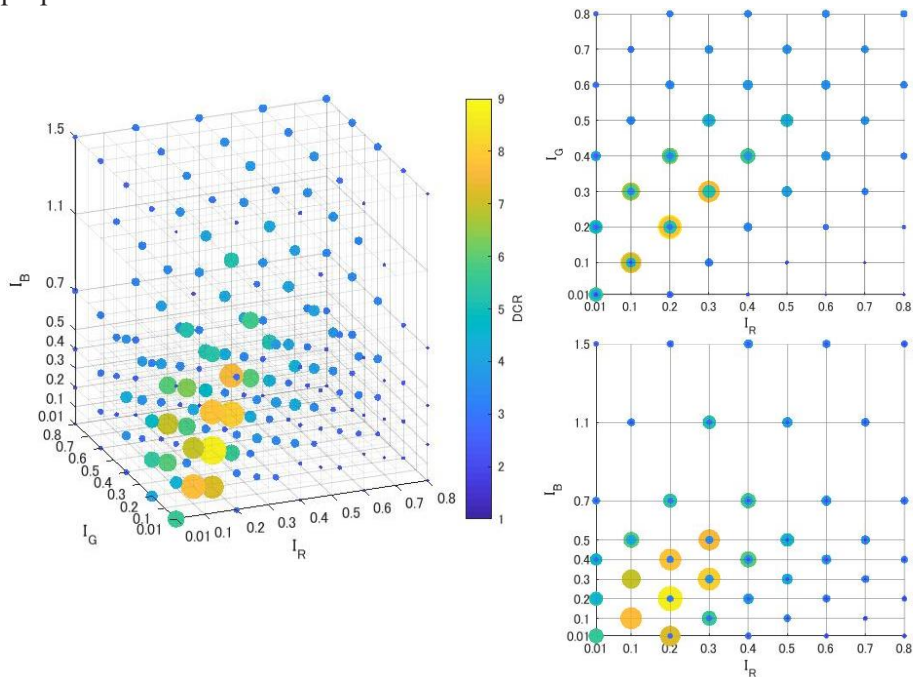


Figure 3. Average of experimental results (24 images viewed by one observer)

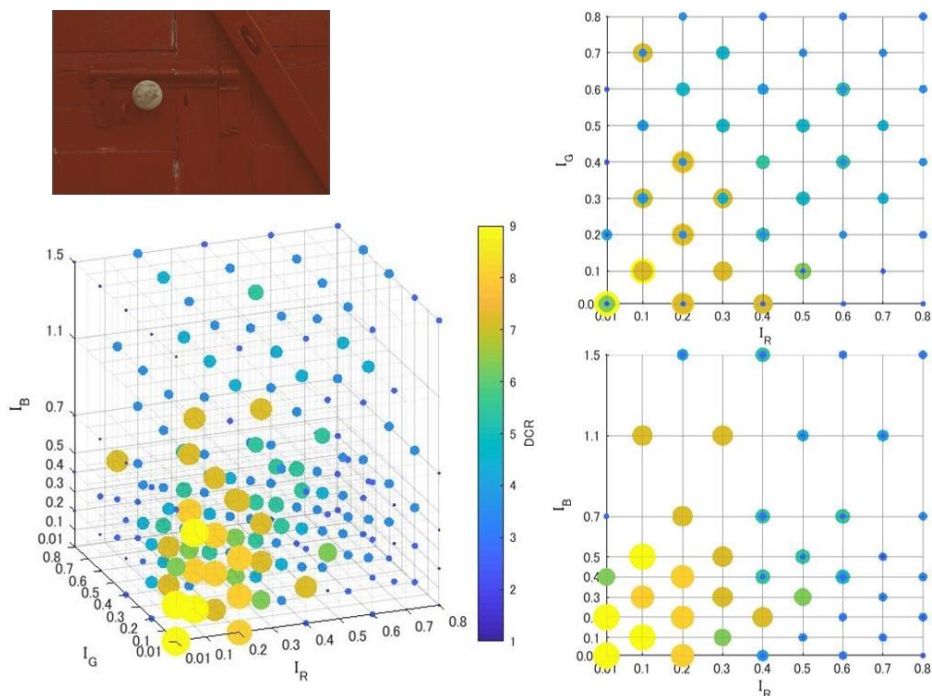


Figure 4. Results for an image containing more R than G and B

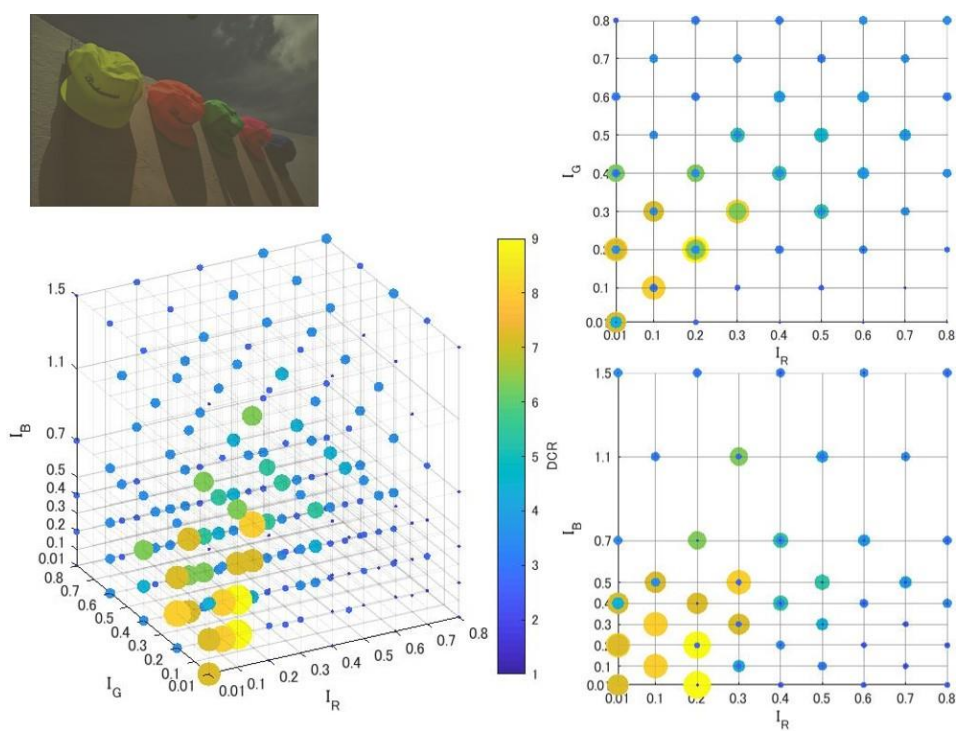


Figure 5. Results for an image containing R, G, and B almost equally

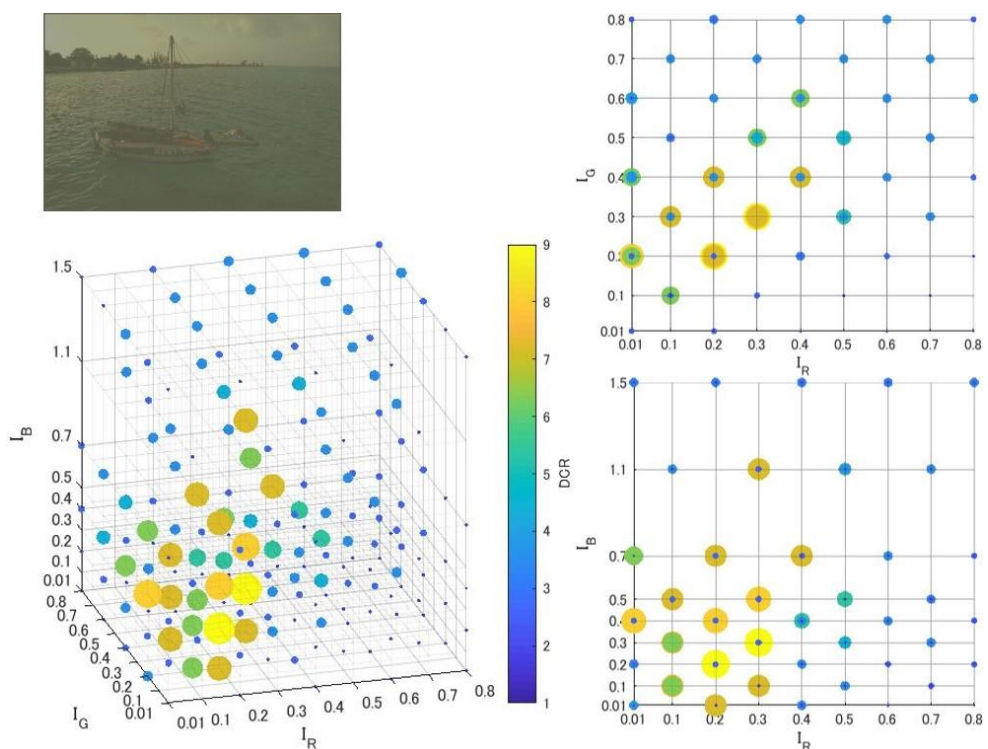


Figure 6. Results for an image containing less R than G and B

DISCUSSION

Although image quality degraded under the additive color shift conditions, it improved under the subtractive color shift conditions. However, too much subtraction caused image quality degradation inversely. Degradation caused by an additive color shift was gradual, but degradation caused by a subtractive color shift was rapid. With regard to this tendency, some observers described that the image with additive color shift was hard to see and that with excessive subtraction caused an unnatural impression.

The results in Figure 4, 5, and 6 showed that subtractive color shifts in the directions of G and B gave higher DCR scores than R did for those three images, indicating that G and B contribute to image quality improvement. However, this tendency may depend on the observer, who is using subjective perception. It should be noted that the effect depends on the characteristics of the image.

For optimal color correction of an image degraded by color light superposition, it is necessary to make adjustments according to the image degradation degree and image characteristics. We would like to achieve image quality improvement by generalizing the experimental results for each image and deriving a function that outputs the image quality when the inputs are brightness, chromaticity and characteristics of the image as input.

REFERENCES

1. Yasuko Kosaka and Hiroyuki Shinoda, Subjective Assessment of Image Quality Degradation Caused by Uniform Color Shift, Japan, ALC2018, 2018.
2. Yasuko Kosaka and Hiroyuki Shinoda, Subjective Assessment of Image Quality Degraded by Uniform Color Shift, ACA2018, 2018.
3. Rich Franzen, Kodak Lossless True Color Image Suite, Retrieved from <http://r0k.us/graphics/kodak/>, 2007.
4. ITU-T Rec. P. 910, Subjective Video Quality Assessment Methods for Multimedia Applications, 2008.
5. David H. Brainard. The Psychophysics Toolbox: Spatial Vision, 10, 443-446, 1997.
6. Denis G. Pelli. The VideoToolbox software for visual psychophysics: Transforming numbers into movies, Spatial Vision, 10, 437-442, 1997.
7. Mario Kleiner, David Brainard, and Denis Pelli. What's new in Psychtoolbox-3?: Perception, 36 ECVF Abstract Supplement, 2007.

CONTRAST EFFECT OF WINDOW VIEW AND INDOOR SPACE ON THE PERCEIVED BRIGHTNESS OF A ROOM EVALUATED BY RATING SCALE

Shun Ito^{1*} and Hiroyuki Shinoda²

¹*Graduate School of Information Science and Engineering, Ritsumeikan University, Japan.*

²*College of Information Science and Engineering, Ritsumeikan University, Japan.*

*Corresponding author: Shun Ito, is0294fx@ed.ritsumeai.ac.jp

Keywords: Spatial brightness, Window, Daylight, Display, Rating scale

ABSTRACT

Various brightness indices have been developed in consideration of the characteristics of visual perception. However, these indicators have been developed only for a windowless room. In this study, we examined the spatial brightness of a room with a window through which daylight enters and outdoor scenery can be viewed. In our previous study, a brightness-matching experiment was created on a computer display. However, the brightness matching was relatively difficult and the results showed large differences between individual observers. In the present study, the brightness of a room presented on a display image was evaluated with a rating scale instead of brightness matching. The obtained results show that the observers' evaluation was consistent and individual differences were small. The experimental result showed a similar tendency to that in our previous study.

INTRODUCTION

The diversification of lighting methods enables us to create various visual environments. However, recent studies have reported many situations in which the horizontal illuminance (generally used as a brightness index) does not correspond to human perception. When people see a space, they overlook not only the floor but also the entire room. This means that the horizontal illuminance does not always represent the perceived brightness. Various brightness indices have been developed in consideration of the characteristics of visual perception. Although these indicators function well for windowless rooms, the influence of daylight is not considered. In this study, we examined the spatial brightness of a room with a window through which daylight enters and outdoor scenery can be viewed.

Previous studies have reported that the spacial brightness of a room with a window was lower than that of a windowless room with equivalent horizontal illuminance [1][2]. Other studies showed that such brightness inhibition was stronger in a room with a scenery viewed through a window, compared to a room with a frosted window [3][4]. In those studies, scale models were used as stimuli for psychophysical evaluation and it was costly and time-consuming to modify the experimental conditions. In our previous study, a brightness-matching experiment was conducted on a computer display [5][6]. The experimental results showed the same tendency as shown in the previous studies using a scale model, suggesting the validity of brightness evaluation on a computer display. However, the brightness matching was relatively difficult and the results showed large differences between individual observers. In the present study, the brightness of a room presented on a display image was evaluated with a rating scale instead of brightness matching.

METHOD

In the experiment the relative luminance distributions in the overall view of a room with window scenery having various illuminance levels were precisely simulated on a liquid crystal display (LCD). The image of the room with a window (Window Room Image) was presented on the display (EIZO CS230), which was created by combining the image of an indoor space illuminated by daylight with scenery viewed through a window (Window-Daylight Image) and an image of the indoor space illuminated only by ceiling light (Ceiling Light Image). When performing the image calculation, calculated luminance values were used instead of the display RGB values. Therefore, the actual physical conditions were faithfully recreated on the display screen. Furthermore, various outdoor and indoor conditions were expressed by multiplying each image with an intensity adjustment coefficient (Figure 1). These images were generated and presented using Matlab and Psychophysics Toolbox version 3 [7][8][9].

$$\begin{array}{c}
 rD \\
 tD
 \end{array}
 \times
 \begin{array}{c}
 \text{Window-Daylight Image} \\
 \text{Image}
 \end{array}
 +
 \begin{array}{c}
 rC \\
 tC
 \end{array}
 \times
 \begin{array}{c}
 \text{Ceiling Light Image} \\
 \text{Image}
 \end{array}
 =
 \begin{array}{c}
 \text{Window Room Image} \\
 \text{Image}
 \end{array}$$

Figure 1. Experimental image

In the experiment, the test image and reference image were alternately presented to 4 observers. In the reference image, the window-daylight intensity adjustment coefficient rD and the ceiling light intensity adjustment coefficient rC were set to predetermined values. In the test image, the window-daylight intensity adjustment coefficient tD and the ceiling light intensity adjustment coefficient tC were set to predetermined values. In a single trial, two achromatic images, reference and test, were successively presented for a duration of 5 sec on the display (Figure 2). Each observer received two different instructions: evaluate the brightness by focusing around the wall and evaluate by focusing around the floor. Observers were also instructed to report the perceived brightness of the room in the test image relative to that in the reference image with the following rating scale: “darker,” “slightly darker,” “same,” “slightly brighter,” and “brighter” (Table 1).

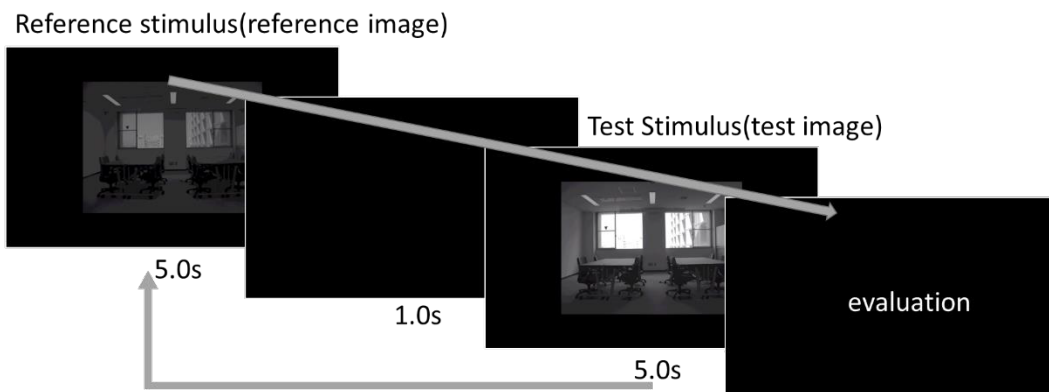


Figure 2. Experimental procedure

Score	Rating Word
1	Darker
2	Slightly darker
3	Same
4	Slightly brighter
5	Brighter

Experiments were conducted in a dark room using a liquid crystal display. Each observer viewed the display through a D-up viewer designed to occlude one eye and restrict the visual field to the display image. The image was perceived as a three-dimensional space because the D-up viewer prevented recognition of a flat display panel by depriving a binocular disparity cue; the image itself also contained several pictorial cues for depth such as a linear perspective.

In order for the image to be displayed within upper luminance limit of the display, the actual luminance was compressed to 1/137. The rD and, rC of the reference image were set to 1, 0.25, or 0.0625 (Table 2). The tD and, tC of the test image were set to 1, 0.5, 0.25, 0.125, or 0.0625 (Table 3).

Table 2. Reference image adjustment coefficient

rD	Combined coefficient for each rC value		
	1	0.25	0.0625
1	(1, 1)	(1, 0.25)	(1, 0.0625)
0.25	(0.25, 1)	(0.25, 0.25)	(0.25, 0.0625)
0.0625	(0.0625, 1)	(0.0625, 0.25)	(0.0625, 0.0625)

Table 3. Test image adjustment coefficient

tD	Combined coefficient for each tC value				
	1	0.5	0.25	0.125	0.0625
1	(1, 1)	(1, 0.5)	(1, 0.25)	(1, 0.125)	(1, 0.0625)
0.5	(0.5, 1)	(0.5, 0.5)	(0.5, 0.25)	(0.5, 0.125)	(0.5, 0.0625)
0.25	(0.25, 1)	(0.25, 0.5)	(0.25, 0.25)	(0.25, 0.125)	(0.25, 0.0625)
0.125	(0.125, 1)	(0.125, 0.5)	(0.125, 0.25)	(0.125, 0.125)	(0.125, 0.0625)
0.0625	(0.0625, 1)	(0.0625, 0.5)	(0.0625, 0.25)	(0.0625, 0.125)	(0.0625, 0.0625)

RESULT AND DISCUSSION

The experimental results are shown in Figures 3 and 4. The graphs show each (rD , rC) setting for the reference image. The different symbols represent differences in tD of the test image. Five data points with the same symbol connected by straight lines correspond to the five test image conditions. The horizontal axes of the graph indicate the mean horizontal illuminance (lx) in the room corresponding to the test image. The vertical axes of the graph indicate the rating scale. The mean illuminance values of the test image were calculated as the sum of the mean illuminance values corresponding to the window-daylight image and the ceiling light image.

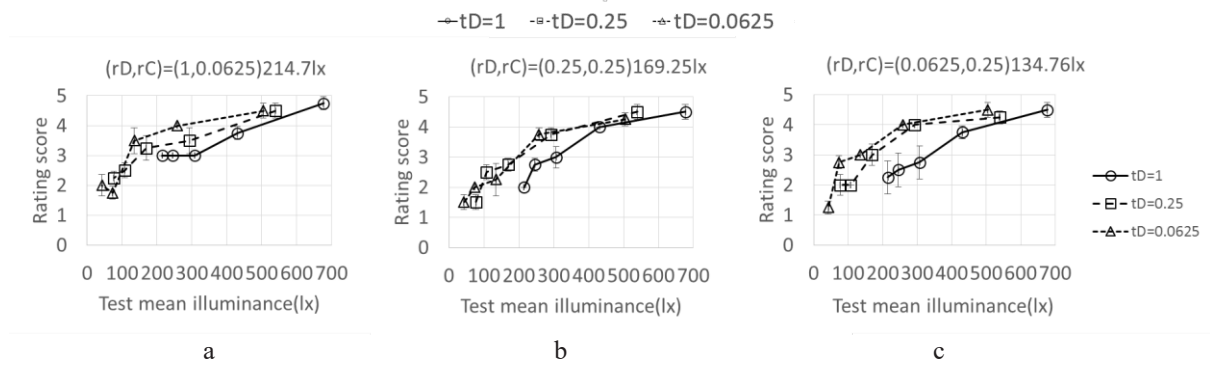


Figure 3. Evaluated brightness around the wall

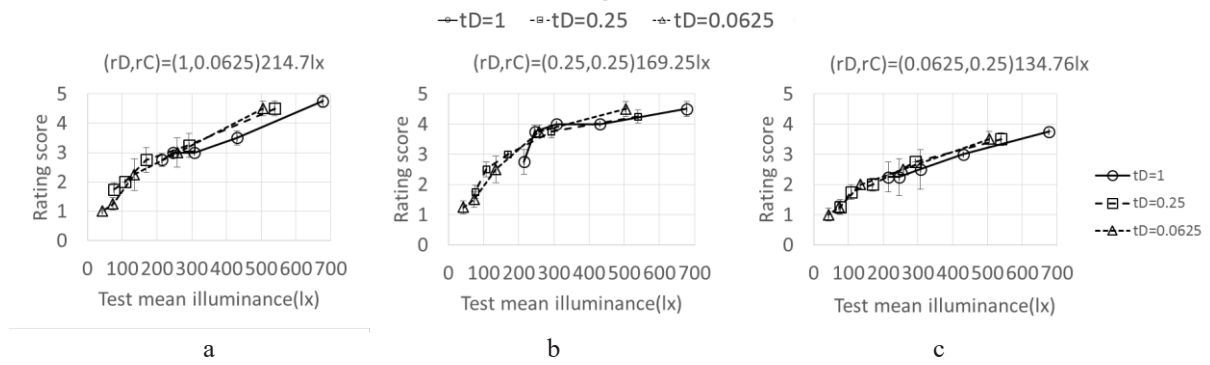


Figure 4. Evaluated the brightness around the floor

The results show that when rD and tD are equal, tD data are plotted on the baseline. For instance, the $tD=1$ line is the baseline in Figure 3a. However, under the condition $tD < rD$, the result is plotted above the baseline, indicating that the subject evaluated the test image with a score higher than that of the reference image. In other words, if the indoor illuminances of the reference image and test image are the same, then the interior of the reference image appears darker. In contrast, under the condition $tD > rD$, the results are plotted below the baseline, indicating that the room illuminance of the test image was set to a lower score. Figure 4 shows that all lines are close to the baseline, indicating that the influence of the window view is reduced.

The above results show that the observers' evaluations were consistent, and individual differences were small. The division of the instructions made the evaluation easier and the results were consistent. The experimental results show a tendency similar to that in our previous study. These results show that the spatial brightness of a windowed room was affected not only by the change in illuminance due to daylight entering the window but also by the perceived brightness for scenery viewed through a window. In other words, even if the illuminance increases owing to daylight incidence, if the scenery viewed through a window is recognized as a bright space, then the indoor space appears darker in comparison.

REFERENCES

- (1) Yamaguchi, H., and Shinoda, H. 2007, Journal of Illuminating Engineering Institute of Japan 91 (5) 266-271 (in Japanese).
- (2) Yamaguchi, H., Maruyama, T., and Shinoda, H. 2014, Journal of Illuminating Engineering Institute of Japan 98 (11) 593-599 (in Japanese).
- (3) Tanaka, R., Shinoda, H., Seya, Y. 2014, Perception 43 (Supplement) 163.
- (4) Yamada, S., Tanaka, R., Shinoda, H., and Seya, Y. 2015, Proc. of AIC2015, 1211-1216.
- (5) Ito, S., Shinoda, H. Y.2018, Proc. of ALC2018, Kobe(Japan)
- (6) Ito, S., Shinoda, H. Y.2018, Proc. of ACA2018, Chiang Mai(Thailand)
- (7) David H. Brainard. The Psychophysics Toolbox: Spatial Vision, 10, 443-446, 1997
- (8) Denis G. Pelli. The VideoToolbox software for visual psychophysics: Transforming numbers into movies, Spatial Vision, 10, 437-442, 1997
- (9) Mario Kleiner, David Brainard, and Denis Pelli. What's new in Psychtoolbox-3: Perception, 36 ECVF Abstract Supplement, 2007

Display Primaries' Spectral Power Distributions Acquired from RGB Images by Using Gradient Descent

Ryuta Tetsuo^{1*} and Hiroyuki Shinoda²

¹Graduate School of Information Science and Engineering, Ritsumeikan University, Japan.

²College of Information Science and Engineering, Ritsumeikan University, Japan

*Corresponding author: Ryuta Tetsuo, e-mail (is0267pf@ed.ritsumei.ac.jp)

Keywords: Display, Digital camera, Sensor's spectral sensitivities, Spectral power distributions, Gradient descent

ABSTRACT

Display calibration is usually performed with XYZ tristimulus values using a colorimeter. In this study, we propose a method by which to estimate the spectral power distribution of a display using a digital camera. The tasks of the proposed method are acquisition of the spectral sensitivities of camera sensors and estimation of the spectral irradiances of display primaries. The proposed algorithm was verified by an experiment using a digital camera and a liquid crystal display. Various colored lights emitted from the display with known spectral power distributions were used to estimate the spectral sensitivities of the camera sensors. Then the spectral irradiances of the display primaries were recovered by photographed image with the camera whose sensors' spectral sensitivities were obtained. Gradient descent was used for all estimations. The recovered spectral irradiances of the display primaries were compared with those measured by a spectrophotometer in order to evaluate the performance of the proposed algorithm.

INTRODUCTION

Colors on a display are created by the additive color mixture of three primaries, i.e., RGB. The additive color mixture is calculated by vector summation in CIEXYZ color space. Therefore, display calibration is usually performed with XYZ tristimulus values using a colorimeter. However, there is a limit to processing the color of the display in CIEXYZ color space. For example, for the case in which an anti-glare or anti-reflection filter is overlaid on display screens, not only the spectral transmittance of the filter but also the spectral power distribution (SPD) of the display is required. With respect to the recovery of the spectral reflectance of surfaces, several methods [1][2][3] have been proposed. However, these methods require specific instruments for measurements. Therefore, in this study, we propose a method for estimating the SPD of a display using a relatively inexpensive digital camera. One of objectives is to develop a method of estimating spectral properties using a normal and relatively inexpensive digital camera. In our previous reports [4][5], the spectral sensitivities of the camera sensors were estimated by the pseudo inverse matrix. In the present study, another estimation method is proposed by applying gradient descent in order to improve the accuracy. The method consists of two tasks: acquisition of the spectral sensitivities of camera sensors and estimation of the spectral irradiances of the display primaries.

PRINCIPLE

Acquisition of spectral sensitivities of camera sensors

Suppose the RGB sensors of a camera respond linearly to light intensity. Then, each response is an integral of the product of the SPD of incident light and the spectral sensitivity of the sensor. Such a

relationship among the RGB values of a captured image, the spectral irradiances of incident light, and the spectral sensitivities of the camera sensors are expressed by Eq. (1).

$$g_{kj} = \sum_{l=1}^L s_{kl} D_{lj} \Delta\lambda, \quad j = 1 \dots J, k = 1, 2, 3 \quad (1)$$

where $\Delta\lambda$ is the wavelength interval, g_{kj} is the j -th RGB values of the captured image for the k -th camera sensor, D_{lj} is the spectral irradiance of the j -th patch at the l -th wavelength, s_{kl} is the spectral sensitivity of the k -th sensor at the l -th wavelength, J is the number of patches, and L is the number of wavelengths.

Therefore, by photographing patches with known spectral irradiances, s_{kl} is derived from the RGB values g_{kj} from the photographed image and the spectral irradiances D_{lj} . Using gradient descent, s_{kl} is estimated so that the sum of squared errors shown by Eq. (2) can be minimized.

$$SSE_k = \sum_{j=1}^J \left\{ g_{jk} - \sum_{l=1}^L s_{lk} D_{jl} \Delta\lambda \right\}^2 \quad (2)$$

Estimation of spectral irradiances of display primaries

Several patches presented on a display are photographed by the digital camera for which the spectral sensitivities s_{kl} of the sensors are obtained in advance. The spectral irradiances D_{lj} of these patches are estimated by the spectral sensitivity s_{kl} of the camera sensors and the RGB values g_{kj} obtained from the photographed image using Eq. (1). The spectral irradiances D_{lj} can be expressed by Eq. (3).

$$D_{lj} = \sum_{m=1}^3 d_{lm} f_{mj}^{\gamma_m} + e_l \quad (3)$$

where f_{mj} is the RGB input values (0~1) of the m -th channel of the display for the j -th patch, e_l is the spectral irradiance of the background when $f_{mj} = 0$ at the l -th wavelength, γ_m is the gamma characteristic of the m -th channel, and d_{lm} is the maximum spectral irradiances of the m -th channel at the l -th wavelength.

In the proposed method, we need to estimate the maximum spectral irradiances d_{lm} and γ_m for the display RGB primaries. All the f_{mj} for the presented patches have non-zero values. Therefore, a single spectral irradiance for one of the display primaries must be derived from the difference between a pair of D_{lj} and D_{li} in which two of the input values f_{mj} and f_{mi} are the same. Finally, using gradient descent, γ_m and d_{lm} are estimated so that the sum of squared errors given by Eq. (4) can be minimized.

$$SSE_m = \sum_{l=1}^L \left\{ (D_{li} - D_{lj}) - d_{lm} (f_{mi}^{\gamma_m} - f_{mj}^{\gamma_m}) \right\}^2 \quad (4)$$

EXPERIMENT

Acquisition of spectral sensitivities of camera sensors

The experiment was conducted in a darkroom to avoid stray light. The distance between the display (Eizo, CE240W) and the digital camera (Nikon, D750) was 70 cm. To limit the wavelength range of incident light onto the camera, a short-wavelength cut filter (Asahi Spectra, LUX400) and a long-wavelength cut filter (Asahi Spectra, SVX690) were attached in front of the camera lens. In the wavelength range of 400-680 nm with an interval $\Delta\lambda$ of 10 nm, spectral sensitivities and spectral irradiances were calculated for 29 wavelengths ($L = 29$). The aperture and sensitivity of the camera

were set F 5.6 and ISO 100, respectively. To obtain a linear RGB response from the captured RAW data and to eliminate blown out highlights or blocked up shadows, high dynamic range (HDR) images [6] were generated at seven different shutter speeds: 1/250, 1/125, 1/60, 1/30, 1/15, 1/8, and 1/4 seconds. MATLAB was used for computation and analysis. Input RGB values for color patches on the display are shown in Table.1.

The procedures were as follows. First, the 26 colors listed in Table.1 were presented on the display successively one by one and their spectral irradiances D_{lj} were measured with an illuminance spectrophotometer (Konica Minolta, CL-500A). Then, a tile of the 26 patches presented on the display was photographed with the digital camera. Using gradient descent, the spectral sensitivities of the camera sensors s_{kl} were obtained so that the sum of squared errors of Eq. (2) can be minimized.

Estimation of spectral irradiances of display primaries

The spectral irradiances d_{lm} and gammas γ_m were recovered for the same display (Eizo, CE240W) used for acquisition of the spectral sensitivities of the camera sensors. The experimental environment and condition were the exact same as in the experiment of acquisition of sensors' sensitivities. First, the spectral irradiances D_{lj} of the 26 patches on the display were estimated via Eq. (1) by the acquired spectral sensitivities s_{kl} of the camera sensors and the RGB values g_{kj} from the captured image. Then, $d_{lm}(f_{mi}^{\gamma_m} - f_{mj}^{\gamma_m})$ for each of the display primaries were derived by subtractions among D_{lj} . Using gradient descent, the best display gammas γ_m and maximum irradiances d_{lm} were obtained so that the sum of squared errors of Eq. (4) can be minimized. The obtained d_{lm} and γ_m were compared with those measured with the CL-500A to evaluate the performance of the proposed algorithm.

Table 1. RGB input values for display color patches

#	R	G	B	#	R	G	B	#	R	G	B	#	R	G	B	#	R	G	B
1	0	0	0	3	160	96	96	9	192	128	64	15	192	64	64	21	192	96	32
2	128	128	128	4	96	160	96	10	192	64	128	16	64	192	64	22	192	32	96
				5	96	96	160	11	64	192	128	17	64	64	192	23	32	192	96
				6	160	160	96	12	128	192	64	18	64	192	192	24	96	192	32
				7	160	96	160	13	128	64	192	19	192	64	192	25	96	32	192
				8	96	160	160	14	64	128	192	20	192	192	64	26	32	96	192

RESULT AND DISCUSSION

Acquisition of spectral sensitivities of camera sensors

The obtained spectral sensitivities s_{kl} of the camera sensors are shown in Fig. 1(right) and the results of previous studies are shown in Fig. 1(left). Since the spectral sensitivities of the camera sensors are not provided by the manufacturer, whether the spectral sensitivities were accurately obtained cannot be judged. However, as in our previous report Fig. 1(left), they have peak values in each preferable wavelength ranges, and the spectral sensitivity are low in the other wavelength range. As shown in Fig. 1(left), smooth spectral sensitivities were obtained in the previous study by applying smoothness constraints for consecutive points on the curves. However, the estimated spectral sensitivities in Fig. 1(right) were jagged because the smoothness was not taken into consideration in the present estimation method.

Gradient descent was used to derive the spectral sensitivities of the camera sensors. This method might change the result depending on the initial value. Therefore, we tried to derive the spectral

sensitivities of the camera sensors using various initial values. As a result, regardless of the initial value, the spectral sensitivities of the camera sensors having a shape similar to that shown in Fig. 1 (right) were obtained. Therefore, the result is not expected to depend on the initial value.

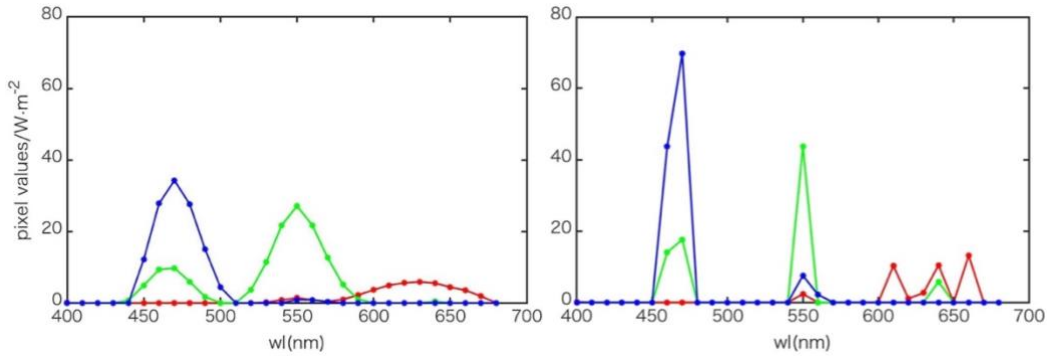


Fig. 1 Spectral sensitivities s_{kl} of the camera sensors

Estimation of spectral irradiances of display primaries

The spectral irradiances $d_{lm}(f_{mi}^{\gamma_m} - f_{mj}^{\gamma_m})$ are shown in Fig. 2 for each of the RGB primaries. They have peak values in each preferable wavelength range.

The maximum spectral irradiances d_{lm} of the display primaries and γ_m are shown in Fig. 3. The d_{lm} values measured using the CL-500A are on the left and the estimated d_{lm} are shown on the right. The estimated d_{lm} have peaks around each preferable wavelength range but they are slightly different from the measured values.

In the proposed method, d_{lm} and γ_m are estimated via $d_{lm}(f_{mi}^{\gamma_m} - f_{mj}^{\gamma_m})$ derived from D_{lj} . The RGB values g_{kj} of the captured images can be expressed as a function of d_{lm} and γ_m in Eq. (5), which is obtained by substituting Eq. (3) into Eq. (1). Therefore, by minimizing the sum of squared errors of g_{kj} in Eq. (6), both d_{lm} and γ_m for display primaries could be directly obtained without the estimation of D_{lj} . This optimization problem only has to be solved with the constraints of $d_{lm} \geq 0$ and $\gamma_m \geq 0$.

$$g_{kj} = \sum_{l=1}^L s_{kl} \left(\sum_{m=1}^3 d_{lm} f_{mj}^{\gamma_m} + e_l \right) \Delta\lambda \quad (5)$$

$$SSE_m = \sum_{j=1}^J \left\{ g_{kj} - \sum_{l=1}^L s_{kl} (d_{lm} f_{mj}^{\gamma_m} + e_l) \Delta\lambda \right\}^2 \quad (6)$$

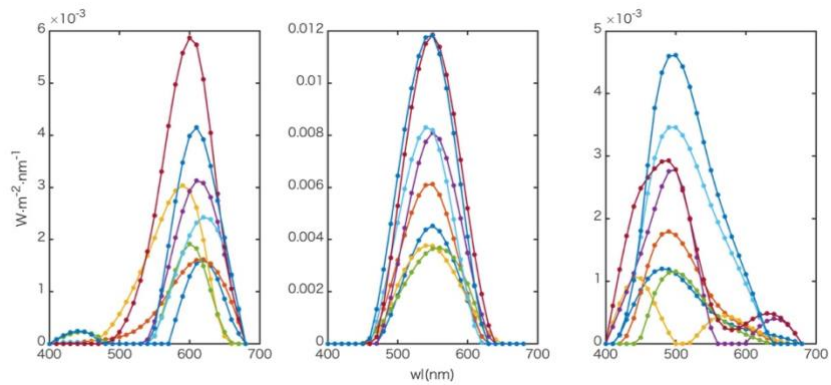


Fig. 2 Spectral irradiances of a RGB $d_{lm}(f_{mi}^{\gamma_m} - f_{mj}^{\gamma_m})$

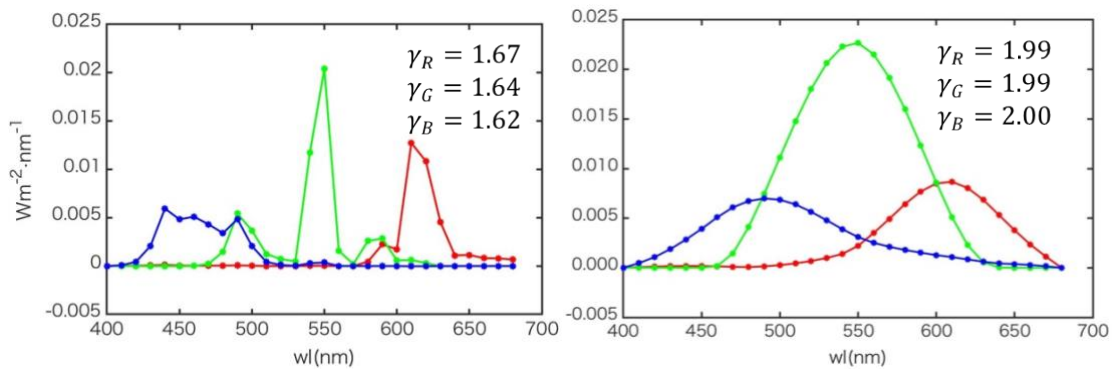


Fig. 3 Maximum spectral irradiances d_{lm} of the display primaries

REFERENCE

1. Tominaga, S., Journal of the Optical Society of America A, 13, pp.2163-2173, 1996.
2. Chi, C., Yoo, H., and Ben-Ezra, M., International Journal on Computer Vision, 86, pp.140-151, 2010.
3. Han, S. et al., International Journal of Computer Vision, 110 (2) pp172–184, 2014.
4. Tetsuo, R. Shinoda, H., Proc. of ALC2018, Kobe (Japan), 2018.
5. Tetsuo, R. Shinoda, H., Proc. of ACA2018, Chieng mai (Thailand), 2018.
6. Debevec, P. E., and Malik, J., Proc. of SIGGRAPH'97, pp369-378, 1997.

EFFECT OF DUAL TASK EXECUTION AND ILLUMINANCE LEVEL DECLINE ON SPATIAL RESOLUTION

Toru Sugiura^{1*} and Hiroyuki Shinoda²

¹ Graduate School of Information Science and Engineering, Ritsumeikan University, Japan.

² College of Information Science and Engineering, Ritsumeikan University, Japan.

*Corresponding author: Toru Sugiura, is0312ir@ed.ritsumei.ac.jp

Keywords: Eyewitness testimony, Dual task, Spatial resolution, Illuminance

ABSTRACT

An assessment of the credibility of eyewitness testimony is necessary for legal justice. In the present study, experiments were conducted to examine how spatial resolution changes due to a dual task. A participant discriminated the orientation of a Landolt ring presented at random times while tracking a moving target using a mouse. The illuminance of an experimental booth was set at various levels from photopic vision to scotopic vision. The luminance of the Landolt ring, the moving target, the mouse cursor, and the background were modulated on a display according to the illuminance level. The result showed a degradation in orientation discrimination due to the dual task. The performance degradation was larger at mesopic illuminance levels than at other illuminance levels.

INTRODUCTION

Eyewitness testimony at a crime scene is treated as important evidence in a trial. Credibility of eyewitness sometimes may put in issue of trials because eyewitness testimony is greatly influenced by visual performance of human. Therefore, it is necessary to establish an index to evaluate the accuracy of eyewitness testimony in order to prevent false charges or overlooking a true criminal. The accuracy of eyewitness testimony has been studied from various perspectives. Most studies took into account the influence of the environment on sight. For instance, one study showed that the distance should be less than 15 m and the illuminance should be more than 15 lx to identify faces [1]. In another study, color response was shown to be inconsistent because color recognition was affected by illuminance, stimulus size, and observation duration [2]. Like color recognition, spatial resolution is an important factor in the credibility of eyewitness testimony because it is important in the recognition of the faces of human or shapes of objects such as number plates. In actual sighting situations, however, witnesses happen to see an event such as an accident or a crime while performing other irrelevant tasks, such as driving. In other words, witnesses may not completely concentrate on the sighting. Therefore, it is necessary to investigate how the accuracy of witness testimony, including spatial resolution, changes as the degree of concentration of the witness changes. In the present study, experiments were conducted to examine how spatial resolution changes due to a dual task that disturbs concentration on sighting.

EXPERIMENTS

In the experiment, participants were instructed to conduct a dual task or a single task. The experimental booth is shown in Figure 1a. The horizontal illuminance on the display screen of the experimental booth was varied at five levels (200, 20, 1.8, 1.0, and 0.2 lx) from photopic to scotopic vision in order to simulate the actual sighting environment. Participants sat on a chair at a distance of 100 cm from the display (EIZO, CG2420) and conducted the dual task. The experimental booth was illuminated at the five illuminance levels by fluorescent lamps (Panasonic, FLR40S D-SDL/M daylight color) set in the ceiling. Color temperature of fluorescent lamps were 6500 K.

The dual task consisted of a tracking task (main task) and an orientation discrimination task of the Landolt ring (sub-task). In the tracking task, participants tracked a circular target that moved along an invisible ∞ -shaped trajectory on the display screen using a computer mouse. The trajectory consisted of two circles, the visual angle of each of which was 7 degrees (see Figure 1b). The visual angles of the tracking target and the mouse cursor were 0.5 degrees. During the tracking task, a Landolt ring was presented at one of the two centers of the trajectory for a period of 1 second as an orientation discrimination task. The visual angle of the cut-out of the ring was randomly set from 2 minutes to 10 minutes. The orientation of the cut-out of the ring was up, down, left, or right, so that the chance level was 25%. The colors of the Landolt ring, the moving target, the mouse cursor, and the background were selected from the achromatic colors of Munsell Color System. The Landolt ring was Munsell N7, and the moving target and the mouse cursor were Munsell N8. The background was Munsell N5. The luminance and chromaticity of the Landolt ring, the moving target, the mouse cursor, and the background were precisely modulated on the display according to the illuminance level. Stimulus presentation and recording responses of participants were performed using MATLAB and the Psychophysics Toolbox Version 3 [3]-[5] on a PC (Apple, MacBook Pro 13 inch). As a control condition, the subject performed a single task that included only the direction discrimination task.

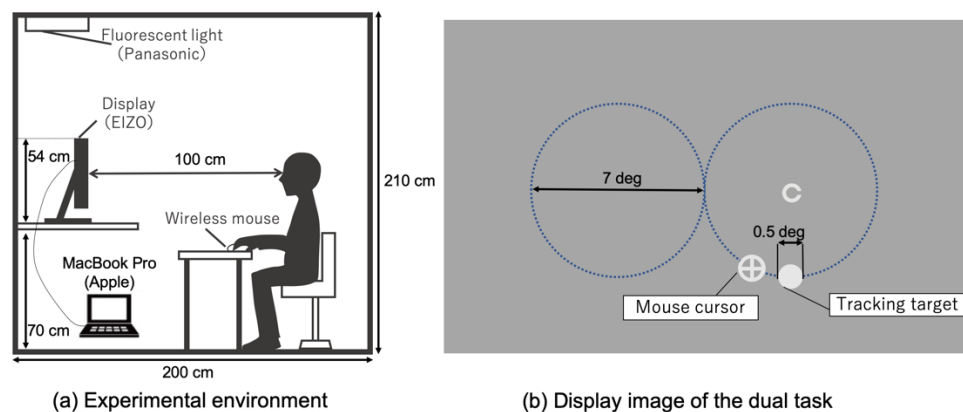


Figure 1. Experimental environment and display image of the dual task

A single session consisted of the repetition of the dual task or the single task and reporting under a constant illuminance level. The order for one trial of the dual task was as follows: wait screen, dual task, and reporting. At the wait screen, the tracking target and the mouse cursor were displayed. The tracking target was displayed at the center of the screen. The dual task started upon mouse click. After the dual task, participants were asked to report the orientation of cut-out of the ring by clicking on the area that corresponded to what he/she believed to be the correct orientation. Participants were asked to report his/her confidence in the orientation discrimination with numerals from 1 (very unconfident) through 5 (very confident) (see Figure 2a). The order for one trial of the single task was as follows: wait screen, single task, and reporting. At the same waiting screen as the dual task, participants click the mouse, but the tracking target does not start to move. The display image was the same as the waiting screen. Participants did not have to track the target by mouse, but only to watch the tracking target. The Landolt ring was displayed in the same manner as in the dual task, and the remainder of the trial was the same as in the dual task case (see Figure 2b). Participants adapted to the illuminance for 10 min before the experimental session started. The percent correct for one size of the Landolt ring was calculated by repeating the trial 20 times.

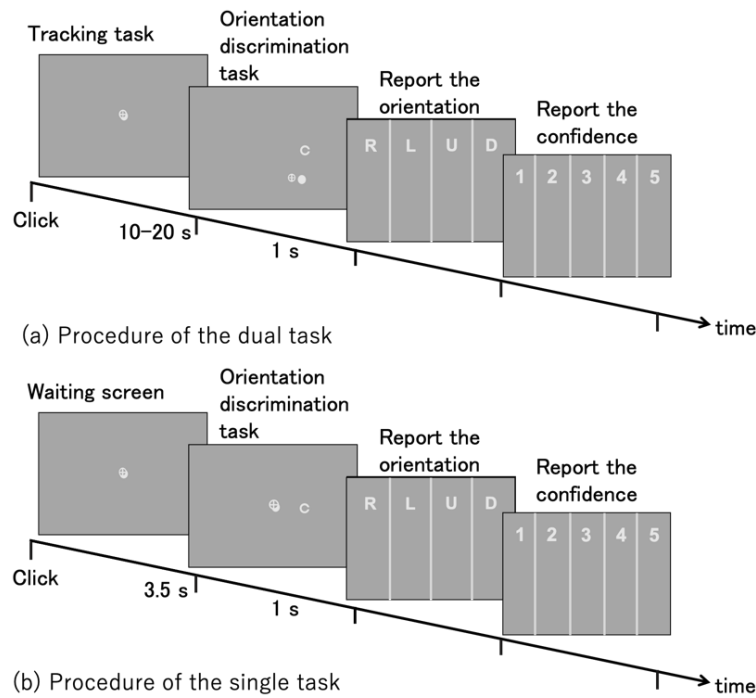


Figure 2. Procedures of the dual task and the single task

RESULT AND DISCUSSION

Figure 3 shows the experimental results summarized by illuminance level for average of three participants. The figure shows (a) the percent correct of each illuminance level, (b) the confidence and (c) relation between confidence and percent correct. Figure 3(c) was fitted by least square method. As the gap size decreased, both the percent correct and the confidence of the orientation discrimination task decreased. Comparing the presence (solid line) or absence of the tracking task (dashed line), the percent correct of the orientation discrimination in the dual task case was lower than that in the case of a single task (no tracking), indicating lower spatial resolution by the tracking task. The decrease in the percent correct due to the tracking task was as large as 25% at maximum at mesopic illuminance levels and was smaller at other illumination levels. The decrease in confidence due to the tracking task is not as remarkable as decline in the percent correct. From Figure 3(c), in same illuminance, the percent correct decrease proportionally as the confidence decreases. In other words, participants didn't underestimate or overestimate confidence on what they saw during tracking task.

Figure 4 shows parameters of linear fitting for relation between confidence and percent correct shown in Figure 3(c). Percent correct can be presented by equation (1), where P represents percent correct, C represents the confidence and a and b represent linear parameter; slope and y intercept.

$$P = aC + b \quad (1)$$

From Figure 4(b), y intercepts of dual task were smaller than that of single task in most conditions. However, difference in y intercepts between dual and single task get lowered in low luminance levels. In other word, the orientation discrimination task was difficult regardless participants did the tracking task or not in these illuminance condition. The upper limit of the confidence and the percent correct

are fixed at 100 and 5. And all fitting lines pass through around this point. This is why slopes of lines for dual task were higher corresponding to y intercepts than single task.

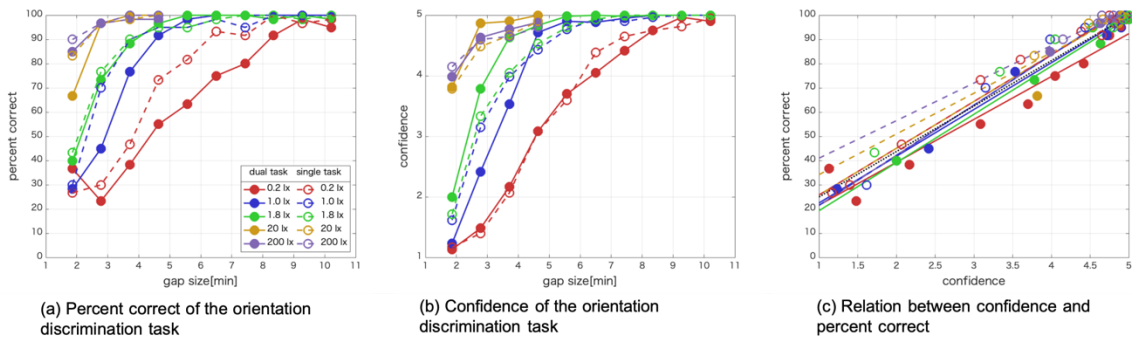


Figure 3. Performance degradation due to decrease of gap size of the Landolt ring

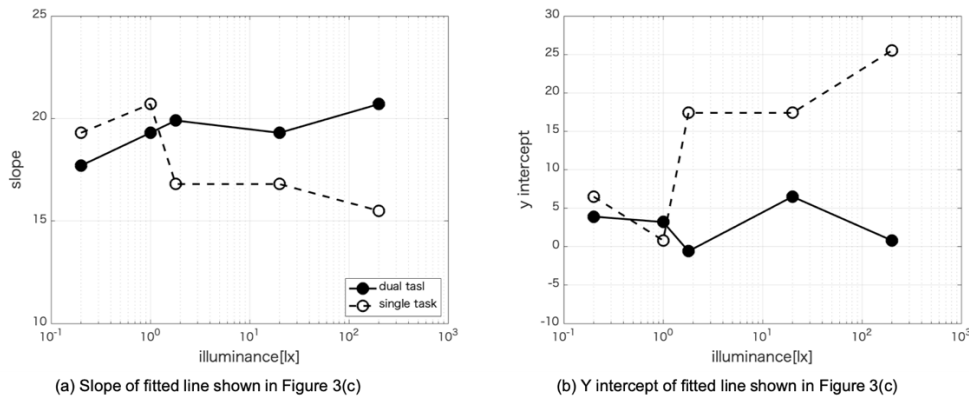


Figure 4. Parameters of fitting line shown in Figure 3(c)

Figure 5 shows the experimental results summarized by gap size. The graph shows only four conditions from the smallest gap size. The figure shows (a) the percent correct of each gap size, (b) the confidence and (c) relation between confidence and percent correct. As the illuminance lowered, both the percent correct and the confidence of the orientation discrimination task decreased. Both the percent correct and the confidence decrease drastically at the mesopic illuminance in most conditions. In case of small gap size, the percent correct and the confidence start to decrease at higher illuminance level than other gap sizes. Comparing the presence (solid line) or absence of the tracking task (dashed line), same tendency as Figure 3(a), (b) is seen. In same gap size, the percent correct decrease proportionally as the confidence decreases. This is same tendency as Figure 3(c).

Figure 6 shows parameters of linear fitting for relation between confidence and percent correct shown in Figure 5(c). From Figure 6 same tendency same tendency as Figure 4 is seen.

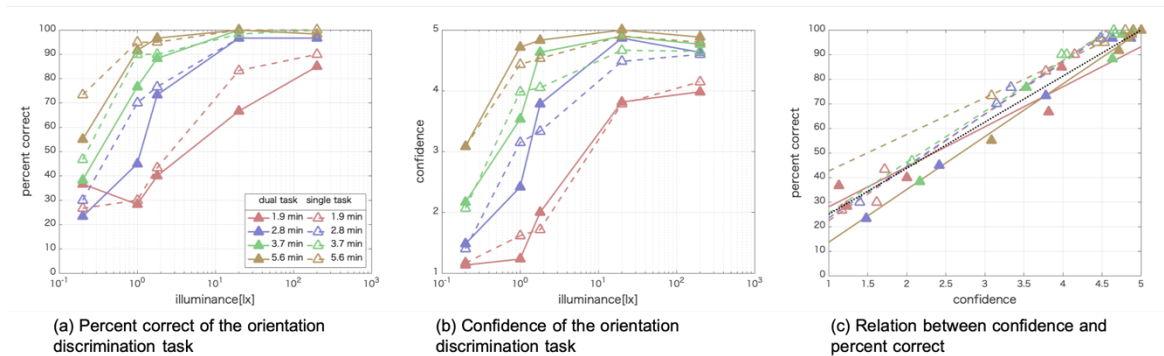


Figure 5. Performance degradation due to illuminance decline

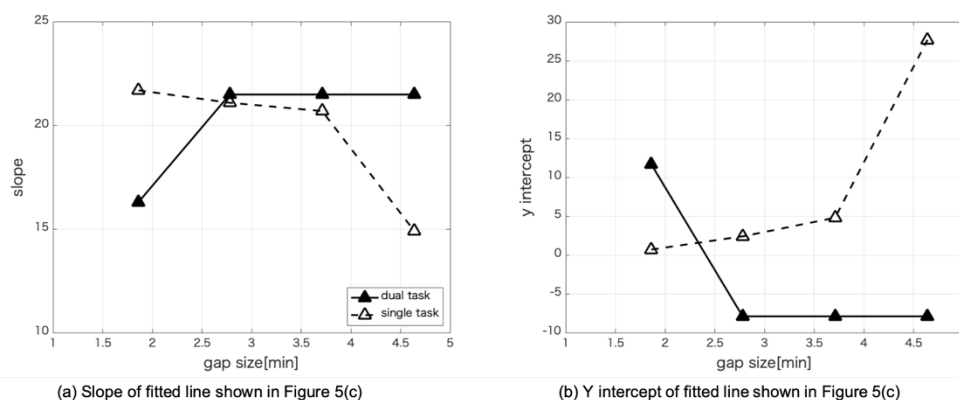


Figure 6. Performance degradation due to illuminance decline

The results suggest that the accuracy of eyewitness testimony under the irrelevant task can deteriorate and that these testimonies should be treated carefully. The results of the present study will not only help judicial officials to correctly evaluate eyewitness statements but will also help to evaluate the concentration on other tasks that demand long-term concentration.

REFERENCES

1. Wagenaar, W. & Van Der Schrier, J. (1996). Familiar face recognition as a function of distance and illumination: A practical tool for use in the courtroom, *PSYCHOLOGY CRIME & LAW* 2, 321-332.
2. Airi H. & Hiroyuki S. (2018). COLOR IDENTIFICATION AFFECTED BY ILLUMINANCE LEVELS, STIMULUS SIZE AND OBSERVATION PERIOD, *11th Asia Lighting Conference Proceedings*, 211-214.
3. David H. B. (1997). The Psychophysics Toolbox, *Spatial Vision* 10, 443-446.
4. Denis G. P. (1997). The Video Toolbox software for visual psychophysics: Transforming numbers into movies, *Spatial Vision* 10, 437-442.
5. Mario K. & David H.B. & Denis G.P. (2007). What's new in Psychtoolbox-3?, *Perception* 36 *ECVP Abstract Supplement*.

CONTRAST OF COLORED PAIRS ENHANCED BY USING 3 SELECTIVE WAVELENGTHS FOR PEOPLE WITH LOW VISION

Anukul Radsamrong¹ Pichayada Katemake^{1*} Éric Dinet² and Alain Tremeau²

¹*Department of Imaging and Printing Technology, Faculty of science, Chulalongkorn University, Thailand.*

²*Univ Lyon, UJM Saint-Étienne, CNRS, Laboratoire Hubert Curien UMR 5516, France*

*Corresponding author: Pichayada Katemake, pichayada.k@chula.ac.th

Keywords: Low vision, Contrast enhancement, Optimized wavelengths, Mixing colored lights

ABSTRACT

This research is aimed to investigate the performance of 3 lamps in enhancing the contrast of colored sample pairs perceived by subjects wearing 2 types of simulated low vision glasses: cloudy vision (CV) and blurred vision (BV) glasses. Previously we optimized 3-wavelengths for 3 lamps based on 1) fastest response lighting condition (L_FR), 2) contrast threshold, minimum color difference of colored pairs, perceived by simulated cloudy vision having visual acuity (VA) of 0.08 (L_CV) and 3) contrast threshold perceived by simulated blurred vision, VA = 0.06 (L_BV). The 1st lamp was the wavelength combination of 425 nm, 540 nm and 635 nm. The 2nd lamp was 475 nm, 595 nm and 700 nm and the 3rd one was 425 nm, 525 nm and 660 nm. In present experiment, the performance of 3 lamps was tested by 80 subjects, half of them worn simulated CV glasses and another half worn BV glasses. Each half was equally separated into 4 groups. The first four groups observed 200 colored pairs under control white LED (W), L_FR, L_CV and L_BV. There were 40 hues of Munsell in our 200 colored pairs. Each hue was paired with the next 5 neighbor hues counter clockwise making 5 pairs. Consequently, there would be 20 pairs in the group of 4 red hues of 2.5R, 5R, 7.5R and 10R, for example. The subjects wearing CV glasses could perceive contrast of 52%, 59%, 63% and 64% of 200 pairs under L_FR, W, L_CV and L_BV respectively, whereas subjects wearing BV glasses perceived contrast 70%, 85%, 85% and 91% under W, L_FR, L_CV and L_BV. We could see that the L_CV gave a good performance with subjects wearing CV glasses as expected because the L_CV was built based on the threshold determined by subjects wearing CV glasses. Similarly, the L_BV gave the highest percentage of the number of colored pairs that subjects wearing BV glasses could perceive contrast. Under W, L_FR and L_BV, subjects with CV glasses could discriminate greater than 50% for each hue (20 pairs) except for Munsell BG and Munsell R, whereas subjects with BV glasses could do better in all colored pairs except for Munsell B. The subjects with BV glasses could discriminate the contrast greater than 50% of all Munsell hues. We could conclude that lighting condition could be used for enhancing the contrast of colors for the low vision, however, it is dependent on type of vision.

INTRODUCTION

According to the world health organization (WHO), the definition for the low vision following used “Low vision is visual acuity less than 6/18 and equal to or better than 3/60 in the better eye with the best correction”. Globally, of the 216.6 million and 188.5 million people alive in 2015 had moderate to severe visual impairment (less than 6/18 but 3/60 or better) and mild visual impairment (less than 6/12 but 6/18 or better) respectively. However, the global predictions of number of people with moderately or severely vision impaired increasing to 237.1 million by 2020 and 587.6 million by 2050 [Rupert et al. 2017]. The people with low vision face difficulty in everyday life and also in their jobs such as less opportunity to improve skills, less freedom to judge, less encouraging in tough

events and less recognition for their operate [Stefania, Alfonso, Daniel, 2010]. This indicated that the health and vision related quality of life indices [Julian 2010]. Moreover, the low vision people cause a significant economic responsibility, which increases the degree of visual impairment for cost and intangible effects [Juliane et al. 2013]. Preparing and improving the environment to facilitate the lives of people with low vision is important to consider in the future.

The illuminance levels are described in lux, as a total luminous flux incident on a surface per unit area. It is a measure of how much the incident light illuminates the surface, wavelength-weighted by the luminosity function to correlate with human brightness perception [Hunt and Pointer, 2011]. A previous study about people with low vision on reading performance, demonstrated that illumination levels have an impact significantly on reading performance of people with low vision, and increasing illumination levels could improve their performance [Eldred, 1992]. William et.al investigated lighting conditions improves reading performance. They found the reading performance might be improved by brighter lighting conditions [William et al., 2018]. Another research study about impact of spectral power distribution on discrimination ability in people with are-related macular degeneration (AMD), the results showed that the full spectral of light source for the illumination better than fluorescent light [Henrik et al. 2011]. James et.al. study effect of correlated colour temperature (CCT) on reading performance in visually impaired people, the results indicated that the reading performance did not be different with correlated color temperature [James et al. 2012]. It seems like the eligible lighting conditions made the people with low vision to see better.

This research is aimed to investigate the performance of 3 lighting conditions in enhancing the contrast of colored pairs perceived by subjects wearing 2 types of simulated low vision glasses, CV and BV. The cloudy and blurred visions are caused by uncorrected refractive errors, cataract that cloudy of the crystalline lens, and vascular occlusions. The people with uncorrected refractive errors and cataract were about 78% of the people with low vision [WHO, 2007; Valrie et al., 1997; Anne, et al., 2010; Navaid et al., 2014].

MATERIAL AND METHODS

Colored samples: Two-hundred physical color pair samples were prepared from 40 hues of matte Munsell color order system including 2.5, 5, 7.5, and 10 of R, RP, P, PB, B, BG, G, GY, Y, and YR. The value and chroma of Munsell colour samples selected were 5 and 8 respectively except for 2.5Y, 5Y, 7.5Y, 10Y, and 2.5GY having value/chroma: 5/6 due to the limitation of chroma. Systematically, the colored pairs were started from 10Y paired with 7.5Y (1st), 5Y (2nd), 2.5Y (3rd), 10YR (4th), and 7.5 YR (5th). Then, 7.5Y was paired with 5Y (6th), 2.5Y(7th), 10YR (8th), 7.5YR (9th), and 5YR (10th) respectively. The size of individual colored pair was 5.0 x 5.0 cm.

Light source and apparatus: LEDCube-Any SPD Simulator with fourteen channels was used in the experiment. The spectral range is 400-700 nm with the correlated colour temperature (CCT) 2000-20000K and CIE Ra:0-100. The size of the light booth is 43 x 43 x 43 cm. The light intensity of LEDCube was controlled by MATLAB codes. Fourteen channels of LEDCube (cool white channel, warm white channel, 405nm, 425nm, 450nm, 475nm, 505nm, 525nm, 540nm, 595nm, 635nm, 660nm, 670nm, and 700nm) were divided into 3 regions (short, medium and long). The short wavelength region included 405nm, 435nm, 450nm and 475nm. The medium one comprised 505nm, 525nm, 540nm, and 595nm. Then, 635nm, 660nm, 670nm, and 700nm were classified in the long wavelength regions. The LEDCube was set up on the top of the light booth. Three walls and the base of the light booth were medium neutral grey. The experiment was set in the dark room.

Lighting conditions: Four lighting conditions including 1) the white LED (W) with correlated color temperature of 5500K, 2) optimized light source with the combination of 425nm, 540nm, and

635nm which was previously tested to have fastest response time for discriminated color pairs (L_FR), 3) optimized light source with the combination of 475nm, 595nm, and 700nm giving the contrast threshold, minimum color difference of colored pairs, perceived by simulated cloudy vision having visual acuity (VA) of 0.08 (L_CV) and 4) optimized light source with the combination of 425nm, 525nm and 660nm giving the contrast threshold perceived by simulated blurred vision, VA = 0.06 (L_BV). The luminance of 4 conditions, measured at observing distance of 50 cm away from sample, were 187 cd/cm².

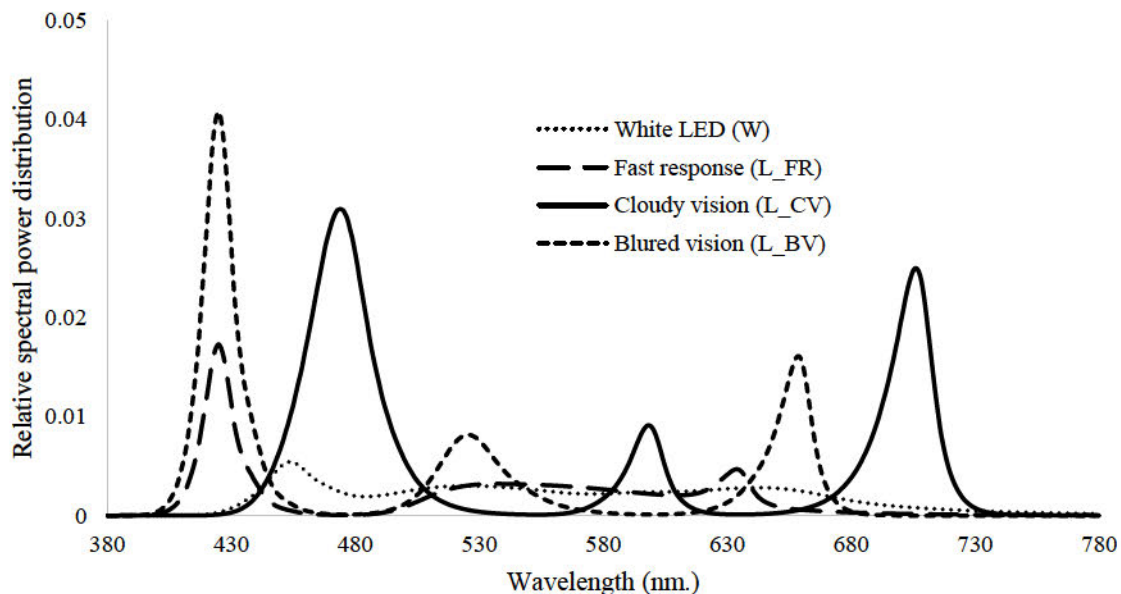


Figure 1. The spectral power distribution (SPD) of 4 lighting conditions W, L_FR, L_CV), and L_BV measured with a Konica Minolta spectroradiometer CS2000a

Measuring of colored samples: Forty physical colored samples were measured using the Konica Minolta spectroradiometer CS2000a under 4 lighting conditions. The CIE color difference 1976 (ΔE^*_{ab}) of individual pair were calculated. The spectral power distributions of 4 light sources were also measured with the spectroradiometer.

Participants: Eighty subjects, 35 males and 45 females, students at Chulalongkorn University, Thailand and at Université Jean Monnet, France were participated in the experiment. The age average was 22 years old (SD = 1.64). They were randomly divided into 2 groups: wearing CV and BV glasses with visual acuity of 0.08 and 0.06 respectively.

Procedure: The experimenter described the process of the experiment as follows: “You will observe 200 colored pair samples at a time. They are divided into ten groups, twenty colored pairs in each group. You will pick up the following pairs and put into the corresponding boxes (G1-G3): 1) colored pairs that you could not observe the contrast, G1; 2) colored pairs that you are not certain of seeing its contrast, G2 and 3) colored pairs that you see the contrast clearly, G3.” The participants then wore stimulated low vision glasses and adapted to the glasses and the room lighting condition for 2 minutes before starting the experiment. The time spent on judging individual colored pairs were recorded.

Analysis: The number of colored pairs in G3 and response time were used for assessing the lighting conditions for 2 groups of participant.

RESULTS AND DISCUSSIONS

Subjects wearing BV glasses could perceive contrast of 200 colored pairs better than wearing CV glasses in all 4 lighting conditions as shown in Table 1. The 3 proposed lighting conditions could significantly enhance the contrast compared to the controlled W. In contrast to BV, subjects with CV glasses, could discriminate colored pairs similarly for all 4 lighting conditions.

Table 1: Percentage of colored pairs that could be discriminated under 4 lighting conditions (right) and average response time of discriminating 200 colored pairs of 20 subjects for each condition.

Lighting conditions	% colored pairs with good contrast (G3)				response time (S)			
	W	L_FR	L_CV	L_BV	W	L_FR	L_CV	L_BV
BV	70 ^{eC}	85 ^{fC}	85 ^{fC}	91 ^{fC}	79±25 ^{aA}	82±25 ^{bA}	72±19 ^{cA}	86±31 ^{dA}
CV	59 ^{eD}	52 ^{eD}	63 ^{eD}	64 ^{eD}	86±23 ^{aA}	108±34 ^{aB}	95±26 ^{aB}	105±33 ^{aB}

Data are shown as the mean ± 1SD, derived from twenty participants for each session. Means followed by a different superscript small letter and capital letter are significantly different ($p < 0.05$; paired sample t-test) in vertical and horizontal groups respectively.

Under W, L_FR and L_BV, subjects with CV glasses could discriminate greater than 50% for each hue (20 pairs) except for colored pairs having Munsell BG or Munsell R, whereas subjects with BV glasses could perform better in all colored pairs except for colored pairs having Munsell B. Subject with BV glasses could discriminate the contrast of 200 colored pairs greater than 50% of all Munsell hue.

The response time of discriminating 200 colored pairs of 3 proposed lighting conditions were significantly different from W, carried out by subjects with BV glasses as shown in Table 1. The L_CV was the only one lighting condition having the less response time than W. The subjects with CV glasses did not give the significant difference in response time for all 4 lighting conditions.

The glasses types (CV and BV), colored pairs (10 hues), and their interactions did not give the difference to the mean of response time under W. In contrast to the W, the 3 proposed lighting conditions showed the difference in response time when wearing BV and CV glasses (Table 1).

By taking the type of vision into consideration, L_FR, L_CV and L_BV lighting conditions are optimized for the simulated blur vision regarding % colored pairs with good contrast (G3) and L_CV regarding response time. From figure 2 we could see that the proposed L_FR could reduce 7% of G1 (not see the contrast at all) and 9% of G2 (not certain of seeing the contrast). Similarly, L_CV and L_BV could decrease the percentage of G1 and G2.

For the simulated cloudy vision, the L_FR, L_CV and L_BV did not give the difference from the controlled W. From figure 2, L_FR did not help to enhance the contrast compared to W. The L_CV could reduce 1% and 4% in G1 and G2 respectively and the L_BV reduces 3% and 2% in G1 and G2 respectively. This does not obviously enhance the contrast compared to the simulated blur vision.

It could be confirmed that lighting condition could be used for enhancing the contrast of colors for the low vision, however, it is dependent on type of vision.

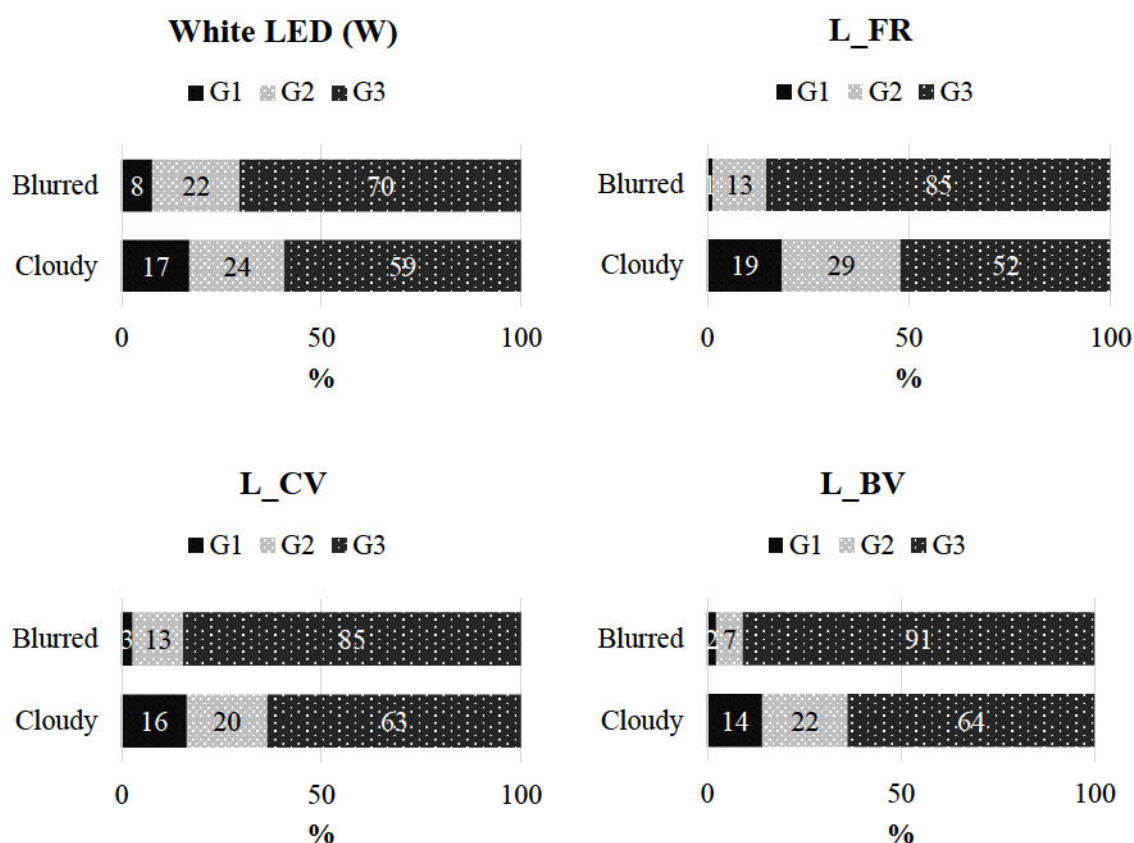


Figure 2. The percentage of 3 groups of colour pairs judged by participants: G1 (not see the contrast at all) , G2 (not certain of seeing the contrast), G3 (perceive contrast clearly).

CONCLUSIONS

Our proposed lighting conditions, L_FR, L_CV and L_BV could significantly enhance the contrast for people wearing simulated blur glasses with visual acuity of 0.06 but not for one wearing simulated cloudy vision glasses with visual acuity of 0.08. We will confirm our L_FR, L_CV and L_BV with the low vision patients.

ACKNOWLEDGEMENT

This work was supported by Chulalongkorn Dusadi Phiphat fund, Chulalongkorn University.

REFERENCES

1. Anne, L.C., Alan, J.K. Foundations of Low Vision: Clinical and Functional Perspectives. AFB Press New York: American Foundation for Blind, 2010.

2. Eldred, K.B. Optimal illumination for reading in patients with age-related maculopathy. *Optometry and Vision Science* 69: 46–50.
3. Henrik, H., Asger B.C., Michael J.A., & Claus R.J. (2011). The impact of light source in discrimination ability in subjects with age-related macular degeneration. *Acta Ophthalmologica* 89: 779-784.
4. Hunt, R. W. G., and Pointer, M.R. Radiometric and Photometric Terms and Units, in *Measuring Colour*, 4th Edition, England: John Wiley & Sons, 2011.
5. James, S.W., Eshmael, P., Martin, R., & Frank, E. (2012). Effect of light-emitting diode colour temperature on magnifier reading performance of the visually impaired. *Clinical and Experimental Optometry* 95: 510-514.
6. Julian, M. (2010) The economic argument for vision 2020. *International Agency for the Prevention of Blindness* :30-33.
7. Juliane, K., Karolina, B., Corinna, S., Robert, P.F. (2013). The economic burden of visual impairment and blindness: a systemic review. *BMK Open* 3:1-14.
8. Navaid, Q., Tabassum, A., & Tahir, A. (2014). Opacities in optical media to cause diminished vision. *Journal of the Society of Surgeons of Pakistan* 1: 63-66.
9. Rupert, R.A.B., Seth, R.F., Tasanee, B., Maria V.C., Aditi, D., Jost B.J., Jill, K., John H.K., Janet, L., Hans, L., Kovin, N. Konrad, P. Serhe, R., Alex, S., Gretchen, A.S., Nuna T., Tien, Y.W., Hugh, R.T. (2017). Magnitude, temporal trends, and projections of the global prevalence of blindness and distance and near vision impairment: a systematic review and meta-analysis. *Lancet Glob Health* 5: 888-897
10. Stefania, M.M.A., Alfonso, S.P., & Daniel, S.M. (2010). Impact of Low Vision on Employment. *Ophthalmologica* 224: 381-388.
11. Valrie, B., Nancy, J.N., & Paul, S. (1997) Retinal Vein Occlusion and Transient Monocular Visual Loss Associated with Hyperhomocystinemia. *American Journal of Ophthalmology* 2: 257-260.
12. William, S., Olga, O., Bruce, R., Tiffany, A., J. Vernon, O., & Alan, R. (2018). Effects of Lighting on Reading Speed as a Function of Letter Size. *American Journal of Occupational Therapy* 72 (2): 7202345020p1–7202345020p7.
13. World Health Organization. *International Classification of Functioning, Disability and Health*. Geneva: WHO Press, 2007.

NEURAL RESPONSES TO COLORS WITH DIFFERENT SALIENCY

Naoko Takahashi¹, Chen Xu¹, Yuki Motomura², and Chihiro Hiramatsu^{2*}

¹Human Science Course, Graduate School of Design, Kyushu University, Japan.

² Department of Human Science, Faculty of Design, Kyushu University, Japan.

*Corresponding author: Chihiro Hiramatsu, chihiro@design.kyushu-u.ac.jp

Keywords: Color Vision Diversity, Color Saliency, Oddball, EEG, ERP

ABSTRACT

Colors are often used to label different categories in readiness for identification. However, salient color combinations may differ from person to person. Most of the human population has three different cone pigments, S, M, and L, i.e., trichromacy. However, people with minor color vision types have deviated sensitivity or lack of sensitivity in any of the cone pigments. These differences cause variations in color perception, which should be based on different neural responses to the same stimulus. However, it is unclear how much difference there is in neural representation of colors with the same physical properties between individuals with different color vision types. In this study, we aimed to investigate the differences in neural responses to colors with different saliency among individuals with different color vision types using a visual oddball task. The stimuli consisted of three different colors—green, blue-green, and red—and each color saturated from the white point by the same amount on the CIE 1976 u'v' color space. We used green as the frequently presented standard color, and blue-green and red as infrequently presented deviant colors. The participants were asked to respond only to the deviant colors. An electroencephalogram (EEG) was recorded during the task, and event related potential (ERP) components were analyzed for attentional changes to each color stimulus. We hypothesized that trichromatic participants would respond faster with less attentional allocation to red than blue-green, and the opposite result would be yielded from dichromatic participants without M or L cone pigments. Our preliminary results with several trichromatic participants showed that the ERP component for attention exhibited shorter latency to red when compared to blue-green. The amplitude, however, did not show clear differences between stimuli. Future work will extend the experiment with participants possessing different color vision types to reveal the variation of neural responses to the same stimuli.

INTRODUCTION

It is known that approximately 5% of males in Japan are born with minor color vision types while a majority possess trichromatic color vision based on S (short-wavelength-sensitive), M (middle-wavelength-sensitive), and L (long-wavelength-sensitive) cone photoreceptor cells in the retina. Most of these minor color vision types either lack one of three cone cells, i.e., dichromacy, or possess cone cells with spectrally close sensitivities i.e., anomalous trichromacy. These deviations from trichromacy occur mostly on either L or M cone cells and much less with S cone cells due to the different amount of genetic variation in the human population. Since our color discrimination mechanism is primarily based on the comparison mechanism that contrasts cone cell responses of different sensitivities, reduction in cone pigment would substantially reduce color variations that one can discriminate [1]. However, despite the difference in photoreceptors, color naming in dichromats is similar to trichromats [2]. Moreover, Sunaga et.al. found that there was a certain color perceived by dichromats with higher saliency than trichromats [3]. These findings question dichromats' sensitivity to color perception and how they fulfill the loss of spectral sensitivity at a photoreceptor level. Using a visual oddball task, our aim is to unveil the neural basis of differences in color saliency

between dichromats and trichromats. We have obtained preliminary data from a few trichromatic participants. Here, we report the results of the preliminary analysis.

METHODS

1. Participants

Several male university students with trichromacy participated in this study. The experiment was carried out in accordance with the Declaration of Helsinki and was approved by the ethical committee of Faculty of Design, Kyushu University. Participants with other color vision types will be studied after this preliminary experiment.

2. Apparatus

MATLAB (MathWorks) and Psychtoolbox were used to prepare and present stimuli. An OEL display (TRIMASTER EL PVM-2541A, Sony; 24.5 inch, full HD, refresh rate 60 Hz) was used to display stimuli. Gamma curves of the display were measured with a spectrometer (CS-2000A, Konika Minolta) and corrected based on the measured data.

3. Stimuli

A combination of stimuli was selected in reference to the color search task experiment reported by Sunaga et. al. [3]. In their study, dichromats were able to detect target blue-green stimuli out from green distractive stimuli faster than trichromats, suggesting that blue-green has higher saliency for dichromats compared to trichromats. In the same study, between dichromatic and trichromatic participants, red was found to have lower saliency for dichromats.

For our oddball experiment, each of the three stimuli was selected from the CIE 1976 $u'v'$ chromaticity diagram in association to the deuteranope confusion line as shown in Figure 1. A circumference with radius 0.03 with D65 at the center was used to find crossover points with the deuteranope confusion line. One of the crossover points (0.2271, 0.4618) was selected as deviant 2 (red stimulus). Deviant 1 (blue-green) and standard (green) points were selected 45° apart from the other crossover point (0.1685, 0.4748) in both the clockwise and counterclockwise directions. Their coordinates were (0.1817, 0.4936) and (0.1725, 0.4522) for standard and deviant 1, respectively. D65 was selected as the background color so that each of the three stimuli was equally saturated from the background with the luminance at 20 cd/m^2 for trichromatic observers.

According to the results of the previous study [3], saliency differences were expected to be significant between the two deviant colors: higher saliency with deviant 1 (blue-green) and lower saliency with deviant 2 (red) for dichromats and vice versa for trichromats. For this preliminary experiment, the saliency difference between the two deviant colors was expected to be subtle due to the acute discrimination ability of trichromats.

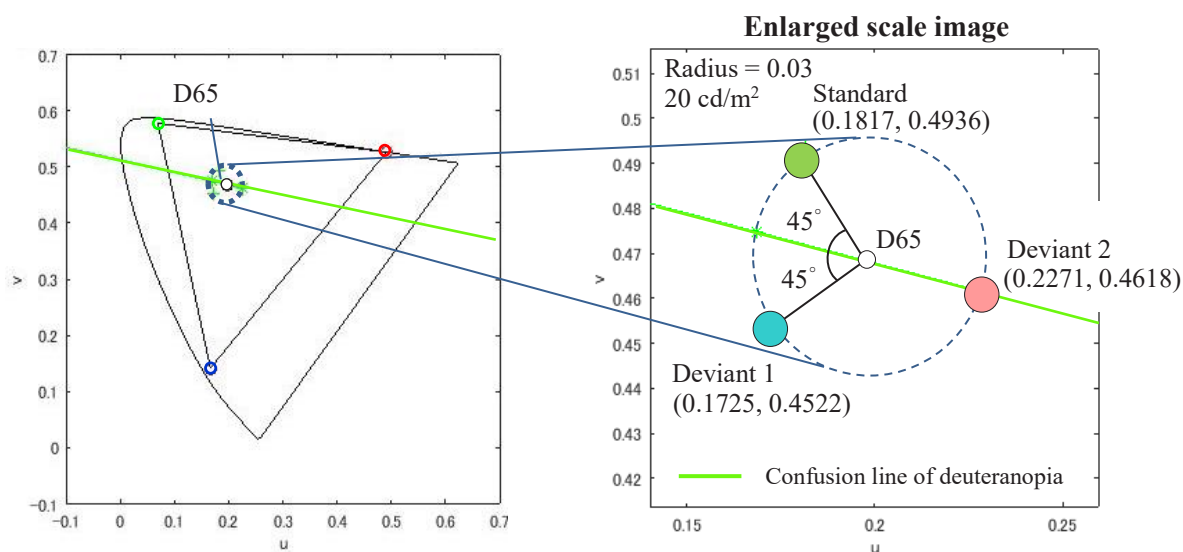


Figure 1. Coordinates of standard and deviant stimuli on the CIE 1976 $u'v'$ chromaticity diagram

4. Procedure

The oddball task consisted of one frequently presented standard stimulus (green) and two infrequently presented deviant stimuli (blue-green and red). Table 1 shows the frequency of stimulus presentation during the task. The frequency of each stimulus was balanced within the entire session in which 80% of the stimuli were standard and the remaining 20% were equally shared between deviant 1 (blue-green) and deviant 2 (red). As specified in Figure 2, there were 40 sessions of 10 trials within an experiment set. The first three trials of the session were always standard stimuli so that the participant would become familiar with the standard stimulus. Each stimulus was presented for 400 ms with a randomized interval of 1200-1600 ms. During the interval, only the gray background was displayed. The participant was allowed to take a break in between sessions so that he could suppress spontaneous body movements, such as eye blinking during stimulus presentation. The experiment was resumed by the participant's press of a space key.

In each trial, a circle filled with a single color chosen from standard, deviant 1, and deviant 2, was presented at the center of the display on a gray background. The outline of the circle was shaded off into the background so that the participant would judge the stimulus based on the inner color of the circle and not based on the saliency difference caused by the boundary of the circle and the background. The stimulus order was randomized and the participant was asked to respond only to the deviant stimuli by pressing a button.

Table 1: Frequency of each stimulus and number of stimulus presentation in an experiment set

	Standard	Deviant 1	Deviant 2
	green 	blue-green 	red 
Frequency (%)	80	10	10
No. of presentation	320	40	40

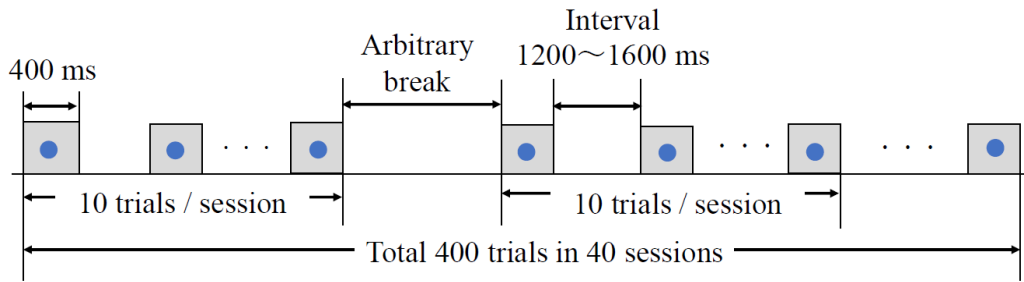


Figure 2. Procedure of the experiment

5. EEG data recording and processing

EEG was recorded with an 8 ch analog bio amplifier BA2008 (Miyuki Giken) at a digitizing rate of 1000 Hz. At the time of recording we applied a 0.05 Hz (time constant 3 s) high-pass filter and a 30 Hz low-pass filter. A hum filter was also applied to remove 60 Hz noise. Electrophysiological data were recorded from 7 electrodes (Fz, CPz, Pz, PO7, O1, O2, and PO8) that were placed on the scalp surface following the extended 10-20 system. Eye blinks and movements were monitored with bi-polar channels placed diagonally, one on the side of the right upper eyelid and the other on the left lower eyelid, to monitor both vertical and horizontal eye movements. EEG channels were referenced to the mean voltage of the right and left ear lobes. An electrode placed on the forehead (FPz) served as ground. All electrodes used were active electrodes.

For analysis, we applied a finite impulse response (FIR) filter, where we placed a 1 Hz low-pass and a 40 Hz high-pass filters. AC noises of 60 Hz and 120 Hz were also removed from the recording. In total, 320 trials for standard stimulus and 38 and 40 trials for deviant 1 and deviant 2 were averaged separately after rejection of the trials with excessive artifacts. Averaged trial data were lasting 1000 ms starting from 100 ms prior to the stimulus onset. As for the baseline, averaged pre-stimulus 100 ms was subtracted from each of the three averaged data. To evaluate the saliency between deviant 1 and 2 within the individual participant, we conducted t-test using trial data at each time point. The records were displayed and analyzed using MATLAB (MathWorks) and MATLAB toolbox EEGLAB.

RESULTS

1. Perceptual component N1 and N2

N1 and N2 are perceptual components that appear around 100 ms and 200 ms after stimulus onset. They reflect sensory level responses to the stimulus presentation [4]. Since the participant was a trichromat, we expected to find a faster latency as well as larger amplitude for deviant 2 on both N1 and N2. However, no significant difference was found between deviant 1 and 2 on both ERPs. On O1, due to the cyclic waveform caused by α waves, N1 could not be identified. For N2, again, the peaks of deviant 1 and 2 did not reach the significant difference (Figure 3).

2. Cognitive level component P2 and P3

P3 is an ERP component that appears around 300-400 ms after stimulus onset and is known to be highly correlated with attention allocation [5]. When the stimulus shows a higher amplitude with delay in latency, it suggests that the stimulus may have lower saliency, thus requiring a larger amount of attention to discriminate the color. P3 is best expressed in the parietal region such as CPz. As shown in Figure 3, although the amplitude did not reach a significant difference, there was a delay in response to deviant 1 recorded on CPz. This may suggest that for this participant, deviant 2 (red

stimulus) had higher saliency. In contrast to P3, P2 recorded at CPz reached a significant difference. P2 modulates attention allocation which appears in P3.

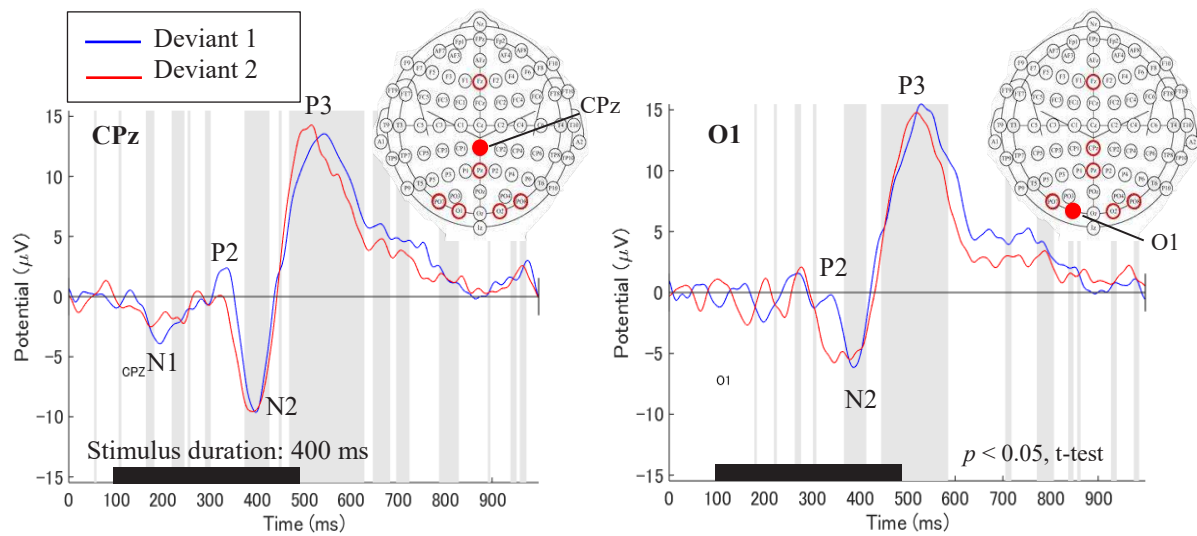


Figure 3. ERP waveforms recorded on CPz (left) and O1 (right)

White area on background of the plot shows the time points that reached significant difference.

3. Visual mismatch negativity (vMMN)

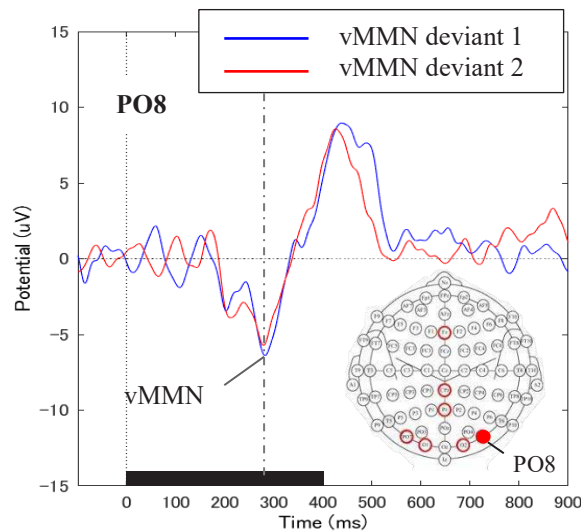


Figure 4. vMMN recorded on PO8

vMMN is an ERP component that appears around 150 to 300 ms after stimulus onset in negative polarity and is expressed well in the right occipital region. It reflects the brain's unconscious response to the violation of the sequential rule established internally within the participant through repetitive stimulus presentation [6]. vMMN was acquired by subtracting the averaged ERP for standard stimuli from the ERP for deviant stimuli. Figure 4 shows vMMN recorded at PO8 appearing around 280 ms after stimulus onset. We expected a higher amplitude for deviant 1 since there would be more difficulty for a trichromat to internally establish the sequential rule with a stimulus with lower

saliency. The peak amplitude of vMMN was observed at 280 ms post-stimulus. However, there was no difference by t-test between ERPs for deviant 1 and 2 when each of the trials was compared to the averaged ERP for standard (vMMN).

DISCUSSION

In this study, we analyzed the ERPs measured from a trichromatic participant conducting a visual oddball task to investigate fundamental neural response to color stimuli. The trichromatic participant had keen color discrimination ability; thus, the neural basis of saliency differences among the stimuli was not clearly observed. Since the current result was derived from a single participant, the data cannot exclude the personal characteristics of this particular individual. Following the same reasoning, we cannot deduce the tendency in neural responses that represent the class of this color vision type. Since the ultimate purpose of this study is to elucidate the neural responses that represent saliency differences between color vision types, we will continue the experiment with a more refined protocol and extend the participants to those with different color vision types.

ACKNOWLEDGEMENT

This work was supported by JSPS KAKENHI Grant Numbers JP17H05952, JP19H04198, and the NTT-Kyushu University Collaborative Research Program for Fundamental Sciences to CH.

REFERENCES

1. Schwartz, S. (1994). Spectral sensitivity of dichromats: role of postreceptor processes. *Vision research*. 34(22). 2983-2990.
2. Montag, E. (1994). Surface color naming in dichromats. *Vision research*. 34(16). 2137-2151.
3. Sunaga, S., Ogura, T., Seno, T. (2013). Evaluation of a dichromatic color-appearance simulation. *Optical review*. 20(2). 83-93.
4. He, X., Witzel, C., Forder, L. et.al. (2014). Color categories only affect post-perceptual processes when same- and different-category colors are equally discriminable. *Journal of the optical society of America*. 31(4). A1-A10.
5. Dujardin, K., Derambure, P., Bourriez, J., Jacquesson, J. et.al. (1993). P300 component of the event-related potentials (ERP) during an attention task: effects of age, stimulus modality and event probability. *International journal of psychophysiology*. 14. 255-267.
6. Kimura, M. (2011). Visual mismatch negativity: An electrophysiological index of temporal-context-based prediction in vision. *Japanese journal of physiological psychology and psychophysiology*. 29(1). 53-71.

DEVELOPMENT OF A COLOR SAMPLE SET FROM THE VIEWPOINT OF DICHROMATS FOR COLOR UNIVERSAL DESIGN

Kajitsu Yoshitake^{1,2*}, Kyoko Kido³, Satoshi Hano⁴, Shigehito Katsura⁵, Shoji Sunaga^{5*}

¹ *Future Creators in Science Project: QFC-SP, Kyushu University, Japan*

² *Oita Hita High School, Japan*

³ *Graduate School of Design, Kyushu University, Japan*

⁴ *Center for Health Sciences and Counseling, Kyushu University, Japan*

⁵ *Faculty of Design, Kyushu University, Japan*

*Corresponding authors: Kajitsu Yoshitake, kajitsu_jp@icloud.com,
Shoji Sunaga, sunaga@design.kyushu-u.ac.jp

Keywords: Color universal design, Dichromat, Color sample set, Color design method

ABSTRACT

A color design method that avoids the use of confusion colors for dichromats is called color universal design. Recently, a new color universal design method, without a dichromatic simulator, has been proposed (Sato, Japan patent 4507641, 2010; Sunaga et al., J. Color Sci. Assoc. Jpn, 42, 209-217, 2018). This new method has two steps. In the first step, a color combination for dichromats is determined based on the colors that dichromats can distinguish. In the next step, the color combination is modified for trichromats by changing each color in the color combination to another color that is difficult for dichromats to distinguish. Despite these changes, the appearance of the color combination determined in the first step for dichromats is preserved, because of the color changes among the confusion colors of dichromats. Although Sunaga et al. (2018) established a new method using a commercial color sample set of 199 colors, they were unable to obtain sufficiently robust results for practical use, because only 199 colors were included. The current study sought to extend the method using the categories of color names proposed by Sunaga et al., to develop a robust color sample set for practical use. We used Natural Colour System®© (NCS) chips containing 1,948 colors as a color sample set. We used our sample set in an on-campus, barrier-free design project at Kyushu University. We present the results of the Kyushu University barrier-free design project.

INTRODUCTION

Typical human color vision is trichromatic, involving the responses of three types of cone photoreceptors. However, some individuals lack one of the three cone photoreceptor types. These individuals are known as “dichromats”, and their color vision is known as “dichromacy”. Dichromats cannot distinguish colors that evoke different responses in only the missing cone type. Such colors are known as “confusion colors”, and are named depending on which cone type is lacking. In designing visual materials, color universal design seeks to avoid using confusion colors. To carry out color universal design, designers check whether confusion colors are contained in visual materials, using a color simulation of dichromacy [1]. Recently, a new color universal design method, which does not require dichromatic simulation, was proposed [2, 3]. This new method comprises two steps. In the first step, a color combination for dichromats is determined based on the colors dichromats can distinguish. In the next step, the color combination is modified for trichromats, by changing each color in the color combination to another color that is difficult for dichromats to distinguish. Despite these changes, the appearance of the color combination determined in the first step for dichromats is preserved, because the color changes are made among the dichromat confusion colors. However, because the protanopic and deuteranopic confusion lines

do not agree, it is difficult to carry out color universal design for protanopes and deuteranopes simultaneously. Therefore, Sunaga et al. [3] introduced an acceptable color shift from each confusion line in the second step, and established the new color universal design method. They then developed a commercial color sample set consisting of 199 colors for their color universal design method. Because Sunaga et al.'s sample set included only 199 colors, the purpose of the present study was to extend the method, using the categories of color name designation proposed by Sunaga et al., to obtain a robust color sample set for practical use. Moreover, because Sunaga et al. used an old colorimetric system, we used the CIE 2015XYZ [4] and the illuminant D65, instead of the CIE 1931XYZ and illuminant C, for calculating the confusion colors.

METHODS

Color samples

We used Natural Colour System[®] (NCS) chips (NCS Box, NCS Colour AB, Stockholm, Sweden), containing 1,948 colors, as a color sample set. Figure 1 shows the CIE 2015 xy chromaticities of these color chips when illuminated by the D65 illuminant. The spectral reflectances of the color chips were measured with a spectrophotometer (CM-2600d, Konica Minolta, Tokyo, Japan).

Introduction of an acceptable color shift from the protanopic and deuteranopic confusion lines

We started with the regions of categories of color name designation proposed by Sunaga et al. [3] to be acceptable shifts. The regions are shown in Figure 2 [5]. The color name designations in Figure 2 are 5PB, N, and 5Y, because the colors with the dominant wavelengths of 475 and 575 nm approximately correspond to the Munsell hues 5PB and 5Y, respectively. The regions of color name designation are defined by the Munsell notation and some Munsell colors are represented by the CIE 1931XYZ tri-stimulus values when the illuminant C is used. Because one of our goals was to use the new color system, CIE 2015XYZ, it was necessary to derive the CIE 2015XYZ tri-stimulus values from the CIE 1931XYZ tri-stimulus values of the regions of color name designation. First, the CIE 1931XYZ tri-stimulus values of the corner colors of the regions of color name designation were interpolated based on the Munsell colors whose CIE 1931XYZ tri-stimulus values are already known [6]. Second, the spectral reflectances of the corners were estimated from those CIE 1931XYZ tri-stimulus values, according to the model proposed by Sobagaki et al. [7]. Finally, the CIE 2015XYZ tri-stimulus values of the corners were calculated from the estimated

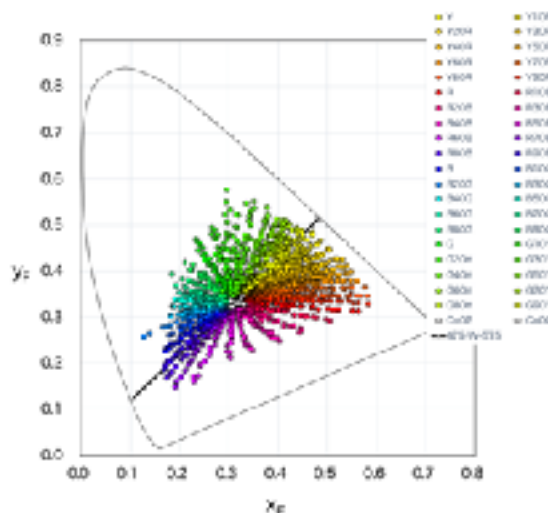


Figure 1. The chromaticities of the 1,948 color chips of NCS

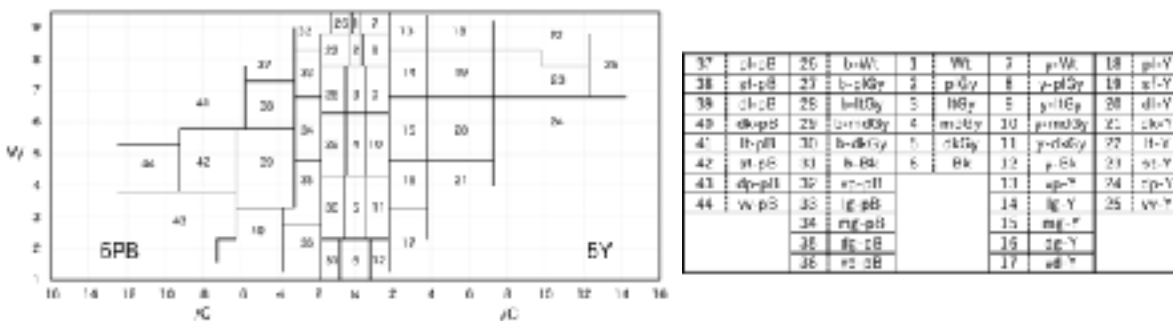


Figure 2. The regions of color name designation of 5PB,N, and 5Y

spectral reflectances of the corners and the spectral power distribution of the D65 illuminant. Figures 3 and 4, respectively, show the protanopic and deuteranopic simulated chromaticities of the 1,948 NCS color chips, with the regions of categories of color name designation in the CIE 2015XYZ. Each region surrounded by the dashed lines indicates the acceptable color-shift region for dichromats when the colors are modified for trichromats in the second step.

The colors included in the same color name designation region of both the protanopic and deuteranopic simulations are candidate colors for trichromats. The algorithm proposed by Brettel et al. [8] was adapted to the dichromatic simulation. However, the D65 chromaticity and Stockman and Sharpe's cone fundamentals [9] were used, instead of the equal-energy white chromaticity and Stockman, MacLeod and Johnson's cone fundamentals [10], in our algorithm.

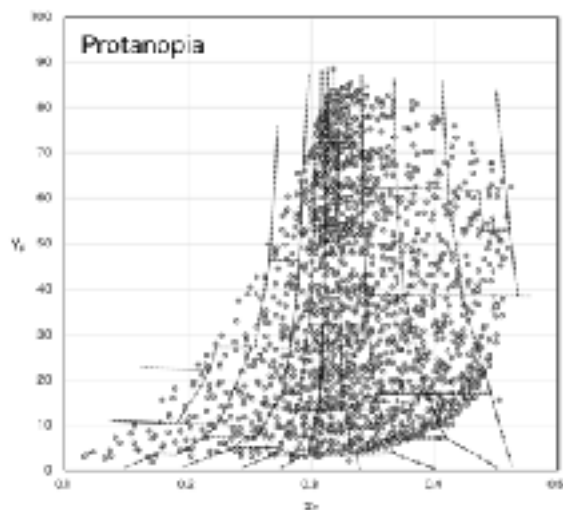


Figure 3. The regions of the color name designation and the x-Y plots of the protanopic simulation

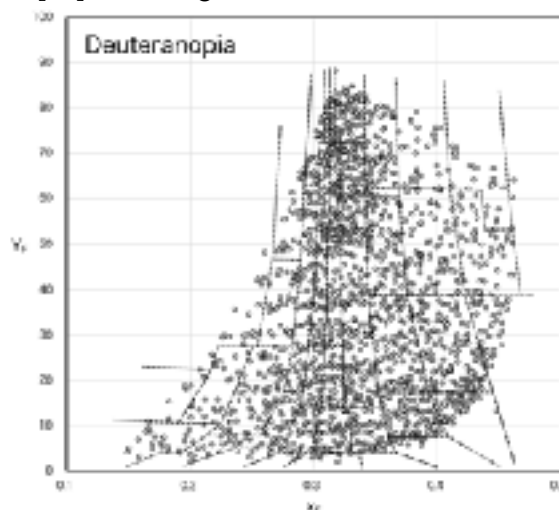


Figure 4. The regions of the color name designation and the x-Y plots of the deuteranopic simulation

RESULTS

Color sample set

The color sample set we made is shown in Figure 5. The 1,948 NCS color chips were assigned to 43 categories out of the 44 categories (all except the bluish-black) of color name designation in the 5PB-N(neutral)-5Y color plane. The 1,107 color chips belonged to the same color name designation region of both the protanopic simulation and deuteranopic simulation.

Color design using the color sample set

In order to examine whether our color sample set was of practical use, we used it for coloring a sign on our campus, in association with the members of the peer supporters of people with



Figure 5. The color sample set for color universal design method using categories of color name designation

disabilities, in the campus barrier-free design project at Kyushu University. Figure 6a shows a target sign for coloring, in this case a route map of the buses across our campus. As shown in Figure 6a, because one shade each of red, orange and yellow, which may be confusing colors for dichromats, were used in the original map, its colors should be modified. The colors for dichromats were chosen from the colors represented in Figure 5. The colors for trichromats were replaced by the colors belonging to the identical bundle of each category of color name designation. The RGB values of the last colors selected for the map were calculated from the CIE 1931XYZ tri-stimulus values of the NCS color chips [11, 12]. Figures 6b and 6c show the coloring of the maps for dichromats and trichromats, respectively.

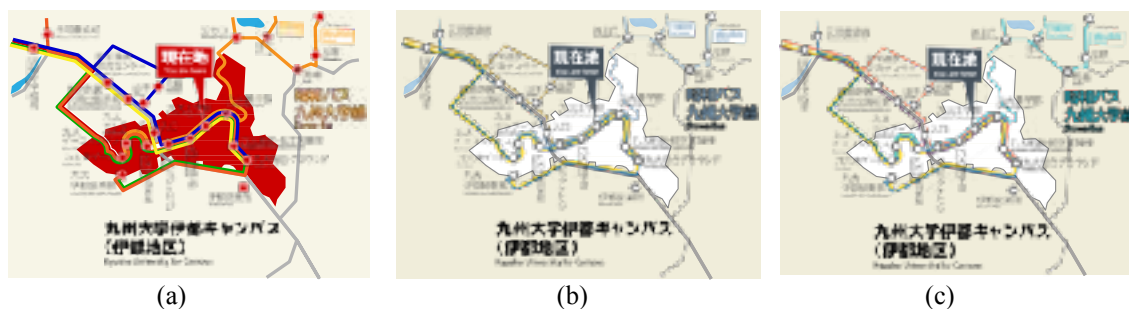


Figure 6. (a) Original map, (b) modified map for dichromats, (c) modified map for trichromats

CONCLUSIONS

We have developed a color sample set consisting of 1,948 color chips, from the viewpoint of dichromats, for color universal design. Moreover, we examined whether our color sample set is fit for practical use. We found that the color sample set is very applicable for color universal design.

ACKNOWLEDGMENTS

This work was supported by JST Global Science Campus and JSPS KAKENHI Grant Number 17H00809. We gratefully acknowledge the members of the peer supporters for people with disabilities, Kyushu University. We thank Claire Barnes, PhD, from Edanz Group (www.edanzediting.com/ac) for editing a draft of this manuscript.

REFERENCES

1. Asada, K. (2013). Chromatic Vision Simulator. <http://asada.tukusi.ne.jp/cvsimulator/e>.
2. Sato, T. (2010). *Iro wo sentaku suru houhou* (A method for selecting colors). Japan patent 4507641 [in Japanese].
3. Sunaga, S., Kido, K., and Katsura, S. (2018). A proposal of a color universal design method based on the viewpoint of dichromacy using categories of color name designation. *Journal of Color Science Association of Japan*, 42(5), 209-217 [in Japanese with English abstract].
4. CIE 170-2. (2015). Fundamental chromaticity diagram with physiological axes – Part II: Spectral luminous efficiency functions and chromaticity diagrams.
5. JIS Z 8102. (2001). Names of non luminous object colours [in Japanese].
6. JIS Z 8712. (1993). Colour specification – Specification according to their three attributes [in Japanese].
7. Sobagaki, H., Takahama, K., and Nayatani, Y. (1984). Analysis on spectral reflectance distributions of the Munsell colors. *Journal of Color Science Association of Japan*, 7(4), 167-174 [in Japanese with English abstract].

8. Brettel, H., Viènot, F., and Mollon, J. D. (1997). Computerized simulation of color appearance for dichromats. *Journal of Optical Society of America A*, 14(10), 2647-2655.
9. CIE 170-1. (2006). Fundamental chromaticity diagram with physiological axes – Part I.
10. Stockman, A., MacLeod, D. I. A., and Johnson, N. E. (1993). Spectral sensitivities of the human cones. *Journal of Optical Society of America A*, 10(12), 2491-2521.
11. Stokes, M., Anderson, M., Chandrasekar, S., and Motta, R. (1996). A standard default color space for the internet – sRGB. <https://www.w3.org/Graphics/Color/sRGB>.
12. Adobe® RGB. (1998). Color image encoding. <http://www.adobe.com>.

Effects of colors on the illusory self-motion perception (vection)

Takeharu Seno^{1*}, Masaki Ogawa², Shoji Sunaga¹ and Hiroyuki Ito¹

¹*Faculty of Design, Kyushu University, 4-9-1 Shiobaru, Minami-ku Fukuoka, Japan.*

²*Faculty of Engineering, Mie University, 1577 Kurimamachiya-cho Tsu city, Mie, Japan.*

*Corresponding author: Takeharu Seno, seno@design.kyushu-u.ac.jp

Keywords: vection, red, colorful, optic flow

ABSTRACT

In this presentation, two articles about the effects of colors on vection were reviewed by the author himself. Two articles are, Seno, Sunaga, & Ito (2010, Attention, perception & Psychophysics) and Ogawa & Seno (2016, TVRSJ). In both articles, expanding optical flows during one's forward self-motion were simulated by moving dots. In the first article, the dots and the background were painted in equiluminant red and green. Experiments showed that vection was weaker when the background was red than when the background was green. In the second article, we measured vection strength induced by six different colors in an optic flow stimulus. Vection strength was inhibited by multiple colored dots but not by uniform grey dots. In conclusion, color has a strong impact on vection.

INTRODUCTION

When stationary observers are exposed to a large visual motion field, simulating the retinal flow generated by self-translation or self-rotation, they often experience an illusory perception of self-motion, known as vection (Fischer & Kornmuller, 1930). In the history of vection research, various stimulus attributes that are effective or ineffective for vection induction have been examined extensively (e.g. Palmisano et al., 2015; Seno et al., 2017, 2018).

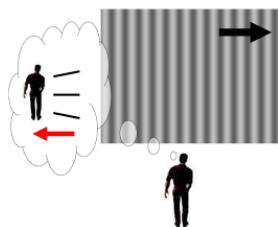


Figure 1. A schematic illustration of vection.

Is red effective or inefficient for vection induction?

First, we investigated the effect of color “red” on vection induction. Expanding dots as optical flows were presented to the participants, as simulated one's forward self-motion. Twelve naive volunteers participated in all experiments. They were either graduate or undergraduate students (20–27 years of age, 8 males and 4 females). All of them had normal color vision that we assessed by the Fransworth–Munsell 100-hue test, and they had not experienced any disease of the vestibular system. Informed consent was obtained from each subject. The white dots and the background were set to be in the equiluminant red and green.

Results showed that vection was weaker when the background was red than when the background was green. Also, vection was weaker when the moving dots were red than when the dots were green. Furthermore, it was revealed that red dots on a red background induced very weak vection, as compared with green dots on a green background. These results could not be explained by some luminance artifacts. We presented these results in the article already published (Seno, Sunaga and Ito, 2010, Attention, Perception & Psychophysics).

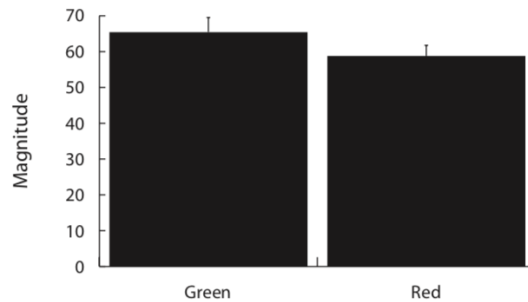


Figure 2. The results in Seno et al., 2010

Is colorful stimulus effective or inefficient for vection induction?

In the other article (Ogawa & Seno, 2016, TVRSJ), we measured vection strength induced by six different colors in an optic flow stimulus. Vection strength was measured by using button pressing and by magnitude estimation. Twenty naive volunteers participated. They were either graduate or undergraduate students and had normal color vision. The six colors were red, green, blue, cyan, magenta and yellow with luminances of 6, 42, 5.09, 3.14, 21.9, 9.23, and 24.2 cd/m² respectively. Those XY chromaticities were X; 0.66, Y; 0.31, (Red), X; 0.29, Y; 0.64, (Green), X; 0.14, Y; 0.06, (Blue), X; 0.19, Y; 0.27, (Cyan), X; 0.29, Y; 0.13, (Magenta), and X; 0.43, Y; 0.52, (Yellow). As a control condition, uniform grey dots were used in the expanding dots optical flow. The luminance of the grey dots was set to 11.5 cd/m².

Vection strength was weaker in the multiple colored dots rather than in the uniform grey dots. Even with brighter background, this inhibition effect was obtained. Too colorful stimulus was not effective for vection induction. This result might be related to the fact that stimuli that are ‘too colorful’ are not a realistic representation of the external world.

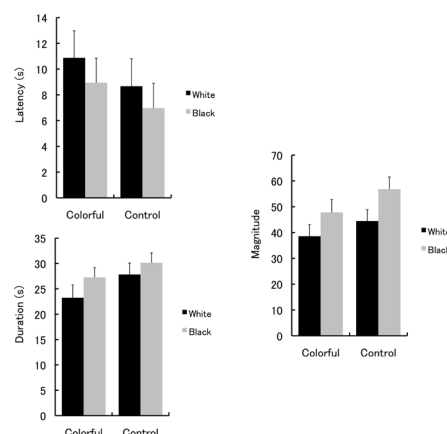


Figure 3. The results in Ogawa & Seno, 2016, TVRSJ

General Discussion

In the two articles, we had reported two findings. First, red is inefficient color for vection induction. Second, very colorful stimuli are also inefficient for vection induction. However, totally the opposite results were reported by Seya, Yamaguchi & Shinoda (2015) and by Bonato & Bubka (2006). They reported that red stimuli and colorful stimuli could enhance perceived vection. We thought that the colors might be special for self-motion perception and the directions of the effects of them could be modulated by the differences in the stimulus types. The further experiments should be done for the integrated understanding of this topic, i.e. color and vection.

ACKNOWLEDGEMENT

This work was supported by MEXT KAKENHI (Grant number JP26700016, JP17K12869, and JP18H01100) to TS. Part of this work was carried out under the Cooperative Research Project Program of the Research Institute of Electrical Communication, Tohoku University.

REFERENCES

1. Seno, T., Sunaga, S. & Ito H. 2009 "Inhibition of vection by red." *Attention, Perception & Psychophysics*, 72, 1642-1653.
2. Ogawa, M. & Seno T. 2016 "Colorful stimuli might inhibit Vection." *Transactions of the Virtual Reality Society of Japan*, 21(1), 31-34.
3. Fischer, M. H. & Kornmuller, A. E. 1930 "Optokinetic ausgeloste Bewegungs-wahrnehmungen und optokinetischer Nystagmus." *Journal of Psychological Neurology*, 41, 273-308.
4. Palmisano, S., Allison, R.S, Schira, M.M. & Barry, R.J. 2015 "Future Challenges for Vection Research: Definitions, Functional Significance, Measures and Neural Bases." *Frontiers in Psychology*, 6(193), 1-15.
5. Seno, T., Sawai, K. I., Kanaya, H., Wakebe, T., Ogawa, M., Fujii, Y., & Palmisano, S. 2017 "The Oscillating Potential Model of Visually Induced Vection." *i-Perception*, 8(6), 2041669517742176.
6. Seno, T., Murata, K., Fuji, Y., Kanaya, H., Ogawa, M., Tokunaga, K. & Palmisano, S. 2018 "Vection is enhanced by increased exposure to optic flow." *i-Perception*, 9(3), 2041669518774069.
7. Bonato F. & Bubka A. 2006 "Chromaticity, spatial complexity, and self-motion perception." *Perception* 35 53-64.
8. Seya, Y., Yamaguchi, M. & Shinoda, H. 2015 "Single stimulus color can modulate vection." *Frontiers in psychology*, 6, 406.

EMOTIONAL RESPONSES OF DICHROMATS TO COLORS AND COLOR NAMES

Shigehito Katsura^{1*}, Yoshino Tanaka², Kei Kawamoto³ and Shoji Sunaga¹

¹*Faculty of Design, Kyushu University, Japan.*

²*School of Design, Kyushu University, Japan.*

³*School of Design, Kawasaki University of medical welfare, Japan.*

*Corresponding author: Shigehito Katsura, katsura.shigehito.997@m.kyushu-u.ac.jp

Keywords: Dichromat, Deuteranope, Trichromat, Color emotion, Semantic differential method

ABSTRACT

Colors are well known to influence emotional responses in humans. For example, the color red is associated with warmth, while blue is associated with cold. The emotional effects of colors are frequent components of visual information encountered in daily life. For instance, red and blue are often used to indicate temperature on water faucets, with the expectation that individuals will implicitly know the color meanings. The emotional effects of colors play an important role in design.

Trichromacy and dichromacy are two types of color vision. While trichromats have three types of retinal cone photoreceptors, dichromats have only two. Therefore, dichromats perceive different colors compared with trichromats. Indeed, Jameson and Hurvich (1978) reported that categorical color naming has been found to differ between trichromats and dichromats. Differences in color perception and categorical color naming likely modulate emotional responses to colors and color names in trichromats vs. dichromats. Kawamoto et al. (2008) reported that while trichromats and dichromats assigned the same names to colors, the two groups reported different emotional responses to colors. In this study, we sought to investigate emotional responses to “color names” and “color stimuli” in trichromats and dichromats.

Ten trichromats and four deuteranopes participated in this experiment. Observers assessed 37 colors and 11 color names on 13 color emotion scales: Passionate-Calm, Warm-Cool, Dynamic-Static, Strong-Weak, Hard-Soft, Deep-Pale, Clear-Muddy, Clean-Dirty, Like-Dislike, Feminine-Masculine, Dangerous-Safe, Sweet-Bitter, and Spicy-Sour. They also assigned colors presented on a monitor to categorical color names (Red, Orange, Yellow, Green, Blue, Purple, Brown, Pink, Black, Gray, and White).

Our results showed that the emotional responses to the color names were similar between trichromats and deuteranopes. The color stimuli with higher consensus in terms of color categorization evoked similar emotions among the observers with different color vision types, with the exception of colors categorized as “Pink” and “White”. It is possible that the emotional responses to the color stimuli with higher consensus resembled the emotional responses to the corresponding color names. Consequently, we suggest that the color stimuli with higher consensus regarding color categorization, such as focal colors, evoked the most consistent emotions from both trichromats and dichromats.

INTRODUCTION

Colors may be characterized in complex ways, such as elegant, romantic, or beautiful, and can elicit emotional responses. They often affect the decisions that people make such as choosing whether one likes or dislikes an object. Thus, colors that consistently evoke particular emotions can be useful components of the visual information that induces people to think or behave in certain ways. For instance, red and blue are often used to indicate hot and cold on a water faucet, based on

the expectation that individuals will implicitly know these color meanings. Colors play an important role in product design and as a component of visual information.

The use of colors to convey specific information relies upon the assumption that color perception is shared among individuals. However, there are multiple types of color vision. Most individuals are trichromatic, and have three types of retinal cone photoreceptors. However, individuals with dichromacy, which make up about 5% of males, have only two of the three types of retinal cone photoreceptors. Therefore, dichromats and trichromats have differing color perception as well as categorical color naming [1]. As a result, it is possible that colors evoke different feelings in dichromats vs. trichromats.

Several previous studies have used the semantic differential rating scale to investigate color emotions in trichromats. Particularly, Oyama et al. (1965) showed that evaluations of emotional responses to colors could be categorized according to three factors: activity, potency, and evaluation [2].

However, few studies have examined color emotions in dichromats. Kawamoto et al. (2008) reported that while trichromats and dichromats assigned the same color names to colors, the colors elicited different emotional responses among the observer groups [3]. Noguchi and Mitsuboshi (2015) reported that trichromats and color deficiencies varied in terms of the emotions elicited by red, orange, and white, but not those elicited by blue, purple, gray, and black [4]. Ichihara (2017) reported that green elicited different emotional responses between trichromats and dichromats [5]. It was not clear whether observers were consistent in how they assigned the color stimuli to color names because the observers were not asked to report the color names.

In the present study, we investigated differences in emotional responses to “color names” and “color stimuli” between trichromats and dichromats. We sought to clarify whether: (i) there was agreement regarding emotional responses to color names, and (ii), whether colors assigned to the same color names in trichromats and dichromats would evoke the same emotions in these groups. Investigation color emotions in dichromats may impact the color universal design such that design choices reflect color emotions in dichromats as well as trichromats.

METHOD

Apparatus and Stimulus

To investigate emotional response to “color stimuli”, observers were asked to look at a color patch presented on a 24-inch LCD monitor (EIZO ColorEdge CS2420-BK) controlled by a computer (Apple Mac mini) while sitting in a dark room. The viewing distance was 60 cm. Each color patch had an area of 4 degrees squared, and was presented on the center of the monitor. The area surrounding the color patch was gray (77.64 cd/m^2) that had Munsell value of N6.5, and a white reference frame (193.05 cd/m^2) surrounded the area. The chromaticity of the white reference frame was the same as the chromaticity of the white standard illuminant D65.

We chose 37 colors from the Munsell color system. The Munsell color notations and the CIE 1931 chromaticity coordinates of the 37 color stimuli are shown in Table 1.

Semantic Differential Scale

We used the semantic differential scale. Observers completed a questionnaire with 13 bipolar seven-step-scaled, which were represented with the words, extremely, quite, slightly, and equally, emotional-word pairs for each color stimulus. Of these, Passionate-Calm, Warm-Cool, Dynamic-Static, Strong-Weak, Hard-Soft, Deep-Pale, Clear-Muddy, and Clean-Dirty were used to confirm whether the evaluations of emotional responses were categorized according to the three primary factors, as in previous research [2]. We used the others, Like-Dislike, Feminine-Masculine, Dangerous-Safe, Sweet-Bitter, and Spicy-Sour, to examine the differences among color vision types because these are most applicable to product design.

Observers

Ten trichromats and four dichromats, all of whom were deuteranopes, participated in the experiments. We asked each observer to undergo color vision tests using Ishihara plates, the Panel D-15 test, the Farnsworth-Munsell 100-hue test, and the Nagel anomaloscope (Anomaloscope OT-II, Neitz), and we identified the type of color vision according to the results.

Procedure

Observers were informed regarding the purpose of the study before the experiments began. The “color stimuli” experiment began after 2 minutes of adaptation to the white reference displayed on the monitor. The color patches were displayed one by one in a random order. The observer’s task was to rate the presented color stimulus and write down their rating on the questionnaire paper. After rating all 13 emotional-word pairs, observers were asked to verbally report an optimal color name for each of the presented color stimuli. They were asked to choose from 11 color names (Red, Orange, Yellow, Green, Blue, Purple, Brown, Pink, Black, Gray, and White). Each observer evaluated 37 color stimuli.

The “color names” experiment was conducted in an experimental booth illuminated by D65 fluorescent lamps. Observers were asked to imagine a color that they associated with the color name given on the questionnaire paper. They rated the color that they imagined using the same method as that used in the “color stimuli” experiment except that they reported a color name. Each observer evaluated the 11 categorical color names described above.

The order of the two experiments was counterbalanced across observers.

Table 1: Munsell color notations and the CIE 1931 chromaticity coordinates for 37 color stimuli

No.	H V/C	Y	x	y	No.	H V/C	Y	x	y
1	5R 3/4	6.3	0.4	0.3	20	10PB 6/8	29	0.3	0.2
2	2.5GY 3/3	6.4	0.4	0.4	21	10R 7/2	42	0.3	0.3
3	7.5B 3/1	6.4	0.3	0.3	22	10R 7/16	41	0.6	0.4
4	10B 3/2	6.4	0.3	0.3	23	5Y 7/10	42	0.4	0.5
5	7.5PB 3/30	6	0.2	0.1	24	7.5PB 7/6	42	0.3	0.3
6	10P 3/16	6.3	0.3	0.2	25	2.5RP 7/3	42	0.3	0.3
7	2.5R 3/1	6.4	0.3	0.3	26	10R 8/4	57	0.4	0.3
8	10PB 4/28	11	0.2	0.1	27	5PB 8/4	58	0.3	0.3
9	5RP 4/4	12	0.4	0.3	28	5R 9/2	77	0.3	0.3
10	5R 5/6	19	0.4	0.3	29	10YR 9/2	77	0.3	0.4
11	5R 5/18	19	0.6	0.3	30	10Y 9/16	77	0.4	0.5
12	2.5Y 5/10	19	0.5	0.5	31	5GY 9/16	77	0.4	0.6
13	5GY 5/4	19	0.3	0.4	32	5BG 9/2	77	0.3	0.3
14	5G 5/8	20	0.3	0.4	33	2.5B 9/3	77	0.3	0.3
15	5B 5/10	20	0.2	0.3	34	2.5RP 9/3	77	0.3	0.3
16	10B 5/4	19	0.3	0.3	35	N 1	1.2	0.3	0.3
17	5RP 5/16	19	0.4	0.2	36	N 7	42	0.3	0.3
18	7.5RP 5/18	19	0.5	0.2	37	N 9	77	0.3	0.3
19	5PB 6/4	29	0.3	0.3					

Table 2: The results of color categorization and the maximum ratio

No.	Trichromats		Deuteranopes		No.	Trichromats		Deuteranopes	
	The ratio	color name	The ratio	color name		The ratio	color name	The ratio	
11	1	Red	0.75		10	0.6	Red	Brown	0.5
22	1	Orange	0.75		33	0.8	Blue	White	1
30	1	Yellow	0.75		16	0.6	Blue	Green	0.5
31	0.9	Yellow	1		8	1	Purple	Blue	1
23	0.9	Yellow	0.75		20	1	Purple	Blue	0.75
14	1	Green	1		7	0.9	Brown	Green	0.75
13	1	Green	1		34	0.8	Pink	White	0.75
2	0.8	Green	0.5		26	0.6	Pink	Orange	0.5
5	1	Blue	1		3	0.6	Gray	Green	1
15	1	Blue	1		4	0.6	Gray	Green	0.75
24	0.4	Blue	1		27	0.5	White	Blue	0.5
6	1	Purple	1		29	0.3, 0.3, 0.3	Oe, Yw, We	White	0.5
1	0.9	Brown	0.75		12	0.4, 0.4	Yellow, Brown	Orange	0.75
17	0.9	Pink	1		32	0.4, 0.4	Blue, White	White	1
18	0.8	Pink	1		19	0.5, 0.5	Purple, Gray	Green, Blue	0.5, 0.5
21	0.6	Pink	0.5		9	0.4, 0.4	Purple, Brown	Gn, Pe, Pk, Gy	0.25 each
35	0.8	Black	1		25	0.8	Pink	Pink, Gray	0.5, 0.5
36	0.6	Gray	0.5						
37	1	White	1						
28	0.5	White	1						

RESULTS AND DISCUSSION

Emotional Responses to “Color Names”

Figure 1 shows the evaluation profiles of the color name “Green”. The black dotted line indicates the mean evaluation values given by the 10 trichromats, and the green solid line indicates those of the four deuteranopes. The seven-step-scales are represented as values. The two groups gave similar evaluations for “Green”, “Red”, “Orange”, “Yellow”, “Pink”, “Blue”, “White”, and “Black” but gave different evaluation results for “Gray”. Specifically, trichromats tended to evaluate “Gray” as weak, pale, and to state that they disliked it whereas deuteranopes tended to evaluate it conversely as strong, deep, and to state that they liked it. We also found differences between the groups for the color names “Purple” and “Brown”. Specifically, trichromats evaluated “Purple” as feminine and stated that they disliked “Brown” while deuteranopes evaluated these using the opposite descriptors.

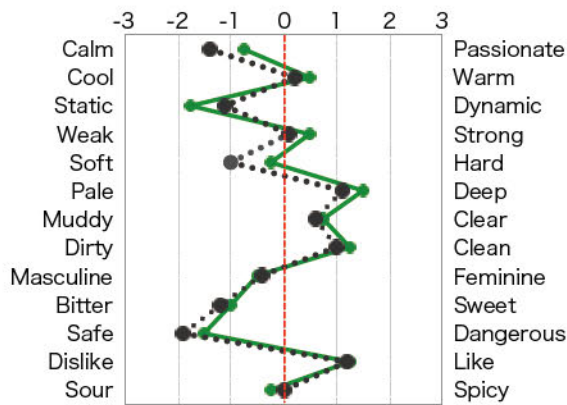


Figure 1. The evaluation profile for the color name “Green”

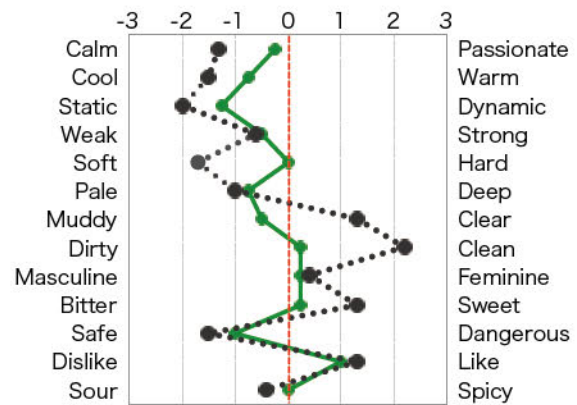


Figure 2. The evaluation profile for the color N9

We further investigated the emotional differences among color vision types using factor analysis with an orthogonal rotation technique. First, we divided the 13 emotional-word pairs into two groups. The first group included the eight pairs used in previous research, and second group included the five pairs that we added and three pairs, Passionate-Calm, Strong-Weak, and Clean-Dirty, extracted from the eight emotional-word pairs.

We calculated the factor loadings for first group and second group, respectively. As in previous research, we extracted three factors from the first group of trichromats and deuteranopes: activity, potency, and evaluation. We found that these factors accounted for 93% and 92% of the total variance in trichromats and deuteranopes, respectively. However, the contribution ratio for potency and evaluation was reversed in trichromats vs. deuteranopes. Moreover, in deuteranopes, the factor loading for Hard-Soft and Deep-Pale was nearly equal for the three factors. The correlation coefficients for each factor score among observer groups were 0.95 (activity), 0.93 (potency), and 0.93 (evaluation).

We extracted four factors from the second group of trichromats and deuteranopes, which accounted for 92% and 87% of the total variance in these observers, respectively. The first factor, regarded as activity, included Feminine-Masculine and Sweet-Bitter. The second factor, regarded as evaluation, included Like-Dislike. The third factor, regarded as potency, included Dangerous-Safe. The fourth factor included Spicy-Sour only. The correlation coefficients for each factor score among observer groups were 0.85 (factor 1), 0.82 (factor 2), 0.90 (factor 3) and 0.83 (factor 4).

These results indicate that the emotional responses to “color names” reflected similar emotions in trichromats and deuteranopes.

Emotional Response to “Color Stimuli”

Table 2 shows the color names categorized by each color vision type for each color stimulus. The values indicate the maximum ratio of observers who categorized the color stimulus according to the color name. While the categorization of 20 colors by color name was consistent among observer groups, the two groups assigned eleven colors to different color name categories. We could not determine whether the six remaining colors were assigned to the same color name in observer groups because these colors were assigned into more than one color name by at least one of observer groups.

Figure 2 shows the evaluation profiles of color N9. The black dotted line indicates the mean evaluation values for the 10 trichromats, and the green solid line indicates those for the four deuteranopes. The color stimulus elicited high consensus regarding color categorization but did not provoke similar emotional responses among the observer groups. Trichromats tended to evaluate the color stimulus categorized as “White” as clear, whereas conversely, deuteranopes tended to

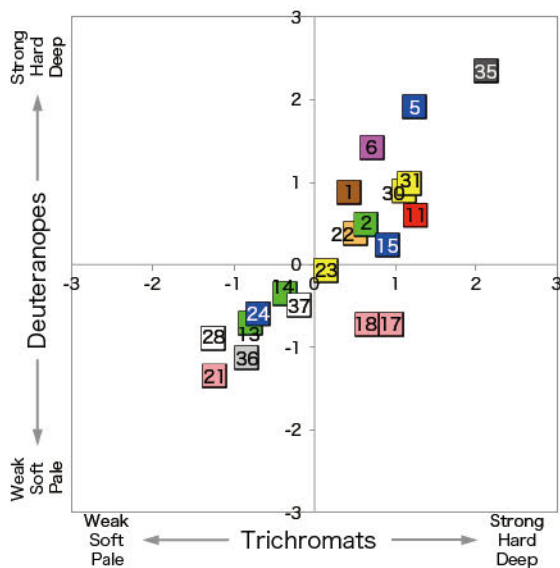


Figure 3. The relationship between the factor scores for “potency”

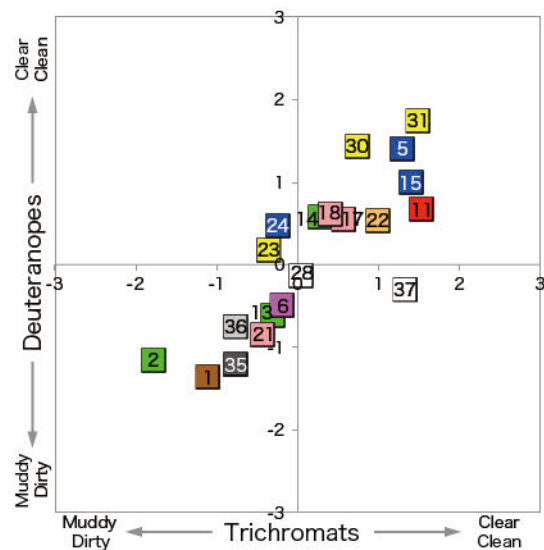


Figure 4. The relationship between the factor scores for “evaluation”

evaluate it as muddy. The two groups gave different evaluation results for another color stimulus. Specifically, trichromats tended to evaluate the color stimulus, 5RP 5/16, categorized as “Pink” as strong, deep, and dangerous, whereas deuteranopes tended to evaluate it instead as weak, pale, and safe. We also found some emotional differences in the response to the eight colors that were regarded as having the same color categorization.

We calculated the factor loadings for first group and second group, respectively. We extracted three factors from the first group of trichromats and deuteranopes, which accounted for 92% and 86% of the total variance in the two groups, respectively. We found no differences in the emotional words clustered into each factor.

To investigate the factor differences between trichromats and deuteranopes, we plotted each factor score. Figures 3 and 4 show the relationships between the factor scores, potency, and evaluation for the 20 colors according to color categorization by observer group. The abscissa represents the factor scores for trichromats, and the ordinate represents those for deuteranopes. The color number indicated in Tables 1 and 2 are shown inside or beside the symbols. In these figures, the data plotted in the first and third quadrants represent the color stimuli for which the two observer groups reported having the same feelings, and those plotted in the second and fourth quadrants represent color stimuli for which the two observer groups had different feelings.

As shown in Figures 3 and 4, most of the colors are plotted in the first or third quadrants. For example, two colors, 10Y 9/16 and 7.5PB 3/30, plotted in the first quadrant were categorized as “Yellow” and “Blue”, respectively. Each of them evoked the same feeling in trichromats and deuteranopes. The colors were highly saturated colors, and had higher consensus regarding color categorization. In contrast, other two colors, 5Y 7/10 and 7.5PB 7/6, plotted in the second quadrant in Figure 4 were also categorized as “Yellow” and “Blue”, respectively, and evoked the different feeling. These color stimuli had low consensus in terms of color categorization, and were less saturated colors than the colors with high consensus categorized as the same color names.

On the other hand, one color stimulus categorized as “White” and two color stimuli categorized as “Pink” elicited high consensus regarding color categorization, but did not provoke similar emotional responses among the observer groups. The “White” color plotted in the fourth quadrant in Figure 4 was N9, and the “Pink” colors plotted in the fourth quadrant in Figure 3 were 5RP 5/16 and 7.5RP 5/18, that were highly saturated colors. In addition, another color categorized as “Pink”

was plotted in the third quadrant in Figure 3. This color stimulus was a desaturated color, 10R 7/2, which evoked the same feeling in trichromats and deuteranopes, and had lower consensus in terms of color categorization. The relationship for the color categorized as “White” or “Pink” between agreement of color emotions in trichromats and deuteranopes and consensus regarding color categorization was opposite to the other colors.

We extracted four factors from the second group of trichromats and deuteranopes, which accounted for 87% and 78% of the total variance, respectively. We found no differences in the factor analysis of “color names”. The color stimuli, categorized as “Pink” and “White” described above, also differed in terms of factor 2 (potency) and factor 3 (evaluation), respectively.

These results indicate that the color stimuli with high consensus in terms of color categorization evoked the same feeling in trichromats and deuteranopes with some exceptions, such as the color stimuli categorized as “Pink” and “White”. It is possible that the emotional responses to color names resembled those to color stimuli for colors that had high consensus regarding color categorization.

CONCLUSION

We compared emotional responses to “color names” and “color stimuli” between trichromats and deuteranopes. Our results indicate that the emotional responses to “color names” were similar in trichromats and deuteranopes with some exceptions. The largest difference was the emotional response to “Purple” as Feminine-Masculine, to “Brown” as Like-Dislike, and to “Gray” as Strong-Weak, Deep-Pale, and Like-Dislike.

The color stimuli with higher consensus in terms of color categorization among color vision types evoked similar emotions between trichromats and deuteranopes, except for the colors categorized as “Pink” and “White”. The highly saturated colors categorized as “Pink” were associated with strong, deep, and dangerous in trichromats but not dichromats, while the color categorized as “White” was associated with muddy in dichromats but not trichromats. The emotional responses to “color names” did not reflect those differences. It is possible that the emotional responses to “color names” resemble those to color stimuli for colors with high consensus regarding color categorization.

Consequently, we infer that color stimuli with higher levels of consensus in terms of color categorization, such as focal colors, are more likely to evoke similar emotions in trichromats and dichromats, at the least deuteranopes.

ACKNOWLEDGEMENTS

This work was supported by JSPS KAKENHI Grant Number 17H00809. We gratefully acknowledge the participants of the experiments. We thank Sydney Koke, MFA, from Edanz Group (www.edanzediting.com/ac) for editing a draft of this manuscript.

REFERENCES

1. Jameson, D., & Hurvich, L. M. (1978). Dichromatic color language: “reds” and “greens” don’t look alike but their colors do. *Sensory processes*, 2, 146-155.
2. Oyama, T., Soma, I., Tomiie, T., & Chijiwa, H. (1965). A factor analytical study on affective responses to color. *Acta Chromatica*, 1(4), 164-173.
3. Kawamoto, K., Wake, T., & Yasuma, T. (2008). Identified color and impression of color deficiencies on color categorization. *The collection of papers of the Color Science Association of Japan*, Supplement 32, 124-125. [in Japanese].
4. Noguchi, Y., & Mitsuboshi, M. (2015). The color image of dichromats and anomalous trichromats. *Proceedings of AIC 2015*, 354-359.
5. Ichihara, Y. (2017). Impression evaluation between colour vision types. *Journal of Color Science Association of Japan*, Supplement 41(6+), 23-24. [in Japanese].

INFLUENCE OF HUE ON THE BRIGHTNESS PERCEPTION OF FACES IN THE DIFFERENT TYPE OF SKIN COLOR

Suguru Tanaka^{1*}, Kumiko Kikuchi², Yoko Mizokami¹

¹*Chiba University, Japan*

²*Shiseido Global Innovation Center, Japan*

*Corresponding author: Suguru Tanaka, normal0214@chiba-u.jp

Keywords: Skin, Face, Brightness, Color

ABSTRACT

Facial skin color is an important clue to obtain information such as health status, emotions, and races. Yoshikawa et al. (2012) showed that reddish skin tended to appear brighter than yellowish skin, even with the same average lightness. However, the experimental stimulus was the average face and skin color of Japanese females, and the observers were also Japanese. Human skin color is diverse, and the characteristics of skin color differ depending on races and other factors such as environments and lifestyles. In this study, we investigated whether the same brightness perception was shown in the skin colors of different races for Japanese observers. The average skin colors of four races (Caucasian, Thai, and African) were reproduced on the average face of Japanese females. We created five test stimuli in each race by changing the hue angle (h_{ab} in CIELAB) of skin colors to positive and negative directions in 4 and 8 degrees from the average skin color. For matching stimulus, we prepared a face image with seventeen lightness levels in each race. The hue angle of matching stimulus was kept at the average skin color of each race. We also tested stimulus with different lightness for Thai, African, and Japanese to examine the influence of hue and lightness on brightness perception. A test stimulus and a matching stimulus were presented side by side on an LCD in a dark room. Observers adjusted the brightness of the matching stimulus to match the brightness of the test stimulus. Observers were seven Japanese (four males and three females). As a result, the reddish skin appeared brighter, and the yellowish skin appeared darker for faces with higher lightness ($L^* = 59.6$ to 65.0) and a part of faces with the middle lightness ($L^* = 46.5$ to 50.0). However, this effect did not occur for faces with low lightness ($L^* = 35.0$). Therefore, it was shown that there is a relation between the influence of hue on the brightness perception of face and the lightness of facial skin. Besides, we examined the relationship between facial impression and the brightness perception of the face. We evaluated the impression of each face stimulus on five items: healthiness, preference, brightness, whiteness, and the visibility of face color. There was a correlation between healthiness and brightness perception in general. We also found a trend that reddish skin appeared healthier than yellowish skin. These results imply that the tendency that reddish skin appears brighter than yellowish skin is associated with facial impressions.

INTRODUCTION

Skin color is an important clue to know information about health, emotions, and race. Japanese skin color distribution data show that reddish skin is darker, and yellowish skin is lighter [1]. However, Yoshikawa et al. showed that reddish skin tends to look brighter, and yellowish skin tends to look darker even with the same average brightness [2]. It has also been shown that this effect is not seen in monochromatic patches. This suggests that we have perceptions specific to human skin color. In the study of Yoshikawa et al. [2], the average face and skin color of Japanese women were used as an experimental stimulus. However, human skin color is diverse, and skin color characteristics

vary depending on race. We verified that the skin color of different races showed similar perceptual characteristics of brightness [3]. Here we further investigate the influence of lightness on the brightness perception of face and the relationship between the impression and brightness perception of each face image.

EXPERIMENT

1. Experimental environment

Figure 1 shows the experimental environment. The experiment was conducted using an LCD monitor in a dark booth. A viewing distance was 60 cm, and the visual angle of a stimulus was $12.9^\circ \times 16.7^\circ$. A test stimulus was presented on the left and a matching stimulus on the right on the black display. Stimuli were framed with white lines, and the background of the face was equivalent to Munsell N5. The viewing angle of the width of the white line was 1.2° .

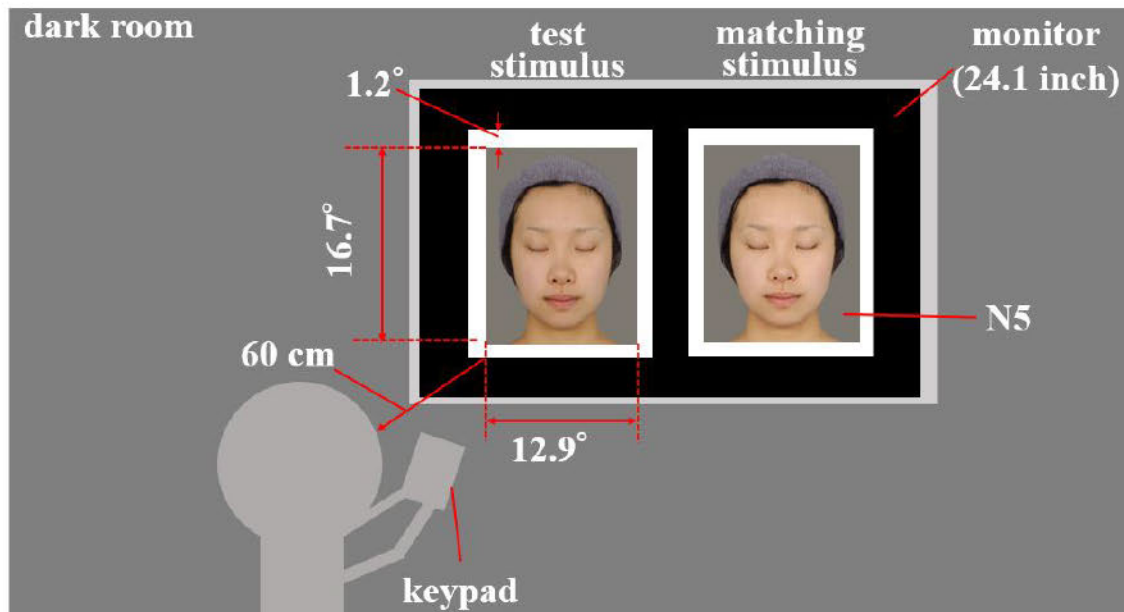


Figure 1. Experimental environment

2. Experimental stimulus

Using the average face of Japanese women, we reproduced the average skin color of Caucasian, Thai [4] and African [5], and performed an evaluation experiment on brightness. The hue angle was calculated from the a^* and b^* of the average skin color in each racial type. Each skin color was modulated in two steps at a 4-degree interval in the positive direction or yellowish direction and negative direction or reddish direction, based on the hue angle. A total of five test stimuli were created for each type. Figure 2 shows the test stimuli used in the experiment. The lightness L^* of the average skin color of each racial type was changed in 17 steps (-8 to +8) and used as a matching stimulus. In order to investigate the effect of skin color brightness and hue angle, stimulus images with varying brightness while maintaining the hue angle were also prepared for Africans, Thais, and Japanese.

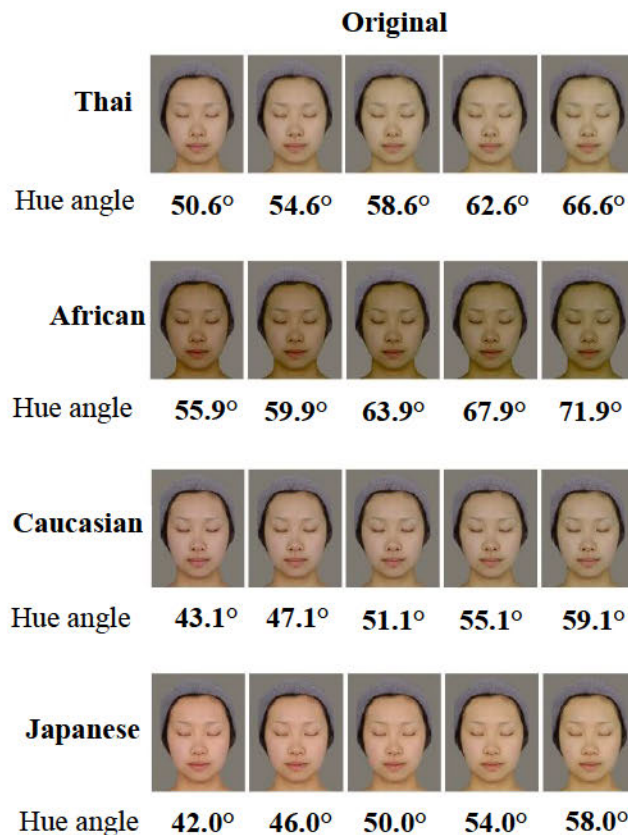


Figure 2. Test stimulus of the face image

2.3. Experimental procedure

The method of adjustment was used in the experiment. First, dark adaptation and light adaptation were performed for one minute each. An observer adjusted the brightness of a matching stimulus to match the brightness of a test stimulus. This procedure continued for all test stimuli in one session. The test stimuli with different hues and races were presented in random order. The observers were seven Japanese with normal color vision, and they conducted the experiment 5 sessions each.

RESULTS

Figure 3 shows the average results of all observers. The horizontal axis shows the hue angle of the test stimuli. The smaller the value is, the redder a face image is. The larger the value is, the yellower the face image. The vertical axis shows brightness that the observer matched to each test stimulus shown by perceived lightness L^* . Error bars are standard deviations. The results show that the reddish skin appeared brighter, and the yellowish skin appeared darker for faces with higher lightness ($L^* = 59.6$ to 65.0) and a part of faces with the middle lightness ($L^* = 46.5$ to 50.0). However, this effect did not occur for faces with low lightness ($L^* = 35.0$). Therefore, it was shown that there is a relation between the lightness of facial skin and the influence of hue on the brightness perception of the face.

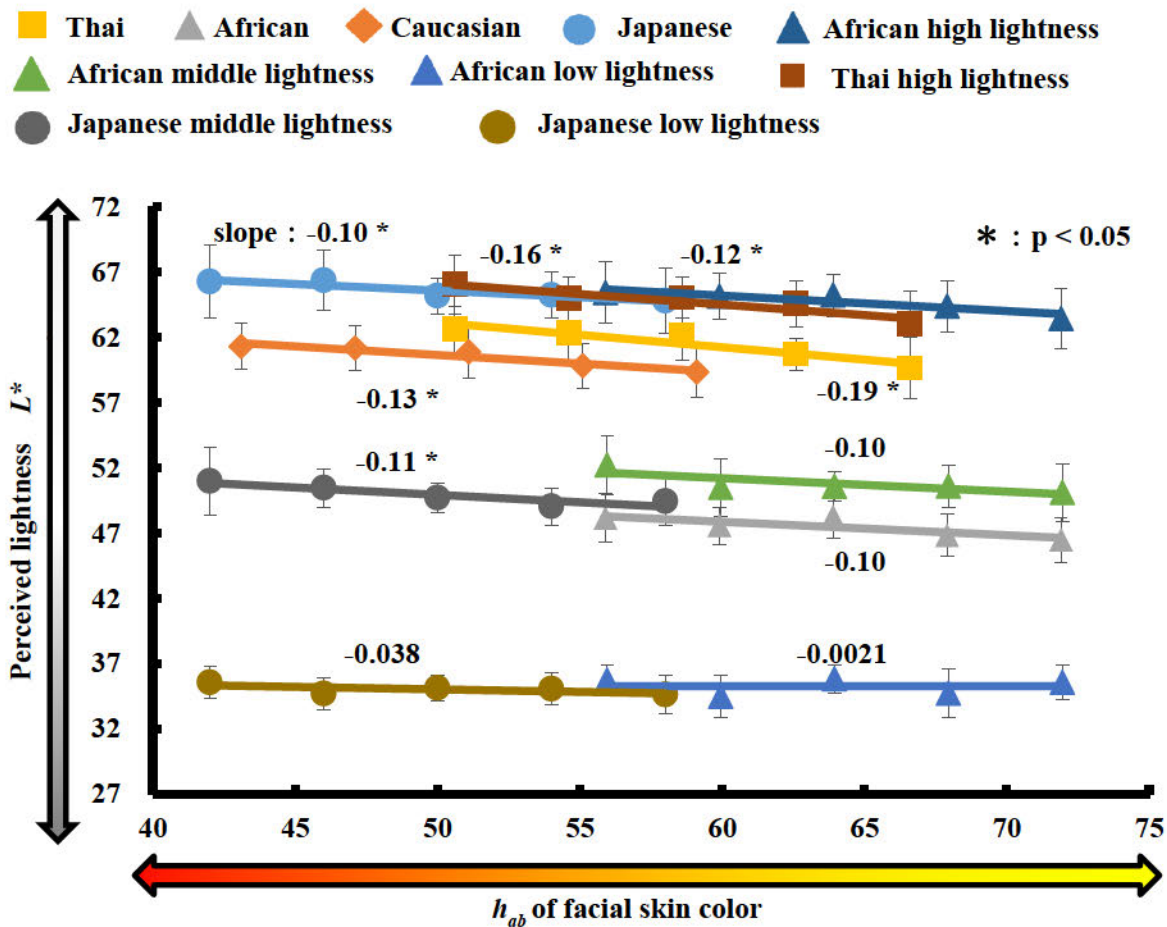


Figure 3. The result of brightness matching to each test stimulus

DISCUSSION

We discuss the reason why the hue of facial skin influences the brightness perception of a face. The observer's recognition of facial image may affect brightness perception. We evaluated the impression of each face stimulus on five items: healthiness, preference, brightness, whiteness, and the visibility of face color. Observers evaluated each item on a 7-point scale (-3 to 3).

The results of healthiness impression in relation to the hue of facial skin and brightness perception are shown in Figure 4 and 5. We found a trend that reddish skin appeared healthier than yellowish skin. There was a correlation between healthiness and brightness perception also. These results imply that the tendency that reddish skin appears brighter than yellowish skin is associated with facial impressions.

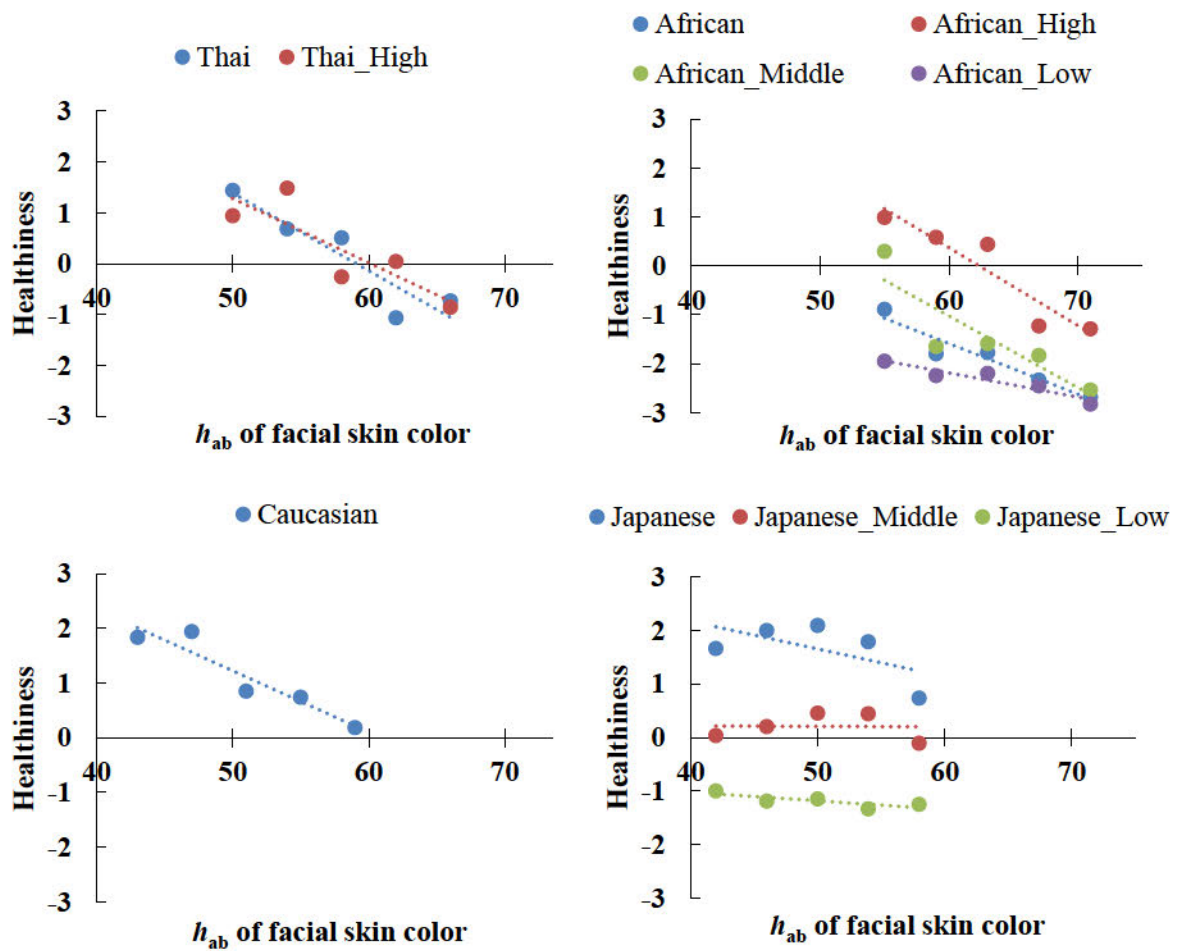
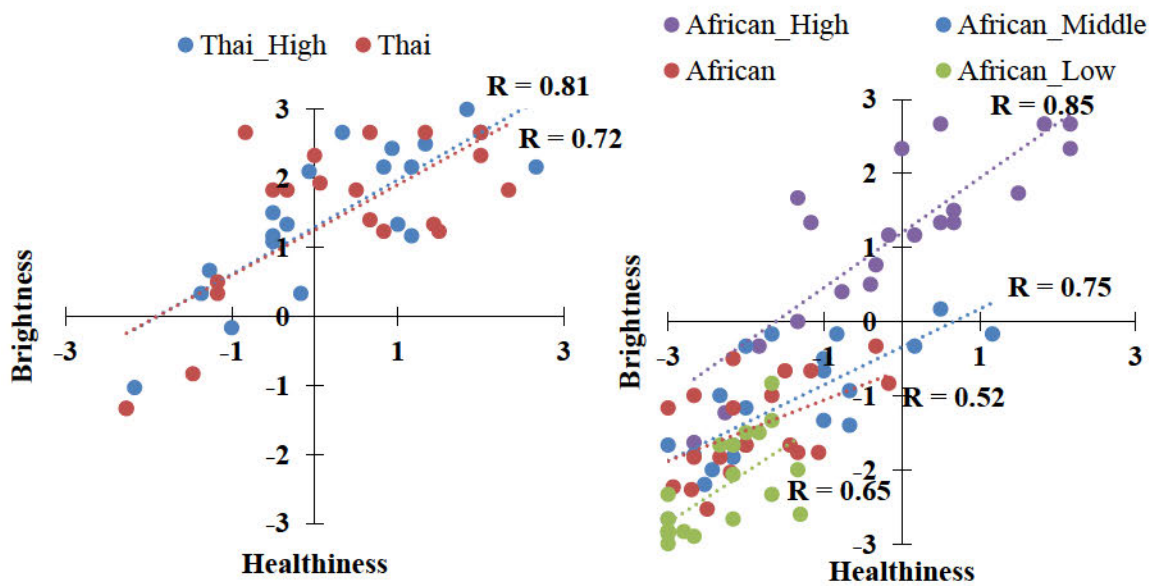


Figure 4. Relationship between healthiness and color for all stimuli



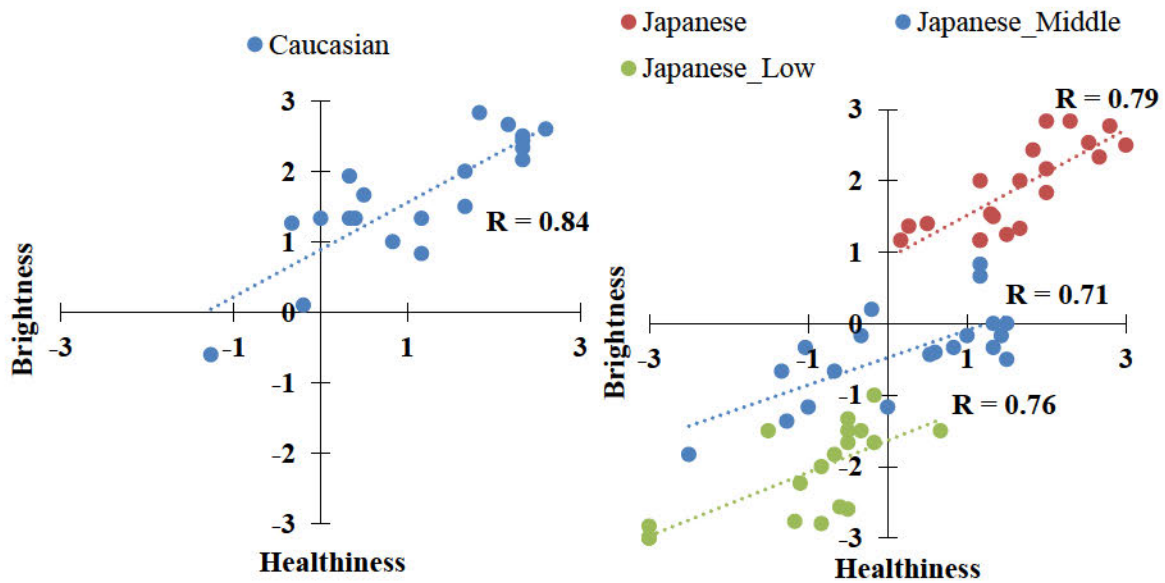


Figure 5. Relationship between brightness and healthiness for all stimuli

CONCLUSION

Our results showed that reddish skin tended to appear brighter than yellowish skin in the high lightness and a part of middle lightness levels. In the low lightness level, there was little influence of hue on the brightness perception. Thus, the influence of hue on brightness perception depends on the lightness of the face image. It was also suggested that the tendency that reddish skin appears brighter than yellowish skin may be associated with facial impressions such as healthiness.

ACKNOWLEDGEMENT

This work was supported by JSPS KAKENHI JP 16H01663 & 18H04183.

REFERENCES

1. Yoshikawa, H. (2005). Colorimetric Approach to the Skin Color. *JOURNAL OF THE COLOR SCIENCE ASSOCIATION OF JAPAN*, 29, 31-34.
2. Yoshikawa, H., Kikuchi, K., Yaguchi, H., Mizokami, Y., & Takata, S. (2012). Effect of chromatic components on facial skin whiteness. *Color Research & Application*, 37 (4), 281-291.
3. Tanaka, S., & Mizokami, M. (2019). Brightness perception on face in different type of skin color. *Asian Pacific Conference on Vision (APCV) 2019*.
4. Xiao, K., Yates, JM., Zardawi, F., Sueprasarn, S., Liao, N., Gill, L., Li, C., & Wuerqer, S. (2017). Characterising the variations in ethnic skin colours: a new calibrated data base for human skin. *Skin Research and Technology* 23, 21-29.
5. Janine, S. Everett, Mia, Budescu., & Marilyn, S. Sommers. (2012). Making Sense of Skin Color in Clinical Care. *Clinical Nursing Research*, 21-4, 1-22.

CONTRIBUTION OF SATURATION AND LIGHTNESS CONTRAST ON COLORFULNESS ADAPTATION OF IMAGES

Taishi Masumitsu^{1*} and Yoko Mizokami²

¹*Department of Imaging Science, Division of Creative Engineering, Graduate School of Science and Engineering, Chiba University, Japan*

²*Department of Imaging Sciences, Division of Creative Engineering, Graduate School of Engineering Chiba University, Japan*

*Corresponding author: Taishi Masumitsu, t.masumitsu@chiba-u.jp

Keywords: Colorfulness adaptation, Saturation, Lightness contrast, Naturalness, Natural image

ABSTRACT

It was shown that our visual system could adapt colorfulness changes in environments, and suggested that the spatial structure of images affects the strength of the colorfulness adaptation (Mizokami et al., 2012). Nakano et al. (2009) showed that the image appeared more natural when the luminance contrast of an image was increased (decreased) according to the increase (decrease) of saturation of the image than when only its saturation was changed. We showed that the effect of colorfulness adaptation was stronger for the natural combination of saturation and lightness contrast than for the unnatural combinations (2018). However, we did not differentiate the contribution of chromatic contrast and lightness contrast. There is a possibility that the modulation of lightness contrast of images enhanced the colorfulness of images and affected colorfulness adaptation. In this research, we examine the effect of colorfulness adaptation from the viewpoint of naturalness and the contribution of lightness contrast on images. In the experiment, four types of modulated images were used as adaptation stimuli: images which only their saturation changed ("Saturation-modulated stimuli"), images which their lightness contrast changed in proportion to the saturation ("Naturally-modulated stimuli"), images which their lightness contrast changed in inverse proportion to the saturation ("Unnaturally-modulated stimuli"), and images which only their lightness contrast changed ("Lightness contrast-modulated stimuli"). Test stimuli for colorfulness judgment were three types of images: "Saturation-modulated stimuli," "Naturally-modulated stimuli," and "Unnaturally-modulated stimuli." Each adaptation stimuli group included six images. Images for test stimuli were not included in adaptation stimuli. Following to three-minute-dark adaptation, observers adapted to images with a certain saturation level chosen from one of the adaptation stimuli groups for two minutes. After that, a test image was presented for three seconds, followed by ten-second re-adaptation to the same adaptation stimuli, and observers judged whether the test image appeared "natural" or "too colorful." This judgment was repeated for seven test images during one session. We examined three saturation levels in three adaptation stimuli groups and three lightness contrast levels in lightness contrast-modulated stimuli. Seven observers participated, and each observer ran three sessions for each condition. Our results showed a colorfulness adaptation in most conditions. When observers adapted to images with higher saturation, the border of "natural" and "too colorful" appearance shifted to higher saturation and vice versa. The effect was stronger when adapting to saturation-modulated stimuli and naturally-modulated stimuli, and weaker when adapting to unnaturally-modulated stimuli. All conditions of test stimuli showed a similar trend. This trend was consistent with the result of the subjective naturalness evaluation of adaptation stimuli. Furthermore, the results showed a weak colorfulness adaptation effect even when adapting to the lightness contrast-modulated stimuli. The border of "natural" and "too colorful" appearance shifted to higher saturation after adapting to images with higher lightness contrast. This suggests the contribution of

lightness contrast on colorfulness perception. However, the difference of colorfulness adaptation effect in naturally-modulated stimuli and unnaturally-modulated stimuli could not be explained solely by lightness contrast. Therefore, colorfulness adaptation would be largely affected by the naturalness of images.

INTRODUCTION

Our visual system can adapt to various changes in the color environment, including colorfulness. Mizokami et al. showed the effect of colorfulness adaptation by using natural and shuffled images consisting and revealed the effect was stronger for the natural images than for the shuffled images [1]. It suggests that the natural structure of images is important for colorfulness adaptation. They examined the condition that only the saturation of images was modified without changing the luminance of images. Nakano et al. showed that the image appeared more natural when the luminance contrast of the image was increased (decreased) according to the increase (decrease) of the saturation of the image than when only saturation was changed [2]. When the saturation and luminance contrast of images are modulated, we can change the naturalness of images without changing the spatial structure and the object recognition of images. Therefore, we measured whether the combination of saturation and lightness contrast in adaptation images influenced the colorfulness adaptation. We showed that the adaptation effect was stronger for the natural combination of saturation and lightness contrast than for the unnatural combinations [3]. However, we did not differentiate the contribution of chromatic contrast and lightness contrast. There is a possibility that the modulation of lightness contrast of images enhanced the colorfulness of images and affected colorfulness adaptation. In this research, we examine the effect of colorfulness adaptation from the viewpoint of naturalness and the contribution of lightness contrast on images.

EXPERIMENT

1. Environment

The experiment was conducted in a dark booth. In the booth, an LCD monitor and a chin rest were installed. An observer fixed the head with the chin rest and kept the viewing distance at 80 cm.

2. Stimuli

Three types of modulated images were used as adaptation stimuli: images which only their saturation changed ("Saturation-modulated stimuli"), images which their lightness contrast changed in proportion to the saturation ("Naturally modulated stimuli"), images which their lightness contrast changed in inverse proportion to the saturation ("Unnaturally modulated stimuli") and images which only their lightness contrast changed ("Lightness contrast-modulated stimuli"). Each stimuli group included six images. Their lightness contrast was modulated by multiplying the modulation coefficient j to the contrast of L^* , and their saturation was modulated by multiplying the modulation coefficient k to the metric chroma C^*_{ab} in the CIE1976 $L^*a^*b^*$ color space. Figure 1 shows the example of adaptation stimuli based on the combination of modulation coefficients (j_a, k_a) . Test stimulus for colorfulness judgment were two types of images which only their saturation was changed, and they were not included in adaptation stimuli. Figure 2 shows the example of test stimuli and their saturation modulation coefficients k_b and the average metric chroma C^*_{ab} of each image.

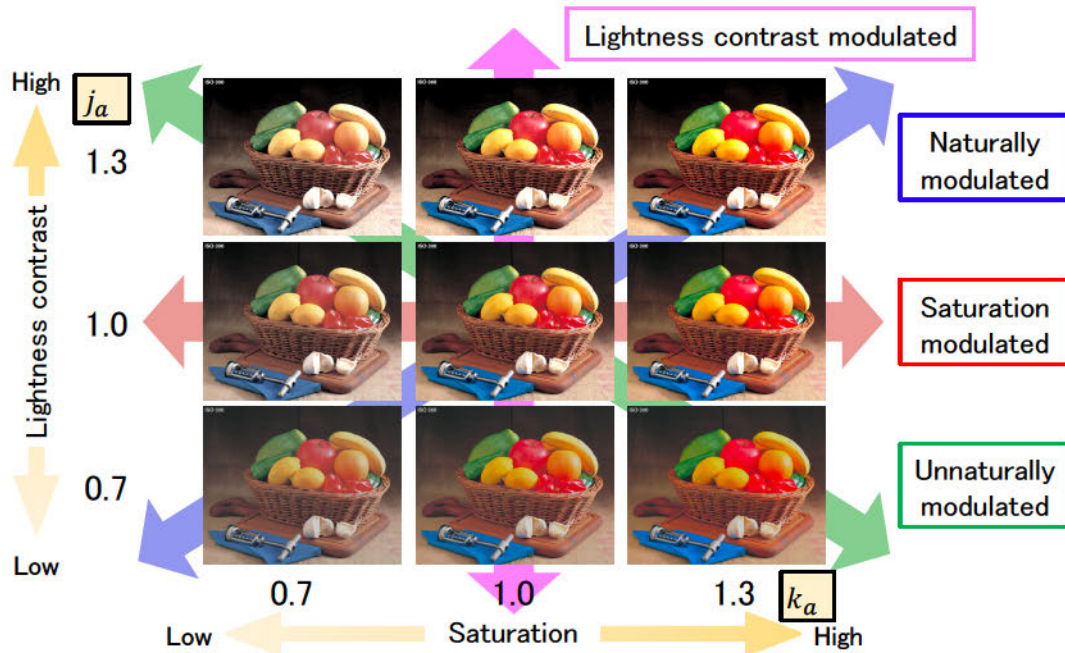


Figure 1. Example of adaptation stimuli

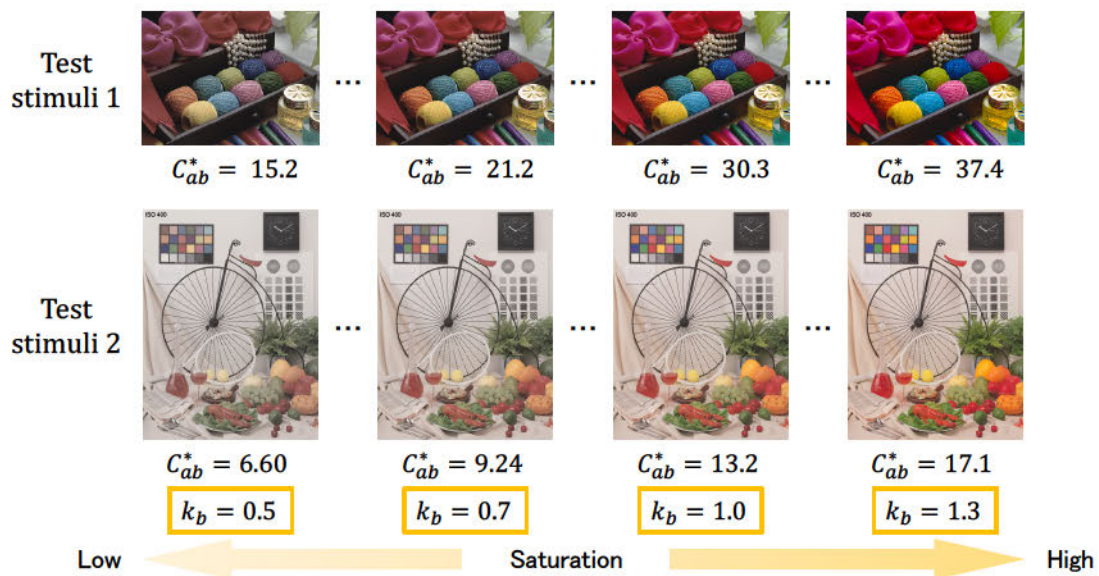


Figure 2. Example of test stimuli

3. Procedure

The experiment was conducted by the method of constant stimuli. After dark adaptation for 3 minutes, six images with a certain saturation level chosen from one of the adaptation stimuli groups were randomly presented at different positions on the monitor every 2 seconds, and observers adapted to them for 2 minutes. After that, a test image was presented for 3 seconds, and observers judged whether the test image appeared “natural” or “too colorful.” After the judgment, observers re-adapted to the same adaptation stimuli for 10 seconds. This judgment was repeated five times for seven test images during one session. We examined three saturation levels in three adaptation stimuli groups and three lightness contrast levels in lightness contrast-modulated stimuli. Seven observers participated, and each observer ran three sessions for each condition.

RESULT

The modulation coefficient k_b when the probability that the observer responded test stimuli “too colorful” was 50% was obtained by the probit analysis and set as the colorfulness threshold k_t . It means the border of “natural” and “too colorful” of test stimuli. Figure 3 shows the relationship between the saturation modulation coefficient of adaptation stimuli k_a and the colorfulness threshold k_t of test stimuli for one observer (Obs.1, Test stimuli 1). Linear fitting lines in Figure 3 show a linear approximation to the result of each modulation condition and that of the original image by the least-squares method. It shows that the adapted saturation of images influenced the perception of colorfulness: when observers adapted to higher saturation, the border of “natural” and “too colorful” appearance became higher and vice versa. The effect of colorfulness adaptation was confirmed in all conditions. Other participants showed a similar tendency.

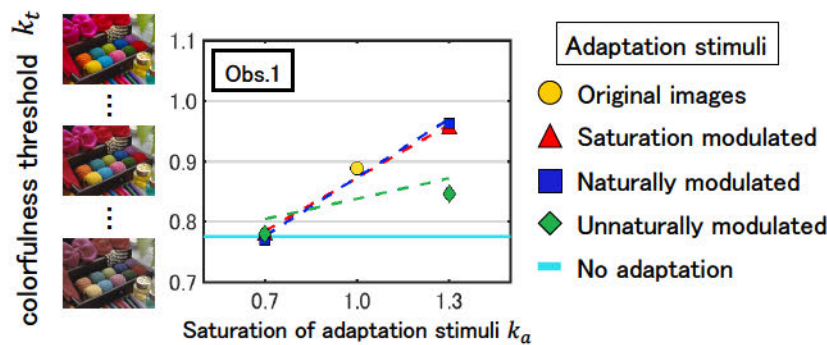


Figure 3. Relationship between the saturation modulation coefficient of adaptation stimuli k_a and the threshold k_t of test stimuli for one observer (Obs.1, Test stimuli 1).

We defined a value that k_t of each adaptation condition minus k_t of “Original images” as an adaptation effect. Figure 4 shows the adaptation effect of each adaptation stimuli on each test stimuli. When adapting to low saturation stimuli, the effect was almost the same on each adaptation stimuli. On the other hand, when adapting to high saturation stimuli, the effect was stronger for saturation-modulated and naturally-modulated stimuli, but weaker for unnaturally-modulated stimuli. This trend is consistent with each test stimuli.

Figure 5 shows the result when adaptation stimuli were images in which only lightness contrast was modulated. The result indicates that the lightness contrast modulation also affected colorfulness adaptation. The effect is a little stronger when adapting to high lightness contrast modulated images than when adapting to low lightness contrast modulated images in test stimuli 1, but not in test stimuli

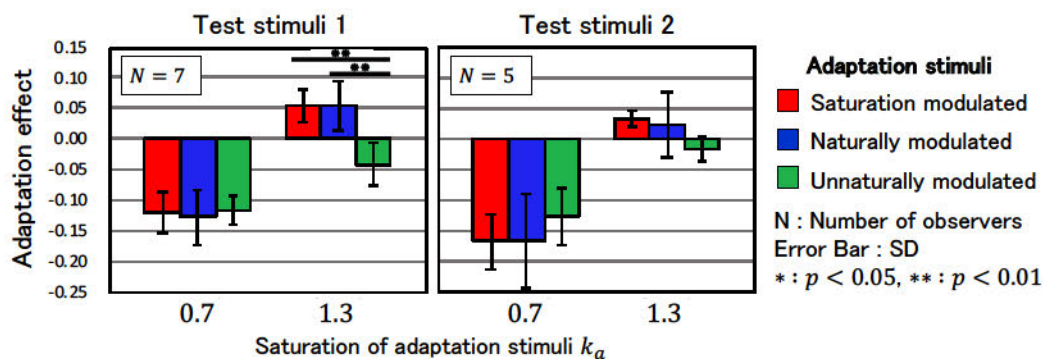


Figure 4. The effect of colorful adaptation on each test stimuli.

2.

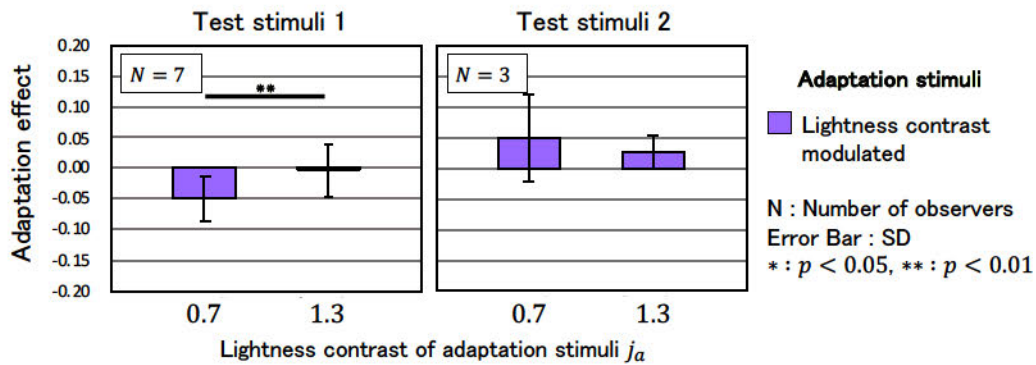


Figure 5. The effect of colorful adaptation by lightness contrast modulated stimuli on each test stimuli.

DISCUSSION

Our results showed that colorfulness adaptation is stronger for the natural combination of saturation and lightness contrast than for the unnatural combinations. The subjective evaluation of the naturalness of adaptation stimuli and the effect of colorfulness adaptation has a relationship at high saturated adaptation stimuli [3]. However, there is a possibility that lightness contrast modulation of images enhanced the colorfulness of images and affected colorfulness adaptation. Therefore, we took the effect of lightness contrast on adaptation (Figure 5) into each result (Figure 4) to measure how much the modulation of lightness contrast contributed to the adaptation effect. We subtracted the adaptation effect of lightness contrast modulated stimuli from the adaptation effect of saturated adaptation stimuli, whose modulation coefficient of lightness contrast was the same as that of them. Figure 6 shows the result of each test stimuli. The purple filled square and dotted lines show how much the adaptation effect has increased or decreased by considering only lightness contrast modulation. It shows that the difference of the adaptation effect between the conditions of high saturated adaptation stimuli becomes smaller at test stimuli 1. It means the lightness contrast of images contributed to the effect of colorfulness adaptation. However, the difference of colorfulness adaptation effect in naturally-modulated stimuli and unnaturally-modulated stimuli could not be explained solely by lightness contrast.

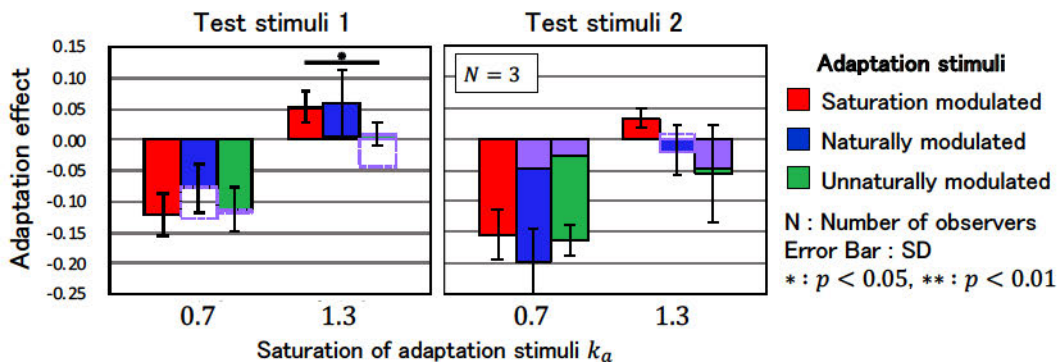


Figure 6. The effect of colorful adaptation considering the effect of lightness contrast.

We also conducted the evaluation of colorfulness for each adaptation stimuli to clarify whether high lightness contrast of images enhanced the colorfulness impression of images. In this experiment, two types of stimuli were used: images whose saturation can be changed in 0.05 steps (“Adjustment stimuli”) and images for standard (“Standard stimuli”). Observers adjusted the saturation of

adjustment stimuli to the overall colorfulness impression of standard stimuli. The standard stimuli were naturally-modulated, unnaturally-modulated stimuli and lightness contrast modulated stimuli. The original images of adjustment stimuli and standard stimuli were always the same. Each observer ran three sessions. Figure 7 shows the results for each standard stimulus. The vertical axis means matching saturation showing how much standard stimuli appeared colorful. The results show that the impression of colorfulness is almost the same in each adaptation condition. These results indicate that the modulation of lightness contrast did not change the colorfulness impression of images. In other words, the difference of the adaptation effect between the condition of adaptation stimuli did not come from the difference of the colorfulness impression by lightness contrast modulation.

From the above, lightness contrast modulation of images solely could not explain the adaptation effect and did not enhance the colorfulness impression of images. Therefore, the adaptation effect would be largely affected by other factors of images, which may be the naturalness of images, as we had shown before [3].

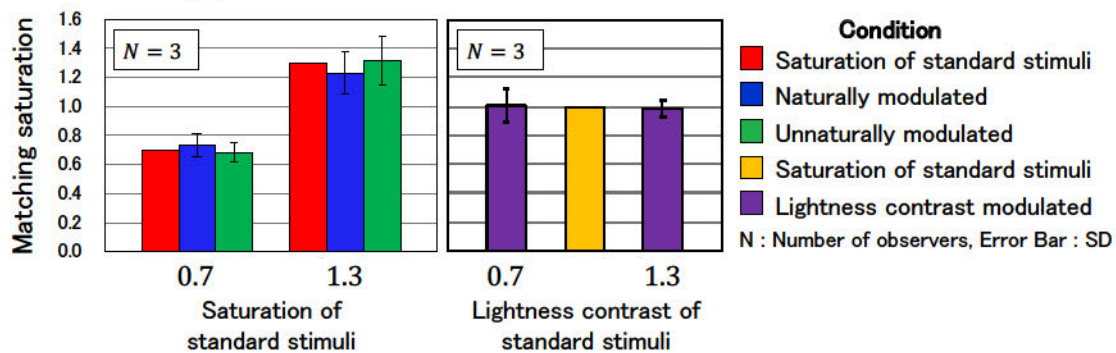


Figure 7. Results of the evaluation of colorfulness of each adaptation stimuli

CONCLUSION

Our results showed that colorfulness adaptation was influenced by the combination of the saturation and lightness in images. When observers adapted to images with higher saturation, the border of “natural” and “too colorful” appearance became higher and vice versa. This colorfulness adaptation effect was stronger when adapting to stimuli with saturation modulation only and those with both saturation and lightness contrast modulation, and weaker when adapting to stimuli with the unnatural combination of saturation and lightness contrast modulation. Although there is the contribution of lightness contrast, the difference of colorfulness adaptation effect in naturally-modulated stimuli and unnaturally-modulated stimuli could not be explained solely by lightness contrast. Therefore, colorfulness adaptation would be largely affected by the naturalness of images.

REFERENCES

1. Mizokami, Y., Kamesaki, C., Ito, N., Sakaibara, S. & Yaguchi (2012). Effect of spatial structure on colorfulness adaptation for natural images. *Journal of the Optical Society of America A*, 29(2), 118-127.
2. Nakano, L., Takeuchi, T., Motoyoshi, I., Li, Y., Adelson, E., & Nishida, S. (2009). The effect of color saturation and luminance contrast on color naturalness. *Journal of Vision*, 9(8), 1040, 1040a
3. Masumitsu, T., & Mizokami, Y. (2018). Effect of natural combination of saturation and lightness contrast on colorfulness adaptation. *The 4th conference of the Asia Color Association Proceeding book*, 278-282.

Effect of the acquired memory color of objects on color constancy

Tomohiro Funaki¹ and Yoko Mizokami²

¹*Department of Imaging Science, Division of Creative Engineering, Graduate School of Science and Engineering, Chiba University, Japan*

²*Department of Imaging Sciences, Division of Creative Engineering, Graduate School of Engineering Chiba University, Japan*

*Corresponding author: Tomohiro Funaki, tomohiro_funaki@chiba-u.jp

Keywords: Color constancy, Memory color, Illumination

ABSTRACT

It is known that memory color affects color constancy. For example, Olkkonen et al. (2008) showed that the memory colors were formed in objects which we were familiar with, such as bananas, and the color constancy for these objects improved. In previous researches, however, it was not clear if color constancy improved even when we newly memorize the unfamiliar color of objects. Our study aims to investigate the influence of memory color made by observing unfamiliar color objects on color constancy. In the experiment, we used a light with a correlated color temperature of 5000K as a reference. We used lights with 2700 K and 66500 K along the black body locus as well as Red and Green lights in a direction perpendicular to black body locus as test lights. The distance between the reference and each test light was set to be equal. In this setting, we can compare if the degree of color constancy is different depending on illumination color along black body locus or an orthogonal locus. Stimuli were the food models of "rice ball," which is familiar to Japanese people and generally remembered as a white object. The stimuli were painted to have chromaticity values under the reference light close to each of five illumination colors. This is to be able to compare the amount of color difference of white stimulus and other color stimuli under the same illumination and to examine if a color judgment was based on the reflectance of object surface (perfect color constancy) or radiance from object surface (no color constancy). Observers evaluated the color appearance of the stimuli using elementary color naming method under each illumination color and evaluated the impression of the illumination and stimuli before memorizing the colors of stimuli. After that, observers memorized the color of stimuli for ten days. After confirming that a stable memory color was formed in the pre-observation, the same experiment evaluating their color appearance was performed again. We analyzed the color constancy by color difference in color response between under the 5000K reference light and the other light colors. The larger this value is, the larger the difference in appearance is, which means that the effect of color constancy is smaller. Our result showed that the color appearance difference generally reduced after the pre-observation and was stable compared to that before the pre-observation. Both before and after the pre-observation, the color difference was small in the white rice ball, which is the general color of the stimulus. However, it is not clear whether this good color constancy was caused by the effect of memory color or the effect of achromatic color. Although there were individual differences in the stimulus color showing better color constancy, the color constancy for stimuli with other colors tended to improve after the pre-observation. This result suggests that acquired memory color by a short-term observation influences color constancy. We partially find a difference in the degree of color constancy among black body locus and an orthogonal locus.

INTRODUCTION

Memory colors are known to affect color constancy. For example, Olkkonen et al. (2008) showed that memory colors were formed with objects we are familiar with, such as bananas, and improved color constancy for these objects [1]. Vurro (2013) et al. showed that the accuracy of memory colors increases with the texture and outline of objects [2]. As for the illumination color, Pearce et al. (2014) show that the color constancy is easier to work with the illumination color in the black body locus direction than the illumination color in the orthogonal locus direction [3]. However, in previous studies, it was not clear whether a new memory of an unfamiliar color of the object would improve color constancy. Our research aims to investigate how color constancy is influenced by memory colors made by observing colored objects with unfamiliar colors.

EXPERIMENT

1. Experimental environment

The experiment was conducted in a 150 cm x 300 cm booth simulating a regular room. Various objects, such as stuffed animals and house plants, were placed in the booth.

2. Illumination and Stimulus

In the experiment, we used five illumination colors and five stimuli for color evaluation.

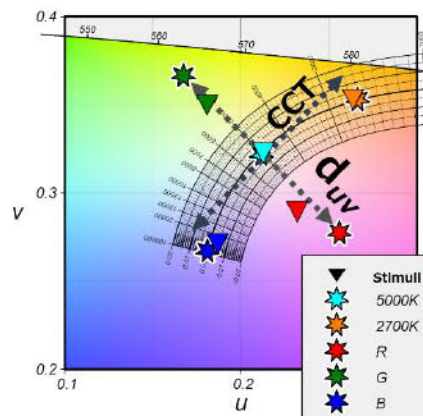


Figure 1. chromaticity diagram of the illumination and stimuli



Figure 2. Stimuli Images

Figure 1 shows the uv chromaticity coordinates of illumination and stimuli used in the experiment. In the experiment, illumination with a correlated color temperature of 5000K was used as a reference. For the test illumination, we used 2700 K and 66500 K illumination along the black body locus, and red and green illumination in the direction perpendicular to the black body locus. The distance between the reference light and each test light was set equal. With this setting, we can compare whether the degree of color constancy varies depending on the color of the illumination along the blackbody locus or the orthogonal locus. For test stimuli, we used “rice ball” food models, which is well known to Japanese and is generally remembered as a white object. Figure 2 shows the images of stimuli. Each stimulus was painted to have a chromaticity value close to each of the five illumination colors, under a reference light. This is to be able to compare the amount of color difference of white stimulus and other color stimuli under the same illumination. We can examine if a color judgment was based on the reflectance of the object surface (perfect color constancy) or radiance from the object surface (no color constancy).

3. Procedure

An observer evaluated the appearance of the stimulus color using an elementary color naming method under each illumination color and evaluated the illumination and the impression of the stimulus before memorizing the stimulus color. The observer then memorized the color of the stimulus for ten days. A memory color test was performed on the 0th, 5th, and 10th days. For each stimulus, the observer chose stimulus colors close to memory from the color chart. After confirming that stable memory colors were formed by prior observation, the same elementary color naming experiment was performed again to evaluate the appearance of those colors. The experiment was performed by six observers with a normal color vision before and after the observation. Each performed two sessions.

RESULTS

The amount of color shift was defined as the difference between the color appearance under the 5000K standard illumination and the color appearance under each test illumination. The larger the difference is, the greater the change in color appearance is when the illumination color changes, meaning that the color constancy is less likely to work.

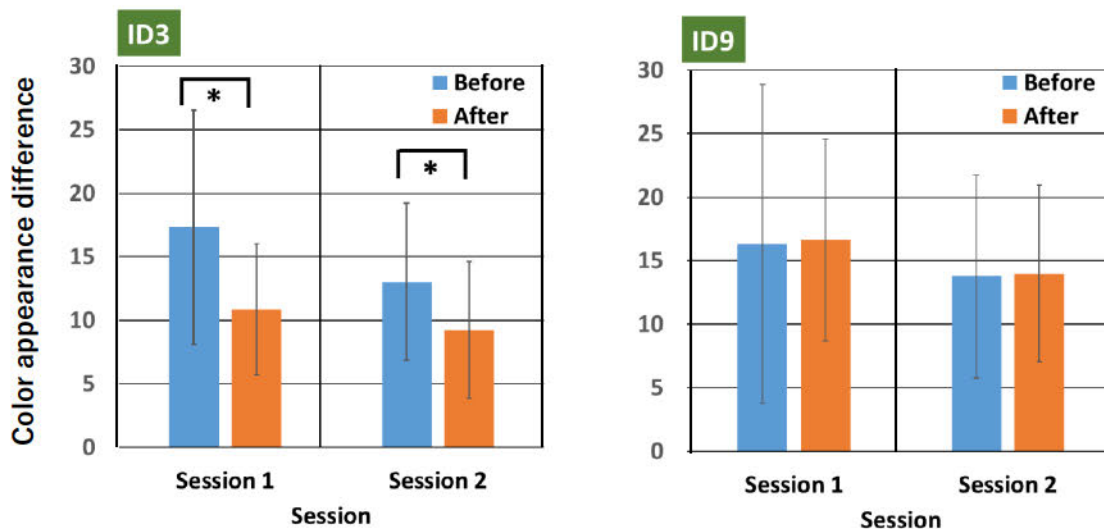


Figure 3. Example of change in color appearance difference before and after observation

Figure 3 shows the results for observers ID3 and ID9. Due to the specifications of the experimental database, the number of observers does not match the numbers of IDs. As the results of ID3, there were differences in the total color shift amount before and after pre-observation in 5 observers. The amount of color shift was smaller after observation, suggesting that color constancy was more likely to work. On the other hand, the results of ID9 showed no difference in a color shift before and after observation.

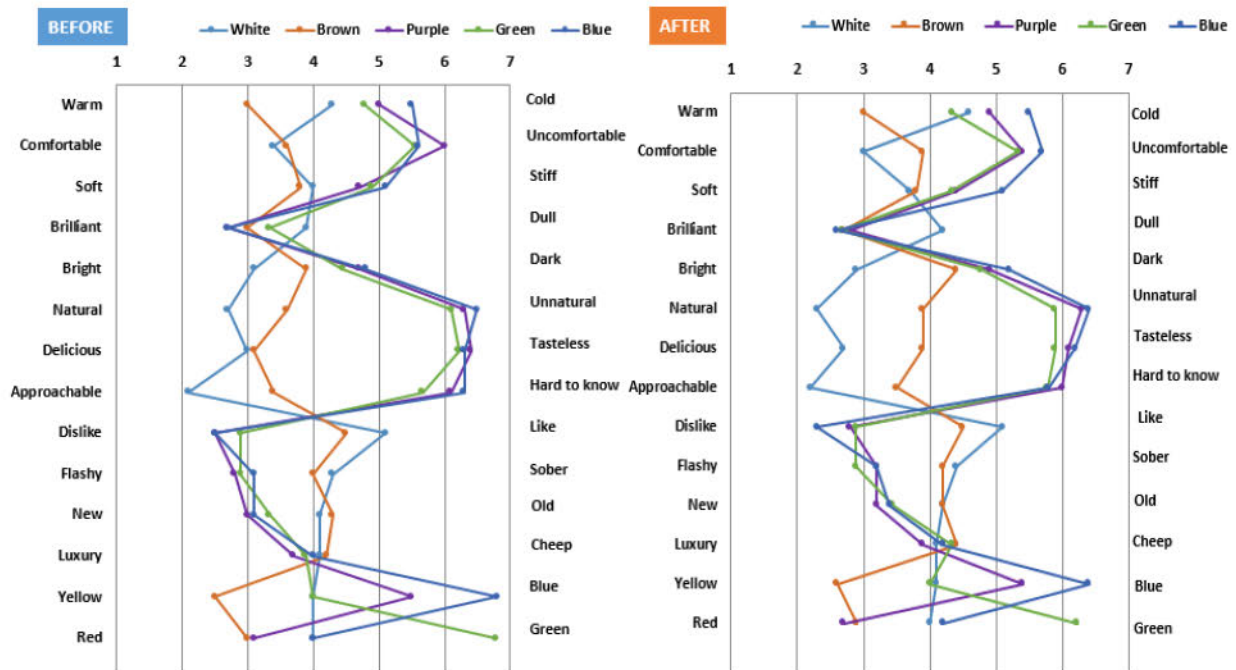


Figure 4. Change in the impression of stimulus before and after observation

Figure 4 shows the results of an impression evaluation experiment on stimuli. There was no significant difference between the values before and after the observation.

DISCUSSION

The experimental results of the elementary color naming method showed that the color constancy was improved after observation for most observers.

Figure 5 shows the change in the average color shift of all observers before and after observation for illumination and stimuli. The effect of the change in the color shift of the white stimulus is small. It is not conclusive if it is because the white stimulus is achromatic, or it is a standard color of rice balls. It can be seen that the color shift in green illumination is reduced after observation. The result of the impression evaluation experiment shows that green illumination gives the impression of incongruity. It implies that memory color is more effective for color constancy in more unnatural illumination.

If we look at the results in detail, there was a significant difference in the change in a color shift before and after observation between 2700K illumination and green illumination. The average change in a color shift under 2700K illumination was -3.4, and the average change in a color shift under green illumination was -9.2. The cluster analysis of the impression evaluation showed that these two illuminations are in different clusters. It would be possible that the difference in impression caused a difference in the effect of color constancy caused by prior observation.

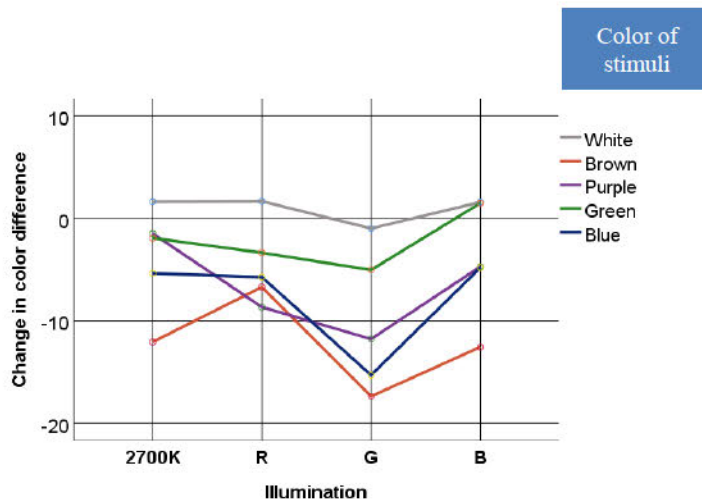


Figure 5. Detail of change in color difference before and after observation

Among the stimuli, there was a significant difference in the color shift change before and after observation between white (Ave: 2.0) and the group of purple (Ave: -6.2) and blue (Ave: -6.9). White and the group of purple and blue are located in different clusters, and purple and blue are located in the same cluster. The difference in impression may have affected the way that color constancy works in the stimuli.

CONCLUSION

There was a tendency for color constancy to work more effectively after ten days of observation. It was also suggested that the influence of the memory color is more considerable under illumination with unfamiliar color.

ACKNOWLEDGEMENT

This work was partially supported by JSPS KAKENHI JP 16K00368 and 19H04196.

REFERENCES

1. Olkkonen, M., Hansen, T., & Gegenfurtner, K. R. (2008). Color appearance of familiar objects: Effects of object shape, texture, and illumination changes. *Journal of Vision*, 8(5),13-13.
2. Vurro, M., Ling Y., & Hurlbert, A. C. (2013). Memory color of natural familiar objects: Effects of surface texture and 3-d shape. *Journal of Vision*, 13 (7): 20, 1–20,
3. Pearce, B., Crichton, S., Mackiewicz, M., Finlayson, G. D., Hurlbert, A. (2014) Chromatic illumination discrimination ability reveals that human colour constancy is optimised for blue daylight illuminations. *PLoS ONE* 9(2): e87989.

EFFECTS OF DISPLAY ON DEPTH DISCRIMINATION OF MOVING STIMULI

Takuto Ito^{1*}, Tomonori Tashiro¹, and Yasuki Yamauchi¹

¹*Department of Informatics, Graduate School of Science and Engineering, Yamagata University, Japan.*

*tke37836@st.yamagata-u.ac.jp

Keywords: Binocular disparity, frames-per-second, 3D, depth perception

ABSTRACT

Video has been presented at higher frame rates as the video technologies have been developed. To investigate the effects of the frame rate on human perception, Kime et al. (2016) conducted a discrimination experiment using videos at two different frame rates: 60 and 1000 frames-per-second (fps). The results showed the threshold under the frame rate with 1000 fps video was clearly higher than that with 60 fps. It means that human perceptual performance improves as the frame rate increases. In recent years, 3D videos have been penetrated on various devices, and have become more familiar to us. In the case of the 3D video, subject perceive depth using binocular disparity which was mediated by showing the left and right eyes the shifted images. The improvement of human perception due to the increase of frame rate may also improve the depth perception by binocular disparity. Nasiri et al. (2015) subjectively evaluated video quality using various frame rates up to 60 fps. As the frame rate increases, the quality of the video is improved and the effect is saturated at around 60 fps. However, their research focuses on the quality of the video, and the effects of the frame rate on the depth perception were not been studied. As such, there are few studies on the effect of frame rate on depth perception due to binocular disparity.

In order to investigate how the frame rate affects the discrimination of depth by binocular disparity, this study examined the quantitative relationship between the frame rate and the discrimination threshold velocity of the depth of the moving stimulus: the maximum speed at which the depth discrimination can be performed. In this experiment, changes in the speed at which the subject's stimulus depth can be differentiated were investigated using five frame rates: 30, 60, 80, 120, and 240 fps.

We used random dot stereogram (RDS) as a stimulus to examine only the discrimination of depth by binocular disparity. Two stimuli were presented successively. One of these two stimuli had disparity to mediate depth perception. Depth and frame rate were selected randomly. The subject responded which stimulus, first or second, had depth with two-alternative forced choice method. The discrimination threshold velocity was obtained with stair-case method. The depth was set to 3 conditions: 0.18, 0.42, 0.62 deg, and the difference in the influence of the frame rate due to the difference in depth was also investigated. 4 subjects participated in the experiments.

As a result, it showed the depth discrimination threshold velocity increased as the frame rate increased. This tendency was saturated at 80 fps. Furthermore, it was found that stimuli with greater depth are more affected by the frame rate. This suggests that the improvement of human perception due to the increase of frame rate improves the depth perception mediated by binocular disparity.

INTRODUCTION

Videos have been presented at higher frame rates as the video technologies have been developed. To investigate the effects of the frame rate on human perception, Kime et al. (2016) conducted a discrimination experiment using videos at two different frame rates: 60 and 1000 frames-per-second (fps). The results showed the threshold under the frame rate with 1000 fps video was clearly higher than that with 60 fps [1]. It means that human perceptual performance improves as the frame rate increases. Recent years, 3D videos have been penetrated on various devices, and have become more familiar to us. In the case of the 3D video, subject perceive depth using binocular disparity which was mediated by showing shifted images to the left and right eyes. The improvement of human perception due to the increase of frame rate may also improve the depth perception by binocular disparity. Nasiri et al. (2015) subjectively evaluated video quality using various frame rates up to 60 fps. As the frame rate increased, the quality of the video was improved, and the effect was saturated at around 60 fps [2]. However, their research focused on the quality of the video, and the effects of the frame rate on the depth perception were not been studied. As such, there are few studies on the effect of frame rate on depth perception mediated with binocular disparity.

In order to investigate how the frame rate affects the discrimination of depth by binocular disparity, this study examined the quantitative relationship between the frame rate and the discrimination threshold velocity of the depth of the moving stimulus: the maximum speed at which the depth discrimination can be performed. In this experiment, changes in the speed at which the subject's stimulus depth can be differentiated were investigated using five frame rates: 30, 60, 80, 120, and 240 fps.

EXPERIMENTAL CONDITION

We used random dot stereogram (RDS) as a stimulus to examine the discrimination of depth by binocular disparity (Figure 1). RDS was used as stimulus for avoiding any pictorial cues. The depth was set to 3 conditions: 0.18, 0.42, 0.62 arcmin.

Schematic diagram of the experimental apparatus is shown in Figure 2. We used mirrors to fuse right and left image. Subjects perceived depth on center of stimuli when fusing right and left images.

Four subjects in their 20s with normal visual acuity participated in the experiment.

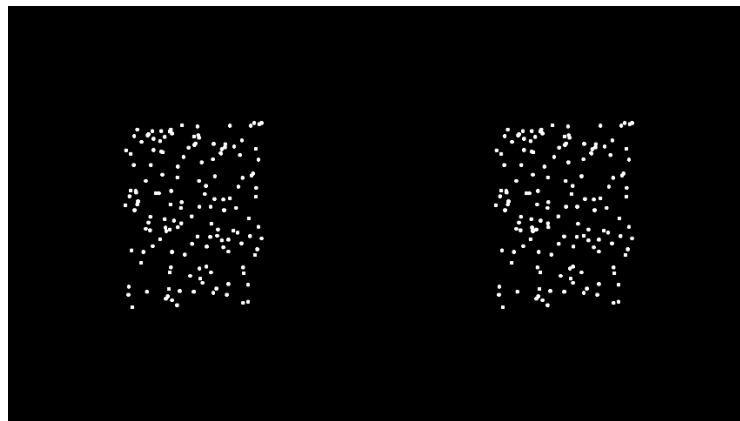


Figure 1. Example of the stimulus (RDS) shown to the subjects

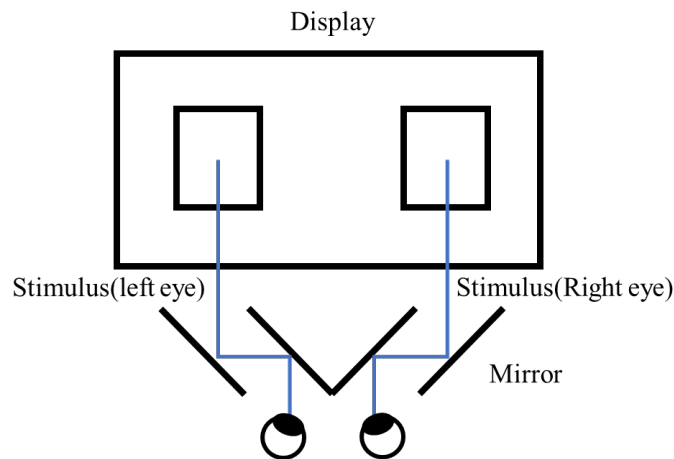


Figure 2. Experimental apparatus : Right and left mirrors deliver images to right and left image, respectively. When stimuli had disparity, a subject could perceive depth.

PROCEDURE

Before starting a session, the subject dark adapted for 60 secs. Then after pressing any key on the keyboard, a trial started. In each trial, two moving stimuli were presented with an interval for 0.5 sec successively. Stimuli moved in vertical direction from top to bottom. One of these two stimuli had disparity to mediate depth perception. Depth and frame rate were selected randomly. The subject responded which stimulus, first or second, had depth with two-alternative forced choice method. 0.5 sec after the response, next trial was started.

The discrimination threshold velocity was obtained with stair-case method. When the subject responded correctly, the velocity of the moving stimuli increased, while the velocity decreased for the wrong response. Each session ended with 15 turns. The average was calculated from the turning points of the last 5 times and used as the threshold.

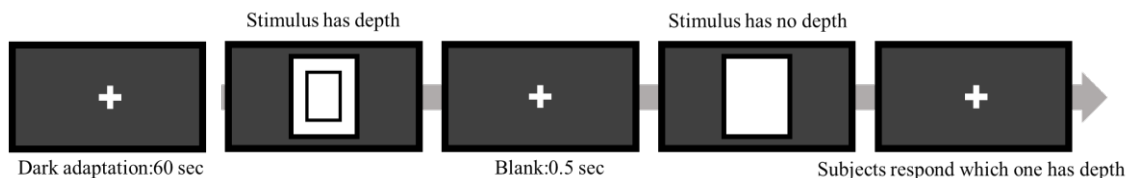


Figure 3. Experimental paradigm : After dark adaptation experiment was started. Displayed a fixed point between the first and second stimuli (0.5 sec) and waiting for a response.

RESULT

Figure 4 shows the depth discrimination threshold velocity increased as the frame rate increased.

As a result of two-way ANOVA, there was a significant difference between 30-60 and 60-80 fps at 0.62 arcmin and there was no significant difference between frame rate conditions 80-120 and 120-240 fps. In 0.42 arcmin, there was a significant difference between 30-80 fps. There was no significant difference between the frame rate conditions at 0.18 arcmin (Table 1).

It was found from the result that the threshold velocity increases with the frame rate as the parameter increases and converges at 80 fps.

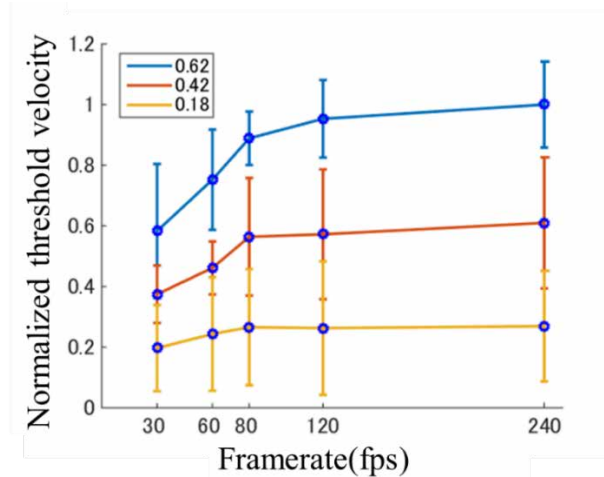


Figure 4. Threshold velocity across frameratess. Normalization was performed with a depth condition of 0.62 arcmin and a frame rate condition of 240 fps as 1. The horizontal and vertical axes denote the frame rate condition and the normalized speed, respectively. The depth discrimination threshold velocity increased as the frame rate increased, saturated around 80 fps.

Table 1. As a result of two-way ANOVA.
 ** means there was a significant ($p < 0.01$), n.s. means there was no significant.

	0.18 deg/sec					0.42 deg/sec					0.62 deg/sec				
	30	60	80	120	240	30	60	80	120	240	30	60	80	120	240
30		n.s.	n.s.	n.s.	n.s.		n.s.	**	**	**		**	**	**	**
60	n.s.		n.s.	n.s.	n.s.	n.s.		n.s.	n.s.	n.s.	**	**	**	**	**
80	n.s.	n.s.		n.s.	n.s.	**	n.s.		n.s.	n.s.	**	**		n.s.	n.s.
120	n.s.	n.s.	n.s.		n.s.	**	n.s.	n.s.		n.s.	**	**	n.s.		n.s.
240	n.s.	n.s.	n.s.	n.s.		**	n.s.	n.s.	n.s.		**	**	n.s.	n.s.	

CONCLUSION & FUTURE WORK

In this study, it was shown the depth discrimination threshold velocity increased as the frame rate increased. This tendency was saturated at around 80 fps. Furthermore, it was found that stimuli with greater depth are more affected by the frame rate. This suggests that the improvement of human perception due to the increase of frame rate improves the depth perception mediated by binocular disparity.

In this experiment, subjects were showed only the vertical movement. However, video contents contain much more complicated directions of motion. We have to verify whether our findings in this study can be also applied to different patterns of motion.

REFERENCES

[1] S.Kime et al, "Psychophysical Assessment of Perceptual Performance With Varying Display Frame Rates", Journal of Display Technology, vol.12, no.11, pp.1372-1382, November, 2016
 [2] R.Nasiri et al, "Perceptual quality assesment of high frame rate video", IEEE 17th International Workshop on Multimedia Signal Processing, pp.19-21, October, 2015

HOW CAN THE WATERCOLOR EFFECT BE ENHANCED BY STIMULUS CONFIGURATION?

Shoko Isawa^{1,2}, Kazutaka Takeo², Nanako Koda³, Tomonori Tashiro² and Yasuki Yamauchi²

¹*Department of Modern Home Economics, Tokyo Kasei Gakuin University, Japan.*

²*Department of Informatics, Graduate School of Science and Engineering, Yamagata University, Japan.*

³*Department of Informatics, Yamagata University, Japan.*

Shoko Isawa, isawa@san.kasei-gakuin.ac.jp

Keywords: Watercolor effect, Color perception, Hue cancellation method, Whiteness

ABSTRACT

Our findings from previous experiments have demonstrated that the intensity of the watercolor effect is influenced by how colors are combined in the stimulus image.^{[1][2]} In this study, we use the hue cancellation method to measure the amount of change in the watercolor effect when curve modulation is performed to quantitatively verify the intensity of the effect.

The experiment was conducted using a liquid crystal display (EIZO ColorEdge CG223W) in an experimental booth where external light was blocked. The distance between the subject and the display was 70 cm. For the experimental stimuli, we used the following color combinations: yellow-blue (YB), red-green (RG), and green-red (GR) (the first color in each pair is the inner color and the second is the outer color). These color combinations give rise to stronger color assimilation effects than the colors used in our previous experiments. The size of each stimulus was 500 pixels by 500 pixels, and it was presented at an angle of approximately 10.7 degrees and a viewing distance of approximately 70 cm. The stimuli were varied across two parameters: frequency modulation, which changes the number of waves, and amplitude modulation, which changes the amplitude of waves. Five levels of modulated stimuli were prepared for each parameter. The subjects adapted to the environment in the experimental booth for approximately 3 minutes before the presentation began. Thereafter, stimulus images corresponding to each parameter configuration were presented in succession at the center of the display. As each stimulus was presented, the subject was asked to use the mouse to adjust the area inside the frame, which initially appeared colored due to the watercolor effect, until it appeared white or achromatic. After the response was received, the next stimulus was presented. The five stimulus images under both modulation conditions (frequency and amplitude) were each presented five times in a randomized order for a total of 75 trials. In addition, photometry (metering) was carried out for each result. The subjects comprised three male, who were in their twenties and had normal color vision.

The results of the experiment showed that under both the frequency and amplitude modulation conditions, the subjects tended to select chromaticity points in a direction complementary to the color that was perceived to have spread into the framed area. Under the frequency modulation conditions, as the frequency increased, the amount of shift from the white point also increased; this proved that the watercolor effect intensifies with increase in frequency. Under the amplitude modulation conditions, the peaks in the intensity of the watercolor effect varied depending on the color pattern. In both the experiments, the influence of frequency and amplitude modulation varied depending on the color pattern.

INTRODUCTION

A colored line running parallel and contiguous to a darker contour will appear to spread its color onto a white area enclosed by the line. When drawing an outline figure with a double line consisting of two chromatic colors, the color inside the double outline appears to seep out of the enclosed region. This phenomenon is called the watercolor effect^[1]. This effect indicates that our perception for the central part can be altered depending on the surrounding color setting.

The results of our previous experiments showed that the intensity of the watercolor effect is influenced by how colors are combined in the stimulus image^{[2][3]}. In this study, we focused on the extent to which the watercolor effect changes when curve modulation is performed. Peggy et al.^[4] conducted experiments using the conjoint measurement method to investigate the joint effects of luminance contrast, contour frequency, and amplitude modulation on the watercolor effect.

In this study, we used the hue cancellation method to measure the amount of change in the watercolor effect when surrounding curves are modulated either in amplitude or in frequency. By comparing the amount of the color shift for the test stimulus to appear white (achromatic), we can quantitatively verify how much the watercolor effects are.

METHOD

Experimental environment and stimuli

The experiment was conducted using a liquid crystal display (EIZO ColorEdge CG223W) in an experimental booth. The distance between the subject and the display was approximately 70 cm. For the experimental stimuli, we used the following color combinations: yellow-blue (YB), red-green (RG), and green-red (GR) (the first and second color in each pair denote the inner and outer colors, respectively). These color combinations give rise to stronger color assimilation effects than the colors in our previous experiments. Figure 1 shows the three types of stimuli used in the experiment. The stimulus was a square of approximately 10.7 degrees. The stimuli were varied across two parameters: frequency modulation, which changes the number of waves, and amplitude modulation, which changes the amplitude of waves. Five levels of modulated stimuli were prepared for each parameter. For frequency modulation, the values 0.4, 0.6, 0.7, 1.2, and 2.1 cycles per degree (cpd) were used, and for amplitude modulation, the values 0.3, 0.4, 0.7, 0.8, and 1.2 degrees were used. Figures 2 and 3 show examples of frequency-modulated and amplitude-modulated stimuli, respectively.

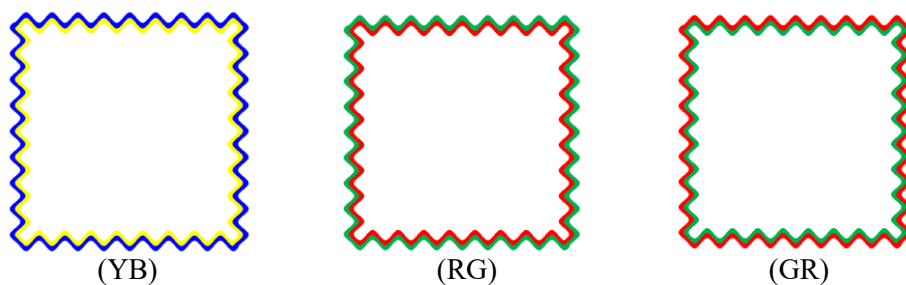


Fig. 1: Examples of stimuli used in the experiment

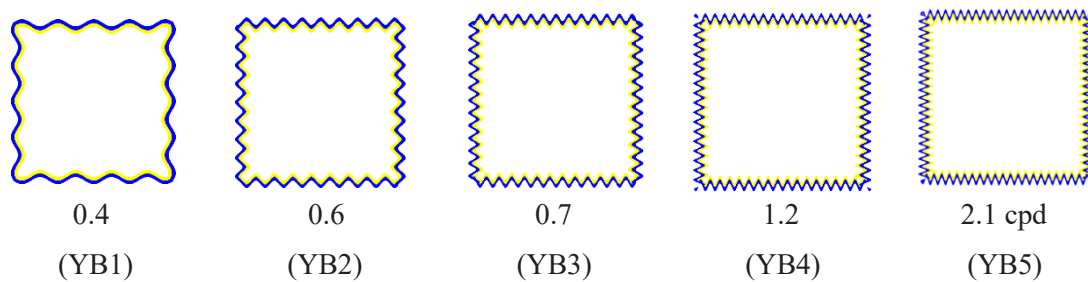


Fig. 2: Examples of frequency-modulated stimuli used in the experiment

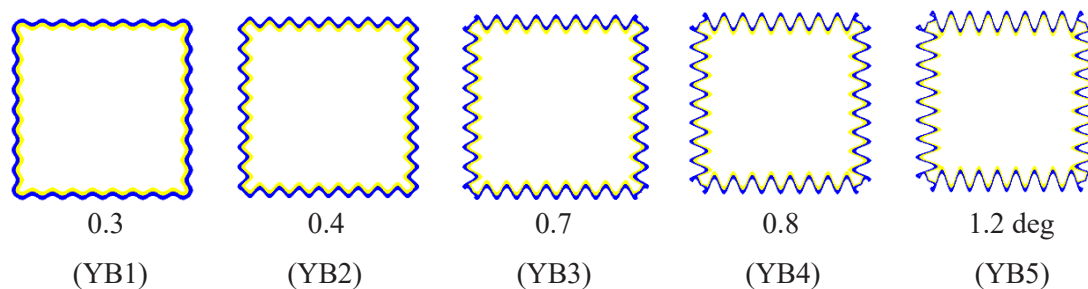


Fig. 3: Examples of amplitude-modulated stimuli used in the experiment

Experimental procedure

The subjects adapted to the environment in the experimental booth for approximately 3 minutes before a session started. Each session was composed of 75 trials, where 5 different configurations for all of the 3 color patterns were randomly displayed, and 5 repetitions for each stimulus. In each trial, the subject was asked to use the mouse to change the color of the area inside the frame, which initially appeared colored due to the watercolor effect, until it appeared white or achromatic. After the response was received, the next stimulus was presented.

Two modulation conditions, frequency modulation and amplitude modulation, were conducted in a different session.

Subjects

Three male students participated in this experiment, who were in their twenties and they had normal color vision.

RESULTS AND DISCUSSION

Frequency modulation condition

The results of the experiment are presented in the $u'v'$ color space.

Figure 4 shows the average chromaticities under the frequency modulation conditions of the GR stimulus, which had caused the watercolor effect to be most pronounced. The subjects' selected chromaticity points under all the modulation conditions were located in a direction complementary to the color that was perceived to have spread into the framed area. The figure shows that as the frequency of the frame increases, the chromaticity points tend to move further away from the white

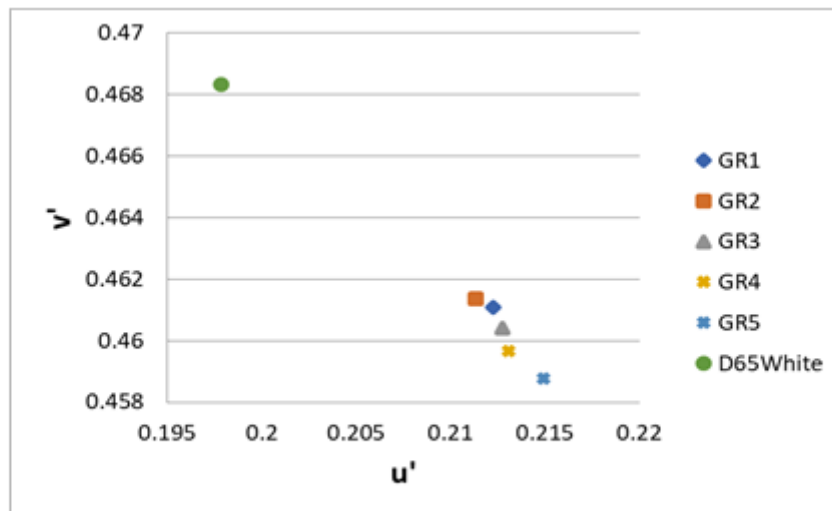


Fig. 4: Average chromaticities under frequency modulation conditions (GR)

point and in the direction of greater saturation.

Figure 5 shows the amount of the shifts for all the stimuli from white point, which represents color differences on the $u' v'$ chromaticity diagram. It shows that for the GR stimulus, the amount of shift from the white point tends to increase noticeably as the spatial frequency increases. This means that as the distance from the white point increased, the chromaticness required to cancel the chromaticness of the center also increased, which indicated the watercolor effect was felt more strongly. It was also found that the amount of shift from the white point varied depending on the color pattern. This suggests that the impact of frequency modulation may be different for different color patterns.

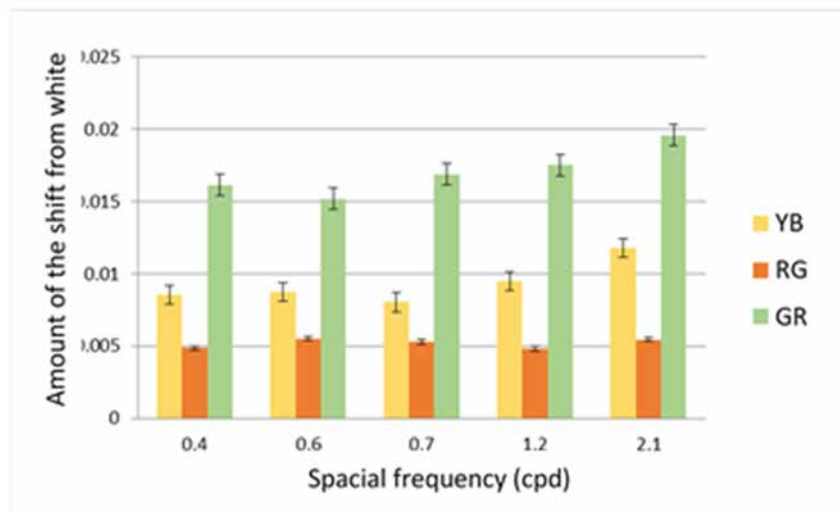


Fig. 5: Amount of the shift from white point for each experimental condition on the $u' v'$ chromaticity diagram under frequency modulation conditions

Amplitude modulation condition

Figure 6 shows the average chromaticities under the amplitude modulation conditions of the GR stimulus, similar to the frequency modulation experiment. Under all the modulation conditions, the subjects selected chromaticities in a direction complementary to the color that spread into the framed area. On the other hand, depending on the color pattern, there were cases where the chromaticity coordinates regressed toward low saturation near the white point at the maximum amplitude.

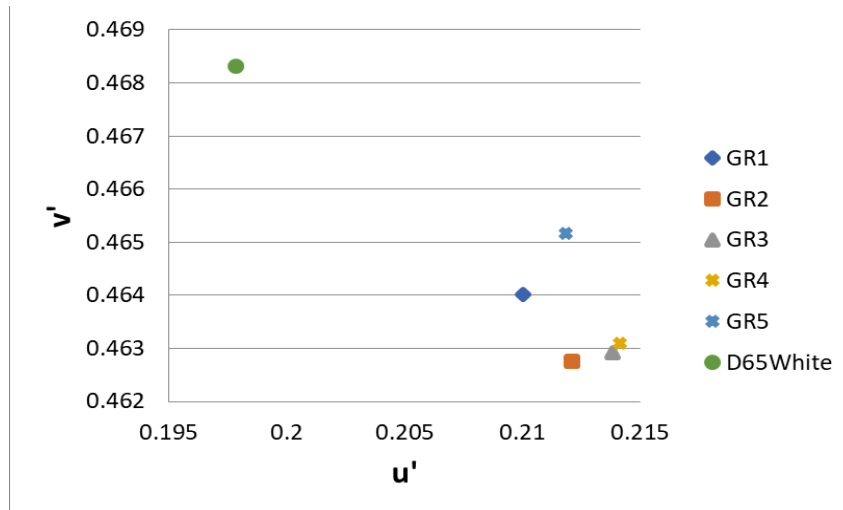


Fig. 6: Average chromaticities under amplitude modulation conditions (GR)

Figure 7 shows the amount of the shifts for all the stimuli from white point, which represents color differences on the u' v' chromaticity diagram. Compared to the results of the frequency modulation experiments, the differences in the amount of shift between different color patterns were smaller. The peaks in the intensity of the watercolor effect varied depending on the color pattern. In addition, there were variations in the amount of shift depending each color patterns, suggesting that the impact of amplitude modulation may be different for different color patterns.

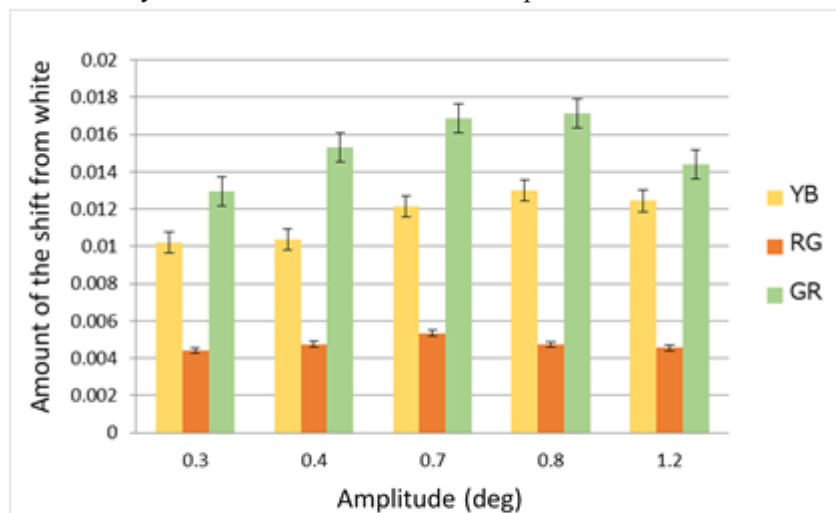


Fig. 7: Amount of the shift from white point for each experimental condition on the u' v' chromaticity diagram under amplitude modulation conditions

CONCLUSIONS

In this study, we used the hue cancellation method to quantitatively verify the intensity of the watercolor effect. By measuring the amount of change in the watercolor effect when the modulation conditions for the curve changed, we obtained the following results:

1. Under both the frequency and amplitude modulation conditions, the subjects tended to select chromaticity points in a direction complementary to the color that was perceived to have spread into the framed area.
2. Under the frequency modulation conditions, as the spatial frequency of the GR stimulus was increased, there was a noticeable increase in the amount of shift away from the white point.
3. Under the amplitude modulation conditions, the peaks in the intensity of the watercolor effect varied depending on the color pattern.
4. Under both the frequency and amplitude modulation conditions, the impact of each modulation condition appeared to vary depending on the color pattern.
5. The influence on the watercolor effect is caused more strongly by frequency modulation.

REFERENCES

1. Pinna, B., Brelstaff, G., Spillmann, L. 2001. Surface color from boundaries: a new 'watercolor' illusion. *Vision Research* 41(20): pp.2669-2676.
2. Isawa, S. 2016. A Study of the Perceived Whiteness Change by the Watercolor illusion. *Journal of Tokyo Kasei Gakuin University* No.56, pp. 27-32.
2. Isawa, S., Tashiro, T., Nagai, T., and Yamauchi, Y. 2018. Whiteness Enhancement Using the Watercolor Effect. *Proceedings of the 4th Conference of Asia Color Association*, pp. 317-321.
3. Peggy, G., Frederic, D., Michel, D., and Kenneth, K. 2014. Contributions of contour frequency, amplitude, and luminance to the watercolor effect illustrated by conjoint measurement. *Journal of Vision* 14 (4): 9, pp. 1-14.

TOWARDS CONSISTENT COLOR APPEARANCE - EVALUATION OF CLOSENESS OF COLOR IMAGES WITH A TRENDLINE -

Tomonori Tashiro^{1*}, Yuto Nakamura², Yuta Terashima², Syori Yamada²,
Takehiro Nagai³, Yasuki Yamauchi¹

¹*Department of Informatics, Graduate School of Science and Engineering, Yamagata University, Japan.*

²*Department of Informatics and Electronics, Faculty of Engineering, Yamagata University, Japan.*

³*Department of Information and Communications Engineering, School of Engineering, Tokyo Institute of Technology, Japan.*

*Corresponding author: Tomonori Tashiro, tomotashiro@yz.yamagata-u.ac.jp

Keywords: Color appearance, Consistent color, Trendline, Closeness evaluation, Color image

ABSTRACT

Recently, many color image output devices such as displays and printers are widely available. They sometimes reproduce different colors even though they are provided with the identical color information because of the different gamut size. In order to deal with this issue, some mapping technique was adopted to convert the color information into the device gamut. Then we need to evaluate whether these mappings are appropriately conducted or not. Several methods to estimate the difference of colors such as CIE DE 2000 and CIE 76 have been proposed. These metrics are able to show quantitative differences between two colors, but they do not necessarily represent subjective differences in color impression or appearance. In order to address this problem, we have proposed a trendline-based approach. In our approach, we assume that each color has several “consistent colors”, which give the same or quite similar impression or the appearance to the original color, even though their saturation and lightness differ, and we can get a trendline by connecting each consistent color. That is, as far as two colors are on the same trendline, they look similar, where consistent color appearance holds. We tried to find consistent colors for 12 reference colors empirically. In order to obtain a trendline for each reference color, an observer changed the test color on the surface of a given gamut until the test color appeared the most similar, or most consistent in appearance to that of the reference color. As a result, we could get a trendline for consistent color appearance by fitting the closest colors of different gamuts. In this study we investigated whether it is possible to quantitatively evaluate the closeness of impressions or appearances for the images using these trendlines. In the experiment, two sets of images were presented to the observer, and he chose which set appeared to have more consistent color appearance. Each set of images were consisted of four images including the original Adobe RGB image. Three other images were created by converting original image to either large, medium, or small size gamuts. Four images: red, green, blue dominant images with a person and multicolor natural image were used. Ten observers in their twenties participated in an experiment, and each observer repeated the evaluation twice. The degree of closeness of each image set was evaluated by expressing the results as Z-scores. The reference color, red, green, and blue was converted by applying the same conditions as converting test images. Euclidian distance between each converted color and the trendline of the same color was calculated. Sum of the three distance values with composed a set of the images were used as the total color difference, compared with Z-scores obtained by image comparison experiment. As a result, the subjective evaluation value decreases as the total color difference increases. This means that a set of images having a small total color difference has a higher evaluation of the closeness of impression or appearance than that having a large difference.

INTRODUCTION

Recently, many color image output devices such as displays and printers are widely available. They sometimes reproduce different colors even though they are provided with the identical color information because of the different gamut size. In order to deal with this issue, many mapping techniques have been developed to convert the color information so that it will be fit into the device gamut. Then we need to evaluate whether these mappings are appropriately conducted or not. Several methods to estimate the difference of colors such as CIE DE 2000 and CIE 76 shown in Eq.1 and Eq.2 have been proposed [1,2]. Color differences mean that the psychological difference that humans perceive, and usually Euclid distance between the two colors in the color space are used to express color differences [3]. These metrics are able to show quantitative differences between two colors, but they do not necessarily represent subjective differences in color impression or appearance. In order to address this problem, we have proposed a trendline-based approach. In this study we investigated whether it is possible to quantitatively evaluate the closeness of impressions or appearances for the images using a trendline-based approach.

$$dE_{00} = \sqrt{\left(\frac{\Delta L'}{k_L S_L}\right)^2 + \left(\frac{\Delta C'}{k_C S_C}\right)^2 + \left(\frac{\Delta H'}{k_H S_H}\right)^2} + R_T \left(\frac{\Delta C'}{k_C S_C}\right) \left(\frac{\Delta H'}{k_H S_H}\right) \quad (1)$$

$$dE = \sqrt{(L_1^* - L_2^*)^2 + (a_1^* - a_2^*)^2 + (b_1^* - b_2^*)^2} \quad (2)$$

TRENDLINE

In our approach, we assume that each color has several “consistent colors”, which give the same or quite similar impression or the appearance to the original color, even though their saturation and lightness differ, and we can get a trendline by connecting each consistent color. That is, as far as two colors are on the same trendline, they look similar, where consistent color appearance holds. Our previous researches tried to find consistent colors for several reference colors empirically [4,5].

In the experiment, 18 reference colors were used in total, 3 different luminance levels for 6 different hues. The hues were chosen as those of Adobe RGB of three primaries (Red, Green, Blue) and their mixtures (Cian, Magenta, Yellow). The test stimulus was the color on the surface of one of the CRPCs (Characterized Reference Printing Condition) proposed by CGATS [6]. We adopted CRPC7, CRPC5, and CRPC3. Adobe RGB space was used to display the reference colors. The reference colors which were shown during the setting increased as the difference of the color gamuts became larger (multiple reference method). In order to obtain a trendline for each reference color, an observer changed the test color on the surface of a given gamut until the test color appeared the most similar, or most consistent in appearance to that of the reference color. As a result, we could get a trendline shown in Figure 1 for a consistent color appearance by fitting the closest colors of different gamuts.

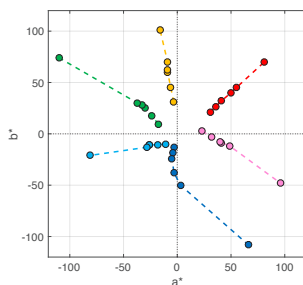


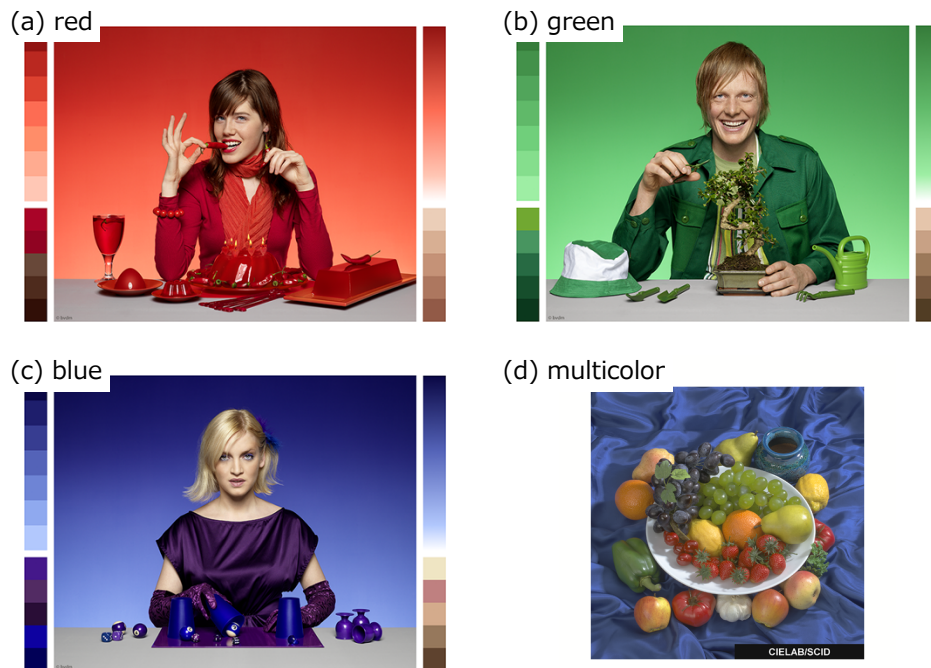
Figure 1. Result of trendline



Figure 2. Presentation example of image sets on display

EXPERIMENTAL METHOD

In the experiment, two sets of images were presented to the observer, as shown in Figure 2, and observer chose which set appeared to have more consistent color appearance. Four images, red, green, and blue dominant images with a person and multicolor natural image, are shown in Figure 3 as the original Adobe RGB images. Each set of images consisted of four images including the original Adobe RGB image. Three other images were created by converting original image to either large, medium, or small size color gamuts. A total of 18 image sets were created with different combinations of color gamuts and mapping strategies (either colorimetric or perceptual intent).



**Figure 3. Images used as a stimulus in the experiment:
(a) red, (b) green, (c) blue, and (d) multicolor**

The experiments were conducted in a booth whose walls were covered with black velvet. Fluorescent light with CCT 5000K lit the inside the booth in order to prevent observers from dark adaptation. The illuminance of the booth was approximately 100 lx. An LCD monitor (BenQ, Color Management Monitors SW320, 32 inch) was placed in front of the observer in order to present stimuli. The gamut of this monitor covered almost the entire Adobe RGB space. The distance between a monitor and an observer was approximately 80 cm. Observers could move their head freely.

Ten observers in their twenties participated in an experiment. The observation time was not limited. Each observer conducted the evaluation for all combinations of image sets. (153 combinations for each image set)

RESULTS AND DISCUSSION

The degree of closeness of each image set was evaluated by expressing the results as Z-scores. Results are shown in Figure 4. The horizontal axis indicates the different image set, and the vertical axis denotes Z-scores for each image set. Z-score was calculated based on the selection rate obtained from all observers. The higher the Z-score, the more consistent the image set. The results showed almost the same tendency regardless of the different color stimuli. Z-scores were high for image set g, h, I, j, and low for image set e, f.

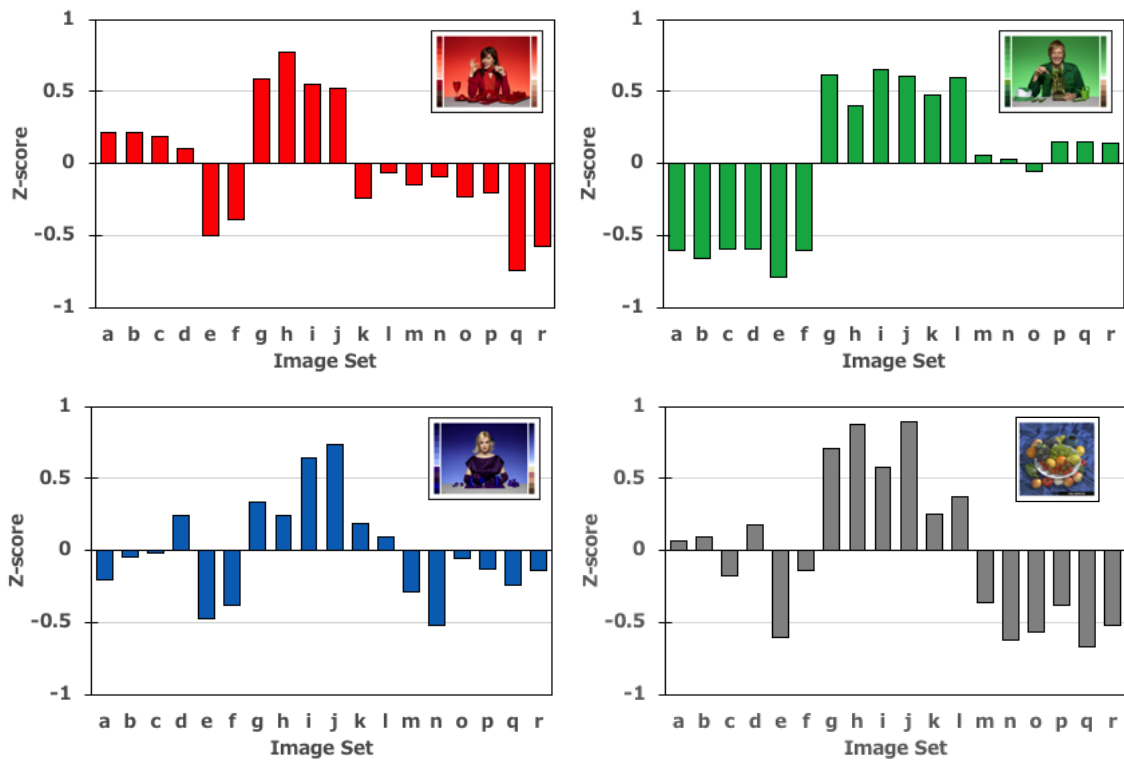


Figure 4. Results of experiment

Based on our trendline concept, a reference color should have a series of consistent colors with different saturation along a straight line or gentle curve towards achromatic point ($(a^*, b^*) = (0,0)$). Therefore, if the colors of the same location in each image are mapped along a sort of line, that image set should have highly consistency, assuming that line denotes a trendline. We tried to examine the relationship between chromaticities of the same location in a set of images and Z-score. The results are as shown in Figure 5. They are adopted from the green patch of the “green” image (Figure 3(b)). In the panel in Figure 5, black point is the chromaticity of the original image, and the other three points are chromaticities obtained by three images included in the set. The solid line is the trendline of the green primary color of Adobe RGB obtained in previous research, and the dotted line is a straight line connecting the chromaticity of the reference and the achromatic point. The results show that Z-scores are large when variations are small in the positional relationship between chromaticity of the original image and the other three points. This means that the concept of a trendline may be applicable to evaluate the closeness of color images. However, as the trendlines obtained so far are created only with the primary colors of Adobe RGB, it is necessary to consider how many trendlines are required for the evaluation in the future.

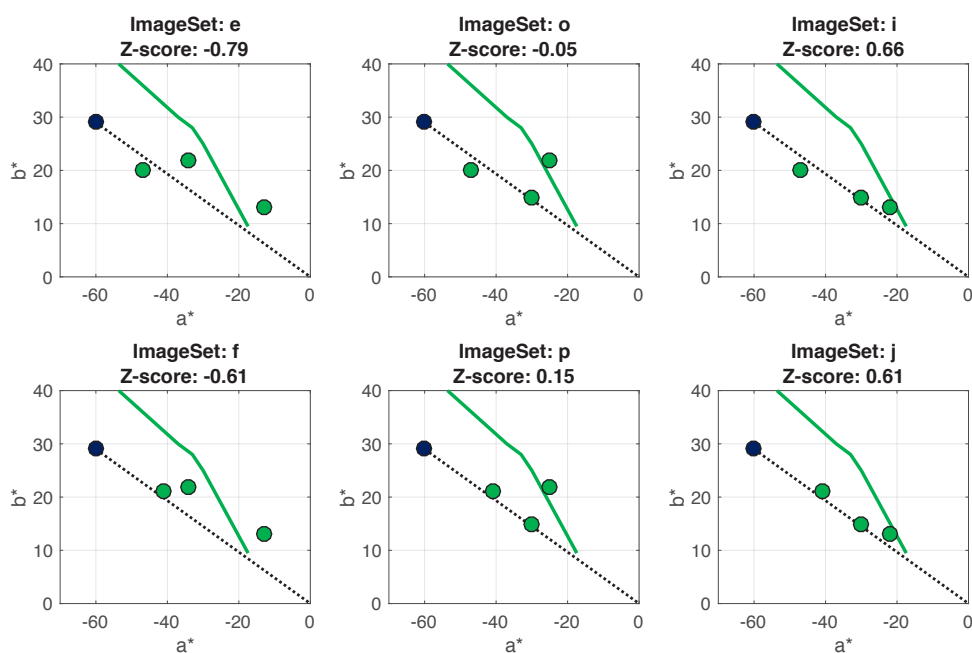


Figure 5. Relationship between Z-score and Chromaticity change

CONCLUSION

In this study we investigated whether it is possible to quantitatively evaluate the closeness of impressions or appearances for the images using a trendline-based approach. When the Z-score is higher, the results indicated that the chromaticity changes on the straight line. This suggested that the trendline-based approach may be applied to evaluate the closeness of color images. In the future, it is necessary to add trendlines with various reference colors

REFERENCES

1. CIE. (2001). Improvement to industrial colour-difference evaluation. *Vienna: CIE Publication No. 142-2001*.
2. CIE. (1986). Colorimetry – official recommendations of the international commission on illumination, *Vienna: CIE Publication No.15.2*.
3. Mokrzycki.W.S., Tatol.M. (2011). Color difference Delta E – A survey. *Machine Graphics and Vision*, Vol.20, No.4, pp.383-411.
4. Yamauchi.Y., Iida.Y., Kawashima.Y., Nagai.T. (2015). A New Metric for Evaluating the Closeness of Two Colors, *Proceedings of AIC2015*, pp.680-684.
5. Iida.Y., Kawashima.Y., Nagai.T., Yamauchi.Y. (2015). A novel metric to evaluate the closeness of the two colors, *Proceedings of CIE2015*, pp.1086-1092.
6. CGATS, <https://www.npes.org/programs/standardsworkroom/cgatstechnicalstandards.aspx>



Design concept behind the ACA2019 Nagoya Logo

This logo was designed based on the letters “A”, “C”, and “A”. The pair of gold figures in both “A” s represents the Kinshachi, golden tiger-fish roof ornaments on the top of Nagoya Castle. The “C” expresses a gathering from many different countries by using the color circle.

In this conference, Japanese traditional colors and texture patterns were used for the sign system and the name tags. One texture pattern was overlaid on one color. Therefore, everyone with any color vision can easily identify all colors. These texture patterns had been used as decorations of the interior of Nagoya Castle in the Edo period (Fig. 1-5). These colors and patterns are useful not only for enjoying Japanese culture but also for providing a universal design.



Color name AKE

It represents sunshine or the flame of a fire.

Pattern name SHIPPO

The repeated circles illustrate eternal happiness.



Fig. 1 Transom window



Color name HON-MURASAKI

The purple of a gromwell root was the most highly ranked color in ancient Japan.

Pattern name AOI

The heart-shaped leaves illustrate meeting your god.



Fig. 2 Transom window



Color name KONZIKI

Gold is a symbol of richness and power.

Pattern name KORAI-BERI

It is the pattern found on the edge of a tatami mat, which originated from ancient Korea.



Fig. 3 Edge of tatami



Color name HANADA-IRO

It is indigo blue.

Pattern name UROKO

This represents scales of a dragon or snake and regarded as protection from bad luck.



Fig. 4 Ceiling ornament



Color name KOKE-IRO

It is the color of a wet moss plant.

Pattern name ICHIMATSU

It represents the stone pavement pattern used in costumes for KABUKI dance.

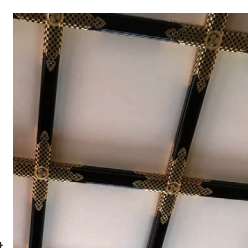


Fig. 5 Ceiling ornament

Sponsors / Exhibitors

Sponsors:

DENTALPRO Co.,Ltd. / JACKS BS SINGAPORE PTE LTD

We support the base for staying healthy forever.

For about 90 years since Sano Shigeru who is the founder found "Sano Shigeru Store" (forerunner of Taihei Kogyo) in 1927, we have been researching and developing products with "Engage in manufacturing and sales, praying for health and happiness of people who use our products" as a basic philosophy.

Moreover, we have proposed new values to the market with unique ideas of DENTALPRO. Base on our policy "We wish the users not only to become healthy when using our products but also to enjoy oral care", we have adopted "fun" and "fashionable" as important spice for product development.



ITO OPTICAL INDUSTRIAL CO., LTD.

Itoh Optical Group was the first Japanese manufacture to put the coating of ophthalmic lenses and contact lenses into the market. In 2007, we released Variantor, a filter simulating color vision deficiency. This new venture was carried out in cooperation with Prof. Nakauchi of Toyohashi University of Technology and Prof. Shinomori of Kochi University of Technology. In addition, in 2019, we released SeniorView, a filter simulating the visibility of the color world seen by the elderly. SeniorView was developed by Prof. Okajima of Yokohama National University. We keep continuing further progress and provide high quality lenses with our updated technology.



KICTEC INC.

KICTEC has worked in the area of transport, which forms the foundation of people's daily lives, the economy, and culture. We have helped to build public environments through the development, manufacture, and construction of products related to traffic safety, such as road markings and traffic signs. We will offer the values of comfort and peace of mind more widely to the world and realize our contribution to society.



KONICA MINOLTA JAPAN, Inc.

KONICA MINOLTA JAPAN, Inc. (Sensing Business Unit) is a leading company of measurement solutions for applications in the fields of Color & Appearance and Light Measurement.

Derived from our state-of-the-art optical and image processing technologies, measuring solutions from Konica Minolta help improve quality control and support R&D in a diverse range of industries.

Our color & appearance management solutions are essential for Quality Assurance & High Design Product Development in industries such as Plastics, Paints & Coatings, Automotive, Building Materials, Chemicals, Cosmetics, Pharmaceuticals and Graphic Arts.



OFFICE COLOR SCIENCE CO.,LTD.

Office Color Science Co., Ltd is specialized in computer system relating to color science. We have mainly developed Computer Color Matching system and Color QC system for Metallic and Pearlescent color. We pursue the possibility of color application and create value through our technology to enrich color design and producing.



Shinto Tsushin Co., Ltd.

SHINTO TSUSHIN is the agency contributes "interesting and exciting things" to the world based on the regions of Japan. We support your sales promotion, branding and business expansion with our crowdfunding, live video streaming and digital promotion services.



SHOFU INC.

SHOFU is a multinational, comprehensive manufacturer of dental materials and equipment. With our extensive research and development capabilities and technological expertise that have cultivated since our company's inception, SHOFU has successfully developed many innovative products that are ahead of the times and has contributed to advancements in dentistry. While maintaining leading market share in the fields of artificial teeth and abrasives in Japan, we now provide our products to more than 100 countries around the world.



TOYODA GOSEI CO., LTD.

Since the company was founded in 1949, Toyoda Gosei has contributed to society through the provision of automotive products that use rubber and plastics technology under the company credo of “Boundless Creativity and Social Contribution.” Today, we have 67 Group companies in 17 countries.



TOYOTA HOUSING CORPORATION

Toyota Housing Corporation has a diversified business portfolio that has detached housing, rental business as its main core, and also includes a stock business, apartment business, and special building business.

We have believed in holding as “customer first” and have put our whole hearts into making and selling products and providing after-sales services. The underlying philosophy for how Toyota Housing builds homes is our founding spirits, “Strive to make Japan’s homes better”

This philosophy is reflected in our brand vision’s motto of “Sincerely for You: Together for Life”, and how we value life-long relationships with our customers more than anything else.



Exhibitors:

EBA JAPAN CO., LTD.

EBA JAPAN develops various types of hyperspectral cameras that can measure what we cannot visualize. We are now launching new cameras called “target spectral cameras,” which are multispectral cameras specialized for each customer. Each camera is designed using optimal wavelength bands selected for the specific purpose.

We also provide a consulting service for customers so that they can solve their technical problems. Our state-of-the-art spectral technology has been bringing innovation to every industry.

We propose a new color management system using spectral information. One of our goals is to make this system a new global standard originating in Japan.



JAPAN COLOR ENTERPRISE CO., LTD.

Japan color enterprise Co., Ltd. manufactures and sells text, equipment, materials, color design tools, etc. for school education, specialized design education, and corporate training.

Our products are made under the supervision of the Japan Color Research Institute.

Since we have a wide variety of products, we would like everyone involved in color to use them.

* PCCS is a color system copyrighted by Japan color enterprise Co., Ltd.



KONICA MINOLTA JAPAN, Inc.

— See the previous page —

NAMOTO Co., Ltd.

We provide various equipment for mainly visual science and plant ecology research and related software that we import from overseas, and maintenance services. For visual science, we sell lighting environment simulation light source, visual stimulus generator, visual stimulus creation software, MRI compatible display, eye tracker, etc.



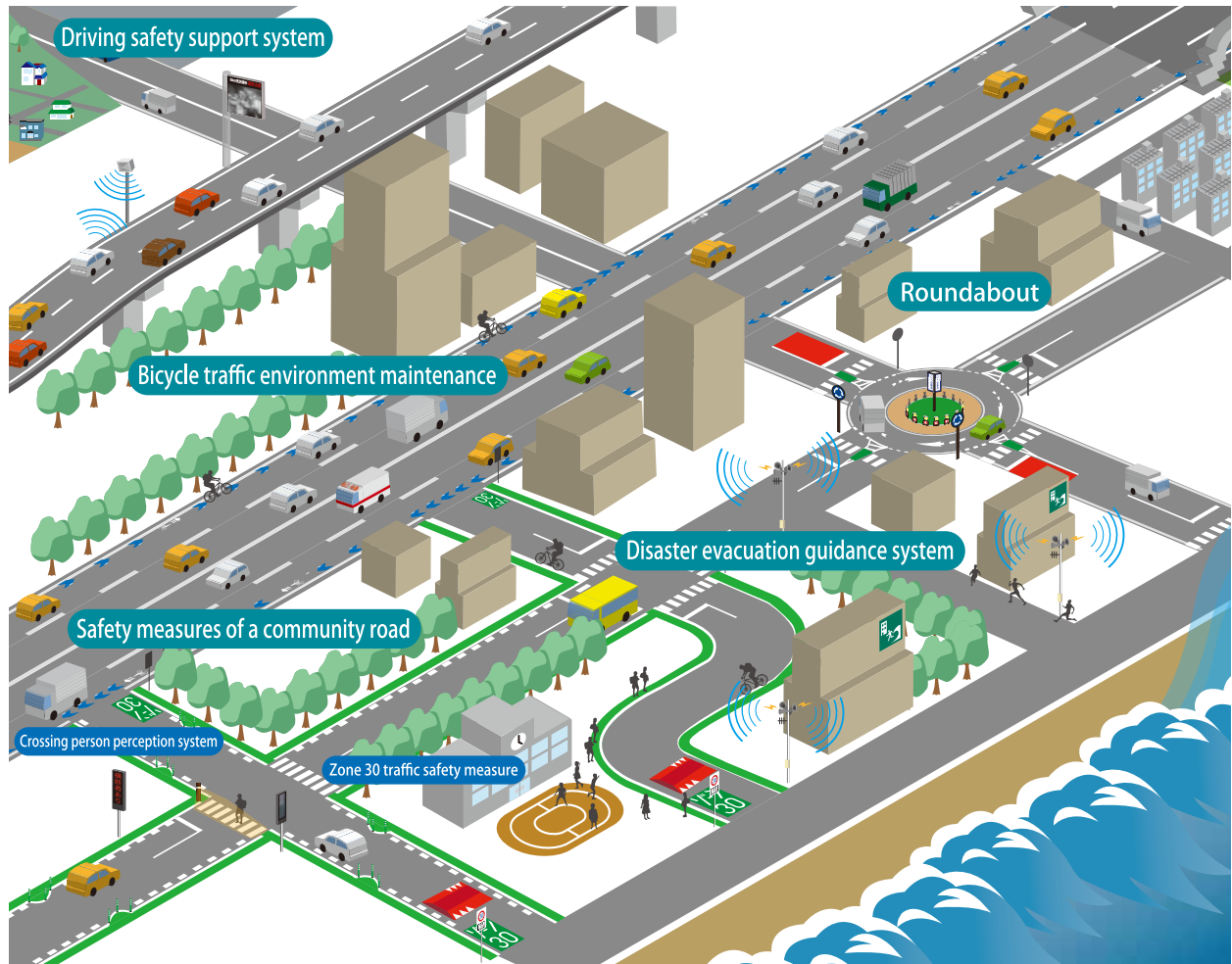
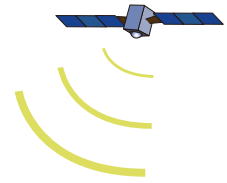
NIPPON DENSHOKU INDUSTRIES CO., LTD

Nippon Denshoku Industries Co.,Ltd is leading pioneer company, Color and light.



A traffic sign painted on the road and a road sign make the safe and safe future.

ICT-ITS society which KICTEC INC.makes



<https://www.kitect.co.jp>

Headquarters

1-26 Kafuku-Hondori, Minami-ku, Nagoya, Aichi 457-0836 Japan
TEL (81) 52-611-0680 FAX (81) 52-613-3934

Tokyo Headquarters

2-12-5 Hirakawa-cho, Chiyoda-ku, Tokyo 102-0093 Japan
TEL (81) 3-5226-0088 FAX (81) 3-5226-2152

Chubu Office

150 Umeogaoka, Usaka, Agui-cho, Chita-gun, Aichi 470-2295 Japan
TEL (81) 569-48-1145 FAX (81) 569-48-8255



Kitect ICT center

1111-7, Se, Araishinden, Shiraoka, Saitama Japan
TEL (81) 480-31-8222 FAX (81) 480-90-0088

Osaka branch (81) 72-987-2241
Shizuoka branch (81) 54-282-1856
Aichi branch (81) 569-48-8078
Mie branch (81) 59-232-6131
Gifu branch (81) 58-272-6833
Sapporo sales office (81) 11-790-6652
Morioka sales office (81) 19-652-6222
Sendai sales office (81) 22-241-4661

Niigata sales office (81) 25-280-1511
Nagano sales office (81) 26-256-8025
Kanazawa sales office (81) 76-262-1157
Hamamatsu sales office (81) 53-475-3396
Nagoya SP business division (81) 52-611-0737
Toyohashi sales office (81) 532-57-3631
Hyogo sales office (81) 78-882-9708
West Japan office (81) 86-253-2538

Hiroshima sales office (81) 82-263-0561
Kyushu sales office (81) 92-472-2012
Sendai Sign factory (81) 22-241-4712
Kikusui Construction Corporation (81) 3-3690-1501
Kitect ICT center (81) 480-31-8222
Kitect (Sendai) (81) 22-241-4661
Hokkaido Corporation (81) 11-790-6711



KONICA MINOLTA

Giving Shape to Ideas

How to measure color & appearance?

If the surface state or internal structure of the measuring objects are different from each other, these color & appearance (reflection characteristics) look also different.

Konica Minolta provides advanced optical technology that precisely measures the elements of color, appearance and light.

KONICA MINOLTA JAPAN, INC.

Sensing Business Unit
<https://sensing.konicaminolta.jp>



A creative group seeking interesting and exciting things, we are constantly striving for self-fulfillment as a way of contributing to the good of society through merchandising of ideas.

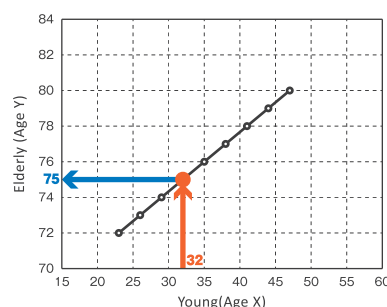
SHINTO TSUSHIN is the agency contributes “interesting and exciting things” to the world based on the regions of Japan. We support your sales promotion, branding and business expansion with our crowdfunding, live video streaming and digital promotion services.

SeniorView™ Elderly Vision Simulator



The relationship between a young observer of age X and an elderly person of age Y

Young(Age X)	Elderly (Age Y)
20	72
24	73
28	74
32	75
34	76
38	77
41	78
44	79
48	80



SeniorView enables you to experience the visibility of the color world seen by the elderly. You can understand the difficulties that aged people suffer in their daily lives.

The filters of SeniorView can precisely simulate the spectral transmittance of an aged human lens. They were designed based on a two-factor model so that the human lens of the standard 32 years old person with healthy eyes can virtually be replaced for the human lens of the standard 75 years old person with healthy yellowish eyes.

SeniorView was developed and supervised by Prof. Katsunori Okajima, Yokohama National University, and was manufactured by Itoh Optical Industrial Co.,Ltd. Gamagori 443-0041, JAPAN.

<http://www.variantor.com/senior/>



The new entry-level intraoral scanner for simple “scan and send-to” solution
TRIOS 3 intraoral scanner (S1P (Basic)) has been launched!!



TRIOS 3 intraoral scanner (S1P pen grip type)

Full set ... ¥5,980,000 License fee (from the 2nd year) ... ¥200,000

NEW

TRIOS 3 intraoral scanner (S1P (Basic))

Full set ... ¥2,980,000 License fee (from the 2nd year) ... ¥150,000

* PC is not included in the set. Please purchase one according to our laptop recommendations.

The prices above are suggested retail prices (tax excluded) as of October 2019



SHOFU INC. 11 Kamitakamatsu-cho, Fukuine, Higashiyama-ku, Kyoto 605-0983, Japan

Technology for a Brighter Global Future

世界のお客様へ「安心」「安全」「快適」をお届けします



 豊田合成

本社 / 〒452-8564 愛知県清須市春日長畑1番地
<https://www.toyoda-gosei.co.jp/>



“TOYOTA QUALITY” を住まいにも。

Also introducing TOYOYA's quality to residences.

「インドネシアの住宅をよくしたい」という想いのもと、
インドネシアのブカシ、カラワン地区で分譲事業を展開しています。

With the desire to make better housing in Indonesia,
we are developing a subdivision business in Bekasi and Karawang.



 トヨタホーム株式会社
TOYOTA HOUSING INDONESIA
<http://www.toyotahousing-id.com/>

